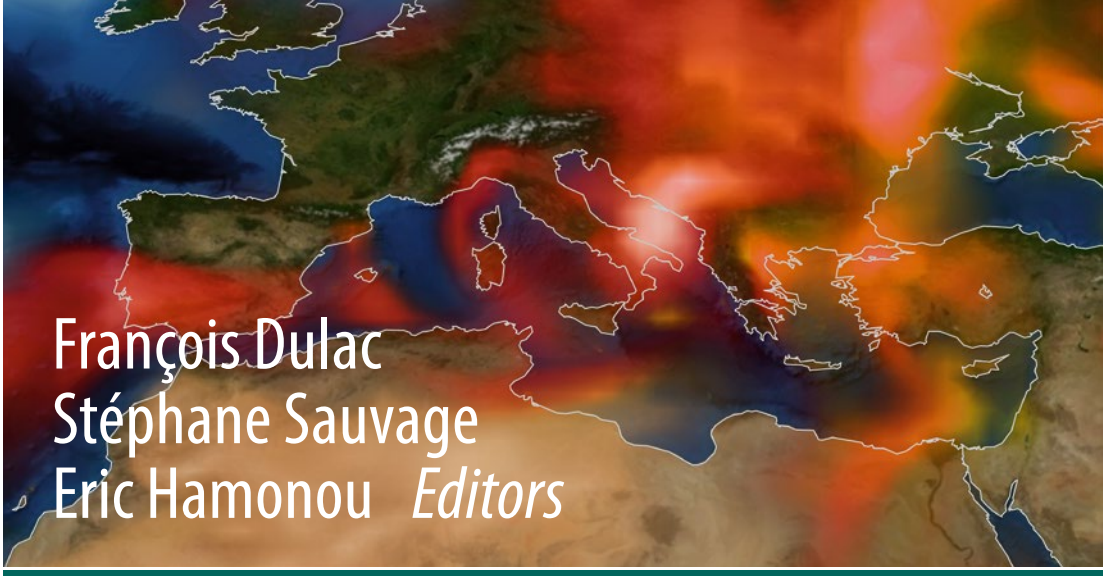

François Dulac
Stéphane Sauvage
Eric Hamonou *Editors*

Atmospheric Chemistry in the Mediterranean Region

Volume 2 - From Air Pollutant Sources to Impacts

Springer

Atmospheric Chemistry in the Mediterranean Region

François Dulac • Stéphane Sauvage
Eric Hamonou
Editors

Atmospheric Chemistry in the Mediterranean Region

Volume 2 - From Air Pollutant Sources to Impacts

Springer

Editors
François Dulac
Laboratoire des Sciences du Climat et de l'Environnement (LSCE)
CEA-CNRS-UVSQ
Université Paris-Saclay
IPSL, CEA Paris-Saclay
Gif-sur-Yvette, France

Eric Hamonou
Science Partners
Paris, France

Stéphane Sauvage
IMT Nord Europe
Institut Mines-Télécom
Univ. Lille
Centre for Energy and Environment
F-59000 Lille, France

ISBN 978-3-030-82384-9 ISBN 978-3-030-82385-6 (eBook)
https://doi.org/10.1007/978-3-030-82385-6

This Springer imprint is published by the registered company Springer Nature Switzerland AG
The registered company address is: Gewerbestrasse 11, 6330 Cham, Switzerland

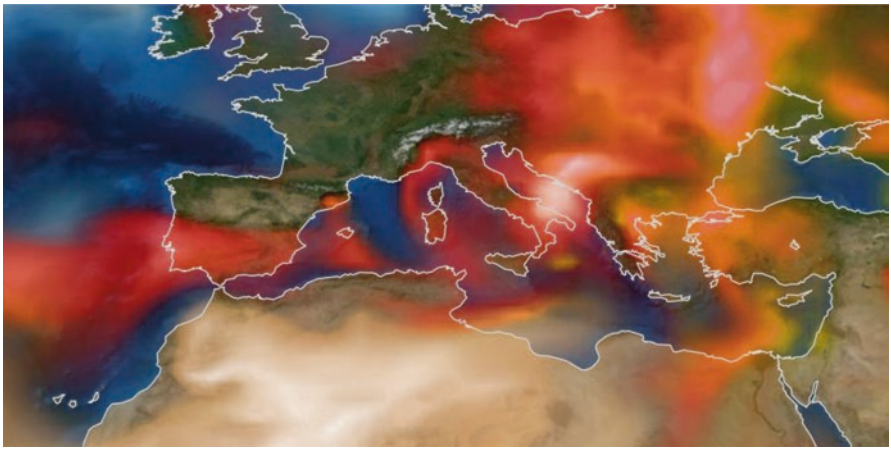

Cover image of Vol. 2: The cover image illustrates the generally complex atmospheric aerosol situation over the Mediterranean basin. It shows the aerosol optical depth at 550 nm over the Mediterranean and surrounding regions (25°N–55°N, 20°W–40°E) on June 29, 2013, 09 UTC, from the ECMWF atmospheric composition reanalysis 4 (EAC4) as produced by the European Copernicus Atmosphere Monitoring Service (CAMS; (https://atmosphere.copernicus.eu). Sea-salt, sulfate, biomass burning, and mineral dust aerosol contributions are plotted with a dark to light blue, yellow, red and beige color scale, respectively. The cover image of Volume 1 shows the situation 2 days before (27 June, 00 UTC). Color scales and more details are given in the introduction chapter of Volume 1. ©ECMWF, courtesy of Miha Razinger and Vincent-Henri Peuch

Foreword

The Chemistry-Aerosol Mediterranean Experiment (ChArMEx) has initiated and coordinated exciting international research, and contributed impressively to the scientific understanding of atmospheric chemical and climate processes in a region that can be characterized as a global environmental change “hot spot”. The Mediterranean region, at the crossroads of three continents, has historically been a pivot of civilization where humanity thrived in a favourable environment. Currently, it houses nearly half a billion people in about two dozen nations, while droughts and heat extremes are becoming increasingly common. In some areas, population growth is rapid, and environmental pressures and socio-economic, cultural and religious differences pose major challenges. Environmental science cannot claim to resolve them but can guide in preventing overexploitation, toxic pollution levels and disruption of ecosystems and help to find the optimum between agricultural, industrial and urban development and healthy living conditions. This provides the necessary framework to achieve prosperity. Because air pollution and climate change in the Mediterranean "hot spot" are indiscriminate concerning national boundaries and political orientation, the region must inter-connect to address them. To me, this is both a challenge and an opportunity.

ChArMEx has analysed biogeochemical cycles that influence the atmospheric composition, and to what degree they are perturbed by anthropogenic emissions. These perturbations have consequences for marine and terrestrial ecosystems, involving eutrophication and exposure to air pollution. As an example, research in the past addressed reactive nitrogen input into Mediterranean ecosystems, while more recently it also includes phosphorus, transition metals and toxic substances, as their human-induced deposition changes nutrient availability. Another example is aeolian dust, of which roughly a quarter is anthropogenic, while the particle composition is perturbed by interactions with air pollutants. The uptake of acids by airborne desert dust, notably nitric acid (from nitrogen oxide emissions), leads to the mobilization of mineral cations. This influences nutrient deposition, and also changes the physicochemical properties of the particles, which affects air quality and the availability of cloud condensation nuclei. Pristine dust particles are poor condensation nuclei, but the interaction with air pollution makes them more

hygroscopic, promoting their growth into clouds droplets with consequences for climate and the water cycle.

Human-induced emissions of a host of gases (primary pollutants) that are chemically converted into secondary pollutants during atmospheric transport influence air quality and climate. For example, volatile organic compounds, of both natural and anthropogenic origins, are photochemically oxidized, and in the presence of nitrogen oxides (NO_x), ozone is formed that damages biological tissue. This is relevant for terrestrial ecosystems and crops, leading to substantial economic losses. Conversely, the increasingly water-stressed vegetation less efficiently removes ozone (as leaves close their stomata), which intensifies air pollution episodes. Ozone is also a potent greenhouse gas and, together with methane, causes a radiative forcing of climate that rivals that of carbon dioxide from the use of fossil fuels. Sulphur dioxide and NO_x from the same sources form sulphate and nitrate particles (aerosols), a process that is promoted by the presence of ammonia from agriculture. Further, primary and secondary organic compounds are key contributors to aerosols. The concentrations of atmospheric particles in the Mediterranean region are very high, even though European emissions have decreased in the past few decades. While the western Mediterranean has profited from the European pollution reductions, in the eastern Mediterranean, with several major megacities, emissions are still increasing. A related issue is the occurrence of forest fires, which have become a major hazard. Next to fossil fuel use, the burning of vegetation is a strong source of air pollution, for example NO_x, organic and black carbon, which is another connection between air pollution and climate change.

The documentation and analysis of these processes by ChArMEx has provided important data and knowledge to develop modelling tools that compute biogeochemical cycles, air quality and climate and enable integral studies of the abovementioned anthropogenic effects. Models are also essential for scenario calculations to support policymaking. There is a need for regional atmospheric and climate modelling of the Mediterranean, as land-sea interactions and the pronounced topography affect the meteorology. Recent projections of the Mediterranean climate indicate that torrential rainfall events could increase, even in areas that are subject to drying. This means that precipitation will occur in fewer but more extreme rainstorms. If this comes true, we can expect major repercussions for water availability and agriculture. Heat extremes and droughts have additional, important ramifications for agriculture, public health and society, with the potential to contribute to political tension and even migration in some parts of the Mediterranean. To be prepared for such developments, it is imperative to pursue high-resolution modelling of future scenarios through the Coordinated Regional Climate Downscaling Experiment (CORDEX) of the World Climate Research Programme.

It has long been known that heat extremes have serious health impacts by aggravating chronic diseases such as cardiovascular and respiratory conditions, leading to premature mortality. In recent decades, heat-related mortality in summer has increased steeply, which was not compensated by a reduction of cold-related mortality in winter. This trend will undoubtedly continue in future. Heatwaves are extended episodes with unusually high temperature, with stagnant weather

conditions during which air pollutants accumulate. Therefore, part of the excess mortality is related to short-term health impacts from poor air quality, for example by ozone and fine particulate matter. Also, the long-term exposure to these pollutants, even at relatively low concentrations, enhances morbidity and mortality, mostly related to the same chronic diseases, including cancer. Recent studies document that a larger variety of diseases is involved than assumed previously, such as diabetes, hypertension and neurological disorders. The World Health Organization has issued air quality guidelines, but they are violated nearly everywhere. Despite the compelling scientific evidence, the health risks are often under-appreciated. Air pollution is a major health hazard, with a public health impact that compares to tobacco smoking, for example. Fossil fuel use is a major pollution source, common to air quality and climate change. Living up to the 2015 Paris climate agreement could, therefore, achieve multiple benefits.

ChArMEx has provided a foundation for environmental policymaking, promoted by its international dimension, which can be further extended in the years to come. It is important to involve Mediterranean countries from all points of the compass, especially those that are still low-performing in environmental science. ChArMEx has furthered inter-disciplinary research, linking aspects of the atmosphere, ocean and climate towards Earth system science with a Mediterranean focus. This needs to continue, as many of the important feedbacks in the system need to be understood more quantitatively, by combining computer modelling with observational studies, and pursue attribution, impact and policy assessments. I am confident that it will continue, as ChArMEx has established a strong research community, being demonstrated by the science presented in the chapters of this book.

Max Planck Institute for Chemistry (MPIC) Jos Lelieveld
Mainz, Germany
Climate and Atmosphere Research Center (CARE-C), The Cyprus Institute
Aglantzia, Nicosia, Cyprus,

Preface and Acknowledgments

Air is fundamental to life on Earth. To speak only of humans, we each breathe 10–15 kg of air every day. Though atmospheric chemistry has been developed quite recently as a science, we now understand how small modifications of the atmospheric composition are important to life and the environment. Our health and, more generally, ecosystems on land and in the ocean, and even the climate, are all deeply` impacted by reactive gases and aerosols, which are at the center of atmospheric chemistry. These trace compounds represent less than 0.1% of the atmospheric composition but can no longer be neglected in our understanding and modeling of the complex Earth system.

The atmosphere is a vast chemical cauldron, in which a quasi-infinite number of trace compounds are mixed and transported, and react together to form new species. This is especially true in the Mediterranean region, which can be seen as an atmospheric chemistry hotspot, which we believe deserves to be highlighted. Indeed, the Mediterranean Sea is a wide oceanic basin of major economic importance, whose marine atmosphere is controlled mainly by long-range transported continental air masses from three different continents to its north, south, and east sides, each contrasted in terms of air pollution sources. In addition, the specific atmospheric circulation in the Mediterranean region, influenced by peripheral mountain ranges and arid areas, and its specific climate with a long dry, warm, and sunny season favor natural emissions as well as the accumulation of pollutants and the photochemical production of secondary species formed within the atmosphere, such as ultrafine secondary aerosol particles and ozone. The Mediterranean coasts also host many large industrial harbors and ever-growing urban centers, increasing regional anthropogenic pressure. Poor air quality combined with impacts of climate change already strongly affects this region and raises the issue of its future inhabitability.

This book intends to augment information from many existing books on the Mediterranean region with an original and comprehensive diagnostic of the regional atmospheric chemistry. Our overview not only considers the full atmospheric chemistry processes including emissions, transport, transformation, and sinks of pollutants but also addresses the main impacts of the regional atmospheric chemistry, including radiative effects, interactions with clouds and precipitation, feedbacks on

climate, adverse health effects, and the transfer of nutrients and pollutants to terrestrial and marine ecosystems.

The three co-editors of this book have a long and complementary expertise in atmospheric chemistry. Altogether, we have been witnessing several decades of scientific progress in this particular field and have contributed to the growing focus of the scientific community on the Mediterranean region.

In the late 1970s and early 1980s, oceanographers realized the importance of long-range atmospheric transport of trace substances on the composition of remote surface marine waters and began sampling atmospheric aerosols at sea during oceanographic cruises. Within his PhD study in the mid-1980s, François Dulac (FD) demonstrated the importance of continental air masses in driving the content of trace elements in the lower troposphere over the Mediterranean basin based on such samples, combining geochemical approaches and some of the first computed 3-D air mass trajectories. He also showed a high variability in the aerosol load and deposition that justified the implementation of continuous monitoring strategies. Early meteorological satellite images showed the impact of ship plumes on cloud properties and the impact of large desert dust plumes on the regional Earth radiative transfer in marine areas.

The progressive development of quantitative aerosol products from passive satellite imagery, to which FD contributed in the Mediterranean region in the 1990s, including the setup of the first near real-time desert dust regional monitoring system as part of the European project MEDUSE (the Mediterranean Dust Experiment), offered a new view of the ubiquity of long-range transport of aerosols in the marine atmosphere. The question of aerosol impacts on climate went beyond the simple issue of a global nuclear winter or major volcanic eruptions. Early use of aerosol lidars, active remote sensing instruments, for the monitoring of the vertical dimension and their combination with passive remote sensing demonstrated the complex vertical structure of the aerosol layers in the Mediterranean troposphere and opened the way to accurate accounts of their radiative impact. This was the basis of the PhD study of Eric Hamonou (EH) in the late 1990s. Awareness levels of the great sensitivity of the Mediterranean environment to climate change and anthropogenic pressure, both enhanced in this region, were rising. In the mid-2000s, this uncertain future led the French science community to call for a large research program in order to investigate the future inhabitability of the Mediterranean region.

At the initiative of the French Institut National des Sciences de l'Univers (INSU), a multidisciplinary and multiagency program entitled MISTRALS (Mediterranean Integrated Studies at Regional and Local Scales) was established for the period 2010–2020, and later endorsed by the Union for the Mediterranean, with the objective of international cooperation. The aim was to study the entire Mediterranean environment and its future in the context of global change and increasing anthropogenic pressures. Besides the major topical issue of the regional water cycle within MISTRALS, FD put forward the question of the aerosol impacts on the regional climate and ecosystems and their possible future evolution. After three years of preliminary studies (supported in particular by the French program LEFE—Les Enveloppes Fluides et l'Environnement) and a joint effort by the aerosol and gas

chemistry communities, the project ChArMEx (the Chemistry-Aerosol Mediterranean Experiment) was established in 2010. Two years later, EH took over the management of the ChArMEx project. In addition to facilitating the organization of the experiments, he promoted scientific dissemination and outreach on the importance of atmospheric chemistry and its impacts in the Mediterranean region. Organic chemistry and secondary organic aerosol formation, which were both poorly understood and reproduced by air quality models, were among the main emerging scientific issues, into which Stéphane Sauvage (SS) deeply invested from the early 2010s through the setup of the first monitoring system of volatile organic compounds in a remote Mediterranean site. This system was successfully operated for over more than two years, including several intensive campaigns at the ChArMEx station installed from scratch in containers of Météo-France and CEA on the heights of Ersa in northern Corsica, in the background atmosphere of the northwestern Mediterranean basin. In the second phase of the project, SS took over the coordination of research actions dealing with the source apportionment of reactive atmospheric pollutants over the Mediterranean basin as a complementary approach for emission inventory assessment.

With important funding support from a variety of French institutions (~12 M€ in total, excluding permanent staff salaries), ChArMEx has federated a large international scientific community on atmospheric chemistry to perform studies in the Mediterranean region. An unprecedented experimental effort was set up, including several large field campaigns with research aircraft, balloons, and vessels, first mainly focused on the western Mediterranean basin before developing more in the eastern basin, but with unfortunate limitations following budget issues.

This academic book is an initiative of the ChArMEx scientific community to conclude the end of the ChArMEx project. It aims to review and update the scientific knowledge in regional atmospheric chemistry by integrating both ChArMEx and non-ChArMEx literature. The book content partially relies on an unpublished white book on Mediterranean aerosols written in 2007–2010 to support the project initiative, which gathered and listed approximately 650 references only considering aerosols. Since then, the literature on regional atmospheric chemistry has increased substantially, in particular in terms of organic chemistry thanks to the development of new measurement techniques, in particular mass spectrometry. As of this writing, more than 140 articles associated with ChArMEx have been published in high-level peer-reviewed journals, including more than one hundred in a special issue jointly published by the two journals *Atmospheric Measurement Techniques* and *Atmospheric Chemistry and Physics*. ChArMEx has produced or contributed to many original results in terms of aerosol properties and climatology, quasi-Lagrangian monitoring of ozone and aerosols with drifting balloons, transport of very large African dust particles, dust and trace metal deposition fluxes, large-scale new particle formation, aerosol chemical composition, gaseous phase chemistry, pollutant emissions in large urban-industrial centers (namely Athens, Beirut, Cairo, Istanbul, Marseille), assimilation of observations from an aerosol lidar network in particulate air quality modeling, improvement of chemical modeling, and more. ChArMEx has developed strong cooperation with the climate and marine

biogeochemistry science communities (with the MISTRALS projects HyMeX and MERMEX, in particular) to quantify the aerosol impact on the regional climate and on marine biogeochemistry. ChArMEx has also established a network (ARCHIMEDES) coordinated by EH and set up a school with the health community to raise interest in the impact of atmospheric pollution on human health, in particular in the eastern and southern Mediterranean countries. Beyond the considerable update to the field of atmospheric chemistry and its impacts that this book attempts to present, many open questions remain, and the two volume conclusions summarize recommendations for future research issued from the different book chapters.

Since this book is closing ChArMEx, we would like to emphasize that this project is the result of an exceptionally large cooperation of the regional atmospheric science community, which built and performed very exciting experimental campaigns and contributed to fruitful scientific exchanges. We have a particular thought for our former colleagues and friends Laura Chiappini, Laurent Gomes, Savvas Kleanthous, and William Lahoz who sadly left us prematurely during the ChArMEx project, as well as for two other highly motivated colleagues from Cyprus and France who were not able to contribute as much as planned due to severe health concerns.

It is also time to acknowledge the many French institutions that funded ChArMEx and favored international cooperation, including ADEME, ANR, CEA, CNRS-INSU, CNES, Météo-France, Ministère des Affaires Étrangères, IMT Nord Europe, Regional institutions of Corsica (CTC) and Provence-Alpes-Côte d'Azur (PACA), and universities of Clermont-Ferrand, Lille, Marseille, Paris, and Versailles-St-Quentin. Even though some of them sometimes made life of the project coordination rather painful and its management particularly heavy, due to multiple independent funding sources and schedules, extremely long administrative delays, strong unexpected budget cuts, and very late decisions, they nevertheless allowed us to organize and achieve an exciting decadal scientific project including our summer 2013 major experimental campaign with more than 3000 person-days in the field, illustrated by the on-line video documentary *Science en Plein Ciel/Science on Air* (in French with possible English subtitles: https://images.cnrs.fr/video/4843, last access 16 May 2022). In particular, the French program LEFE/CHAT (Les Enveloppes Fluides et l'Environnement/Chimie Atmosphérique), which supported the preparation phase of ChArMEx, and the early funding from ADEME have been crucial for the successful initiation of our project. Among too many other supporting teams to be listed, the SAFIRE aircraft teams, the CNES balloon teams, the SEDOO data and service center staff, the French AERONET component PHOTONS (Photométrie pour le Traitement Opérationnel de Normalisation Satellitaire; http://www-loa.univ-lille1.fr/photons; last access 16 May 2022), the MISTRALS administrative group, and the LSCE direction and administrative group played a particularly important role for the success of ChArMEx-France. We also thank in particular for their essential support and help Aurélien Bourdon (SAFIRE), Véronique Chagué (INSU), Marie-Anne Clair (CNES), Elsa Cortijo (CEA/LSCE), Hélène Ferré (OMP/SEDOO), Laurence Fleury (OMP/SEDOO), Dominique Le Quéau (INSU), Vanessa

Martray (INSU), Nathalie Poisson (ADEME), Etienne Ruellan (INSU), Michèle Schaldembrand (INSU), and Nicolas Verdier (CNES). Setting up a comprehensive monitoring station at a remote location in Cape Corsica was a challenge and, among the many people involved in its success, we are especially grateful to Pierre Chiarelli, Jean-Luc Pajolet, and Jean-Luc Savelli (Qualit'air Corse) for their important support, and to Florent Bordier (Qualit'air Corse), Thierry Bourrianne (CNRM), Zineb Liraki (CIRMED), José Nicolas (LSCE), Véronique Pont (LAero), Jean Sciare (LSCE), Emmanuel Tison (IMT Nord Europe), for their crucial contribution to operate the station.

International cooperation has been wide all along the project despite our lack (within a hair) of significant EU funding, which unfortunately prevented the participation of two major European research aircrafts, namely the British BAe-146 and the German HALO. We would like to warmly thank all international contributors, with special thanks to Michaël Sicard and Xavier Querol (Spain), Giorgio di Sarra (Italy), Raymond Ellul (Malta), Nikos Mihalopoulos (Greece), Jean Sciare (Cyprus), Noureddine Yassaa (Algeria), Mohamed Labiadh (Tunisia), Wolfgang Junkermann (Germany), John Wenger (Ireland), Uri Dayan (Israel), Fatma Öztürk (Turkey), Charbel Afif (Lebanon), and Claire Reeves (UK) for their role and contributions to the overall building and execution of our experimental effort. International teams and institutes involved at some point in ChArMEx are too many to be acknowledged individually, but we would like to emphasize (i) the NASA AERONET network and the many scientists involved in the management of the Mediterranean AERONET stations for their long-term effort to provide particularly useful high-quality data, with special thanks to Alexander Smirnov for supporting the ChArMEx AERONET/MAN campaigns at sea, and (ii) the ACTRIS/EARLiNET network and the many scientists who made possible a continuous 3-D lidar monitoring for a model assimilation exercise. We also wish to especially thank the Universitat Politécnica de Catalunya, Barcelona, Spain; the International Centre for Theoretical Physics (ICTP), Trieste, Italy; and the Cyprus Institute, Nicosia, Cyprus, for hosting and sponsoring one of the five ChArMEx international conferences and, in the case of ICTP, an international school made accessible for the first time by internet following our request. We apologize to the National Observatory of Athens (NOA) and panhellenic PANACEA research infrastructure that the Sixth ChArMEx conference planned in fall 2019 with their support was not held due to a severe ChArMEx-France budget cut.

Finally, we are very grateful to (i) the book section coordinators and all contributing authors – one hundred coming from institutions in 16 different countries – for their rich contributions, (ii) all – about 50 – chapter and section reviewers for their valuable help and inputs on the initial manuscript, (iii) Miha Razinger for providing the cover and related ECMWF/MACC model images, and (iv) Jos Lelieveld for the "Foreword" to this publication.

We do hope that our book will meet its objective and be a source of interest for the academic community involved in atmospheric chemistry in the Mediterranean region and beyond.

Laboratoire des Sciences du Climat
et de l'Environnement (LSCE)
CEA-CNRS-UVSQ, Université Paris-Saclay
IPSL, CEA Paris-Saclay
Gif-sur-Yvette, France
François Dulac

IMT Nord Europe, Institut Mines-Télécom
Univ. Lille, Centre for Energy and Environment
F-59000 Lille, France
Stéphane Sauvage

Science Partners
Paris, France
Eric Hamonou

14 May 2021

Abstract (same as Vol. 1)

The Mediterranean region is heavily polluted by particulate and gaseous reactive pollutants from a great variety of natural and anthropogenic sources originating from the basin itself and from its three different bordering continents (namely Europe, North Africa, and the Middle East). It is undergoing increasing anthropogenic and climate change pressures, which questions its future inhabitability. *Atmospheric Chemistry in the Mediterranean Region* presents a review of an abundant literature on the topic of air pollution and includes yet unpublished results. Its 41 peer-reviewed chapters have been contributed by a large international panel of 100 scientists all recognized in their field, from institutes in 16 different countries, among which a great number have been involved in the Chemistry-Aerosol Mediterranean Experiment (ChArMEx), the largest ever research project dedicated to the study of the Mediterranean atmospheric chemistry. It is an invaluable source of scientific information for anyone interested in the Mediterranean atmospheric pollution and its impacts, reviewing several decades of studies on atmospheric chemistry in the Mediterranean region, starting with radioactive aerosol measurements in the 1960s, including the ChArMEx project contribution all along the 2010s. Volume 1 first considers background information relevant to the regional tropospheric chemistry and its future evolution, including atmospheric circulation and climate, and anthropogenic pressures. It also describes the spatial and temporal distributions and trends of aerosols, ozone, inorganic aerosol precursors and organic volatile compounds. Volume 2 first addresses the various aspects of the atmospheric cycle of aerosols and reactive gases including emissions, chemical processes, various aerosol properties, and deposition. The last parts are dedicated to the major impacts of atmospheric pollutants on the regional radiative budget and climate, on human health, and on marine and terrestrial ecosystems. Conclusion chapters of the two volumes summarize recommendations for future research issued from the different chapters.

Contents

Part X Impacts of Air Pollution on Human Health and Ecosystems

List of Figures

Sea Spray Emissions

Emissions from the Mediterranean Vegetation

Soil Dust Emissions

Anthropogenic Emissions of Reactive Compounds in the Mediterranean Region

Ultrafine Particle Emissions in the Mediterranean

Total OH Reactivity

Ozone Photochemical Production Rates in the Western Mediterranean

Nucleation in the Mediterranean Atmosphere

Secondary Aerosol Formation and Their Modeling

Particle-Gas Multiphasic Interactions

Aerosol Size Distribution

Aerosol Composition and Reactivity

Aerosol Optical Properties

Aerosol Hygroscopicity

Mass Deposition

Aerosol and Tropospheric Ozone Direct Radiative Impacts

Aerosol-Cloud Interactions and Impact on Regional Climate

Aerosol Impacts on Atmospheric and Precipitation Chemistry

Air Quality and Health Impacts

Impact of Atmospheric Deposition on Marine Chemistry and Biogeochemistry

Impact of Air Pollution on Terrestrial Ecosystems

Appendix

List of Tables

Aerosol Composition and Reactivity

Aerosol Optical Properties

Aerosol Hygroscopicity

Mass Deposition

Nutrient Deposition and Variability

Trace Metals and Contaminants Deposition

Aerosol and Tropospheric Ozone Direct Radiative Impacts

Aerosol Impacts on Atmospheric and Precipitation Chemistry

Air Quality and Health Impacts

Impact of Atmospheric Deposition on Marine Chemistry and Biogeochemistry

Impact of Air Pollution on Terrestrial Ecosystems

Contributors

Charbel Afif Emissions, Measurements, and Modeling of the Atmosphere (EMMA) Laboratory, CAR, Faculty of Sciences, Saint Joseph University, Beirut, Lebanon

Climate and Atmosphere Research Center (CARE-C), The Cyprus Institute, Aglantzia, Nicosia, Cyprus

Laurent Alleman IMT Nord Europe, Institut Mines-Télécom, Univ. Lille, Centre for Energy and Environment, F-59000 Lille, France

Isabella Annesi-Maesano INSERM, Université de Montpellier, DESP IURC, Montpellier, France

Thomas Audoux Université Paris Cité and Univ. Paris Est Créteil, CNRS, LISA, F-75013 Paris, France

Anna Ávila Castell Centro de Investigación Ecológica y Applicaciones Forestales (CREAF), Universitat Autònoma de Barcelona, Ballaterra, Spain

Rima Baalbaki University of Helsinki, Helsinki, Finland

Dominique Baisnée Laboratoire des Sciences du Climat et de l'Environnement (LSCE), CEA-CNRS-UVSQ, IPSL, Univ. Paris-Saclay, Gif-sur-Yvette, France

Sara Basart Barcelona Supercomputing Center, Barcelona, Spain

Silvia Becagli Department of Chemistry Ugo Schiff, University of Florence, Sesto Fiorentino (FI), Italy

Matthias Beekmann Université Paris Cité and Univ. Paris Est Créteil, CNRS, LISA, Paris, France

Gilles Bergametti Université Paris Cité and Univ. Paris Est Créteil, CNRS, LISA, F-75013, Paris, France

Bertrand Bessagnet CITEPA, Paris, France

Mariem Bibi Physics Department, Faculty of Sciences of Sfax, Sfax University, Sfax, Tunisia

Christophe Boissard Université Paris Cité and Univ. Paris Est Créteil, CNRS, LISA, F-75013, Paris, France

Laboratoire des Sciences du Climat et de l'Environnement (LSCE), CEA-CNRS-UVSQ, IPSL, Univ. Paris-Saclay, Gif-sur-Yvette, France

Agnès Borbon Université Clermont Auvergne, CNRS, Laboratoire de Météorologie Physique UMR 6016 (LaMP), Clermont-Ferrand, France

Olivier Boucher Laboratoire de Météorologie Dynamique (LMD), Sorbonne Université, Ecole Polytechnique, Ecole Normale Supérieure, Université Paris-Saclay, CNRS, Ecole des Ponts ParisTech, IPSL, Paris, France

Patrick Chazette Laboratoire des Sciences du Climat et de l'Environnement (LSCE), CEA-CNRS-UVSQ, IPSL, Univ. Paris-Saclay, Gif-sur-Yvette, France

Semia Cherif Institut Supérieur des Sciences Biologiques Appliquées de Tunis (ISSBAT), University of Tunis El Manar, Tunis Jebari, Tunisia

Isabelle Chiapello Université de Lille, CNRS, UMR 8518 Laboratoire d'Optique Atmosphérique (LOA), Villeneuve d'Ascq, France

Gerrit de Leeuw Koninklijk Nederlands Meteorologisch Instituut (KNMI), De Bilt, The Netherlands

Claire Delon Laboratoire d'Aérologie (LAERO), Université de Toulouse III Paul Sabatier, CNRS, Observatoire Midi-Pyrénées, Toulouse, France

Cyrielle Denjean Centre National de Recherches Météorologiques (CNRM), Université de Toulouse, Météo France, CNRS, Toulouse, France

Frank J. Dentener Joint Research Centre (JRC), European Commission, Ispra (VA), Italy

Karine Desboeufs Université Paris Cité and Univ. Paris Est Créteil, CNRS, LISA, F-75013 Paris, France

Claudia Di Biagio Université Paris Cité and Université Paris Est Créteil, CNRS, LISA, F-75013 Paris, France

Alcide Giorgio di Sarra Laboratory for Observations and Measurements for Environment and Climate, Italian National Agency for New Technologies, Energy, and Sustainable Economic Development (ENEA), Rome, Italy

François Dulac Laboratoire des Sciences du Climat et de l'Environnement (LSCE), CEA-CNRS-UVSQ, IPSL, Univ. Paris-Saclay, Gif-sur-Yvette Cedex, France

Silvano Fares Institute of Bioeconomy, CNR, Rome, Italy

Catherine Fernandez Institut Méditerranéen de Biodiversité et d'Ecologie marine et continentale (IMBE), Aix-Marseille Université, Avignon Université, CNRS, IRD, Marseille, France

Paola Formenti Université Paris Cité and Univ. Paris Est Créteil, CNRS, LISA, F-75013, Paris, France

François Gheusi Laboratoire d'Aérologie (LAERO), CNRS, Univ. Toulouse III Paul Sabatier, Observatoire Midi-Pyrénées, Toulouse, France

Claire Granier Université de Toulouse III Paul Sabatier, CNRS, Observatoire Midi-Pyrénées, Toulouse, France

Valérie Gros Laboratoire des Sciences du Climat et de l'Environnement (LSCE), CEA-CNRS-UVSQ, IPSL, University of Paris-Saclay, Gif-sur-Yvette, France

Cécile Guieu Laboratoire d'Océanographie de Villefranche (LOV), UMR 7093 CNRS, Sorbonne Université, Chemin du Lazaret, Villefranche-sur-Mer, France

Claudia Gutiérrez Environmental Science Institute, University of Castilla-La Mancha (UCLM), Toledo, Spain

Valérie Gros Eric Hamonou Science-Partners, Paris, France

Eric Hamonou Science-Partners, Paris, France

Nikos Hatzianastassiou Laboratory of Meteorology, Department of Physics, University of Ioannina, Ioannina, Greece

Didier Hauglustaine Université de Toulouse III Paul Sabatier, CNRS, Observatoire Midi-Pyrénées, Toulouse, France

Corinne Jambert Laboratoire d'Aerologie (LAERO), Université de Toulouse III Paul Sabatier, Observatoire Midi-Pyrénées, Toulouse, France

Wolfgang Junkermann Institute of Meteorology and Climate Research (IMK-IFU), Karlsruhe Institute of Technology, Campus-Alpine, Garmisch-Partenkirchen, Germany

Markus Kalberer University of Basel, Department of Environmental Sciences, Basel, Switzerland

Nikolaos Kalivitis Environmental Chemical Processes Laboratory (ECPL), Department of Chemistry, University of Crete, Heraklion, Greece

Maria Kanakidou Environmental Chemical Processes Laboratory (ECPL), Department of Chemistry, University of Crete, Heraklion, Greece

Konrad Kandler Institut für Angewandte Geowissenschaften, Technische Universität Darmstadt, Darmstadt, Germany

Zamin A. Kanji Swiss Federal Institute of Technology (ETH), Zurich, Switzerland

Dimitris Kaskaoutis Institute for Environmental Research and Sustainable Development, National Observatory of Athens (NOA/IERSD), Athens, Greece

Martina Klose Barcelona Supercomputing Center, Barcelona, Spain

Juliette Lathière Laboratoire des Sciences du Climat et de l'Environnement (LSCE), CEA-CNRS-UVSQ, IPSL, Univ. Paris-Saclay, Gif-sur-Yvette, France

Benoît Laurent Université Paris Cité and Univ. Paris Est Créteil, CNRS, LISA, Paris, France

Jos Lelieveld Max Planck Institute for Chemistry (MPIC), Mainz, Germany

Climate and Atmosphere Research Center (CARE-C), The Cyprus Institute, Aglantzia, Nicosia, Cyprus

Simone Lolli Istituto di Metodologie per l'Analisi Ambientale (IMAA), CNR, Tito Scalo (PZ), Italy

Cara Nichole Maesano INSERM, Université de Montpellier, DESP IURC, Montpellier, France

Sylvain Mailler Laboratoire de Météorologie Dynamique (LMD), Ecole Polytechnique, Ecole Normale Supérieure, Université Paris-Saclay, Sorbonne Université, CNRS, Ecole des Ponts ParisTech, IPSL, Palaiseau, France

Marc Mallet Centre National de Recherches Météorologiques (CNRM), Université de Toulouse, Météo France, CNRS, Toulouse, France

Emilio Marañón Dept. of Ecology and Animal Biology, Univ. of Vigo, Vigo, Spain

Laurent Menut Laboratoire de Météorologie Dynamique (LMD), Ecole Polytechnique, Ecole Normale Supérieure, Université Paris-Saclay, Sorbonne Université, CNRS, Ecole des Ponts ParisTech, IPSL, Palaiseau, France

Vincent Michoud Université Paris Cité and Univ. Paris Est Créteil, CNRS, LISA, F-75013, Paris, France

Lucia Mona Istituto di Metodologie per l'Analisi Ambientale (IMAA), CNR, Tito Scalo (PZ), Italy

Stelios Myriokefalitakis Institute for Environmental Research and Sustainable Development, National Observatory of Athens (NOA/IERSD), Lofos Koufou, Penteli, Greece

Pierre Nabat Centre National de Recherches Météorologiques (CNRM), Université de Toulouse, Météo France, CNRS, Toulouse, France

Panayiotis Nektarios School of Agricultural Sciences, Department of Agriculture, Hellenic Mediterranean University, Heraklion, Crete, Greece

Athanasios Nenes School of Architecture, Civil and Environmental Engineering, Ecole Polytechnique Fédérale de Lausanne, Lausanne, Switzerland

Institute for Chemical Engineering Sciences, Foundation for Research and Technology Hellas, Patras, Greece

Elena Ormeño Institut Méditerranéen de Biodiversité et d'Ecologie marine et continentale (IMBE), Aix-Marseille Université, Avignon Université, CNRS, IRD, Marseille, France

Anastasia Panopoulou IMT Nord Europe, Institut Mines-Télécom, Univ. Lille, Centre for Energy and Environment, F-59000 Lille, France

Institute for Environmental Research and Sustainable Development, National Observatory of Athens (NOA/IERSD), Palaia Penteli, Athens, Greece

Environmental Chemical Processes Laboratory (ECPL), Department of Chemistry, University of Crete, Heraklion, Greece

Vassileios C. Papadimitriou Laboratory of Photochemistry and Chemical Kinetics, Department of Chemistry, University of Crete, Heraklion, Crete, Greece

Stefania Papatheodorou Department of Epidemiology, Harvard TH Chan School of Public Health, Boston, MA, USA

Francesc Peters Institut de Ciències del Mar (ICM), CSIC, Barcelona, Spain

Jorge Pey Betrán ARAID-Instituto Pirenaico de Ecología, CSIC, Zaragoza, Spain

Michael Pikridas Climate and Atmosphere Research Center (CARE-C), The Cyprus Institute, Aglantzia, Nicosia, Cyprus

Andreas Pozzer Max Planck Institute for Chemistry (MPIC), Mainz, Germany

Anne Probst Laboratoire Ecologie Fonctionnelle et Environnement, Observatoire Midi-Pyrénées, Université de Toulouse, CNRS, Toulouse, France

Alexandru Rap School of Earth and Environment, University of Leeds, Leeds, UK

Céline Ridame Laboratoire d'Océanographie et du Climat: Expérimentations et Approches Numériques (LOCEAN), UMR 7159 CNRS, IRD, MNHN, Sorbonne Université, IPSL, Paris, France

Clémence Rose Université Clermont Auvergne, CNRS, Laboratoire de Météorologie Physique UMR 6016, Clermont-Ferrand, France

Daniel Rosenfeld Institute of Earth Sciences, The Hebrew University of Jerusalem, The Edmond J. Safra Campus, Jerusalem, Israel

Matthew Rowlinson National Centre for Atmospheric Science, University of York, York, UK

Thérèse Salameh IMT Nord Europe, Institut Mines-Télécom, Univ. Lille, Centre for Energy and Environment, F-59000 Lille, France

Roland Sarda-Estève Laboratoire des Sciences du Climat et de l'Environnement (LSCE), CEA-CNRS-UVSQ, IPSL, Univ. Paris-Saclay, Gif-sur-Yvette, France

Climate and Atmosphere Research Center (CARE-C), The Cyprus Institute, Aglantzia, Nicosia, Cyprus

Réseau National de Surveillance Aérobiologique, Le Plat du Pin, Brussieu, France

Karine Sartelet Centre d'Enseignement et de Recherche en Environnement Atmosphérique (CEREA), École des Ponts ParisTech, EDF R&D, Marne-la-Vallée, France

Stéphane Sauvage IMT Nord Europe, Institut Mines-Télécom, Univ. Lille, Centre for Energy and Environment, F-59000 Lille, France

Karine Sellegri Université Clermont Auvergne, CNRS, Laboratoire de Météorologie Physique UMR 6016 (LaMP), Clermont-Ferrand, France

Maria Sfakianaki Environmental Chemical Processes Laboratory (ECPL), Department of Chemistry, University of Crete, Heraklion, Greece

Vinayak Sinha IISER, Mohali Campus, Mohali, Punjab, India

Fabien Solmon Laboratoire d'Aérologie (LAERO), Université de Toulouse III Paul Sabatier, CNRS, Observatoire Midi-Pyrénées, Toulouse, France

Michael Staudt Centre d'Ecologie Fonctionnelle et Evolutive (CEFE), UMR CNRS, EPHE, IRD, Université Montpellier, Université Paul Valéry, Montpellier, France

Oksana Tarasova Atmospheric Environment Research Division, World Meteorological Organization (WMO), Geneva, Switzerland

Baye Toulaye P. Thera Université Clermont Auvergne, CNRS, Laboratoire de Météorologie Physique UMR 6016 (LaMP), Clermont-Ferrand, France

Erwin Ulrich Office National des Forêts (ONF), Pôle Recherche-Développement-Innovation de Fontainebleau-Compiègne, Fontainebleau, France

Gaëlle Uzu Institut des Géosciences de l'Environnement (IGE), CNRS, Université de Grenoble Alpes, Grenoble INP, IRD, OSUG, Saint Martin d'Hères, France

Eric Villenave Environnements et Paléoenvironnements Océaniques et Continentaux (EPOC), CNRS, Université de Bordeaux, Pessac, France

Heike Wex Leibniz Institute for Tropospheric Research (TROPOS), Leipzig, Germany

Henri Wortham Laboratoire Chimie de l'Environnement (LCE), UMR 7376, CNRS, Aix-Marseille Université, Marseille, France

Nora Zannoni Laboratoire des Sciences du Climat et de l'Environnement (LSCE), CEA-CNRS-UVSQ, IPSL, University of Paris-Saclay, Gif-sur-Yvette, France

Max Planck Institute for Chemistry (MPIC), Mainz, Germany

Introduction to the Volume 2 of Atmospheric Chemistry in the Mediterranean Region

Stéphane Sauvage, Eric Hamonou, and François Dulac

Contents

Abstract This chapter is a brief introduction to the second volume of the present book reviewing atmospheric chemistry and most important impacts of atmospheric pollutants in the Mediterranean region. We list the various topics addressed in Vol. 2, which is structured in six thematic sections (book parts V to X) dedicated to: (V) regional emissions of natural and anthropogenic pollutants, a critical term in understanding atmospheric pollution; (VI) important chemical processes that impact gas and aerosol concentrations; (VII) aerosol properties that mediate their impact on chemistry and climate; (VIII) atmospheric deposition, which controls the transfer from land to the Mediterranean Sea of mineral dust, nutrients, and contaminants; (IX) impacts on climate and precipitation chemistry; and (X) impacts of air pollution on human health and ecosystems. A conclusive chapter of

*Reviewed by **Eric Villenave** (Environnements et Paléoenvironnements Océaniques et Continentaux (EPOC), CNRS, Université de Bordeaux, Pessac, France) and **Gaëlle Uzu** (Institut des Géosciences de l'Environnement (IGE), CNRS, Université de Grenoble Alpes, Grenoble INP, IRD, OSUG, Saint Martin d'Hères, France)*

S. Sauvage (✉)
IMT Nord Europe, Institut Mines-Télécom, Univ. Lille, Centre for Energy and Environment, F-59000 Lille, France
e-mail: stephane.sauvage@imt-nord-europe.fr

E. Hamonou
Science Partners, Paris, France

F. Dulac
Laboratoire des Sciences du Climat et de l'Environnement (LSCE), CEA-CNRS-UVSQ, Université Paris-Saclay, IPSL, CEA Paris-Saclay, Gif-sur-Yvette, France

F. Dulac et al. (eds.), *Atmospheric Chemistry in the Mediterranean Region*,
https://doi.org/10.1007/978-3-030-82385-6_1

Vol. 2 summarizes recent progress and issues some recommendations relative to the topics reviewed in the volume.

1 Introduction

This introduction is a review of tropospheric chemistry and its main impacts on the Mediterranean region. It comes after more than four decades of related scientific studies, from the first publications in the late 1970s up to the very active last decade (2010–2020) that has seen many national and international research projects dedicated to the Mediterranean atmospheric chemistry. Of particular note is the greatest ever federative research and networking effort in this field, the Chemistry-Aerosol Mediterranean Experiment (ChArMEx; see in particular the ChArMEx special issue that gathers more than 100 articles: https://www.atmos-chem-phys.net/special_issue334.html; last access 21 July 2022). The book is an initiative of the ChArMEx scientific community to conclude the project, prepared as of 2007 and officially started in 2010 as part of the French 2010–2020 program MISTRALS (Mediterranean Studies at Regional and Local Scales; https://programmes.insu.cnrs.fr/mistrals/; last access 21 July 2022).

Atmospheric chemistry is considered as the study of reactive trace compounds in the lower Earth's atmosphere, that is, thousands of species present in both aerosol and gaseous phases, with relatively short lifetimes and subsequently a high temporal and spatial variability, with a possible order of magnitude variability in atmospheric concentrations on typical daily and regional scales. Atmospheric chemistry has been the subject of many general books from Mészáros (1981) to Seinfeld and Pandis (2016), and from Jacobson (2005) to Brasseur and Jacob (2017) for its modeling. The objective of this new book on atmospheric chemistry focused on the Mediterranean region is an updated assessment of our understanding of the regional cycle of short-lived species in the lower atmosphere and their impacts on the inhabitability of the region. This includes their sources, transport, transformations, sinks, interactions with and feedback on climate and ecosystems, variability, past trends, and future evolution.

This is an ambitious journey through the abundant past and recent literature and represents a very large amount of knowledge to compile in order to cover major results from field campaigns, surface monitoring stations, satellite observations, laboratory studies, air quality surveys, and chemistry-transport and climate modeling. In addition, the book also presents original material, in particular from ChArMEx. The total amount of contributions needed two volumes (Dulac, Sauvage, & Hamonou, 2022, 2023).

The first volume (Dulac, Sauvage, & Hamonou, 2023) is dedicated to the description of the Mediterranean atmospheric chemistry hotspot, reviewing general aspects that make this region one of the most important places in the world for both atmospheric chemistry and its impacts. At first, an introduction presents the

ChArMEx-related field operations in the Mediterranean region during the last decade, from which many recent results presented in this book are issued (Dulac et al., 2023). This observational effort is further illustrated by a series of maps presented in an appendix. Volume 1 is structured in four different parts that respectively address: (I) general aspects, including climate and anthropogenic pressures (Dulac, 2023); (II) the regional dynamics and its relation with atmospheric pollution, with a focus on the highly polluted summer season (Dayan, 2023); (III) aerosol distribution and variability from the diurnal scale to long-term trends, including the consideration of radionuclides (Mihalopoulos, 2023a); and (IV) reactive gas distribution and variability, including ozone, inorganic aerosol precursors, and organic gases (Mihalopoulos, 2023b). Finally, a concluding chapter summarizes the main conclusions of the volume and draws recommendations for future research (Sauvage et al., 2023).

This second volume (Dulac, Sauvage, & Hamonou, 2023) complements the first one by reviewing the main emissions, processes, and impacts relevant to atmospheric chemistry in the Mediterranean region. Its content is introduced in the following.

2 Content of Volume 2: From Atmospheric Chemistry to the Mediterranean Inhabitability

Volume 2 is entirely focused on the life cycle of pollutants, how they are emitted, processed, and deposited and how they ultimately impact on some key aspects of the Mediterranean region's inhabitability. The 23 following chapters of this second volume are organized into six thematic sections, which constitute the book Parts V to X.

Part V (Sauvage, 2022) explores regional natural and anthropogenic emissions of atmospheric pollutants, a critical term in the understanding and modeling of atmospheric pollution. The first chapter (Sellegri & Mallet, 2022) is dedicated to the emission processes of sea spray aerosol particles, which constitute one of the most important natural components of the Mediterranean atmosphere. The chapter devotes to the physical and biological drivers of the sea sprays and to the chemical composition of the resulting particles. The second chapter (Gros et al., 2022) is mainly dedicated to the emissions of the Mediterranean vegetation, which is an important source of biogenic Volatile Organic Compounds (VOCs). It presents the emission processes, speciation, and fluxes for different Mediterranean plant species from the branch to the larger scales. The end of the chapter is dedicated to bioaerosols. The third chapter (Laurent & Bergametti, 2022) addresses the physics of soil dust emission and focuses on the identification of Mediterranean dust sources by a combination of satellite observations and models. It also discusses how human activities in the northern fringe of the Saharan desert could affect dust emissions in the future. The fourth chapter (Borbon et al., 2022) is an account of the progress in

the study of anthropogenic emissions. Intensities, variabilities, and trends are discussed on a regional perspective. A focus is made on some of the largest urban centers, for which recent observations have enabled an evaluation of the emission inventories of anthropogenic VOCs. Based in particular on measurements onboard an ultralight aircraft, the fifth and last chapter in this section (Junkermann, 2022) discusses ultrafine particles, their sources in the Mediterranean basin, their potential properties as cloud condensation nuclei (CCN), and their strong concentration increase compared to historical data.

Part VI in Vol. 2 (Beekmann, 2022, this volume) details the chemical processes that strongly modify the tropospheric composition in gases and aerosols over the Mediterranean basin and that also affect exchanges between both phases. The first chapter in Part VI (Gros & Zannoni, 2022) presents total OH reactivity measurements performed in the Mediterranean and discusses their use to infer the measurement efficiency to capture the diversity of atmospheric reactive species, especially volatile organic compounds (VOCs). The second chapter (Gheusi, 2022) presents quasi-Lagrangian monitoring of ozone growth rate performed in the Mediterranean thanks to boundary-layer pressurized balloons (BLPBs). Results are compared with previous similar measurements made in southeastern France. This chapter ends by a discussion on ozone net photochemical formation rates. The third chapter (Sellegri & Rose, 2022) gives an overview of new particle formation (NPF) in the Mediterranean basin and points to possible precursors. It discusses impacts of NPF on cloud condensation nuclei (CCN) and cloud droplet number (CDN). The fourth chapter (Sartelet, 2022) compares different formation schemes of secondary organic aerosol (SOA) to measurements performed in the Mediterranean and tests their ability to account for measured characteristics and variabilities. The chapter highlights the importance of the scheme used for studying SOA trends in a warmer climate. Finally, the fifth and last chapter of this section (Michoud, 2022) discusses the often large discrepancies between predicted and measured partition coefficients between the particle and the gas phase of semi-volatile organic compounds during ChArMEx-related campaigns.

Part VII (Formenti, 2022) presents the latest observations of Mediterranean aerosol properties that are important to the regional climate and air quality. The first chapter (Di Biagio, 2022) reviews current knowledge on the size distribution of atmospheric aerosols observed in the Mediterranean basin. This includes remote sensing observations, as well as ground-based and airborne in situ measurements. The second chapter (Becagli, 2022) deals with the Mediterranean aerosol chemical composition and the potential reactivity of the components at the gas-particle interface. It is demonstrated how such processes impact the chemical and physical properties of aerosol particles. The third chapter (Mallet et al., 2022a) reports observations of optical properties for different aerosol types observed in the Mediterranean region. The chapter focuses on parameters that are important to radiative forcing calculations, including the aerosol optical depth and its wavelength dependence, the single scattering albedo, and the asymmetry parameter. It also addresses the aerosol backscatter to extinction ratio, a key parameter in the inversion of lidar

measurements for deriving the vertical profile of the aerosol extinction. The fourth and last chapter in this section (Denjean, 2022) reviews existing results on the aerosol hygroscopic properties at sub-saturated and supersaturated conditions (relative humidity below and above 100%, respectively). It also discusses the ice nucleation properties of aerosols from measurements at multiple sites in the Mediterranean.

Part VIII (Desboeufs, 2022a) examines composition, seasonality, and spatial heterogeneity of atmospheric deposition to the Mediterranean Sea. It focuses on the atmospheric deposition of mineral dust and species like major nutrients (nitrogen and phosphorus), trace metals, and organic contaminants, which play an important role in marine biogeochemical cycles. The first chapter in this section (Laurent et al., 2022) briefly recalls dry and wet deposition processes and their parameterizations and discusses the variability of aerosol mass deposition over the Mediterranean basin thanks to a dataset spanning over more than half a century. The second chapter (Desboeufs, 2022b) compares recently published results on fluxes and sources of nitrogen and phosphorus to historical data in the Mediterranean basin. It discusses present and future trends and also addresses the relative importance of organic/inorganic and dissolved/particulate forms of nutrients. The third and last chapter (Desboeufs, 2022c) presents the latest insights on the atmospheric deposition and fluxes of trace metals and organic contaminants such as organochlorine compounds or Polycyclic Aromatic Hydrocarbons (PAHs).

Parts IX (Kanakidou, 2022a) and X (Kanakidou, 2022b) of the book report on the progress made in our understanding of important impacts of the atmospheric composition in the Mediterranean region. Part IX focuses on interactions with precipitation chemistry and climate. The first chapter in this section (Mallet al., 2022b) is dedicated to current knowledge on aerosol and tropospheric ozone direct radiative impacts in the region, including radiation extinction relevant to renewable energy production. The second chapter (Nabat et al., 2022) summarizes knowledge on the indirect climatic effects of aerosols. It details their impact on the number and properties of cloud condensation nuclei and ice nuclei and, in turn, their impact on cloud properties over the Mediterranean basin. The third chapter (Kanakidou, et al., 2022a) discusses the involvement of aerosols in precipitation chemistry and impact on atmospheric composition through multiphase reactions.

Part X (Kanakidou, 2022b) is a highlight on the current knowledge on the impacts of air pollution on the Mediterranean inhabitability for humans and ecosystems. The first chapter in this section (Kalivitis et al., 2022) summarizes our knowledge on the exposure of the Mediterranean population to atmospheric pollutants, with special attention to both short- and long-term effects of air quality on health. It also explores mitigation and adaptation strategies. The second chapter (Guieu & Ridame, 2022) sums up our understanding of the impact of atmospheric deposition on the chemistry and biogeochemistry of the Mediterranean Sea. Results include process studies, observations at sea, and state-of-the-art numerical simulations. The third and last chapter (Kanakidou et al., 2022b) reports on the current knowledge on the impacts of air pollution on the terrestrial vegetation, which can take place through a number of direct and indirect pathways.

Finally, the last chapter (Dulac et al., 2022) summarizes conclusions from the 23 different chapters of Vol. 2, highlighting recent progress in tropospheric chemistry and its impacts in the Mediterranean region. It also issues some recommendations for future research to address major remaining gaps in our knowledge.

3 Conclusion

Intense climate change and increasing anthropogenic pressure already seen in the Mediterranean region might impair its future inhabitability, which calls for a better understanding of the present chemical environment and its expected future evolution. The Mediterranean atmospheric chemical system and its impacts needs a wide interdisciplinary field of expertise and long and combined efforts from the scientific community. As an unprecedented initiative, the decadal ChArMEx research program and partner initiatives provided new relevant knowledge, thanks in particular to an intensive field observation program throughout the basin that has been summarized in the introduction of Vol. 1 and its appendix (Dulac, Sauvage, & Hamonou, 2023). Observations from monitoring networks, supersites, and many regional and local campaigns, together with some laboratory studies and integrative approaches, allowed a better understanding of processes driving atmospheric composition evolution and its impacts on health, climate, and ecosystems. This effort has resulted in a ChArMEx special issue jointly published by the two journals *Atmospheric Measurement and Techniques* and *Atmospheric Physics and Chemistry* providing online access to more than one hundred articles with detailed results (https://acp.copernicus.org/articles/special_issue334.html, last access 21 July 2022). In the present book, as many as one hundred authors joined their scientific expertise to provide an updated review of the abundant available literature on atmospheric chemistry and its impact in the Mediterranean region, compiling results from the ChArMEx special issue and other ChArMEx-related publications and from many other available studies, and some yet unpublished data. The resulting edited book in two volumes includes ten different sections and more than 40 reviewed chapters including conclusion chapters with recommendations for future research. The first four parts of Volume 1 address general background information of interest, relationships between the regional dynamics and atmospheric pollution, and the distribution and variability at different local and spatial scales of aerosols and reactive gases. The present Volume 2 includes six more thematic parts focused on the pollutant lifecycles, including emissions, chemical processes, aerosol properties, atmospheric deposition, and on important impacts of the atmospheric composition in the Mediterranean region, from climate-related aspects to marine and terrestrial ecosystems and human health, that is, key aspects of the regional inhabitability.

Acknowledgments ChArMEx has many partners to thank for its achievements, and relevant acknowledgments can be found in the book preface.

References

Becagli, S. (2022). Aerosol composition and reactivity. In F. Dulac, S. Sauvage, & E. Hamonou (Eds.), *Atmospheric chemistry in the Mediterranean Region* (Vol. 2, From air pollutant sources to impacts). Springer, this volume. https://doi.org/10.1007/978-3-030-82385-6_13

Beekmann, M. (Coord.). (2022). Recent progress on chemical processes. In F. Dulac, S. Sauvage, & E. Hamonou (Eds.), *Atmospheric chemistry in the Mediterranean Region* (Vol. 2, From air pollutant sources to impacts, Part VI). Springer, this volume. https://doi.org/10.1007/978-3-030-82385-6

Borbon, A., Afif, C., Salameh, T., Thera, B., & Panopoulou, A. (2022). Anthropogenic emissions of reactive compounds in the Mediterranean region. In F. Dulac, S. Sauvage, & E. Hamonou (Eds.), *Atmospheric chemistry in the Mediterranean Region* (Vol. 2, From air pollutant sources to impacts). Springer, this volume. https://doi.org/10.1007/978-3-030-82385-6_5

Brasseur, G. P., & Jacob, D. J. (2017). *Modeling of atmospheric chemistry* (xxiv+606 pp.). Cambridge Univ. Press. https://doi.org/10.1017/9781316544754

Dayan, U. (2023). Synoptic and dynamic conditions affecting pollutant concentrations over the Mediterranean basin. In F. Dulac, S. Sauvage, & E. Hamonou (Eds.), *Atmospheric chemistry in the Mediterranean Region* (Vol. 1, Background information and pollutant distribution, Part II). Springer.

Denjean, C. (2022). Aerosol hygroscopicity. In F. Dulac, S. Sauvage, & E. Hamonou (Eds.), *Atmospheric chemistry in the Mediterranean Region* (Vol. 2, From air pollutant sources to impacts). Springer, this volume. https://doi.org/10.1007/978-3-030-82385-6_15

Desboeufs, K. (Coord.). (2022a). Deposition in the Mediterranean region. In F. Dulac, S. Sauvage, & E. Hamonou (Eds.), *Atmospheric chemistry in the Mediterranean Region* (Vol. 2, From air pollutant sources to impacts, Part VIII). Springer, this volume. https://doi.org/10.1007/978-3-030-82385-6

Desboeufs, K. (2022b). Nutrient deposition and variability. In F. Dulac, S. Sauvage, & E. Hamonou (Eds.), *Atmospheric chemistry in the Mediterranean Region* (Vol. 2, From air pollutant sources to impacts). Springer, this volume. https://doi.org/10.1007/978-3-030-82385-6_17

Desboeufs, K. (2022c). Trace metals and contaminants deposition. In F. Dulac, S. Sauvage, & E. Hamonou (Eds.), *Atmospheric chemistry in the Mediterranean Region* (Vol. 2, From air pollutant sources to impacts). Springer, this volume. https://doi.org/10.1007/978-3-030-82385-6_18

Di Biagio, C. (2022). Aerosol size distribution. In F. Dulac, S. Sauvage, & E. Hamonou (Eds.), *Atmospheric chemistry in the Mediterranean Region* (Vol. 2, From air pollutant sources to impacts). Springer, this volume. https://doi.org/10.1007/978-3-030-82385-6_12

Dulac, F. (Coord.). (2023). The Mediterranean atmospheric chemistry hotspot. In F. Dulac, S. Sauvage, & E. Hamonou (Eds.), *Atmospheric chemistry in the Mediterranean Region* (Vol. 1, Background information and pollutant distribution, Part I). Springer.

Dulac, F., Sauvage, S., & Hamonou, E. (Eds.) (2023). *Atmospheric chemistry in the mediterranean Region* (Vol. 1, Background information and pollutant distribution). Springer.

Dulac, F., Sauvage, S., & Hamonou, E. (Eds.) (2022). *Atmospheric chemistry in the Mediterranean Region* (Vol. 2, From air pollutant sources to impacts). Springer, this volume. https://doi.org/10.1007/978-3-030-82385-6

Dulac, F., Sauvage, S., Hamonou, E., & Debevec, C. (2023). Introduction to the volume 1 of Atmospheric Chemistry in the Mediterranean Region and to the experimental effort during the ChArMEx decade. In F. Dulac, S. Sauvage, & E. Hamonou (Eds.), *Atmospheric chemistry in the Mediterranean Region* (Vol. 1, Background information and pollutant distribution). Springer.

Dulac, F., Hamonou, E., Sauvage, S., Kanakidou, M., Beekmann, M., Desboeufs, K., Formenti, P., Becagli, S., Di Biagio, C., Borbon, A., Denjean, C., Gheusi, F., Gros, V., Guieu, C., Junkermann, W., Kalivitis, N., Laurent, B., Mallet, M., Michoud, V., … Sellegri, K. (2022). Summary of recent progress and recommendations for future research regarding air pollutant sources, processes, deposition and impacts in the Mediterranean region. In F. Dulac, S. Sauvage, & E. Hamonou

(Eds.), *Atmospheric chemistry in the mediterranean Region* (Vol. 2, From air pollutant sources to impacts). Springer, this volume. https://doi.org/10.1007/978-3-030-82385-6_25

Formenti, P. (Coord.). (2022). Mediterranean aerosol properties. In F. Dulac, S. Sauvage, & E. Hamonou (Eds.), *Atmospheric chemistry in the Mediterranean Region* (Vol. 2, From air pollutant sources to impacts, Part VII). Springer, this volume. https://doi.org/10.1007/978-3-030-82385-6

Gheusi, F. (2022). Ozone photochemical production rates in the western Mediterranean. In F. Dulac, S. Sauvage, & E. Hamonou (Eds.), *Atmospheric chemistry in the Mediterranean Region* (Vol. 2, From air pollutant sources to impacts). Springer, this volume. https://doi.org/10.1007/978-3-030-82385-6_8

Gros, V., & Zannoni, N. (2022). Total OH reactivity. In F. Dulac, S. Sauvage, & E. Hamonou (Eds.), *Atmospheric chemistry in the Mediterranean Region* (Vol. 2, From air pollutant sources to impacts). Springer, this volume. https://doi.org/10.1007/978-3-030-82385-6_7

Gros, V., Lathière, J., Boissard, C., Jambert, C., Delon, C., Staudt, M., Fernandez, C., Ormeño, E., Baisnée, D., & Sarda Estève, R. (2022). Emissions from the Mediterranean vegetation. In F. Dulac, S. Sauvage, & E. Hamonou (Eds.), *Atmospheric chemistry in the Mediterranean Region* (Vol. 2, From air pollutant sources to impacts). Springer, this volume. https://doi.org/10.1007/978-3-030-82385-6_3

Guieu, C., & Ridame, C. (2022). Impact of atmospheric deposition on marine chemistry and biogeochemistry. In F. Dulac, S. Sauvage, & E. Hamonou (Eds.), *Atmospheric chemistry in the Mediterranean Region* (Vol. 2, From air pollutant sources to impacts). Springer, this volume. https://doi.org/10.1007/978-3-030-82385-6_23

Jacobson, M. Z. (2005). *Fundamentals of atmospheric modeling.* (2nd edn., 813 pp.). Cambridge University Press. https://doi.org/10.1017/CBO9781139165389.

Junkermann, W. (2022). Ultrafine particle emissions in the Mediterranean. In F. Dulac, S. Sauvage, & E. Hamonou (Eds.), *Atmospheric chemistry in the Mediterranean Region* (Vol. 2, From air pollutant sources to impacts). Springer, this volume. https://doi.org/10.1007/978-3-030-82385-6_6

Kalivitis, N., Papatheodorou, S., Maesano, C. N., & Annesi-Maesano, I. (2022). Air quality and health impacts. In F. Dulac, S. Sauvage, & E. Hamonou (Eds.), *Atmospheric chemistry in the Mediterranean Region* (Vol. 2, From air pollutant sources to impacts). Springer, this volume. https://doi.org/10.1007/978-3-030-82385-6_22

Kanakidou, M. (Coord.). (2022a). Impact of air pollution on precipitation chemistry and climate. In F. Dulac, S. Sauvage, & E. Hamonou (Eds.), *Atmospheric chemistry in the Mediterranean Region* (Vol. 2, From air pollutant sources to impacts, Part IX). Springer, this volume. https://doi.org/10.1007/978-3-030-82385-6

Kanakidou, M. (Coord.). (2022b). Impact of air pollution on human health and ecosystems. In F. Dulac, S. Sauvage, & E. Hamonou (Eds.), *Atmospheric chemistry in the Mediterranean Region* (Vol. 2, From air pollutant sources to impacts, Part X). Springer, this volume. https://doi.org/10.1007/978-3-030-82385-6

Kanakidou, M., Myriokefalitakis, S., Papadimitriou, V. C., & Nenes, A. (2022a). Aerosol impacts on atmospheric and precipitation chemistry. In F. Dulac, S. Sauvage, & E. Hamonou (Eds.), *Atmospheric chemistry in the Mediterranean Region* (Vol. 2, From air pollutant sources to impacts). Springer, this volume. https://doi.org/10.1007/978-3-030-82385-6_21

Kanakidou, M., Sfakianaki, M., & Probst, A. (2022b). Impact of air pollution on terrestrial ecosystems. In F. Dulac, S. Sauvage, & E. Hamonou (Eds.), *Atmospheric chemistry in the Mediterranean Region* (Vol. 2, From air pollutant sources to impacts). Springer, this volume. https://doi.org/10.1007/978-3-030-82385-6_24

Laurent, B., & Bergametti, G. (2022). Soil dust emissions. In F. Dulac, S. Sauvage, & E. Hamonou (Eds.), *Atmospheric chemistry in the Mediterranean Region* (Vol. 2, From air pollutant sources to impacts). Springer, this volume. https://doi.org/10.1007/978-3-030-82385-6_4

Laurent, B., Audoux, T., Bibi, M., Dulac, F., & Bergametti, G. (2022). Mass deposition. In F. Dulac, S. Sauvage, & E. Hamonou (Eds.), *Atmospheric chemistry in the Mediterranean*

Region (Vol. 2, From air pollutant sources to impacts). Springer, this volume. https://doi.org/10.1007/978-3-030-82385-6_16

Mallet, M., Chazette, P., Dulac, F., Formenti, P., Di Biagio, C., Denjean, C., & Chiapello, I. (2022a). Aerosol optical properties. In F. Dulac, S. Sauvage, & E. Hamonou (Eds.), *Atmospheric chemistry in the Mediterranean Region* (Vol. 2, From air pollutant sources to impacts). Springer, this volume. https://doi.org/10.1007/978-3-030-82385-6_14

Mallet, M., Nabat, P., di Sarra, A. G., Solmon, F., Gutierrez, C., Mailler, S., Menut, L., Kaskaoutis, D., Rowlinson, M., Rap, A., & Dulac, F. (2022b). Aerosol and tropospheric ozone direct radiative impacts. In F. Dulac, S. Sauvage, & E. Hamonou (Eds.), *Atmospheric chemistry in the Mediterranean Region* (Vol. 2, From air pollutant sources to impacts). Springer, this volume. https://doi.org/10.1007/978-3-030-82385-6_19

Mészáros, E. (1981). *Atmospheric chemistry: Fundamental aspects.* Elsevier, 201 pp., ISBN 978-0444997531.

Michoud, V. (2022). Particle-gas multiphasic interactions. In F. Dulac, S. Sauvage, & E. Hamonou (Eds.), *Atmospheric chemistry in the Mediterranean Region* (Vol. 2, From air pollutant sources to impacts). Springer, this volume. https://doi.org/10.1007/978-3-030-82385-6_11

Mihalopoulos, N. (Coord.). (2023a). Aerosol concentrations and variability. In F. Dulac, S. Sauvage, & E. Hamonou (Eds.), *Atmospheric chemistry in the Mediterranean Region* (Vol. 1, Background information and pollutant distribution, Part III). Springer.

Mihalopoulos, N. (Coord.). (2023b). Reactive gas concentrations and variability. In F. Dulac, S. Sauvage, & E. Hamonou (Eds.), *Atmospheric chemistry in the Mediterranean Region* (Vol. 2, Background information and pollutant distribution, Part IV). Springer.

Nabat, P., Kanji, Z., Mallet, M., Denjean, C., & Solmon, F. (2022). Aerosol-cloud interactions and impact on regional climate. In F. Dulac, S. Sauvage, & E. Hamonou (Eds.), *Atmospheric chemistry in the Mediterranean Region* (Vol. 2, From air pollutant sources to impacts). Springer, this volume. https://doi.org/10.1007/978-3-030-82385-6_20

Sartelet, K. (2022). Secondary aerosol formation and their modeling. In F. Dulac, S. Sauvage, & E. Hamonou (Eds.), *Atmospheric chemistry in the Mediterranean Region* (Vol. 2, From air pollutant sources to impacts). Springer, this volume. https://doi.org/10.1007/978-3-030-82385-6_10

Sauvage, S. (Coord.). (2022). Emissions and sources. In F. Dulac, S. Sauvage, & E. Hamonou (Eds.), *Atmospheric chemistry in the Mediterranean Region* (Vol. 2, From air pollutant sources to impacts, Part V). Springer, this volume. https://doi.org/10.1007/978-3-030-82385-6

Sauvage, S., Dulac, F., Hamonou, E., Dayan, U., Mihalopoulos, N., Debevec, C., Doussin, J.-F., Giorgi, F., Kalabokas, P., Kaskaoutis, D. G., Liakakou, E., & Masson, O. (2023). Summary of recent progress and recommendations for future research regarding the Mediterranean context and atmospheric pollutant distributions. In F. Dulac, S. Sauvage, & E. Hamonou (Eds.), *Atmospheric chemistry in the Mediterranean Region* (Vol. 1, Background information and pollutant distribution). Springer.

Seinfeld, J. H., & Pandis, S. N. (2016). *Atmospheric chemistry and physics: From air pollution to climate change* (3rd Ed., 1152 pp). Wiley. ISBN 978–1–119-22117-3.

Sellegri, K., & Mallet, M. (2022). Sea spray emissions. In F. Dulac, S. Sauvage, & E. Hamonou (Eds.), *Atmospheric chemistry in the Mediterranean Region* (Vol. 2, From air pollutant sources to impacts). Springer, this volume. https://doi.org/10.1007/978-3-030-82385-6_2

Sellegri, K., & Rose, C. (2022). Nucleation in the Mediterranean atmosphere. In F. Dulac, S. Sauvage, & E. Hamonou (Eds.), *Atmospheric chemistry in the Mediterranean Region* (Vol. 2, From air pollutant sources to impacts). Springer, this volume. https://doi.org/10.1007/978-3-030-82385-6_9

Part V
Emissions and Sources

Coordinated by ***Stéphane Sauvage***

IMT Nord Europe, Institut Mines-Télécom, Univ. Lille, Centre for Energy and Environment, F-59000 Lille, France

Reviewed by Claire Granier (Laboratoire d'Aérologie, CNRS – Univ. Toulouse III Paul Sabatier, Toulouse, France)

Abstract

The Mediterranean basin is the recipient of anthropogenic emissions from Europe and densely populated coastal urban areas combined with natural emissions from the surrounding vegetation, the sea, and African and Middle East deserts. Accurate emission assessment of gaseous and particulate pollutants is among the prerequisites to study atmospheric pollution and climate change in this region. It is especially crucial to evaluate how much sources contribute to air pollution in order to target pollution remediation and define air quality policies. Source types are numerous and both natural and anthropogenic emitters have to be identified and evaluated in terms of chemical composition of emitted pollutants as well as their emission processes.

Sea Spray Emissions

Karine Sellegri and Marc Mallet

Contents

Abstract Sea spray aerosol particles constitute one of the most important natural components of the atmosphere and are emitted from the Mediterranean Sea with characteristics linked to the high temperatures and oligotrophic properties of the seawater. Sea spray aerosol production results from the action of wind stress on the sea surface, creating waves and bubbles, and is traditionally assumed to be mainly composed of inorganic sea salt, an organic fraction, and water. While the inorganic matter present in sea spray is relatively well documented and parameterized in models, much more uncertainties are associated with the emission of marine organic matter. Biochemical processes in the seawater and surface microlayer are at play in determining the fraction of organic matter in sea spray, but also the number of sea

Chapter reviewed by ***Gerrit de Leeuw*** *(Koninklijk Nederlands Meteorologisch Instituut (KNMI) De Bilt, The Netherlands), as part of the book Part V Emissions and Sources also reviewed by* ***Claire Granier*** *(Laboratoire d'Aérologie (LAERO), CNRS – Univ. Toulouse III Paul Sabatier, Observatoire Midi-Pyrénées, Toulouse, France)*

K. Sellegri (✉)
Université Clermont Auvergne, CNRS, Laboratoire de Météorologie Physique UMR 6016 (LaMP), Clermont-Ferrand, France
e-mail: K.Sellegri@opgc.univ-bpclermont.fr

M. Mallet
Centre National de Recherches Météorologiques (CNRM), Université de Toulouse, Météo-France, CNRS, Toulouse, France

F. Dulac et al. (eds.), *Atmospheric Chemistry in the Mediterranean Region*,
https://doi.org/10.1007/978-3-030-82385-6_2

spray particles emitted into the atmosphere. Under environmental conditions specific to the Mediterranean Sea, the relationship between seawater biology and sea spray properties has specificities that will be presented in the present chapter.

1 Introduction

Marine aerosol particles constitute one of the most important natural components of the atmosphere that significantly contribute to the Earth's radiative budget, but they also have local effects on regional air quality (O'Dowd & De Leeuw, 2007). Marine aerosols influence cooling or warming at the top of the atmosphere (Randles et al., 2004, Claeys et al., 2017; Mallet et al., 2022). These aerosols may also have indirect effects by becoming cloud droplets or ice crystals (Novakov & Corrigan, 1996; Novakov & Penner, 1993). Despite their importance, our ability to correctly describe and simulate marine aerosols is still limited by the poor understanding of the link between the properties of the seawater below and the formation of aerosol particles at the air-sea interface and their subsequent evolution in the atmosphere. Mesoscale models are unable to reproduce the number concentrations of aerosol particles in the marine boundary layer and their impact on cloud properties (Merikanto et al., 2009), and a large uncertainty in the projection of future climate can be attributed to a lack of knowledge on marine aerosols (Carslaw et al., 2013). In the Mediterranean area, the marine aerosol emission pathways may be different from those in other parts of the world, firstly due to the specific temperature range and oligotrophic properties of the seawater. Furthermore, high radiation and ozone levels in the atmosphere lead to an intense photochemical activity over a large period of the year. Marine aerosol particles may be produced via two different pathways. Primary marine aerosol production results from wind stress at the sea surface which gives rise to the mechanical production of sea spray aerosol (SSAer), traditionally assumed to be mainly composed of inorganic sea salt, an organic fraction, and water. Secondary marine aerosol production may occur via nucleation or the condensation of gas-phase species onto pre-existing particles. Primary marine aerosol sources (sea spray) are addressed in the present chapter, while nucleation processes from marine precursors are addressed in Sellegri & Rose (2022), as well as marine sources as precursors to SOA in Sartelet (2022).

2 Parameters Influencing the Sea Spray Emission Fluxes

At horizontal wind speeds greater than 4 m s^{-1}, breaking waves generate bubbles that rise in the water column and burst when protruding the surface. The disrupting film cap produces film drops; the rising jet produces jet drops. At wind speeds exceeding about 9 m s^{-1}, sea spray droplets, referred to as spume droplets, are

directly blown off the wave tops. Sea spray aerosols make up a large portion of the natural aerosol emissions, with an estimated global contribution between 2000 and 10,000 Tg per year (Gantt & Meskhidze, 2013). Mulcahy et al. (2008) report a relationship between aerosol optical depth (AOD) in clean oceanic air and squared surface wind speed with AODs value of 0.3–0.4 under high wind speed conditions of 15–18 m s^{-1}. Sea spray particle emissions are mainly dependent on wind speed, but also on the sea surface temperature, the sea state (wave height, shape, etc.), and salinity (Grythe et al., 2014). Sea spray number fluxes may depend also on other seawater parameters such as organic matter of biological origin with surfactant properties (Fuentes et al., 2010). Laboratory measurements indicate that the number concentrations of sea spray aerosols produced by bubble bursting mainly peak at sizes of 100 nm and 40 nm for Atlantic Ocean waters (Mårtensson et al., 2003; Fuentes et al., 2010), which does not differ significantly in Mediterranean waters. Indeed, laboratory characterization of sea spray from Mediterranean waters shows that the SSAer size distribution can be best described by two main modes around 40–50 nm and 100 nm, an additional nucleation mode (around 20–25 nm), and a second accumulation mode at 260 nm (Schwier et al., 2015, 2017). The presence of surface-active components may influence the bubble bursting process and hence the size distribution of SSAer. A shift toward smaller particles was observed when artificial surfactants (Sellegri et al., 2006) or biogenic exudates (Fuentes et al., 2010) were added to artificial (inorganic) seawater. Also, several authors report an increase of the 200–300 nm mode number concentrations when organic matter is present (Sellegri et al., 2006; King et al., 2012). However, changes in the shape of SSAer size distribution due to the presence of organic matter in the seawater are not relevant for climate-relevant impact (see Section 4 hereafter).

However, changes in the relative contribution of the different modes to Mediterranean SSAer due to the presence of organic matter are relatively low. Figure 1 shows the mode decomposition of sea spray generated from Mediterranean surface waters from four different experiments. Modes are always found at about 40 nm and 100 nm with similar contributions that dominate the size distributions and at 250 nm with a minor contribution. The most variable mode presence is the nucleation mode at 20 nm. This mode is likely more dependent on the presence of surfactants, although there is still a lot of uncertainty in the factors influencing it and some further research is necessary.

Several parameterizations of the sea spray fluxes published in the literature and used in modelling exercises include a sea surface temperature (SST) dependence (Forestieri et al., 2018; Grythe et al., 2014; Jaeglé et al., 2011; Mårtensson et al., 2003; Ovadnevaite et al., 2014; Salter et al., 2014; Zábori et al., 2012; Albert et al., 2016). Some of these studies agree on a sharp SST dependence of the SSAer number fluxes, with concentrations increasing when temperature decreases below 10 °C (Salter et al., 2014; Zábori et al., 2012). In the SST range representative of the Mediterranean seawater, parameterizations derived from synthetic inorganic seawater experiments show little dependence of the SSAer number concentrations on temperature (Mårtensson et al., 2003; Salter et al., 2014). From laboratory experiments of SSAer generation from natural Mediterranean seawaters, Schwier et al. (2017)

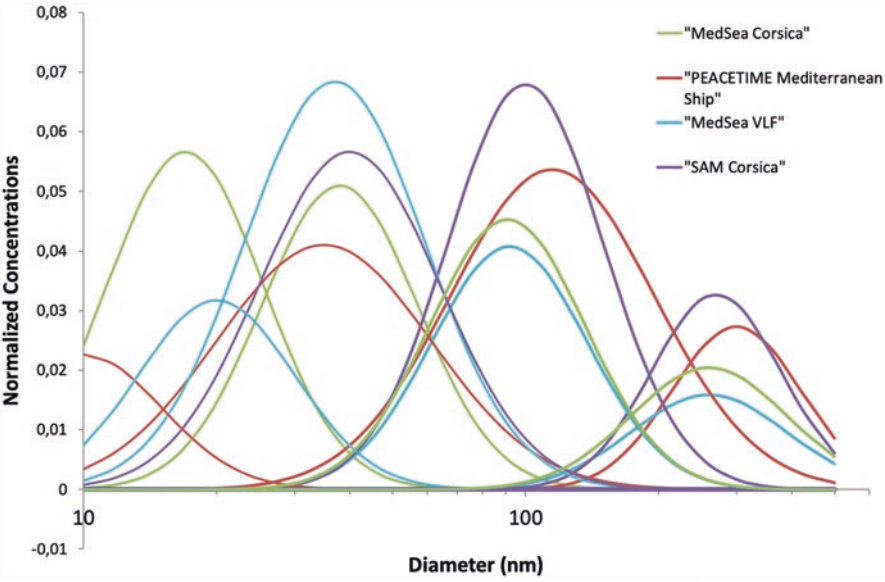

Fig. 1 Lognormal decomposition of the normalized size distributions (fractions of the total number concentration) obtained from sea spray generation experiments during four experiments (MedSea Corsica, MedSea Villefranche-sur-Mer, SAM Corsica, and PEACETIME over a ship cruise across the western Mediterranean Sea) performed with the support of ChArMEx. Thickness of lines is increasing with mode size (from nucleation to accumulation mode)

show that there is a factor of 2 increase in the total number concentration of SSAer when temperature changes from 22 to 30 °C. The same tendency was found in Jaeglé et al. (2011) for SST higher than 20 °C at the global scale, from the comparison of modelled versus observed SSAer concentrations constrained with Tropical Pacific, Tropical Atlantic, and Indian Ocean data.

Given the large variability of SST dependence of sea spray fluxes in the literature, it is likely that other factors influence this SST dependence in natural seawaters. Several laboratory sea spray generation experiments showed differences between number fluxes generated from synthetic inorganic seawaters and those generated from natural seawaters (Tyree et al., 2007; Fuentes et al., 2010; Alpert et al., 2015; Forestieri et al., 2018) or differences between fluxes measured in non-biologically versus biologically rich seawaters (Keene et al., 2017). In general, seawater enriched in biologically derived organics show higher number fluxes. In oligotrophic seawaters such as those found in the Mediterranean Sea, sea spray fluxes were measured as a function of the seawater biogeochemical properties during the PEACETIME ship campaign (a joint MERMEX-ChArMEx initiative; Guieu et al., 2020). Results show that a clear relationship was found between the number fluxes of sea spray and the abundance of nanophytoplankton cells (Sellegri et al., 2021). This relationship was also found in a data set from the South-West Pacific and reinforced when these two data sets are merged, indicating that Mediterranean

seawater contains biologically originating organic material with the same properties as found in the global ocean (Sellegri et al., 2021). The mechanism behind the impact of seawater microorganisms on sea spray number emission fluxes is thought to be the production of organic compounds by these microorganisms, which affects the bubble's film stability and hence their thickness.

3 Chemical Composition of Sea Spray

Sea spray contains both inorganic sea salts and organic material. Primary emissions can acquire organic material either as bubbles traverse through the water column or at the ocean surface from the organic rich microlayer (Bigg & Leck, 2008; Blanchard, 1964; Lion & Leckie, 1981) which can exhibit different physical, chemical, and biological properties to oceanic subsurface water (Cunliffe et al., 2013; Walker et al., 2016). Concentrations of marine organic aerosol particles were found to be highly dependent on the biological productivity at the ocean surface, following a seasonal bloom cycle (O'Dowd et al., 2004; Sciare et al., 2009). Organic matter found in sea spray was mainly found as insoluble colloids during a bloom period of the North Atlantic Ocean (Facchini et al., 2008). Current mesoscale and some global atmospheric models use Chl-a in seawater as a proxy to calculate sea spray organic fractions (OMSS) (Langmann et al., 2008; Vignati et al., 2010). They are based on the results from different studies that have linked the total submicron organic mass fraction of sea spray aerosol to chlorophyll-a (Chl-a) levels observed by satellite (Vignati et al., 2010; Albert et al., 2012; Rinaldi et al., 2013). These studies use the organic fraction of marine aerosols sampled at a receptor site, and hence organic found in the samples can be of primary origin, but they can also be the result of condensation of organic gas-phase species during transport. In order to isolate the sea spray fraction of organic concentration from the total organic content of ambient marine aerosols, aerosols may be generated artificially from seawater. Using this approach, Prather et al. (2013) showed a link between the marine particles' organic content and heterotrophic bacteria abundance instead of Chl-a. Also using a sea spray generation system with Mediterranean seawaters sample, Schwier et al. (2015) showed a correlation between the organic fraction of small sea spray particles and Chl-a and heterotrophic and autotrophic bacteria abundance in seawater. The linear relationship found between the organic fraction of sea spray and seawater Chl-a was however not found during a mesocosm experiment using Mediterranean seawater in which the biological activity was sustained with the addition of nutrients (Schwier et al., 2017). The hypothesis is that the nature of the organic matter produced by microorganisms determines the amount of organic matter that is enriched in the sea surface microlayer, and therefore the ratio of organic matter to total sea spray mass transferred to the atmosphere as bubble film drops. When merging data from three different mesocosm experiments performed with Mediterranean seawaters, and excluding the mesocosms that had been enriched with nutriments, one can derive a parameterization that can be applied for the oligotrophic waters of

the Mediterranean Sea (Fig. 2). Different aerosol size ranges (Aitken mode and PM_1) need to be considered separately, as a strong increase in the fraction of organics was found with decreasing particle size, as already reported by Facchini et al. (2008) for North Atlantic waters. The resulting parameterizations are the following:

$$\mathrm{OMSS}_{\mathrm{Aitken}} = 0.63 + 0.12\mathrm{Ln}\left(\mathrm{Chl} - a\right) \quad (1)$$

$$\mathrm{OMSS}_{\mathrm{PM1}} = 0.33 + 0.04\mathrm{Ln}\left(\mathrm{Chl} - a\right) \quad (2)$$

For the inorganic fraction, Schwier et al. (2015) also showed that the composition of Mediterranean SSAer was very similar to the composition of the seawater as reported by Seinfeld and Pandis (2016), although a deficit in chloride compared to the seawater chloride-to-sodium ratio was observed. Since this deficit is observed before SSAer is transported in the atmosphere, one can hypothesize that chemical reactions modifying the Na/Cl ratio already occur within the Mediterranean seawater or at the sea surface. Close to the coasts such as the Mediterranean ones, river inputs and the pollution from urbanized coastal sites with large population densities can cause an excess of phosphate and nitrate compounds (Jamet et al., 2001) that may result in specific reactions.

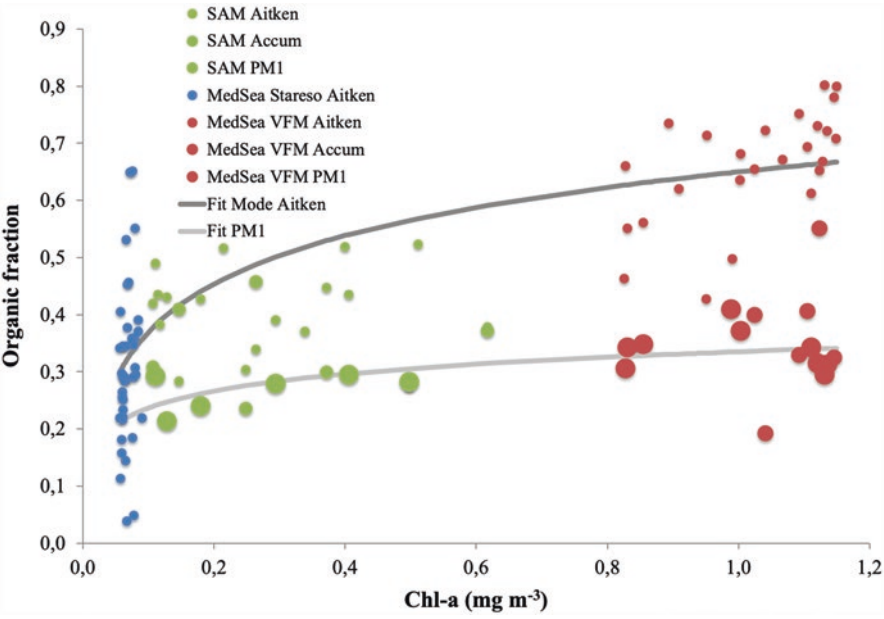

Fig. 2 Organic fraction of sea spray aerosols as a function of Chl-a concentration in the seawater measured from three different mesocosm campaigns (MedSea Stareso (Corsica, bay of Calvi), MedSea VFM (France, bay of Villefranche), and SAM (Corsica, bay of Calvi)) and for different size ranges of the sea spray (Aitken mode, accumulation mode, and total submicron aerosol PM_1). Fit of the organic fraction of each size range (Aitken and PM_1) with a logarithmic law

4 Sea Spray Emissions and Derived Cloud Condensation and Ice Nuclei

Sea spray can act as cloud condensation nuclei (CCN), and thus influences cloud properties, with an efficiency that is dependent on its size and hygroscopicity. CCN properties of sea spray generated from Mediterranean seawater were measured during the SAM experiment in May 2013, showing that the sea spray originating CCN fluxes varied like the total number of sea spray fluxes, with no impact of the organic content of sea spray on its CCN ability (around 60% of sea spray number concentration act as CCN at the 0.3% supersaturation) (Schwier et al., 2017). This conclusion was also observed from seawaters of other origins (King et al., 2012; Moore et al., 2011) and confirmed for Mediterranean seawater during the PEACETIME cruise (Sellegri et al., 2021). The lack of effect of the organic content on CCN properties of sea spray can be explained by the lack of impact of the marine organics on the shape of the sea spray size distribution (and hence its size) (see Fig. 1) and by the little variability of the organic content itself (and hence its hygroscopicity) in oligotrophic waters for a given season (see Fig. 2). The large impact of organic matter on the total sea spray number fluxes that was evidenced from diverse seawater types, including Mediterranean seawater (Sellegri et al., 2021), would however significantly influence the total number of sea spray derived CCN flux to the atmosphere as a function of the seawater biogeochemical properties.

Sea spray ice nuclei (IN) properties are thought to be lower than those of dust particles at low freezing temperatures, but may be significant at warmer temperatures and of major importance in areas where particles of terrestrial origin are absent (DeMott et al., 2016). IN properties of sea spray are poorly understood, although there is evidence that biological factors influence these properties with increased IN efficiencies for higher biological productivities (Bigg, 1973; Schnell & Vali, 1976; DeMott et al., 2016). It appears that sea spray IN properties depend differently on biological factors when considering either cold IN (for temperatures below −18 °C) or warm IN (for temperatures above −18 °C) (McCluskey et al., 2018). While cold ice nucleating sea spray particles are linked to a heat-labile microbial type in the seawater, the warm ice nucleating sea spray particles are rather linked to surface-active DOC enriched in the sea surface microlayer (McCluskey et al., 2018). This finding of two classes of IN sea spray was recently confirmed from Mediterranean seawaters and further conceptualized into a biology-dependent marine IN parameterization (Trueblood et al., 2021).

5 Conclusion and Recommendations

The relationship between sea spray and the seawater biogeochemical properties is complex, due to the presence of processes of physical, chemical, photochemical, and biological nature interacting with each other. Nowadays, parameterizations of

sea spray aerosol fluxes include an organic component that is at best a function of Chl-a in the seawater, although a recent modelling study has integrated the different nature of organic classes in the seawater (originating from proteins, lipids, polysaccharides, or humic-like substances) and their surfactant properties for prescribing their transfer to the atmosphere (Burrows et al., 2014). The Mediterranean Sea is oligotrophic, and hence sea spray aerosol particles emitted from Mediterranean waters contain a low level of biologically originating carbon except during phytoplanktonic bloom conditions. Besides, sea surface temperatures are relatively high throughout the year, implying that organic matter will not have a large impact on sea spray number emissions via their impact on the temperature dependence of surfactants. However, the Mediterranean Sea experiences a large amount of radiation which effect on emissions is largely unknown and should be the focus of future research on sea spray aerosol emissions in this area of the world.

References

Albert, M. F. M. A., Schaap, M., Manders, A. M. M., Scannell, C., O'Dowd, C. D., & de Leeuw, G. (2012). Uncertainties in the determination of global sub-micron marine organic matter emissions. *Atmospheric Environment, 57*, 289–300. https://doi.org/10.1016/j.atmosenv.2012.04.009

Albert, M. F. M. A., Anguelova, M. D., Manders, A. M. M., Schaap, M., & de Leeuw, G. (2016). Parameterization of oceanic whitecap fraction based on satellite observations. *Atmospheric Chemistry and Physics, 16*, 13725–13751. https://doi.org/10.5194/acp-16-13725-2016

Alpert, P. A., Kilthau, W. P., Bothe, D. W., Radway, J. C., Aller, J. Y., & Knopf, D. A. (2015). The influence of marine microbial activities on aerosol production: A laboratory mesocosm study. *Journal of Geophysical Research – Atmospheres, 120*, 8841–8860. https://doi.org/10.1002/2015JD023469

Bigg, E. K. (1973). Ice nucleus concentrations in remote areas. *Journal of the Atmospheric Sciences, 30*, 1153–1157. https://doi.org/10.1175/1520-0469(1973)030<1153:INCIRA>2.0.CO;2

Bigg, E. K., & Leck, C. (2008). The composition of fragments of bubbles bursting at the ocean surface. *Journal of Geophysical Research, 113*, D11209. https://doi.org/10.1029/2007JD009078

Blanchard, D. C. (1964). Sea-to-air transports surface active material. *Science, 146*, 396–397. https://doi.org/10.1126/science.146.3642.396

Burrows, S. M., Ogunro, O., Frossard, A. A., Russell, L. M., Rasch, P. J., & Elliott, S. M. (2014). A physically based framework for modeling the organic fractionation of sea spray aerosol from bubble film Langmuir equilibria. *Atmospheric Chemistry and Physics, 14*, 13601–13629. https://doi.org/10.5194/acp-14-13601-2014

Carslaw, K. S., Lee, L. A., Reddington, C. L., Pringle, K. J., Rap, A., Forster, P. M., Mann, G. W., Spracklen, D. V., Woodhouse, M. T., Regayre, L. A., & Pierce, J. R. (2013). Large contribution of natural aerosols to uncertainty in indirect forcing. *Nature, 503*, 67–71. https://doi.org/10.1038/nature12674

Claeys, M., Roberts, G., Mallet, M., Arndt, J., Sellegri, K., Sciare, J., Wenger, J., & Sauvage, B. (2017). Optical, physical and chemical properties of aerosols transported to a coastal site in the western Mediterranean: A focus on primary marine aerosols. *Atmospheric Chemistry and Physics, 17*, 7891–7915. https://doi.org/10.5194/acp-17-7891-2017

Cunliffe, M., Engel, A., Frka, S., Gašparović, B., Guitart, C., Murrell, J. C., Salter, M., Stolle, C., Upstill-Goddard, R., & Wurl, O. (2013). Sea surface microlayers: A unified physicochemical and biological perspective of the air−ocean interface. *Progress in Oceanography, 109*, 104–116. https://doi.org/10.1016/j.pocean.2012.08.004

DeMott, P. J., Hill, T. C. J., McCluskey, C. S., Prather, K. A., Collins, D. B., Sullivan, R. C., Ruppel, M. J., Mason, R. H., Irish, V. E., Lee, T., Hwang, C. Y., Rhee, T. S., Snider, J. R., McMeeking, G. R., Dhaniyala, S., Lewis, E. R., Wentzell, J. J. B., Abbatt, J., Lee, C., … Franc, G. D. (2016). Sea spray aerosol as a unique source of ice nucleating particles. *Proceedings of the National Academy of Sciences USA, 113*, 5797–5803. https://doi.org/10.1073/pnas.1514034112

Facchini, M. C., Rinaldi, M., Decesari, S., Carbone, C., Finessi, E., Mircea, M., Fuzzi, S., Ceburnis, D., Flanagan, R., Nilsson, E. D., de Leeuw, G., Martino, M., Woeltjen, J., & O'Dowd, C. D. (2008). Primary submicron marine aerosol dominated by insoluble organic colloids and aggregates. *Geophysical Research Letters, 35*, L17814. https://doi.org/10.1029/2008GL034210

Forestieri, S. D., Moore, K. A., Martinez Borrero, R., Wang, A., Stokes, M. D., & Cappa, C. D. (2018). Temperature and composition dependence of sea spray aerosol production. *Geophysical Research Letters, 45*, 7218–7225. https://doi.org/10.1029/2018GL078193

Fuentes, E., Coe, H., Green, D., de Leeuw, G., & McFiggans, G. (2010). On the impacts of phytoplankton-derived organic matter on the properties of the primary marine aerosol – Part 1: Source fluxes. *Atmospheric Chemistry and Physics, 10*, 9295–9317. https://doi.org/10.5194/acp-10-9295-2010

Gantt, B., & Meskhidze, N. (2013). The physical and chemical characteristics of marine primary organic aerosol: A review. *Atmospheric Chemistry and Physics, 13*, 3979–3996. https://doi.org/10.5194/acp-13-3979-2013

Grythe, H., Ström, J., Krejci, R., Quinn, P., & Stohl, A. (2014). A review of sea-spray aerosol source functions using a large global set of sea salt aerosol concentration measurements. *Atmospheric Chemistry and Physics, 14*, 1277–1297. https://doi.org/10.5194/acp-14-1277-2014

Guieu, C., D'Ortenzio, F., Dulac, F., Taillandier, V., Doglioli, A., Petrenko, A., Barrillon, S., Mallet, M., Nabat, P., & Desboeufs, K. (2020). Introduction: Process studies at the air–sea interface after atmospheric deposition in the Mediterranean Sea – Objectives and strategy of the PEACETIME oceanographic campaign (May–June 2017). *Biogeosciences, 17*, 5563–5585. https://doi.org/10.5194/bg-17-5563-2020

Jaeglé, L., Quinn, P. K., Bates, T. S., Alexander, B., & Lin, J. T. (2011). Global distribution of sea salt aerosols: New constraints from in situ and remote sensing observations. *Atmospheric Chemistry and Physics, 11*, 3137–3157. https://doi.org/10.5194/acp-11-3137-2011

Jamet, J.-L., Bogé, G., Richard, S., Geneys, C., & Jamet, D. (2001). The zooplankton community in bays of Toulon area (northwest Mediterranean Sea, France). *Hydrobiologia, 457*, 155–165. https://doi.org/10.1023/A:1012279417451

Keene, W. C., Long, M. S., Reid, J. S., Frossard, A. A., Kieber, D. J., Maben, J. R., Russell, L. M., Kinsey, J. D., Quinn, P. K., & Bates, T. S. (2017). Factors that modulate properties of primary marine aerosol generated from ambient seawater on ships at sea. *Journal of Geophysical Research – Atmospheres, 122*, 11961–11990. https://doi.org/10.1002/2017JD026872

King, S. M., Butcher, A. C., Rosenoern, T., Coz, E., Lieke, K. I., de Leeuw, G., Nilsson, E. D., & Bilde, M. (2012). Investigating primary marine aerosol properties: CCN activity of sea salt and mixed inorganic-organic particles. *Environmental Science & Technology, 246*, 10405–10412. https://doi.org/10.1021/es300574u

Langmann, B., Scannell, C., & O'Dowd, C. (2008). New directions: Organic matter contribution to marine aerosols and cloud condensation nuclei. *Atmospheric Environment, 42*, 7821–7822. https://doi.org/10.1016/j.atmosenv.2008.09.002

Lion, L. W., & Leckie, J. O. (1981). The biogeochemistry of the air-sea interface. *Annual Review of Earth and Planetary Sciences, 9*, 449–486. https://doi.org/10.1146/annurev.ea.09.050181.002313

Mallet, M., Nabat, P., di Sarra, A., Solmon, F., Gutiérrez, C., Mailler, S., Menut, L., Kaskaoutis, D., Rowlinson, M., Rap, A., & Dulac, F. (2022). Aerosol and tropospheric ozone direct radiative impact. In F. Dulac, S. Sauvage, & E. Hamonou (Eds.), Atmospheric chemistry in the Mediterranean Region (Vol. 2, From air pollutant sources to impacts). Springer, this volume. https://doi.org/10.1007/978-3-030-82385-6_19

Mårtensson, E. M., Nilsson, E. D., De Leeuw, G., Cohen, L. H., & Hansson, H. C. (2003). Laboratory simulations and parameterization of the primary marine aerosol production. *Journal of Geophysical Research, 108*, 4297. https://doi.org/10.1029/2002JD002263

McCluskey, C. S., Hill, T. C. J., Sultana, C. M., Laksina, O., Trueblood, J., Santander, M. V., Beall, C. M., Michaud, J. M., Kreidenweis, S. M., Prather, K. A., Grassian, V., & DeMott, P. J. (2018). A mesocosm double feature: Insights into the chemical makeup of marine ice nucleating particles. *Journal of the Atmospheric Sciences, 75*, 2405–2423. https://doi.org/10.1175/JAS-D-17-0155.1

Merikanto, J., Spracklen, D. V., Mann, G. W., Pickering, S. J., & Carslaw, K. S. (2009). Impact of nucleation on global CCN. *Atmospheric Chemistry and Physics, 9*, 8601–8616. https://doi.org/10.5194/acp-9-8601-2009

Moore, M. J. K., Furutani, H., Roberts, G. C., Moffet, R. C., Gilles, M. K., Palenik, B., & Prather, K. A. (2011). Effect of organic compounds on cloud condensation nuclei (CCN) activity of sea spray aerosol produced by bubble bursting. *Atmospheric Environment, 45*, 7462–7469. https://doi.org/10.1016/j.atmosenv.2011.04.034

Mulcahy, J. P., O'Dowd, C. D., Jennings, S. G., & Ceburnis, D. (2008). Significant enhancement of aerosol optical depth in marine air under high wind conditions. *Geophysical Research Letters, 35*, L16810. https://doi.org/10.1029/2008GL034303

Novakov, T., & Corrigan, C. E. (1996). Cloud condensation nucleus activity of the organic component of biomass smoke particles. *Geophysical Research Letters, 23*, 2141–2144. https://doi.org/10.1029/96GL01971

Novakov, T., & Penner, J. E. (1993). Large contribution of organic aerosols to cloud-condensation-nuclei concentrations. *Nature, 365*, 823–826. https://doi.org/10.1038/365823a0

O'Dowd, C. D., & De Leeuw, G. (2007). Marine aerosol production: A review of the current knowledge. *Philosophical Transactions of the Royal Society A, 365*, 1753–1774. https://doi.org/10.1098/rsta.2007.2043

O'Dowd, C. D., Facchini, M. C., Cavalli, F., Ceburnis, D., Mircea, M., Decesari, S., Fuzzi, S., Yoon, Y. J., & Putaud, J.-P. (2004). Biogenically driven organic contribution to marine aerosol. *Nature, 431*, 676–680. https://doi.org/10.1038/nature02959

Ovadnevaite, J., Manders, A., de Leeuw, G., Ceburnis, D., Monahan, C., Partanen, A. I., Korhonen, H., & O'Dowd, C. D. (2014). A sea spray aerosol flux parameterization encapsulating wave state. *Atmospheric Chemistry and Physics, 14*, 1837–1852. https://doi.org/10.5194/acp-14-1837-2014

Prather, K. A., Bertram, T. H., Grassian, V. H., Deane, G. B., Stokes, M. D., DeMott, P. J., Aluwihare, L. I., Palenik, B. P., Azam, F., Seinfeld, J. H., Moffet, R. C., Molina, M. J., Cappa, C. D., Geiger, F. M., Roberts, G. C., Russell, L. M., Ault, A. P., Baltrusaitis, J., Collins,D. B., ... Zhao, D. (2013). Bringing the ocean into the laboratory to probe the chemical complexity of sea spray aerosol. *Proceedings of the National Academy of Sciences, 110*, 7550–7555. https://doi.org/10.1073/pnas.1300262110

Randles, C. A., Russell, L. M., & Ramaswamy, V. (2004). Hygroscopic and optical properties of organic sea salt aerosol and consequences for climate forcing. *Geophysical Research Letters, 31*, L16108. https://doi.org/10.1029/2004GL020628

Rinaldi, M., Fuzzi, S., Decesari, S., Marullo, S., Santoleri, R., Provenzale, A., von Hardenberg, J., Ceburnis, D., Vaishya, A., O'Dowd, C. D., & Facchini, M. C. (2013). Is chlorophyll-a the best surrogate for organic matter enrichment in submicron primary marine aerosol? *Journal of Geophysical Research – Atmospheres, 118*, 4964–4973. https://doi.org/10.1002/jgrd.50417

Salter, M. E., Nilsson, E. D., Butcher, A., & Bilde, M. (2014). On the seawater temperature dependence of the sea spray aerosol generated by a continuous plunging jet. *Journal of Geophysical Research – Atmospheres, 119*, 9052–9072. https://doi.org/10.1002/2013JD021376

Sartelet, K. (2022). Secondary aerosol formation and their modeling. In F. Dulac, S. Sauvage, & E. Hamonou (Eds.), *Atmospheric chemistry in the Mediterranean Region* (Vol. 2, From air pollutant sources to impacts). Springer, this volume. https://doi.org/10.1007/978-3-030-82385-6_10

Schnell, R. C., & Vali, G. (1976). Biogenic ice nuclei: Part I. Terrestrial and marine sources. *Journal of the Atmospheric Sciences, 33*, 1554–1564. https://doi.org/10.1175/1520-0469(1976)033<1554:BINPIT>2.0.CO;2

Schwier, A. N., Rose, C., Asmi, E., Ebling, A. M., Landing, W. M., Marro, S., Pedrotti, M.-L., Sallon, A., Iuculano, F., Agusti, S., Tsiola, A., Pitta, P., Louis, J., Guieu, C., Gazeau, F., & Sellegri, K. (2015). Primary marine aerosol emissions from the Mediterranean Sea during pre-bloom and oligotrophic conditions: Correlations to seawater chlorophyll-a from a mesocosm study. *Atmospheric Chemistry and Physics, 15*, 7961–7976. https://doi.org/10.5194/acp-15-7961-2015

Schwier, A. N., Sellegri, K., Mas, S., Charrière, B., Pey, J., Rose, C., Temime-Roussel, B., Parin, D., Jaffrezo, J.-L., Picard, D., Sempéré, R., Marchand, N., & D'Anna, B. (2017). Primary marine aerosol physical and chemical emissions during a nutriment enrichment experiment in mesocosms of the Mediterranean Sea. *Atmospheric Chemistry and Physics, 17*, 14645–14660. https://doi.org/10.5194/acp-17-14645-2017

Sciare, J., Favez, O., Sarda-Estève, R., Oikonomou, K., Cachier, H., & Kazan, V. (2009). Long-term observations of carbonaceous aerosols in the Austral Ocean atmosphere: Evidence of a biogenic marine organic source. *Journal of Geophysical Research, 114*, D15302. https://doi.org/10.1029/2009JD011998

Sellegri, K., & Rose, C. (2022). Nucleation in the Mediterranean atmosphere. In F. Dulac, S. Sauvage, & E. Hamonou (Eds.), *Atmospheric chemistry in the Mediterranean Region* (Vol. 2, From air pollutant sources to impacts). Springer, this volume. https://doi.org/10.1007/978-3-030-82385-6_9

Sellegri, K., O'Dowd, C. D., Yoon, Y. J., Jennings, S. G., & De Leeuw, G. (2006). Surfactants and submicron sea spray generation. *Journal of Geophysical Research, 111*, D22215. https://doi.org/10.1029/2005JD006658

Sellegri, K., Nicosia, A., Freney, E., Uitz, J., Thyssen, M., Grégori, G., Engel, A., Zäncker, B., Haëntjens, N., Mas, N., Picard, D., Saint-Macary, A., Peltola, M., … Law, C. S. (2021). Surface ocean microbiota determine cloud precursors. *Scientific Reports, 11*, 281. https://doi.org/10.1038/s41598-020-78097-5

Seinfeld, J. H., & Pandis, S. N. (2016). Atmospheric Chemistry and Physics: from Air Pollution to Climate Change, 3rd Ed., Wiley, 1152 pp., ISBN 978-1-118-94740-1

Trueblood, J. V., Nicosia, A., Engel, A., Zäncker, B., Rinaldi, M., Freney, E., Thyssen, M., Obernosterer, I., Dinasquet, J., Belosi, F., Tovar-Sánchez, A., Rodriguez-Romero, A., Santachiara, G., Guieu, C., & Sellegri, K. (2021). A two-component parameterization of marine ice nucleating particles based on seawater biology and sea spray aerosol measurements in the Mediterranean Sea. *Atmospheric Chemistry and Physics, 21*, 4659–4676. https://doi.org/10.5194/acp-21-4659-2021

Tyree, C. A., Hellion, V. M., Alexandrova, O. A., & Allen, J. O. (2007). Foam droplets generated from natural and artificial seawaters. *Journal of Geophysical Research, 112*, D12204. https://doi.org/10.1029/2006JD007729

Vignati, E., Facchini, M. C., Rinaldi, M., Scannell, C., Ceburnis, D., Sciare, J., Kanakidou, M., Myriokefalitakis, S., Dentener, F., & O'Dowd, C. D. (2010). Global scale emission and distribution of sea-spray aerosol: Sea-salt and organic enrichment. *Atmospheric Environment, 44*, 670–677. https://doi.org/10.1016/j.atmosenv.2009.11.013

Walker, C. F., Harvey, M., Smith, M. J., Bell, T. G., Saltzman, E. S., Marriner, A. S., McGregor, J. A., & Law, C. S. (2016). Assessing the potential for dimethylsulfide enrichment at the sea surface and its influence on air–sea flux. *Ocean Science, 12*, 1033–1048. https://doi.org/10.5194/os-12-1033-2016

Zábori, J., Matisāns, M., Krejci, R., Nilsson, E. D., & Ström, J. (2012). Artificial primary marine aerosol production: A laboratory study with varying water temperature, salinity, and succinic acid concentration. *Atmospheric Chemistry and Physics, 12*, 10709–10724. https://doi.org/10.5194/acp-12-10709-2012

Emissions from the Mediterranean Vegetation

Valérie Gros, Juliette Lathière, Christophe Boissard, Corinne Jambert, Claire Delon, Michael Staudt, Catherine Fernandez, Elena Ormeño, Dominique Baisnée, and Roland Sarda-Estève

Contents

*Chapter reviewed by **Silvano Fares** (Institute of Bioeconomy, CNR, Rome, Italy), as part of the book Part V Emissions and Sources also reviewed by **Claire Granier** (Laboratoire d'Aérologie (LAERO), CNRS – Univ. Toulouse III Paul Sabatier, Observatoire Midi-Pyrénées, Toulouse, France)*

V. Gros (✉) · J. Lathière · D. Baisnée
Laboratoire des Sciences du Climat et de l'Environnement (LSCE), CEA-CNRS-UVSQ, IPSL, Univ. Paris-Saclay, Gif-sur-Yvette, France
e-mail: valerie.gros@lsce.ipsl.fr

C. Boissard
Université de Paris and Univ Paris Est Creteil, CNRS, LISA, Paris, France

C. Jambert · C. Delon
Laboratoire d'Aérologie (LAERO), CNRS-Univ. de Toulouse, Observatoire Midi-Pyrénées, Toulouse, France

M. Staudt
Centre d'Ecologie Fonctionnelle et Evolutive (CEFE), UMR CNRS, EPHE, IRD, Université Montpellier, Montpellier, France

C. Fernandez · E. Ormeño
Institut Méditerranéen de Biodiversité et d'Ecologie marine et continentale (IMBE), Aix Marseille Université, CNRS, IRD, Marseille, France

R. Sarda-Estève
Laboratoire des Sciences du Climat et de l'Environnement (LSCE), CEA-CNRS-UVSQ, IPSL, Univ. Paris-Saclay, Gifsur-Yvette, France

Climate and Atmosphere Research Center, The Cyprus Institute, Aglantzia, Nicosia, Cyprus

Réseau National de Surveillance Aérobiologique, Le Plat du Pin, Brussieu, France

F. Dulac et al. (eds.), *Atmospheric Chemistry in the Mediterranean Region*,
https://doi.org/10.1007/978-3-030-82385-6_3

Abstract The vegetation is a source of various compounds in the gas phase and particulate phase ("bioaerosols"). Global emissions of volatile organic compounds (VOCs) are largely dominated by biogenic sources. Due to the high vegetation biodiversity and favorable climatic conditions, the Mediterranean area has been identified as a huge potential source of biogenic VOCs (BVOCs), which are precursors of tropospheric ozone and secondary organic aerosols. Therefore, this chapter is mainly dedicated to BVOCs although emissions of bioaerosols are briefly reviewed. First, we present shortly the processes leading to BVOC emissions by terrestrial vegetation. Then we focus on BVOC speciation, emissions, and fluxes, from the branch to the canopy level and larger scales. A review of emissions from typical Mediterranean plant species follows, as well as a synthesis of the mean BVOC fluxes measured by micrometeorological techniques in the Mediterranean area. Factors controlling BVOCs and their evolution in the Mediterranean context are then examined from a modelling perspective. Finally, we present a brief overview of measurements and studies of bioaerosols (pollens, fungal spores, etc.) in the Mediterranean basin.

1 Introduction

The vegetation is a source of various compounds in the gas phase and the particulate phase ("bioaerosols"). Globally, VOC emissions are largely dominated by biogenic sources (Guenther et al., 1995). Given the high biodiversity and favorable climatic conditions (sunny and warm), the Mediterranean area has been identified as a huge potential source of biogenic VOCs (BVOCs). VOCs are known to be precursors of both tropospheric ozone and secondary organic aerosols (SOA). In the Mediterranean basin, BVOCs could be responsible of an additional 5–15 ppb of tropospheric ozone in summertime (Curci et al., 2009) and could also contribute significantly to the SOA formation (Sartelet et al., 2012; Cholakian et al., 2018). For this reason, the following sub-chapter is mainly dedicated to BVOCs. It is completed with a subchapter focusing on bioaerosol emissions.

2 Biogenic Volatile Organic Compounds

The countries located at the border of the Mediterranean Sea have BVOC emission rates (by surface unit) two to three times higher than the other European countries. Steinbrecher et al. (2009) have estimated that the European countries with the highest BVOC emissions are Portugal, Cyprus, Spain, and Greece, all located in the Mediterranean basin and all covered with vegetation associated with high BVOC emission potentials (oak, eucalyptus, aromatic plants, etc.). Despite these high emissions, their mixing ratios in the atmosphere stay usually below the ppb levels due to the high reactivity of some of them such as isoprene and terpenes (Cerqueira

et al., 2003; Liakakou et al., 2009; Davison et al., 2009; Seco et al., 2011). Some higher values (up to 20 ppb for isoprene) can be detected in environments where the surrounding vegetation is associated with very large emission rates (Harrison et al., 2001; Kalogridis et al., 2014). Keenan et al. (2009) give an overview of isoprenoid emissions from European forest types. Some studies on VOC source apportionment have been performed based on observation periods at rural sites in the Mediterranean area allowing to estimate the contribution of BVOCs to total VOCs. At a remote site in northern Corsica (Ersa) in summer, more than 20% of VOCs were attributed to biogenic sources (primary or secondary) based on a Positive Matrix Factorization (PMF) approach (Michoud et al., 2017). In Cyprus, based on a measurement campaign in spring and corresponding PMF simulations, a contribution of 40% of biogenic sources was found for VOCs (Debevec et al., 2017). Nevertheless, one should keep in mind that these calculated contributions depend on the atmospheric VOC concentrations that had been measured and implemented in the PMF model and do not consider the potential photochemical decay from the site of emission to the site of measurement. These quite high contributions of BVOCs to total VOCs found in the two aforementioned studies are partly due to the important weight of oxygenated compounds like methanol and acetone. At Ersa in Corsica, a PMF exercise was applied to a 2-year dataset of 14 VOCs measured twice a week (Debevec et al., 2021). The average BVOC contribution was only 4% on an annual basis, highlighting the strong seasonal variability of biogenic emissions.

In the following, we focus on BVOC emission sources in terrestrial ecosystems and the determination of BVOC speciation, emissions, and fluxes at different scales and finally will examine the main factors controlling BVOC and their evolution in the Mediterranean region.

2.1 BVOC Emission Sources in Terrestrial Ecosystems

Field studies in terrestrial ecosystems have historically focused on BVOCs from living above-ground foliar biomass. All plant organs (leaves, flowers, fruits, trunk, roots) release BVOCs although foliage is considered as the main source of VOCs (Guenther, 2013). Mature fully developed foliage mainly releases isoprenoids, especially hemiterpene isoprene and monoterpenes, whereas the VOC release from young developing foliage is frequently dominated by methanol (Bracho-Nunez et al., 2011). Major Mediterranean plant emitters can be inferred from European BVOC inventories (Karl et al., 2009; Keenan et al., 2009; Oderbolz et al., 2013). Thus, considering plant emission rates and projected leaf dry mass per unit area (g m^{-2}) reported in these inventories, *Quercus pubescens* (sub-Mediterranean oak species) appears as the major isoprene emitter in the French Mediterranean region, while *Q. ilex* and other closely related evergreen oak species are the major monoterpene emitters (Kesselmeier & Staudt, 1999; Bracho-Nunez et al., 2013; Keenan et al., 2009; Genard-Zielinski et al., 2018).

Once BVOCs are synthesized in leaves, they are released through several ways including the cuticle, stomata, and damaged leaf surfaces. The highest emission rates are well known to occur in late spring and summer, since climatic conditions (high temperatures, high photon flux densities) and/or plant physiological activity (BVOC metabolism, photosynthesis) favors BVOC synthesis and release (Llusià & Peñuelas, 2000; Staudt et al., 2003; Genard-Zielinski et al., 2018). With a few exceptions, foliar BVOC fluxes from typical Mediterranean evergreen shrubs and trees (e.g., *Q. coccifera*, *Q. ilex*, *Rosmarinus officinalis*, *Arbutus unedo*, *Erica arborea*, *Cistus* spp.) do not cease during the winter season (Llusià & Peñuelas, 2000; Staudt et al., 2000, 2002; Olivier et al., 2011a, 2011b). This unique feature of Mediterranean biomes has potentially important implications for BVOC inventories.

The exchanges of BVOCs between the ground (bare soil and decomposing plant material) and the atmosphere are very small, especially in Mediterranean ecosystems, as recently reviewed (Peñuelas et al., 2014). The forest floor has been suggested to contribute between 10 and 100 times less than above-ground vegetation to the total BVOC emissions. It is a source of both C_1–C_3 oxygenated compounds (methanol, acetic acid, and acetone) and isoprenoids (Peñuelas et al., 2014). A study involving 40 root-free soil and litter samples revealed that decomposing plant material (litter), rather than bare soil, mostly contributes to VOC emissions in terms of both, diversity and quantity (Leff & Fierer, 2008). The floor from a natural Mediterranean holm oak forest mostly released methanol with negligible terpene emissions (Asensio et al., 2007). Bare soil as well as soil from an evergreen Mediterranean shrub ecosystem acted as a sink rather than a source of VOCs (Asensio et al., 2008). Litter VOC emission rates (from Mediterranean and non-Mediterranean species) vary according to both, biotic factors (e.g., type of litter, decomposing rate, and associated microbiota) and abiotic factors (mainly temperature and humidity; Asensio et al., 2007; Gray et al., 2010), although it remains unclear which is the main driver of VOC emissions (Peñuelas et al., 2014). Since many BVOC-storing Mediterranean species produce a rather important amount of litter (e.g., 500 g m^{-2} $year^{-1}$ for *P. halepensis*), which decomposes slowly (Asensio et al., 2008), it is plausible that litter significantly contributes to total BVOCs in Mediterranean forests and shrubs as recently evidenced in a maritime pine forest in Southwest France (Staudt et al., 2019). Some efforts have been done to incorporate BVOC emissions from soil and litter into VOC models at global scale (Jacob, 2005). This step is however constrained by the scarcity and highly variable emission data, and this variability may be explained by the contribution of soil microorganisms.

2.2 *Determination of BVOCs: Speciation and Emissions/ Fluxes at Different Scales*

Branch Scale

Field-based research studies on BVOC emissions from living above-ground vegetation have mostly been performed at the branch scale using dynamic enclosure systems. These systems allow the optimal quantification of low volatility and highly

reactive BVOCs including very light BVOCs (C_1–C_3), C6 compounds, and isoprenoids. A full description of this method and the associated potential instrumentation to measure BVOCs are described by Ortega et al., 2008. The enclosure is typically made of Teflon materials such as PFA and PTFE consisting of a rigid skeleton and transparent Teflon sheet. A lower-cost Nalophan-made sheet can also alternatively be used (Olivier et al., 2011a, b; Yáñez-Serrano et al., 2018) although the former materials limit to a greater extent the memory effect due to BVOC stickiness. Transparency of these sheets is also a prerequisite so that ~99% of the photosynthetically active radiation goes through the sheet and reaches the enclosed foliage, which uses light for photosynthesis. A continuous air stream is maintained through the enclosure, while a smaller fraction of the flow is used for offline or online analysis of BVOCs or other gases such as CO_2. The air flow through the enclosure should be high enough to ensure air renewal within a few minutes or less in order to avoid BVOC reactions with ambient oxidants (O_3, OH, NO_3), CO_2 depletion, and excessive humidity and temperature inside the enclosure. In addition, ozone scrubbers before the chamber might be required before collecting BVOCs, in order to prevent the reaction of BVOCs with ozone. Even though air is rapidly renewed in the enclosures (<5 min), some terpenes (e.g., a-terpinene) still readily (1 min) react with ozone (Atkinson & Arey, 2003). This technical point is of special importance in Mediterranean semi-natural ecosystems where ozone pollution peaks are often reached (~100 ppb). Dynamic enclosure systems also allow the online measurement of CO_2 and H_2O exchanges (net photosynthesis, transpiration, and derived parameters such as stomatal conductance), by diverting part of the air flow to adequate analyzers (most often infrared gas analyzers) (Fig. 1).

Many other systems can be used as extensively described by Tholl et al. (2006). Among them, two other methods are mainly used in BVOC research: (i) leaf-scale measurements using commercial photosynthesis measurement systems equipped with small cuvettes (2–6 cm^2) (Lavoir et al., 2011; Genard-Zielinski et al., 2014), requiring special care during leaf clipping since Mediterranean species typically feature leaves with a short petiole, and (ii) static systems at leaf or branch scales involving no continuous air flow through the enclosed plant material. Static systems are particularly useful to detect trace emissions but should be avoided when the aim is to obtain accurate emission rates under close to ambient conditions. Static systems or systems with low air exchange rates generate non-steady-state environmental conditions inside the enclosures including raising temperature and air humidity, CO_2 depletion, and unrealistic BVOC concentrations that all can directly affect the net exchange rates of BVOCs and/or cause artifacts during sampling and subsequent analysis of BVOCs (see, e.g., Niinemets et al., 2011 for a review on this topic).

Special caution should be taken when using any of these systems to characterize emissions of Mediterranean aromatic species since these species feature specific BVOC reservoirs which store vast amounts of volatiles (mainly terpenes) in the order of several mg per g of dry matter (1–20, Ormeño et al., 2011; Valor et al., 2017). For example, Lamiaceae spp. (e.g., *Lavandula* spp., rosemary) and Cistaceae spp. (*Cistus* spp.) present an external secretory glandular trichome on the leaf and stem surface (Ormeño et al., 2007). Species from the Pinaceae family feature

Fig. 1 Dynamic branch enclosure (60 L) system used in the field to study BVOC emissions from *Q. pubescens* in southern France at O_3HP deployed during the CANOPEE campaigns (Genard-Zielinski et al., 2015)

secretory cavities and canals located within needle and stem tissues, respectively, which also contain large amounts of volatile terpene compounds. Enclosure of branches from these species may easily result in mechanical stress causing huge emission bursts from these BVOC reservoirs (see, e.g., Niinemets et al., 2011). This may lead to a large overestimation of BVOC emission rates especially if emissions are measured just after enclosure. Therefore, emissions should be collected several hours after branch enclosure, although VOCs can also be collected within the first hour if entire individuals are enclosed (typically possible when using potted plants).

Using either branch- or leaf-scale systems, Mediterranean species have been classified as high, moderate, low, and negligible emitters. As a whole, high emitters are plant species that present, at least for a given seasonal period, an average emission factor higher than 10 μg g^{-1} h^{-1}, while moderate, low, and negligible emitters present emission rates from 5 to 10 μg g^{-1} h^{-1}, 1 to 5 μg g^{-1} h^{-1}, and < 1 μg g^{-1} h^{-1}, respectively (Owen et al., 1997, 2001). According to such classification and considering only natural plant species, high terpene tree emitters in the Northern Mediterranean region are the evergreen *Quercus* spp., including the monoterpene emitters *Quercus ilex* (10–60 μg g^{-1} h^{-1}; Street et al., 1997; Owen & Hewitt, 2000; Staudt et al., 2001; Nuñez et al., 2002) and *Quercus suber* (20–30 μg g^{-1} h^{-1}) (Staudt et al., 2004; Pio et al., 2005). Although it is not a typical Mediterranean tree species, *Q. pubescens* (deciduous *Quercus* spp.) accounts for the main isoprene emitter in the Mediterranean region, since it is both a high isoprene emitter (20 and 100 μg g^{-1} h^{-1}) and it is highly widespread occupying more than 2 million ha

(Ormeño et al., 2007; Saunier et al., 2017; Genard-Zielinski et al., 2018). Note that all these emission rates mostly refer to late spring, summer, and beginning autumn, while negligible emissions occur both during leaf senescence in autumn and budbreak in spring when most often only negligible emissions occur (<0.1 μg g^{-1} h^{-1}). Unlike these broad-leaf species, all typical *Pinus* species in the Northern Mediterranean area (e.g., *Pinus pinea*, *Pinus halepensis*) feature low to intermediate emission rates characterized by monoterpene compounds and a smaller fraction of sesquiterpene compounds (Nuñez et al., 2002; Ormeño et al., 2007).

Several typical Mediterranean shrub species also feature high terpenoid emission rates although they are not represented in BVOC inventories. The major emitters are isoprene emitters and include *Myrtus communis* (~100–140 μg g^{-1} h^{-1}), *Erica arborea, E. multiflora* (~20 μg g^{-1} h^{-1}), *Cytisus* spp. (>20 μg g^{-1} h^{-1}), and *Spartium junceum* (Owen et al., 1997; Owen & Hewitt, 2000). *Cistus albidus* has also been reported as a high monoterpene emitter (~20–30 μg g^{-1} h^{-1}; Llusià & Peñuelas, 2000) like other *Cistus* species.

Canopy Scale

The determination of the chemical reactivity of the atmosphere requires the integration of exchanges at canopy scale. This allows the link with modelling involving ecosystem characteristics at kilometric scales or more. The heterogeneity of vegetation at small scale and the variability of emission factors within and among species can thus be integrated by measurements of emissions at canopy scale with micrometeorological methods above homogeneous plant canopies (Baldocchi et al., 1988; Dabberdt et al., 1993). Flux determination is based on eddy measurement methods involving turbulence characterization and turbulent exchange coefficient determination (Lenchow, 1995). For VOCs, methodologies have been reviewed by Fowler et al. (2009) and Hewitt et al. (2011).

The flux measurements were initially based on the gradient method, which requires vertical profiles of meteorological and chemical quantities (Park et al., 2013, 2014) but can suffer from strong assumptions on turbulent exchange coefficients and on the possible chemical reactions of the compounds within the profile (Darmais et al., 2000). Applications of eddy covariance methodologies were limited by the low VOC concentrations measured in ambient air and slow chemical sensor response time and therefore required the accumulation of VOC onto adsorbent cartridges. The relaxed eddy accumulation (REA) has been proposed, with sampling depending on updraft or downdraft winds, by Businger and Oncley (1990) and was subsequently used to determine VOC fluxes over various Mediterranean ecosystems. For example, Valentini et al. (1997) applied the REA technique over a mixed forest (oak and forest) at Castelporziano (Italy) characterized by non-oxygenated monoterpene emissions and observed a good consistency between measured VOC fluxes and those obtained from branch enclosure systems. Schade and Goldstein (2001) carried out the first long-term flux measurements of highly volatile oxygenated BVOC above the canopy of a Mediterranean climate-type ponderosa pine

plantation and revealed that 2-methyl-3-buten-2-ol (hemiterpene, C5) and methanol were the dominant volatiles, while ethanol, acetaldehyde, and acetone fluxes were roughly fivefold lower. However, this latter study also strongly suggested that above-canopy measurements of methanol, acetaldehyde, and acetone came from soil and litter emissions as well.

The eddy covariance (EC) method is largely applied for energy flux determination (latent heat, sensible heat fluxes) over ecosystems, by calculating the covariance of a scalar (e, T) with turbulent vertical wind speed and parameters sampled at 10–20 Hz. The determination of BVOC fluxes with the EC method was first made over isoprene-emitting forests using a fast isoprene sensor (FIS) coupled to a sonic wind sensor (Guenther & Hills, 1998). The disjunct eddy covariance (DEC) method is based on statistical analysis of EC data, suggesting that sub-sampling of a scalar may introduce a maximum underestimation of 5–20% of the flux compared to EC (Lenschow et al., 1993; Rinne et al., 2001), as long as the sample is grabbed quickly (<0.2 s). For example, Baghi et al. (2012) found a good agreement between the isoprene fluxes measured by EC, and DEC with a dedicated grab sampler system (MEDEE), with a FIS over a *Quercus pubescens* forest at the OHP site.

In the last decades, the development of proton transfer mass spectrometry technologies (PTR-QMS and PTR-TOF-MS with quadrupole and time-of-flight detectors, respectively) allowed the online measurement of many VOCs including oxygenated volatile organic compounds (OVOCs). The sequential measurements of selected compounds by PTR-MS allow the application of virtual DEC (v-DEC), i.e., DEC without a physical grab sampler (Karl et al., 2002). DEC and EC methods are now applied to most biogenic VOC flux measurements. Recently, Jensen et al. (2018) compared for the first time BVOCs mixing ratios and fluxes over a deciduous oak forest in northern Italy by three different instruments (PTR-QMS, PTR-TOF-MS, and FIS) and reported a good agreement for isoprene (the only compound measured by the three instruments). Furthermore, the observed 24 h-mean isoprene flux of 5.2 ± 2.4 nmol m^{-2} s^{-1} was comparable to the fluxes found in previous studies over forests dominated by other strong isoprene-emitting oak species. Thus, Schallhart et al. (2016) reported an isoprene flux of 6.5 nmol m^{-2} s^{-1} from a mixed oak and hornbeam forest in northern Italy (located 250 km from the previous one), and Kalogridis et al. (2014) reported a mean flux (11 h–17 h) of 11.3 nmol m^{-2} s^{-1} from a *Quercus pubescens* forest in southern France (OHP). These values are much higher than the isoprene fluxes of 0.300–1.183 nmol m^{-2} s^{-1} measured by Davison et al. (2009) over a Mediterranean scrubland at the site of Castelporziano near Rome, which is mainly composed of evergreen monoterpene-emitting species (Fares & Loreto, 2015). Concerning monoterpene fluxes, they were indeed much higher at the Castelporziano site (0.489–1.753 nmol m^{-2} s^{-1}; Davison et al., 2009) compared to the abovementioned forests (0.209 nmol m^{-2} s^{-1}; Schallhart et al., 2016; 0.08 ± 0.05 nmol m^{-2} s^{-1}; Jensen et al., 2018). Nevertheless, monoterpenes can also be the most emitted compounds in some forest environments, as, for example, in Mediterranean forests dominated by the evergreen holm oak (Buysse et al., 2019). *Citrus* trees are also potential strong monoterpene and sesquiterpene emitters especially during flowering, as measured in the orange orchards in Spain (Ciccioli

et al., 1999) and California (Fares et al., 2012). The PTR-MS technique development has allowed the measurements of other BVOC fluxes, especially oxygenated compounds. Mean fluxes of oxygenated BVOCs (as well as isoprene and monoterpenes) measured by micrometeorological methods in the Mediterranean area are given in Table 1. Methanol has been often measured as the most emitted oxygenated VOCs in the different ecosystems studied, whereas acetone and acetaldehyde presented lower fluxes (see Table 1). Fluxes of methyl vinyl ketone and methacrolein (MVK + MAK) have been determined as well in these studies, showing values usually one or two orders of magnitude lower than isoprene, their main precursor.

The previous paragraph has focused on the dominant BVOCs, but two important points need to be underlined. Firstly, the technical development (especially PTR-TOF-MS) now allows the measurement of hundreds of masses/compounds. Secondly, BVOC deposition has also to be taken into account and can sometimes constitute their main sink (Park et al., 2013).

Landscape Scale

Airborne flux measurements are based on micrometeorological methodologies, and the main difficulty is to deduce the flux at surface level from the measurements. Different approaches have been proposed and are reviewed by Hewitt et al. (2011): (i) the mixed layer budget (MLB), where the flux at the surface is deduced from measured concentrations in a well-mixed layer, the reactivity at the measurement level z, and the entrainment flux at the top of the mixed layer (Eerdekens et al., 2009); (ii) the mean mixed layer gradient (MLG), where gradient profile is established in the mixed layer and surface flux deduced from simulations (Karl et al., 2007); (iii) the mixed layer variance (MLV), which relies the variability of a quantity to surface and entrainment fluxes using convective-scale parameterization (Karl et al., 2007); and (iv) the airborne eddy covariance (AEC) methodologies. For this last case, the difference with the tower-based EC measurements is that AEC is based on spatial rather than time domain, based on Taylor's hypothesis of a frozen turbulence.

As for canopy-scale measurements, the rapidity and sensibility of the analytical instruments are critical for airborne VOC flux measurements. First VOC airborne flux measurements were done with REA methodology. Applications above a Central African forest in Congo during the EXPRESSO campaign can be found in Delon et al. (2000). PTR-MS and PTR-TOF-MS techniques allow now AEC measurements. Aircraft DEC measurements (Baghi et al., 2012), coupled with PTR-MS instrumentation, were done above the Landes forest with MEDEE grab sampler, and results are in good agreement with the isoprene and monoterpene 2000 emission inventory from Luchetta et al. (2000). Wavelets methodologies may be applied for the data treatment for EC flux calculations (Karl et al., 2009). Few studies were dedicated to VOC aircraft flux measurements, and to our knowledge, none has been published yet for the Mediterranean region.

Table 1 Mean BVOC fluxes (nmol m^{-2} s^{-1}) measured by aerodynamic techniques in the Mediterranean area

Vegetation (location)	Isoprene	Terpene (sum)	MVK + MAK	Methanol	Acetone	Acetaldehyde	Reference
Pine oak (Castelporziano, Italy)		8.3–9.0 (11 h–16 h)					Valentini et al. (1997)
		0.37–13.2 (11 h–12 h)					Schween et al. (1997)
Orange orchard (Valencia, Spain)		0.48–1.68 (9 h30–14 h)			6.1 (11 h–18 h)	32.2 (11 h–18 h)	Ciccioli et al. (1999)
Scrub (Castelporziano, Italy)	0.30–1.18	0.49–1.75		3.21–3.82	0.86–2.15	1.14–2.27	Davison et al. (2009)
Downy oak (O3HP, SE France)	8.77 (10 h–17 h)						Baghi et al. (2012)
Downy oak (O3HP, SE France)	11.29 (10 h–17 h)		0.12 (10 h–17 h)	2.69 (10 h–17 h)			Kalogridis et al. (2014)
Oak and hornbeam (Bosco Fontana, Po Valley, Italy)	6.47	0.21	0.31	1.17	0.34	0.23	Schallhart et al. (2016)
Deciduous common oak, etc. (JRC Ispra, Italy)	5.2 ± 2.4	0.08 ± 0.05	0.06 ± 0.04	0.85 ± 0.41	0.13 ± 0.06	0.10 ± 0.24	Jensen et al. (2018)

All measurements represent mean diurnal (24 h) values, except when specified in brackets

OH Reactivity as an Approach to Determine the Completeness of Measured BVOCs

The increase of measurement capabilities, especially since the use of PTR-TOF-MS technology, has led in the last decade to a tremendous increase in the number of measured VOCs (see, e.g., Schallhart et al., 2016 and references therein). Nevertheless, our analytical capabilities are still far away from exhaustive measurements of all existing VOCs (Goldstein & Galbally, 2007). Therefore, other approaches, like the measurement of total OH reactivity, are necessary to address the issue of the completeness of measured compounds. The total OH reactivity represents the OH sink and therefore takes into account the contributions from all compounds reacting with OH (Gros & Zannoni, 2022). It can be either calculated (by summing all individual OH reactivity, which are the compounds concentrations multiplied by their reaction constant rate with OH) or directly measured by different techniques (see the dedicated chapter in this volume (Gros & Zannoni, 2022), the review of OH reactivity by Yang et al. (2016), and the intercomparison of OH reactivity techniques in Fuchs et al. (2017)). If both results agree (within the uncertainties), it shows that all compounds playing a significant role on OH reactivity of the studied environment have been taken into account. If not, the difference between measured and calculated reactivity points out a missing reactivity, which needs to be investigated to understand which compounds were not measured or identified. So far, there are a limited number of OH reactivity measurements on Mediterranean vegetation, but they show their potential to evaluate the completeness of measured BVOCs. For example, at the French Mediterranean forest site of the Observatoire de Haute Provence (OHP) largely dominated by *Quercus pubescens*, a known large emitter of isoprene, Zannoni et al. (2016) have performed OH reactivity measurements inside and above the canopy. During daytime and at both heights, measured and calculated OH reactivity agreed very well, showing that for this environment, measured VOCs explain well the OH reactivity. We note that isoprene was by far the largest contributor to the OH reactivity (up to 80% during daytime). Nevertheless, a missing reactivity of up to 50% was observed during the night, probably due to some non-measured oxidation products.

2.3 Factors Controlling Future BVOC Emissions in the Mediterranean Context: A Modelling Perspective

Regarding the modelling of BVOC emissions, two main approaches have been considered so far: (i) empirically based parameterizations to represent observed emission variations in relation to easily accessible environmental drivers and (ii) process-based mechanistic relationships built on the understanding of the biological regulation of isoprene synthesis from the carbon assimilated during photosynthesis (Ashworth et al., 2013). Both types of models are adapted for global and regional modelling. Their aim is to reproduce the intensity and variation of BVOC emissions

depending mostly on light and temperature conditions. Empirical approaches are commonly used for applications in the field of atmospheric chemistry, especially for air quality exercises for which mechanistic models remain far too complex. Grote et al. (2014) indicate that mechanistic models are fairly effective in accounting for the mild stress effects on seasonal monoterpene emission variations of *Quercus ilex*, for instance, but the large number of parameters required in these models represents an obstacle for their broad and routine use in air quality studies (Ashworth et al., 2013). The development of empirical BVOC emission models, especially the most widely used empirical model MEGAN (Model of Emissions of Gases and Aerosols from Nature; Guenther et al., 2006, 2012), was partly based on measurements carried out under "optimum" growing conditions and/or obtained from very few emitters. They depict a fair picture of the general level and global distribution of BVOC emission, but remain somewhat deficient in assessing BVOC variability under a large range of stress conditions. The impact of drought stress on BVOC emissions, and especially isoprene, was implemented in MEGAN based on one laboratory study focused on young (2-year-old) *Quercus virginiana* Mill., an isoprene emitter and fast-growing evergreen and drought-sensitive tree (Pegoraro et al., 2004). Based on the difference between the soil moisture and the wilting point characteristic of soil (the soil moisture below which plants cannot extract water from soil), a soil moisture activity parameterization was developed in MEGAN for isoprene emission to account for drought effects. Considering drought in BVOC models is of crucial importance in the Mediterranean region. However, the study by Genard-Zielinski et al. (2018) in a natural site under Mediterranean climate demonstrated that this parameterization was unable to reproduce the effect of drought on isoprene emissions of mature *Q. pubescens* trees (~70 years old), a drought-adapted and slow-growing species, whatever the drought intensity (natural or amplified). Interestingly, MEGAN captured the seasonal variation of isoprene emissions from *Q. pubescens* very efficiently (more than 80%) when the soil moisture activity factor was not considered in the simulation. However, this performance was reduced by 50% when drought was amplified. Genard-Zielinski et al. (2018) suggested that the formulation of drought stress impact in MEGAN could be improved by distinguishing at least two distinct types of isoprene emitters: drought-sensitive species such as *Q. virginiana* and *Populus deltoides* and drought-resistant emitters such as *Q. pubescens*. The chemical transport model CHIMERE (Menut et al., 2013), which includes the classical form of the MEGAN model to simulate biogenic emissions, is routinely used by air quality agencies in different Mediterranean areas such as southern France (e.g., Martin 2010) to assess concentrations of air pollutants (e.g., O_3; see also Kalabokas et al., 2020) and their precursors (e.g., BVOCs). For example, using CHIMERE, AtmoSud (the official network in charge of pollution survey and forecast in the southeastern French region of Provence-Alpes-Côte d'Azur) is able to generate regional maps of surface emissions of BVOC and atmospheric concentrations of ozone (Fig. 2; Saunier, 2017; Saunier et al., 2020).

The version of CHIMERE used for such modelling relies on (i) concentration of 15 precursors (e.g., NO, NO_2, ethane, *n*-butane, isoprene) where anthropogenic compounds come from the EMEP 2007 database and from the AtmoSud database,

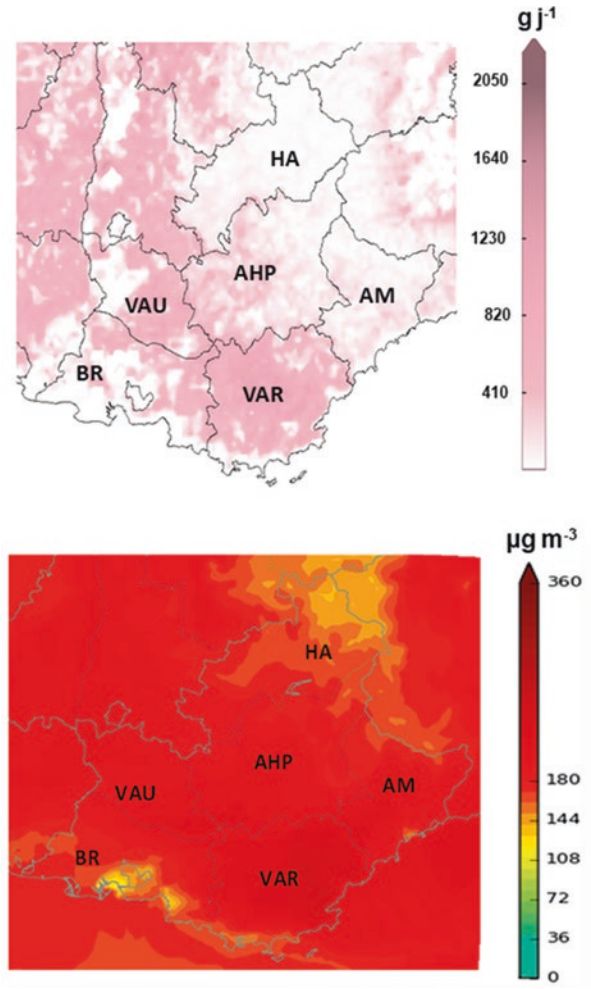

Fig. 2 *Top* Simulated maximum isoprene emissions (µg g_{DW}^{-1} h^{-1}) over the PACA region (southern France) using the MEGAN model and climatic conditions for one particular day during the heat wave in 2003 (August 13). *Bottom* Simulated maximum tropospheric ozone levels (µg m^{-3}) on the same day, showing one of the most severe O_3 peaks of the year over the region (simulation performed with the air quality model CHIMERE (HA, Hautes-Alpes; AHP, Alpes-de-Haute-Provence; VAU, Vaucluse; VAR, Var; AM, Alpes-Maritimes; BR, Bouches-du-Rhône). Courtesy of Damien Piga, AtmoSud

whereas biogenic data (i.e., emission factors from plant species) come from the MEGAN database with some modifications for a few local plant species (Aleppo pine, kermes oak, rosemary, and *Cistus* spp.) studied in the region (Ormeño et al., 2007; Rivoal et al., 2010; Olivier et al., 2011a, 2011b); (ii) the land use database (CORINE Land Cover 2006, https://land.copernicus.eu/paneuropean/corine-land-cover/clc-2006); and (iii) meteorological data from the WRF model. Considering

the isoprene parameterization proposed by Genard-Zielinski et al. (2018) for a drought-resistant species, which is based on results from a drought-sensitive species as explained above, instead of the classical MEGAN model, would probably improve O_3 estimates in Mediterranean areas where most species are naturally adapted to drought.

In the future, changes in climate and land use could significantly affect BVOC emission levels and geographical distribution at local to global scales. Regional models including online BVOC emission schemes can help in depicting emissions in the Mediterranean region under future possible scenarios of climate and land use changes. Based on four ICCP Representative Concentration Pathways scenarios (RCP2.6, RCP4.5, RCP6.0, and RCP8.5; van Vuuren et al., 2011) for three different periods (2000, 2030, and 2100), Jaidan et al. (2018) estimated the changes in the future ozone concentration over the Mediterranean basin. A net decrease in the mean surface ozone in 2030 (2100) was calculated for the Mediterranean for three RCPs, −14% (−38%) for RCP2.6, −9% (−24%) for RCP4.5, and −10% (−29%) for RCP6.0, mainly due to the reduction in ozone precursors. At the European scale, Bauwens et al. (2018), using the MEGAN-MOHYCAN model, calculated a future increase in isoprene emissions ranging from 7% to 83% depending on the RCP scenario considered. Considering other impacts such as the CO_2 fertilization effect on plant growth or the known CO_2 inhibition effect on isoprene emissions would further significantly affect the estimated emissions. The future changes in BVOC emissions, in relation with future changes in climate and vegetation distribution expected to be important in the broad Mediterranean region, could also significantly change atmospheric chemistry processes and affect the regional air quality.

3 Bioaerosols

Primary biological aerosol particles (PBAPs), which include airborne pollen grains, fungal spores, and bacteria, are crucial in the Earth system through their roles on biosphere, atmosphere, climate, and public health (Pöschl & Shiraiwa, 2015; Fröhlich-Nowoisky et al., 2016). Their physicochemical properties are mainly relative to their size range, which extends from 100 nm to 100 µm (Pöschl & Shiraiwa, 2015). For instance, they can act as nuclei for cloud droplets (giant cloud condensation nuclei, GCCN, or CCN) and as ice nucleating particles (INP), which consequently affect the precipitation, the hydrological cycle, and the climate (Pope, 2010; Pöschl et al., 2010; Morris et al., 2011; Mason et al., 2016). Less is known about their survival mechanism during atmospheric transport and about their role as nutrients for marine ecosystems, especially in the Mediterranean region (Kellogg & Griffin, 2006; Myriokefalitakis et al., 2016). The Mediterranean region is particularly interesting because of the variety of ecosystems encountered over the same latitude range but at different longitudes (Aguilera et al., 2015). Indeed, marked under-domain climatological patterns lead to a contrasted longitudinal seasonality, characterized, however, by a general hydrological stress (Polymenakou et al., 2008;

Recio et al., 2010; Mescioglu et al., 2019). The different sources of PBAPs in the atmosphere, mixed with combustion and terrigenous aerosols, in particular mineral dust, are not yet well characterized and therefore constitute a large gap in the scientific understanding of the interaction between biosphere and atmosphere compartments (Abu-Dieyeh et al., 2010; Raisi et al., 2010; Katra et al., 2014; Rahav et al., 2019). This last aspect is of major importance as the Mediterranean habitat will be strongly affected by the global warming in the future (Giorgi & Lionello, 2008; see also the chapter by Giorgi & Raffaele, 2023), along with atmospheric invasion of PBAPs from non-native species (Peñuelas et al., 2002; Belmonte & Vilà, 2004; Cecchi et al., 2010). In this context, it is important to increase the bioaerosol monitoring network (Scheifinger et al., 2013; Pollen Monitoring Map of the World, https://www.zaum-online.de/pollen/pollen-monitoring-map-of-the-world.html, last accessed 22 July 2022) in the eastern part of the Mediterranean area, including intensive campaigns. Figure 3 illustrates results from a campaign performed at the Cyprus Atmospheric Observatory (CAO; https://www.cyi.ac.cy/cao/, last accessed 22 July 2022), a rural background atmospheric station at Agia Marina Xyliatou in Cyprus. It shows a measurement time series of airborne bacteria, fungal spores, and pollen every 2 hours from 4 to 12 April 2016. The bioaerosol observatory in Cyprus is currently under development in close collaboration with the French aerobiological monitoring network (RNSA; https://www.pollens.fr, last accessed 22 July 2022). The genuine data collected will allow feeding robust statistical models for predicting the evolution of the concentrations in the Mediterranean area. This last aspect is of primary importance to characterize and evaluate the means employed by biodiversity to cope with global climate change and Earth system evolution (Damialis et al., 2007, 2015).

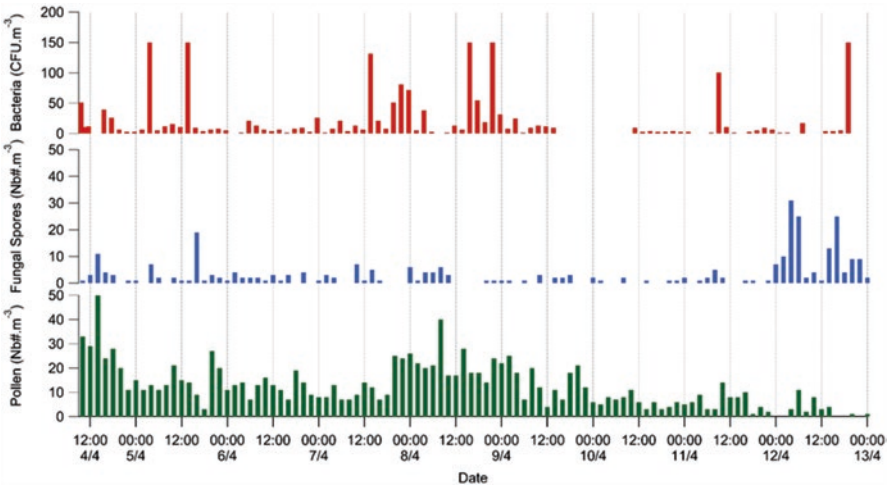

Fig. 3 Variability of bioaerosol concentrations at Agia Marina Observatory in the center of Cyprus during the April 2016 INUIT campaign of the BACCHUS EU Project: *top* culturable bacteria, *middle* fungal spores, and *bottom* pollen

4 Conclusion and Recommendations

Biogenic VOCs have been studied in the Mediterranean area since the 1990s, most often in the western basin. BVOC emissions have been measured from the branch to the canopy scale through various approaches and over different ecosystems. Since two decades, the development of the PTRMS technology has favored canopy flux measurements as well as the measurements of hitherto largely neglected BVOC classes, especially methanol and other oxygenated compounds, that can be largely emitted by terrestrial vegetation. But we still miss measurements to characterize BVOC emissions and chemistry. The total OH reactivity approach is an independent measurement method helping to estimate the completeness of direct VOC measurements. A missing OH reactivity is pointed out in several ecosystems, showing that important VOCs for atmospheric chemistry are still not measured. We also note that there are still plenty of Mediterranean species which are poorly investigated, and we recommend extending measurements to a larger number of different plants. Standardized measurements are needed in order to facilitate comparisons from one study to the other and model applications (see, e.g., the study of Langford et al., 2017). Although emissions from bare soil are very low, VOC emissions from litter may also need to be considered. More measurements are needed to better characterize this source and enable its implementation in emission models. At a larger scale, BVOC airborne measurements to characterize fluxes at the landscape scale are scarce in the Mediterranean area (Freney et al., 2018).

Concerning modelling, good progress has been made in simulating BVOC emissions through different approaches. The most commonly used model in the community is the empirical model MEGAN, enabling to determine distributions and intensities of BVOC emissions at local to global scales. However, emission models have limitations to account for biome-specific stress conditions. Studies having estimated drought stress on diverse VOC emitters emphasize that its impact largely depends on the species ability to withstand drought. This impact of drought stress on isoprene is still poorly described in emission models.

We still need more data (1) to refine our knowledge on drought effects on BVOC emissions and (2) to parameterize and validate empirical approaches over a broader range of environmental stress conditions and emitters. Our capability to correctly assess the impact of drought in VOC emission inventories is especially crucial for regions that are covered with a large quantity of strong VOC emitters and that experience frequent drought episodes, like the Mediterranean region. Therefore, we recommend to expand manipulative experiments, like the one performed recently in southern France (Genard-Zielinski et al., 2018), to other Mediterranean ecosystems to better understand their responses to climate change. All these improvements in BVOC emission parameterization will help as well to improve modelling of the secondary species (ozone, secondary organic aerosols) and better assess biosphere-atmosphere interactions (and their feedback) in the context of regional climate change.

Bioaerosol is an emerging important topic through its potential impact on health and on climate. The situation is contrasted. While pollen measurements are routinely performed in the western part of the Mediterranean basin, the eastern part is much less documented. In addition, measurements of fungal spores and bacteria are still very scarce in the whole basin. Therefore, current efforts to enlarge the bioaerosol measurement network should be encouraged, in parallel with implementation of bioaerosols in regional models.

References

Abu-Dieyeh, M. H., Barham, R., Abu-Elteen, K., Al-Rashidi, R., & Shaheen, I. (2010). Seasonal variation of fungal spore populations in the atmosphere of Zarqa area, Jordan. *Aerobiologia, 26*, 263–276. https://doi.org/10.1007/s10453-010-9162-2

Aguilera, F., Dhiab, A. B., Msallem, M., Orlandi, F., Bonofiglio, T., Ruiz-Valenzuela, L., Galán, C., Díaz-de la Guardia, C., Giannelli, A., & del Mar Trigo, M. (2015). Airborne-pollen maps for olive-growing areas throughout the Mediterranean region: Spatio-temporal interpretation. *Aerobiologia, 31*, 421–434. https://doi.org/10.1007/s10453-015-9375-5

Asensio, D., Peñuelas, J., Ogaya, R., & Llusià, J. (2007). Seasonal soil VOC exchange rates in a Mediterranean holm oak forest and their responses to drought conditions. *Atmospheric Environment, 41*, 2456–2466. https://doi.org/10.1016/j.atmosenv.2006.05.007

Asensio, D., Owen, S. M., Llusià, J., & Peñuelas, J. (2008). The distribution of volatile isoprenoids in the soil horizons around Pinus halepensis trees. *Soil Biology and Biochemistry, 40*, 2937–2947. https://doi.org/10.1016/j.soilbio.2008.08.008

Ashworth, K., Boissard, C., Folberth, G., Lathière, J., & Schurgers, G. (2013). Global modeling of volatile organic compound emissions. In Ü. Niinemets & R. Monson (Eds.), *Biology, controls and models of tree volatile organic compound emissions* (Tree physiology) (Vol. 5, pp. 451–487). https://doi.org/10.1007/978-94-007-6606-8_16

Atkinson, R., & Arey, J. (2003). Gas-phase tropospheric chemistry of biogenic volatile organic compounds: A review. *Atmospheric Environment, 37*(Suppl. 2), 197–219. https://doi.org/10.1016/S1352-2310(03)00391-1

Baghi, R., Durand, P., Jambert, C., Jarnot, C., Delon, C., Serca, D., Striebig, N., Ferlicoq, M., & Keravec, P. (2012). A new disjunct eddy-covariance system for BVOC flux measurements – Validation on CO_2 and H_2O fluxes. *Atmospheric Measurement Techniques, 5*, 3119–3132. https://doi.org/10.5194/amt-5-3119-2012

Baldocchi, D. D., Hincks, B. B., & Meyers, T. P. (1988). Measuring biosphere-atmosphere exchanges of biologically related gases with micrometeorological methods. *Ecology, 69*, 1331–1340. https://doi.org/10.2307/1941631

Bauwens, M., Stavrakou, T., Müller, J. F., Van Schaeybroeck, B., De Cruz, L., De Troch, R., Giot, O., Hamdi, R., Termonia, P., Laffineur, Q., Amelynck, C., Schoon, N., Heinesch, B., Holst, T., Arneth, A., Ceulemans, R., Sanchez-Lorenzo, A., & Guenther, A. (2018). Recent past (1979–2014) and future (2070–2099) isoprene fluxes over Europe simulated with the MEGAN-MOHYCAN model. *Biogeosciences, 15*, 3673–3690. https://doi.org/10.5194/bg-15-3673-2018

Belmonte, J., & Vilà, M. (2004). Atmospheric invasion of non-native pollen in the Mediterranean region. *American Journal of Botany, 91*, 1243–1250. https://doi.org/10.3732/ajb.91.8.1243

Bracho-Nunez, A., Welter, S., Staudt, M., & Kesselmeier, J. (2011). Plant-specific volatile organic compound emission rates from young and mature leaves of Mediterranean vegetation. *Journal of Geophysical Research, 116*, D16304. https://doi.org/10.1029/2010JD015521

Bracho-Nunez, A., Knothe, N. M., Welter, S., Staudt, M., Costa, W. R., Liberato, M. A. R., Piedade, M. T. F., & Kesselmeier, J. (2013). Leaf level emissions of volatile organic compounds (VOC) from some Amazonian and Mediterranean plants. *Biogeosciences, 10*, 5855–5873. https://doi.org/10.5194/bg-10-5855-2013

Businger, J. A., & Oncley, S. T. (1990). Flux measurement with conditional sampling. *Journal of Atmospheric and Oceanic Technology, 7*, 349–352. https://doi.org/10.1175/1520-0426(1990)007<0349:FMWCS>2.0.CO;2

Buysse, P., Lafouge, F., Kammer, J., Ciuraru, J., Staudt, M., Bsaibes, S., Truong, F., Gros, V., Piquemal, K., Ourcival, J.-M., Piel, F., & Loubet, B. (2019) Fluxes of biogenic volatile organic compounds in a green oak forest. *Geophysical Research Abstracts*, *21*, EGU2019-8640. https://meetingorganizer.copernicus.org/EGU2019/EGU2019-8640.pdf.

Cecchi, L., d'Amato, G., Ayres, J., Galan, C., Forastiere, F., Forsberg, B., Gerritsen, J., Nunes, C., Behrendt, H., & Akdis, C. (2010). Projections of the effects of climate change on allergic asthma: The contribution of aerobiology. *Allergy, 65*, 1073–1081. https://doi.org/10.1111/j.1398-9995.2010.02423.x

Cerqueira, M. A., Pio, C. A., Gomes, P. A., Matos, J. S., & Nunes, T. V. (2003). Volatile organic compounds in rural atmospheres of central Portugal. *Science of the Total Environment, 313*, 49–60. https://doi.org/10.1016/S0048-9697(03)00250-X

Ciccioli, P., Brancaleoni, E., Frattoni, M., Di Palo, V., Valentini, R., Tirone, G., Seufert, G., Bertin, N., Hansen, U., Csiky, O., Lenz, R., & Sharma, M. (1999). Emission of reactive terpene compounds from orange orchards and their removal by within-canopy processes. *Journal of Geophysical Research, 104*, 8077–8094. https://doi.org/10.1029/1998JD100026

Cholakian, A., Beekmann, M., Colette, A., Coll, I., Siour, G., Sciare, J., Marchand, N., Couvidat, F., Pey, J., & Gros, V. (2018). Simulation of fine organic aerosols in the western Mediterranean area during the ChArMEx 2013 summer campaign. *Atmospheric Chemistry and Physics, 18*, 7287–7312. https://doi.org/10.5194/acp-18-7287-2018

Curci, G., Beekmann, M., Vautard, R., Smiatek, G., Steinbrecher, R., Theloke, J., & Friedrich, R. (2009). Modelling study of the impact of isoprene and terpene biogenic emissions on European ozone levels. *Atmospheric Environment, 43*, 1444–1455. https://doi.org/10.1016/j.atmosenv.2008.02.070

Dabberdt, W. F., Lenschow, D. H., Horst, T. W., Zimmerman, P. R., Oncley, S. P., & Delany, A. C. (1993). Atmosphere-surface exchange measurements. *Science, 260*, 1472–1481. https://doi.org/10.1126/science.260.5113.1472

Damialis, A., Halley, J. M., Gioulekas, D., & Vokou, D. (2007). Long-term trends in atmospheric pollen levels in the city of Thessaloniki, Greece. *Atmospheric Environment, 41*, 7011–7021. https://doi.org/10.1016/j.atmosenv.2007.05.009

Damialis, A., Vokou, D., Gioulekas, D., & Halley, J. M. (2015). Long-term trends in airborne fungal-spore concentrations: A comparison with pollen. *Fungal Ecology, 13*, 150–156. https://doi.org/10.1016/j.funeco.2014.09.010

Darmais, S., Dutaur, L., Larsen, B., Cieslick, S., Luchetta, L., Simon, V., & Torres, L. (2000). Emission flux of VOC by orange trees determined by both eddy accumulation and vertical gradient approaches. *Chemosphere, 2*, 47–56. https://doi.org/10.1016/S1465-9972(99)00050-1

Davison, B., Taipale, R., Langford, B., Misztal, P., Fares, S., Matteucci, G., Loreto, F., Cape, J. N., Rinne, J., & Hewitt, C. N. (2009). Concentrations and fluxes of biogenic volatile organic compounds above a Mediterranean macchia ecosystem in western Italy. *Biogeosciences, 6*, 1655–1670. https://doi.org/10.5194/bg-6-1655-2009

Debevec, C., Sauvage, S., Gros, V., Sciare, J., Pikridas, M., Stavroulas, I., Salameh, T., Leonardis, T., Gaudion, V., Depelchin, L., Fronval, I., Sarda-Esteve, R., Baisnée, D., Bonsang, B., Savvides, C., Vrekoussis, M., & Locoge, N. (2017). Origin and variability in volatile organic compounds observed at an Eastern Mediterranean background site (Cyprus). *Atmospheric Chemistry and Physics, 17*, 11355–11388. https://doi.org/10.5194/acp-17-11355-2017

Debevec, C., Sauvage, S., Gros, V., Salameh, T., Sciare, S., Dulac, F., & Locoge, N. (2021). Seasonal variation and origins of volatile organic compounds observed during two years at a

western Mediterranean remote background site (Ersa, Cape Corsica). *Atmospheric Chemistry and Physics, 21*, 1449–1484. https://doi.org/10.5194/acp-21-1449-2021

Delon, C., Druilhet, A., Delmas, R., & Greenberg, J. (2000). Aircraft assessment of trace compound fluxes in the atmosphere with relaxed eddy accumulation: Sensitivity to the conditions of selection. *Journal of Geophysical Research: Atmospheres, 105, 20461–20472.* https://doi.org/10.1029/2000JD900186

Detlef P., van Vuuren Jae, Edmonds Mikiko, Kainuma Keywan, Riahi Allison, Thomson Kathy, Hibbard George C., Hurtt Tom, Kram Volker, Krey Jean-Francois, Lamarque Toshihiko, Masui Malte, Meinshausen Nebojsa, Nakicenovic Steven J., Smith Steven K., Rose (2011) The representative concentration pathways: an overview. *Climatic Change 109(1–2), 5–31.* https://doi.org/10.1007/s10584-011-0148-z

Eerdekens, G., Ganzeveld, L., Vilà-Guerau de Arellano, J., Klüpfel, T., Sinha, V., Yassaa, N., Williams, J., Harder, H., Kubistin, D., Martinez, M., & Lelieveld, J. (2009). Flux estimates of isoprene, methanol and acetone from airborne PTR-MS measurements over the tropical rainforest during the GABRIEL 2005 campaign. *Atmospheric Chemistry and Physics, 9*, 4207–4227. https://doi.org/10.5194/acp-9-4207-2009

Fares, S., & Loreto, F. (2015). Isoprenoid emissions by the Mediterranean vegetation in Castelporziano. *Rendiconti Fis. Accademia Lincei, 26*, 493–498. https://doi.org/10.1007/s12210-014-0331-z

Fares, S., Park, J. H., Gentner, D. R., Weber, R., Ormeño, E., Karlik, J., & Goldstein, A. H. (2012). Seasonal cycles of biogenic volatile organic compound fluxes and concentrations in a California *Citrus* orchard. *Atmospheric Chemistry and Physics, 12*, 9865–9880. https://doi.org/10.5194/acp-12-9865-2012

Fowler, D., Pilegaard, K., Sutton, M. A., Ambus, P., Raivonen, M., Duyzer, J., Simpson, D., Fagerli, H., Fuzzi, S., Schjoerring, J. K., Granier, C., Neftel, A., Isaksen, I. S. A., Laj, P., Maione, M., Monks, P. S., Burkhardt, J., Daemmgen, U., Neirynck, J., … Erisman, J. W. (2009). Atmospheric composition change: Ecosystems–Atmosphere interactions. *Atmospheric Environment, 43*, 5193–5267. https://doi.org/10.1016/j.atmosenv.2009.07.068

Fröhlich-Nowoisky, J., Kampf, C. J., Weber, B., Huffman, J. A., Pöhlker, C., Andreae, M. O., Lang-Yona, N., Burrows, S. M., Gunthe, S. S., & Elbert, W. (2016). Bioaerosols in the Earth system: Climate, health, and ecosystem interactions. *Atmospheric Research, 182*, 346–376. https://doi.org/10.1016/j.atmosres.2016.07.018

Fuchs, H., Novelli, A., Rolletter, M., Hofzumahaus, A., Pfannerstill, E. Y., Kessel, S., Edtbauer, A., Williams, J., Michoud, V., Dusanter, S., Locoge, N., Zannoni, N., Gros, V., Truong, F., Sarda-Esteve, R., Cryer, D. R., Brumby, C. A., Whalley, L. K., Stone, D., … Wahner, A. (2017). Comparison of OH reactivity measurements in the atmospheric simulation chamber SAPHIR. *Atmospheric Measurement Techniques, 10*, 4023–4053. https://doi.org/10.5194/amt-10-4023-2017

Genard-Zielinski, A.-C., Ormeño, E., Boissard, C., & Fernandez, C. (2014). Isoprene emissions from downy oak under water limitation during an entire growing season: What cost for growth? *PLoS One, 9*, e112418. https://doi.org/10.1371/journal.pone.0112418

Genard-Zielinski, A.-C., Boissard, C., Fernandez, C., Kalogridis, C., Lathière, J., Gros, V., Bonnaire, N., & Ormeño, E. (2015). Variability of BVOC emissions from a Mediterranean mixed forest in southern France with a focus on *Quercus pubescens*. *Atmospheric Chemistry and Physics, 15*, 431–446. https://doi.org/10.5194/acp-15-431-2015

Genard-Zielinski, A.-C., Boissard, C., Ormeño, E., Lathière, J., Reiter, I. M., Wortham, H., Orts, J.-P., Temime-Roussel, B., Guenet, B., Bartsch, S., Gauquelin, T., & Fernandez, C. (2018). Seasonal variations of *Quercus pubescens* isoprene emissions from an *in natura* forest under drought stress and sensitivity to future climate change in the Mediterranean area. *Biogeosciences, 15*, 4711–4730. https://doi.org/10.5194/bg-15-4711-2018

Giorgi, F., & Lionello, P. (2008). Climate change projections for the Mediterranean region. *Global Planet Change, 63*, 90–104. https://doi.org/10.1016/j.gloplacha.2007.09.005

Giorgi, F., & Raffaele, F. (2023). The climate of the Mediterranean region and future projections in relation to air quality issues. In F. Dulac, S. Sauvage, & E. Hamonou (Eds.), *Atmospheric chemistry in the Mediterranean Region* (Vol. 1, Background information and pollutants distribution) (). Springer.

Goldstein, A. H., & Galbally, I. E. (2007). Known and unexplored organic constituents in the Earth's atmosphere. *Environmental Science & Technology, 41*, 1514–1521. https://doi.org/10.1021/es072476p

Gray, C. M., Monson, R. K., & Fierer, N. (2010). Emissions of volatile organic compounds during the decomposition of plant litter. *Journal of Geophysical Research, 115*, G03015. https://doi.org/10.1029/2010JG001291

Grote, R., Morfopoulos, C., Niinemets, Ü., Sun, Z., Keenan, T. F., Pacifico, F., & Butler, T. M. (2014). A fully integrated isoprenoid emissions model coupling emissions to photosynthetic characteristics. *Plant, Cell & Environment, 37*, 1965–1980. https://doi.org/10.1111/pce.12326

Gros, V., & Zannoni, N. (2022). Total OH reactivity. In F. Dulac, S. Sauvage, & E. Hamonou (Eds.), *Atmospheric chemistry in the Mediterranean Region* (Vol. 2, From air pollutant sources to impacts). Springer, this volume. https://doi.org/10.1007/978-3-030-82385-6_7

Guenther, A. (2013). Biological and Chemical Diversity of Biogenic Volatile Organic Emissions into the Atmosphere. ISRN *Atmospheric Sciences 20131-27*. https://doi.org/10.1155/2013/786290

Guenther, A., Hewitt, C. N., Erickson, D., Fall, R., Geron, C., Graedel, T., Harley, P., Klinger, L., Lerdau, M., Mckay, W. A., Pierce, T., Scholes, B., Steinbrecher, R., Tallamraju, R., Taylor, J., & Zimmerman, P. (1995). A global model of natural volatile organic compound emissions. *Journal of Geophysical Research, 100*, 8873. https://doi.org/10.1029/94JD02950

Guenther, A. B., & Hills, A. J. (1998). Eddy covariance measurement of isoprene fluxes. *Journal of Geophysical Research, 103*, 13145–13152. https://doi.org/10.1029/97JD03283

Guenther, A., Karl, T., Harley, P., Wiedinmyer, C., Palmer, P. I., & Geron, C. (2006). Estimates of global terrestrial isoprene emissions using MEGAN (Model of Emissions of Gases and Aerosols from Nature). *Atmospheric Chemistry and Physics, 6*, 3181–3210. https://doi.org/10.5194/acp-6-3181-2006

Guenther, A. B., Jiang, X., Heald, C. L., Sakulyanontvittaya, T., Duhl, T., Emmons, L. K., & Wang, X. (2012). The Model of Emissions of Gases and Aerosols from Nature version 2.1 (MEGAN2.1): An extended and updated framework for modeling biogenic emissions. *Geoscientific Model Development, 5*, 1471–1492. https://doi.org/10.5194/gmd-5-1471-2012

Harrison, D., Hunter, M. C., Lewis, A. C., Seakins, P. W., Nunes, T. V., & Pio, C. A. (2001). Isoprene and monoterpene emission from the coniferous species Abies borisii-regis - implications for regional air chemistry in Greece. *Atmospheric Environment, 35, 4687–4698*. https://doi.org/10.1016/S1352-2310(01)00092-9

Hewitt, C., Karl, T., Langford, B., Owen, S., & Possell, M. (2011). Quantification of VOC emission rates from the biosphere. *Trends in Analytical Chemistry, 30*, 937–944. https://doi.org/10.1016/j.trac.2011.03.008

Jacob, D. J., Field B.D., Li Q., Blake D.R., de Gouw J., Warneke C., Hansel A., Wisthaler A., Singh H.B. and Guenther A. (2005). Global budget of methanol: Constraints from atmospheric observations. *Journal of Geophysical Research, 110*, D08303. https://doi.org/10.1029/2004JD005172

Jaidan, N., El Amraoui, L., Attié, J.-L., Ricaud, P., & Dulac, F. (2018). Future changes in surface ozone over the Mediterranean Basin in the framework of the Chemistry-Aerosol Mediterranean Experiment (ChArMEx). *Atmospheric Chemistry and Physics, 18*, 9351–9373. https://doi.org/10.5194/acp-18-9351-2018

Jensen, N. R., Gruening, C., Goded, I., Müller, M., Hjorth, J., & Wisthaler, A. (2018). Eddy-covariance flux measurements in an Italian deciduous forest using PTR-Tof-MS, PTR-QMS and FIS. *International Journal of Environmental Analytical Chemistry, 98*, 758–788. https://doi.org/10.1080/03067319.2018.1502758

Kalabokas, P., Jensen, N. R., Roveri, M., Hjorth, J., Eremenko, M., Cuesta, J., Dufour, G., Foret, G., & Beekmann, M. (2020). A study of the influence of tropospheric subsidence on spring and

summer surface ozone concentrations at the JRC Ispra station in northern Italy. *Atmospheric Chemistry and Physics, 20*, 1861–1885. https://doi.org/10.5194/acp-20-1861-2020

Kalogridis, C., Gros, V., Sarda-Esteve, R., Langford, B., Loubet, B., Bonsang, B., Bonnaire, N., Nemitz, E., Genard, A.-C., Boissard, C., Fernandez, C., Ormeño, E., Baisnée, D., Reiter, I., & Lathière, J. (2014). Concentrations and fluxes of isoprene and oxygenated VOCs at a French Mediterranean oak forest. *Atmospheric Chemistry and Physics, 14*, 10085–10102. https://doi.org/10.5194/acp-14-10085-2014

Karl, T. G., Spirig, C., Rinne, J., Stroud, C., Prevost, P., Greenberg, J., Fall, R., & Guenther, A. (2002). Virtual disjunct eddy covariance measurements of organic compound fluxes from a subalpine forest using proton transfer reaction mass spectrometry. *Atmospheric Chemistry and Physics, 2*, 279–291. https://doi.org/10.5194/acp-2-279-2002

Karl, T., Guenther, A., Yokelson, R. J., Greenberg, J., Potosnak, M., Blake, D. R., & Artaxo, P. (2007). The tropical forest and fire emissions experiment: Emission, chemistry, and transport of biogenic volatile organic compounds in the lower atmosphere over Amazonia. *Journal of Geophysical Research, 112*, D18302. https://doi.org/10.1029/2007JD008539

Karl, M., Guenther, A., Köble, R., Seufert, G., Leip, A., & Seufert, G. (2009). A new European plant-specific emission inventory of biogenic volatile organic compounds for use in atmospheric transport models. *Biogeosciences, 6*, 1059–1087. https://doi.org/10.5194/bg-6-1059-2009

Katra, I., Arotsker, L., Krasnov, H., Zaritsky, A., Kushmaro, A., & Ben-Dov, E. (2014). Richness and diversity in dust stormborne biomes at the southeast Mediterranean. *Scientific Reports, 4*, 5265. https://doi.org/10.1038/srep05265

Keenan, T., Niinemets, Ü., Sabate, S., Gracia, C., & Peñuelas, J. (2009). Process based inventory of isoprenoid emissions from European forests: Model comparisons, current knowledge and uncertainties. *Atmospheric Chemistry and Physics, 9*, 4053–4076. https://doi.org/10.5194/acpd-9-6147-2009

Kellogg, C. A., & Griffin, D. W. (2006). Aerobiology and the global transport of desert dust. *Trends in Ecology & Evolution, 21*, 638–644. https://doi.org/10.1016/j.tree.2006.07.004

Kesselmeier, J., & Staudt, M. (1999). Biogenic Volatile Organic Compounds (VOC): An overview on emission, physiology and ecology. *Journal of Atmospheric Chemistry, 33*, 23–88. https://doi.org/10.1023/A:1006127516791

Langford, B., Cash, J., Acton, W. J. F., Valach, A. C., Hewitt, C. N., Fares, S., Goded, I., Gruening, C., House, E., Kalogridis, A.-C., Gros, V., Schafers, R., Thomas, R., Broadmeadow, M., & Nemitz, E. (2017). Isoprene emission potentials from European oak forests derived from canopy flux measurements: An assessment of uncertainties and inter-algorithm variability. *Biogeosciences, 14*, 5571–5594. https://doi.org/10.5194/bg-14-5571-2017

Luchetta, L., Simon, V., Torres, L. (2000). Emission of the main biogenic volatile organic compounds in France, Pollution atmosphérique, N°167, p. 387–412

Lavoir, A. V., Duffet, C., Mouillot, F., Rambal, S., Ratte, J. P., Schnitzler, J. P., & Staudt, M. (2011). Scaling-up leaf biogenic monoterpene emissions from water-limited Mediterranean landscapes: A case study with *Quercus ilex* woodlands. *Atmospheric Environment, 45*, 2888–2897. https://doi.org/10.1016/j.atmosenv.2011.02.005

Leff, J. W., & Fierer, N. (2008). Volatile organic compound (VOC) emissions from soil and litter samples. *Soil Biology and Biochemistry, 40*, 1629–1636. https://doi.org/10.1016/j.soilbio.2008.01.018

Lenschow, D. H. (1995). Micrometeorological techniques for measuring biosphere-atmosphere trace gas exchange. In P. A. Matson & R. C. Hariss (Eds.), Biogenic Trace Gases: Measuring Emissions from Soil and Water (pp. 126–163). Oxford: Blackwell Science.

Lenschow, D. H., Mann, J., & Kristensen, I. (1993). How long is long enough when measuring fluxes and other turbulent statistics? *Journal of Atmospheric and Oceanic Technology, 11*, 661–673. https://doi.org/10.1175/1520-0426(1994)011<0661:HLILEW>2.0.CO;2

Liakakou, E., Bonsang, B., Williams, J., Kalivitis, N., Kanakidou, M., & Mihalopoulos, N. (2009). C_2–C_8 NMHCs over the Eastern Mediterranean: Seasonal variation and impact on regional oxidation chemistry. *Atmospheric Environment, 43*, 5611–5621. https://doi.org/10.1016/j.atmosenv.2009.07.067

Llusià, J., & Peñuelas, J. (2000). Seasonal patterns of terpene content and emission from seven Mediterranean woody species in field conditions. *American Journal of Botany, 87*, 133–140. https://doi.org/10.2307/2656691

Martin, N. (2010). Performances des modélisations déterministes d'ozone à méso-échelle et à micro-échelle dans les Alpes-Maritimes, Cybergeo, doc. 503. https://doi.org/10.4000/cybergeo.23183.

Mason, R. H., Si, M., Chou, C., Irish, V. E., Dickie, R., Elizondo, P., Wong, R., Brintnell, M., Elsasser, M., Lassar, W. M., Pierce, K. M., Leaitch, W. R., MacDonald, A. M., Platt, A., Toom-Sauntry, D., Sarda-Estève, R., Schiller, C. L., Suski, K. J., Hill, T. C. J., … Bertram, A. K. (2016). Size-resolved measurements of ice-nucleating particles at six locations in North America and one in Europe. *Atmospheric Chemistry and Physics, 16*, 1637–1651. https://doi.org/10.5194/acp-16-1637-2016

Menut, L., Bessagnet, B., Khvorostyanov, D., Beekmann, M., Blond, N., Colette, A., Coll, I., Curci, G., Foret, G., Hodzic, A., Mailler, S., Meleux, F., Monge, J.-L., Pison, I., Siour, G., Turquety, S., Valari, M., Vautard, R., & Vivanco, M. G. (2013). CHIMERE 2013: A model for regional atmospheric composition modelling. *Geoscientific Model Development, 6*, 981–1028. https://doi.org/10.5194/gmd-6-981-2013

Mescioglu, E., Rahav, E., Belkin, N., Xian, P., Eigenza, J. M., Vichik, A., Herut, B., & Paytan, A. (2019). Aerosol microbiome over the Mediterranean Sea diversity and abundance. *Atmosphere, 10*, 440. https://doi.org/10.3390/atmos10080440

Michoud, V., Sciare, J., Sauvage, S., Dusanter, S., Léonardis, T., Gros, V., Kalogridis, C., Zannoni, N., Féron, A., Petit, J.-E., Crenn, V., Baisnée, D., Sarda-Estève, R., Bonnaire, N., Marchand, N., DeWitt, H. L., Pey, J., Colomb, A., Gheusi, F., … Locoge, N. (2017). Organic carbon at a remote site of the western Mediterranean Basin: Sources and chemistry during the ChArMEx SOP2 field experiment. *Atmospheric Chemistry and Physics, 17*, 8837–8865. https://doi.org/10.5194/acp-17-8837-2017

Morris, C. E., Sands, D., Bardin, M., Jaenicke, R., Vogel, B., Leyronas, C., Ariya, P., & Psenner, R. (2011). Microbiology and atmospheric processes: Research challenges concerning the impact of airborne micro-organisms on the atmosphere and climate. *Biogeosciences, 8*, 17–25. https://doi.org/10.5194/bg-8-17-2011

Myriokefalitakis, S., Nenes, A., Baker, A. R., Mihalopoulos, N., & Kanakidou, M. (2016). Bioavailable atmospheric phosphorous supply to the global ocean: A 3-D global modeling study. *Biogeosciences, 13*, 6519–6543. https://doi.org/10.5194/bg-2016-215

Niinemets, Ü., Kuhn, U., Harley, P. C., Staudt, M., Arneth, A., Cescatti, A., Ciccioli, P., Copolovici, L., Geron, C., Guenther, A., Kesselmeier, J., Lerdau, M. T., Monson, R. K., & Peñuelas, J. (2011). Estimations of isoprenoid emission capacity from enclosure studies: Measurements, data processing, quality and standardized measurement protocols. *Biogeosciences, 8*, 2209–2246. https://doi.org/10.5194/bg-8-2209-2011

Nuñez, L., Plaza, J., Perez-Pastor, R., Pujadas, M., Gimeno, B. S., Bermejo, V., & Garcia-Alonso, S. (2002). High water vapour pressure deficit influence on *Quercus ilex* and *Pinus pinea* field monoterpene emission in the central Iberian Peninsula (Spain). *Atmospheric Environment, 36*, 4441–4452. https://doi.org/10.1016/S1352-2310(02)00415-6

Oderbolz, D. C., Aksoyoglu, S., Keller, J., Barmpadimos, I., Steinbrecher, R., Skjøth, C. A., Plaß-Dülmer, C., & Prévôt, A. S. H. (2013). A comprehensive emission inventory of biogenic volatile organic compounds in Europe: Improved seasonality and land-cover. *Atmospheric Chemistry and Physics, 13*, 1689–1712. https://doi.org/10.5194/acp-13-1689-2013

Olivier, R., Staudt, M., Lavoir, A. V., Ormeño, E., Rizvi, S. H., Baldy, V., Rivoal, A., Greff, S., Lecareux, C., & Fernandez, C. (2011a). Direct and indirect impact of sewage sludge compost spreading on *Quercus coccifera* monoterpene emissions in a Mediterranean shrubland. *Environmental Pollution, 159*, 963–969. https://doi.org/10.1016/j.envpol.2010.12.003

Olivier, R., Lavoir, A.-V., Ormeño, E., Mouillot, F., Greff, S., Lecareux, C., Staudt, M., & Fernandez, C. (2011b). Compost spreading in Mediterranean shrubland indirectly increases biogenic emissions by promoting growth of VOC-emitting plant parts. *Atmospheric Environment, 45*, 3631–3639. https://doi.org/10.1016/j.atmosenv.2011.03.060

Ormeño, E., Fernandez, C., Bousquet-Melou, A., Greff, S., Morin, E., Robles, C., Vila, B., & Bonin, G. (2007). Monoterpene and sesquiterpene emissions of three Mediterranean species through calcareous and siliceous soils in natural conditions. *Atmospheric Environment, 41*, 629–639. https://doi.org/10.1016/j.atmosenv.2006.08.027

Ormeño, E., Goldstein, A., & Niinemets, U. (2011). Extracting and trapping biogenic volatile organic compounds stored in plant species. *Trends in Analytical Chemistry, 30*, 978–989. https://doi.org/10.1016/j.trac.2011.04.006

Ortega, J., Helmig, D., Daly, R. W., Tanner, D. M., Guenther, A. B., & Herrick, J. D. (2008). Approaches for quantifying reactive and low-volatility biogenic organic compound emissions by vegetation enclosure techniques – Part B: Applications. *Chemosphere, 72*, 365–380. https://doi.org/10.1016/j.chemosphere.2008.02.054

Owen, S. M., & Hewitt, N. H. (2000). Extrapolating branch enclosure measurements to estimates of regional scale biogenic VOC fluxes in the north-western Mediterranean basin. *Journal of Geophysical Research, 105*, 11573–11583. https://doi.org/10.1029/1999JD901154

Owen, S. M., Boissard, C., Street, R. A., Duckham, S. C., Csiky, O., & Hewitt, C. N. (1997). Screening of 18 Mediterranean plant species for volatile organic compounds emissions. *Atmospheric Environment, 31*, 101–117. https://doi.org/10.1016/S1352-2310(97)00078-2

Owen, S. M., Boissard, C., & Hewitt, C. N. (2001). Volatile organic compounds (VOCs) emitted from 40 Mediterranean plant species: VOC speciation and extrapolation to habitat scale. *Atmospheric Environment, 35*, 5393–5409. https://doi.org/10.1016/S1352-2310(01)00302-8

Park, J.-H., Goldstein, A. H., Timkovsky, J., Fares, S., Weber, R., Karlik, J., & Holzinger, R. (2013). Eddy covariance emission and deposition flux measurements using proton transfer reaction – Time of flight – Mass spectrometry (PTR-TOF-MS): Comparison with PTR-MS measured vertical gradients and fluxes. *Atmospheric Chemistry and Physics, 13*, 1439–1456. https://doi.org/10.5194/acp-13-1439-2013

Park, J.-H., Fares, S., Weber, R., & Goldstein, A. H. (2014). Biogenic volatile organic compound emissions during BEARPEX 2009 measured by eddy covariance and flux–Gradient similarity methods. *Atmospheric Chemistry and Physics, 14*, 231–244. https://doi.org/10.5194/acp-14-231-2014

Pegoraro, E., Rey, A., Greenberg, J., Harley, P., Grace, J., Malhi, Y., & Guenther, A. (2004). Effect of drought on isoprene emission rates from leaves of *Quercus virginiana* Mill. *Atmospheric Environment, 38*, 6149–6156. https://doi.org/10.1016/j.atmosenv.2004.07.028

Peñuelas, J., Filella, I., & Comas, P. (2002). Changed plant and animal life cycles from 1952 to 2000 in the Mediterranean region. *Global Change Biology, 8*, 531–544. https://doi.org/10.1046/j.1365-2486.2002.00489.x

Peñuelas, J., Asensio, D., Tholl, D., Wenke, K., Rosenkranz, M., Piechulla, B., & Schnitzler, J. P. (2014). Biogenic volatile emissions from the soil. *Plant, Cell & Environment, 37*, 1866–1891. https://doi.org/10.1111/pce.12340

Pio, C. A., Silva, P. A., Cerqueira, M. A., & Nunes, T. V. (2005). Diurnal and seasonal emissions of volatile organic compounds from cork oak (*Quercus suber*) trees. *Atmospheric Environment, 39*, 1817–1827. https://doi.org/10.1016/j.atmosenv.2004.11.018

Polymenakou, P. N., Mandalakis, M., Stephanou, E. G., & Tselepides, A. (2008). Particle size distribution of airborne microorganisms and pathogens during an intense African dust event in the Eastern Mediterranean. *Environmental Health Perspectives, 116*, 292–296. https://doi.org/10.1289/ehp.10684

Pope, F. D. (2010). Pollen grains are efficient cloud condensation nuclei. *Environmental Research Letters, 5*, 044015. https://doi.org/10.1088/1748-9326/5/4/044015

Pöschl, U., & Shiraiwa, M. (2015). Multiphase chemistry at the atmosphere–biosphere interface influencing climate and public health in the anthropocene. *Chemical Reviews, 115*, 4440–4475. https://doi.org/10.1021/cr500487s

Pöschl, U., Martin, S. T., Sinha, B., Chen, Q., Gunthe, S. S., Huffman, J. A., Borrmann, S., Farmer, D. K., Garland, R. M., Helas, G., Jimenez, J. L., King, S. M., Manzi, A., Mikhailov, E., Pauliquevis, T., Petters, M. D., Prenni, A. J., Roldin, P., Rose, D., … Andreae, M. O. (2010).

Rainforest aerosols as biogenic nuclei of clouds and precipitation in the Amazon. *Science, 329*, 1513–1516. https://doi.org/10.1126/science.1191056

Rahav, E., Belkin, N., Paytan, A., & Herut, B. (2019). The relationship between air-mass trajectories and the abundance of dust-borne prokaryotes at the SE Mediterranean Sea. *Atmosphere, 10*, 280. https://doi.org/10.3390/atmos10050280

Raisi, L., Lazaridis, M., & Katsivela, E. (2010). Relationship between airborne microbial and particulate matter concentrations in the ambient air at a Mediterranean site. *Global NEST Journal, 12*, 84–91. https://doi.org/10.30955/gnj.000694

Recio, M., Docampo, S., García-Sánchez, J., Trigo, M. M., Melgar, M., & Cabezudo, B. (2010). Influence of temperature, rainfall and wind trends on grass pollination in Malaga (western Mediterranean coast). *Agricultural and Forest Meteorology, 150*, 931–940. https://doi.org/10.1016/j.agrformet.2010.02.012

Rinne, H. J. I., Guenther, A. B., Warneke, C., de Gouw, J. A., & Luxembourg, S. L. (2001). Disjunct eddy covariance technique for trace gas flux measurements. *Geophysical Research Letters, 28*, 3139–3142. https://doi.org/10.1029/2001GL012900

Rivoal, A., Fernandez, C., Lavoir, A.-V., Olivier, R., Lecareux, C., Greff, S., Roche, P., & Vila, B. (2010). Environmental control of terpene emissions from *Cistus monspeliensis* L. in natural Mediterranean shrublands. *Chemosphere, 78*, 942–949. https://doi.org/10.1016/j.chemosphere.2009.12.047

Sartelet, K. N., Couvidat, F., Seigneur, C., & Roustan, Y. (2012). Impact of biogenic emissions on air quality over Europe and North America. *Atmospheric Environment, 53*, 131–141. https://doi.org/10.1016/j.atmosenv.2011.10.046

Saunier, A. (2017). Réponse de la forêt à des scénarios de sécheresse appliqués à moyen et long terme en milieu naturel : Étude des COVB du chêne pubescent, principal émetteur d'isoprène en région mediterranéenne, PhD dissertation, Aix Marseille Université, Marseille, 184 pp. http://www.theses.fr/2017AIXM0106/document

Saunier, A., Ormeño, E., Wortham, H., Temime-Roussel, B., Lecareux, C., Boissard, C., & Fernandez, C. (2017). Chronic drought decreases anabolic and catabolic BVOC emissions of *Quercus pubescens* in a Mediterranean forest. *Frontiers in Plant Science, 8*, 71. https://doi.org/10.3389/fpls.2017.00071

Saunier, A., Ormeéno, E., Piga, D., Armengaud, A., Boissard, C., Lathière, J., Szopa, S., Genard-Zielinski, A.-C., & Fernandez, C. (2020). Isoprene contribution to ozone production under climate change in the French Mediterranean area. *Regional Environmental Change, 20*, 111. https://doi.org/10.1007/s10113-020-01697-4

Schade, G. W., & Goldstein, A. H. (2001). Fluxes of oxygenated volatile organic compounds from a ponderosa pine plantation. *Journal of Geophysical Research, 106*, 3111–3123. https://doi.org/10.1029/2000JD900592

Schallhart, S., Rantala, P., Nemitz, E., Taipale, D., Tillmann, R., Mentel, T. F., Loubet, B., Gerosa, G., Finco, A., Rinne, J., & Ruuskanen, T. M. (2016). Characterization of total ecosystem-scale biogenic VOC exchange at a Mediterranean oak–hornbeam forest. *Atmospheric Chemistry and Physics, 16*, 7171–7194. https://doi.org/10.5194/acp-16-7171-2016

Scheifinger, H., Belmonte, J., Buters, J., Celenk, S., Damialis, A., Dechamp, C., García-Mozo, H., Gehrig, R., Grewling, L., Halley, J. M., Hogda, K.-A., Jäger, S., Karatzas, K., Karlsen, S.-R., Koch, E., Pauling, A., Peel, R., Sikoparija, B., Smith, M., Galán-Soldevilla, C., Thibaudon, M., Vokou, D., and de Weger L. A.: Monitoring, modelling and forecasting of the pollen season, in Allergenic pollen, Sofiev, M., Bergmann, K. C., 71–126, Springer., https://doi.org/10.1007/978-94-007-4881-1_4, 2013.

Schween, J., Dlugi, R., Hewitt, C. N., & Foster, P. (1997). Determination and accuracy of VOC-fluxes above the pine/oak forest at Castelporziano. *Atmospheric Environment, 31*(Suppl. 1), 199–215. https://doi.org/10.1016/S1352-2310(97)00111-8

Seco, R., Peñuelas, J., Filella, I., Llusià, J., Molowny-Horas, R., Schallhart, S., Metzger, A., Müller, M., & Hansel, A. (2011). Contrasting winter and summer VOC mixing ratios at a forest site in the Western Mediterranean Basin: The effect of local biogenic emissions. *Atmospheric Chemistry and Physics, 11*, 13161–13179. https://doi.org/10.5194/acp-11-13161-2011

Staudt, M., Bertin, N., Frenzel, B., & Seufert, G. (2000). Seasonal variations in amount and composition of monoterpenes emitted by young *Pinus pinea* trees – Implications for emission modeling. *Journal of Atmospheric Chemistry, 35*, 77–99. https://doi.org/10.1023/A:1006233010748

Staudt, M., Mandl, N., Joffre, R., & Rambal, S. (2001). Intraspecific variability of monoterpene composition emitted by *Quercus ilex* leaves. *Canadian Journal of Forest Research, 31*, 174–180. https://doi.org/10.1139/x00-153

Staudt, M., Rambal, S., Joffre, R., & Kesselmeier, J. (2002). Impact of drought on seasonal monoterpene emissions from *Quercus ilex* in southern France. *Journal of Geophysical Research, 107*, 4602. https://doi.org/10.1029/2001JD002043

Staudt, M., Joffre, R., & Rambal, S. (2003). How growth conditions affect the capacity of Quercus ilex leaves to emit monoterpenes. *The New Phytologist, 158*, 61–73. https://doi.org/10.1046/j.1469-8137.2003.00722.x

Staudt, M., Céline, M., Joggre, R., Rambal, S., Bonin, A., Landais, D., & Lumaret, R. (2004). Isoprenoid emissions of *Quercus* spp. (*Q. suber* and *Q. ilex*) in mixed stands contrasting in interspecific genetic introgression. *The New Phytologist, 163*, 573–584. https://doi.org/10.1111/j.1469-8137.2004.01140.x

Staudt, M., Byron, J., Piquemal, K., & Williams, J. (2019). Compartment specific chiral pinene emissions identified in a Maritime pine forest. *Science of the Total Environment, 654*, 1158–1166. https://doi.org/10.1016/j.scitotenv.2018.11.146

Steinbrecher, R., Smiatek, G., Köble, R., Seufert, G., Theloke, J., Hauff, K., Ciccioli, P., Vautard, R., & Curci, G. (2009). Intra- and inter-annual variability of VOC emissions from natural and semi-natural vegetation in Europe and neighbouring countries. *Atmospheric Environment, 43*, 1380–1391. https://doi.org/10.1016/j.atmosenv.2008.09.072

Street, R. A., Owen, S., Duckham, S. C., Boissard, C., & Hewitt, C. N. (1997). Effect of habitat and age on variations in volatile organic compound (VOC) emissions from *Quercus ilex* and *Pinus pinea*. *Atmospheric Environment, 31*, 89–100. https://doi.org/10.1016/S1352-2310(97)00077-0

Tholl, D., Boland, W., Hansel, A., Loreto, F., Röse, U. S. R., & Schnitzler, J. P. (2006). Practical approaches to plant volatile analysis. *The Plant Journal, 45*, 540–560. https://doi.org/10.1111/j.1365-313X.2005.02612.x

Valentini, R., Greco, S., Seufert, G., Bertin, N., Ciccioli, P., Cecinato, A., Brancaleoni, E., & Frattoni, M. (1997). Fluxes of biogenic VOC from Mediterranean vegetation by trap enrichment relaxed eddy accumulation. *Atmospheric Environment, 31*(Suppl. 1), 229–238. https://doi.org/10.1016/S1352-2310(97)00085-X

Valor, T., Ormeño, E., & Casals, P. (2017). Temporal effects of prescribed burning on terpene production in Mediterranean pines. *Tree Physiology, 37*, 1622–1636. https://doi.org/10.1093/treephys/tpx069

Yang, Y., Shao, M., Wang, X., Nölscher, A. C., Kessel, S., Guenther, A., & Williams, J. (2016). Towards a quantitative understanding of total OH reactivity: A review. *Atmospheric Environment, 134*, 147–161. https://doi.org/10.1016/j.atmosenv.2016.03.010

Yáñez-Serrano, A. M., Fasbender, L., Kreuzwieser, J., Dubbert, D., Haberstroh, S., Lobo-do-Vale, R., Caldeira, M. C., & Werner, C. (2018). Volatile diterpene emission by two Mediterranean Cistaceae shrubs. *Scientific Reports, 8*, 6855. https://doi.org/10.1038/s41598-018-25056-w

Soil Dust Emissions

Benoit Laurent and Gilles Bergametti

Contents

Abstract In this chapter, we first discuss the basis of the physics of soil dust emission, underlining that the processes controlling these emissions are strongly (and non-linearly) related to meteorological parameters (especially the wind speed and precipitation). Consequently, dust emissions are sensitive to climatic changes. Moreover, dust emissions from soils result from complex interactions between these meteorological parameters and the soil surface, making their assessment even more difficult. Indeed, dust emission only occurs when the wind speed exceeds the wind speed threshold for erosion, which depends on the characteristics of the surface (roughness, soil grain size, vegetation cover, soil moisture, etc.). Some arid and semi-arid areas are thus more prone to emitting dust into the atmosphere than others. After providing estimates of the magnitude of dust emissions as simulated by models, the meteorological mechanisms leading to dust emission and transport in the Mediterranean are illustrated. Then, Saharan source regions that contribute the

Chapter reviewed by ***Sara Basart*** *and* ***Martina Klose*** *(Barcelona Supercomputing Center (BSC), Barcelona, Spain), as part of the book Part V Emissions and Sources also reviewed by* ***Claire Granier*** *(Laboratoire d'Aérologie (LAERO), CNRS – Univ. Toulouse III Paul Sabatier, Observatoire Midi-Pyrénées, Toulouse, France)*

B. Laurent (✉) · G. Bergametti
Université Paris Cité and Univ. Paris Est Créteil, CNRS, LISA, Paris, France
e-mail: Benoit.Laurent@lisa.ipsl.fr

F. Dulac et al. (eds.), *Atmospheric Chemistry in the Mediterranean Region*,
https://doi.org/10.1007/978-3-030-82385-6_4

most to dust fallout in the western Mediterranean region are discussed from deposition measurements, satellite aerosol observations, and air mass trajectories. The way by which human activities (especially agriculture) could affect dust emissions is briefly illustrated.

1 Introduction

The Mediterranean basin is surrounded on its southern border by the Sahara desert, the largest desert of the world, and on its eastern border by the Middle East deserts. Dust emission regions were first identified using the records of dust storms and associated events as reported in meteorological stations located in or close to the main deserts (e.g., Dubief, 1953; Middleton et al., 1986). Shao et al. (2013) compiled synoptic meteorological records to establish the global distribution of frequencies of dust situations for the period 1974–2012. Even if these observations are often done in the margins of the main desert areas, they give us a global view of the main dust emission regions. In particular, the data gathered in Fig. 1 illustrate the high dust event frequencies encountered in the regions of the Sahara and Middle East deserts in agreement with the main dust source regions identified from space using the TOMS absorbing aerosol index (Prospero et al., 2002).

Mineral dust is a major component of the Mediterranean atmospheric aerosol (Basart et al., 2009; Pey et al., 2013; Gkikas et al., 2016). For example, Bergametti et al. (1989) showed that the concentrations of mineral aerosols, as traced by aluminum measured in the Mediterranean atmosphere, vary over several orders of magnitude, from several tens to several thousands of μg m^{-3}, in less than 48 h. This results from (1) strong of dust concentrations gradients due to sporadic events and short lifetimes in the atmosphere and (2) preferential areas for high dust concentrations.

Figure 2 provides an example of the rapid change in dust concentration as it can be observed in dust source regions. It reports the 5-minute mean and maximum wind speeds and PM_{10} (i.e., the particulate matter having a diameter < 10 μm) concentrations measured at the Institute of Arid Region station of El Fjé in Médénine, South Tunisia (33.499°N, 10.642°E), on May 13, 2014 (Bouet et al., 2019). A sudden huge increase in 5-min PM_{10} concentration (from about 50 up to about 3400 μg m^{-3}) occurred concomitantly with an increase in 5-min maximum wind speed from about 3 to 15 m s^{-1}, and large concentrations (>500 μg m^{-3}) persisted as long as the maximum wind speed remained >13 m s^{-1}. This illustrates the pulsed and sporadic nature of dust events emitted from desert areas: dust concentrations can increase by several orders of magnitude within very short periods of time (<1 hour) and for relatively short durations (here less than 2 hours).

Indeed, dust emissions only occur when the surface wind speed exceeds a threshold value controlled by the surface soil properties. Thus, any part of the Sahara desert and semi-arid peripheral regions can be a dust source provided the wind

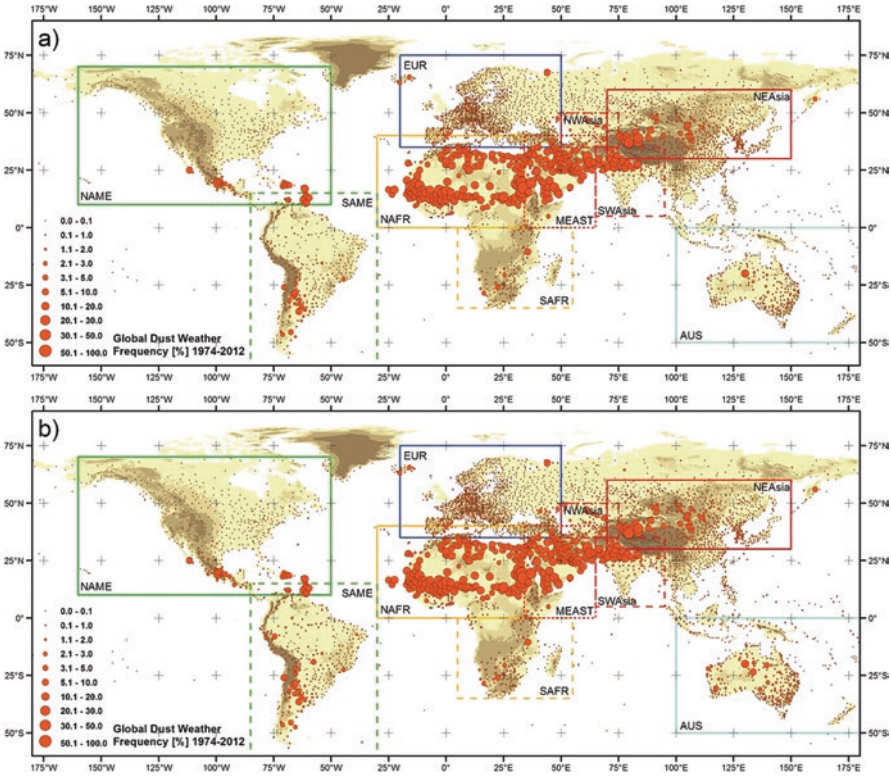

Fig. 1 Global distribution of the frequencies of dust situations estimated from synoptic records (weak and strong events) for the period from January 1974 to December 2012. The different regions are framed: N and S Africa, N and S America, Middle East, NO Asia, NE Asia, SW Asia, Europe, and Australia. (Reprinted from Fig. 2 in Shao et al., 2013)

speed is above the threshold, but preferential areas for dust emissions do exist. They generally correspond to regions where both high wind speeds are frequently observed and smooth and easily erodible surfaces are present. However, the assessment of the dust sources, especially of their intensity, remains challenging. Indeed, the most frequent and the most intense dust sources are generally not the same (e.g., Laurent et al., 2006; Bergametti et al., 2017).

In this chapter, a brief description of the dust emission processes and their quantification is presented as well as the role of human activities in northern Africa and the way by which they could affect soil dust emissions. Meteorological mechanisms leading to dust emission and transport and their temporal variability are illustrated. Finally, the main locations of dust sources for the Mediterranean region are discussed.

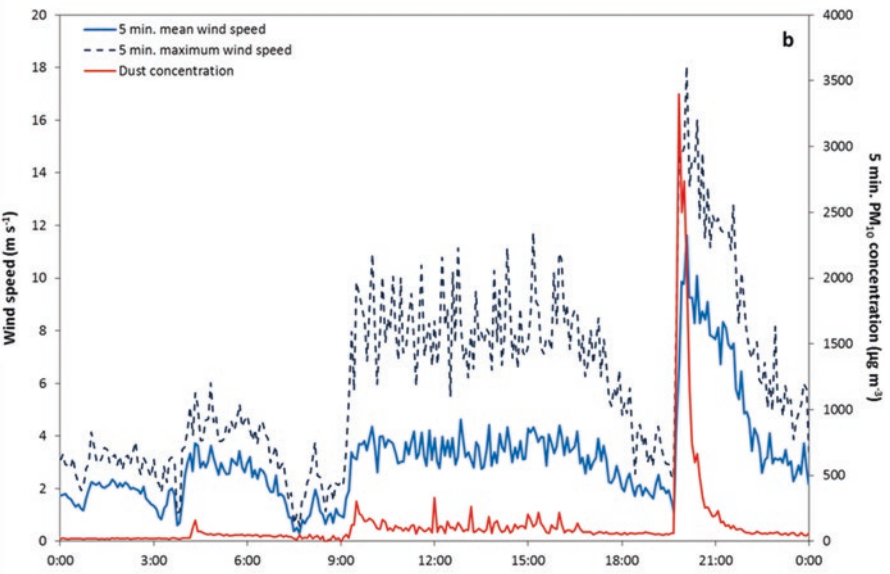

Fig. 2 Temporal evolution of the 5-minute PM_{10} concentration (in µg m^{-3}, red line) and 5-minute mean (light blue line) and maximum (dark blue dashed line) wind speed (in m s^{-1}) observed at Médénine, Tunisia, on May 13, 2014. (Figure reprinted from Fig. A1 Bouet et al. (2019))

2 Processes and Quantification of Dust Emissions

2.1 Dust Emission Physical Processes

Mineral dust emissions result from the force exerted by wind on an erodible soil surface (i.e., generally bare or sparsely vegetated and dry). The force exerted by the wind on the surface is the shear stress (τ):

$$\tau = \rho_a U^{*2} \tag{1}$$

with ρ_a, the air density, and U^*, the wind friction velocity. Under thermal neutral conditions, U^* can be expressed from the wind speed (U) at a given height (z) and the aerodynamic roughness length (Z_0) using the logarithmic wind speed profile (Priestley, 1959):

$$\text{for } z > Z_0, \quad U(z) = \left(U^* / k\right) \ln\left(z / Z_0\right) \tag{2}$$

where k is the von Karman constant ($k \sim 0.4$). Z_0 quantitatively translates the effect of erodible elements (soil grains) or non-erodible elements (gravels, pebbles, stones, vegetation) on the transfer of energy from the wind to the surface.

A key point to have in mind is that dust emission into the atmosphere only occurs when the energy provided by the surface wind is higher than the energy maintaining the soil grains at the surface. Gravity, inter-particle cohesion, as well as capillary forces, which can be observed when the soils have a significant water content, contribute to maintain the soil grains and aggregates on the ground. These forces oppose the mechanical action of the wind, which tends to tear the grains off the ground. The setting in motion of soil grains and aggregates is observed when the wind friction velocity is higher than a threshold value to overcome the forces maintaining the soil grains on the surface (e.g., Bagnold, 1941). The threshold wind friction velocity for erosion, U^*_t, is defined as the wind friction velocity at which the movement of soil grains is initiated. Gillette et al. (1982) and Nickling and Gillies (1989) performed measurements carried out using portable wind tunnels in various arid and semi-arid sites in the United States, They documented variations in U^*_t from a few tenths to several m s^{-1} in natural conditions. On Earth, for smooth, loose, and dry soil, and assuming spherical soil grains, U^*_t depends mainly on the grain diameter (D_p) and density (ρ_p). There is an optimal grain diameter, around 70–100 μm, for which the threshold speed required for the mobilization of soil particles is minimal (Chepil, 1951; Iversen & White, 1982) and close to 18–20 cm s^{-1}. Furthermore, Shao and Lu (2000) proposed a formulation of U^*_t based on an explicit expression of the van der Waals and electrostatic forces involved in the inter-particle cohesion forces. For larger grains, U^*_t increases because their greater weight increases the energy required to set them in motion. For the grains having a diameter smaller than the optimum grain diameter for wind erosion, U^*_t increases on average when the grain size decreases. Indeed, relative to the weight of individual particles, the inter-particle forces become increasingly significant as the particle size decreases (e.g., Stringer et al., 2020). However, the dust particles emitted from soils and transported in the atmosphere (i.e., soil particles with a diameter less than a few micrometers to some tens of micrometers) are most often linked together in the soil by cohesive forces in the form of aggregates of greater sizes, from several tens to hundreds of micrometers. Free particles in the atmospheric dust size range are generally rare in soils (e.g., Chatenet et al., 1996; Mei et al., 2004).

The gravels, pebbles, micro-reliefs, as well as sparse vegetation that can be encountered in desert areas partly protect the surface, which is then less subject to wind erosion. Beyond this covering effect of the surface, these non-erodible elements also dissipate a fraction of the wind energy that is no longer available to mobilize the grains of the soil. This leads to an apparent increase in the threshold wind friction velocity (e.g., Raupach, 1992; Marticorena et al., 1997).

When the soil is sufficiently moist, the presence of water between the soil grains increases the capillary forces and then reinforces the cohesion between the soil grains (Chepil, 1956; McKenna-Neuman & Nickling, 1989; Chen et al., 1996). The threshold wind friction velocity does not increase as a function of the total soil moisture (w), but of the difference between *w and of the so-called residual moisture (w')* (Fécan et al., 1999). This residual moisture reflects the amount of water that must be trapped in a film of water around the grains before the interstices between

the soil grains begin to fill. This residual soil moisture depends on the soil texture (i.e., relative proportions of sand, silt, and clay).

Other environmental factors, such as snow cover or frost, can also limit or even inhibit wind erosion of soils. In addition, surface crusts strongly reduce or even inhibit dust emissions. The formation of crusts depends on the soil texture (in particular % of clay, i.e. the finest size fraction) and the composition (% of salts) of the soil surface layer, as well as humidification by precipitation and drying processes of the soils (e.g., Valentin & Bresson, 1992; Belnap & Gillette, 1998; Rajot et al., 2003).

When the threshold wind friction velocity is exceeded, the soil grains and aggregates follow a ballistic trajectory in a horizontal movement above the surface known as saltation. The disaggregation of aggregates in saltation when they collide the surface or when they are bombarded on the ground by soil grains in saltation releases into the atmosphere the finer dust particles that were previously linked in larger aggregates (Gillette & Goodwin, 1974; Gomes et al., 1990). This process is generally called sandblasting. Saltation is thus often considered as a prerequisite to generate significant dust emission fluxes. It must be noted that a fractionation in size but also in composition (mineralogical, chemical) between the soil and the aerosol takes place during these saltation and sandblasting processes (e.g., Gomes et al., 1990; Shao, 2001; Kok, 2011).

The grains in saltation constitute the horizontal mass flux (G). It is generally accepted that only dust particles smaller than a few tens of micrometers can be extracted from the saltation layer and then transported over longer distances (e.g., Gillette, 1977; Nickling, 1994; Shao, 2008). The emission of these fine particles into the atmosphere is referred to as the vertical dust flux (F). Nevertheless, "giant" particles with sizes up to >100 μm can be found at remote distances (Betzer et al., 1988; Weinzierl et al., 2009; van der Does et al., 2018; Ryder et al., 2019; Toth III et al., 2020) although their theoretical gravitational velocity of thousands meters by day is not compatible with their long-range transport. Their abundance is still debated especially because they are difficult to collect quantitatively in the atmosphere. Based on in situ measurements with quasi-Lagrangian balloons drifting within Saharan dust plumes over the western Mediterranean, Renard et al. (2018) report the persistence of a particle size mode around 30 μm in diameter during transport.

Numerical models have been developed to compute saltation and dust fluxes taking into account a description of the threshold wind friction velocity, the saltation process, and the efficiency of sandblasting. It is therefore essential to pay particular attention to the key parameters chosen to model G and F. From a dimensional analysis, Bagnold (1941) established a first formulation of G as a function of U^*:

$$G = c^{4/3} \rho_a / g U^{*3} \tag{3}$$

with G in g cm^{-1} s^{-1}, c an empirical coefficient function of the grain size (between 1.5 and 2.8), ρ_a the air density in g cm^{-3}, g the gravity in cm s^{-2}, and U^* in cm s^{-1}.

Based on field and wind tunnel experiments or theoretical studies, many authors have proposed semi-empirical expressions of the horizontal flux G. For example,

the equation from (White 1979 derived from Kawamura 1964) represents the influence of the threshold friction speed on G (with $c = 2.6$):

$$G = c\frac{\rho_a}{g}U^{*3}\left(1+\frac{U_t^*}{U^*}\right)\left(1-\frac{U_t^{*2}}{U^{*2}}\right) \tag{4}$$

Different conceptual relationships have been established relating the F/G ratio (i.e., sandblasting efficiency, α) to the kinetic energy of impacting particles and the resistance of the surface (Shao et al., 1993) or to the proportion of fine particles in the soil (% of clay) (Marticorena & Bergametti, 1995). These approaches provide an estimate of the mass of emitted dust. However, an explicit description of the phenomenon leading to the disruption of aggregates is necessary to model the size distribution of the particles constituting F. Alfaro and Gomes (2001) developed a sandblasting scheme based on the balance between the kinetic energy (e_c) of grains in saltation impacting the surface and the cohesion energy (e_i) of aggregated particles. A mass flux of dust is emitted if e_c is greater than e_i. Another approach is to estimate the amount of fine particles present in the volume of soil that a grain in saltation can eject by impacting on the surface (Shao, 2001, 2004). This scheme, which also includes the disaggregation of saltating aggregates, uses the texture and an estimate of the plastic pressure of the soil to relate F to G. Finally, an analogy between the dust emission due to saltation and the impact fragmentation of brittle materials such as glass has been proposed by Kok (2011) and Kok et al. (2014), which also requires knowledge of the soil texture.

2.2 Quantification of Dust Emission

Estimates of dust emission are only provided by modeling studies, since direct measurements and observations cannot quantitatively measure dust emissions at the scale of the desert source areas. Dust emission parameterizations derived from the physical description of the processes were included in chemical transport models (CTM) (e.g., Schulz et al., 1998; Ginoux et al., 2001; Zender et al., 2003; Menut et al., 2005; Albani et al., 2014). Modeling studies suggest that the amount of desert aerosols emitted each year into the atmosphere at global scale ranges between 1000 and 4000 Mt year^{-1} and between 200 and 2900 Mt year^{-1} for North Africa (see Huneeus et al., 2011 and references therein). In order to document the state of the art in terms of aerosol modeling, the AeroCom project (https://aerocom.met.no) intercompared the simulations of global aerosol models and also compared them with a large number of satellite observations and measurements (AERONET measurements, surface concentrations) (Textor et al., 2006, 2007; Huneeus et al., 2011). Based on the AeroCom work of Textor et al. (2006, 2007), Bergametti and Forêt (2014) selected seven models, with similar representation of the aerosol size distribution, for which they compared the yearly emissions budget and average

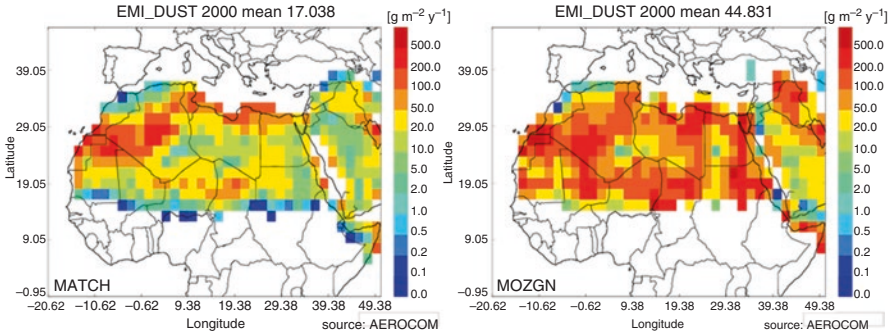

Fig. 3 Dust emission simulated for 2000 by MATCH and MOZGN (Huneeus et al., 2011) in the framework of the AeroCom-Experiment-A model intercomparison exercise. (Figures from https://aerocom.met.no/cgi-bin/surfobs_annualrs.pl (last accessed April 25, 2020))

atmospheric dust load simulated on a global scale: the dust load simulated by the different models ranges from 17 to 29 Tg, whereas model dust emissions vary by a much larger ratio of up to 4. From a second AeroCom intercomparison exercise, Huneeus et al. (2011) confirmed that the simulations of the aerosol optical depth (AOD, which is a proxy of the aerosol content integrated over the whole atmospheric column) performed by global models are quite consistent with no more than a difference of a factor of 2, while there may be a factor of 10 in surface concentrations and deposition. These results illustrate how the mass budget between simulated dust emissions and deposition can differ from one model to another.

As an example, Fig. 3 reports the dust emissions simulated for North Africa and western Middle East by the MATCH and MOZGN global models (see more information about the these CTM and the aerosol modules in Textor et al., 2006, 2007), pointing out the differences in (i) the mean annual dust emission fluxes simulated for 2000 and (ii) the relative importance of the main dust sources. With MOZGN, the simulated dust emissions are almost three times higher than the ones with MATCH (45 vs 17 g m^{-2} $year^{-1}$), and the eastern and southern Sahara as well as the Middle East sources are much more active in MOZGN simulations.

This large difference in simulated dust emissions reflects the uncertainties that persist in modeling dust emissions. In fact, our ability to document the surface and soil parameters as well as the surface winds is a key point to model dust emissions. Figure 4 illustrates the erosion threshold wind speeds computed at high resolution for the Sahara and Middle Eastern deserts combining Z_0 derived from POLDER satellite observations (Marticorena et al., 2004; Laurent et al., 2008) and soil in situ measurements representative of large desert landscapes. This shows that the 10-m wind speed required for dust emissions from most of the desert source areas range from about 6 to 20 m s^{-1}, which are generally not, and by far, the most frequent wind speeds of the wind speed distribution (e.g., Menut, 2008). For example, in the Sahel, the time during which the wind speed exceeds the wind threshold for wind erosion is of the order of only 36–48 hours by year (Bergametti et al., 2017). This means that meteorological fields used in 3D models should reproduce precisely the part of

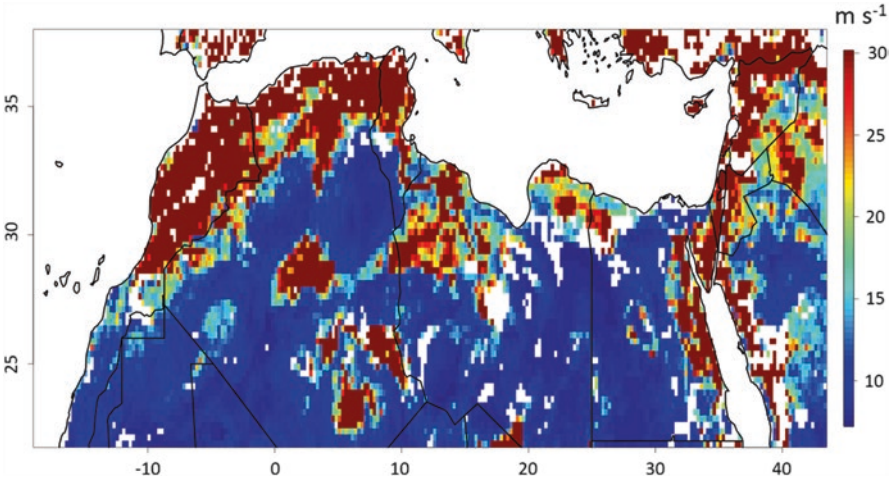

Fig. 4 Map of the minimum 10m erosion threshold wind speed (in m s^{-1}) over North Africa ¼° × ¼° spatial resolution. (After data from Laurent et al., 2008)

the wind speed distribution corresponding to the highest wind speeds and, generally, they do not (e.g., Cowie et al., 2015; Torralba et al., 2017).

Using a semi-empirical model (Marticorena & Bergametti, 1995) and this database specifically developed to document the erosion wind threshold for North African desert areas, annual dust emission of 670 Mt was simulated for the Sahara desert: 480 being emitted from the western Sahara (16° N–38°N; 19°W–14°E) and 190 from the eastern Sahara (16° N–38°N; 14°E–40°E) (Laurent et al., 2008). These simulations were in agreement with the early proposed estimation by d'Almeida (1986) (630–710 Mt $year^{-1}$ for 1981 and 1982). A significant part of the dust emitted from these regions can be transported over the Mediterranean area. It was estimated that between 80 and 120 Mt of dust are transported per year northward from the Sahara (d'Almeida, 1986).

Mineral dust emissions could also result from soil disturbance due to changes in human activities, desertification, and intensification of high surface winds connected to climate change. The quantification of anthropogenic dust emissions and their relative contribution to the global dust emissions remain uncertain and under debate (e.g., Mahowald et al., 2010; Ginoux et al., 2012), although progress has been made in understanding the human impact on these areas. For a given site, each ecological state (e.g., grassland, shrub-invaded grassland, or shrubland) has some ranges of potential wind erodibility based on the ground cover dynamics and soil disturbance frequency. These characteristics are modulated by land use intensity and management practices, which may also be drivers of ecological state change (Bestelmeyer et al., 2015; Webb & Pierre, 2018). For instance, the Mediterranean basin, on both its eastern and southern borders, has been subject to major changes in land uses, including deforestation and increase in surfaces devoted to agricultural and urban activities. Moreover, the semi-arid areas that contribute to the dust

content observed over the Mediterranean basin are especially vulnerable to changes in precipitation patterns which could generate drought periods that favor dust emissions. These different conditions have certainly already modified the mineral dust content of the Mediterranean region and its composition even if the magnitude of these effects remains unknown at that time. The socioeconomic development in North African countries has induced a growing pressure on natural soils with an expansion of cultivated areas and the introduction of modern techniques (e.g., Khatteli et al., 2016). While most plowing operations in North Africa during the 1960s were based on draft animals and traditional tools, tractors and disc plows have progressively replaced these former techniques (Labiadh et al., 2013 and references therein). Labiadh et al. (2013) measured saltation flux and micrometeorological parameters in South Tunisia over agricultural plots constituted of very fine sand (Labiadh et al., 2011) that have been tilled with different plowing tools (moldboard, tiller, disc). Their results show that the saltation fluxes are significantly higher over agricultural surfaces tilled by disc plow, a technique recently introduced in North Africa, compared to those measured on the plot tilled with tiller plows (by a factor 4) or with moldboard (by one order of magnitude), a technique more similar to traditional practices. These results strongly suggest that new techniques of tillage, like disc, could modify drastically the soil erosion by wind, at least on agricultural plots constituted of loose soils (Labiadh et al., 2013). This also suggests that changes in agricultural management practices could have similar or even higher impacts on dust emissions than those induced by the increase in agricultural surfaces.

3 Meteorological Situations Favorable to Dust Emission and Transport Toward the Mediterranean

Different meteorological mechanisms are responsible for high wind speeds and thus dust emission. In this section, some of the most frequent situations are illustrated. For instance, in the Sahara, they are mainly connected to (i) the diurnal cycle of the nocturnal low-level jet, (ii) large-scale synoptic systems and associated fronts, and (iii) convective cells of various sizes.

The diurnal cycle of the nocturnal low-level jet (NLLJ), associated with a wind speed maximum frequently forming in the lower troposphere at nighttime, is responsible for most of the high wind speeds, especially during morning in the Sahelian and Saharan regions (e.g., Fiedler et al., 2013; Knippertz, 2008; Marsham et al., 2013). The most common process responsible for the formation of NLLJ is a decoupling of the airflow from surface friction which then oscillates around the geostrophic wind (Blackadar, 1957). One of the requirements for the formation of the NLLJ is a radiative cooling creating a surface inversion that stabilizes the surface layer. In the morning, from sunrise to about midday, the turbulence grows by surface heating, allowing downward mixing of momentum from the NLLJ to produce surface wind speeds that can be sufficient to initiate wind erosion and dust emission.

At the synoptic scale, the key feature for dust emission is the existence of an intense, low-level pressure gradient that can generate sufficiently high wind speeds. Depending on the season, different positions of troughs and high-pressure systems occur over the Sahara. As an example, in spring, a season especially favorable to Saharan dust transport toward Europe and the Mediterranean region, dust emissions are frequently due to intense low-level cyclones linked to the penetration to low latitudes of an upper level trough moving eastward along the northern margin of the Sahara (e.g., Moulin et al., 1998; Kubilay et al., 2000; Barkan et al., 2005, Barkan & Alpert, 2008; Knippertz & Todd, 2012). The associated dust events are the well-known Khamsin in Libya and Egypt or Sharav in the Middle East. More details can be found in Alpert and Ziv (Alpert & Ziv, 1989), Bou Karam et al. (2010), and Knippertz and Todd (2012).

Lastly, the gust front outflows caused by moist convection are also responsible for high wind speeds and intense dust emission. Typical cases of such events are haboobs that occur frequently in the Sahel as a consequence of the passing of mesoscale convective systems and other squall lines. This type of process linked to strong evaporation and downdraft caused by dry air at mid-level can also be observed in the foothills of mountain ranges such as along the Atlas chain (Knippertz et al., 2007).

Because various meteorological situations control the frequency of dust events in the North of Africa, their occurrence varies significantly on seasonal, annual, and decadal time scales (Goudie & Middleton, 2001; Klose et al., 2010). For instance, dust emissions show marked seasonal cycles driven by both local surface winds and large-scale atmospheric dynamics. Multiannual simulations performed by Laurent et al. (2008) point out different seasonal cycles of dust emissions between the western and eastern parts of the Sahara, with a maximum in summer for the western Sahara and in spring for the eastern Sahara. This is in good agreement with observations: the highest dust event frequencies are recorded in late spring and summer in the western basin and spring (and to a lesser extent in fall) in the eastern basin (Bergametti et al., 1989; Ganor, 1994; Kubilay & Saydam, 1995; Prospero, 1996; Moulin et al., 1998; Koçak et al., 2004; Meloni et al., 2007). Even if dust emissions exhibit a different seasonal pattern from one part of the basin to another, dust events can be observed in the Mediterranean all along the year. Depending on the sub-Mediterranean region, between 15 and 30 sporadic and pulsed dust events having generally a 2–3-day duration occur every year (Loÿe-Pilot & Martin, 1996; Bergametti et al., 1989; Ganor, 1994; Barkan et al., 2005; Meloni et al., 2008), but are observed more frequently in the southern part of the basin (Pey et al., 2013). During these sporadic dust events, the concentration in particulate matter measured in the Mediterranean atmosphere can increase drastically in a very short time (e.g., Pey et al., 2013).

The main atmospheric configurations favoring the transport of dust from North Africa toward the western Mediterranean are illustrated in Fig. 5 (Bout-Roumazeilles et al., 2007, based on the works of Coudé-Gaussen, 1982; Coudé-Gaussen et al., 1987; Bergametti et al., 1989; Rodrıguez et al., 2001).

It appears that (1) a SW-NE transport toward the northern Mediterranean occurs mostly in winter when a large depression system develops between the Canary

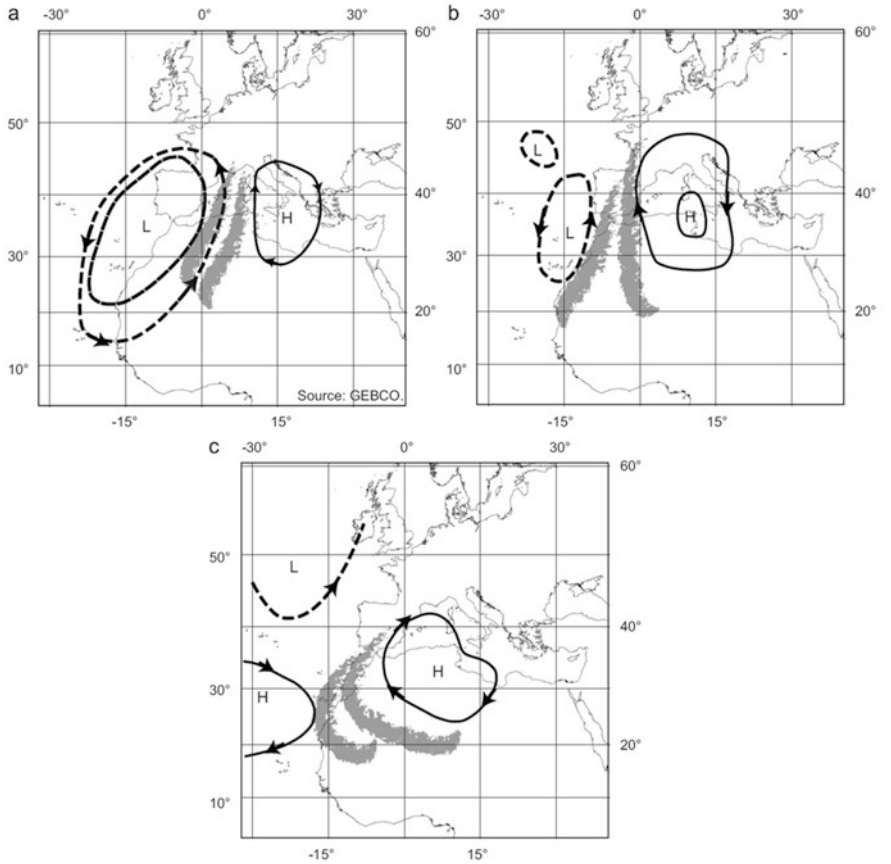

Fig. 5 Three main atmospheric configurations favoring the meridional transport of Saharan dust toward Europe: (**a**) during winter with a strong low pressure (L) over the Iberian Peninsula; (**b**) during fall with a strong high pressure (H) over the central Mediterranean combined with a low pressure off Portugal; and (**c**) during summer with a strong low pressure over North Africa and tropical Atlantic and a low pressure over the North Atlantic. (Figure reprinted from Fig. 2 in Bout-Roumazeilles et al., 2007)

Islands and the Iberian Peninsula; (2) during inter-seasons, a SE-NW transport is initiated by the simultaneous occurrence of a strong central European anticyclone and of a depression off Portugal; and (3) summer dust transport may result from the westward shift of the North African anticyclone associated with the remoteness of the Azores High, which provides a SW-NE depression trench along the African coasts toward the Iberian Peninsula and western part of the Mediterranean (Bout-Roumazeilles et al., 2007). Dust events in the eastern Mediterranean are usually associated with strong south-westerly and southerly flows in the region, although events have been reported under easterly flow conditions in the easternmost part of the basin (Dayan et al., 1991; Levi & Rosenfeld, 1996).

4 Dust Source Regions of Interest for the Mediterranean

Far from dust source regions, the earlier works to identify the provenance of dust transported over the Mediterranean basin were mainly based on backward air mass trajectories, sometimes associated with elemental or mineralogical tracers and/or qualitative analysis of satellite images (e.g. Prodi & Fea, 1979; Reiff et al., 1986; Bergametti et al., 1989). Most of these studies focused on the western part of the basin. It was found that the dust sources contributing the most to long-range transport were located in the northern part of the Sahara (the southern border of the Atlas Mountain in Morocco and Algeria, the Jeffara area in Tunisia, and Libya) and some events could also result from dust sources located deeper inside the Sahara south of 30°N (e.g., Bergametti et al., 1989; Avila et al., 1997). Studies of dust plume events over the Sahara using Infrared Difference Dust Index derived from METEOSAT observations were also conducted (Legrand et al. (1994), and from METEOSAT observations, Moulin et al. (1998). They confirmed the importance of dust source regions around 30°N from Morocco to Egypt for the Mediterranean region.

Middleton and Goudie (2001) and Prospero et al. (2002) used the TOMS (Total Ozone Mapping Spectrometer) Absorbing Aerosol Index to localize the main source areas of mineral dust. The analysis of these observations averaged over decadal periods (Prospero et al., 2002; Washington et al., 2003) also suggests that the main sources for the Mediterranean basin are located in eastern Algeria-Tunisia, and Libya and Egypt for the easternmost part of the basin. TOMS data points out the extensive system of chotts (i.e., salty depression) and dry lakes located on the southern flanks of the Atlas, as the region of most intense dust activity. Sources are also active in a large area of the eastern Libyan Desert. In Egypt, the main source identified by TOMS is ranging from 24°N to 27°N and from 29°E and 33°E, i.e., the Ghurd Abu Muharrik region, also called the Abu Mukharri Dunes.

Another analysis of the TOMS data performed by Israelevich et al. (2002) disagrees with the previous studies regarding the respective importance of the northern and southern Saharan sources of dust for the Mediterranean basin. The authors point out two regions, also identified by Prospero et al. (2002) and Washington et al. (2003), deeply inside the Sahara, one centered around 16°N and 16°E and corresponding roughly to the Chad basin and one located around 19°N and 6°W (Eljouf basin) as the primary sources of dust for the Mediterranean basin. These authors assume that the dust events over the Mediterranean are not caused directly by the increased dust supply (dust storms) from the main source regions but by the occurrence of favorable synoptic conditions (Sharav cyclones). The role of these source regions would be to maintain a reservoir of desert aerosol above the whole of northern Africa during spring and summer, this dust being transported northward and eastward to the Mediterranean region each time a cyclone is formed.

Based on a global-scale high-resolution (0.1°) mapping of sources using MODIS (Moderate Resolution Imaging Spectroradiometer) Deep Blue estimates of dust optical depth (M-DB2 DOD) and land use data sets, Ginoux et al. (2012) investigated dust sources worldwide. They ascribed dust sources to natural and

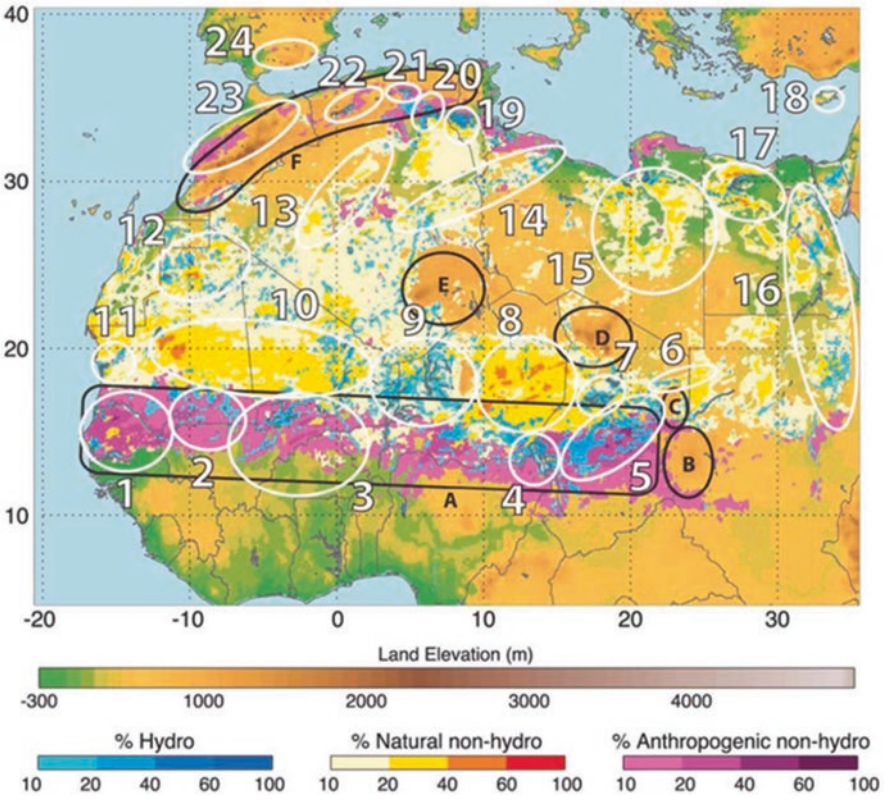

Fig. 6 Distribution of the relative number of days per year (%) with M-DB2 DOD >0.2 over North Africa overplotted on shaded orography. The frequencies associated with (hydro) and without (non-hydro) ephemeral water bodies and with less (natural) and more (anthropogenic) than 30% land use are shaded in blue; yellow, red, and orange; and magenta, respectively. The frequency levels are 10%, 20%, 40%, 60%, and 100%. The topography shading varies from dark green (300 m) to brown (1000–4000 m) and then to gray for higher elevation. Some source areas, discussed in the text, are contoured in white and are numbered as follows: 1, Senegal River Basin; 2, Aoukar depression; 3, upper Niger River Basin; 4, Lake Chad; 5, river drainage basin of the Ennedi and Ouaddaï Highlands; 6, Mourdi depression; 7, Bodélé depression; 8, Grand Erg of Bilma; 9, river drainage basin of the Aïir; 10, Erg El Djouf; 11, Sebkhet te-n-Dgâmcha; 12, Tiris Zemmour region; 13, Grand Erg Occidental; 14, Grand Erg Oriental; 15, Libyan Desert; 16, Nile River Basin; 17, Qattara depression; 18, Mesaoria plain in Cyprus; 19, Chott el Jerïd; 20, Chott Melrhir; 21, Chott el Hodna; 22, Chott Ech Chergui; 23, Morocco coastal plains; and 24, Andalusia in Spain. Some geographic features are contoured in black and are labeled as follows: A, the Sahel; B, the Ouaddaï Highlands; C, Ennedi; D, Tibesti; E, Ahaggar; and F, Atlas Mountains. (Reprinted from Fig. 7 in Ginoux et al., 2012)

anthropogenic (primarily agricultural) origins and estimated their respective contributions to dust emissions. They estimated that 8% of North African dust emissions were anthropogenic, mostly from the Sahel. Moreover, sources in the Atlas Mountains and along the Mediterranean coast were generally anthropogenic (Fig. 6). According to these authors, local dust activity observed in Southern Spain and Cyprus is also mainly associated with anthropogenic activities.

More recently, Vincent et al. (2016) discussed how different Saharan dust regions can contribute to dust deposition in the western Mediterranean from a joint analysis of weekly deposition measurements performed between 2011 and 2013 at five locations, MODIS AOD and HYSPLIT air mass trajectories(see also the chapter by Laurent et al., 2022). For each identified dust deposition event, the most southerly location of the highest AOD along the modelled air mass trajectory defined a region where dust originated. The identified regions were relatively large to account for the uncertainties of the trajectory model and the associated meteorological data. It should also be kept in mind that other sources located along the pathway of the dust plume can also contribute to the dust uplifts. Vincent et al. (2016) defined seven areas of dust provenance by grouping together the closest dust localizations (Fig. 7): Niger and Chad (DPA1), northern Mali and southern Mauritania (DPA2), western Sahara and southern Morocco (DPA3), central Algeria (DPA4), Libya (DPA5), Tunisia and eastern Algeria (DPA6), and northern Morocco and northwestern Algeria (DPA7). Almost 3/4 of the dust deposition collected in the northwestern Mediterranean and south of France comes from the western part of the Sahara, when source provenance areas, even south of 20° N, like Niger and Chad, and northern Mali and southern Mauritania, could contribute to dust deposition in the western Mediterranean but are definitely not dominant. Western Sahara and Tunisia were the most frequent origins of dust deposited in Majorca. Salvador et al. (2014) identified Tunisian and Libyan sources for specific dust outbreaks observed in spring in Balearic Islands and central Mediterranean. Dust deposited in Corsica generally came from the Western Sahara and southern Morocco, Tunisia and eastern Algeria, and Libya (Vincent et al., 2016). The authors also noted that dust deposited in Lampedusa generally came from the Tunisian and Libyan regions and central Algeria. Marconi et al. (2014) also pointed out source regions located in Tunisia-Algeria and Libya to explain atmospheric dust content in Lampedusa, and Meloni et al. (2008) indicated Morocco, Algeria, and Tunisia as dust loading areas, as well as southern areas in Mauritania-Mali. These results illustrate that Saharan dust coming from different regions contributes in different proportions to the dust deposition in the different parts of the western Mediterranean basin.

Achilleos et al. (2020) investigated the spatiotemporal variability of desert dust storms in the eastern Mediterranean between 2006 and 2017. They used PM_{10} and dust-AOD obtained in Finokalia (Crete, Greece), Ayia Marina Xyliatos (Cyprus), and Beer Sheva (Israel) combined with HYSPLIT trajectories to determine the influence of Saharan and Middle Eastern desert dust sources on the eastern Mediterranean on an annual level. Finokalia station was influenced almost exclusively by dust coming from the Sahara desert, only a small number of events being influenced at the same time by air masses originating from both Saharan and Middle Eastern deserts. However, during the years 2012 and 2015 in Cyprus and 2013 in Israel, the number of dust events originating from Middle Eastern deserts increased. On average, desert dust storms originating from North Africa and the Middle East were of higher intensity in Ayia Marina station, and those originating from the Sahara desert, in Beer Sheva station. Linear trends analysis showed that desert dust

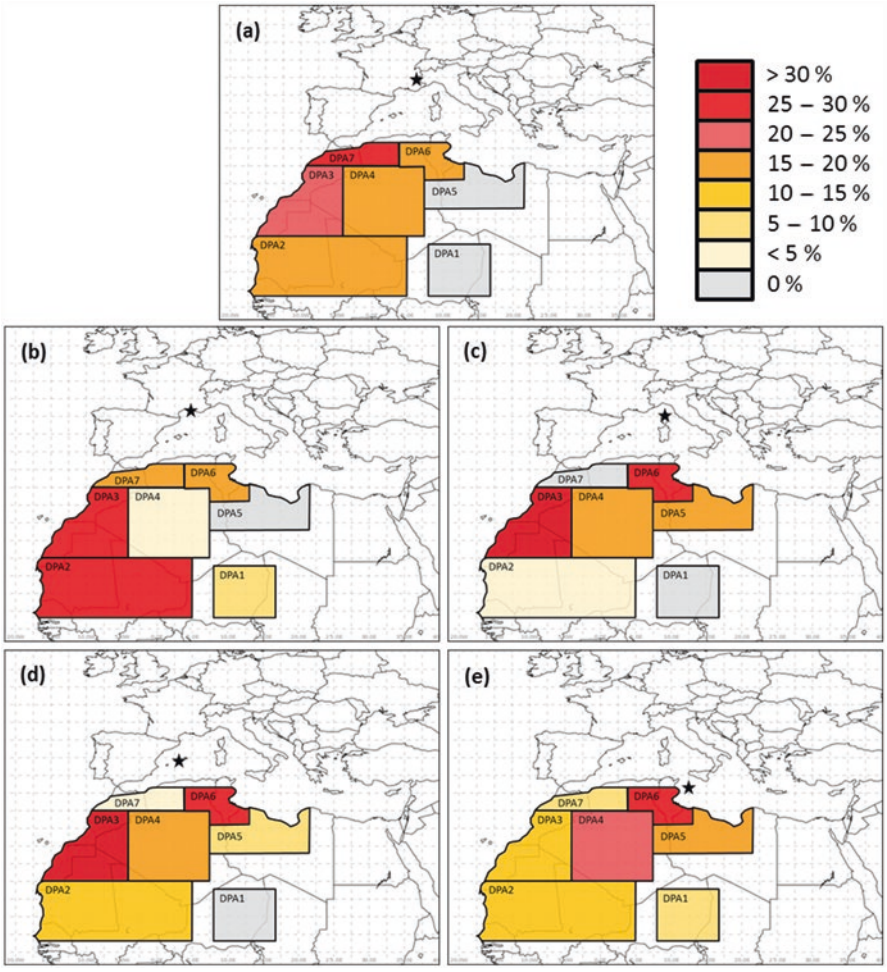

Fig. 7 Frequency of dust provenance areas identified using MODIS AOD and HYSPLIT air mass trajectories for the dust deposition events recorded at five stations indicated by a star: (**a**) Le Casset, (**b**) Frioul, (**c**) Corsica, (**d**) Majorca, and (**e**) Lampedusa. (Reprinted from Fig. 6 in Vincent et al., 2016)

storms originating solely from Sahara or from both Saharan and Middle Eastern deserts in Cyprus, and from pure Saharan dust in Israel, decreased over years (Achilleos et al., 2020). From the analysis of long time series of dust falls, Ganor (1991) suggested also that North Africa is the main source of desert dust transported in Israel, while dust from sources in the Middle East is more typically transported to the Mediterranean in autumn (Dayan, 1986; Kubilay et al., 2000, 2005).

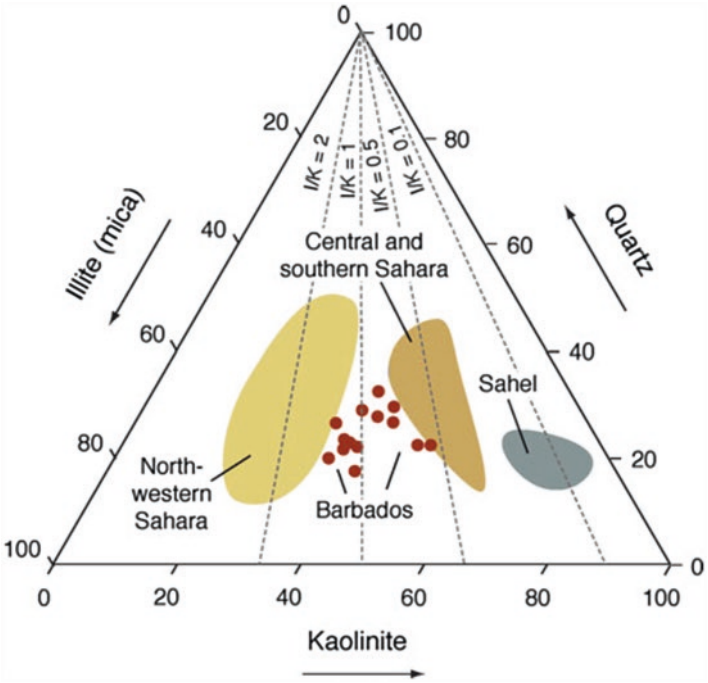

Fig. 8 Ternary diagram showing abundances of quartz, illite (mica), and kaolinite in dust samples collected off the coast of Africa attributed to various regions of origin (shaded polygons) based on back-trajectory analyses. Also shown are values of dust samples collected in Barbados. Dashed lines correspond to various illite/kaolinite ratios (I/K). (Reprinted from Fig. 3.5 in Muhs et al., 2014)

5 Dust Composition as a Tracer of Source Regions

The intrinsic composition of emitted dust is linked to the composition of its parent soil through the physical emission processes. Tracers, as specific as possible and conservative throughout the dust cycle, have been sought in order to trace the dust back to its source area. Indeed, the location of the source regions controls the chemical and mineralogical composition of dust particles (Bergametti et al., 1989; Lafon et al., 2004; Moreno et al., 2006). Mineral dust particles are dominated by clay minerals (illite, kaolinite, smectite, chlorite, etc.), calcium carbonates (calcite $CaCO_3$, dolomite $CaMgCO_3$), quartz, and feldspars (Ganor, 1991; Molinari, 1996; Caquineau et al., 1998; Falkovich et al., 2001). Iron oxides and gypsum ($CaSO_4$) are also frequently observed in dust but in minor proportions (Glaccum & Prospero, 1980; Lafon et al., 2004). Illite is the dominant clay mineral in dust emitted from the north and east Sahara, whereas kaolinite exhibits significant amounts in dust emitted from southern and central Sahara (Avila et al., 1997; Chiapello et al., 1997; Caquineau et al., 1998) and is often dominant in Sahelian dust (Fig. 8).

Dust emitted from the large sedimentary areas in the northern Sahara exhibits high carbonate contents (Löye-Pilot et al., 1986; Losno et al., 1991; Chiapello et al., 1997; Avila & Rodà, 2002; Avila et al., 2007). However, one of the problems addressed by chemical and mineralogical tracers is that the proportions of the various minerals change during transport due to the deposition of the largest particles and/or chemical transformations. In fact, the consequence of deposition is generally an increase in the proportion of clay minerals (mainly located in the smallest part of the dust size distribution) and a decrease in quartz (generally associated with coarser grains). Chemical transformations occurring during transport affect the mineralogical mixture (Usher et al., 2003), like the transformation of calcium carbonates into fresh gypsum or calcium nitrates by reaction with acidic sulfur and nitrogen species in the moist atmosphere (Glaccum & Prospero, 1980; Yuan et al., 2006; Gibson et al., 2006; see also the chapter by Becagli, (2022)).

Finally, radiogenic isotopes, especially Sr and Nd, the contents of which depend both on the lithology and on the age of the parent rocks from which dust is derived, have proved to be the most discriminating array of tracers, especially when used in conjunction with others (such as clay mineralogy) (Scheuvens et al., 2013 and references therein; Table 1). Studies in the Mediterranean and in southeastern Europe showed that this approach could also be profitably applied to investigate dust provenance in this region. The Nd isotopic composition has been particularly well documented. The $^{143}Nd/^{144}Nd$ ratio (often defined as $\mathcal{E}_{Nd}(0) = ((^{143}Nd/^{144}Nd/0.512638) - 1) \times 10{,}000$ where 0.512638 is a standard reference ratio) has the advantage over the $^{87}Sr/^{86}Sr$ ratio to be less affected by grain size (Goldstein et al., 1984; Grousset & Biscaye, 2005). The $^{87}Sr/^{86}Sr$ ratio is also highly sensitive to the calcium carbonate content, which generally bears a distinct isotopic composition (often seawater-like) from the silicate fraction of the dust, and may therefore, when not removed, obliterate some of the provenance information.

Most of the $^{143}Nd/^{144}Nd$ and $^{87}Sr/^{86}Sr$ ratios for dust particles in the Mediterranean region roughly match the isotopic composition of Saharan dust (Grousset et al., 1998). Extensive mapping of the isotopic composition in North African potential source areas (Grousset et al., 1992, 1998, 2003), combined with air-mass backtrajectories and Nd isotopes, in particular, has permitted locating the source areas of some dust events crossing the Mediterranean Sea with a relatively good precision.

Table 1 Geographical regions of northern Africa with representative $^{87}Sr/^{86}Sr$ and $\mathcal{E}_{Nd}(0)$ values (Scheuvens et al., 2013 and references therein)

Source region	$^{87}Sr/^{86}Sr$	$\mathcal{E}_{Nd}(0)$ (per 10,000)
Northern region (Morocco, Algeria)	0.717–0.727	−17.1 to −8.3
West (western Sahara, Mauritania)	0.720–0.738	−17.9 to −13.5
Senegal	0.715–0.737	−16.2 to −14.5
Tunisia	0.714	−9.5
Libya	0.715	−15.4 to −10.7
Egypt and northern Sudan	0.705–0.718	−11.0 to −3.9
Sub-Saharan (without Senegal)	0.715–0.724	−12.4 to −10.0

Distinct contributing sources, in Mauritania and in Libya, for instance, have been identified (Grousset et al., 2003), substantiating independent evidence for varying sources and transport pathways (Bergametti et al., 1989; Bout-Roumazeilles et al., 2007, and references therein).

6 Conclusion and Perspectives

The different perspectives considered in this chapter, both meteorological and geochemical, whether based on observations or models, suggest in a convergent way that the entire Sahara, even its southernmost part, can contribute to the dust events observed in the Mediterranean basin. It seems that the northern sources, especially those located on the border of the Atlas Mountains, in Tunisia, Libya, and Egypt are probably the most frequent dust providers for the western and central Mediterranean. But, it is also probable that large-scale dust events, originating from well-known active dust sources like the Bodélé depression or the western Sahara, are responsible for the most intense dust transport events toward the Mediterranean basin. The Middle Eastern deserts also appear to be seasonal major sources of dust in the eastern Mediterranean basin. However, a more systematic identification of the source regions distinguishing between the most intense and the most frequent sources remains to be done. This should be assessed in a context of semi-arid area evolution under anthropogenic activities and climate change. The ongoing advancement of remote sensing techniques (e.g., high-resolution and high-frequency satellite imagery) and to a lesser degree of meteorological data (e.g., model air-mass trajectories), combined with chemical and mineralogical approaches, provide invaluable tools for mineral dust source identification. Jointly used with isotopic techniques, this helps to pinpoint the provenance of the dust when it is deposited up to thousands of kilometers from its desert source area in the Mediterranean region.

References

Achilleos, S., Mouzourides, P., Kalivitis, N., Katra, I., Kloog, I., Kouis, P., Middleton, N., Mihalopoulos, N., Neophytou, M., Panayiotou, A., Papatheodoroua, S., Savvides, C., Tymvios, P., Vasiliadou, E., Yiallouros, P., & Koutrakis, P. (2020). Spatio-temporal variability of desert dust storms in Eastern Mediterranean (Crete, Cyprus, Israel) between 2006 and 2017 using a uniform methodology. *Science of the Total Environment, 714*, 136693. https://doi.org/10.1016/j.scitotenv.2020.136693

Albani, S., Mahowald, N. M., Perry, A. T., Scanza, R. A., Zender, C. S., Heavens, N. G., Maggi, V., Kok, J. F., & Otto-Bliesner, B. L. (2014). Improved dust representation in the Community Atmosphere Model. *Journal of Advances in Modeling Earth Systems, 6*, 541–570. https://doi.org/10.1002/2013MS000279

Alfaro, S. C., & Gomes, L. (2001). Modeling mineral aerosol production by wind erosion: Emission intensities and aerosol size distributions in source areas. *Journal of Geophysical Research, 106*, 18075–18084. https://doi.org/10.1029/2000JD900339

Alpert, P., & Ziv, B. (1989). The Sharav cyclone: Observations and some theoretical considerations. *Journal of Geophysical Research, 94*, 18495–18514. https://doi.org/10.1029/JD094iD15p18495

Avila, A., Alarcón, M., Castillo, S., Escudero, M., García Orellana, J., Masqué, P., & Querol, X. (2007). Variation of soluble and insoluble calcium in red rains related to dust sources and transport patterns from North Africa to northeastern Spain, *Journal of Geophysical Research, 112*, D05210. https://doi.org/10.1029/2006JD007153

Avila, A., & Rodà, F. (2002). Assessing decadal changes in rainwater alkalinity at a rural Mediterranean site in the Montseny Mountains (NE Spain). *Atmospheric Environment, 36*, 2881–2890. https://doi.org/10.1016/S1352-2310(02)00098-5

Avila, A., Queralt-Mitjans, I., & Alarcón, M. (1997). Mineralogical composition of African dust delivered by red rains over northeastern Spain. *Journal of Geophysical Research, 102*, 21977–21996. https://doi.org/10.1029/97JD00485

Bagnold, R. A. (1941). *The physics of blown sand and desert dunes*. Methuen and Co, 286 pp. + 16 plates.

Barkan, J., & Alpert, P. (2008). Synoptic patterns associated with dusty and non-dusty seasons in the Sahara, Theor. Appl. Climatol., 94, 153–162. https://doi.org/10.1007/s00704-007-0354-9

Barkan, J., Alpert, P., Kutiel, H., & Kishcha, P. (2005). Synoptics of dust transportation days from Africa toward Italy and central Europe. *Journal of Geophysical Research, 110*, D07208. https://doi.org/10.1029/2004JD005222

Basart, S., Pérez García-Pando, C., Cuevas, E., Baldasano Recio, J. M., & Gobbi, G. P. (2009). Aerosol characterization in Northern Africa, Northeastern Atlantic, Mediterranean basin and Middle East from direct-sun AERONET observations. *Atmospheric Chemistry and Physics, 9*, 8265–8282. https://doi.org/10.5194/acp-9-8265-2009

Becagli, S. (2022). Aerosol composition and reactivity. In F. Dulac, S. Sauvage, & E. Hamonou (Eds.), *Atmospheric chemistry in the Mediterranean Region* (Vol. 2, From air pollutant sources to impacts). Springer, this volume. https://doi.org/10.1007/978-3-030-82385-6_13

Belnap, J., & Gillette, D. A. (1998). Vulnerability of desert biological soil crusts to wind erosion: The influences of crust development, soil texture, and disturbance. *Journal of Arid Environments, 39*, 133–142. https://doi.org/10.1006/jare.1998.0388

Bergametti, G., & Forêt, G. (2014). Dust deposition. In P. Knippertz & J.-B. W. Stuut (Eds.), *Mineral dust: A key player in the earth system* (pp. 179–200). Springer. https://doi.org/10.1007/978-94-017-8978-3_8

Bergametti, G., Gomes, L., Remoudaki, E., Desbois, M., Martin, D., & Buat-Ménard, P. (1989). Present transport and deposition patterns of African dusts to the North-Western Mediterranean. In M. Leinen & M. Sarnthein (Eds.), *Paleoclimatology and paleometeorology: Modern and past patterns of global atmospheric transport* (NATO ASI Series, Series C) (Vol. 282, pp. 227–252). Kluwer. https://doi.org/10.1007/978-94-009-0995-3_9

Bergametti, G., Marticorena, B., Rajot, J. L., Chatenet, B., Féron, A., Gaimoz, C., Siour, G., Coulibaly, M., Koné, I., Maman, A., & Zakou, A. (2017). Dust uplift potential in the central Sahel: An analysis based on 10 years of meteorological measurements at high temporal resolution. *Journal of Geophysical Research, 122*, 12433–12448. https://doi.org/10.1002/2017JD027471

Bestelmeyer, B. T., Okin, G. S., Duniway, M. C., Archer, S. R., Sayre, N. F., Williamson, J. C., & Herrick, J. E. (2015). Desertification, land use, and the transformation of global dryland. *Frontiers in Ecology and the Environment, 13*, 28–36. https://doi.org/10.1890/140162

Betzer, P., Carder, K., Duce, R., Merrill, J. T., Tindale, N. W., Uematsu, M., Costello, D. K., Young, R. W., Feely, R. A., Breland, J. A., Bernstein, R. E., & Greco, A. M. (1988). Long-range transport of giant mineral aerosol particles. *Nature, 336*, 568–571. https://doi.org/10.1038/336568a0

Blackadar, A. K. (1957). Boundary layer wind maxima and their significance for the growth of nocturnal inversions. *Bulletin of the American Meteorological Society, 83*, 283–290. https://doi.org/10.1175/1520-0477-38.5.283

Bou Karam, D., Flamant, C., Cuesta, J., Pelon, J., & Williams, E. (2010). Dust emission and transport associated with Saharan depression: February 2007 case. *Journal of Geophysical Research, 115*, D00H27. https://doi.org/10.1029/2009JD012390

Bouet, C., Labiadh, M. T., Rajot, J.-L., Bergametti, G., Marticorena, B., Henry des Tureaux, T., Ltifi, M., Sekrafi, S., & Féron, A. (2019). Impact of desert dust on air quality: What is the meaningfulness of daily PM standards in regions close to the sources? The example of southern Tunisia. *Atmosphere, 10*, 452. https://doi.org/10.3390/atmos10080452

Bout-Roumazeilles, V., Combourieu Nebout, N., Peyron, O., Cortijo, E., Landais, A., & Masson-Delmotte, V. (2007). Connection between South Mediterranean climate and North African atmospheric circulation during the last 50,000 yr BP North Atlantic cold events. *Quaternary Science Reviews, 26*, 3197–3215. https://doi.org/10.1016/j.quascirev.2007.07.015

Caquineau, S., Gaudichet, A., Gomes, L., Magonthier, M.-C., & Chatenet, B. (1998). Saharan dust: Clay ratio as a relevant tracer to assess the origin of soil-derived aerosols. *Geophysical Research Letters, 25*, 983–986. https://doi.org/10.1029/98GL00569

Chatenet, B., Marticorena, B., Gomes, L., & Bergametti, G. (1996). Assessing the micropeds-size distribution of desert soils erodible by wind. *Sedimentology, 43*, 901–911. https://doi.org/10.1111/j.1365-3091.1996.tb01509.x

Chen, W., Zhibao, D., Zhenshan, L., & Zuotao, Y. (1996). Wind tunnel test of the influence of soil moisture on erodibility of loessial sandy loam soil by wind. *Journal of Arid Environments, 34*, 391–402. https://doi.org/10.1006/jare.1996.0119

Chepil, W. S. (1951). Properties of soil that influence wind erosion: IV. State of dry aggregate structure. *Soil Science, 72*, 387–401.

Chepil, W. S. (1956). Influence of moisture on erodibility of soil by wind. *Soil Science Society of America Proceedings, 20*, 288–292.

Chiapello, I., Bergametti, G., Chatenet, B., Bousquet, P., Dulac, F., & Santos-Soares, E. (1997). Origins of African dust transported over the northeastern tropical Atlantic. *Journal of Geophysical Research, 102*, 13701–13709. https://doi.org/10.1029/97JD00259

Coudé-Gaussen, G. (1982). Les poussières éoliennes sahariennes. Mise au point. *Rev. Géomorph. Dyn, 31*, 49–69.

Coudé-Gaussen, G., Rognon, P., Bergametti, G., Gomes, L., Strauss, B., & Le Coustumer, M. N. (1987). Saharan dust on Fuerteventura island (Canaries): Chemical and mineralogical characteristics, air mass trajectories, and probable sources. *Journal of Geophysical Research, 92*, 9753–9771. https://doi.org/10.1029/JD092iD08p09753

Cowie, S. M., Marsham, J. M., & Knippertz, P. (2015). The importance of rare, high-wind events for dust uplift in northern Africa. *Geophysical Research Letters, 42*, 8208–8215. https://doi.org/10.1002/2015GL065819

d'Almeida, G. A. (1986). A model for Saharan dust transport. *Journal of Applied Meteorology, 25*, 903–916. https://doi.org/10.1175/1520-0450(1986)025<0903:AMFSDT>2.0.CO;2

Dayan, U. (1986). Climatology of back trajectories from Israel based on synoptic analysis. *Journal of Applied Meteorology, 25*, 591–595. https://doi.org/10.1175/1520-0450(1986)025<0591:COBTFI>2.0.CO;2

Dayan, U., Heffter, J. L., Miller, J. M., & Gutman, G. (1991). Dust intrusion events into the Mediterranean basin. *Journal of Applied Meteorology, 30*, 1185–1199. https://doi.org/10.1175/1520-0450(1991)030<1185:DIEITM>2.0.CO;2

Dubief, J. (1953). Les vents de sable dans le Sahara Français. In *Colloques Internationaux du CNRS* (Vol. 35, pp. 45–70). CNRS.

Falkovich, A. H., Ganor, E., Levin, Z., Formenti, P., & Rudich, Y. (2001). Chemical and mineralogical analysis of individual mineral dust particles. *Journal of Geophysical Research, 106*, 18029–18036. https://doi.org/10.1029/2000JD900430

Fécan, F., Marticorena, B., & Bergametti, G. (1999). Parameterization of the increase of the aeolian erosion threshold wind friction velocity due to soil moisture for arid and semi-arid areas. *Annales de Geophysique, 17*, 149–157. https://doi.org/10.1007/s00585-999-0149-7

Fiedler, S., Schepanski, K., Heinold, B., Knippertz, P., & Tegen, I. (2013). Climatology of nocturnal low-level jets over North Africa and implications for modeling mineral dust emission. *Journal of Geophysical Research, 118*, 6100–6121. https://doi.org/10.1002/jgrd.50394

Ganor, E. (1991). The composition of clay minerals transported to Israel as indicators of Saharan dust emission. *Atmospheric Environment, 25*, 2657–2664. https://doi.org/10.1016/0960-1686(91)90195-D

Ganor, E. (1994). The frequency of Saharan dust episodes over Tel Aviv, Israel. *Atmospheric Environment, 28*, 2867–2871. https://doi.org/10.1016/1352-2310(94)90087-6

Gibson, E. R., Hudson, P. K., & Grassian, V. H. (2006). Aerosol chemistry and climate: Laboratory studies of the carbonate component of mineral dust and its reaction products. *Geophysical Research Letters, 33*, L13811. https://doi.org/10.1029/2006GL026386

Gillette, D. A. (1977). Fine particulate emissions due to wind erosion. *Transactions of the American Society of Agricultural Engineers, 20*, 890–897. https://doi.org/10.13031/2013.35670

Gillette, D. A., & Goodwin, P. A. (1974). Microscale transport of sand-sized soil aggregates eroded by wind. *Journal of Geophysical Research, 79*, 4080–4084. https://doi.org/10.1029/JC079i027p04080

Gillette, D. A., Adams, J., Muhs, D., & Kihl, R. (1982). Threshold friction velocities and rupture moduli for crusted desert soils for the input of soil particles into the air. *Journal of Geophysical Research, 87*, 9003–9015. https://doi.org/10.1029/JC087iC11p09003

Ginoux, P., Chin, M., Tegen, I., Prospero, J. M., Holben, B., Dubovik, O., & Lin, S. J. (2001). Sources and distributions of dust aerosols simulated with the GOCART model. *Journal of Geophysical Research, 106*, 20255–20273. https://doi.org/10.1029/2000JD000053

Ginoux, P., Prospero, J. M., Gill, T. E., Hsu, N. C., & Zhao, M. (2012). Global-scale attribution of anthropogenic and natural dust sources and their emission rates based on MODIs Deep Blue aerosol products. *Reviews of Geophysics, 50*, RG3005. https://doi.org/10.1029/2012RG000388

Gkikas, A., Basart, S., Hatzianastassiou, N., Marinou, E., Amiridis, V., Kazadzis, S., Pey, J., Querol, X., Jorba, O., Gassó, S., & Baldasano, J. M. (2016). Mediterranean intense desert dust outbreaks and their vertical structure based on remote sensing data. *Atmospheric Chemistry and Physics, 16*, 8609–8642. https://doi.org/10.5194/acp-16-8609-2016

Glaccum, R. A., & Prospero, J. M. (1980). Saharan aerosols over the tropical North Atlantic–Mineralogy. *Marine Geology, 37*, 295–321. https://doi.org/10.1016/0025-3227(80)90107-3

Goldstein, S. L., O'Nions, R. K., & Hamilton, P. J. (1984). A Sm–Nd isotopic study of dusts and particulates from major river systems. *Earth and Planetary Science Letters, 70*, 221–236. https://doi.org/10.1016/0012-821X(84)90007-4

Gomes, L., Bergametti, G., Coudé-Gaussen, G., & Rognon, P. (1990). Submicron desert dust: A sandblasting process. *Journal of Geophysical Research, 95*, 13927–13935. https://doi.org/10.1029/JD095iD09p13927

Goudie, A. S., & Middleton, N. J. (2001). Saharan dust storms: Nature and consequences. *Earth Science Reviews, 56*, 179–204. https://doi.org/10.1016/S0012-8252(01)00067-8

Grousset, F. E., & Biscaye, P. E. (2005). Tracing dust sources and transport patterns using Sr, Nd and Pb isotopes. *Chemical Geology, 222*, 149–167. https://doi.org/10.1016/j.chemgeo.2005.05.006

Grousset, F. E., Rognon, P., Coudé-Gaussen, G., & Pédemay, P. (1992). Origins of peri-Saharan dust deposits traced by their Nd and Sr isotopic composition. *Palaeogeography Palaeoclimatology Palaeoecology, 93*, 203–212. https://doi.org/10.1016/0031-0182(92)90097-O

Grousset, F. E., Parra, M., Bory, A., Martinez, P., Bertrand, P., Shimmield, G., & Ellam, R. M. (1998). Saharan wind regimes traced by the Sr–Nd isotopic composition of subtropical Atlantic sediments: Last glacial maximum vs. today. *Quaternary Science Reviews, 17*, 385–409. https://doi.org/10.1016/S0277-3791(97)00048-6

Grousset, F. E., Ginoux, P., Bory, A., & Biscaye, P. E. (2003). Case study of a Chinese dust plume reaching the French Alps. *Geophysical Research Letters, 30*, 1277. https://doi.org/10.1029/2002GL016833

Huneeus, N., Schulz, M., Balkanski, Y., Griesfeller, J., Prospero, J. M., Kinne, S., Bauer, S., Boucher, O., Chin, M., Dentener, F., Diehl, T., Easter, R., Fillmore, D., Ghan, S., Ginoux, P., Grini, A., Horowitz, L., Koch, D., Krol, M. C., … Zender, C. S. (2011). Global dust model intercomparison in AeroCom phase I. *Atmospheric Chemistry and Physics, 11*, 7781–7816. https://doi.org/10.5194/acp-11-7781-2011

Israelevich, P. L., Levin, Z., Joseph, J. H., & Ganor, E. (2002). Desert aerosol transport in the Mediterranean region as inferred from the TOMS aerosol index. *Journal of Geophysical Research, 107*, 4572. https://doi.org/10.1029/2001JD002011

Iversen, J. D., & White, B. R. (1982). Saltation threshold on Earth, Mars and Venus. *Sedimentology, 29*, 111–119. https://doi.org/10.1111/j.1365-3091.1982.tb01713.x

Kawamura, R. (1964). Study of sand movement by wind. In *Hydraulic Eng. Lab. Tech. Rep. HEL-2-8* (pp. 99–108). Univ. California.

Khatteli, H., Ali, R. R., Bergametti, G., Bouet, C., Hachicha, M., Hamdi-Aissa, B., Labiadh, M., Montoroi, J.-P., Podwojewski, P., Rajot, J.-L., Zaghloul, A. M., & Valentin, C. (2016). Soils and desertification in the Mediterranean region. In S. Thiébault, & J.-P. Moatti (Eds.), *The Mediterranean region under climate change: A scientific update* (IRD ed., pp. 617–625). https://www.researchgate.net/profile/M_Hachicha2/publication/311481928_Soils_and_desertification_in_the_Mediterranean_region/links/5875351d08ae329d62205e8b/Soils-and-desertification-in-the-Mediterranean-region.pdf. Last accessed 15 Sept 2020.

Klose, M., Shao, Y., Karremann, M. K., & Fink, A. H. (2010). Sahel dust zone and synoptic background. *Geophysical Research Letters, 37*, L09802. https://doi.org/10.1029/2010GL042816

Knippertz, P. (2008). Dust emissions in the West African heat trough: The role of the diurnal cycle and of extratropical disturbances. *Meteorologische Zeitschrift, 17*(5), 553–563. https://doi.org/10.1127/0941-2948/2008/0315

Knippertz, P. (2014). Meteorological aspects of dust storms. In P. Knippertz & J.-B. W. Stuut (Eds.), *Mineral dust: A key player in the earth system* (pp. 121–147). Springer. https://doi.org/10.1007/978-94-017-8978-3_6

Knippertz, P., & Todd, M. C. (2012). Mineral dust aerosols over the Sahara: Meteorological controls on emission and transport and implications for modeling. *Reviews of Geophysics, 50*, RG1007. https://doi.org/10.1029/2011RG000362

Knippertz, P., Deutscher, C., Kandler, K., Müller, T., Schulz, O., & Schütz, L. (2007). Dust mobilization due to density currents in the Atlas region: Observations from the SAMUM 2006 field campaign. *Journal of Geophysical Research, 112*, D21109. https://doi.org/10.1029/2007JD008774

Koçak, M., Kubilay, N., & Mihalopoulos, N. (2004). Ionic composition of lower tropospheric aerosols at a Northeastern Mediterranean site: Implications regarding sources and long-range transport. *Atmospheric Environment, 38*, 2067–2077. https://doi.org/10.1016/j.atmosenv.2004.01.030

Kok, J. (2011). A scaling theory for the size distribution of emitted dust aerosols suggests climate models underestimate the size, of the global dust cycle. *PNAS, 108*, 1016–1021. https://doi.org/10.1073/pnas.1014798108

Kok, J. F., Mahowald, N. M., Fratini, G., Gillies, J. A., Ishizuka, M., Leys, J. F., Mikami, M., Park, M. S., Park, S. U., Van Pelt, R. S., & Zobeck, T. M. (2014). An improved dust emission model – Part 1: Model description and comparison against measurements. Atmospheric Chemistry and Physics, 14, 13023–13041. https://doi.org/10.5194/acp-14-13023-2014.

Kubilay, N., & Saydam, A. C. (1995). Trace elements in atmospheric particulates over the Eastern Mediterranean; Concentrations, sources, and temporal variability. *Atmospheric Environment, 29*, 2289–2300. https://doi.org/10.1016/1352-2310(95)00101-4

Kubilay, N., Nickovic, S., Moulin, C., & Dulac, F. (2000). An illustration of the transport and deposition of mineral dust onto the eastern Mediterranean. *Atmospheric Environment, 34*, 1293–1303. https://doi.org/10.1016/S1352-2310(99)00179-X

Kubilay, N., Oguz, T., Koçak, M., & Torres, O. (2005). Ground-based assessment of Total Ozone Mapping Spectrometer (TOMS) data for dust transport over the northeastern Mediterranean. *Global Biogeochemical Cycles, 19*, GB1022. https://doi.org/10.1029/2004GB002370

Labiadh, M. T., Bergametti, G., Attoui, B., & Sekrafi, S. (2011). Particle size distributions of south Tunisian soils erodible by wind. *Geodinamica Acta, 24*, 37–47. https://doi.org/10.3166/ga.24.37-472011

Labiadh, M., Bergametti, G., Kardous, M., Perrier, S., Grand, N., Attoui, B., Sekrafi, S., & Marticorena, B. (2013). Soil erosion by wind over tilled surfaces in South Tunisia. *Geoderma, 202–203*, 8–17. https://doi.org/10.1016/j.geoderma.2013.03.007

Lafon, S., Rajot, J. L., Alfaro, S. C., & Gaudichet, A. (2004). Quantification of iron oxides in desert aerosol. *Atmospheric Environment, 38*, 1211–1218. https://doi.org/10.1016/j.atmosenv.2003.11.006

Laurent, B., Audoux, T., Bibi, M., Dulac, F., & Bergametti, G. (2022). Mas deposition. In F. Dulac, S. Sauvage, & E. Hamonou (Eds.), *Atmospheric chemistry in the Mediterranean Region* (Vol. 2, From air pollutant sources to impacts). Springer, this volume. https://doi.org/10.1007/978-3-030-82385-6_16

Laurent, B., Marticorena, B., Bergametti, G., & Mei, F. (2006). Modeling mineral dust emissions from Chinese and Mongolian deserts. *Global and Planetary Change, 52*, 121–141. https://doi.org/10.1016/j.gloplacha.2006.02.012

Laurent, B., Marticorena, B., Bergametti, G., Léon, J.-F., & Mahowald, N. M. (2008). Modeling mineral dust emissions from the Sahara desert using new surface and soil developments. *Journal of Geophysical Research, 113*, D14218. https://doi.org/10.1029/2007JD009484

Legrand, M., N'Doumé, C., & Jankowiak, I. (1994). Satellite-derived climatology of the Saharan Aerosol, In D. K. Lynch (Ed.), *Passive infrared remote sensing of clouds and the atmosphere II: Proc. SPIE 2309* (pp. 127–135).

Levi, Y., & Rosenfeld, D. (1996). Ice nuclei, rainwater chemical composition, and static cloud seeding effects in Israel. *Journal of Applied Meteorology, 35*, 1494–1501. https://doi.org/10.1175/1520-0450(1996)035<1494:INRCCA>2.0.CO;2

Losno, R., Bergametti, G., Carlier, P., and Mouvier, G. (1991). Major ions in marine rainwater with attention to sources of alkaline and acidic species, *Atmospheric Environment, 25A*, 763D. K. 770. https://doi.org/10.1016/0960-1686(91)90074-H.

Loÿe-Pilot, M.-D., & Martin, J.-M. (1996). Saharan dust input to the western Mediterranean: An eleven years record in Corsica. In S. Guerzoni & R. Chester (Eds.), *The impact of desert dust across the Mediterranean* (pp. 191–199). Springer. https://doi.org/10.1007/978-94-017-3354-0_18

Löye-Pilot, M. D., Martin, J. M., & Morelli, J. (1986). Influence of Saharan dust on the rain acidity and the atmospheric input to the Mediterranean. *Nature, 321*, 427–428. https://doi.org/10.1038/321427a0

Mahowald, N. M., Kloster, S., Engelstaedter, S., Moore, J. K., Mukhopadhyay, S., McConnell, J. R., Albani, S., Doney, S. C., Bhattacharya, A., Curran, M. A. J., Flanner, M. G., Hoffman, F. M., Lawrence, D. M., Lindsay, K., Mayewski, P. A., Neff, J., Rothenberg, D., Thomas, E., Thornton, P. E., & Zender, C. S. (2010). Observed 20th century desert dust variability: Impact on climate and biogeochemistry. *Atmospheric Chemistry and Physics, 10*, 10875–10893. https://doi.org/10.5194/acp-10-10875-2010

Marconi, M., Sferlazzo, D. M., Becagli, S., Bommarito, C., Calzolai, G., Chiari, M., di Sarra, A., Ghedini, C., Gómez-Amo, J. L., Lucarelli, F., Meloni, D., Monteleone, F., Nava, S., Pace, G., Piacentino, S., Rugi, F., Severi, M., Traversi, R., & Udisti, R. (2014). Saharan dust aerosol over the central Mediterranean Sea: PM_{10} chemical composition and concentration versus optical columnar measurements. *Atmospheric Chemistry and Physics, 14*, 2039–2054. https://doi.org/10.5194/acp-14-2039-2014

Marsham, J. H., Hobby, M., Allen, C. J. T., Banks, J. R., Bart, M., Brooks, B. J., Cavazos-Guerra, C., Engelstaedter, S., Gascoyne, M., Lima, A. R., Martins, J. V., McQuaid, J. B., O'Leary, A., Ouchene, B., Ouladichir, A., Parker, D. J., Saci, A., Salah-Ferroudh, M., Todd, M. C., & Washington, R. (2013). Meteorology and dust in the central Sahara: Observations from Fennec supersite-1 during the June 2011 Intensive Observation Period. *Journal of Geophysical Research, 118*, 4069–4089. https://doi.org/10.1002/jgrd.50211

Marticorena, B., & Bergametti, G. (1995). Modeling the atmospheric dust cycle: 1-Design of a soil derived dust production scheme. *Journal of Geophysical Research, 100*, 16415–16430. https://doi.org/10.1029/95JD00690

Marticorena, B., Bergametti, G., Gillette, D. A., & Belnap, J. (1997). Factors controlling threshold friction velocities in semi-arid areas of the United States. *Journal of Geophysical Research, 102*, 23277–23288. https://doi.org/10.1029/97JD01303

Marticorena, B., Chazette, P., Bergametti, G., Dulac, F., & Legrand, M. (2004). Mapping the aerodynamic roughness length of desert surfaces from the POLDER/ADEOS bi-directional

reflectance product. *International Journal of Remote Sensing, 25*, 603–626. https://doi.org/10.1080/0143116031000116976

McKenna-Neuman, C., & Nickling, W. G. (1989). A theoretical and wind tunnel investigation of the effect of capillarity water on the entrainment of sediment by wind. *Canadian Journal of Soil Science, 69*, 79–96. https://doi.org/10.4141/cjss89-008

Mei, F., Zhang, X., Lu, H., Shen, Z., & Wang, Y. (2004). Characterization of MASDs of surface soils in north China and its influence on estimating dust emission, Chinese Sci. *Bull, 49*(20), 2169–2176.

Meloni, D., di Sarra, A., Biavati, G., De Luisi, J. J., Monteleone, F., Pacea, G., Piacentino, S., & Sferlazzo, D. M. (2007). Seasonal behavior of Saharan dust events at the Mediterranean island of Lampedusa in the period 1999–2005. *Atmospheric Environment, 41*, 3041–3056. https://doi.org/10.1016/j.atmosenv.2006.12.001

Meloni, D., di Sarra, A., Monteleone, F., Pace, G., Piacentino, S., & Sferlazzo, D. M. (2008). Seasonal transport patterns of intense Saharan dust events at the Mediterranean island of Lampedusa. *Atmospheric Research, 88*, 134–148. https://doi.org/10.1016/j.atmosres.2007.10.007

Menut, L. (2008). Sensitivity of hourly Saharan dust emissions to NCEP and ECMWF modeled wind speed. *Journal of Geophysical Research, 113*, D16201. https://doi.org/10.1029/2007JD009522

Middleton, N. J., & Goudie, A. S. (2001). Saharan dust: Sources and trajectories. *Transactions of the Institute of British Geographers, 26*, 165–181. https://doi.org/10.1111/1475-5661.00013

Middleton, N. J., Goudie, A. S., & Wells, G. L. (1986). The frequency and source areas of dust storms. In W. G. Nickling (Ed.), *Aeolian geomorphology* (pp. 237–259). Unwin Hyman.

Molinari, E. (1996). Mineralogical characterization of Saharan dust with a view to its final destination in Mediterranean sediments. In S. Guerzoni & R. Chester (Eds.), *The impact of African dust across the Mediterranean* (pp. 153–162). Kluwer. https://doi.org/10.1007/978-94-017-3354-0_14

Moreno, T., Querol, X., Castillo, S., Alastuey, A., Cuevas, E., Herrmann, L., Mounkaila, M., Elvira, J., & Gibbons, W. (2006). Geochemical variations in aeolian mineral particles from the Sahara–Sahel dust corridor. *Chemosphere, 65*, 261–270. https://doi.org/10.1016/j.chemosphere.2006.02.052

Moulin, C., Lambert, C. E., Dayan, U., Masson, V., Ramonet, M., Bousquet, P., Legrand, M., Balkanski, Y. J., Guelle, W., Marticorena, B., Bergametti, G., & Dulac, F. (1998). Satellite climatology of African dust transport in the Mediterranean atmosphere. *Journal of Geophysical Research, 103*, 13137–13144. https://doi.org/10.1029/98JD00171

Muhs, D. R., Prospero, J. M., Baddock, M. C., & Gill, T. E. (2014). Identifying sources of aeolian mineral dust: Present and past. In P. Knippertz & J.-B. W. Stuut (Eds.), *Mineral dust: A key player in the earth system* (pp. 51–74). Springer. https://doi.org/10.1007/978-94-017-8978-3_3

Nickling, W. G. (1994). Aeolian sediment transport and deposition. In K. Pye (Ed.), *Sediment transport and depositional processes*. Blackwell Scientific.

Nickling, W. G., & Gillies, J. A. (1989). Emission of fine-grained particulates from desert soils. In M. Leinen & M. Sarnthein (Eds.), *Paleoclimatology and paleometeorology: Modern and past patterns of global atmospheric transport* (NATO ASI Series) (Vol. 282, pp. 133–165). Kluwer. https://doi.org/10.1007/978-94-009-0995-3_5

Pey, J., Querol, X., Alastuey, A., Forastiere, F., & Stafoggia, M. (2013). African dust outbreaks over the Mediterranean Basin during 2001–2011: PM_{10} concentrations, phenomenology and trends, and its relation with synoptic and mesoscale meteorology. *Atmospheric Chemistry and Physics, 13*, 1395–1410. https://doi.org/10.5194/acp-13-1395-2013

Priestley, C. H. B. (1959). *Turbulent transfer in the lower atmosphere* (130 pp). University of Chicago Press.

Prodi, F., & Fea, G. (1979). A case study of transport and deposition of Saharan dust over the Italian peninsula and southern Europe. *Journal of Geophysical Research, 84*, 6951–6960. https://doi.org/10.1029/JC084iC11p06951

Prospero, J. M. (1996). Saharan dust transport over the North Atlantic Ocean and Mediterranean: An overview. In S. Guerzoni & R. Chester (Eds.), *The impact of desert dust across the Mediterranean* (pp. 133–151). Springer. https://doi.org/10.1007/978-94-017-3354-0_13

Prospero, J. M., Ginoux, P., Torres, O., & Nicholson, S. E. (2002). Environmental characterization of global sources of atmospheric soil dust derived from the NIMBUS-7 TOMS absorbing aerosol product. *Reviews of Geophysics, 40*, 2–31. https://doi.org/10.1029/2000RG000095

Rajot, J.-L., Alfaro, S. C., Gomes, L., & Gaudichet, A. (2003). Soil crusting on sandy soils and its influence on wind erosion. *Catena, 53*, 1–16. https://doi.org/10.1016/S0341-8162(02)00201-1

Raupach, M. (1992). Drag and drag partition on rough surfaces. *Boundary-Layer Meteorology, 60*(4), 375–395. https://doi.org/10.1007/BF00155203

Reiff, J., Forbes, G. S., Spieksma, F. T. M., & Reynders, J. J. (1986). African dust reaching northwestern Europe: A case study to verify trajectory calculations. *Journal of Applied Meteorology, 25*, 1543–1567. https://doi.org/10.1175/1520-0450(1986)025<1543:ADRNEA>2.0.CO;2

Renard, J.-B., Dulac, F., Durand, P., Bourgeois, Q., Denjean, C., Vignelles, D., Couté, B., Jeannot, M., Verdier, N., & Mallet, M. (2018). In situ measurements of desert dust particles above the western Mediterranean Sea with the balloon-borne Light Optical Aerosol Counter/sizer (LOAC) during the ChArMEx campaign of summer 2013. *Atmospheric Chemistry and Physics, 18*, 3677–3699. https://doi.org/10.5194/acp-18-3677-2018

Rodrıguez, S., Querol, X., Alastuey, A., Kallos, G., & Kakaliagou, O. (2001). Saharan dust contributions to PM_{10} and TSP levels in Southern and Eastern Spain. *Atmospheric Environment, 35*, 2433–2447. https://doi.org/10.1016/S1352-2310(00)00496-9

Ryder, C. L., Highwood, E. J., Walser, A., Seibert, P., Philipp, A., & Weinzierl, B. (2019). Coarse and giant particles are ubiquitous in Saharan dust export regions and are radiatively significant over the Sahara. *Atmospheric Chemistry and Physics, 19*, 15353–15376. https://doi.org/10.5194/acp-19-15353-2019

Salvador, P., Alonso-Pérez, S., Pey, J., Artíñano, B., de Bustos, J. J., Alastuey, A., & Querol, X. (2014). African dust outbreaks over the western Mediterranean Basin: 11-year characterization of atmospheric circulation patterns and dust source areas. *Atmospheric Chemistry and Physics, 14*, 6759–6775. https://doi.org/10.5194/acp-14-6759-2014

Scheuvens, D., Schütz, L., Kandler, K., Ebert, M., & Weinbruch, S. (2013). Bulk composition of northern African dust and its source sediments — A compilation. *Earth-Science Reviews, 116*, 170–194. https://doi.org/10.1016/j.earscirev.2012.08.005

Schulz, M., Balkanski, Y. J., Guelle, W., & Dulac, F. (1998). Role of aerosol size distribution and source location in a three-dimensional simulation of a Saharan dust episode tested against satellite-derived optical thickness. *Journal of Geophysical Research, 103*, 10579–10592. https://doi.org/10.1029/97JD02779

Shao, Y. (2001). A model for mineral dust emission. *Journal of Geophysical Research, 106*, 20239–20254. https://doi.org/10.1029/2001JD900171

Shao, Y. (2004). Simplification of a dust emission scheme and comparison with data. *Journal of Geophysical Research, 109*, D10202. https://doi.org/10.1029/2003JD004372

Shao, Y. (2008). *Physics and modelling of wind erosion* (2nd and revised ed., 452 pp). Springer.

Shao, Y., & Lu, H. (2000). A simple expression for wind erosion threshold friction velocity. *Journal of Geophysical Research, 105*, 22437–22443. https://doi.org/10.1029/2000JD900304

Shao, Y., Raupach, M. R., & Findlater, P. A. (1993). The effect of saltation bombardment on the entrainment of dust by wind. *Journal of Geophysical Research, 98*, 12719–12726. https://doi.org/10.1029/93JD00396

Shao, Y., Klose, M., & Wyrwoll, K.-H. (2013). Recent global dust trend and connections to climate forcing. *Journal of Geophysical Research, 118*, 11107–11118. https://doi.org/10.1002/jgrd.50836

Stringer, M. E., Cerna-Alvarez, E., & Kutter, B. L. (2020). Effects of the ratio between body forces and inter-particle forces on maximum void ratio. *Soils and Foundations, 60*, 1–12. https://doi.org/10.1016/j.sandf.2019.12.012

Textor, C., Schulz, M., Guibert, S., Kinne, S., Balkanski, Y., Bauer, S., Berntsen, T., Berglen, T., Boucher, O., Chin, M., Dentener, F., Diehl, T., Easter, R., Feichter, H., Fillmore, D., Ghan, S.,

Ginoux, P., Gong, S., Grini, A., … Tie, X. (2006). Analysis and quantification of the diversities of aerosol life cycles within AeroCom. *Atmospheric Chemistry and Physics, 6*, 1777–1813. https://doi.org/10.5194/acp6-1777-2006

Textor, C., Schulz, M., Guibert, S., Kinne, S., Balkanski, Y., Bauer, S., Berntsen, T., Berglen, T., Boucher, O., Chin, M., Dentener, F., Diehl, T., Feichter, J., Fillmore, D., Ginoux, P., Gong, S., Grini, A., Hendricks, J., Horowitz, L., … Tie, X. (2007). The effect of harmonized emissions on aerosol properties in global models – An AeroCom experiment. *Atmospheric Chemistry and Physics, 7*, 4489–4501. https://doi.org/10.5194/acp-7-4489-2007

Torralba, V., Doblas-Reyes, F. J., & Gonzalez-Reviriego, N. (2017). Uncertainty in recent near-surface wind speed trends: A global reanalysis intercomparison. *Environmental Research Letters, 12*, 114019. https://doi.org/10.1088/1748-9326/aa8a58

Toth, J. R., III, Rajupet, S., Squire, H., Volbers, B., Zhou, J., Xie, L., Sankaran, R. M., & Lacks, D. J. (2020). Electrostatic forces alter particle size distributions in atmospheric dust. *Atmospheric Chemistry and Physics, 20*, 3181–3190. https://doi.org/10.5194/acp-20-3181-2020

Usher, C. R., Michel, A. E., & Grassian, V. H. (2003). Reactions on mineral dust. *Chemical Reviews, 103*, 4883–4939. https://doi.org/10.1021/cr020657y

Valentin, C., & Bresson, L. M. (1992). Morphology, genesis and classification of surface crusts in loamy and sandy soils. *Geoderma, 55*, 225–245. https://doi.org/10.1016/0016-7061(92)90085-L

van der Does, M., Knippertz, P., Zschenderlein, P., Harrison, R. G., & Stuut, J. B. W. (2018). The mysterious long-range transport of giant mineral dust particles. *Science Advances, 4*, eaau2768. https://doi.org/10.1126/sciadv.aau2768

Vincent, J., Laurent, B., Losno, R., Bon Nguyen, E., Roullet, P., Sauvage, S., Chevaillier, S., Coddeville, P., Ouboulmane, N., di Sarra, A. G., Tovar-Sánchez, A., Sferlazzo, D., Massanet, A., Triquet, S., Morales Baquero, R., Fornier, M., Coursier, C., Desboeufs, K., Dulac, F., & Bergametti, G. (2016). Variability of mineral dust deposition in the western Mediterranean basin and south-east of France. *Atmospheric Chemistry and Physics, 16*, 8749–8766. https://doi.org/10.5194/acp-16-8749-2016

Washington, R., Todd, M., Middleton, N. J., & Goudie, A. S. (2003). Dust-storm source areas determined by the Total Ozone Monitoring Spectrometer and surface observations. *Annals of the American Association of Geographers, 93*, 297–313. https://doi.org/10.1111/1467-8306.9302003

Webb, N. J., & Pierre, C. (2018). Quantifying anthropogenic dust emissions. *Earth's Future, 6*, 286–295. https://doi.org/10.1002/2017EF000766

Weinzierl, B., Petzold, A., Esselborn, M., Wirth, M., Rasp, K., Kandler, K., Schütz, L., Koepke, P., & Fiebig, M. (2009). Airborne measurements of dust layer properties, particle size distribution and mixing state of Saharan dust during SAMUM 2006. *Tellus B, 61*, 96–117. https://doi.org/10.1111/j.1600-0889.2008.00392.x

White, B. (1979). Soil transport by winds on Mars. *Journal of Geophysical Research, 84*, 4643–4651. https://doi.org/10.1029/JB084iB09p04643

Yuan, H., Zhuang, G., Rahn, K. A., Zhang, X., & Li, Y. (2006). Composition and mixing of individual particles in dust and non-dust conditions of north China, spring 2002. *Journal of Geophysical Research, 111*, D20208. https://doi.org/10.1029/2005JD006478

Zender, C. S., Bian, H., & Newman, D. (2003). Mineral Dust Entrainment and Deposition (DEAD) model: Description and 1990s dust climatology. *Journal of Geophysical Research, 108*(D14), 4416. https://doi.org/10.1029/2002JD002775

Anthropogenic Emissions of Reactive Compounds in the Mediterranean Region

Agnès Borbon, Charbel Afif, Thérèse Salameh, Baye Toulaye P. Thera, and Anastasia Panopoulou

Contents

*Chapter reviewed by **Bertrand Bessagnet** (CITEPA, Paris, France), as part of the book Part V Emissions and Sources also reviewed by **Claire Granier** (Laboratoire d'Aérologie (LAERO), CNRS – Univ. Toulouse III Paul Sabatier, Observatoire Midi-Pyrénées, Toulouse, France)*

A. Borbon (✉) · B. T. P. Thera
Université Clermont Auvergne, CNRS, Laboratoire de Météorologie Physique UMR 6016 (LaMP), Clermont-Ferrand, France
e-mail: agnes.borbon@uca.fr

C. Afif
Emissions, Measurements, and Modeling of the Atmosphere (EMMA) Laboratory, CAR, Faculty of Sciences, Saint Joseph University, Beirut, Lebanon

Climate and Atmosphere Research Center (CARE-C), The Cyprus Institute, Aglantzia, Nicosia, Cyprus

T. Salameh
IMT Nord Europe, Institut Mines-Télécom, Univ. Lille, Centre for Energy and Environment, F-5900 Lille, France

A. Panopoulou
IMT Nord Europe, Institut Mines-Télécom, Univ. Lille, Centre for Energy and Environment, F-5900 Lille, France

Institute for Environmental Research and Sustainable Development, National Observatory of Athens (NOA/IERSD), Palaia Penteli, Athens, Greece

Environmental Chemical Processes Laboratory (ECPL), Department of Chemistry, University of Crete, Heraklion, Greece

F. Dulac et al. (eds.), *Atmospheric Chemistry in the Mediterranean Region*,
https://doi.org/10.1007/978-3-030-82385-6_5

Abstract In this chapter, we present the current knowledge of the anthropogenic emissions of major gaseous and particulate pollutants in the Mediterranean basin. Anthropogenic emissions affect air quality and/or climate through (i) direct emission of greenhouse gases (mainly carbon dioxide), (ii) emission of indirect greenhouse gases (precursors of tropospheric ozone or gases affecting the oxidative capacity of the atmosphere, such as nitrogen oxides (NO_x), carbon monoxide (CO), and volatile organic compounds (VOC)), and (iii) emission of aerosols and their precursors (black carbon BC, organic carbon OC, sulfur compounds, NO_x, VOC, and ammonia). Here we tackle reactive gases and $PM_{2.5}$ on two levels: the first focuses on the entire Mediterranean basin and the second on urban areas distributed along its surroundings where human-made activities concentrate. At the basin level, the emission intensities along with their spatial and temporal variabilities per major sector are discussed. In addition, different perspectives are presented: past and future evolutions, West vs. East basin, and basin vs. global. This discussion relies mostly on global emission inventories downscaled to the basin. At the urban level, we emphasize on the way recent observations collected in the frame of ChArMEx (like the TRANSEMED initiative in the eastern Mediterranean basin) have provided relevant constraints to disentangle anthropogenic emissions and to evaluate the uncertainties in emission inventories.

1 Anthropogenic Emissions at the Scale of the Mediterranean Basin: Intensity and Variability

Identifying emission sources and quantifying their releases are essential steps in the understanding of atmospheric processes and environmental management. Various types of anthropogenic emission inventories exist with different spatial domains around the world that provide crucial information to modelling and observational systems. However, no specific inventory was developed for the Mediterranean region which benefits at present from the global inventories or the regional inventories like EMEP to access gridded emissions. The European part of the Mediterranean has its own local gridded emissions which are reported to European agencies like the European Environment Agency. But even European emissions are still a challenge when comparing different European inventories of urban areas (Trombetti et al., 2018) or countries (e.g., Cyprus: Kushta et al., 2018). It is also worth noting that some of the non-European countries of the basin have developed local emission inventories at national levels (e.g., Waked et al., 2012 for Lebanon) which are being updated (e.g., Lebanon) and developed at an institutional level for other countries (e.g., Egypt and Turkey). These local inventories in the non-European countries are of high importance since regulations are less enforced and technical practices exist (Waked et al., 2012). The implementation of these emission datasets in global and regional inventories where possible is a crucial step toward regional policy making at the basin level involving EU and non-EU countries. The uncertainty analysis and

objective assessment are considerable challenges for the development of these inventories. This chapter focuses on emissions of Particulate matter 2,5 μm or less ($PM_{2.5}$) and reactive gases, when the following one considers the particular case of ultrafine particle emissions (Junkermann, 2022).

1.1 Emission Inventories

The GEIA initiative through its ECCAD portal provides access to different emission inventories for several concerned pollutants, time spans, and covered domains, along with different resolutions but also sectors (ECCAD Database; https://eccad3.sedoo.fr/). Some of these inventories are presented hereafter.

The ACCMIP inventory was developed in support of the fifth IPCC-AR5 (Intergovernmental Panel for Climate Change – Assessment Report 5; Lamarque et al., 2010), together with the global emission projections of the Representative Concentration Pathways (RCP; van Vuuren et al., 2011). ACCMIP covers the period 1850–2000 including biomass burning. The RCP projections of future emissions are based on four selected scenarios. The RCP are named according to their 2100 radiative forcing level, i.e., RCP 8.5 corresponds to a radiative forcing of 8.5 W m^{-2} in 2100. As part of MACC and CityZen EU projects, the ACCMIP and the RCP 8.5 emissions datasets have been interpolated on a yearly basis for the period 1960–2020 for the anthropogenic emissions to form the MACCity anthropogenic inventory for each sector and each year between 1960 and 2020. For the IPCC's sixth Coupled Model Intercomparison Project phase 6 (CMIP6, Eyring et al., 2016), the Shared Socioeconomic Pathways (SSPs) global scenarios were developed and describe how the future emissions might evolve according to socioeconomic development, demographics, and technological advances within the context of climate change mitigation and adaptation throughout the twenty-first century (Riahi et al., 2017). There are five main scenarios, each representing a different pathway. For example, SSP2 presents the "Middle of the Road (Medium challenges to mitigation and adaptation)," while SSP5 presents the "Fossil-fuelled Development – Taking the Highway (High challenges to mitigation, low challenges to adaptation)" pathway. These SSP can be combined with a radiative forcing from the RCP, like 4.5 W m^{-2} which gives SSP245 for the SSP2 or an 8.5 W m^{-2} combined with SSP5 to give SSP585.

The European Joint Research Centre in collaboration with the Netherlands Environmental Assessment Agency developed the Emissions Database for Global Atmospheric Research (EDGAR) from 1970 until 2015, based on public available activity data and proxies for greenhouse and non-greenhouse gases and particles (Crippa et al., 2018). In its updates, it relies on several aspects from other guidance/inventories like the technology-based emission factors and end-of-pipe reductions, which followed the recommendations of the European Monitoring and Evaluation Programme (EMEP)/European Environment Agency (EEA) air pollutant emission inventory guidebook (EMEP/EEA, 2013), the HTAP_v2 dataset

(Janssens-Maenhout et al., 2015), and the PEGASOS study (Crippa et al., 2016). The Task Force on Hemispheric Transport of Air Pollution (HTAP) was established by the UNECE Convention on Long-Range Transboundary Air Pollution (LRTAP Convention). HTAP_v2 is a compilation of grid maps from officially reported datasets (from the United States Environmental Protection Agency, European Monitoring and Evaluation Programme (EMEP), etc.). Efforts were made to combine EDGAR and HTAP in the European Union. In addition to that, the EMEP has developed a European emission inventory over a domain including Europe and some of its adjacent countries. On the other hand, the European Copernicus Atmosphere Monitoring Service (CAMS) developed a historical global emission inventory for the years 2000–2020 based on EDGAR (version 4.3.2) and the Community Emissions Data System (CEDS) inventories (Elguindi et al., 2020). The CAMS inventory is used as input data in the air quality CAMS global model.

One of the well-known global emission inventories is the Evaluating of the CLimate and Air Quality ImPacts of Short-livEd pollutants (ECLIPSE) emission dataset used with the Greenhouse Gas and Air Pollution Interactions and Synergies (GAINS) model. It assesses the different emission abatement techniques and their cost-effectiveness with the base years of 2005 and 2010 and project emissions until 2050 (Höglund-Isaksson, 2012; Klimont et al., 2013). The model relies on international and national statistics of activity data. It considers two scenarios: a baseline scenario 2005–2050 (current legislation – CLE) and a maximum technically feasible reduction scenario for 2030 and 2050 (MTFR).

Other inventories are more specific like the Global Fire Assimilation System (GFAS), which focuses on biomass burning emissions by assimilating the Fire Radiative Power (FRP) observations from the MODIS instruments onboard the Terra and Aqua satellites (Kaiser et al., 2012). It takes into account the land cover type with a resolution of $0.1° \times 0.1°$ from 2003 until the present day.

1.2 The Regional Mediterranean Emissions

With a population of around 500 million inhabitants, the Mediterranean region accounts for about 7% of the total world inhabitants. The emissions from 22 Mediterranean countries (namely, Albania, Algeria, Bosnia and Herzegovina, Croatia, Cyprus, Egypt, France, Gibraltar, Greece, Israel, Italy, Lebanon, Libya, Malta, Monaco, Morocco, Palestine, Slovenia, Spain, Syria, Tunisia, Turkey) reported by the emission inventories described above have been extracted from the ECCAD portal. The countries have been grouped in four different regions (Fig. 1), and the emissions of all anthropogenic sectors have been summed and are reported for trace gases and $PM_{2.5}$ in Fig. 2. The data on targeted sectors and pollutants were selected and extracted solely from ECCAD, whenever inventories encompass the entire Mediterranean basin. Figure 2 covers the future years for targeted sectors and pollutants when available, whereas for the past years the data selection was made in a way not to duplicately use inventories with common databases (e.g., ACCMIP and

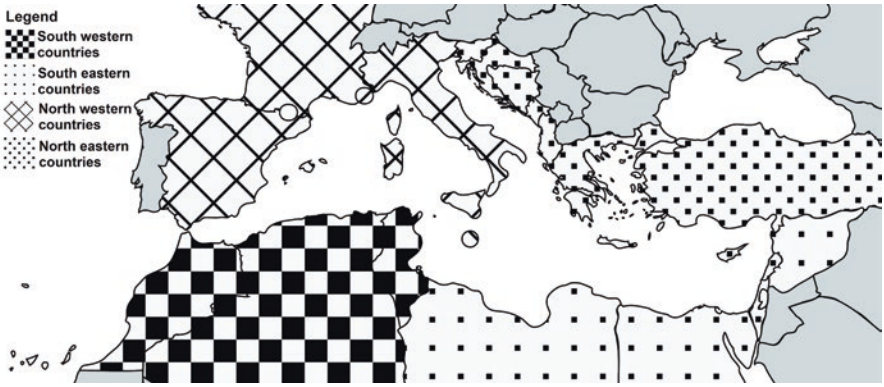

Fig. 1 Considered subdivisions of the Mediterranean countries

MACCity). The objective is to assess the trend in emissions while looking at discrepancies between the selected inventories.

Trends in Anthropogenic Emissions

The different inventories generally agree on the decrease of gaseous emissions in the Mediterranean basin in the twenty-first century after reaching a maximum in the 1990s (Fig. 2a–l), whereas $PM_{2.5}$ increased slightly from the last century with a slight downward decrease after the year 2000 (Fig. 2m–o).

NO_x emissions from the entire basin increased from the 1850s to the year 2000 from 0.16 Tg to 5.14 Tg as per the ACCMIP inventory (Fig. 2d). A decrease is then calculated by the CAMS inventory in line with ECLIPSE-CLE (indicated as ECLIPSE in the rest of the text) and the SSP245 and SSP585 in general till 2020. However, the discrepancy between these inventories, excluding ECLIPSE, is in the range of 20–35% which is acceptable. ECLIPSE on the other hand shows emissions higher by 50–60%. At the beginning of the twenty-first century, the Mediterranean basin contributed by around 8% of the global nitrogen oxides (NO_x) emissions, while this contribution is decreasing over time to almost 5% in 2019. According to the SSP245 and SSP585, emissions are expected to reach values of 2 and 3.5 Tg in 2100, respectively, equivalent to 1960–1975 emissions.

The same trend is depicted for Non-Methan Hydrocarbons (NMHC)(Fig. 2g) with a maximum in the 1990–2000 period (10 Tg) followed by a decrease. The contribution to worldwide emissions from the beginning of the century accounts for around 6.5% with lower values of around 3.5–4% in 2019. The discrepancy between inventories is lower than for NOx, including ECLIPSE, with values below 20%. At the end of this century, emissions based on SSP245 and SSP585 are predicted to be in the range of 1950–1965 emissions.

After a maximum in the 1980s, both CAMS and MACCity show a downward trend for Sulfur Dioxide (SO_2) (Fig. 2j) in the twenty-first century with a value

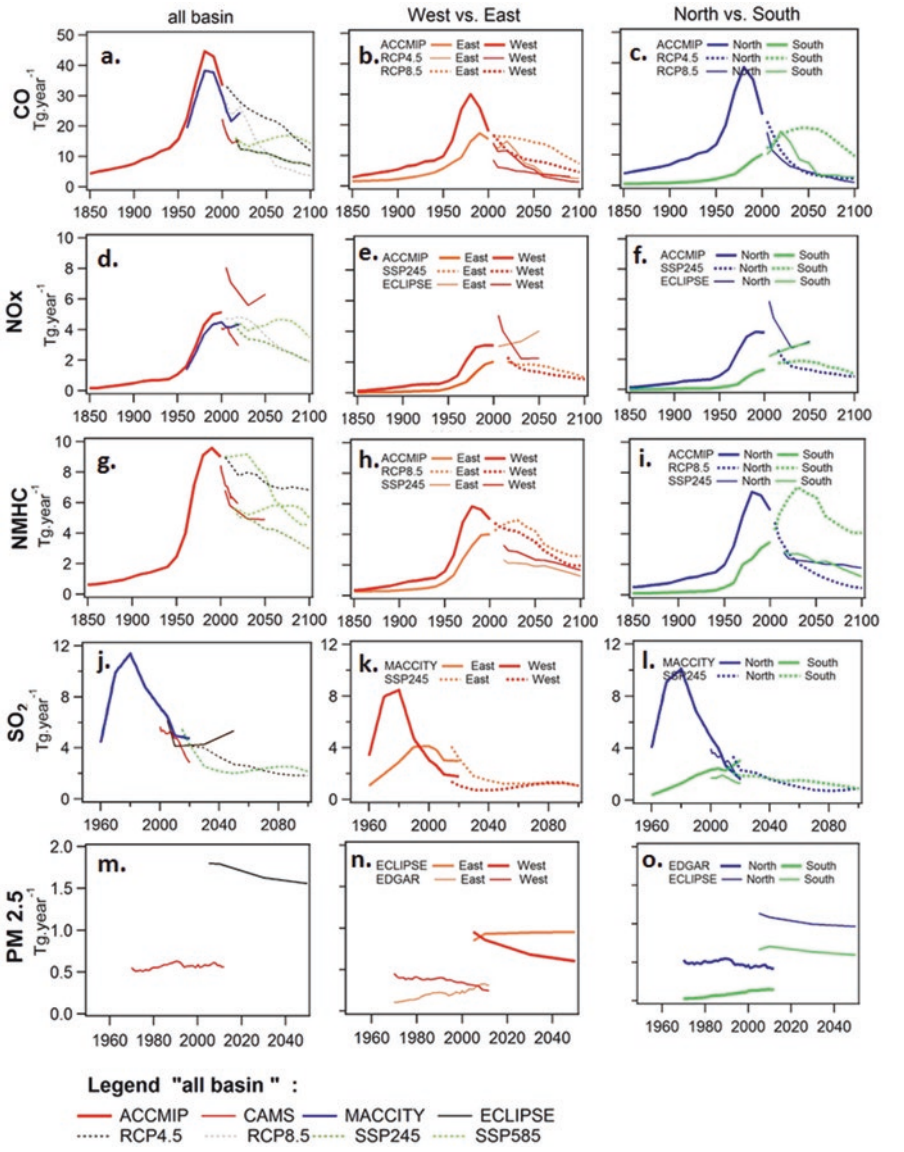

Fig. 2 Past and future emissions (1850–2100) of reactive trace gases and $PM_{2.5}$ in the Mediterranean basin. (Data extracted from selected emission inventories from the ECCAD database; https://eccad3.sedoo.fr/)

ranging from around 3.5–5 Tg year^{-1} in 2020. The contribution to worldwide emissions accounted for 7%, while it has now been reduced to 3% (2020).

EDGAR inventory shows that $PM_{2.5}$ emissions increased slightly from the mid of the last century until 2012 with values ranging from 0.50 to 0.65 Tg year^{-1} over the

basin (Fig. 2m). ECLIPSE shows emissions threefold higher than EDGAR for the common period of 2005–2010 with a decrease expected of 10–15% by the mid-twenty-first century compared to the 2005–2010 period.

Comparing Western-Eastern Basins and Northern-Southern Basins

The emissions of NO_x (Fig. 2e), NMHC (Fig. 2h), and $PM_{2.5}$ (Fig. 2n) of the western countries of the Mediterranean exhibit higher values than those of the eastern part with values of 20–30% higher in 2000 (ACCMIP for NO_x non methane volatile organic compounds (NMVOC) and EDGAR for $PM_{2.5}$). NO_x and NMVOC were increasing historically from 1850 until they began decreasing between 1980 and 2000 on the entire basin. However, $PM_{2.5}$ emissions began decreasing in the western countries of the basin around 1990, while the eastern part had continuous increasing emissions exceeding those of the western part around 2008. Western NO_x and NMVOC emissions declined after 2000 significantly compared to the East. Lelieveld et al. (2015a) processed NO_2 column from the satellite instrument Dutch OMI (DOMINO v2) between 2005 and 2014 over the eastern Mediterranean and the Middle East. They show that the combination of political factors, including economic crisis and armed conflict, has changed significantly the NOx emissions in the region where some countries exhibit increases in emissions like Lebanon due to mass displacements from Syria where armed conflicts caused the decrease of NOx emissions as also suggested by Georgoulias et al. (2019). The authors also add that such short-term changes cannot be captured by inventories and future projections. All future scenarios, namely, SSP245, SSP585, and ECLIPSE, exhibit a decrease in the NOx and NMVOC emissions for both parts of the basin: NMVOCs will reach values similar to those of 1960 between 1.5 and 3 Tg $year^{-1}$ with the western part always emitting higher quantities, while NOx decrease will achieve values between those of 1960 and 1970 of 1–2 Tg $year^{-1}$. However, ECLIPSE shows that the eastern part will have an increase of NOx emissions reaching a historical high value of 4 Tg $year^{-1}$. $PM_{2.5}$ emissions are expected to increase very slightly from 2010 to 2050 in the eastern part while decreasing by around 25% in the western part and reaching around 0.6 Tg $year^{-1}$, according to ECLIPSE.

On the other hand, NO_x and NMVOC from both ACCMIP and CAMS were both released in higher quantities from the northern countries of the basin until the year 2000 for NOx and the year 1980 for NMVOC after which the emissions of both pollutants begin declining, while the southern countries exhibit a continual increase until present. SSPs show decrease of NO_x emissions from both northern and southern countries, while ECLIPSE shows a continual increase for southern countries with a tipping point in trend from decrease to increase starting in 2030 for northern countries. As for NMVOC future emissions, all inventories show decreasing trends for the entire basin with emissions below 2 Tg $year^{-1}$ for each of the northern and southern parts of the basin by 2100 except for the northern countries in the SSP585 which shows an increase all over the century reaching a fairly constant value of 3.32 Tg $year^{-1}$ by the end of the twenty-first century. ECLIPSE shows that $PM_{2.5}$

emissions decline in both parts, the northern and the southern, reaching around 1 and 0.6 Tg year^{-1} in 2050, respectively.

Western Mediterranean countries exhibit a decrease in SO_2 emissions (Fig. 2k), while the eastern part shows decreasing values in CAMS while steady values of 3 Tg year^{-1} in MACCity. On the other hand, northern countries present in both inventories lower emissions trends, while the southern countries show a slowly decreasing trend for CAMS in contrast to MACCity where the trend is slightly upward. SSPs both show a decrease of SO_2 emissions in western, eastern, northern, and southern parts of the basin, while ECLIPSE shows an increase in these parts in 2050 compared to 2030.

The Road Transport Sector

The road transport is one important anthropogenic emission sector for gases like NOx, COV, and Carbon monoxide (CO). For instance, in CAMS, road transport accounts for 45% of NO_x Mediterranean emissions on average over the last two decades. While it accounted for one third of NMVOC emissions in 2000, road transport still release 20% of NMVOC in 2020. EDGAR shows that NO_x, NMVOC, and $PM_{2.5}$ total emissions increased with time until the mid-1990s and declined afterward. Comparing the western/eastern and northern/southern countries reveals that European countries emit more quantities of pollutants for this sector. Because they are applying stricter regulations over time, they drive the emissions trend over the basin. This was true until the period of 2000–2010 where the main emitter is no longer the European countries, but the non-European countries. On the other hand, the eastern and southern countries have a continuous increasing trend for the pollutants except for NMVOC, and this is mainly due to Libya whose emissions have more than tripled from 2000 until 2019 based on CAMS values.

Through the gridded emission inventory established for Lebanon using a bottom-up approach, Waked et al. (2012) showed that the road transportation sector drives the CO, NO_x, and NMVOC emissions, in Lebanon. This is also the case in Istanbul (Markakis et al., 2012; Kara et al., 2014). Waked and Afif (2012) compared road transport emissions in the Middle East which includes the East Mediterranean and showed that emissions per capita are linearly related to GDP. Moreover, in their comparison of different touristic cities in the Mediterranean, namely, Barcelona, Athens, and Beirut, they highlight the heterogeneity of trends and emission intensity despite several common factors. In addition to that, Waked and Afif (2012) show that local traditions and conditions (e.g., removal of catalyst, level of law enforcement, etc.) are an important factor to take into consideration in the basin.

The Maritime Sector

The Mediterranean Sea is an important path along the world network of maritime shipping especially with the Suez Canal. Johansson et al. (2017) indicate that the Mediterranean Sea is responsible for almost 4% of the total maritime emissions

with higher emissions in the eastern part than the western part. CAMS emissions of NO_x and NMVOC show a similar trend whether on the entire basin or western/eastern or even northern/southern parts with a slight increase until 2010 followed by a slight decrease until present. The maritime sector in the Mediterranean Sea contributes to around 2% of total basin anthropogenic NO_x emissions in the last two decades and around 1% of NMVOC emissions, according to CAMS. However, $PM_{2.5}$ emissions from EDGAR show an increase from the 1990s until 2010, like for CAMS, and a decline after 2010. On the other hand, SSP NO_x emissions are higher than CAMS for the 2015–2020 period by a factor of 4–5 and show a decrease by 30–50% until the end of the century reaching 0.2–0.35 Tg year^{-1} depending on the SSP. However, the NMVOC emissions exhibit a decrease until 2040 followed by an increase until the end of the century. SO_2 emission from shipping in the Mediterranean Sea contributes to 0.07% of total SO_2 emissions worldwide, while it contributes to around 2% of the total Mediterranean emissions in 2020 according to CAMS which is equivalent at present to road transport emissions. Historically, emissions were higher, reaching around 0.25 Tg year^{-1} in 2005–2010 according to MACCity, while they reached almost 0.09 Tg year^{-1} around 2014–2015 according to CAMS and dropped significantly after that following EU regulations on the sulfur content of marine diesel. SSP future scenarios exhibit a further decrease in SO_2 emissions, while the northern countries will still dominate these releases into the air. Shipping also appears to be an important source of ultrafine particles and CCN in the Mediterranean, as documented in the following chapter (Junkermann, 2022).

The Biomass Burning

Biomass burning is occurring at a higher frequency and more intensively in the last years in the Mediterranean basin. ACCMIP shows an increase in the years 1990–2000 for NO_x and NMVOC emissions reaching 0.03 and 0.16 Tg year^{-1}, respectively, with a contribution to total emissions of 1–2% for both pollutants while keeping these steady emissions over the century as per the RCP8.5. On the other hand, GFAS show values at the beginning of the twenty-first century higher by a factor of almost 9 and 4 for NO_x and NMVOC, respectively, when compared to RCP8.5. $PM_{2.5}$ emissions from GFAS show a very slight decrease on a yearly average from 2003 till 2016 where the value reaches 0.78 Tg year^{-1}. When looking more in depth, the Western Mediterranean countries dominate the emissions, and even when North/South comparison is conducted, South dominates according to GFAS for all pollutants.

Finally, emission inventories usually show consistent trends with discrepancies generally not exceeding 40%. However, different patterns are depicted between western, eastern, northern, and southern basins. For the latter, the emissions are expected to increase in the future. The general good consistency between emission inventories does not prevent from an evaluation of their uncertainties, an essential task in policy making.

2 Anthropogenic Emissions at Urban Scale

2.1 Past Studies in the Mediterranean Basin Prior to ChArMEx

Historically, identifying the activity sources and the areas contributing to pollutant concentration has been a fundamental task to design and implement effective abatement strategies and air quality plans. Dense urban areas along the Mediterranean border experiencing high air pollution loads like Barcelona (North-East Iberia), Marseille (southern France), and Athens (Greece) have been some of the first targets. All these coastal cities have in common a complex mixture of sources due to the presence of industries and port activities in addition to traffic and a complex orographic terrain favoring air pollution events. The first emission model developed in Barcelona in the early 1990s attributed one third of the emissions of NO_x, CO, SO_2, VOC, and particles to industrial activities against 50% for traffic (Costa & Baldasano, 1996). At that time, the primary concern was photochemical smog by the implementation of regional chemical transport models (CTM) for which emissions needed to be documented. These models investigated the interplay between ozone transport dynamics and chemistry in meteorology-controlled areas due to orography and land-sea alternate breeze regime (Menut et al., 2005). The ESCOMPTE program (Cros et al., 2004) conducted in summer 2001 in the Marseille area is emblematic of those concerns. ESCOMPTE was designed to closely evaluate and improve CTM at the regional scale. A bottom-up emission inventory was built at 1 km resolution, and physical and chemical measurements of ozone precursors were performed. Ten years later, the various VOC observations collected during the ESCOMPTE campaigns were used to evaluate the VOC emission inventory (Coll et al., 2010). In Athens, some measurements of VOC ozone precursors have been extensively reported since 1993 but with no attempt in the allocation of their sources (Moschonas & Glavas, 1996; Rappenglück et al., 1998, 1999; Moschonas et al., 2001; Petrakis et al., 2003, 2008; Giakoumi et al., 2009). The reasons were: (i) the studies were conducted mainly during warm months, with often short sampling durations and data acquisition, and (ii) a reduced spectrum of VOC measured with lighter VOC (from 2 to 3 atoms of carbon) was rarely monitored. Indeed, observations are an alternative to the non-effectiveness of the traditional approach by dispersion modeling. Source apportionment based on field observations was made possible by the development of receptor models and the continuous improvement of analytical technologies that refined the temporal scale of observations and our capacities in quantifying the chemical composition of key atmospheric components. The development of online techniques like online gas chromatography with flame-ionization detection (GC-FID) and high-resolution mass spectrometers like Proton-Transfer Reaction Mass Spectrometry (PTR-MS) or Aerosol Mass Spectrometry (AMS) represented a technological leap by increasing the number of collected data and their representativity, a prerequisite for the application of source-receptor models. Among receptor models, the massive use of the Positive Matrix Factorization

model (PMF) started in the late 2000s (Karagulian & Belis, 2012). Receptor models are mostly used for source contribution estimation at local and regional level. They apportion the measured mass of an atmospheric pollutant at a given site to its emission sources by assuming mass conservation between sources and receptor (Hopke, 2016). While Spanish groups had reported the first source apportionment studies on VOCs for the city of Martorell 20 km NW of Barcelona (Baldasano et al., 1998) and particulate matter (PM) (Querol et al., 2001), numerous studies were conducted from 2010 toward the understanding of the origin of the primary and secondary fractions of submicronic PM (Karanasiou et al., 2009; El Haddad et al., 2011; Mohr et al., 2012; Alier et al., 2013). This kind of source apportionment study is also reported in the eastern Mediterranean basin for the cities of Antalya (Öztürk et al., 2012), Istanbul (Koçak et al., 2011), Cairo (Abu-Allaban et al., 2007), and Beirut (Waked et al., 2013). In parallel to those studies, more recent programs have been implemented with usually a focus on PM rather than gaseous precursors: DAURE (Determination of the Sources of Atmospheric Aerosols in Urban and Rural Environments in the Western Mediterranean) (Pandolfi et al., 2014), APICE (Common Mediterranean strategy and local practical Actions for the mitigation of Port, Industries and Cities Emissions) for estimating the impact of harbor emissions of PM_{10} and $PM_{2.5}$ (Pérez et al., 2016), and CITIZEN (Kanakidou et al., 2011 and reference therein) on the effects of megacities and hot spot emissions on their local, regional, and global environment. In CITIZEN, the East Mediterranean was one of the regions of interest with the Great Athens area, Istanbul, and Cairo as targets from the emission inventory effort.

2.2 The TRANSEMED Initiative in the Eastern Mediterranean

Context

The eastern Mediterranean basin (EMB) is a highly sensitive environment under considerable anthropogenic pressures (see the other book chapter by Doussin, 2023). With rapidly growing populations, the EMB may be one of the most populous areas on Earth to suffer severe impacts of climate change, with continuous and gradual warming in the region (see the other book chapter by Giorgi & Raffaele, 2023), much stronger than in other regions. In this region, both ozone, in summer, and particulate limit values are often exceeded (Afif et al., 2009; Kanakidou et al., 2011; Massoud et al., 2011). Given that the population of these regions will continue to grow, this will contribute to the increase and accumulation of anthropogenic emissions of gaseous and particulate pollutants from surrounding urban areas, as well as of photochemical air pollution in a climate change context. EMB includes two large megacities, Istanbul (13.8 million inhabitants) and Cairo (16 million inhabitants), which experience extremely high levels of pollution (Kanakidou et al., 2011). Waked and Afif (2012) showed that the emissions of NO_x and CO rapidly increased by a factor of 1.5 and 2.8, respectively, in the countries of the EMB

between 2000 and 2005 as a result of the increase in fuel consumption. They also found that the road transport sector in the EMB is a significant contributor to the global emissions of CO and NO_x as road transport in Western Europe and North America. According to Salameh et al. (2017) and based on the 2015 ECCAD database (http://eccad.sedoo.fr), NMVOC emissions have been constantly increasing in the Middle Eastern region (MEA) over the last 30 years, while they have been strongly decreasing in the USA and Europe. All inventories suggest that NMVOC emissions from the MEA region are as significant as or even higher than the ones from post-industrialized regions. Considering that no source regions clearly dominate global anthropogenic emissions, an accurate representation of anthropogenic emissions is of importance in developing regions like the MEA where highest uncertainties are expected (Salameh et al., 2017). A recent study of Lelieveld et al. (2015b) estimated the number of premature deaths due to ozone and $PM_{2.5}$ in Istanbul at 5600 in 2010, to increase to 8500 in 2025, and to 13,200 in 2050. This work was based on a global atmospheric chemistry model, which in particular does not take into account the urban heterogeneity. Consequently, it is crucial to better characterize the sources and their composition at a finer scale, which are fundamental input data of the model used.

On the basis of these findings, TRANSEMED (TRANSport Emissions and Mitigation in the East meDiterranean) initiative was established in 2010. The overall objective of TRANSEMED is to assess the state of atmospheric anthropogenic pollution at EMB representative urban scales at present and for the next decades and create region-specific mitigation scenarios in a changing climate, through (i) assessing urban atmospheric composition and emission source identification and contribution and (ii) evaluation of anthropogenic emission inventories. Target urban areas are Beirut (Lebanon, Middle East), Athens (Greece, Europe), and Istanbul and Cairo megacities.

Source-apportionment Methodology Based on Ambient and Near-Source Measurements

The strategy of TRANSEMED is based on the implementation of dedicated observation campaigns in order to assess the spatiotemporal variability of the emissions. Here, we focus on two of the urban areas of interest: Beirut in 2011 and Istanbul in 2014. The observations combined both continuous ambient measurements at one suburban site, with a very high temporal resolution, for a year-round monitoring or intensive field campaigns and near-field measurements in the vicinity of specific sources. The ambient measurements include air quality parameters (nitrogen monoxide (NO), nitrogen dioxide (NO2), nitrogen oxides (NO_x), ozone (O_3), carbon monoxide (CO)), a detailed analysis of the organic fraction composition in gas and particulate phases (NMVOC measured by GC-FID, PTR-MS, sorbent tubes), primary and secondary organic aerosol tracers, polycyclic aromatic hydrocarbons (PAH), elemental carbon (EC), organic carbon (OC), trace metals, ions, meteorological parameters, and NO_2 photolysis frequency. In parallel, for near-field

measurements, offline devices (sorbent tubes and canisters) were deployed to analyze the NMVOC composition in the vicinity of some targeted sources. We combine the collected observations and complementary source apportionment approaches (urban enhancement emission ratios, emission source profiles determined by near-field measurements, multivariate receptor model like PMF) (Paatero & Tapper, 1994; Paatero, 1997) for NMVOC source identification and contribution. Over the past years, a very detailed database of ambient and near-field source observations has been built up especially regarding the composition of gaseous organic carbon.

In Lebanon, a developing country located in the Middle East on the eastern shore of the Mediterranean Sea, available information and data on air quality were limited to only a few pollutants, excluding NMVOCs. Within the TRANSEMED-ECOCEM framework, the experimental strategy included near-field measurements close to major emission sources and two intensive field campaigns (July 2–18, 2011, and Jan. 28–Feb. 12, 2012). A set of eight speciated profiles of four major NMHC sources in Lebanon, including road transport, gasoline vapor, power generation, and solvent use sources, were proposed by Salameh et al. (2014). During intensive field campaigns, the measurements were taken on the roof of the Faculty of Sciences building of Saint Joseph University (33°87′N, 35°56′E), located in the eastern suburbs of the city of Beirut (6 km south-east of Beirut downtown) at an altitude of 230 m above sea level. The site is appropriately located in order to receive air masses coming from the Greater Beirut Area, which includes the city of Beirut and close suburbs. Over 70 compounds of C_2-C_9 NMHCs, including alkanes, alkenes, alkynes, and aromatics, were continuously analyzed (Salameh et al., 2014, 2015). The NMHC total emissions in Lebanon were estimated to be 115 Gg for the year 2010 by the National Emissions Inventory established by Waked et al. (2012). According to this inventory, transport is the main source of NMHC with a relative contribution of 67% of total emissions. Moreover, there is no direct speciation information for NMHC emissions in this inventory.

The city of Istanbul is located between Europe and Asia and is characterized by Mediterranean, humid subtropical, and oceanic climates. The meteorological conditions in Istanbul (warm-dry summers and cold-wet winters) are driven by the heat gradient produced by both the Black Sea in the north and the Marmara Sea in the south. The wind direction in the city is mainly northeast. According to Markakis et al. (2012), road transport is the most dominant emission source of NMHCs (44.8%) followed by solvent use (29.7%) and activities linked to waste treatment and disposal (20.3%). Within TRANSEMED-Istanbul, the experimental strategy included one intensive field campaign from September 14 to 30 in 2014 and some near-field measurements close to major emission sources (one residential area, one roadside site, and two seashore sites) (Thera et al., 2019). The supersite studied in the case of Istanbul was located along the Barbaros Boulevard in the district of Besiktas, on the European shore of the Bosporus strait (4 Km away from the Haydarpasa Port) (41°02′33″N, 29°00′26″E). Barbaros Boulevard is characterized by high traffic density. The sampling site was also 500 m away from the Besiktas shore and was surrounded by *Pinus* (terpene emitters) which represents the maximum overall vegetation in Istanbul and *Quercus* (isoprene emitter). More than 70

species including non-methane hydrocarbons, oxygenated VOCs, and organic compounds of intermediate volatility have been quantified by GC-FID and PTR-MS techniques.

Source Apportionment of Anthropogenic VOC Emission Contribution

Comparison of Source Apportionment of VOCs

The PMF model has been applied to the datasets collected at the two sites (Beirut, with 59 NMHCs from C_2 to C_9 in summer 2011 and winter 2012; Istanbul, with 23 NMHC and oxygenated VOC in September 2014). The results are reported in Fig. 3. Beirut's PMF results show several common factors in winter and summer, but their relative contribution was slightly different. The contribution of traffic-related sources dominates in Beirut. It includes the combustion and the gasoline evaporation accounting for 51% in winter and 74% in summer (Salameh et al., 2016). If we consider the gasoline evaporation sources (episodic and related to traffic) in Beirut, we obtain a significant contribution of 43% in winter and 46% in summer reflecting the importance of gasoline evaporation in Beirut. Additional factors were found in winter but absent in summer, for instance, gas leakage due to the use of liquefied petroleum gas (LPG) in residential heating. On the opposite, in Istanbul, the traffic, including exhaust and fuel evaporation, only contributes to 16% of the NMVOC concentrations, whereas natural gas evaporation contributes to 26% of the NMVOC concentrations (Thera et al., 2019). Other factors as sources resolved by the model

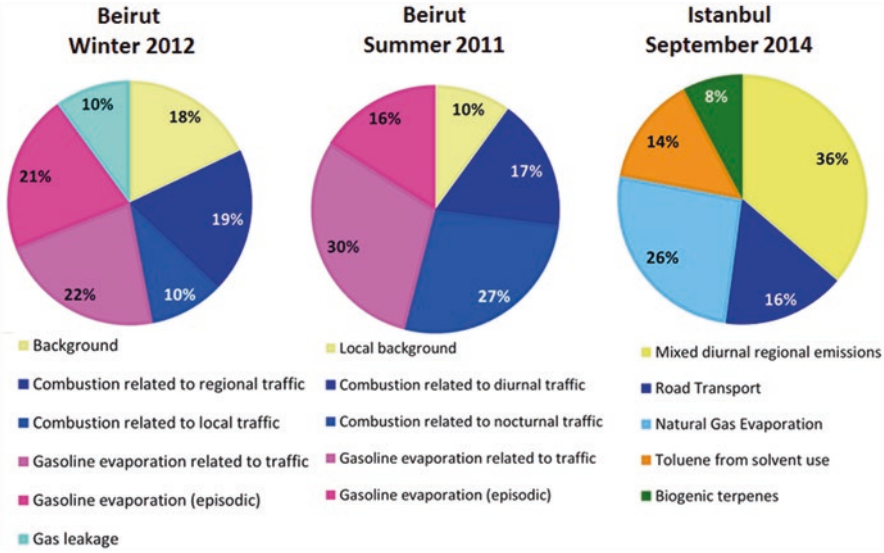

Fig. 3 Relative contribution of sources-PMF factors to NMVOC measured concentrations in Beirut, winter and summer, and Istanbul. (Reprinted from Salameh et al. (2016) and Thera et al. (2019))

were toluene (14.2%), biogenic terpenes (7.8%), and a last factor characterized by mixed regional emissions (36.3% and composed of most of the species) (Thera et al., 2019).

2.3 *Observations as Relevant Constraints to Evaluate Emission Inventories: VOCs as Target Compounds*

Methodology: Emission Ratios Derived from Direct Observations and PMF Factors

Emission inventories usually combine bottom-up and top-down calculations to estimate emissions. Comprehensive bottom-up calculations aggregate multiple local statistics on different emission source categories where possible. Top-down calculations use regional or national activity data and reallocate emissions to a finer scale using spatial surrogates (e.g., population statistics at the local level). Therefore, the uncertainties of numerous data sources are cumulated in the overall estimation of emission amounts and along increasing scales (local to regional to global). In general, the global inventories do not describe the methodologies applied nor the data used (emission factors, NMVOC species considered, etc.). Following these approaches, some highly resolved inventories have been developed at the regional scale in the EMB area for Beirut (Waked et al., 2012) and Istanbul (Markakis et al., 2012), but their uncertainties are unknown, and speciation of NMVOC is usually disregarded.

Evaluation of Emissions Based on Observations and PMF Results and National and Global Emission Inventories

The objective of this section is to estimate NMVOC emissions from anthropogenic sources with focus on the road transport sector from PMF results and NMVOC and CO observations and to compare these values to the ones derived from the various emission inventories described above, MACCity (Granier et al., 2011) for 2014, EDGAR (Crippa et al., 2018) for 2012, and ACCMIP (Lamarque et al., 2010) for 2000, at a spatial resolution of 0.5° downscaled to Beirut and Istanbul, following Eq. 1 (Salameh et al., 2016; Thera et al., 2019):

$$\mathrm{NMVOC}_{\mathrm{estimated}} = \mathrm{ratio}\left(\frac{\mathrm{NMVOC}}{\mathrm{CO}}\right)_{\text{all observations, PMF Road transport factor}} \times \mathrm{CO}_{\mathrm{inventory}} \quad (1)$$

with:

- $\mathrm{NMVOC}_{\mathrm{estimated}}$: the estimated emission for an individual NMVOC or a group of NMVOC in tons/year for all anthropogenic emissions or road transport emissions

- $CO_{inventory}$: the extracted emission of CO from either ACCMIP (Tg year^{-1}), MACCity (Tg year^{-1}), EDGAR (tons year^{-1}), or the National Emissions Inventory (NEI) for Beirut (Waked & Afif, 2012; Waked et al., 2012)
- NMVOC/CO: the NMVOC-to-CO emission ratio determined by Thera et al. (2019) for Istanbul or from each NMVOC contribution in the PMF road transport factor

The comparison of the PMF results to the NEI for Lebanon as well as for Beirut and its suburbs suggests that the inventory underestimates the road transport emissions in a reasonable way (20–39%; Fig. 4a), whereas the comparison of the PMF results to the global emission inventories (ACCMIP, EDGARv4.2) shows

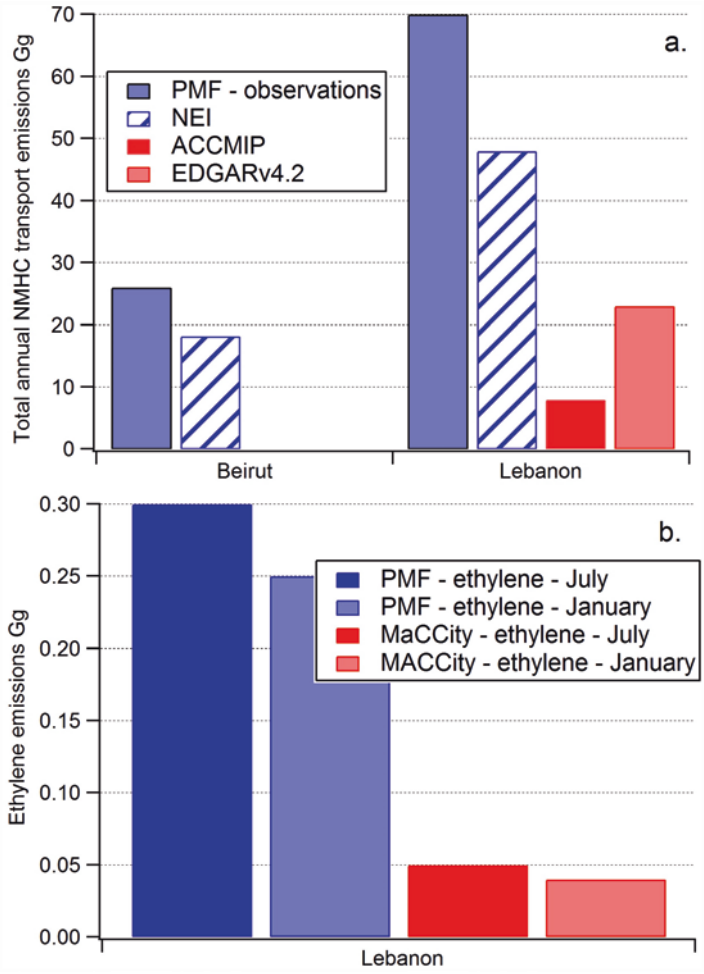

Fig. 4 Comparison of anthropogenic emissions derived from observations and PMF to emission inventories in Beirut and Lebanon: (**a**) total NMHC; (**b**) ethylene. (Reproduced from Fig. 12 Salameh et al. (2016))

significant differences reaching a factor of 10 (Fig. 4b; Salameh et al., 2016). This comparison reveals that global and national inventories are not consistent between each other. For a more detailed evaluation, we compared the emissions of ethylene, obtained by the PMF results according to Eq. 1 (with NMHC representing ethylene) to the emissions from a speciated inventory having a monthly temporal resolution, over the same period, called MACCity (Granier et al., 2011). The difference between MACCity and the PMF results is by a factor of 6.

In Istanbul, the total annual NMVOC anthropogenic emissions by global inventories are usually either within the same range by a factor of 2–3 for alkanes and aromatics or largely underestimated especially for oxygenated compounds (Fig. 5a; Thera

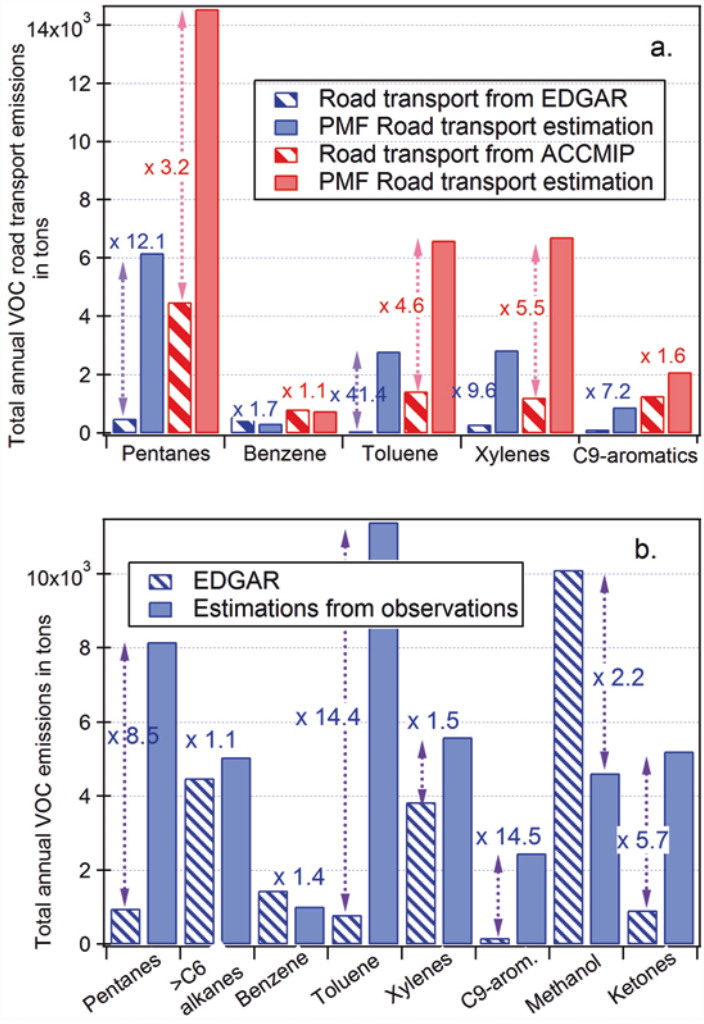

Fig. 5 Comparison of speciated NMVOC emissions (VOC excluding methane) derived from observations and PMF to emission inventories for (**a**) the road transport sector and (**b**) all anthropogenic sectors. (Reprinted from Fig. 11 in Thera et al. (2019))

et al., 2019). The evaluation of the road transport emissions is limited to the compounds from the unburned fuel fraction, and there is again an underestimation by the emission inventories (up to 12 times) except for benzene (Fig. 5b; Thera et al., 2019).

Evaluation of the Speciation of Global Emission Inventories Downscaled to Beirut

In situ observations are therefore necessary constraints for the development of reliable emission inventories. Urban emission ratios of various NMVOCs relative to a tracer of incomplete combustion (CO, acetylene) or relative to another NMVOC to each of the other NMVOC have been used as high-quality field constraints to evaluate regional emission inventories in cities of post-industrialized countries (Warneke et al., 2007; Coll et al., 2010; Borbon et al., 2013). In order to evaluate global NMVOC speciated emission inventories, in the absence of regional emission inventories for EMB, the observations collected in Beirut including detailed near-source field measurements and ambient measurements at a suburban site were used (Salameh et al., 2017). We used speciated regional (EMEP) and global (ACCMIP shown here and MACCity) emission inventories downscaled to Lebanon as well at a spatial resolution of 0.5° (Salameh et al., 2017).

The urban enhancement ratios (ERs) obtained from ACCMIP vs. those obtained from the observations are reported in Fig. 6. It appears that benzene is

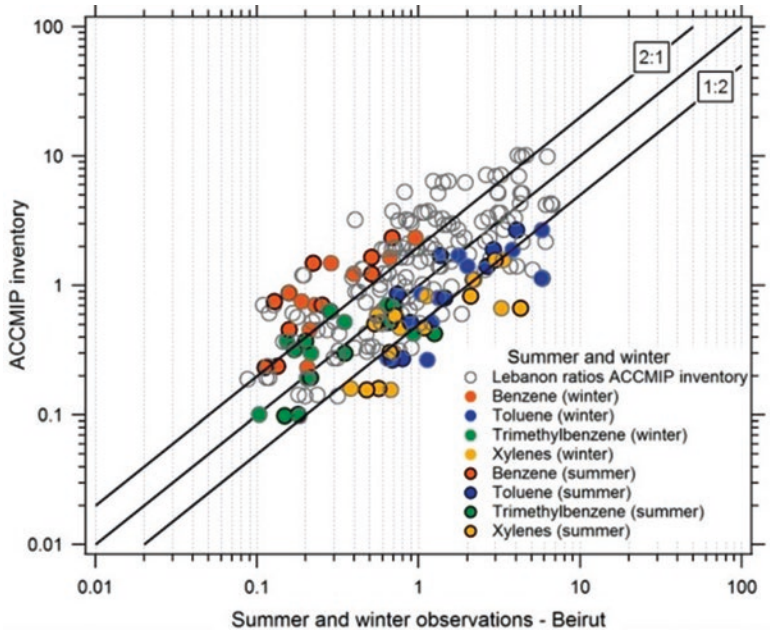

Fig. 6 Comparison of the emission ratios of NMVOC vs. $NMVOC_i$ from ACCMIP to the measured ones in Beirut, in summer and in winter, for all the anthropogenic sectors, for all data of all compound classes (in gray dots), and for a given NMVOC (colored dots). (Reprinted from Fig. 9 in Salameh et al. (2017))

systematically overestimated up to a factor of 5 in ACCMIP. Conversely, xylenes are underestimated in the ACCMIP global emission inventory but not systematically. The other compounds are closer to the line of the slope (=1), below a factor of 2. Finally, comparisons between ACCMIP and observations suggest that the overall speciation of anthropogenic sources for major hydrocarbons that act as ozone and SOA precursors in ACCMIP is better represented than the other species, but it still needs improvement (Salameh et al., 2017).

It should be emphasized that when a consensus is met between observed and inventory ERs (the ERs fall around the ratio of 1), this does not necessarily mean that the absolute emissions are correct. Indeed, Salameh et al. (2016) showed that global inventories (ACCMIP, EDGAR, MACCity) could underestimate the NMVOC emissions by up to a factor of 10 for the transportation sector. Both speciation and absolute emissions have to be taken into consideration.

3 Conclusion and Recommendations

While multi-year trends suggest a global decrease in anthropogenic emissions over the whole Mediterranean basin, the trajectories are different when comparing western-eastern regions to northern-southern regions. Detailed observations provide very useful constraints for source-apportionment studies and evaluation of emission inventories as illustrated by the works developed within the ChArMEx-TRANSEMED initiative for NMVOC. Very high uncertainties keep on being associated with global emission inventories. Given the complex environment the basin exhibits due to the different levels of regulations, technology implemented and practices, but also law enforcement, highly spatially and temporally resolved local emission inventories are essential for the future to build a more realistic regional inventory taking into account these heterogeneities like the work of Waked et al. (2012), for example. The quality assurance/quality control of the inventories is recommended to maintain a minimum level of reliability in the proposed results. Different approaches exist and shall be used to sustain the development of emission inventories and validate their results at the local and regional scale, going from a combination of remote sensing and modelling, especially with better performance of new satellites, a combination of a priori highly resolved local emission inventories and remote sensing, or even measurements solely like the work conducted within TRANSEMED. This step is crucial and shall be more focused on assessing uncertainties in future emission inventories. Since local practices play an important part in the technology performances, whether in road transport, industries, etc., the characterization of the source profiles is a future must. These will help extend the inventories to more speciated species that play a considerable role in atmospheric chemistry and composition. The TRANSEMED initiative now continues with Greater Athens, Greece (Panopoulou et al., 2018), and, more recently, with the POLCAIR campaigns in Cairo, Egypt (November 2019 to July 2021). After almost one decade of experimental efforts, this dataset constitutes a benchmark for the East

Mediterranean. These field data have also been useful to address the health impacts of air pollution like in Beirut where the cumulative cancer risk was estimated (Dhaini et al., 2017) or Cairo through long-term exposure assessment (Wheida et al., 2018). Other ongoing projects are taking place in the western part of the Mediterranean basin at Marseille, France, since February 2019, with a focus on the impact of shipping emissions. Another project was launched recently with concrete quick achievements like field campaigns in Nicosia, Cyprus, participation to POLCAIR campaign in Cairo, etc., namely, the Eastern Mediterranean and Middle East-Climate and Atmosphere Research Centre (EMME-CARE) through the creation of a Centre of Excellence at the Cyprus Institute, tackling air pollution and climate change and their health impact coupled to policy making over the next decades in the region, using a combination of modelling, remote sensing, observations, etc. and based on a dense network of strategic collaborations. Such sustained projects are much needed and vital in the long run especially in the southern part of the basin. Another level of collaboration shall also be established with decision-makers especially in the southern countries with the help of the northern ones to enhance policy making related to emissions and the future of the atmospheric environment in the Mediterranean basin.

References

Abu-Allaban, M., Lowenthal, D. H., Gertler, A. W., & Labib, M. (2007). Sources of PM_{10} and $PM_{2.5}$ in Cairo's ambient air. *Environmental Monitoring and Assessment, 133*, 417–425. https://doi.org/10.1007/s10661-006-9596-8

Afif, C., Dutot, A., Jambert, C., Abboud, M., Adjizian-Gerard, J., Farah, W., Perros, P., & Rizk, T. (2009). Statistical approach for the characterization of NO_2 concentrations in Beirut. *Air Quality, Atmosphere and Health, 2*, 57. https://doi.org/10.1007/S11869-009-0034-2

Alier, M., Van Drooge, B. L., Dall'Osto, M., Querol, X., Grimalt, J. O., & Tauler, R. (2013). Source apportionment of submicron organic aerosol at an urban background and a road site in Barcelona (Spain) during SAPUSS. *Atmospheric Chemistry and Physics, 13*, 10353–10371. https://doi.org/10.5194/acp-13-10353-2013

Baldasano, J. M., Delgado, R., & Calbó, J. (1998). Applying receptor models to analyze urban/suburban VOCS air quality in Martorell (Spain). *Environmental Science & Technology, 32*, 405–412. https://doi.org/10.1021/es970008h

Borbon, A., Gilman, J. B., Kuster, W. C., Grand, N., Chevaillier, S., Colomb, A., Dolgorouky, C., Gros, V., Lopez, M., Sarda-Esteve, R., Holloway, J., Stutz, J., Petetin, H., McKeen, S., Beekmann, M., Warneke, C., Parrish, D. D., & De Gouw, J. A. (2013). Emission ratios of anthropogenic volatile organic compounds in northern mid-latitude megacities. Observations versus emission inventories in Los Angeles and Paris. *Journal of Geophysical Research – Atmospheres, 118*, 2041–2057. https://doi.org/10.1002/jgrd.50059

Coll, I., Rousseau, C., Barletta, B., Meinardi, S., & Blake, D. R. (2010). Evaluation of an urban NMHC emission inventory by measurements and impact on CTM results. *Atmospheric Environment, 44*, 3843–3855. https://doi.org/10.1016/j.atmosenv.2010.05.042

Costa, M., & Baldasano, J. M. (1996). Development of a source emission model for atmospheric pollutants in the Barcelona area. *Atmospheric Environment, 30*, 309–318. https://doi.org/10.1016/1352-2310(95)00221-J

Crippa, M., Janssens-Maenhout, G., Dentener, F., Guizzardi, D., Sindelarova, K., Muntean, M., Van Dingenen, R., & Granier, C. (2016). Forty years of improvements in European air quality: Regional policy-industry interactions with global impacts. *Atmospheric Chemistry and Physics, 16*, 3825–3841. https://doi.org/10.5194/acp-16-3825-2016

Crippa, M., Guizzardi, D., Muntean, M., Schaaf, E., Dentener, F., van Aardenne, J. A., Monni, S., Doering, U., Olivier, J. G. J., Pagliari, V., & Janssens-Maenhout, G. (2018). Gridded emissions of air pollutants for the period 1970–2012 within EDGAR v4.3.2. *Earth System Science Data, 10*, 1987–2013. https://doi.org/10.5194/essd-10-1987-2018

Cros, B., Durand, P., Cachier, H., Drobinski, P., Frejafon, E., Kottmeier, C., Perros, P. E., Peuch, V. H., Ponche, J. L., Robin, D., Saïd, F., Toupance, G., & Wortham, H. (2004). The ESCOMPTE program: An overview. *Atmospheric Research, 69*, 241–279. https://doi.org/10.1016/j.atmosres.2003.05.001

Dhaini, H. R., Salameh, T., Waked, A., Sauvage, S., Borbon, A., Formenti, P., Doussin, J. F., Locoge, N., & Afif, C. (2017). Quantitative cancer risk assessment and local mortality burden for ambient air pollution in an eastern Mediterranean City. *Environmental Science and Pollution Research, 24*, 14151–14162. https://doi.org/10.1007/s11356-017-9000-y

Doussin, J.-F. (2023). The Mediterranean atmosphere under anthropogenic pressures. In F. Dulac, S. Sauvage, & E. Hamonou (Eds.), *Atmospheric chemistry in the Mediterranean Region* (Vol. 1, Background information and pollutants distribution). Springer.

El Haddad, I., Marchand, N., Wortham, H., Piot, C., Besombes, J. L., Cozic, J., Chauvel, C., Armengaud, A., Robin, D., & Jaffrezo, J. L. (2011). Primary sources of $PM_{2.5}$ organic aerosol in an industrial Mediterranean city, Marseille. *Atmospheric Chemistry and Physics, 11*, 2039–2058. https://doi.org/10.5194/acp-11-2039-2011

Elguindi, N., Granier, C., Stavrakou, T., Darras, S., Bauwens, M., Cao, H., Chen, C., Denier van der Gon, H. A. C., Dubovik, O., Fu, T. M., Henze, D., Jiang, Z., Kuenen, J. J. P., … Zheng, B. (2020). Analysis of recent anthropogenic surface emissions from bottom-up inventories and top-down estimates: Are future emission scenarios vali`d for the recent past? *Earth's Future*. https://doi.org/10.1002/essoar.10502317.1, under review.

EMEP/EEA. (2013). EMEP/EEA air pollutant emission inventory guidebook 2013 – Technical guidance to prepare national emission inventories, European Environment Agency, European Environmental Agency Tech. Rept. 12/2013, Publ. Office of the European Union, Luxembourg, 23 pp. https://doi.org/10.2800/92722

Eyring, V., Bony, S., Meehl, G. A., Senior, C. A., Stevens, B., Stouffer, R. J., & Taylor, K. (2016). Overview of the Coupled Model Intercomparison Project Phase 6 (CMIP6) experimental design and organization. *Geoscientific Model Development, 9*, 1937–1958. https://doi.org/10.5194/gmd-9-1937-2016

Georgoulias, A. K., van der A, R. J., Stammes, P., Boersma, K. F., & Eskes, H. J. (2019). Trends and trend reversal detection in 2 decades of tropospheric NO_2 satellite observations. *Atmospheric Chemistry and Physics, 19*, 6269–6294. https://doi.org/10.5194/acp-19-6269-2019

Giakoumi, A., Maggos, T., Michopoulos, J., Helmis, C., & Vasilakos, C. (2009). $PM_{2.5}$ and volatile organic compounds (VOCs) in ambient air: A focus on the effect of meteorology. *Environmental Monitoring and Assessment, 152*, 83. https://doi.org/10.1007/s10661-008-0298-2

Giorgi, F., & Raffaele, F. (2023). The climate of the Mediterranean region and future projections in relation to air quality issues. In F. Dulac, S. Sauvage, & E. Hamonou (Eds.), *Atmospheric chemistry in the Mediterranean Region* (Vol. 1, Background information and pollutants distribution). Springer.

Granier, C., Bessagnet, B., Bond, T., D'Angiola, A., Denier van der Gon, H., Frost, G. J., Heil, A., Kaiser, J. W., Kinne, S., Klimont, Z., Kloster, S., Lamarque, J.-F., Liousse, C., Masui, T., Meleux, F., Mieville, A., Ohara, T., Raut, J.-C., Riahi, K., … van Vuuren, D. P. (2011). Evolution of anthropogenic and biomass burning emissions of air pollutants at global and regional scales during the 1980–2010 period. *Climatic Change, 109*, 163–190. https://doi.org/10.1007/s10584-011-0154-1

Höglund-Isaksson, L. (2012). Global anthropogenic methane emissions 2005–2030: Technical mitigation potentials and costs. *Atmospheric Chemistry and Physics, 12*, 9079–9096. https://doi.org/10.5194/acp-12-9079-2012

Hopke, P. K. (2016). Review of receptor modeling methods for source apportionment. *Journal of the Air & Waste Management Association (1995), 66*, 237–259. https://doi.org/10.1080/10962247.2016.1140693

Janssens-Maenhout, G., Crippa, M., Guizzardi, D., Dentener, F., Muntean, M., Pouliot, G., Keating, T., Zhang, Q., Kurokawa, J., Wankmüller, R., Denier van der Gon, H., Kuenen, J. J. P., Klimont, Z., Frost, G., Darras, S., Koffi, B., & Li, M. (2015). HTAP_v2.2: A mosaic of regional and global emission grid maps for 2008 and 2010 to study hemispheric transport of air pollution. *Atmospheric Chemistry and Physics, 15*, 11411–11432. https://doi.org/10.5194/acp-15-11411-2015

Johansson, L., Jalkanen, J.-P., & Kukkonen, J. (2017). Global assessment of shipping emissions in 2015 on a high spatial and temporal resolution. *Atmospheric Environment, 167*, 403–415. https://doi.org/10.1016/j.atmosenv.2017.08.042

Junkermann, W. (2022). Anthropogenic emissions of ultrafine particles in the Mediterranean. In F. Dulac, S. Sauvage, & E. Hamonou (Eds.), *Atmospheric chemistry in the Mediterranean Region* (Vol. 2, From air pollutant sources to impacts). Springer, this volume. https://doi.org/10.1007/978-3-030-82385-6_6

Kaiser, J. W., Heil, A., Andreae, M. O., Benedetti, A., Chubarova, N., Jones, L., Morcrette, J.-J., Razinger, M., Schultz, M. G., Suttie, M., & van der Werf, G. R. (2012). Biomass burning emissions estimated with a global fire assimilation system based on observed fire radiative power. *Biogeosciences, 9*, 527–554. https://doi.org/10.5194/bg-9-527-2012

Kanakidou, M., Mihalopoulos, N., Kindap, T., Im, U., Vrekoussis, M., Gerasopoulos, E., Dermitzaki, E., Unal, A., Koçak, M., Markakis, K., Melas, D., Kouvarakis, G., Youssef, A. F., Richter, A., Hatzianastassiou, N., Hilboll, A., Ebojie, F., Wittrock, F., von Savigny, C., … Moubasher, H. (2011). Megacities as hot spots of air pollution in the East Mediterranean. *Atmospheric Environment, 45*, 1223–1235. https://doi.org/10.1016/j.atmosenv.2010.11.048

Kara, M., Mangir, N., Bayram, A., & Elbir, T. (2014). A spatially high resolution and activity based emissions inventory for the metropolitan area of Istanbul, Turkey. *Aerosol and Air Quality Research, 14*, 10–20. https://doi.org/10.4209/aaqr.2013.04.0124

Karagulian, F., & Belis, C. A. (2012). Enhancing source apportionment with receptor models to foster the air quality directive implementation. *International Journal of Environment and Pollution, 50*. https://doi.org/10.1504/IJEP.2012.051192

Karanasiou, A. A., Siskos, P. A., & Eleftheriadis, K. (2009). Assessment of source apportionment by Positive Matrix Factorization analysis on fine and coarse urban aerosol size fractions. *Atmospheric Environment, 43*, 3385–3395. https://doi.org/10.1016/j.atmosenv.2009.03.051

Klimont, Z., Smith, S. J., & Cofala, J. (2013). The last decade of global anthropogenic sulfur dioxide: 2000–2011 emissions. *Environmental Research Letters, 8*, 014003. https://doi.org/10.1088/1748-9326/8/1/014003

Koçak, M., Theodosi, C., Zarmpas, P., Im, U., Bougiatioti, A., Yenigun, O., & Mihalopoulos, N. (2011). Particulate matter (PM_{10}) in Istanbul: Origin, source areas and potential impact on surrounding regions. *Atmospheric Environment, 45*, 6891–6900. https://doi.org/10.1016/j.atmosenv.2010.10.007

Kushta, J., Georgiou, G. K., Proestos, Y., Christoudias, T., & Lelieveld, J. (2018). Modelling study of the atmospheric composition over Cyprus. *Atmospheric Pollution Research, 9*, 257–269. https://doi.org/10.1016/j.apr.2017.09.007

Lamarque, J.-F., Bond, T. C., Eyring, V., Granier, C., Heil, A., Klimont, Z., Lee, D., Liousse, C., Mieville, A., Owen, B., Schultz, M. G., Shindell, D., Smith, S. J., Stehfest, E., Van Aardenne, J., Cooper, O. R., Kainuma, M., Mahowald, N., McConnell, J. R., … van Vuuren, D. P. (2010). Historical (1850–2000) gridded anthropogenic and biomass burning emissions of reactive gases and aerosols: Methodology and application. *Atmospheric Chemistry and Physics, 10*, 7017–7039. https://doi.org/10.5194/acp-10-7017-2010

Lelieveld, J., Beirle, S., Hormann, C., Stenchikov, G., & Wagner, T. (2015a). Abrupt recent trend changes in atmospheric nitrogen dioxide over the Middle East. *Science Advances, 1*, e1500498. https://doi.org/10.1126/sciadv.1500498

Lelieveld, J., Evans, J. S., Fnais, M., Giannadaki, D., & Pozzer, A. (2015b). The contribution of outdoor air pollution sources to premature mortality on a global scale. *Nature, 525*, 367–371. https://doi.org/10.1038/nature15371

Markakis, K., Im, U., Unal, A., Melas, D., Yenigun, O., & Incecik, S. (2012). Compilation of a GIS based high spatially and temporally resolved emission inventory for the greater Istanbul area. *Atmospheric Pollution Research, 3*, 112–125. https://doi.org/10.5094/APR.2012.011

Massoud, R., Shihadeh, A., Roumie, M., Youness, M., Gerard, J., Saliba, N., Zaarour, R., Abboud, M., Farah, W., & Saliba, N. A. (2011). Intraurban variability of PM_{10} and $PM_{2.5}$ in an Eastern Mediterranean city. *Atmospheric Research, 101*, 893. https://doi.org/10.1016/J.ATMOSRES.2011.05.019

Menut, L., Coll, I., & Cautenet, S. (2005). Impact of meteorological data resolution on the forecasted ozone concentrations during the ESCOMPTE IOP 2a and 2b. *Atmospheric Research, 74*, 139–159. https://doi.org/10.1016/j.atmosres.2004.04.008

Mohr, C., DeCarlo, P. F., Heringa, M. F., Chirico, R., Slowik, J. G., Richter, R., Reche, C., Alastuey, A., Querol, X., Seco, R., Peñuelas, J., Jiḿenez, J. L., Crippa, M., Zimmermann, R., Baltensperger, U., & Prévôt, A. S. H. (2012). Identification and quantification of organic aerosol from cooking and other sources in Barcelona using aerosol mass spectrometer data. *Atmospheric Chemistry and Physics, 12*, 1649–1665. https://doi.org/10.5194/acp-12-1649-2012

Moschonas, N., & Glavas, S. (1996). C_3-C_{10} hydrocarbons in the atmosphere of Athens, Greece. *Atmospheric Environment, 30*, 2769–2772. https://doi.org/10.1016/1352-2310(95)00488-2

Moschonas, N., Glavas, S., & Kouimtzis, T. (2001). C_3 to C_9 hydrocarbon measurements in the two largest cities of Greece, Athens and Thessaloniki. Calculation of hydrocarbon emissions by species. Derivation of hydroxyl radical concentrations. *Science of the Total Environment, 271*, 117–133. https://doi.org/10.1016/S0048-9697(00)00838-X

Öztürk, F., Zararsz, A., Dutkiewicz, V. A., Husain, L., Hopke, P. K., & Tuncel, G. (2012). Temporal variations and sources of Eastern Mediterranean aerosols based on a 9-year observation. *Atmospheric Environment, 61*, 463–475. https://doi.org/10.1016/j.atmosenv.2012.07.051

Paatero, P. (1997). A weighted non-negative least squares algorithm for three-way "PARAFAC" factor analysis. *Chemometrics and Intelligent Laboratory, 38*, 223–242. https://doi.org/10.1016/S0169-7439(97)00031-2

Paatero, P., & Tapper, U. (1994). Positive Matrix Factorization: A nonnegative factor model with optimal utilization of error estimates of data values. *Environmetrics, 5*, 111–126. https://doi.org/10.1002/env.3170050203

Pandolfi, M., Querol, X., Alastuey, A., Jimenez, J. L., Jorba, O., Day, D., Ortega, A., Cubison, M. J., Comerón, A., Sicard, M., Mohr, C., Prévôt, A. S. H., Minguillón, M. C., Pey, J., Baldasano, J. M., Burkhart, J. F., Seco, R., Peñuelas, J., van Drooge, B. L., … Szidat, S. (2014). Effects of sources and meteorology on particulate matter in the Western Mediterranean Basin: An overview of the DAURE campaign. *Journal of Geophysical Research*. https://doi.org/10.1002/2013JD021079

Panopoulou, A., Liakakou, E., Gros, V., Sauvage, S., Locoge, N., Bonsang, B., Psiloglou, B. E., Gerasopoulos, E., & Mihalopoulos, N. (2018). Non-methane hydrocarbon variability in Athens during wintertime: The role of traffic and heating. *Atmospheric Chemistry and Physics, 18*, 16139–16154. https://doi.org/10.5194/acp-18-16139-2018

Pateraki, S., Maggos, T., Michopoulos, J., Flocas, H. A., Asimakopoulos, D. N., & Vasilakos, C. (2008). Ions species size distribution in particulate matter associated with VOCs and meteorological conditions over an urban region. *Chemosphere, 72*, 496–503. https://doi.org/10.1016/j.chemosphere.2008.02.061

Pérez, N., Pey, J., Reche, C., Cortés, J., Alastuey, A., Querol, X., et al. (2016). *Science of the Total Environment, 571*, 237–250. https://doi.org/10.1016/j.scitotenv.2016.07.025

Petrakis, M., Psiloglou, B., Kassomenos, P. A., & Cartalis, C. (2003). Summertime measurements of benzene and toluene in Athens using a differential optical absorption spectroscopy system. *Journal of the Air & Waste Management Association (1995), 53*, 1052–1064. https://doi.org/10.1080/10473289.2003.10466266

Querol, X., Alastuey, A., Rodriguez, S., Plana, F., Ruiz, C. R., Cots, N., Massagué, G., & Puig, O. (2001). PM_{10} and $PM_{2.5}$ source apportionment in the Barcelona Metropolitan area, Catalonia, Spain. *Atmospheric Environment, 35*, 6407–6419. https://doi.org/10.1016/S1352-2310(01)00361-2

Rappenglück, B., Fabian, P., Kalabokas, P., Viras, L. G., & Ziomas, I. C. (1998). Quasi-continuous measurements of nonmethane hydrocarbons (NMHC) in the Greater Athens area during medcaphot-trace. *Atmospheric Environment, 32*, 2103–2121. https://doi.org/10.1016/S1352-2310(97)00430-5

Rappenglück, B., Kourtidis, K., Melas, D., & Fabian, P. (1999). Observations of biogenic and anthropogenic NMHC in the greater Athens area during the PAUR campaign. *Physics and Chemistry of the Earth, Part B, 24*, 717–724. https://doi.org/10.1016/S1464-1909(99)00071-4

Riahi, K., van Vuuren, D. P., Kriegler, E., Edmonds, J., O'Neill, B. C., Fujimori, S., Bauer, N., Calvin, K., Dellink, R., Fricko, O., Lutz, W., Popp, A., Crespo Cuaresma, J., Kc, S., Marian Leimbach, M., Jiang, L., Kram, T., Rao, S., Emmerling, J., … Tavoni, M. (2017). The shared socioeconomic pathways and their energy, land use, and greenhouse gas emissions implications: An overview. *Global Environmental Change, 42*, 153–168. https://doi.org/10.1016/j.gloenvcha.2016.05.009

Salameh, T., Afif, C., Sauvage, S., Borbon, A., & Locoge, N. (2014). Speciation of Non-Methane Hydrocarbons (NMHC) from anthropogenic sources in Beirut, Lebanon. *Environmental Science and Pollution Research, 21*, 10867–10877. https://doi.org/10.1007/s11356-014-2978-5

Salameh, T., Sauvage, S., Afif, C., Borbon, A., Leonardis, T., Brioude, J., Waked, A., & Locoge, N. (2015). Exploring the seasonal NMHC distribution in an urban area of the Middle East during ECOCEM campaigns: Very high loadings dominated by local emissions and dynamics. *Environment and Chemistry, 12*, 316–328. https://doi.org/10.1071/EN14154

Salameh, T., Sauvage, S., Afif, C., Borbon, A., & Locoge, N. (2016). Source apportionment vs. emission inventories of non-methane hydrocarbons (NMHC) in an urban area of the Middle East: Local and global perspectives. *Atmospheric Chemistry and Physics, 16*, 3595–3607. https://doi.org/10.5194/acp-16-3595-2016

Salameh, T., Borbon, A., Afif, C., Sauvage, S., Leonardis, T., Gaimoz, C., & Locoge, N. (2017). Composition of gaseous organic carbon during ECOCEM in Beirut, Lebanon: New observational constraints for VOC anthropogenic emission evaluation in the Middle East. *Atmospheric Chemistry and Physics, 17*, 193–209. https://doi.org/10.5194/acp-17-193-2017

Thera, B. T. P., Dominutti, P., Öztürk, F., Salameh, T., Sauvage, S., Afif, C., Çetin, B., Gaimoz, C., Keleş, M., Evan, S., & Borbon, A. (2019). Composition and variability of gaseous organic pollution in the port megacity of Istanbul: Source attribution, emission ratios, and inventory evaluation. *Atmospheric Chemistry and Physics, 19*, 15131–15156. https://doi.org/10.5194/acp-19-15131-2019

Trombetti, M., Thunis, P., Bessagnet, B., Clappier, A., Couvidat, F., Guevara, M., Kuenen, J., & López-Aparicio, S. (2018). Spatial inter-comparison of top-down emission inventories in European urban areas. *Atmospheric Environment, 173*, 142–156. https://doi.org/10.1016/j.atmosenv.2017.10.032

van Vuuren, D., Edmonds, J., Kainuma, M., Riahi, K., & Weyant, J. (2011). A special issue on the RCPs. *Climatic Change, 109*, 1–4. https://doi.org/10.1007/s10584-011-0157-y

Waked, A., & Afif, C. (2012). Emissions of air pollutants from road transport in Lebanon and other countries in the Middle East region. *Atmospheric Environment, 61*, 446–452. https://doi.org/10.1016/j.atmosenv.2012.07.064

Waked, A., Afif, C., & Seigneur, C. (2012). An atmospheric emission inventory of anthropogenic and biogenic sources for Lebanon. *Atmospheric Environment, 50*, 88–96. https://doi.org/10.1016/j.atmosenv.2011.12.058

Waked, A., Afif, C., Brioude, J., Formenti, P., Chevaillier, S., El Haddad, I., Doussin, J. F., Borbon, A., & Seigneur, C. (2013). Composition and source apportionment of organic aerosol in Beirut, Lebanon, during winter 2012. *Aerosol Science and Technology, 47*, 1258–1266. https://doi.org/10.1080/02786826.2013.831975

Warneke, C., McKeen, S. A., de Gouw, J. A., Goldan, P. D., Kuster, W. C., Holloway, J. S., Williams, E. J., Lerner, B. M., Parrish, D. D., Trainer, M., Fehsenfeld, F. C., Kato, S., Atlas, E. L., Baker, A., & Blake, D. R. (2007). Determination of urban volatile organic compound emission ratios and comparison with an emissions database. *Journal of Geophysical Research, 112*, D10S47. https://doi.org/10.1029/2006JD007930

Wheida, A., Nasser, A., El Nazer, M., Borbon, A., Abo El Ata, G. A., Wahab, M. A., & Alfaro, S. C. (2018). Tackling the mortality from long-term exposure to outdoor air pollution in megacities: Lessons from the Greater Cairo case study. *Environmental Research, 160*, 223–231. https://doi.org/10.1016/j.envres.2017.09.028

Ultrafine Particle Emissions in the Mediterranean

Wolfgang Junkermann

Contents

Abstract An overview of ultrafine particles (UFP) and their sources in the Mediterranean basin is presented based on historical and new measurements in the framework of ChArMEx (the Chemistry-Aerosol Mediterranean Experiment). UFP and meteorological variables were measured from an ultralight aircraft focusing on particles in the nucleation and Aitken modes, and their potential properties as cloud condensation nuclei (CCN). Observed UFP could be assigned to different source areas and occasionally to certain types of emitters. An assessment of ship emissions contribution to the nucleation and Aitken particle modes budget over the Mediterranean is derived. Shipping along the main route from Suez to Gibraltar is a source of UFP in a similar order of magnitude or even larger than anthropogenic emissions along the shorelines and well above any natural sources. In areas far from major emission sources, the majority of UFP were identified as CCN in concentrations far above natural abundance and significantly enhanced compared to

Chapter reviewed by ***Daniel Rosenfeld*** *(Institute of Earth Sciences, The Hebrew University of Jerusalem, The Edmond J. Safra Campus, Jerusalem, Israel), as part of the book Part V Emissions and Sources also reviewed by* ***Claire Granier*** *(Laboratoire d'Aérologie (LAERO), CNRS – Univ. Toulouse III Paul Sabatier, Observatoire Midi-Pyrénées, Toulouse, France)*

W. Junkermann (✉)
Institute of Meteorology and Climate Research (IMK-IFU), Karlsruhe Institute of Technology, Garmisch-Partenkirchen, Germany

F. Dulac et al. (eds.), *Atmospheric Chemistry in the Mediterranean Region*,
https://doi.org/10.1007/978-3-030-82385-6_6

pre-climate change (~1970) conditions. This enhancement in CCN concentrations over the whole basin by anthropogenic UFP is an important input parameter for aerosol-cloud interaction models and could be a timely, well-correlated, and essential factor for the observed changes in rainfall patterns within the last decades.

1 Introduction

The preceding chapter reviewed anthropogenic emissions of various reactive gases and fine particulate compounds in the Mediterranean region (Borbon et al., 2022). Here the focus is put on the anthropogenic contribution to the budget of ultrafine particles (UFP) in the Mediterranean atmosphere. Most emission inventories are based on mass emissions, and UFP represents only a minor fraction of the mass. Despite their climate relevance, the number emission is not included in emission databases like those considered in the preceding chapter. To our knowledge, the first number emission scenario was published by Paasonen et al. (2016). The main sources were industrial and residential combustion processes and traffic. However, these numbers are still highly uncertain, and they cover only continental sources, whereas in the Mediterranean, the contribution from intense ship traffic (see the chapter in Vol. 1 by Doussin, 2023) has to be taken into account given documented UFP emissions by large ship engines (e.g., Contini et al., 2015; Villa et al., 2019 and references therein).

UFP constitute the fraction of the airborne particle size spectrum below 100 nm in diameter. This size range covers particles in both the nucleation mode, <1–20 nm, and the Aitken mode, 20–100 nm (Young & Keeler, 2007). In the upper range of the Aitken mode (>40 nm) and further extending into the accumulation mode (>100 nm), ultrafine particles may act as cloud condensation nuclei (CCN) (Charlson et al., 1987; Andreae, 2009). The threshold for CCN activity at sizes >40 nm is not fixed as it depends on aerosol chemistry, the fraction of water-soluble and water-insoluble compounds, and their physical distribution within the particle. Further on, meteorological and cloud dynamical parameters like updraft velocity and supersaturation of water vapor in clouds control the growth of cloud condensation nuclei to real cloud droplets (Rosenfeld et al., 2019). A reduction in droplet size by additional UFP-derived CCN is expected to delay rainfall from shallow clouds (Rosenfeld, 2000; Bigg, 2008), although a direct causality for regional drought is difficult to prove (Heinzeller et al., 2016). On the other hand, more latent heat energy originates from more rapid evaporation of warm shallow cloud droplets and also from in-cloud processes involving condensation on UFP/CCN inside strong convective cells. This latent energy invigorates torrential rains leading locally to even more intense precipitation (Bell et al., 2008; Rosenfeld et al., 2008; Fan et al., 2018; Guerreiro et al., 2018). Increased lightning intensity over major shipping lines was also reported (Thornton et al., 2017).

Due to the impact of ultrafine particles as CCN on clouds and subsequently on the hydrological cycle, knowledge about these particles and their emissions and budgets is crucial for climate modelling (Charlson et al., 1987). The Mediterranean is suffering from changes of the hydrological cycle, rainfall, drought, and surface runoff as well as torrential rains and Mediterranean tropical-like cyclones called medicanes (Gudmundsson et al., 2016). Understanding UFP and the fraction of the UFP active as CCN might be contributing to the understanding of these changes. Enhanced CCN might even be responsible not only for longer droughts but also for an increase in lower troposphere water vapor as a major greenhouse gas and thus directly affect the earth's radiation balance (Riuttanen et al., 2016; Bister & Kulmala, 2011).

Ultrafine particles in the atmosphere, especially in the lowest size ranges, originate from a production from gas phase molecules or gas to particle conversion (GPC). The initial step, the nucleation, is the production of a more or less stable cluster of about 1 nm in diameter that then further grows and stabilizes within a few hours (Kulmala et al., 2013). This nucleation and growth process may happen everywhere in the atmosphere where a suitable mixture of chemical compounds is available. It has already been observed by Aitken at the Scottish northwest coast and also at the coastline of Tasmania at Cape Grim. Such a natural particle production from maritime emissions or related compounds (O'Dowd et al., 2005) has, however, never been observed in the Mediterranean although volcanic emissions could emit additionally the required chemical precursors. Key substances for the initial cluster production are compounds like sulfuric or nitric acid as well as ammonia, and the intensity of new particle formation is, like in all other chemical reactions, depending on the "ambient" "laboratory" conditions. Natural UFP in the maritime environment are either derived from biogenic emissions of organic sulfur compounds oxidizing in the atmosphere to reactive sulfur and subsequently slowly growing GPC particles (Charlson et al., 1987) or derived from sea spray and bursting gas bubbles. Particle concentrations over pristine ocean surfaces are in the order of a few hundred cm^{-3}, of which about 100 to 150 are cloud condensation nuclei (Schmale et al., 2018). However, under conditions with marine biogenic material exposed to sunlight at some coastal sites, locally enhanced number concentrations well exceeding 10,000 cm^{-3} were observed (O'Dowd et al., 2005, 2007). Everywhere in the atmosphere, sulfur dioxide emitted naturally from volcanic activity or from marine emissions like DMS, or emitted by anthropogenic sources, may produce nanoparticles upon interaction with ammonia from agriculture. The natural continental background source strength, however, is not well known. Bigg and Turvey (1978) estimated the natural background for remote Australia to ~700 particles cm^{-3}. Strong anthropogenic induced gas to particle conversion was observed to produce large numbers of particles in sulfur-rich plumes released from power stations (Kiang et al., 1973) and smelters (Ayers et al., 1979) or also in the industrial applications burning at high temperatures sulfur containing fossil fuel (Bai et al., 1992) as part of the SCR flue gas cleaning systems. For these applications, the addition of ammonia was proposed as a technique to convert harmful gaseous compounds SO_2 and NO_x into filterable particulate matter.

The growth of the initial nucleation clusters in the atmosphere with growth rates of a few nm per hour is finally dependent on the presence of additional condensable substances like extreme low volatility organic compounds (ELVOC) (Kulmala et al., 2013; Ehn et al., 2014). Such VOCs would be readily available from the Mediterranean vegetation. After several hours, particles grown into the size range of cloud condensation nuclei are then composed of a mixture of an inorganic core, i.e., ammonium sulfate or nitrate, and organic compounds with a more or less hydrophilic composition which controls the later droplet activation process in the cloud and the probability of the UFP to become a CCN (Wang et al., 2019).

Frequent biomass burning over and around the Mediterranean is an alternate source for particles in the CCN range, but it is producing large amounts of mainly accumulation mode particles. The main emission mode is larger, and the number size distribution main mode of fresh biomass burning aerosol is normally above 80 nm with a tail well into the visible size range >300 nm (Alonso-Blanco et al., 2014). Besides the number concentration thus, to disentangle different sources and production processes, the size distribution is a powerful key to investigate the origin, or age, of ultrafine particulate matter. For example, in case that the nucleation mode is suppressed and only particles >10 nm are observed, this is normally an indication of a medium- to long-range transport due to the fast growth of freshly produced particles from the nucleation into the Aitken mode (Boy & Kulmala, 2002; Dal Maso et al., 2005). Also, the shape of the observed modes can be used as an indicator of underlying production and aging processes. Unfortunately, ultrafine particles are invisible and thus not detectable by remote sensing techniques which would allow a better spatial coverage and monitoring. They have to be measured in situ, and spatial investigation requires aircraft.

An extended overview about the historical and technological development of instrumentation for the measurement of UFP is given by Mohnen and Hidy (2010). Although instrumentation for the detection of particles >15 nm has been available since the late nineteenth century (Coulier, 1875; Aitken, 1888), the knowledge of ultrafine particles and their sources and budget is still limited. One reason for the limited database is the fact that, despite the early knowledge of particle numbers as a proxy for pollution levels (Aitken, 1890; Landsberg, 1938), regulations concerning particles normally consider the mass fraction, particulate matter with size ranges <10 μm or 2.5 μm (PM_{10} or $PM_{2.5}$). This was one of the initial parameters reproducible measurable and claimed to be health relevant (Pope et al., 2002). Environmental monitoring sites were thus normally equipped with instrumentation neither for long-term monitoring of particle number concentration nor for the particle size distribution. That ultrafine particles may be even more health relevant than particulate mass came up about a decade ago (Franck et al., 2011) and is now generally accepted. The health effect is described to be due to the smaller size and subsequent deeper penetration of UFP into the lung. However, only a few monitoring networks have been established since (Birmili et al., 2016). In the Mediterranean, only two sites were installed since 2000 following the detection of more or less regular diurnal patterns of ultrafine particles within the nucleation mode in a boreal forest

environment (Kulmala et al., 2004). The instrumentation is relatively complex so that data are mostly available from short-term campaign activities. In Italy, the first site in the eastern Po Valley was established at San Pietro Capofiume about 30 km from the Adriatic coast in a predominant agricultural area surrounded by several large pollution sources (Laaksonen et al., 2005). Data are covering several years, for example, from the QUEST-EU (Quantification of Aerosol Nucleation) campaign, and long-term measurements were analyzed and published by Hamed et al. (2007). In the eastern Mediterranean, a station has been established in Crete (Finokalia), and analyses covering several years are now reported (Kalivitis et al., 2019). A station on the island of Gozo was installed in 2012, but to our knowledge, no data have been published yet.

To cover the gaps in observations, a few more stations were installed to extend the existing infrastructure temporarily in relatively clean locations on the islands of Mallorca and Corsica, and aircraft were used for additional three-dimensional investigations within the framework of the Chemistry-Aerosol Mediterranean Experiment (ChArMEx; https://www.atmos-chem-phys.net/special_issue334.html). Field operations were mainly over the western basin (Rose et al., 2015) and over the island of Corsica in summer 2012 (project VESSAER: Vertical Structure, Sources, and Evolution of Aerosols in the Mediterranean Region; Roberts et al., 2013) and extended further south east over Malta and Gozo islands in summer 2013. On a short time scale and on a campaign basis, further ultrafine particle data are available from campaign activities in ChArMEx from field sites in Mallorca Isl. and at Ersa (north of Cap Corse on Corsica Isl.) in the western Mediterranean and at Finokalia (Crete Isl.) in the eastern Mediterranean (Berland et al., 2017; Kalivitis et al., 2019). Data from a later campaign in Madrid in 2017 (Carnerero et al., 2018) fit well into the overall picture.

One advantage of the available database for the characterization of the anthropogenic contribution to the particle budget is the fact that besides measurements with the latest available instrumentation, at least a few historical data on particle number concentrations are published. John Aitken spent at the end of the nineteenth century already several weeks on the French coastline east of Toulon with his mobile counter. Later, in the early 1970s, a ship cruise for the investigation of ultrafine particle number concentrations was performed in the Sardinia and Sicily Channels which were considered at that time as remote maritime areas (Colacino & Dalu, 1972), followed by a cruise in 1975 throughout the whole western and eastern Mediterranean (Elliott, 1976). These measurements now can be compared to number concentrations measured during ChArMEx in 2012 and 2013 considering that the early Aitken and Pollak (Metnieks & Pollak, 1959) counters are comparable in the lower detectable size limit but were not able to measure nucleation mode particles below ~15 nm. Nevertheless, the currently available size distributions down to ~3 nm allow a comparison.

2 Airborne Experiments in the Mediterranean

Several aircraft were involved in aerosol investigations in the western Mediterranean: the French Safire ATR-42 flew in 2012 during a campaign of the Hydrological Cycle Mediterranean Experiment (HyMeX; Rose et al., 2015) and in cooperation with the Safire Falcon F-20 in 2013 during a ChArMEx campaign (Mallet et al., 2016). A small aircraft operated by Karlsruhe Institute of Technology (KIT) in Germany was used already earlier between 1999 and 2008 in the western Mediterranean for investigations of the regional three-dimensional distribution of aerosols and radiation. These first campaigns included ultrafine particles from a > 10 nm particle counter (CPC) to characterize photochemistry in southern France between Avignon and Marseille (Junkermann, 2005) and the vertical structure of the planetary boundary layer (PBL) over the island of Lampedusa for Saharan dust studies (Meloni et al., 2015). To gather first information on nucleation mode particles, extensive flights over the eastern Po Valley within the QUEST project (Laaksonen et al., 2005) used a twin counter setup with 3 and 10 nm cutoffs.

With a similar two-counter setup plus an additional SMPS (20–480 nm), Rose et al. (2015) indeed found nanoparticles between 5 and 10 nm in elevated layers especially over the Gulf of Lyon and assigned these particles to new particle formation. The data presented do not allow us to identify or to quantify the emission source or the contribution to the CCN budget. A contribution of marine emissions to new particle formation in the elevated layers would require at least convective vertical and synoptic horizontal transport most likely with some anthropogenic contamination. The corresponding three-dimensional distribution and temporal, day and night occurrence, could be as well in agreement with continental emission, meteorology, and long-range transport (Junkermann & Hacker, 2018).

Within the framework of ChArMEx, two airborne campaigns specially focusing on ultrafine particles and CCN followed over islands of Corsica and Malta during summer of 2012 and 2013, respectively. Aerosol particle size distributions and their potential to serve as cloud condensation nuclei were investigated during the VESSAER 2012 campaign on the eastern side of Corsica up to an altitude of about 3500 m a.s.l., probing both the planetary boundary layer and the lower free troposphere. The objective was to characterize ultrafine particle number, size distributions, and cloud condensation nuclei spectra in local (PBL) and long-range transported air masses (lower free troposphere) (Roberts et al., 2013). The aircraft, an instrumented weight shift microlight, carried a set of aerosol sensors, CPC (>10 nm), nano-SMPS (4.5–350 nm with 15 size bins between 4.5 and 20 nm, 120–sec time resolution), optical particle spectrometer (0.3–20 μm), as well as comprehensive meteorological instrumentation, i.e., temperature, dew point, radiation, wind speed, and turbulence (Junkermann et al., 2016). An additional miniaturized cloud condensation nuclei spectrometer was provided for the Corsica campaign by G. Roberts, Météo-France, Toulouse. During summer 2013, the KIT ultralight flew with a more sensitive CPC (>4.5 nm) from the island of Malta with vertical profiles over Malta and the neighboring island of Gozo to characterize ship emissions close to the Sicilian Channel, nowadays one of the world's major shipping routes (see chapter on anthropogenic pressures; Doussin, 2023).

The results for both island locations were quite different. Corsica is located relatively close to the coastline of Italy with 200 km of Genova and ~ 120 km of Civitavecchia, and ~ 900 km of the Spanish coast, but further away from major shipping routes than Malta. The island is large enough to be subject to thermal convection, mixing planetary boundary layer air up to the mountain summits at 2700 m. During VESSAER, we experienced mainly westerly winds with 24 h back trajectories originating on the Iberian Peninsula and fast transport over ~900 km. Number concentrations of ultrafine particles were always moderate, in the range of 2000–4000 cm^{-3} up to an altitude of ~2500–3000 m, but occasionally even higher up to 6000 cm^{-3} in an elevated layer above 1800 m. For westerly winds encountered, the mountain range on Corsica is a barrier with open channels at about 1600 m. Thus, below 1600 m, likely more local conditions prevail. The island is covered with dense Mediterranean vegetation, the source of VOC required for rapid aerosol growth (Ehn et al., 2014). However, during 2 weeks of campaign, no significant signature of fresh nucleation in any of these air masses was ever observed. Geometric mean particle size was normally between 70 and 100 nm and more than 50%, up to 100% of these particles were cloud condensation nuclei at 0.3% supersaturation. In one case, we found a direct transport or smaller particles at mid-elevation (1600–2300 m) passing over Ajaccio and possibly affected by emissions from the local fossil fuel power station (Roberts et al., 2013). The data compare well with the size distributions at the surface site of Ersa at 535 m a.s.l. in altitude north of Corsica and with the traces of nucleation mode aerosol in elevated layers reported by Rose et al. (2015) (Fig. 1). From continuous measurements at Ersa (Cap Corse; Berland et al., 2017; see also the chapter on nucleation by Sellegri & Rose, 2022),

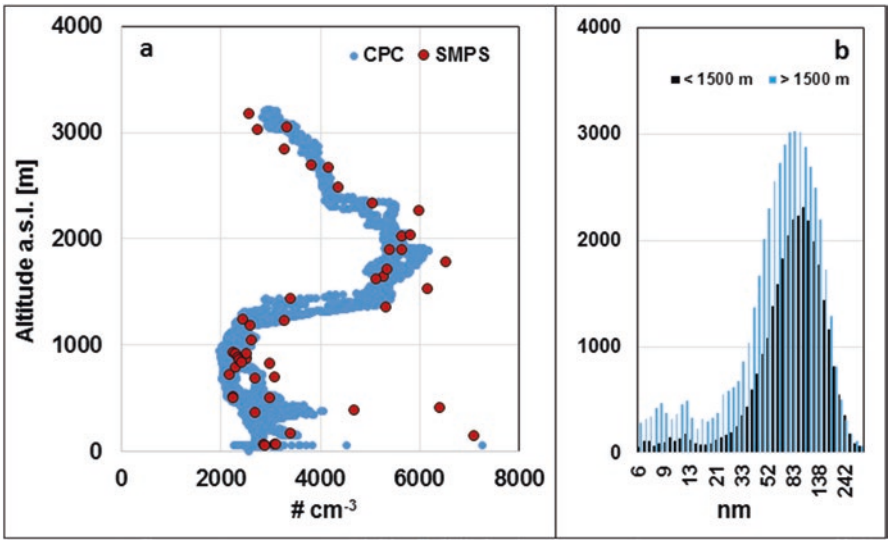

Fig. 1 (**a**) Vertical profiles of ultrafine particles >10 nm (CPC, light blue) and total number concentration (SMPS, dark red) over Ghisonaccia (Corsica) July 9, 2012. (**b**) Average size distribution: (diameter) in the PBL below 1500 m (black) and between 1500 and 2300 m (light blue)

<10 nm nucleation mode particles were visible only occasionally, and the "typical" diurnal "banana curve" patterns, which are often observed at surface sites on the continent, began at or above 15 nm, an indication that favors rather long-range transport advected particles compared to local particle production (Boy & Kulmala, 2002; Dal Maso et al., 2005). During the time of the flights and also at Ersa, the size of the main UFP mode was already generally >50 nm.

The Malta flights revealed a completely different picture. The nucleation mode dominated the atmospheric marine boundary layer (MBL) with concentrations about an order of magnitude larger than observed over Corsica and previously in the campaigns at Lampedusa, where normally several distinct layers of UFP were observed, the first one just marking the top of the MBL (Di Iorio et al, 2003). These stable aerosol layers are a result of the normally stable stratification of the marine planetary boundary MBL compared to the continent, and Lampedusa is too small to significantly produce such a thermal convection as observed over Corsica (Junkermann, 2001; Meloni et al., 2015). Over Malta and Gozo, the UFP in the MBL were not perfectly mixed, an indication of a nearby source, but the average concentrations over both islands were the same each day. Contrary to the moderate number concentrations over Corsica with up to ~6000 cm^{-3} over Malta up to 150,000 cm^{-3}, typically 40,000–80,000 cm^{-3} were found. Figure 2a shows the vertical structure of ultrafine particles during a morning flight (08:00 to 10:00 UTC) over Malta and Gozo with slight northerly winds on June 14, 2013.

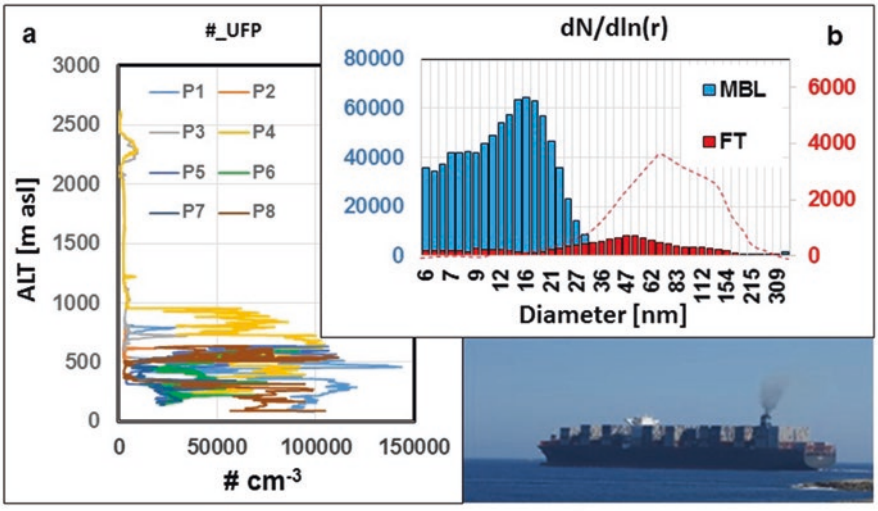

Fig. 2 UFP over the island of Malta and Gozo: (**a**) Eight vertical soundings from ~50 m a.g.l. to ~2500 m a.g.l. for particle number concentrations >4.5 nm. (**b**) Corresponding averaged size distributions above the MBL and within the MBL. The flight was performed under conditions with about 2.5 ms^{-1} northerly winds downwind of the main shipping route between Malta and Sicily. For comparison, a typical MBL size distribution from Corsica is included (dotted line). The photo taken during the campaign shows a cargo ship off Malta with its smoke plume

Due to airspace restrictions with Malta airport, all vertical profiles >600 m were flown over the island of Gozo. Here on June 14, a thin layer with ~10,000 particles cm^{-3} (already more than in Corsica) was found at 2300 m. The origin of this layer with low concentration for Malta but high compared to Corsica is not known; however, the back trajectory passed quite close to the summit of Mt. Etna. This layer can thus be both natural and anthropogenic. The corresponding size distributions in the MBL (see Fig. 2b) had a major and slightly asymmetric mode at 18–20 nm diameter, while the size distribution above the MBL peaked at ~60 nm more similar to the observations of aged particles over Corsica. A size distribution with a main mode at that small diameter is probably a mixture of primary emission and fast secondary production in agreement with the ships emitting high amounts of sulfur dioxide and NO_x. A pure secondary production during the morning time window would, however, require a significantly faster growth than known from recent literature. It is interesting to note that the UFP main mode is clearly smaller than the one reported for a container ship burning heavy marine oil outside the SECA (Sulfur Emission Control Area) area of the British channel (~80 nm; Petzold et al., 2008) and much closer to the sizes emitted from modern continental power stations (Junkermann et al., 2016; Junkermann & Hacker, 2018). Such stations apply flue gas cleaning techniques like SCR or SNCR (selective (non)-catalytic reduction) where large amounts of added ammonia suppress the NO_2 emission but favor the production of new particles. Nucleation then already occurs within the power station, respectively, within the flue gas cleaning section (Bai et al., 1992; Srivastava et al., 2004) or directly after emission in the cooling and spreading flue gas plume. A later comparison with a hybrid ferry in the Baltic Sea operating at low sulfur fuel (<0.1%) and including a pollution scrubber system revealed even higher number emissions under totally overcast conditions. The ferry emitted a clear single particle mode at 30 nm without any indication of fresh nucleation. For the Mediterranean under bright sunshine downwind of the main shipping channel, a slightly smaller main size mode (18 nm) which was found extending into the lowest nucleation mode size bins, a signature of gas to particle conversion.

During the airborne campaign over Malta, an additional ground-based particle counter (TSI 3010) and an optical particle spectrometer (model GRIMM 1.108) were installed on a rooftop (fifth floor) at the harbor of Marsaxlokk on the east side of Malta island as a ground-based reference. On the average over the campaign the instruments measured ~15,000 particles cm^{-3} with particle numbers reaching >50,000 cm^{-3} (Fig. 3a). An obvious diurnal pattern with maxima around noon (Fig. 3b) indicates that Malta, although smaller than Corsica, is also likely subject to diurnal convection regularly advecting sulfur- and particle-rich air from ships either passing by or on berth to the island. The pattern is not in agreement with the local car traffic in the area. However, here the size of the UFP and the mixture of primary and secondary particles remains unknown due to the missing size distribution.

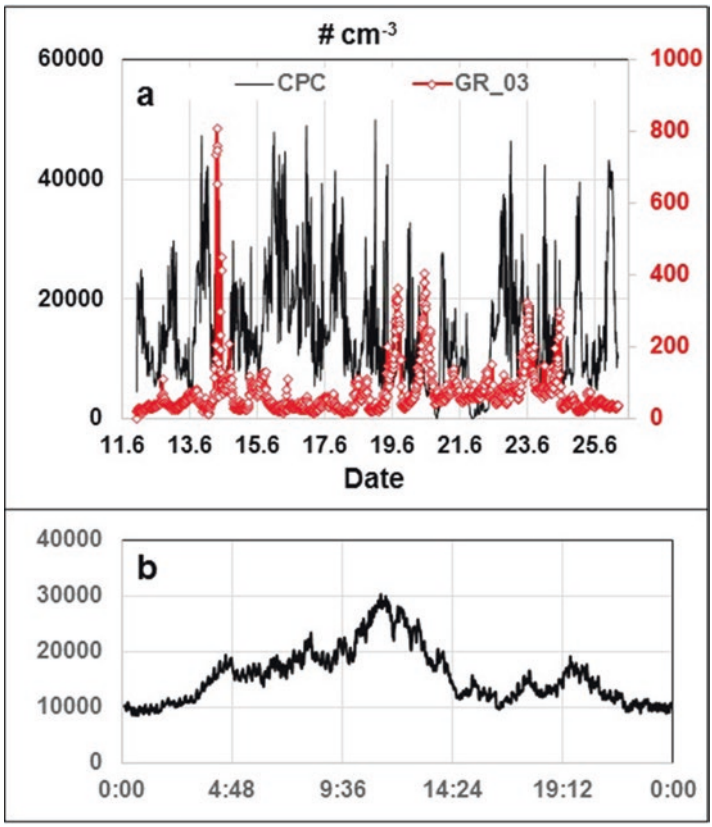

Fig. 3 Ground-based UFP measurements during the June 11–26, 2013, campaign on the island of Malta, at a rooftop fifth floor at the harbor front of Marsaxlokk: (**a**) concentration levels of particles >10 nm (CPC-TSI 3010; left axis) and the particle number concentration of fine particles >300 nm (GR0_03, right axis); high values of fine particles indicate Saharan dust events; (**b**) diurnal cycle of the UFP concentration as a running average for the campaign

3 History of Ultrafine Particle Concentration Levels in the Mediterranean

It is interesting to note how particle number concentrations and potential cloud condensation nuclei concentrations changed in the Mediterranean within the last decades. Already back in 1890 John Aitken (1890) identified anthropogenic activities at the harbor town of Toulon as one of the major sources of Aitken particles and other pollution, but, he was not able to identify any chemical process involved. During his measurements, about 30 km from Toulon he found, from the clean maritime sector, ~600 particles cm^{-3}. Polluted air reached up to 45,000 particles cm^{-3} downwind the city and port of Toulon.

Colacino and Dalu (1972) found 80 years later about 800 to 1000 particles cm^{-3} over the open water of the Sicily and Sardinia Channels, also most probably upwind of the industry in Sicily, and on the mainland. At that time, clean oceanic conditions over the Atlantic and Pacific were expected to have about 300 to 400 particles cm^{-3}, and the Mediterranean, as expected, was no longer completely clean. Compared to Aitken's measurements 80 years earlier, there was no obvious change in cleaner parts of the Mediterranean Sea. Elliott (1976) found a few years later on a cruise extending into the eastern basin and into the northern Aegean Sea between 1000 and 2000 cm^{-3} and occasionally up to 15,000 cm^{-3}, which were assigned to anthropogenic sources at the coast. The increase in background number concentrations could be already related to growing shipping traffic emissions that finally in the twenty-first century led to ~15,000–20,000 particles cm^{-3} in 2013 in the same area.

Especially within the central part of the Mediterranean, the emissions changed significantly in the last decades. Power stations and refineries were in operation in the 1970s in Sicily and at the southern tip of the Italian mainland, where one of the largest industrial sites is located, in Taranto, since the late 1960s. However, these particle sources were not equipped with flue gas cleaning systems until the end of the twentieth century and emitted a major fraction as fine particles. Fine particles serve as a condensation sink and suppress the number of ultrafine ones. Thus, although the total emitted mass (PM) was higher, number concentrations was probably lower than today as a drawback of modern "clean" technology.

Despite the introduction of air polluton control measures the levels in urban environments in the twenty-first century did not change much compared to 1890 with the exception of black carbon and fine dust, which is significantly reduced. This is due to the more intense traffic now. The coastline with expanding urban settlements and increasing traffic is thus becoming a continuous line source these days, compared to the patchy patterns at the turn of the nineteenth century. Traffic emissions in urban environments and also from in between these agglomerations are now one of the larger sources of primary nanoparticles (Olin et al., 2020; Rönkkö et al., 2017). From the available data we have, it is impossible to estimate whether and how far UFP emissions changed. However, a number of new, important and dominating sources have been introduced. Growing emissions from fossil fuel power stations and refineries have shifted from fine particles to ultrafine ones since ~1980. Different to urban and car emissions, these UFP emitters release into elevated altitudes of about 200–300 m. These emissions occur during the day into the boundary layer, during night above the nocturnal inversion, favoring mid-elevation transport up to a few hundred km (Junkermann & Hacker, 2018). This agrees with the elevated layers observed over the less convective MBL (Junkermann, 2001; Meloni et al., 2015; Rose et al., 2015) and with the diurnal pattern of size distributions at the ground-based field sites (Berland et al., 2017; Junkermann & Hacker, 2018). Within the Mediterranean, large industrial UFP sources are found in increasing numbers and increasing size. Currently, about 35 units burning coal (https://www.endcoal.org) are located along and ~ 200 km inland of the coastline from Gibraltar, along the Spanish coast over southern France towards Italy and further east to Greece and

Turkey. Additionally, several large refineries and heavy oil-fired units are also now operational (Malta, etc.). The source for ultrafine mode aerosol identified by Kalkavouras et al. (2017) for particles observed at the Finokalia site is such a region with several coal fired power stations. Intense UFP events at the Cyprus coast can be traced back to stations at the Turkish south coast (Brilke et al., 2020). The Italian field site at San Pietro Capofiume (Laaksonen et al., 2005) is similarly affected by fossil fuel emissions from nearby Mestre, Porto Tolle, and Rimini. Correspondingly, the local fossil fuel-fired power stations located in Mallorca, Corsica, Malta, Crete, and Cyprus have to be considered. The possible nucleation source areas identified by Berland et al. (2017) are close to such UFP emission hotspots. In addition, maritime fossil fuel extraction sites like gas and oil rigs have not been investigated yet. The fuel there is not burnt in significant amounts, but they could contribute, especially in the eastern Mediterranean where their number could increase rapidly following recent hydrocarbon fields' discoveries (Ellinas et al., 2016).

4 Major Contributions to the Mediterranean UFP Budget

Local traffic, urban environments, fossil fuel processing (refineries), power generation, and ship traffic all contribute to the ultrafine particle budget over the Mediterranean (Junkermann & Hacker, 2015, 2018) with, depending on the source, different emission heights. Ships are emitting always into the MBL, and power stations at night above the nocturnal MBL, leading to different transport patterns day and night. Above the MBL, long-range transport might cover the whole basin (Elliott, 1976), and diurnal convection is rapidly mixing these layered emissions both down to the ground and up to the cloud base. Ships in the Sicilian Channel were identified to be a major source of ultrafine particles initially too small for CCN activity but growing within a few hours into the respective size range. Ships burning sulfur-rich fuel were estimated to emit slightly less per MW, but at larger sizes (Petzold et al., 2008), their emission is also dependent on speed, size, engine, and fuel. However, cleaner fuel as required after 2020 also for the Mediterranean does not mean that the UFP emission is decreasing. Experiments in the Baltic Sea indicated that with a reduction of fine particles, the primary emission of ultrafine or nanoparticles might be even increasing to similar values as were obtained from the modern continental power stations in the order of 3 10^{15} particles per MW. This would agree with the results of Hamed et al. (2010) who observed that the number of cloud condensation nuclei at a field site surrounded by several lignite power stations increased during transition from "dirty" to "clean" operation, despite sulfur dioxide reduction. A doubling of nucleation mode particles was observed a few hours downwind of a modern power station, and even after transport for 48 h and about 800 km downwind of a major UFP source, the signature of enhanced nucleation appeared under "clean Mediterranean" conditions over Australia (Junkermann & Hacker, 2015; see also Rosenfeld 2000). That indicates that even in a diluted plume still sufficient precursor material is available.

Using the Malta vertical profiles for shipping emissions, an emission rate estimate can be calculated although it cannot be disentangled how primary emission and fast secondary gas to particle production are contributing. Measurements a few km downwind from large point sources always summarize the primary and immediate secondary production. It is thus a measure of the direct contribution of a single source to the total budget, and this is the number emission finally needed for a model grid cell. Using the information from the flight of Fig. 2, an average particle number concentration along the shipping line over ~40 km (Malta-Gozo) of 30,000 cm^{-3}, a height of the MBL of 800 m, and an average perpendicular wind vector of 2.6 ms^{-1}, the effective particle production from the shipping line is on the order of ~6 10^{16} s^{-1} km^{-1}. Extrapolated to the full distance from Suez to Gibraltar, that would be equivalent to more than 70 medium-size fossil fuel-fired power stations (Junkermann et al., 2011, 2016). Maritime UFP emissions in the Mediterranean are thus in a similar order of magnitude as continental emissions along the coast. Data about shipping intensity are available from the AIS data archive (https://www.marinetraffic.com/). These data contain at least the type, size, and speed of all individual ships, especially all cargo ships, and allow a calculation how much cargo (gross register tonnage) is transported along the shipping route. Ship emission reported by Petzold et al. (2008) and calculation of particle emission for the amount of cargo shipped through the Mediterranean are in good agreement with the above shipping emission estimate for the summer time conditions from the Malta campaign.

5 Conclusion and Recommendations

Ultrafine particles over the Mediterranean are dominated by anthropogenic activities along the surrounding coastline, by emissions from urban agglomerations, from industrial installations, and from shipping. These emissions are spread over the basin by regional-scale horizontal advection, often in distinct layers, and are finally vertically mixed by thermal convection during daytime. This thermal convection is stronger over land, and larger islands than over the open water. Considering the lifetime of small ultrafine particles, transport distances of about 500 km have to be considered, occasionally even more, similar to Saharan dust transport. Single events can be analyzed for source apportionment, for example, using HYSPLIT or FLEXPART back trajectory models. In many cases, the most likely source can be identified (e.g., Junkermann & Hacker, 2015). Aging and loss processes involved during transport modify size distributions, mainly to larger sizes, toward CCN sizes and to the accumulation mode. A reduction in fine particles due to emission control measures, the condensation sink of UFP, might even increase the lifetime for smaller particles in the ultrafine mode. Important for the climate impact of ultrafine aerosols, among changes in size distributions and chemistry of UFP with aging, the fraction of cloud condensation nuclei is increasing (close to 100% CCN in aged particles over Corsica). Compared to 1970 with a maximum of 600–800 CCN cm^{-3},

in the unlikely case that all particles at that time were active CCN, nowadays >2000 and more CCN cm^{-3} are normal over the Mediterranean. This is due to the aging UFP from continental sources along the coastline and to the emissions from shipping.

Due to missing data, no trend or even a quantitative estimate can be made for coastal and urban emissions throughout the basin. However, the source from increasing global ship transport is obvious. Shipping is nowadays a major source of ultrafine particulate matter, especially in the marine environment of the central Mediterranean, which was originally remote or only moderately polluted (at least up to the 1970s). ChArMEx results allow a better estimate of the shipping contribution and provide new insights into size distributions related to particulate shipping emissions. Given the large impact of ultrafine particle-derived CCN on the hydrologic cycle through aerosol-cloud interactions, it is suspected that these additional emissions contributed to the observed modification of rainfall patterns with the last decades and the subsequent changes in horizontal and vertical water vapor distributions. There is also experimental evidence that in other areas with reported exceptional rainfall deficiencies, the number concentrations of UFP were enhanced in a similar way to the Mediterranean and that rainfall decline timely correlates with an increase in ultrafine particles, respectively, CCN (Bigg, 2008; Junkermann et al., 2009, 2011; Junkermann & Hacker, 2015; Heinzeller et al., 2016). These climate-relevant processes need more observations and further sophisticated climate modelling with updated primary emission scenarios and detailed aerosol and cloud physics.

Acknowledgments The European Facility for Airborne Research (EUFAR; https://www.eufar.net/, last accessed July 29, 2020) is acknowledged for supporting the VESSAER campaign of the KIT ultralight aircraft.

References

Aitken, J. (1888). On the number of dust particles in the atmosphere. *Nature, 37*, 428–430. https://doi.org/10.1038/037428a0

Aitken, J. (1890). On the number of dust particles in the atmosphere of certain places in Great Britain and on the continent, with remarks on the relation between the amount of dust and meteorological phenomena. *Nature, 41*, 394–396. https://doi.org/10.1038/041394e0

Alonso-Blanco, E., Calvo, A. I., Pont, V., Mallet, M., Fraile, R., & Castro, A. (2014). Impact of biomass burning on aerosol size distribution, aerosol optical properties and associated radiative forcing. *Aerosol and Air Quality Research, 14*, 708–724. https://doi.org/10.4209/aaqr.2013.05.0163

Andreae, M. O. (2009). Correlation between cloud condensation nuclei concentration and aerosol optical thickness in remote and polluted regions. *Atmospheric Chemistry and Physics, 9*, 543–556, . www.atmos-chem-phys.net/9/543/2009/

Ayers, G. P., Bigg, E. K., & Turvey, D. E. (1979). Aitken particle and cloud condensation nucleus fluxes in the plume from an isolated industrial source. *Journal of Applied Meteorology, 187*, 449–459. https://doi.org/10.1175/1520-0450

Bai, H., Biswas, P., & Keener, T. (1992). Particle formation by NH_3-SO_2 reactions at trace water conditions. *Industrial and Engineering Chemistry Research, 31*, 88–94. https://doi.org/10.1021/ie00001a013

Bell, T. L., Rosenfeld, D., Kim, K.-M., Yoo, J.-M., Lee, M.-I., & Hahnenberger, M. (2008). Midweek increase in U.S. summer rain and storm heights suggests air pollution invigorates rainstorms. *Journal of Geophysical Research, 113*, D02209. https://doi.org/10.1029/2007JD008623

Berland, K., Rose, C., Pey, J., Culot, A., Freney, E., Kalivitis, N., Kouvarakis, G., Cerro, J. C., Mallet, M., Sartelet, K., Beckmann, M., Bourriane, T., Roberts, G., Marchand, N., Mihalopoulos, N., & Sellegri, K. (2017). Spatial extent of new particle formation events over the Mediterranean Basin from multiple ground-based and airborne measurements. *Atmospheric Chemistry and Physics, 17*, 9567–9583. https://doi.org/10.5194/acp-17-9567-2017

Bigg, E. K. (2008). Trends in rainfall associated with sources of air pollution. *Environment and Chemistry, 5*, 184–193. https://doi.org/10.1071/EN07086n

Bigg, E. K., & Turvey, D. E. (1978). Sources of atmospheric particles over Australia. *Atmospheric Environment, 12*, 1643–1655. https://doi.org/10.1016/0004-6981(78)90313-X

Birmili, W., Weinhold, K., Rasch, F., Sonntag, A., Sun, J., Merkel, M., Wiedensohler, A., Bastian, S., Schladitz, A., Löschau, G., Cyrys, J., Pitz, M., Gu, J., Kusch, T., Flentje, H., Quass, U., Kaminski, H., Kuhlbusch, T. A. J., Meinhardt, F., … Fiebig, M. (2016). Long-term observations of tropospheric particle number size distributions and equivalent black carbon mass concentrations in the German Ultrafine Aerosol Network (GUAN). *Earth System Science Data, 8*, 355–382. https://doi.org/10.5194/essd-8-355-2016

Bister, M., & Kulmala, M. (2011). Anthropogenic aerosols may have increased upper troposphere humidity in the 20th century. *Atmospheric Chemistry and Physics, 11*, 4577–4586. https://doi.org/10.5194/acp-11-4577-2011

Borbon, A., Afif, C., Salameh, T., Thera, B., & Panopoulou, A. (2022). Anthropogenic emissions of reactive compounds in the Mediterranean region. In F. Dulac, S. Sauvage, & E. Hamonou (Eds.), *Atmospheric chemistry in the Mediterranean Region* (Vol. 2, From air pollutant sources to impacts). Springer, this volume. https://doi.org/10.1007/978-3-030-82385-6_5

Boy, M., & Kulmala, M. (2002). Nucleation events in the continental boundary layer: Influence of physical and meteorological parameters. *Atmospheric Chemistry and Physics, 2*, 1–16. https://doi.org/10.5194/acp-2-1-2002

Brilke, S., Fölker, N., Müller, T., Kandler, K., Gong, X., Peischl, J., Weinzierl, B., & Winkler, P. M. (2020). New particle formation and sub-10 nm size distribution measurements during the A-LIFE field experiment in Paphos, Cyprus. *Atmospheric Chemistry and Physics, 20*, 5645–5656. https://doi.org/10.5194/acp-20-5645-2020

Carnerero, C., Pérez, N., Reche, C., Ealo, M., Titos, G., Lee, H.-K., Eun, H.-R., Park, Y.-H., Dada, L., Paasonen, P., Kerminen, V.-M., Mantilla, E., Escudero, M., Gómez-Moreno, F. J., Alonso-Blanco, E., Coz, E., Saiz-Lopez, A., Temime-Roussel, B., Marchand, N., … Querol, X. (2018). Vertical and horizontal distribution of regional new particle formation events in Madrid. *Atmospheric Chemistry and Physics, 18*, 16601–16618. https://doi.org/10.5194/acp-18-16601-2018

Charlson, R. J., Lovelock, J. M., Andreae, M. O., & Warren, S. G. (1987). Oceanic phytoplankton, atmospheric sulphur, cloud albedo and climate. *Nature, 326*, 655–661. https://doi.org/10.1038/326655a0

Colacino, M., & Dalu, G. A. (1972). Condensation nuclei measurements in marine atmosphere (Mediterranean Sea). *Pure and Applied Geophysics, 93*, 205–213. https://doi.org/10.1007/BF00875237

Contini, D., Donateo, A., Gambaro, A., Argiriou, A., Melas, D., Cesari, D., Poupkou, A., Karagiannidis, A., Tsakis, A., Merico, E., Cesari, R., & Dinoi, A. (2015). Impact of ship traffic to $PM_{2.5}$ and particle number concentrations in three port-cities of the Adriatic/Ionian area. *International Journal of Environmental and Ecological Engineering, 9*, 533–538, . https://publications.waset.org/pdf/10000904

Coulier, P. J. (1875). Note sur une nouvelle propriété de l'air. *Journal de Pharmacie et de Chimie, 4*, 165–172.

Dal Maso, M., Kulmala, M., Riipinen, I., Wagner, R., Hussein, T., Aalto, P. P., & Lehtinen, K. E. J. (2005). Formation and growth of fresh atmospheric aerosols: Eight years of aerosol size distribution data from SMEAR II, Hyytiälä, Finland. *Boreal Environment Research, 10*, 323–336. https://doi.org/10.1029/2001JD001053

Di Iorio, T., di Sarra, A., Junkermann, W., Cacciani, M., Fiocco, G., & Fuà, D. (2003). Tropospheric aerosols in the Mediterranean: 1. Microphysical and optical properties. *Journal of Geophysical Research, 108*, 4316. https://doi.org/10.1029/2002jd002815

Doussin, J.-F. (2023). The Mediterranean atmosphere under anthropogenic pressures. In F. Dulac, S. Sauvage, & E. Hamonou (Eds.), *Atmospheric chemistry in the Mediterranean Region* (Vol. 1, Background information and pollutants distribution). Springer.

Ehn, M., Thornton, J. A., Kleist, E., Sipila, M., Junninen, H., Pullinen, I., Springer, M., Rubach, F., Tillmann, R., Lee, B., Lopez-Hilfiker, F., Andres, S., Acir, I.-H., Rissanen, M., Jokinen, T., Schobesberger, S., Kangasluoma, J., Kontkanen, J., Nieminen, T., … Mentel, T. F. (2014). A large source of low-volatility secondary organic aerosol. *Nature, 506*, 476–479. https://doi.org/10.1038/nature13032

Ellinas, C., Roberts, J., & Tzimitras, H. (2016). *Hydrocarbon developments in the Eastern Mediterranean – The case for pragmatism*. Washington, DC: Atlantic Council. 34 pp. https://euagenda.eu/upload/publications/untitled-6644-ea.pdf, last accessed 15 June 2020.

Elliott, W. P. (1976). Condensation nuclei concentrations over the Mediterranean Sea. *Atmospheric Environment, 10*, 1091–1094. https://doi.org/10.1016/0004-6981(76)90119-0

Fan, J., Rosenfeld, D., Zhang, Y., Giangrande, S. E., Li, Z., Machado, L. A., Martin, S. T., Yang, Y., Wang, J., Artaxo, P., & Barbosa, H. M. (2018). Substantial convection and precipitation enhancements by ultrafine aerosol particles. *Science, 359*, 411–418. https://doi.org/10.1126/science.aan8461

Franck, U., Odeh, S., Wiedensohler, A., Wehner, B., & Herbarth, O. (2011). The effect of particle size on cardiovascular disorders — The smaller the worse. *Science of the Total Environment, 409*, 4217–4221. https://doi.org/10.1016/j.scitotenv.2011.05.049

Gudmundsson, L., Seneviratne, S. I., & Zhang, Z. (2016). Anthropogenic climate change detected in European renewable freshwater resources. *Nature Climate Change, 7*, 813–816. https://doi.org/10.1038/NCLIMATE3416

Guerreiro, S., Fowler, H. J., Barbero, R., Westra, S., Lenderink, G., Blenkinsop, S., Lewis, E., & Li, X.-F. (2018). Detection of continental-scale intensification of hourly rainfall extremes. *Nature Climate Change, 8*, 803–806. https://doi.org/10.1038/s41558-018-0245-3

Hamed, A., Joutsensaari, J., Mikkonen, S., Sogacheva, L., Dal Maso, M., Kulmala, M., Cavalli, F., Fuzzi, S., Facchini, M. C., Decesari, S., Mircea, M., Lehtinen, K. E. J., & Laaksonen, A. (2007). Nucleation and growth of new particles in Po Valley, Italy. *Atmospheric Chemistry and Physics, 7*, 355–376. https://doi.org/10.5194/acp-7-355-2007

Hamed, A., Birmili, W., Joutsensaari, J., Mikkonen, S., Asmi, A., Wehner, B., Spindler, G., Jaatinen, A., Wiedensohler, A., Korhonen, H., Lehtinen, K. E. J., & Laaksonen, A. (2010). Changes in the production rate of secondary aerosol particles in Central Europe in view of decreasing SO2 emissions between 1996 and 2006. *Atmospheric Chemistry and Physics, 10*, 1071–1091. https://doi.org/10.5194/acp-10-1071-2010

Heinzeller, D., Junkermann, W., & Kunstmann, H. (2016). Anthropogenic aerosol emissions and rainfall decline in South-West Australia: Coincidence or causality. *Journal of Climate, 29*, 8471–8493. https://doi.org/10.1175/JCLI-D-16-0082.1

Junkermann, W. (2001). An ultralight aircraft as platform for research in the lower troposphere: System performance and first results from radiation transfer studies in stratiform aerosol layers and broken cloud conditions. *Journal of Atmospheric and Oceanic Technology, 18*, 934–946. https://doi.org/10.1175/1520-0426(2001)018<0934:AUAAPF>2.0.CO;2

Junkermann, W. (2005). The actinic UV-radiation budget during the ESCOMPTE campaign 2001: Results of airborne measurements with the microlight research aircraft D-MIFU. *Atmospheric Research, 74*, 461–475. https://doi.org/10.1016/j.atmosres.2004.06.009

Junkermann, W., & Hacker, J. M. (2015). Ultrafine particles over Eastern Australia: An airborne survey. *Tellus B, 67*, 25308. https://doi.org/10.3402/tellusb.v67.25308

Junkermann, W., & Hacker, J. M. (2018). Ultrafine particles in the lower troposphere: Major sources, invisible plumes and meteorological transport processes. *Bulletin of the American Meteorological Society, 99*, 2587–2622. https://doi.org/10.1175/BAMS-D-18-0075.1

Junkermann, W., Hacker, J., Lyons, T., & Nair, U. (2009). Land use change suppresses precipitation. *Atmospheric Chemistry and Physics, 9*, 6531–6539. https://doi.org/10.5194/acp-9-6531-2009

Junkermann, W., Vogel, B., & Sutton, M. A. (2011). The climate penalty for clean fossil fuel combustion. *Atmospheric Chemistry and Physics, 11*, 12917–12924. https://doi.org/10.5194/acp-11-12917-2011

Junkermann, W., Vogel, B., & Bangert, M. (2016). Ultrafine particles over Germany – An aerial survey. *Tellus B, 68*, 29250. https://doi.org/10.3402/tellusb.v68.29250

Kalivitis, N., Kerminen, V.-M., Kouvarakis, G., Stavroulas, I., Tzitzikalaki, E., Kalkavouras, P., Daskalakis, N., Myriokefalitakis, S., Bougiatioti, A., Manninen, H. E., Roldin, P., Petäjä, T., Boy, M., Kulmala, M., Kanakidou, M., & Mihalopoulos, N. (2019). Formation and growth of atmospheric nanoparticles in the eastern Mediterranean: Results from long-term measurements and process simulations. *Atmospheric Chemistry and Physics, 19*, 2671–2686. https://doi.org/10.5194/acp-19-2671-2019

Kalkavouras, P., Bossioli, E., Bezantakos, S., Bougiatioti, A., Kalivitis, N., Stavroulas, I., Kouvarakis, G., Protonotariou, A. P., Dandou, A., Biskos, G., Mihalopoulos, N., Nenes, A., & Tombrou, M. (2017). New particle formation in the southern Aegean Sea during the Etesians: Importance for CCN production and cloud droplet number. *Atmospheric Chemistry and Physics, 17*, 175–192. https://doi.org/10.5194/acp-17-175-2017

Kiang, C. S., Stauffer, D., Mohnen, V. A., Bricard, J., & Vigla, D. (1973). Heteromolecular nucleation theory applied to gas to particle conversion. *Atmospheric Environment, 7*, 1279–1283. https://doi.org/10.1016/0004-6981(73)90137-6

Kulmala, M., Laakso, L., Lehtinen, K. E. J., Riipinen, I., Dal Maso, M., Anttila, T., Kerminen, V.-M., Hõrrak, U., Vana, M., & Tammet, H. (2004). Initial steps of aerosol growth. *Atmospheric Chemistry and Physics, 4*, 2553–2560. https://doi.org/10.5194/acp-4-2553-2004

Kulmala, M., Kontkanen, J., Junninen, H., Lehtipalo, K., Manninen, H. E., Nieminen, T., Petäjä, T., Sipilä, M., Schobesberger, S., Rantala, P., Franchin, A., Jokinen, T., Järvinen, E., Äijälä, M., Kangasluoma, J., Hakala, J., Aalto, P. P., Paasonen, P., Mikkilä, J., … Worsnop, D. R. (2013). Direct observations of atmospheric aerosol nucleation. *Science, 339*, 943–946. https://doi.org/10.1126/science.1227385

Laaksonen, A., Hamed, A., Joutsensaari, J., Hiltunen, L., Cavalli, F., Junkermann, W., Asmi, A., Fuzzi, S., & Facchini, M. C. (2005). Cloud condensation nucleus production from nucleation events at a highly polluted region. *Geophysical Research Letters, 32*, L06812. https://doi.org/10.1029/2004GL022092

Landsberg, H. E. (1938). Atmospheric condensation nuclei. In *Gerlands Beiträge zur Geophysik, Dritter Supplementband, Ergebnisse der Kosmischen Physik III, Akademische Verlagsgesellschaft M. B. H* (pp. 155–252), editor Victor Conrad.

Mallet, M., Dulac, F., Formenti, P., Nabat, P., Sciare, J., Roberts, G., Pelon, J., Ancellet, G., Tanré, D., Parol, F., Denjean, C., Brogniez, G., di Sarra, A., Alados-Arboledas, L., Arndt, J., Auriol, F., Blarel, L., Bourrianne, T., Chazette, P., … Zapf, P. (2016). Overview of the chemistry-aerosol Mediterranean experiment/aerosol direct radiative forcing on the Mediterranean climate (ChArMEx/ADRIMED) summer 2013 campaign. *Atmospheric Chemistry and Physics, 16*, 455–504. https://doi.org/10.5194/acp-16-455-2016

Meloni, D., Junkermann, W., di Sarra, A., Cacciani, M., De Silvestri, L., Di Iorio, T., Estelles, V., Gomez-Amo, J. L., Pace, G., & Sferlazzo, D. M. (2015). Altitude resolved shortwave and longwave radiative effects of desert dust in the Mediterranean during the GAMARF campaign: Indications of a net daily cooling in the dust layer. *Journal of Geophysical Research: Atmospheres, 120*, 3386–3407. https://doi.org/10.1002/2014JD022312

Metnieks, A. L., & Pollak, L. W. (1959). Instruction for use of photo-electric condensation nucleus counters–Their care and maintenance together with calibration and auxiliary tables. *Geophysical Bulletin, 16*, Tech. note 6, AFCRC-TN-59-640, AD-232273, School of Cosmic Physics, Dublin Institute for Advanced Studies, 18 pp.

Mohnen, V., & Hidy, G. M. (2010). Measurements of atmospheric nanoparticles (1875–1980). *Bulletin of the American Meteorological Society, 91*, 1525–1540. https://doi.org/10.1175/2010BAMS2929

O'Dowd, C. D., Jimenez, J. L., Bahreini, R., Flagan, R. C., Seinfeld, J. H., Pirjola, L., Kulmala, M., Jennings, S. G., & Hoffmann, T. (2005). Marine aerosols and iodine emissions. *Nature, 433*, 1501. https://doi.org/10.1038/nature03373

O'Dowd, C. D., Yoon, Y. J., Junkermann, W., Aalto, P., Kulmala, M., Lihavainen, H., & Viisanen, Y. (2007). Airborne measurements of nucleation mode particles I: Coastal nucleation and growth rates. *Atmospheric Chemistry and Physics, 7*, 1491–1501. https://doi.org/10.5194/acp-7-1491-2007

Olin, M., Kuuluvainen, H., Aurela, M., Kalliokoski, J., Kuittinen, N., Isotalo, M., Timonen, H. J., Niemi, J. V., Rönkkö, T., & Dal Maso, M. (2020). Traffic-originated nanocluster emission exceeds H2SO4-driven photochemical new particle formation in an urban area. *Atmospheric Chemistry and Physics, 20*, 1–13. https://doi.org/10.5194/acp-20-1-2020

Paasonen, P., Kupiainen, K., Klimont, Z., Visschedijk, A., Denier van der Gon, H. A. C., & Amann, M. (2016). Continental anthropogenic primary particle number emissions. *Atmospheric Chemistry and Physics, 16*, 6823–6840. https://doi.org/10.5194/acp-16-6823-2016

Petzold, A., Hasselbach, J., Lauer, P., Baumann, R., Franke, K., Gurk, C., Schlager, H., & Weingartner, E. (2008). Experimental studies on particle emissions from cruising ship, their characteristic properties, transformation and atmospheric lifetime in the marine boundary layer. *Atmospheric Chemistry and Physics, 8*, 2387–2403. https://doi.org/10.5194/acp-8-2387-2008

Pope, C. A., Burnett, R. T., Thun, M. J., Calle, E. E., Krewski, D., Ito, K., & Thurston, G. D. (2002). Lung cancer, cardiopulmonary mortality, and long-term exposure to fine particulate air pollution. *Journal of the American Medical Association, 287*, 1132–1141. https://doi.org/10.1001/jama.287.9.1132

Riuttanen, L., Bister, M., Kerminen, V.-M., John, V. O., Sundström, A.-M., Dal Maso, M., Räisänen, J., Sinclair, V. A., Makkonen, R., Xausa, F., de Leeuw, G., & Kulmala, M. (2016). Observational evidence for aerosols increasing upper tropospheric humidity. *Atmospheric Chemistry and Physics, 16*, 14331–14342. https://doi.org/10.5194/acp-16-14331-2016

Roberts, G., Bourrianne, T., Léon, J.-F., Pont, V., Mallet, M., Lambert, D., Augustin, P., Dulac, F., & Junkermann, W. (2013). The vertical structure, sources, and evolution of aerosols in the Mediterranean region. *Geophysical Research Abstracts, 15*. EGU2013-4174-4. https://meetingorganizer.copernicus.org/EGU2013/EGU2013-4174-4.pdf.

Rönkkö, T., Kuuluvainen, H., Karjalainen, P., Keskinen, J., Hillamo, R., Niemi, J. V., Pirjola, L., Timonen, H. J., Saarikoski, S., Saukko, E., Järvinen, A., Silvennoinen, H., Rostedt, A., Olin, M., Yli-Ojanperä, J., Nousiainen, P., Kousa, A., & Dal Maso, M. (2017). Traffic is a major source of atmospheric nanocluster aerosol. *Proceedings of the National Academy of Sciences of the United States of America, 114*, 7549–7554. https://doi.org/10.1073/pnas.1700830114

Rose, C., Sellegri, K., Freney, E., Dupuy, R., Colomb, A., Pichon, J.-M., Ribeiro, M., Bourianne, T., Burnet, F., & Schwarzenboeck, A. (2015). Airborne measurements of new particle formation in the free troposphere above the Mediterranean Sea during the HYMEX campaign. *Atmospheric Chemistry and Physics, 15*, 10203–10218. https://doi.org/10.5194/acp-15-10203-2015

Rosenfeld, D. (2000). Suppression of Rain and Snow by Urban and Industrial Air Pollution, *Science, 287, 1793*

Rosenfeld, D., Lohmann, U., Raga, G. B., O'Dowd, C. D., Kulmala, M., Fuzzi, S., Reissell, A., & Andreae, M. O. (2008). Flood or drought: How do aerosols affect precipitation? *Science, 321*, 1309–1313. https://doi.org/10.1126/science.1160606

Rosenfeld, D., Zhu, Y., Wang, M., Zheng, Y., Goren, T., & Yu, S. (2019). Aerosol-driven droplet concentrations dominate coverage and water of oceanic low level clouds. *Science, 363*, eaav0599. https://doi.org/10.1126/science.aav0566

Schmale, J., Henning, S., Decesari, S., Henzing, B., Keskinen, H., Sellegri, K., Ovadnevaite, J., Pöhlker, M. L., Brito, J., Bougiatioti, A., Kristensson, A., Kalivitis, N., Stavroulas, I., Carbone, S., Jefferson, A., Park, M., Schlag, P., Iwamoto, Y., Aalto, P., … Gysel, M. (2018). Long-

term cloud condensation nuclei number concentration, particle number size distribution and chemical composition measurements at regionally representative observatories. *Atmospheric Chemistry and Physics, 18*, 2853–2881. https://doi.org/10.5194/acp-18-2853-2018

Sellegri, K., & Rose, C. (2022). Nucleation. In F. Dulac, S. Sauvage, & E. Hamonou (Eds.), *Atmospheric chemistry in the Mediterranean Region* (Vol. 2, From air pollutant sources to impacts). Springer, this volume. https://doi.org/10.1007/978-3-030-82385-6_9

Srivastava, R. K., Miller, C. A., Erickson, C., & Jambhekar, R. (2004). Emissions of sulfur trioxide from coal-fired power plants. *Journal of the Air & Waste Management Association, 54*, 750–762. https://doi.org/10.1080/10473289.2004.10470943

Thornton, J. A., Virts, K. S., Holzworth, R. H., & Mitchell, T. P. (2017). Lightning enhancement over major oceanic shipping lanes. *Geophysical Research Letters, 44*, 9102–9111. https://doi.org/10.1002/2017GL074982

Villa, T. F., Brown, R. A., Jayaratne, E. R., Gonzalez, L. F., Morawska, L., & Ristovski, Z. D. (2019). Characterization of the particle emission from a ship operating at sea using an unmanned aerial vehicle. *Atmospheric Measurement Techniques, 12*, 691–702. https://doi.org/10.5194/amt-12-691-2019

Wang, J., Shilling, J. E., Liu, J., Zelenyuk, A., Bell, D. M., Petters, M. D., Thalman, R., Mei, F., Zaveri, R. A., & Zheng, G. (2019). Cloud droplet activation of secondary organic aerosol is mainly controlled by molecular weight, not water solubility. *Atmospheric Chemistry and Physics, 19*, 941–954. https://doi.org/10.5194/acp-19-941-2019

Young, L. H., & Keeler, G. J. (2007). Summertime ultrafine particles in urban and industrial air: Aitken and nucleation mode particle events. *Aerosol and Air Quality Research, 7*, 379–402. https://doi.org/10.4209/aaqr.2007.02.0012

Part VI
Recent Progress on Chemical Processes

Coordinated by ***Matthias Beekmann***
Université Paris Cité and Univ. Paris Est Créteil, CNRS, LISA, F-75013 Paris, France
matthias.beekmann@lisa.ipsl.fr
Reviewed by ***Andrea Pozzer*** *(Max Planck Institute for Chemistry, Mainz, Germany)*

Abstract

Chemical processes strongly modify the tropospheric composition in gases and aerosols over the Mediterranean basin (MB), and physico-chemical processes affect exchanges between both phases. Main results from the ChArMEx program dealing with these issues are highlighted in this chapter. Observations of total OH reactivity of molecules over the MB made evident larger reactivity over the western than the eastern part of the basin, due to stronger biogenic VOC emissions, reflecting more favorable (especially less dry) climatic conditions over the western part. Quasi-Lagrangian boundary-layer isopycnic balloons over the gulfs of Lion and Genoa revealed net ozone growth, at intermediate rates between those reported in polluted regions and remote areas. Nucleation and growth of new particles were found to be ubiquitous in the MB, from coastal sites to the open sea boundary layer and lower free troposphere. We are discussing the role of compounds such as isoprene, terpenes, methane-sulphonic acid and iodine as precursors for new particle formation. Extremely low-volatile compounds from monoterpene autoxidation, which may contribute to secondary organic aerosols (SOA) mass by up to 10%, could also be involved. Origins and formation pathways of secondary aerosols are investigated from their concentrations and properties (carbon origin, oxidation state, solubility, mixing state), e.g., the absorption of soluble non-marine biogenic SOA in sea-salt particles. Overall, 3D models simulate well SOA levels over the basin and their seasonal variability. Still, field measurements over the basin show that theoretical partition coefficients of semi-volatile compounds between aerosol and gas phases, the basis used in 3D chemistry-transport models, are under-estimated, suggesting a potential role of particle viscosity in phase exchanges.

Total OH Reactivity

Valérie Gros and Nora Zannoni

Contents

Abstract Total OH reactivity is defined as the total loss rate of reaction of the hydroxyl radical OH with atmospheric chemical compounds. It represents the inverse of the OH radical lifetime. Since OH is the main atmospheric oxidant during daytime, measuring the total OH reactivity represents an estimate of the total loading of reactive molecules in the atmosphere. This chapter presents the measurement principle of total OH reactivity and then results from measurements in the Mediterranean basin, which are placed in the general context of worldwide measurements. The major applications of such measurements are highlighted: first, the total OH reactivity is compared to the sum of OH reactivities of individual VOCs,

Chapter reviewed by ***Vinayak Sinha*** *(IISER, Mohali Campus, Mohali, Punjab, India), as part of the book Part VI Recent Progress on Chemical Processes also reviewed by* ***Andrea Pozzer*** *(Max Planck Institute for Chemistry, Mainz, Germany)*

V. Gros (✉)
Laboratoire des Sciences du Climat et de l'Environnement (LSCE), CEA-CNRS-UVSQ, IPSL, Université Paris-Saclay, Gif-sur-Yvette, France
e-mail: valerie.gros@lsce.ipsl.fr

N. Zannoni
Laboratoire des Sciences du Climat et de l'Environnement (LSCE), CEA-CNRS-UVSQ, IPSL, Université Paris-Saclay, Gif-sur-Yvette, France

Max Planck Institute for Chemistry (MPIC), Mainz, Germany

F. Dulac et al. (eds.), *Atmospheric Chemistry in the Mediterranean Region*,
https://doi.org/10.1007/978-3-030-82385-6_7

which allows one deriving a missing non-measured part. Then instantaneous photochemical ozone formation rates, and the chemical regime of such ozone formation, are presented.

1 Total OH Reactivity Concept and Applications

Total OH reactivity (R) is defined as the total loss rate of reaction of the hydroxyl radical OH with atmospheric chemical compounds and represents the inverse of the OH radical lifetime. Since OH is the main atmospheric oxidant during daytime, measuring the total OH reactivity represents an estimate of the total loading of reactive molecules in the atmosphere. Concurrently, a large number of reactive atmospheric compounds can be measured with the available current technologies in order to determine their concentration, therefore their reactivity to OH. The latter is done by considering the sum of the products between the concentration X_i of each measured molecule i and the rate constant of reaction k of i with OH (Eq. 1). This parameter is often named calculated OH reactivity.

$$R = \sum_i k_{\mathrm{Xi + OH}} X_i \tag{1}$$

Total OH reactivity and calculated OH reactivity represent, respectively, an experimental and theoretical approach of the same parameter, used to examine the number and abundance of reactive hydrocarbons in the atmosphere. Measuring the OH reactivity is relevant for many aspects as listed below.

1.1 OH Radical Sources

Measures of the total OH sink (OH reactivity) are helpful to constrain the total OH source when the concentration of the hydroxyl radical is known. Whalley et al. (2011) compared OH production rates, OH sink, and OH measurements carried out in the tropical rainforest of Borneo and found out that OH in the tropics is produced at a rate ten times greater than the identified OH sources. Their predictions of OH concentration further highlighted that this parameter is underestimated by measurements, with important implications for understanding VOC degradation and methane lifetime in the tropics.

1.2 Unmeasured Atmospheric Constituents

Measurements of OH reactivity can be performed together with measurements of ambient air constituents. In an environment where every single air component has been quantified and its reaction rate constant with the hydroxyl radical is known, the measured OH reactivity and the calculated OH reactivity will be the same. If the calculated OH reactivity is smaller than the measured OH reactivity, then a fraction of the composition of the air remains unidentified. This fraction is usually regarded as "missing OH reactivity". Missing OH reactivity was found to different extents in many environments and was generally highest where biogenic VOCs dominated (Di Carlo et al., 2004; Nölscher et al., 2016; Zannoni et al., 2017). Comparisons of missing OH reactivity results should be done with caution, as the unidentified fraction depends on the number and type of chemical compounds monitored and used to determine the calculated OH reactivity. Nevertheless, this approach is useful for analyzing time series and improving our current understanding of environmental and atmospheric processes. It can also be used as a quality control measure of the deployed techniques.

1.3 Ozone Production Potential

Rates of instantaneous ozone production potential and regimes can be derived from measurements of OH reactivity when combined with measurements of NO_x, OH, and peroxy radicals. Sinha et al. (2012) developed this type of approach to analyze the impact of point sources on regional ozone levels during the DOMINO campaign on the southwestern coast of Spain. They found out that the ozone production potential was higher when the coastal site was more influenced by continental air masses. They also identified the NO_x point sources that were limiting such an effect. Nevertheless, a limitation of the method is that the ozone production potential so determined assumes that ozone production is not limited by availability of NO_x. An alternative method to determine net ozone production from quasi-Lagrangian isopycnic balloon measurements is presented in the following chapter (Gheusi, 2022).

1.4 Particle Formation

OH reactivity offers a direct link between VOC emission and new particle formation, which will be addressed in the three following chapters by Sellegri & Rose (2022), Sartelet (2022), and Michoud (2022). Mogensen et al. (2011) analyzed the particle formation events that occurred during 1 month of field campaign in the Finnish boreal forest with the measured OH reactivity. They found out that the missing OH reactivity increased during the particle formation event. Correlations between measured and missing reactivity with the condensation sink confirmed that the missing

reactivity could not be explained by OH loss on particle surface, but rather by OH oxidation with VOCs forming higher oxidized semi-volatile compounds.

2 Measuring the OH Reactivity

In 1993, William H. Brune conceived for the first time the concept of total OH reactivity as the direct measurement of OH loss rate (Kovacs & Brune, 2001). A few years later, the first measurements of total OH reactivity were performed independently by two research groups, (i) in the laboratory using a differential absorption lidar technique (Calpini et al., 1999) and (ii) in ambient air based on laser-induced fluorescence for detecting OH (Kovacs & Brune, 2001). Currently, the total OH reactivity can be measured using two main approaches: the direct measurement of the decay of artificially produced OH and indirectly measuring the concentration of a reference molecule whose reactivity to OH is established. Direct measurement of OH reactivity is achieved with three main types of instruments. The first type consists in detecting the OH decay in a flow tube where ambient air is drawn, whereas OH is continuously produced from photolysis of H_2O and monitored through laser-induced fluorescence (Mao et al., 2009). The second type deploys a flow tube combined with chemical ionization mass spectrometry (CIMS) in order to detect H_2SO_4 from the chemical conversion of OH (Muller et al., 2018). The third type, laser photolysis-laser-induced fluorescence (LP-LIF), detects OH through LIF, whereas OH is artificially produced by ozone photolysis using short laser pulses at a low repetition rate (Sadanaga et al., 2004; Fuchs et al., 2017a). The indirect method, known as comparative reactivity method (CRM), generally uses proton transfer reaction mass spectrometry (PTR-MS) to monitor the concentration of a reference molecule reactive to OH mixed in a glass reactor with artificially produced OH and ambient air (Sinha et al., 2008). Alternatively, a gas chromatography-photoionization detector (GC-PID) can be used instead of a PTR-MS (Nölscher et al., 2012). Intercomparisons of the same method (Zannoni et al., 2015) or different methods (Hansen et al., 2015) and of all methods (Fuchs et al., 2017b) have been carried out in recent years aiming at assessing the performances of the discussed techniques. Direct methods demonstrated to be more precise, have a better time resolution and lower limit of detection. Nevertheless, indirect methods have the advantage that they do not require a large sampling flow and therefore can be assembled from instruments already in use in many laboratories studying VOCs.

3 OH Reactivity Measurements in the Mediterranean Basin

Total OH reactivity was measured in a few studies conducted in the Mediterranean basin, including at background sites located in the western basin (Corsica; Zannoni et al., 2017) and eastern basin (Cyprus; Keßel, 2016), over open waters (Pfannerstill

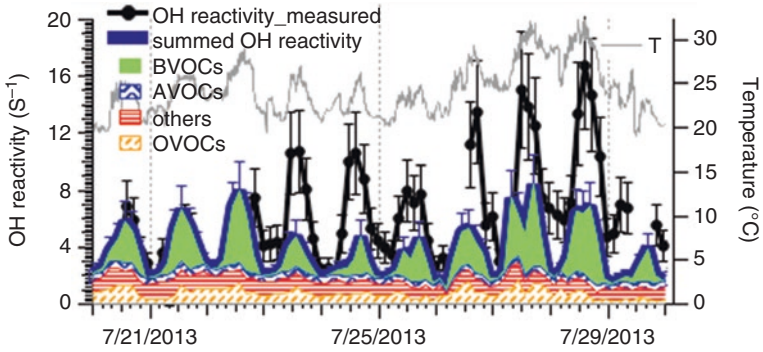

Fig. 1 Total measured and calculated (summed) OH reactivity and ambient temperature (in grey) during summer 2013 at the remote site of Ersa (42.969°N, 9.380°E) in Cape Corsica (France). The origins of the air masses for the reported time were classified as from the North (21–23/07), West (23–26/07), and South (26–30/07). Summed OH reactivity represents the sum of reactivities of biogenic volatile organic compounds (BVOCs), anthropogenic volatile organic compounds (AVOCs), oxygenated organic compounds (OVOCs), and others (sum of CO, methane, and NO_x contributions). More information can be found in Zannoni et al. (2017) and Michoud et al. (2017)

et al., 2019), in a forest (Zannoni et al., 2016), over an agricultural region in the Po Valley (Kaiser et al., 2016), and at a near coastal SW Spanish site in vicinity of the basin (Sinha et al., 2012). The main objectives of these studies were either to determine and investigate OH missing reactivity or to investigate the ozone formation potential. In parallel to other efforts, the ChArMEx program added to existing literature new measurement points in the region, especially over the western part of the basin (Zannoni et al., 2016, 2017).

Zannoni et al. (2017) investigated the OH reactivity based on CRM measurements performed at the station of Ersa (42.969°N, 9.380°E) on the north of Cape Corsica ("Cap Corse" in French) in July 2013, on a crest at the northeastern tip of Corsica island, within the ChArMEx program (see Dulac et al., 2023 and the book appendix). This site can be considered as a background site, with low local anthropogenic influence, and is under the influence of various air masses with different origins (marine influenced or anthropogenically influenced as those from southern France or northern Italy). Nevertheless, in the absence of major pollution events, and with relatively clean local air, the air masses' origin had little effect on the measured reactivity. In contrast, local biogenic emissions from the scrub type of vegetation surrounding the measurement site (specifically, macchia and low aromatic plants) had the largest impact on OH reactivity. OH reactivity in Corsica was on average 17 ± 6 s^{-1} and had a campaign maximum of 22 s^{-1}. Despite this, a significant missing OH reactivity was found (up to 50%) and attributed to oxidation products of BVOCs (Fig. 1).

Significantly lower levels (mean campaign value of 1.8 s^{-1}; Keßel, 2016) were found in spring-summer 2014 in Cyprus island, in the eastern Mediterranean basin. The main explanation for the observed differences is given by the local ecosystems

and impact of direct biogenic VOC emissions to the OH reactivity. Indeed, the measurement site in Corsica was influenced by dense macchia, while the site in Cyprus was very dry and with very little vegetation, showing only low biogenic VOC concentrations (sum of isoprene and terpenes maximum typically about 500 pptv; see Derstroff et al., 2017).

In September 2017, Pfannerstill et al. (2019) performed shipborne OH reactivity measurements with CRM during the AQABA campaign, departing from southern France, crossing the Mediterranean eastward to reach the Suez Canal, and then exploring the surroundings of the Arabian Peninsula. Aged and therefore rather clean air masses were encountered during the crossing of the Mediterranean, and the corresponding mean OH reactivity was low ($7.2 \pm 2.9\ s^{-1}$) with the OVOC group accounting for the largest calculated OH reactivity. Higher OH reactivity levels were measured only during short periods corresponding to polluted air from the mainland. The levels were significantly higher in the Arabian Gulf, Gulf of Suez, and Suez Canal, where atmospheric composition was influenced by various anthropogenic sources (urban, industrial, and from oil and gas production and processing). These measurements were used to derive ozone production regimes in terms of the OH reactivities of VOCs and NO_x. In the Mediterranean, it was then found that 97% of the time, a regime with a VOC-to-NO_x ratio suitable for ozone formation was encountered (i.e., it was intermediate between NO_x and VOC limitation).

Also in the framework of the ChArMEx and CANOPEE programs, Zannoni et al. (2016) measured the OH reactivity (CRM method) in June 2014 in a forest of downy oaks (*Quercus pubescens*), a typical Mediterranean species known as a high isoprene emitter (Keenan et al., 2009). Measurements at the geophysical station of Observatoire de Haute Provence (OHP) (43°55′54″N, 5°42′44″E) were performed at two heights, inside and above the canopy (respectively, 2 and 10 m as the canopy height was about 5 m). High OH reactivity was found (daytime mean of $29\ s^{-1}$ and campaign maximum of $69\ s^{-1}$ at 2 m), and as expected, isoprene was its main contributor during daytime (83% and 72% inside and above the canopy, respectively). The comparison between measured total OH reactivity and calculated OH reactivity from the measured VOCs showed that no significant missing reactivity was present during daytime (neither inside nor above the canopy). This suggests that intracanopy oxidation was low, in agreement with the measurements of low levels of isoprene oxidation products and with previous studies with isoprene and oxidation products' flux measurements (Kalogridis et al., 2014). In contrast, a missing reactivity up to 50% was found during night-time, possibly due to unmeasured oxidation products, very likely oxygenated compounds. During night, local isoprene emissions are lower, and transport from more distant sources is thus relatively more important.

Another study performed directly in a forested area is the one by Bsaibes et al. (2020) which is based on measurements (CRM method) obtained during the LANDEX campaign in summer 2017 over a pine forest in SW France. Maritime pine (*Pinus pinaster*) is mostly found in Portugal forests but also at sites from the French and Italian Mediterranean coasts and is known to be a terpene emitter. This study is also based on measurements inside and above the canopy (respectively, at 6

and 12 m with a mean canopy height of 10 m). Measured OH reactivity was very high with values up to 99 s^{-1} inside the canopy and 70 s^{-1} above the canopy (respective means of 19.2 s^{-1} and 16.5 s^{-1}), with maximum values of OH reactivity mostly recorded during the nights. For this site, the main contributor to calculated OH reactivity was by far the monoterpene class (about 68–65% during daytime and 92–89% during night-time inside and above the canopy, respectively) followed by isoprene (25–27% during daytime). Missing OH reactivity showed a day-night variability. The authors suggest that it was mainly related to temperature-enhanced primary emissions and secondary oxidation products during the day and could be linked to transported and accumulated long-lived species in the stable nocturnal boundary layer during the night.

Kaiser et al. (2015) have determined a vertical gradient in OH reactivity during the PEGASOS campaign, which took place on-board a Zeppelin over the Po Valley (Italy) in July 2012. They have measured an OH reactivity of 5 s^{-1} at the ground level (with NO_x contributing to 40%) and only 2 s^{-1} at 800 m over an agricultural area (with OVOCs and CO contributing to 60%). These values are close to typical values for background air, i.e., an environment not influenced locally by anthropogenic or biogenic sources.

Finally, Sinha et al. (2012) measured OH reactivity during the DOMINO campaign in southwestern Spain in fall 2008. They classified their results according to the air mass origins, and the levels of OH reactivity were varying from background levels (6.3 ± 6.6 s^{-1}) when sampling marine air masses up to 31.4 ± 4.5 s^{-1} under the influence of northeastern continental air masses. They proposed an approach to use the measured OH reactivity (combined with NO_x and peroxy radical measurements) to constrain both diel instantaneous ozone production potential rates and regimes. They found a peak value of about 20 ppbV O_3 h^{-1} for the studied site (and have estimated that this value would be double if the site was not NO_x-limited). These values are much larger than those derived from quasi-Lagrangian ozone measurements under boundary-layer pressurized balloons drifting over the western Mediterranean Sea (1–2 ppbV O_3 h^{-1}; Gheusi et al., 2016; Gheusi, 2022). Nevertheless, we note that these latter values are net production (versus gross production); therefore, the comparison must be considered with caution.

4 Conclusions and Recommendations

Only a few studies of OH reactivity have been conducted in the Mediterranean basin so far (Fig. 2; see Yang et al. (2016) for the corresponding references). Among those, we can distinguish measurements in the western and eastern basin, over open water, in forests, and at anthropogenically influenced sites. Studies in the western and eastern basins have shown that the western basin has a larger OH reactivity, which was mainly attributed to biogenic VOC, specifically terpenes, and possibly their oxidation products. Biogenic VOCs are very reactive compounds; therefore, their influence on OH reactivity is mainly local, although they can have a wider

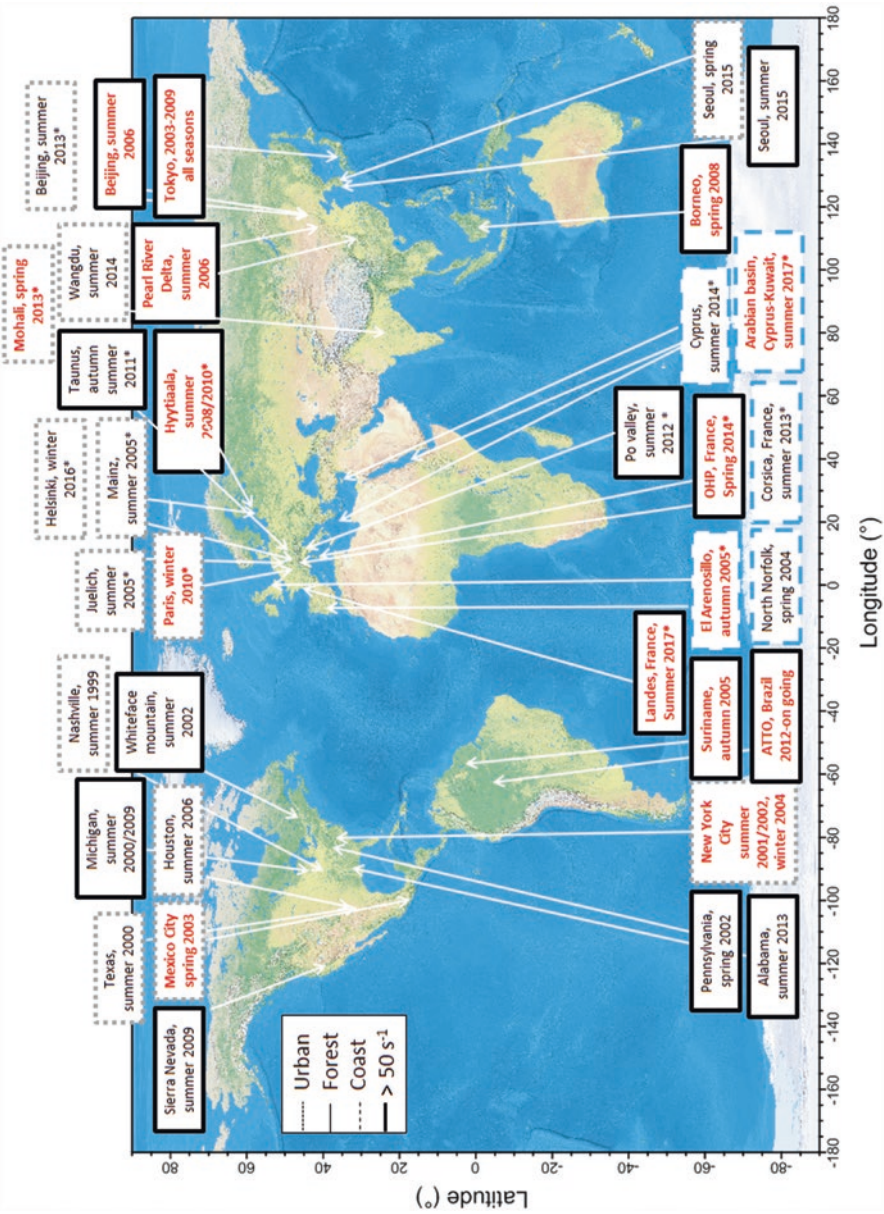

Fig. 2 Existing OH reactivity studies around the world. Studies conducted in the Mediterranean region are indicated with a *. High OH reactivity (and high concentration of very reactive VOCs) was reported in sites indicated in red. (Adapted from Zannoni, 2015)

impact through the transport of their oxidation products. Campaign periods with higher ambient temperature and sunlight triggered larger plant emissions and photochemistry, which explained the reported missing reactivity. The sites located in both the western and eastern basin were background sites, with weak pollution events; therefore, the different vegetation due to different latitudes was the driving factor for reactivity. The values measured at these sites are comparable to the reactivity measured over open water. Over open water, no local event occurred, and processed air masses, mainly containing OVOCs and CO, had a similar reactivity to the one measured in the western basin without the contribution of the local BVOCs. Sites under anthropogenic influence can also show high reactivity, when measurements are directly performed close to emission sources (see the case of megacities and urban agglomerates; Fig. 2).

As reported in Fig. 2, most measurements performed at coastal sites have been performed in the Mediterranean region. Therefore, the comparison with other non-Mediterranean coastal sites is limited. Nevertheless, as seen in other areas of the world, the environments usually associated with high OH reactivity (and often higher missing OH reactivity) are forested areas. This shows the importance to better characterize BVOC and their oxidation products. The development of a plant chamber facility (Hohaus et al., 2016) and similar facilities enabling controlled experiments will be of great help to investigate these chemical reactions and therefore to identify and quantify the oxidation products issued from BVOC compounds and their corresponding OH reactivity. In addition, for a complete understanding of OH reactivity in the Mediterranean basin, more measurements in different environments and seasons are needed. As an example, the Mediterranean region being often under the influence of biomass burning, OH reactivity measurements could also be useful to better characterize the corresponding pollution plumes, as done in another region of the world by Kumar et al. (2018). We note that OH reactivity is mostly useful when combined with other measurements. Therefore, we recommend to associate OH reactivity measurements to each field campaign deploying a large set of gaseous compound measurements, especially reactive VOCs. The objective is to determine whether there are any not measured compounds which lead to a significant missing OH reactivity and possibly investigate which ones when this is the case. If combined with measurements of NO_x, O_3, and OH radicals, the OH reactivity is also a useful parameter to help better constrain the OH budget and estimate the O_3 production potential. Finally, the explicit calculation of the total OH reactivity derived by atmospheric chemistry models (Whalley et al., 2016) with detailed chemical schemes would be very valuable to perform a direct comparison with measurements, but it is still challenging due to the large number of compounds (especially issued from multi-oxidation) involved.

References

Bsaibes, S., Al Ajami, M., Mermet, K., Truong, F., Batut, S., Hecquet, C., Dusanter, S., Léornadis, T., Sauvage, S., Kammer, J., Flaud, P.-M., Perraudin, E., Villenave, E., Locoge, N., Gros, V., & Schoemaecker, C. (2020). Variability of hydroxyl radical (OH) reactivity in the Landes maritime pine forest: Results from the LANDEX campaign 2017. *Atmospheric Chemistry and Physics, 20*, 1277–1300. https://doi.org/10.5194/acp-20-1277-2020

Calpini, B., Jeanneret, F., Bourqui, M., Clappier, A., Vajtai, R., & van den Bergh, H. (1999). Direct measurement of the total reaction rate of OH in the atmosphere. *Analusis, 27*, 328–336. https://doi.org/10.1051/analusis:1999270328

Derstroff, B., Hüser, I., Bourtsoukidis, E., Crowley, J. N., Fischer, H., Gromov, S., Harder, H., Janssen, R. H. H., Kesselmeier, J., Lelieveld, J., Mallik, C., Martinez, M., Novelli, A., Parchatka, U., Phillips, G. J., Sander, R., Sauvage, C., Schuladen, J., Stönner, C., … Williams, J. (2017). Volatile organic compounds (VOCs) in photochemically aged air from the eastern and western Mediterranean. *Atmospheric Chemistry and Physics, 17*, 9547–9566. https://doi.org/10.5194/acp-17-9547-2017

Di Carlo, P. D., Brune, W. H., Martinez, M., Harder, H., Lesher, R., Ren, X., Thornberry, T., Carroll, M. A., Young, V., Shepson, P. B., Riemer, D., Apel, E., & Campbell, C. (2004). Missing OH reactivity in a forest: Evidence for unknown reactive biogenic VOCs. *Science, 304*, 722–725. https://doi.org/10.1126/science.1094392

Dulac, F., Sauvage, S., Hamonou, E., & Debevec, C. (2023). Introduction to the volume 1 of Atmospheric Chemistry in the Mediterranean Region and to the experimental effort during the ChArMEx decade. In F. Dulac, S. Sauvage, & E. Hamonou (Eds.), *Atmospheric chemistry in the Mediterranean Region* (Vol. 1, Background information and pollutant distribution). Springer.

Fuchs, H., Tan, Z., Lu, K., Bohn, B., Broch, S., Brown, S. S., Dong, H., Gomm, S., Häseler, R., He, L., Hofzumahaus, A., Holland, F., Li, X., Liu, Y., Lu, S., Min, K.-E., Rohrer, F., Shao, M., Wang, B., … Zhang, Y. (2017a). OH reactivity at a rural site (Wangdu) in the North China Plain: Contributions from OH reactants and experimental OH budget. *Atmospheric Chemistry and Physics, 17*, 645–661. https://doi.org/10.5194/acp-17-645-2017

Fuchs, H., Novelli, A., Rolletter, M., Hofzumahaus, A., Pfannerstill, E. Y., Kessel, S., Edtbauer, A., Williams, J., Michoud, V., Dusanter, S., Locoge, N., Zannoni, N., Gros, V., Truong, F., Sarda-Esteve, R., Cryer, D. R., Brumby, C. A., Whalley, L. K., Stone, D., … Wahner, A. (2017b). Comparison of OH reactivity measurements in the atmospheric simulation chamber SAPHIR. *Atmospheric Measurement Techniques, 10*, 4023–4053. https://doi.org/10.5194/amt-10-4023-2017

Gheusi, F. (2022). Ozone photochemical production rates. In F. Dulac, S. Sauvage, & E. Hamonou (Eds.), *Atmospheric chemistry in the Mediterranean Region* (Vol. 2, From air pollutant sources to impacts). Springer, this volume. https://doi.org/10.1007/978-3-030-82385-6_8

Gheusi, F., Durand, P., Verdier, N., Dulac, F., Attié, J.-L., Commun, P., Barret, B., Basdevant, C., Clenet, A., Derrien, S., Doerenbecher, A., El Amraoui, L., Fontaine, A., Hache, E., Jambert, C., Jaumouillé, E., Meyerfeld, Y., Roblou, L., & Tocquer, F. (2016). Adapted ECC ozonesonde for long-duration flights aboard boundary-layer pressurised balloons. *Atmospheric Measurement Techniques, 9*, 5811–5832. https://doi.org/10.5194/amt-9-5811-2016

Hansen, R. F., Blocquet, M., Schoemaecker, C., Léonardis, T., Locoge, N., Fittschen, C., Hanoune, B., Stevens, P. S., Sinha, V., & Dusanter, S. (2015). Intercomparison of the comparative reactivity method (CRM) and pump–probe technique for measuring total OH reactivity in an urban environment. *Atmospheric Measurement Techniques, 8*, 4243–4264. https://doi.org/10.5194/amt-8-4243-2015

Hohaus, T., Kuhn, U., Andres, S., Kaminski, M., Rohrer, F., Tillmann, R., Wahner, A., Wegener, R., Yu, Z., & Kiendler-Scharr, A. (2016). A new plant chamber facility, PLUS, coupled to the atmosphere simulation chamber SAPHIR. *Atmospheric Measurement Techniques, 9*, 1247–1259. https://doi.org/10.5194/amt-9-1247-2016

Kaiser, J., Wolfe, G. M., Bohn, B., Broch, S., Fuchs, H., Ganzeveld, L. N., Gomm, S., Häseler, R., Hofzumahaus, A., Holland, F., Jäger, J., Li, X., Lohse, I., Lu, K., Prévôt, A. S. H., Rohrer, F., Wegener, R., Wolf, R., Mentel, T. F., … Keutsch, F. N. (2015). Evidence for an unidentified non-photochemical ground-level source of formaldehyde in the Po Valley with potential implications for ozone production. *Atmospheric Chemistry and Physics, 15*, 1289–1298. https://doi.org/10.5194/acp-15-1289-2015

Kaiser, J., Skog, K. M., Baumann, K., Bertman, S. B., Brown, S. B., Brune, W. H., Crounse, J. D., de Gouw, J. A., Edgerton, E. S., Feiner, P. A., Goldstein, A. H., Koss, A., Misztal, P. K., Nguyen, T. B., Olson, K. F., St. Clair, J. M., Teng, A. P., Toma, S., Wennberg, P. O., … Keutsch, F. N. (2016). Speciation of OH reactivity above the canopy of an isoprene-dominated forest. *Atmospheric Chemistry and Physics, 16*, 9349–9359. https://doi.org/10.5194/acp-16-9349-2016

Kalogridis, C., Gros, V., Sarda-Esteve, R., Langford, B., Loubet, B., Bonsang, B., Bonnaire, N., Nemitz, E., Genard, A.-C., Boissard, C., Fernandez, C., Ormeño, E., Baisnée, D., Reiter, I., & Lathière, J. (2014). Concentrations and fluxes of isoprene and oxygenated VOCs at a French Mediterranean oak forest. *Atmospheric Chemistry and Physics, 14*, 10085–10102. https://doi.org/10.5194/acp-14-10085-2014

Keenan, T., Niinemets, Ü., Sabate, S., Gracia, C., & Peñuelas, J. (2009). Process based inventory of isoprenoid emissions from European forests: Model comparisons, current knowledge and uncertainties. *Atmospheric Chemistry and Physics, 9*, 4053–4076. https://doi.org/10.5194/acp-9-4053-2009

Keßel, S. (2016). Entwicklung und Charakterisierung der Comparative Reactivity Method zur Messung von Hydroxylradikal- und Chlorradikal-Reaktivitäten – Troposphärische Oxidationschemie in drei unterschiedlich stark anthropogen beeinflussten Gebieten, PhD dissertation, Johannes Gutenberg-Universität Mainz.

Kovacs, T. A., & Brune, W. H. (2001). Total OH loss rate measurement. *Journal of Atmospheric Chemistry, 39*, 105–122. https://doi.org/10.1023/A:1010614113786

Kumar, V., Chandra, B. P., & Sinha, V. (2018). Large unexplained suite of chemically reactive compounds present in ambient air due to biomass fires. *Scientific Reports, 8*, 626. https://doi.org/10.1038/s41598-017-19139-3

Mao, J., Ren, X., Brune, W. H., Olson, J. R., Crawford, J. H., Fried, A., Huey, L. G., Cohen, R. C., Heikes, B., Singh, H. B., Blake, D. R., Sachse, G. W., Diskin, G. S., Hall, S. R., & Shetter, R. E. (2009). Airborne measurement of OH reactivity during INTEX-B. *Atmospheric Chemistry and Physics, 9*, 163–173. https://doi.org/10.5194/acp-9-163-2009

Michoud, V. (2022). Particle-gas multiphasic interactions. In F. Dulac, S. Sauvage, & E. Hamonou (Eds.), *Atmospheric chemistry in the Mediterranean Region* (Vol. 2, From air pollutant sources to impacts). Springer, this volume. https://doi.org/10.1007/978-3-030-82385-6_11

Michoud, V., Sciare, J., Sauvage, S., Dusanter, S., Léonardis, T., Gros, V., Kalogridis, C., Zannoni, N., Féron, A., Petit, J.-E., Crenn, V., Baisnée, D., Sarda-Estève, R., Bonnaire, N., Marchand, N., DeWitt, H. L., Pey, J., Colomb, A., Gheusi, F., … Locoge, N. (2017). Organic carbon at a remote site of the western Mediterranean Basin: Sources and chemistry during the ChArMEx SOP2 field experiment. *Atmospheric Chemistry and Physics, 17*, 8837–8865. https://doi.org/10.5194/acp-17-8837-2017

Mogensen, D., Smolander, S., Sogachev, A., Zhou, L., Sinha, V., Guenther, A., Williams, J., Nieminen, T., Kajos, M. K., Rinne, J., Kulmala, M., & Boy, M. (2011). Modelling atmospheric OH-reactivity in a boreal forest ecosystem. *Atmospheric Chemistry and Physics, 11*, 9709–9719. https://doi.org/10.5194/acp-11-9709-2011

Muller, J. B. A., Elste, T., Plass-Dülmer, C., Stange, G., Holla, R., Claude, A., Englert, J., Gilge, S., & Kubistin, D. (2018). A novel semi-direct method to measure OH reactivity by chemical ionization mass spectrometry (CIMS). *Atmospheric Measurement Techniques, 11*, 4413–4433. https://doi.org/10.5194/amt-11-4413-2018

Nölscher, A. C., Sinha, V., Bockisch, S., Klüpfel, T., & Williams, J. (2012). Total OH reactivity measurements using a new fast Gas Chromatographic Photo-Ionization Detector (GC-PID). *Atmospheric Measurement Techniques, 5*, 2981–2992. https://doi.org/10.5194/amt-5-2981-2012

Nölscher, A. C., Yañez-Serrano, A. M., Wolff, S., Carioca de Araujo, A., Lavrič, J. V., Kesselmeier, J., & Williams, J. (2016). Unexpected seasonality in quantity and composition of Amazon rainforest air reactivity. *Nature Communications, 7*, 10383. https://doi.org/10.1038/ncomms10383

Pfannerstill, E. Y., Wang, N., Edtbauer, A., Bourtsoukidis, E., Crowley, J. N., Dienhart, D., Eger, P. G., Ernle, L., Fischer, H., Hottmann, B., Paris, J.-D., Stönner, C., Tadic, I., Walter, D., Lelieveld, J., & Williams, J. (2019). Shipborne measurements of total OH reactivity around the Arabian Peninsula and its role in ozone chemistry. *Atmospheric Chemistry and Physics, 19*, 11501–11523. https://doi.org/10.5194/acp-19-11501-2019

Sadanaga, Y., Yoshino, A., Watanabe, K., Yoshioka, A., Wakazono, Y., Kanaya, Y., & Kajii, Y. (2004). Development of a measurement system of OH reactivity in the atmosphere by using a laser-induced pump and probe technique. *The Review of Scientific Instruments, 75*, 2648–2655. https://doi.org/10.1063/1.1775311

Sartelet, K. (2022). Secondary aerosol formation and their modeling. In F. Dulac, S. Sauvage, & E. Hamonou (Eds.), *Atmospheric chemistry in the Mediterranean Region* (Vol. 2, From air pollutant sources to impacts). Springer, this volume. https://doi.org/10.1007/978-3-030-82385-6_10

Sellegri, K., & Rose, C. (2022). Nucleation in the Mediterranean atmosphere. In F. Dulac, S. Sauvage, & E. Hamonou (Eds.), *Atmospheric chemistry in the Mediterranean Region* (Vol. 2, From air pollutant sources to impacts). Springer, this volume. https://doi.org/10.1007/978-3-030-82385-6_9

Sinha, V., Williams, J., Crowley, J. N., & Lelieveld, J. (2008). The comparative reactivity method – A new tool to measure total OH reactivity in ambient air. *Atmospheric Chemistry and Physics, 8*, 2213–2227. https://doi.org/10.5194/acp-8-2213-2008

Sinha, V., Williams, J., Diesch, J. M., Drewnick, F., Martinez, M., Harder, H., Regelin, E., Kubistin, D., Bozem, H., Hosaynali-Beygi, Z., Fischer, H., Andrés-Hernández, M. D., Kartal, D., Adame, J. A., & Lelieveld, J. (2012). Constraints on instantaneous ozone production rates and regimes during DOMINO derived using in-situ OH reactivity measurements. *Atmospheric Chemistry and Physics, 12*, 7269–7283. https://doi.org/10.5194/acp-12-7269-2012

Whalley, L. K., Edwards, P. M., Furneaux, K. L., Goddard, A., Ingham, T., Evans, M. J., Stone, D., Hopkins, J. R., Jones, C. E., Karunaharan, A., Lee, J. D., Lewis, A. C., Monks, P. S., Moller, S. J., & Heard, D. E. (2011). Quantifying the magnitude of a missing hydroxyl radical source in a tropical rainforest. *Atmospheric Chemistry and Physics, 11*, 7223–7233. https://doi.org/10.5194/acp-11-7223-2011

Whalley, L. K., Stone, D., Bandy, B., Dunmore, R., Hamilton, J. F., Hopkins, J., Lee, J. D., Lewis, A. C., & Heard, D. E. (2016). Atmospheric OH reactivity in central London: Observations, model predictions and estimates of in situ ozone production. *Atmospheric Chemistry and Physics, 16*, 2109–2122. https://doi.org/10.5194/acp-16-2109-2016

Yang, Y., Shao, M., Wang, X., Nölscher, A. C., Kessel, S., Guenther, A., & Williams, J. (2016). Towards a quantitative understanding of total OH reactivity: A review. *Atmospheric Environment, 134*, 147–161. https://doi.org/10.1016/j.atmosenv.2016.03.010

Zannoni, N. (2015). OH reactivity measurements in the Mediterranean region, PhD Dissertation, Université Paris-Saclay, p. 188.

Zannoni, N., Dusanter, S., Gros, V., Sarda Esteve, R., Michoud, V., Sinha, V., Locoge, N., & Bonsang, B. (2015). Intercomparison of two comparative reactivity method instruments in the Mediterranean basin during summer 2013. *Atmospheric Measurement Techniques, 8*, 3851–3865. https://doi.org/10.5194/amt-8-3851-2015

Zannoni, N., Gros, V., Lanza, M., Sarda, R., Bonsang, B., Kalogridis, C., Preunkert, S., Legrand, M., Jambert, C., Boissard, C., & Lathiere, J. (2016). OH reactivity and concentrations of biogenic volatile organic compounds in a Mediterranean forest of downy oak trees. *Atmospheric Chemistry and Physics, 16*, 1619–1636. https://doi.org/10.5194/acp-16-1619-2016

Zannoni, N., Gros, V., Sarda Esteve, R., Kalogridis, C., Michoud, V., Dusanter, S., Sauvage, S., Locoge, N., Colomb, A., & Bonsang, B. (2017). Summertime OH reactivity from a receptor coastal site in the Mediterranean Basin. *Atmospheric Chemistry and Physics, 17*, 12645–12658. https://doi.org/10.5194/acp-17-12645-2017

Ozone Photochemical Production Rates in the Western Mediterranean

François Gheusi

Contents

Abstract In the context of 3 ChArMEx field campaigns conducted in summer 2012 and 2013, 16 boundary-layer pressurized balloons (BLPBs), carrying ozone payloads, were launched over the western Mediterranean from 3 sites, in order to measure photochemical ozone formation. Such balloons allow a quasi-Lagrangian monitoring approach, at least over selected measurement periods. Rather slow net ozone growth rates, ranging from +1.2 to +2.2 ppbv h^{-1}, were observed in the Mediterranean lower troposphere during ChArMEx. On the contrary, larger values, up to about +15 ppbv h^{-1}, had been encountered during the 2001 ESCOMPTE summer campaign around Marseille, mostly over land. Differences could be due to different meteorological and flight conditions during both periods. Also decreased precursor emissions (NO_x, VOC), as well as enhanced dilution during long-range flights over the sea, should contribute to smaller photochemical ozone formation rates.

Chapter reviewed by ***Vinayak Sinha*** *(IISER, Mohali Campus, Mohali, Punjab, India), as part of the book Part VI Recent Progress on Chemical Processes also reviewed by* ***Andrea Pozzer*** *(Max Planck Institute for Chemistry, Mainz, Germany)*

F. Gheusi (✉)
Laboratoire d'Aérologie (LAERO), CNRS, Univ. Toulouse III Paul Sabatier, Observatoire Midi-Pyrénées, Toulouse, France
e-mail: francois.gheusi@aero.obs-mip.fr

F. Dulac et al. (eds.), *Atmospheric Chemistry in the Mediterranean Region*,
https://doi.org/10.1007/978-3-030-82385-6_8

1 Introduction

The Mediterranean basin is one of the world's hot spots for tropospheric ozone (e.g., Richards et al., 2013; Sicard et al., 2013; Gaudel et al., 2018). For the western basin, Richards et al. (2013) report summertime average surface ozone mole fractions of more than 55–60 ppbv for rural stations in Italy, eastern Spain, and Malta. In their review paper on tropospheric ozone, Monks et al. (2015) point out the various deleterious impacts of this gas: on human health (up to 20% of casualties related to atmospheric pollution), on vegetation (affecting forest and crop yield, as well as the capacity of CO_2 uptake into the biosphere), and also as a greenhouse gas.

The photochemical production rate of ozone – thereafter $P(O_3)$ – is triggered by the radical or light-induced oxidation of volatile organic compounds (VOCs) and carbon monoxide (CO) in the presence of Nitrogen oxides (NOx). $P(O_3)$ thus depends on the availability of ozone precursors, VOCs/CO and NO_x, and on the availability of radicals formed by photolysis processes (see also the chapter by Gros & Zannoni, 2022). Relationships between these factors and $P(O_3)$ are complex and lead to the existence of chemical regimes, in which $P(O_3)$ is limited by the availability of either VOCs or NO_x (e.g., Kleinman, 2005) or both of them. The regimes are delineated by the reactivity of OH radicals to NO_x or VOC precursors (Kirchner et al., 2001; Sinha et al., 2012). Summertime photochemical ozone production over the western Mediterranean basin is generally NO_x-limited (Beekmann & Vautard, 2010).

$P(O_3)$ from both natural and anthropogenic species emitted in the atmosphere is now recognized as being the dominant source term in the global tropospheric ozone budget, relative to transport from the stratosphere (Monks et al., 2015 and references therein). The tropospheric ozone budget was typically studied by means of numerical models (e.g., Young et al., 2013), but nevertheless, attempts have been made to estimate ozone photochemical production in the troposphere from in situ measurements. Coll et al. (2005), for instance, report estimations of ozone production in a polluted boundary layer on the French Mediterranean coast by means of ground-based measurement of peroxy radicals and NO at a rural site, and airborne measurements of the photo-stationary state (NO, NO_2, O_3, and photolysis rate JNO_2) in the area.

Estimations of $P(O_3)$ are most often made in Eulerian frames. A difficulty with the Eulerian point of view is that advection is a major term in the local ozone budget, but difficult to assess unless a numerical chemical transport model is used. Although being challenging in field studies, the Lagrangian approach is especially relevant, since chemical reactions are the only cause of air composition changes in a Lagrangian volume (assumed to be transported by the local wind with negligible mass exchange across its boundaries). Among the different strategies to carry out in situ observations in a Lagrangian frame (reviewed in Businger et al., 1996, 2006, and Gheusi et al., 2016), the use of constant-volume balloons (CVBs) offers the capability to drift with the wind at constant density (isopycnic) levels and thus to follow quasi-Lagrangian trajectories. In this chapter, we report ozone net production rates obtained over the western Mediterranean with CVBs deployed in summer 2012 and 2013 in the framework of the Chemistry-Aerosol Mediterranean Experiment (ChArMEx) field campaigns (Di Biagio et al., 2015; Mallet et al., 2016).

2 Boundary-Layer Pressurized Balloons and Adapted ECC Sondes

Boundary-layer pressurized balloons (hereafter abbreviated as BLPBs) are a class of CVBs developed since 1972 for scientific applications in the tropical atmospheric marine boundary layer (Cadet & Ovarlez, 1976) and operated by the French Space Agency CNES (Centre National d'Etudes Spatiales; https://cnes.fr/en). These balloons have the capability to transport light scientific payloads for several weeks (depending on the amount of energy needed) and to transmit data via satellite communication. They have been deployed for atmospheric dynamics studies over the Arabian Sea and Indian Ocean (Cadet & Ovarlez, 1976; Cadet, 1981; Reverdin & Sommeria, 1983; Ethé et al., 2002; Duvel et al., 2009), the South Atlantic Ocean (Ethé, 2001), the Sahel in Africa, and the Mediterranean Sea (Doerenbecher et al., 2016). For the ChArMEx project in the Mediterranean, the balloon was further developed to offer flight possibilities higher up in the lower free troposphere and to accommodate atmospheric chemistry payloads, namely, for aerosol (Renard et al., 2018) and ozone measurements (Gheusi et al., 2016).

Electrochemical concentration cell (ECC) sensors (Komhyr, 1969) are used worldwide below light balloons for tropospheric and stratospheric ozone soundings (Smit and the ASOPOS panel, 2011). Ambient air is pumped at constant volumetric flow rate and bubbles into a cathode chamber filled with a potassium iodide solution, thus generating a current (of a few μA) proportional to ozone mole fraction in air. During two ESCOMPTE field campaigns in 2000 and 2001 near Marseille on the French Mediterranean coast (Cros et al., 2004), conventional ECC sondes were operated under CVBs for up to 6 hours within the continental boundary layer (Bénech et al., 2008). However, the lifetime of a conventional ECC sonde is limited to a few hours (mainly due to electrolyte evaporation in the cathode chamber). In collaboration with the ChArMEx research community, CNES also developed in 2011–2012 a new ozone payload based on the ECC technology, but suited for long-duration flights aboard BLPBs. To increase the sonde autonomy, a strategy was adopted of short measurement sequences (2–3 min) repeated, e.g., every 15 minutes. The rest of the time, the sondes were quiescent (pump off). All details concerning the payload, laboratory validation, and field deployment are given in Gheusi et al. (2016), including outdoor ground-based tests prior to the ChArMEx campaigns that demonstrated the ability to provide 10% accurate measurements over 5 days, at a rate of one data point every 15 minutes, and to capture ozone diurnal cycles as well as variations on shorter time scales. Figure 1 shows the balloon and ozone payload.

3 Ozone Production over the Mediterranean as Seen from the BLPBs

In the context of 3 ChArMEx field campaigns conducted in summer 2012 and 2013, 16 BLPBs carrying ozone payloads were launched over the western Mediterranean from 3 sites, as represented in Fig. 2a, b, and detailed in Table 1. The TRAQA

Fig. 1 (**a**) Photo of the BLPB B54 launch unpressurized from Minorca Island in June 2013. (**b**) Photo of the ozone payload hanging below the balloon B59 before launch from the Levant Island in July 2013. Details on the ozone-equipped balloon flights are given in Table 1. (Photographs by courtesy of François Dulac, CEA/LSCE)

(June–July 2012) and the SAFMED (July–August 2013) campaigns were mainly designed to study anthropogenic pollution transport and chemistry over the western Mediterranean basin (Di Biagio et al., 2015). The two respective launch sites – Martigues (43°19.96′ N, 5°05.22′ E) and the Levant Island (43°01.31′ N, 6°27.61′ E) – were located on the southeast French coast, a major source region of anthropogenic pollution in France (Cachier et al., 2005). The balloon ceiling levels, ranging within 200–700 m above the sea, were chosen to sample the atmospheric marine boundary layer. The ADRIMED campaign (June–July 2013) was mainly devoted to characterizing aerosol optical properties during dust transport episodes from the Sahara (Mallet et al., 2016), again over the western Mediterranean basin. The chosen launch site – Sant Lluís (39°51.98′ N, 4°15.30′E) – was on Minorca Island, which is remote from anthropogenic emission sources, but located on the pathway of Saharan dust plumes to the north and north-west. The higher flight levels around 2–3 km targeted the free troposphere, where dust transport mainly occurs (Chazette et al., 2016).

Fig. 2 (continued) Other plots show selected flight segments during which the role of photochemistry in the observed ozone trend is considered as most likely (see Table 1). Middle plots show boundary-layer flight segments: (**c**) from Martigues; (**d**) from the Levant Island. Bottom plots show free tropospheric flights from Minorca Isl.: (**e**) balloon B55; (**f**) balloon B57. Common to all panels but only displayed in panel a, the color code refers to observed ozone mole fraction (in ppbv), and the dot size refers to on-board measurement of global solar irradiance (in W m^{-2}). (Data from Gheusi et al., 2016)

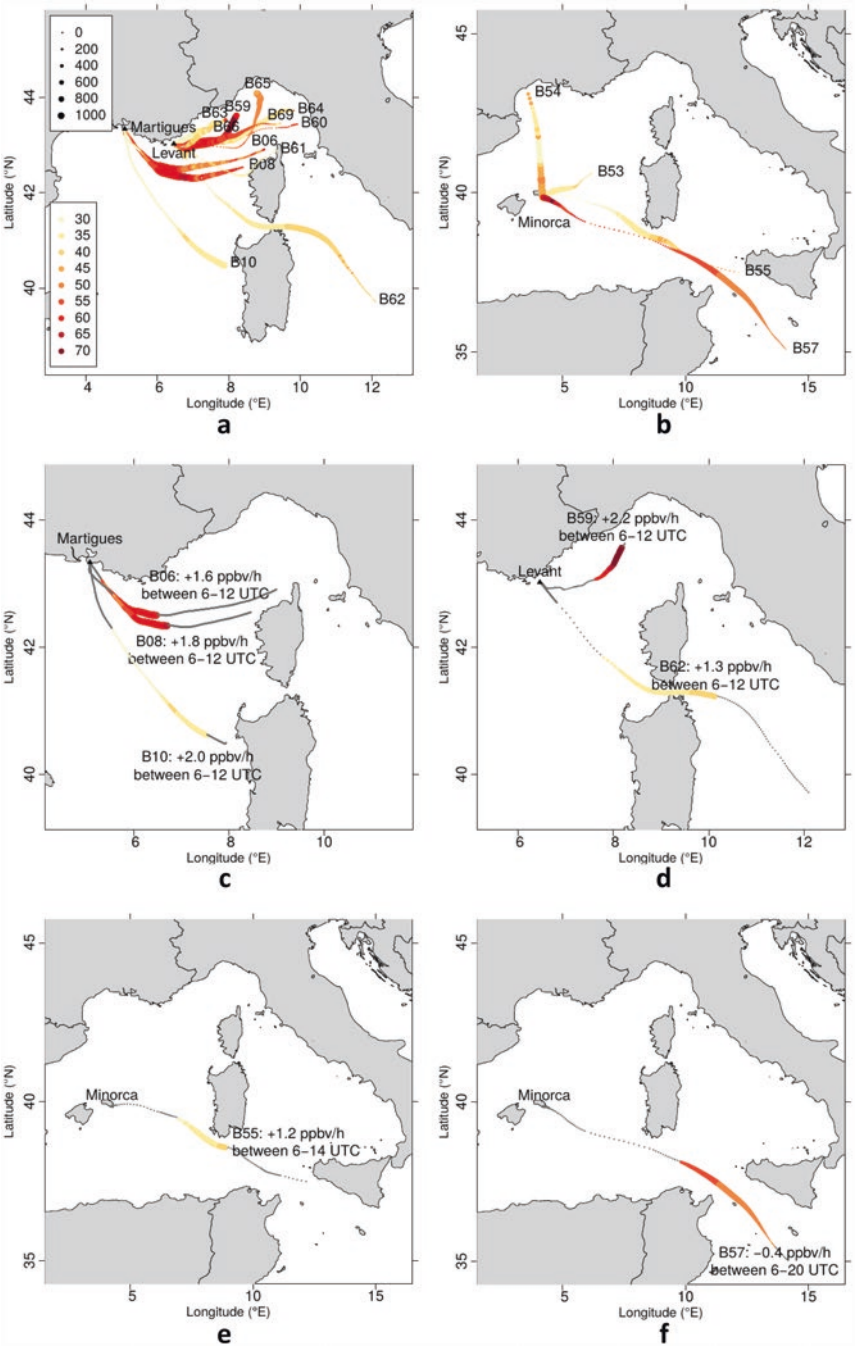

Fig. 2 Top plots provide an overview of the 16 BLPB-ozone flights during 3 ChArMEx campaigns: (**a**) boundary-layer flights during TRAQA 2012 (from Martigues) and SAFMED 2013 (from Levant Isl.); (**b**) free tropospheric flights during ADRIMED 2013 (from Minorca Isl.).

Table 1 Overview of the 16 BLPB-ozone flights operated in 2012 and 2013. Data after Gheusi et al. (2016) and complementary data

BLPB balloon number	Launch site	Launch date/time (UTC)	Flight duration (h)/range (km)	Altitude at ceiling (m)	Ozone range at ceiling (ppbv)	Ozone trend over at least 4 h ($ppbh^{-1}$)	Day period (UTC) of ozone trend occurrence	Integrated ozone buildup (ppbv)	Evidence of in situ chemistry	Surface O_3 during the flight (ppbv)[a]
B06	Martigues 43°20′N 5°05′E	6 July 2012, 04:46	15.4/371	470–609	45–67	+1.6	06–12	+9.6	Yes	18–52
B08	6 July 2012, 02:37	15.5/336	417–574	55–69	+1.8	06–12	+10.8	Yes	10–52	B10
27 June 2012, 01:00		9.5/175	566–720	20–46	+2.0	05–10	+10.0	Yes	13–55	B53
Minorca Island 39°52′N 4°15′E		16 June 2013, 09:56	14.1/193	2996–3065	39–44	No	–	–	No	52–59
B54	17 June 2013, 09:45	7.0/367	1836–2020	36–54	No	–	–	No	48–61	B55
2 July 2013, 18:00		32.0/732	2429–477	23–54	+1.2	06–14	+9.6	Yes	27–41	B57
2 July 2013, 13:12		33.0/1014	3083–3198	49–75	−0.4	06–20	−5.6	Yes	27–42	B59
Levant Island 43°01′N 6°28′E		22 July 2013, 21:05	15.4/189	242–395	45–85	+2.2	06–12	+13.2	Yes	43–77

B60	25 July 2013, 06:00	19.1/296	526–649	54–66	*+0.9*	*06–12*	*+5.4*	*Poor*	17–56	B61
29 July 2013, 21:56		5.5/279	300,733	39–42	No	–	–	No	36–39	B62
30 July 2013, 02:59		17.4/626	207–634	36–48	+1.3	06–12	+7.8	Yes	32–55	B63
3 August 2013, 06:54		9.9/118	467–630	30–53	*+6.5*	*12–16*	*+26.0*	*Poor*	38–55	B64
3 August 2013, 20:57		21.6/304	773–907	39–58	*+1.3*	*13–18*	*+6.5*	*Poor*	27–84	B65
3 August 2013, 20:57		15.3/299	391–615	52–61	*−0.7*	*06–12*	*−4.2*	*Poor*	27–74	B66
4 August 2013, 02:52		13.3/176	798–943	42–59	No	–	–	No	27–84	B69
25 July 2013, 04:00		19.4/265	208–0621	41–67	*−0.6*	*06–19*	*−7.8*	*Poor*	17–56	

[a]Surface ozone at the balloon launch pad (right column) was continuously measured by a UV-absorption analyzer TEI 49i. The values correspond to surface ozone ranges observed at the launch pad during each flight period

As it can be deduced from the ozone levels reported in Table 1, Fig. 1a, b, and Fig. 2a, no major ozone pollution episode was experienced during the 2012–2013 balloon campaigns. During a given flight, ozone varied by less than 25 ppb around flight averages ranging between 30 and 60 ppbv. Except in two cases (22 July and 4 August 2013), surface ozone values measured on the balloon launch pad did not exceed 60 ppbv (Table 1).

A decade earlier, two field campaigns were held on the French Mediterranean coast in summer 2000 and 2001 during the ESCOMPTE program (Cros et al., 2004). To quantify net photochemical ozone production within air masses sampled by ozone-equipped CVBs during these campaigns, Bénech et al. (2008) developed a method for identifying flight segments, during which the balloon trajectory could be considered as quasi-Lagrangian. Constant specific humidity was an indication that the balloon flew within a homogeneous and coherent air mass. Conversely, changes in specific humidity indicated turbulent transport or the fact that the isopycnic trajectory crossed the boundary between two air layers. Gheusi et al. (2016) adopted a similar strategy of selecting flight segments when analyzing the data from the ChArMEx BLPBs. Flight segments showing noteworthy ozone growth were retained, and in situ production/destruction was considered to cause the ozone trend, only if (i) the event had a duration of at least 4 h and (ii) no concurrent specific humidity trend was observed. Unlike specific humidity, which is a passive tracer in unsaturated air, temperature may vary in a Lagrangian air mass by diabatic heating/cooling. Therefore, temperature was not considered in our criteria. Flight segments during which the role of chemistry on the ozone trend is the most likely are tagged "Yes" in Table 1 and illustrated in Fig. 2c–f. If concurrent humidity changes occurred, the segments were tagged "Poor." Observed ozone trends were more or less linear with time, and rates (reported both in Gheusi et al., 2016 and here in Table 1) were estimated manually from curves. These trends all occurred during the daytime and mostly in the morning (Table 1). Given the flight altitudes between 200 and 900 m over sea indicated in Table 1, and given a typical marine boundary layer height of about several hundred meters without large diurnal variation (Stull, 1988), encountered air masses were either located within the marine boundary layer, or above, in a residual layer probably still influenced by continental emissions. In both cases, turbulence is expected to be much less pronounced than in a continental boundary layer.

A feature common to both Bénech et al. (2008) and Gheusi et al. (2016) is that ozone increase was found in a majority of cases (Fig. 2b). Among the ChArMEx cases with likely ozone photochemical production, flight B55 (Fig. 2e) is especially interesting because the balloon was not designed to fly in the boundary layer, but higher in the free troposphere. Despite this, a positive trend of +1.2 ppbv h^{-1} was observed, lasting more than 7 hours during the daytime. This was one of the rare direct observations of ozone production in the free troposphere (if not the first in a Lagrangian frame). Like during ESCOMPTE, few cases with negative ozone change rates were also reported by Gheusi et al. (2016). Among them, B57 (Fig. 2f) was a free tropospheric flight with presumably slow ozone destruction. In absence of any other data, it is hard to speculate on a cause for such destruction during the daytime.

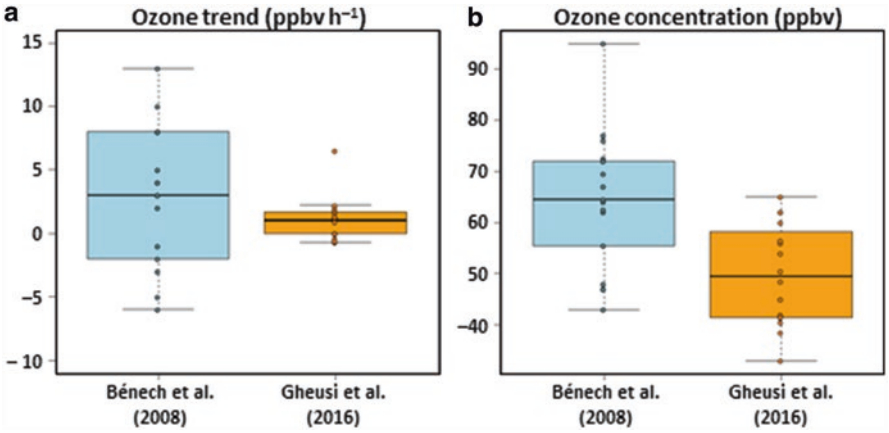

Fig. 3 Box-and-whisker comparison of values reported by Bénech et al. (2008) and Gheusi et al. (2016) from tropospheric constant-volume balloons carrying ozone sensors: (**a**) ozone change rates (ppbv h^{-1}) during selected flight segments; (**b**) in-flight average ozone mole fraction (ppbv)

The role of destruction in the observed ozone decrease is less certain in two other cases (B65 and B69, Table 1) given the concurrent variation in specific humidity.

Focusing on the boundary layer, i.e., on TRAQA and SAFMED flight segments below 700 m with qualified ozone trend, the net photochemical ozone production rates range from +1.2 to +2.2 ppbv h^{-1} (Table 1). When integrated over the measurement intervals (generally ~6 h in the morning), those rates correspond to an ozone buildup of 8–13 ppb (Table 1). Larger, but also more variable, net photochemical production rates than during TRAQA and SAFMED were reported by Bénech et al. (2008) during ESCOMPTE, with a median value of about 3 ppbv h^{-1} (Fig. 3a). Like during TRAQA and SAFMED, the ESCOMPTE CVBs were launched from the French southeast coast, but this time, they flew mostly inland, where higher ozone concentrations were observed than over sea during ChArMEx (Fig. 3b).

Based on surface and airborne observations, as well as a chemical transport model, Coll et al. (2005) reported estimations of ozone gross production rates of a few tens of ppbv h^{-1} for an ESCOMPTE intensive observation period, characterized by intensive photochemistry and strong ozone pollution. The production rates reported for this case are even higher than those in Bénech et al. (2008) with CVBs. For a coastal site in south-west Spain and surface observations, Sinha et al. (2012) similarly found gross ozone production rates above 10 ppb h^{-1} near the surface during most of the daytime.

Unlike gross ozone production rates calculated from surface measurements, production rates derived from CVB ozone observation reflect the net ozone buildup, in which chemical sinks are taken into account. Thus, gross ozone production rates are by definition larger than net ones, an effect which is largest in remote conditions. This is seen at the Finokalia coastal background site in Crete, where chemical ozone production and destruction rates nearly cancel out when averaged over a whole

summer season: summer net ozone change rates typically vary between ±2 ppbv h^{-1} (Gerasopoulos et al., 2006). In Sinha et al. (2012), the net ozone growth rate directly derived from surface ozone measurement was reported to be of 1.9 ppbv/ h^{-1} on average over their experimental campaign, so much smaller than the gross production rates above 10 ppb h^{-1}. These net results are much more in line with our balloon observations.

Beyond distinguishing gross vs. net values, how can such large differences in ozone production rate estimations be explained? First, the altitude of measurements can play a major role, ozone precursor concentrations being expected to be larger at the ground than a few hundred meters above (our typical balloon ceiling altitude), even within the boundary layer. Second, the results depend on the distance to source regions, again because of the availability of ozone precursors. This is consistent with larger $P(O_3)$ values observed during the ESCOMPTE campaign near the source regions around the Marseille and Fos-Berre industrial regions, than during the ChArMEx flights, where distances from sources were in the range 100–1000 km. The ESCOMPTE values are also larger than those at Finokalia in Crete, typically several hundreds of km away from any pollution source regions in eastern Europe, Greece, and Turkey. To quantify the remoteness of the experimental areas considered in the different studies, we indicate here ranges of daytime NO concentrations for each region: during ESCOMPTE, they were typically between 0.5 and 1.5 ppbv when the studied rural site of Dupail was affected by the urban-industrial plume from Marseille-Fos-Berre (Coll et al., 2005); during ChArMEx 2013, they were generally in the range 0.1–0.3 ppbv at 535 m altitude at Ersa (Corsica), a remote coastal site on the northern tip of Corsica (Lambert et al., 2011) representative of the marine boundary layer in the western Mediterranean (daily 75 percentiles over the period 1 June–12 August 2013 were considered here as representative of NO daytime values); and they were typically less than 0.1 ppbv at Finokalia (Gerasopoulos et al., 2006). In terms of both distance from source regions and NO_x levels, it appears that ChArMEx oversea balloon flights encountered intermediate conditions between polluted and remote areas, not yet covered by former measurements. This is an important result from this campaign.

Also, the meteorological context of CVB flights during ESCOMPTE, and during TRAQA and SAFMED on the other hand, was different. For public safety reasons, wind conditions in which the balloons could fly over the land were systematically avoided during TRAQA and SAFMED. Thus, moderate conditions of the regional northwesterly land wind called mistral were preferred to calm and warm anticyclonic conditions, although the latter are more favorable to ozone production. Indeed, coastal sea breezes generally develop during the daytime in such conditions and could bring back the balloons inland. During ESCOMPTE in contrast, flights over the land were in majority (Bénech et al., 2008). Also, the chemical compositions of the continental and marine boundary layers are expected to be different. In the marine case, there are no precursor emissions from the sea surface nor dry deposition, but more humidity, which favors radical formation, via the $O(^1D) + H_2O$ reaction, and may enhance both ozone chemical production and destruction, depending on NO levels. These factors could thus strongly influence the comparison.

One last reason is long-term changes in ozone precursor emissions and atmospheric composition. Obviously, the atmospheric context encountered in 2000–2001 during ESCOMPTE was more favorable to photochemical ozone production, than later in 2012–2013 during ChArMEx. Sicard et al. (2013) studied the decadal evolution of ozone levels over 2000–2010 from a large panel of European air quality stations around the western Mediterranean basin. They found an overall decrease of ozone peak values (98th percentile) over the decade, attributed to European reduction policies of ozone precursor emissions (NO_x, non-methane VOCs, and CO). A similar result (decrease in ozone 95th percentile) was reported by Yan et al. (2018) for all Europe for the 1995–2014 period. Richards et al. (2013) model results further indicate that Mediterranean surface O_3 levels are the most sensitive to regional NO_x emissions. French, Italian, and Spanish anthropogenic NO_x emissions decreased by 56%, 44%, and 38%, respectively, between 2001 and 2013, and those of anthropogenic VOC by 38%, 35%, and 38% according to the EMEP emission database (https://www.ceip.at/webdab_emepdatabase/emissions_emepmodels, consulted in March 2020). Decreasing trends in high ozone percentiles are consistent with ozone pollution episodes of weaker intensity in 2012–2013 than in 2000–2001.

4 Conclusions and Recommendations

As seen from space and atmospheric modeling, the Mediterranean basin is well known as a summer hot spot for surface and tropospheric ozone (Richards et al., 2013). This is supported by land surface observation data from the dense network of air quality stations deployed around the basin (Sicard et al., 2013; Gaudel et al., 2018). Yet, the marine lower troposphere remained largely unexplored in situ, in terms of both ozone levels and production rates. Sixteen ozone-equipped BLPB flights conducted during the three ChArMEx field campaigns in 2012 and 2013 intended to fill this gap. In situ net ozone production was found over sea during daytime in a majority of cases, in both the marine boundary layer and the free troposphere, but at lower rates than generally observed over the land in polluted coastal areas in the Mediterranean basin. Ozone levels and net production rates were nevertheless higher than those found in very remote marine environments (e.g., Williams et al., 2010). The interpretation of ozone concentration dynamics observed during each flight remains here limited by the absence of concurrent measurement of ozone precursors. Based on literature data, we nevertheless conjecture that, although launched from relatively polluted areas, the balloons flew in air masses with limited availability of ozone precursors, likely present at intermediate concentration levels between polluted and remote atmospheres. Despite this, daytime ozone buildup of ~10 ppbv in 6 h was frequently observed and could contribute to forming the Mediterranean tropospheric ozone pool, in the absence of surface deposition and titration at night.

This original data set composed of both ozone levels and derived net production rates should now be considered as an important observational constraint for

numerical chemical transport modeling studies, which would provide a quantification of precursor concentrations and actinic fluxes and help to characterize the main chemical processes in play in the lower troposphere over the sea. This also would allow a more quantitative discussion of determining factors of $P(O_3)$. Although the difference has not been properly quantified, the operational air quality model forecasts used during the ChArMEx campaigns to help balloon flight planning were generally overestimating ozone concentrations over the basin. A better understanding of ozone chemistry processes should improve air quality models and forecasts around the Mediterranean basin, which is important in a context of changing climate and emissions, that will affect regional ozone levels.

Acknowledgments The ozone balloons were funded by CNES. The NO concentration data from Ersa were downloaded from the ChArMEx database (https://mistrals.sedoo.fr/ChArMEx/) by courtesy of Aurélie Colomb and Jean-Marc Pichon (LaMP, OPGC, Clermont-Ferrand, France). We especially thank the editors Matthias Beekmann and François Dulac for their numerous and helpful inputs and comments while writing this chapter. We also thank François Dulac, Pierre Durand, and Nicolas Verdier for their central scientific role before, during and after, the 2012 and 2013 balloon campaigns, as well as all other people having participated in ozone measurements and data management.

References

Beekmann, M., & Vautard, R. (2010). A modelling study of photochemical regimes over Europe: Robustness and variability. *Atmospheric Chemistry and Physics, 10*, 10067–10084. https://doi.org/10.5194/acp-10-10067-2010

Bénech, B., Ezcurra, A., Lothon, M., Said, F., Campistron, B., Lohou, F., & Durand, P. (2008). Constant volume balloons measurements in the urban Marseille and Fos-Berre industrial ozone plumes during ESCOMPTE experiment. *Atmospheric Environment, 42*, 5589–5601. https://doi.org/10.1016/j.atmosenv.2008.03.011

Businger, S., Chiswell, S. R., Ulmer, W. C., & Johnson, R. (1996). Balloons as a Lagrangian measurement platform for atmospheric research. *Journal of Geophysical Research, 101*, 4363–4376. https://doi.org/10.1029/95JD00559

Businger, S., Johnson, R., & Talbot, R. (2006). Scientific insights from four generations of Lagrangian smart balloons in atmospheric research. *Bulletin of the American Meteorological Society, 87*, 1539–1554. https://doi.org/10.1175/BAMS-87-11-1539

Cachier, H., Aulagnier, F., Sarda, R., Gautier, F., Masclet, P., Besombes, J.-L., Marchand, N., Despiau, S., Croci, D., Mallet, M., Laj, P., Marinoni, A., Deveau, P.-A., Roger, J.-C., Putaud, J.-P., Van Dingenen, R., Dell'Acqua, A., Viidanoja, J., Martins-Dos Santos, S., … Galy-Lacaux, C. (2005). Aerosol studies during the ESCOMPTE experiment: An overview. *Atmospheric Research, 74*, 547–563. https://doi.org/10.1016/j.atmosres.2004.06.013

Cadet, D. (1981). Low-level circulation during the 1979 Indian summer monsoon. *Advances in Space Research, 1*, 113–120. https://doi.org/10.1016/0273-1177(81)90054-5

Cadet, D., & Ovarlez, H. (1976). Low-level air flow circulation over the Arabian Sea during the summer monsoon as deduced from satellite-tracked superpressure balloons. Part I—Balloon trajectories. *Quarterly Journal of the Royal Meteorological Society, 102*, 805–816. https://doi.org/10.1002/qj.49710243410

Chazette, P., Totems, J., Ancellet, G., Pelon, J., & Sicard, M. (2016). Temporal consistency of lidar observations during aerosol transport events in the framework of the ChArMEx/ADRIMED

campaign at Minorca in June 2013. *Atmospheric Chemistry and Physics, 16*, 2863–2875. https://doi.org/10.5194/acp-16-2863-2016

Coll, I., Pinceloup, S., Perros, P. E., Laverdet, G., & Le Bras, G. (2005). 3D analysis of high ozone production rates observed during the ESCOMPTE campaign. *Atmospheric Research, 74*, 477–505. https://doi.org/10.1016/j.atmosres.2004.06.008

Cros, B., Durand, P., Cachier, H., Drobinski, P., Fréjafon, E., Kottmeier, C., Perros, P., Peuch, V.-H., Ponche, J., Robin, D., Saïd, F., Toupance, G., & Wortham, H. (2004). The ESCOMPTE program: An overview. *Atmospheric Research, 69*, 241–279. https://doi.org/10.1016/j.atmosres.2003.05.001

Di Biagio, C., Doppler, L., Gaimoz, C., Grand, N., Ancellet, G., Raut, J.-C., Beekmann, M., Borbon, A., Sartelet, K., Attié, J.-L., Ravetta, F., & Formenti, P. (2015). Continental pollution in the western Mediterranean basin: Vertical profiles of aerosol and trace gases measured over the sea during TRAQA 2012 and SAFMED 2013. *Atmospheric Chemistry and Physics, 15*, 9611–9630. https://doi.org/10.5194/acp-15-9611-2015

Doerenbecher, A., Basdevant, C., Drobinski, P., Durand, P., Fesquet, C., Bernard, F., Cocquerez, P., Verdier, N., & Vargas, A. (2016). Low atmosphere drifting balloons: Platforms for environment monitoring and forecast improvement. *Bulletin of the American Meteorological Society, 97*, 1583–1599. https://doi.org/10.1175/BAMS-D-14-00182.1

Duvel, J. P., Basdevant, C., Bellenger, H., Reverdin, G., Vargas, A., & Vialard, J. (2009). The Aeroclipper: A new device to explore convective systems and cyclones. *Bulletin of the American Meteorological Society, 90*, 63–72. https://doi.org/10.1175/2008BAMS2500.1

Ethé, C. (2001). Modélisation et simulation de trajectoires de ballons dérivants: Applications à l'étude de la circulation atmosphérique sur l'océan Indien, PhD dissertation, Univ. Paris-XI Orsay.

Ethé, C., Basdevant, C., Sadourny, R., Appu, K. S., Harenduprakash, L., Sarode, P. R., & Viswanathan, G. (2002). Air mass motion, temperature and humidity over the Arabian Sea and western Indian Ocean during the INDOEX intensive phase, as obtained from a set of superpressure drifting balloons. *Journal of Geophysical Research, 107*, 8023. https://doi.org/10.1029/2001JD001120

Gaudel, A., Cooper, O. R., Ancellet, G., Barret, B., Boynard, A., Burrows, J. P., Clerbaux, C., Coheur, P.-F., Cuesta, J., Cuevas, E., Doniki, S., Dufour, G., Ebojie, F., Foret, G., Garcia, O., Granados Muños, M. J., Hannigan, J. W., Hase, F., Huang, G., … Ziemke, J. (2018). Tropospheric ozone assessment report: Present-day distribution and trends of tropospheric ozone relevant to climate and global atmospheric chemistry model evaluation. *Elementa: Science of the Anthropocene, 6*, 39. https://doi.org/10.1525/elementa.291

Gerasopoulos, E., Kouvarakis, G., Vrekoussis, M., Donoussis, C., Mihalopoulos, N., & Kanakidou, M. (2006). Photochemical ozone production in the Eastern Mediterranean. *Atmospheric Environment, 40*, 3057–3069. https://doi.org/10.1016/j.atmosenv.2005.12.061

Gheusi, F., Durand, P., Verdier, N., Dulac, F., Attié, J.-L., Commun, P., Barret, B., Basdevant, C., Clenet, A., Derrien, S., Doerenbecher, A., El Amraoui, L., Fontaine, A., Hache, E., Jambert, C., Jaumouillé, E., Meyerfeld, Y., Roblou, L., & Tocquer, F. (2016). Adapted ECC ozonesonde for long-duration flights aboard boundary-layer pressurised balloons. *Atmospheric Measurement Techniques, 9*, 5811–5832. https://doi.org/10.5194/amt-9-5811-2016

Gros, V., & Zannoni, N. (2022). Total OH reactivity. In F. Dulac, S. Sauvage, & E. Hamonou (Eds.), *Atmospheric chemistry in the Mediterranean Region* (Vol. 2, From air pollutant sources to impacts). Springer, this volume. https://doi.org/10.1007/978-3-030-82385-6_7

Kirchner, F., Jeanneret, F., Clappier, A., Kruger, B., van den Bergh, B., van den Bergh, H., & Calpini, B. (2001). Total VOC reactivity in the planetary boundary layer: 2. A new indicator for determining the sensitivity of the ozone production to VOC and NO_x. *Journal of Geophysical Research, 106*, 3095–3110. https://doi.org/10.1029/2000jd900603

Kleinman, L. I. (2005). The dependence of tropospheric ozone production rate on ozone precursors. *Atmospheric Environment, 39*, 575–586. https://doi.org/10.1016/j.atmosenv.2004.08.047

Komhyr, W. (1969). Electrochemical concentration cells for gas analysis. *Annales de Geophysique, 25*, 203–210.

Lambert, D., Mallet, M., Ducrocq, V., Dulac, F., Gheusi, F., & Kalthoff, N. (2011). CORSiCA: A Mediterranean atmospheric and oceanographic observatory in Corsica within the framework of HyMeX and ChArMEx. *Advances in Geosciences, 26*, 125–131. https://doi.org/10.5194/adgeo-26-125-2011

Mallet, M., Dulac, F., Formenti, P., Nabat, P., Sciare, J., Roberts, G., Pelon, J., Ancellet, G., Tanré, D., Parol, F., Denjean, C., Brogniez, G., di Sarra, A., Alados-Arboledas, L., Arndt, J., Auriol, F., Blarel, L., Bourrianne, T., Chazette, P., … Zapf, P. (2016). Overview of the Chemistry-Aerosol Mediterranean Experiment/Aerosol Direct Radiative Forcing on the Mediterranean Climate (ChArMEx/ADRIMED) summer 2013 campaign. *Atmospheric Chemistry and Physics, 16*, 455–504. https://doi.org/10.5194/acp-16-455-2016

Monks, P. S., Archibald, A. T., Colette, A., Cooper, O., Coyle, M., Derwent, R., Fowler, D., Granier, C., Law, K. S., Mills, G. E., Stevenson, D. S., Tarasova, O., Thouret, V., von Schneidemesser, E., Sommariva, R., Wild, O., & Williams, M. L. (2015). Tropospheric ozone and its precursors from the urban to the global scale from air quality to short-lived climate forcer. *Atmospheric Chemistry and Physics, 15*, 8889–8973. https://doi.org/10.5194/acp-15-8889-2015

Renard, J.-B., Dulac, F., Durand, P., Bourgeois, Q., Denjean, C., Vignelles, D., Couté, B., Jeannot, M., Verdier, N., & Mallet, M. (2018). In situ measurements of desert dust particles above the western Mediterranean Sea with the balloon-borne Light Optical Aerosol Counter/sizer (LOAC) during the ChArMEx campaign of summer 2013. *Atmospheric Chemistry and Physics, 18*, 3677–3699. https://doi.org/10.5194/acp-18-3677-2018

Reverdin, G., & Sommeria, G. (1983). The dynamical structure of the planetary boundary layer over the Arabian Sea, as deduced from constant-level balloon trajectories. *Journal of the Atmospheric Sciences, 40*, 1435–1452. https://doi.org/10.1175/1520-0469(1983)040<1435:TDSOTP>2.0.CO;2

Richards, N. A. D., Arnold, S. R., Chipperfield, M. P., Miles, G., Rap, A., Siddans, R., Monks, S. A., & Hollaway, M. J. (2013). The Mediterranean summertime ozone maximum: Global emission sensitivities and radiative impacts. *Atmospheric Chemistry and Physics, 13*, 2331–2345. https://doi.org/10.5194/acp-13-2331-2013

Sicard, P., De Marco, A., Troussier, F., Renou, C., Vas, N., & Paoletti, E. (2013). Decrease in surface ozone concentrations at Mediterranean remote sites and increase in the cities. *Atmospheric Environment, 79*, 705–715. https://doi.org/10.1016/j.atmosenv.2013.07.042

Sinha, V., Williams, J., Diesch, J. M., Drewnick, F., Martinez, M., Harder, H., Regelin, E., Kubistin, D., Bozem, H., Hosaynali-Beygi, Z., Fischer, H., Andrés-Hernández, M. D., Kartal, D., Adame, J. A., & Lelieveld, J. (2012). Constraints on instantaneous ozone production rates and regimes during DOMINO derived using in-situ OH reactivity measurements. *Atmospheric Chemistry and Physics, 12*, 7269–7283. https://doi.org/10.5194/acp-12-7269-2012

Smit, H. G. J., & ASOPOS Panel. (2011). Quality assurance and quality control for ozonesonde measurements in GAW, Global Atmosphere Watch Rept. 201, World Meteorological Organization, Geneva, Switzerland, 92 pp. Available at: https://www.en-sci.com/wp-content/uploads/2018/05/GAW-Report-201-Quality-Assurance-and-Quality-Control-For-Ozonesonde-Measurements-In-GAW.pdf. Last access: 31 January 2022.

Stull, R. B. (1988). *An introduction to boundary layer meteorology* (670 pp). Kluwer Academic Publishers. https://doi.org/10.1007/978-94-009-3027-8.

Williams, J., Custer, T., Riede, H., Sander, R., Jöckel, P., Hoor, P., Pozzer, A., Wong-Zehnpfennig, S., Hosaynali Beygi, Z., Fischer, H., Gros, V., Colomb, A., Bonsang, B., Yassaa, N., Peeken, I., Atlas, E. L., Waluda, C. M., Van Aardenne, J. A., & Lelieveld, J. (2010). Assessing the effect of marine isoprene and ship emissions on ozone, using modelling and measurements from the South Atlantic Ocean. *Environment and Chemistry, 7*, 171–182. https://doi.org/10.1071/EN09154

Yan, Y., Pozzer, A., Ojha, N., Lin, J., & Lelieveld, J. (2018). Analysis of European ozone trends in the period 1995–2014. *Atmospheric Chemistry and Physics, 18*, 5589–5605. https://doi.org/10.5194/acp-18-5589-2018

Young, P. J., Archibald, A. T., Bowman, K. W., Lamarque, J.-F., Naik, V., Stevenson, D. S., Tilmes, S., Voulgarakis, A., Wild, O., Bergmann, D., Cameron-Smith, P., Cionni, I., Collins, W. J., Dalsøren, S. B., Doherty, R. M., Eyring, V., Faluvegi, G., Horowitz, L. W., Josse, B., … Zeng, G. (2013). Pre-industrial to end 21st century projections of tropospheric ozone from the Atmospheric Chemistry and Climate Model Intercomparison Project (ACCMIP). *Atmospheric Chemistry and Physics, 13*, 2063–2090. https://doi.org/10.5194/acp-13-2063-2013

Nucleation in the Mediterranean Atmosphere

Karine Sellegri and Clémence Rose

Contents

Abstract Among the formation pathways of secondary aerosols, nucleation is the process responsible for the formation of new nanoparticle clusters (as opposed to the process of condensation onto pre-existing particles), observed in a variety of environments. The processes of nucleation and early growth lead to the occurrence of new particle formation (NPF) in the atmosphere. NPF has frequently been observed in the Mediterranean basin, and a full overview of measurements of this process over the Mediterranean is given. The nature of the precursors to new particles in the marine environment is however an open question, which is addressed by correlative studies between NPF burst and enhanced concentrations of potential precursors. NPF events contribute to the production of cloud condensation nuclei

*Chapter reviewed by **Michael Pikridas** (Climate and Atmosphere Research Center (CARE-C), The Cyprus Institute, Aglantzia, Nicosia, Cyprus), and by **Rima Baalbaki** (University of Helsinki, Helsinki, Finland), as part of the book Part VI Recent Progress on Chemical Processes also reviewed by **Andrea Pozzer** (Max Planck Institute for Chemistry, Mainz, Germany)*

K. Sellegri (✉) · C. Rose
Université Clermont Auvergne, CNRS, Laboratoire de Météorologie Physique UMR 6016 (LaMP), Clermont-Ferrand, France
e-mail: K.Sellegri@opgc.univ-bpclermont.fr

F. Dulac et al. (eds.), *Atmospheric Chemistry in the Mediterranean Region*,
https://doi.org/10.1007/978-3-030-82385-6_9

(CCN), but competition effects for available water vapour need to be taken into account and limit the increase in the cloud droplet number (CDN) due to Mediterranean NPF events.

1 Introduction

Nucleation is a process responsible for the formation of new nanoparticle clusters from gas-phase precursors, observed in a variety of environments. Triggered by photochemical processes, oxidized lower volatility products are formed, of which some have the properties of nucleating into new particulate clusters. There are relatively few precursor species for nucleation as this requires that they have an extremely low saturation vapour. The species most commonly considered to trigger nucleation is sulphuric acid (Spracklen et al., 2008), although it was more recently shown that ammonia (Dunne et al., 2016), iodide (O'Dowd et al. 2002; Sipilä et al., 2016) or biogenic organic compounds (Kirkby et al., 2016; Rose et al., 2018) are also involved. Once particle clusters are formed by nucleation, they may be scavenged onto pre-existing particles by coagulation if they do not rapidly grow to larger sizes by condensation of compounds that may be of different nature than the nucleating ones. Thus, the early growth of newly formed clusters is also an important process. The processes of nucleation and early growth lead to the occurrence of new particle formation (NPF) in the atmosphere.

2 Overview of Observations of NPF in the Mediterranean Basin

NPF has frequently been observed in the Mediterranean basin. At Finokalia, Crete, NPF events were detected with an average frequency close to 30% (Pikridas et al., 2012; Berland et al., 2017; Kalivitis et al., 2019). The highest frequency of NPF events was detected during late winter/spring time (as usually observed at continental stations; Manninen et al., 2010), reaching during this season close to 50% (Pikridas et al., 2012; Berland et al., 2017; Kalivitis et al., 2019). In Corsica, measurements performed at Ersa in the framework of the ChArMEx project show the same seasonal variation as the one observed at Finokalia (35.335°N, 25.670°E) in Crete for the NPF events frequency (Berland et al., 2017). In Cyprus, new particle formation events, also analysed in the framework of ChArMEx, occurred with a 66% frequency over a 3-week period in spring at the CAO regional background site (35.039°N, 33.058°E; Debevec et al., 2018). The majority of the NPF events started from the nanometric size (2 nm), indicating that nucleation occurred locally. Newly formed clusters then showed a clear and continuous growth to larger sizes,

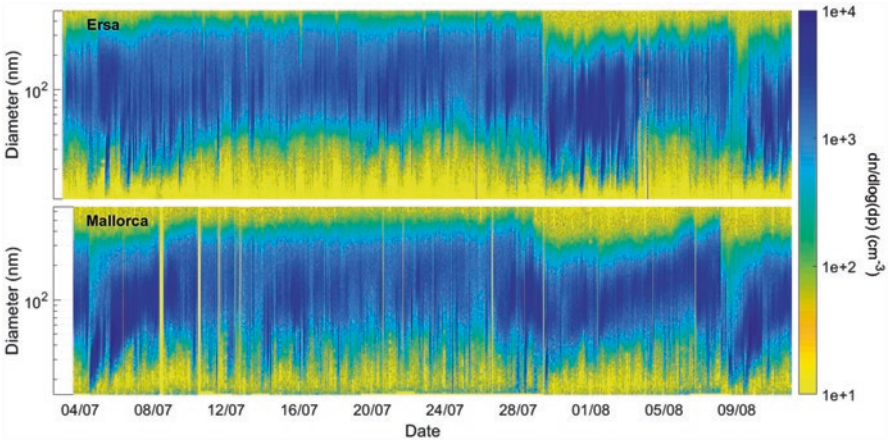

Fig. 1 Number size distribution of particles measured simultaneously in Corsica (Ersa) and Mallorca in July 2013 and showing that NPF occurs at the two sites during the same period. (Adapted from Berland et al., 2017)

indicating nucleation also occurred at the regional scale. High new particle number concentrations were detected, exceeding 3 10^4 cm^{-3} on two thirds of the detected events (Sciare et al., "personal communication"). New particle formation rates of 10 nm particles observed in the Mediterranean area (seasonal medians 0.4–0.6 cm^{-3} s^{-1}; Kalivitis et al., 2019) are, however, at the lower end of NPF rates reported in the literature for coastal sites of the Baltic Sea and Atlantic and Pacific Oceans (0.4–1.5 cm^{-3} s^{-1}; Kulmala et al., 2004), but particle diameter growth rates are similar to those measured in other marine environments (2.6–6.8 nm h^{-1} at Mediterranean sites, Kalivitis et al., 2019, vs 5.4–6.7 nm h^{-1} for Atlantic Ocean and Baltic Sea coastal sites, Manninen et al., 2010). As often reported in the literature, the seasonal variation of nucleation rates has a different pattern than the one observed for the newly formed particles' growth rates, indicating different precursors to each of these NPF successive steps. A slightly decreasing trend in the new particle growth rates has been reported at Finokalia over the years 2008–2015 and attributed to a decrease in anthropogenic SO_2 concentrations in the Eastern Mediterranean sector (Kalivitis et al., 2019). In the work by Berland et al. (2017), a statistical analysis on ChArMEx and other data was performed on NPF occurrence and characteristics at three Mediterranean sites (Mallorca, Corsica and Crete) during the same period of several months. The study revealed that NPF is observed simultaneously at all stations, confirming the spatial extent of the nucleation and growth process over several hundred kilometres (Fig. 1).

Airborne measurements performed above the Mediterranean Sea between 500 and 3000 m above sea level revealed contrasting situations, with particle clusters either formed in the marine boundary layer, or initially nucleated above the continent or in the free troposphere (FT) and further transported above the sea (Berland

et al., 2017). The large spatial extent of NPF events over the Mediterranean Sea, independent of the air mass origin, indicates the potential contribution of marine precursors to nucleation.

3 Nucleation from Marine Sources?

Despite their importance, our ability to correctly describe and numerically simulate marine aerosols is still limited by the poor understanding of the link between aerosol formation/evolution at the air-sea interface and the properties of the seawater below. Mesoscale models are unable to reproduce the number concentrations of aerosol particles in the marine boundary layer and their impact on cloud properties (Merikanto et al., 2009), and a large uncertainty in the projection of future climate can be attributed to a lack of knowledge on marine aerosols (Carslaw et al., 2013). Tidal coastal areas display one of the highest nucleation rates (Kulmala et al., 2004) when macroalgae are exposed to ambient air during low-tide conditions (O'Dowd et al. 2002). However, in the open marine boundary layer, nucleation has never been directly evidenced, although it has been strongly suspected from measurements of grown nucleated particles at 20 nm in pure marine air masses of the Atlantic Ocean (O'Dowd et al., 2010). In the Mediterranean area, the marine aerosol emission pathways may be different from other parts of the world, due to the specific temperature range and oligotrophic properties of the seawater (Moutin et al., 2012) and due to high radiation and ozone levels in the atmosphere (Berresheim et al., 2003) that lead to an intense photochemical activity over a large period of the year. Airborne measurements within HYMEX, a sister project of ChArMEx under the MISTRALS programme umbrella (https://programmes.insu.cnrs.fr/en/mistrals-en/), showed high levels of nanoparticles in the 5–10 nm size range above the Mediterranean Sea, particularly at altitudes between 1 and 3 km (Fig. 2; Rose et al., 2015).

The nature of the precursors to new particles in the marine environment remains an open question. The major constituents of secondary marine aerosol are considered the nss-sulphates and methane sulfonic acid (MSA), but also iodine and organic species have been proposed as possible secondary aerosol precursors (O'Dowd et al., 2002; O'Dowd and De Leeuw 2007). In tidal coastal areas where NPF have been observed, iodine species released by macroalgae were identified as the main precursor to new particles through indirect measurements (O'Dowd et al. 2002; McFiggans et al., 2004; Sellegri et al., 2005) and direct measurements (Allan et al., 2015). Over open oceans, the link between phytoplankton and iodine emissions is still unclear (Thorenz et al., 2014), and dimethyl sulfide (DMS) is commonly proposed as the main species driving secondary aerosol number production and influencing the number of CCN since the early 1990s (Charlson et al., 1987; Fitzgerald, 1991). Thus, DMS is the one species still implemented in present global models (Bopp et al., 2003; Boucher et al., 2003), even though it is recognized that other CCN sources are required to explain observations (Sorooshian et al., 2009; Quinn & Bates, 2011). However, the capacity of DMS to form new particles has only been

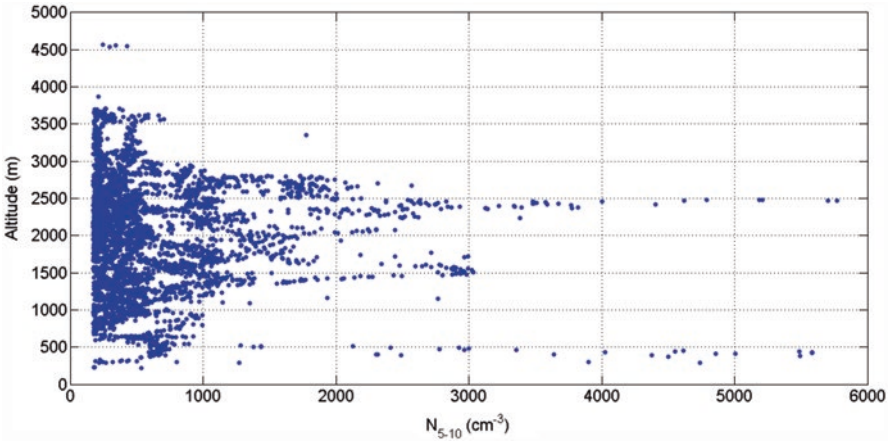

Fig. 2 Particle concentration in the size range 5–10 nm as a function of altitude observed from airborne measurements above the Mediterranean Sea in the frame of the HYMEX project. (After data from Rose et al., 2015)

demonstrated from recent laboratory measurements (Chen et al. 2017; Li et al., 2018; Wen et al., 2019), but not from ambient measurements.

It is difficult to detangle different precursor sources from ambient measurements. Hypothesis on the aerosol precursor has to be driven from indirect evidences such as covariations between precursors to oxidized, low volatility species and nanoparticle concentrations. Using this method, Debevec et al. (2018) found that NPF events detected at the Cyprus station within ChArMEx could not be explained by sulphuric acid concentrations. On some occasions they were strongly correlated to biogenic organic precursors (isoprene and monoterpene oxidation products), but on other occasions neither the vegetation nor anthropogenic sources could explain the high nucleation rates. In the case of Crete, Pikridas et al. (2012) as well concluded that nucleation was not limited by the availability of SO_2 alone, as nucleation events did not systematically take place during periods with high sulphuric acid concentrations. Other measurements, performed on the Island of Porquerolles in 2007, show that NPF events are favoured by the sea breeze/land breeze local dynamics that bring land-originating compounds over the sea during the night, where these compounds are oxidized to nucleate during the day before being transported back to the island (Piazzola et al., 2012). In coastal areas, a mixture of compounds from different origins likely coexists that may induce an enhanced production of condensable vapours. In the framework of the SAM (Sources of Aerosols in the Mediterranean) project as part of the MISTRALS/ChArMEx and MERMEX projects, mesocosms enclosing both seawater and a portion of the atmosphere above have been used to derive direct fluxes of nanoparticles formed from seawater emissions. These experiments were performed on seawater from the bay of Calvi, Corsica. Results showed that (1) new particle clusters can be formed with a high formation rate from marine

emissions in non-tidal waters in a confined volume; (2) cluster concentrations correlate with iodine compounds that have condensed onto larger particles; (3) iodine concentrations in the particulate phase correlate with phytoplanktonic species; (4) amines of biological origin are linked to the early growth of newly formed clusters; and (5) no correlation was found between DMS and MSA or a proxy of sulphuric acid and cluster concentrations (Sellegri et al., 2016). Over the Mediterranean Sea, it is possible that the high level of ozone promotes the formation of new particle clusters from iodine oxides rather than from DMS oxidation products, which might be a specificity of the region compared to other oceanic environments.

In Lampedusa, one of the sites with intensive measurements during the ChArMEx project, located in the far southeastern part of the Mediterranean Sea (36°4′24″ N, 14°13′9″ E), hence less prone to coastal anthropogenic activities from the northern coast of the Mediterranean Sea, NPF events were detected only in air masses originated from the Atlantic Ocean (either "Mistral" cases or "Atlantic" cases) (Mallet et al., 2019). The most pronounced event was a night-time event, hence not triggered by photochemical processes, and it had a signature of MSA in the accumulation mode suggesting possible condensation from marine biogenic vapours.

4 Impact of NPF on Cloud Condensation Nuclei (CCN) and Cloud Droplet Number (CDN)

The growth of newly formed particles to size ranges relevant for the formation of cloud droplets (i.e. about 100 nm for a supersaturation of 0.2%) was investigated at Finokalia (Kalivitis et al., 2015; Kalkavouras et al., 2019) and Cyprus (Gong et al., 2019). NPF events contribute to the production of cloud condensation nuclei (CCN) on the day NPF occurs (Gong et al., 2019), but also when new particles formed the previous day are grown to CCN sizes (Kalivitis et al., 2015). The average contribution of NPF to CCN concentrations is 29% at 0.1% supersaturation, but this contribution varies according to the level of pre-existing particles. Under clean conditions that represent 40% of NPF event days, the contribution of NPF particles to CCN concentration at 0.1% supersaturation reaches 40% of CCN concentrations (Kalkavouras et al., 2019). However, an impact on CCN does not necessarily translate into a similar impact on cloud droplet numbers (CDNs). In a CCN chamber, water vapour availability is infinite, which is not the case in a real cloud. In real clouds, there are competition effects for available water vapour. Due to these competing effects and to the low water supersaturations reached in Mediterranean clouds, NPF-issued particles would contribute to only 7–13% of the totally formed cloud droplet number.

5 Conclusion and Recommendations

Nucleation and growth of new particles were found to be ubiquitous in the Mediterranean atmosphere, from coastal sites to the open Mediterranean Sea atmospheric boundary layer and free troposphere. However, the identification of the exact chemical precursors to this process is missing. The measurement of the concentration of nanometric cluster particles, simultaneously with potential precursor gases of low volatility, is a prerequisite to understand the contribution from the different sources (marine, anthropogenic, vegetation, or a combined effect of different sources) to the process of nucleation. These measurements should be performed both in the ambient atmosphere and in semi-controlled environments representative of each source type. There has also been a lack of modelling studies dedicated to the study of nucleation in the Mediterranean atmosphere that would have helped in testing the different hypotheses for potential nucleating species (H_2SO_4 vs iodine oxides, for instance). For the purpose of testing the nucleation process, mesoscale chemical transport models should include an aerosol dynamical module that deals with the evolution of the aerosol population number concentration, while most models solve transfer processes by mass. At last, for documenting the evolution of new particle formation frequency and intensity in the Mediterranean atmosphere in the future years, it is necessary to rely on background monitoring research stations, such as the Cyprus Atmospheric Observatory (CAO; https://emme-care.cyi.ac.cy/cyprus-atmospheric-observatory-cao/, last access 22 July 2022) in Cyprus and Finokalia Atmospheric Observatory (FKL; https://deims.org/d16cc035-054d-4b0e-9e19-6e9ec10aecd0, last access 22 July 2022) in Crete.

References

Allan, J. D., Williams, P. I., Najera, J., Whitehead, J. D., Flynn, M. J., Taylor, J. W., Liu, D., Darbyshire, E., Carpenter, L. J., Chance, R., Andrews, S. J., Hackenberg, S. C., & McFiggans, G. (2015). Iodine observed in new particle formation events in the Arctic atmosphere during ACCACIA. *Atmospheric Chemistry and Physics, 15*, 5599–5609. https://doi.org/10.5194/acp-15-5599-2015

Berresheim, H., Plass-Dülmer, C., Elste, T., Mihalopoulos, N., & Rohrer, F. (2003). OH in the coastal boundary layer of Crete during MINOS: Measurements and relationship with ozone photolysis. *Atmospheric Chemistry and Physics, 3*, 639–649. https://doi.org/10.5194/acp-3-639-2003

Berland, K., Rose, C., Pey, J., Culot, A., Freney, E., Kalivitis, N., Kouvaratis, G., Cerro, J., Mallet, M., Sartelet, K., Beekmann, M., Bourriane, T., Roberts, G., Marchand, N., Mihalopoulos, N., & Sellegri, K. (2017). Spatial extent of new particle formation events over the Mediterranean Basin from multiple ground-based and airborne measurements. *Atmospheric Chemistry and Physics, 17*, 9567–9583. https://doi.org/10.5194/acp-17-9567-2017

Bopp, L., Aumont, O., Belviso, S., & Monfray, P. (2003). Potential impact of climate change on marine dimethyl sulfide emissions. *Tellus B, 55*, 11–22. https://doi.org/10.3402/tellusb.v55i1.16359

Boucher, O., Moulin, C., Belviso, S., Aumont, O., Bopp, L., Cosme, E., von Kuhlmann, R., Lawrence, M. G., Pham, M., Reddy, M. S., Sciare, J., & Venkataraman, C. (2003). DMS atmospheric concentrations and sulphate aerosol indirect radiative forcing: A sensitivity study to the DMS source representation and oxidation. *Atmospheric Chemistry and Physics, 3*, 49–65. https://doi.org/10.5194/acp-3-49-2003

Carslaw, K. S., Lee, L. A., Reddington, C. L., Pringle, K. J., Rap, A., Forster, P. M., Mann, G. W., Spracklen, D. V., Woodhouse, M. T., Regayre, L. A., & Pierce, J. R. (2013). Large contribution of natural aerosols to uncertainty in indirect forcing. *Nature, 503*, 67–71. https://doi.org/10.1038/nature12674

Charlson, R. J., Lovelock, J. E., Andreae, M. O., & Warren, S. G. (1987). Oceanic phytoplankton, atmospheric sulphur, cloud albedo and climate. *Nature, 326*, 655–661. https://doi.org/10.1038/326655a0

Chen, H., & Finlayson-Pitts, B. J. (2017). New particle formation from methanesulfonic acid and amines/ammonia as a function of temperature. *Environmental Science & Technology, 51*, 243–252. https://doi.org/10.1021/acs.est.6b04173

Debevec, C., Sauvage, S., Gros, V., Sellegri, K., Sciare, J., Pikridas, M., Stavroulas, I., Leonardis, T., Gaudion, V., Depelchin, L., Fronval, I., Sarda-Esteve, R., Baisnee, D., Bonsang, B., Savvides, C., Vrekoussis, M., & Locoge, N. (2018). Driving parameters of biogenic volatile organic compounds and consequences on new particle formation observed at an eastern Mediterranean background site. *Atmospheric Chemistry and Physics, 18*, 14297–14325. https://doi.org/10.5194/acp-18-14297-2018

Dunne, E. M., Gordon, H., Kürten, A., Almeida, J., Duplissy, J., Williamson, C., Ortega, I. K., Pringle, K. J., Adamov, A., Baltensperger, U., Barmet, P., Benduhn, F., Bianchi, F., Breitenlechner, M., Clarke, A., Curtius, J., Dommen, J., Donahue, N. M., Ehrhart, S., … Carslaw, K. S. (2016). Global atmospheric particle formation from CERN CLOUD measurements. *Science, 354*, 1119–1124. https://doi.org/10.1126/science.aaf2649

Fitzgerald, J. W. (1991). Marine aerosols: A review. *Atmospheric Environment, 25*, 533–545. https://doi.org/10.1016/0960-1686(91)90050-H

Gong, X., Wex, H., Müller, T., Wiedensohler, A., Höhler, K., Kandler, K., Ma, N., Dietel, B., Schiebel, T., Möhler, O., & Stratmann, F. (2019). Characterization of aerosol properties at Cyprus, focusing on cloud condensation nuclei and ice-nucleating particles. *Atmospheric Chemistry and Physics, 19*, 10883–10900. https://doi.org/10.5194/acp-19-10883-2019

Kalivitis, N., Kerminen, V.-M., Kouvarakis, G., Stavroulas, I., Bougiatioti, A., Nenes, A., Manninen, H. E., Petäjä, T., Kulmala, M., & Mihalopoulos, N. (2015). Atmospheric new particle formation as a source of CCN in the eastern Mediterranean marine boundary layer. *Atmospheric Chemistry and Physics, 15*, 9203–9215. https://doi.org/10.5194/acp-15-9203-2015

Kalivitis, N., Kerminen, V.-M., Kouvarakis, G., Stavroulas, I., Tzitzikalaki, E., Kalkavouras, P., Daskalakis, N., Myriokefalitakis, S., Bougiatioti, A., Manninen, H. E., Roldin, P., Petäjä, T., Boy, M., Kulmala, M., Kanakidou, M., & Mihalopoulos, N. (2019). Formation and growth of atmospheric nanoparticles in the eastern Mediterranean: Results from long-term measurements and process simulations. *Atmospheric Chemistry and Physics, 19*, 2671–2686. https://doi.org/10.5194/acp-19-2671-2019

Kalkavouras, P., Bougiatioti, A., Kalivitis, N., Stavroulas, I., Tombrou, M., Nenes, A., & Mihalopoulos, N. (2019). Regional new particle formation as modulators of cloud condensation nuclei and cloud droplet number in the eastern Mediterranean. *Atmospheric Chemistry and Physics, 19*, 6185–6203. https://doi.org/10.5194/acp-19-6185-2019

Kirkby, J., Duplissy, J., Sengupta, K., Frege, C., Gordon, H., Williamson, C., Heinritzi, M., Simon, M., Yan, C., Almeida, J., Tröstl, J., Nieminen, T., Ortega, I. K., Wagner, R., Adamov, A., Amorim, A., Bernhammer, A.-K., Bianchi, F., Breitenlechner, M., … Curtius, J. (2016). Ion-induced nucleation of pure biogenic particles. *Nature, 533*, 521–526. https://doi.org/10.1038/nature17953

Kulmala, M., Vehkamäki, H., Petäjä, T., Dal Maso, M., Lauri, A., Kerminen, V.-M., Birmili, W., & McMurry, P. H. (2004). Formation and growth rates of ultrafine atmospheric particles: A

review of observations. *Journal of Aerosol Science, 35*, 143–176. https://doi.org/10.1016/j.jaerosci.2003.10.003

Li, H., Zhang, X., Zhong, J., Liu, L., Zhang, H., Chen, F., Li, Z., Li, Q., & Ge, M. (2018). The role of hydroxymethanesulfonic acid in the initial stage of new particle formation. *Atmospheric Environment, 189*, 244–251. https://doi.org/10.1016/j.atmosenv.2018.07.003

Mallet, M. D., D'Anna, B., Même, A., Bove, M. C., Cassola, F., Pace, G., Desboeufs, K., Di Biagio, C., Doussin, J.-F., Maille, M., Massabò, D., Sciare, J., Zapf, P., di Sarra, A. G., & Formenti, P. (2019). Summertime surface PM_1 aerosol composition and size by source region at the Lampedusa island in the central Mediterranean Sea. *Atmospheric Chemistry and Physics, 19*, 11123–11142. https://doi.org/10.5194/acp-19-11123-2019

Manninen, H. E., Nieminen, T., Asmi, E., Gagné, S., Häkkinen, S., Lehtipalo, K., Aalto, P., Vana, M., Mirme, A., Mirme, S., Hõrrak, U., Plass-Dülmer, C., Stange, G., Kiss, G., Hoffer, A., Tör'o, N., Moerman, M., Henzing, B., de Leeuw, G., … Kulmala, M. (2010). EUCAARI ion spectrometer measurements at 12 European sites – Analysis of new particle formation events. *Atmospheric Chemistry and Physics, 10*, 7907–7927. https://doi.org/10.5194/acp-10-7907-2010

McFiggans, G., Coe, H., Burgess, R., Allan, J., Cubison, M., Alfarra, M. R., Saunders, R., Saiz-Lopez, A., Plane, J. M. C., Wevill, D., Carpenter, L., Rickard, A. R., & Monks, P. S. (2004). Direct evidence for coastal iodine particles from Laminaria macroalgae – Linkage to emissions of molecular iodine. *Atmospheric Chemistry and Physics, 4*, 701–713. https://doi.org/10.5194/acp-4-701-2004

Merikanto, J., Spracklen, D. V., Mann, G. W., Pickering, S. J., & Carslaw, K. S. (2009). Impact of nucleation on global CCN. *Atmospheric Chemistry and Physics, 9*, 8601–8616. https://doi.org/10.5194/acp-9-8601-2009

Moutin, T., Van Wambeke, F., & Prieur, L. (2012). Introduction to the Biogeochemistry from the Oligotrophic to the Ultraoligotrophic Mediterranean (BOUM) experiment. *Biogeosciences, 9*, 3817–3825. https://doi.org/10.5194/bg-9-3817-2012

O'Dowd, C. D., & De Leeuw, G. (2007). Marine aerosol production: a review of the current knowledge. Philosophical Transactions of the Royal Society A: *Mathematical, Physical and Engineering Sciences, 365*, 1753-1774. https://doi.org/10.1098/rsta.2007.2043

O'Dowd, C. D., Jimenez, J. L., Bahreini, R., Flagan, R. C., Seinfeld, J. H., Hämeri, K., Pirjola, L., Kulmala, M., Jennings, S. G., & Hoffmann, T. (2002). Marine aerosol formation from biogenic iodine emissions. *Nature, 417*, 632–636. https://doi.org/10.1038/nature00775

O'Dowd, C. D., Monahan, C., & Dall'Osto, M. (2010). On the occurrence of open ocean particle production and growth events. *Geophysical Research Letters, 37*, L19805. https://doi.org/10.1029/2010GL044679

Piazzola, J., Sellegri, K., Bourcier, L., Mallet, M., Tedeschi, G., & Missamou, T. (2012). Physicochemical characteristics of aerosols measured in the spring time in the Mediterranean coastal zone. *Atmospheric Environment, 54*, 545–556. https://doi.org/10.1016/j.atmosenv.2012.02.057

Pikridas, M., Riipinen, I., Hildebrandt, L., Kostenidou, E., Manninen, H., Mihalopoulos, N., Kalivitis, N., Burkhart, J. F., Stohl, A., Kulmala, M., & Pandis, S. N. (2012). New particle formation at a remote site in the eastern Mediterranean. *Journal of Geophysical Research, 117*, D12205. https://doi.org/10.1029/2012JD017570

Quinn, P., & Bates, T. (2011). The case against climate regulation via oceanic phytoplankton sulphur emissions. *Nature, 480*, 51–56. https://doi.org/10.1038/nature10580

Rose, C., Sellegri, K., Freney, E., Dupuy, R., Colomb, A., Pichon, J.-M., Ribeiro, M., Bourianne, T., Burnet, F., & Schwarzenboeck, A. (2015). Airborne measurements of new particle formation in the free troposphere above the Mediterranean Sea during the HYMEX campaign. *Atmospheric Chemistry and Physics, 15*, 10203–10218. https://doi.org/10.5194/acp-15-10203-2015

Rose, C., Zha, Q., Dada, L., Yan, C., Lehtipalo, K., Junninen, H., Buenrostro Mazon, S., Jokinen, T., Sarnela, N., Sippilä, M., Petäjä, T., Verminen, V.-M., Bianchi, F., & Kulmala, M. (2018). Observations of biogenic ion-induced cluster formation in the atmosphere. *Science Advances, 4*, eaar5218. https://doi.org/10.1126/sciadv.aar5218

Sellegri, K., Yoon, Y. J., Jennings, S. G., O'Dowd, C. D., Pirjola, L., Cautenet, S., Chen, H., & Hoffmann, T. (2005). Quantification of coastal new ultra-fine particles formation from in situ and chamber measurements during the BIOFLUX campaign. *Environment and Chemistry, 2*, 260–270. https://doi.org/10.1071/EN05074

Sellegri, K., Pey, J., Rose, C., Culot, A., DeWitt, H. L., Mas, S., Schwier, A. N., Temime-Roussel, B., Charriere, B., Saiz-Lopez, A., Mahajan, A. S., Parin, D., Kukui, A., Sempere, R., D'anna, B., & Marchand, N. (2016). Evidence of atmospheric nanoparticle formation from emissions of marine microorganisms. *Geophysical Research Letters, 43*, 6596–6603. https://doi.org/10.1002/2016GL069389

Sipilä, M., Sarnela, N., Jokinen, T., Henshel, H., Junninen, H., Kontkanen, J., Richters, S., Kangasluoma, J., Franchin, A., Peräkylä, O., Rissanen, M. P., Ehn, M., Vekhamäki, H., Kurten, T., Berndt, T., Petäjä, T., Worsnop, D., Ceburnis, D., Kerminen, V.-M., … O'Dowd, C. (2016). Molecular-scale evidence of aerosol particle formation via sequential addition of HIO_3. *Nature, 537*, 532–534. https://doi.org/10.1038/nature19314

Sorooshian, A., Padró, L. T., Nenes, A., Feingold, G., McComiskey, A., Hersey, S. P., Gates, H., Jonsson, H. H., Miller, S. D., Stephens, G. L., Flagan, R. C., & Seinfeld, J. H. (2009). On the link between ocean biota emissions, aerosol, and maritime clouds: Airborne, ground, and satellite measurements off the coast of California. *Global Biogeochemical Cycles, 23*, GB40007. https://doi.org/10.1029/2009GB003464

Spracklen, D. V., Carslaw, K. S., Kulmala, M., Kerminen, V.-M., Sihto, S.-L., Riipinen, I., Merikanto, J., Mann, G. W., Chipperfield, M. P., Wiedensohler, A., Birmili, W., & Lihavainen, H. (2008). Contribution of particle formation to global cloud condensation nuclei concentrations. Geophysical Research Letters, 35, L06808. https://doi.org/10.1029/2007GL033038

Thorenz, U. R., Carpenter, L. J., Huang, R.-J., Kundel, M., Bosle, J., & Hoffmann, T. (2014). Emission of iodine-containing volatiles by selected microalgae species. *Atmospheric Chemistry and Physics, 14*, 13327–13335. https://doi.org/10.5194/acp-14-13327-2014

Wen, H., Wang, C.-Y., Wang, Z.-Q., Hou, X.-F., Han, Y.-J., Liu, Y.-R., Jiang, S., Huang, T., & Huang, W. (2019). Formation of atmospheric molecular clusters consisting of methanesulfonic acid and sulfuric acid: Insights from flow tube experiments and cluster dynamics simulations. *Atmospheric Environment, 199*, 380–390. https://doi.org/10.1016/j.atmosenv.2018.11.043

Secondary Aerosol Formation and Their Modeling

Karine Sartelet

Contents

Abstract Measurement studies using particle into liquid sampler coupled with an ion chromatograph (PILS-IC), aerosol mass spectrometer (AMS), or aerosol chemical speciation monitor (ACSM) show a large fraction of organics and sulfate in fine particles in summer over the western and eastern Mediterranean. Different formation pathways of organic aerosol (OA), from anthropogenic and biogenic precursors of continental or marine origin, are discussed and quantified, using observations and modeling. The contribution of specific formation pathways, such as autoxidation of biogenic VOC precursors, is estimated. OA properties and their seasonal variation, in particular oxidation state and related solubility, are discussed. The temperature sensitivity of secondary OA formation differs for different aerosol modeling schemes, which is important to take into account when predicting aerosol in a future warmer climate. Over the Mediterranean, sea salt is an important fraction of the coarse aerosol and interacts with the soluble organic aerosol.

Chapter reviewed by ***Didier Hauglustaine*** *(Laboratoire des Sciences du Climat et de l'Environnement (LSCE), CEA-CNRS-UVSQ, IPSL, Université Paris-Saclay, Gif-sur-Yvette, France), as part of the book Part VI Recent Progress on Chemical Processes also reviewed by* ***Andrea Pozzer*** *(Max Planck Institute for Chemistry, Mainz, Germany)*

K. Sartelet (✉)
Centre d'Enseignement et de Recherche en Environnement Atmosphérique (CEREA), École des Ponts ParisTech, EDF R&D, Marne-la-Vallée, France
e-mail: karine.sartelet@enpc.fr

F. Dulac et al. (eds.), *Atmospheric Chemistry in the Mediterranean Region*,
https://doi.org/10.1007/978-3-030-82385-6_10

1 Introduction

The Mediterranean region is considered as one of the prominent regions that could be detrimentally impacted by climate change with an increase in temperature and in formation of secondary aerosols (Cholakian et al., 2019a). Depending on the atmospheric circulation, natural aerosols (desert dust and sea salt) are dominant compounds of PM_{10} concentrations over the western Mediterranean (Menut et al., 2015; Rea et al., 2015; Di Biagio et al., 2016; Schepanski et al., 2016; Guth et al., 2018), which are also influenced by sporadic wildfires (e.g., Pace et al., 2003; Ancellet et al., 2016). Fine particles (PM_1 and $PM_{2.5}$) are dominated by organics (compounds formed from the atmospheric transformation of organic species) and inorganics (mostly sulfate but also nitrate, ammonium, sodium, and chloride) both over the western and the eastern Mediterranean, as shown by PILS-IC, ACSM, and AMS measurements. ACSM and AMS instruments measure the real-time chemical composition and mass loading of non-refractory aerosol compounds (sulfate, nitrate, ammonium, chloride, and organic compounds) of particles with aerodynamic diameters typically between 70 and 1000 nm (PM_1). A large fraction of these inorganic and organic aerosols (OA) is secondary (Stavroulas et al., 2019), with influences from different sources (biogenic, marine, anthropogenic: traffic, residential heating, agriculture, etc.). These fine particles affect both climate and human health. They influence the direct radiation budget mostly by scattering sunlight resulting in negative direct radiative forcing. Moreover, they can act as cloud condensation nuclei and hence modify cloud microphysical properties and lifetime. Considering health effects, oxidative stress, which is induced by the generation of reactive oxygen species (ROS), is suggested as one pathway of OA toxicity. The oxidative potential may differ for the different organic precursors. The different measurement stations where campaigns were based or long-term observations performed are displayed in Fig. 1.

Fig. 1 Map of the ground-based stations involved in campaigns mentioned in this chapter

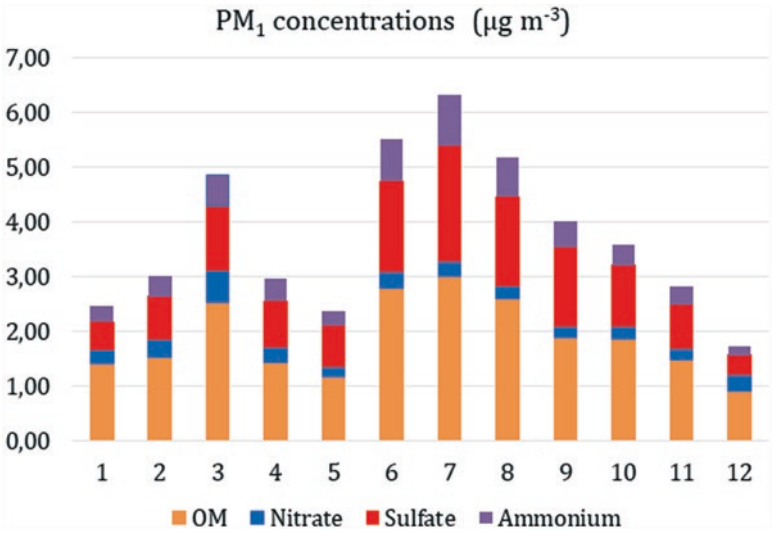

Fig. 2 Submicron aerosol composition at Ersa obtained from ACSM measurements between June 2012 and July 2014. (Data courtesy of Jean Sciare)

In summer, over the western Mediterranean, several measurement studies using ACSM or AMS stressed the high fraction of organics and sulfate in fine particles, for instance, at Montseny (Minguillón et al., 2015) and at Lampedusa (Mallet et al., 2019). Measurements performed in the framework of ChArMEx (Chemistry-Aerosol Mediterranean Experiment) at Ersa (Corsica, France) are shown in Fig. 2. Organics and sulfate represent the two main fractions of the fine aerosols observed (Arndt et al., 2017; Chrit et al., 2018a; Mallet et al., 2019), with higher concentrations during summer time. Although the fractions of organic matter (OM) and sulfate depend on air masses, during summer 2013, the PM_1 composition was similar between Mallorca and Ersa: organics dominate the PM_1 fraction (45% of OM and 40% to 42% of sulfate in PM_1 at both Cap Corse and Mallorca, respectively, between 10 July and 10 August 2013).

The eastern Mediterranean is also strongly influenced by sulfate and organics. Over the Aegean Archipelago, measurements performed in summer at Vigla and Finokalia showed that sulfate and OM accounted for about 40–45% and 20–32% of PM_1 mass, respectively (Pikridas et al., 2010; Athanasopoulou et al., 2015; Bougiatioti et al., 2016). High organic concentrations were also observed in Beirut: about 35% of $PM_{2.5}$ during the year 2014 (Abdallah et al., 2018), with higher organic fractions in summer. In July 2011, organics accounted for about 50% of $PM_{2.5}$ against about 30% for sulfate (Waked et al., 2013). Using 2-year measurements, Theodosi et al. (2018) showed that organics and inorganics make about 38% and 31%, respectively, of $PM_{2.5}$ concentrations in Athens. In summer, Stavroulas et al. (2019) measured that 46% of PM_1 are organics, while 31% are made of sulfate.

Secondary organic aerosols (SOA) are produced through chemical oxidation of gaseous organic compounds, among which volatile organic compounds (VOCs). The condensable products formed may then condense on organic or aqueous particulate matter, depending on their affinity with water. In summer, because solar radiation and temperature are high, a large fraction of emitted VOCs is biogenic. These biogenic VOC emissions are oxidized and are strongly affected by anthropogenic compounds, leading to the formation of SOA. The most important biogenic precursors of SOA are isoprene, monoterpenes, and sesquiterpenes. The formation of biogenic SOA is enhanced by anthropogenic plumes, because of an increase of oxidant concentrations and of absorbing mass on which SOA can condense. Therefore, reducing anthropogenic emissions may actually reduce the biogenic SOA concentration (Carlton et al., 2010; Sartelet et al., 2012). Over the United States and over Europe, Carlton et al. (2010) and Sartelet et al. (2012) estimated that as much as 50% of biogenic OA may be controllable.

In winter, the precursors of OA may predominantly be anthropogenic VOCs and I/S-VOCs (intermediate and semi-volatile organic compounds). Over Europe, the seasonality of OA due to wood burning and biogenic emissions in winter and summer, respectively, was pointed out by different studies based on either modeling (Couvidat et al., 2012) or measurements (Theodosi et al., 2018; Daellenbach et al., 2019; Yttri et al., 2019). Organic concentrations are higher during winter than summer in large cities, such as Athens (Stavroulas et al., 2019). The origins and formation pathways of these fine particles are now investigated into details using measurement and modeling studies.

2 Organic Aerosols

In order to understand the origins and formation pathways of organic aerosols, their properties are first described. For modeling purposes, it is important that not only the concentrations but also the properties of OA are well understood and represented, in order to make sure that their formation processes included in the models are as close as possible to the reality. Because of the large number of organic compounds that may partition between the gas and particle phases, they are grouped into classes in 3D air quality models. Different approaches may be used, depending on the model and/or precursor. Over the Mediterranean, two main approaches have been used to represent the compounds formed by oxidation of the precursors: a VBS approach where the classes are defined depending on the volatility of the compounds (Cholakian et al., 2018; Chrit et al., 2018b) and a surrogate approach where each class is represented by a surrogate (Chrit et al., 2017, 2018a, b). The surrogate approach differs from the VBS approach by the characterization of each class not only by the volatility of the compounds but also by the definition of specific properties (oxidation, affinity with water, molecular structure).

2.1 Organic Aerosol Properties

Carbon Origin

From experiments, the biogenic origin can be studied using high-volume quartz filter sampling ^{14}C measurements, which can determine if the organic carbon OC has a fossil or a non-fossil origin. Measurements performed over the western Mediterranean in summer suggest that most of the OA is from biogenic origins: biogenic precursors are processed and nucleate and/or condense to form OA.

At remote locations, this is illustrated by the ^{14}C measurements performed in July 2013 during the ChArMEx summer campaign at Ersa and Mallorca. OC is mainly of non-fossil origin at both Ersa (84.7 ± 3.1%) and Mallorca (70.1 ± 9.5%). We can also note the stability of the contribution of non-fossil OC at Ersa all along the summer 2013 campaign indicating a relative independence of the SOA sources toward air masses' history, while Mallorca, due to its location (low altitude and closer to anthropogenic emissions sources), is, as expected, more influenced by fossil carbon emissions, than Ersa. Even in cities, this biogenic influence dominates during summer. El Haddad et al. (2011a, b) showed, by combining data from an AMS (aerosol mass spectrometer), organic markers, and ^{14}C measurements obtained in downtown Marseille in summer, that more than 70% of the OA was from secondary and with contemporary origins. These high biogenic concentrations in an urban area are partly explained by the influence of anthropogenic emissions on biogenic SOA formation.

In modeling studies, the carbon origin is determined by tracing the SOA surrogates formed from the different precursors. Simulations performed using the surrogate and the VBS approaches over the western Mediterranean agree well with measurements performed at Ersa during summer 2013 (Chrit et al., 2017; Cholakian et al., 2018). Figure 3 shows the ratio of biogenic SOA to OA in $PM_{2.5}$ (in %) at surface during the summer 2013 using the concentrations simulated by Chrit et al. (2017). The biogenic contribution reaches 95% at remote locations and is higher than 70% over cities. The lowest biogenic SOA contribution to OA is along the ship lines (about 55%). However, at higher altitudes (300–450 m), the local anthropogenic contribution becomes lower due to slow mixing in the boundary layer over marine areas, while biogenic contributions are transported from more distant sources and are better mixed (Cholakian et al., 2018).

Oxidation

From ACSM or HR-ToF-AMS measurements, the ratios of OM/OC and O/C and the oxidation state of organics are estimated following Kroll et al. (2011). Positive matrix factorization may also be used to identify different "types" of oxidized OA (Lanz et al., 2010): HOA (hydrocarbon-like organic aerosol), LVOOA (low volatile oxygenated OA), and SVOOA (semi-volatile oxygenated OA). Positive matrix

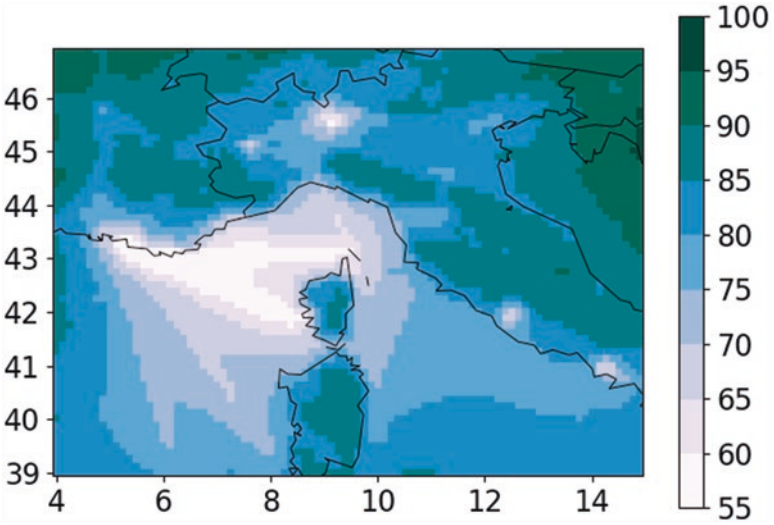

Fig. 3 BSOA/OA ratio in $PM_{2.5}$ (in %) at surface during the summer 2013, using the concentrations simulated by Chrit et al. (2017)

Table 1 Average (standard deviation) of atomic ratios derived from HR-ToF-AMS results for Ersa and Mallorca

Station	O/C	H/C	OM/OC	OSc
Ersa	0.92 (±0.11)	1.30 (±0.08)	2.34 (±0.14)	0.53 (±0.28)
Mallorca	0.64 (±0.10)	1.25 (±0.05)	1.97 (±0.13)	0.03 (±0.02)

Courtesy of Nicolas Marchand
The oxidation state (OSc) measures the degree of oxidation of organic compounds

factorization (PMF) on the combined organic-inorganic matrices separate the oxidized organic aerosol into a more oxidized organic aerosol (MOOA equivalent to LVOOA) and a less oxidized organic aerosol (LOOA equivalent to SVOOA).

In summer, at remote locations, the organic fractions of the aerosols are very oxidized (see Table 1; Chrit et al., 2017; Michoud et al., 2017; Cholakian et al., 2018; Mallet et al., 2019) with differences depending on time and location. For example, the organic fraction of the aerosols collected at Ersa in July 2013 (O:C ~ 0.92) is clearly more oxidized than at Mallorca (O:C ~ 0.64). There was a global stability of all the atomic ratios all along the campaign of July 2013 at both Ersa and Mallorca, suggesting a constant income of highly oxidized OA (LVOOA). Mallet et al. (2019) showed that at Lampedusa in June 2013, OA is also very oxidized with a ratio O:C about 1. They also found that MOOA was the dominant factor (53% of the PM_1 OA mass) and it was well correlated with sulfate.

In the framework of the ChArMEx and the ANR project SAFMED (Secondary Aerosol Formation over the Mediterranean), Freney et al. (2018) measured in late June–early July 2013 that 60–72% of PM_1 aerosols are organics and very oxidized

(O:C ~ 1.05) over forested regions in the south of France. The MOOA component was strongly associated with inorganic species, in opposition to the LOOA factor, which correlated well with biogenic volatile organic species measured with mass spectrometry, such as isoprene and its oxidation products.

To compare the observed oxidation properties to the simulations using the VBS modeling approach, Cholakian et al. (2018) distributed the different classes among HOA, LVOOA, and SVOOA: primary OA was assumed to correspond to HOA, while secondary OA was distributed among LVOOA and SVOOA depending on the saturation concentration of the class. Using the surrogate approach, Chrit et al. (2017, 2018b) and Freney et al. (2018) calculated the OM/OC and O/C ratios by weighting the OM/OC and O/C ratios of each surrogate species. Cholakian et al. (2018) found good agreement between the modeled and simulated oxidation properties after adding the formation of low volatility compounds in the VBS approach; and Chrit et al. (2017) and Freney et al. (2018) added the formation of extremely low volatility compounds (ELVOCs) from the ozonolysis of monoterpenes and organic nitrates from the monoterpene oxidation.

During winter, the oxidation state was observed to stay very high at Ersa (see Fig. 4), as well as the oxygenation level (O/C). The modeling study of Chrit et al. (2018a) managed to reproduce the high concentration observed in March 2014 at Ersa (Fig. 2) by adding emissions of intermediate and semi-volatile organic compounds (I/S-VOCs) in their model. These compounds are emitted by combustion processes (traffic and residential heating), and their volatility distribution at the emission influences the concentrations strongly. These high oxygenation levels observed in winter may stress the importance of emissions from residential heating, which may be more oxidized than those from traffic (Ciarelli et al., 2017). However, the observed organic oxidation and oxygenation states were underestimated in the

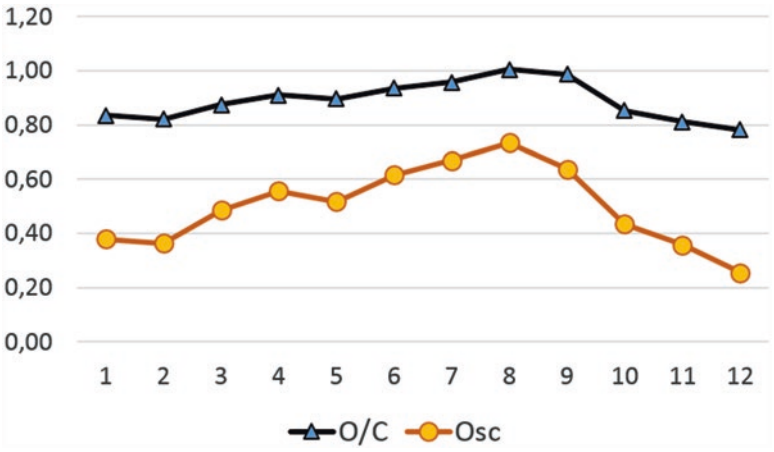

Fig. 4 Monthly averaged submicron aerosol oxidation properties (triangles, O/C ratio; circles, OSc) at Ersa (Corsica) obtained from ACSM measurements between June 2012 and July 2014. (Data courtesy of Jean Sciare)

simulations (O/C was about 0.7 in the simulations against 0.8 in the measurements), even when multigenerational aging of I/S-VOCs was modeled. This suggests that some aging processes of anthropogenic emissions still need to be elucidated, with a potential formation of ELVOCs from anthropogenic emissions (e.g., aromatics) and organic nitrate.

Solubility

Organic aerosols are observed to be highly soluble over the Mediterranean in summer. In the eastern Mediterranean, at Finokalia, Pikridas et al. (2010) estimated that at much as 80% of OC is water-soluble. At Ersa, measurements performed using a PILS-TOC-UV to estimate the water-soluble fraction of organics (Sciare et al., 2011) showed that 64% of OC is soluble (Chrit et al., 2017). Measurements using Raman lidar have also been used to characterize aerosol hygroscopicity (Navas-Guzmán et al., 2019).

Using the surrogate approach for modeling organics, the water-soluble mass of OC can be estimated from the mass of the surrogates that are water-soluble, which depends on the Henry constants of the surrogates. Chrit et al. (2017) report a good agreement between measured and simulated water-soluble organic carbon (WSOC) at Ersa (Fig. 5), with a large contribution of surrogates formed from the oxidation of biogenic precursors. The evolution of WSOC with time is due to variations in the aerosol composition depending on air mass origins. At Finokalia in the eastern Mediterranean, Bougiatioti et al. (2016) derived a hygroscopicity parameter from

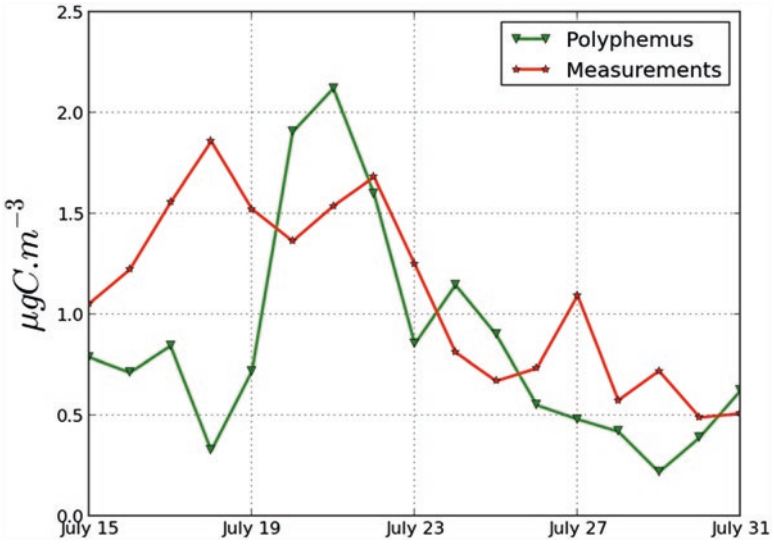

Fig. 5 Submicron WSOC measured (in red) and simulated (in green) at Ersa during the summer of 2013. (Reprinted from Chrit et al. (2017))

CCN and hygroscopic tandem differential mobility analyzer (HTDMA) measurements and linked it to distinct chemical constituents identified with PMF of the chemical constituents measured with an ACSM. Hygroscopicity was found to increase with size, as particles are more atmospherically processed. Furthermore, freshly emitted biomass burning OA was found to be around two to three times less hygroscopic than atmospherically processed biomass burning OA and highly oxidized organic aerosols.

2.2 Origins and Formation Pathways

As discussed in the introduction, a large fraction of PM_1 and $PM_{2.5}$ is organic. The study of the properties of OA in the previous sections shed lights on the origins and formation pathways of OA. Note that the interactions between chemical compounds of different origins are strong. For example, in summer over the Mediterranean, Chrit et al. (2018a) simulated a strong sensitivity of OA concentrations to meteorology. This sensitivity is not only because the temperature influences the partitioning between the gaseous and particulate phases but also because the meteorology influences the emissions of biogenic precursors and inorganic sea salt emissions, which are both involved in the formation of OA as discussed below.

Biogenic

In summer, at least 70% of OA was observed to be biogenic at both remote and urban sites. However, the influence of anthropogenic emissions on the formation of biogenic organic aerosols is clearly important, as shown by the modeling work (Sartelet et al., 2012). Freney et al. (2018) showed that less oxidized organic aerosols correlate well with biogenic precursors over forests in the south of France. The contribution of specific signatures for isoprene epoxydiols SOA (IEPOXSOA) was very weak, suggesting that isoprene SOA was not formed through IEPOX.

The modeling studies of Chrit et al. (2017) and Freney et al. (2018) suggest that, at ERSA site and over forests, non-IEPOX SOA from isoprene forms 15–35% of the OA mass, with a large part of OA being formed from the oxidation of monoterpenes (30–50%) and sesquiterpenes (about 10%). A large fraction of oxidation products of biogenic precursors may be hydrophilic, explaining the high fraction of water-soluble carbon observed. The contribution of ELVOCs from monoterpenes was found to be as high as 10%, partly explaining the high oxidation state observed. These compounds may also be involved in new particle formation (NPF), as suggested in the preceding chapter on nucleation (Sellegri & Rose, 2022).

The temperature sensitivity of biogenic SOA (BSOA) formation has been addressed in a modeling study, comparing BSOA under a future climate scenario with different organic aerosol schemes (Cholakian et al., 2019a). Five years of historical simulations and 5 years of future simulations according to a RCP8.5 scenario

have been conducted with a modeling chain described in Colette et al. (2013), involving for boundary conditions the IPSL-CM5A-MR global climate model and the LMDz-INCA global CTM, the EURO-CORDEX WRF regional climate simulations, and CHIMERE regional CTM simulations with different organic aerosol schemes. Over Europe and the Mediterranean, BSOA increases for all aerosol schemes as a consequence of increased BVOC emissions triggered by higher temperature. However, a scheme based on the volatility basis set formalism and including functionalization and fragmentation of semi-volatile organic species as well as formation of non-volatile BSOA (Shrivastava et al., 2015) leads to two times higher relative BSOA increases than the molecular standard scheme in CHIMERE without chemical aging (Menut et al., 2013). For the latter scheme, the BVOC increase is partly compensated by increased evaporation of semi-volatile BSOA in a hotter climate, while for the former scheme, this effect is more limited due to the formation of non-volatile BSOA (Cholakian et al., 2019a). Thus, exact knowledge of chemical formation pathways of BSOA is necessary to correctly predict its sensitivity to a future warmer climate.

Marine Aerosol

Satellites (MODIS) show important phytoplankton activity near coasts in the Mediterranean (Chrit et al., 2017) with sea-derived organic particles emitted in the Aitken mode (Schwier et al., 2015, 2017). However, Chrit et al. (2017) showed that the contribution of the sea-origin organic particles to organic concentrations is low (at most 2% in summer) if parameterizations using chlorophyll a (Chl a) as a proxy are used. This agrees with the measurements of Schwier et al. (2017), who found that the correlation between the particle organic fraction and the seawater Chl a was poor in their measurements.

Measurements at Lampedusa found correlations between sulfate and organics (Mallet et al., 2019). For Mallorca and Ersa, the ME2 (Multilinear Engine 2, SoFi toolkit; Canonaco et al., 2013) was used to perform PMF calculation with the whole AMS mass spectra (i.e., including sulfate, nitrate, and ammonium fragments in addition to organic fragments) measured in July 2013 in Mallorca and Ersa. A factor mixing sulfate and oxidized organic fragments (named sulfate-OOA) represents between 15% in Mallorca and 25% in Ersa of the total PM_1 mass. As shown for Mallorca (Fig. 6), the sulfate-OOA factor is, at both sites, extremely well correlated with $CH_3SO_2^+$ fragment, a well-known fragment of methane sulfonic acid (MSA) which is an oxidation of product of dimtehyl sulfide (DMS). Therefore, a significant biogenic marine contribution to the secondary organic aerosol budget is expected.

This biogenic marine contribution may be direct and linked to DMS, as discussed by Sellegri and Rose (Sellegri & Rose, 2022), but it may also be an indirect contribution, for example, by providing an absorbing aqueous mass for condensing non-marine biogenic oxidation products. As shown in Pun et al. (2006) and Couvidat and Seigneur (2011), biogenic oxidation products tend to be strongly hydrophilic. They may condense onto the aqueous phase formed by marine primary inorganic

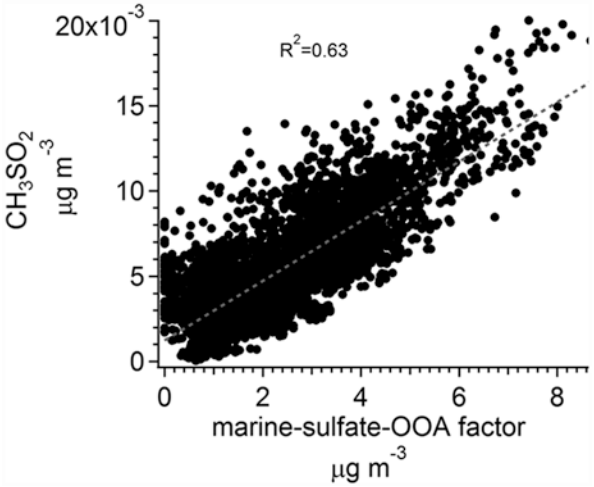

Fig. 6 Correlation, fitted by the dotted line, between the sulfate-OOA factor and the main MSA fragment ($CH_3SO_2^+$) at Mallorca in July 2013. (Courtesy of Nicolas Marchand)

aerosols. In Chrit et al. (2018a), biogenic SOA is formed from the condensation on marine aerosols of hydrophilic oxidation products of monoterpenes, such as pinonaldehyde and pinic acid, and a strong sensitivity of OM_1 concentrations to sea salt emissions is simulated. Other processes may also be involved: the experiments of Wang et al. (2019) showed that particulate sulfate may be formed through the oxidation of dissolved sulfur dioxide by organic peroxides from monoterpene oxidation.

Anthropogenic

The estimate of the anthropogenic contribution to organic aerosols is highly dependent on the quality of the emission inventory. In some parts of the eastern Mediterranean, the anthropogenic contribution is difficult to establish because of difficulties to have accurate emission inventories, as pointed out by Abdallah et al. (2016 and 2018) and Salameh et al. (Salameh et al., 2016; Salameh et al., 2017) for Lebanon and Beirut (see also Borbon et al., 2022). In summer, although the anthropogenic contribution from organic precursors was found to be low, anthropogenic emissions influence the formation of biogenic aerosols by enhancing oxidant concentrations and increasing the absorbing mass (Sartelet et al., 2012). The contribution of anthropogenic precursors, as shown by the ^{14}C measurements, is low in summer. Using modeling, the contribution of single-ring aromatics (toluene, xylene) is simulated to be low (<5%) in both summer and winter (Couvidat et al., 2012; Chrit et al., 2017, 2018b). In summer, I/S-VOCs are found to contribute about 20% or less to OA, while their contribution is major in winter (about 80%). However, other volatile organic compounds emitted from residential wood combustion may strongly influence the OA formation, potentially explaining the high organic

oxidation state observed (Stefenelli et al., 2019). At Athens, in the PMF receptor modeling on measured data, Theodosi et al. (2018) estimated that biomass burning is the main source of $PM_{2.5}$ (31%), followed by vehicular emissions (19%) and heavy oil combustion linked to maritime traffic (7%).

Maritime Traffic

Using markers of heavy fuel oil combustion, Becagli et al. (2017) estimated that during summer 2013, the minimum ship emission contributions to PM_{10} were 11% at Lampedusa and 8.6% at Capo Granitola, respectively. Large differences exist in emission inventory of ships (Chrit et al., 2017; Cholakian et al., 2018). However, ships strongly influence OA concentrations over the Mediterranean (Fig. 3). They emit not only primary organic particles and organic precursors but also NO_x leading to an increase of oxidants and hence SOA formation. Organic nitrate is also estimated to be important over the sea during low-wind periods (Chrit et al., 2017).

Wildfires

Although wildfires are sporadic, they can lead to high aerosol loading in the atmosphere. For example, intense wildfire episodes have been reported in Greece and the Balkans (Majdi et al., 2019a). Because wildfires involve large amounts of aerosols, wildfires from other continents, especially the North American continent or Siberia (Brocchi et al., 2018; Guth et al., 2018), impact the Mediterranean domain. Wildfires contribute to high organic aerosol loading (Bougiatioti et al., 2016), with a large contribution of I/S-VOCs (Konovalov et al., 2015; Konovalov et al., 2019; Majdi et al., 2019a). Although their contribution to OA could be as large as 70% during severe fire episodes, volatile organic compounds (phenol, catechol, cresol, xylene, toluene, benzene, naphthalene) may significantly contribute to OA (Majdi et al., 2019b). During wildfires, atmospheric processes of particles affect the hygroscopicity as well as the mixing state of the particles (Bougiatioti et al., 2016).

3 Inorganic Aerosols

Over the Mediterranean, sulfate makes a large fraction of fine aerosols (see introduction and Fig. 2). Sea salt aerosols contain sulfate (Schwier et al., 2015). However, the contribution of sea salt sulfate to PM_1 is small, and sulfate is highly sensitive to the emission inventory (maritime traffic) (Chrit et al., 2018a). Ammonium, sodium, nitrate, and chloride to a lesser extent (Chrit et al., 2018a) are measured to contribute significantly to PM_{10} and PM_1 concentrations. Note that the contribution of sodium is included in the composition depicted in Fig. 2, because ACSM and AMS measurements can only estimate the concentrations of non-refractory compounds.

Sodium and chloride originate mostly from sea salt emission. Although sodium is non-volatile, sea salt chloride evaporates from sea salt aerosols to be replaced by nitrate (Claeys et al., 2017), influencing the gas/particle partitioning of inorganic semi-volatile compounds. The precursors of aerosol nitrate and ammonium are mostly anthropogenic: nitrogen dioxide and ammonia, with a large fraction emitted by traffic and agriculture, respectively. The mixing state of particles influences the gas/particle partitioning. For example, semi-volatile inorganic compounds are strongly influenced by the mixing state of sea salt aerosols. Those may not be well mixed to urban aerosols, with a dynamic exchange between the gas and particle phases (Chrit et al., 2018a; Freney et al., 2018).

Using sensitivity simulations, several studies pointed to the strong influence of maritime traffic, meteorology, and sea salt emissions on inorganic aerosol concentrations in the western Mediterranean region (Cholakian et al., 2018; Chrit et al., 2018a; Guth et al., 2018). Maritime traffic affects inorganic aerosol concentrations, because it emits their precursors (nitrogen dioxide and sulfur dioxide). Meteorology influences the gas-/particle-phase partitioning of semi-volatile inorganics, nitrate, ammonium, and chloride, because of the influence of the temperature. However, temperature influences not only the gas-/particle-phase partitioning but also photochemistry and the formation of semi-volatile compounds, such as inorganic nitrates or organic species (see above) from their precursors, explaining the strong sensitivity of these compounds to climate change (Cholakian et al., 2019b).

4 Conclusions and Recommendations

Organic and inorganic aerosols make a large fraction of fine particles over the Mediterranean. In summer, organics are mostly of biogenic origins, water-soluble, and highly oxidized. Biogenic precursors are monoterpenes, isoprene, and sesquiterpenes. Anthropogenic emissions influence the formation of biogenic organics by influencing the formation of oxidants and by providing an absorbing mass for condensation. The formation processes of biogenic aerosols are fairly well modeled, and 3D air quality models manage to represent the concentrations and properties of OA at remote sites and over forests, despite large uncertainties in biogenic emissions (Jiang et al., 2019). ELVOCs are found to contribute to up to 10% of organics in the western Mediterranean. They may also contribute to the formation and growth of NPF, as suggested in Chapter 6.3. In winter, precursors are mostly anthropogenic, with formation processes that still need to be studied further. The models suggest a strong influence of IS/VOC emissions, whose gas phase is missing in emission inventories. However, as the organic oxidation state is not well modeled in winter, formation processes may need to be revisited, by considering the formation of extremely low volatility organic compounds and organic nitrate from anthropogenic precursors. Note that the viscosity of OA may also influence gas/particle partitioning of organics (Kim et al., 2019).

Among inorganics, sulfate concentrations are especially high, because of ship emissions, as discussed in chapter "Anthropogenic Emissions of Ultrafine Particles in the Mediterranean". The influence of sulfate sea salt is simulated to be low compared to the influence of ship emissions. Because of the diversity of sources (anthropogenic, sea salt, biogenic) and the high photochemistry in summer, an accurate representation of gas/particle partitioning is required to represent inorganic concentrations in summer, with a large influence of thermodynamic and aerosol mixing state. Primary sea salt organic emissions are also estimated to have a low contribution to organics. However, sea salt emissions strongly enhance the formation of organic aerosols by providing an absorbing aqueous mass to the hydrophilic semi-volatile organics formed from the oxidation of biogenic precursors. Inorganics provide not only an aqueous absorbing mass, but their interactions with organics need to be better understood and modeled, e.g., deviation from ideal thermodynamic behavior as represented by activity coefficients is important.

The concentrations of secondary organic aerosols have been simulated to increase in the Mediterranean in 2050 because of climate change. Increased temperatures lead to an increase in biogenic VOC emissions and to a shift of gas-particulate phase equilibrium toward gas phase. The increase in biogenic emissions was shown to be the most impacting factor, explaining the increase of secondary organic aerosols. Over cities, the increase of secondary aerosols may also be due to an increase in oxidant concentrations, because of NO_x emission reductions. Land-use changes could also affect these NO_x and biogenic emissions and should be taken into account in future simulations.

References

Abdallah, C., Sartelet, K., & Afif, C. (2016). Influence of boundary conditions and anthropogenic emission inventories on simulated O_3 and $PM_{2.5}$ concentrations over Lebanon. *Atmospheric Pollution Research, 7*, 971–979. https://doi.org/10.1016/j.apr.2016.06.001

Abdallah, C., Afif, C., El Masri, N., Öztürk, F., Keleç, M., & Sartelet, K. (2018). A first annual assessment of air quality modeling over Lebanon using WRF/Polyphemus. *Atmospheric Pollution Research, 9*, 643–654. https://doi.org/10.1016/j.apr.2018.01.003

Ancellet, G., Pelon, J., Totems, J., Chazette, P., Bazureau, A., Sicard, M., Di Iorio, T., Dulac, F., & Mallet, M. (2016). Long-range transport and mixing of aerosol sources during the 2013 North American biomass burning episode: Analysis of multiple lidar observations in the western Mediterranean basin. *Atmospheric Chemistry and Physics, 16*, 4725–4742. https://doi.org/10.5194/acp-16-4725-2016

Arndt, J., Sciare, J., Mallet, M., Roberts, G. C., Marchand, N., Sartelet, K., Sellegri, K., Dulac, F., Healy, R. M., & Wenger, J. C. (2017). Sources and mixing state of summertime background aerosol in the north-western Mediterranean basin. *Atmospheric Chemistry and Physics, 17*, 6975–7001. https://doi.org/10.5194/acp-17-6975-2017

Athanasopoulou, E., Protonotariou, A. P., Bossioli, E., Dandou, A., Tombrou, M., Allan, J. D., Coe, H., Mihalopoulos, N., Kalogiros, J., Bacak, A., Sciare, J., & Biskos, G. (2015). Aerosol chemistry above an extended archipelago of the eastern Mediterranean basin during strong northern winds. *Atmospheric Chemistry and Physics, 15*, 8401–8421. https://doi.org/10.5194/acp-15-8401-2015

Becagli, S., Anello, F., Bommarito, C., Cassola, F., Calzolai, G., Di Iorio, T., di Sarra, A., Gómez-Amo, J.-L., Lucarelli, F., Marconi, M., Meloni, D., Monteleone, F., Nava, S., Pace, G., Severi, M., Sferlazzo, D. M., Traversi, R., & Udisti, R. (2017). Constraining the ship contribution to the aerosol of the central Mediterranean. *Atmospheric Chemistry and Physics, 17*, 2067–2084. https://doi.org/10.5194/acp-17-2067-2017

Borbon, A., Afif, C., Salameh, T., Liousse, C., Thera, B., & Panopoulou, A. (2022). Anthropogenic emissions in the Mediterranean region. In F. Dulac, S. Sauvage, & E. Hamonou (Eds.), *Atmospheric chemistry in the Mediterranean Region* (Vol. 2, From air pollutant sources to impacts). Springer, this volume. https://doi.org/10.1007/978-3-030-82385-6_5

Bougiatioti, A., Bezantakos, S., Stavroulas, I., Kalivitis, N., Kokkalis, P., Biskos, G., Mihalopoulos, N., Papayannis, A., & Nenes, A. (2016). Biomass-burning impact on CCN number, hygroscopicity and cloud formation during summertime in the eastern Mediterranean. *Atmospheric Chemistry and Physics, 16*, 7389–7409. https://doi.org/10.5194/acp-16-7389-2016

Brocchi, V., Krysztofiak, G., Catoire, V., Guth, J., Marécal, V., Zbinden, R., El Amraoui, L., Dulac, F., & Ricaud, P. (2018). Intercontinental transport of biomass burning pollutants over the Mediterranean Basin during the summer 2014 ChArMEx-GLAM airborne campaign. *Atmospheric Chemistry and Physics, 18*, 6887–6906. https://doi.org/10.5194/acp-18-6887-2018

Canonaco, F., Crippa, M., Slowik, J. G., Baltensperger, U., & Prévôt, A. S. H. (2013). SoFi, an IGOR-based interface for the efficient use of the generalized multilinear engine (ME-2) for the source apportionment: ME-2 application to aerosol mass spectrometer data. *Atmospheric Measurement Techniques, 6*, 3649–3661. https://doi.org/10.5194/amt-6-3649-2013

Carlton, A., Pinder, R., Bhave, P., & Pouliot, G. (2010). To what extent can biogenic SOA be controlled? *Environmental Science & Technology, 44*, 3376e3380. https://doi.org/10.1021/es903506b

Cholakian, A., Beekmann, M., Colette, A., Coll, I., Siour, G., Sciare, J., Marchand, N., Couvidat, F., Pey, J., Gros, V., Sauvage, S., Michoud, V., Sellegri, K., Colomb, A., Sartelet, K., Langley DeWitt, H., Elser, M., Prévot, A. S. H., Szidat, S., & Dulac, F. (2018). Simulation of fine organic aerosols in the western Mediterranean area during the ChArMEx 2013 summer campaign. *Atmospheric Chemistry and Physics, 18*, 7287–7312. https://doi.org/10.5194/acp-18-7287-2018

Cholakian, A., Beekmann, M., Coll, I., Ciarelli, G., & Colette, A. (2019a). Biogenic secondary organic aerosol sensitivity to organic aerosol simulation schemes in climate projections. *Atmospheric Chemistry and Physics, 19*, 13209–13226. https://doi.org/10.5194/acp-19-13209-2019

Cholakian, A., Colette, A., Coll, I., Ciarelli, G., & Beekmann, M. (2019b). Future climatic drivers and their effect on PM10 components in Europe and the Mediterranean Sea. *Atmospheric Chemistry and Physics, 19*, 4459–4484. https://doi.org/10.5194/acp-19-4459-2019

Chrit, M., Sartelet, K., Sciare, J., Pey, J., Marchand, N., Couvidat, F., Sellegri, K., & Beekmann, M. (2017). Modelling organic aerosol concentrations and properties during ChArMEx summer campaigns of 2012 and 2013 in the western Mediterranean region. *Atmospheric Chemistry and Physics, 17*, 12509–12531. https://doi.org/10.5194/acp-17-12509-2017

Chrit, M., Sartelet, K., Sciare, J., Majdi, M., Nicolas, J., Petit, J.-E., & Dulac, F. (2018a). Modeling organic aerosol concentrations and properties during winter 2014 in the northwestern Mediterranean region. *Atmospheric Chemistry and Physics, 18*, 18079–18100. https://doi.org/10.5194/acp-18-18079-2018

Chrit, M., Sartelet, K., Sciare, J., Pey, J., Nicolas, J. B., Marchand, N., Freney, E., Sellegri, K., Beekmann, M., & Dulac, F. (2018b). Aerosol sources in the western Mediterranean during summertime: A model-based approach. *Atmospheric Chemistry and Physics, 18*, 9631–9659. https://doi.org/10.5194/acp-18-9631-2018

Ciarelli, G., Aksoyoglu, S., El Haddad, I., Bruns, E. A., Crippa, M., Poulain, L., Äijälä, M., Carbone, S., Freney, E., O'Dowd, C., Baltensperger, U., & Prévôt, A. S. H. (2017). Modelling winter organic aerosol at the European scale with CAMx: Evaluation and source apportionment with a

VBS parameterization based on novel wood burning smog chamber experiments. *Atmospheric Chemistry and Physics, 17*, 7653–7669. https://doi.org/10.5194/acp-17-7653-2017

Claeys, M., Roberts, G., Mallet, M., Arndt, J., Sellegri, K., Sciare, J., Wenger, J., & Sauvage, B. (2017). Optical, physical and chemical properties of aerosols transported to a coastal site in the western Mediterranean: A focus on primary marine aerosols. *Atmospheric Chemistry and Physics, 17*, 7891–7915. https://doi.org/10.5194/acp-17-7891-2017

Colette, A., Bessagnet, B., Vautard, R., Szopa, S., Rao, S., Schucht, S., Klimont, Z., Menut, L., Clain, G., Meleux, F., Curci, G., & Rouïl, L. (2013). European atmosphere in 2050, a regional air quality and climate perspective under CMIP5 scenarios. *Atmospheric Chemistry and Physics, 13*, 7451–7471. https://doi.org/10.5194/acp-13-7451-2013

Couvidat, F., & Seigneur, C. (2011). Modeling secondary organic aerosol formation from isoprene oxidation under dry and humid conditions. *Atmospheric Chemistry and Physics, 11*, 893–909. https://doi.org/10.5194/acp-11-893-2011

Couvidat, F., Debry, E., Sartelet, K. N., & Seigneur, C. (2012). A hydrophilic/hydrophobic organic (H_2O) aerosol model: Development, evaluation and sensitivity analysis. *Journal of Geophysical Research, 117*, D10304. https://doi.org/10.1029/2011JD017214

Daellenbach, K. R., Kourtchev, I., Vogel, A. L., Bruns, E. A., Jiang, J., Petäjä, T., Jaffrezo, J.-L., Aksoyoglu, S., Kalberer, M., Baltensperger, U., El Haddad, I., & Prévôt, A. S. H. (2019). Impact of anthropogenic and biogenic sources on the seasonal variation in the molecular composition of urban organic aerosols: A field and laboratory study using ultra-high-resolution mass spectrometry. *Atmospheric Chemistry and Physics, 19*, 5973–5991. https://doi.org/10.5194/acp-19-5973-2019

Di Biagio, C., Formenti, P., Doppler, L., Gaimoz, C., Grand, N., Ancellet, G., Attié, J.-L., Bucci, S., Dubuisson, P., Fierli, F., Mallet, M., & Ravetta, F. (2016). Continental pollution in the Western Mediterranean basin: Large variability of the aerosol single scattering albedo and influence on the direct shortwave radiative effect. *Atmospheric Chemistry and Physics, 16*, 10591–10607. https://doi.org/10.5194/acp-16-10591-2016

El Haddad, I., Marchand, N., Wortham, H., Piot, C., Besombes, J.-L., Cozic, J., Chauvel, C., Armengaud, A., Robin, D., & Jaffrezo, J.-L. (2011a). Primary sources of $PM_{2.5}$ organic aerosol in an industrial Mediterranean city, Marseille. *Atmospheric Chemistry and Physics, 11*, 2039–2058. https://doi.org/10.5194/acp-11-2039-2011

El Haddad, I., Marchand, N., Temime-Roussel, B., Wortham, H., Piot, C., Besombes, J.-L., Baduel, C., Voisin, D., Armengaud, A., & Jaffrezo, J.-L. (2011b). Insights into the secondary fraction of the organic aerosol in a Mediterranean urban area: Marseille. *Atmospheric Chemistry and Physics, 11*, 2059–2079. https://doi.org/10.5194/acp-11-2059-2011

Freney, E., Sellegri, K., Chrit, M., Adachi, K., Brito, J., Waked, A., Borbon, A., Colomb, A., Dupuy, R., Pichon, J.-M., Bouvier, L., Delon, C., Jambert, C., Durand, P., Bourianne, T., Gaimoz, C., Triquet, S., Féron, A., Beekmann, M., … Sartelet, K. (2018). Aerosol composition and the contribution of SOA formation over Mediterranean forests. *Atmospheric Chemistry and Physics, 18*, 7041–7056. https://doi.org/10.5194/acp-18-7041-2018

Guth, J., Marécal, V., Josse, B., Arteta, J., & Hamer, P. (2018). Primary aerosol and secondary inorganic aerosol budget over the Mediterranean Basin during 2012 and 2013. *Atmospheric Chemistry and Physics, 18*, 4911–4934. https://doi.org/10.5194/acp-18-4911-2018

Jiang, J., Aksoyoglu, S., Ciarelli, G., Oikonomakis, E., El-Haddad, I., Canonaco, F., O'Dowd, C., Ovadnevaite, J., Minguillón, M. C., Baltensperger, U., & Prévôt, A. S. H. (2019). Effects of two different biogenic emission models on modelled ozone and aerosol concentrations in Europe. *Atmospheric Chemistry and Physics, 19*, 3747–3768. https://doi.org/10.5194/acp-19-3747-2019

Kim, Y., Sartelet, K., & Couvidat, F. (2019). Modeling the effect of non-ideality, dynamic mass transfer and viscosity on SOA formation in a 3-D air quality model. *Atmospheric Chemistry and Physics, 19*, 1241–1261. https://doi.org/10.5194/acp-19-1241-2019

Konovalov, I. B., Beekmann, M., Berezin, E. V., Petetin, H., Mielonen, T., Kuznetsova, I. N., & Andreae, M. O. (2015). The role of semi-volatile organic compounds in the mesoscale

evolution of biomass burning aerosol: A modeling case study of the 2010 mega-fire event in Russia. *Atmospheric Chemistry and Physics, 15*, 13269–13297. https://doi.org/10.5194/acp-15-13269-2015

Konovalov, I. B., Beekmann, M., Golovushkin, N. A., & Andreae, M. O. (2019). Nonlinear behavior of organic aerosol in biomass burning plumes: A microphysical model analysis. *Atmospheric Chemistry and Physics, 19*, 12091–12119. https://doi.org/10.5194/acp-19-12091-2019

Kroll, J. H., Donahue, N. M., Jimenez, J. L., Kessler, S. H., Canagaratna, M., Wilson, K. R., Altieri, K. E., Mazzoleni, L. R., Wozniak, A. S., Bluhm, H., Mysak, E. R., Smith, J. D., Kolb, C. E., & Worsnop, D. R. (2011). Carbon oxidation state as a metric for describing the chemistry of atmospheric organic aerosol. *Nature Chemistry, 3*, 133–139. https://doi.org/10.1038/NCHEM.948

Lanz, V. A., Prévôt, A. S. H., Alfarra, M. R., Weimer, S., Mohr, C., DeCarlo, P. F., Gianini, M. F. D., Hueglin, C., Schneider, J., Favez, O., D'Anna, B., George, C., & Baltensperger, U. (2010). Characterization of aerosol chemical composition with aerosol mass spectrometry in Central Europe: An overview. *Atmospheric Chemistry and Physics, 10*, 10453–10471. https://doi.org/10.5194/acp-10-10453-2010

Majdi, M., Turquety, S., Sartelet, K., Legorgeu, C., Menut, L., & Kim, Y. (2019a). Impact of wildfires on particulate matter in the Euro-Mediterranean in 2007: Sensitivity to some parameterizations of emissions in air quality models. *Atmospheric Chemistry and Physics, 19*, 785–812. https://doi.org/10.5194/acp-19-785-2019

Majdi, M., Sartelet, K., Lanzafame, G. M., Couvidat, F., Kim, Y., Chrit, M., & Turquety, S. (2019b). Precursors and formation of secondary organic aerosols from wildfires in the Euro-Mediterranean region. *Atmospheric Chemistry and Physics, 19*, 5543–5569. https://doi.org/10.5194/acp-19-5543-2019

Mallet, M. D., D'Anna, B., Même, A., Bove, M. C., Cassola, F., Pace, G., Desboeufs, K., Di Biagio, C., Doussin, J.-F., Maille, M., Massabò, D., Sciare, J., Zapf, P., di Sarra, A. G., & Formenti, P. (2019). Summertime surface PM_1 aerosol composition and size by source region at the Lampedusa island in the central Mediterranean Sea. *Atmospheric Chemistry and Physics, 19*, 11123–11142. https://doi.org/10.5194/acp-19-11123-2019

Menut, L., Bessagnet, B., Khvorostyanov, D., Beekmann, M., Blond, N., Colette, A., Coll, I., Curci, G.,Foret, G., Hodzic, A., Mailler, S., Meleux, F., Monge, J.-L., Pison, I., Siour, G., Turquety, S., Valari, M., Vautard, R.,and Vivanco, M. G. (2013). CHIMERE a model for regional atmospheric composition modelling, Geosci. *Model Dev.,6*, 981–1028. https://doi.org/10.5194/gmd-6-981-2013

Menut, L., Mailler, S., Siour, G., Bessagnet, B., Turquety, S., Rea, G., Briant, R., Mallet, M., Sciare, J., Formenti, P., & Meleux, F. (2015). Ozone and aerosol tropospheric concentrations variability analyzed using the ADRIMED measurements and the WRF and CHIMERE models. *Atmospheric Chemistry and Physics, 15*, 6159–6182. https://doi.org/10.5194/acp-15-6159-2015

Michoud, V., Sciare, J., Sauvage, S., Dusanter, S., Léonardis, T., Gros, V., Kalogridis, C., Zannoni, N., Féron, A., Petit, J.-E., Crenn, V., Baisnée, D., Sarda-Estève, R., Bonnaire, N., Marchand, N., DeWitt, H. L., Pey, J., Colomb, A., Gheusi, F., … Locoge, N. (2017). Organic carbon at a remote site of the western Mediterranean Basin: Sources and chemistry during the ChArMEx SOP2 field experiment. *Atmospheric Chemistry and Physics, 17*, 8837–8865. https://doi.org/10.5194/acp-17-8837-2017

Minguillón, M. C., Ripoll, A., Pérez, N., Prévôt, A. S. H., Canonaco, F., Querol, X., & Alastuey, A. (2015). Chemical characterization of submicron regional background aerosols in the western Mediterranean using an Aerosol Chemical Speciation Monitor. *Atmospheric Chemistry and Physics, 15*, 6379–6391. https://doi.org/10.5194/acp-15-6379-2015

Navas-Guzmán, F., Martucci, G., Collaud Coen, M., Granados-Muñoz, M. J., Hervo, M., Sicard, M., & Haefele, A. (2019). Characterization of aerosol hygroscopicity using Raman lidar measurements at the EARLINET station of Payerne. *Atmospheric Chemistry and Physics, 19*, 11651–11668. https://doi.org/10.5194/acp-19-11651-2019

Pace, G., Meloni, D., & di Sarra, A. (2003). Forest fire aerosol over the Mediterranean basin during summer 2003. *Journal of Geophysical Research, 110*, D21202. https://doi.org/10.1029/2005JD005986

Pikridas, M., Bougiatioti, A., Hildebrandt, L., Engelhart, G. J., Kostenidou, E., Mohr, C., Prévôt, A. S. H., Kouvarakis, G., Zarmpas, P., Burkhart, J. F., Lee, B.-H., Psichoudaki, M., Mihalopoulos, N., Pilinis, C., Stohl, A., Baltensperger, U., Kulmala, M., & Pandis, S. N. (2010). The Finokalia Aerosol Measurement Experiment – 2008 (FAME-08): An overview. *Atmospheric Chemistry and Physics, 10*, 6793–6806. https://doi.org/10.5194/acp-10-6793-2010

Pun, B. K., Seigneur, C., & Lohman, K. (2006). Modeling secondary organic aerosol formation via multiphase partitioning with molecular data. *Environmental Science & Technology, 40*, 4722–4731. https://doi.org/10.1021/es0522736

Rea, G., Turquety, S., Menut, L., Briant, R., Mailler, S., & Siour, G. (2015). Source contributions to 2012 summertime aerosols in the Euro-Mediterranean region. *Atmospheric Chemistry and Physics, 15*, 8013–8036. https://doi.org/10.5194/acp-15-8013-2015

Salameh, T., Sauvage, S., Afif, C., Borbon, A., & Locoge, N. (2016). Source apportionment vs. emission inventories of non-methane hydrocarbons (NMHC) in an urban area of the Middle East: Local and global perspectives. *Atmospheric Chemistry and Physics, 16*, 3595–3607. https://doi.org/10.5194/acp-16-3595-2016

Salameh, T., Borbon, A., Afif, C., Sauvage, S., Leonardis, T., Gaimoz, C., & Locoge, N. (2017). Composition of gaseous organic carbon during ECOCEM in Beirut, Lebanon: New observational constraints for VOC anthropogenic emission evaluation in the Middle East. *Atmospheric Chemistry and Physics, 17*, 193–209. https://doi.org/10.5194/acp-17-193-2017

Sartelet, K. N., Couvidat, F., Seigneur, C., & Roustan, Y. (2012). Impact of biogenic emissions on air quality over Europe and North America. *Atmospheric Environment, 53*, 131–141. https://doi.org/10.1016/j.atmosenv.2011.10.046

Schepanski, K., Mallet, M., Heinold, B., & Ulrich, M. (2016). North African dust transport toward the western Mediterranean basin: Atmospheric controls on dust source activation and transport pathways during June–July 2013. *Atmospheric Chemistry and Physics, 16*, 14147–14168. https://doi.org/10.5194/acp-16-14147-2016

Schwier, A. N., Rose, C., Asmi, E., Ebling, A. M., Landing, W. M., Marro, S., Pedrotti, M.-L., Sallon, A., Iuculano, F., Agusti, S., Tsiola, A., Pitta, P., Louis, J., Guieu, C., Gazeau, F., & Sellegri, K. (2015). Primary marine aerosol emissions from the Mediterranean Sea during pre-bloom and oligotrophic conditions: Correlations to seawater chlorophyll a from a mesocosm study. *Atmospheric Chemistry and Physics, 15*, 7961–7976. https://doi.org/10.5194/acp-15-7961-2015

Schwier, A. N., Sellegri, K., Mas, S., Charrière, B., Pey, J., Rose, C., Temime-Roussel, B., Jaffrezo, J.-L., Parin, D., Picard, D., Ribeiro, M., Roberts, G., Sempéré, R., Marchand, N., & D'Anna, B. (2017). Primary marine aerosol physical flux and chemical composition during a nutrient enrichment experiment in mesocosms in the Mediterranean Sea. *Atmospheric Chemistry and Physics, 17*, 14645–14660. https://doi.org/10.5194/acp-17-14645-2017

Sciare, J., d'Argouges, O., Sarda-Estève, R., Gaimoz, C., Dolgorouky, C., Bonnaire, N., Favez, O., Bonsang, B., & Gros, V. (2011). Large contribution of water-insoluble secondary organic aerosols in the region of Paris (France) during wintertime. *Journal of Geophysical Research, 116*, d22203. https://doi.org/10.1029/2011JD015756

Sellegri, K., & Rose, C. (2022). *Nucleation in the Mediterranean atmosphere*, In F. Dulac, S. Sauvage, & E. Hamonou (Eds.), *Atmospheric chemistry in the Mediterranean Region* (Vol. 2, From air pollutant sources to impacts). Springer, this volume. https://doi.org/10.1007/978-3-030-82385-6_9

Shrivastava, M., Easter, R. C., Liu, X., Zelenyuk, A., Singh, B., Zhang, K., Ma, P., Chand, D., Ghan, S., Jimenez, J. L., Zhang, Q., Fast, J., Rasch, P. J., & Tiitta, P. (2015). Global transformation and fate of SOA: Implications of low-volatility SOA and gas-phase fragmentation reactions. *Journal of Geophysical Research – Atmospheres, 120*, 4169–4195. https://doi.org/10.1002/2014JD022563

Stavroulas, I., Bougiatioti, A., Grivas, G., Paraskevopoulou, D., Tsagkaraki, M., Zarmpas, P., Liakakou, E., Gerasopoulos, E., & Mihalopoulos, N. (2019). Sources and processes that control the submicron organic aerosol composition in an urban Mediterranean environment (Athens): A high temporal-resolution chemical composition measurement study. *Atmospheric Chemistry and Physics, 19*, 901–919. https://doi.org/10.5194/acp-19-901-2019

Stefenelli, G., Jiang, J., Bertrand, A., Bruns, E. A., Pieber, S. M., Baltensperger, U., Marchand, N., Aksoyoglu, S., Prévôt, A. S. H., Slowik, J. G., & El Haddad, I. (2019). Secondary organic aerosol formation from smoldering and flaming combustion of biomass: A box model parameterization based on volatility basis set. *Atmospheric Chemistry and Physics, 19*, 11461–11484. https://doi.org/10.5194/acp-19-11461-2019

Theodosi, C., Tsagkaraki, M., Zarmpas, P., Grivas, G., Liakakou, E., Paraskevopoulou, D., Lianou, M., Gerasopoulos, E., & Mihalopoulos, N. (2018). Multi-year chemical composition of the fine-aerosol fraction in Athens, Greece, with emphasis on the contribution of residential heating in wintertime. *Atmospheric Chemistry and Physics, 18*, 14371–14391. https://doi.org/10.5194/acp-18-14371-2018

Waked, A., Seigneur, C., Couvidat, F., Kim, Y., Sartelet, K., Afif, C., Borbon, A., Formenti, P., & Sauvage, S. (2013). Modeling air pollution in Lebanon: Evaluation at a suburban site in Beirut during summer. *Atmospheric Chemistry and Physics, 13*, 5873–5886. https://doi.org/10.5194/acp-13-5873-2013

Wang, S., Zhou, S., Tao, Y., Tsui, W. G., Ye, J., Zhen Yu, J., Murphy, J. G., McNeill, V. F., Abbatt, J. P. D., & Chan, A. W. H. (2019). Organic peroxides and sulfur dioxide in aerosol: Source of particulate sulfate. *Environmental Science & Technology, 53*, 10695–10704. https://doi.org/10.1021/acs.est.9b02591

Yttri, K. E., Simpson, D., Bergström, R., Kiss, G., Szidat, S., Ceburnis, D., Eckhardt, S., Hueglin, C., Nøjgaard, J. K., Perrino, C., Pisso, I., Prevot, A. S. H., Putaud, J.-P., Spindler, G., Vana, M., Zhang, Y.-L., & Aas, W. (2019). The EMEP Intensive Measurement Period campaign, 2008–2009: Characterizing carbonaceous aerosol at nine rural sites in Europe. *Atmospheric Chemistry and Physics, 19*, 4211–4233. https://doi.org/10.5194/acp-19-4211-2019

Particle-Gas Multiphasic Interactions

Vincent Michoud

Contents

Abstract A partition coefficient of Semi-Volatile Organic Compounds (SVOC) is defined as the ratio between concentrations of the compound in the particulate to gas phases normalized by the mass of aerosol. It is determined by the thermodynamic equilibrium between the particle (aerosol) and gas phase. This equilibrium is thought to be dominated by absorption phenomena. However, the validity of the instantaneous equilibrium between both phases and the predominance of absorption processes during the phase transfer are uncertain. It is therefore crucial to test the theoretical partition coefficient against measured ones in the field, for which in situ measurement of organic compounds in both phases needs to be performed. Such measurements have been performed at several sites in the western Mediterranean region during the ChArMEx project. It was found that the experimental values were

Chapter reviewed by ***Markus Kalberer*** *(University of Basel, Department of Environmental Sciences, Basel, Switzerland), as part of the book Part VI Recent Progress on Chemical Processes also reviewed by* ***Andrea Pozzer*** *(Max Planck Institute for Chemistry, Mainz, Germany)*

V. Michoud (✉)
Université Paris Cité and Univ. Paris Est Créteil, CNRS, LISA, F-75013 Paris, France
e-mail: vincent.michoud@lisa.ipsl.fr

F. Dulac et al. (eds.), *Atmospheric Chemistry in the Mediterranean Region*,
https://doi.org/10.1007/978-3-030-82385-6_11

systematically higher, often by several orders of magnitude, than the theoretical ones. Reasons for these discrepancies and implications for aerosol modeling are discussed.

1 Introduction

Organic aerosol can be primary or secondary. Primary organic aerosols (POA) are directly emitted into the atmosphere. Secondary organic aerosols (SOA) are formed through the oxidation of anthropogenic or biogenic gaseous organic precursors such as volatile organic compounds(VOC) by atmospheric oxidants (OH, O_3, and NO_3). This oxidation process is progressive and multigenerational. The O/C ratio of the product formed rises with growing generation of products, and their volatility decreases. This allows them to condense on existing particles leading to SOA formation or to form new particles. The semi-volatile organic compounds (SVOC) formed during the process can be in both the particulate and the gaseous phase.

Furthermore, models suggest that gaseous organic compounds can be transported over long distances and are still reactive several days after emission (Aumont et al., 2005; Madronich, 2006). They can, therefore, affect the oxidant budget as well as the formation of secondary pollutants, such as ozone and SOA, far from emission areas. The Mediterranean basin is impacted by strong natural and anthropogenic emissions and undergoes intense photochemical events (Lelieveld et al., 2002). It is, thus, a key region to study the fate of organic compounds during long-range transport and especially the interactions between gas and particle phase.

The aerosol and gaseous phase chemical composition on a molecular level is generally observed by separate analytical methods. Therefore, the multiphasic partitioning of organic compounds can usually not be addressed. Nevertheless, the study of mechanisms controlling the partitioning of SVOC between both phases is crucial to understand the formation and fate of SOA. A partition coefficient is defined according to the thermodynamic equilibrium to calculate the mass transfer of SVOC into the particulate phase (Pankow, 1994). This equilibrium is thought to be dominated by absorption phenomena (Liang et al., 1997). However, the validity of the instantaneous equilibrium between both phases and the predominance of absorption processes in the mass transfer are questionable (Healy et al., 2008; Virtanen et al., 2010; Rossignol et al., 2012; Bateman et al., 2015). It is therefore crucial to test the theoretical partition coefficient against measured ones in the real atmosphere, and this requires in situ measurement of organic compounds in both phases.

This chapter describes these interactions between particle and gaseous phases and relies mainly on the observations that have been made during the ChArMEx summer 2013 field campaign at Ersa.

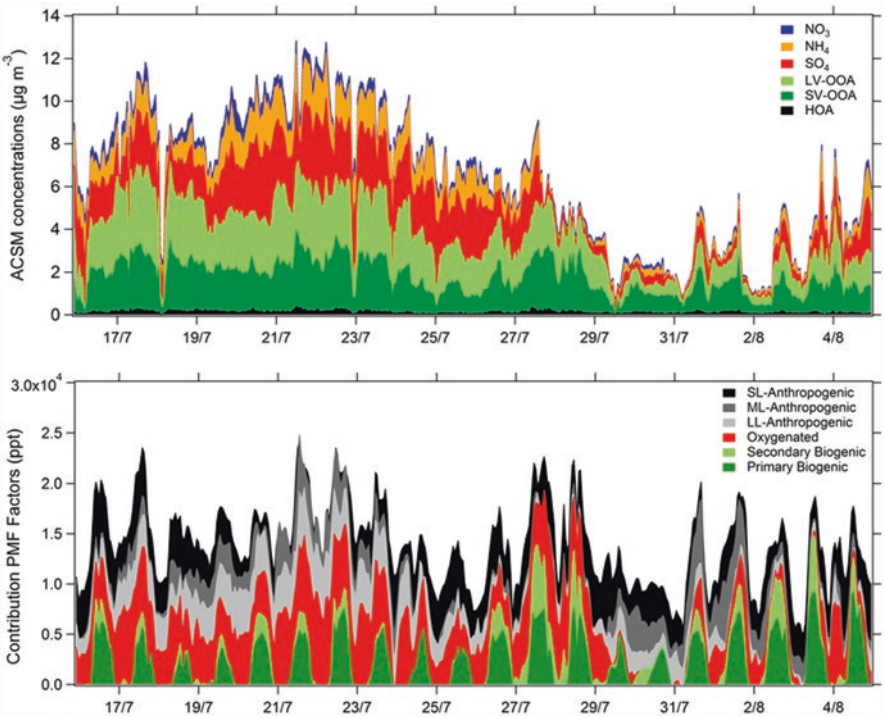

Fig. 1 Time series of accumulated aerosol fractions (top panel) and of accumulated gas phase PMF factors (bottom panel). LL-, ML-, and SL-Anthropogenic refer to the long-lived, medium-lived, and short-lived anthropogenic factors, respectively. (Adapted from Fig. 12 of Michoud et al. (2017))

2 Interconnection Between Gas Phase and Aerosol Compounds During the Summer 2013 ChArMEx Field Campaign

Figure 1 shows the time series of the accumulated different fractions (inorganic and organic) of aerosol measured by the Aerosol Chemical Speciation Monitor (ACSM) (top panel) as well as time series of accumulated contributions of Positive Matrix Factorization (PMF) factors (middle panel) for the VOCs during the summer 2013 ChArMEx field campaign at Cap Corse. This figure aims at drawing a parallel between aerosol and gas phase composition in order to highlight the link between both phases.

During the campaign, two periods correspond to aged anthropogenic air masses reaching the site (between 19 and 27 July and between 30 July and 03 August 2013; see Michoud et al., 2017). The first period is characterized by high contributions of anthropogenic and oxygenated gas PMF factors as well as an aerosol with inorganic and organic fractions in approximately similar proportions, where most inorganic

aerosol fractions have anthropogenic sources. This period also corresponds to air masses with the lowest photochemical age of the campaign (corresponding to the highest propane/ethane and butane/ethane ratios used as relative photochemical clock sensitive for anthropogenic emissions; Michoud et al., 2017), coinciding with wind coming from the north-east and therefore north of Italy, an highly industrialized region. The second period of incoming transported anthropogenic emissions from north of Italy is characterized by less intense anthropogenic gas phase PMF factors, especially for the long-lived anthropogenic factor (LL), and a clear predominance of the organic fraction for aerosols. Aerosol concentrations are also lower by approximately 50% than in the first period. During both periods, a non-negligible biogenic influence is also observed from primary and secondary biogenic PMF factors. This is even more pronounced for the second "anthropogenic" period. During these periods it is, therefore, likely that oxygenated volatile organic compounds (OVOCs) and oxygenated organic aerosols (OOA) have both biogenic and anthropogenic origins in variable proportions.

The period between 26 and 28 July corresponds to intense biogenic influence without significant long-range transport of anthropogenic emissions. This period is characterized by high contributions of the primary and secondary biogenic gas phase PMF factors. The oxygenated gas phase factor also rises during this period, and the aerosol composition is mainly dominated by the organic fraction. Indeed, the inorganic aerosol fraction decreased during this period to reach less than 10% of the aerosol composition at the end on 28 July. This strong decrease occurred when the wind sector changed from west (marine influence) to south (Cap Corse influence) at the end of this period on 28 July. This is consistent with an absence of close

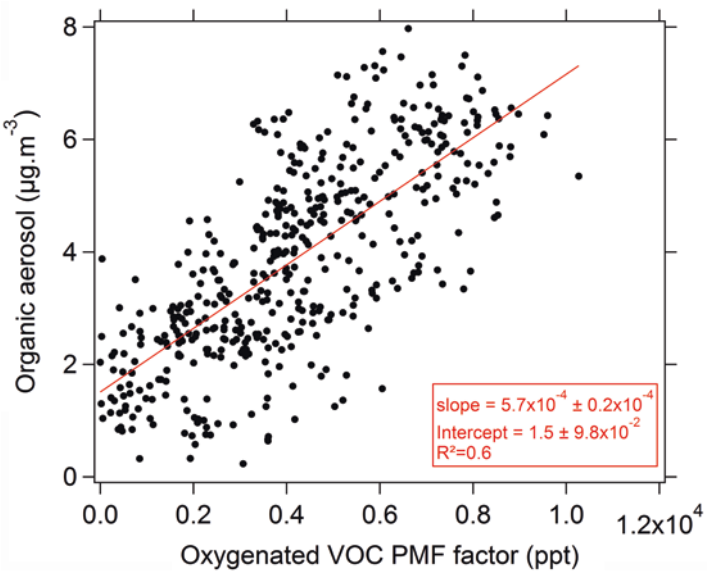

Fig. 2 Scatter plots between the organic fraction of aerosols and the contribution of the gas phase oxygenated PMF factor for the whole ChArMEx summer 2013 field campaign. (Adapted from Fig. S8 of Michoud et al. (2017))

anthropogenic influence during this period. It is therefore likely that the oxygenated VOCs and the organic fraction of aerosols during these days are mainly influenced by biogenic sources.

Such evidence for similar processes leading to aging of organics in both the gas phase and aerosols, observed during periods dominated by either anthropogenic or biogenic influence, is supported by the good correlation between organic aerosols and the PMF-derived gas phase oxygenated factor illustrated in Fig. 2.

This correlation suggests a close link between gaseous oxidation products observed at the site and measured organic aerosol (OA), while primary OA remains low despite the high concentration of OA with respect to inorganic aerosol. This also reveals that they originate from similar processes. During the campaign, very low levels of primary organic aerosols were observed (hydrocarbon-like organic aerosol (HOA) determined by ACSM measurements below 0.6 μg m^{-3}; top panel in Fig. 1). Thus, this good correlation is most likely due to the secondary fraction of OA, which can come from the oxidation of both biogenic and anthropogenic gaseous precursors, explaining the similar behavior of the organic aerosol mass and the gas phase oxygenated factor.

3 Partitioning of Organic Carbon Between the Gaseous and Particulate Phase

This close link observed between gas phase oxygenated compounds and organic aerosol highlights the interactions between both phases and, more especially, the partitioning of these oxygenated species between the gas phase and the aerosol phase. This is particularly true for the special case of the Mediterranean basin where anthropogenic and biogenic influenced air masses are mixed and undergo intense photo-oxidation over several days.

Understanding the processes governing the equilibrium between both phases requires the determination of the partitioning coefficient. An experimental partitioning coefficient can be determined by Eq. 1 (Pankow, 1994) for the compounds detected and quantified in both phases:

$$K_{pe,i} = \left(F_i / \mathrm{TSP}\right) / A_i \tag{1}$$

where $K_{pe,i}$ is the experimental partitioning coefficient for the compounds i (m^3 μg^{-1}), F_i the concentration in the particulate phase (ng m^{-3}), A_i the concentration in gaseous phase (ng m^{-3}), and TSP (total suspended particulate matter) the total mass concentration of particles measured by TEOM-FDMS (μg m^{-3}). Uncertainties for experimental partitioning coefficients taking into account averaged relative uncertainties of all parameters are estimated to be ±25% on average.

Theoretical partitioning coefficients are determined, considering an equilibrium between gaseous phase and a homogeneous liquid organic particle phase, using Eq. 2:

$$K_{pt\_i} = \left(760 \cdot R \cdot T \cdot f_{\text{om}}\right) / \left(M \cdot W_{\text{om}} \cdot \zeta_i \cdot 10^6 \cdot P^0_{L,i}\right) \quad (2)$$

where $K_{pt,i}$ corresponds to the theoretical partitioning coefficient for the compounds i ($m^3\ \mu g^{-1}$), R the ideal gas constant (m^3 atm mol^{-1} K^{-1}), T the temperature in Kelvin, f_{om} the organic matter (OM) mass fraction, MW_{om} the averaged molar mass of compounds constituting organic particulate matter (g mol^{-1}), ζ_i the activity coefficient, and $P^0_{L,i}$ the saturation vapor pressure (in Torr). Saturation vapor pressures are determined using three different models (Myrdal & Yalkowsky, 1997; Moller et al., 2008; Nannoolal et al., 2008).

Experimental and theoretical partitioning coefficients obtained during three different field campaigns (Hallemans, 2016; Rossignol et al., 2016) in the western Mediterranean basin, respectively, in the framework and 2 years before ChArMEx SOP 1b field campaign, and one campaign in the EUPHORE simulation chamber in Spain (Rossignol et al., 2016) for compounds identified in both phases are presented in Table 1. For most compounds, experimental partitioning coefficients obtained for the four campaigns compare well with a difference that can reach up to an order of magnitude (e.g., dimethylglyoxal or acrolein). These observed differences are small compared to the differences recorded between experimental and theoretical coefficients. Indeed, the theoretical coefficients differ from two to seven orders of magnitude compared to the experimental coefficients.

It is worth noting that the three models used for theoretical coefficient determination are in good agreement. For all compounds, the equilibrium determined experimentally is shifted toward the particulate phase. It is worth noting that a denuder was used upstream the filter collection for all campaigns presented in Table 1. This allows to avoid overestimation of particulate organic matter due to adsorption of semi-volatile compounds onto the filter. It excludes overestimation of experimental partitioning coefficients due to positive artifact for concentrations of compounds in the particulate phase. Underestimation of gaseous concentrations for these compounds is also unlikely since careful inter-comparisons have been performed for OVOCs between several different measurement techniques to exclude this possibility (Hallemans, 2016).

The differences observed between experimental and theoretical partitioning coefficient for some compounds (e.g., organic acids) may be explained by the high humidity conditions encountered. Indeed, the theoretical partitioning coefficient as described by Pankow equilibrium does not take into account the presence of an aqueous phase or a deliquescent aerosol, while soluble organic compounds can split between gaseous, aqueous, and non-aqueous particulate phases. This hypothesis is however not plausible for insoluble compounds such as aldehydes and ketones, for example. These differences could also be explained by the fact that the equilibrium between both phases is not reached, i.e., a kinetic delay in establishing the equilibrium. This could be due to the viscosity of particles. Some studies show that organic aerosols can be found in various states, from liquid to semi-solid (viscous) (Virtanen et al., 2010; Shiraiwa et al., 2011; Booth et al., 2014; Bateman et al., 2016). The viscosity of the particle can limit the diffusion inside the particle and therefore cause inhomogeneity in the composition with the formation of a gradient in

Table 1 Experimental ($K_{pe,i}$) and theoretical ($K_{pt,i}$) partitioning coefficients of various VOCs

	$K_{pe,i}$ from field campaigns			$K_{pe,i}$ from chamber	$K_{pt,i}$		
Compound	ChArMEx (Ersa, Corsica)[a]	CANOPEE (OHP)[a]	Citrus fruit field, Corsica[b]	EUPHORE[b]	MOL[c,f]	NAN[d,f]	MYR[e,f]
Propanal	6.1 10^{-3} ± 75%	9.7 10^{-3} ± 62%	2.2 10^{-3} ± 50%	–	2.6 10^{-10}	2.6 10^{-10}	4.7 10^{-10}
Pentanal	6.5 10^{-4} ± 106%	9.8 10^{-4} ± 92%	1.8 10^{-4} ± 51%	–	3.2 10^{-9}	3.2 10^{-9}	3.8 10^{-9}
Hexanal	1.3 10^{-3} ± 61%	–	–	–	1.0 10^{-8}	1.0 10^{-8}	1.1 10^{-8}
Heptanal	5.1 10^{-4} ± 91%	–	–	–	3.3 10^{-8}	3.2 10^{-8}	3.4 10^{-8}
Nonanal	–	1.6 10^{-4} ± 79%	5.5 10^{-2} ± 57%	–	3.1 10^{-7}	2.8 10^{-7}	3.1 10^{-7}
Acrolein	7.3 10^{-4} ± 74%	7.6 10^{-4} ± 51%	6.1 10^{-3} ± 50%	–	3.6 10^{-10}	3.6 10^{-10}	3.7 10^{-7}
Methacrolein	7.3 10^{-4} ± 69%	–	–	–	7.2 10^{-10}	7.2 10^{-10}	9.0 10^{-10}
2-butanone	–	9.5 10^{-5} ± 86%	–	–	9.8 10^{-10}	9.5 10^{-10}	7.1 10^{-10}
Acetone	–	9.2 10^{-5} ± 51%	–	–	2.7 10^{-10}	2.6 10^{-10}	2.6 10^{-10}
Hydroxyacetone	–	7.9 10^{-3} ± 107%	–	–	4.7 10^{-8}	3.4 10^{-8}	3.0 10^{-8}
Methyl vinyl ketone	5.8 10^{-4} ± 57%	–	–	–	1.3 10^{-9}	1.3 10^{-9}	5.6 10^{-10}
Nopinone	5.5 10^{-4} ± 53%	–	–	–	1.7 10^{-7}	1.7 10^{-7}	1.9 10^{-7}
4-Oxopentanal	–	7.0 10^{-3} ± 51%	5.6 10^{-4} ± 50%	6.5 10^{-4} ± 34%	1.6 10^{-8}	1.5 10^{-8}	2.9 10^{-8}
Dimethylglyoxal	5.0 10^{-3} ± 65%	2.6 10^{-3} ± 86%	5.6 10^{-4} ± 70%	6.2 10^{-4} ± 47%	–	3.4 $10^{-9\,g}$	7.0 $10^{-9\,g}$
Glyoxal	6.9 10^{-5} ± 56%	3.6 10^{-3} ± 79%	9.8 10^{-3} ± 110%		–	3.3 $10^{-8\,g}$	6.7 $10^{-10\,g}$
Methylglyoxal	3.6 10^{-3} ± 60%	3.3 10^{-3} ± 51%	2.2 10^{-2} ± 132%	1.3 10^{-3} ± 84%	–	8.6 $10^{-10\,g}$	2.1 $10^{-9\,g}$
Propenoic acid	–	3.7 10^{-4} ± 185%	–	–	5.0 10^{-8}	4.3 10^{-8}	3.7 10^{-8}
Benzoic acid	–	1.3 10^{-3} ± 240%	–	–	3.8 10^{-5}	1.9 10^{-5}	8.7 10^{-6}
Levulinic acid	5.1 10^{-3} ± 77%	5.4 10^{-3} ± 67%	–	–	1.7 10^{-5}	4.4 10^{-6}	2.9 10^{-6}
Methacrylic acid	1.5 10^{-4} ± 198%	–	–	–	8.4 10^{-8}	7.6 10^{-8}	8.9 10^{-8}
Undecanoic acid	–	1.2 10^{-3} ± 110%	–	–	3.2 10^{-3}	4.8 10^{-4}	1.8 10^{-4}

(continued)

Table 1 (continued)

Compound	$K_{pe,i}$ from field campaigns			$K_{pe,i}$ from chamber	$K_{pt,i}$		
	ChArMEx (Ersa, Corsica)[a]	CANOPEE (OHP)[a]	Citrus fruit field, Corsica[b]	EUPHORE[b]	MOL[c,f]	NAN[d,f]	MYR[e,f]
Glycolic acid	3.1 10^{-2} ± 268%	3.1 10^{-3} ± 104%	–	–	8.5 10^{-5}	1.3 10^{-5}	2.0 10^{-6}
4-Hydroxybenzoic acid	–	2.6 10^{-3} ± 59%	–	–	2.1 10^{-4}	9.9 10^{-5}	1.9 10^{-4}
Glutaric acid	–	3.4 10^{-3} ± 95%	–	–	3.9 10^{-3}	1.3 10^{-3}	2.5 10^{-4}
Succinic acid	–	1.0 10^{-2} ± 71%	–	3.2 10^{-2}	1.1 10^{-3}	3.6 10^{v4}	1.1 10^{-4}
Glycerol	1.1 10^{-2} ± 62%	5.4 10^{-4} ± 88%	–	–	7.1 10^{-4}	8.4 10^{-4}	1.3 10^{-5}

[a]Myrdal and Yalkowsky (1997)
[b]Hallemans (2016)
[c]Rossignol et al. (2016)
[d]Moller et al. (2008)
[e]Nannoolal et al. (2008)
[f]coupled with Nannoolal et al. (2004) method for boiling point determination
[g]Coefficients extracted from Rossignol et al. (2012) at temperature of 300 K; other parameters (MW_{om} et ζ_i) similar to the ChArMEx campaign

concentration between the surface and the center of the particle (Zobrist et al., 2011; Chan et al., 2014; Davies & Wilson, 2015). The equilibrium could therefore only be reached between an outer layer of the particle and the gaseous phase (Davies & Wilson, 2015). Or on the contrary, a semi-solid external layer, caused by the aging of the particle, could prevent the equilibrium to be reached between the particulate bulk and the gaseous phase. These aspects are critical for the Mediterranean basin where aging is promoted by intense photochemical activity and oxidation that occurs over a relatively long time period in the year.

Furthermore, Soonsin et al. (2010) showed that the physical state of the particle can influence the activity coefficient of some compounds and especially of dicarboxylic acids that are the dominant contributors of OA during ChArMEx campaign in Ersa/Cap Corse, for example (see Fig. 3). Partitioning coefficients are calculated considering a liquid aerosol phase. Considering a solid or semi-solid aerosol phase would lead to a decrease in the vapor pressure estimation for such compounds and therefore to higher theoretical partitioning coefficients.

In addition, oligomerization processes in the particulate phase have been highlighted in previous studies through the identification of compounds with high molecular masses (Kalberer et al., 2004; Tolocka et al., 2004; Hallquist et al., 2009; Lim et al., 2010). The formation of oligomers increases the viscosity of the particle during its aging (Abramson et al., 2013) which, as discussed above, can partly cause the disagreement observed. These reactions could also explain the presence of semi-volatile compounds in the particulate phase in such high proportion, especially for

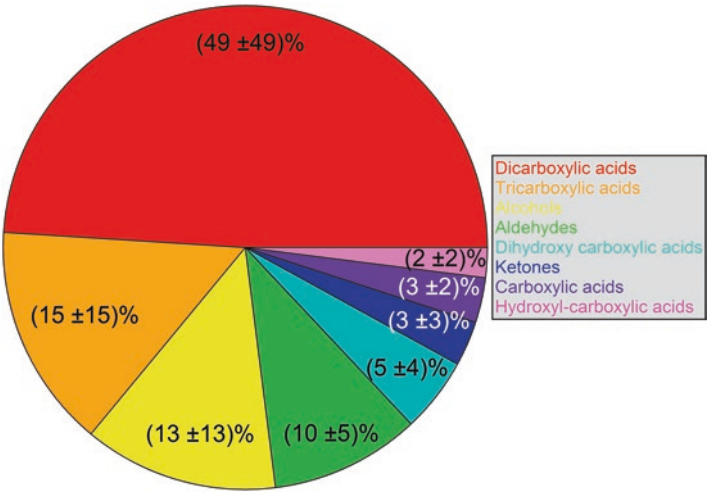

Fig. 3 Campaign averaged relative composition of the sum of all compound concentrations measured by thermal desorption and coupled gas chromatography-mass spectrometry (TD-GC/MS). (Adapted from Fig. 85 of Hallemans (2016))

carbonyls. It is worth noting that carbonyls have high vapor pressure and should not be present in the particle phase. Indeed, numerous studies reveal the possibility of formation of oligomers, inside the particle, from carbonyls such as α-di-carbonyls, for example, from glyoxal or methylglyoxal (e.g., Jang & Kamens, 2001; Iinuma et al., 2004; Tolocka et al., 2004; Hastings et al., 2005; Lim et al., 2010). These reactions are favored under low water content in the particles. On the contrary, under higher humidity conditions, oligomers can decompose back into monomer compounds which in case of a viscous layer at the surface of the particles can be trapped into the particulate phase. In that case, the equilibrium between the gaseous and the particle phase could be shifted notably in favor of the particle phase for the monomer compounds.

4 Conclusions and Recommendations

Good correlation between organic aerosols and the gas phase oxygenated component implies that similar processes lead to the formation and aging of organics in gas and particulate phases. It highlights the interactions between both phases and, more especially, the partitioning of these oxygenated species between the gas phase and the aerosol phase. This is particularly true over the Mediterranean basin where air masses under anthropogenic and biogenic influences are mixed and undergo intense photo-oxidation during several days.

However, the partitioning of the semi-volatile compounds between the gaseous particulate phases is influenced by the meteorology (humidity, temperature) and the

state of particles (viscosity, water content, organic fraction concentrations, acidity, etc.). The impact of these conditions strongly depends on the properties of the considered compounds (solubility, vapor pressure, reactivity, etc.).

This leads to differences between experimental and theoretical partitioning coefficients, which have important implications for organic aerosol modeling. It indicates that the partitioning theory, which is the base for this modeling, is most often inappropriate, unless the processes that explain the differences between experimental and theoretical partitioning coefficients are included. These processes might partly also occur in chamber experiments, from which empirical partitioning coefficients for model compounds are derived. Coefficients obtained in this way would then partly include processes shifting semi-volatile material into the particulate phase. This could explain why current aerosol schemes used in the preceding chapter (Sartelet, 2022) do not systematically underestimate organic aerosol by orders of magnitude. Furthermore, the SOA models used in this chapter (Chrit et al., 2017; Cholakian et al., 2018) were revisited in the framework of ChArMEx to take into account the formation of non-volatile organic aerosols from biogenic precursors. In addition, some schemes (Shiraiwa et al., 2011; Shrivastava et al., 2015; Couvidat & Sartelet, 2015) can take into account the viscosity of particles in order to account for deviations from ideal partitioning theory.

The study of experimental partitioning coefficients should be carried on in various types of environments and systematically compared to theoretical ones. This could help to understand under which conditions a thermodynamic control of gas/particle partitioning is effective. For other conditions, hypotheses of multi-layer particles of various viscosities and/or phases as proposed by Shiraiwa et al. (2010), Couvidat and Sartelet (2015) and as investigated in 3D by Kim et al. (2019), or of reactivity in the particulate phase should be tested comparing measurements to simulations.

References

Abramson, E., Imre, D., Beránek, J., Wilson, J., & Zelenyuk, A. (2013). Experimental determination of chemical diffusion within secondary organic aerosol particles. *Physical Chemistry Chemical Physics, 15*, 2983–2991. https://doi.org/10.1039/C2CP44013J

Aumont, B., Szopa, S., & Madronich, S. (2005). Modelling the evolution of organic carbon during its gas-phase tropospheric oxidation: Development of an explicit model based on a self generating approach. *Atmospheric Chemistry and Physics, 5*, 2497–2517. https://doi.org/10.5194/acp-5-2497-2005

Bateman, A. P., Bertram, A. K., & Martin, S. T. (2015). Hygroscopic influence on the semisolid-to-liquid transition of secondary organic materials. *The Journal of Physical Chemistry A, 119*, 4386–4395. https://doi.org/10.1021/jp508521c

Bateman, A. P., Gong, Z., Liu, P., Sato, B., Cirino, G., Zhang, Y., Artaxo, P., Bertram, A. K., Manzi, A. O., Rizzo, L. V., Souza, R. A. F., Zaveri, R. A., & Martin, S. T. (2016). Sub-micrometre particulate matter is primarily in liquid form over Amazon rainforest. *Nature Geoscience, 9*, 34–37. https://doi.org/10.1038/ngeo2599

Booth, A. M., Murphy, B., Riipinen, I., Percival, C. J., & Topping, D. O. (2014). Connecting bulk viscosity measurements to kinetic limitations on attaining equilibrium for a model aerosol

composition. *Environmental Science & Technology, 48*, 9298–9305. https://doi.org/10.1021/es501705c

Chan, M. N., Zhang, H., Goldstein, A. H., & Wilson, K. R. (2014). Role of water and phase in the heterogeneous oxidation of solid and aqueous succinic acid aerosol by hydroxyl radicals. *Journal of Physical Chemistry C, 118*, 28978–28992. https://doi.org/10.1021/jp5012022

Chrit, M., Sartelet, K., Sciare, J., Pey, J., Marchand, N., Couvidat, F., Sellegri, K., and Beekmann, M. (2017). Modelling organic aerosol concentrations and properties during ChArMEx summer campaigns of 2012 and 2013 in the western Mediterranean region, *Atmospheric Chemistry and Physics, 17, 12509–12531,* https://doi.org/10.5194/acp-17-12509-2017

Cholakian, A., Beekmann, M., Colette, A., Coll, I., Siour, G., Sciare, J., Marchand, N., Couvidat, F., Pey, J., Gros, V., Sauvage, S., Michoud, V., Sellegri, K., Colomb, A., Sartelet, K., Langley DeWitt, H., Elser, M., Prévot, A. S. H., Szidat, S., and Dulac, F.: Simulation of fine organic aerosols in the western Mediterranean area during the ChArMEx 2013 summer campaign, *Atmospheric Chemistry and Physics, 18, 7287–7312,* https://doi.org/10.5194/acp-18-7287-2018

Couvidat, F., & Sartelet, K. (2015). The Secondary Organic Aerosol Processor (SOAP v1.0) model: A unified model with different ranges of complexity based on the molecular surrogate approach. *Geoscientific Model Development, 8*, 1111–1138. https://doi.org/10.5194/gmd-8-1111-2015

Davies, J. F., & Wilson, K. R. (2015). Nanoscale interfacial gradients formed by the reactive uptake of OH radicals onto viscous aerosol surfaces. *Chemical Science, 6*, 7020–7027. https://doi.org/10.1039/C5SC02326B

Hallemans, E. (2016). Étude de la formation, du vieillissement et de la composition chimique de l'aérosol organique secondaire dans le bassin méditerranéen, PhD dissertation, Université Paris Est, Créteil, 400 pp. https://tel.archives-ouvertes.fr/tel-01542908/document

Hallquist, M., Wenger, J. C., Baltensperger, U., Rudich, Y., Simpson, D., Claeys, M., Dommen, J., Donahue, N. M., George, C., Goldstein, A. H., Hamilton, J. F., Herrmann, H., Hoffmann, T., Iinuma, Y., Jang, M., Jenkin, M. E., Jimenez, J. L., Kiendler-Scharr, A., Maenhaut, W., … Wildt, J. (2009). The formation, properties and impact of secondary organic aerosol: Current and emerging issues. *Atmospheric Chemistry and Physics, 9*, 5155–5236. https://doi.org/10.5194/acp-9-5155-2009

Hastings, W. P., Koehler, C. A., Bailey, E. L., & De Haan, D. O. (2005). Secondary organic aerosol formation by glyoxal hydration and oligomer formation: Humidity effects and equilibrium shifts during analysis. *Environmental Science & Technology, 39*, 8728–8735. https://doi.org/10.1021/es050446l

Healy, R. M., Wenger, J. C., Metzger, A., Duplissy, J., Kalberer, M., & Dommen, J. (2008). Gas/particle partitioning of carbonyls in the photooxidation of isoprene and 1,3,5-trimethylbenzene. *Atmospheric Chemistry and Physics, 8*, 3215–3230. https://doi.org/10.5194/acp-8-3215-2008

Iinuma, Y., Böge, O., Gnauk, T., & Herrmann, H. (2004). Aerosol-chamber study of the α-pinene/O3 reaction : Influence of particle acidity on aerosol yields and products. *Atmospheric Environment, 38*, 761–773. https://doi.org/10.1016/j.atmosenv.2003.10.015

Jang, M., & Kamens, R. M. (2001). Atmospheric secondary aerosol formation by heterogeneous reactions of aldehydes in the presence of a sulfuric acid aerosol catalyst. *Environmental Science & Technology, 35*, 4758–4766. https://doi.org/10.1021/es010790s

Kalberer, M., Paulsen, D., Sax, M., Steinbacher, M., Dommen, J., Prevot, A. S. H., Fisseha, R., Weingartner, E., Frankevich, V., Zenobi, R., & Baltensperger, U. (2004). Identification of polymers as major components of atmospheric organic aerosols. *Science, 303*, 1659–1662. https://doi.org/10.1126/science.1092185

Kim, Y., Sartelet, K., & Couvidat, F. (2019). Modeling the effect of non-ideality, dynamic mass transfer and viscosity on SOA formation in a 3-D air quality model. *Atmospheric Chemistry and Physics, 19*, 1241–1261. https://doi.org/10.5194/acp-19-1241-2019

Lelieveld, J., Berresheim, H., Borrmann, S., Crutzen, P. J., Dentener, F. J., Fischer, H., Feichter, J., Flatau, P. J., Heland, J., Holzinger, R., Korrmann, R., Lawrence, M. G., Levin, Z., Markowicz, K. M., Mihalopoulos, N., Minikin, A., Ramanathan, V., de Reus, M., Roelofs, G. J., … Ziereis, H. (2002). Global air pollution crossroads over the Mediterranean. *Science, 298*, 794–799. https://doi.org/10.1126/science.1075457

Liang, C., Pankow, J. F., Odum, J. R., & Seinfeld, J. H. (1997). Gas/particle partitioning of semivolatile organic compounds to model inorganic, organic, and ambient smog aerosols. *Environmental Science & Technology, 31*, 3086–3092. https://doi.org/10.1021/es9702529

Lim, Y. B., Tan, Y., Perri, M. J., Seitzinger, S. P., & Turpin, B. J. (2010). Aqueous chemistry and its role in secondary organic aerosol (SOA) formation. *Atmospheric Chemistry and Physics, 10*, 10521–10539. https://doi.org/10.5194/acp-10-10521-2010

Madronich, S. (2006). Chemical evolution of gaseous air pollutants downwind of tropical megacities: Mexico City case study. *Atmospheric Environment, 40*, 6012–6018. https://doi.org/10.1016/j.atmosenv.2005.08.047

Michoud, V., Sciare, J., Sauvage, S., Dusanter, S., Léonardis, T., Gros, V., Kalogridis, C., Zannoni, N., Féron, A., Petit, J.-E., Crenn, V., Baisnée, D., Sarda-Estève, R., Bonnaire, N., Marchand, N., DeWitt, H. L., Pey, J., Colomb, A., Gheusi, F., … Locoge, N. (2017). Organic carbon at a remote site of the western Mediterranean Basin: Sources and chemistry during the ChArMEx SOP2 field experiment. *Atmospheric Chemistry and Physics, 17*, 8837–8865. https://doi.org/10.5194/acp-17-8837-2017

Moller, B., Rarey, J., & Ramjugernath, D. (2008). Estimation of the vapour pressure of non-electrolyte organic compounds via group contributions and group interactions. *Journal of Molecular Liquids, 143*, 52–63. https://doi.org/10.1016/j.molliq.2008.04.020

Myrdal, P. B., & Yalkowsky, S. H. (1997). Estimating pure component vapor pressures of complex organic molecules. *Industrial and Engineering Chemistry Research, 36*, 2494–2499. https://doi.org/10.1021/ie9502421

Nannoolal, Y., Rarey, J., Ramjugernath, D., & Cordes, W. (2004). Estimation of pure component properties: Part 1. Estimation of the normal boiling point of non-electrolyte organic compounds via group contributions and group interactions. *Fluid Phase Equilibria, 226*, 45–63. https://doi.org/10.1016/j.fluid.2004.09.001

Nannoolal, Y., Rarey, J., & Ramjugernath, D. (2008). Estimation of pure component properties: Part 3. Estimation of the vapor pressure of non-electrolyte organic compounds via group contributions and group interactions. *Fluid Phase Equilibria, 269*, 117–133. https://doi.org/10.1016/j.fluid.2008.04.020

Pankow, J. F. (1994). An absorption model of gas/particle partitioning of organic compounds in the atmosphere. *Atmospheric Environment, 28*, 185–188. https://doi.org/10.1016/1352-2310(94)90093-0

Rossignol, S., Chiappini, L., Perraudin, E., Rio, C., Fable, S., Valorso, R., & Doussin, J. F. (2012). Development of a parallel sampling and analysis method for the elucidation of gas/particle partitioning of oxygenated semi-volatile organics: A limonene ozonolysis study. *Atmospheric Measurement Techniques, 5*, 1459–1489. https://doi.org/10.5194/amt-5-1459-2012

Rossignol, S., Couvidat, F., Rio, C., Fable, S., Grignion, G., Savelli, Pailly, O., Leoz-Garziandia, E., Doussin, J.-F., & Chiappini, L. (2016). Organic aerosol molecular composition and gas-particle partitioning coefficients at a Mediterranean site (Corsica). *Journal of Environmental Sciences, 40*, 92–104. https://doi.org/10.1016/j.jes.2015.11.017

Sartelet, K. (2022). Secondary aerosol formation and their modeling. In F. Dulac, S. Sauvage, & E. Hamonou (Eds.), *Atmospheric chemistry in the Mediterranean Region* (Vol. 2, From air pollutant sources to impacts). Springer, this volume. https://doi.org/10.1007/978-3-030-82385-6_10

Shiraiwa, M., Pfrang, C., & Poschl, U. (2010). Kinetic multi-layer model of aerosol surface and bulk chemistry (KM-SUB): The influence of interfacial transport and bulk diffusion on the

oxidation of oleic acid by ozone. *Atmospheric Chemistry and Physics, 10*, 3673–3691. https://doi.org/10.5194/acp-10-3673-2010

Shiraiwa, M., Ammann, M., Koop, T., & Pöschl, U. (2011). Gas uptake and chemical aging of semisolid organic aerosol particles. *Proceedings of the National Academy of Sciences, 108*, 11003–11008. https://doi.org/10.1073/pnas.1103045108

Shrivastava, M., Easter, R. C., Liu, X., Zelenyuk, A., Singh, B., Zhang, K., Ma, P., Chand, D., Ghan, S., Jimenez, J. L., Zhang, Q., Fast, J., Rasch, P. J., & Tiitta, P. (2015). Global transformation and fate of SOA: Implications of low-volatility SOA and gas-phase fragmentation reactions. *Journal of Geophysical Research – Atmospheres, 120*, 4169–4195. https://doi.org/10.1002/2014JD022563

Soonsin, V., Zardini, A. A., Marcolli, C., Zuend, A., & Krieger, U. K. (2010). The vapor pressures and activities of dicarboxylic acids reconsidered: The impact of the physical state of the aerosol. *Atmospheric Chemistry and Physics, 10*, 11753–11767. https://doi.org/10.5194/acp-10-11753-2010

Tolocka, M. P., Jang, M., Ginter, J. M., Cox, F. J., Kamens, R. M., & Johnston, M. V. (2004). Formation of oligomers in secondary organic aerosol. *Environmental Science & Technology, 38*, 1428–1434. https://doi.org/10.1021/es035030r

Virtanen, A., Joutsensaari, J., Koop, T., Kannosto, J., Yli-Pirilä, P., Leskinen, J., Mäkelä, J. M., Holopainen, J. K., Pöschl, U., Kulmala, M., Worsnop, D. R., & Laaksonen, A. (2010). An amorphous solid state of biogenic secondary organic aerosol particles. *Nature, 467*, 824–827. https://doi.org/10.1038/nature09455

Zobrist, B., Soonsin, V., Luo, B. P., Krieger, U. K., Marcolli, C., Peter, T., & Koop, T. (2011). Ultra-slow water diffusion in aqueous sucrose glasses. *Physical Chemistry Chemical Physics, 13*, 3514–3526. https://doi.org/10.1039/C0CP01273D

Part VII
Mediterranean Aerosol Properties

Coordinated by ***Paola Formenti***
Université Paris Cité and Univ. Paris Est Créteil, CNRS, LISA, F-75013 Paris, France
paola.formenti@lisa.ipsl.fr

Reviewed by ***Jorge Pey Betrán*** *(ARAID-Instituto Pirenaico de Ecología, CSIC, Zaragoza, Spain)*

Abstract

In this section we review the properties of the Mediterranean aerosols that determine their effects on the regional climate and air quality. Analysed observations from the most recent large-scale experiments are presented, and put into the larger historical context. The emphasis is on fundamental variables, such as inorganic and organic composition, particle size distribution, optical properties of scattering and absorption, and hygroscopicity at sub- and super-saturation conditions.

Aerosol Size Distribution

Claudia Di Biagio

Contents

Abstract Particle size is a fundamental parameter to understand and predict the lifetime, transport processes, and the diverse impacts of atmospheric aerosols. In this chapter, we review current knowledge on the size distribution of atmospheric aerosols observed in the Mediterranean basin. This includes remote sensing observations, as well as ground-based and airborne in situ measurements from intensive field campaigns over the last two decades. Observations show that the volume aerosol size distribution above 100 nm diameter is basically bimodal in the whole Mediterranean basin, with anthropogenic particles mostly contributing to the fine mode and dust, smoke, and marine particles contributing to the coarse mode. Coarse and giant dust particles measured for Saharan outbreaks agree with similar observations in the Atlantic, supporting the efficient transport of dust aerosols with diameters above 10μm over long distances. Ultrafine particles (<100 nm diameter) are ubiquitous over the basin and observed both in the boundary layer and the free troposphere. While past observations provide significant knowledge, at present we still miss a complete regional characterization of the aerosol size over the whole basin

Chapter reviewed by ***Konrad Kandler*** *(Institut für Angewandte Geowissenschaften, Technische Universität Darmstadt, Darmstadt, Germany) and* ***Marc Mallet*** *(Centre National de Recherches Météorologiques, Toulouse, France), as part of the book Part VII Mediterranean Aerosol Properties also reviewed by* ***Jorge Pey Betrán*** *(ARAID-Instituto Pirenaico de Ecología, CSIC, Zaragoza, Spain)*

C. Di Biagio (✉)
Université Paris Cité and Univ. Paris Est Créteil, CNRS, LISA, F-75013 Paris, France
e-mail: claudia.dibiagio@lisa.ipsl.fr

F. Dulac et al. (eds.), *Atmospheric Chemistry in the Mediterranean Region*,
https://doi.org/10.1007/978-3-030-82385-6_12

including seasonal effects. Further observation and retrieval capabilities from satellites need to be developed to fulfill this gap.

1 Preamble and Definitions

We define in this section the basic information concerning the atmospheric aerosol size distribution, and we introduce the parameters presented and discussed in the chapter. For a complete discussion and analysis of theoretical bases, we redirect the reader to Seinfeld and Pandis (2016).

Atmospheric aerosols cover a vast size spectrum, from few nanometers to tens of micrometers. Particles with diameters less than 1μm are classified as "fine aerosols," while particles greater than 1μm are "coarse aerosols." Fine aerosols are additionally divided into Aitken or ultrafine mode particles (diameter < 0.1μm) and accumulation mode particles (diameter between 0.1 and 1.0μm; to note that in some literature studies the separation between Aitken and accumulation modes is at radius of 0.1μm instead of the diameter). The size distribution and the partitioning between the fine and coarse modes for different aerosol types depend first on their formation mechanism. Coarse mode aerosols are usually made of primary particles, mostly of natural origin. Primary aerosol particles are defined as particles directly entrained into the atmosphere by the drag of wind on continental and oceanic surfaces (desert dust or sea salt aerosols), as a product of biomass burning (soot and ashes), volcanic eruptions, or biological debris, among others. In contrast, anthropogenic aerosols occur mostly in the fine mode, and they are often secondary in origin. Secondary aerosols are formed in the atmosphere from gaseous precursors (e.g., new particle formation (NPF) from gas-to-particle conversion), and they can be both natural and anthropogenic. Once in the atmosphere, the aerosol size distribution continuously modifies due to processes like coagulation, sedimentation, heterogeneous reactions with gases, water adsorption, and mixing (Seinfeld & Pandis, 2016).

The size distribution of the aerosols is typically expressed as the number distribution $dN(D)/d\log D$ where $dN(D)$ is the number concentration of particles, i.e., the number of particles per cm^3 of air, per size interval expressed in logarithmic scale ($d\log D = \log(D_2/D_1)$, with D_1 and D_2 the lower and upper diameters of the size bin. Similarly, the number distribution can be expressed as a function of the particle radius (R) as $dN(R)/d\log R$ knowing that the two definitions are equivalent since $d\log D = d\log R$. Both the decimal ($d\log_{10} D$) and the natural ($d\ln D$) logarithm can be used in the size formulation, and both are currently found in the literature. The decimal and logarithmic formulations are related by a constant proportionality that is $dN/d\log D = \ln(10)\, dN/d\ln D$.

Because several aerosol properties depend on the aerosol surface, volume, and mass, it is often convenient to express the aerosol size distribution in the form of surface size distribution ($dS/d\log D = \pi D^2\, dN/d\log D$ in the approximation of spherical particles, unit of $\mu m^2\ cm^{-3}$), volume distribution ($dV/d\log D = \pi/6\, D^3\, dN/d\log D$, unit of $\mu m^3\ cm^{-3}$), and mass distribution ($dM/d\log D = \rho\, dV/d\log D$, units of

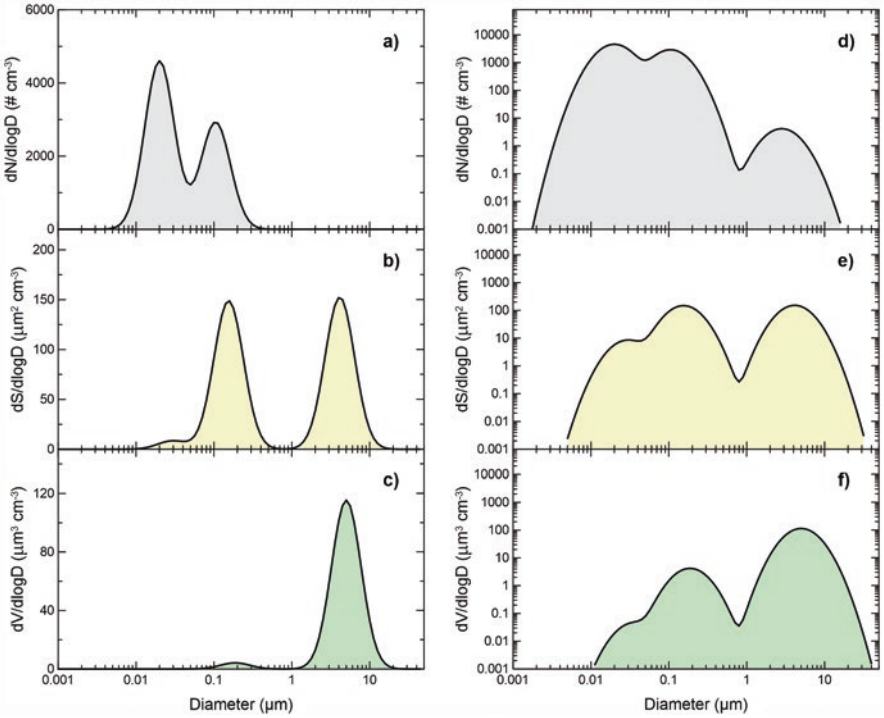

Fig. 1 Example of an atmospheric aerosol size distribution composed of three lognormal modes; **a and d** number size distribution; **b and e** surface size distribution; **c and f** volume size distribution. Distributions are plotted in linear and logarithmic ordinate scales (left and right plots, respectively). (Modified from Fig. 8.6 in Seinfeld and Pandis (2016))

μg cm^{-3}, where ρ is the aerosol particle density, e.g., as g cm^{-3}). These formulations represent the distribution of the surface area, volume, and mass of particles per cm^3 of air.

The size distribution of atmospheric aerosols usually appears as the sum of main modes, each of them well represented by a lognormal distribution, i.e., the log$D$ or ln$D$ are normally distributed. In Fig. 1, we report an example of number, surface, and volume distribution for a typical atmospheric aerosol population composed of the sum of three lognormal modes including both submicronic and supermicronic particles. The number modal diameter, which is the diameter at which the derivative of the distribution is zero (in other words the mode maximum), is 0.02, 0.10, and 2.8μm for the three modes. Figure 1 shows that the submicronic aerosol modes dominate the number distribution (Fig. 1a and d), whereas the supermicronic aerosol mode dominates the volume size (Fig. 1c and f). This is because the volume of a particle of 1 or 10μm in diameter is 10^3 or 10^6 times larger than that of a particle of 100 nm in diameter. Showing the size distribution data as a function of number or volume can permit therefore to better evidence the contribution of fine or ultrafine particles (number representation) or coarse mode diameters (volume representation) to the whole dust size spectrum.

The number-, surface-, volume-, and mass-median diameter (NMD, SMD, VMD, and MMD, units of length) are respectively the diameters for which half of the number, surface, volume, and mass of the aerosol population is for diameters below the median diameter and the other half above. For lognormal distributed aerosols, the median diameter coincides with the modal diameter of the distribution. The different median diameters represent different properties of the size distribution, and their values are not directly comparable, with the only exception for the VMD and the MMD that coincide if the aerosol density is constant with size. As an example, for the three modes in Fig. 1, the NMD is 0.02, 0.10, and 2.8μm, and the VMD is 0.04, 0.2, and 5μm. The aerosol particle size distribution is generally represented by a sum of lognormal modes, with the advantage that a lognormal size distribution has the same geometric standard deviation (σ) in number, size, or volume and that a simple relationship relates the various median numbers (e.g., VMD = NMD $\exp\{3(\ln\sigma)^2\}$; Jaenicke, 1988).

Other size-related parameters frequently used to describe the aerosol size distribution are the (optical) effective radius (R_{eff}; or the effective diameter D_{eff}, that is twice R_{eff}), the effective variance (v_{eff}), and the Angström exponent of scattering/extinction (α). These are defined as follows.

- **The effective radius (R_{eff}), effective diameter (D_{eff}), and effective variance (v_{eff})**

The effective radius R_{eff} (unit of length), or area-weighted mean radius, is calculated by weighting each radius by the cross-sectional area of the particles (πR^2 d$N(R)$ / dlog$R$):

$$R_{\text{eff}} = \frac{\int R\pi R^2 \frac{\mathrm{d}N}{\mathrm{d}\log R}\mathrm{d}\log R}{\int \pi R^2 \frac{\mathrm{d}N}{\mathrm{d}\log R}\mathrm{d}\log R} = \frac{\int \pi R^3 \frac{\mathrm{d}N}{\mathrm{d}\log R}\mathrm{d}\log R}{\int \pi R^2 \frac{\mathrm{d}N}{\mathrm{d}\log R}\mathrm{d}\log R} \tag{1}$$

The corresponding definition of D_{eff} is:

$$D_{\text{eff}} = \frac{\int \pi D^3 \frac{\mathrm{d}N}{\mathrm{d}\log D}\mathrm{d}\log D}{\int \pi D^2 \frac{\mathrm{d}N}{\mathrm{d}\log D}\mathrm{d}\log D} \tag{2}$$

In parallel, we can also define the effective variance, that is, a measure of the width of the aerosol distribution (unitless), as:

$$v_{\text{eff}} = \frac{\int \left(R - R_{\text{eff}}\right)^2 R^2 \frac{\mathrm{d}N}{\mathrm{d}\log R}\mathrm{d}\log R}{R_{\text{eff}^2} \int R^2 \frac{\mathrm{d}N}{\mathrm{d}\log R}\mathrm{d}\log R} \tag{3}$$

The term "effective" refers to the light extinction properties of the aerosol population, since the capacity of aerosols to extinct radiation is proportional to the cross-sectional area in the limit of geometric optics, i.e., when the radius of the particle is similar or larger than the wavelength of the incident light. Therefore, the effective radius or effective diameter are particularly useful when referring to the optical properties of aerosols. Aerosol populations with both the same R_{eff} (or D_{eff}) and v_{eff} will show a similar optical behavior. The R_{eff} or D_{eff} can be calculated for the entire aerosol size distribution (entire range of documented radius or diameters) or evaluated separately for the fine and coarse fractions of the aerosols size, for instance, by integrating Eq. 2 for diameters ≤1μm ($D_{\text{eff, fine}}$) and >1μm ($D_{\text{eff, coarse}}$), respectively. It should be mentioned that the retrieved values for the fine and coarse effective radius or diameter critically depend on the selected size range of calculation, i.e., the lower and upper limit of the documented size distribution. As a consequence, the R_{eff} and D_{eff} from sizes measured with instruments with different dynamical ranges are not always directly comparable.

- **The Angström Exponent (AE)**

The unitless Angström exponent (AE) represents the spectral dependence of extinction or aerosol optical depth (AOD). The AOD depends on the wavelength (λ) of light according to the power law (Angström, 1929):

$$AOD_{\lambda} = AOD_{\lambda_0} \left(\frac{\lambda}{\lambda_0} \right)^{-AE} \tag{4}$$

The Angström exponent is the exponent of the power law in Eq. 4. For non-absorbing aerosols, the Angström exponent is a good proxy for the aerosol particle size distribution: in general, the larger the particles, the lower AE, and vice versa.

2 Observations

Currently, most of the knowledge on the Mediterranean aerosol size distribution is derived from in situ and remote sensing measurements. The majority were made at coastal sites around the basin or at island locations. Also, local- and regional-scale intensive studies including aircraft and balloon-borne observations importantly contributed.

2.1 Ground-Based Remote Sensing Measurements

The AERONET (Aerosol Robotic Network; https://aeronet.gsfc.nasa.gov), due to its extensive coverage of the area and the long-term track of observations available (more than 20 years for some stations), is the first source of information on the size

distribution for Mediterranean aerosols. The AERONET network is a global network of ground-based multi-spectral sun and sky photometers measuring daytime aerosol load and properties (Holben et al., 1998). The AERONET operational analysis protocol retrieves the aerosol size distribution in the range 0.1–30μm in diameter by mathematical inversion of combined direct solar irradiance and sky radiance measurements (Dubovik & King, 2000; Dubovik et al., 2006). In this case, the retrieved size distribution is column-integrated, that is, it represents the mean size distribution of the various aerosol layers encountered from ground level up to the top of the atmosphere. The AERONET retrievals, being based on remote sensing measurements of the aerosol optical signature, depend on particle shape (Dubovik et al., 2006). The latest AERONET retrieval scheme works considering an aerosol mixture of polydisperse randomly oriented homogeneous spheroids with a fixed distribution of aspect ratios (Mishchenko et al., 1997; Dubovik et al., 2006).

As of mid-2022, there are about 50 active AERONET sites around the Mediterranean basin (see Fig. A1 in the volume annex; Dulac et al., 2023). Their regional distribution is quite homogeneous and covers the western and the eastern parts, from southern Europe to the coasts of Middle East and North Africa, including also many island locations throughout the area (Ersa, Palma de Mallorca, Lampedusa, Alboran, Malta, Crete, etc.). This spatial extent allows for capturing the diversity of the Mediterranean aerosol population resulting from the different contributing sources, such as desert dust, marine, urban/industrial pollution, and biomass burning, showing particles in the 0.1–30μm optically active range sensed by AERONET. On the other hand, AERONET observations do not provide information on the aerosol ultrafine mode, therefore no indications of NPF events.

Various studies reporting AERONET observations across the Mediterranean discuss the retrieved column-integrated volume distributions (e.g., Kubilay et al., 2003; Masmoudi et al., 2003a, b; Derimian et al., 2006; Toledano et al., 2007; Mallet et al., 2013, 2016; Sicard et al., 2016; Logothetis et al., 2020) or the Angström exponent (e.g., Sabbah et al., 2001; Pace et al., 2006; Basart et al., 2009; Formenti et al., 2018; Logothetis et al., 2020). A statistical study of the long-term AERONET size data across the Mediterranean basin was performed by Mallet et al. (2013) using datasets from 22 AERONET coastal stations with more than 2.5 yr of data. They showed that the volume size distribution of the aerosols in the basin is bimodal and that the coarse mode usually dominates over the fine mode (Fig. 2): in the eastern (western) part of the Mediterranean, they found a 31% (37%) average contribution from the fine mode and 69% (63%) contribution from the coarse mode to the total particle's volume size. The average modal diameter for the fine mode is located around 0.3μm, whereas for the coarse mode, it is between 4.5 and 5.0μm (Mallet et al., 2013, 2016). Daily and seasonal data show nonetheless a spread of both modal diameters and concentration values for the fine and coarse modes due to the variable contribution of different aerosol types and loading conditions (Mallet et al., 2016; Sicard et al., 2016).

Gkikas et al. (2016) made a similar statistical study than Mallet et al. (2013), but also included inland areas around the basin for a total of 109 stations from the year 2000 to 2013. They found that the two distinct fine and coarse modes in the

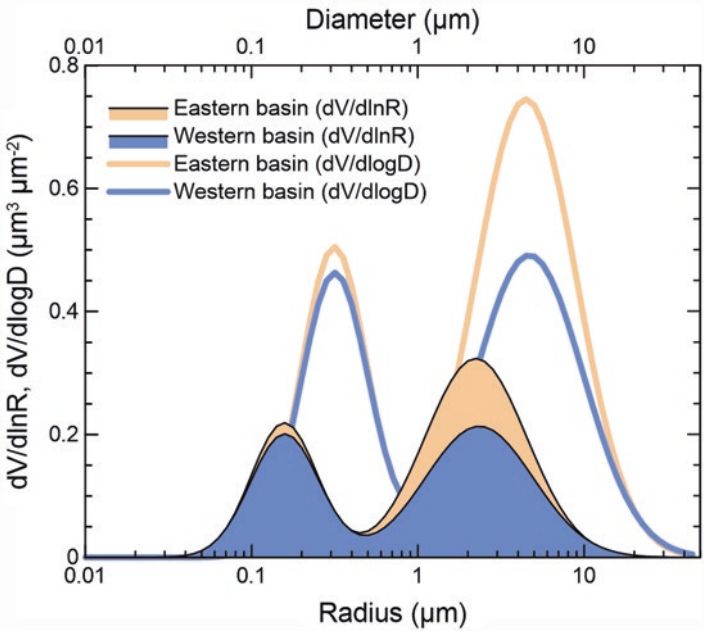

Fig. 2 Average volume size distribution retrieved from AERONET inversions at 8 coastal sites in the eastern Mediterranean basin and 14 coastal sites in the western basin. We show here both the d*V*/dln*R* distributions as provided by Mallet et al. (2013) and given as AERONET output and also the conversion into d*V*/dlog*D* formulation. Note that the unit for the volume distribution is μm^3 μm^{-2} in AERONET as it refers to a column-averaged quantity. (Modified from Fig. 8 in Mallet et al. (2013))

climatological aerosol size distribution (average modal diameters at 0.3 and 4.4μm) equally contribute to the volume size, differently from Mallet et al. (2013), where this difference was due to the larger contribution of finer aerosols from continental Europe included in their study. They also analyzed the shape of the distribution under strong and severe dust episodes and found in these cases that the size is still bimodal (about 0.3 and 3.4–4.5μm modal diameters for the fine and coarse modes), but the peak of the coarse mode increases by up to 15 times due to the contribution of coarse dust, in accordance with other studies (e.g., Kubilay et al., 2003; Tafuro et al., 2006). Also for fresh smoke plumes measured in coastal Spain, the size is bimodal. The fine mode is centered at 0.26–0.29μm (volume modal diameter), similarly to dust, and the coarse mode is at about 5.0μm (Alados-Arboledas et al., 2011; Gómez-Amo et al., 2017). This agrees with AERONET values reported for biomass burning aerosols all over the world (Sayer et al., 2014). Similar to dust and smoke, marine aerosols observations at the Ersa site in northern Corsica in summer 2013 show a fine mode located around 0.3μm, but a larger coarse mode at about 7μm, consistently with in situ surface data taken at the same site (Claeys et al., 2017). The study by Gerasopoulos et al. (2007) compared the mass size distributions obtained by cascade impactor sampling to those retrieved by AERONET between

2004 and 2006 at a remote coastal station in Greece. Seven distinct modes are identified in the diameter range 0–10μm. Of these, the "Accumulation 1" (0.25–0.55μm) and "Coarse 2" (3–7μm) modes are dominant, in line with the AERONET studies.

2.2 In Situ Measurements

In order to more thoroughly characterize the impacts of atmospheric aerosols on climate and health, one has to know their number, surface, and volume/mass size distributions on the largest possible size spectrum, including ultrafine and coarse diameters. This type of measurement is complex, as it requires a combination of various in situ analyzers based on different physical principles for different size classes. The submicron fraction of atmospheric aerosols is commonly sized in terms of the electrical mobility diameter (i.e., the diameter of a sphere with the same migration velocity in a constant electric field as the particle of interest) by using the differential mobility particle sizer (DMPS), working in the range going from few nm up to 900 nm. Optical particle counters (OPCs) use the light scattering technique to provide the aerosol number size distribution between approximately 300 nm to 100μm as optical equivalent diameter (i.e., the diameter of a sphere of given or assumed refractive index scattering the same amount of radiation into a given solid angle). Aerosol sizing over a large diameter range including supermicron diameters can be also performed by individual particle characterization by transmission and/or scanning electron microscopy on particles collected by filtration or impaction; in this case, the size distribution is expressed as a function of the projected−area equivalent diameter (i.e., the diameter of a circle with the same area of the particle under investigation as obtained from the 2-dimensional aerosol image projection). The aerosol size distribution in terms of the aerodynamic diameter (i.e., the diameter of a sphere of unit density having the same terminal velocity in an accelerated airflow as the irregularly shaped particles) can be measured by Aerodynamic Particle Sizers (APS), working in the range going from about 500 nm to 20μm. Finally, multistage filtration or cascade impaction sampling coupled with gravimetric or chemical analysis can be applied to retrieve the mass size distributions of aerosols. The full aerosol number/mass size distribution over the entire sub- to supermicron diameter range can be reconstructed from the combination of these different measurement techniques, an exercise which however is far from being without ambiguity (e.g., DeCarlo et al., 2004; Formenti et al., 2011; Ryder et al., 2013) for two main reasons: first, the necessity to refer to a same diameter definition (electrical mobility, optical, projected-area, aerodynamic) when combining different datasets, which implies performing a priori assumptions on the physicochemical properties of the (generally unknown) aerosol population and, second, the possible occurrence of size-dependent biases possibly varying with the sizing technique as a function of the specific sampling conditions, i.e., lowered sampling efficiencies for specific size ranges. This second issue may particularly affect airborne data from research aircraft

due to the low pressure and high speed (Ryder et al., 2013). In order to ensure the robustness of the obtained aerosol size distribution, whenever it is possible, the accuracy of the collected data should be evaluated through validation/intercomparison studies based on mass and optical closures.

Numerous intensive campaigns using both ground-based, airborne, and balloon-borne platforms reported on in situ measurements of the number and mass size distributions across the Mediterranean basin using mostly optical and condensation counters and multistage impactor sampling (Table 1). Although spatially sparse and often focused on specific events, these data constitute the most accurate method for describing in detail the spatial and vertical variability of the aerosol size distribution on scales ranging from local to regional. In particular, airborne observations are among the only in situ data of aerosol size distribution over the sea surface. Often the mass size distribution is reported for individual chemical components by using a combination of impactor sampling and analysis by ion beam or chemical extraction techniques (e.g., Dulac et al., 1989; Ichoku et al., 1999; Maenhaut et al., 1999; Formenti et al., 2001; Masmoudi et al., 2003b; Smolík et al., 2003; Kuloglu & Tuncel, 2005). This allows distinguishing the relative contribution of anthropogenic and natural sources to the aerosol load. As an example, at Sde Boker in Israel, the fine mode mass distribution is dominated by anthropogenic aerosols generated by conversion of long-range transported SO_2 and other combustion products, whereas an enhancement in the coarse mode is related to intrusion of Saharan mineral dust (Maenhaut et al., 1999). These authors were also able to identify the seasonal cycle in the relative contributions of pollution and dust to size distribution.

Recent airborne data, and in particular those acquired during the project ChArMEx (Chemistry-Aerosol Mediterranean Experiment) including the TRAQA, SAFMED, and ADRIMED surface and airborne campaigns in summers 2012 and 2013, have provided new data of the ultrafine and coarsest aerosol modes and their vertical and spatial distribution across the Mediterranean, which we explore further in the two following paragraphs.

2.3 In Situ Observations of the Ultrafine Particle Mode

As part of ChArMEx, the TRAQA and SAFMED airborne campaigns in the northwestern Mediterranean basin have evidenced the presence of both fine and ultrafine aerosols as far as 250 km from the coastline (and up to 4 km in height) in summertime (Di Biagio et al., 2015, 2016). The combined analysis of the plumes chemical composition and size suggested the mixing of fresh and aged pollution air masses mostly corresponding to export from inland areas and coastal cities in southern Europe. Below 350 m in the boundary layer, the volume size distribution had two equally abundant main modes, occurring frequently in the Mediterranean as indicated from AERONET observations. The fine mode is centered between 0.13 and 0.23μm and the coarse one between 5 and 8μm as number modal diameter (NMD), corresponding to a fine mode of 0.15–0.25μm and a coarse mode between 4 and

Table 1 Summary of intensive studies targeted at aerosol physicochemical and radiative properties and including size observations performed in the Mediterranean basin in the last two decades based on in situ measurements using ground-based and airborne platforms

Location	Level/ Platform	Campaign	Period	References
Negev desert, Israel	Surface	ARACHNE (Aerosol, RAdiation and CHemistry Experiment)	Summer 1996	Ichoku et al. (1999) Maenhaut et al. (1999), Formenti et al. (2001), Andreae et al. (2002)
Thessaloniki, Greece	Surface	MEDUSE (MEditerranean DUSt Experiment)	June 1997	Chazette and Liousse (2001)
Southern Aegean Sea and Finokalia, Crete	Airborne and surface	STAAARTE (Scientific Training and Access to Aircraft for Atmospheric Research Throughout Europe)	June 1997	Dulac and Chazette (2003)
Aegean Sea	Airborne	STAAARTE-MED (Scientific Training and Access to Aircraft for Atmospheric Research Throughout Europe - Mediterranean campaign)	Summer 1998	Formenti et al. (2002)
Lampedusa Isl., Italy	Airborne, Surface	PAUR (Photochemical Activity and Ultraviolet Radiation)	May 1999	Junkermann (2001), Di Iorio et al. (2003)
Mt. Cimone, Italy	Surface	MINATROC (Mineral Dust and Tropospheric Chemistry)	June–Dec. 2000	Bonasoni et al. (2004)
			June–July 2000	Van Dingenen et al. (2005)
Lampedusa Isl., Italy	Surface	C–MARE (Central Mediterranean Aerosol and Radiation Experiment)	Sept.–Oct. 2004	di Sarra et al. (2005)
	Airborne, Surface	GAMARF (Ground–based and Airborne Measurement of the Aerosol Radiative Forcing)	April–May 2008	Meloni et al. (2015)
Basilicata, Italy	Airborne	MORE (Marine Ozone and Radiation Experiment)	June 2010	Pace et al. (2015)
Southern France	Surface	ESCOMPTE (Expérience sur Site pour Contraindre les Modèles de Pollution atmosphérique et de Transport d'Emissions)	June–July 2001	Mallet et al. (2003)
Barcelona, Spain	Surface	–	Nov. 2003–Dec. 2004	Pey et al. (2008) Pey et al. (2009) Dall'Osto et al. (2012)
	Surface	SAPUSS (Solving Aerosol Problems by Using Synergistic Strategies)	Fall 2010	Brines et al. (2014)

(continued)

Table 1 (continued)

Location	Level/ Platform	Campaign	Period	References
Montseny, Spain	Surface	–	Nov. 2010–May 2011 and mid-Oct. 2011–mid-Dec. 2011	Cusack et al. (2013a, 2013b)
Western Mediterranean	Airborne	HYMEX (HYdrological cycle in Mediterranean Experiment)	Sept.–Nov. 2012	Rose et al. (2015)
	Balloon-borne	ChArMEx (the Chemistry-Aerosol Mediterranean Experiment)	Summer 2013	Renard et al. (2018)
	Airborne	TRAQA (Transport and Air QuAlity)	June–July 2012	Di Biagio et al. (2015, 2016)
	Airborne	SAFMED (Secondary Aerosol Formation in the MEDiterranean)	July 2013	
	Airborne, Surface	ADRIMED (Aerosol Direct Radiative Impact on the regional climate in the MEDiterranean region)	June 2013	Denjean et al. (2016), Mallet et al. (2016)
Lampedusa Isl., Italy	Surface		June 2013	Mallet et al. (2016, 2019)
Ersa (Corsica Isl.), France and Finokalia (Crete Isl.), Greece	Surface	ChArMEx (the Chemistry-Aerosol Mediterranean Experiment) enhanced observation period (EOP)	May 2012–August 2013	Berland et al. (2017)

9.6μm as VMD. High number concentrations (up to 20,000 cm^{-3}) of ultrafine or Aitken particles, measured in the size range 4–100 nm, were observed in several cases, both in the boundary layer and in the free troposphere during the TRAQA and SAFMED campaigns. Examples of different Aitken and accumulation mode aerosol vertical concentration profiles during TRAQA showing layers with enhanced Aitken mode particles are shown in Fig. 3.

Some of the cases observed during TRAQA and SAFMED corresponded to a concurrent increase in the concentration of accumulation mode particles. As shown for instance in Fig. 3a, which refers to the SAFIRE ATR-42 flight V31, the dN_{Aitken} increase between 1000 and 3000 m corresponds to simultaneous increase of dN_{Acc} (but also CO and ozone not reported in the figure), suggesting a layer directly transported from a region emitting in the Aitken size range. In other cases, the ultrafine aerosol was not related to simultaneous accumulation mode and ozone increases in the layer, suggesting the occurrence of NPF events over the basin. Panel (b) corresponds to flight V28b: the enhanced dN_{Aitken} layer at about 100 m, not related to dN_{Acc} increase, is possibly related to surface emissions over the sea surface (e.g., ship emissions) and NPF events. Panel (c) corresponds to flight V26: the layer

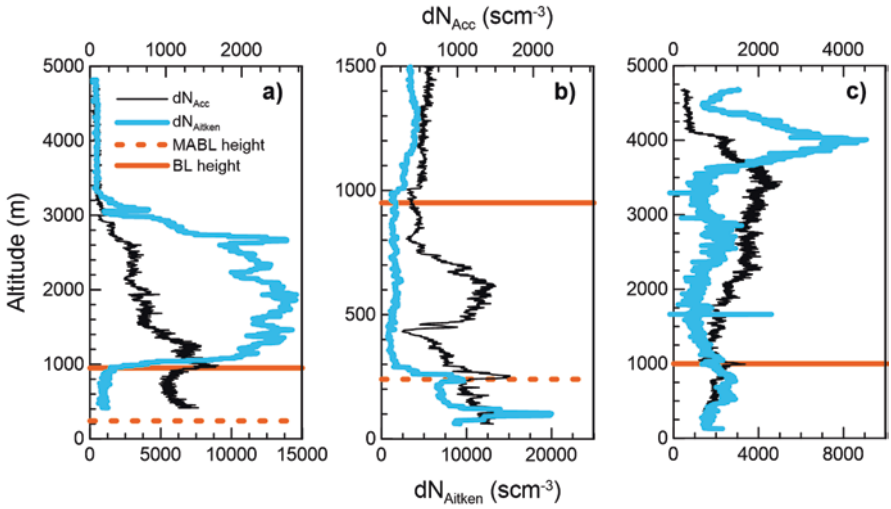

Fig. 3 Vertical profiles of the accumulation and Aitken number particle concentrations (dN_{Acc}, dN_{Aitken}) for three flights of the SAFIRE ATR-42 during the TRAQA campaign. The horizontal lines indicate the height of the marine atmospheric boundary layer (MABL; dotted line) and the planetary boundary layer (BL; continuous line): (**a**) flight V31; (**b**) flight V28b; (**c**) flight V26. Particle concentrations are expressed as the number of particles per standard cubic centimeter (i.e., at standard temperature and pressure (STP) conditions T = 293.15 K and p = 1013.25 hPa). (Modified from Fig. 10 in Di Biagio et al. (2015))

of enhanced dN_{Aitken} in the free troposphere between 3500 and 4500 m is possibly related to a NPF event.

Measurements of ultrafine particles are rare in the Mediterranean with only few long-term time series of in situ observations available in coastal areas in the western (Pey et al., 2008; Cusack et al., 2013a) and eastern (Kopanakis et al., 2013; Kalivitis et al., 2019) parts of the basin. Additional data are available over the sea surface from past intensive field campaigns. Airborne measurements during the C–MARE and GAMARF campaigns in the open sea site of Lampedusa reported ultrafine particle concentrations lower than 3000 cm^{-3} in the boundary layer (di Sarra et al., 2005; Meloni et al., 2015). Concentrations up to 12,000 cm^{-3} for ultrafine aerosols were obtained at a coastal site with complex orography in Southern Italy during the MORE experiment with evidence of local pollution and possibly nucleation phenomena associated with the events (Pace et al., 2015). The study by Rose et al. (2015) based on HYMEX observations also reported on NPF events over the open sea in the western basin. These authors showed that NPF events occur over large areas above the sea in mass types with different origins. Observations by Rose et al. further indicate that significant high concentrations of particles in the size range 5–10 nm correspond to fetches (time spent by the airmass over the sea surface) spanning between 0 and 60 h and that ultrafine concentration maxima do not consistently correspond to low fetches, therefore supporting the hypothesis that local marine precursors may significantly contribute to NPF over the basin. Mallet

et al. (2005) reported on ultrafine aerosol measurements during a summertime photochemical pollution event in the Marseille area, Southern France, 60 km inland. They measured vertical profiles of particles' concentration larger than 7 nm in two consecutive days in the early morning and at noon. The aerosol concentration in the boundary layer was observed in both days to be lower in the morning (4000 cm^{-3}) than at noon, when it reached values of 12,000 cm^{-3} in the first day and more than 40,000 cm^{-3} in the second day of measurements. Berland et al. (2017) reported on ground-based measurements at Ersa (Corsica) and Finokalia (Crete) over a 1-year period (2013) and for the 2013 summer season also at Mallorca (Spain) and combined to aircraft data during ADRIMED and SAFMED to study the contribution of NPF at the scale of the basin. They found that NPF events leading to enhanced ultrafine particle concentrations occurred about 35% of the time at Ersa and Finokalia with a similar seasonal pattern showing a maximum in spring. The NPF formation was interestingly observed for 20% of the cases to occur simultaneously at least at two of the three stations considered, which suggests the regional–scale character of NPF events and ultrafine particle distribution in the Mediterranean area. In another chapter of this book, Junkermann (2022) also reports ultrafine particle size distribution measurements performed with an ultralight aircraft up to 3.5 km in altitude in Corsica and Malta during TRAQA and ADRIMED campaigns, respectively. The role of shipping as a large source of ultrafine particles over the Mediterranean is highlighted.

2.4 In Situ Observations of the Coarse Mineral Dust Particle Mode

Airborne measurements during the ChArMEx campaign in 2013 have also provided new data on the size of Saharan dust under transport conditions with particular focus on its coarsest sizes. First observations of the coarse dust size distribution were provided in few studies over the basin (e.g., De Falco et al., 1996).

An accurate description of the coarse mode of mineral dust is vital since the presence of large particles enhances the capacity of mineral dust in absorbing shortwave and longwave radiation (e.g., Ryder et al., 2013) and affects cloud formation (e.g., Koehler et al., 2009) and atmospheric chemistry (e.g., Bauer et al., 2004). Aircraft observations of dust aerosols above 1.5 km in the western Mediterranean during ADRIMED were reported in Denjean et al. (2016). The dust number size distribution was parameterized as a four-mode lognormal function, and the coarse mode was located between 1.3 and 2.5μm (number modal diameter or NMD, corresponding to values between about 7 and 19μm for the VMD) regardless of the altitude, indicating a vertically well-mixed coarse mode. Below 300 nm in diameter, the dust aerosols were externally mixed with pollution particles. The effective coarse diameter ($D_{\text{eff, coarse}}$, calculated between 1 and 20μm) was within 3.8 and 14.2μm independently of the transport time (estimated at 1–5 days for the measured episodes during

ADRIMED), suggesting that the dust transported over the Mediterranean conserves its coarse mode. This persistence of the coarse mode was explained in Denjean et al. (2016) by the presence of temperature inversions in the middle troposphere, as observed from aircraft sondes, which kept the dust confined in a stable stratified layer. Additional observations were performed with sounding and quasi-Lagrangian drifting balloons launched from Menorca island in the western Mediterranean and embarking a new OPC counter (Renard et al., 2016, 2018). The balloon OPC measured persistently aerosols larger than 15μm in diameter within a dust plume sampled between the 16th and the 19th of June originated a few days before in northern Africa, in agreement with aircraft observations over the same area by Denjean et al. (2016). The size distribution could be fitted by a sum of three lognormal modes centered at (0.26 ± 0.04), (3.7 ± 0.4), and (30.4 ± 2.8) μm as volume median diameter, which remained fairly stable during the transport over the basin. The persistence of unexpected large particles (up to 50μm in diameter) as observed in Renard et al. (2018) suggests that a giant mode of dust aerosols is also efficiently transported in the Mediterranean basin, even if the mechanisms for this transport are still unknown since gravitational settling should quickly scavenge such a mode from the transported plume (e.g., Foret et al., 2006; Weinzierl et al., 2011).

Similarly, to the Mediterranean basin, particles larger than 10μm are measured after mid-range transport over the Atlantic Ocean (e.g., Ryder et al., 2013, 2018; Weinzierl et al., 2011, 2017), and indications for the long-range transport of giant mode dust also over the Atlantic are provided by van der Does et al. (2018). Figure 4 compares the datasets of dust volume distribution measured in the Mediterranean by Denjean et al. (2016) with observations performed in the outflow of African dust in the eastern tropical Atlantic. Despite some differences in the submicron size fraction, i.e., an enhanced fine mode in the Denjean et al. (2016) dataset due to the mixing of dust aerosols with pollution particles in the Mediterranean, the data comparison in Fig. 4 suggests the consistency of the dust coarse mode conservation after mid- to long-range transport in the atmosphere.

3 Synthesis of Observations

As discussed in the previous paragraphs, a large body of observations of the Mediterranean aerosols size distribution is available thanks to long-term monitoring and intensive field campaigns. Data have been acquired with different techniques measuring number or mass/volume particle size distributions and different size-related diameters (e.g., optically effective, projected cross area, aerodynamic equivalent, etc.), and more or less constrained hypotheses, often different from a study to another, are necessary to convert one distribution to the other. Despite these difficulties, Tables 2 and 3, respectively, present (i) a synthesis of mass median diameters (MMD) given as EAD (equivalent aerodynamic diameter) obtained by cascade impactor sampling at various ground-based locations and for various

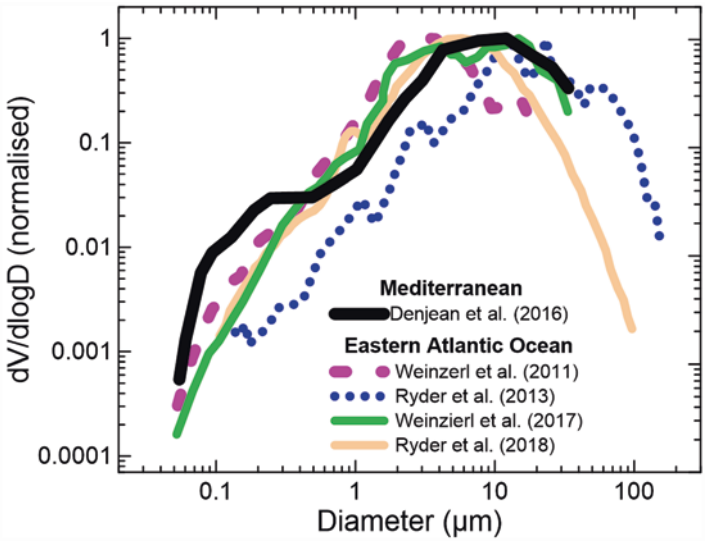

Fig. 4 Volume size distributions of dust aerosols measured airborne during the ADRIMED campaign and comparison to in situ dust size distribution measurements from campaigns in the eastern Atlantic Ocean. Data from Denjean et al. (2016) refer to the average dust size distribution in Fig. 7b; data from Weinzierl et al. (2011) are retrieved from the average number size distribution for dust in their Fig. 13; data from Ryder et al. (2013) refer to the dust "aged" category that is dust emitted 12–70 h prior in the Sahara Desert and are from their Fig. 2; data from Weinzierl et al. (2017) refer to observations at Cape Verde during a Lagrangian experiment and are retrieved from number distribution data in their Fig. 9; data from Ryder et al. (2018) are for the average of dust observations in the Saharan Air Layer (SAL) in their Fig. 6. For the sake of comparison, and in order to eliminate differences linked to different sampled concentrations, all size data are normalized to 1 at the maximum of the volume distribution. (Data are retrieved from cited publications)

aerosol types and (ii) effective diameters D_{eff} obtained by AERONET or sun photometer retrievals across the basin.

In the case of mineral dust, MMD values vary between 2.3 and 6μm at various sampling sites located in transport regions, the highest values being obtained for the Israeli site of Sde Boker (Formenti et al., 2001; Maenhaut et al., 1999), possibly the closest to North African sources and itself located in a semi-arid environment. The effective diameter values for the coarse mode retrieved by AERONET are in the range 3.2–5μm for observations conducted in the proximity of source regions in Tunisia (Masmoudi et al., 2003a) and over transport areas in Turkey (Kubilay et al., 2003), Italy (Masmoudi et al., 2003a), and Spain (Gómez-Amo et al., 2017). In agreement with the in situ airborne observations during ChArMEx (Denjean et al., 2016; Renard et al., 2018), these observations suggest that changes in the coarse mode size distribution of dust aerosols due to transport are not important (or detectable) within the precision of optical and aerodynamic measurements.

From these studies, it is also indicated that, apart from dust, there are other contributors to the aerosol coarse mode. Among the non-dust types, the largest coarse

Table 2 Mass median diameter (MMD) as equivalent aerodynamic diameter obtained by impactor sampling and elemental analysis at various ground-based locations and for various aerosol types

Aerosol type	Location	Tracer	MMD (μm)	References
Sea salt	Western Mediterranean Sea	Na	4.6–10.8, median 5.9	Dulac et al. (1989)
	Antalya, Southern Turkey	Cl	5.3	Kuloglu and Tuncel (2005)
	Finokalia, Crete, and Aegean Sea		5	Smolík et al. (2003)
Mineral dust	Capo Cavallo, Corsica	Al	2.3 ± 0.4	Dulac et al. (1989)
	Western Mediterranean Sea		1.9–5.2, median 2.8	
	Sde Boker, Negev Desert, Israel		6	Maenhaut et al. (1999) Formenti et al. (2001)
	Finokalia, Crete, and Aegean Sea		4	Smolík et al. (2003)
	Antalya, Southern Turkey		3.45	Kuloglu and Tuncel (2005)
Anthropogenic pollution	Sde Boker, Negev Desert, Israel	V	0.3 and 6	Maenhaut et al. (1999) Formenti et al. (2001)
	Finokalia, Crete, and Aegean Sea		0.3 and 3	Smolík et al. (2003)
	Antalya, Southern Turkey		1.21	Kuloglu and Tuncel (2005)
	Western Mediterranean Sea	Pb	0.69	Dulac et al. (1989)
	Finokalia, Crete, and Aegean Sea		1	Smolík et al. (2003)
	Antalya, Southern Turkey		0.77	Kuloglu and Tuncel (2005)
	Finokalia, Crete, and Aegean Sea	S	0.3 and 3	Smolík et al. (2003)
	Antalya, Southern Turkey		0.63[a]	Kuloglu and Tuncel (2005)
		Zn	1.24	

[a]As SO_4^{2-}

effective diameters are observed during extremely intense biomass burning events (> 4.0μm in Gómez-Amo et al. (2017) for a biomass burning smoke event with an exceptional AOD of 8 at 500 nm wavelength as estimated from AERONET observations). These intense fires can lift large carbon aggregates, ashes, and unburnt material quite efficiently.

Another important finding of recent studies is that the aerosol number and mass concentration – in particular for the fine mode – measured in remote regions over the sea surface across the basin are comparable to that measured in coastal cities and

Table 3 Overview of mean effective diameter (D_{eff}) of column-integrated volume distributions of aerosols retrieved over the Mediterranean basin by AERONET or other sun photometer observations. Fine, coarse, and total indicate that data refer to the fine mode, coarse mode, and total size distribution, respectively. Data for Kubilay et al. (2003) and Gómez-Amo et al. (2017) for fine and coarse effective diameters have been recalculated from the published size distribution by applying Eq. (2) and by assuming that the separation between fine and coarse particles occurs for a radius (diameter) of 0.5 (1) μm. Note that the same criteria is not applied in all datasets: Logothetis et al. (2020) assume fine and coarse particles for radius respectively below and above 0.992 μm in their calculations

Location	Dominant aerosol type	D_{eff} (μm)	References
Erdemli, South coastal Turkey (36°N, 34°E), 3 m a.s.l.	Desert dust	0.12 (fine) 3.9 (coarse)	Kubilay et al. (2003)
Thala, Tunisia (35°N, 8°E), 1091 m a.s.l.	Average over April–June 2001	4.6 ± 0.84 (coarse)	Masmoudi et al. (2003a)
Oristano, Sardinia Isl., Italy (39°N, 8°E), 10 m a.s.l.		4.7 ± 0.60 (coarse)	
Rome Tor Vergata, Italy (41°N, 12°E), 130 m a.s.l.		5.0 ± 0.58 (coarse)	
Crete Isl., Greece (35.3°N, 25.3°E), 20 m a.s.l.	Average over Jan. 2003–Dec. 2004	0.26 (fine) 4.2 (coarse)	Fotiadi et al. (2006)
Granada, Spain (37°N, 4°W), 680 m a.s.l.	Biomass burning	0.3–0.4 (total)	Alados-Arboledas et al. (2011)
109 stations within 29–47°N, 11°W–39°E	Aerosol climatology 2000–2013	0.7 (total, median)	Gkikas et al. (2016)
	Desert dust climatology 2000–2013	1.1–2.8 (total) 1.5 (total, median)	
Valencia, Spain (40°N, 0.4°W), 60 m a.s.l.	Summer background	0.22 (fine) 4.1 (coarse) 0.6 (total)	Gómez-Amo et al. (2017)
	Desert dust	0.25–0.36 (fine) 3.2–3.8 (coarse) 1.0–1.6 (total)	
	Smoke	0.25–0.27 (fine) 4.0–4.3 (coarse) 0.4–0.7 (total)	
	Residual smoke	0.22 (fine) 4.1–4.4 (coarse) 0.7–0.8 (total)	
South Europe (9 stations)	Aerosol climatology 2008–2017	0.28–0.38 (fine) 3.86–4.92 (coarse) 0.6–1.0 (total)	Logothetis et al. (2020)
North Africa and the Middle East (10 coastal stations)		0.22–0.30 (fine) 3.46–3.80 (coarse) 1.00–1.42 (total)	

Table 4 Comparison of the number concentrations (in number per standard cm^{-3}) in the Aitken (dN_{Aitken}, 4–100 nm) and accumulation (dN_{Acc}, 0.1–1μm) modes observed during the two ChArMEx/TRAQA and ChArMEx/SAFMED airborne field campaigns, together with those reported in the literature for airborne observations in continental Europe

Atmospheric layer	Particle mode	Particle number concentration (scm^{-3})	
		TRAQA and SAFMED campaigns	Other literature over continental Europe
Free troposphere	dN_{Aitken}	0–19250	812–9149[a]; 0–980[b]
	dN_{Acc}	34–3233	20–80[c]; 25–85[b]; 0–500[d]
Boundary layer	dN_{Aitken}	4–22471	1037–31370[a]; 1000–20000[e]; 0–30000[f]; 0–19000[b]
	dN_{Acc}	90–3215	70–560[c]; 10–50[e]; 400–1200[b]; 0–2000[d]

Adapted from Table 2 in Di Biagio et al. (2015)
[a]Mallet et al. (2005), south-eastern France, June 2001; size range dN_{Aitken} (0.006–0.6μm)
[b]Hamburger et al. (2012), central Europe, May 2008; size range dN_{Aitken} (0.004–0.15μm), dN_{Acc} (>0.15μm)
[c]Petzold et al. (2002), central Europe, July–August 1998; size range dN_{Acc} (>0.15μm)
[d]Highwood et al. (2012), central Europe, May 2008; size range dN_{Aitken} (0.004–0.15μm), dN_{Acc} (>0.15μm)
[e]Wiegner et al. (2006), Germany, May 2003; size range dN_{Aitken} (>0.01μm), dN_{Acc} (>0.3μm)
[f]Junkermann (2009), Po Valley, July–August 2002 and September–October 2003; size range dN_{Aitken} (>0.01μm)

continental Europe, suggesting that a non-polluted atmosphere over the Mediterranean is very rare. This point is illustrated in Table 4 where the number concentrations for Aitken and accumulation mode particles measured over the sea in the Western Mediterranean basin in Di Biagio et al. (2015) are compared to literature values for continental Europe. On the contrary, in clear conditions, as often observed in case of high wind speeds (Mallet et al., 2019), the ultrafine particles concentration over the basin can be lower than 500 cm^{-3} and the accumulation mode concentration lower than 20 cm^{-3} (Pace et al., 2015; Di Biagio et al., 2015). For comparison, the number concentration for the coarse mode (>1μm diameter) may reach 4–40 cm^{-3} for moderate to intense dust events (Bonasoni et al., 2004; Di Biagio et al., 2015; Pace et al., 2015; Denjean et al., 2016).

4 Summary and Challenges for Future Research

The ensemble of observations discussed in this section points out different aspects of the size distribution for Mediterranean aerosols: (i) in the Mediterranean basin, the volume size distribution above 100 nm in diameter is basically bimodal, with anthropogenic particles mostly contributing to the fine mode, while different particle types contributing to the coarse mode (dust, smoke, marine particles); (ii) ultrafine particles (<100 nm diameter) are ubiquitous over the basin, and NPF events mostly leading to these ultrafine particles occur at the regional scale over the basin,

independently of the air mass origin, and both in the boundary layer and the free troposphere; (iii) observations of coarse and giant particles during dust events are in agreement with similar observations in the Atlantic and support the efficiency of atmospheric transport of dust aerosols with diameters above 10μm over long distances; (iv) pristine conditions are very rarely encountered over the basin.

While much information on the Mediterranean aerosol size distribution has been acquired in recent years, at present, we still miss a complete regional characterization of the aerosol size over the whole basin including seasonal effects. Such regional-scale dataset could be efficiently derived from satellite observations. Many studies reports on data over the Mediterranean from the Moderate Resolution Imaging Spectroradiometer (MODIS) (Papadimas et al., 2008, 2009; Gkikas et al., 2009, 2016), the combination of MODIS and the Total Ozone Mapping Spectrometer (TOMS) (Hatzianastassiou et al., 2009), the Sea-Viewing Wide Field-of-View Sensor (SeaWiFS) (Antoine & Nobileau, 2006), the POLarization and Directionality of the Earth's Reflectances (POLDER) radiometer on PARASOL (Polarization & Anisotropy of Reflectances for Atmospheric Sciences coupled with Observations from a Lidar) (Formenti et al., 2018), or combination of different products (Nabat et al., 2013). Today satellites allow retrieving only partial information, as the column-averaged aerosol Angström exponent or the effective aerosol diameter. Further observation and retrieval capabilities need to be developed in the future to allow retrieving the aerosol size distribution from satellites. This is crucial to improve our understanding of the regional, seasonal, annual, and long-term aerosol size distribution.

Acknowledgments The author wishes to thank P. Formenti for providing a first draft of this section, based on which she developed the full work presented and discussed here.

References

Alados-Arboledas, L., Müller, D., Guerrero-Rascado, J. L., Navas-Guzmán, F., Pérez-Ramírez, D., & Olmo, F. J. (2011). Optical and microphysical properties of fresh biomass burning aerosol retrieved by Raman lidar, and star-and sun-photometry. *Geophysical Research Letters, 38*, L01807. https://doi.org/10.1029/2010GL045999

Andreae, T. W., Andreae, M. O., Ichoku, C., Maenhaut, W., Cafmeyer, J., Karnieli, A., & Orlovsky, L. (2002). Light scattering by dust and anthropogenic aerosol at a remote site in the Negev desert, Israel. *Journal of Geophysical Research, 107*, 4008. https://doi.org/10.1029/2001JD900252

Angström, A. (1929). On the atmospheric transmission of sun radiation and on dust in the air. *Geografiska Annaler, 11*, 156–166. https://doi.org/10.1080/20014422.1929.11880498

Antoine, D., & Nobileau, D. (2006). Recent increase of Saharan dust transport over the Mediterranean Sea, as revealed from ocean color satellite (SeaWiFS) observations. *Journal of Geophysical Research, 111*, D12214. https://doi.org/10.1029/2005JD006795

Basart, S., Pérez, C., Cuevas, E., Baldasano, J. M., & Gobbi, G. P. (2009). Aerosol characterization in Northern Africa, Northeastern Atlantic, Mediterranean Basin and Middle East from direct-sun AERONET observations. *Atmospheric Chemistry and Physics, 9*, 8265–8282. https://doi.org/10.5194/acp-9-8265-2009

Bauer, S. E., Balkanski, Y., Shulz, M., Hauglustaine, D. A., & Dentener, F. (2004). Global modelling of heterogeneous chemistry on mineral aerosol surfaces: The influence of ozone chemistry and comparison to observations. *Journal of Geophysical Research, 109*, D02304. https://doi.org/10.1029/2003JD003868

Berland, K., Rose, C., Pey, J., Culot, A., Freney, E., Kalivitis, N., Kouvarakis, G., Cerro, J. C., Mallet, M., Sartelet, K., Beckmann, M., Bourriane, T., Roberts, G., Marchand, N., Mihalopoulos, N., & Sellegri, K. (2017). Spatial extent of new particle formation events over the Mediterranean Basin from multiple ground-based and airborne measurements. *Atmospheric Chemistry and Physics, 17*, 9567–9583. https://doi.org/10.5194/acp-17-9567-2017

Bonasoni, P., Cristofanelli, P., Calzolari, F., Bonafè, U., Evangelisti, F., Stohl, A., Zauli Sajani, S., van Dingenen, R., Colombo, T., & Balkanski, Y. (2004). Aerosol-ozone correlations during dust transport episodes. *Atmospheric Chemistry and Physics, 4*, 1201–1215. https://doi.org/10.5194/acp-4-1201-2004

Brines, M., Dall'Osto, M., Beddows, D. C. S., Harrison, R. M., & Querol, X. (2014). Simplifying aerosol size distributions modes simultaneously detected at four monitoring sites during SAPUSS. *Atmospheric Chemistry and Physics, 14*, 2973–2986. https://doi.org/10.5194/acp-14-2973-2014

Chazette, P., & Liousse, C. (2001). A case study of optical and chemical apportionment for urban aerosols in Thessaloniki. *Atmospheric Environment, 35*, 2497–2506. https://doi.org/10.1016/S1352-2310(00)00425-8

Claeys, M., Roberts, G., Mallet, M., Arndt, J., Sellegri, K., Sciare, J., Wenger, J., & Sauvage, B. (2017). Optical, physical and chemical properties of aerosols transported to a coastal site in the western Mediterranean: A focus on primary marine aerosols. *Atmospheric Chemistry and Physics, 17*, 7891–7915. https://doi.org/10.5194/acp-17-7891-2017

Cusack, M., Pérez, N., Pey, J., Wiedensohler, A., Alastuey, A., & Querol, X. (2013a). Variability of sub-micrometer particle number size distributions and concentrations in the Western Mediterranean regional background. *Tellus, 65B*, 19243. https://doi.org/10.3402/tellusb.v65i0.19243

Cusack, M., Pérez, N., Pey, J., Alastuey, A., & Querol, X. (2013b). Source apportionment of fine PM and sub-micron particle number concentrations at a regional background site in the western Mediterranean: A 2.5 year study. *Atmospheric Chemistry and Physics, 13*, 5173–5187. https://doi.org/10.5194/acp-13-5173-2013

Dall'Osto, M., Beddows, D. C. S., Pey, J., Rodriguez, S., Alastuey, A., Harrison, R. M., & Querol, X. (2012). Urban aerosol size distributions over the Mediterranean city of Barcelona, NE Spain. *Atmospheric Chemistry and Physics, 12*, 10693–10707. https://doi.org/10.5194/acp-12-10693-2012

De Falco, G., Molinaroli, E., & Rabitti, S. (1996). Grain size analysis of aerosol and rain particles: A methodological comparison. In *The impact of desert dust across the Mediterranean, environmental science and technology library* (Vol. 11, pp. 233–238). Springer. https://doi.org/10.1007/978-94-017-3354-0_23

DeCarlo, P., Slowik, J. G., Worsnop, D. R., Davidovits, P., & Jimenez, J. L. (2004). Particle morphology and density characterization by combined mobility and aerodynamic diameter measurements. Part 1: Theory. *Aerosol Science and Technology, 38*, 1185–1205. https://doi.org/10.1080/027868290903907

Denjean, C., Cassola, F., Mazzino, A., Triquet, S., Chevaillier, S., Grand, N., Bourrianne, T., Momboisse, G., Sellegri, K., Schwarzenbock, A., Freney, E., Mallet, M., & Formenti, P. (2016). Size distribution and optical properties of mineral dust aerosols transported in the western Mediterranean. *Atmospheric Chemistry and Physics, 16*, 1081–1104. https://doi.org/10.5194/acp-16-1081-2016

Derimian, Y., Karnieli, A., Kaufman, Y. J., Andreae, M. O., Andreae, T. W., Dubovik, O., Maenhaut, W., Koren, I., & Holben, B. N. (2006). Dust and pollution aerosols over the Negev desert, Israel: Properties, transport, and radiative effect. *Journal of Geophysical Research, 111*, D05205. https://doi.org/10.1029/2005JD006549

Di Biagio, C., Doppler, L., Gaimoz, C., Grand, N., Ancellet, G., Raut, J.-C., Beekmann, M., Borbon, A., Sartelet, K., Attié, J.-L., Ravetta, F., & Formenti, P. (2015). Continental pollution in the western Mediterranean basin: Vertical profiles of aerosol and trace gases measured over the sea during TRAQA 2012 and SAFMED 2013. *Atmospheric Chemistry and Physics, 15*, 9611–9630. https://doi.org/10.5194/acp-15-9611-2015

Di Biagio, C., Formenti, P., Doppler, L., Gaimoz, C., Grand, N., Ancellet, G., Attié, J.-L., Bucci, S., Dubuisson, P., Fierli, F., Mallet, M., & Ravetta, F. (2016). Continental pollution in the Western Mediterranean basin: Large variability of the aerosol single scattering albedo and influence on the direct shortwave radiative effect. *Atmospheric Chemistry and Physics, 16*, 10591–10607. https://doi.org/10.5194/acp-16-10591-2016

Di Iorio, T., di Sarra, A., Junkermann, W., Cacciani, M., Fiocco, G., & Fuà, D. (2003). Tropospheric aerosols in the Mediterranean: 1. Microphysical and optical properties. *Journal of Geophysical Research, 108*, 4316. https://doi.org/10.1029/2002JD002815

di Sarra, A., Anello, F., Bommarito, C., Chamard, P., De Silvestri, L., Di Iorio, T., Fiocco, G., Junkermann, W., Mastrilli, A., Meloni, D., Monteleone, F., Pace, G., Piacentino, S., & Sferlazzo, D. (2005). *The Central-Mediterranean Aerosol and Radiation Experiment (C-MARE): Overview of meteorology and measurements* (Technical Rept. RT-2005-21-CLIM). ENEA.

Dubovik, O., & King, M. D. (2000). A flexible inversion algorithm for retrieval of aerosol optical properties from sun and sky radiance measurements. *Journal of Geophysical Research, 105*, 20673–20696. https://doi.org/10.1029/2000JD900282

Dubovik, O., Sinyuk, A., Lapyonok, T., Holben, B. N., Mishchenko, M., Yang, P., Eck, T. F., Volten, H., Muñoz, O., Veihelmann, B., van der Zande, W. J., Leon, J.-F., Sorokin, M., & Slutsker, I. (2006). Application of spheroid models to account for aerosol particle non sphericity in remote sensing of desert dust. *Journal of Geophysical Research, 111*, D11208. https://doi.org/10.1029/2005JD006619

Dulac, F., & Chazette, P. (2003). Airborne study of a multi-layer aerosol structure in the eastern Mediterranean observed with the airborne polarized lidar ALEX during a STAAARTE campaign (7 June 1997). *Atmospheric Chemistry and Physics, 3*, 1817–1831. https://doi.org/10.5194/acp-3-1817-2003

Dulac, F., Buat-Ménard, P., Ezat, U., Melki, S., & Bergametti, G. (1989). Atmospheric input of trace metals to the western Mediterranean: Uncertainties in modelling dry deposition from cascade impactor data. *Tellus, 41B*, 362–378. https://doi.org/10.1111/j.1600-0889.1989.tb00315.x

Dulac, F., Sauvage, S., Hamonou, E., & Debevec, C. (2023). Introduction to the volume 1 of Atmospheric Chemistry in the Mediterranean Region and to the experimental effort during the ChArMEx decade. In F. Dulac, S. Sauvage, & E. Hamonou (Eds.), *Atmospheric chemistry in the Mediterranean Region* (Vol. 1, Background information and pollutant distribution). Springer.

Foret, G., Bergametti, G., Dulac, F., & Menut, L. (2006). An optimized particle size bin scheme for modeling mineral dust aerosol. *Journal of Geophysical Research, 111*, D17310. https://doi.org/10.1029/2005JD006797

Formenti, P., Andreae, M. O., Ichoku, C., Andreae, T. W., Schebeske, G., Kettle, A. J., Maenhaut, W., Cafmeyer, J., Ptasinsky, J., Karnieli, A., & Lelieveld, J. (2001). Physical and chemical characteristics of aerosols over the Negev desert (Israel) during summer 1996. *Journal of Geophysical Research, 106*, 4871–4890. https://doi.org/10.1029/2000JD900556

Formenti, P., Reiner, T., Sprung, D., Andreae, M. O., Wendisch, M., Wex, H., Kindred, D., Dewey, K., Kent, J., Tzortziou, M., Vasaras, A., & Zerefos, C. (2002). STAAARTE-MED 1998 summer airborne measurements over the Aegean Sea: 1. Aerosol particles and trace gases. *Journal of Geophysical Research, 107*, 4450. https://doi.org/10.1029/2001JD001337

Formenti, P., Schütz, L., Balkanski, Y., Desboeufs, K., Ebert, M., Kandler, K., Petzold, A., Scheuvens, D., Weinbruch, S., & Zhang, D. (2011). Recent progress in understanding physical and chemical properties of African and Asian mineral dust. *Atmospheric Chemistry and Physics, 11*, 8231–8256. https://doi.org/10.5194/acp-11-8231-2011

Formenti, P., Mbemba Kabuiku, L., Chiapello, I., Ducos, F., Dulac, F., & Tanré, D. (2018). Aerosol optical properties derived from POLDER-3/PARASOL (2005–2013) over the western Mediterranean Sea – Part 1: Quality assessment with AERONET and in situ airborne observations. *Atmospheric Measurement Techniques, 11*, 6761–6784. https://doi.org/10.5194/amt-11-6761-2018

Fotiadi, A., Hatzianastassiou, N., Drakakis, E., Matsoukas, C., Pavlakis, K. G., Hatzidimitriou, D., Gerasopoulos, E., Mihalopoulos, N., & Vardavas, I. (2006). Aerosol physical and optical properties in the Eastern Mediterranean Basin, Crete, from Aerosol Robotic Network data. *Atmospheric Chemistry and Physics, 6*, 5399–5413. https://doi.org/10.5194/acp-6-5399-2006

Gerasopoulos, E., Koulouri, E., Kalivitis, N., Kouvarakis, G., Saarikoski, S., Mäkelä, T., Hillamo, R., & Mihalopoulos, N. (2007). Size-segregated mass distributions of aerosols over Eastern Mediterranean: Seasonal variability and comparison with AERONET columnar size-distributions. *Atmospheric Chemistry and Physics, 7*, 2551–2561. https://doi.org/10.5194/acp-7-2551-2007

Gkikas, A., Hatzianastassiou, N., & Mihalopoulos, N. (2009). Aerosol events in the broader Mediterranean basin based on 7-year (2000–2007) MODIS C005 data. *Annales de Geophysique, 27*, 3509–3522. https://doi.org/10.5194/angeo-27-3509-2009

Gkikas, A., Basart, S., Hatzianastassiou, N., Marinou, E., Amiridis, V., Kazadzis, S., Pey, J., Querol, X., Jorba, O., Gassó, S., & Baldasano, J. M. (2016). Mediterranean intense desert dust outbreaks and their vertical structure based on remote sensing data. *Atmospheric Chemistry and Physics, 16*, 8609–8642. https://doi.org/10.5194/acp-16-8609-2016

Gómez-Amo, J. L., Estellés, V., Marcos, C., Segura, S., Esteve, A. R., Pedrós, R., Utrillas, M. P., & Martínez-Lozano, J. A. (2017). Impact of dust and smoke mixing on column-integrated aerosol properties from observations during a severe wildfire episode over Valencia (Spain). *The Science of the Total Environment, 599–600*, 2121–2134. https://doi.org/10.1016/j.scitotenv.2017.05.041

Hamburger, T., McMeeking, G., Minikin, A., Petzold, A., Coe, H., & Krejci, R. (2012). Airborne observations of aerosol microphysical properties and particle ageing processes in the troposphere above Europe. *Atmospheric Chemistry and Physics, 12*, 11533–11554. https://doi.org/10.5194/acp-12-11533-2012

Hatzianastassiou, N., Gkikas, A., Mihalopoulos, N., Torres, O., & Katsoulis, B. D. (2009). Natural versus anthropogenic aerosols in the eastern Mediterranean basin derived from multiyear TOMS and MODIS satellite data. *Journal of Geophysical Research, 114*, D24202. https://doi.org/10.1029/2009JD011982

Highwood, E. J., Northway, M. J., McMeeking, G. R., Morgan, W. T., Liu, D., Osborne, S., Bower, K., Coe, H., Ryder, C., & Williams, P. (2012). Aerosol scattering and absorption during the EUCAARI-LONGREX flights of the Facility for Airborne Atmospheric Measurements (FAAM) BAe-146: Can measurements and models agree? *Atmospheric Chemistry and Physics, 12*, 7251–7267. https://doi.org/10.5194/acp-12-7251-2012

Holben, B. N., Eck, T. F., Slutsker, I., Tanré, D., Buis, J. P., Setzer, A., Vermote, E., Reagan, J. A., Kaufman, Y. J., Nakajima, T., Lavenu, F., Jankowiak, I., & Smirnov, A. (1998). AERONET – A federated instrument network and data archive for aerosol characterization. *Remote Sensing of Environment, 66*, 1–16. https://doi.org/10.1016/S0034-4257(98)00031-5

Ichoku, C., Andreae, M. O., Andreae, T. W., Meixner, F. X., Shebeske, G., & Formenti, P. (1999). Interrelationships between aerosol characteristics and light scattering during late winter in an eastern Mediterranean arid environment. *Journal of Geophysical Research, 104*, 24371–24393. https://doi.org/10.1029/1999JD900781

Jaenicke, R. (1988). Aerosol physics and chemistry. In *Landolt-Börnstein numerical data and functional relationships in science and technology, 4b* (pp. 391–457). Springer.

Junkermann, W. (2001). An ultralight aircraft as platform for research in the lower troposphere: System performance and first results from radiation transfer studies in stratiform aerosol layers and broken cloud conditions. *Journal of Atmospheric and Oceanic Technology, 18*, 934–946. https://doi.org/10.1175/1520-0426(2001)018<0934:AUAAPF>2.0.CO;2

Junkermann, W. (2009). On the distribution of formaldehyde in the western Po-Valley, Italy, during 2002/2003. *Atmospheric Chemistry and Physics, 9*, 9187–9196. https://doi.org/10.5194/acp-9-9187-2009

Junkermann, W. (2022). Ultrafine particle emissions in the Mediterranean. In F. Dulac, S. Sauvage, & E. Hamonou (Eds.), *Atmospheric chemistry in the Mediterranean Region* (Vol. 2, From air pollutant sources to impacts). Springer, this volume. https://doi.org/10.1007/978-3-030-82385-6_6

Kalivitis, N., Kerminen, V.-M., Kouvarakis, G., Stavroulas, I., Tzitzikalaki, E., Kalkavouras, P., Daskalakis, N., Myriokefalitakis, S., Bougiatioti, A., Manninen, H. E., Roldin, P., Petäjä, T., Boy, M., Kulmala, M., Kanakidou, M., & Mihalopoulos, N. (2019). Formation and growth of atmospheric nanoparticles in the eastern Mediterranean: Results from long-term measurements and process simulations. *Atmospheric Chemistry and Physics, 19*, 2671–2686. https://doi.org/10.5194/acp-19-2671-2019

Koehler, K. A., Kreidenweis, S. M., DeMott, P. J., Petters, M. D., Prenni, A. J., & Carrico, C. M. (2009). Hygroscopicity and cloud droplet activation of mineral dust aerosol. *Geophysical Research Letters, 36*, L08805. https://doi.org/10.1029/2009GL037348

Kopanakis, I., Chatoutsidou, S. E., Torseth, K., Glytsos, T., & Lazaridis, M. (2013). Particle number size distribution in the eastern Mediterranean: Formation and growth rates of ultrafine airborne atmospheric particles. *Atmospheric Environment, 77*, 790–802. https://doi.org/10.1016/j.atmosenv.2013.05.066

Kubilay, N., Cokacar, T., & Oguz, T. (2003). Optical properties of mineral dust outbreaks over the northeastern Mediterranean. *Journal of Geophysical Research, 108*, 4666. https://doi.org/10.1029/2003JD003798

Kuloglu, E., & Tuncel, G. (2005). Size distribution of trace elements and major ions in the eastern Mediterranean atmosphere. *Water, Air, and Soil Pollution, 167*, 221–241. https://doi.org/10.1007/s11270-005-8651-3

Logothetis, S. A., Salamalikis, V., & Kazantzidis, A. (2020). Aerosol classification in Europe, Middle East, North Africa and Arabian Peninsula based on AERONET version 3. *Atmospheric Research, 239*, 15, 104893. https://doi.org/10.1016/j.atmosres.2020.104893

Maenhaut, W., Ptasinski, J., & Cafmeyer, J. (1999). Detailed mass size distributions of atmospheric aerosol species in the Negev desert, Israel, during ARACHNE-96. *Nuclear Instruments and Methods in Physics Research Section B, 150*, 422–427. https://doi.org/10.1016/S0168-583X(98)01069-6

Mallet, M., Roger, J. C., Despiau, S., Dubovik, O., & Putaud, J. P. (2003). Microphysical and optical properties of aerosol particles in urban zone during ESCOMPTE. *Atmospheric Research, 69*, 73–97. https://doi.org/10.1016/j.atmosres.2003.07.001

Mallet, M., Van Dingenen, R., Roger, J. C., Despiau, S., & Cachier, H. (2005). In situ airborne measurements of aerosol optical properties during photochemical pollution events. *Journal of Geophysical Research, 110*, D03205. https://doi.org/10.1029/2004JD005139

Mallet, M., Dubovik, O., Nabat, P., Dulac, F., Kahn, R., Sciare, J., Paronis, D., & Léon, J. F. (2013). Absorption properties of Mediterranean aerosols obtained from multi-year ground-based remote sensing observations. *Atmospheric Chemistry and Physics, 13*, 9195–9210. https://doi.org/10.5194/acp-13-9195-2013

Mallet, M., Dulac, F., Formenti, P., Nabat, P., Sciare, J., Roberts, G., Pelon, J., Ancellet, G., Tanré, D., Parol, F., Denjean, C., Brogniez, G., di Sarra, A., Alados-Arboledas, L., Arndt, J., Auriol, F., Blarel, L., Bourrianne, T., Chazette, P., … Zapf, P. (2016). Overview of the Chemistry-Aerosol Mediterranean Experiment/Aerosol Direct Radiative Forcing on the Mediterranean Climate (ChArMEx/ADRIMED) summer 2013 campaign. *Atmospheric Chemistry and Physics, 16*, 455–504. https://doi.org/10.5194/acp-16-455-2016

Mallet, M. D., D'Anna, B., Même, A., Bove, M. C., Cassola, F., Pace, G., Desboeufs, K., Di Biagio, C., Doussin, J.-F., Maille, M., Massabò, D., Sciare, J., Zapf, P., di Sarra, A. G., & Formenti, P. (2019). Summertime surface PM_1 aerosol composition and size by source region at the Lampedusa island in the central Mediterranean Sea. *Atmospheric Chemistry and Physics, 19*, 11123–11142. https://doi.org/10.5194/acp-19-11123-2019

Masmoudi, M., Chaabane, M., Tanré, D., Gouloup, P., Blarel, L., & Elleuch, F. (2003a). Spatial and temporal variability of aerosol: Size distribution and optical properties. *Atmospheric Research, 66*, 1–19. https://doi.org/10.1016/S0169-8095(02)00174-6

Masmoudi, M., Chaabane, M., Medhioub, K., & Euch, F. (2003b). Variability of aerosol optical thickness and atmospheric turbidity in Tunisia. *Atmospheric Research, 66*, 175–188. https://doi.org/10.1016/S0169-8095(02)00175-8

Meloni, D., Junkermann, W., di Sarra, A., Cacciani, M., De Silvestri, L., Di Iorio, T., Estellés, V., Gómez-Amo, J. L., Pace, G., & Sferlazzo, D. M. (2015). Altitude-resolved shortwave and longwave radiative effects 1 of desert dust in the Mediterranean during the GAMARF campaign: Indications of a net daily cooling in the dust layer. *Journal of Geophysical Research, 120*, 3386–3407. https://doi.org/10.1002/2014JD022312

Mishchenko, M. I., Travis, L. D., Kahn, R. A., & West, R. A. (1997). Modeling phase function for dustlike tropospheric aerosols using a shape mixture of randomly oriented poly-disperse spheroids. *Journal of Geophysical Research, 102*, 16831–16847. https://doi.org/10.1029/96JD02110

Nabat, P., Somot, S., Mallet, M., Chiapello, I., Morcrette, J. J., Solmon, F., Szopa, S., Dulac, F., Collins, W., Ghan, S., Horowitz, L. W., Lamarque, J. F., Lee, Y. H., Naik, V., Nagashima, T., Shindell, D., & Skeie, R. (2013). A 4-D climatology (1979–2009) of the monthly tropospheric aerosol optical depth distribution over the Mediterranean region from a comparative evaluation and blending of remote sensing and model products. *Atmospheric Measurement Techniques, 6*, 1287–1314. https://doi.org/10.5194/amt-6-1287-2013

Pace, G., di Sarra, A., Meloni, D., Piacentino, S., & Chamard, P. (2006). Aerosol optical properties at Lampedusa (Central Mediterranean). 1. Influence of transport and identification of different aerosol types. *Atmospheric Chemistry and Physics, 6*, 697–713. https://doi.org/10.5194/acp-6-697-2006

Pace, G., Junkermann, W., Vitali, L., di Sarra, A., Meloni, D., Cacciani, M., Cremona, G., Iannarelli, A. M., & Zanini, G. (2015). On the complexity of the boundary layer structure and aerosol vertical distribution in the coastal Mediterranean regions: A case study. *Tellus B: Chemical and Physical Meteorology, 67*, 27721. https://doi.org/10.3402/tellusb.v67.27721

Papadimas, C. D., Hatzianastassiou, N., Mihalopoulos, N., Querol, X., & Vardavas, I. (2008). Spatial and temporal variability in aerosol properties over the Mediterranean basin based on 6-year (2000–2006) MODIS data. *Journal of Geophysical Research, 113*, D11205. https://doi.org/10.1029/2007JD009189

Papadimas, C. D., Hatzianastassiou, N., Mihalopoulos, N., Kanakidou, M., Katsoulis, B. D., & Vardavas, I. (2009). Assessment of the MODIS collections C005 and C004 aerosol optical depth products over the Mediterranean basin. *Atmospheric Chemistry and Physics, 9*, 2987–2999. https://doi.org/10.5194/acp-9-2987-2009

Petzold, A., Fiebig, M., Flentje, H., Keil, A., Leiterer, U., Schroder, F., Stifter, A., Wendisch, M., & Wendling, P. (2002). Vertical variability of aerosol properties observed at a continental site during the Lindenberg Aerosol Characterization Experiment (LACE 98). *Journal of Geophysical Research, 107*, 8128. https://doi.org/10.1029/2001JD001043

Pey, J., Rodríguez, S., Querol, X., Alastuey, A., Moreno, T., Putaud, J. P., & Van Dingenen, R. (2008). Variations of urban aerosols in the western Mediterranean. *Atmospheric Environment, 42*, 9052–9062. https://doi.org/10.1016/j.atmosenv.2008.09.049

Pey, J., Querol, X., Alastuey, A., Rodríguez, S., Putaud, J. P., & Van Dingenen, R. (2009). Source apportionment of urban fine and ultra fine particle number concentration in a Western Mediterranean city. *Atmospheric Environment, 43*, 4407–4415. https://doi.org/10.1016/j.atmosenv.2009.05.024

Renard, J.-B., Dulac, F., Berthet, G., Lurton, T., Vignelles, D., Jégou, F., Tonnelier, T., Jeannot, M., Couté, B., Akiki, R., Verdier, N., Mallet, M., Gensdarmes, F., Charpentier, P., Mesmin, S., Duverger, V., Dupont, J.-C., Elias, T., Crenn, V., … Daugeron, D. (2016). LOAC: A small aerosol optical counter/sizer for ground-based and balloon measurements of the size distribution and nature of atmospheric particles – Part 2: First results from balloon and unmanned aerial

vehicle flights. *Atmospheric Measurement Techniques, 9*, 3673–3686. https://doi.org/10.5194/amt-9-3673-2016

Renard, J.-B., Dulac, F., Durand, P., Bourgeois, Q., Denjean, C., Vignelles, D., Couté, B., Jeannot, M., Verdier, N., & Mallet, M. (2018). In situ measurements of desert dust particles above the western Mediterranean Sea with the balloon-borne Light Optical Aerosol Counter/sizer (LOAC) during the ChArMEx campaign of summer 2013. *Atmospheric Chemistry and Physics, 18*, 3677–3699. https://doi.org/10.5194/acp-18-3677-2018

Rose, C., Sellegri, K., Freney, E., Dupuy, R., Colomb, A., Pichon, J.-M., Ribeiro, M., Bourianne, T., Burnet, F., & Schwarzenboeck, A. (2015). Airborne measurements of new particle formation in the free troposphere above the Mediterranean Sea during the HYMEX campaign. *Atmospheric Chemistry and Physics, 15*, 10203–10218. https://doi.org/10.5194/acp-15-10203-2015

Ryder, C. L., Highwood, E. J., Lai, T. M., Sodemann, H., & Marsham, J. H. (2013). Impact of atmospheric transport on the evolution of microphysical and optical properties of Saharan dust. *Geophysical Research Letters, 40*, 2433–2438. https://doi.org/10.1002/grl.50482

Ryder, C. L., Marenco, F., Brooke, J. K., Estelles, V., Cotton, R., Formenti, P., McQuaid, J. B., Price, H. C., Liu, D., Ausset, P., Rosenberg, P. D., Taylor, J. W., Choularton, T., Bower, K., Coe, H., Gallagher, M., Crosier, J., Lloyd, G., Highwood, E. J., & Murray, B. J. (2018). Coarse-mode mineral dust size distributions, composition and optical properties from AER-D aircraft measurements over the tropical eastern Atlantic. *Atmospheric Chemistry and Physics, 18*, 17225–17257. https://doi.org/10.5194/acp-18-17225-2018

Sabbah, I., Ichoku, C., Kaufman, Y. J., & Remer, L. (2001). Full year cycle of desert dust spectral optical thickness and precipitable water vapor over Alexandria, Egypt. *Journal of Geophysical Research, 106*, 18305–18316. https://doi.org/10.1029/2000JD900410

Sayer, A. M., Hsu, N. C., Eck, T. F., Smirnov, A., & Holben, B. N. (2014). AERONET-based models of smoke-dominated aerosol near source regions and transported over oceans, and implications for satellite retrievals of aerosol optical depth. *Atmospheric Chemistry and Physics, 14*, 11493–11523. https://doi.org/10.5194/acp-14-11493-2014

Seinfeld, J. H., & Pandis, S. N. (2016). *Atmospheric chemistry and physics: From air pollution to climate change* (3rd ed.). Wiley, 1152 pp.

Sicard, M., Barragan, R., Dulac, F., Alados-Arboledas, L., & Mallet, M. (2016). Aerosol optical, microphysical and radiative properties at regional background insular sites in the western Mediterranean. *Atmospheric Chemistry and Physics, 16*, 12177–12203. https://doi.org/10.5194/acp-16-12177-2016

Sanchez-Marroquin, A., Hedges, D. H. P., Hiscock, M., Parker, S. T., Rosenberg, P. D., Trembath, J., Walshaw, R., Burke, I. T., McQuaid, J. B., & Murray, B. J. (2019). Characterisation of the filter inlet system on the FAAM BAe-146 research aircraft and its use for size-resolved aerosol composition measurements, *Atmospheric Measurements Techniques, 12*, 5741–5763. https://doi.org/10.5194/amt-12-5741-2019, 2019

Smolík, J., Ždímal, V., Schwarz, J., Lazaridis, M., Havárnek, V., Eleftheriadis, K., Mihalopoulos, N., Bryant, C., & Colbeck, I. (2003). Size resolved mass concentration and elemental composition of atmospheric aerosols over the Eastern Mediterranean area, *Atmos. Chem. Phys., 3*, 2207–2216. https://doi.org/10.5194/acp-3-2207-20033/

Tafuro, A. M., Banaba, F., De Tomasi, F., Perrone, M. R., & Gobbi, G. P. (2006). Saharan dust particle properties over the central Mediterranean. *Atmospheric Research, 81*, 67–93. https://doi.org/10.1016/j.atmosres.2005.11.008

Toledano, C., Cachorro, V. E., Berjon, A., de Frutos, A. M., Sorribas, M., de la Morena, B. A., & Goloub, P. (2007). Aerosol optical depth and Ångström exponent climatology at El Arenosillo AERONET site (Huelva, Spain). *Quarterly Journal of the Royal Meteorological Society, 133*, 795–807. https://doi.org/10.1002/qj.54

van der Does, M., Knippertz, P., Zschenderlein, P., Harrison, R. G., & Stuut, J.-B. W. (2018). The mysterious long-range transport of giant mineral dust particles. *Science Advances, 4*, eaau2768. https://doi.org/10.1126/sciadv.aau2768

Van Dingenen, R., Putaud, J.-P., Martins-Dos Santos, S., & Raes, F. (2005). Physical aerosol properties and their relation to air mass origin at Monte Cimone (Italy) during the first MINATROC campaign. *Atmospheric Chemistry and Physics, 5*, 2203–2226. https://doi.org/10.5194/acp-5-2203-2005

Weinzierl, B., Sauer, D., Esselborn, M. M., Petzold, A., Veira, A., Rose, M., Mund, S., Wirth, M., Ansmann, A., Tesche, M., Gross, S., & Freudenthaler, V. (2011). Microphysical and optical properties of dust and tropical biomass burning aerosol layers in the Cape Verde region–an overview of the airborne in situ and lidar measurements during SAMUM–2. *Tellus B: Chemical and Physical Meteorology, 63*, 589–618. https://doi.org/10.1111/j.1600-0889.2011.00566.x

Weinzierl, B., Ansmann, A., Prospero, J. M., Althausen, D., Benker, N., Chouza, F., Dollner, M., Farrell, D., Fomba, W. K., Freudenthaler, V., Gasteiger, J., Groß, S., Haarig, M., Heinold, B., Kandler, K., Kristensen, T. B., Mayol-Bracero, O. L., Müller, T., Reitebuch, O., … Walser, A. (2017). The Saharan aerosol long–range transport and aerosol–cloud–interaction experiment: Overview and selected highlights. *Bulletin of the American Meteorological Society, 98*, 1427–1451. https://doi.org/10.1175/BAMS-D-15-00142.1

Wiegner, M., Emeis, S., Freudenthaler, V., Heese, B., Junkermann, W., Münkel, C., Schäfer, K., Seefeldner, M., & Vogt, S. (2006). Mixing layer height over Munich, Germany: Variability and comparisons of different methodologies. *Journal of Geophysical Research, 111*, D13201. https://doi.org/10.1029/2005JD006593

Aerosol Composition and Reactivity

Silvia Becagli

Contents

Abstract Aerosol over the Mediterranean region is composed of a challenging mix of aerosol components from natural and anthropic sources, primary emitted or secondary formed in the atmosphere. In this chapter, we report a synthesis of the reactivity of the main aerosol components in the Mediterranean region. In particular, the reaction between Saharan dust, sea salt, ammonia, carbonaceous components with acids (and their gaseous precursor) and oxidant (e.g., ozone) are reported. The knowledge of aerosol reactivity is crucial in a climate change context environment because reactions are able to change the chemical and physical properties of aerosol particles, especially the gas/condensed phase interface. The products of the reactions usually present higher solubility than precursors, therefore altering the original particles optical property and their capability to form cloud condensation nuclei. For these reasons, studies on aerosol chemical reactivity in the Mediterranean atmosphere are highly appreciated.

Chapter reviewed by ***Konrad Kandler*** *(Institut für Angewandte Geowissenschaften, Technische Universität Darmstadt, Darmstadt, Germany) and* ***Cyrielle Denjean*** *(Centre National de Recherches Météorologiques, Université de Toulouse, Météo France, CNRS, Toulouse France), as part of the book Part VII Mediterranean Aerosol Properties also reviewed by* ***Jorge Pey Betrán*** *(ARAID-Instituto Pirenaico de Ecología, CSIC, Zaragoza, Spain)*

S. Becagli (✉)
Department of Chemistry Ugo Schiff, University of Florence, Sesto Fiorentino (FI), Italy
e-mail: silvia.becagli@unifi.it

F. Dulac et al. (eds.), *Atmospheric Chemistry in the Mediterranean Region*,
https://doi.org/10.1007/978-3-030-82385-6_13

1 Preamble and Definitions

Due to the presence of a high number of primary and secondary sources over the Mediterranean basin, the knowledge of mixing and reactions between the different aerosol types is important. The degree of particle mixing and aging changes the aerosol composition and possibly its optical and hygroscopic properties as well as its lifetime.

Many different reactive aerosol particle types occur in the Mediterranean region such as mineral dust, sea salt, natural and anthropogenic organic, black carbon and sulphate/sulphuric acid particles. In the following, a summary of the main inorganic and organic components found in the Mediterranean is given.

1.1 Non-carbonaceous Aerosol Composition

In the Mediterranean region, sulphate (SO_4^{2-}) and ammonium (NH_4^+) have been identified as the main ionic components of the submicron aerosol soluble fraction independent of the season, accounting for up to 90% of the total ionic content in the fine fraction both for the eastern (Bardouki et al., 2003; Sciare et al., 2005) and western (Sellegri et al., 2001; Putaud et al., 2004a; Carbone et al., 2014; Cerro et al., 2020) basin as well as the Adriatic (Tursic et al., 2006) areas. Significant correlation between non-sea-salt (nss) sulphate and ammonium has been observed in the northeastern and the southern Mediterranean region (Guerzoni et al., 1995; Mihalopoulos et al., 1997; Koçak et al., 2004). The correlation between these two species in the fine mode indicates a gas-to-particle conversion of this aerosol. Indeed, the heavy emission of gaseous precursors, such as SO_2 and NH_3 from continental anthropized areas in central and eastern Europe in combination to efficient vertical transport due to surface heating, can constitute a significant source of particles to the free troposphere (Carbone et al., 2014). These particles can eventually be transported over long distances, in particular towards the less anthropized areas over Mediterranean Sea.

For the coarse mode, nitrate, chloride, sodium and calcium are identified as main ionic soluble components. Among the ions arising from sea spray, chloride and sodium are the dominant species especially in coastal sites (e.g., Querol et al., 2009; Becagli et al., 2017). The calcium contribution is directly correlated to the dust intrusions when air masses originated from North Africa or the Middle East (Koçak et al., 2004; Marconi et al., 2014; Gobbi et al., 2019). Mineral dust originating from the Sahara is one of the most abundant aerosols encountered in the Mediterranean (e.g., Pey et al., 2013), but it has a sporadic character. For instance, at Lampedusa island in the central Mediterranean Sea in the time period 2004–2010, the crustal contribution to PM_{10} has an annual average value of 5.42 μg m^{-3} and reaches a value as high as 67.9 μg m^{-3} (corresponding to 49% of PM_{10}) during an intense Saharan dust event (Marconi et al., 2014). Saharan dust chemistry is variable depending on

the history of geological basement (e.g., Formenti et al., 2008; Scheuvens et al., 2013) and distinctly different from dust originating from other desert areas (Guieu et al., 2002 and references therein; Saydam & Senyuva, 2002; Krueger et al., 2004). In particular, Saydam and Senyuva (2002) suggest that the presence of specific fungi releasing oxalate in cloud water favours the photochemical production of bioavailable iron by Saharan dust.

The knowledge of Saharan dust mineralogical composition is useful to understand its surface reactivity. By XRD analysis of bulk aerosol samples, the most important mineral phases of northern African dust were identified: quartz, feldspars (plagioclase, K-feldspar), carbonates (calcite, dolomite, rarely Mg-calcite), sulphates (gypsum, anhydrite), chlorides (halite), micas (muscovite, biotite), iron oxides (hematite, magnetite), iron hydroxides (goethite) and titanium oxide phases (amphibole, pyroxene; Scheuvens et al., 2013 and references therein).

The northern region of the Saharan desert is characterized by higher carbonate contents, whereas the Sahelian zone contains lower amounts of carbonates (Moreno et al., 2006; Formenti et al., 2008; Kandler et al., 2011; Klaver et al., 2011).

1.2 Carbonaceous Aerosol

Carbonaceous aerosol constitutes a significant fraction of atmospheric particle mass concentrations in the continental areas of the Mediterranean region (Querol et al., 2009; Contini et al., 2018; Galindo et al., 2019). The carbonaceous fraction is usually classified into organic carbon (OC) and elemental carbon (EC). EC is a primary particulate pollutant emitted directly from fossil fuel combustion and biomass burning. In contrast, OC can either be emitted directly from combustion processes and other sources (primary organic carbon or POC) or formed in the atmosphere by oxidation reactions (secondary organic carbon or SOC). In urban areas, vehicle emissions are an important source of POC, whereas secondary organic aerosols (SOA) may be formed from the oxidation of both anthropogenic and biogenic volatile organic compounds (De Gouw & Jimenez, 2009). An actual separation between POC and SOC, however, is challenging when the timescales of emission and gas-to-particle formation overlap.

In contrast to inorganic aerosol, which is mostly composed of a few well-characterized components, organic aerosol is composed of thousands of species, many of them not characterized in detail (Goldstein & Galbally, 2007). Furthermore, the organic aerosol is dynamic and may have multiple gas-to-particle conversion pathways: most of its components are semi-volatile and can evaporate under atmospheric conditions; as gases, they can diffuse easily, be further processed in the atmosphere and undergo re-partitioning to the aerosol phase (Robinson et al., 2007). In a number of studies, positive matrix factorization (PMF) was used for the source apportionment of organic aerosols (e.g., Hildebrandt et al., 2010, 2011; Bougiatioti et al., 2014; Minguillón et al., 2016; Arndt et al., 2017; Michoud et al., 2017), sometimes combined with meteorological information (Petit et al., 2017). For PM_1

samples collected at Lampedusa, Mallet et al. (2019) show that the dominant factor in summer (53% of the PM_1 organic aerosol mass) consists of more oxygenated (therefore oxidized) organic aerosol. It is correlated with SO_4^{2-} and is generally dominant when air masses originate from the eastern Mediterranean and central Europe. The formation of oxidized compounds from precursors is due to the meteorology of the basin, and to other conditions such as high solar irradiation and summer temperature, and high relative humidity favouring secondary aerosol formation processes (Pey et al., 2009; Im et al., 2012; Pérez et al., 2016). Conversely, less oxidized oxygenated organic aerosol was more prevalent during westerly winds with air masses originating from the Atlantic Ocean, the western Mediterranean and at high altitudes over France and Spain from mistral winds (Mallet et al., 2019).

Biomass-burning aerosol (BBA) constitutes a significant fraction of primary organic aerosol (POA) (Bond et al., 2004) and secondary organic aerosol (SOA), derived from oxidative aging of volatile and semi-volatile organic vapours emitted from biomass-burning plumes (Decesari et al., 2002; Hallquist et al., 2009; Carrico et al., 2010). In summertime, air masses affected by wildfires sampled at Finokalia (Crete) hundreds of kilometres far from the source, showed that of the total organic aerosol (OA), about 20% is freshly emitted biomass-burning organic aerosol (BBOA), 30% is oxidized organic aerosol originating from BBOA (BB-OOA), and the remaining 50% is highly oxidized aerosol that results from extensive atmospheric ageing (Bougiatioti et al., 2014).

Water-soluble organic carbon (WSOC) compounds from gas-to-particle conversion or heterogeneous reactions on pre-existing particles are found in the sub- and supermicron modes. The contribution of WSOC to the total ionic content and its composition is highly variable and depends on the sampling location. Oxalate is the main ionic species independent of particle size (Bardouki et al., 2003; Tursic et al., 2006). During summer, the concentrations of oxalate, associated with acetate and formate, can account for up to 90% of the total organic ionic mass (Bardouki et al., 2003), oxalate being an end-product of the photochemical degradation of the higher dicarboxylic acids and fatty acids after reaction with O_3 (Kawamura & Sakaguchi, 1999). On the contrary, Tursic et al. (2006) show that the organic mono−/di-acids represent between 0.13% and 3.3% to the WSOC, assuming a large contribution of polycarboxylic acids, as humic or fulvic acids.

Regarding the carbonaceous particles emitted by incomplete combustion processes, casually referred to as soot, black carbon (BC) or elemental carbon (EC) particles depending on measurement method, it is necessary to specify the meaning of the many terms used in literature. The term black carbon (BC) is used to refer, in a general sense, to the most refractory, insoluble and strongly light-absorbing component of combustion particles. BC is essentially elemental carbon (EC), i.e., almost pure carbon with a graphitic-like chemical microstructure. These features distinguish BC from OC. The term BC-containing particle is used to refer to BC internally mixed with other particulate matter (Petzold et al., 2013). EC (or BC) represents a small fraction of the European atmospheric aerosol, typically contributing less than 10% to the total mass concentration of particles in both size

fractions smaller than 2.5 μm and 10 μm in diameter (Putaud et al., 2004a; Sciare et al., 2008; Zanatta et al., 2016). Despite being a minor mass fraction only, it has been argued that anthropogenic BC might cause the second largest positive radiative forcing after CO_2 (Jacobson 2000; Bond et al., 2013).

2 Aerosol Mixing and Reactivity

The aerosol particle mixing state can be external (i.e., two or more particulate constituents coexist in the same air mass, but in separate particles) or internal (i.e., two or more particulate constituents form mixed particles).

Using analytical electron microscopy, Ganor et al. (1998), Chabas and Lefèvre (2000) and Levin et al. (2005) investigated the individual particle composition of Mediterranean aerosols in land and sea breezes and in dust-laden air masses and reported on the internal mixing between soot, dust and sea salt, possibly as a result of cloud processing. Similar observations were made in other areas of the globe (Pósfai et al., 1994, 1995, 1999; Hasegawa & Ohta, 2002). Cook et al. (2007) also report internal mixing between sulphate and soot in airborne samples in the Northern Adriatic.

These studies, as well as various others (e.g., Caquineau et al., 1998; Falkovich et al., 2001; Formenti et al., 2001; Sobanska et al., 2003), reported on the abundance of sulphate particles in the form of gypsum ($CaSO_4$) resulting from the heterogeneous reaction of gaseous H_2SO_4 on the surface of mineral $CaCO_3$ particles and not from the coagulation of sulphate particles onto mineral dust.

In addition to microscopic analysis, the aerosol mixing state has also been investigated in many studies using hygroscopic tandem differential mobility analyser (HTDMA) measurements (see the chapter by Denjean, 2022).

3 Aerosol Chemical Reactivity

The atmospheric reactivity is highly affected by aerosols, as they offer to the surrounding gas a surface that may potentially favour surface-mediated chemical reactions (e.g., due to lower activation energies as in heterogeneous catalysis) and also a bulk condensed phase, in which reactions can take place that are not possible in the gas phase (such as electron transfer, acid-base reactions, hydrolysis, etc.) (see George et al., 2015 for a review). In this section, the common reactions of the main aerosol components with each other and with reactive gases are summarized. In particular, the surface reactivity of dust, sea salt, NH_3 and organic aerosols with inorganic acidic species (H_2SO_4, HNO_3), their precursors (SO_2, NO_x) and O_3 (and related radical species) is reported focusing on the Mediterranean region.

3.1 Mineral Dust

The reactivity of mineral dust substrates with atmospheric trace gases can be summarized as follows. In regard to the substrate, we may distinguish (i) reactive systems, owing to the presence of $CaCO_3$ leading to formation of a gaseous reaction product (CO_2) (Hanisch & Crowley, 2001a, b; Santschi & Rossi, 2006), and (ii) nonreactive systems leading to solid adsorbates such as nitrates, sulphites and sulphates without formation of a gas phase product except water vapour (Dentener et al., 1996; Ullerstam et al., 2003; Bauer et al., 2004a, b; Seisel et al., 2004; Bauer et al., 2007a, b; Mogili et al., 2006; Astitha et al., 2010; Crowley et al., 2010). The key to an understanding of the reactivity of calcite is the presence of a bifunctional surface intermediate $Ca(OH)(HCO_3)$; the involved reactions are:

$$\mathrm{Ca(OH)(HCO_3)} + \mathrm{HX} \rightarrow \mathrm{Ca(X)(HCO_3)} + \mathrm{H_2O} \tag{1}$$

$$\mathrm{Ca(X)(HCO_3)} + \mathrm{HX} \rightarrow \mathrm{Ca(X)y} + \mathrm{H_2O} + \mathrm{CO_2} \tag{2}$$

where X = NO_3, Cl, SO_4, C_2O_4, CH_3COO, or HCOO.

In the case of HNO_3, the final solid reaction product is $Ca(NO_3)_2$. This reaction is rapid, corresponding to atmospheric timescales of hours. At low to moderate HNO_3 exposures, the increase in the hygroscopicity of the particles is a linear function of the HNO_3(g) exposure (Sullivan et al., 2009a; Fig. 1). Besides, the hygroscopic conversion of the calcite component of atmospheric mineral dust aerosol will be controlled by the availability of nitric acid and similar reactants, and not by the atmospheric residence time (Sullivan et al., 2009a).

Calcium nitrate and calcium chloride are both more hygroscopic than calcite ($CaCO_3$), activating similarly to ammonium sulphate. Conversely, calcium sulphate and calcium oxalate are significantly less CCN-active than calcite; therefore, the common assumption that all mineral dust particles become more hygroscopic and CCN-active after atmospheric processing should be smoothed, calcium sulphate and calcium oxalate are two realistic proxies for aged mineral dust that remain non-hygroscopic (Sullivan et al., 2009b).

Measurements in the Mediterranean (Koçak et al., 2007; Pey et al., 2009; Athanasopoulou et al., 2016; Cesari et al., 2016) result in correlations of mineral species with sulphate and nitrates. Besides, Falkovich et al. (2004) clearly showed the interaction of oxalic, acetic and formic acids with mineral dust particles, demonstrating the occurrence of reaction (1) and (2) in the dust plume. The extent of the reaction with the different species is highly variable; very low increases of sulphate, nitrate and various organic acids onto mineral dust particles were found by Aymoz et al. (2004) from measurements at the high-altitude site (Monte Cimone); Putaud et al. (2004b) have indicated that there was no significant SO_4^{2-} formation onto mineral dust particles while NO_3^- shifted to the super-μm fraction due to the adsorption of HNO_3 onto dust particles during Saharan dust plumes. Athanasopoulou et al. (2016) found that the formation of nitrate on Saharan dust is seasonally

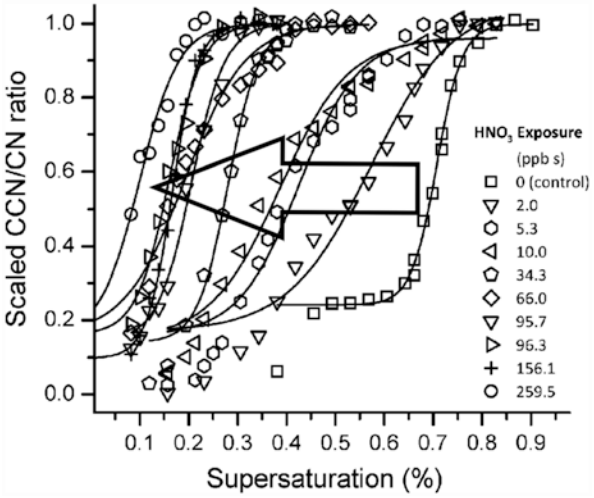

Fig. 1 CCN activation curves of unreacted and reacted calcite aerosol at 50% relative humidity (RH). The arrow in the plot indicates the increase in CCN activity (critical supersaturation decreases) as HNO_3(g) exposure (= concentration of HNO_3 × reaction time) increases. Reaction time is in the range 4–25 s. After Sullivan et al. (2009a)

dependent in eastern Mediterranean due to the abundant availability of nitric acid during summer compared to the winter and to the accumulation of aerosol particles in the atmosphere that is favoured by the low precipitation rates during summertime.

Rutile (the most stable crystal structure of TiO_2) has been proposed as a photoactive redox-reactive ingredient of Saharan dust (George et al., 2007). The role of nonreactive substrates may be either a mere support of surface-adsorbed water (SAW) or simply an inert substrate onto which trace gases may be irreversibly lost. Surface hydrolysis and surface disproportionation reactions are most frequently occurring. HNO_3 has a high affinity towards basic surface hydroxyl groups leading to rapid uptake kinetics for both reactive and nonreactive substrates and resulting in the formation of surface nitrates:

$$M^+OH + HNO_3 \rightarrow M^+ONO_2 + H_2O \quad (3)$$

Surface hydroxyl groups may be acidic (M-O^-H^+ leading to M-O^- after titration of the proton by a strong base) or basic (M^+OH^- such in reaction (3), in which HNO_3 as a strong acid neutralize the hydroxyl ion of the metal(oxide)). Actually, M^+ is not a metal cation because there are oxygen atoms/oxide anions surrounding M that are not shown in representation (3). Surface hydroxyl groups on rutile span the whole pH spectrum, from strongly basic to strongly acidic (Setyan et al., 2009, 2010). Börensen et al. (2000) also highlight the importance of adsorbed H_2O in the uptake of HNO_3 on metal oxide surfaces and therefore on the yield of the reaction (3).

N_2O_5 reacts by surface hydrolysis with SAW, both on reactive and on nonreactive substrates. Akin to HNO_3, N_2O_5 most rapidly reacts with the OH group of the

bifunctional intermediate on $CaCO_3$, reaction (1). The $NO_3^{\bullet}$ free radical reactivity is characterized by fast irreversible adsorption on any mineral dust surrogate without formation of a volatile, thus a detectable reaction product (Karagulian & Rossi, 2005).

N_2O_4 (the dimer of NO_2 that can be described as $NO^+NO_3^-$) is reactive because it leads to two stable species and it undergoes heterogeneous disproportionation on the mineral dust surface to surface nitrite and nitrate as well as to HONO when acidified:

$$N_2O_4(g) + H_2O(ads) \rightarrow HONO(g) + HNO_3(ads) \quad (4)$$

An interesting photocatalytic reaction of N_2O_4 with Saharan dust from Algeria, Tunisia, Morocco and Mauritania resulting in HONO has been found by George et al. (2007).

NH_4NO_3, which is a semi-volatile aerosol owing to its re-dissociation into NH_3 and HNO_3 under ambient conditions, is often associated with mineral dust aerosol. It can form coatings around the particles, which recrystallize upon reaching the efflorescence RH (Han et al., 2002). This transformation changes the solubility of the originally insoluble pristine particles and alters the aerosol size distribution and its optical properties.

H_2SO_3 reacts with the HCO_3^- surface functional group on $CaCO_3$ in contrast to all investigated surface acids including H_2CO_3. It generates surface sulphites and bisulphites on nonreactive substrates that may be oxidized to surface sulphates and bisulphates on contact with atmospheric oxidants (e.g., O_3 or NO_2; Ullerstam et al., 2002, 2003).

Due to the observed anticorrelation between O_3 levels and the presence of aerosol particles in the same atmospheric strata, many studies on its heterogeneous chemistry with mineral dust surrogates have been performed (e.g., Usher et al., 2003). However, it became clear very soon that the uptake kinetics of O_3 on mineral dust proxies is slow compared to the uptake of ozone precursors such as HNO_3 and N_2O_5. Bauer et al. (2004a, b) modelled Saharan dust aerosol, O_3 and HNO_3 for a 3-month period at Monte Cimone. They showed that uptake of atmospheric HNO_3 onto mineral dust aerosol is the most important factor in the reduction of tropospheric ozone during dust storm episodes whereas the direct heterogeneous destruction of ozone is negligible.

Another important atmospheric ageing process of dust is the redox chemistry and dissolution of Fe- and P-containing minerals. The kinetics of these processes are of crucial importance in determining the speciation and thus the bioavailability of these elements, since most photosynthetic aquatic organisms can take up iron and phosphorus only in the dissolved form (see also Kanakidou et al., 2022).

Acidification of airborne dust particles increases the amount of bioavailable P and Fe deposited on the surface ocean (Shi et al., 2011; Stockdale et al., 2016).

Iron-containing mineral particles dissolve by three different mechanisms: (1) proton-promoted dissolution, (2) ligand-controlled dissolution, and (3) reductive

dissolution (Wiederhold et al., 2006; Cwiertny et al., 2008; Key et al., 2008). The first two processes ultimately increase Fe bioavailability through the generation of dissolved forms of Fe(III). The third mechanism, reductive dissolution, involves electron transfer to Fe(III) atoms on the particle surface to produce Fe(II), which is readily released into solution (Larsen & Postma, 2001). In the presence of light, oxalate dissolves goethite (a Fe(III) mineral) by a photochemical reductive mechanism, producing aqueous Fe(II) and CO_2 (Sulzberger & Laubscher, 1995).

Fu et al. (2010) suggested that the Fe solubility is dependent on pH, light, O_2, type of acids (e.g., HCl, H_2SO_4, HNO_3), rather than temperature and reaction time. Indeed, the high concentration of nitric acid necessary to promote iron dissolution was also capable of suppressing the release of dissolved Fe(II) as nitrate could act as oxidant, favouring the formation of Fe(III) (Cwiertny et al., 2008).

Fe dissolution is much slower than P dissolution (Shi et al., 2011). Acid dissolution of P occurs rapidly (seconds to minutes) and is controlled by the amount of H^+ ions present. For $H^+ < 10^{-4}$ mol g^{-1} of dust, 1–10% of the total P is dissolved, largely as a result of dissolution of surface-bound forms (Stockdale et al., 2016). When the aerosol particles are activated into clouds at lower pH, the Fe is likely to reprecipitate as nanoparticles (Shi et al., 2009), whereas P does not reprecipitate (Stockdale et al., 2016).

Finally, Shi et al. (2011) indicate that the solubility of Fe depends on the dust mineralogical composition and, due to the differences in chemical weathering and aging of Fe oxides, there is a significant regional variability in the chemical and Fe mineralogical compositions of dusts across North African sources.

3.2 Sea Salt

Atmospheric sea salt particles undergo complex multiphase reactions (Finlayson-Pitts, 2003; Rossi, 2003) that have profound consequences on their evolving physicochemical properties, especially in the areas influenced by anthropogenic emissions. A noticeable depletion of chloride in sea salt particles was reported in a number of field studies conducted in both polluted and pristine marine environments (Bardouki et al., 2003; Pio et al., 1996; Sellegri et al., 2001; Bardouki et al., 2003; Koçak et al., 2004). The acid displacement reactions of sea salt chlorides with inorganic acids present in the atmosphere are attributed to the chloride depletion that can be expressed in a generalized form as follows:

$$\mathrm{NaCl}_{(\mathrm{aer})} + \mathrm{HA}_{(\mathrm{aer\,or\,gas})} \rightarrow \mathrm{NaA}_{(\mathrm{aer})} + \mathrm{HCl}_{(\mathrm{gas})} \tag{5}$$

NaCl denotes chloride salts in sea salt aerosol, and HA are atmospheric acids such as nitric acid, sulphuric acid, and methanesulphonic acid (MSA). These reactions release volatile HCl(gas) to the atmosphere, leaving particles enriched in corresponding salts (present as dissociate ions in the aerosol) and depleted in

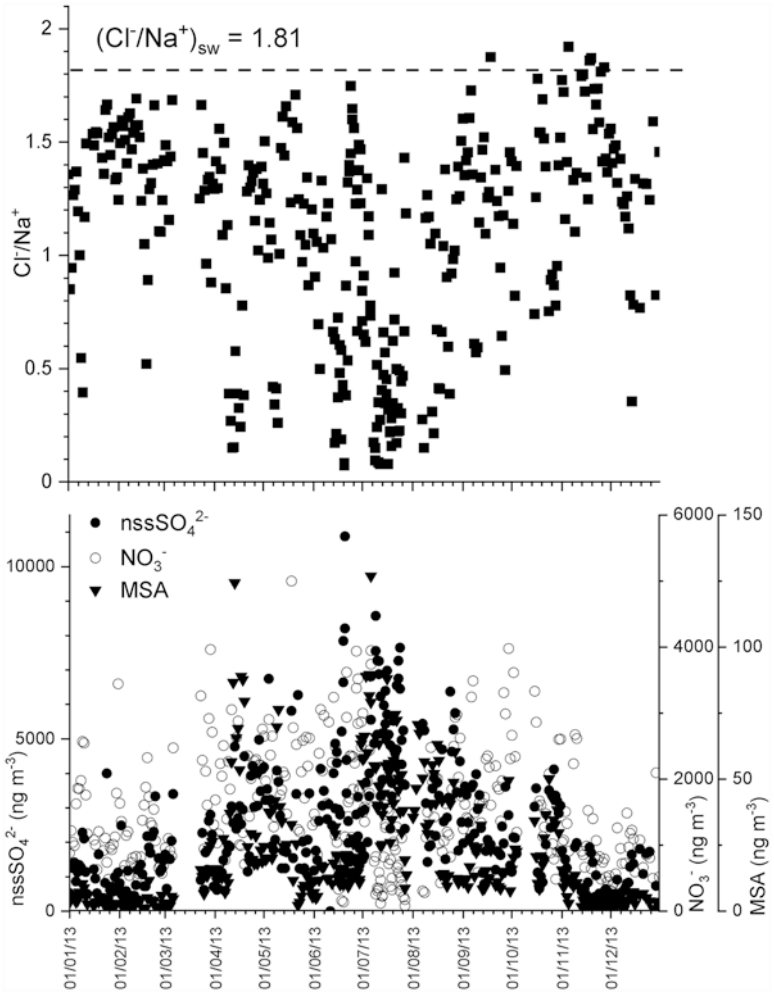

Fig. 2 Nitrate, non-sea-salt sulphate, methanesulphonate (*top*) and Cl^-/Na^+ mass concentration ratio (*bottom*) in PM_{10} sampled at Lampedusa during the year 2013. Dashed line represents the Cl^- to Na^+ ratio in seawater. Data show that the maximum chloride depletion (Cl^-/Na^+ ratio in the aerosol samples is lower than Cl^-/Na^+ in theoretical seawater) occurs in correspondence of maximum concentration of NO_3^-, $nssSO_4^{2-}$ and MSA. (Data from Becagli et al., 2017)

chloride (Fig. 2). The chloride deficit is mainly due to HNO_3, H_2SO_4; organic acids (MSA and low-molecular-weight carboxylic acids) can also contribute, even if their concentrations in the atmosphere are lower than inorganic acids (Falkovich et al., 2004).

The interaction between sea salt and weak organic acids has been discussed by Kerminen et al. (1998) and further investigated by Laskin et al. (2012), but studies in the Mediterranean region are scarce. While formation of the organic salt products is not thermodynamically favoured in bulk aqueous chemistry, these reactions in

aerosols are driven by high volatility and evaporation of the HCl product from drying particles. Field evidence shows that chloride components in sea salt particles may effectively react with organic acids releasing HCl gas to the atmosphere, leaving particles depleted in chloride and enriched in the corresponding organic salts on the surface. This process becomes more evident as transport times become longer (Laskin et al., 2012).

Sellegri et al. (2001) found significant chloride depletion reaching 50% also for continental samples in the northwestern Mediterranean. In these samples, chloride depletion is associated with supermicron nitrate and $NaNO_3$ formation. Conversely, samples collected from air masses originating from the North Atlantic Ocean between Britain and Iceland before passing over Spain or southwestern France were rain-scavenged over continents and showed high relative mass of NO_{3-} in the Aitken mode. In this case, chloride depletion is limited, supermicron NO_{3-} is very low, and chloride and nitrate are independent from each other. In some cases, the observed chloride deficit may reach up to 90%. A high Cl^- deficit is usually observed during summer, which may result from HNO_3 adsorption on sea salt particles, explaining also the high values of NO_3^- in the coarse mode (Bardouki et al., 2003; Koçak et al., 2004). A significant interaction between HNO_3 and coarse particles has also been observed by Putaud et al. (2004b) via the displacement of NO_{3-} towards the aerosol supermicrometer fraction in the presence of dust. As noted by Keene et al. (1990), such a deficit cannot be explained by acid displacement alone. Additional atmospheric chemistry processes contribute to the chloride depletion; these processes can be partially attributed to heterogeneous and interfacial chemistry with a variety of atmospheric trace species, including OH, HO_2, O_3, NO_2, N_2O_5 and $ClONO_2$ (Finlayson-Pitts, 2003; Rossi, 2003).

Reactions between sea salt aerosols and oxides of nitrogen generate inorganic halogen compounds that easily release atomic halogens upon photolysis (Finlayson-Pitts, 2003; Rossi, 2003).

3.3 Aerosol Neutralization by NH_3

The most important sources of ammonia (NH_3) are agricultural excreta, by abiotic and biotic decomposition of urea, from domestic and wild animals, and synthetic fertilizers (Bouwman et al., 1997; Paulot et al., 2014). In the troposphere, NH_3 is the main neutralizing agent for sulphuric acid (H_2SO_4) and nitric acid (HNO_3) (Hauglustaine et al., 2014).

Firstly, NH_3 will react instantaneously and irreversibly with H_2SO_4 to produce ammonium bisulphate $(NH_4)HSO_4$; the less abundant of the two species is the limitation for the subsequent formation of $(NH_4)_2SO_4$ or for the excess of H_2SO_4, respectively (Fig. 3). This reaction takes priority over ammonium nitrate formation due to a higher rate constant of the pseudo-first-order reaction between NH_3 and H_2SO_4 ($k_{S\text{-}1}$) than those (k_N) between NH_3 and HNO_3 (Baek et al., 2004 and references therein). Secondly, if all NH_3 is consumed by the previous reactions with H_2SO_4, no

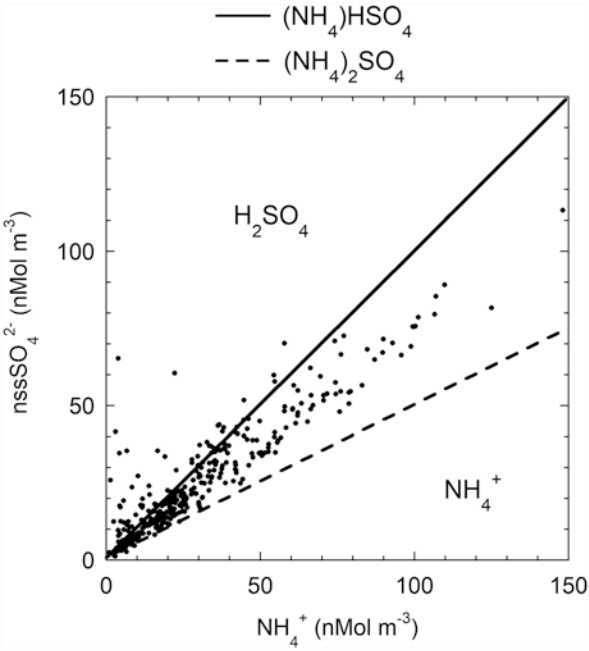

Fig. 3 Scatter plot of $nssSO_4^{2-}$ and NH_4^+ in PM_{10} samples collected at Lampedusa for the year 2013. The dashed line represents the $(NH_4)_2SO_4$ molar ratio; the area below this line represents the excess of NH_4^+ (that could be eventually counterbalanced by other anions (NO_3^-, Cl^-, methanesulphonate). The continuous line represents the $(NH_4)HSO_4$ molar ratio; the area above this line represents the excess of H_2SO_4. Experimental data are mainly between the two lines demonstrating the simultaneous presence of $(NH_4)HSO_4$ and $(NH_4)_2HSO_4$ in the investigated PM_{10} samples. (Reprinted from Becagli et al., 2017)

ammonium nitrate is formed. If there is still some NH_3, it will neutralize the HNO_3 to create NH_4NO_3 (Hauglustaine et al., 2014).

In the whole Mediterranean region, a significant correlation between NH_4^+ and SO_4^{2-} is found, especially in the fine aerosol fraction (Karageorgos & Rapsomanikis, 2007) with molar ratios in the range 1.22–1.35 (Sellegri et al., 2001; Bardouki et al., 2003; Karageorgos & Rapsomanikis, 2007; Theodosi et al., 2011). This suggests the presence of a mixture of $(NH_4)HSO_4$ and $(NH_4)_2SO_4$. It is indicative of an ammonium-poor atmosphere. In accordance, the correlation between NH_4^+ and NO_3^- is poor as expected. The formation of NH_4NO_3 is usually not expected to occur to a significant extent in an ammonium-poor atmosphere in summer. Actually, the rate constant $k_{S\text{-}1}$ was found to increase as ambient temperature and solar radiation increases and decreases with increasing relative humidity (Baek et al., 2004).

Conversely, ammonium is significantly correlated to nitrate in winter in a highly polluted environment in the Mediterranean (greater Athens area: Karageorgos & Rapsomanikis, 2007; Theodosi et al., 2011; Remoundaki et al., 2013; Paraskevopoulou et al., 2015; Po valley: Squizzato et al., 2013). The formation of ammonium nitrate was observed during the cold period under conditions of low

temperature, high relative humidity and the greater availability of HNO_3 from higher emissions of NO_x (peculiar for cold periods). Therefore, nitrate formation may occur at a local scale, enhanced by high availability of NO_2 and conditions of low temperature and high relative humidity, whereas sulphate is mainly transported on a regional scale (Squizzato et al., 2013).

With the reduction in SO_2 emissions, less atmospheric NH_3 is required to neutralize the strong acid H_2SO_4. Excess of NH_3 will form NH_4NO_3 aerosols so that its importance will likely increase over this century (Bauer et al., 2007a, b, 2016; Hauglustaine et al., 2014; Li et al., 2014).

3.4 Carbonaceous Aerosol

As reported above, carbonaceous aerosol is composed of organic compounds and elemental carbon (EC), the former being generally highly reactive species in the atmosphere. Although the EC presents a lower chemical reactivity than organic compounds, it presents a great adsorbing surface in terms of the optical absorption cross section in the near UV and in the visible range (e.g., Bond et al., 2013). Their great surface area allows the accumulation of other substances onto the surface of the EC particles, owing to the presence of high concentrations of species on the surface. Some reactions may occur more easily at the gas-solid interface than in the gas phase (Brooks et al., 2014). Indeed, the presence of ammonium sulphate was found on EC particles by Arndt et al. (2017) in a recent ChArMEx study combining mass spectrometry with other high-resolution chemical and physical measurements from the western Mediterranean. In the same study, eight classes of EC-rich particles could be distinguished (EC-SOx; EC-oxalate; EC-K; EC-K-SOx; EC-K-oxalate; K-EC-NOx; K-EC-SOx; K-EC-Oxalate), accounting for 53% of the total number of detected particles that is significantly representative of the total particles number (details may be found in Arndt et al., 2017). The importance of EC internal mixing is highlighted in a comprehensive data set over Europe by Zanatta et al. (2016), which provides evidence that internal mixing of BC with other aerosol components enhances the light absorption by BC owing to a lensing effect by less than a factor of two.

Similar to other aerosol types, the reactions involving organic aerosol enable some changes in the particles physical and chemical properties (Brooks et al., 2014; Ellison et al., 1999; Rudich, 2003; Pöschl, 2005; Rudich et al., 2007; George & Abbatt, 2010; Brooks et al., 2014). Laboratory and field studies have shown that biomass-burning aerosol is highly hygroscopic and water soluble, exhibiting up to approximately half the water uptake capacity of ammonium sulphate (Asa-Awuku et al., 2008; Cerully et al., 2015). Studies able to identify functional groups in the molecules have shown that fresh wood burning particles are composed of polyols and aromatic compounds, while aged samples are clearly depleted in alcohols and enriched in aliphatic acids with a smaller contribution of aromatic compounds (Paglione et al., 2014).

Heterogeneous OH oxidation of organic aerosol can initiate reactions that result in the production of oxidized polar functional groups. These can reduce the droplet surface tension (George et al., 2009) and increase the particle water solubility (Suda et al., 2014), thus enabling greater water uptake and higher cloud condensation nuclei (CCN) activity (Decesari et al., 2002; Petters et al., 2006; George et al., 2009). The hygroscopicity of ambient biogenic SOA processed by the OH radical was shown to increase at higher OH exposures with increasing oxygen-to-carbon (O:C) ratio (Wong et al., 2011).

Due to the high oxidation capacity of the Mediterranean atmosphere, such oxidation processes are particularly efficient in this area. Bougiatioti et al. (2016) report that over the Mediterranean region, the transformation of freshly emitted BBOA into more OOA-BB can result in a twofold increase in the organic hygroscopicity; approximately 10% of the total aerosol hygroscopicity is related to two biomass-burning components, which in turn contribute almost 35% to the fine-particle organic water (i.e., water associated to organic components) of the aerosol.

It is interesting to note that oxidative processes on biogenic aerosol, in addition to increasing its capability of forming CCN, are also able to change its optical properties. Laboratory studies find that as aerosol becomes more oxidized, the less optical absorbing it becomes, presumably due to oxidative degradation of the chromophores. The kinetics of this process depend on the type of oxidant. In particular, heterogeneous oxidation by OH in the presence of ozone results in a "bleaching" (i.e., decrease in absorptivity or optical absorption cross section) of the brown carbon (BrC) active over long timescales (timescale of days), suggesting a sustained change of BrC optical properties throughout the aerosol atmospheric lifetime (Laskin et al., 2015; Browne et al., 2019).

Due to its optical properties, BrC is receiving increasing attention in the Mediterranean region. BrC optical properties are reported by Tasoglou et al. (2020) for a remote site in eastern Mediterranean and by Liakakou et al. (2020) for urban background sites of Athens; in the latter study, also BrC sources daily and seasonal trends are reported.

4 Summary and Challenges for Future Research

The Mediterranean is a crossroads for air masses transporting different types of aerosols from natural and anthropogenic origins. Owing to the presence of a high number of primary and secondary sources and gaseous precursors, the high irradiance and the specific boundary layer dynamic is of particular relevance with respect to the knowledge of mixing of and reactions between the different aerosol components in this region. The main reactions occurring in the Mediterranean atmosphere are resumed and sketched in Table 1 (see also Kanakidou et al., 2022).

The aerosol reactivity is a key issue especially in a climate change environment because reactions enable changes in the chemical and physical features of the aerosol particle surfaces. In particular, chemical reactions are able, on the one hand,

Table 1 Reactions and processes between aerosol components and gaseous compounds present in the Mediterranean environment

Aerosol type	Reaction with/process	Reaction products	Consequences
Saharan dust	Inorganic acids and precursors (H_2SO_4, NO_x, HNO_3) and organic (oxalic, acetic, formic) acids	Formation of $CaSO_4$, $CaNO_3$, and Ca oxalate, acetate, and formate	Increased solubility of the particle surface
	O_3		O_3 destruction
	Acidity (HNO_3, H_2SO_4, HCl), organic ligands, sun light	Soluble Fe and P compounds	Ocean fertilization
Sea salt	Inorganic acids and precursors (H_2SO_4, N_2O_5, HNO_3)	Formation of Na_2SO_4, $NaNO_3$ and HCl(g)	Chloride depletion
	OH, HO_2, O_3, NO_2, N_2O_5, $ClONO_2$	Formation of Cl_2	Chloride depletion
Ammonia	H_2SO_4	Formation of $(NH_4)HSO_4$ and $(NH4)_2SO_4$	Preferred reaction compared to HNO_3
	HNO_3	Formation of $(NH_4)NO_3$	Occurs only if NH_3 is in molar excess with respect to H_2SO_4
Organic aerosol	OH, O_3, NO_3	Formation of oxygenated organic compounds (e.g., aliphatic acids)	Increased solubility of organic aerosol
	Equilibrium with gas phase		Transport over long distances
Elemental carbon	Adsorption of inorganic and organic compounds at its surface		Enhanced adsorption properties and CCN ability

to alter the optical properties of the particles and, on the other hand, to change the aerosol solubility that in turn is related to the capability of forming cloud condensation or ice nuclei, and therefore aerosol particles removal from the atmosphere. Furthermore, the continuous geochemical variations in the atmospheric composition over this region will be of interest. Specifically, the reduction in anthropogenic emissions from vehicles, power generation and maritime transport in Europe is occurring in parallel with the accentuation of new climatic scenarios.

Acknowledgements The author wishes to thank M. J. Rossi and P. Formenti for providing the first draft of this section, based on which she developed the work presented and discussed here.

References

Arndt, J., Sciare, J., Mallet, M., Roberts, G. C., Marchand, N., Sartelet, K., Sellegri, K., Dulac, F., Healy, R. M., & Wenger, J. C. (2017). Sources and mixing state of summertime background aerosol in the north-western Mediterranean basin. *Atmospheric Chemistry and Physics, 17*, 6975–7001. https://doi.org/10.5194/acp-17-6975-2017

Asa-Awuku, A., Sullivan, A. P., Hennigan, C. J., Weber, R. J., & Nenes, A. (2008). Investigation of molar volume and surfactant characteristics of water-soluble organic compounds in biomass burning aerosol. *Atmospheric Chemistry and Physics, 8*, 799–812. https://doi.org/10.5194/acp-8-799-2008

Astitha, M., Kallos, G., Spyrou, C., O'Hirok, W., Lelieveld, J., & Denier van der Gon, H. A. C. (2010). Modelling the chemically aged and mixed aerosols over the eastern central Atlantic Ocean – potential impacts. *Atmospheric Chemistry and Physics, 10*, 5797–5822. https://doi.org/10.5194/acp-10-5797-2010

Athanasopoulou, E., Protonotariou, A., Papangelis, G., Tombrou, M., Mihalopoulos, N., & Gerasopoulos, E. (2016). Long-range transport of Saharan dust and chemical transformations over the Eastern Mediterranean. *Atmospheric Environment, 140*, 592–604. https://doi.org/10.1016/j.atmosenv.2016.06.041

Aymoz, G., Jaffrezo, J.-L., Jacob, V., Colomb, A., & George, C. (2004). Evolution of organic and inorganic components of aerosol during a Saharan dust episode observed in the French Alps. *Atmospheric Chemistry and Physics, 4*, 2499–2512. https://doi.org/10.5194/acp-4-2499-2004

Baek, B. H., Aneja, V. P., & Tong, Q. (2004). Chemical coupling between ammonia, acid gases, and fine particles. *Environmental Pollution, 129, 89–98.* https://doi.org/10.1016/j.envpol.2003.09.022

Bardouki, H., Liakakou, H., Ecobomou, C., Sciare, J., Smolik, J., Zdimal, V., Eleftheriadis, K., Lazaridis, M., Dye, C., & Mihalopolos, N. (2003). Chemical composition of size resolved aerosols in the eastern Mediterranean during summer and winter. *Atmospheric Environment, 37*, 195–208. https://doi.org/10.1016/S1352-2310(02)00859-2

Bauer, S. E., Balkanski, Y., Schulz, M., Hauglustaine, D. A., & Dentener, F. (2004a). Global modeling of heterogeneous chemistry on mineral aerosol surfaces: Influence on tropospheric ozone chemistry and comparison to observations. *Journal of Geophysical Research – Atmospheres, 109*, D02304. https://doi.org/10.1029/2003JD003868

Bauer, S. E., Balkanski, Y., Schulz, M., & Hauglustaine, D. A. (2004b). Global modeling of heterogeneous chemistry on mineral aerosol surfaces: Influence on tropospheric ozone chemistry and comparison to observations. *Journal of Geophysical Research, 109*, D02304. https://doi.org/10.1029/2005JD006977

Bauer, S. E., Koch, D., Unger, N., Metzger, S. M., Shindell, D. T., & Streets, D. G. (2007a). Nitrate aerosols today and in 2030: A global simulation including aerosols and tropospheric ozone. *Atmospheric Chemistry and Physics, 7*, 5043–5059. https://doi.org/10.5194/acp-7-5043-2007

Bauer, S. E., Mishchenko, M. I., Lacis, A. A., Zhang, S., Perlwitz, J., & Metzger, S. M. (2007b). Do sulfate and nitrate coatings on mineral dust have important effects on radiative properties and climate modeling? *Journal of Geophysical Research, 112*, D0630. https://doi.org/10.1029/2005JD006977

Bauer, S. E., Tsigaridis, K., & Miller, R. (2016). Significant atmospheric aerosol pollution caused by world food cultivation. *Geophysical Research Letters, 43*, 5394–5400. https://doi.org/10.1002/2016GL068354

Becagli, S., Anello, F., Bommarito, C., Cassola, F., Calzolai, G., Iorio, T. D., di Sarra, A., Gómez-Amo, J.-L., Lucarelli, F., & Marconi, M. (2017). Constraining the ship contribution to the aerosol of the central Mediterranean. *Atmospheric Chemistry and Physics, 17*, 2067–2084. https://doi.org/10.5194/acp-17-2067-2017

Bond, T., Streets, D., Yarber, K., Nelson, S., Woo, J.-H., & Klimont, Z. (2004). A technology-based global inventory of black and organic carbon emissions from combustion. *Journal of Geophysical Research, 109*, D14203. https://doi.org/10.1029/2003JD003697

Bond, T. C., Doherty, S. H., Fahey, D. W., Forster, P. M., Berntsen, T., DeAngelo, B. J., Flanner, M. G., Ghan, G., Kärcher, B., Koch, D., Kinne, S., Kondo, Y., Quinn, P. K., Sarofim, M. C., Schultz, M. G., Schulz, M., Venkataraman, C., Zhang, H., Zhang, S., … Zender, C. S. (2013). Bounding the role of black carbon in the climate system: A scientific assessment. *Journal of Geophysical Research – Atmospheres, 118*, 5380–5552. https://doi.org/10.1002/jgrd.50171

Börensen, C., Kirchner, U., Scheer, V., Vogt, R., & Zellner, R. (2000). Mechanism and kinetics of the reaction of NO_2 or HNO_3 with alumina as a mineral dust model compound. *The Journal of Physical Chemistry. A, 104*, 5036–5045. https://doi.org/10.1021/jp994170d

Bougiatioti, A., Stavroulas, I., Kostenidou, E., Zarmpas, P., Theodosi, C., Kouvarakis, G., Canonaco, F., Prévôt, A., Nenes, A., & Pandis, S. (2014). Processing of biomass-burning aerosol in the eastern Mediterranean during summertime. *Atmospheric Chemistry and Physics, 14*, 4793–4807. https://doi.org/10.5194/acp-14-4793-2014

Bougiatioti, A., Bezantakos, S., Stavroulas, I., Kalivitis, N., Kokkalis, P., Biskos, G., Mihalopoulos, N., Papayannis, A., & Nenes, A. (2016). Biomass-burning impact on CCN number, hygroscopicity and cloud formation during summertime in the eastern Mediterranean. *Atmospheric Chemistry and Physics, 16*, 7389–7409. https://doi.org/10.5194/acp-16-7389-2016

Bouwman, A. F., Lee, D. S., Asman, W., Dentener, F. J., Van Der Hoek, K. W., & Olivier, J. G. J. (1997). A global high-resolution emission inventory for ammonia. *Global Biogeochemical Cycles, 11*, 561–587. https://doi.org/10.1029/97GB02266

Brooks, S. D., Suter, K., & Olivarez, L. (2014). Effects of chemical aging on the ice nucleation activity of soot and polycyclic aromatic hydrocarbon aerosols. *The Journal of Physical Chemistry. A, 118*, 10036–10047. https://doi.org/10.1021/jp508809y

Browne, E. C., Zhang, X., Franklin, J. P., Ridley, K. J., Kirchstetter, T. W., Wilson, K. R., Cappa, C. D., & Kroll, J. H. (2019). Effect of heterogeneous oxidative aging on light absorption by biomass burning organic aerosol. *Aerosol Science and Technology, 53*, 663–679. https://doi.org/10.1080/02786826.2019.1599321

Caquineau, S., Gaudichet, A., Gomes, L., Magonthier, M. C., & Chatenet, B. (1998). Saharan dust: Clay ratio as a relevant tracer to assess the origin of soil derived aerosols. *Geophysical Research Letters, 25*, 983–986. https://doi.org/10.1029/98GL00569

Carbone, C., Decesari, S., Paglione, M., Giulianelli, L., Rinaldi, M., Marinoni, A., Cristofanelli, P., Didiodato, A., Bonasoni, P., Fuzzi, S., & Facchini, M. C. (2014). 3-year chemical composition of free tropospheric PM_1 at the Mt. Cimone GAW global station – South Europe – 2165 m a.s.l. *Atmospheric Environment, 87*, 218–227. https://doi.org/10.1016/j.atmosenv.2014.01.048

Carrico, C. M., Petters, M. D., Kreidenweis, S. M., Sullivan, A. P., McMeeking, G. R., Levin, E. J. T., Engling, G., Malm, W. C., & Collett, J. L., Jr. (2010). Water uptake and chemical composition of fresh aerosols generated in open burning of biomass. *Atmospheric Chemistry and Physics, 10*, 5165–5178. https://doi.org/10.5194/acp-10-5165-2010

Cerro, J. C., Cerdà, V., Querol, X., Alastuey, A., & Pey, J. (2020). Variability of air pollutants, and PM composition and sources at a regional background site in the Balearic Islands: Review of western Mediterranean phenomenology from a 3-year study. *Science of the Total Environment, 717*, 137177. https://doi.org/10.1016/j.scitotenv.2020.137177

Cerully, K. M., Bougiatioti, A., Hite, J. R., Jr., Guo, H., Xu, L., Ng, N. L., Weber, R., & Nenes, A. (2015). On the link between hygroscopicity, volatility, and oxidation state of ambient and water-soluble aerosols in the southeastern United States. *Atmospheric Chemistry and Physics, 15*, 8679–8694. https://doi.org/10.5194/acp-15-8679-2015

Cesari, D., Donateo, A., Conte, M., Merico, E., Giangreco, A., Giangreco, F., & Contini, D. (2016). An inter-comparison of $PM_{2.5}$ at urban and urban background sites: Chemical characterization and source apportionment. *Atmospheric Research, 174–175*, 106–119. https://doi.org/10.1016/j.atmosres.2016.02.004

Chabas, A., & Lefèvre, R. A. (2000). Chemistry and microscopy of atmospheric particulates at Delos (Cyclades–Greece). *Atmospheric Environment, 34*, 225–238. https://doi.org/10.1016/S1352-2310(99)00255-1

Contini, D., Vecchi, R., & Viana, M. (2018). Carbonaceous aerosols in the atmosphere. *Atmosphere, 9*, 181. https://doi.org/10.3390/atmos9050181

Cook, J., Highwood, E. J., Coe, H., Formenti, P., Haywood, J. M., & Crosier, J. (2007). A comparison of aerosol optical and chemical properties over the Adriatic and Black Seas during summer 2004: Two case studies from ADRIEX. *Quarterly Journal of the Royal Meteorological Society, 133*(Suppl. 1), 33–45. https://doi.org/10.1002/qj.93

Crowley, J. N., Ammann, M., Cox, R. A., Hynes, R. G., Jenkin, M. E., Mellouki, A., Rossi, M. J., Troe, J., & Wallington, T. J. (2010). Evaluated kinetic and photochemical data for atmospheric chemistry: Volume V – Heterogeneous reactions on solid substrates. *Atmospheric Chemistry and Physics, 10*, 9059–9223. https://doi.org/10.5194/acp-10-9059-2010

Cwiertny, D. M., Baltrusaitis, J., Hunter, G. J., Laskin, A., Scherer, M. M., & Grassian, V. H. (2008). Characterization and acid-mobilization study of iron-containing mineral dust source materials. *Journal of Geophysical Research, 113*, D05202. https://doi.org/10.1029/2007JD009332

De Gouw, J., & Jimenez, J. L. (2009). Organic aerosols in the earth atmosphere. *Environmental Science & Technology, 43*, 7614–7618. https://doi.org/10.1021/es9006004

Decesari, S., Facchini, M. C., Matta, E., Mircea, M., Fuzzi, S., Chughtai, A. R., & Smith, D. M. (2002). Water soluble organic compounds formed by oxidation of soot. *Atmospheric Environment, 36*, 1827–1832. https://doi.org/10.1016/S1352-2310(02)00141-3

Denjean, C. (2022). Aerosol hygroscopicity. In F. Dulac, S. Sauvage, & E. Hamonou (Eds.), *Atmospheric chemistry in the Mediterranean Region* (Vol. 2, From air pollutant sources to impacts). Springer, this volume. https://doi.org/10.1007/978-3-030-82385-6_15

Dentener, F. J., Carmichael, G. R., Zhang, Y., Lelieveld, J., & Crutzen, P. J. (1996). Role of mineral aerosol as a reactive surface in the global troposphere. *Journal of Geophysical Research, 101*, 22869. https://doi.org/10.1029/96JD01818

Ellison, G. B., Tuck, A. F., & Vaida, V. (1999). Atmospheric processing of organic aerosols. *Journal of Geophysical Research – Atmospheres, 104*, 11633–11641. https://doi.org/10.1029/1999JD900073

Falkovich, A., Ganor, E., Levin, Z., Formenti, P., & Rudich, Y. (2001). Chemical and mineralogical analysis of individual mineral dust particles. *Journal of Geophysical Research, 106*, 18029–18036. https://doi.org/10.1029/2000JD900430

Falkovich, A. H., Schkolnik, G., Ganor, E., & Rudich, Y. (2004). Adsorption of organic compounds pertinent to urban environments onto mineral dust particles. *Journal of Geophysical Research, 109*, D02208. https://doi.org/10.1029/2003JD003919

Finlayson-Pitts, B. J. (2003). The tropospheric chemistry of sea salt: A molecular-level view of the chemistry of NaCl and NaBr. *Chemical Reviews, 103, 12*, 4801–4822. https://doi.org/10.1021/cr020653t

Formenti, P., Andreae, M. O., Ichoku, C., Andreae, T. W., Schebeske, G., Kettle, A. J., Maenhaut, W., Cafmeyer, J., Karnieli, A., & Lelieveld, J. (2001). Physical and chemical characteristics of aerosols over the Negev Desert (Israel). *Journal of Geophysical Research, 106*, 4871–4890. https://doi.org/10.1029/2000JD900556

Formenti, P., Rajot, J. L., Desboeufs, K., Caqineau, S., Chevaillier, S., Nava, S., Gaudichet, A., Journet, E., Triquet, S., Alfaro, S., Chiari, M., Haywood, J., Coe, H., & Highwood, E. (2008). Regional variability of the composition of mineral dust from western Africa: Results from the AMMA SOP0/DABEX and DODO field campaigns. *Journal of Geophysical Research, 113*, D00C13. https://doi.org/10.1029/2008JD009903

Fu, H., Cwiertny, D. M., Carmichael, G. R., Scherer, M. M., & Grassian, V. H. (2010). Photoreductive dissolution of Fe-containing mineral dust particles in acidic media. *Journal of Geophysical Research, 115*, D11304. https://doi.org/10.1029/2009JD012702

Galindo, N., Yubero, E., Clemente, A., Nicolas, J. F., Navarro-Selma, B., & Crespo, J. (2019). Insights into the origin and evolution of carbonaceous aerosols in a mediterranean urban environment. *Chemosphere, 235*, 636–642. https://doi.org/10.1016/j.chemosphere.2019.06.202

Ganor, E., Levin, Z., & Van Grieken, R. (1998). Composition of individual aerosol particles above the israelian Mediterranean coast during the summer time. *Atmospheric Environment, 32*, 1631–1642. https://doi.org/10.1016/S1352-2310(97)00397-X

George, I. J., & Abbatt, J. P. D. (2010). Heterogeneous oxidation of atmospheric aerosol particles by gas-phase radicals. *Nature Chemistry, 2*, 713–722. https://doi.org/10.1038/nchem.806

George, C., Ndour, M., Balkanski, Y., & Ka, O. (2007). Photoenhanced uptake of NO_2 on mineral dust. In W. Mellouki & A. R. Ravishankara (Eds.), *Regional climate variability and its impacts in the Mediterranean area* (NATO science series IV earth and environmental sciences) (Vol. 79, pp. 219–233). https://doi.org/10.1007/978-1-4020-6429-6_16

George, I. J., Chang, R. Y.-W., Danov, V., Vlasenko, A., & Abbatt, J. P. D. (2009). Modification of cloud condensation nucleus activity of organic aerosols by hydroxyl radical heterogeneous oxidation. *Atmospheric Environment, 43*, 5038–5045. https://doi.org/10.1016/j.atmosenv.2009.06.043

George, C., Ammann, M., D'Anna, B., Donladson, D. J., & Nizkodrov, S. A. (2015). Heterogeneous photochemistry in the atmosphere. *Chemical Reviews, 115*, 4218–4258. https://doi.org/10.1021/cr500648z

Gobbi, G. P., Barnaba, F., Di Liberto, L., Bolignano, A., Lucarelli, F., Nava, S., Perrino, C., Pietrodangelo, A., Basart, S., Costabile, F., Dionisi, D., Rizza, U., Canepari, S., Sozzi, R., Morelli, M., Manigrasso, M., Drewnick, F., Struckmeier, C., Poenitz, K., & Wille, H. (2019). An inclusive view of Saharan dust advections to Italy and the Central Mediterranean. *Atmospheric Environment, 201*, 242–256. https://doi.org/10.1016/j.atmosenv.2019.01.002

Goldstein, A. H., & Galbally, I. E. (2007). Known and unexplored organic constituents in the Earth's atmosphere. *Environmental Science & Technology, 41*, 1515–1521. https://doi.org/10.1021/es072476p

Guerzoni, S., Cristini, A., Caboi, R., Le Bolloch, O., Marras, I., & Rundeddu, L. (1995). Ionic composition of rainwater and atmospheric aerosols in Sardinia Southern Mediterranean. *Water, Air Soil & Pollution, 85*, 2077–2082. https://doi.org/10.1007/BF01186140

Guieu, C., Loÿe-Pilot, M.-D., Ridame, C., & Thomas, C. (2002). Chemical characterization of the Saharan dust end-member: Some biogeochemical implications for the western Mediterranean Sea. *Journal of Geophysical Research, 107*, 4258. https://doi.org/10.1029/2001JD000582

Hallquist, M., Wenger, J. C., Baltensperger, U., Rudich, Y., Simpson, D., Claeys, M., Dommen, J., Donahue, N. M., George, C., Goldstein, A. H., Hamilton, J. F., Herrmann, H., Hoffmann, T., Iinuma, Y., Jang, M., Jenkin, M. E., Jimenez, J. L., Kiendler-Scharr, A., Maenhaut, W., … Wildt, J. (2009). The formation, properties and impact of secondary organic aerosol: Current and emerging issues. *Atmospheric Chemistry and Physics, 9*, 5155–5236. https://doi.org/10.5194/acp-9-5155-2009

Han, J.-H., Hung, H.-M., & Martin, S. T. (2002). Size effect of hematite and corundum inclusions on the efflorescence relative humidities of aqueous ammonium nitrate particles. *Journal of Geophysical Research, 107*, 4086. https://doi.org/10.1029/2001JD001054

Hanisch, F., & Crowley, J. N. (2001a). Heterogeneous reactivity of gaseous nitric acid on Al_2O_3, $CaCO_3$ and atmospheric dust samples: A Knudsen cell study. *The Journal of Physical Chemistry. A, 105*, 3096–3106. https://doi.org/10.1021/jp001254+

Hanisch, F., & Crowley, J. N. (2001b). The heterogeneous reactivity of gaseous nitric acid on authentic mineral dust samples, and on individual mineral and clay mineral components. *Physical Chemistry Chemical Physics, 3*, 2474–2482. https://doi.org/10.1039/B101700O

Hasegawa, S., & Ohta, S. (2002). Some measurements of the mixing state of soot-containing particles at urban and non-urban areas. *Atmospheric Environment, 36*, 3899–3908. https://doi.org/10.1016/S1352-2310(02)00343-6

Hauglustaine, D. A., Balkanski, Y., & Schulz, M. (2014). A global model simulation of present and future nitrate aerosols and their direct radiative forcing of climate. *Atmospheric Chemistry and Physics, 14*, 11031–11063. https://doi.org/10.5194/acp-14-11031-2014

Hildebrandt, L., Engelhart, G., Mohr, C., Kostenidou, E., Lanz, V., Bougiatioti, A., DeCarlo, P., Prevot, A., Baltensperger, U., & Mihalopoulos, N. (2010). Aged organic aerosol in the Eastern Mediterranean: The Finokalia aerosol measurement experiment–2008. *Atmospheric Chemistry and Physics, 10*, 4167–4186. https://doi.org/10.5194/acp-10-4167-2010

Hildebrandt, L., Kostenidou, E., Lanz, V., Prevot, A., Baltensperger, U., Mihalopoulos, N., Laaksonen, A., Donahue, N. M., & Pandis, S. N. (2011). Sources and atmospheric processing of organic aerosol in the Mediterranean: Insights from aerosol mass spectrometer factor analysis. *Atmospheric Chemistry and Physics, 11*, 12499–12515. https://doi.org/10.5194/acp-11-12499-2011

Im, U., Markakis, K., Kocak, M., Gerasopoulos, E., Daskalakis, N., Mihalopoulos, N., Poupkou, A., Kinda, T., Unal, A., & Kanakidou, M. (2012). Summertime aerosol chemical composition in the eastern Mediterranean and its sensitivity to temperature. *Atmospheric Environment, 50*, 164–173. https://doi.org/10.1016/j.atmosenv.2011.12.044

Jacobson, M. Z. (2000). A physically-based treatment of elemental carbon optics: implications for global direct forcing of aerosols. *Geophysical Research Lettters, 27, 217–220.* https://doi.org/10.1029/1999GL010968

Kanakidou, M., Myriokefalitakis, S., Papadimitriou, V. C., & Nenes, A. (2022). Aerosol impact on atmospheric and precipitation chemistry. In F. Dulac, S. Sauvage, & E. Hamonou (Eds.), *Atmospheric chemistry in the Mediterranean Region (Vol. 2, From air pollutant sources to impacts). Springer, this volume. https://doi.org/10.1007/978-3-030-82385-6_21*

Kandler, K., Schütz, L., Jäckel, S., Lieke, K., Emmel, C., Müller-Ebert, D., Ebert, M., Scheuvens, D., Schladitz, A., Wiedensohler, A., & Weinbruch, S. (2011). Ground-based off-line aerosol measurements at Praia, Cape Verde, during the Saharan 2 mineral dust experiment: Microphysical properties and mineralogy. *Tellus B: Chemical and Physical Meteorology, 63*, 459–474. https://doi.org/10.3402/tellusb.v63i4.16240

Karageorgos, E. T., & Rapsomanikis, S. (2007). Chemical characterization of the inorganic fraction of aerosols and mechanisms of the neutralization of atmospheric acidity in Athens, Greece. *Atmospheric Chemistry and Physics, 7*, 3015–3033. https://doi.org/10.5194/acp-7-3015-2007

Karagulian, F., & Rossi, M. J. (2005). The heterogeneous chemical kinetics of NO_3 on atmospheric mineral dust surrogates. *Physical Chemistry Chemical Physics, 7*, 3150–3162. https://doi.org/10.1039/B506750M

Kawamura, K., & Sakaguchi, F. (1999). Molecular distributions of water soluble dicarboxylic acids in marine aerosols over the Pacific Ocean including tropics. *Journal of Geophysical Research: Atmospheres, 104*, 3501–3509. https://doi.org/10.1029/1998JD100041

Keene, W. C., Pszenny, A. A. P., Jacob, D. J., Duce, R. A., Galloway, J. N., Schultz-Tokos, J. J., Sievering, H., & Boatman, J. F. (1990). The geochemical cycling of reactive chlorine through marine troposphere. *Global Biogeochemical Cycles, 4*, 407–430. https://doi.org/10.1029/GB004i004p00407

Kerminen, V. M., Teinila, K., Hillamo, R., & Pakkanen, T. (1998). Substitution of chloride in sea-salt particles by inorganic and organic anions. *Journal of Aerosol Science, 29*, 929–942. https://doi.org/10.1016/S0021-8502(98)00002-0

Key, J. M., Paulk, N., & Johansen, A. M. (2008). Photochemistry of iron in simulated crustal aerosols with dimethyl sulfide oxidation products. *Environmental Science & Technology, 42*, 133–139. https://doi.org/10.1021/es071469y

Klaver, A., Formenti, P., Caquineau, S., Chevaillier, S., Ausset, P., Calzolai, G., Osborne, S., Johnson, B., Harrsion, M., & Dubovik, O. (2011). Physico-chemical and optical properties of Sahelian and Saharan mineral dust: In situ measurements during the GERBILS campaign. *Quarterly Journal of the Royal Meteorological Society, 137*, 1193–1210. https://doi.org/10.1002/qj.889

Koçak, M., Kubilay, N., & Mihalopolos, N. (2004). Ionic composition of lower tropospheric aerosols at a Northeastern Mediterranean site: Implications regarding sources and long-range transport. *Atmospheric Environment, 38*, 2067–2077. https://doi.org/10.1016/j.atmosenv.2004.01.030

Koçak, M., Mihalopoulos, N., & Kubilay, N. (2007). Chemical composition of the fine and coarse fraction of aerosols in the northeastern Mediterranean. *Atmospheric Environment, 41*, 7351–7368. https://doi.org/10.1016/j.atmosenv.2007.05.011

Krueger, B. J., Grassian, V. H., Cowin, J. P., & Laskin, A. (2004). Heterogeneous chemistry of individual mineral dust particles from different dust source regions: The importance of particle mineralogy. *Atmospheric Environment, 38*, 6253–6261. https://doi.org/10.1016/j.atmosenv.2004.07.010

Larsen, O., & Postma, D. (2001). Kinetics of reductive bulk dissolution of lepidocrocite, ferrihydrite, and goethite. *Geochimica et Cosmochimica Acta, 65*, 1367–1379. https://doi.org/10.1016/S0016-7037(00)00623-2

Laskin, A., Moffet, R. C., Gilles, M. K., Fast, J. D., Zaveri, R. A., Wang, B., Nigge, P., & Shutthanandan, J. (2012). Tropospheric chemistry of internally mixed sea salt and organic particles: Surprising reactivity of NaCl with weak organic acids. *Journal of Geophysical Research, 117*, D15302. https://doi.org/10.1029/2012JD017743

Laskin, A., Laskin, J., & Nizkodrov, S. A. (2015). Chemistry of atmospheric brown carbon. *Chemical Reviews, 115*, 4335–4382. https://doi.org/10.1021/cr5006167

Levin, Z., Teller, A., Ganor, E., & Yin, Y. (2005). On the interactions of mineral dust, sea-salt particles, and clouds: A measurement and modeling study from the Mediterranean Israeli Dust Experiment campaign. *Journal of Geophysical Research, 110*, D20202. https://doi.org/10.1029/2005JD005810

Li, J., Wang, W.-C., Liao, H., & Chang, W. (2014). Past and future direct radiative forcing of nitrate aerosol in East Asia. *Theoretical and Applied Climatology, 121*, 445–458. https://doi.org/10.1007/s00704-014-1249-1

Liakakou, E., Kaskaoutis, D. G., Grivas, G., Stavroulas, I., Tsagkaraki, M., Paraskevopoulou, D., Bougiatioti, A., Dumka, U. C., Gerasopoulos, E., & Mihalopoulos, N. (2020). Long-term brown carbon spectral characteristics in a Mediterranean city (Athens). *The Science of the Total Environment, 708*, 135019. https://doi.org/10.1016/j.scitotenv.2019.135019

Mallet, M. D., D'Anna, B., Même, A., Bove, M. C., Cassola, F., Pace, G., Desboeufs, K., Di Biagio, C., Doussin, J.-F., Maille, M., Massabò, D., Sciare, J., Zapf, P., di Sarra, A. G., & Formenti, P. (2019). Summertime surface PM_1 aerosol composition and size by source region at the Lampedusa island in the central Mediterranean Sea. *Atmospheric Chemistry and Physics, 19*, 11123–11142. https://doi.org/10.5194/acp-19-11123-2019

Marconi, M., Sferlazzo, D. M., Becagli, S., Bommarito, C., Calzolai, G., Chiari, M., di Sarra, A., Ghedini, C., Gómez-Amo, J. L., Lucarelli, F., Meloni, D., Monteleone, F., Nava, S., Pace, G., Piacentino, S., Rugi, F., Severi, M., Traversi, R., & Udisti, R. (2014). Saharan dust aerosol over the central Mediterranean Sea: PM_{10} chemical composition and concentration versus optical columnar measurements. *Atmospheric Chemistry and Physics, 14*, 2039–2054. https://doi.org/10.5194/acp-14-2039-2014

Michoud, V., Sciare, J., Sauvage, S., Dusanter, S., Léonardis, T., Gros, V., Kalogridis, C., Zannoni, N., Féron, A., & Petit, J.-E. (2017). Organic carbon at a remote site of the western Mediterranean Basin: Sources and chemistry during the ChArMEx SOP2 field experiment. *Atmospheric Chemistry and Physics, 17*, 8837–8865. https://doi.org/10.5194/acp-17-8837-2017

Mihalopoulos, N., Stephanou, E., Kanakidou, M., Pilitsidis, S., & Bousquet, P. (1997). Tropospheric aerosol ionic composition in the Eastern Mediterranean region. *Tellus B: Chemical and Physical Meteorology, 49*, 314–326. https://doi.org/10.1034/j.1600-0889.49.issue3.7.x

Minguillón, M., Pérez, N., Marchand, N., Bertrand, A., Temime-Roussel, B., Agrios, K., Szidat, S., van Drooge, B., Sylvestre, A., & Alastuey, A. (2016). Secondary organic aerosol origin in an urban environment: Influence of biogenic and fuel combustion precursors. *Faraday Discussions, 189*, 337–359. https://doi.org/10.1039/C5FD00182J

Mogili, P. K., Kleiber, P. D., Young, M. A., & Grassian, V. H. (2006). Heterogeneous uptake of ozone on reactive components of mineral dust aerosol: An environmental aerosol reaction chamber study. *The Journal of Physical Chemistry. A, 110*, 13799–13807. https://doi.org/10.1021/jp063620g

Moreno, T., Querol, X., Castillo, S., Alastuey, A., Cuevas, E., Herrmann, L., Mounkaila, M., Elvira, J., & Gibbons, W. (2006). Geochemical variations in aeolian mineral particles from the Sahara–Sahel Dust Corridor. *Chemosphere, 65*, 261–270. https://doi.org/10.1016/j.chemosphere.2006.02.052

Paglione, M., Saarikoski, S., Carbone, S., Hillamo, R., Facchini, M. C., Finessi, E., Giulianelli, L., Carbone, C., Fuzzi, S., Moretti, F., Tagliavini, E., Swietlicki, E., Stenström, K. E., Prévôt, A. S. H., Massoli, P., Canaragatna, M., Worsnop, D., & Decesari, S. (2014). Primary and secondary biomass burning aerosols determined by proton nuclear magnetic resonance (1H-NMR) spectroscopy during the 2008 EUCAARI campaign in the Po Valley (Italy). *Atmospheric Chemistry and Physics, 14*, 5089–5110. https://doi.org/10.5194/acp-14-5089-2014

Paraskevopoulou, D., Liakakou, E., Gerasopoulos, E., & Mihalopoulos, N. (2015). Sources of atmospheric aerosol from long-term measurements (5 years) of chemical composition in Athens, Greece. *The Science of the Total Environment, 527–528*, 165–178. https://doi.org/10.1016/j.scitotenv.2015.04.022

Paulot, F., Jacob, D. J., Pinder, R., Bash, J., Travis, K., & Henze, D. (2014). Ammonia emissions in the United States, European Union, and China derived by high-resolution inversion of ammonium wet deposition data: Interpretation with a new agricultural emissions inventory (MASAGE_NH3). *Journal of Geophysical Research – Atmospheres, 119*, 4343–4364. https://doi.org/10.1002/2013JD021130

Pérez, N., Pey, J., Reche, C., Cortés, J., Alastuey, A., & Querol, X. (2016). Impact of harbour emissions on ambient PM_{10} and $PM_{2.5}$ in Barcelona (Spain): Evidences of secondary aerosol formation within the urban area. *The Science of the Total Environment, 571*, 237–250. https://doi.org/10.1016/j.scitotenv.2016.07.025

Petit, J.-E., Favez, O., Albinet, A., & Canonaco, F. (2017). A user-friendly tool for comprehensive evaluation of the geographical origins of atmospheric pollution: Wind and trajectory analyses. *Environmental Modelling and Software, 88*, 183–187. https://doi.org/10.1016/j.envsoft.2016.11.022

Petters, M. D., Prenne, A. J., Kreidenweis, S. M., DeMott, P. J., Matsunaga, A., Lim, Y. B., & Ziemann, P. J. (2006). Chemical aging and the hydrophobic-to-hydrophilic conversion of carbonaceous aerosol. *Geophysical Research Letters, 33*, L24806. https://doi.org/10.1029/2006GL027249

Pey, J., Querol, X., & Alastuey, A. (2009). Variations of levels and composition of PM_{10} and $PM_{2.5}$ at an insular site in the Western Mediterranean. *Atmospheric Research, 94*, 285–299. https://doi.org/10.1016/j.atmosres.2009.06.006

Pey, J., Querol, X., Alastuey, A., Forastiere, F., & Stafoggia, M. (2013). African dust outbreaks over the Mediterranean Basin during 2001–2011: PM_{10} concentrations, phenomenology and trends, and its relation with synoptic and mesoscale meteorology. *Atmospheric Chemistry and Physics, 13*, 1395–1410. https://doi.org/10.5194/acp-13-1395-2013

Petzold, A., Ogren, J. A., Fiebig, M., Laj, P., Li, S.-M., Baltensperger, U., Holzer-Popp, T., Kinne, S., Pappalardo, G., Sugimoto, N., Wehrli, C., Wiedensohler, A., & Zhang, X.-Y. (2013). Recommendations for reporting "black carbon" measurements. *Atmospheric Chemistry and Physics, 13, 8365–8379.* https://doi.org/10.5194/acp-13-8365-2013

Pio, C. A., Cerqueira, M. A., Castro, L. M., & Salgueiro, M. L. (1996). Sulphur and nitrogen compounds in variable marine/continental air masses at the southwest European coast. *Atmospheric Environment, 30*, 3115–3127. https://doi.org/10.1016/1352-2310(96)00059-3

Pöschl, U. (2005). Atmospheric aerosols: Composition, transformation, climate and health effects. *Angewandte Chemie, International Edition, 44*, 7520–7540. https://doi.org/10.1002/anie.200501122

Pósfai, M., Anderson, J. R., Buseck, P. R., Shattuck, T. W., & Tindale, N. W. (1994). Constituents of a remote pacific marine aerosol: A TEM study. *Atmospheric Environment, 28*, 1747–1756. https://doi.org/10.1016/1352-2310(94)90137-6

Pósfai, M., Anderson, J. R., Buseck, P. R., & Sievering, H. (1995). Compositional variations of sea-salt-mode aerosol particles from the North Atlantic. *Journal of Geophysical Research, 100*, 23063–23074. https://doi.org/10.1029/95JD01636

Pósfai, M., Anderson, J. R., Buseck, P. R., & Sievering, H. (1999). Soot and sulfate aerosol particles in the remote marine troposphere. *Journal of Geophysical Research, 104*, 21685–21694. https://doi.org/10.1029/1999JD900208

Putaud, J. P., Raes, F., Van Dingenen, R., Bruggemann, E., Facchini, M. C., Decesari, S., Fuzzi, S., Gehrig, R., Huglin, C., Laj, P., Lorbeer, G., Maenhaut, W., Mihalopoulos, N., Muller, K., Querol, X., Rodriguez, S., Schneider, J., Spindler, G., ten Brink, H., … Wiedensohler, A. (2004a). A European aerosol phenomenology 2: Chemical characteristics of particulate matter at kerbside, urban, rural and background sites in Europe. *Atmospheric Environment, 38*, 2579–2595. https://doi.org/10.1016/j.atmosenv.2004.01.041

Putaud, J.-P., Van Dingenen, R., Dell'Acqua, A., Raes, F., Matta, E., Decesari, S., Facchini, M. C., & Fuzzi, S. (2004b). Size-segregated aerosol mass closure and chemical composition in Monte Cimone (I) during MINATROC. *Atmospheric Chemistry and Physics, 4*, 889–902. https://doi.org/10.5194/acp-4-889-2004

Querol, X., Alastuey, A., Pey, J., Cusack, M., Pérez, N., Mihalopoulos, N., Theodosi, C., Gerasopoulos, E., Kubilay, N., & Koçak, M. (2009). Variability in regional background aerosols within the Mediterranean. *Atmospheric Chemistry and Physics, 9*, 4575–4591. https://doi.org/10.5194/acp-9-4575-2009

Remoundaki, E., Kassomenos, P., Mantas, E., Mihalopoulos, N., & Tsezos, M. (2013). Composition and mass closure of $PM_{2.5}$ in urban environment (Athens, Greece). *Aerosol and Air Quality Research, 13*, 72–82. https://doi.org/10.4209/aaqr.2012.03.0054

Robinson, A. L., Donahue, N. M., Shrivastava, M. K., Weitkamp, E. A., Sage, A. M., Grieshop, A. P., Lane, T. E., Pierce, J. R., & Pandis, S. N. (2007). Rethinking organic aerosols: Semivolatile emissions and photochemical aging. *Science, 315*, 1259–1262. https://doi.org/10.1126/science.1133061

Rossi, M. J. (2003). Heterogeneous reactions on salts. *Chemical Reviews, 103*, 4823–4882. https://doi.org/10.1021/cr020507n

Rudich, Y. (2003). Laboratory perspectives on the chemical transformations of organic matter in atmospheric particles. *Chemical Reviews, 103*, 5097–5124. https://doi.org/10.1021/cr020508f

Rudich, Y., Donahue, N. M., & Mentel, T. F. (2007). Aging of organic aerosol: Bridging the gap between laboratory and field studies. *Annual Review of Physical Chemistry, 58*, 321–352. https://doi.org/10.1146/annurev.physchem.58.032806.104432

Santschi, C., & Rossi, M. J. (2006). The uptake of CO_2, SO_2, HNO_3 and HCl on $CaCO_3$ at 300K: Mechanism and the role of adsorbed water. *The Journal of Physical Chemistry. A, 110*, 6789–6802. https://doi.org/10.1021/jp056312b

Saydam, A. C., & Senyuva, H. Z. (2002). Deserts: Can they be the potential suppliers of bioavailable iron? *Geophysical Research Letters, 29*, 1524. https://doi.org/10.1029/2001GL013562

Scheuvens, D., Schütz, L., Kandler, K., Ebert, M., & Weinbruch, S. (2013). Bulk composition of northern African dust and its source sediments – A compilation. *Earth-Science Reviews, 116*, 170–194. https://doi.org/10.1016/j.earscirev.2012.08.005

Sciare, J., Oikonomou, K., Cachier, H., Mihalopoulos, N., Andreae, M. O., Maenhaur, W., & Sarda-Estève, R. (2005). Aerosol mass closure and reconstruction of the light scattering coefficient over the Eastern Mediterranean Sea during the MINOS campaign. *Atmospheric Chemistry and Physics, 5*, 2253–2265. https://doi.org/10.5194/acp-5-2253-2005

Sciare, J., Oikonomou, K., Favez, O., Liakakou, E., Markaki, Z., Cachier, H., & Mihalopoulos, N. (2008). Long-term measurements of carbonaceous aerosols in the Eastern Mediterranean: Evidence of long-range transport of biomass burning. *Atmospheric Chemistry and Physics, 8*, 5551–5563. https://doi.org/10.5194/acp-8-5551-2008

Seisel, S., Börensen, C., Vogt, R., & Zellner, R. (2004). The heterogeneous reaction of HNO_3 on mineral dust and alumina surfaces: A combined Knudsen cell and DRIFTS study. *Physical Chemistry Chemical Physics, 6*, 5498–5508. https://doi.org/10.1039/b410793d

Sellegri, K., Gourdeau, J., Putaud, J.-P., & Despiau, S. (2001). Chemical composition of marine aerosol in a Mediterranean coastal zone during the FETCH experiment. *Journal of Geophysical Research, 106*, 12023–12037. https://doi.org/10.1029/2000JD900629

Setyan, A., Sauvain, J.-J., & Rossi, M. J. (2009). The use of heterogeneous chemistry for the characterization of functional groups at the gas/particle interface of soot and TiO_2 nanoparticles. *Physical Chemistry Chemical Physics, 11*, 6205–6217. https://doi.org/10.1039/B902509J

Setyan, A., Sauvain, J.-J., Guillemin, M., Riediker, M., Demirdjian, B., & Rossi, M. J. (2010). Probing functional groups at the gas–aerosol interface using heterogeneous titration reactions: A tool for predicting aerosol health effects? *ChemPhysChem, 11*, 3823–3835. https://doi.org/10.1002/cphc.201000490

Shi, Z., Krom, M. D., Bonneville, S., Baker, A. R., Jickells, T. D., & Benning, L. G. (2009). Formation of iron nanoparticles and increase in iron reactivity in the mineral dust during simulated cloud processing. Environmental Science & Technology, 43, 6592–6596. https://doi.org/10.1021/es901294g

Shi, Z., Krom, M. D., Bonneville, S., Baker, A. R., Bristow, C., Drake, N., Mann, G., Carslaw, K., McQuaid, J. B., Jickells, T., & Benning, L. G. (2011). Influence of chemical weather-

ing and aging of iron oxides on the potential iron solubility of Saharan dust during simulated atmospheric processing. *Global Biogeochemical Cycles, 25*, GB2010. https://doi.org/10.1029/2010GB003837

Sobanska, S., Coeur, C., Maenhaut, W., & Adams, F. (2003). SEM-EDX characterisation of tropospheric aerosols in the Negev desert (Niger). *Journal of Atmospheric Chemistry, 44*, 299–322. https://doi.org/10.1023/A:1022969302107

Squizzato, S., Masiol, M., Brunelli, A., Pistollato, S., Tarabotti, E., Rampazzo, G., & Pavoni, B. (2013). Factors determining the formation of secondary inorganic aerosol: A case study in the Po Valley (Italy). *Atmospheric Chemistry and Physics, 13*, 1927–1939. https://doi.org/10.5194/acp-13-1927-2013

Stockdale, A., Kroma, M. D., Mortimer, R. J. G., Benninga, L. G., Carslawa, K. S., Herberta, R. J., Shi, Z., Myriokefalitakis, S., Kanakidou, M., & Nenes, A. (2016). Understanding the nature of atmospheric acid processing of mineral dusts in supplying bioavailable phosphorus to the oceans. *Proceeding of National Academy Science, 113*, 14639–14644. https://doi.org/10.1073/pnas.1608136113

Suda, S. R., Petters, M. D., Yeh, G. K., Strollo, C., Matsunaga, A., Faulhaber, A., Ziemann, P. J., Prenni, A. J., Carrico, C. M., Sullivan, R. C., & Kreidenweis, S. M. (2014). Influence of functional groups on organic aerosol cloud condensation nucleus activity. *Environmental Science & Technology, 48*, 10182–10190. https://doi.org/10.1021/es502147y

Sullivan, R. C., Moore, M. J. K., Petters, M. D., Kreidenweis, S. M., Roberts, G. C., & Prather, K. A. (2009a). Timescale for hygroscopic conversion of calcite mineral particles through heterogeneous reaction with nitric acid. *Physical Chemistry Chemical Physics, 11*, 7826–7837. https://doi.org/10.1039/b904217b

Sullivan, R. C., Moore, M. J. K., Petters, M. D., Kreidenweis, S. M., Roberts, G. C., & Prather, K. A. (2009b). Effect of chemical mixing state on the hygroscopicity and cloud nucleation properties of calcium mineral dust particles. *Atmospheric Chemistry and Physics, 9*, 3303–3316. https://doi.org/10.5194/acp-9-3303-2009

Sulzberger, B., & Laubscher, H. (1995). Reactivity of various types of iron(III) (hydr) oxides towards light-induced dissolution. *Marine Chemistry, 50*, 103–115. https://doi.org/10.1016/0304-4203(95)00030-U

Tasoglou, A., Louvaris, E., Florou, K., Liangou, A., Karnezi, E., Kaltsonoudis, C., Wang, N., & Pandis, S. N. (2020). Aerosol light absorption and the role of extremely low volatility organic compounds. *Atmospheric Chemistry and Physics, 20*, 11625–11637. https://doi.org/10.5194/acp-20-11625-2020

Theodosi, C., Grivas, G., Zarmpas, P., Chaloulakou, A., & Mihalopoulos, N. (2011). Mass and chemical composition of size-segregated aerosols (PM_1, $PM_{2.5}$, PM_{10}) over Athens, Greece: Local versus regional sources. *Atmospheric Chemistry and Physics, 11*, 11895–11911. https://doi.org/10.5194/acp-11-11895-2011

Tursic, J., Podkrajsek, B., Grgic, I., Ctyroky, P., Berner, A., Dusek, U., & Hitzenberger, R. (2006). Chemical composition and hygroscopic properties of size-segregated aerosol particles collected at the Adriatic coast of Slovenia. *Chemosphere, 63*, 1193–1202. https://doi.org/10.1016/j.chemosphere.2005.08.040

Ullerstam, M., Vogt, R., Langer, S., & Ljungström, E. (2002). The kinetics and mechanism of SO_2 oxidation by O_3 on mineral dust. *Physical Chemistry Chemical Physics, 4*, 4694–4699. https://doi.org/10.1039/b203529b

Ullerstam, M., Johnson, M. S., Vogt, R., & Ljungström, E. (2003). DRIFTS and Knudsen cell study of the heterogeneous reactivity of SO_2 and NO_2 on mineral dust. *Atmospheric Chemistry and Physics, 3*, 2043–2051. https://doi.org/10.5194/acp-3-2043-2003

Usher, C. R., Michel, A. E., & Grassian, V. H. (2003). Reactions on mineral dust. *Chemical Reviews, 103*, 4883–4939. https://doi.org/10.1021/cr020657y

Wiederhold, J. G., Kraemer, S. M., Teutsch, N., Borer, P. M., Halliday, A. N., & Kretzschmar, R. (2006). Iron isotope fractionation during proton-promoted, ligand-controlled, and reductive dissolution of goethite. *Environmental Science & Technology, 40*, 3787–3793. https://doi.org/10.1021/es052228y

Wong, J. P. S., Lee, A. K. Y., Slowik, J. G., Cziczo, D. J., Leaitch, W. R., Macdonald, A., & Abbatt, J. P. D. (2011). Oxidation of ambient biogenic secondary organic aerosol by hydroxyl radicals: Effects on cloud condensation nuclei activity. *Geophysical Research Letters, 38*, L22805. https://doi.org/10.1029/2011GL049351

Zanatta, M., Gysel, M., Bukowiecki, N., Müller, T., Weingartner, E., Areskoug, H., Fiebig, M., Yttri, K. E., Mihalopoulos, N., Kouvarakis, G., Beddows, D., Harrison, R. M., Cavalli, F., Putaud, J. P., Spindler, G., Wiedensohler, A., Alastuey, A., Pandolfi, M., Sellegri, K., … Laj, P. (2016). A European aerosol phenomenology-5: Climatology of black carbon optical properties at 9 regional background sites across Europe. *Atmospheric Environment, 145*, 346–364. https://doi.org/10.1016/j.atmosenv.2016.09.035

Aerosol Optical Properties

Marc Mallet, Patrick Chazette, François Dulac, Paola Formenti, Claudia Di Biagio, Cyrielle Denjean, and Isabelle Chiapello

Contents

*Chapter reviewed by **Nikos Hatzianastassiou** (Laboratory of Meteorology, Department of Physics, University of Ioannina, Greece), and **Silvia Becagli** (Department of Chemistry Ugo Schiff, University of Florence, Sesto Fiorentino, Florence, Italy), as part of the book Part VII Mediterranean Aerosol Properties also reviewed by **Jorge Pey Betrán** (ARAID-Instituto Pirenaico de Ecología, CSIC, Zaragoza, Spain)*

M. Mallet (✉) · C. Denjean
Centre National de Recherches Météorologiques (CNRM), Université de Toulouse, Météo France, CNRS, Toulouse, France
e-mail: marc.mallet@meteo.fr

P. Chazette · F. Dulac
Laboratoire des Sciences du Climat et de l'Environnement (LSCE), CEA-CNRS-UVSQ, IPSL, Université Paris-Saclay, Gif-sur-Yvette, France

P. Formenti · C. Di Biagio
Université Paris Cité and Univ. Paris Est Créteil, CNRS, LISA, F-75013 Paris, France

I. Chiapello
Université de Lille, CNRS, Laboratoire d'Optique Atmosphérique (LOA), Villeneuve d'Ascq, France

F. Dulac et al. (eds.), *Atmospheric Chemistry in the Mediterranean Region*,
https://doi.org/10.1007/978-3-030-82385-6_14

Abstract In this chapter, we review the measured optical properties of different aerosol types observed in the Mediterranean region, from both ground-based and aircraft in situ measurements and from remote sensing. We focus our description on the most relevant optical parameters used in radiative forcing calculations, namely, the aerosol optical depth (AOD) and its spectral dependence (Angström exponent, AE), the single scattering albedo (SSA) and the asymmetry parameter (g). We also consider the aerosol backscatter to extinction ratio (BER), which is a key parameter in the inversion of lidar profiles for deriving the vertical distribution of the aerosol extinction.

1 Introduction

Aerosol optical properties observed over the Mediterranean region are very variable in both space and time (e.g., Moulin et al., 1998; Markowicz et al., 2002; Barnaba & Gobbi, 2004; Bryant et al., 2006; Pace et al., 2006; Papadimas et al., 2008; De Meij & Lelieveld, 2011; Mallet et al., 2013, 2016; Ealo et al., 2016, 2018; Pandolfi et al., 2018). Here, the discussion is focused on the optical parameters that are mostly used in direct radiative forcing calculations. This includes the spectral aerosol optical depth (AOD_λ, extinction at the wavelength λ integrated over the whole atmospheric column) and its spectral dependence, namely, the Ångstrom exponent ($AE = -\log(AOD_{\lambda 1}/AOD_{\lambda 2}) / \log(\lambda_1/\lambda_2)$), the single scattering albedo (SSA: ratio of aerosol scattering to the total extinction, i.e., scattering + absorption) and the asymmetry parameter (g: cosine-weighted average of the aerosol scattering phase function). Among the different radiative parameters, knowledge of the SSA (and its spectral variation) is essential for the estimation of the aerosol direct radiative effect, as it determines its sign (i.e., cooling vs. heating), depending on the underlying earth surface albedo, vertical distribution of aerosol types and total AOD. We additionally consider the aerosol backscatter-to-extinction ratio (BER: the product of the aerosol single scattering albedo by the probability that a photon is backscattered by the aerosol), which depends on the aerosol types and has to be hypothesized in under-constrained inversions of lidar profiles for deriving the aerosol extinction vertical profile (Klett, 1983).

2 Dataset

The aerosol optical properties presented in this section include different techniques of observations, based on in situ local estimates, as well as remote sensing retrievals from both the surface (AERONET sun photometer network in particular) and different satellites. Satellite-derived aerosol optical parameters such as AOD, AE and more recently SSA can be retrieved, but results are much more reliable in terms of AOD than the two other parameters (e.g., Thieuleux et al., 2005; Antoine & Nobileau, 2006; Bréon et al., 2011). Satellite aerosol products have been used in the literature for describing the AOD geographical distribution over the Mediterranean basin and its seasonal and interannual variability as described in other chapters of this book (Kaskaoutis et al., 2023a, 2023b). Here we focus on long-term regional AOD averages. A synthesis of available satellite-derived regional mean AOD is given in Table 1. In Table 2, we list the main

Table 1 Satellite remote sensing of the aerosol optical depth (AOD) over seawater pixels of the Mediterranean basin and averaged from mean monthly products, unless specified

Satellite/sensor (product; resolution)	Period	Wavelength λ (nm)	AOD ± std. dev.	References
METEOSAT/MVIRI (from ISCCP-B2, »35 km)	1984–1994	550	0.11 ± 0.04[a, b]	Moulin et al. (1998)
CALIOP (CALIPSO L3-V2; 1°)	2007–2015	532	0.09[a, c1] 0.06[a,c2]	Derived from Marinou et al. (2017)
SeaWiFS (Antoine & Nobileau, 2006; 8 km)	1998–2004	865	0.165 ± 0.004 0.205 ± 0.016[d]	Derived from Antoine and Nobileau (2006)
SeaWiFS (Hsu et al., 2012; 0.5°)	2000–2007	550[e]	0.168	Nabat et al. (2013)
NOAA/AVHRR (Stowe et al., 1997; 0.5°)	2000–2007	550	0.179	
TERRA/MISR (MIL3MAE v. F15_0031; 0.5°)	2001–2010	550	0.211	
TERRA/MODIS (MOD08_M3 Coll. 5.1; 1°)	2001–2010	550	0.206	
AQUA/MODIS (MYD08_M3 coll. 5.1; 1°)	2003–2010	550	0.197	
ENVISAT/MERIS (MER_T550M; 8 km)	2003–2010	550	0.151	
PARASOL/POLDER-3 (PR_ATM_M Coll. 2; 1/6°)	2006–2010	550[e, f]	0.244	
MSG/SEVIRI (AER-OC-M3; 12.5–18 km^2)	2006–2010	550	0.185	
MSG/SEVIRI (AER-OC-D3; 12.5–18 km^2)	June 2005–May 2010		0.26 ± 0.04[g]	Lionello et al. (2012)
			0.23 ± 0.04[g]	This work
	Feb. 2004–Jan. 2016		0.21 ± 0.04[g]	
TERRA/MODIS (MOD08_M3 Coll. 4; 1°)	March 2000–Feb. 2006	550	0.27 ± 0.21[h]	Papadimas et al. (2009)
TERRA/MODIS (MOD08_M3 Coll. 5; 1°)			0.22 ± 0.07[h]	
AQUA/MODIS (MYD08_D3 Coll. 6; 1°)	Mid-2002–2014	550	0.20 ± 0.05	Floutsi et al. (2016)
Merged TERRA/ and AQUA/MODIS Coll. 6.1 (Sayer et al., 2014; 1°)	2000–2017	550	0.20	Nabat et al. (2020)
MISR (MILMAE; 0.5°)			0.16	
PARASOL/POLDER-3 (OC2 Coll. 3; 1/6°)	2006–2012	550[e,f]	0.164 ± 0.115	This work
		865	0.116 ± 0.103	
	Mar. 2005–Oct. 2013		0.111 ± 0.026[i]	Formenti et al. (2018)

(continued)

Table 1 (continued)

[a]Mineral dust estimated contribution only
[b]Nabat et al. (2013) highlight possible drifts and discontinuities in the calibration of the five successive MVIRI sensors used
[c1, c2]Respectively, central and East Med. (10°E–30°E, 30°N–45°N) and central and West Med. (10°W–10°E, 35°N–45°N), including land areas
[d]Only where and when mineral dust is detected
[e]Recomputed based on AE and AOD at another λ
[f]The difference between Nabat et al. (2013) and our new estimation can be partly explained by the fact that POLDER AOD over ocean from collection 2 is larger than from collection 3, especially at the beginning of the observation period (Didier Tanré, personal communication); in addition, since the Angström relationship is not linear, the method used by Nabat et al. (2013) to compute POLDER average AOD_{550} based on monthly averages of AOD_{865} and AE can yield some bias compared to our estimation based on averaging AOD_{550} recomputed daily
[g]Mean of all available daily data; note that this type of averaging gives more weight to the more numerous days with clear sky and more turbid conditions available during the Mediterranean summer periods than the monthly mean averaging shown in the preceding line; here the standard deviation does not account for variability of the 12 basin scale annual averages but for the daily variability over the whole period at the pixel level
[h]Broad Mediterranean region including Black Sea, Atlantic and some land areas within the domain 29.5°N–46.5°N and 10.5°W–38.5°E
[i]Western basin only

available observations of the AOD, AE, SSA and *g* estimated for various types of aerosols from local measurements, either in situ or columnar in the case of passive remote sensing. Note that an extensive list of existing ground-based and ship-based AERONET observations in the broad Mediterranean region is given in another chapter of volume 1 (Dulac et al., 2023a).

3 Aerosol Optical Depth

Satellite observations over the Mediterranean Sea have been analysed for describing the AOD geographical distribution. The seasonal variability and trends are discussed in other chapters of this book (Kaskaoutis et al., 2023a, 2023b). The various satellite climatologies of AOD reported in Table 1 indicate an average AOD_{550} over the Mediterranean basin in the range of 0.16–0.24. Among the lowest reported values, those from SeaWiFS and MERIS products were found much less reliable than products from other satellite sensors when compared to AERONET (Nabat et al., 2013). Sulphate-like and desert dust aerosols are the dominant species over the Mediterranean basin with yearly average AOD values of the order of 0.08, with an East-West and a South-North decreasing gradient, respectively (Nabat et al., 2013). Antoine and Nobileau (2006) have indicated that the 1998–2004 climatological average AOD (at 865 nm) derived from SeaWiFS over the Mediterranean is 0.165 and increases to 0.208 in the presence of mineral dust aerosols. The overall basin average AE varies in the range 0.6–0.9 but decreases to 0.40–0.45 in case of dust plumes, which are detected with an average time and space occurrence of ∼11% with a maximum of

Table 2 Surface land (unless specified) local measurements of aerosol optical depth (AOD), Ångstrom exponent (AE), single scattering albedo (SSA) and asymmetry parameter (g) estimated at $\lambda = 550$ nm (unless specified)

Location	Period	Aerosol type	AOD	AE	SSA	g	References
Jerusalem (Israel)	1930–1934 (3880 obs.) 1961–1968 (7142 obs.)	Continental urban	0.037[a] 0.048[a]	1.5–1.9[b] 1.45–1.8[b]	–	–	Joseph and Manes (1971)
Mediterranean Sea (from ship)	Aug.–Sept. 1986	Continental	0.19	1.18	–	–	Gulyaev et al. (1990) cited by Smirnov et al. (1995)
Cagliari and Carloforte (San Pietro Island) (Sardinia, Italy)	28 May, and 7 June 1994, resp.	Maritime	0.11 and 0.09[c]	0.7	–	–	Dalu et al. (1995)
Carloforte (San Pietro Island, Sardinia) and Finokalia (Crete Isl.)	Spring and summer 1996 and 1997	Marine background	0.077[d]	1.80	–	–	Paronis et al. (1998)
Sde Boker and Ness Ziona (Israel)	Feb. 2000– Oct. 2001 (monthly averages)	Continental, dusty	0.20–0.39[e] 0.06–0.16[f]	0.7–1.2	–	–	Israelevich et al. (2003)
Marseille (SE France)	June 2001	Continental urban	0.30	–	0.83–0.85	0.60–0.65	Mallet et al. (2003, 2006), Roger et al. (2006)
Toulon (SE France)	June 2006		0.23	–	0.85	0.85	Saha et al. (2008)
ESCOMPTE domain (around Marseille, France)	25–26 June 2006		–	–	0.86–0.89[g]	–	Mallet et al. (2005a), Mallet et al., 2005b)
Almeria (South Spain)	June 1999		0.40	–	0.86–0.90	0.62–0.72	Horvath et al. (2002)

(continued)

Table 2 (continued)

Location	Period	Aerosol type	AOD	AE	SSA	*g*	References
Finokalia (Crete Isl.)	July 2001	Anthropogenic	0.21	–	0.87	–	Markowicz et al. (2002)
Sde Boker, Negev Desert (Israel)	Summer 1996		0.19 ± 0.08[c]	1.5 ± 0.04[c]	0.92 ± 0.03[g] [0.87–0.96][g] pollut.: 0.89[g] Clear: 0.94[g]	–	Formenti et al. (2001a)
Capo Cavallo (Corsica Isl.)	22 March 1986	Continental pollution	0.25–0.35	1.1–1.4			Moulin et al. (1997)
Mount Athos Observatory (MAO, Greece)	Jun.–Sep. 1998		0.1–0.5	–	0.78–0.80[g]	–	Formenti et al. (2001b)
MAO and Thessaloniki (Greece)	1999–2002	Continental pollution and urban	0.23	–	–	–	Gerasopoulos et al. (2003)
Thessaloniki (Greece)	Apr. 1996– Jun. 1997	Continental urban	0.14[h]	–	–	–	Léon et al. (1999)
	June 1997		–	1.5	0.82	0.61	Chazette and Liousse (2001)
	Apr. 1996–Jun. 1997 (monthly values)		0.12–0.37[i]	1.2–2.2[i]			Balis et al. (2000)
	1997–2004		0.45 ± 0.11[e]	–			Balis et al. (2006)
	Mid Aug.-Sept. 2003	Desert dust	0.6–1.4[e]	0.7–1			
Finokalia (Crete Isl.)			0.2–0.6[j]	0.2–1			
Capo Cavallo (Corsica Isl.)	26 Mar.–22 Apr. 1986	Marine background aerosols	0.05–0.19	0.8–2	–	–	Moulin et al. (1997)
Lampedusa Island (Italy)	July 2001–Sep 2003		0.15[k]	–	–	–	Pace et al. (2006)
	25 May 1999	Anthropogenic	0.16[l]	–	0.83[l]	0.67[l]	Meloni et al. (2003)
	27 May 1999		0.22[l]	–	0.79[l]	0.65[l]	
Lecce (southern Italy)	Summer 2003–2004		0.25	–	0.94	–	Tafuro et al. (2007)

Location	Period	Aerosol type	AOD	AE	SSA	*g*	References
Finokalia (Crete Isl.)	Jul. 2001– Nov. 2002	All aerosols (overall average)	–	–	0.89 ± 0.04[m]	–	Vrekoussis et al. (2005)
	8–13 Aug. 2001	Biomass burning	–	–	≥0.74[m]	–	
MAO (Greece)	14 Aug. 1998		0.39	–	0.89[g]	–	Formenti et al. (2002)
Lampedusa Island (Italy)	Aug. 2003		0.25–0.8[l]	–	0.82[l]	0.63[l]	Meloni et al. (2006)
	July 2001– Sept. 2003	Mixed biomass burning and urban-industrial	0.27[k]	–	0.87[k]	–	Pace et al. (2006)
	July 2001– Sept. 2003	Desert dust	0.37[k]	–	0.81[k]	–	
	16 July 2002	North African dust	0.26[l]	–	0.88–0.89[l]	0.81–0.82[l]	Meloni et al. (2004)
	18 May 1999	Saharan dust	0.51[l]	–	0.74[l]	0.79[l]	Meloni et al. (2003)
	14 July 2002		0.23[l]	–	0.96–0.97[l]	0.79–0.80[l]	Meloni et al. (2004)
	26–28 March 2004		1.18	–	–	–	Meloni et al. (2008)
	1999–2005		–	–	0.77	–	Meloni et al. (2007)
	2004–2007		0.33	0.24	0.78[l] 0.91[n]	0.84[l] 0.73[n]	Di Biagio et al. (2009)
5 stations, central-western Med.	15–26 July 2003		–		0.87–0.91[j]	–	Tafuro et al. (2006)
Toulon (SE France)	19 June 2006		0.75		0.90	0.80	Saha et al. (2008)
Mediterranean basin	June 2006		0.20–0.35	0.6–0.9	0.93–0.98	–	De Meij and Lelieveld (2011)
Erdemli (S Turkey)	Apr 2000		1.30–1.80[j]		0.97[j]	0.78[j]	Kubilay et al. (2003)
	Oct 2000	Middle East-Arabian dust	0.50[j]		0.99[j]	0.70[j]	
	Aug. 2000	Mixed pollution and dust	1.30[j]		0.85–0.90[j]	0.68[j]	

(continued)

Table 2 (continued)

Location	Period	Aerosol type	AOD	AE	SSA	*g*	References
Lampedusa Island (Italy)	2004–2007	Urban–industrial/biomass burning	0.20	1.64	0.89[l] 0.80[n]	0.65[l] 0.60[n]	Di Biagio et al. (2009)
		Mixed aerosols (pure marine, marine polluted, and mixtures of various aerosol types)	–	–	0.81[l] 0.82[n]	0.69[l] 0.68[n]	
Montseny (NE Spain)	Nov. 2009–Oct. 2010	Polluted	–	1.3	0.90[o]	–	Pandolfi et al. (2011)
Barcelona (NE Spain)	July 2009	Dust and smoke	0.59[j]	~0.3	0.83 ± 0.04[j]	–	Sicard et al. (2012)
		Fresh biomass burning	0.41[j]	2.0	0.86 ± 0.04[j]	–	
Western Mediterranean	Summer 2013	Marine	0.10	–	0.98	–	Claeys et al. (2017)
		Dust	–	–	0.90–1.00	0.7–0.8	Denjean et al. (2016)
Mediterranean (22 AERONET stations)	1996–2012	Polluted	–	–	0.94–0.95	–	Mallet et al. (2013)
		Dust	–	–	0.91	–	
Alboran Island, Spain (southwestern Mediterranean	Jul. 2011–Jan. 2012	Dust	>0.3[c]	<0.8	–	–	Lyamani et al. (2015)
	30 Sep.–4 Oct. 2011	Polluted	0.2–0.6[c]	1–1.7			
Western Mediterranean	Mar. 2005–Oct. 2013	Dust	0.1–0.2[h]	–	–	–	Formenti et al. (2018)
	Summer 2012	Polluted	–	–	0.84–0.98[p] 0.70–0.99[q]	–	Di Biagio et al. (2016)
Valencia (eastern Spain)	Summer 2012	Background	<0.2	1–1.4	0.82–0.86[r]	0.57[r]	Gómez-Amo et al. (2017)
		Smoke	0.31–4.13	2.08–2.34	0.87[r]	0.55–0.60[r]	
		Dust	0.2–0.8	0.1–0.8	0.93–0.97[r]	0.66–0.71[r]	

Table 2 (continued)

[a]At λ = 1000 nm for the column
[b]Monthly averages
[c]At λ = 500 nm for the column
[d]At 870 nm for the column
[e]At 340 nm for the column
[f]At 1020 nm for the column
[g]For the aerosol in dry state
[h]At 865 nm for the column
[i]At 532 nm for the column
[j]At 440 nm for the column
[k]At 496 nm for the column
[l]At 416 nm for the total atmospheric column
[m]At 550 nm at the surface from in situ scattering and absorption measurements
[n]At 868.7 nm for the column
[o]At 635 nm for the column
[p]At 370 nm for the column
[q]At 950 nm for the column
[r]At 675 nm for the column

16% in the central basin between June and November (Antoine & Nobileau, 2006). Estimates of the basin average, yearly mean contribution from desert dust range between 0.07 (Marinou et al., 2017) and 0.11 ± 0.04 (Moulin et al., 1998) (top of Table 1). By combining sun photometer and Polder-1 satellite data, Léon et al. (1999) report that 42% of the days with observed $AOD_{865} > 0.18$ between April 1996 and June 1997 in the suburban area of Thessaloniki, Greece, were associated with desert dust transport events, particularly observed in the period March–July.

Indeed, many dust events over the Mediterranean region have been documented in the literature based on local optical measurements (Table 2). Three different cases of Saharan dust transport that occurred on 18 May 1999 and 14 and 16 July 2002 on the island of Lampedusa, in the central Mediterranean, were studied by Meloni et al. (2003), Meloni et al. (2004), respectively. Their results indicate moderate values of AOD (at 415.6 nm) for the 14 and 16 July 2002 event (0.23–0.26) and a significantly larger one (0.51) for the event of 18 May 1999 (Table 2). Pace et al. (2006) report observed values of AOD and AE for the period July 2001–September 2003 at Lampedusa, with values of 0.37 and 0.81, respectively. Meloni et al. (2008) report AOD (at 500 nm) measurements at Lampedusa for the 1999 to 2006 period, indicating daily values comprised between 0.29 and 1.18. The highest AOD values were measured in March 2004 (a peak daily value of 1.35 on 28 March 2004, with a 3-day average of 1.18). In almost all cases, African aerosols display high AOD values (average value of 0.37 at 496 nm over the whole observing period; Table 2). At a different site (coastal French Mediterranean region), Saha et al. (2008) have also documented a dust event observed on 19 June 2006, characterized by a high AOD (0.75 at 550 nm). Finally, Kubilay et al. (2003) documented three dust intrusion events at Erdemli (Turkish coast of the northeastern Mediterranean), occurring in spring (originating from central Sahara), in summer (from eastern Sahara) and in autumn (from the Middle East/Arabian Peninsula). In each case, the presence of dust particles significantly increased AOD, up to 1.8 (Table 2). Over the eastern basin, Papayannis et al. (2005) have also reported dust AOD of about 0.6 (at 355 nm) during a dust event in August 2000. Dust AOD values have also been reported in the Mediterranean based on satellite (MODIS, OMI) algorithms (Gkikas et al., 2013, 2016a). During strong dust episodes, AOD values can be as high as about 0.8 over the Algerian coast and 1 over the Gulf of Sidra (Gkikas et al., 2016a). The respective values for extreme dust episodes are 1.5 and 2.5.

In the framework of the ChArMEx/ADRIMED project, Mallet et al. (2016) reported dust AOD around 0.3–0.4 over the western Mediterranean during the summer of 2013, based on different techniques of observations. At the regional scale and during the same period, Menut et al. (2015) confirmed important transport of mineral dust in June–July 2013 over the central Mediterranean with local maxima around 1 and a mean value of 0.3–0.4 (at 550 nm), using the regional chemical transport model (CTM) CHIMERE model. Nabat et al. (2012) have simulated dust AOD between 0.15 and 0.3 (at 550 nm) over the Mediterranean Sea using the RegCM regional climate model over the 2000–2009 decade. Based on the POLDER-3/PARASOL satellite data set (2005–2013) over the western Mediterranean Sea, Formenti et al. (2018) consistently report high values of AOD_{865}, ranging between 0.10 and 0.20 on average, over areas with the lowest AE, as

illustrated by Fig. 1. This figure also shows an important contribution of about 0.078 from the coarse particle mode to the total AOD_{865}, of 0.111 on a regional average.

In addition to mineral dust particles, various studies have documented AOD for urban/industrial (UI) Mediterranean aerosols (Table 2). According to early actinometric measurements performed at Jerusalem, the AOD followed an increasing

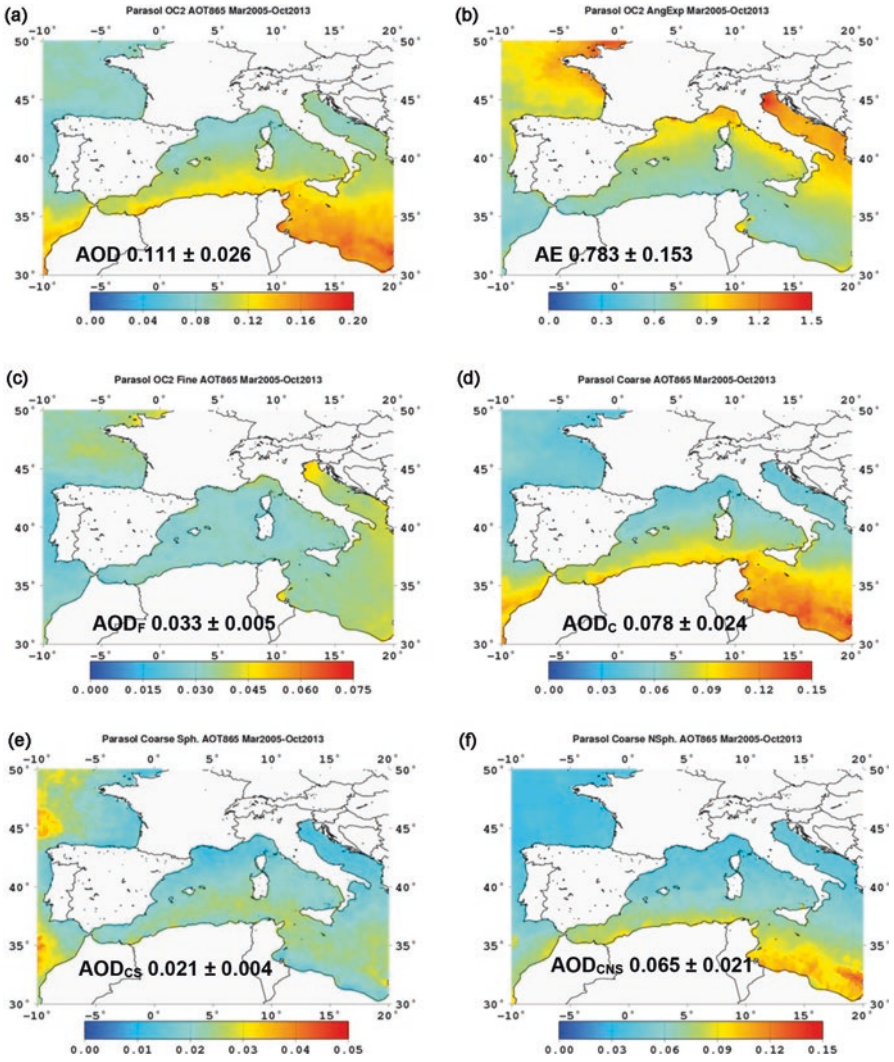

Fig. 1 Regional maps of aerosol optical properties over marine areas as retrieved from POLDER-3 averaged over the period March 2005–October 2013: (**a**) AOD_{865}, (**b**) AE, (**c**) fine and (**d**) coarse aerosol mode AOD_{865} (AOD_F and AOD_C, respectively, with $AOD_F + AOD_C = AOD_{865}$), and (**e**) spherical and (**f**) non-spherical coarse mode AOD (AOD_{CS} and AOD_{CNS}, respectively, with $AOD_{CS} + AOD_{CNS} = AOD_C$). The mean and standard deviation over the whole marine area of the window are reported for each parameter. (Reprinted from Fig. 11 in Formenti et al., 2018)

trend of +10% per decade between the 1930s and 1960s, also seen in a few continental stations of the northern hemisphere, and attributed to non-local factors (Joseph & Manes, 1971). The different surface observations performed under polluted conditions have reported AOD values ranging between 0.1 and 0.5, i.e., clearly lower than those for dust regimes. Over southeastern France, AOD values have been documented, more specifically, during summer periods (Mallet et al., 2005a, b; Roger et al., 2006; Saha et al., 2008). These studies show AOD of about 0.30 at visible wavelengths (400–500 nm). Over Spain and Greece, similar AOD ranges are reported. Horvath et al. (2002) indicated a mean value of 0.40 (at 520 nm) in Almeria (South Spain) under polluted conditions. Gerasopoulos et al. (2003) reported an averaged AOD value of 0.23 (at 500 nm) in the city of Thessaloniki and at Mount Athos Observatory (MAO), Ouranoupolis, over a time span of 3 years, lower than values of 0.3–0.5 (at 500 nm) observed during summer (Table 2). Similar observations were reported by Formenti et al. (2001b), who indicated an average value of AOD between June and September 1998 of 0.28 at MAO, which peaks up to 0.50. In parallel, measurements performed in Thessaloniki by Chazette and Liousse (2001) on 12 and 13 June 1997 indicate a mean value of 0.17 and 0.34 (at 550 nm), respectively. Such values are consistent with spaceborne and ground-based remote sensing observation of pollution aerosols performed between April 1996 and June 1997 in Thessaloniki by Léon et al. (1999). These authors reported a mean AOD of 0.12 ± 0.04 at 865 nm (implying a value of 0.33 at 440 nm, estimated by using AE = 1.5, as measured by Chazette & Liousse, 2001). Over Crete Island, Fotiadi et al. (2006) reported an AERONET-based AOD_{500} value of 0.21 ± 0.11 for the 2-year period 2003–2004. Finally, over southeastern Italy (Lecce, 40.33°N, 18.10°E), Tafuro et al. (2007) reported monthly mean values of AOD larger than 0.15 during summer (averaged over the 2003–2004 period), when pollution dominates the AOD. Using satellite TOMS and MODIS observations, Hatzianastassiou et al. (2009) also indicated high AOD values (up to 0.8) over large urban areas surrounding megacities. At the regional scale and based on climatological ALADIN-Climate regional simulations (1979–2016 period), Drugé et al. (2019) have recently indicated that anthropogenic nitrates could also contribute to the total AOD over the Euro-Mediterranean region, with values between 0.05 and 0.1 (at 550 nm) associated with local maxima over the Po valley. Finally, Gkikas et al. (2016b) reported high frequencies and intensity (AOD of about 0.5) of biomass-burning/urban-industrial aerosols over the northern coasts of the Mediterranean Sea.

Formenti et al. (2001a) reported observations of AOD performed in the frame of the Aerosol, Radiation and Chemistry Experiment (ARACHNE-96) at Sde Boker, in the Negev Desert of Israel, for polluted air masses transported from Southern Europe, mainly from the Balkan region and Greece. In that case, AOD values are certainly more representative of "aged polluted" aerosols and are characterized by lower values (mean of 0.19 at 500 nm). "Aged" anthropogenic aerosols over the eastern Mediterranean have also been documented during the Mediterranean Intensive Oxidant Study (MINOS), which took place in summer 2001 in the Greek island of Crete (Lelieveld et al., 2002). During this experimental campaign, the mean AOD value (0.21 at 500 nm) was close to the one observed during ARACHNE-96.

Up to now, only few studies have been dedicated to biomass burning aerosol (BBA) over the Mediterranean region, which are mainly observed in July and August (driest months of the year), when the development of forest fires is favoured (Meloni et al., 2006). The STAAARTE-MED experiment (August 1998 in the eastern Mediterranean) results, relevant for BBA emitted from Canadian fires (Formenti et al., 2002), have documented a mean AOD of 0.39 (at 550 nm). Furthermore, AOD values in the range between 0.3 and 0.8 (Pace et al., 2005, 2006; Meloni et al., 2006) have also been observed at Lampedusa island from 5 to 22 August 2003, originating from intense fires that took place in Southern Europe and being transported over the Mediterranean basin during a regional heat wave. At the present time, data available for BBA suggest "intermediate" AOD values compared to those observed for mineral and urban/industrial particles (Table 2). For a specific event occurring in Barcelona, Sicard et al. (2012) observed AOD due to smoke aerosols around 0.4–0.5 during July 2009. A BBA episode from North America was also observed over the western Mediterranean in late June 2013 (Ancellet et al., 2016)

Concerning primary sea spray aerosols, Fotiadi et al. (2006) reported a background AOD value of 0.15 in Crete island, corresponding to marine aerosols, and Mishra et al. (2014) found a mean AOD over the eastern Mediterranean (June–August 2010) of 0.06 ± 0.01. More recently, Claeys et al. (2017) have reported marine AOD_{500} (22–26 June 2013) of about 0.11 ± 0.08, based on AERONET retrievals. From sun photometer measurements in spring and summer 1997 in coastal Sardinia and Crete, Paronis et al. (1998) reported a marine background AOD_{870} of 0.077.

Finally, assessing the different contributions based on MODIS Terra and Aqua observations, Georgoulias et al. (2016) report that anthropogenic aerosols, dust and fine mode natural aerosols account for ~51%, ~34% and ~15% of the total AOD_{550} over land, respectively, while over the sea, anthropogenic aerosols, dust and marine aerosols account for ~40%, ~34% and ~26%, respectively.

4 Aerosol Single-Scattering Albedo

Mineral dust particles observed over the Mediterranean region show significant variations in SSA (Table 2) with columnar values ranging from as high as 0.96–0.99 at various wavelengths between 400 and 800 nm, down to quite low values, e.g., of 0.74, 0.77 or 0.81 at 416 nm at Lampedusa, suggesting considerably high absorption by dust (Pace et al., 2006; Meloni et al., 2003, 2006, 2007; Di Biagio et al., 2009; Ealo et al., 2018). More recently, Denjean et al. (2016) have reported in situ aircraft measurements of dust SSA during several dust plumes advected over the Mediterranean basin. These authors indicate moderate absorption of light by the dust plumes, with SSA values (at 530 nm) ranging from 0.90 to 1.00 (Fig. 2). At the high-altitude Alpine Jungfraujoch station, SSA values are generally >0.9 in case of African dust plumes, but occasional values as low as 0.75–0.80 were reported by Collaud Coen et al. (2004). Their measurements show a clearly different spectral dependence of SSA in the case of dust events, characterized by increasing SSA with

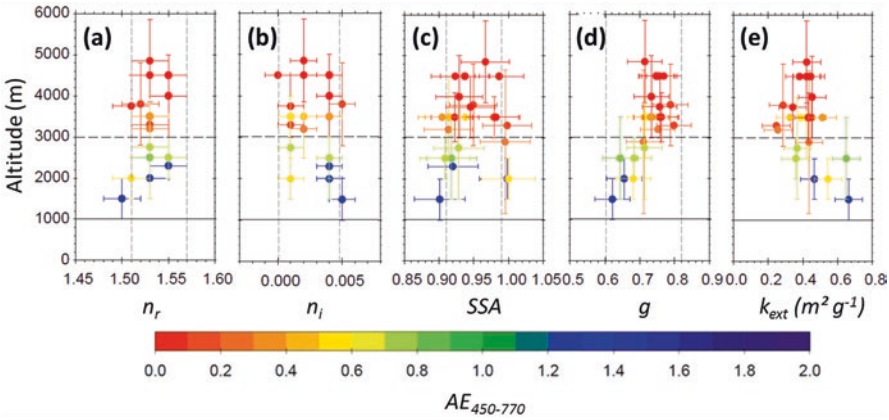

Fig. 2 Scatter plots showing aerosol optical properties at $\lambda = 530$ nm as a function of the altitude, from all airborne straight level runs and vertical profiles within the dust layers measured during the ADRIMED campaign: (**a**) the real part of the complex refractive index n_r, (**b**) the imaginary part of the complex refractive index n_i, (**c**) the single scattering albedo SSA, (**d**) the asymmetry parameter g, and (**e**) the mass extinction efficiency of aerosols k_{ext}. The markers are coloured according to the scattering Angström exponent ($AE_{450–770}$) calculated between 450 and 770 nm. (Reproduced from Fig. 8 in Denjean et al., 2016)

λ. Intermediate dust SSA (0.85–0.92, see Table 2) have also been reported over the Mediterranean basin (Kubilay et al., 2003; Meloni et al., 2004; Saha et al., 2008). These estimates clearly indicate that significantly different SSA values are observed depending on the dust particle origins, transport pathways and/or possible mixing of mineral aerosols with other species. For example, Kubilay et al. (2003) underline the importance of such mixing of mineral aerosols, showing SSA values clearly lower (0.85–0.90) at 440 nm in case of mixed dusts and urban industrial or biomass burning particles, as compared to pure mineral dust (0.96–0.97). Similarly, the effect on SSA of dust mixing with pollution (Fig. 2) is identified in the variable SSA values reported by Denjean et al. (2016).

When columnar remote sensing observations are considered, as it is the case of many studies in Table 2, it should be kept in mind that these may integrate the contribution of different aerosols types present within the tropospheric column and therefore they may not be representative of a single species or even a single plume. This issue is clearly illustrated by Di Biagio et al. (2009) who reported 3 years of columnar measurements of dust SSA at 416 and 868 nm at Lampedusa Island. These authors show that the dust SSA exhibits a large variability, with values between 0.7 and 0.8 at $\lambda = 416$ nm and between 0.8 and 0.9 at 868 nm. The same authors performed a back-trajectory analysis to explain the observed variability and found that the majority of cases with SSA < 0.75 at 416 nm and SSA < 0.85 at 868 nm corresponded to air masses below 1 km, being dominated by polluted particles from continental Europe, while dust was dominant above. Instead, cases with SSA between 0.8 and 0.9 at 416 nm corresponded to air masses with a strong contribution by marine particles below 1 km, together with dust plumes in higher altitude levels.

Apart from SSA associated with mineral dust regimes, SSA observed in the case of urban/industrial regimes have also been well documented over the Mediterranean Sea and at coastal sites (see Table 2). In most cases, moderate or low SSA (0.78–0.94) are observed due to emissions containing black carbon aerosols. Over southeastern France, optical computations performed by Mallet et al. (2004) and Saha et al. (2008) indicate SSA values of 0.83 and 0.85 (at 550 nm) near the cities of Marseille and Toulon, respectively. Aircraft observations performed over the Marseille-Etang de Berre area during the ESCOMPTE campaign showed values ranging between 0.88 and 0.93 (at 550 nm) in the Planetary Boundary Layer (Mallet et al., 2005a). These SSA values are close to those observed in South Spain (0.86–0.90) by Horvath et al. (2002), though those observed over Greece look slightly lower: 0.78–0.80 at MAO (Formenti et al., 2002) and 0.82 at Thessaloniki (Chazette & Liousse, 2001). Over southeastern Italy, Tafuro et al. (2007) have recently reported a value of 0.94 during summer time corresponding to anthropogenic particles. A very low mean SSA value of 0.71 ± 0.07 (at 550 nm) was reported by Titos et al. (2012) at Granada, suggesting a large fraction of absorbing material. Finally, anthropogenic polluted particles transported over the Mediterranean basin were also associated with relatively low SSA values, as reported by Markowicz et al. (2002) over Crete Island (0.87) and by Di Iorio et al. (2003) (0.79–0.83) over Lampedusa Island for two cases (25 and 27 May 1999) of "aged" anthropogenic aerosols originating from Europe. Di Biagio et al. (2009) reported average SSA values of 0.80 (at 416 nm) and 0.89 (868 nm) from 3 years of observations of polluted plumes over Lampedusa. Based on AERONET climatological retrievals (17-year period 1996–2012), Mallet et al. (2013) showed that the Mediterranean urban-industrial aerosols appear "moderately" absorbing, with values of SSA close to about 0.94–0.95 ± 0.04 (at 440 nm). Finally, in situ airborne observations from Di Biagio et al. (2016) during the ChArMEx/TRAQA campaign in summer 2012 show a large variability of polluted aerosol SSA over the northwestern Mediterranean, with values in the range 0.84–0.98 (370 nm).

As opposed to dust and polluted aerosols, few studies reported SSA for BBA over the Mediterranean Sea. One such estimation has been obtained during STAAARTE-MED by Formenti et al. (2002) who reported a mean dry SSA of 0.89 (at 500 nm) obtained from aircraft in situ observations over the Aegean Sea (Greece). Meloni et al. (2006) reported quite different estimations at Lampedusa Island, with column-averaged values of 0.82 ± 0.04 (at 415 nm) and 0.80 ± 0.05 (at 868 nm), for BBA over the Mediterranean region. These SSA estimates are representative of two different periods corresponding to intense active fires in the Balkans, southern Italy and Sicily for the 31 July–4 August 2001 period, and in southern Europe in August 2003 (Pace et al., 2006). The observed differences between the SSA values reported by Formenti et al. (2002) and Meloni et al. (2006) could be due to the fact that the BBA events described by Meloni et al. (2006) are more "local" and not (or somewhat less) mixed with other secondary species, as opposed to BBA particles documented by Formenti et al. (2002), which were emitted from very distant Canadian Arctic fires (and underwent mixing during their very long transatlantic pathway). More recently, over Barcelona, Sicard et al. (2012) have also reported very low SSA

for smoke (0.86 ± 0.04 at 440 nm) particles observed in July 2009. Additionally, Gómez-Amo et al. (2017) have reported an average SSA value of 0.87 at 675 nm during a severe fire event in coastal Spain.

5 Asymmetry Parameter

As previously mentioned, the asymmetry parameter (g) represents an important radiative parameter for the derivation of the direct radiative effect of aerosols. Different estimations have been made over the Mediterranean basin aiming at characterizing this optical property under diverse aerosol regimes. For mineral dust aerosols, Meloni et al. (2003, 2004) indicated high important values of about 0.79–0.82, which are typical of aerosols including an important coarse fraction. Such values are of similar magnitude with those published by Saha et al. (2008) or Kubilay et al. (2003). Due to the smaller size of aerosols produced by anthropogenic or biomass burning emissions, g is found to be generally lower for such aerosols. For smoke particles, a value of ∼0.63 (at 550 nm) has been reported by Meloni et al. (2006). The same order of magnitude is reported for polluted aerosols, with values between 0.60 and 0.65 (Chazette & Liousse, 2001; Meloni et al., 2003; Roger et al., 2006). Finally, some estimations have been also proposed over the Mediterranean basin for mixed aerosols, that generally indicate intermediate values. For polluted aerosols mixed with mineral dust, Kubilay et al. (2003) reported an asymmetry parameter value ∼0.68 (at 440 nm). This variability of g for different aerosol regimes has been clearly demonstrated by Denjean et al. (2016) using aircraft observations (Fig. 2). These recent in situ data obtained over the western Mediterranean basin indicate a general increase of g (at 550 nm) with altitude, from ∼0.60 at 1.5 km to ∼0.75 at altitudes higher than 3 km. These changes are mainly due to the presence of fine polluted aerosols between 1 and 3 km and mineral dust above 3 km.

6 Aerosol Extinction-to-Backscatter Ratio

Active remote sensing of tropospheric aerosols by lidar systems over the Mediterranean region has strongly developed in the past two decades for aerosol vertical profiling (e.g., Hamonou et al., 1999; Balis et al., 2000, 2004, 2006; Gobbi et al., 2000; Sicard et al., 2002, 2011, 2012; De Tomasi et al., 2003; Dulac & Chazette, 2003; Berthier et al., 2006; Mona et al., 2006; Papayannis et al., 2008a; Royer et al., 2010; Mamouri et al., 2013; Chazette et al., 2014, 2016, 2019a; Nisantzi et al., 2014, 2015; Flamant et al., 2015; Barragan et al., 2017; Mandija et al., 2017; Marinou et al., 2017; Ortiz-Amezcua et al., 2017; Ansmann et al., 2019; Benkhalifa et al., 2019; Fernandez et al., 2019; Chazette, 2020). Thanks to transportable systems, it is now a relatively common technique deployed during field campaigns either ground based (e.g., Chazette et al., 2014, 2016, 2019a, b) or airborne (Mallet

et al., 2016; Chazette, 2020). Southern Europe and the Mediterranean region host several stations of the European research lidar monitoring network EARLINET (Pappalardo et al., 2014), making possible lidar data assimilation in aerosol transport modelling (Wang et al., 2014).

The lidar ratio (LR), i.e., the ratio of the extinction to backscatter aerosol coefficients, is one of the key parameters that can be derived from lidar measurements. It does not have a direct physical meaning unlike its opposite, the backscatter-to-extinction ratio (BER = LR^{-1}), which has also been widely used by the pioneers of lidar remote sensing of the atmosphere in both the troposphere and stratosphere. The BER is the product of the aerosol single scattering albedo by the probability that a photon is backscattered by the aerosol. It is therefore, like LR, an insightful parameter, rich in information on the aerosol nature, even though it does not provide as precise discrimination as chemical analyses (mainly performed at the ground level, however). The LR (or BER) allows one differentiating between the 3 main classes of aerosols, typically: (i) mineral aerosols (e.g., Saharan dust over the Mediterranean region), (ii) pollution and biomass burning aerosols and (iii) marine aerosols (e.g., sea salt), as illustrated in Fig. 3. Three main aerosol types could be identified based on the combination of lidar-derived values of the BER and particle depolarization ratio (PDR) (Burton et al., 2012), e.g., at a wavelength of 355 nm: (i) dust-like, non-spherical aerosols, with values of BER and PDR centred on 0.022 sr^{-1} and 20–30%, respectively, (ii) pollution aerosols, with BER and PDR centred on 0.015 sr^{-1} and 2–5%, respectively, and (iii) marine aerosols with mean values of BER and PDR centred on 0.04 sr^{-1} and 0%, respectively (Chazette et al., 2016). The

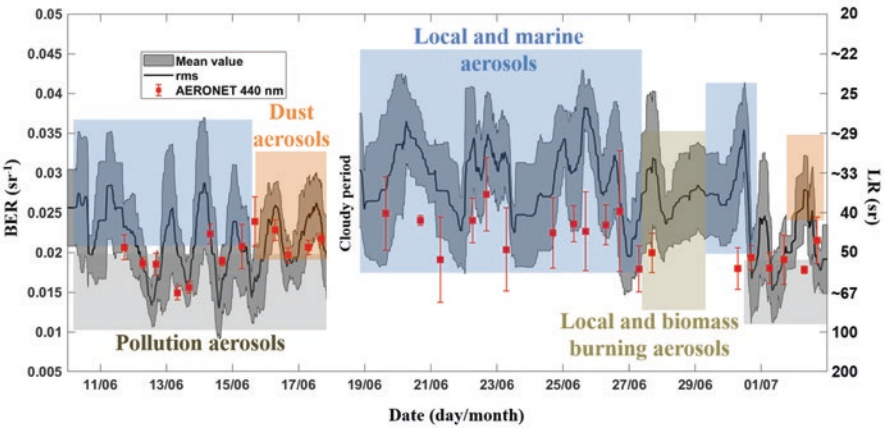

Fig. 3 Temporal evolution of the BER (left axis) or LR (right axis) from 10 June to 1 July 2013 at Cap d'en Font, Minorca Isl., Spain, during the ChArMEx/ADRIMED summer field campaign described by Mallet et al. (2016) (see also Figs. A11 and A12 in the book appendix; Dulac et al., 2023b). The black line shows lidar-derived values with their root mean square error given by the grey area (variability over 20 min). Red dots show sun-photometer-derived values with bars showing their standard deviation (variability over a half day). The reported aerosol categories were identified based on the lidar-derived BER and PDR. After Fig. 4a in Chazette et al. (2016)

figure highlights the high variability of LR values associated with a given aerosol type. This variability can partly be related to mixtures of aerosols of different natures. Furthermore, LR values may overlap significantly between different aerosol types, as discussed hereafter.

More aerosol types may have to be considered in operational aerosol classification from lidar data. This is the case for Earth observation missions using lidar onboard sun-synchronous satellites such as (i) the Cloud-Aerosol LIdar with Orthogonal Polarization (CALIOP; Winker et al., 2007) flying onboard the Cloud-Aerosol Lidar Pathfinder Satellite Observation (CALIPSO) since 2006 (https://www-calipso.larc.nasa.gov/products/) and (ii) for a shorter period of time, the Cloud-Aerosol Transport System (CATS; Yorks et al., 2016) orbited between 375 and 435 km onboard the non-sun-synchronous International Space Station between January 2015 and October 2017. The choice of LR values to invert the lidar data of these spaceborne instruments in order to retrieve the vertical profiles of the aerosol extinction coefficient is dictated by the spectral dependence, backscatter level and particle depolarization ratio, as explained in Omar et al. (2009), Burton et al. (2012) and Kim et al. (2018). Multiple scattering, especially in more turbid layers often associated with desert dust, also tends to increase the LR value, and this should be considered in unconstrained inversion of space lidar observations, as shown by Berthier et al. (2006) and Wandinger et al. (2010). Table 3 from Chazette et al. (2019b) gives the LR values of main aerosol types considered by operational inversion algorithms associated to both CALIPSO/CALIOP and CATS spaceborne missions. The table shows several aerosol types which overlap if one considers the uncertainty in the LR, which is of the order of 5–10 sr. Note that the LR values derived from ground-based lidar measurements are obtained with similar uncertainties, which often incorporate the natural variability of the aerosol layers. Care must be taken in order to avoid confusion between the uncertainties associated with the initial assumptions needed for the inversion algorithms and with the temporal variability of the atmosphere sampled by the lidar. It is mainly the statistical detection noise that influences the uncertainties. Nevertheless, there may be significant biases related to optical misalignments, and these biases must be considered along with the statistical noise. Values from Table 3 are commonly used as references to retrieve the vertical profiles of aerosol optical properties over the Mediterranean area from lidar systems. However, actual aerosols may present different LR values as shown in Chazette (2020), and this can lead to significant biases in the retrieved optical

Table 3 Lidar ratio (LR) values corresponding to the CATS- and CALIOP-derived aerosol typing from Table 2 in Chazette et al. (2019a)

CALIOP/CATS aerosol typing	Respective lidar ratio at 532 nm (sr)
Polluted continental or smoke/Polluted continental	70/65
Clean continental/Clean background	53/55
Clean marine/Marine	23/25
Dust/Dust	44/45
Polluted dust/Dust mixture	55/35
Elevated smoke/Smoke	70/70
Dusty marine/Marine mixture	37/45

properties of aerosols. The advent of high spectral resolution lidar systems such as Earthcare/ATLID should make it possible to remove this ambiguity (Groß et al., 2015).

Compared to reference values in Table 3, many intermediate LR values can be encountered knowing that different types of particles can be mixed within the lower and middle troposphere. In addition, a wide range of LR values can be encountered for a given type of aerosol as shown in Tables 4 and 5. This is the case of dust aerosol (Table 4), which can originate from different sources with varying soil characteristics. The lidar-derived LRs values range from 25 (29) to more than 80 (61) sr at 355 (resp. 532) nm in case of particularly coarse non-spherical particles.

In the same way, biomass burning aerosols, whose nature will depend on the type of biomass burned, the temperature of the fire and even the hygrometric level of the soil, show LR values between 23 (47) and 94 (87) sr at 355 (532) nm (Table 5). Less variability is reported for pollution aerosols (Table 5). The hydrophilic nature of aerosols can also affect the LR values, but to a lesser extent as shown by Raut and Chazette (2008).

7 Challenges for Future Research

Atmospheric aerosol, especially that present in the lower and middle troposphere, is one of the key components for improving our understanding of the Earth-atmosphere system. It directly influences the radiation balance of the Earth system, the cloud cover, albedo and precipitation via the so-called indirect effect, and the vertical stability of the atmosphere via the semi-direct effect. Yet, the aerosol influence does not stop there, as it also modifies actinic fluxes, thus photochemistry, and brings nutrients or toxins to the surface, influencing the terrestrial and marine biodiversity (see other chapters by Kanakidou et al., 2022 and Guieu and Ridame, 2022, respectively).

As illustrated in this chapter, great progress has been made over the last two decades in assessing main optical properties of the different types of aerosols, and their mixing, in the Mediterranean region, which is a hot spot identified by climate projections. Nevertheless, we still need to improve the accuracy of measurements and numerical methodologies in order to obtain better assessments of the various geophysical parameters of atmospheric aerosols, including optical properties, aiming at reducing uncertainties in aerosol radiative impact and climate projections.

In relation with the results presented above, a better assessment of the spectral SSA of the different aerosol types is clearly needed over the Mediterranean Sea, especially for biomass burning particles, but also for mixed aerosols in this region that hosts complex mixtures (presence of primary dust, black and organic carbon, secondary aerosols as sulphate, nitrate and secondary organic aerosol particles). One specific question to be addressed is the effect of the mixing state (external and/or internal) of absorbing aerosols (urban/industrial black carbon, biomass burning and even mineral dust) on the particle optical properties, especially SSA. It is also

Table 4 Lidar ratio (LR) reported in the literature for pure and mixed mineral dust aerosol types in the Mediterranean region, at various wavelengths in the ultraviolet (UV, at 351 or 355 nm), visible (VIS, at 500, 532 or 550 nm) and near-infrared (NIR, at 1064 nm)

Aerosol type	Site, campaign	Instrument, inversion method	λ (nm) UV VIS NIR	LR (sr)	References
Pure dust	AERONET network	Sun photometers	550	42 ± 4	Cattrall et al. (2005)
	Lampedusa Isl.	Sun photometer	532	40	Di Iorio et al. (2003)
	Rome, Italy	MFRSR radiometer	500	53	Ciardini et al. (2012)
	Lecce, S Italy, EARLINET	N_2 Raman lidar	351	45–60	De Tomasi et al. (2003)
	French Riviera, ChArMEx		355	32 ± 5	Chazette et al. (2019a)
	Thessaloniki, Greece, EARLINET			84 ± 20	Balis et al. (2004)
				57 ± 29[a]	Amiridis et al. (2005)
				44 ± 2	Papayannis et al. (2005)
	Athens, Greece, EARLINET			58 ± 1	
	Potenza, Italy, EARLINET			38 ± 2	Mona et al. (2006)
	Barcelona, NE Spain, EARLINET		532	51	Sicard et al. (2012)
			1064	47	
	Limassol, Cyprus, EARLINET		532	34–39[b]	Mamouri et al. (2013)
	Minorca Isl., Spain, ChArMEx		355	45 ± 6	Chazette et al. (2016)
	Central Mediterranean Sea, MEDUSE	Calculation using Meteosat/MVIRI	532	29 ± 10	Hamonou et al. (1999)
	8 EARLINET stations	N_2 Raman lidar	355	30–80	Papayannis et al. (2008a)
	Barcelona, NE Spain, EARLINET		532	46–52	Sicard et al. (2011)
	Limassol, Cyprus, EARLINET			53 ± 6[c]	Nisantzi et al. (2015)
				41 ± 4[d]	
	Iberian Peninsula, EARLINET			38–61	Fernandez et al. (2019)
			355	40–55	
	San Pedro Alcantara and Gibraltar Strait	N_2 Raman lidar and airborne lidar		34	Chazette (2020)
Polluted dust				45 ± 8	
Dust and marine	Minorca Isl., Spain, ChArMEx	N_2 Raman lidar		25 ± 6	Chazette et al. (2016)
Dusty mix	Balearic Islands, HyMeX			47–63	Chazette et al. (2014)
	Central Mediterranean Sea, STAAARTE	Airborne lidar and Meteosat	532	59 ± 17	Dulac and Chazette (2003)

[a]West Sahara dust,
[b]Syrian dust,
[c]Sahara dust,
[d]Middle-East dust

Table 5 Same as Table 4 but for biomass burning and pollution aerosols

Aerosol type	Site, campaign	Instrument, inversion method	λ (nm)	LR (sr)	References
Biomass burning	AERONET network	Sun photometers	550	60 ± 8	Cattrall et al. (2005)
	Western Med., ChArMEx	CALIOP	532	60 ± 20	Ancellet et al. (2016)
	Thessaloniki, Greece	N_2 Raman lidar	355	39–94[a]	Amiridis et al. (2009)
	Athens, Greece, EARLINET			60–80	Papayannis et al. (2008b)
			532	55–90	
	Barcelona, NE Spain, EARLINET			36	Sicard et al. (2012)
			1064	20	
	Granada, S Spain, EARLINET		532	47–58	Ortiz-Amezcua et al. (2017)
			355	23–34	
	Évora, Portugal EARLINET			42 ± 7	Sicard et al. (2019)
			532	55 ± 14	
Pollution	AERONET network	Sun photometers	550	71 ± 10	Cattrall et al. (2005)
	Po Valley, N Italy	CALIOP and MODIS synergy	532	83 ± 25	Royer et al. (2010)
	Minorca Island, Spain, ChArMEx	N_2 Raman lidar	355	67 ± 6	Chazette et al. (2016)
	French Riviera, ChArMEx			42–62	Chazette et al. (2019a)

[a]From Russia, Ukraine

very important to find, when possible, analytical relationships linking the SSA variability to the chemical composition and/or mixing state of the particles, in order to develop adapted parameterizations that can be implemented in regional models used over the Mediterranean basin. This will improve the accuracy of available aerosol optical properties and the direct and semi-direct radiative effect estimates of absorbing aerosols over the basin. Moreover, the SSA is estimated by various indirect methods with higher or lower accuracy, and it is necessary to achieve a consistency among their results. In particular, further in situ observations, both at the surface and airborne, are required to overcome the limitations of columnar data. In fact, even if columnar observations provide a good description of the whole aerosol population in the atmosphere, they are not sufficient for a detailed and accurate description of the SSA and its variability over such a complex environment as the Mediterranean, which is characterized by the coexistence of different aerosol types. This should be linked as much as possible with recent satellite observations, which provide now information on absorbing properties of aerosols (Lacagnina et al., 2015).

In this chapter, we have presented, in the most exhaustive possible way, the scientific work carried out over the last 20 years on aerosol optical properties over the

Mediterranean region. This work has often required heavy means of investigation and has improved our understanding of the processes involving natural and anthropogenic atmospheric aerosols. Spaceborne, airborne and in situ observations have been coupled in order to assess the properties of aerosols, not only on the surface but also in the atmospheric column. They involved sampling of the chemical composition, particle size distribution and optical properties of particle mixtures. The coherence of all these data sets still needs to be better specified using closure approaches combining inverse methods and numerical modelling. Initial tests have been conducted in order to assimilate raw lidar data into chemical transport models for air quality forecasting around the western Mediterranean basin (e.g., Wang et al., 2014), using an approach similar to that used in operational meteorology and based on the construction of an observable simulator. This type of approach allows a better integration of aerosol mixtures but needs to be validated through cross-comparisons with key parameters such as the single scattering albedo, which is indirectly obtained through synergies between different types of measurements. Innovative methods to precisely assess the single-scattering albedo, coupling observation and modelling, have already been implemented within the framework of large campaigns (Randriamiarisoa et al., 2004) and should be expanded over the Mediterranean basin.

Acknowledgements Michaël Sicard and Alexandros Papayannis are warmly acknowledged for providing some lidar references.

References

Amiridis, V., Balis, D. S., Kazadzis, S., Bais, A., Giannakaki, E., Papayannis, A., & Zerefos, C. (2005). Four-year aerosol observations with a Raman lidar at Thessaloniki, Greece, in the framework of European Aerosol Research Lidar Network (EARLINET). *Journal of Geophysical Research, 110*, D21203. https://doi.org/10.1029/2005JD006190

Amiridis, V., Balis, D. S., Giannakaki, E., Stohl, A., Kazadzis, S., Koukouli, M. E., & Zanis, P. (2009). Optical characteristics of biomass burning aerosols over Southeastern Europe determined from UV-Raman lidar measurements. *Atmospheric Chemistry and Physics, 9*, 2431–2440. https://doi.org/10.5194/acp-9-2431-2009

Ancellet, G., Pelon, J., Totems, J., Chazette, P., Bazureau, A., Sicard, M., Di Iorio, T., Dulac, F., & Mallet, M. (2016). Long-range transport and mixing of aerosol sources during the 2013 North American biomass burning episode: Analysis of multiple lidar observations in the western Mediterranean basin. *Atmospheric Chemistry and Physics, 16*, 4725–4742. https://doi.org/10.5194/acp-16-4725-2016

Ansmann, A., Mamouri, R.-E., Bühl, J., Seifert, P., Engelmann, R., Hofer, J., Nisantzi, A., Atkinson, J. D., Kanji, Z. A., Sierau, B., Vrekoussis, M., & Sciare, J. (2019). Ice-nucleating particle versus ice crystal number concentration in altocumulus and cirrus layers embedded in Saharan dust: A closure study. *Atmospheric Chemistry and Physics, 19*, 15087–15115. https://doi.org/10.5194/acp-19-15087-2019

Antoine, D., & Nobileau, D. (2006). Recent increase of Saharan dust transport over the Mediterranean Sea, as revealed from ocean color satellite (SeaWiFS) observations. *Journal of Geophysical Research, 111*, D12214. https://doi.org/10.1029/2005JD006795

Balis, D., Papayannis, A., Galani, E., Marenco, F., Santasecaria, V., Hamonou, E., Chazette, P., Ziomas, I., & Zerefos, C. (2000). Tropospheric LIDAR aerosol measurements and sun photometric observations at Thessaloniki, Greece. *Atmospheric Environment, 34*(6), 925–933. https://doi.org/10.1016/S1352-2310(99)00317-9

Balis, D. S., Amiridis, V., Nickovic, S., Papayannis, A., & Zerefos, C. (2004). Optical properties of Saharan dust layers as detected by a Raman lidar at Thessaloniki, Greece. *Geophysical Research Letters, 31*, L13104. https://doi.org/10.1029/2004GL019881

Balis, D., Amiridis, V., Kazadzis, S., Papayannis, A., Tsaknakis, G., Tzortzakis, S., Kalivitis, N., Vrekoussis, M., Kanakidou, M., Mihalopoulos, N., Chourdakis, G., Nickovic, S., Pérez, C., Baldasano, J., & Drakakis, M. (2006). Optical characteristics of desert dust over the East Mediterranean during summer: A case study. *Annales de Geophysique, 24*, 807–821. https://doi.org/10.5194/angeo-24-807-2006

Barnaba, F., & Gobbi, G. P. (2004). Aerosol seasonal variability over the Mediterranean region and relative impact of maritime, continental and Saharan dust particles over the basin from MODIS data in the year 2001. *Atmospheric Chemistry and Physics, 4*, 2367–2391. https://doi.org/10.5194/acp-4-2367-2004

Barragan, R., Sicard, M., Totems, J., Léon, J.-F., Dulac, F., Mallet, M., Pelon, J., Alados-Arbodelas, L., Amodeo, A., Augustin, P., Boselli, A., Bravo-Aranda, J. A., Burlizzi, P., Chazette, P., Comeron, A., D'Amico, G., Granados-Muñoz, M. J., Leto, G., Guerrero-Rascado, J. L., … Zanmar-Sanchez, R. (2017). Spatio-temporal monitoring by ground-based and air- and space-borne lidars of a moderate Saharan dust event affecting southern Europe in June 2013 in the framework of the ADRIMED/ChArMEx campaign. *Air Quality, Atmosphere and Health, 10*, 261–285. https://doi.org/10.1007/s11869-016-0447-7

Benkhalifa, J., Léon, J. F., & Chaabane, M. (2019). Aerosol vertical distribution, optical properties and dust transport in the Western Mediterranean basin (case study: Summer, 2012). *Atmospheric Pollution Research, 10*, 1291–1298. https://doi.org/10.1016/j.apr.2019.02.013

Berthier, S., Chazette, P., Couvert, P., Pelon, J., Dulac, F., Thieuleux, F., Moulin, C., & Pain, T. (2006). Desert dust aerosol columnar properties over ocean and continental Africa from Lidar in-Space Technology Experiment (LITE) and Meteosat synergy. *Journal of Geophysical Research, 111*, D21202. https://doi.org/10.1029/2005JD006999

Bréon, F.-M., Vermeulen, A., & Descloitres, J. (2011). An evaluation of satellite products against sunphotometer measurements. *Remote Sensing of Environment, 115*, 3102–3111. https://doi.org/10.1016/j.rse.2011.06.017

Bryant, C., Eleftheriadis, K., Smolik, J., Zdimal, V., Mihalopoulos, N., & Colbeck, I. (2006). Optical properties of aerosols over the eastern Mediterranean. *Atmospheric Environment, 40*, 6229–6244. https://doi.org/10.1016/j.atmosenv.2005.06.009

Burton, S. P., Ferrare, R. A., Hostetler, C. A., Hair, J. W., Rogers, R. R., Obland, M. D., Butler, C. F., Cook, A. L., Harper, D. B., & Froyd, K. D. (2012). Aerosol classification using airborne High Spectral Resolution Lidar measurements – methodology and examples. *Atmospheric Measurement Techniques, 5*, 73–98. https://doi.org/10.5194/amt-5-73-2012

Cattrall, C., Reagan, J., Thome, K., & Dubovik, O. (2005). Variability of aerosol and spectral lidar and backscatter and extinction ratios of key aerosol types derived from selected Aerosol Robotic Network locations. *Journal of Geophysical Research, 110*, D10S11. https://doi.org/10.1029/2004JD005124

Chazette, P. (2020). Aerosol optical properties as observed from an ultralight aircraft over the Strait of Gibraltar. *Atmospheric Measurement Techniques, 13*, 4461–4477. https://doi.org/10.5194/amt-13-4461-2020

Chazette, P., & Liousse, C. (2001). A case study of optical and chemical ground apportionment for urban aerosols in Thessaloniki. *Atmospheric Environment, 35*, 2497–2506. https://doi.org/10.1016/S1352-2310(00)00425-8

Chazette, P., Marnas, F., & Totems, J. (2014). The mobile Water vapor Aerosol Raman LIdar and its implication in the frame of the HyMeX and ChArMEx programs: Application to a dust trans-

port process. *Atmospheric Measurement Techniques, 7*, 1629–1647. https://doi.org/10.5194/amt-7-1629-2014

Chazette, P., Totems, J., Ancellet, G., Pelon, J., & Sicard, M. (2016). Temporal consistency of lidar observations during aerosol transport events in the framework of the ChArMEx/ADRIMED campaign at Minorca in June 2013. *Atmospheric Chemistry and Physics, 16*, 2863–2875. https://doi.org/10.5194/acp-16-2863-2016

Chazette, P., Totems, J., & Shang, X. (2019a). Transport of aerosols over the French Riviera – Link between ground-based lidar and spaceborne observations. *Atmospheric Chemistry and Physics, 19*, 3885–3904. https://doi.org/10.5194/acp-19-3885-2019

Chazette, P., Flamant, C., Totems, J., Gaetani, M., Smith, G., Baron, A., Landsheere, X., Desboeufs, K., Doussin, J.-F., & Formenti, P. (2019b). Evidence of the complexity of aerosol transport in the lower troposphere on the Namibian coast during AEROCLO-sA. *Atmospheric Chemistry and Physics, 19*, 14979–15005. https://doi.org/10.5194/acp-19-14979-2019

Ciardini, V., Di Iorio, T., Di Liberto, L., Tirelli, C., Casasanta, G., di Sarra, A., Fiocco, G., Fuà, D., & Cacciani, M. (2012). Seasonal variability of tropospheric aerosols in Rome. *Atmospheric Research, 118*, 205–214. https://doi.org/10.1016/j.atmosres.2012.06.026

Claeys, M., Roberts, G., Mallet, M., Arndt, J., Sellegri, K., Sciare, J., Wenger, J., & Sauvage, B. (2017). Optical, physical and chemical properties of aerosols transported to a coastal site in the western Mediterranean: A focus on primary marine aerosols. *Atmospheric Chemistry and Physics, 17*, 7891–7915. https://doi.org/10.5194/acp-17-7891-2017

Collaud Coen, M., Weingartner, E., Schaub, D., Hueglin, C., Corrigan, C., Henning, S., Schwikowski, M., & Baltensperger, U. (2004). Saharan dust events at the Jungfraujoch: Detection by wavelength dependence of the single scattering albedo and first climatology analysis. *Atmospheric Chemistry and Physics, 4*, 2465–2480. https://doi.org/10.5194/acp-4-2465-2004

Dalu, G., Rao, R., Pompei, A., Boi, P., Tonna, G., & Olivieri, B. (1995). Aerosol optical properties retrieved from solar aureole measurements over southern Sardinia. *Journal of Geophysical Research, 100*, 26135–26140. https://doi.org/10.1029/95JD02598

De Meij, A., & Lelieveld, J. (2011). Evaluating aerosol optical properties observed by ground-based and satellite remote sensing over the Mediterranean and the Middle East in 2006. *Atmospheric Research, 99*, 415–433. https://doi.org/10.1016/j.atmosres.2010.11.005

De Tomasi, F., Blanco, A., & Perrone, M. R. (2003). Raman lidar monitoring of extinction and backscattering of African dust layers and dust characterization. *Applied Optics, 42*, 1699–1709. https://doi.org/10.1364/AO.42.001699

Denjean, C., Cassola, F., Mazzino, A., Triquet, S., Chevaillier, S., Grand, N., Bourrianne, T., Momboisse, G., Sellegri, K., Schwarzenbock, A., Freney, E., Mallet, M., & Formenti, P. (2016). Size distribution and optical properties of mineral dust aerosols transported in the western Mediterranean. *Atmospheric Chemistry and Physics, 16*, 1081–1104. https://doi.org/10.5194/acp-16-1081-2016

Di Biagio, C., di Sarra, A., Meloni, D., Monteleone, F., Piacentino, S., & Sferlazzo, D. (2009). Measurements of Mediterranean aerosol radiative forcing and influence of the single scattering albedo. *Journal of Geophysical Research, 114*, D06211. https://doi.org/10.1029/2008JD011037

Di Biagio, C., Formenti, P., Doppler, L., Gaimoz, C., Grand, N., Ancellet, G., Attié, J.-L., Bucci, S., Dubuisson, P., Fierli, F., Mallet, M., & Ravetta, F. (2016). Continental pollution in the Western Mediterranean basin: Large variability of the aerosol single scattering albedo and influence on the direct shortwave radiative effect. *Atmospheric Chemistry and Physics, 16*, 10591–10607. https://doi.org/10.5194/acp-16-10591-2016

Di Iorio, T., Di Sarra, A., Junkermann, W., Cacciani, M., Fiocco, G., & Fuà, D. (2003). Tropospheric aerosols in the Mediterranean: 1. Microphysical and optical properties. *Journal of Geophysical Research, 108*, 4316. https://doi.org/10.1029/2002JD002815

Di Iorio, T., Di Sarra, A., Sferlazzo, D. M., Cacciani, M., Meloni, D., Monteleone, F., Fuà, D., & Fiocco, G. (2009). Seasonal evolution of the tropospheric aerosol vertical profile in the central Mediterranean and role of desert dust. *Journal of Geophysical Research, 114*, D02201. https://doi.org/10.1029/2008JD010593

Drugé, T., Nabat, P., Mallet, M., & Somot, S. (2019). Model simulation of ammonium and nitrate aerosols distribution in the Euro-Mediterranean region and their radiative and climatic effects over 1979–2016. *Atmospheric Chemistry and Physics, 19*, 3707–3731. https://doi.org/10.5194/acp-19-3707-2019

Dulac, F., & Chazette, P. (2003). Characterization of a multi-layer aerosol structure in the eastern Mediterranean observed with the airborne polarized lidar ALEX during a STAAARTE campaign (June 1997). *Atmospheric Chemistry and Physics, 3*, 2393–2426. https://doi.org/10.5194/acp-3-1817-2003

Dulac, F., Mihalopoulos, N., Kaskaoutis, D. G., di Sarra, A., Masson, O., Pey, J., Querol, X., Sciare, J., & Sicard, M. (2023a). History of Mediterranean aerosol observations. In F. Dulac, S. Sauvage, & E. Hamonou (Eds.), *Atmospheric chemistry in the Mediterranean Region* (Vol. 1, Background information and pollutant distribution). Springer.

Dulac, F., Hamonou, E., Sauvage, S., & Debevec, C. (2023b). Introduction to the volume 1 of atmospheric chemistry in the Mediterranean Region and to the experimental effort during the ChArMEx decade. In F. Dulac, S. Sauvage, & E. Hamonou (Eds.), *Atmospheric chemistry in the Mediterranean Region* (Vol. 1, Background information and pollutants distribution). Springer.

Ealo, M., Alastuey, A., Ripoll, A., Pérez, N., Minguillón, M. C., Querol, X., & Pandolfi, M. (2016). Detection of Saharan dust and biomass burning events using near-real-time intensive aerosol optical properties in the north-western Mediterranean. *Atmospheric Chemistry and Physics, 16*, 12567–12586. https://doi.org/10.5194/acp-16-12567-2016

Ealo, M., Alastuey, A., Pérez, N., Ripoll, A., Querol, X., & Pandolfi, M. (2018). Impact of aerosol particle sources on optical properties in urban, regional and remote areas in the north-western Mediterranean. *Atmospheric Chemistry and Physics, 18*, 1149–1169. https://doi.org/10.5194/acp-18-1149-2018

Fernandez, A. J., Sicard, M., Costa, M. J., Guerrero-Rascado, J. L., Gómez-Amo, J. L., Molero, F., Barragán, R., Basart, S., Bortoli, D., Bedoya-Velásquez, A. E., Utrillas, M. P., Salvador, P., Granados-Muñoz, M. J., Potes, M., Ortiz-Amezcua, P., Martínez-Lozano, J. A., Artíñano, B., Muñoz-Porcar, C., Salgado, R., … Pujadas, M. (2019). Extreme, wintertime Saharan dust intrusion in the Iberian Peninsula: Lidar monitoring and evaluation of dust forecast models during the February 2017 event. *Atmospheric Research, 228*, 223–241. https://doi.org/10.1016/j.atmosres.2019.06.007

Flamant, C., Chaboureau, J.-P., Chazette, P., Di Girolamo, P., Bourrianne, T., Totems, J., & Cacciani, M. (2015). The radiative impact of desert dust on orographic rain in the Cévennes–Vivarais area: A case study from HyMeX. *Atmospheric Chemistry and Physics, 15*, 12231–12249. https://doi.org/10.5194/acp-15-12231-2015

Floutsi, A. A., Korras-Carraca, M. B., Matsoukas, C., Hatzianastassiou, N., & Biskos, G. (2016). Climatology and trends of aerosol optical depth over the Mediterranean basin during the last 12 years (2002–2014) based on Collection 006 MODIS-Aqua data. *Science of The Total Environment, 551-552*, 292–303. https://doi.org/10.1016/j.scitotenv.2016.01.192

Formenti, P., Andreae, M. O., Andreae, T. W., Ichoku, C., Schebeske, G., Kettle, J., Maenhaut, W., Kafmeyer, J., Ptasinsky, J., Karnieli, A., & Lelieveld, J. (2001a). Physical and chemical characteristics of aerosols over the Negev Desert (Israel) during summer 1996. *Journal of Geophysical Research, 106*, 4871–4890. https://doi.org/10.1029/2000JD900556

Formenti, P., Andreae, M. O., Andreae, T. W., Galani, E., Vasaras, A., Zerefos, C., Amiridis, V., Orlovsky, L., Karnieli, A., Wendisch, M., Wex, H., Holben, B. N., Maenhaut, W., & Lelieveld, J. (2001b). Aerosol optical properties and large-scale transport of air masses: Observations at a coastal and a semiarid site in the eastern Mediterranean during summer 1998. *Journal of Geophysical Research, 106*, 9807–9826. https://doi.org/10.1029/2000JD900609

Formenti, P., Boucher, O., Reiner, T., Sprung, D., Andreae, M. O., Wendisch, M., Wex, H., Kindred, D., Tzortziou, M., Vasaras, A., & Zerefos, C. (2002). STAAARTE-MED 1998 summer airborne measurements over the Aegean Sea, 2. Aerosol scattering and absorption, and radiative calculations. *Journal of Geophysical Research, 107*, 4451. https://doi.org/10.1029/2001JD001536

Formenti, P., Mbemba Kabuiku, L., Chiapello, I., Ducos, F., Dulac, F., & Tanré, D. (2018). Aerosol optical properties derived from POLDER-3/PARASOL (2005–2013) over the western Mediterranean Sea – Part 1: Quality assessment with AERONET and in situ airborne observations. *Atmospheric Measurement Techniques, 11*, 6761–6784. https://doi.org/10.5194/amt-11-6761-2018

Fotiadi, A., Hatzianastassiou, N., Drakakis, E., Matsoukas, C., Pavlakis, K. G., Hatzidimitriou, D., Gerasopoulos, E., Mihalopoulos, N., & Vardavas, I. (2006). Aerosol physical and optical properties in the Eastern Mediterranean Basin, Crete, from Aerosol Robotic Network data. *Atmospheric Chemistry and Physics, 6*, 5399–5413. https://doi.org/10.5194/acp-6-5399-2006

Georgoulias, A. K., Alexandri, G., Kourtidis, K. A., Lelieveld, J., Zanis, P., Pöschl, U., Levy, R., Amiridis, V., Marinou, E., & Tsikerdekis, A. (2016). Spatiotemporal variability and contribution of different aerosol types to the aerosol optical depth over the Eastern Mediterranean. *Atmospheric Chemistry and Physics, 16*, 13853–13884. https://doi.org/10.5194/acp-16-13853-2016

Gerasopoulos, E., Andreae, M. O., Zerefos, C. S., Andreae, T. W., Balis, D., Formenti, P., Merlet, P., Amiridis, V., & Papastefanou, C. (2003). Climatological aspects of aerosol optical properties in Northern Greece. *Atmospheric Chemistry and Physics, 3*, 2025–2041. https://doi.org/10.5194/acp-3-2025-2003

Gkikas, A., Hatzianastassiou, N., Mihalopoulos, N., Katsoulis, V., Kazadzis, S., Pey, J., Querol, X., & Torres, O. (2013). The regime of intense desert dust episodes in the Mediterranean based on contemporary satellite observations and ground measurements. *Atmospheric Chemistry and Physics, 13*, 12135–12154. https://doi.org/10.5194/acp-13-12135-2013

Gkikas, A., Basart, S., Hatzianastassiou, N., Marinou, E., Amiridis, V., Kazadzis, S., Pey, J., Querol, X., Jorba, O., Gassó, S., & Baldasano, J. M. (2016a). Mediterranean intense desert dust outbreaks and their vertical structure based on remote sensing data. *Atmospheric Chemistry and Physics, 16*, 8609–8642. https://doi.org/10.5194/acp-16-8609-2016

Gkikas, A., Hatzianastassiou, N., Mihalopoulos, N., & Torres, O. (2016b). Characterization of aerosols episodes in the greater Mediterranean Sea area from satellite observations (2000–2007). *Atmospheric Environment, 128*, 286–304. https://doi.org/10.1016/j.atmosenv.2015.11.056

Gobbi, G. P., Barnaba, F., Giorgi, R., & Santacasa, A. (2000). Altitude-resolved properties of a Saharan dust event over the Mediterranean. *Atmospheric Environment, 34*, 5119–5127. https://doi.org/10.1016/S1352-2310(00)00194-1

Gómez-Amo, J. L., Estellés, V., Marcos, C., Segura, S., Esteve, A. R., Pedrós, R., Utrillas, M. P., & Martínez-Lozano, J. A. (2017). Impact of dust and smoke mixing on column-integrated aerosol properties from observations during a severe wildfire episode over Valencia (Spain). *Science of The Total Environment, 599–600*, 2121–2134. https://doi.org/10.1016/j.scitotenv.2017.05.041

Groß, S., Freudenthaler, V., Wirth, M., & Weinzierl, B. (2015). Towards an aerosol classification scheme for future EarthCARE lidar observations and implications for research needs. *Atmospheric Science Letters, 16*, 77–82. https://doi.org/10.1002/asl2.524

Guieu, C., & Ridame, C. (2022). Impact of atmospheric deposition on marine chemistry and biogeochemistry. In F. Dulac, S. Sauvage, & E. Hamonou (Eds.), *Atmospheric chemistry in the Mediterranean Region* (Vol. 2, From air pollutant sources to impacts). Springer, this volume. https://doi.org/10.1007/978-3-030-82385-6_23

Gulyaev, Y. N., Yershov, O. A., Smirnov, A. V., & Shifrin, K. S. (1990). The air masses influence on spectral transmittance in typical maritime regions (in Russian). In K. S. Shifrin (Ed.), *Atmospheric and Marine Optics* (pp. 96–97). State Optical Institute Leningrad.

Hamonou, E., Chazette, P., Balis, D., Dulac, F., Schneider, X., Galani, E., Ancellet, G., & Papayannis, A. (1999). Characterisation of the vertical structure of Saharan dust export to the Mediterranean basin. *Journal of Geophysical Research, 18*, 2257–2270. https://doi.org/10.1029/1999JD900257

Hatzianastassiou, N., Gkikas, A., Mihalopoulos, N., Torres, O., & Katsoulis, B. D. (2009). Natural versus anthropogenic aerosols in the eastern Mediterranean basin derived from multiyear TOMS and MODIS satellite data. *Journal of Geophysical Research, 114*, D24202. https://doi.org/10.1029/2009JD011982

Horvath, H., Alados Arboledas, L., Olmo, F. J., Jovanovic, O., Gangl, M., Sanchez, C., Sauerzopf, H., & Seidl, S. (2002). Optical characteristics of the aerosol in Spain and Austria and its effect on radiative forcing. *Journal of Geophysical Research, 107*, 4386. https://doi.org/10.1029/2001JD001472

Hsu, N. C., Gautam, R., Sayer, A. M., Bettenhausen, C., Li, C., Jeong, M. J., Tsay, S.-C., & Holben, B. N. (2012). Global and regional trends of aerosol optical depth over land and ocean using SeaWiFS measurements from 1997 to 2010. *Atmospheric Chemistry and Physics, 12*, 8037–8053. https://doi.org/10.5194/acp-12-8037-2012

Israelevich, P. L., Ganor, E., Levin, Z., & Joseph, J. H. (2003). Annual variations of physical properties of desert dust over Israel. *Journal of Geophysical Research, 108*, 4381. https://doi.org/10.1029/2002JD003163

Joseph, J. H., & Manes, A. (1971). Secular and seasonal variations of atmospheric turbidity at Jerusalem. *Journal of Applied Meteorology, 10*, 453–462, https://journals.ametsoc.org/doi/pdf/. https://doi.org/10.1175/1520-0450(1971)010<0453:SASVOA>2.0.CO;2

Kanakidou, M., Sfakianaki, M., & Probst, A. (2022). Impact of air pollution on terrestrial ecosystems. In F. Dulac, S. Sauvage, & E. Hamonou (Eds.), *Atmospheric chemistry in the Mediterranean Region* (Vol. 2, From air pollutant sources to impacts). Springer, this volume. https://doi.org/10.1007/978-3-030-82385-6_24

Kaskaoutis, D. G., Stavroulas, I., Bougiatioti, A., Gerasopoulos, E., Mihalopoulos, N., Alastuey, A., Minguillón, M. C., Rashki, A., Sciare, J., & Titos, G. (2023a). Diurnal to seasonal variability of aerosols above the Mediterranean. In F. Dulac, S. Sauvage, & E. Hamonou (Eds.), *Atmospheric chemistry in the Mediterranean Region* (Vol. 1, Background information and pollutant distribution). Springer.

Kaskaoutis, D. G., Liakakou, E., Grivas, G., Gerasopoulos, E., Mihalopoulos, N., Alastuey, A., Dulac, F., Dumka, U. C., Pandolfi, M., Pikridas, M., Sciare, J., & Titos, G. (2023b). Interannual variability and long-term trends of aerosols above the Mediterranean. In F. Dulac, S. Sauvage, & E. Hamonou (Eds.), *Atmospheric chemistry in the Mediterranean Region* (Vol. 1, Background information and pollutants distribution). Springer.

Kazadzis, S., Bais, A., Kouremeti, N., Gerasopoulos, E., Garane, K., Blumthaler, M., Schallhart, B., & Cede, A. (2005). Direct spectral measurements with a Brewer spectroradiometer: Absolute calibration and aerosol optical depth retrieval. *Applied Optics, 44*, 1681–1690. https://doi.org/10.1364/AO.44.001681

Kim, M.-H., Omar, A. H., Tackett, J. L., Vaughan, M. A., Winker, D. M., Trepte, C. R., Hu, Y., Liu, Z., Poole, L. R., Pitts, M. C., Kar, J., & Magill, B. E. (2018). The CALIPSO version 4 automated aerosol classification and lidar ratio selection algorithm. *Atmospheric Measurement Techniques, 11*, 6107–6135. https://doi.org/10.5194/amt-11-6107-2018

Klett, J. D. (1983). Lidar calibration and extinction coefficients. *Applied Optics, 22*, 514–515. https://doi.org/10.1364/AO.22.000514

Kubilay, N., Cokacar, T., & Oguz, T. (2003). Optical properties of mineral dust outbreaks over the northeastern Mediterranean. *Journal of Geophysical Research, 108*, 4666. https://doi.org/10.1029/2003JD003798

Lacagnina, C., Hasekamp, O. P., Bian, H., Curci, G., Myhre, G., van Noije, T., Schulz, M., Skeie, R. B., Takemura, T., & Zhang, K. (2015). Aerosol single-scattering albedo over the global oceans: Comparing PARASOL retrievals with AERONET, OMI, and AeroCom models estimates. *Journal of Geophysical Research – Atmospheres, 120*, 9814–9836. https://doi.org/10.1002/2015JD023501

Lelieveld, J., Berresheim, H., Borrmann, S., Crutzen, P. J., Dentener, F. J., Fischer, H., Feichter, J., Flatau, P. J., Heland, J., Holzinger, R., Korrmann, R., Lawrence, M. G., Levin, Z., Markowicz, K. M., Mihalopoulos, N., Minikin, A., Ramanathan, V., de Reus, M., Roelofs, G. J., … Ziereis, H. (2002). Global air pollution crossroads over the Mediterranean. *Science, 298*, 794–799. https://doi.org/10.1126/science.1075457

Léon, J.-F., Chazette, P., & Dulac, F. (1999). Retrieval and monitoring of aerosol optical thickness over an urban area using spaceborne and ground-based remote sensing. *Applied Optics, 38*, 6918–6926. https://doi.org/10.1364/AO.38.006918

Lionello, P., Abrantes, F., Congedi, L., Dulac, F., Gacic, M., Gomiz, D., Goodess, C., Hoff, H., Kutiel, H., Luterbacher, J., Planton, S., Reale, M., Schröder, K., Struglia, M. V., Toreti, A., Tsimplis, M., Ulbrich, U., & Xoplaki, E. (2012). Introduction: Mediterranean climate–background information. In P. Lionello (Ed.), *The climate of the Mediterranean region: From the past to the future* (pp. xxxv–xc). Elsevier. https://doi.org/10.1016/B978-0-12-416042-2.00012-4

Lyamani, H., Valenzuela, A., Perez-Ramirez, D., Toledano, C., Granados-Muñoz, M. J., Olmo, F. J., & Alados-Arboledas, L. (2015). Aerosol properties over the western Mediterranean basin: Temporal and spatial variability. *Atmospheric Chemistry and Physics, 15*, 2473–2486. https://doi.org/10.5194/acp-15-2473-2015

Mallet, M., Roger, J. C., Despiau, S., Dubovik, O., & Putaud, J. P. (2003). Microphysical and optical properties of aerosol particles in urban zone during ESCOMPTE. *Atmospheric Research, 69*, 73–97. https://doi.org/10.1016/j.atmosres.2003.07.001

Mallet, M., Roger, J. C., Despiau, S., Putaud, J. P., & Dubovik, O. (2004). A study of the mixing state of black carbon in urban zone. *Journal of Geophysical Research, 109*, D04202. https://doi.org/10.1029/2003JD003940

Mallet, M., Van Dingenen, R., Roger, J. C., Despiau, S., & Cachier, H. (2005a). In situ airborne measurements of aerosol optical properties during photochemical pollution events. *Journal of Geophysical Research, 110*, D03205. https://doi.org/10.1029/2004JD005139

Mallet, M., Pont, V., & Liousse, C. (2005b). Modelling of strong heterogeneities in aerosol single scattering albedos over a polluted region. *Geophysical Research Letters, 32*, L09807. https://doi.org/10.1029/2005GL022680

Mallet, M., Pont, V., Liousse, C., Roger, J. C., & Dubuisson, P. (2006). Simulation of aerosol radiative properties with the ORISAM-RAD model during a pollution event (ESCOMPTE 2001). *Atmospheric Environment, 40*, 7696–7705. https://doi.org/10.1016/j.atmosenv.2006.08.031

Mallet, M., Dubovik, O., Nabat, P., Dulac, F., Kahn, R., Sciare, J., Paronis, D., & Léon, J. F. (2013). Absorption properties of Mediterranean aerosols obtained from multi-year ground-based remote sensing observations. *Atmospheric Chemistry and Physics, 13*, 9195–9210. https://doi.org/10.5194/acp-13-9195-2013

Mallet, M., Dulac, F., Formenti, P., Nabat, P., Sciare, J., Roberts, G., Pelon, J., Ancellet, G., Tanré, D., Parol, F., Denjean, C., Brogniez, G., di Sarra, A., Alados-Arboledas, L., Arndt, J., Auriol, F., Blarel, L., Bourrianne, T., Chazette, P., … Zapf, P. (2016). Overview of the Chemistry-Aerosol Mediterranean Experiment/Aerosol Direct radiative Forcing on the Mediterranean Climate (ChArMEx/ADRIMED) summer 2013 campaign. *Atmospheric Chemistry and Physics, 16*, 455–504. https://doi.org/10.5194/acp-16-455-2016

Mamouri, R. E., Ansmann, A., Nisantzi, A., Kokkalis, P., Schwarz, A., & Hadjimitsis, D. (2013). Low Arabian dust extinction-to-backscatter ratio. *Geophysical Research Letters, 40*, 4762–4766. https://doi.org/10.1002/grl.50898

Mandija, F., Sicard, M., Comerón, A., Alados-Arboledas, L., Guerrero-Rascado, J. L., Barragan, R., Bravo-Aranda, J. A., Granados-Muñoz, M. J., Lyamani, H., Porcar, C. M., & Rocadenbosch, F. (2017). Origin and pathways of the mineral dust transport to two Spanish EARLINET sites: Effect on the observed columnar and range-resolved dust optical properties. *Atmospheric Research, 187*, 69–83. https://doi.org/10.1016/j.atmosres.2016.12.002

Marinou, E., Amiridis, V., Binietoglou, I., Tsikerdekis, A., Solomos, S., Proestakis, E., Konsta, D., Papagiannopoulos, N., Tsekeri, A., Vlastou, G., Zanis, P., Balis, D., Wandinger, U., & Ansmann, A. (2017). Three-dimensional evolution of Saharan dust transport towards Europe based on a 9-year EARLINET-optimized CALIPSO dataset. *Atmospheric Chemistry and Physics, 17*, 5893–5919. https://doi.org/10.5194/acp-17-5893-2017

Markowicz, K. M., Flatau, P. J., Ramana, M. V., Crutzen, P. J., & Ramanathan, V. (2002). Absorbing mediterranean aerosols lead to a large reduction in the solar radiation at the surface. *Geophysical Research Letters, 29*, 1968. https://doi.org/10.1029/2002GL015767

Meloni, D., di Sarra, A., DeLuisi, J., Di Iorio, T., Fiocco, G., Junkermann, W., & Pace, G. (2003). Tropospheric aerosols in the Mediterranean: 2. Radiative effects through model simulations and measurements. *Journal of Geophysical Research, 108*, 4317. https://doi.org/10.1029/2002JD002807

Meloni, D., di Sarra, A., Di Iorio, T., & Fiocco, G. (2004). Direct radiative forcing of Saharan dust in the Mediterranean from measurements at Lampedusa Island and MISR space-borne observations. *Journal of Geophysical Research, 109*, D08206. https://doi.org/10.1029/2003JD003960

Meloni, D., di Sarra, A., Pace, G., & Monteleone, F. (2006). Aerosol optical properties at Lampedusa (Central Mediterranean). 2. Determination of single scattering albedo at two wavelengths for different aerosol types. *Atmospheric Chemistry and Physics, 6*, 715–727. https://doi.org/10.5194/acp-6-715-2006

Meloni, D., di Sarra, A., Biavati, G., DeLuisi, J. J., Monteleone, F., Pace, G., Piacentino, S., & Sferlazzo, D. M. (2007). Seasonal behavior of Saharan dust events at the Mediterranean island of Lampedusa in the period 1999-2005. *Atmospheric Environment, 41*, 3041–3056. https://doi.org/10.1016/j.atmosenv.2006.12.001

Meloni, D., di Sarra, A., Monteleone, F., Pace, G., Piacentino, S., & Sferlazzo, D. M. (2008). Seasonal transport patterns of intense Saharan dust events at the Mediterranean island of Lampedusa. *Atmospheric Research, 88*, 134–148. https://doi.org/10.1016/j.atmosres.2007.10.007

Menut, L., Mailler, S., Siour, G., Bessagnet, B., Turquety, S., Rea, G., Briant, R., Mallet, M., Sciare, J., Formenti, P., & Meleux, F. (2015). Ozone and aerosol tropospheric concentrations variability analyzed using the ADRIMED measurements and the WRF and CHIMERE models. *Atmospheric Chemistry and Physics, 15*, 6159–6182. https://doi.org/10.5194/acp-15-6159-2015

Mishra, A. K., Klingmueller, K., Fredj, E., Lelieveld, J., Rudich, Y., & Koren, I. (2014). Radiative signature of absorbing aerosol over the eastern Mediterranean basin. *Atmospheric Chemistry and Physics, 14*, 7213–7231. https://doi.org/10.5194/acp-14-7213-2014

Mona, L., Amodeo, A., Pandolfi, M., & Pappalardo, G. (2006). Saharan dust intrusions in the Mediterranean area: Three years of Raman lidar measurements. *Journal of Geophysical Research, 111*, D16203. https://doi.org/10.1029/2005JD006569

Moulin, C., Dulac, F., Lambert, C. E., Chazette, P., Jankowiak, I., Chatenet, B., & Lavenu, F. (1997). Long-term daily monitoring of Saharan dust load over marine areas using Meteosat ISCCP-B2 data. Part II: Accuracy of the method and validation using sunphotometer measurements. *Journal of Geophysical Research, 102*, 16959–16969. https://doi.org/10.1029/96JD02598

Moulin, C., Lambert, C. E., Dayan, U., Masson, V., Ramonet, M., Bousquet, P., Legrand, M., Balkanski, Y. J., Guelle, W., Marticorena, B., Bergametti, G., & Dulac, F. (1998). Satellite climatology of African dust transport in the Mediterranean atmosphere. *Journal of Geophysical Research, 103*, 13137–13144. https://doi.org/10.1029/98JD00171

Nabat, P., Solmon, F., Mallet, M., Kok, J. F., & Somot, S. (2012). Dust emission size distribution impact on aerosol budget and radiative forcing over the Mediterranean region: A regional climate model approach. *Atmospheric Chemistry and Physics, 12*, 10545–10567. https://doi.org/10.5194/acp-12-10545-2012

Nabat, P., Somot, S., Mallet, M., Chiapello, I., Morcrette, J. J., Solmon, F., Szopa, S., Dulac, F., Collins, W., Ghan, S., Horowitz, L. W., Lamarque, J. F., Lee, Y. H., Naik, V., Nagashima, T., Shindell, D., & Skeie, R. (2013). A 4-D climatology (1979–2009) of the monthly tropospheric aerosol optical depth distribution over the Mediterranean region from a comparative evaluation and blending of remote sensing and model products. *Atmospheric Measurement Techniques, 6*, 1287–1314. https://doi.org/10.5194/amt-6-1287-2013

Nabat, P., Somot, S., Cassou, C., Mallet, M., Michou, M., Bouniol, D., Decharme, B., Drugé, T., Roehrig, R., & Saint-Martin, D. (2020). Modulation of radiative aerosols effects by atmospheric circulation over the Euro-Mediterranean region. *Atmospheric Chemistry and Physics, 20*, 8315–8349. https://doi.org/10.5194/acp-20-8315-2020

Nisantzi, A., Mamouri, R. E., Ansmann, A., & Hadjimitsis, D. (2014). Injection of mineral dust into the free troposphere during fire events observed with polarization lidar at Limassol, Cyprus. *Atmospheric Chemistry and Physics, 14*, 12155–12165. https://doi.org/10.5194/acp-14-12155-2014

Nisantzi, A., Mamouri, R. E., Ansmann, A., Schuster, G. L., & Hadjimitsis, D. G. (2015). Middle East versus Saharan dust extinction-to-backscatter ratios. *Atmospheric Chemistry and Physics, 15*, 7071–7084. https://doi.org/10.5194/acp-15-7071-2015

Omar, A., Winker, D., Kittaka, C., Vaughan, M., Liu, Z., Hu, Y., Trepte, C., Rogers, R., Ferrare, R., Lee, K., Kuehn, R., & Hostetler, C. (2009). The CALIPSO automated aerosol classification and lidar ratio selection algorithm. *Journal of Atmospheric and Oceanic Technology, 26*, 1994–2014. https://doi.org/10.1175/2009JTECHA1231.1

Ortiz-Amezcua, P., Guerrero-Rascado, J. L., Granados-Muñoz, M. J., Benavent-Oltra, J. A., Böckmann, C., Samaras, S., Stachlewska, I. S., Janicka, Ł., Baars, H., Bohlmann, S., & Alados-Arboledas, L. (2017). Microphysical characterization of long-range transported biomass burning particles from North America at three EARLINET stations. *Atmospheric Chemistry and Physics, 17*, 5931–5946. https://doi.org/10.5194/acp-17-5931-2017

Pace, G., Meloni, D., & Di Sarra, A. (2005). Forest fire aerosol over the Mediterranean basin during summer 2003. *Journal of Geophysical Research, 110*, D21202. https://doi.org/10.1029/2005JD005986

Pace, G., Di Sarra, A., Meloni, D., Piacentino, S., & Chamard, P. (2006). Aerosol optical properties at Lampedusa (Central Mediterranean). 1. Influence of transport and identification of different aerosol types. *Atmospheric Chemistry and Physics, 6*, 697–713. https://doi.org/10.5194/acp-6-697-2006

Pandolfi, M., Cusack, M., Alastuey, A., & Querol, X. (2011). Variability of aerosol optical properties in the Western Mediterranean Basin. *Atmospheric Chemistry and Physics, 11*, 8189–8203. https://doi.org/10.5194/acp-11-8189-2011

Pandolfi, M., Alados-Arboledas, L., Alastuey, A., Andrade, M., Angelov, C., Artiñano, B., Backman, J., Baltensperger, U., Bonasoni, P., Bukowiecki, N., Collaud Coen, M., Conil, S., Coz, E., Crenn, V., Dudoitis, V., Ealo, M., Eleftheriadis, K., Favez, O., Fetfatzis, P., … Laj, P. (2018). A European aerosol phenomenology – 6: Scattering properties of atmospheric aerosol particles from 28 ACTRIS sites. *Atmospheric Chemistry and Physics, 18*, 7877–7911. https://doi.org/10.5194/acp-18-7877-2018

Papadimas, C. D., Hatzianastassiou, N., Mihalopoulos, N., Querol, X., & Vardavas, I. (2008). Spatial and temporal variability in aerosol properties over the Mediterranean basin based on 6-year (2000–2006) MODIS data. *Journal of Geophysical Research, 113*, D11205. https://doi.org/10.1029/2007JD009189

Papadimas, C. D., Hatzianastassiou, N., Mihalopoulos, N., Kanakidou, M., Katsoulis, B. D., & Vardavas, I. (2009). Assessment of the MODIS Collections C005 and C004 aerosol optical depth products over the Mediterranean basin. *Atmospheric Chemistry and Physics, 9*, 2987–2999. https://doi.org/10.5194/acp-9-2987-2009

Papayannis, A., Balis, D., Amiridis, V., Chourdakis, G., Tsaknakis, G., Zerefos, C., Castanho, A. D. A., Nickovic, S., Kazadzis, S., & Grabowski, J. (2005). Measurements of Saharan dust aerosols over the Eastern Mediterranean using elastic backscatter-Raman lidar, spectrophotometric and satellite observations in the frame of the EARLINET project. *Atmospheric Chemistry and Physics, 5*, 2065–2079. https://doi.org/10.5194/acp-5-2065-2005

Papayannis, A., Amiridis, V., Mona, L., Tsaknakis, G., Balis, D., Bösenberg, J., Chaikovski, A., De Tomasi, F., Grigorov, I., Mattis, I., Mitev, V., Müller, D., Nickovic, S., Pérez, C., Pietruczuk, A., Pisani, G., Ravetta, F., Rizi, V., Sicard, M., … Pappalardo, G. (2008a). Systematic lidar observations of Saharan dust over Europe in the frame of EARLINET (2000–2002). *Journal of Geophysical Research, 113*, D10204. https://doi.org/10.1029/2007JD009028

Papayannis, A., Mamouri, R. E., Nenes, A., Tsaknakis, G., Georgoussis, G., Avdikos, G., Böckmann, C., Osterloh, L., Eleftheridais, K., Böhme, D., & Stohl, A. (2008b). Optical, microphysical and chemical properties of tropospheric aerosols retrieved by a 6-wavelength RAMAN lidar system during a biomass burning event over Athens, Greece. In *Proceedings of 24th International laser radar Conference* (Vol. I, pp. 381–384., http://www.academia.edu/download/44389828/PAPAYANNIS_et_al.pdf).

Pappalardo, G., Amodeo, A., Apituley, A., Comeron, A., Freudenthaler, V., Linné, H., Ansmann, A., Bösenberg, J., D'Amico, G., Mattis, I., Mona, L., Wandinger, U., Amiridis, V., Alados-Arboledas, L., Nicolae, D., & Wiegner, M. (2014). EARLINET. Towards an advanced sustainable European aerosol lidar network. *Atmospheric Measurement Techniques, 7*, 2389–2409. https://doi.org/10.5194/amt-7-2389-2014

Paronis, D., Dulac, F., Chazette, P., Hamonou, E., & Liberti, G. L. (1998). Aerosol optical thickness monitoring in the Mediterranean. *Journal of Aerosol Science, 29*(Suppl. 1), 671–672. https://doi.org/10.1016/S0021-8502(98)90518-3

Randriamiarisoa, H., Chazette, P., & Mégie, G. (2004). Retrieving the aerosol single-scattering albedo from the NO_2 photolysis rate coefficient. *Tellus B: Chemical and Physical Meteorology, 56*, 118–127. https://doi.org/10.1111/j.1600-0889.2004.00093.x

Raut, J.-C., & Chazette, P. (2008). Vertical profiles of urban aerosol complex refractive index in the frame of ESQUIF airborne measurements. *Atmospheric Chemistry and Physics, 8*, 901–919. https://doi.org/10.5194/acp-8-901-2008

Roger, J. C., Mallet, M., Dubuisson, P., Cachier, H., Vermote, E., Dubovik, O., & Despiau, S. (2006). A synergetic approach for estimating the local direct aerosol forcing: Application to an urban zone during the Expérience sur Site pour Contraindre les Modèles de Pollution et de Transport d'Emission (ESCOMPTE) experiment. *Journal of Geophysical Research, 111*, D13208. https://doi.org/10.1029/2005JD006361

Royer, P., Raut, J.-C., Ajello, G., Berthier, S., & Chazette, P. (2010). Synergy between CALIOP and MODIS instruments for aerosol monitoring: Application to the Po Valley. *Atmospheric Measurement Techniques, 3*, 893–907. https://doi.org/10.5194/amt-3-893-2010

Saha, A., Mallet, M., Roger, J. C., Dubuisson, P., Piazzola, J., & Despiau, S. (2008). One year measurements of aerosol optical properties in a coastal zone. Implication on the local radiative effects. *Atmospheric Research, 90*, 195–202. https://doi.org/10.1016/j.atmosres.2008.02.003

Sayer, A. M., Munchak, L. A., Hsu, N. C., Levy, R. C., Bettenhausen, C., & Jeong, M. (2014). MODIS Collection 6 aerosol products: Comparison between Aqua's e-Deep Blue, Dark Target, and "merged" data sets, and usage recommendations. *Journal of Geophysical Research – Atmospheres, 119*, 13965–13989. https://doi.org/10.1002/2014JD022453

Sicard, M., Chazette, P., Pelon, J., Won, J. G., & Yoon, S. C. (2002). Variational method for the retrieval of the optical thickness and the backscatter coefficient from multiangular lidar profiles. *Applied Optics, 41*, 493–502. https://doi.org/10.1364/ao.41.000493

Sicard, M., Rocadenbosch, F., Reba, M. N. M., Comerón, A., Tomás, S., García-Vízcaino, D., Batet, O., Barrios, R., Kumar, D., & Baldasano, J. M. (2011). Seasonal variability of aerosol optical properties observed by means of a Raman lidar at an EARLINET site over Northeastern Spain. *Atmospheric Chemistry and Physics, 11*, 175–190. https://doi.org/10.5194/acp-11-175-2011

Sicard, M., Mallet, M., García-Vizcaíno, D., Comerón, A., Rocadenbosch, F., Dubuisson, P., & Muñoz-Porcar, C. (2012). Intense dust and extremely fresh biomass burning outbreak in Barcelona, Spain: Characterization of their optical properties and estimation of their direct radiative forcing. *Environmental Research Letters, 7*, 034016. https://doi.org/10.1088/1748-9326/7/3/034016

Sicard, M., Granados-Muñoz, M. J., Alados-Arboledas, L., Barragán, R., Bedoya-Velásquez, A. E., Benavent-Oltra, J. A., Bortoli, D., Comerón, A., Córdoba-Jabonero, C., Costa, M. J., del Águila, A., Fernández, A. J., Guerrero-Rascado, J. L., Jorba, O., Molero, F., Muñoz-Porcar, C., Ortiz-Amezcua, P., Papagiannopoulos, N., Potes, M., … Yela, M. (2019). Ground/space, passive/active remote sensing observations coupled with particle dispersion modelling to understand the inter-continental transport of wildfire smoke plumes. *Remote Sensing of Environment, 232*, 111294. https://doi.org/10.1016/j.rse.2019.111294

Smirnov, A., Villevalde, Y., O'Neill, N. T., Royer, A., & Tarussov, A. (1995). Aerosol optical depth over the oceans: Analysis in terms of synoptic air mass types. *Journal of Geophysical Research, 100*, 16639–16650. https://doi.org/10.1029/95JD01265

Stowe, L. L., Ignato, A. M., & Singh, R. R. (1997). Development, validation, and potential enhancements to the second-generation operational aerosol product at the National Environmental Satellite, Data, and Information Service of the National Oceanic and Atmospheric Administration. *Journal of Geophysical Research, 102*, 16923–16934. https://doi.org/10.1029/96JD02132

Tafuro, A. M., Barnaba, F., De Tomasi, F., Perrone, M. R., & Gobbi, G. P. (2006). Saharan dust particle properties over the Central Mediterranean. *Atmospheric Research, 81*, 67–93. https://doi.org/10.1016/j.atmosres.2005.11.008

Tafuro, A. M., Kinne, S., De Tomasi, F., & Perrone, M. R. (2007). Annual cycle of direct radiative effect over Southeast Italy and sensitivity studies. *Journal of Geophysical Research, 112*, D20202. https://doi.org/10.1029/2006JD008265

Thieuleux, F., Moulin, C., Bréon, F. M., Maignan, F., Poitou, J., & Tanré, D. (2005). Remote sensing of aerosols over the oceans using MSG/SEVIRI imagery. *Annales de Geophysique, 23*, 3561–3568. https://doi.org/10.5194/angeo-23-3561-2005

Titos, G., Foyo-Moreno, I., Lyamani, H., Querol, X., Alastuey, A., & Alados-Arboledas, L. (2012). Optical properties and chemical composition of aerosol particles at an urban location: An estimation of the aerosol mass scattering and absorption efficiencies. *Journal of Geophysical Research, 117*, D04206. https://doi.org/10.1029/2011JD016671

Vrekoussis, M., Liakakou, E., Koçak, M., Kubilay, N., Oikonomou, K., Sciare, J., & Mihalopoulos, N. (2005). Seasonal variability of optical properties of aerosols in the Eastern Mediterranean. *Atmospheric Environment, 39*, 7083–7094. https://doi.org/10.1016/j.atmosenv.2005.08.011

Wandinger, U., Tesche, M., Seifert, P., Ansmann, A., Müller, D., & Althausen, D. (2010). Size matters: Influence of multiple scattering on CALIPSO light-extinction profiling in desert dust. *Geophysical Research Letters, 37*, L10801. https://doi.org/10.1029/2010GL042815

Wang, Y., Sartelet, K. N., Bocquet, M., Chazette, P., Sicard, M., D'Amico, G., Léon, J. F., Alados-Arboledas, L., Amodeo, A., Augustin, P., Bach, J., Belegante, L., Binietoglou, I., Bush, X., Comerón, A., Delbarre, H., García-Vízcaino, D., Guerrero-Rascado, J. L., Hervo, M., … Dulac, F. (2014). Assimilation of lidar signals: Application to aerosol forecasting in the western Mediterranean basin. *Atmospheric Chemistry and Physics, 14*, 12031–12053. https://doi.org/10.5194/acp-14-12031-2014

Winker, D. M., Hunt, W. H., & McGill, M. J. (2007). Initial performance assessment of CALIOP. *Geophysical Research Letters, 34*, L19803. https://doi.org/10.1029/2007GL030135

Yorks, J. E., McGill, M. J., Palm, S. P., Hlavka, D. L., Selmer, P. A., Nowottnick, E. P., Vaughan, M. A., Rodier, S. D., & Hart, W. D. (2016). An overview of the CATS level 1 processing algorithms and data products. *Geophysical Research Letters, 43*, 4632–4639. https://doi.org/10.1002/2016GL068006

Aerosol Hygroscopicity

Cyrielle Denjean

Contents

Abstract The hygroscopic and ice nucleation properties play a vital role for the direct and indirect effects of aerosols on climate by determining the interactions of aerosol particles with atmospheric water vapour, ice and cloud microphysical processes. This chapter reviews the existing published results on the aerosol hygroscopic properties at subsaturated (relative humidity below 100%) and supersaturated (relative humidity above 100%) conditions, and on the ice nucleation properties of aerosols from measurements at multiple sites in the Mediterranean. Rapid progress has been made in the last 20 years in understanding how different chemical and physical properties affect the aerosol hygroscopic growth. Some early investigations have yielded comprehensive information regarding the main sources and chemical composition of the atmospheric cloud condensation nuclei (CCN) and ice-nucleating particles (INP) in the Mediterranean region. Despite these advances, process-level understanding of aerosol hygroscopic properties and related ice nucleation remains

*Chapter reviewed by **Heike Wex** (Leibniz Institute for Tropospheric Research, Leipzig, Germany) and **Claudia Di Biagio** (Laboratoire Interuniversitaire des Systèmes Atmosphériques, Créteil, France), as part of the book Part VII Mediterranean Aerosol Properties also reviewed by **Jorge Pey Betrán** (ARAID-Instituto Pirenaico de Ecología, CSIC, Zaragoza, Spain)*

C. Denjean (✉)
Centre National de Recherches Météorologiques (CNRM), Université de Toulouse, Météo France, CNRS, Toulouse, France
e-mail: cyrielle.denjean@meteo.fr

F. Dulac et al. (eds.), *Atmospheric Chemistry in the Mediterranean Region*,
https://doi.org/10.1007/978-3-030-82385-6_15

insufficient, causing unacceptably large uncertainties when simulating aerosol radiative effects in future climate projections.

1 Preamble and Definitions

The hygroscopic properties of aerosols determine the interactions between the aerosol particles and water vapour both at subsaturated (i.e. relative humidity (RH) <100%) and supersaturated (i.e. RH >100%) conditions. They determine their climatic impacts via the following physical mechanisms:

1. When water vapour is subsaturated, an aerosol particle in equilibrium with the surrounding environment can contain some amount of absorbed water. Aerosol water uptake changes the particle size and spectral optical properties with profound implications for the atmospheric radiative transfer. For example, at RH of 90%, the aerosol scattering cross section can increase by a factor of 5 compared to that of the dry particle if the diameter increases by a factor of 2.3 (Tang, 1996). Because of this, the water uptake of the aerosol is the most important contributor to direct radiative cooling by aerosols (Pilinis et al., 1995).
2. When water vapour is supersaturated, aerosol particles can act as cloud condensation nuclei (CCN) to form cloud droplets. Consequently, aerosols are a major player in the water cycle by possibly inducing changes in the cloud microphysical properties, precipitation patterns and cloud radiative effects (Lohmann & Feichter, 2005). This second physical mechanism is referred to as the aerosol indirect radiative effect.

Atmospheric particles can absorb water at relative humidity well below 100% depending on their chemical composition and their size. A large portion of hygroscopic particles in subsaturated conditions is usually related to inorganic species, such as ammonium nitrate, ammonium sulphate and sodium chloride, whose hygroscopic growth behaviour is known relatively accurately (Tang & Munkelwitz, 1994). In contrast, the understanding of the hygroscopic behaviour of organic aerosol is sparser, due to the myriad of individual species involved (Saxena & Hildemann, 1996). This lack of understanding has also hampered a better understanding of the role of organic aerosols on climate (Kanakidou et al., 2005). One way to explore the hygroscopic properties of aerosols at supersaturated conditions is to measure the so-called hygroscopic growth factor (GF), defined as the ratio of the particle diameter at a certain RH divided by its dry diameter. The most common instrument for measurements of GF is the hygroscopicity tandem differential mobility analyser (HTDMA; Swietlicki et al., 2008). It explores the GF of particles in the dry size range 20–260 nm and was employed successfully in most ground-based campaigns in the Mediterranean, as discussed below. The probability distribution of GF measured by the HTDMA is independent of the particle mixing state. Hygroscopic properties of aerosol particles are usually categorized according to the value of GF,

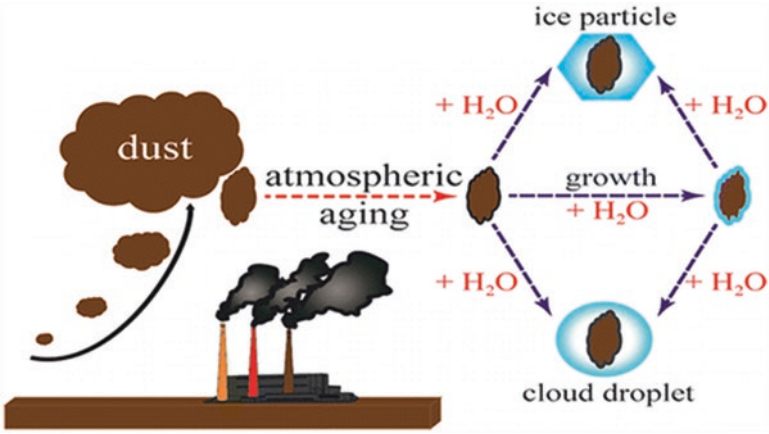

Fig. 1 Schematic diagram of mineral dust particles and water interactions. Reactions with reactive trace gases during transport can increase mineral dust hygroscopicity. (Reprinted with permission from Tang et al. (2016), © American Chemical Society)

typically at 90% RH, into hydrophobic particles (GF below 1.05), nearly hydrophobic particles (GF between 1.05 and 1.2), less hygroscopic particles (GF ranging between 1.2 and 1.4), moderately hygroscopic particles (GF in the range 1.4–1.6) and the most hygroscopic particles (GF > 1.7). For instance, sea salt particles are very hygroscopic with GF values larger than 2 (e.g. Zieger et al., 2017), and mineral dust particles are typically hydrophobic with GF values around 1 (e.g. Tang et al., 2016). However, atmospheric aging caused by reactions with trace gases and cloud processing during transport can enhance the hygroscopic growth of aerosol particles (see the review by Tang et al., 2016; Fig. 1). For a given type of multicomponent aerosol particles, the hygroscopic growth may be size dependent (Laskina et al., 2015).

CCNs constitute the direct microphysical link between aerosols and clouds. The ability of an aerosol particle to act as a CCN at a given supersaturation depends primarily on its size and secondarily on its chemical composition (Dusek et al., 2006). CCN are emitted directly to the atmosphere by a variety of natural and anthropogenic sources, in addition to which CCN can also be produced in the atmosphere by the growth of both primary and secondary aerosol particles (Andreae & Rosenfeld, 2008). Measurements of the CCN concentration are usually made using CCN counters at different supersaturations (SS) levels.

To obtain a comprehensive understanding of the contribution of different groups of aerosols to the overall aerosol hygroscopicity under sub- and supersaturated conditions, the hygroscopicity parameter κ was introduced by Petters and Kreidenweis (2007) as a single variable to account for chemical effects on aerosol water uptake at any humidity. The κ value can be calculated from either GF measured by an HTDMA, CCN concentration measured by a CCN counter or aerosol chemical composition measured by an aerosol mass spectrometer.

Ice-nucleating particles (INPs) act as a seed surface for water vapour and liquid water to enable the emergence and growth of ice crystals in the atmosphere. Despite their low abundance in the atmosphere, INPs are crucial for the evolution of ice in clouds (Pruppacher & Klett, 2010). Without their existence, the ice phase in clouds would solely arise from homogeneous ice nucleation at temperatures below about −38 °C. In the presence of INPs, water freezes at much higher temperatures by heterogeneous ice nucleation. The process of ice nucleation can occur by immersion, condensation, deposition or contact ice nucleation (Vali et al., 2015). Although the number of studies on INP properties for different kinds of aerosol particles has been continuously increasing in recent years, our knowledge about which physical and chemical properties favour the formation of ice on the surface of an aerosol particle is still very rudimentary. General requirements for INPs have been identified in Pruppacher and Klett (2010) but have more recently been revised (Kanji et al., 2017). Certain particle types are considered to be more efficient at nucleating ice in the atmosphere than others. Aerosols that can act as INP are mostly insoluble particles that often mimic ice lattice structure. Only a few aerosol types have this property including mineral dust, volcanic ash, and bioaerosols such as bacteria, fungal spores and pollen (Hoose & Möhler, 2012).

2 Hygroscopic Properties at Subsaturated Conditions

Over the last 20 years, field measurements have been dedicated to the study of the GF of aerosols at various sites in the Mediterranean, including polluted continental sites, background marine environments and high-altitude sites. Studied air masses were influenced by various sources, such as fresh and aged anthropogenic particles, marine particles, dust particles, aged biomass burning and their mixtures. Figure 2 shows the GF values classified as a function of the aerosol type for the different studies across the Mediterranean. Owing to the frequent observations of externally mixed aerosols (multi-modal probability distribution of GF), the data are presented as averages in order to provide an overview of particle hygroscopicity. Most data were acquired at 90% RH, but the reported RH was as low as 80% for some data sets. For comparison between observations, the average GF was recalculated at 90% RH using the *K*-Köhler theory introduced by Petters and Kreidenweis (2007).

Measurements of average GF in polluted continental environments (long dashed lines in Fig. 2) have been reported in the Po Valley (Adam et al., 2012; Bialek et al., 2014; Rosati et al., 2016) and the cities of Marseille in France and Athens in Greece (Petäjä et al., 2007). The GF varies greatly. Petäjä et al. (2007) reported an average GF of 1.3 and 1.45 for particles of 50-nm diameter at Marseille and Athens, respectively, suggesting differences in the average chemical composition between the two urban sites. In the Po Valley, the summertime aerosol at Ispra (Adam et al., 2012) seems to be slightly less hygroscopic than at San Pietro Capofiume (Rosati et al., 2016). Adam et al. (2012) found diurnal and seasonal variations in both the

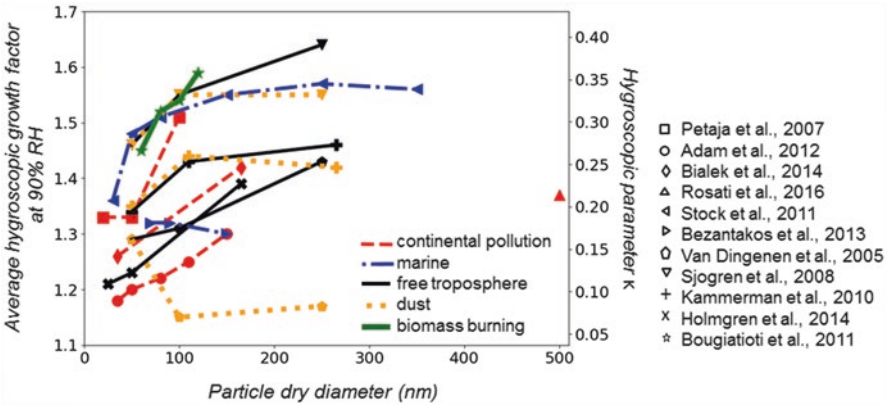

Fig. 2 Average growth factor as a function of particle dry diameter observed at various sites across the Mediterranean. Values from Sjogren et al. (2008), Bezantakos et al. (2013) and Rosati et al. (2016) have been converted at 90% RH using the *K*-Köhler theory (Petters & Kreidenweis, 2007). All measurements were performed using an HTDMA with the exception of Rosati et al. (2016) who used a white-light humidified optical particle spectrometer (WHOPS) to measure the growth factor of particles with a dry diameter of 500 nm

anthropogenic–natural and primary–secondary components, which can explain some of the variability in the average GF.

Although the variability in average GF values appears to be large, a consistent picture emerges when looking at the probability distribution of GF (not shown in Fig. 2). Overall, the various studies reported persistent externally mixed particles with at least two or sometimes three hygroscopic modes that can be classified as being nearly hydrophobic, less hygroscopic and more hygroscopic particles. The most hygroscopic fraction was predominantly the largest one and was attributed to an aged regional background aerosol. The various studies showed that the number fraction of the nearly hydrophobic and less hygroscopic particle groups decreases with size at all sites. These particles were assigned mainly to freshly emitted combustion particles, more specifically to vehicle emissions consisting of large mass fractions of black-carbon or containing some water-insoluble organic compounds. In addition, chemical composition measurements in the Po Valley feature the nitrate fraction as an important driver for the decrease of GF overnight (Bialek et al., 2014; Rosati et al., 2016).

Only two studies report on hygroscopic measurements in background marine environments (blue points in Fig. 2). These measurements were conducted in the region of the Aegean Sea at Finokalia, in Crete, from August to October 2005 (Stock et al., 2011), and during two flights from Crete to Lemnos in August and September 2011 (Bezantakos et al., 2013). Particles were mainly found in an internal mixing state, as a result of coagulation and condensation of gaseous species during a long atmospheric residence time (Heintzenberg, 1989). At Finokalia, the average GF was about 1.55 at 90% RH for 150 nm particles (Stock et al., 2011), which is within the broad range observed in oceanic areas (Swietlicki et al., 2008). By contrast, the average GF measured by Bezantakos et al. (2013) was significantly lower (average

GF of about 1.3 at 90% RH for 150-nm particles) and more representative of continental aerosol particles. This was attributed to the contribution of polluted air from Athens over the Aegean Sea. Values of average GF were negatively correlated with the concentration of particulate organic matter, which contributed almost 50% to the volume of the particles. The exact chemical nature of these organic particles that were either of biogenic or anthropogenic origin was not reported.

Air masses influenced by aged biomass burning originating from central eastern Europe (green points in Fig. 2) have been studied at Finokalia by Bougiatioti et al. (2011). The average GF values were among the highest reported over the Mediterranean with an average value of 1.6 at 90% RH. Bimodal hygroscopicity distributions, respectively classified as moderately hygroscopic and nearly hydrophobic, were observed during the arrival of the smoke plumes. The moderately hygroscopic mode was dominant in number for all sampled particles. Larger particle sizes exhibited higher hygroscopic growth and degree of mixing than smaller particles sizes, which was attributed to the effects of condensational growth and cloud processing. The number concentration of nearly hydrophobic mode exhibited considerable variability (up to 100% for particles of the same size) and coincided with the fraction of organic components in the sub-100 nm size. The fact that smaller particles were less mixed than larger particles suggests that the smaller particles were an external mixture of freshly emitted and secondarily formed particles.

Measurements of average GF in the free troposphere (FT) (black points in Fig. 2) have been reported at the high alpine research station Jungfraujoch in Switzerland (~3580 m a.s.l.; Weingartner et al., 2002; Sjogren et al., 2008; Kammermann et al., 2010), the Monte Cimone observatory in northern Italy (~2300 m asl.; Van Dingenen et al., 2005) and the Puy de Dôme in central France (~1465 m asl.; Holmgren et al., 2014). Although these sites are located in the lower FT, they can also be influenced by injections of more polluted atmospheric boundary layer (BL) air. At Jungfraujoch, field campaigns were conducted during summer and winter in the years 2000, 2002, 2004 and 2005 (Weingartner et al., 2002; Sjogren et al., 2008) and during a 13-month period in the years 2008 and 2009 (Kammermann et al., 2010). Aerosol hygroscopicity was independent of the season and of the synoptic wind direction during advective weather situations. From a climatology analysis, Kammermann et al. (2010) reported that the hygroscopic behaviour of the aerosol at Jungfraujoch can be considered representative of the lower FT, with limited influence of the BL. Moreover, they found that the annual average GF was independent to particle diameters (by considering the Kelvin effect). This suggests that a constant and size independent value of average GF (~1.5 at 90% RH) is a good approximation in models that need a simple description of the Aitken and accumulation mode aerosol at the Jungfraujoch site. The Monte Cimone and Puy de Dôme sites are located in the transition zone between the BL and the FT. As for the Jungfraujoch site, the majority of particles measured were found to be moderately hygroscopic. However, the observed hygroscopic behaviour of the aerosol was strongly dependent on the air mass origin and history at both sites. Injections of BL air in the FT lead to a decrease in average GF, attributed to a higher contribution of hydrophobic black carbon and/or organic particles in the accumulation mode.

Finally, the impact of Saharan dust events on average GF has been studied at these FT sites (orange points in Fig. 2). Van Dingenen et al. (2005), Sjogren et al. (2008), and Kammermann et al. (2010) reported that the accumulation mode (represented by 100 and 250 nm particles) during dust events displayed a high degree of external mixing with an increase of nearly hydrophobic particles. The average GF of larger particles were obtained in the western (Granados-Muñoz et al., 2015) and eastern (Tutsak & Koçak, 2019) Mediterranean by using a newly developed methodology based on combining active and passive remote sensing and collocated radiosounding data. These studies showed that a substantial fraction of particles was nearly hydrophobic when mineral dust dominated the aerosol population. Most of the non-hygroscopic dust particles were observed in spring and altered significantly the RH dependence of integral optical properties of aerosol (Tutsak & Koçak, 2019).

Table 1 CCN concentrations and κ-derived values observed at various sites across the Mediterranean at 0.2% supersaturation

Location	Site category	Period	Mean CCN concentration at 0.2% SS (cm^{-3})	Mean κ	References
Finokalia, Crete Isl.	Coastal background	Sept.–Oct. 2007	1321	0.25[a]	Bougiatioti et al. (2009)
		July–Aug. 2007	1373	0.22[b]	Bougiatioti et al. (2011)
		Nov. 2014–Sep. 2015	340	0.46[a]	Schmale et al. (2018)
		June 2008–May 2015	–	0.36[a]	Kalkavouras et al. (2019)
	Biomass burning influence	Aug.–Sep. 2012	–	0.2–0.3[b]	Bougiatioti et al. (2016)
Cyprus	Continental pollution	2–30 April 2017	1065	0.49[b]	Gong et al. (2019)
Jungfraujoch, Swiss Alps	Mountain background	May 2008–Sep. 2009	94.7	0.23[b]	Jurányi et al. (2011)
		Jan. 2012–Dec. 2014	152	0.39[a]	Schmale et al. (2018)
Puy de Dôme, France		Nov. 2014–Sep. 2015	312	–	

[a]Derived from the measurements of aerosol chemical composition data
[b]Derived from the measurements of CCN concentration at 0.2% supersaturation (SS) and the aerosol number size distribution

3 Hygroscopic Properties at Supersaturated Conditions

As shown in Table 1, measurements of the CCN concentration were performed in the marine location of Finokalia in the eastern Mediterranean (Bougiatioti et al., 2009, 2011, 2016; Kalivitis et al., 2015; Schmale et al., 2018; Kalkavouras et al., 2019), the continental polluted area of Cyprus (Gong et al., 2019) and the high-altitude sites of Jungfraujoch (Jurányi et al., 2011) and Puy de Dôme (Schmale et al., 2018).

Long-term observations explored the frequency and seasonal cycles of CCN number concentration at regionally representative sites, while some observations focused on relatively short time periods to capture specific circumstances and in particular new particle formation (NPF) or biomass-burning events. Schmale et al. (2018) found that the CCN number concentrations varied considerably with region, across site categories and also seasonally within one measurement station. The lowest CCN concentrations were observed at the mountain sites Jungfraujoch and Puy de Dôme, with almost no observation higher than 1000 cm^{-3}. This is expected as they represent FT and continental background conditions, as discussed in the previous section. Higher CCN concentrations (between 200 and 2000 cm^{-3} at a supersaturation of 0.2%) were found in the marine environment of Finokalia due to particular pollution influences, which, for example, include long-range transport of N-E European pollution and biomass-burning events in summer. During an intensive measurement campaign at Cyprus, Gong et al. (2019) found even higher values of CCN concentrations up to 3730 cm^{-3} at a supersaturation of 0.3%. Strong seasonal cycles of CCN number concentrations were reported at the different sites, most strongly at the FT sites Puy de Dôme and Jungfraujoch due to BL air masses uplifted in summer (Schmale et al., 2018). A similar seasonal cycle exists, although less pronounced, at the marine site of Finokalia, characterized by pollution events occurring in summer.

Large-scale modelling studies suggest that a significant fraction of CCN in the global atmosphere originates from NPF (Spracklen et al., 2006; Makkonen et al., 2012; Dunne et al., 2016; Gordon et al., 2017). Although initially too small (1–2 nm; Kerminen et al., 2012) to act as CCN, particles from NPF may grow to sufficient size and hygroscopicity over a period of a few hours to days and eventually act as efficient CCN. According to our current understanding, molecular cluster formation appears to take place almost everywhere and all the time in the atmosphere, whereas the formation of growing nanoparticles to CCN sizes requires more specific atmospheric conditions (Kulmala et al., 2014). Atmospheric observations in the Mediterranean region support the current view, obtained from large-scale model simulations, that atmospheric NPF is an important source of CCN. Evidence for substantial local enhancement in CCN number from NPF have been reported at the coastal site of Finokalia (Bougiatioti et al., 2011, 2016; Kalivitis et al., 2015; Kalkavouras et al., 2017, 2019; Schmale et al., 2018) and at the continental polluted site in Cyprus (Gong et al., 2019). At Finokalia, Kalkavouras et al. (2019) found from 7 years of continuous aerosol measurements that the average contribution of

NPF to the CCN budget varied from 29% to 77% in the 0.1% to 1% supersaturation range. This phenomenon appears to be sporadic in nature and requires specific conditions to occur like a minimum concentration of pre-existing aerosol particles. As a result, the frequency of enhancement in CCN number from NPF varies over the course of a year, since most of the variables influencing NPF and particle growth have a pronounced seasonal variation. The active period for CCN associated with NPF tends to be the afternoon in summertime (Kalkavouras et al., 2019) and was partly attributed to either marine emissions (Kalivitis et al., 2015) or anthropogenic emissions transported from central eastern Europe (Bougiatioti et al., 2011).

The CCN properties of air masses influenced by biomass-burning events have been studied at the Finokalia site by Bougiatioti et al. (2016). They found a direct influence of fire events on the total CCN concentration across all particle sizes, with an enhancement of CCN concentrations by a factor from 1.6 to 2.5 compared to background conditions. Particle sizes larger than 100 nm exhibited an increase in CCN number of more than 50% and up to 30% for particles in the 60–80 nm range compared to background conditions. This clearly suggested a size-dependent chemical composition of particles.

Overall it seems that at the different sites investigated, the mixing between anthropogenic and natural (marine) sources leads to a complex behaviour of particle activation. The composition-derived κ values suggest that sulphate play important roles in growing nucleated particles to CCN sizes at Finokalia and Cyprus during summertime (Kalivitis et al., 2015; Kalkavouras et al., 2017; Gong et al., 2019). However, increased organic particle mass is observed during the biomass burning season at Finokalia with 40% mass contribution when κ reaches a minimum (Bougiatioti et al., 2016). At the alpine site of Jungfraujoch, the influence of organic matter (up to 70% mass contribution) becomes most important in summer because of BL air mass uplift, and again the impact on the calculated κ is evident (Jurányi et al., 2011; Schmale et al., 2018).

4 Ice Nuclei Particles

Ground-based observations in the Mediterranean have generally identified an increase in INP concentration in the presence of mineral dust (Santachiara et al., 2010; Belosi et al., 2017), with up to a twofold increase compared to dust-free conditions (Levi & Rosenfeld, 1996; Ardon-Dryer & Levin, 2014; Rinaldi et al., 2017). Based on unmanned aerial vehicle (UAV) measurements over Cyprus, Schrod et al. (2017) found an increase in the INP concentration by a factor 10 in elevated plumes compared to ground level due to Sahara dust layers travelling at several kilometres in altitude. This suggests that mineral dust particles can remain ice-active even after long transport in the atmosphere and thus over considerable distances, making them a major contributor to the ice-nucleating properties of the aerosol in the Mediterranean region. Excluding situations characterized by transport of dust plumes, Rinaldi et al. (2017) found that INP concentration at a measurement station in the Po valley basin was roughly double that of what they observed at the Apennine mountain of Monte

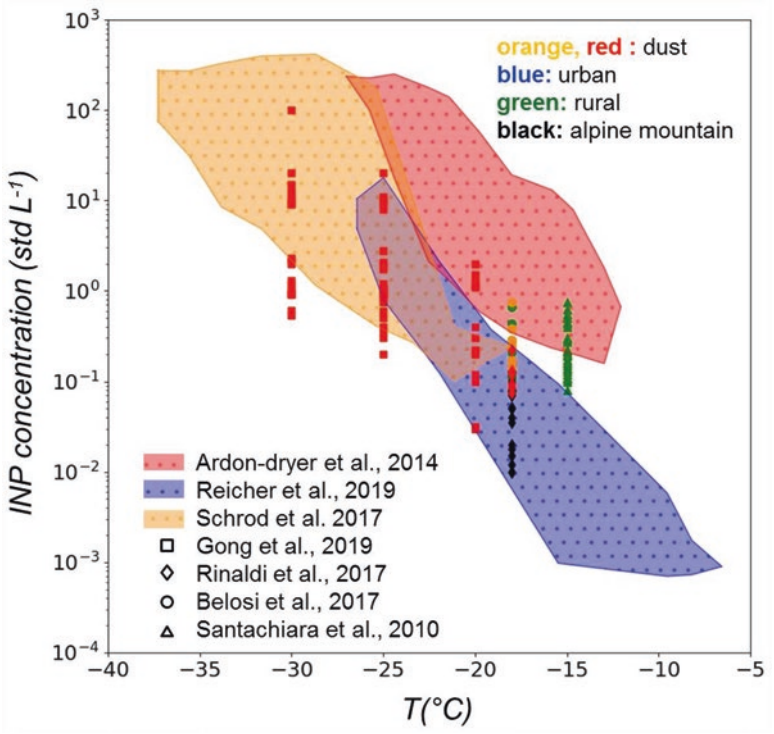

Fig. 3 Summary of INP concentrations taken from field measurements conducted in the Mediterranean

Cimone. Gong et al. (2019) observed elevated concentrations of INP at temperature $T \geq -18$ °C on the anthropogenically polluted island of Cyprus. Specifically, INP concentration spanned about 1 order of magnitude below −20 °C and about 2 orders of magnitude at the warmer temperatures ($T \geq 18$ °C), without correlation to the surface area concentration of the total aerosol. INP at the lower temperatures were likely dust particles, while the larger concentration range observed at higher temperatures may be due to varying concentrations of biological particles.

Figure 3 shows a summary of INP concentrations as a function of the temperature taken from field measurements conducted in the Mediterranean. Measurements are classified based on aerosol types. A general observation that has already been made early on (as described in Kanji et al., 2017) is roughly an exponential increase in INP concentrations with decreasing temperature. However, at a given temperature, the spread in observed INP concentrations in dust plumes is of several orders of magnitude, suggesting that a parameterization based on a simple exponential fit does not describe the observations. Parameterizations of ice formation in climate models are often based on the freezing properties of surface natural or standard dust (Niemand et al., 2012), which have been shown to overestimate the activity of airborne dust (Reicher et al., 2019) and anthropogenic polluted aerosol (Gong et al.,

2019) in the eastern Mediterranean. Though the exact properties of dust particles that determine their ice nucleation ability are not known, it was consistently shown that the mineral composition plays an important role (Atkinson et al., 2013; Kanji et al., 2017). Recently, Reicher et al. (2019) corroborated that the INP activity of particles collected during several mineral dust events in Israel is size dependent. The size dependence of ice nucleation, which for dust particles is typically seen as a relation between ice activity and surface area, has already been shown in laboratory studies for different dusts (e.g. Niedermeier et al., 2015; Hartmann et al., 2016). Reicher et al. (2019) further suggested that the freezing activity of dust particles is dominated by feldspar and quartz for the supermicron- and submicron-sized particles, respectively. Given that the dust size distribution evolves during transport in the atmosphere due to deposition processes of the largest particles (Mahowald et al., 2014), accounting for a time-dependent particle size for the dust fraction of the aerosol and for a dust mineralogy using a two-moment scheme could improve the prediction of ice clouds formation. Regarding dust-free environments, observations highlight the importance of developing new parameterizations including biological INP to be incorporated in climate models (Gong et al., 2019).

5 Summary and Challenges for Future Research

Most ambient measurements of aerosol hygroscopic properties were conducted at the ground level in the Mediterranean. However, surface measurements are not always representative for aerosol properties at elevated altitudes. Previous airborne studies showed that aerosol chemical composition can vary with height over the Mediterranean basin (Formenti et al., 2002; Dulac & Chazette, 2003; Di Biagio et al., 2015; Denjean et al., 2016). Accordingly, aerosol hygroscopicity, which depends on chemical composition, is also expected to be height dependent. New airborne studies that allow direct measurements or aerosol hygroscopicity at high altitudes can be very valuable.

While CCN measurements can provide useful information about the origin of CCN particles in the atmosphere and their activation rate into cloud droplets, the missing link in the aerosol–cloud interactions is the connection of CCN concentrations to the ambient cloud droplet number concentration (CDNC). The latter distinction is important, given that CDNC exhibits a sublinear response to aerosol increases, owing to the elevated competition for water vapour and reduction in cloud supersaturation (Nenes et al., 2001; Ramanathan et al., 2001). However, very few studies actually go beyond CCN measurements to calculations of CDNC in the Mediterranean, and particularly, to our knowledge, no study has compared CCN concentrations to direct CDNC measurements. Kalkavouras et al. (2017, 2019) reported much higher CCN number enhancement (87%) at two marine sites in the eastern Mediterranean (namely, Santorini and Finokalia) than in CDNC (12%) during NPF episodes in summer. Similarly, Bougiatioti et al. (2016) found that biomass burning increases droplet number only by 8.5% although strongly elevating CCN

concentrations. The reason for this discrepancy is due in part to the different supersaturations used to quantify CCN enhancement (0.2%, 0.4%, 0.6% and 0.8%) compared to values used to compute CDNC (ranging from 0.03% to 0.27%) and also because supersaturation drops due to increasing CCN concentrations because of water vapour competition effects during the process of droplet formation. These issues are important, because a misrepresentation of CDNC would result in precipitation underestimation at locations with shallow cloud formation, as precipitation efficiency in shallow convection is reduced with increasing CDNC (Andreae & Rosenfeld, 2008). If filled, this gap could greatly improve our understanding of the processes and feedbacks within the aerosol–cloud–climate interactions and enhance the performance and accuracy of climate models in the Mediterranean region (see also the chapter by Nabat et al., 2022).

During the last decade, significant progress in INP measurements has been made in the Mediterranean. Studies show that the lower tropospheric INP population is composed of mineral dust and carbonaceous particles of biological origins. However, the INP ability of different types of particles and the extent to which anthropogenic aerosols can play a role in cloud ice formation are still open questions. It still remains largely unclear, and it is crucial to assess the abundance, variability and nature of INPs, both in continental and marine environments. Insufficient understanding of ice production is limiting our ability to quantify aerosol effects on ice crystal concentrations and subsequent cloud properties. In particular, attention should focus on anthropogenic perturbations to these relationships and the implications for climate forcing.

References

Adam, M., Putaud, J. P., Martins dos Santos, S., Dell'Acqua, A., & Gruening, C. (2012). Aerosol hygroscopicity at a regional background site (Ispra) in Northern Italy. *Atmospheric Chemistry and Physics, 12*, 5703–5717. https://doi.org/10.5194/acp-12-5703-2012

Andreae, M. O., & Rosenfeld, D. (2008). Aerosol-cloud-precipitation interactions. Part 1. The nature and sources of cloud-active aerosols. *Earth-Science Reviews, 89*, 13–41. https://doi.org/10.1016/j.earscirev.2008.03.001

Ardon-Dryer, K., & Levin, Z. (2014). Ground-based measurements of immersion freezing in the eastern Mediterranean. *Atmospheric Chemistry and Physics, 14*, 5217–5231. https://doi.org/10.5194/acp-14-5217-2014

Atkinson, J., Murray, B. J., Woodhouse, M. T., Whale, T. F., Baustian, K. J., Carslaw, K. S., Dobbie, S., O'Sullivan, D., & Malkin, T. L. (2013). The importance of feldspar for ice nucleation by mineral dust in mixed-phase clouds. *Nature, 498*, 355–358. https://doi.org/10.1038/nature12278

Belosi, F., Rinaldi, M., Decesari, S., Tarozzi, L., Nicosia, A., & Santachiara, G. (2017). Ground level ice nuclei particle measurements including Saharan dust events at a Po Valley rural site (San Pietro Capofiume, Italy). *Atmospheric Research, 186*, 116–126. https://doi.org/10.1016/j.atmosres.2016.11.012

Bezantakos, S., Barmpounis, K., Giamarelou, M., Bossioli, E., Tombrou, M., Mihalopoulos, N., Eleftheriadis, K., Kalogiros, J., Allan, J. D., Bacak, A., Percival, C. J., Coe, H., & Biskos, G. (2013). Chemical composition and hygroscopic properties of aerosol particles over the

Aegean Sea. *Atmospheric Chemistry and Physics, 13*, 11595–11608. https://doi.org/10.5194/acp-13-11595-2013

Bialek, J., Dall Osto, M., Vaattovaara, P., Decesari, S., Ovadnevaite, J., Laaksonen, A., & O'Dowd, C. (2014). Hygroscopic and chemical characterisation of Po Valley aerosol. *Atmospheric Chemistry and Physics, 14*, 1557–1570. https://doi.org/10.5194/acp-14-1557-2014

Bougiatioti, A., Fountoukis, C., Kalivitis, N., Pandis, S. N., Nenes, A., & Mihalopoulos, N. (2009). Cloud condensation nuclei measurements in the marine boundary layer of the Eastern Mediterranean: CCN closure and droplet growth kinetics. *Atmospheric Chemistry and Physics, 9*, 7053–7066. https://doi.org/10.5194/acp-9-7053-2009

Bougiatioti, A., Nenes, A., Fountoukis, C., Kalivitis, N., Pandis, S. N., & Mihalopoulos, N. (2011). Size-resolved CCN distributions and activation kinetics of aged continental and marine aerosol. *Atmospheric Chemistry and Physics, 11*, 8791–8808. https://doi.org/10.5194/acp-11-8791-2011

Bougiatioti, A., Bezantakos, S., Stavroulas, I., Kalivitis, N., Kokkalis, P., Biskos, G., Mihalopoulos, N., Papayannis, A., & Nenes, A. (2016). Biomass-burning impact on CCN number, hygroscopicity and cloud formation during summertime in the eastern Mediterranean. *Atmospheric Chemistry and Physics, 16*, 7389–7409. https://doi.org/10.5194/acp-16-7389-2016

Denjean, C., Cassola, F., Mazzino, A., Triquet, S., Chevaillier, S., Grand, N., Bourrianne, T., Momboisse, G., Sellegri, K., Schwarzenbock, A., Freney, E., Mallet, M., & Formenti, P. (2016). Size distribution and optical properties of mineral dust aerosols transported in the western Mediterranean. *Atmospheric Chemistry and Physics, 16*, 1081–1104. https://doi.org/10.5194/acp-16-1081-2016

Di Biagio, C., Doppler, L., Gaimoz, C., Grand, N., Ancellet, G., Raut, J.-C., Beekmann, M., Borbon, A., Sartelet, K., Attié, J.-L., Ravetta, F., & Formenti, P. (2015). Continental pollution in the western Mediterranean basin: Vertical profiles of aerosol and trace gases measured over the sea during TRAQA 2012 and SAFMED 2013. *Atmospheric Chemistry and Physics, 15*, 9611–9630. https://doi.org/10.5194/acp-15-9611-2015

Dulac, F., & Chazette, P. (2003). Airborne study of a multi-layer aerosol structure in the eastern Mediterranean observed with the airborne polarized lidar ALEX during a STAAARTE campaign (7 June 1997). *Atmospheric Chemistry and Physics, 3*, 1817–1831. https://doi.org/10.5194/acp-3-1817-2003

Dunne, E. M., Gordon, H., Kürten, A., Almeida, J., Duplissy, J., Williamson, C., Ortega, I. K., Pringle, K. J., Adamov, A., Baltensperger, U., Barmet, P., Benduhn, F., Bianchi, F., Breitenlechner, M., Clarke, A., Curtius, J., Dommen, J., Donahue, N. M., Ehrhart, S., … Carslaw, K. S. (2016). Global atmospheric particle formation from CERN CLOUD measurements. *Science, 354*, 1119–1124. https://doi.org/10.1126/science.aaf2649

Dusek, U., Reischl, G. P., & Hitzenberg, R. (2006). CCN activation of pure and coated carbon black particles. *Environmental Science & Technology, 40*, 1223–1230. https://doi.org/10.1021/es0503478

Formenti, P., Reiner, T., Sprung, D., Andreae, M. O., Wendisch, M., Wex, H., Kindred, D., Dewey, K., Kent, J., Tzortziou, M., Vasaras, A., & Zerefos, C. (2002). STAAARTE-MED 1998 summer airborne measurements over the Aegean Sea 1. Aerosol particles and trace gases. *Journal of Geophysical Research, 107*, 4450. https://doi.org/10.1029/2001JD001337

Gong, X., Wex, H., Müller, T., Wiedensohler, A., Höhler, K., Kandler, K., Ma, N., Dietel, B., Schiebel, T., Möhler, O., & Stratmann, F. (2019). Characterization of aerosol properties at Cyprus, focusing on cloud condensation nuclei and ice-nucleating particles. *Atmospheric Chemistry and Physics, 19*, 10883–10900. https://doi.org/10.5194/acp-19-10883-2019

Gordon, H., Kirkby, J., Baltensperger, U., Bianchi, F., Breitenlechner, M., Curtius, J., Dias, A., Dommen, J., Donahue, N. M., Dunne, E. M., Duplissy, J., Ehrhart, S., Flagan, R. C., Frege, C., Fuchs, C., Hansel, A., Hoyle, C. R., Kulmala, M., Kürten, A., … Carslaw, K. S. (2017). Causes and importance of new particle formation in the present-day and preindustrial atmospheres. *Journal of Geophysical Research – Atmospheres, 122*, 8739–8760. https://doi.org/10.1002/2017JD026844

Granados-Muñoz, M. J., Navas-Guzmán, F., Bravo-Aranda, J. A., Guerrero-Rascado, J. L., Lyamani, H., Valenzuela, A., Titos, G., Fernández-Gálvez, J., & Alados-Arboledas, L. (2015). Hygroscopic growth of atmospheric aerosol particles based on active remote sensing and radiosounding measurements: Selected cases in southeastern Spain. *Atmospheric Measurement Techniques, 8*, 705–718. https://doi.org/10.5194/amt-8-705-2015

Hartmann, S., Wex, H., Clauss, T., Augustin-Bauditz, S., Niedermeier, D., Rösch, M., & Stratmann, F. (2016). Immersion freezing of kaolinite - scaling with particle surface area. *Journal of the Atmospheric Sciences, 73*, 263–278. https://doi.org/10.1175/JAS-D-15-0057.1

Heintzenberg, J. (1989). Fine particles in the global troposphere a review. *Tellus B: Chemical and Physical Meteorology, 41*, 149–160. https://doi.org/10.3402/tellusb.v41i2.15064

Holmgren, H., Sellegri, K., Hervo, M., Rose, C., Freney, E., Villani, P., & Laj, P. (2014). Hygroscopic properties and mixing state of aerosol measured at the high-altitude site Puy de Dôme (1465 m a.s.l.), France. *Atmospheric Chemistry and Physics, 14*, 9537–9554. https://doi.org/10.5194/acp-14-9537-2014

Hoose, C., & Möhler, O. (2012). Heterogeneous ice nucleation on atmospheric aerosols: A review of results from laboratory experiments. *Atmospheric Chemistry and Physics, 12*, 9817–9854. https://doi.org/10.5194/acp-12-9817-2012

Jurányi, Z., Gysel, M., Weingartner, E., Bukowiecki, N., Kammermann, L., & Baltensperger, U. (2011). A 17 month climatology of the cloud condensation nuclei number concentration at the high alpine site Jungfraujoch. *Journal of Geophysical Research, 116*, D10204. https://doi.org/10.1029/2010JD015199

Kalivitis, N., Kerminen, V.-M., Kouvarakis, G., Stavroulas, I., Bougiatioti, A., Nenes, A., Manninen, H. E., Petäjä, T., Kulmala, M., & Mihalopoulos, N. (2015). Atmospheric new particle formation as a source of CCN in the eastern Mediterranean marine boundary layer. *Atmospheric Chemistry and Physics, 15*, 9203–9215. https://doi.org/10.5194/acp-15-9203-2015

Kalkavouras, P., Bossioli, E., Bezantakos, S., Bougiatioti, A., Kalivitis, N., Stavroulas, I., Kouvarakis, G., Protonotariou, A. P., Dandou, A., Biskos, G., Mihalopoulos, N., Nenes, A., & Tombrou, M. (2017). New particle formation in the southern Aegean Sea during the Etesians: Importance for CCN production and cloud droplet number. *Atmospheric Chemistry and Physics, 17*, 175–192. https://doi.org/10.5194/acp-17-175-2017

Kalkavouras, P., Bougiatioti, A., Kalivitis, N., Stavroulas, I., Tombrou, M., Nenes, A., & Mihalopoulos, N. (2019). Regional new particle formation as modulators of cloud condensation nuclei and cloud droplet number in the eastern Mediterranean. *Atmospheric Chemistry and Physics, 19*, 6185–6203. https://doi.org/10.5194/acp-19-6185-2019

Kammermann, L., Gysel, M., Weingartner, E., & Baltensperger, U. (2010). 13-month climatology of the aerosol hygroscopicity at the free tropospheric site Jungfraujoch (3580 m a.s.l.). *Atmospheric Chemistry and Physics, 10*, 10717–10732. https://doi.org/10.5194/acp-10-10717-2010

Kanakidou, M., Seinfeld, J. H., Pandis, S. N., Barnes, I., Dentener, F. J., Facchini, M. C., Van Dingenen, R., Ervens, B., Nenes, A., Nielsen, C. J., Swietlicki, E., Putaud, J. P., Balkanski, Y., Fuzzi, S., Horth, J., Moortgat, G. K., Winterhalter, R., Myhre, C. E. L., Tsigaridis, K., … Wilson, J. (2005). Organic aerosol and global climate modelling: A review. *Atmospheric Chemistry and Physics, 5*, 1053–1123. https://doi.org/10.5194/acp-5-1053-2005

Kanji, Z. A., Ladino, L. A., Wex, H., Boose, Y., Burkert-Kohn, M., Cziczo, D. J., & Krämer, M. (2017). Overview of ice nucleating particles. *Meteorological Monographs, 58*, 1.1–1.33. https://doi.org/10.1175/AMSMONOGRAPHS-D-16-0006.1

Kerminen, V.-M., Paramonov, M., Anttila, T., Riipinen, I., Fountoukis, C., Korhonen, H., Asmi, E., Laakso, L., Lihavainen, H., Swietlicki, E., Svenningsson, B., Asmi, A., Pandis, S. N., Kulmala, M., & Petäjä, T. (2012). Cloud condensation nuclei production associated with atmospheric nucleation: A synthesis based on existing literature and new results. *Atmospheric Chemistry and Physics, 12*, 12037–12059. https://doi.org/10.5194/acp-12-12037-2012

Kulmala, M., Petäjä, T., Ehn, M., Thornton, J., Sipilä, M., Worsnop, D. R., & Kerminen, V.-M. (2014). Chemistry of atmospheric nucleation: On the recent advances on precursor

characterization and atmospheric cluster composition in connection with atmospheric new particle formation. *Annual Review of Physical Chemistry, 65*, 21–37. https://doi.org/10.1146/annurev-physchem-040412-110014

Laskina, O., Morris, H. S., Grandquist, J. R., Qin, Z., Stone, E. A., Tivanski, A. V., & Grassian, V. H. (2015). Size matters in the water uptake and hygroscopic growth of atmospherically relevant multicomponent aerosol particles. *The Journal of Physical Chemistry. A, 119*, 4489–4497. https://doi.org/10.1021/jp510268p

Levi, Y., & Rosenfeld, D. (1996). Ice nuclei, rainwater chemical composition, and static cloud seeding effects in Israel. *Journal of Applied Meteorology, 35*, 1494–1501. https://doi.org/10.1175/1520-0450(1996)035<1494:INRCCA>2.0.CO;2

Lohmann, U., & Feichter, J. (2005). Global indirect aerosol effects: A review. *Atmospheric Chemistry and Physics, 5*, 715–737. https://doi.org/10.5194/acp-5-715-2005

Mahowald, N., Albani, S., Kok, J., Engelstaeder, S., Scanza, R., Ward, G., & Flanner, M. (2014). The size distribution of desert dust aerosols and its impact on the Earth system. *Aeolian Research, 15*, 53–71. https://doi.org/10.1016/j.aeolia.2013.09.002

Makkonen, R., Asmi, A., Kerminen, V.-M., Boy, M., Arneth, A., Guenther, A., & Kulmala, M. (2012). BVOC-aerosol-climate interactions in the global aerosol-climate model ECHAM5.5-HAM2. *Atmospheric Chemistry and Physics, 12*, 10077–10096. https://doi.org/10.5194/acp-12-10077-2012

Nabat, P., Kanji, Z. A., Mallet, M., Denjean, C., & Solmon, F. (2022). Aerosol-cloud interactions and impact on regional climate. In F. Dulac, S. Sauvage, & E. Hamonou (Eds.), *Atmospheric chemistry in the Mediterranean Region* (Vol. 2, From air pollutant sources to impacts). Springer, this volume. https://doi.org/10.1007/978-3-030-82385-6_20

Nenes, A., Ghan, S., Abdul-Razzak, H., Chuang, P. Y., & Seinfeld, J. H. (2001). Kinetic limitations on cloud droplet formation and impact on cloud albedo. *Tellus B: Chemical and Physical Meteorology, 53*, 133–149. https://doi.org/10.1034/j.1600-0889.2001.d01-12.x

Niedermeier, D., Augustin-Bauditz, S., Hartmann, S., Wex, H., Ignatius, K., & Stratmann, F. (2015). Can we define an asymptotic value for the ice active surface site density for heterogeneous ice nucleation? *Journal of Geophysical Research, 120*, 5036–5046. https://doi.org/10.1002/2014JD022814

Niemand, M., Möhler, O., Vogel, B., Vogel, H., Hoose, C., Connolly, P., Klein, H., Bingemer, H., DeMott, P., Skrotzki, J., & Leisner, T. (2012). A particle-surface-area-based parameterization of immersion freezing on desert dust particles. *Journal of the Atmospheric Sciences, 69*, 3077–3092. https://doi.org/10.1175/JAS-D-11-0249.1

Petäjä, T., Kerminen, V.-M., Dal Maso, M., Junninen, H., Koponen, I. K., Hussein, T., Aalto, P. P., Andronopoulos, S., Robin, D., Hämeri, K., Bartzis, J. G., & Kulmala, M. (2007). Sub-micron atmospheric aerosols in the surroundings of Marseille and Athens: Physical characterization and new particle formation. *Atmospheric Chemistry and Physics, 7*, 2705–2720. https://doi.org/10.5194/acp-7-2705-2007

Petters, M. D., & Kreidenweis, S. M. (2007). A single parameter representation of hygroscopic growth and cloud condensation nucleus activity. *Atmospheric Chemistry and Physics, 7*, 1961–1971. https://doi.org/10.5194/acp-7-1961-2007

Pilinis, C., Pandis, S. N., & Seinfeld, J. H. (1995). Sensitivity of a direct climate forcing by atmospheric aerosols to aerosol size and composition. *Journal of Geophysical Research, 100*, 18739–18754. https://doi.org/10.1029/95JD02119

Pruppacher, H. R., & Klett, J. D. (2010). *Microphysics of Clouds and Precipitation*. Springer, Dordrecht, XXII+954 pp. https://doi.org/10.1007/978-0-306-48100-0

Ramanathan, V., Crutzen, P. J., Kiehl, J. T., & Rosenfeld, D. (2001). Aerosols, climate and the hydrological cycle. *Science, 294*, 2119–2124. https://doi.org/10.1126/science.1064034

Reicher, N., Budke, C., Eickhoff, L., Raveh-Rubin, S., Kaplan-Ashiri, I., Koop, T., & Rudich, Y. (2019). Size-dependent ice nucleation by airborne particles during dust events in the eastern Mediterranean. *Atmospheric Chemistry and Physics, 19*, 11143–11158. https://doi.org/10.5194/acp-19-11143-2019

Rinaldi, M., Santachiara, G., Nicosia, A., Piazza, M., Decesari, S., Gilardoni, S., Paglione, M., Cristofanelli, P., Marinoni, A., Bonasoni, P., & Belosi, F. (2017). Atmospheric Ice Nucleating Particle measurements at the high mountain observatory Mt. Cimone (2165 m a.s.l., Italy). *Atmospheric Environment, 171*, 173–180. https://doi.org/10.1016/j.atmosenv.2017.10.027

Rosati, B., Gysel, M., Rubach, F., Mentel, T. F., Goger, B., Poulain, L., Schlag, P., Miettinen, P., Pajunoja, A., Virtanen, A., Klein Baltink, H., Henzing, J. S. B., Größ, J., Gobbi, G. P., Wiedensohler, A., Kiendler-Scharr, A., Decesari, S., Facchini, M. C., Weingartner, E., & Baltensperger, U. (2016). Vertical profiling of aerosol hygroscopic properties in the planetary boundary layer during the PEGASOS campaigns. *Atmospheric Chemistry and Physics, 16*, 7295–7315. https://doi.org/10.5194/acp-16-7295-2016

Santachiara, G., Di Matteo, L., Prodi, F., & Belosi, F. (2010). Atmospheric particles acting as Ice Forming Nuclei in different size ranges. *Atmospheric Research, 96*, 266–272. https://doi.org/10.1016/j.atmosres.2009.08.004

Saxena, P., & Hildemann, L. (1996). Water-soluble organics in atmospheric particles: A critical review of the literature and application of thermodynamics to identify candidate compounds. *Journal of Atmospheric Chemistry, 24*, 57–109. https://doi.org/10.1007/BF00053823

Schmale, J., Henning, S., Decesari, S., Henzing, B., Keskinen, H., Sellegri, K., Ovadnevaite, J., Pöhlker, M. L., Brito, J., Bougiatioti, A., Kristensson, A., Kalivitis, N., Stavroulas, I., Carbone, S., Jefferson, A., Park, M., Schlag, P., Iwamoto, Y., Aalto, P., … Gysel, M. (2018). Long-term cloud condensation nuclei number concentration, particle number size distribution and chemical composition measurements at regionally representative observatories. *Atmospheric Chemistry and Physics, 18*, 2853–2881. https://doi.org/10.5194/acp-18-2853-2018

Schrod, J., Weber, D., Drücke, J., Keleshis, C., Pikridas, M., Ebert, M., Cvetković, B., Nickovic, S., Marinou, E., Baars, H., Ansmann, A., Vrekoussis, M., Mihalopoulos, N., Sciare, J., Curtius, J., & Bingemer, H. G. (2017). Ice nucleating particles over the Eastern Mediterranean measured by unmanned aircraft systems. *Atmospheric Chemistry and Physics, 17*, 4817–4835. https://doi.org/10.5194/acp-17-4817-2017

Sjogren, S., Gysel, M., Weingartner, E., Alfarra, M. R., Duplissy, J., Cozic, J., Crosier, J., Coe, H., & Baltensperger, U. (2008). Hygroscopicity of the submicrometer aerosol at the high-alpine site Jungfraujoch, 3580 m a.s.l., Switzerland. *Atmospheric Chemistry and Physics, 8*, 5715–5729. https://doi.org/10.5194/acp-8-5715-2008

Spracklen, D. V., Carslaw, K. S., Kulmala, M., Kerminen, V.-M., Mann, G. W., & Sihto, S.-L. (2006). The contribution of boundary layer nucleation events to total particle concentrations on regional and global scales. *Atmospheric Chemistry and Physics, 6*, 5631–5648. https://doi.org/10.5194/acp-6-5631-2006

Stock, M., Cheng, Y. F., Birmili, W., Massling, A., Wehner, B., Müller, T., Leinert, S., Kalivitis, N., Mihalopoulos, N., & Wiedensohler, A. (2011). Hygroscopic properties of atmospheric aerosol particles over the Eastern Mediterranean: Implications for regional direct radiative forcing under clean and polluted conditions. *Atmospheric Chemistry and Physics, 11*, 4251–4271. https://doi.org/10.5194/acp-11-4251-2011

Swietlicki, E., Hansson, H.-C., Hämeri, K., Svenningsson, B., Massling, A., McFiggans, G., McMurry, P. H., Petäjä, T., Tunved, P., Gysel, M., Topping, D., Weingartner, E., Baltensperger, U., Rissler, J., Wiedensohler, A., & Kulmala, M. (2008). Hygroscopic properties of submicrometer atmospheric aerosol particles measured with H-TDMA instruments in various environments – A review. *Tellus B: Chemical and Physical Meteorology, 60*, 432–469. https://doi.org/10.1111/j.1600-0889.2008.00350.x

Tang, I. N. (1996). Chemical and size effects of hygroscopic aerosols on light scattering coefficients. *Journal of Geophysical Research, 101*, 19245–19250. https://doi.org/10.1029/96JD03003

Tang, I. N., & Munkelwitz, H. R. (1994). Aerosol phase transformation and growth in the atmosphere. *Journal of Applied Meteorology, 33*, 791–796. https://doi.org/10.1175/1520-0450(1994)033<0791:APTAGI>2.0.CO;2

Tang, M., Cziczo, D. J., & Grassian, V. H. (2016). Interactions of water with mineral dust aerosol: Water adsorption, hygroscopicity, cloud condensation, and ice nucleation. *Chemical Reviews, 116*, 4205–4259. https://doi.org/10.1021/acs.chemrev.5b00529

Tutsak, E., & Koçak, M. (2019). Long-term measurements of aerosol optical and physical properties over the Eastern Mediterranean: Hygroscopic nature and source regions. *Atmospheric Environment, 207*, 1–15. https://doi.org/10.1016/j.atmosenv.2019.03.007

Vali, G., DeMott, P. J., Möhler, O., & Whale, T. F. (2015). Technical note: A proposal for ice nucleation terminology. *Atmospheric Chemistry and Physics, 15*, 10263–10270. https://doi.org/10.5194/acp-15-10263-2015

Van Dingenen, R., Putaud, J.-P., Martins-Dos Santos, S., & Raes, F. (2005). Physical aerosol properties and their relation to air mass origin at Monte Cimone (Italy) during the first MINATROC campaign. *Atmospheric Chemistry and Physics, 5*, 2203–2226. https://doi.org/10.5194/acp-5-2203-2005

Weingartner, E., Gysel, M., & Baltensperger, U. (2002). Hygroscopicity of aerosol particles at low temperatures. 1. New low-temperature H-TDMA instrument: Setup and first applications. *Environmental Science & Technology, 36*, 55–62. https://doi.org/10.1021/es010054o

Zieger, P., Väisänen, O., Corbin, J. C., Partridge, D. G., Bastelberger, S., Mousavi-Fard, M., Rosati, B., Gysel, M., Krieger, U. K., Leck, C., Nenes, A., Riipinen, I., Virtanen, A., & Salter, M. E. (2017). Revising the hygroscopicity of inorganic sea salt particles. *Nature Communications, 8*, 15883. https://doi.org/10.1038/ncomms15883

Part VIII
Deposition in the Mediterranean Region

Coordinated by ***Karine Desboeufs***
Université Paris Cité and Univ. Paris Est Créteil, CNRS, LISA, F-75013 Paris, France
karine.desboeufs@lisa.u-pec.fr

Reviewed by ***Francesc Peters*** *(ICM/CSIC, Barcelona, Spain)*

Abstract
Deposition is a key term to correctly model the atmospheric aerosol mass burden, which results from the balance between emission and deposition fluxes. In the Mediterranean basin (MB), the spring season is marked by occasional and sometimes very intense dust storms. The particulate mass budget is highly influenced by those dust events which provide a major contribution to the PM_{10} atmospheric mass measured at regional background sites located in the southern MB. In addition to intense inputs of Saharan dust, the MB also receives both noticeable pulsed and continuous anthropogenic inputs. In this context, atmospheric deposition constitutes major external sources of nutrients and contaminants for Mediterranean terrestrial and marine ecosystems. In this section, we examine composition, seasonality and heterogeneity of atmospheric deposition to the Mediterranean Sea. We focus on the atmospheric deposition of dust and species being of marine biogeochemical interest.

Mass Deposition

Benoit Laurent, Thomas Audoux, Mariem Bibi, François Dulac, and Gilles Bergametti

Contents

Abstract In this chapter, we briefly recall dry and wet deposition processes and their parameterizations and examine the aerosol mass deposition over the Mediterranean basin and its temporal and spatial variability, mainly through a review of available dust deposition measurements. Even if deposition sampling was performed at various periods and places with different devices and for different purposes, the dataset provides a quite complete picture of deposition in the sub-regions of the Mediterranean over more than half a century, from historical observations to recent studies in the framework of the Chemistry-Aerosol Mediterranean Experiment (ChArMEx). Atmospheric deposition mass fluxes in the western, central and eastern regions of the Mediterranean are illustrated focusing on

Chapter reviewed by ***Anna Ávila Castell*** *(Centro de Investigación Ecológica y Applicaciones Forestales (CREAF), Universitat Autònoma de Barcelona, 08193, Ballaterra, Spain), as part of the book Part VIII Deposition in the Mediterranean Region also reviewed by* ***Francesc Peters*** *(ICM/CSIC, Barcelona, Spain)*

B. Laurent (✉) · T. Audoux · G. Bergametti
Université Paris Cité and Univ. Paris Est Créteil, CNRS, LISA, F-75013 Paris, France
e-mail: benoit.laurent@lisa.ipsl.fr

M. Bibi
Physics Department, Faculty of Sciences of Sfax, Sfax University, Sfax, Tunisia

F. Dulac
Laboratoire des Sciences du Climat et de l'Environnement (LSCE), CEA-CNRS-UVSQ, Université Paris-Saclay, IPSL, CEA Paris-Saclay, Gif-sur-Yvette, France

F. Dulac et al. (eds.), *Atmospheric Chemistry in the Mediterranean Region*,
https://doi.org/10.1007/978-3-030-82385-6_16

mineral dust. As in other regions, the spatial and temporal variability of the Mediterranean aerosol deposition is controlled by relative changes in pulsed and sporadic dust emission sources, atmospheric pathways, and balance between wet and dry deposition processes. A better understanding of past and future deposition evolution and trends requires joint studies of direct measurements, satellite observations and model simulations of natural and anthropogenic changes in the Mediterranean context.

1 Introduction

The Mediterranean Sea lies between highly industrialized areas to the north and arid regions to the south. Different kinds of aerosols are emitted from these contrasting regions, which upon transport and deposition affect the marine and terrestrial ecosystems of the basin (see the chapters by Guieu & Ridame, 2022; Kanakidou et al., 2022). Aerosol deposition measurements have been carried out since the mid-1960s in the Mediterranean region. Several studies have thus been done to investigate the deposition of dust aerosols. Deposition tends to be dominated by pulsed and sporadic events (see also the chapter by Laurent & Bergametti, 2022) that nevertheless represent a major contribution of the total mass deposition flux (dry and wet deposition) in the Mediterranean basin.

The main physical processes involved in the dry deposition of aerosol particles are sedimentation, interception, impaction, Brownian diffusion and rebound (e.g., Slinn & Slinn, 1980; Slinn, 1982; Seinfeld & Pandis, 1998). These processes depend on the aerosol characteristics (diameter, density, shape, hygroscopicity, electrostatic charge, etc.) but also on the meteorological conditions (turbulence, wind speed, friction speed, sensible heat flux, atmospheric stability, relative humidity, etc.) and surface properties (roughness, temperature, electrostatic properties, humidity, etc.). Wet deposition occurs when particles are scavenged from the atmosphere to the surface by precipitation. Two phenomena are involved: scavenging of particles below the cloud by precipitating rain drops (below-cloud scavenging) and incorporation of particles in the cloud water, followed by their precipitation (in-cloud scavenging) (e.g., Slinn, 1983; Seinfeld & Pandis, 1998; Duhanyan & Roustan, 2011). In the atmosphere, water usually condenses on particles that act as cloud condensation nuclei (CCN) or ice nuclei (IN) in a colder atmosphere. The ability of a particle to act as CCN or IN depends on its physicochemical properties, its size and its mineralogical and chemical composition (e.g., Seinfeld & Pandis, 1998; Atkinson et al., 2013). When a particle is incorporated into a droplet, it may partially or completely be dissolved. It may therefore be necessary to collect together or separately the soluble and insoluble fractions of the aerosol deposited by precipitation.

In situ deposition measurements have to be referred to the method employed to sample the dry, wet, total (dry plus wet) or bulk deposition, the target components

(soluble, insoluble) and the temporal scale (short or long term). They can be sampled with specific sampling devices (e.g., Laurent et al., 2015, and references therein). When a wet only/dry only collector is used, the sampling bucket is only exposed during rain/no rain period, respectively. When collectors are continuously open to the atmosphere, the bulk deposition is collected, so that the dry deposition fraction is included. Deposition mass is generally obtained by the weighing of the samples (e.g., Loÿe-Pilot and Martin, 1996; Laurent et al., 2015). However, the elemental analysis of deposition samples can also allow one to estimate the dust deposited mass. Especially aluminium can be used to estimate the mass of the deposition flux of dust by considering that this element contributes to about 7–8% of their total mass (e.g., Kubilay et al., 2000; Guieu et al., 2002). It can also be derived from atmospheric dust concentrations by applying a deposition rate for dry deposition or a scavenging efficiency for wet deposition (e.g., Jickells et al., 1987; Duce & Tindale, 1991).

Deposition of aerosols emitted from different natural sources and sources related to human activity impacts the Mediterranean. Studies performed on both sides of the Mediterranean basin have investigated only the mineral fraction of the deposition (Vincent et al., 2016) or the contribution of mineral, organic and anthropogenic sources to deposition (e.g., Fu et al., 2017; Lequy et al., 2018; Cerro et al., 2020). The heterogeneity, variability and source apportionment of deposition based on chemical measurements are discussed in the two following chapters on nutrient deposition and variability, and trace metals and contaminants deposition, respectively (Desboeufs, 2022a, 2022b). After a brief description of the dry and wet deposition processes, the spatial and temporal mass deposition pattern in the Mediterranean is discussed in this chapter by focusing on mineral dust deposition.

2 Deposition Processes

Particles in the atmosphere are subject to gravitational settling, which depends mainly on their size and density. The gravitational settling velocity (V_s) is controlled by the balance of the forces exerted on a falling particle in the air (gravity, Archimedes' principle, drag force). V_s is expressed from the Stokes' law (Stokes, 1851) which represents the force exerted by a fluid on a particle moving in this fluid:

$$V_s = \frac{D_{aero}^2 \left(\rho_{aero} - \rho_a\right) g Cu}{18 \mu_a} \quad (1)$$

with D_{aero} the aerosol diameter, ρ_{aero} and ρ_a the aerosol and air densities, respectively, g the gravity, μ_a the air dynamic viscosity. and *Cu the Cunningham's correction factor.*

A particle close to a surface can also be subject to other processes which are the impaction, the inertial interception, the Brownian diffusion or rebound. These processes depend on particle properties and on the air flow near the surface and are

characterized by aerodynamic (r_a) and surface (r_s) resistances. These different processes are considered in the deposition velocity (V_d) which is generally expressed as a function of V_s (m s^{-1}), r_a and r_s (s m^{-1}) according to Slinn (1982):

$$V_d = V_s + \frac{1}{f(r_a, r_s)} \tag{2}$$

V_d is minimum for particles whose diameter is between 0.1 µm and 1 µm. Indeed, Brownian diffusion controls the deposition of particles with a diameter lower than 0.1 µm, while gravitational settling and impaction control dry deposition of particles larger than 1 µm. However, the physical representation of the rebound of atmospheric particles remains an open question (Figgis et al., 2018).

The dry deposition flux (F_s) is expressed as a function of V_d and the aerosol concentration ($C_{aero,\,h}$) in an air layer of height h (e.g., Seinfeld & Pandis, 1998):

$$F_s = V_d C_{aero,h} \tag{3}$$

The wet deposition flux of aerosol particles (F_h) is expressed as the product of the concentration of particles in rainwater ($C_{aero,\,rain}$) by the rainfall rate (P) (e.g., Slinn, 1983; Seinfeld & Pandis, 1998).

The below-cloud scavenging corresponds to the collection of atmospheric particles trapped under the cloud by precipitating hydrometeors. This phenomenon takes place in the air column between the cloud and the ground. The main processes involved are the impaction, interception and Brownian diffusion induced by the fall of the raindrops. This leads to a decrease with time of the atmospheric particle concentration (C_{aero}) which can be expressed as a function of a below-cloud scavenging coefficient Λ_{below} (in s^{-1}) (e.g., Slinn, 1977; Seinfeld & Pandis, 1998; Loosmore & Cederwall, 2004):

$$\frac{dC_{aero}}{dt} = -\Lambda_{below} C_{aero} \text{ with } \Lambda_{below} = \frac{3}{2}\frac{E(D_{aero})P}{D_g} \tag{4}$$

where D_{aero} is the diameter of the particles, P is the rainfall rate, which is expressed as a function of the diameter of the drops (D_g) and their fall velocity (v_g), and $E(D_{aero}, D_g)$ is the wet collection efficiency, i.e., the ratio of the particles captured by the rain drops to the total particles in the atmosphere. Slinn (1977) expresses E as the sum of the collection effects by impaction (E_{Impa}), interception (E_{Inter}) and Brownian diffusion (E_{Brown}). Numerous studies add electrostatic and phoretic effects to the Slinn model in order to compensate for its underestimation in the 0.1–3 µm particle size range (Wang et al., 1978; Andronache, 2004; Chate, 2005; Andronache et al., 2006).

The variation in aerosol concentration (C_{aero}) with time by in-cloud deposition can also be expressed from a scavenging coefficient Λ_{in} (in s^{-1}) (e.g., Tsyro, 2002):

$$\frac{\mathrm{d}C_{\mathrm{aero}}}{dt} = -\Lambda_{\mathrm{in}} C_{\mathrm{aero}} \text{ with } \Lambda_{\mathrm{in}} = \frac{\varepsilon P_{\mathrm{r}}}{m_{\mathrm{w}} \Delta z} \tag{5}$$

P_{r} corresponds to the rate of precipitation released in the considered mesh, m_{w} is the density of cloud water and Δz is the height of the mesh. ε is the efficiency of incorporation of the particles in the aqueous phase of the cloud. It corresponds to the ratio of the particle concentration in the aqueous phase to the total particle concentration.

For dust particles, which present a large size range from less than a tenth to several tens of micrometres, the dry processes generally dominate their deposition near their source regions of emission. This is due to the high concentration of large particles and to the dry climate prevailing most of the time in desert regions. Far from the dust source regions, since the largest particles have been previously deposited, the size range of dust particles is tightened, with a typical median mass diameter close to 2 μm (e.g., Schütz, 1980). Wet deposition allows the removal from the atmosphere of the small particles that are less subject to dry deposition. It can be an efficient process for removing particles from the atmosphere during long-range transport (e.g., Slinn, 1977; Bergametti et al., 1989). Observations of the long-range transport of coarse particles of several tens of μm in diameter (e.g., Betzer et al., 1988; Weinzierl et al., 2009; van der Does et al., 2018) suggest, however, that the sedimentation of dust particles is counterbalanced, possibly by electric forces (Renard et al., 2018; Toth III et al., 2020).

3 Mass Deposition in the Mediterranean

Mineral dust largely contributes to the high PM_{10} atmospheric mass concentrations measured at regional background sites in the southern Mediterranean basin (35–50% of PM_{10}), and locally up to 80% of the total PM_{10} mass (Pey et al., 2013; Kaskaoutis et al., 2023). After first dust deposition measurements made in the 1960s in Israel (e.g., Ganor & Foner, 2001), dust deposition was studied in the 1980s in the western and eastern parts of the Mediterranean basin (e.g., Usero & Gracia, 1986; Loÿe-Pilot et al., 1986; Bergametti et al., 1989; Mattson & Nihlén, 1994; Loÿe-Pilot & Martin, 1996; Guerzoni et al., 1999; Kubilay et al., 2000). However, these studies were not connected in time and most of them used different sampling strategies. In 2001, as part of the ADIOS project, nine measurement stations were equipped to measure in a similar way the atmospheric deposition during 1 year (June 2001–May 2002) all around the Mediterranean basin, in France, Spain, Morocco, Tunisia, Egypt, Turkey, Cyprus, Crete and Greece (e.g., Guieu et al., 2010; Markaki et al., 2010). Other studies were carried out at several sites but for a limited period (e.g., Usero & Gracia, 1986; Guieu et al., 2010) or sometimes at a single site for periods longer than 10 years (Avila et al., 1997, 2007; Loÿe-Pilot & Martin, 1996; Fiol et al., 2005). In the framework of the ChArMEx project, Vincent et al. (2016)

deployed a network of deposition samplers between 2011 and 2013 in the western Mediterranean, from the north African coast to southern France, to measure the total insoluble atmospheric deposition on a weekly basis. Moreover, Cerro et al. (2020) collected separately wet and dry deposition from June 2010 to August 2012 at a rural background site on Mallorca Island to determine ions, and major and trace elements, in both the soluble and insoluble fractions.

Dust aerosol deposition fluxes measured in the Mediterranean, and additional information on the type of sampling (total, soluble, insoluble), on the dust flux measurement method (directly weighed or estimated from the concentrations of chemical elements), and on the periods and durations of the samples, are compiled in Table 1. One of the reasons why such a small number of field studies has been performed is the heavy workload that both sampling and measurement of dust deposition represent over long periods of time. Deposition measurements are difficult to perform, and the devices used are generally study dependent; some of the mass deposition measurements are bulk or can just be done for the insoluble or the soluble deposition fractions. A key point when interpreting mass deposition data is knowing the size distribution of the deposited aerosol particles. Direct observations documenting jointly these parameters are challenging to perform as deposition sampling itself can modify the aggregation state of the collected particles. Regional and global models often considered only the dust fraction smaller than 20 μm in diameter, while "giant particles" with diameters from several tens up to one hundred microns have been collected far from emission source areas (Renard et al., 2018; van der Does et al., 2018; Ryder et al., 2019; Toth III et al., 2020). However, overall, these measurements provide a quite complete and realistic picture of dust deposition in the Mediterranean basin.

Dust deposition measurements close to the North African dust sources are scarce. Dust deposition fluxes have been measured in northern Algeria, Morocco, Tunisia and Libya. In northern Algeria, Lequy et al. (2018) registered a deposition flux around 65 g m^{-2} yr^{-1} in 2011–2012. The deposition samples from Morocco and Tunisia (Guieu et al., 2010) were collected at sampling sites located along the Mediterranean coasts and ranged from 7 to 23 g m^{-2} yr^{-1}, respectively. Annual deposition fluxes (2000–2001) over 24 sampling sites in Libya were higher, averaging 129 g m^{-2} yr^{-1} (O'Hara et al., 2006). Deposition at 14 sites located in the northern part of the country ranges from 30 to 103 g m^{-2} yr^{-1} for the particle size fraction <20 μm (O'Hara et al., 2006).

Regarding dust measurements in the eastern Mediterranean, insoluble deposition was measured for a long time period (1965–1995) at different locations in Israel, ranging from 30 to 90 g m^{-2} yr^{-1} (Ganor & Foner, 2001). From elemental measurements and assuming Al is 7.1% of the dust mass, Guieu et al. (2010) estimated dust deposition of around 20 g m^{-2} yr^{-1} in northern Egypt. In the northeastern part of the basin, the annual deposition flux of dust was 5.4 g m^{-2} yr^{-1} in Cyprus between June 2001 and May 2002 (Guieu et al., 2010). Kubilay et al. (2000) estimated the annual total dust deposition at the Erdemli station (36°N, 34°E) in Turkey at around 13 g m^{-2} yr^{-1} for 1992. From several sites on the island of Crete, Mattson and Nihlén (1994) measured deposition ranging from 11 to

Table 1 Mineral dust or total mass deposition fluxes measured in the Mediterranean basin and northern Africa. Measurement types are bulk (B), insoluble only (I), soluble only (S) or wet only (W) . (Adapted and completed from Vincent et al., 2016)

Location	Period	Duration	Deposition flux (g m)$^{-2}$ yr^{-1}	Type	References
Western Mediterranean					
France					
Cap Ferrat and 3 sites in SE France and NW Corsica Isl.	2003–2007	4 yr[a]	11.4	I	Ternon et al. (2010)
Cap bear, SW France	2001–2002	12 mo	10.6[c]	B	Guieu et al. (2010)
Le Casset, SE France	2011–2013	28 mo	0.9	I	Vincent et al. (2016)
Frioul Isl., SE France	2011–2013	28 mo	3.5	I	Vincent et al. (2016)
Capo Cavallo, NW Corsica Isl.	1985–1986	12.5 mo	12.5[c]	B	Bergametti et al. (1989)
	1986–1987	20 mo	9.7	B	Remoudaki (1990)
3 inland sites, Corsica Isl.	1984–1994	10 yr[b]	4–26	B	Loÿe-Pilot and Martin (1996)
Ostriconi, N Corsica Isl.	2001–2002	12 mo	27.4[c]	B	Guieu et al. (2010)
Pirio, NW Corsica Isl.	1995–1997	27 mo	2–4[c]	B	Ridame et al. (1999)
	1999–2000	13 mo[a]	9–14[c]	B	Loÿe-Pilot et al. (2001)
Ersa, NW Corsica Isl.	2012–2013	18 mo	2.1	I	Vincent et al. (2016)
Cap Cuittone (Galeria), W Corsica Isl.	2008–2011	3.5 yr	1.7[c]	B	Desboeufs et al. (2018)
Italy					
Lampedusa Isl., S Italy	2011–2013	23 mo	7.4	I	Vincent et al. (2016)
Capo Carbonara, SE Sardinia Isl.	1990–1992	19 mo	12.8[c]	B	Guerzoni et al. (1999)
Spain					
Montseny, NE Spain	1983–1994	11 yr	5.2[d]	B	Avila et al. (1997)
	2002–2003	12 mo	5.4	B	Castillo et al. (2017)
	2011–2012	18 mo	18.1	B	Lequy et al. (2018)
Palma de Mallorca, Mallorca Isl.	1982–2003	22 yr	~14[d]	B	Fiol et al. (2005)
Can Llompart, Mallorca Isl.	2010–2012	26.5 mo	22.8	B	Cerro et al. (2020)
			5.2	I	
			6.6[c]	I	
Ses Salines, Mallorca Isl.	2011–2013	27 mo	5.8	I	Vincent et al. (2016)

(continued)

Table 1 (continued)

Location	Period	Duration	Deposition flux (g m)$^{-2}$ yr^{-1}	Type	References
Campo de Gibraltar, S Spain	1982–1983	12 mo	22.8[c]	S + I	Usero and Gracia (1986)
Lanjaron, SE Spain	2001–2002	23 mo	11.1	B	Morales-Baquero et al. (2006)
Granada depression, SE Spain	1992–1993	12 mo	26	B	Díaz-Hernández et al. (2011)
Eastern Mediterranean					
Greece					
6 sites, Crete Isl.	1988–1994	6 yr	11–23	B	Mattson and Nihlén (1994)
7 sites, Crete Isl.	1988–1990	34 mo	10–100	B	Pye (1992)
Heraklion and Finokalia, N Crete Isl.	1996	12 mo	6[c]	W	Ezat et al. (1997)
Finokalia, NE Crete Isl.	2001–2002	12 mo	8.8[c]	B	Guieu et al. (2010)
Mytilene, Lesbos Isl.	2001–2002	12 mo	5.4[c]	B	Guieu et al. (2010)
Other countries					
Cavo Greco, SE Cyprus Isl.	2001–2002	12 mo	4.2[c]	B	Guieu et al. (2010)
Various sites, Israel	1965–1995	(a)	30–90	I	Ganor and Foner (2001)
Erdemli, SE Turkey	1991–1992	16 mo	13.0	B	Kubilay et al. (2000)
Akkuyu, SE Turkey	2001–2002	12 mo	10.1[c]	B	Guieu et al. (2010)
North Africa					
Alexandria, N Egypt	2001–2002	8.5 mo	20.3[c]	B	Guieu et al. (2010)
14 inland sites, N Libya	2000–2001	12 mo	58[e]	B	O'Hara et al. (2006)
Cap Spartel, N Morocco	2001–2002	12 mo	7.2[c]	B	Guieu et al. (2010)
Mahdia, E Tunisia	2001–2002	12 mo	23.3[c]	B	Guieu et al. (2010)
Tizi Rached, N Algeria	2011–2012	20 mo	65.4	B	Lequy et al. (2018)

[a]Sampling performed in different places and periods
[b]Sampling in different places
[c]Assuming Al is 7.1% of total dust (Guieu et al., 2002)
[d]Dust rains only
[e]Particles <20 μm only

23 g m^{-2} yr^{-1}, between 1988 and 1990, when Pye (1992) observed a wider range of deposition, from 10 to 100 g m^{-2} yr^{-1} between 1988 and 1992.

In the western Mediterranean, from wet deposition measured in Mallorca between 1982 and 2003, Fiol et al. (2005) estimate an average dust deposition of 14 g m^{-2} yr^{-1} (ranging from 2.5 to 35.5 g m^{-2} yr^{-1}). Two more recent studies with more than 2-year continuous monitoring of insoluble deposition in Mallorca report fluxes of 5.2 and 5.8 g m^{-2} yr^{-1} in the 2010–2013 period (Vincent et al., 2016; Cerro et al., 2020). Also from long-term precipitation measurements (1983–1994), Avila et al. (1997) estimate an average dust deposition in the northeast Spanish Montseny

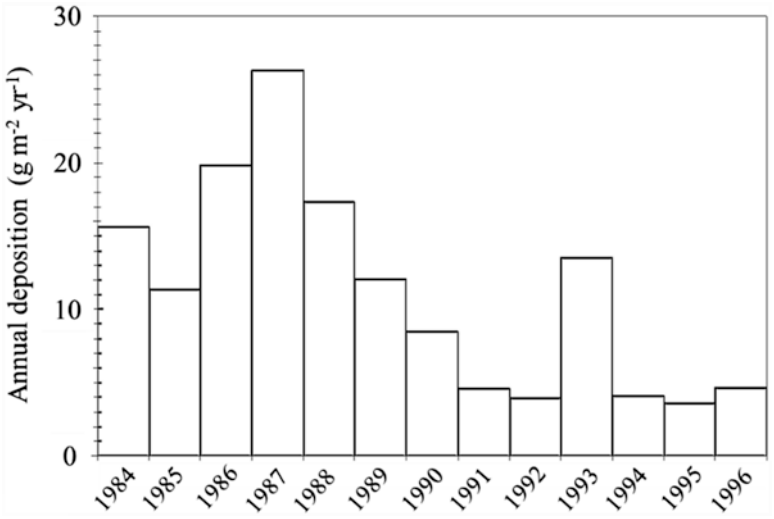

Fig. 1 Annual input of Saharan dust to Corsica from 1984 to 1996. (Adapted from Fig. 5 in Ridame et al. (1999))

Mountains around 5.2 g m^{-2} yr^{-1} associated with rain events. At the same site, Castillo et al. (2017) measured deposition of 5.4 g m^{-2} yr^{-1} in 2002–2003 and Lequy et al. (2018) measured around 18 g m^{-2} yr^{-1} in 2011–2012. Several studies were also conducted in the southern Iberian Peninsula to document deposition: around 23 g m^{-2} yr^{-1} near Gibraltar in 1982–1983 (Usero & Gracia, 1986), 26 g m^{-2} yr^{-1} near Granada during the year 1992 (Díaz-Hernández et al., 2011) and 11 g m^{-2} yr^{-1} in Lanjarón (southeastern Spain) over the 2002–2003 period (Morales-Baquero et al., 2006, 2013). Annual deposition fluxes in Sardinia, Corsica and the south of France range between 2 and 27 g m^{-2} yr^{-1} (Bergametti et al., 1989; Le Bolloch et al., 1996; Loÿe-Pilot & Martin, 1996; Guerzoni et al., 1999; Ridame et al., 1999; Loÿe-Pilot et al., 2001; Guieu et al., 2010; Desboeufs et al., 2018). The study performed by Loÿe-Pilot and Martin (1996) in Corsica over an 11-year period illustrated deposition fluxes ranging from 4 to 26 g m^{-2} yr^{-1} between a dusty (mid-1980s) and a less dusty year (mid-1990s) (Fig. 1).

North of the Mediterranean, the chemical study of glacial archives in the Alps has also made it possible to estimate atmospheric contributions of desert aerosols. Wagenbach and Geis (1989) estimate annual desert dust fluxes of 0.4 g m^{-2} yr^{-1} from a 50-year glacial record at the Gnifetti Pass in the Swiss Alps. The elementary analyses of Al concentrations performed by De Angelis and Gaudichet (1991) in a Mont Blanc archived sample allowed them to estimate a dust flux around 0.7 g m^{-2} yr^{-1} between 1955 and 1969 and an order of magnitude larger flux, 11 g m^{-2} yr^{-1}, between 1983 and 1985.

Using a network of autonomous CARAGA collectors installed in the western Mediterranean (Fig. 2), Vincent et al. (2016) collected weekly total insoluble atmospheric deposition with a temporal recovery rate of 77–91% depending on the

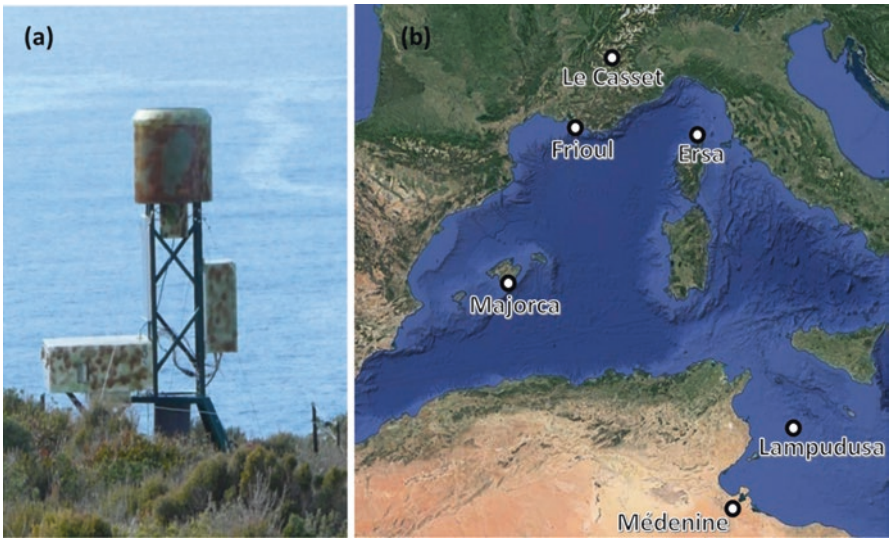

Fig. 2 (**a**) CARAGA collector in Ersa, Cap Corse (photo by Rémi Losno; see Laurent et al., 2015 for details on the sampler); (**b**) CARAGA deposition measurement sites with published data in the western Mediterranean basin: Medenine (33°30′N, 10°38′E), Lampedusa (35°31′N, 12°37′E), Mallorca (39°16′N, 3°03′E), Ersa (43°00′N, 9°21′E), Frioul (43°16′N, 5°17′E), Le Casset (44°59′N, 6°28′E)

sites for a multiannual sampling period. The annual deposition flux measured for the years 2012–2013 were 7.4 g m^{-2} yr^{-1} at Lampedusa; 5.8 g m^{-2} yr^{-1} in Mallorca; 2.1 g m^{-2} yr^{-1} in Ersa, Corsica; 3.5 g m^{-2} yr^{-1} at Frioul and 0.9 g m^{-2} yr^{-1} at Le Casset in the southern French Alps. The annual deposition collected with a CARAGA in 2014 near Medenine in south Tunisia was 60 g m^{-2} yr^{-1}. The values for the western basin and the south of France suggested that this recent period corresponds to a low deposition period when compared to the studies carried out over the previous 30 years (e.g., Loÿe-Pilot & Martin, 1996; Ridame et al., 1999; Desboeufs et al., 2018), while deposition of the same order of magnitude is observed in south Tunisia compared to previous measurements in northern Africa (e.g., O'Hara et al., 2006; Guieu et al., 2010; Lequy et al., 2018).

From these network measurements performed along the basin, a south–north decreasing gradient in the intensity of mineral dust deposition is observed over the western Mediterranean basin with a flux about 2–8 times lower in the northern part of the basin and southern France than in the southern basin (Vincent et al., 2016). CARAGA measurements also illustrate the northward decrease in deposition fluxes with much higher mass deposition at Medenine than at Lampedusa located about 250 km further northeast on the major pathway of African dust plumes exported from south Tunisia. From measurements between about mid-2011 and late 2012, Lequy et al. (2018) also pointed out the relative decrease in Saharan event contribution to the deposition from northern Algeria to northeastern Spain and France.

The compilation of these studies illustrates the large variability in dust deposition in the Mediterranean basin itself, both spatially and between years with ranges spanning over more than one order of magnitude, from 2 to more than 27 g m^{-2} yr^{-1} in the western basin and from 4 to about 100 g m^{-2} yr^{-1} in the eastern basin.

4 Daily, Seasonal and Annual Variability of Dust Deposition

The pulsed and sporadic behaviour of mineral dust emissions from various arid and semi-arid source areas, the aerosol dispersion during atmospheric transport and the rainfall pattern induce a high spatial and temporal variability in dust deposition. Loÿe-Pilot and Martin (1996) related the inter-annual deposition variability over their 1984–1994 sampling period in Corsica to the occurrence of "high" dust deposition events with fluxes >1 g m^{-2}. During 1 year of deposition measurements in Corsica from 1985 to 1986, Bergametti et al. (1989) observed that a single dust event of 3 days occurring in March 1986 contributed to more than a third of the 1986 annual mass deposition flux. Ternon et al. (2010) further measured an extreme event at 22 g m^{-2} at Cap Ferrat in February 2004 which represents more than 90% of the annual deposition flux. From the CARAGA measurements, almost 100 intense deposition events attributed to Saharan dust occurred over the period 2011–2013: 34 in Lampedusa and 20 in Mallorca (Fig. 3), 11 in Corsica, 18 in Frioul and 15 in Le Casset. These samples only correspond to 12–35% of the total number of samples collected at each station but represent between 50% and 85% of the total mass deposition flux (Vincent et al., 2016). These studies illustrate the need to conduct long-term continuous studies accounting for the deposition event variability in order to estimate the annual dust deposition mass.

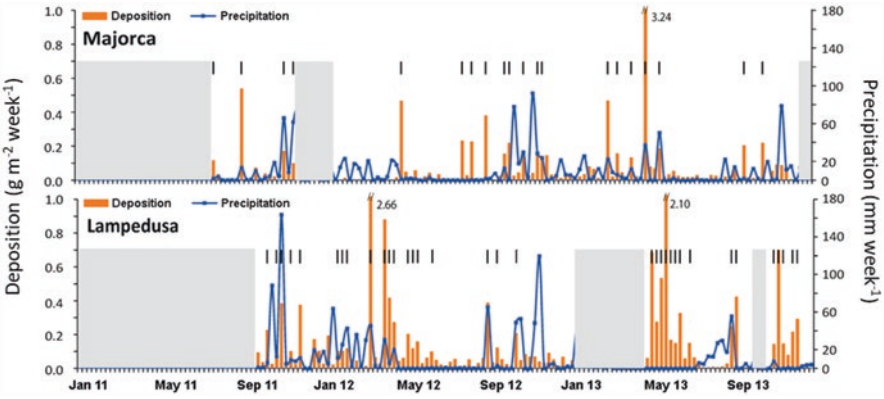

Fig. 3 Weekly insoluble mineral deposition (bars in orange) and precipitation (blue line) in Lampedusa and Mallorca between January 2011 and December 2013. The grey areas correspond to periods without sampling. The most intense dust deposition events are indicated by the black dashes: 34 in Lampedusa and 20 in Mallorca. (Adapted from Fig. 3 in Vincent et al., 2016)

Vincent et al. (2016) also pointed out the existence of spatial and temporal variability within the western Mediterranean basin itself during periods of intense deposition. Although 82% of intense deposition events were collected when at least 4 of the 5 network sites were in operation, 77% of cases of intense deposition were recorded at a single site. From the interpretation of these deposition measurements, air mass trajectories and satellite observations of the north of Africa and the Mediterranean, seven zones of origin of these high dust deposition events have been defined (see Laurent & Bergametti, 2022). For instance, the deposition events in the north and west of the western basin mainly come from western Saharan sources, while those in the southeast of the western basin are linked to Tunisian and Libyan sources. It is therefore generally not the same events that contribute the most to Saharan dust deposition in the different parts of the western basin (Vincent et al., 2016).

Regarding the seasonality of deposition in the eastern Mediterranean, from 39 rains collected on the northern side of Crete between November 1995 and January 1997, Ezat et al. (1997) reported 5 high deposition events (>0.5 g m^{-2}) representing 68% of the total wet dust deposition flux measured. They all occurred in late winter (1) and spring (4). The analyses of aerosol samples and wet deposition measurements between August 1991 and December 1992 at Erdemli, on the Turkish coast of the eastern Mediterranean, have also shown a marked seasonal cycle with higher dust concentration and deposition during spring (maximum) and autumn (secondary maximum) and lower ones in winter (Fig. 4; Kubilay et al., 2000). About 30% of the

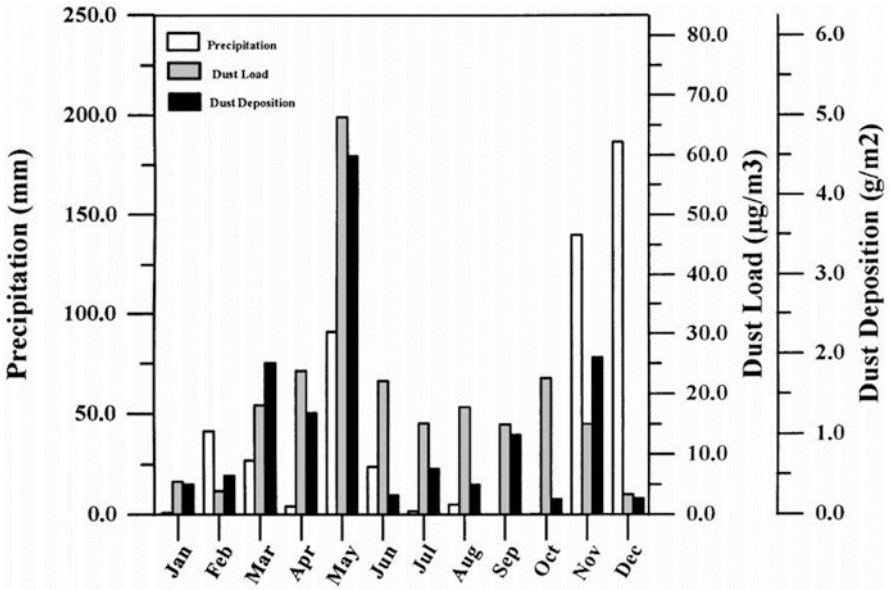

Fig. 4 Temporal variation of the dust flux, atmospheric dust concentration and the precipitation at Erdemli in 1992. (Reprinted from Fig. 3 in Kubilay et al., 2000)

annual deposition for 1992 occurred during two Saharan dust episodes in May. Although the mean dust concentration in summer was about two times higher than in winter, the amount of dust deposited within these two seasons was comparable in 1992. The higher winter deposition rate is attributable to the fact that in 1992, 70% of the annual rainfall occurred in the winter months, whereas only 5% occurred in the summer months. Kubilay et al. (2000) pointed out that high dust deposition rates require the co-existence of dust and rain, which is achieved in the transitional season at Erdemli. They report relative percentages of the wet and dry deposition to the annual deposition of 44 and 56%, respectively. These authors also show that the dry deposition flux was dominant on a seasonal basis: in the dry summer season of 1992, only 7% of the total deposition was estimated to be due to wet deposition and the remaining 93% to dry deposition (Kubilay et al., 2000).

In the western Mediterranean, the seasonality of dust deposition has been observed at various locations. The long-term measurements in Corsica showed maximum frequency and magnitude of the events in spring and autumn and minimum in winter but with a high variability (Loÿe-Pilot & Martin, 1996). For instance, these authors pointed out the high average and standard deviation values in December due to a deposition event of high magnitude in December 1987. Avila et al. (1997) also showed that the occurrence of red rain episodes at the Montseny site in northeastern Spain between 1983 and 1994 were higher in autumn and spring. Combining time series of chemistry of wet deposition in Montseny and daily levels of suspended particulate matter measured in the eastern Iberian Peninsula for the period 1996–2002, Escudero et al. (2005) pointed out that wet dust deposition events showed a relatively higher monthly frequency in May. They analyzed its seasonality and the meteorological configurations responsible of the main dust transport routes to northwestern Mediterranean. Ternon et al. (2010) observed high deposition in spring and summer with a maximum in June and a very high variability from their measurements performed in the Ligurian area between 2003 and 2007. Vincent et al. (2016) indicated that larger deposition is generally observed at their sites in the western Mediterranean between March and June with a second peak in autumn. Based on model simulations, Gallisai et al. (2016) studied large and very large Saharan dust deposition events between 2000 and 2007 to discuss their impact on the dynamics of marine phytoplankton in the Mediterranean Sea. They concluded that these events showed a high spatial, seasonal and inter-annual variability but with patterns of increased frequency in autumn and winter. The variability of deposition is also related to precipitation, since studies in the western basin suggest that wet deposition represents at least 65–75% of the total dust deposition (Bergametti et al., 1989; Guerzoni et al., 1995; Loÿe-Pilot & Martin, 1996). From the interpretation of deposition measurements, precipitation and trajectories of the dust-loaded air masses, Vincent et al. (2016) concluded that the deposition in southern France and Corsica sites is dominated by wet deposition, from 60% to 80% of the total mass deposition. At southern sites of Lampedusa and Mallorca, wet deposition contributes around 50% and 40% to the total deposition mass, respectively. The highest deposition sample in Lampedusa (2.7 g m^{-2} wk^{-1}; 20% of the total deposition flux) corresponds to a single wet deposition event, when the

second highest deposition sample (2.1 g m^{-2} wk^{-1}; 16% of the total annual deposition flux) corresponds to two successive dry deposition events in the same sampling week (Vincent et al., 2016). Cerro et al. (2020) also report a strong seasonality of the wet to dry contribution to both soluble and insoluble total deposition in Mallorca, driven by the precipitation cycle and the occurrence of African or stagnant air masses associated with increased dry deposition of dust during the dry season (from late spring to most of fall).

In order to document the spatiotemporal variability of the dust atmospheric content and deposition flux along the North African coast of the Mediterranean Sea, Bibi et al. (2019) used the MERRA-2 (Modern-Era Retrospective Analysis for Research and Applications V.2) monthly reanalysis data of the 1980–2018 period available from NASA (https://disc.gsfc.nasa.gov/datasets). The MERRA-2 of the Global Modelling and Assimilation Office (GMAO) is an up-to-date reanalysis for the satellite era (1980 onwards). Details on the aerosol module prognostic model are given in Gelaro et al. (2017) and Randles et al. (2017) and are based on the Goddard Earth Observing System Version 5 (GEOS-5) with the Goddard Chemistry Aerosol Radiation and Transport (GOCART) model. Surface PM concentrations and aerosol optical depth from the AErosol RObotic NETwork (AERONET) and satellite observations are currently used to validate dust transport model simulations (e.g., Basart et al., 2012; Wang et al., 2014; Huneeus et al., 2016). Deposition measurements were also used, for instance, to evaluate model simulations of transfers of atmospheric chemical elements to the Mediterranean surface waters (e.g., Richon et al., 2018) even if additional measurements are still needed to better constrain the mass budget in dust models (e.g., Mahowald et al., 2005; Bergametti & Forêt, 2014). Bibi et al. (2019) have extracted the dust optical depth (AOD_{dust}), surface concentrations (C_{dust}), precipitations (Prcp) and deposition fluxes (F_{dry}, F_{wet} and F_{tot}) of 14 areas (7 coastal and 7 offshore) from the Strait of Gibraltar in the west to Egypt and Cyprus in the east of the basin (Fig. 5).

Over the 1980–2018 period, averaged F_{tot} ranges from 2.9 to 7.6 g m^{-2} yr^{-1} for the seven African coastal areas and from 3.1 to 5.8 g m^{-2} yr^{-1} for the seven offshore areas (Bibi et al., 2019). Even if these values are comparable to deposition measured in the western Mediterranean by Vincent et al. (2016) at Lampedusa, Mallorca and Corsica in 2011–2013 and by Cerro et al. (2020) at Mallorca in 2010–2012, much larger deposition fluxes have been reported in the 1980s. No significant increasing or decreasing trend of F_{tot} is observed over the 39 years of MERRA2 data. However, at decadal time scales, an increase of F_{tot} from 1990 to about 2004 and a decrease from 2004 to 2018 are observable in the CW-Tun and OW-SarE areas. Superposed to these slow trends, an important inter-annual variability of the deposition is noted by Bibi et al. (2019). Because of the spatial variability of precipitation, the largest deposition fluxes do not necessarily coincide with the regions of the largest atmospheric dust content. Along the coast of the eastern basin, the low precipitation (from 6.1 to 10.5 mm $month^{-1}$ on average) explains that dry deposition accounts for a significant proportion (45–53%) of the total deposition. Everywhere else, wet deposition dominates and particularly in the marine areas where it represents at least 85% of the total deposition in agreement with observations (Bibi et al., 2019).

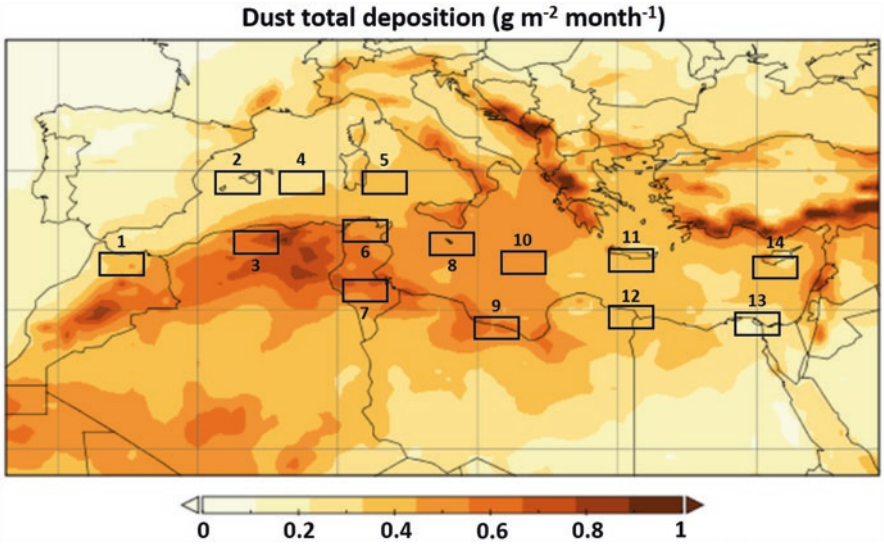

Fig. 5 MERRA-2 average total monthly deposition fluxes of mineral dust in g m^{-2} $month^{-1}$ during the 1980–2018 period for the North Africa and Mediterranean Sea region. The 14 studied areas: 1 CW-Mor, 2 OW-Bal, 3 CW-Alg, 4 OW-SarW, 5 OW-SarE, 6 CW-Tun, 7 CE-Tun, 8 OE-Mal, 9 CE-Lib, 10 OE-Lib, 11 OE-Cre, 12 CE-EgyW, 13 CE-EgyE, 14 OE-Cyp. (Adapted from Fig. 7 in Bibi et al. (2019))

As mentioned, the variability in dust mass deposition on daily, annual and inter-annual scales in the Mediterranean can be caused by different factors from the dust emission sources to air masses circulation and precipitation changes. The recent low deposition fluxes measured in the western Mediterranean (Vincent et al., 2016; Desboeufs et al., 2018) seem concomitant with a decrease in PM_{10} concentrations (Pey et al., 2013). This could be linked to large-scale atmospheric circulation, such as lower North Atlantic Oscillation indices during the last two decades, affecting dust atmospheric contents (Pey et al., 2013), and/or be related to a lower dust activity period in the Sahara as proposed by Evan et al. (2016) from wind variability patterns. However, climate change simulations indicate a dryer and warmer climate in the Mediterranean basin (e.g., Hertig & Jacobeit, 2008), a situation that could enhance dust emissions and transport (Moulin et al., 2006), as well as intense precipitation events (Beaulant et al., 2011). On the other hand, from MERRA-2 global model outputs over the 1980–2018 period, no clear tendency of a decrease in atmospheric dust concentration and total deposition fluxes can be identified in the southern part of the basin (Bibi et al., 2019). Neither do satellite data show a decrease in dust optical depth between the 1980–1990s and recent years (Mallet et al., 2022) compatible with an order of magnitude decrease in deposition fluxes. One hypothesis is that the drying of the Mediterranean basin due to climate change might induce less wet deposition over the basin and longer northward and northeastward transport of the dust before being scavenged.

5 Conclusion

Even though aerosol deposition sampling is difficult to perform, the Mediterranean is one of the most documented regions worldwide regarding deposition fluxes. Since the 1960s, sampling has been carried out at various places and using various devices to investigate soluble, insoluble or bulk deposition, up to an unprecedented effort conducted in the framework of ChArMEx to operate a network of several stations in the western Mediterranean and measure weekly deposition fluxes over several years. This ensemble of measurements performed for different purposes provide a quite complete and realistic picture of the dust deposition in the Mediterranean basin. Mineral dust, which controls annual to short-term aerosol mass deposition fluxes in this region, was specifically studied. The high variability in dust deposition in the Mediterranean, which is linked to nonlinear emission and deposition processes, challenges the study of past and future trends in mass deposition in the Mediterranean under climate change and anthropogenic pressure on land. Direct dust deposition measurements indicate a recent strong decrease in the deposition, for example, in the northwestern Mediterranean, whereas long-term simulations point out an important inter-annual variability of dust deposition. A trend towards more stability is found in the southern part of the basin. This illustrates the need to pursue a combined monitoring of both atmospheric dust load and deposition and to better integrate direct observations and model simulations to document a possible evolution in this Mediterranean region subject to climate change and anthropogenic pressure. Moreover, the estimation of the relative contribution of the different aerosol particles to the total mass deposition in the Mediterranean requires joint studies of air mass trajectories and chemical composition of the deposition. Finally, deposition fluxes can provide an improved constraint to the dust transport models than the current validation by only surface PM concentrations and aerosol optical depth. This will allow a more accurate computing of the atmospheric desert dust mass budgets and associated transfers of chemical elements from arid areas to the marine and terrestrial ecosystems of the Mediterranean basin.

Acknowledgments Authors of this chapter are grateful to Anna Ávila Castell and Francesc Peters for their detailed and helpful review of the manuscript. José Carlos Cerro Garrido is also acknowledged for his suggestions.

References

Andronache, C. (2004). Diffusion and electric charge contributions to below-cloud wet removal of atmospheric ultra-fine aerosol particles. *Journal of Aerosol Science, 35*, 1467–1482. https://doi.org/10.1016/j.jaerosci.2004.07.005

Andronache, C., Grönholm, T., Laakso, L., Phillips, V., & Venäläinen, A. (2006). Scavenging of ultrafine particles by rainfall at a boreal site: Observations and model estimations. *Atmospheric Chemistry and Physics, 6*, 4739–4754. https://doi.org/10.5194/acp-6-4739-2006

Atkinson, J. D., Murray, B. J., Woodhouse, M. T., Whale, T. F., Baustian, K. J., Carslaw, K. S., Whale, T. F., Baustian, K. J., Dobbie, S., O'Sullivan, D., & Malkin, T. L. (2013). The importance of feldspar for ice nucleation by mineral dust in mixed-phase clouds. *Nature, 498*, 355–358. https://doi.org/10.1038/nature12278

Avila, A., Queralt-Mitjans, I., & Alarcón, M. (1997). Mineralogical composition of African dust delivered by red rains over northeastern Spain. *Journal of Geophysical Research, 102*, 21977–21996. https://doi.org/10.1029/97JD00485

Avila, A., Alarcon, M., Castillo, S., Escudero, M., Garcıa Orellana, J., Masque, P., & Querol, X. (2007). Variation of soluble and insoluble calcium in red rains related to dust sources and transport patterns from North Africa to northeastern Spain. *Journal of Geophysical Research, 112*, D05210. https://doi.org/10.1029/2006JD007153

Basart, S., Pérez, C., Nickovic, S., Cuevas, E., & Baldasano, J. M. (2012). Development and evaluation of the BSC-DREAM8b dust regional model over Northern Africa, the Mediterranean and the Middle East. *Tellus B: Chemical and Physical Meteorology, 64*, 18539. https://doi.org/10.3402/tellusb.v64i0.18539

Beaulant, A.-L., Joly, B., Nuissier, O., Somot, S., Ducrocq, V., Joly, A., Sevault, F., Deque, M., & Ricard, D. (2011). Statistico-dynamical downscaling for Mediterranean heavy precipitation. *Quarterly Journal of the Royal Meteorological Society, 137*, 736–748. https://doi.org/10.1002/qj.796

Bergametti, G., & Forêt, G. (2014). Dust deposition. In P. Knippertz & J.-B. W. Stuut (Eds.), *Mineral dust: A key player in the earth system* (pp. 179–200). Springer Verlag. https://doi.org/10.1007/978-94-017-8978-3_8

Bergametti, G., Gomes, L., Remoudaki, E., Desbois, M., Martin, D., & Buat-Ménard, P. (1989). Present transport and deposition patterns of African dusts to the North-Western Mediterranean. In M. Leinen & M. Sarnthein (Eds.), *Paleoclimatology and Paleometeorology: Modern and past patterns of global atmospheric transport* (NATO ASI Ser) (Vol. 282, pp. 227–252). Kluwer. https://doi.org/10.1007/978-94-009-0995-3_9

Betzer, P., Carder, K., Duce, R., Merrill, J. T., Tindale, N. W., Uematsu, M., Costello, D. K., Young, R. W., Feely, R. A., Breland, J. A., Bernstein, R. E., & Greco, A. M. (1988). Long-range transport of giant mineral aerosol particles. *Nature, 336*, 568–571. https://doi.org/10.1038/336568a0

Bibi, M., Saad, M., Masmoudi, M., Laurent, B., & Alfaro, S. C. (2019). Spatial and temporal variability of the atmospheric dust load and deposition fluxes along the North-African coast of the Mediterranean Sea. *Atmospheric Research, 234*, 104689. https://doi.org/10.1016/j.atmosres.2019.104689

Castillo, S., Alastuey, A., Cuevas, E., Querol, X., & Avila, A. (2017). Quantifying dry and wet deposition fluxes in two regions of contrasting African influence: The NE Iberian Peninsula and the Canary Islands. *Atmosphere, 8*, 86. https://doi.org/10.3390/atmos8050086

Cerro, J. C., Cerdà, V., Caballero, S., Bujosa, C., Alastuey, A., Querol, X., & Pey, J. (2020). Chemistry of dry and wet atmospheric deposition over the Balearic Islands, NW Mediterranean: Source apportionment and African dust areas. *Science of The Total Environment, 747*, 141187. https://doi.org/10.1016/j.scitotenv.2020.141187

Chate, D. (2005). Study of scavenging of submicron-sized aerosol particles by thunderstorm rain events. *Atmospheric Environment, 39*, 6608–6619. https://doi.org/10.1016/j.atmosenv.2005.07.063

De Angelis, M., & Gaudichet, A. (1991). Saharan dust deposition over Mont Blanc (French Alps) during the last 30 years. *Tellus, 43B*, 61–75. https://doi.org/10.1034/j.1600-0889.1991.00005.x

Desboeufs, K. (2022a). Nutrient deposition and variability. In F. Dulac, S. Sauvage, & E. Hamonou (Eds.), *Atmospheric chemistry in the Mediterranean Region* (Vol. 2, From air pollutant sources to impacts). Springer, this volume. https://doi.org/10.1007/978-3-030-82385-6_17

Desboeufs, K. (2022b). Trace metals and contaminants deposition. In F. Dulac, S. Sauvage, & E. Hamonou (Eds.), *Atmospheric chemistry in the Mediterranean Region* (Vol. 2, From air pollutant sources to impacts). Springer, this volume. https://doi.org/10.1007/978-3-030-82385-6_18

Desboeufs, K., Bon Nguyen, E., Chevaillier, S., Triquet, S., & Dulac, F. (2018). Fluxes and sources of nutrient and trace metal atmospheric deposition in the northwestern Mediterranean. *Atmospheric Chemistry and Physics, 18*, 14477–14492. https://doi.org/10.5194/acp-18-14477-2018

Díaz-Hernández, J. L., Martín-Ramos, J. D., & López-Galindo, A. (2011). Quantitative analysis of mineral phases in atmospheric dust deposited in the south-eastern Iberian Peninsula. *Atmospheric Environment, 45*, 3013–3024. https://doi.org/10.1016/j.atmosenv.2011.03.024

Duce, R. A., & Tindale, N. W. (1991). Atmospheric transport of iron and its deposition to the ocean. *Limnology and Oceanography, 36*, 1715–1726. https://doi.org/10.4319/lo.1991.36.8.1715

Duhanyan, N., & Roustan, Y. (2011). Below-cloud scavenging by rain of atmospheric gases and particulates. *Atmospheric Environment, 45*, 7201–7217. https://doi.org/10.1016/j.atmosenv.2011.09.002

Escudero, M., Castillo, S., Querol, X., Avila, A., Alarcón, M., Viana, M. M., Alastuey, A., Cuevas, E., & Rodríguez, S. (2005). Wet and dry African dust episodes over eastern Spain. *Journal of Geophysical Research, 110*, D18S08. https://doi.org/10.1029/2004JD004731

Evan, A. T., Flamant, C., Gaetani, M., & Guichard, F. (2016). The past, present and future of African dust. *Nature, 531*, 493–495. https://doi.org/10.1038/nature17149

Ezat, U., Dulac, F., Lambert, C., Kanakidou, M., Mihalopoulos, N., & Kouvarakis, G. (1997). Dust and lead in rainwaters of Crete. *Journal of Aerosol Science, 28*(Suppl. 1), 579–580. https://doi.org/10.1016/S0021-8502(97)85289-5

Figgis, B., Guo, B., Javed, W., Ahzi, S., & Rémond, Y. (2018). Dominant environmental parameters for dust deposition and resuspension in desert climates. *Aerosol Science and Technology, 52*, 788–798. https://doi.org/10.1080/02786826.2018.1462473

Fiol, L. A., Fornós, J. J., Gelabert, B., & Guijarro, J. A. (2005). Dust rains in Mallorca (Western Mediterranean): Their occurrence and role in some recent geological processes. *Catena, 63*, 64–84. https://doi.org/10.1016/j.catena.2005.06.012

Fu, Y., Desboeufs, K., Vincent, J., Bon Nguyen, E., Laurent, B., Losno, R., & Dulac, F. (2017). Estimating chemical composition of atmospheric deposition fluxes from mineral insoluble particles deposition collected in the western Mediterranean region. *Atmospheric Measurement Techniques, 10*, 4389–4401. https://doi.org/10.5194/amt-10-4389-2017

Gallisai, R., Volpe, G., & Peters, F. (2016). Large Saharan dust storms: Implications for chlorophyll dynamics in the Mediterranean Sea. *Global Biogeochemical Cycles, 30*, 1725–1737. https://doi.org/10.1002/2016GB005404

Ganor, E., & Foner, H. A. (2001). Mineral dust concentrations, deposition fluxes and deposition velocities in dust episodes over Israel. *Journal of Geophysical Research, 106*, 18431–18437. https://doi.org/10.1029/2000JD900535

Gelaro, R., McCarty, W., Suárez, M. J., Todling, R., Molod, A., Takacs, L., Randles, C. A., Darmenov, A., Bosilovich, M. G., Reichle, R., Wargan, K., Coy, L., Cullather, R., Draper, C., Akella, S., Buchard, V., Conaty, A., da Silva, A. M., Gu, W., … Zhao, B. (2017). The modern-era retrospective analysis for research and applications, version 2 (MERRA-2). *Journal of Climate, 30*, 5419–5454. https://doi.org/10.1175/JCLI-D-16-0758.1

Guerzoni, S., Quarantotto, G., Molinaroli, E., & Rampazzo, G. (1995). More data on source signature and seasonal fluxes to the central Mediterranean Sea of aerosol dust originated in desert areas. *Water Pollution Research Reports, 32*, 267–274.

Guerzoni, S., Molinaroli, E., Rossini, P., Rampazzo, G., Quarantotto, G., De Falco, G., & Cristini, S. (1999). Role of desert aerosol in metal fluxes in the Mediterranean area. *Chemosphere, 39*, 229–246. https://doi.org/10.1016/S0045-6535(99)00105-8

Guieu, C., & Ridame, C. (2022). Impact of atmospheric deposition on marine chemistry and biogeochemistry. In F. Dulac, S. Sauvage, & E. Hamonou (Eds.), *Atmospheric chemistry in the Mediterranean Region* (Vol. 2, From air pollutant sources to impacts). Springer, this volume. https://doi.org/10.1007/978-3-030-82385-6_23

Guieu, C., Loÿe-Pilot, M. D., Ridame, C., & Thomas, C. (2002). Chemical characterization of the Saharan dust end-member: Some biogeochemical implications for the western Mediterranean Sea. *Journal of Geophysical Research, 107*, 4258. https://doi.org/10.1029/2001JD000582

Guieu, C., Loÿe-Pilot, M. D., Benyahya, L., & Dufour, A. (2010). Spatial variability of atmospheric fluxes of metals (Al, Fe, Cd, Zn and Pb) and phosphorus over the whole Mediterranean from a one year monitoring experiment: Biogeochemical implications. *Marine Chemistry, 120*, 164–178. https://doi.org/10.1016/j.marchem.2009.02.004

Hertig, E., & Jacobeit, J. (2008). Downscaling future climate change: Temperature scenarios for the Mediterranean area. *Global and Planetary Change, 63*, 127–131. https://doi.org/10.1016/j.gloplacha.2007.09.003

Huneeus, N., Basart, S., Fiedler, S., Morcrette, J.-J., Benedetti, A., Mulcahy, J., Terradellas, E., Pérez García-Pando, C., Pejanovic, G., Nickovic, S., Arsenovic, P., Schulz, M., Cuevas, E., Baldasano, J. M., Pey, J., Remy, S., & Cvetkovic, B. (2016). Forecasting the northern African dust outbreak towards Europe in April 2011: A model intercomparison. *Atmospheric Chemistry and Physics, 16*, 4967–4986. https://doi.org/10.5194/acp-16-4967-2016

Jickells, T. D., Church, T. M., & Deuser, W. G. (1987). A comparison of atmospheric inputs and deepocean particle fluxes for the Sargasso Sea. *Global Biogeochemical Cycles, 1*, 117–130. https://doi.org/10.1029/GB001i002p00117

Kanakidou, M., Sfakianaki, M., & Probst, A. (2022). Impact of air pollution on terrestrial ecosystems. In F. Dulac, S. Sauvage, & E. Hamonou (Eds.), *Atmospheric chemistry in the Mediterranean Region* (Vol. 2, From air pollutant sources to impacts). Springer, this volume. https://doi.org/10.1007/978-3-030-82385-6_24

Kaskaoutis, D. G., Liakakou, E., Grivas, G., Gerasopoulos, E., Mihalopoulos, N., Alastuey, A., Dulac, F., Pandolfi, M., Sciare, J., & Titos, G. (2023). Chemical composition and levels of concentrations of aerosols in the Mediterranean. In F. Dulac, S. Sauvage, & E. Hamonou (Eds.), *Atmospheric chemistry in the Mediterranean Region* (Vol. 1, Background information and pollutant distribution). Springer.

Kubilay, N., Nickovic, S., Moulin, C., & Dulac, F. (2000). An illustration of the transport and deposition of mineral dust onto the eastern Mediterranean. *Atmospheric Environment, 34*, 1293–1303. https://doi.org/10.1016/S1352-2310(99)00179-X

Laurent, B., & Bergametti, G. (2022). Soil dust emissions. In F. Dulac, S. Sauvage, & E. Hamonou (Eds.), *Atmospheric chemistry in the Mediterranean Region* (Vol. 2, From air pollutant sources to impacts). Springer, this volume. https://doi.org/10.1007/978-3-030-82385-6_4

Laurent, B., Losno, R., Chevaillier, S., Vincent, J., Roullet, P., Bon Nguyen, E., Ouboulmane, N., Triquet, S., Fornier, M., Raimbault, P., & Bergametti, G. (2015). An automatic collector to monitor insoluble atmospheric deposition: An application for mineral dust deposition. *Atmospheric Measurement Techniques, 8*, 2801–2811. https://doi.org/10.5194/amt-8-2801-2015

Le Bolloch, O., Guerzoni, S., & Molinaroli, E. (1996). Atmosphere-ocean mass fluxes at two coastal sites in Sardinia. In S. Guerzoni & R. Chester (Eds.), *The impact of desert dust across the Mediterranean* (pp. 217–222). Springer. https://doi.org/10.1007/978-94-017-3354-0_21

Lequy, E., Avila, A., Boudiaf Nait Kaci, M., & Turpault, M.-P. (2018). Atmospheric deposition of particulate matter between Algeria and France: Contribution of long and short-term sources. *Atmospheric Environment, 191*, 181–193. https://doi.org/10.1016/j.atmosenv.2018.08.013

Loosmore, G., & Cederwall, R. (2004). Precipitation scavenging of atmospheric aerosols for emergency response applications: Testing an updated model with new real-time data. *Atmospheric Environment, 38*, 993–1003. https://doi.org/10.1016/j.atmosenv.2003.10.055

Loÿe-Pilot, M.-D., & Martin, J.-M. (1996). Saharan dust input to the western Mediterranean: An eleven years records in Corsica. In S. Guerzoni & R. Chester (Eds.), *The impact of desert dust across the Mediterranean* (Environmental science and technology library) (Vol. 11, pp. 191–199). Springer. https://doi.org/10.1007/978-94-017-3354-0_18

Löye-Pilot, M. D., Martin, J. M., & Morelli, J. (1986). Influence of Saharan dust on the rain acidity and the atmospheric input to the Mediterranean. *Nature, 321*, 427–428. https://doi.org/10.1038/321427a0

Loÿe-Pilot, M. D., Guieu, C., & Ridame, C. (2001). Atmospheric bulk fluxes of natural and pollutant metals to the north western mediterranean; their trend over the past 15 years (1985–2000),

in Atmospheric Transport and Deposition of Pollutants into the Mediterranean Sea, UNEP/MAP. *Technical Reports Series, 133*, 35–54.

Mahowald, N. M., Baker, A. R., Bergametti, G., Brooks, N., Duce, R. A., Jickells, T. D., Kubilay, N., Prospero, J. M., & Tegen, I. (2005). Atmospheric global dust cycle and iron inputs to the ocean. *Global Biogeochemical Cycles, 19*, GB4025. https://doi.org/10.1029/2004GB002402

Mallet, M., Chazette, P., Dulac, F., Formenti, P., Di Biagio, C., Denjean, C., & Chiapello, I. (2022). Aerosol optical properties. In F. Dulac, S. Sauvage, & E. Hamonou (Eds.), *Atmospheric chemistry in the Mediterranean Region* (Vol. 2, From air pollutant sources to impacts). Springer, this volume. https://doi.org/10.1007/978-3-030-82385-6_14

Markaki, Z., Loÿe-Pilot, M. D., Violaki, K., Benyahya, L., & Mihalopoulos, N. (2010). Variability of atmospheric deposition of dissolved nitrogen and phosphorus in the Mediterranean and possible link to the anomalous seawater N/P ratio. *Marine Chemistry, 120*, 187–194. https://doi.org/10.1016/j.marchem.2008.10.005

Mattson, J. O., & Nihlén, T. (1994). The transport of Saharan dust to southern Europe: A scenario. *Journal of Arid Environments, 32*, 111–119. https://doi.org/10.1006/jare.1996.0011

Morales-Baquero, R., Pulido-Villena, E., & Reche, I. (2006). Atmospheric inputs of phosphorus and nitrogen to the southwest Mediterranean region: Biogeochemical responses of high mountain lakes. *Limnology and Oceanography, 51*, 830–837. https://doi.org/10.4319/lo.2006.51.2.0830

Morales-Baquero, R., Pulido-Villena, E., & Reche, I. (2013). Chemical signature of Saharan dust on dry and wet atmospheric deposition in the south-western Mediterranean region. *Tellus B: Chemical and Physical Meteorology, 65*, 18720. https://doi.org/10.3402/tellusb.v65i0.18720

Moulin, C., Chiapello, I., Moulin, C., & Chiapello, I. (2006). Impact of human-induced desertification on the intensification of Sahel dust emission and export over the last decades. *Geophysical Research Letters, 33*. https://doi.org/10.1029/2006GL025923

O'Hara, S. L., Clarke, M. L., & Elatrash, M. S. (2006). Field measurements of desert dust deposition, in Libya. *Atmospheric Environment, 40*, 3881–3897. https://doi.org/10.1016/j.atmosenv.2006.02.020

Pey, J., Querol, X., Alastuey, A., Forastiere, F., & Stafoggia, M. (2013). African dust outbreaks over the Mediterranean Basin during 2001-2011: PM_{10} concentrations, phenomenology and trends, and its relation with synoptic and mesoscale meteorology. *Atmospheric Chemistry and Physics, 13*, 1395–1410. https://doi.org/10.5194/acp-13-1395-2013

Pye, K. (1992). Aeolian dust transport and deposition over Crete and adjacent parts of the Mediterranean Sea. *Earth Surface Processes and Landforms, 17*, 271–288. https://doi.org/10.1002/esp.3290170306

Randles, C. A., Da Silva, A. M., Buchard, V., Colarco, P. R., Darmenov, A., Govindaraju, R., Smirnov, A., Holben, B., Ferrare, R., Hair, J., Shinozuka, Y., & Flynn, J. (2017). The MERRA-2 aerosol reanalysis, 1980 onward. Part I: System description and data assimilation evaluation. *Journal of Climate, 30*, 6823–6850. https://doi.org/10.1175/JCLI-D-16-0609.1

Remoudaki, E. (1990). Etude des processus contrôlant la variabilité temporelle des flux atmosphériques de polluants et de poussières minérales en Méditerranée occidentale, Thèse de doctorat, Univ. Paris 7, 244 pp.

Renard, J.-B., Dulac, F., Durand, P., Bourgeois, Q., Denjean, C., Vignelles, D., Couté, B., Jeannot, M., Verdier, N., & Mallet, M. (2018). In situ measurements of desert dust particles above the western Mediterranean Sea with the balloon-borne Light Optical Aerosol Counter/sizer (LOAC) during the ChArMEx campaign of summer 2013. *Atmospheric Chemistry and Physics, 18*, 3677–3699. https://doi.org/10.5194/acp-18-3677-2018

Richon, C., Dutay, J.-C., Dulac, F., Wang, R., Balkanski, Y., Nabat, P., Aumont, O., Desboeufs, K., Laurent, B., Guieu, C., Raimbault, P., & Beuvier, J. (2018). Modeling the impacts of atmospheric deposition of nitrogen and desert dust-derived phosphorus on nutrients and biological budgets of the Mediterranean Sea. *Progress in Oceanography, 163*, 21–39. https://doi.org/10.1016/j.pocean.2017.04.009

Ridame, C., Guieu, C., & Loÿe-Pilot, M. D. (1999). Trend in total atmospheric fluxes of aluminium, iron and trace metals in the northwestern Mediterranean over the past decade (1985–1997). *Journal of Geophysical Research, 104*, 30127–30138. https://doi.org/10.1029/1999JD900747

Ryder, C. L., Highwood, E. J., Walser, A., Seibert, P., Philipp, A., & Weinzierl, B. (2019). Coarse and giant particles are ubiquitous in Saharan dust export regions and are radiatively significant over the Sahara. *Atmospheric Chemistry and Physics, 19*, 15353–15376. https://doi.org/10.5194/acp-19-15353-2019

Schütz, L. (1980). Long range transport of desert dust with special emphasis on the Sahara. In P. J. Lioy (Ed.), *Aerosols: Anthropogenic and natural, source and transport* (pp. 515–532). Annals of the New York Academy of Sciences. https://doi.org/10.1111/j.1749-6632.1980.tb17144.x

Seinfeld, J. H., & Pandis, S. N. (1998). *Atmospheric Chemistry and Physics: From Air Pollution to Climate Change*. Wiley, 1326 pp., ISBN 978-0471178163.

Slinn, W. G. N. (1977). Some approximations for the wet and dry removal of particles and gases from the atmosphere. *Water, Air, and Soil Pollution, 7*, 513–543. https://doi.org/10.1007/BF00285550

Slinn, W. G. N. (1982). Predictions for particle deposition to vegetative canopies. *Atmospheric Environment, 16*, 1785–1794. https://doi.org/10.1016/0004-6981(82)90271-2

Slinn, W. G. N. (1983). Precipitation scavenging. In *Atmospheric Sciences and Power Production, chap 11*. US Department of Energy, Washington, DC, 466–532.

Slinn, S. A., & Slinn, W. G. N. (1980). Prediction for particle deposition on natural waters. *Atmospheric Environment, 14*, 1013–1016. https://doi.org/10.1016/0004-6981(80)90032-3

Stokes, G. G. (1851). On the effect of the internal friction of fluids on the motion of pendulums. *Transaction of the Cambridge Philosophical Society, 9*, 8–106. https://doi.org/10.1017/CBO9780511702266.002

Ternon, E., Guieu, C., Loÿe-Pilot, M. D., Leblond, N., Bosc, E., Gasser, B., Miquel, J. C., & Martin, J. (2010). The impact of Saharan dust on the particulate export in the water column of the North Western Mediterranean Sea. *Biogeosciences, 7*, 809–826. https://doi.org/10.5194/bg-7-809-2010

Toth, J. R., III, Rajupet, S., Squire, H., Volbers, B., Zhou, J., Xie, L., Sankaran, R. M., & Lacks, D. J. (2020). Electrostatic forces alter particle size distributions in atmospheric dust. *Atmospheric Chemistry and Physics, 20*, 3181–3190. https://doi.org/10.5194/acp-20-3181-2020

Tsyro, S. (2002). *First estimates of the effect of aerosol dynamics in the calculation of PM_{10} and $PM_{2.5}$* (Report EMEP/MSC-W Note 4/2002, 40 pp.). Norwegian Meteorological Institute. ISSN 0332-9879.

Usero, J., & Gracia, I. (1986). Trace and major elements in atmospheric deposition in the "Campo de Gibraltar" region. *Atmospheric Environment, 20*, 1639–1646. https://doi.org/10.1016/0004-6981(86)90254-4

van der Does, M., Knippertz, P., Zschenderlein, P., Harrison, R. G., & Stuut, J.-B. W. (2018). The mysterious long-range transport of giant mineral dust particles. *Science Advances, 4*, eaau2768. https://doi.org/10.1126/sciadv.aau2768

Vincent, J., Laurent, B., Losno, R., Bon Nguyen, E., Roullet, P., Sauvage, S., Chevaillier, S., Coddeville, P., Ouboulmane, N., di Sarra, A. G., Tovar-Sánchez, A., Sferlazzo, D., Massanet, A., Triquet, S., Morales Baquero, R., Fornier, M., Coursier, C., Desboeufs, K., Dulac, F., & Bergametti, G. (2016). Variability of mineral dust deposition in the western Mediterranean basin and south-east of France. *Atmospheric Chemistry and Physics, 16*, 8749–8766. https://doi.org/10.5194/acp-16-8749-2016

Wagenbach, D., & Geis, K. (1989). The mineral dust record in a high altitude Alpine glacier (Colle Gnifetti, Swiss Alps). In M. Leinen & M. Sarnthein (Eds.), *Paleoclimatology and paleometeorology: Modern and past patterns of global atmospheric transport* (NATO ASI Ser) (Vol. 282, pp. 543–564). Kluwer. https://doi.org/10.1007/978-94-009-0995-3_23

Wang, P., Grover, S., & Pruppacher, H. (1978). On the effect of electric charges on the scavenging of aerosol particles by clouds and small raindrops. *Journal of the Atmospheric Sciences, 35*, 1735–1743. https://doi.org/10.1175/1520-0469(1978)035<1735:OTEOEC>2.0.CO;2

Wang, Y., Sartelet, K. N., Bocquet, M., Chazette, P., Sicard, M., D'Amico, G., Léon, J. F., Alados-Arboledas, L., Amodeo, A., Augustin, P., Bach, J., Belegante, L., Binietoglou, I., Bush, X.,

Comerón, A., Delbarre, H., García-Vízcaino, D., Guerrero-Rascado, J. L., Hervo, M., … Dulac, F. (2014). Assimilation of lidar signals: Application to aerosol forecasting in the western Mediterranean basin. *Atmospheric Chemistry and Physics, 14*, 12031–12053. https://doi.org/10.5194/acp-14-12031-2014

Weinzierl, B., Petzold, A., Esselborn, M., Wirth, M., Rasp, K., Kandler, K., Schütz, L., Koepke, P., & Fiebig, M. (2009). Airborne measurements of dust layer properties, particle size distribution and mixing state of Saharan dust during SAMUM 2006. *Tellus B: Chemical and Physical Meteorology, 61*, 96–117. https://doi.org/10.1111/j.1600-0889.2008.00392.x

Nutrient Deposition and Variability

Karine Desboeufs

Contents

Abstract Atmospheric deposition of major nutrients such as nitrogen (N) and phosphorus (P) is of primary importance for the oligotrophic Mediterranean Sea, since atmospheric inputs are of the same order of magnitude or even larger than the riverine inputs. This chapter reviews recently published results on measured nutrient fluxes within the Mediterranean, the identification of their sources and the recent trends in comparison to historical data. Nutrients fluxes show a decreasing trend especially for N, probably associated with air pollution mitigation policies. The recent studies addressing the speciation between organic/inorganic and dissolved/particulate forms show that organic forms are critical for N and P fluxes. The chapter concludes on the prediction of atmospheric fluxes in a context of climate changes and N-containing pollutant emission control.

Chapter reviewed by ***Erwin Ulrich*** *(Office National des Forêts (ONF), Pôle Recherche-Développement-Innovation de Fontainebleau-Compiègne, F-77300 Fontainebleau, France), as part of the book Part VIII Deposition in the Mediterranean Region also reviewed by* ***Francesc Peters*** *(ICM/CSIC, Barcelona, Spain)*

K. Desboeufs (✉)
Université Paris Cité and Univ. Paris Est Créteil, CNRS, LISA, F-75013 Paris, France
e-mail: karine.desboeufs@lisa.ipsl.fr

F. Dulac et al. (eds.), *Atmospheric Chemistry in the Mediterranean Region*,
https://doi.org/10.1007/978-3-030-82385-6_17

1 Introduction

Deposition of nutrients is of primary importance for the Mediterranean region, since atmospheric inputs are of the same order of magnitude or larger than the riverine inputs (Koçak et al., 2010; Christodoulaki et al., 2013; Moon et al., 2016; Djaoudi et al., 2018) and hence of primary importance for the marine ecosystem in this region. Owing to the reduced dimension of the Mediterranean oceanic basin (2.51×10^6 km^2) and to numerous and intense land-based emission sources, open waters receive significant loads from atmospheric deposition, in particular noticeable pulsed inputs of Saharan dust, as well as anthropogenic aerosols and seasonal biomass burning inputs. The existence of marked dry and wet Mediterranean seasons, the occurrence of sporadic and intense events (dust event, fires…) and the important dichotomy of aerosols sources between the North and the South of the basin induce a large space-time variability in deposition fluxes both in terms of intensity and chemical composition.

It has been shown that atmospheric deposition of inorganic nitrogen (Loÿe-Pilot et al., 1990; Kouvarakis et al., 2001) and phosphorus (Bergametti et al., 1992; Ridame & Guieu, 2002; Markaki et al., 2003; Bartoli et al., 2005) represents significant inputs to support the primary production in surface waters. In addition to new production, it has been shown that leachable nutrients from atmospheric inputs may enhance N_2 fixation, changes in phytoplankton species composition and carbon sequestration (e.g., Bressac et al., 2014; Guieu et al., 2014; Rahav et al., 2016).

Deposition of inorganic nutrients were surveyed on a long-term basis in Corsica (Loÿe-Pilot & Morelli, 1988; Loÿe-Pilot et al., 1990, 2005; Guieu et al., 2010; Desboeufs et al., 2018), in northeastern Spain (Avila, 1996; Avila & Rodà, 2002; Àvila & Rodà, 2012; Izquierdo et al., 2012; Izquieta-Rojano et al., 2016; Lequy et al., 2018), in Crete (Kouvarakis et al., 2001; Markaki et al., 2003; Mara et al., 2009; Violaki et al., 2010, 2018) and in southeastern Turkey (Özsoy, 2003; Mace et al., 2003; Markaki et al., 2003; Koçak et al., 2010; Nehir & Koçak, 2018). For shorter time periods, measurements are also available at the Israeli coast (Herut et al., 1999, 2002), in Sardinia (Guerzoni et al., 1993; Le Bolloch & Guerzoni, 1995) and more recently in south and east of Spain (Morales-Baquero et al., 2013; Morales-Baquero & Pérez-Martínez, 2016; Cerro et al., 2020). The data are mainly focused on the countries in the northern part of Mediterranean. Only limited information on short periods or for one site are available for the southern part of the Mediterranean (Markaki et al., 2010; Lequy et al., 2018; Ounissi et al., 2018). One of the main problems in assessing the atmospheric deposition to the Mediterranean region is due to the difficulty in intercomparing the existing measurements. Indeed, the various studies that have been performed occurred at different periods and places and used different methodologies. Assessing the atmospheric deposition of one substance and its spatial variations with the available data is then challenging. The results from the ADIOS network are the only data obtained for nutrients over the same 12-month period at nine different sites throughout the Mediterranean basin (Guieu et al., 2010; Markaki et al., 2010). Quantification of spatial and temporal

trends in nutrient deposition was also investigated by modelling approaches in order to estimate the nutrient concentrations and their impacts in the Mediterranean Sea (Im et al., 2013; Christodoulaki et al., 2016; Lazzari et al., 2016; Moon et al., 2016; Richon et al., 2018a, b). In the following, we tentatively review existing observations of the deposition fluxes of the two major limiting nutrients, nitrogen and phosphorus, obtained in the Mediterranean region.

The available data sets are limited and heterogeneous, both for nitrogen (Table 1) and for phosphorus (Table 2). In order to compare with the oceanic biological demand, the deposition of nutrients is generally expressed in mmol m^{-2} yr^{-1}. Available data concern mainly the total/dissolved or inorganic/organic forms of nutrients.

2 Nitrogen Fluxes

Atmospheric deposition of N is issued from the scavenging by wet or dry deposition of all the atmospheric nitrogen forms. Most estimations of atmospheric N deposition mainly consider the inorganic soluble forms of N (ammonium (NH_4^+) and nitrate (NO_3^-) ions), gathering under the term dissolved inorganic nitrogen (DIN). The nitrite (NO_2^-) is also included in the DIN, but it is usually negligible (Herut et al., 1999). The DIN is known to be bioavailable by aquatic organisms. However, recent works emphasized that particulate or organic forms of N can be also assimilated by many organisms (Sipler & Bronk, 2015). The anthropogenic sources and deposition patterns of inorganic nitrogen are well understood, i.e., gaseous species NOy (sum of HNO_3, NO, NO_2) and ammonia (NH_3) and secondary inorganic aerosols ($(NH_4)_2SO_4$, NH_4HSO_4) and particulate NO_3^-. It is known that nitrate was mainly associated with coarse particles in Mediterranean atmosphere, due to the reactivity of nitric acid on sea salt or desert dust (e.g., Bardouki et al., 2003). On the contrary, ammonium is mainly associated with the fine mode of particles. In general, the wet deposition of inorganic nitrogen, as ammonium (NH_4^+) and nitrate (NO_3^-) ions in precipitation, is measured. Deposition measurements on collector surfaces underestimate deposition for gaseous compounds, and for submicron particles, total inorganic nitrogen deposition fluxes are obtained either by bulk sampling or by summing the wet and the dry deposition (total deposition). Thus, the additional dry deposition of nitrogen-containing gases and particles is rarely included in the deposition estimate, due to the difficulty of measurement. Yet, dry deposition of the gaseous phase of DIN could be comparable to, or even greater than, dry deposition of the particulate phase (Kouvarakis et al., 2001; Àvila & Rodà, 2012). For instance, when the gaseous forms are considered, the total inorganic nitrogen deposition flux of ~86 μmol m^{-2} d^{-1} in Crete (Markaki et al., 2003) increases to 105 μmol m^{-2} d^{-1} (Kouvarakis et al., 2001).

Organic nitrogen is a ubiquitous, yet still poorly characterized, component of atmospheric precipitation (Violaki & Mihalopoulos, 2010). Like the inorganic nitrogen ions, organic nitrogen may be incorporated in rainwater by direct dissolution

Table 1 Annual deposition fluxes of nitrogen reported for the Mediterranean basin (mmol m^{-2} yr^{-1})

Location	Type of deposition	Period	TDN fluxes	DIN fluxes	DIN wet/ total	DON fluxes	DON/TDN	References
Israel (Tel Shikmona)	Wet	1992–1998		34.3				Herut et al. (1999)
	Wet + dry	1996–1998		88.3	39%			Herut et al. (2002)
Turkey (Erdemli)	Wet	1996–1997		16.4				Özsoy (2003)
	Wet + dry	1999		60.1				Markaki et al. (2003)
		1999–2007		88.0	51%			Koçak et al. (2010)
		2014–2015	57.8	37.3	63%	20.5	29% (wet) 46% (dry)	Nehir and Koçak (2018)
Turkey (Akkuyu)	Bulk	2001–2002		30.6				Markaki et al. (2010)
Crete Isl. (Finokalia)	Wet + dry	1996–1999		38.4				Kouvarakis et al. (2001)
		1999		38.3	63%			Markaki et al. (2003)
		1999–2005	60.8					Theodosi et al. (2019)
		2003–2006	66.2	44.0	32%	22.2		Violaki et al. (2010)
	Bulk	2001–2002		39.3				Markaki et al. (2010)
Malta Isl. (Gozo)	Bulk	2002–2003		46.1				
Mahdia (Tunisia)	Bulk	2001–2002		18.1				
Corsica Isl. (Bavella)	Bulk	1984–1986		52.2				Loÿe-Pilot et al. (1990)
Corsica Isl. (Ostriconi)	Bulk	2001–2002		25.4				Markaki et al. (2010)
Corsica Isl. (Cap Cuittone)	Bulk	2009–2011		10.2	84%			Desboeufs et al. (2018)
Sardinia Isl. (Capo Carbonara)	Wet + dry	1991–1994		17.2				Guerzoni et al. (1995)
France (Cap Ferrat)	Dry	2004–2005	60.2	43.1		17.2	28%	Sandroni et al. (2007)
France (Frioul Isl.)	Bulk	2015–2016	40.0	23.6		16.4	41%	Djaoudi et al. (2018)
France (Cap Bear)	Bulk	2001–2002		45.9				Markaki et al. (2010)

(continued)

Table 1 (continued)

Location	Type of deposition	Period	TDN fluxes	DIN fluxes	DIN wet/ total	DON fluxes	DON/TDN	References
Spain (Montseny)	Bulk	1983–2000		40.2				Avila and Rodà (2002)
		19,832,009		42.0				
		2012–2013	65.9	43.7		22.2	34%	Izquieta-Rojano et al. (2016)
Spain (Sierra Nevada)	Wet + dry	2000–2002	42.0					Morales-Baquero et al. (2013)
		2004–2005	24.4					Morales-Baquero and Pérez-Martínez (2016)
Algeria (Annaba)	Wet	2014	17.8	14.4		3.43	19%	Ounissi et al. (2018)
Average (for bulk and total)			*46.9 ±18.8*	*40.7 ±20.5*		*17.0 ± 7.9*		

Averages are calculated from bulk and total deposition data for total dissolved, dissolved inorganic and dissolved organic nitrogen (TDN, DIN and DON, respectively)

of gaseous species or by scavenging of atmospheric N-organic containing aerosols. The majority of studies focused only on the dissolved organic nitrogen (DON or WSON (water-soluble organic nitrogen)) (Mace et al., 2003; Violaki & Mihalopoulos, 2010; Violaki et al., 2010, 2015; Izquieta-Rojano et al., 2016; Nehir & Koçak, 2018; Djaoudi et al., 2018). DON is usually estimated from the difference between the total dissolved N (TDN) content of precipitation and the inorganic N (DIN), a process which can lead to large uncertainties. Some data are also available on the speciation of N-organic compounds, such as urea, amines or free amino acids (mainly glycine), but these generally only contribute a small proportion of the organic N fraction (Mace et al., 2003; Violaki & Mihalopoulos, 2010). Available data indicate a variety of sources of organic nitrogen, both of natural and anthropogenic origin, such as fossil fuel and biomass burning (Violaki & Mihalopoulos, 2010) and agricultural activities, notably by resuspension of cultivated soil (Nehir & Koçak, 2018) or pollutants generated in metropolitan areas (Izquieta-Rojano et al., 2016). Indeed, the aerosol-associated DON concentrations obtained in Mediterranean are usually higher than the ones found in the open ocean (Amsterdam Island, Barbados, Pacific Ocean, etc.) due to the anthropogenic influence in comparison to marine emissions (Nehir & Koçak, 2018). Since the Mediterranean Sea is heavily impacted by mineral dust deposition originating from Sahara and Middle East deserts, the potential origin of DON from dust deposition was studied (generally via the relation between DON and no-sea-salt-Ca^{2+} fluxes). Several observations support desert dust as a main source of DON, both in the western and eastern Mediterranean, notably during spring (Mace et al., 2003;

Table 2 Annual deposition fluxes of phosphorus (total phosphorus (TP) including particulate (TPP) and dissolved (TDP), total inorganic phosphorus (TIP) and dissolved organic (DOP) and inorganic (DIP) phosphorus) reported for the Mediterranean basin (mmol m^{-2} yr^{-1}), adapted and completed after Violaki et al. (2018). The period is indicative given that years are not always complete (e.g., the observation period of Guieu et al. (2010) is 12 months from June 2001 to May 2002)

Location	Period	Wet	Dry	Total	Wet / Total	References
TP						
Spain (Sierra Nevada)	2000–2001	0.37	0.22	0.58	63%	Morales-Baquero et al. (2013)
	2000			0.15		
	2001–2002	0.14	0.37	0.51	28%	Morales-Baquero et al. (2006)
	2004–2005	0.42	0.26	0.68	61%	Morales-Baquero and Pérez-Martínez (2016)
France (Cap Ferrat)	1997–1998	0.16				Migon and Sandroni (1999)
NW Corsica Isl., France (Capo Cavallo)	1986–1987			1.29		Bergametti et al. (1992)
W Corsica Isl., France (Cap Cuittone)	2008–2011			4.81	49%	Desboeufs et al. (2018)
Crete Isl., Greece (Finokalia)	2012–2013	1.05	1.03	2.07	50%	Violaki et al. (2018)
Morocco (Cap Spartel)	2001–2002			1.07		Guieu et al. (2010)
France (Cap Béar)				1.20		
Corsica Isl., France (Ostriconi)				1.36		
Tunisia (Mahdia)				1.52		
Crete Isl., Greece (Finokalia)				0.42		
Lebos Isl., Greece (Mytilene)				0.52		
Turkey (Akkuyu)				1.07		
Cyprus Isl. (Cavo Greco)				0.61		
Egypt (Alexandria)				1.23		
TPP						
Spain (Montseny, NE)	2002–2003	0.29	0.29	0.58	50%	Izquierdo et al. (2012)
Spain (Can Llompart, Mallorca Isl.)	2010–2012	0.15	0.45	0.60	25%	Cerro et al. (2020)
France (Cap Ferrat)	1997–1998	0.07				Migon and Sandroni (1999)
Crete Isl. (Finokalia)	2012–2013	0.23	0.34[a]	0.57[a]		Violaki et al. (2018)
TDP						

(continued)

Table 2 (continued)

Location	Period	Wet	Dry	Total	Wet / Total	References
France (Cap Ferrat)	1997–1998	0.10				Migon and Sandroni (1999)
France (Frioul Isl.)	2015–2016			0.39		Djaoudi et al. (2018)
France (Cap Béar)	2005–2011			2.16		Violaki et al. (2018)
Crete Isl. (Finokalia)	2012	0.81	0.69[a]	1.6	51%	Violaki et al. (2018)
TIP						
France (Cap Béar)	2005–2011			1.22		Violaki et al. (2018)
Crete Isl. (Finokalia)	2012–2013	0.21	0.39[a]	0.6	35%	Violaki et al. (2018)
Israel (Tel Shikmona)	1995–1998	0.29	1.0	1.29	22%	Herut et al. (2002)
DOP						
France (Frioul Isl.)	2015–2016			0.07		Djaoudi et al. (2018)
France (Cap Béar)	2005–2011			0.94		Violaki et al. (2018)
Crete Isl. (Finokalia)	2012–2013	0.7	0.46[a]	1.16	60%	Violaki et al. (2018)
DIP or PO_4^{3-}						
Annaba, Algeria	2014	0.88				Ounissi et al. (2018)
Sierra Nevada, Spain[b]	2000–2001	0.15	0.04	0.18	80%	Morales-Baquero et al. (2013)
France (Cap Béar)	2001–2002			0.62		Markaki et al. (2010)
	2005–2011			0.48		Violaki et al. (2018)
France (Cap Ferrat)	1997–1998	0.16				Migon and Sandroni (1999)
	2010–2011−2013	0.11	0.63	0.74	15%	Pasqueron de Fommervault et al. (2015)
Corsica Isl. (Ostriconi)	2001–2003			0.45		Markaki et al. (2010)
Crete Isl. (Finokalia)	1999–2000	0.07	0.13	0.19	37%	Markaki et al. (2003)
	2001–2003	0.076[c]	0.124[c]	0.29	38%	Markaki et al. (2010)
	2012	0.03	0.13[a]	0.16	19%	Violaki et al. (2018)
	2013	0.09	0.03[a]	0.12	75%	
Erdemli (Turkey)	1996–1997	0.31				Özsoy (2003)
	1999		0.17			Markaki et al. (2003)
	1999–2007	0.34	0.22	0.56	61%	Koçak et al. (2010)

[a]Measured only for dry periods
[b]As soluble reactive phosphorus (SRP)
[c]Only for 2001–2002

Violaki et al., 2010; Pulido-Villena et al., 2008; Nehir & Koçak, 2018). Organic nitrogen might either be due to (a) mineral-dust-borne microorganisms and/or (b) interaction (e.g., adsorption or acid-based reaction) between mineral dust and organic nitrogen compounds (Mace et al., 2003; Rahav et al., 2016; Nehir & Koçak, 2018). However, these observations contrast with Djaoudi et al. (2018) who reported the atmospheric fluxes of DON, soluble organic carbon and phosphorus are minimal during Saharan rain events. Maximum values occurred when a combination of

anthropogenic influence and heavy precipitation occurred. The rain effect is also proposed by Morales-Baquero and Pérez-Martínez (2016), who observed a low contribution of dust deposition to N inputs during the weeks without rain. Izquieta-Rojano et al. (2016) found no clear correlation with DON and nss-Ca^{2+} in mountain sites, whereas a positive correlation was observed for a site near Barcelona, suggesting influence of dust deposition could be due to the altitude of transport of Saharan air masses. Finally, the contribution of each source (anthropogenic and natural) defines the distribution of DON between coarse and fine fractions. A recent study in the eastern Mediterranean reports that DON is mainly associated, at 66%, with the coarse fraction of aerosols on Turkish coasts (Nehir & Koçak, 2018), while only 32% of WSON was attributed to this fraction in Crete (Violaki & Mihalopoulos, 2010).

Annual deposition of total dissolved N (TDN) in remote sites varies from 22 to 72 mmol m^{-2} yr^{-1}, the highest values being obtained close to or under anthropogenic influence (Table 1). It is also probably the case for the high values observed in Cap Ferrat and Finokalia (Sandroni et al., 2007; Theodosi et al., 2019), in agreement with modelling studies which show a spatial distribution of N deposition fluxes reflecting emission distribution, with higher deposition over the coastal regions (Im et al., 2013; Richon et al., 2018a). Thus, inter-seasonal spatial variability of this deposition is low, most of the mass being deposited in the northern part of the basin (Richon et al., 2018a). The average TDN flux is 51.0 ± 15.9 mmol m^{-2} yr^{-1}, for the whole Mediterranean, including all the available measurements between 1990 and 2011. DIN is generally the major contributor of the N-fluxes ranging from 10 to 54 mmol m^{-2} yr^{-1}, whereas DON is typically around 20 mmol m^{-2} yr^{-1}, representing between 12% and 80% of total fluxes depending on the study area, and around 30% on average (Table 1). The low values of DIN flux in Corsica (10.2 mmol m^{-2} yr^{-1}; Desboeufs et al., 2018) and in Sardinia (17.1 mmol m^{-2} yr^{-1}; Guerzoni et al., 1995) could be due to a very low estimation of dry gaseous deposition. However, Desboeufs et al. (2018) hypothesized that the low value obtained recently in the coast of Corsica might be connected to the European decrease of N deposition owing to mitigation. This assumption agrees with the decreasing trend observed on DIN fluxes in the Eastern Mediterranean (e.g., by 45% in Erdemli between 2000 and 2015; Nehir & Koçak, 2018). More generally, since the 1990s, a constant decline of the atmospheric deposition fluxes of DIN over the whole Mediterranean has been observed in modelling approaches (Moon et al., 2016; Christodoulaki et al., 2016) in agreement with the decreasing trend in pollutant nitrogen emissions in Europe (Theobald et al., 2019).

NO_3^- fluxes typically dominate the DIN fluxes (e.g., Violaki & Mihalopoulos, 2010). An explanation for the highest fluxes of NO_3^- in comparison to NH_4^+ is the importance of dry deposition together with the presence of NO_3^- mainly in the coarse mode of particles (Herut et al., 2001; Violaki et al., 2010). In the eastern Mediterranean, the atmospheric fluxes of DON and NO_3^- are of the same order of magnitude (around 10 mmol m^{-2} yr^{-1}) and independent of the pathway of deposition. The highest fluxes of NH_4^+ (14 mmol m^{-2} yr^{-1}) are mainly associated with wet deposition, which represents 92% of total flux (Nehir & Koçak, 2018). This trend is

also observed in the western Mediterranean basin in remote environments, with comparable fluxes of NO_3^- and DON and lower fluxes of NH_4^+ (Izquieta-Rojano et al., 2016). Wet TN and NO_3^- deposition dominates the total fluxes in southern Spain, but it could be due to an underestimation of dry deposition of gaseous N species by dry collectors (Morales-Baquero et al., 2013; Morales-Baquero & Pérez-Martínez, 2016). Wet scavenging also appears to be the main deposition pathway in Corsica as suggested by the observed increase in the annual DIN flux with the annual rainfall at a given site (Loÿe-Pilot et al., 1990; Desboeufs et al., 2018). Wet deposition is also reported to strongly dominate (79%) the NO_3^- deposition flux in Mallorca, which is mainly associated with air masses of European origin or stagnant over the basin (Cerro et al., 2020). In the eastern basin, the situation is contrasted: in Turkey, the wet DIN deposition is dominant on the total deposition of inorganic nitrogen species (Markaki et al., 2003; Nehir & Koçak, 2018). On the Israeli coast and in Crete, dry deposition predominates and wet deposition represents less than 40% of the total deposition of particulate nitrogen species, except in winter (Herut et al., 2002; Markaki et al., 2003; Violaki et al., 2010). Over the East Mediterranean, wet deposition fluxes of TN are less than half the dry deposition with maxima in winter and minima in summer (Im et al., 2013), due to the rainfall regime in this area. At the scale of Mediterranean, observations (Kouvarakis et al., 2001; Violaki et al., 2010; Desboeufs et al., 2018) and models (Im et al., 2013; Richon et al., 2017) show that the dry deposition of DIN has higher values during summer and lower values during winter, whereas a maximum of wet deposition of DIN is observed in winter.

3 Phosphorus Fluxes

As for nitrogen, deposited atmospheric phosphorus is measured in both dissolved and particulate pools and in organic and inorganic forms. Traditional terms for P chemical forms include total phosphorus (TP), in both dissolved (TDP) and particulate fractions (TPP), TIP (total inorganic phosphorus) or also TRP (total reactive inorganic phosphorus), DIP (dissolved inorganic phosphorus), also referenced as phosphate (PO_4^{3-}) or SRP (soluble reactive phosphorus) according to the used analytical methods, TOP (total organic phosphorus) and DOP (dissolved organic phosphorus). TRP and SRP correspond to the analysis of phosphorus using the molybdenum blue colorimetric method in unfiltered and filtered samples, respectively. Inorganic phosphorus or phosphate is obtained either by ion chromatography or by stannous chloride colorimetry method. Organically bound phosphorus is generally estimated in soluble (DOP) and total matter (TOP) by subtracting TIP from TDP and TP, respectively. Those notably include nucleic acids, phospholipids, organo-phosphate pesticides, phosphoamines and organic phosphates condensed on particle-associated forms (Karl & Björkman, 2015). Inorganic P species are considered as the bioavailable P forms, and they have been mainly measured in atmospheric deposition over Mediterranean (Bergametti et al.,

1992; Herut et al., 1999, 2002; Migon & Sandroni, 1999; Markaki et al., 2003, 2010; Özsoy, 2003; Morales-Baquero et al., 2006, 2013; Izquierdo et al., 2012; Pasqueron de Fommervault et al., 2015; Desboeufs et al., 2018; Violaki et al., 2018; Theodosi et al., 2019; Cerro et al., 2020). Recent works focused on organic phosphorus in order to estimate the contribution of these compounds in the P cycle and as source of P for marine biosphere (Markaki et al., 2010; Violaki et al., 2018; Djaoudi et al., 2018).

Phosphorus in the atmosphere is predominantly in the forms of aerosols, even if gaseous phosphorus compounds exist, as organophosphate pesticides or ester flame retardants (Castro-Jiménez et al., 2016; Degrendele et al., 2016). The major sources of P in aerosols are combustion processes, such as incinerator, coal/oil combustion and biomass burning in heavily industrialized areas whereas mineral dust dominates the atmospheric phosphorus budget close to desert source areas (Mahowald et al., 2008). At the scale of Mediterranean, Richon et al. (2018b) showed combustion to be a more important source of atmospheric phosphate at the basin scale than natural dust. In consequence, the distribution of P between coarse and fine mode, and hence the deposition rate, depends on the contribution of each source (Markaki et al., 2003; Morales-Baquero et al., 2013). Few data exist on phosphorus aerosol concentrations and sources in Mediterranean, because it is rarely measured in aerosol characterization studies (e.g., Calzolai et al., 2015; Arndt et al., 2017). Starting with Bergametti et al. (1992), most studies about atmospheric P and its sources in the Mediterranean refer to P deposition measurements.

The total phosphorus deposition flux measured in the northwestern Mediterranean (Table 2) varied from 0.5 mmol m^{-2} yr^{-1} in SE Spain (Morales-Baquero et al., 2006) to 1.3–4.8 mmol m^{-2} yr^{-1} in NW Corsica (Bergametti et al., 1992; Desboeufs et al., 2018). Phosphorus atmospheric deposition is estimated at ~0.5 mmol m^{-2} yr^{-1} in the eastern Mediterranean (Herut & Krom, 1996; Carbo et al., 2005), but 2 mmol m^{-2} yr^{-1} was measured in Crete (Violaki et al., 2018). An average around 1 mmol m^{-2} yr^{-1} on all the Mediterranean basins is calculated by Guieu et al. (2010) from the results of the ADIOS network. The ADIOS data set allows to compare the DIP deposition over the same period at various sites across the Mediterranean basin: it shows that the annual deposition fluxes range from 0.24 (in Crete) to 0.61 (in Spain) mmol m^{-2} yr^{-1} (Guieu et al., 2010; Markaki et al., 2010). It also suggests that the deposition fluxes could be higher in the western part of the basin, maybe due to higher anthropogenic emissions. This trend is confirmed by the individual measurements over the basin, with typically the highest fluxes observed in the Western part, except in Turkey (Table 2). The anthropogenic deposition of TP and DIP predominates the annual fluxes whatever the location in Mediterranean, representing sometimes more than 75% of annual fluxes (Bergametti et al., 1992; Migon et al., 2001; Markaki et al., 2003; Guieu et al., 2010; Desboeufs et al., 2018). The role of biomass burning, including incinerators, is pointed as a major combustion source based on the correlation between phosphorus and K^+ in deposition samples (Markaki et al., 2010; Desboeufs et al., 2018). The predominance of anthropogenic phosphate is particularly visible over the northern basin (Adriatic and Aegean seas in particular). For these regions in the vicinity of anthropogenic sources, P deposition from combustion sources has a low variability, whereas P deposition associated with dust

occurs during transient events and is therefore highly variable on a monthly basis (Richon et al., 2018a, b). Indeed, the dust deposition is also found to significantly contribute to the fluxes of total P due to the intense but sporadic inputs, reaching more than 50% of TP fluxes during dust events (Bergametti et al., 1992; Herut et al., 2002; Özsoy, 2003; Morales-Baquero & Pérez-Martínez, 2016; Desboeufs et al., 2018). Thus, the total P fluxes by dry deposition shows a seasonal pattern similar to Saharan dust export over the Mediterranean, with a minimum during winter and maximum during spring-summer, meaning that dust intrusion is the main factor controlling dry deposition of P (Markaki et al., 2010; Morales-Baquero & Pérez-Martínez, 2016). The ratio DIP/TIP is lower than 0.3 in wet deposition during dust intrusions, whereas it is higher than 0.35 without dust influence (Herut et al., 2002; Markaki et al., 2010). This low solubility of P in dust limits the impact of dust deposition on the fluxes of DIP (Ridame & Guieu, 2002; Markaki et al., 2003), and DIP fluxes are similar in wet deposition influenced or not by dust (Özsoy, 2003). Longo et al. (2014) showed that aerosols from Europe deliver more soluble P in comparison to North African aerosols, meaning that these aerosols are a significant source of soluble phosphorus to the Mediterranean Sea. No specific pathway of deposition seems to dominate the total phosphorus fluxes (Table 2). Wet deposition contributes 15 to 80% of DIP fluxes for the different sites (Table 2). This variability is also observed for the same site, with a contribution of wet deposition being 19% in 2012 and 75% in 2013 in Finokalia (Violaki et al., 2018). This high variability could be explained by the inter-annual variability of wet dust deposition (Markaki et al., 2003). In terms of seasonal variability, the lowest values for TIP and DIP fluxes are observed in winter, during wet periods, both in the western and eastern part of Mediterranean (Bergametti et al., 1992; Markaki et al., 2003; Morales-Baquero & Pérez-Martínez, 2016).

The fluxes of DOP range from 0.07 to 1.16 mmol m^{-2} yr^{-1} in Frioul Island and Crete, respectively. This large range shows higher values in Crete in comparison to measurements on the French coast (Table 2) due to larger sources of organic P species in the eastern basin (Violaki et al., 2018). The main organic source could be pollen deposition (Morales-Baquero & Pérez-Martínez, 2016). However, the contribution of soluble organic forms on TDP shows a very high inter-annual variability for a specific site: the DOP/TDP ranges from 38% in 2001–2002 to 90% in 2012–2013 in Crete (Markaki et al., 2010; Violaki et al., 2018). However, no clear spatial variability of DOP contribution is observed from ADIOS results (Markaki et al., 2010). Nevertheless, it is difficult to bring robust conclusions on DOP contribution since the dataset is limited and shows large inter-annual variability (Violaki et al., 2018).

4 Conclusion and Recommendations

The importance of atmospheric deposition for the biogeochemical cycling of N and P in the Mediterranean spurred several long time-series of nutrient deposition measurements across the basin, some of which are 30 years old. The results

emphasize no clear long-term trend for P but a decreasing trend for DIN fluxes possibly associated with anthropogenic emission mitigation. However, it is difficult to analyse long-term trends due to the uncertainties in N measurements. The usual devices to measure N deposition still neglect the gaseous part of nitrogen by dry deposition, which could be a significant form of atmospheric input of N in Mediterranean systems due to NO_x concentrations (Àvila & Rodà, 2012). The synopsis of survey data is complicated by a strong dependence of the results on sampling and analytical methods. Hence, we encourage the definition of common procedures for sampling between the different long time-series sites, as it is the case of the harmonized method for monitoring of air pollution effects on European forests (http://icp-forests.net/; last access 07 July 2022). In spite of recent efforts to estimate the deposition of organic forms, the data on organic nutrient deposition are still fragmented. The contribution of organic forms is often similar to, or even higher than, the inorganic fraction in the total deposition, both for N and P. However, the exact source of these organic forms remains unresolved, notably as the analytical work on chemical speciation is very complex. Thus, the lack of data constitutes another factor that greatly increases the uncertainties and hinders our knowledge of the nitrogen and phosphorus cycles in this region. The literature is slowly growing in studies addressing organic deposition in the Mediterranean basin, but these efforts need to be continued.

A high inter-annual variability is observed in N and P fluxes in all Mediterranean locations. This variability is mainly linked both to the frequency of dust intrusion and of precipitation. If dust deposition controls in part the highest fluxes of N and P, the results show the importance of anthropogenic inputs on the annual fluxes. The contribution of anthropogenic sources is the major factor playing on the spatial variability of nutrient fluxes, but no clear north-south or longitudinal gradient is observed. The variability between measurement sites is usually related to the vicinity of local anthropogenic sources or to anthropogenically influenced air masses. The temporal dynamics of marine N and P concentrations since 1985 show a high sensitivity to anthropogenic atmospheric deposition and are expected to decline in the coming decades due to pollutant emissions mitigation/control (Moon et al., 2016). The regulation of emissions of anthropogenic nutrients could be a key driver affecting seawater nutrient cycles and hence the marine ecosystem in the future. However, atmospheric trace metal sources and effects need to be taken into account as well to provide high-quality projections in a context of future changes. Modelling is the optimal method to differentiate spatial and temporal variations of anthropogenic deposition. However, the quantification of the atmospheric nutrient deposition over the Mediterranean basin has still to be taken with caution. Aerosol and dust atmospheric transport and deposition simulations differ widely from model to model, regarding the total mass of nutrient deposition and its spatial and temporal structure (Basart et al., 2016). The observational time series are spatially spotty and tend to exist for short time periods. We underline the need for more deposition measurements in order to better constrain the modelling of such important nutrient sources for the Mediterranean.

References

Arndt, J., Sciare, J., Mallet, M., Roberts, G. C., Marchand, N., Sartelet, K., Sellegri, K., Dulac, F., Healy, R. M., & Wenger, J. C. (2017). Sources and mixing state of summertime background aerosol in the north-western Mediterranean basin. *Atmospheric Chemistry and Physics, 17*, 6975–7001. https://doi.org/10.5194/acp-17-6975-2017

Avila, A. (1996). Time trends in the precipitation chemistry at a mountain site in northeastern Spain for the period 1983–1994. *Atmospheric Environment, 30*, 1363–1373. https://doi.org/10.1016/1352-2310(95)00472-6

Avila, A., & Rodà, F. (2002). Assessing decadal changes in rainwater alkalinity at a rural Mediterranean site in the Montseny Mountains (NE Spain). *Atmospheric Environment, 36*, 2881–2890. https://doi.org/10.1016/S1352-2310(02)00098-5

Àvila, A., & Rodà, F. (2012). Changes in atmospheric deposition and streamwater chemistry over 25 years in undisturbed catchments in a Mediterranean mountain environment. *The Science of the Total Environment, 434*, 18–27. https://doi.org/10.1016/j.scitotenv.2011.11.062

Bardouki, H., Liakakou, H., Economou, C., Sciare, J., Smolik, J., Zdimal, V., Eleftheriadis, K., Lazaridis, M., Dye, C., & Mihalopoulos, N. (2003). Chemical composition of size-resolved atmospheric aerosols in the eastern Mediterranean during summer and winter. *Atmospheric Environment, 37*, 195–208. https://doi.org/10.1016/S1352-2310(02)00859-2

Bartoli, G., Migon, C., & Losno, R. (2005). Atmospheric input of dissolved inorganic phosphorus and silicon to the coastal northwestern Mediterranean Sea: Fluxes, variability and possible impact on phytoplankton dynamics. *Deep Sea Research Part I: Oceanographic Research Papers, 52*, 2005–2016. https://doi.org/10.1016/j.dsr.2005.06.006

Basart, S., Dulac, F., Baldasano, J. M., Nabat, P., Mallet, M., Solmon, F., Laurent, B., Vincent, J., Menut, L., Amraoui, L. E., Sic, B., Chaboureau, J.-P., Léon, J.-F., Schepanski, K., Renard, J.-B., Ravetta, F., Pelon, J., Di Biagio, C., Formenti, P., … Attié, J.-L. (2016). Extensive comparison between a set of European dust regional models and observations in the western Mediterranean for the summer 2012 pre-ChArMEx/TRAQA campaign. In D. G. Steyn & N. Chaumerliac (Eds.), *Air pollution modeling and its application XXIV* (pp. 79–83). Springer. https://doi.org/10.1007/978-3-319-24478-5_13

Bergametti, G., Remoudaki, E., Losno, R., Steiner, E., Chatenet, B., & Buat-Ménard, P. (1992). Sources, transport and deposition of atmospheric phosphorus over the northwestern Mediterranean. *Journal of Atmospheric Chemistry, 14*, 501–513. https://doi.org/10.1007/BF00115254

Bressac, M., Guieu, C., Doxaran, D., Bourrin, F., Desboeufs, K., Leblond, N., & Ridame, C. (2014). Quantification of the lithogenic carbon pump following a simulated dust-deposition event in large mesocosms. *Biogeosciences, 11*, 1007–1020. https://doi.org/10.5194/bg-11-1007-2014

Calzolai, G., Nava, S., Lucarelli, F., Chiari, M., Giannoni, M., Becagli, S., Traversi, R., Marconi, M., Frosini, D., Severi, M., Udisti, R., di Sarra, A., Pace, G., Meloni, D., Bommarito, C., Monteleone, F., Anello, F., & Sferlazzo, D. M. (2015). Characterization of PM_{10} sources in the central Mediterranean. *Atmospheric Chemistry and Physics, 15*, 13939–13955. https://doi.org/10.5194/acp-15-13939-2015

Carbo, P., Krom, M. D., Homoky, W. B., Benning, L. G., & Herut, B. (2005). Impact of atmospheric deposition on N and P geochemistry in the southeastern Levantine basin. *Deep Sea Research Part II: Topical Studies in Oceanography, 52*, 3041–3053. https://doi.org/10.1016/j.dsr2.2005.08.014

Castro-Jiménez, J., González-Gaya, B., Pizarro, M., Casal, P., Pizarro-Álvarez, C., & Dachs, J. (2016). Organophosphate ester flame retardants and plasticizers in the global oceanic atmosphere. *Environmental Science & Technology, 50*, 12831–12839. https://doi.org/10.1021/acs.est.6b04344

Cerro, J. C., Cerdà, V., Caballero, S., Bujosa, C., Alastuey, A., Querol, X., & Pey, J. (2020). Chemistry of dry and wet atmospheric deposition over the Balearic Islands, NW Mediterranean:

Source apportionment and African dust areas. *Science of The Total Environment, 747*, 141187. https://doi.org/10.1016/j.scitotenv.2020.141187

Christodoulaki, S., Petihakis, G., Kanakidou, M., Mihalopoulos, N., Tsiaras, K., & Treiantafyllou, G. (2013). Atmospheric deposition in the Eastern Mediterranean. A driving force for ecosystem dynamics. *Journal of Marine Systems, 109–110*, 78–93. https://doi.org/10.1016/j.jmarsys.2012.07.007

Christodoulaki, S., Petihakis, G., Mihalopoulos, N., Tsiaras, K., Triantafyllou, G., & Kanakidou, M. (2016). Human-driven atmospheric deposition of N and P controls on the East Mediterranean marine ecosystem. *Journal of the Atmospheric Sciences, 73*, 1611–1619. https://doi.org/10.1175/JAS-D-15-0241.1

Degrendele, C., Okonski, K., Melymuk, L., Landlová, L., Kukučka, P., Audy, O., Kohoutek, J., Čupr, P., & Klánová, J. (2016). Pesticides in the atmosphere: A comparison of gas-particle partitioning and particle size distribution of legacy and current-use pesticides. *Atmospheric Chemistry and Physics, 16*, 1531–1544. https://doi.org/10.5194/acp-16-1531-2016

Desboeufs, K., Bon Nguyen, E., Chevaillier, S., Triquet, S., & Dulac, F. (2018). Fluxes and sources of nutrient and trace metal atmospheric deposition in the northwestern Mediterranean. *Atmospheric Chemistry and Physics, 18*, 14477–14492. https://doi.org/10.5194/acp-18-14477-2018

Djaoudi, K., Van Wambeke, F., Barani, A., Hélias-Nunige, S., Sempéré, R., & Pulido-Villena, E. (2018). Atmospheric fluxes of soluble organic C, N, and P to the Mediterranean Sea: Potential biogeochemical implications in the surface layer. *Progress in Oceanography, 163*, 59–69. https://doi.org/10.1016/j.pocean.2017.07.008

Guerzoni, S., Landuzzi, W., Lenaz, R., Quarantotto, G., Rampazzo, G., Molinaroli, E., Turetta, C., Visin, F., Cesari, G., & Cristini, S. (1993). Fluxes of soluble and insoluble metals and nutrients from the atmosphere to the central Mediterranean Sea. In J.-M. Martin & H. Barth (Eds.), *Water pollution research report 30: EROS 2000 fourth workshop on the North-West Mediterranean Sea* (pp. 253–260). Commission of the European Communities.

Guerzoni, S., Cristini, A., Caboi, R., Le Bolloch, O., Marras, I., & Rundeddu, L. (1995). Ionic composition of rainwater and atmospheric aerosols in Sardinia, southern Mediterranean. *Water Air and Soil Pollution, 85*, 2077–2082. https://doi.org/10.1007/BF01186140

Guieu, C., Loÿe-Pilot, M. D., Benyahya, L., & Dufour, A. (2010). Spatial variability of atmospheric fluxes of metals (Al, Fe, Cd, Zn and Pb) and phosphorus over the whole Mediterranean from a one-year monitoring experiment: Biogeochemical implications. *Marine Chemistry, 120*, 164–178. https://doi.org/10.1016/j.marchem.2009.02.004

Guieu, C., Ridame, C., Pulido-Villena, E., Bressac, M., Desboeufs, K., & Dulac, F. (2014). Impact of dust deposition on carbon budget: A tentative assessment from a mesocosm approach. *Biogeosciences, 11*, 5621–5635. https://doi.org/10.5194/bg-11-5621-2014

Herut, B., & Krom, M. (1996). Atmospheric input of nutrients and dust to the SE Mediterranean. In S. Guerzoni & R. Chester (Eds.), *The impact of desert dust across the Mediterranean* (Environmental science and technology library) (Vol. 11, pp. 349–358). Springer. https://doi.org/10.1007/978-94-017-3354-0_35

Herut, B., Krom, M. D., Pan, G., & Mortimer, R. (1999). Atmospheric input of nitrogen and phosphorus to the Southeast Mediterranean: Sources, fluxes, and possible impact. *Limnology and Oceanography, 44*, 1683–1692. https://doi.org/10.4319/lo.1999.44.7.1683

Herut, B., Nimmo, M., Medway, A., Chester, R., & Krom, M. D. (2001). Dry atmospheric inputs of trace metals at the Mediterranean coast of Israel (SE Mediterranean): Sources and fluxes. *Atmospheric Environment, 35*, 803–813. https://doi.org/10.1016/S1352-2310(00)00216-8

Herut, B., Collier, R., & Krom, M. D. (2002). The role of dust in supplying nitrogen and phosphorus to the Southeast Mediterranean. *Limnology and Oceanography, 47*, 870–878. https://doi.org/10.4319/lo.2002.47.3.0870

Im, U., Christodoulaki, S., Violaki, K., Zarmpas, P., Kocak, M., Daskalakis, N., Mihalopoulos, N., & Kanakidou, M. (2013). Atmospheric deposition of nitrogen and sulfur over southern Europe with focus on the Mediterranean and the Black Sea. *Atmospheric Environment, 81*, 660–670. https://doi.org/10.1016/j.atmosenv.2013.09.048

Izquierdo, R., Benítez-Nelson, C. R., Masqué, P., Castillo, S., Alastuey, A., & Àvila, A. (2012). Atmospheric phosphorus deposition in a near-coastal rural site in the NE Iberian Peninsula and its role in marine productivity. *Atmospheric Environment, 49*, 361–370. https://doi.org/10.1016/j.atmosenv.2011.11.007

Izquieta-Rojano, S., García-Gomez, H., Aguillaume, L., Santamaría, J. M., Tang, Y. S., Santamaría, C., Valiño, F., Lasheras, E., Alonso, R., Àvila, A., Cape, J. N., & Elustondo, D. (2016). Throughfall and bulk deposition of dissolved organic nitrogen to holm oak forests in the Iberian Peninsula: Flux estimation and identification of potential sources. *Environmental Pollution, 210*, 104–112. https://doi.org/10.1016/j.envpol.2015.12.002

Karl, D. M., & Björkman, K. M. (2015). Chapter 5 - Dynamics of dissolved organic phosphorus. In D. A. Hansell & C. A. Carlson (Eds.), *Biogeochemistry of marine dissolved organic matter* (2nd ed., pp. 233–334). Academic Press. https://doi.org/10.1016/B978-0-12-405940-5.00005-4

Koçak, M., Kubilay, N., Tugrul, S., & Mihalopoulos, N. (2010). Atmospheric nutrient inputs to the northern levantine basin from a long-term observation: Sources and comparison with riverine inputs. *Biogeosciences, 7*, 4037–4050. https://doi.org/10.5194/bg-7-4037-2010

Kouvarakis, G., Mihalopoulos, N., Tselepides, A., & Stavrakakis, S. (2001). On the importance of atmospheric inputs of inorganic nitrogen species on the productivity of the eastern Mediterranean Sea. *Global Biogeochemical Cycles, 15*, 805–817. https://doi.org/10.1029/2001GB001399

Lazzari, P., Solidoro, C., Salon, S., & Bolzon, G. (2016). Spatial variability of phosphate and nitrate in the Mediterranean Sea: A modeling approach. *Deep Sea Research Part I: Oceanographic Research Papers, 108*, 39–52. https://doi.org/10.1016/j.dsr.2015.12.006

Le Bolloch, O., & Guerzoni, S. (1995). Acid and alkaline deposition in precipitation on the Western coast of Sardinia, Central Mediterranean (40° N, 8° E). *Water, Air, and Soil Pollution, 85*, 2155–2160. https://doi.org/10.1007/BF01186153

Lequy, E., Avila, A., Boudiaf Nait Kaci, M., & Turpault, M.-P. (2018). Atmospheric deposition of particulate matter between Algeria and France: Contribution of long and short-term sources. *Atmospheric Environment, 191*, 181–193. https://doi.org/10.1016/j.atmosenv.2018.08.013

Longo, A. F., Ingall, E. D., Diaz, J. M., Oakes, M., King, L. E., Nenes, A., Mihalopoulos, N., Violaki, K., Avila, A., Benitez-Nelson, C. R., Brandes, J., McNulty, I., & Vine, D. J. (2014). P-NEXFS analysis of aerosol phosphorus delivered to the Mediterranean Sea. *Geophysical Research Letters, 41*, 4043–4049. https://doi.org/10.1002/2014GL060555

Loÿe-Pilot, M. D., & Morelli, J. (1988). Fluctuations of ionic composition of precipitations collected in Corsica related to changes in the origins of incoming aerosols. *Journal of Aerosol Science, 19*, 577–585. https://doi.org/10.1016/0021-8502(88)90209-1

Loÿe-Pilot, M. D., Martin, J. M., & Morelli, J. (1990). Atmospheric input of inorganic nitrogen to the Western Mediterranean. *Biogeochemistry, 9*, 117–134. https://doi.org/10.1007/BF00692168

Loÿe-Pilot, M.-D., Guieu, C., Klein, C., Mihalopoulos, N., Ridame, C., Dufour, A., Kouvarakis, G., Markaki, Z., & Oikonomou, C. (2005). Les apports atmosphériques en milieu méditerranéen nord occidental et leur évolution. Etude dans la Réserve de Biosphère du Fango. *Travaux scientifiques du Parc naturel régional et des réserves naturelles de Corse, 62*, 29–40.

Mace, K. A., Kubilay, N., & Duce, R. A. (2003). Organic nitrogen in rain and aerosol in the eastern Mediterranean atmosphere: An association with atmospheric dust. *Journal of Geophysical Research, 108*, 4320. https://doi.org/10.1029/2002JD002997

Mahowald, N., Jickells, T. D., Baker, A. R., Artaxo, P., Benitez-Nelson, C. R., Bergametti, G., Bond, T. C., Chen, Y., Cohen, D. D., Herut, B., Kubilay, N., Losno, R., Luo, C., Maenhaut, W., McGee, K. A., Okin, G. S., Siefert, R. L., & Tsukuda, S. (2008). Global distribution of atmospheric phosphorus sources, concentrations and deposition rates, and anthropogenic impacts. *Global Biogeochemical Cycles, 22*, GB4026. https://doi.org/10.1029/2008gb003240

Mara, P., Mihalopoulos, N., Gogou, A., Daehnke, K., Schlarbaum, T., Emeis, K.-C., & Krom, M. (2009). Isotopic composition of nitrate in wet and dry atmospheric deposition on Crete in the eastern Mediterranean Sea. *Global Biogeochemical Cycles, 23*, GB4002. https://doi.org/10.1029/2008GB003395

Markaki, Z., Oikonomou, K., Kocak, M., Kouvarakis, G., Chaniotaki, A., Kubilay, N., & Mihalopoulos, N. (2003). Atmospheric deposition of inorganic phosphorus in the Levantine Basin, eastern Mediterranean: Spatial, temporal variability and its role in seawater productivity. *Limnology and Oceanography, 48*, 1557–1568. https://doi.org/10.4319/lo.2003.48.4.1557

Markaki, Z., Loÿe-Pilot, M. D., Violaki, K., Benyahya, L., & Mihalopoulos, N. (2010). Variability of atmospheric deposition of dissolved nitrogen and phosphorus in the Mediterranean and possible link to the anomalous seawater N/P ratio. *Marine Chemistry, 120*, 187–194. https://doi.org/10.1016/j.marchem.2008.10.005

Migon, C., & Sandroni, V. (1999). Phosphorus in rainwater: Partitioning, inputs and impact on the surface coastal ocean. *Limnology and Oceanography, 44*, 1160–1165. https://doi.org/10.4319/lo.1999.44.4.1160

Migon, C., Sandroni, V., & Béthoux, J.-P. (2001). Atmospheric input of anthropogenic phosphorus to the northwest Mediterranean under oligotrophic conditions. *Marine Environmental Research, 52*, 413–426. https://doi.org/10.1016/S0141-1136(01)00095-2

Moon, J.-Y., Lee, K., Tanhua, T., Kress, N., & Kim, I.-N. (2016). Temporal nutrient dynamics in the Mediterranean Sea in response to anthropogenic inputs. *Geophysical Research Letters, 43*, 5243–5251. https://doi.org/10.1002/2016GL068788

Morales-Baquero, R., & Pérez-Martínez, C. (2016). Saharan versus local influence on atmospheric aerosol deposition in the southern Iberian Peninsula: Significance for N and P inputs. *Global Biogeochemical Cycles, 30*, 501–513. https://doi.org/10.1002/2015gb005254

Morales-Baquero, R., Pulido-Villena, E., & Reche, I. (2006). Atmospheric inputs of phosphorus and nitrogen to the southwest Mediterranean region: Biogeochemical responses of high mountain lakes. *Limnology and Oceanography, 51*, 830–837. https://doi.org/10.4319/lo.2006.51.2.0830

Morales-Baquero, R., Pulido-Villena, E., & Reche, I. (2013). Chemical signature of Saharan dust on dry and wet atmospheric deposition in the south-western Mediterranean region. *Tellus B: Chemical and Physical Meteorology, 65*, 18720. https://doi.org/10.3402/tellusb.v65i0.18720

Nehir, M., & Koçak, M. (2018). Atmospheric water-soluble organic nitrogen (WSON) in the eastern Mediterranean: Origin and ramifications regarding marine productivity. *Atmospheric Chemistry and Physics, 18*, 3603–3618. https://doi.org/10.5194/acp-18-3603-2018

Ounissi, M., Amira, A. B., & Dulac, F. (2018). Riverine and wet atmospheric inputs of materials to a North Africa coastal city (Annaba Bay, Algeria). *Progress in Oceanography, 165*, 19–34. https://doi.org/10.1016/j.pocean.2018.04.001

Özsoy, T. (2003). Atmospheric wet deposition of soluble macro-nutrients in the Cilician Basin, north-eastern Mediterranean sea. *Journal of Environmental Monitoring, 5*, 971–976. https://doi.org/10.1039/B309636J

Pasqueron de Fommervault, O., Migon, C., Dufour, A., D'Ortenzio, F., Kessouri, F., Raimbault, P., Garcia, N., & Lagadec, V. (2015). Atmospheric input of inorganic nitrogen and phosphorus to the Ligurian Sea: Data from the Cap Ferrat coastal time-series station. *Deep Sea Research Part I: Oceanographic Research Papers, 106*, 116–125. https://doi.org/10.1016/j.dsr.2015.08.010

Pulido-Villena, E., Wagener, T., & Guieu, C. (2008). Bacterial response to dust pulses in the western Mediterranean: Implications for carbon cycling in the oligotrophic ocean. *Global Biogeochemical Cycles, 22*, GB1020. https://doi.org/10.1029/2007gb003091

Rahav, E., Shun-Yan, C., Cui, G., Liu, H., Tsagaraki, T. M., Giannakourou, A., Tsiola, A., Psarra, S., Lagaria, A., Mulholland, M. R., Stathopoulou, E., Paraskevi, P., Herut, B., & Berman-Frank, I. (2016). Evaluating the impact of atmospheric depositions on springtime dinitrogen fixation in the Cretan Sea (Eastern Mediterranean)—A mesocosm approach. *Frontiers in Marine Science, 3*, 180. https://doi.org/10.3389/fmars.2016.00180

Richon, C., Dutay, J.-C., Dulac, F., Wang, R., Balkanski, Y., Nabat, P., Aumont, O., Desboeufs, K., Laurent, B., Guieu, C., Raimbault, P., & Beuvier, J. (2018a). Modeling the impacts of atmospheric deposition of nitrogen and desert dust-derived phosphorus on nutrients and biological budgets of the Mediterranean Sea. *Progress in Oceanography, 163*, 21–39. https://doi.org/10.1016/j.pocean.2017.04.009

Richon, C., Dutay, J.-C., Dulac, F., Wang, R., & Balkanski, Y. (2018b). Modeling the biogeochemical impact of atmospheric phosphate deposition from desert dust and combustion sources to the Mediterranean Sea. *Biogeosciences, 15*, 2499–2524. https://doi.org/10.5194/bg-15-2499-2018

Ridame, C., & Guieu, C. (2002). Saharan input of phosphate to the oligotrophic water of the open Western Mediterranean Sea. *Limnology and Oceanography, 47*, 856–869. https://doi.org/10.4319/lo.2002.47.3.0856

Sandroni, V., Raimbault, P., Migon, C., Garcia, N., & Gouze, E. (2007). Dry atmospheric deposition and diazotrophy as sources of new nitrogen to northwestern Mediterranean oligotrophic surface waters. *Deep Sea Research Part I: Oceanographic Research Papers, 54*, 1859–1870. https://doi.org/10.1016/j.dsr.2007.08.004

Sipler, R. E., & Bronk, D. A. (2015). Chapter 4 - Dynamics of dissolved organic nitrogen. In D. A. Hansell & C. A. Carlson (Eds.), *Biogeochemistry of marine dissolved organic matter* (2nd ed., pp. 127–232). Academic Press. https://doi.org/10.1016/B978-0-12-405940-5.00004-2

Theobald, M. R., Vivanco, M. G., Aas, W., Andersson, C., Ciarelli, G., Couvidat, F., Cuvelier, K., Manders, A., Mircea, M., Pay, M.-T., Tsyro, S., Adani, M., Bergström, R., Bessagnet, B., Briganti, G., Cappelletti, A., D'Isidoro, M., Fagerli, H., Mar, K., … Colette, A. (2019). An evaluation of European nitrogen and sulfur wet deposition and their trends estimated by six chemistry transport models for the period 1990–2010. *Atmospheric Chemistry and Physics, 19*, 379–405. https://doi.org/10.5194/acp-19-379-2019

Theodosi, C., Markaki, Z., Pantazoglou, F., Tselepides, A., & Mihalopoulos, N. (2019). Chemical composition of downward fluxes in the Cretan Sea (Eastern Mediterranean) and possible link to atmospheric deposition: A 7 year survey. *Deep Sea Research Part II: Topical Studies in Oceanography, 164*, 89–99. https://doi.org/10.1016/j.dsr2.2019.06.003

Violaki, K., & Mihalopoulos, N. (2010). Water-soluble organic nitrogen (WSON) in size-segregated atmospheric particles over the Eastern Mediterranean. *Atmospheric Environment, 44*, 4339–4345. https://doi.org/10.1016/j.atmosenv.2010.07.056

Violaki, K., Zarbas, P., & Mihalopoulos, N. (2010). Long-term measurements of dissolved organic nitrogen (DON) in atmospheric deposition in the Eastern Mediterranean: Fluxes, origin and biogeochemical implications. *Marine Chemistry, 120*, 179–186. https://doi.org/10.1016/j.marchem.2009.08.004

Violaki, K., Sciare, J., Williams, J., Baker, A. R., Martino, M., & Mihalopoulos, N. (2015). Atmospheric water-soluble organic nitrogen (WSON) over marine environments: A global perspective. *Biogeosciences, 12*, 3131–3140. https://doi.org/10.5194/bg-12-3131-2015

Violaki, K., Bourrin, F., Aubert, D., Kouvarakis, G., Delsaut, N., & Mihalopoulos, N. (2018). Organic phosphorus in atmospheric deposition over the Mediterranean Sea: An important missing piece of the phosphorus cycle. *Progress in Oceanography, 163*, 50–58. https://doi.org/10.1016/j.pocean.2017.07.009

Trace Metals and Contaminants Deposition

Karine Desboeufs

Contents

Abstract Atmospheric deposition is a process of atmospheric removal for various metals and organic contaminants, as organochlorine compounds or polycyclic aromatic hydrocarbons (PAHs). This chapter presents a discussion on atmospheric deposition and fluxes of trace and heavy metals and organic contaminants in the Mediterranean basin. Recent studies used statistical methods to address the source apportionment of deposited metals. They generally show that anthropogenic sources dominate the fluxes of metals, although atmospheric mineral dust deposition is critical for some of them during strong desert dust events. Atmospheric metal fluxes are typically too low to have a toxicological impact on the marine biosphere. Organic contaminants show low deposition fluxes due to the air-sea equilibrium and degradation processes in the water column and, hence, may only have a small impact on marine ecosystems. However, the atmospheric fluxes of these species are

Chapter reviewed by ***Laurent Alleman*** *(IMT Nord Europe, Institut Mines-Télécom, Univ. Lille, Lille, France), as part of the book Part VIII Deposition in the Mediterranean Region also reviewed by* ***Francesc Peters*** *(ICM/CSIC, Barcelona, Spain)*

K. Desboeufs (✉)
Université Paris Cité and Univ. Paris Est Créteil, CNRS, LISA, F-75013 Paris, France
e-mail: karine.desboeufs@lisa.ipsl.fr

F. Dulac et al. (eds.), *Atmospheric Chemistry in the Mediterranean Region*,
https://doi.org/10.1007/978-3-030-82385-6_18

still poorly studied and need to be complemented to improve our knowledge of their impact in this region.

1 Particulate Trace Metals

1.1 Introduction

Aerosol particles are the predominant conveyor of trace metals (hereafter called TMs) in the atmosphere, except for mercury, highly present in the gas phase and not considered in this review. In addition to the major nutrients, TMs such as iron (Fe), chromium (Cr), copper (Cu), nickel (Ni), manganese (Mn), or zinc (Zn) are known to have a biological role, often as cofactors or part of cofactors in enzymes and as structural elements in proteins (Morel & Price, 2003; Annett et al., 2008). Several of these trace metals, like Fe, cobalt (Co), Ni, Cu, cadmium (Cd), vanadium (V) and molybdenum (Mo), are present at low concentrations in oligotrophic oceans and the Mediterranean Sea and therefore possibly limiting the phytoplankton production (Pinedo-González et al., 2015). It is known that iron atmospheric deposition represents a significant input to support the primary production in surface waters of the Mediterranean basin (MB) (Bonnet & Guieu, 2006). Other TMs supplied by atmospheric aerosol deposition to the oceans could also be important in enhancing or inhibiting phytoplankton growth rates and in modifying plankton community structure, thus impacting marine biogeochemistry (Mahowald et al., 2018). Seeding experiments of surface Mediterranean seawater emphasized a fertilizing effect of dust on phytoplankton communities, which was superior to a direct addition of equivalent content of Fe, N and P (Ridame et al., 2011). In incubation experiments, Mackey et al. (2012) showed that this fertilizing effect could be linked to the dissolved metals concentrations from added aerosol particles. This conclusion is supported by the results of Tovar-Sánchez et al. (2014), who showed a correlation of the atmospheric deposition of mineral dust with dissolved trace metals (Cd, Co, Cu, Fe) enrichment of the sea-surface microlayer. However, a negative effect of atmospheric deposition on chlorophyll concentrations was observed in the Mediterranean Sea under a large influence of European aerosol sources (Gallisai et al., 2014). It has been suggested that the atmospheric deposition of aerosols was responsible for the contamination of the Mediterranean waters in trace and heavy metals (Béthoux et al., 1990; Ruiz-Pino et al., 1990; Migon & Nicolas, 1998; Guerzoni et al., 1999; Guieu et al., 2010). For example, the input of anthropogenic aerosols, such as Cu-rich particles, has been suspected to inhibit phytoplankton growth (Jordi et al., 2012).

Trace and heavy metal deposition fluxes available in the literature are summarized in Table 1 for the Mediterranean Sea background and not, or moderately impacted coastal sites. The table reports annual fluxes estimated from at least 1 year of survey, but several other studies tried to estimate the deposition fluxes on shorter

Table 1 Trace and heavy metals annual deposition fluxes (in mg m^{-2} yr^{-1}) at remote and coastal sites of the Mediterranean basin

Location	Period	Type of deposition	Al	As	Cd	Co	Cr	Cu	Fe	Mn	Ni	Pb	V	Zn	References
Israel (Maagan Michael)	Oct. 1994–Dec. 1997	Dry	497		0.007		0.13	0.23	432	11		1.54		1.98	Herut et al. (2001)
Israel (Tel Shikmona)			545		0.008		0.075	0.18	496	10		1.08		2.81	
	Jan. 1999–Dec. 2002		520		0.007			2.9	420	9		6.36		7.58	Koçak et al. (2005)
Turkey (Ankara)	Nov. 1992–Jan. 1994	Wet	25		1.500		0.31	0.52	4		0.28	2.2	0.34	3.4	Kaya and Tuncel (1997)
Turkey (Antalya)	Jan. 1992–Jan. 1994		92		0.720		1.4	0.79			4	1.6		22	Al-Momani et al. (1998)
Turkey (Erdemli)	Jan. 1999–Dec. 2002	Dry	320		0.004			2.6	230	3.8		5.65		5.33	Koçak et al. (2005)

(continued)

Table 1 (continued)

Location	Period	Type of deposition	Al	As	Cd	Co	Cr	Cu	Fe	Mn	Ni	Pb	V	Zn	References
Turkey (Izmir)	Oct. 2003–Jun. 2004	Total			0.15		0.66	1.09			0.58	0.43		5.6	Muezzinoglu and Cizmecioglu (2006)
Greece, Crete Isl. (Finokalia)	Jan. 2005–Dec. 2006				0.063		7.7[a]	2.35	391	8.7		1.25	1.4[a]	7.5	Theodosi et al. (2010)
	Jun. 2001–May 2002	Bulk	672		0.025				408			0.876		8.88	Guieu et al. (2010)
Greece (Mytilene)			384		0.034				264			1.44		12	
Turkey (Akkuyu)			720		0.045				504			2.4		4.8	
Cyprus (Cavo Greco)			288		0.023				228			0.852		6	
Egypt (Alexandria)			1260		0.021				972			1.056		7.2	
Morocco (Cap Spartel)			495		0.061				366			1.9		24.59	
France (Cap Bear)			744		0.042				444			0.96		10.8	
Tunisia (Madhia)			1728		0.045				1224			2.16		7.2	
Tunisia (Medenine)	Oct. 2013–Dec. 2014	Total insoluble	2592			1.6	2.9	2.1	1215	21	1.4		3.8	4.6	Fu et al. (2017) Fu (2018)
Italy (Lampedusa)	Jan. 2013–Dec. 2014		719			0.85	1.55		653	6.7	1.45		1.15	8.3[b]	
France, Corsica Isl. (Ersa)			154			0.1	0.75	0.15	94	1	0.2		0.2	0.5	
Spain, Mallorca Isl. (Ses Salines)			490			0.3	0.7	0.3	280	2.6	0.5		0.8	0.8	
Spain, Mallorca Isl. (Can Llompart)	Jun. 2010–Aug. 2012		472					1.0	280	4.2	0.5	0.4	0.7	5.4	Cerro et al. (2020)

Location	Period	Type of deposition	Al	As	Cd	Co	Cr	Cu	Fe	Mn	Ni	Pb	V	Zn	References
France, Corsica Isl. (Cap Cavallo)	Feb. 1985–Apr.1986	Bulk	970		1.0			4.2		22		31		34	Bergametti (1987) Remoudaki et al. (1991 b)
France, Corsica Isl. (Pirio)	Jan. 1995–Mar. 1997		221		0.055			1.05	137	6.4	0.4	0.9		5.15	Ridame et al. (1999)
France, Corsica Isl. (Ostriconi)	Jun. 2001–May 2002		2028		0.026				1188			0.96		6	Guieu et al. (2010)
France, Corsica Isl. (Cap Cuittone)	Mar. 2008–Feb. 2011			0.14[c]			0.16	1.06	67	3.7[c]	0.21[c]	0.4	0.4	5.7	Desboeufs et al. (2018)
Spain (Montseny)	Jun. 1995–Jun. 1996							0.63				0.65		2.2	Avila and Rodrigo (2004)

(continued)

Table 1 (continued)

Location	Period	Type of deposition	Al	As	Cd	Co	Cr	Cu	Fe	Mn	Ni	Pb	V	Zn	References
Italy, Sardinia Isl. (Capo Carbonara)	Oct. 1990–Apr. 1992	Total	907		0.050		0.62		416			2.29			Guerzoni et al. (1999)
France (Tour du Valat)	May 1988–Jun. 1989		918		1.3	0.4		2	840	20	1.3	4		100	Guieu et al. (1997)
France (Cap Ferrat)	1986–1987				0.173			1.85				3.3–18		9	Migon et al. (1991)
	Sep. 1988–Feb. 1989		195			0.084		2.65	88[d]	2.07[d]	0.69	3.76		3.2[d]	Chester et al. (1997 and 1999)
	Oct. 1992–Sep. 1993				0.066			2.19			1.35	3.14		80.3	Migon et al. (1997)
	Feb. 1997–Jul. 1998		141		0.060			1.28			1.1	1.2		41.2	Sandroni and Migon (2002)
	Jan. 2004–Feb. 2005	Bulk							1118						Bonnet and Guieu (2006)

Aluminium is given as a reference for soil dust particle deposition (see Laurent et al., 2022) but is not considered as a trace metal
[a]Only 2006
[b]Only 2014
[c]From Sept. 2009 only
[d]Only dry

periods as Chester et al. (1997) at Cap Ferrat, Guerzoni et al. (1999) in Sardinia or Fu (2018) during an oceanographic cruise in the western Mediterranean. Even if there exists a European standard procedure for trace metal atmospheric deposition measurements (EN15841: 2009 Ambient air quality – Standard method for determination of arsenic, cadmium, lead and nickel in atmospheric deposition), this method is unfortunately not used in research studies, which makes it very difficult to compare measurements and assess the atmospheric deposition of TMs to the Mediterranean. Indeed, past studies focused on different metals, different periods and different locations, using different methodologies. Many trace metals measurements mainly focus on Fe (for its potential role in marine productivity) and certain heavy metals, such as Cd, Pb and Zn. More occasionally, data exist for other trace metals such as Cu or Mn. Considering the metals identified as playing a role in the marine biosphere, there is little data on V, Co, Cr and Mo. Moreover, atmospheric inputs of trace metals to the Mediterranean sea have been hardly addressed in the recent period (Theodosi et al., 2010; Desboeufs et al., 2018; Fu et al., 2017, 2018) and data mainly come from the 1990s and the beginning of 2000s, especially for the eastern basin. Thus, measurements are relatively heterogeneous, and assessing the atmospheric deposition of one metal and its spatial variations is challenging. Only data of bulk TMs deposition from the Mediterranean ADIOS network (Guieu et al., 2010) and data of insoluble TMs deposition from the CARAGA network in the western basin (Fu et al., 2017, 2018) provide a spatial distribution of fluxes using the same collectors and same protocols for at least a year.

1.2 Sources and Variability

Wet deposition processes are very efficient and can scavenge the tropospheric aerosol in a short period of time during rain events. On the opposite, dry deposition is a more monotonic process leading to continuous deposition. Wet deposition is usually measured by wet-only collectors or using collectors deployed only during rainy periods (e.g., Özsoy & Örnektekin, 2009). Measuring dry deposition is less straightforward than wet deposition. Direct measurement of dry deposition is difficult since it depends on many factors, including meteorological conditions and characteristics of the surface on which deposition occurs. Dry deposition was either collected with different devices, either estimated as the difference between total and wet deposition (e.g., Desboeufs et al., 2018) or computed as the product of aerosols concentrations by settling rates (e.g., Chester et al., 1999). This last method, which is the most common, is based on an assumed steady-state relationship:

$$F = V_d C \tag{1}$$

where the dry deposition flux or rate (F) is a product of the dry deposition velocity (V_d) and the concentration (C) of an airborne TM. However, even if this method is

recommended for estimating dry deposition, the estimated fluxes of trace metals are highly dependent on the adopted average depositional velocities, which are directly linked to the particle size distribution of TMs in aerosols (Dulac et al., 1989; Theodosi et al., 2010). The measurements of particle size distributions of TMs were rarely carried out during deposition studies, creating uncertainties in the measurements of dry deposition fluxes (Chester et al., 1999; Koçak et al., 2005, 2007). The Mediterranean basin is continuously affected by a background of anthropogenic aerosols, which is perturbed by sporadic mixing with biomass burning particles or desert dust from the Sahara and the Middle East in its easternmost part. Metals from anthropogenic or combustion sources are mainly associated with the fine mode, whereas metals from dust origin are linked for a large part with the coarse mode. The partitioning of TMs between these two modes is therefore a key parameter to evaluate more accurately their settling velocities and, hence, their dry deposition.

Severalstudies focused on the source apportionment of metals in deposition samples (Chester et al., 1997; Guerzoni et al., 1999; Ridame et al., 1999; Sandroni & Migon, 2002; Özsoy & Örnektekin, 2009; Guieu et al., 2010; Fu et al., 2017, 2018; Desboeufs et al., 2018; Cerro et al., 2020). Indeed, investigations on TMs sources need to be carried out directly on deposition samples, since results of aerosols sources apportionment algorithms could depend on the deposition, which may in-turn depend on aerosols size distribution, hygroscopicity, rain frequency, etc. Due to its insignificant concentrations in anthropogenic background aerosols, Al can be considered as a tracer of natural aerosols. Consequently, is can be used to distinguish the natural and anthropogenic origins of TMs. In the MB, Al may be considered entirely associated with Saharan dust aerosols. Typically, enrichment factors (EF) or crustal elemental ratios (X/Al) serve as a tool to identify Saharan and anthropogenic components in dry/wet deposition samples and to quantify their relative contributions (Chester et al., 1997; Guerzoni et al., 1999; Ridame et al., 1999; Sandroni & Migon, 2002; Özsoy & Örnektekin, 2009; Guieu et al., 2010; Fu et al., 2017, 2018; Cerro et al., 2020). The EF relative to crustal material is calculated for any element X as follows:

$$EF_{\text{crust}} = \left(\text{X} / Al\right)_{\text{Sample}} / \left(\text{X} / Al\right)\text{Crust} \tag{2}$$

where $(X/Al)_{sample}$ refers to the concentration ratio of the trace element X to Al in the deposition sample and $(X/Al)_{crust}$ in the average ratio for crustal material. Some surrogate compositions are used as reference of crustal material, including the upper continental crust (Mason, 1966; Wedepohl, 1995; Rudnick & Gao, 2003) or Saharan dust composite (Guieu & Thomas, 1996). However, due to the diversity of the dust chemical composition for various emission sources in the Sahara and their physicochemical evolution during atmospheric transport (Formenti et al., 2011), the use of EF can create uncertainties in the estimation of dust contribution. More recently, the source apportionment of particles in the Mediterranean Sea has been also investigated using statistical methods such as the PMF (positive matrix

factorization) (Desboeufs et al., 2018; Cerro et al., 2020) or PCA (principal component analysis) (Özsoy & Örnektekin, 2009; Fu et al., 2017, 2018) methods. These methods identify factors, which can be attributed to chemical source profiles in order to distinguish various natural and anthropogenic sources such as heavy oil combustion, biomass or waste burning.

All these studies show a large predominance of anthropogenic sources for the majority of metals, except Fe, which is mainly attributed to crustal origin (higher than 75%). The signature of continental pollution sources was observed even in remote areas like Lampedusa or Mallorca (Fu et al., 2017; Cerro et al., 2020). Zn and Cd display the highest fractions of total deposition that were not of Saharan origin, typically higher than 95%. Cr, Co, Cu, Mn, Ni and V present values, which are more mixed but are mainly associated with anthropogenic sources (60 to 90%). During intense dust deposition events, the trace metals fluxes are increased either during dry and wet deposition events (Guerzoni et al., 1999; Özsoy & Örnektekin, 2009; Guieu et al., 2010; Desboeufs et al., 2018; Cerro et al., 2020). Yet, the contribution of anthropogenic aerosol deposition remains largely significant for certain metals such as Cd or Zn (Guieu et al., 2010; Desboeufs et al., 2018). For example, the increase in concentrations from background rain to dusty rain in Turkey ranges from 1.1 for Zn and Cd to 14 for Fe or Mn (Özsoy & Örnektekin, 2009). To put it differently, the high-dust-deposition events represent around 50% of annual fluxes for Fe and 33% for Cr, Mn, Ni and V, whereas their contribution is <10% for As, Cu and Zn in Corsica (Desboeufs et al., 2018). The influence of dust source on Mn deposition fluxes depends on the season, since it is correlated with Fe during winter and spring, but presents a peak in summer at Finokalia, associated with air masses from industrialized areas (Theodosi et al., 2010). In Corsica, the deposition flux seasonality of Cr and V also reflects the dust event period in spring (Desboeufs et al., 2018). Concerning Zn and Cu, the statistical apportionment and the correlation with K deposition fluxes enable to emphasize the biomass/waste combustion as their major anthropogenic source (Özsoy & Örnektekin, 2009; Fu et al., 2017; Desboeufs et al., 2018). Even if the heavy oil combustion (ship traffic) was identified as an important source of particulate V and Ni over the Mediterranean Sea (Becagli et al., 2017), it does not seem to be the case for deposition in Corsica (Desboeufs et al., 2018) and still needs to be tested at other sites. The case of Pb is particular, since the data from the 1990s show that Pb was mainly of anthropogenic origin (EF generally higher than 100; e.g., Chester et al., 1999; Koçak et al., 2007), whereas the most recent works found a link with dust deposition (Theodosi et al., 2010; Desboeufs et al., 2018; Fu, 2018). This could be explained by the decreasing temporal evolution of anthropogenic Pb concentrations in aerosols (Migon et al., 2008; Heimbürger et al., 2010) and concurrent Pb deposition fluxes. Indeed, Pb, as Cd and Zn, exhibits deposition fluxes about 100 times lower for the most recent measurements in comparison with data from the 1980s (Table 1). In Corsica, the observed decrease in Pb deposition reached more than one order of magnitude between 1985–1986 (Bergametti, 1987; Remoudaki et al., 1991a) and the beginning of the 2000s (Ridame et al., 1999; Loÿe-Pilot et al., 2001; Guieu et al., 2010) and further decreased by a factor of 2 in the 2010s (Desboeufs et al., 2018). This

behaviour reflects the regulation in atmospheric emissions of this metal in western Europe since the beginning of the 1990s, for example, by the phasing out of lead additives in gasoline, which was identified as the major Pb contributors (~70%) in the Mediterranean atmosphere at that time (Pirrone et al., 1999). Cerro et al. (2020) report greater Pb/Al values under the influence of Libyan dust source areas in comparison to western Sahara, Hoggar Massif or Tunisia, which could point out that anthropogenic emissions from Libya could accompany crustal particles. The decrease in emission is common for the majority of trace metals: e.g., Pb, Cr, Cd, Ni and Zn anthropogenic emissions went down by 93%, 72%, 65%, 70% and 36%, respectively, from 1990 to 2016 in Europe; only Cu increased by 8%, according to the European Union emission inventory report 1990–2016 (EEA, 2018). However, except for Cd, Pb and Zn, no clear trend was registered in deposition samples for other metals (Loÿe-Pilot et al., 2001), due to the lack of long-term datasets.

As a consequence of mass deposition of natural sources, annual fluxes of Fe predominate on the other trace metal fluxes, followed by Zn and Mn, while the weakest flux is found for Cd. Despite the high spatial and time variability of precipitation and aerosol concentrations over the Mediterranean Sea, it appears that the fluxes for one particular TM always present the same order of magnitude of fluxes for dry deposition or wet deposition (e.g., Özsoy & Örnektekin, 2009), except specific sites with local contamination (Koçak et al., 2005; Guieu et al., 2010; Fu et al., 2017). This could be explained by a certain uniformity of metal atmospheric concentrations. The air pollution caused by the metals is most often localized and is typically related to specific industrial plants (EEA, 2018). This uniformity of aerosol concentrations implies that for a given site, the inter-annual variability is low and within a factor 2 at best, except in case of dust intrusion for Fe or in case of local pollution (Ridame et al., 1999; Sandroni & Migon, 2002; Desboeufs et al., 2018). Theodosi et al. (2010) concluded that the long-range transport of anthropogenic aerosols is limited to the MB, and hence, the origin of the TMs deposition fluxes could mainly result from local or regional contaminations. From this idea, the coastal measurements of deposition would not be representative of actual deposition in remote areas and the estimations of representative deposition fluxes should be operated on remote islands or during cruises across the MB, as long as the contamination from the vessel during sampling could be controlled.

The predominance of dry or wet deposition is different from one trace metal to another and from one site to another. Mn and Cu are mainly deposited by dry deposition (around 70% of the total atmospheric inputs) in Finokalia (Theodosi et al., 2010) and Mallorca (Cerro et al., 2020), whereas the wet deposition represents around 60% of their total deposition in Corsica (Desboeufs et al., 2018). In the open sea, the most important wet deposition fluxes for TMs are observed when a rain event occurs after at least three consecutive dry days, leading to higher TM concentrations in the atmosphere (Remoudaki et al., 1991a). Thus, the rain events occurring at that time scavenge highly loaded air masses with anthropogenic aerosols or dust, leading to higher wet deposition fluxes (Remoudaki et al., 1991a; Migon et al., 1997). During summer, due to the lack of precipitation in the MB, the aerosol loading is higher, enhancing the dry deposition during this period

(Remoudaki et al., 1991a; Desboeufs et al., 2018; Cerro et al., 2020). High fluxes can also occur in some cases of intense summer storms (Bergametti et al., 1989). Thus, the seasonality of fluxes would be mainly linked to the seasonality of the rainfall occurrence (Remoudaki et al., 1991a, b). However, deposition fluxes obtained in Corsica show that TMs deposition presented a clear seasonal pattern, which was different for each metal, emphasizing the effect of TM sources variability (Desboeufs et al., 2018). Moreover, due to the high anthropogenic background in the Mediterranean atmosphere, the variability of monthly fluxes was smaller for elements mainly of anthropogenic origin (Cd, Zn and Pb) than for crustal elements (e.g., Fe) (Guieu et al., 2010; Theodosi et al., 2010). For Fe, the time variability of the deposition fluxes is highly linked to the spring fluxes concomitant to the dust intrusions over the MB and the end of the wet season (e.g., Bonnet & Guieu, 2006).

1.3 Solubility

Deposition delivers aerosols directly to the sea surface and TMs can solubilize to some extent according to several parameters: sources and chemical speciation of TMs, pathways of deposition (wet vs. dry), chemical processes during aerosol transport, seawater conditions, and chemical and biological processes in the ocean (Mahowald et al., 2018). Thus, the major challenge for marine biogeochemistry is the conversion of aerosol deposited fluxes of TMs to those that are bioavailable, i.e., fluxes that can directly affect marine ecosystem productivity. The partitioning between the particulate and the dissolved fractions is currently used to estimate the bioavailable fractions of TMs in wet or dry deposition. This partition is defined through the solubility measurement, i.e., the ratio between dissolved concentrations of TMs in water and their total content in deposition samples.

For wet deposition, the solubility is constrained by the aerosol-rain water reactivity and corresponds to the percentage of the dissolved metal concentration divided by its total (soluble plus particulate) concentration. In the case of dry deposition, the solubility is controlled by aerosol-seawater interactions. The solubility calculation implies to perform dissolution/leaching experiments on sampled aerosol filters for mimicking this reactivity (e.g., Chester et al., 1999). Metal dissolution can be influenced by a number of factors both related to aerosol (source/mineralogy, size, atmospheric chemical processing), rainwater (pH, aqueous phase aerosol concentration, organic ligands concentrations, bacteria concentration) and seawater (binding ligands, biological influences, adsorption of particles) (Baker et al., 2016). Thus, the main difficulty to compare the values of solubility for dry deposition is the diversity of dissolution protocols, for example, concerning the type and pH of water (seawater, ultrapure water, acid solution), the exposure time between water and filters in water. However, dissolution experiments carried out on a set of filters collected at the same site enable the study of the variability of solubility in homogeneous conditions. The solubilities of trace metals measured in rains collected at different coastal sites and at sea in the Mediterranean are presented in Table 2.

An important variability in solubility values is observed for the majority of the studied TMs, with up to one or two orders of magnitude, and is observed for most of the studied TMs. Iron presents the highest range with a solubility <1% in dust-rich rain in Turkey (Özsoy & Örnektekin, 2009) and up to 88% in the rain water with anthropogenic influence in the Ionian Sea (Fu, 2018). Only three metals have a limited range of solubility, and they are the most soluble: Cd (72–99%), V (68–99%) and Zn (62–99%). From dry deposition samples, the solubility values of metals show also a significant variability; for example, Zn solubility ranges from 58% to 98% in dry deposition samples collected in Turkey (Muezzinoglu & Cizmecioglu, 2006). For both dry and wet deposition, Cd, Zn and V are the most soluble metals on average, whereas Fe and, to a lesser extent, Cr are the least soluble. These solubility values measured in the Mediterranean region are in the same range as in different oceanic parts of the world under the influence of various aerosols sources, e.g., the Atlantic Ocean (Shelley et al., 2018), the China Sea (Hsu et al., 2010) or the Pacific Ocean (Buck et al., 2013).

The partitioning/mixing between anthropogenic and natural atmospheric inputs is a key parameter in determining the variability of solubility in the Mediterranean Sea (Guieu et al., 1997; Kaya & Tuncel, 1997; Guerzoni et al., 1999; Chester et al., 1999; Fu, 2018). It is known that the metals associated with anthropogenic or combustion aerosols are more soluble than metals linked to mineral dust (Desboeufs et al., 2005). Consequently, the diversity of aerosol sources in deposition samples over the MB could lead to the variability in the observed solubility values. For example, the solubility of all metals is lower in dusty rains than in rains influenced by anthropogenic aerosols (Table 2). The highest solubility of Cd and Zn is also in agreement with the important contribution of anthropogenic aerosol deposition for these metals (higher than 90%, e.g., Chester et al., 1999). However, no clear link was observed between EF and solubility values (Fu, 2018).

In the case of wet deposition, a clear influence of pH and particulate load (or dust load) is also reported on solubility values (Losno et al., 1988; Kaya & Tuncel, 1997; Guerzoni et al., 1999; Kuloglu & Tuncel, 2005; Özsoy & Örnektekin, 2009; Theodosi et al., 2010). The lower the pH, the higher the TM solubility, although the relation is not linear. For example, the soluble fraction for metals in Finokalia rains is usually higher than 60–80% (especially for Mn, Ni, Cu and Cd) in the low pH range (3.5–6.5), whereas these percentages decrease considerably at higher pH values (Theodosi et al., 2010). However, it is difficult to discriminate between the effect of aerosols sources, the effect of the pH or the effect of the particulate load. Dust can partially buffer acids, for example, due to the presence of calcium carbonate and hence significantly increases the pH of rain (e.g., Loÿe-Pilot et al., 1986) or water during dissolution experiments (Desboeufs et al., 2003). Thus, the low solubility observed for pH higher than 6.5 in rain could be related to the dissolution of metals from dust rather than a pH effect or both. The observed inverse relationship between particulate load and solubility of metals can be explained through the mass of dust in comparison to the mass of anthropogenic aerosols. No single process has been identified as the dominant controlling factor for TMs aerosol solubility, and it is likely that combinations of competing factors are important depending on the

Table 2 Solubility values (%) of trace metals found in wet and bulk deposition

Location		Cd	Co	Cr	Cu	Fe	Mn	Ni	Pb	V	Zn	References
Crete Isl., Greece	Finokalia	72 ± 30		44 ± 36	68 ± 28	18 ± 23	69 ± 26	59 ± 26	47 ± 36	70 ± 29	62 ± 31	Theodosi et al. (2010)
Turkey	Ankara	88 ± 17		35 ± 29	49 ± 27	17 ± 16		72 ± 31	40 ± 35	61 ± 26	43 ± 29	Kaya and Tuncel (1997)
	Antalya	96		41	63			46	64		91	Al-Momani et al. (1998)
	Mersin			26 ± 25	35 ± 30	5 ± 13	41 ± 25	30 ± 34			63 ± 34	Özsoy and Örnektekin (2009)
	Izmir	86		79				85			91	Muezzinoglu and Cizmecioglu (2006)
France	Tour Valat	75±26			71 ± 21	11 ± 16	63 ± 28	58 ± 36	52 ± 30		68 ± 30	Guieu et al. (1991, 1997)
	Cap Ferrat	92			82		60	54	65			
	Cap Ferrat		36		76			53	65			Chester et al. (1997)
	Corsica Island				49	13	67		48		76	Losno (1989)
	Corsica Island				48 ± 32				53 ± 37		72 ± 30	Lim et al. (1994)
Sardinia, Italy	Dusty rain	87		49		0.8			32			Guerzoni et al. (1999)
	Background rain	90		63		10			77			
Rains collected at sea during oceanographic cruises												
40°37′N, 07°10′E	Dusty						57					Dulac (1986)
43°06′N, 07°56′E	Anthropogenic						83					
37°56′N, 02°55′E	Dusty	85	52	18	70	8	60	71	27	68	86	Desboeufs et al. (2022)
35°22′N, 19°55′E	Anthropogenic	98	93	38	97	84	92	78	97	99	98	

region and the season. The difficulty to interpret observed metal solubility in aerosol concentrations and deposition is also discussed for other regions and still remains a large subject of study (Mahowald et al., 2018).

2 Organic Contaminants

The Mediterranean Sea is particularly vulnerable because human activities in neighbouring countries (urbanization, agriculture, industries, aquaculture, tourism, harbour activities, etc.) induce significant inputs of chemical contaminants from rivers, runoff, groundwater or atmospheric deposition. Among these contaminants, the Mediterranean Sea is largely impacted by legacy POPs (persistent organic pollutants) and other organic contaminants, such as polycyclic aromatic hydrocarbon compounds (PAHs) (Mandalakis & Stephanou, 2004; Berrojalbiz et al., 2011; The MerMex Group, 2011) and plastic fragments (Schmidt et al., 2018). These organic contaminants are known to act on ecosystems through disruptive effects and can constitute a risk for the sustainability of these fragile ecosystems and for human health. These contaminants have been forbidden by the Stockholm Convention of POPs and regulated by the Water and Marine Strategy Framework Directives at the European level. However, little information exists on their background levels and stocks in the Mediterranean Sea. Thus, despite an increased monitoring of chemical pollution in this region in support of public policies for many years, there remains a crucial need for scientific research on these questions.

Atmospheric deposition was identified as an important vector for the entrance of the organic contaminants into coastal aquatic systems and open oceans (Jurado et al., 2005; Castro-Jiménez et al., 2015). Mass balance studies have shown that the atmosphere is an important pathway for polychlorobiphenyls (PCBs) and PAHs to the Mediterranean marine ecosystem (Lipiatou et al., 1997; Tolosa et al., 1997; Tsapakis et al., 2006). Yet, these estimations are based on very fragmented existing data of deposition and mainly limited to studies carried out on dry deposition. Indeed, a wide literature is available on atmospheric concentrations of organic contaminants in the Mediterranean Sea background and at not, to moderately impacted coastal sites (see Castro-Jiménez et al., 2013, and references therein), but few data about their atmospheric deposition are reported (Table 3).

Deposition data on organic contaminants is available for PAHs and for POPs, including organochlorines (OCs) comprising polychlorinated biphenyls (PCBs) and organochlorine pesticides (OCPs), and polychlorinated dibenzo-p-dioxins and dibenzofurans (PCDD/Fs). Values are also reported for polybrominated diphenyl ethers (PBDEs) and emerging pollutants like organophosphate esters (OPEs), which are used as substitutes of PBDEs since their recent ban by the Stockholm Convention in 2009. If the production and use of POPs is restricted by the Stockholm convention, PAHs are still highly emitted. PAHs are mainly released in the atmosphere by incomplete combustion of organic material, such as waste incineration, vehicles exhaust, residential heating and industrial processes, even if natural sources

Table 3 Annual deposition fluxes of POPs and PAHs reported for the Mediterranean basins, adapted and completed from Castro-Jiménez et al. (2015)

Compounds	Deposition flux			Location	Year[d]	References
	Dry	Wet	Diffusive			
PCDD/Fs (ng m^{-2} yr^{-1})						
Σ2,3,7,8-PCDD/Fs[a]	2–60	n.r.	3–25	All basins (open Med. cruises)	2006, 2007	Castro-Jiménez et al. (2010)
Σ17PCDD/Fs	2–81	n.r.	n.r.	Western Med. (Marseille, France)	2015	Castro-Jiménez et al. (2017)
Σ17PCDD/Fs	2–69	n.r.	n.r.	Western Med. (Bizerte, Tunisia)		
Σ2,3,7,8-PCDD/Fs[a,c]	23	19	n.r.	Western Med. (Thau lagoon, France)	2007–2008	Castro-Jiménez et al. (2011)
PCBs (ng m^{-2} yr^{-1})						
Σ20PCBs	22–690	n.r.	n.r.	Western Med. (Bizerte, Tunisia)	2015	Barhoumi et al. (2018)
Σ18PCBs	36–216	n.r.	n.r.			Castro-Jiménez et al. (2017)
Σ18PCBs	21–115	n.r.	n.r.	Western Med. (Marseille, France)		
Σ18PCBs[a]	136	125	n.r.	Western Med. (Thau lagoon, France)	2007–2008	Castro-Jiménez et al. (2011)
Σ54PCBs[b]	36–400	820[c]	n.r.	Eastern Med. (Finokalia, Crete)	2000–2001	Mandalakis and Stephanou (2004)
Σ41PCBs[a]	50–2250	n.r.	187–4585	All basins (open Med. cruises)	2006, 2007	Berrojalbiz et al. (2014)
PAHs (μg m^{-2} yr^{-1})						
Σ30PAHs[c]	70–80	n.r.	600–1400	All basins (open Med. cruises)	2006, 2007	Castro-Jiménez et al. (2012)
Σ35PAHs[b,c]	58	165	700	Eastern Med. (Finokalia, Crete)	2001, 2002	Tsapakis et al. (2006)
Σ15PAHs	5–41	n.r.	335–510	Western Med. (Barcelona, Spain, and Banyuls, France)	2002	Guitart et al. (2010)
Σ11PAHs[a]	10–30	n.r.	n.r.	Western Med. (Mallorca, Spain)	1989	Lipiatou et al. (1997)
Σ11PAHs[a]	15–35	10–40	n.r.		1990	Lipiatou and Albaigés (1994)
Σ34PAHs[c]	30–1120	n.r.	n.r.	Western Med. (Bizerte, Tunisia)	2015	Barhoumi et al. (2018)
OCPs (ng m^{-2} yr^{-1})						
HCB[a]	4–18	n.r.	30–1400	All basins (open Med. cruises)	2006, 2007	Berrojalbiz et al. (2014)
HCHs[a]	n.r	n.r.	1000–90,000			
Σ6OCP	13–230	n.r.	n.r.	Western Med. (Bizerte, Tunisia)	2015	Barhoumi et al. (2018)
PBDEs (ng m^{-2} yr^{-1})						

(continued)

Table 3 (continued)

Compounds	Deposition flux			Location	Year[d]	References
	Dry	Wet	Diffusive			
Σ27PBDEs	141–1110	n.r.	n.r.	Western Med. (Marseille, France)	2015	Castro-Jiménez et al. (2017))
Σ27PBDEs	69–3386	n.r.	n.r.	Western Med. (Bizerte, Tunisia)		
Σ8PBDEs[a]	230	n.r.	n.r.	Western Med. (Thau lagoon, France)	2007–2008	Estimated from Castro-Jiménez et al. (2011)
Σ5PBDEs[b]	4–90	n.r.	n.r.	Western Med. (Coastal)	2001–2003	Méjanelle et al. unpublished
OPEs (μg m^{-2} yr^{-1})						
Σ14OPEs[a]	26–320	n.r.	n.r.	All basins (open Med. cruises)	2006, 2007	Castro-Jiménez et al. (2014)
Σ9OPEs[a, c]	80	n.r.	n.r.	Western Med. (Bizerte, Tunisia)	2015	Castro-Jiménez and Sempéré (2018)

n.r. not reported
[a]Samples collected using high-volume samplers + polyurethane foam (gas + aerosol)
[b]Samples collected using deposition samplers
[c]Mean values
[d]The period is indicative, given years are not always complete

(volcanoes, forest fires) are not negligible in some environments (Lammel, 2015). All the atmospheric forms of these organic contaminants have obtained relevant attention due to their environmental persistence, bioaccumulation potential and proven toxic effect on aquatic ecosystems and human health (WHO, 2004). For example, in the Mediterranean Sea, the organic fraction of atmospheric aerosols has been shown as biologically active and capable of inducing adverse effects on aquatic species, with strong correlations with the concentration of particle-bound PAHs (Mesquita et al., 2014, 2016).

Depending on the vapour pressure, most organic contaminants are present in both gaseous and particulate phases at ambient temperature in the atmosphere. For the majority of POPs and associated contaminants, the gaseous phase is predominant with a contribution higher than 90% both in the eastern and western Mediterranean (e.g., for PCBs: Mandalakis & Stephanou, 2002; for PAHs: Gambaro et al., 2004; Tsapakis & Stephanou, 2005). When associated with atmospheric particles, organic pollutants can be more resistant to atmospheric degradation processes (e.g., photodegradation), therefore increasing their atmospheric lifetimes and hence long-range transport before their deposition (Castro-Jiménez et al., 2017). Thus, the atmospheric dry deposition is considered as the main pathway for the input of the most hydrophobic contaminants in aquatic ecosystems. It is the reason why the majority of existing data are mainly limited to dry deposition. Most of them are derived from studies performed in coastal sites (Lipiatou & Albaigés, 1994; Lipiatou et al., 1997; Tsapakis et al., 2006; Castro-Jiménez et al., 2017; Barhoumi et al., 2018). As no network on POPs deposition has been implemented yet over the MB,

only two surveys performed during oceanographic cruises enable us to obtain a broad spatial coverage (Castro-Jiménez et al., 2010, 2012, 2014; Berrojalbiz et al., 2014). In these studies, the particulate phase was mainly collected using filters, and dry deposition was estimated from the aerosol concentration and the fine particle settling velocity (typically 0.2 cm s^{-1}). However, atmospheric deposition of organic contaminants is not only represented by dry and wet fluxes but includes air-sea diffusive exchange, i.e., absorption and volatilization fluxes on the seawater surface (e.g., Castro-Jiménez et al., 2012). Generally, the diffusive fluxes are estimated by determining the absorption and volatilization fluxes from an air-water mass transfer coefficient, the contaminant concentrations in the gas phase and in the surface seawater, and the Henry's law constant. Thus, wet deposition of organic contaminants implies both particle/gas scavenging and dissolution of gaseous compounds in cloud droplets according to Henry's law constant (Mandalakis & Stephanou, 2004).

When sampling both gaseous and particulate phases, the studies showed that the distribution of organic contaminants between the particle and gas phases in the atmosphere controls their pathway and hence their removal rate. The air-sea exchange is generally the dominant pathway of organic contaminant deposition. For example, the comparison of air-sea gas exchange with dry deposition shows the greater importance of diffusive exchange by a factor 3 to 5 for PCBs and HCB (Berrojalbiz et al., 2014). In the same way, due to the predominance of PAHs concentrations in the gas phase, air-sea exchange clearly dominates the PAHs deposition processes (Guitart et al., 2010). Thus, gas absorption contributes to 86% and 91% of the total net flux for fluorene and phenanthrene, respectively, at Finokalia (Tsapakis et al., 2006). In addition, net absorption was observed in all transects during Mediterranean cruises for the PAH components with three and four aromatic rings, which are the main constituents of PAH gas phase concentrations (e.g., phenanthrene, anthracene, chrysene) (Castro-Jiménez et al., 2012). Thus, $\sum_{30}$PAH average dry deposition accounted for the 5–11% (15–70 tons per year) of the average total annual inputs in the Mediterranean depending on the basins. Conversely, PAHs with high molecular weight or higher chlorinated PCDD/Fs are introduced in the MB primarily through dry and wet deposition (Tsapakis et al., 2006; Castro-Jiménez et al., 2010, 2013). The effect of weight is not visible for PCBs in wet deposition: particle-bound fractions of heavier congeners are not statistically different from the fractions of lighter ones (Mandalakis & Stephanou, 2004).

The data on dry deposition show that among the POPs, PBDEs present the highest fluxes, followed by PCBs and OCPs, whereas PCDD/Fs have the lowest fluxes (Table 3). The PAHs fluxes are one order of magnitude higher than POPs, as are OPEs fluxes. In addition to background deposition, important fluxes of PAHs have been recorded in the Mediterranean Sea during intense forest fires (Theodosi et al., 2013). The spatial pattern of dry deposition emphasized high fluxes in the western basin in comparison to the eastern one, whatever PAHs, PCBs or HCB, but it is not the case for PCDD/Fs and OPEs, which present similar fluxes in both basins (Castro-Jiménez et al., 2010, 2012, 2014; Berrojalbiz et al., 2014). This difference could be due to the highest aerosol loads in the western basin, associated with air masses

circulating to the north African coast. This fact highlights the potential PAHs/POPs sources from North Africa or the potential association of PCBs and other POPs to dust aerosols (Castro-Jiménez et al., 2012; Berrojalbiz et al., 2014).

From the data reported in Table 3, Castro-Jiménez et al. (2015) estimated that the total atmospheric fluxes of organic contaminants (sum of all studied families) to the open Mediterranean Sea varied from 2100 to 4600 t yr^{-1}. These inputs are dominated by PAHs (2000–4100 t yr^{-1}), then OPEs (13–260 t yr^{-1}), OCPs (3–230 t yr^{-1}), PCBs (~3–20 t yr^{-1}), PBDEs (~1 t yr^{-1}) and 2,3,7,8-PCDD/Fs (60–260 kg yr^{-1}). The fluxes are expected to be higher in areas with high rainfall due to wet deposition (Castro-Jiménez et al., 2010). The concomitant inputs of these various contaminants could favour an effect of contaminant-aerosol cocktail (Castro-Jiménez et al., 2013). Nevertheless, the Mediterranean Sea is not a sink for all organic contaminants as net volatilization for some PAHs or PCDD congeners have been observed mainly in the South-East Mediterranean, in particular close to the Nile delta and Alexandria for PAHs, due to the high concentrations of water-dissolved PAHs (Guitart et al., 2010; Castro-Jiménez et al., 2010, 2012). In addition, several PAHs, PCBs and OCPs are found close to phase equilibrium or net volatilization (upward flux) in the Aegean Sea (Lammel et al., 2015).

3 Conclusion and Recommendations

Atmospheric deposition is one of the significant pathways of trace metals and organic contaminants to the open Mediterranean Sea. The atmospheric deposition dataset shows that anthropogenic inputs largely predominate, even if dust deposition could be at times important for some metals. Due to their environmental impact and, in particular, their impact on marine ecosystems, metals and organic contaminants have been targeted by different protocols of regulation and mitigation to control their emission or use in Europe in order to reduce their atmospheric concentrations. Similar regulations are under process in North African countries. In this context of air quality improvement, the impact of atmospheric deposition of these pollutants could change. For example, the fluxes of metals could be orders of magnitude less such that they are no longer a source of contamination but at the same time are sufficient to support the needs of the marine biosphere in this region. The studies of climate conditions in the future indicate a dryer and warmer climate in the MB, a situation that could change the rain regime (e.g., Déqué et al., 2007), and hence the soluble inputs of metals by wet deposition. Thus, the findings on the atmospheric trace metals sources and effects need to be complemented to provide high-quality projections in a context of climate change. Inversely, new emerging organic contaminants, including flame retardants, perfluoroalkyl substances, surfactants, personal care products and pharmaceutical compounds, have been identified (Barroso et al., 2019) and could prove to be problematic for marine ecosystems in the coming years. In addition, phosphorus is a limiting nutrient in the oligotrophic

Mediterranean Sea. The contribution of OPEs and other potential families of organic compounds containing P as a source of phosphorus could be a relevant aspect of the atmospheric deposition of organic chemicals in the Mediterranean Sea. The studies of these emerging and P-rich contaminants are also key to estimate the effect of atmospheric deposition on marine biogeochemistry.

However, the limited available data do not enable us to observe and quantify the potential subsequent decrease in the atmospheric deposition fluxes of trace metals and conventional organic contaminants or the potential increase of emerging contaminants. Indeed, our extended review of reported data shows the lack of information on the recent deposition fluxes and on the spatial distribution of these fluxes both for trace metals and organic contaminants. For the latter, the deposition measurements are often limited to one or two studies for each POP or associated pollutants, and the emerging organic pollutants have received little consideration yet. Thus, the investigation on the occurrence and behaviour of these compounds in atmospheric deposition is a significant and challenging task due to the lack of regional data representative of the atmosphere over the Mediterranean Sea. In addition, the majority of deposition measurements are carried out at coastal sites, where local/regional contamination is often visible. We recommend increasing representative measurements of atmospheric concentrations and wet deposition of these compounds on isolated islands and during oceanographic cruises (Desboeufs et al., 2022) in remote waters of the Mediterranean basin.

References

Al-Momani, I. F., Aygun, S., & Tuncel, G. (1998). Wet deposition of major ions and trace elements in the eastern Mediterranean basin. *Journal of Geophysical Research, 103*, 8287–8299. https://doi.org/10.1029/97JD03130

Annett, A. L., Lapi, S., Ruth, T. J., & Maldonado, M. T. (2008). The effects of Cu and Fe availability on the growth and Cu: C ratios of marine diatoms. *Limnology and Oceanography, 53*, 2451–2461. https://doi.org/10.4319/lo.2008.53.6.2451

Avila, A., & Rodrigo, A. (2004). Trace metal fluxes in bulk deposition throughfall and stemflow at two evergreen oak stands in NE Spain subject to different exposure to the industrial environment. *Atmospheric Environment, 38*, 171–180. https://doi.org/10.1016/j.atmosenv.2003.09.067

Baker, A. R., Landing, W. M., Bucciarelli, E., Cheize, M., Fietz, S., Hayes, C. T., Kadko, D., Morton, P. L., Rogan, N., Sarthou, G., Shelley, R. U., Shi, Z., Shiller, A., & Hulten, M. M. P. (2016). Trace element and isotope deposition across the air–sea interface: Progress and research needs. *Philosophical Transactions of the Royal Society A, 374*, 20160190. https://doi.org/10.1098/rsta.2016.0190

Barhoumi, B., Castro-Jiménez, J., Guigue, C., Goutx, M., Sempéré, R., Derouiche, A., Achour, A., Touil, S., Driss, M. R., & Tedetti, M. (2018). Levels and risk assessment of hydrocarbons and organochlorines in aerosols from a North African coastal city (Bizerte Tunisia). *Environmental Pollution, 240*, 422–431. https://doi.org/10.1016/j.envpol.2018.04.109

Barroso, P. J., Santos, J. L., Martín, J., Aparicio, I., & Alonso, E. (2019). Emerging contaminants in the atmosphere: Analysis, occurrence and future challenges. *Critical Reviews in Environmental Science and Technology, 49*, 104–171. https://doi.org/10.1080/10643389.2018.1540761

Becagli, S., Anello, F., Bommarito, C., Cassola, F., Calzolai, G., Di Iorio, T., di Sarra, A., Gómez-Amo, J.-L., Lucarelli, F., Marconi, M., Meloni, D., Monteleone, F., Nava, S., Pace, G., Severi, M., Sferlazzo, D. M., Traversi, R., & Udisti, R. (2017). Constraining the ship contribution to the aerosol of the central Mediterranean. *Atmospheric Chemistry and Physics, 17*, 2067–2084. https://doi.org/10.5194/acp-17-2067-2017

Bergametti, G. (1987). *Apports de matière par voie atmosphérique à la Méditerranée Occidentale: Aspects géochimiques et météorologiques* (PhD Dissertation, 296 pp.). University of Paris VII - Paris Diderot - Paris Cité.

Bergametti, G., Dutot, A. L., Buat-Ménard, P., Losno, R., & Remoudaki, E. (1989). Seasonal variability of the elemental composition of atmospheric aerosol particles over the Northwestern Mediterranean. *Tellus, 41B*, 353–361. https://doi.org/10.1111/j.1600-0889.1989.tb00314.x

Berrojalbiz, N., Dachs, J., Del Vento, S., Ojeda, M. J., Valle, M. C., Castro-Jiménez, J., Mariani, G., Wollgast, J., & Hanke, G. (2011). Persistent organic pollutants in Mediterranean seawater and processes affecting their accumulation in plankton. *Environmental Science & Technology, 45*, 4315–4322. https://doi.org/10.1021/es103742w

Berrojalbiz, N., Castro-Jiménez, J., Mariani, G., Wollgast, J., Hanke, G., & Dachs, J. (2014). Atmospheric occurrence, transport and deposition of polychlorinated biphenyls and hexachlorobenzene in the Mediterranean and Black seas. *Atmospheric Chemistry and Physics, 14*, 8947–8959. https://doi.org/10.5194/acp-14-8947-2014

Béthoux, J.-P., Courau, P., Nicolas, E., & Ruiz-Pino, D. (1990). Trace-metal pollution in the Mediterranean Sea. *Oceanologica Acta, 13*, 481–488, https://archimer.ifremer.fr/doc/00103/21418/18995.pdf

Bonnet, S., & Guieu, C. (2006). Atmospheric forcing on the annual iron cycle in the western Mediterranean Sea: A 1-year survey. *Journal of Geophysical Research, Oceans, 111*, C090110. https://doi.org/10.1029/2005JC003213

Buck, C. S., Landing, W. M., & Resing, J. (2013). Pacific Ocean aerosols: Deposition and solubility of iron aluminum and other trace elements. *Marine Chemistry, 157*, 117–130. https://doi.org/10.1016/j.marchem.2013.09.005

Castro-Jiménez, J., & Sempéré, R. (2018). Atmospheric particle-bound organophosphate ester flame retardants and plasticizers in a North African Mediterranean Coastal City (Bizerte Tunisia). *The Science of the Total Environment, 642*, 383–393. https://doi.org/10.1016/j.scitotenv.2018.06.010

Castro-Jiménez, J., Eisenreich, S. J., Ghiani, M., Mariani, G., Skejo, H., Umlauf, G., Wollgast, J., Zaldívar, J. M., Berrojalbiz, N., Reuter, H. I., & Dachs, J. (2010). Atmospheric occurrence and deposition of polychlorinated dibenzo-p-dioxins and dibenzofurans (PCDD/Fs) in the open Mediterranean Sea. *Environmental Science & Technology, 44*, 5456–5463. https://doi.org/10.1021/es100718n

Castro-Jiménez, J., Mariani, G., Vives, I., Skejo, H., Umlauf, G., Zaldívar, J. M., Dueri, S., Messiaen, G., & Laugier, T. (2011). Atmospheric concentrations occurrence and deposition of persistent organic pollutants (POPs) in a Mediterranean Coastal Site (Etang de Thau France). *Environmental Pollution, 159*, 1948–1956. https://doi.org/10.1016/j.envpol.2011.03.012

Castro-Jiménez, J., Berrojalbiz, N., Wollgast, J., & Dachs, J. (2012). Polycyclic aromatic hydrocarbons (PAHs) in the Mediterranean Sea: Atmospheric occurrence, deposition and decoupling with settling fluxes in the water column. *Environmental Pollution, 166*, 40–47. https://doi.org/10.1016/j.envpol.2012.03.003

Castro-Jiménez, J., Berrojalbiz, N., Mejanelle, L., & Dachs, J. (2013). Sources transport and deposition of atmospheric organic pollutants in the Mediterranean Sea. In *Occurrence, fate and impact of atmospheric pollutants on environmental and human health* (ACS Symposium Series) (Vol. 11, pp. 231–260). American Chemical Society. https://doi.org/10.1021/bk-2013-1149.ch011

Castro-Jiménez, J., Berrojalbiz, N., Pizarro, M., & Dachs, J. (2014). Organophosphate ester (OPE) flame retardants and plasticizers in the open Mediterranean and Black Seas atmosphere. *Environmental Science & Technology, 48*, 3203–3209. https://doi.org/10.1021/es405337g

Castro-Jiménez, J., Dachs, J., & Eisenreich, S. J. (2015). Chapter 8 - Atmospheric deposition of POPs: Implications for the chemical pollution of aquatic environments. In E. Y. Zeng (Ed.), *Comprehensive analytical chemistry* (Vol. 67, pp. 295–322). Elsevier. https://doi.org/10.1016/B978-0-444-63299-9.00008-9

Castro-Jiménez, J., Barhoumi, B., Paluselli, A., Tedetti, M., Jiménez, B., Muñoz-Arnanz, J., Wortham, H., Ridha Driss, M., & Sempéré, R. (2017). Occurrence loading and exposure of atmospheric particle-bound POPs at the African and European edges of the western Mediterranean Sea. *Environmental Science & Technology, 51*, 13180–13189. https://doi.org/10.1021/acs.est.7b04614

Cerro, J. C., Cerdà, V., Caballero, S., Bujosa, C., Alastuey, A., Querol, X., & Pey, J. (2020). Chemistry of dry and wet atmospheric deposition over the Balearic Islands, NW Mediterranean: Source apportionment and African dust areas. *Science of The Total Environment, 747*, 141187. https://doi.org/10.1016/j.scitotenv.2020.141187

Chester, R., Nimmo, M., & Corcoran, P. A. (1997). Rain water-aerosol trace metal relationships at Cap Ferrat: A coastal site in the Western Mediterranean. *Marine Chemistry, 58*, 293–312. https://doi.org/10.1016/S0304-4203(97)00056-X

Chester, R., Nimmo, M., & Preston, M. R. (1999). The trace metal chemistry of atmospheric dry deposition samples collected at Cap Ferrat: A coastal site in the Western Mediterranean. *Marine Chemistry, 68*, 15–30. https://doi.org/10.1016/S0304-4203(99)00062-6

Déqué, M., Rowell, D. P., Lüthi, D., Giorgi, F., Christensen, J. H., Rockel, B., Jacob, D., Kjellström, E., de Castro, M., & van den Hurk, B. (2007). An intercomparison of regional climate simulations for Europe: Assessing uncertainties in model projections. *Climatic Change, 81*, 53–70. https://doi.org/10.1007/s10584-006-9228-x

Desboeufs, K., Losno, R., & Colin, J.-L. (2003). Relation between droplet pH and aerosol dissolution kinetics: Effect of incorporated aerosol particles on droplet pH during cloud process. *Journal of Atmospheric Chemistry, 46*, 159–172. https://doi.org/10.1023/A:1026011408748

Desboeufs, K. V., Sofikitis, A., Losno, R., Colin, J. L., & Ausset, P. (2005). Dissolution and solubility of trace metals from natural and anthropogenic aerosol particulate matter. *Chemosphere, 58*, 195–203. https://doi.org/10.1016/j.chemosphere.2004.02.025

Desboeufs, K., Bon Nguyen, E., Chevaillier, S., Triquet, S., & Dulac, F. (2018). Fluxes and sources of nutrient and trace metal atmospheric deposition in the northwestern Mediterranean. *Atmospheric Chemistry and Physics, 18*, 14477–14492. https://doi.org/10.5194/acp-18-14477-2018

Desboeufs, K., Fu, F., Bressac, M., Tovar-Sánchez, A., Triquet, S.,Doussin, J.-F., Giorio, C., Chazette, P., Disnaquet, J., Feron, A.,Formenti, P., Maisonneuve, F., Rodríguez-Romero, A., Zapf, P., Dulac, F., & Guieu, C. (2022). Wet deposition in the remote western and central Mediterranean as a source of trace metals to surface seawater, *Atmos. Chem. Phys., 22*, 2309–2332. https://doi.org/10.5194/acp-22-2309-2022

Dulac, F. (1986). *Dynamique du transport et des retombées d'aérosols métalliques en Méditerranée occidentale* (PhD dissertation, 241 pp.). University of Paris VII - Paris-Diderot - Paris Cité.

Dulac, F., Buat-Ménard, P., Ezat, U., Melki, S., & Bergametti, G. (1989). Atmospheric input of trace metals to the western Mediterranean: Uncertainties in modelling dry deposition from cascade impactor data. *Tellus, 41B*, 362–378. https://doi.org/10.1111/j.1600-0889.1989.tb00315.x

EEA (2018). European Union emission inventory report 1990–2016 under the UNECE Convention on Long-range Transboundary Air Pollution (LRTAP), EEA Report No 6/2018, European Environment Agency, Luxembourg, https://doi.org/10.2800/571876

Formenti, P., Schütz, L., Balkanski, Y., Desboeufs, K., Ebert, M., Kandler, K., Petzold, A., Scheuvens, D., Weinbruch, S., & Zhang, D. (2011). Recent progress in understanding physical and chemical properties of African and Asian mineral dust. *Atmospheric Chemistry and Physics, 11*, 8231–8256. https://doi.org/10.5194/acp-11-8231-2011

Fu, Y. (2018). *Etude des apports des métaux traces par le dépôt atmosphérique en Méditerranée occidentale* (PhD dissertation, V+235 pp.). University of Paris-Diderot - Paris Cité. https://tel.archives-ouvertes.fr/tel-03566619/document. Last access 8 July 2022.

Fu, Y., Desboeufs, K., Vincent, J., Bon Nguyen, E., Laurent, B., Losno, R., & Dulac, F. (2017). Estimating chemical composition of atmospheric deposition fluxes from mineral insoluble particles deposition collected in the western Mediterranean region. *Atmospheric Measurement Techniques, 10*, 4389–4401. https://doi.org/10.5194/amt-10-4389-2017

Gallisai, R., Peters, F., Volpe, G., Basart, S., & Baldasano, J. M. (2014). Saharan dust deposition may affect phytoplankton growth in the Mediterranean Sea at ecological time scales. *PLoS One, 9*, e110762. https://doi.org/10.1371/journal.pone.0110762

Gambaro, A., Manodori, L., Moret, I., Capodaglio, G., & Cescon, P. (2004). Transport of gas-phase polycyclic aromatic hydrocarbons to the Venice lagoon. *Environmental Science & Technology, 38*, 5357–5364. https://doi.org/10.1021/es049084s

Guerzoni, S., Molinaroli, E., Rossini, P., Rampazzo, G., Quarantotto, G., De Falco, G., & Cristini, S. (1999). Role of desert aerosol in metal fluxes in the Mediterranean area. *Chemosphere, 39*, 229–246. https://doi.org/10.1016/S0045-6535(99)00105-8

Guieu, C., & Thomas, A. J. (1996). Saharan aerosols: From the soil to the ocean. In S. Guerzoni & R. Chester (Eds.), *The impact of desert dust across the Mediterranean* (Environ. Sci. Technol. Lib) (Vol. 11, pp. 207–216). Springer. https://doi.org/10.1007/978-94-017-3354-0_20

Guieu, C., Martin, J. M., Thomas, A. J., & Elbaz-Poulichet, F. (1991). Atmospheric versus river inputs of metals to the Gulf of Lions. Total concentrations partitioning and fluxes. *Marine Pollution Bulletin, 22*, 176–183. https://doi.org/10.1016/0025-326X(91)90467-7

Guieu, C., Chester, R., Nimmo, M., Martin, J.-M., Guerzoni, S., Nicolas, E., Mateu, J., & Keyse, S. (1997). Atmospheric input of dissolved and particulate metals to the northwestern Mediterranean. *Deep Sea Research Part II: Topical Studies in Oceanography, 44*, 655–674. https://doi.org/10.1016/S0967-0645(97)88508-6

Guieu, C., Loÿe-Pilot, M. D., Benyahya, L., & Dufour, A. (2010). Spatial variability of atmospheric fluxes of metals (Al, Fe, Cd, Zn and Pb) and phosphorus over the whole Mediterranean from a one-year monitoring experiment: Biogeochemical implications. *Marine Chemistry, 120*, 164–178. https://doi.org/10.1016/j.marchem.2009.02.004

Guitart, C., García-Flor, N., Miquel, J. C., Fowler, S. W., & Albaigés, J. (2010). Effect of the accumulation of polycyclic aromatic hydrocarbons in the sea surface microlayer on their coastal air–sea exchanges. *Journal of Marine Systems, 79*, 210–217. https://doi.org/10.1016/j.jmarsys.2009.09.003

Heimbürger, L.-E., Migon, C., Dufour, A., Chiffoleau, J.-F., & Cossa, D. (2010). Trace metal concentrations in the North-western Mediterranean atmospheric aerosol between 1986 and 2008: Seasonal patterns and decadal trends. *The Science of the Total Environment, 408*, 2629–2638. https://doi.org/10.1016/j.scitotenv.2010.02.042

Herut, B., Nimmo, M., Medway, A., Chester, R., & Krom, M. D. (2001). Dry atmospheric inputs of trace metals at the Mediterranean coast of Israel (SE Mediterranean): Sources and fluxes. *Atmospheric Environment, 35*, 803–813. https://doi.org/10.1016/S1352-2310(00)00216-8

Hsu, S.-C., Wong, G. T. F., Gong, G.-C., Shiah, F.-K., Huang, Y.-T., Kao, S.-J., Tsai, F., Candice Lung, S.-C., Lin, F.-J., Lin, I.-I., Hung, C.-C., & Tseng, C.-M. (2010). Sources solubility and dry deposition of aerosol trace elements over the East China Sea. *Marine Chemistry, 120*, 116–127. https://doi.org/10.1016/j.marchem.2008.10.003

Jordi, A., Basterretxea, G., Tovar-Sánchez, A., Alastuey, A., & Querol, X. (2012). Copper aerosols inhibit phytoplankton growth in the Mediterranean Sea. *Proceedings of the National Academy of Sciences of the United States of America, 109*, 21246. https://doi.org/10.1073/pnas.1207567110

Jurado, E., Jaward, F., Lohmann, R., Jones, K. C., Simó, R., & Dachs, J. (2005). Wet deposition of persistent organic pollutants to the global oceans. *Environmental Science & Technology, 39*, 2426–2435. https://doi.org/10.1021/es048599g

Kaya, G., & Tuncel, G. (1997). Trace element and major ion composition of wet and dry deposition in Ankara Turkey. *Atmospheric Environment, 31*, 3985–3998. https://doi.org/10.1016/S1352-2310(97)00221-5

Koçak, M., Kubilay, N., Herut, B., & Nimmo, M. (2005). Dry atmospheric fluxes of trace metals (Al, Fe, Mn, Pb, Cd, Zn, Cu) over the Levantine basin: A refined assessment. *Atmospheric Environment, 39*, 7330–7341. https://doi.org/10.1016/j.atmosenv.2005.09.010

Koçak, M., Mihalopoulos, N., & Kubilay, N. (2007). Chemical composition of the fine and coarse fraction of aerosols in the northeastern Mediterranean. *Atmospheric Environment, 41*, 7351–7368. https://doi.org/10.1016/j.atmosenv.2007.05.011

Kuloglu, E., & Tuncel, G. (2005). Size distribution of trace elements and major ions in the Eastern Mediterranean atmosphere. *Water, Air, and Soil Pollution, 167*, 221–241. https://doi.org/10.1007/s11270-005-8651-3

Lammel, G. (2015). Polycyclic aromatic compounds in the atmosphere – A review identifying research needs. *Polycyclic Aromatic Compounds, 35*, 316–329. https://doi.org/10.1080/10406638.2014.931870

Lammel, G., Audy, O., Besis, A., Efstathiou, C., Eleftheriadis, K., Kohoutek, J., Kukučka, P., Mulder, M. D., Přibylová, P., Prokeš, R., Rusina, T. P., Samara, C., Sofuoglu, A., Sofuoglu, S. C., Taşdemir, Y., Vassilatou, V., Voutsa, D., & Vrana, B. (2015). Air and seawater pollution and air–sea gas exchange of persistent toxic substances in the Aegean Sea: Spatial trends of PAHs PCBs OCPs and PBDEs. *Environmental Science and Pollution Research International, 22*, 11301–11313. https://doi.org/10.1007/s11356-015-4363-4

Laurent, B., Audoux, T., Bibi, M., Dulac, F., & Bergametti, G. (2022). Mass deposition. In F. Dulac, S. Sauvage, & E. Hamonou (Eds.), *Atmospheric Chemistry in the Mediterranean Region – Vol. 2, From Air Pollutant Sources to Impacts*. Springer, this volume. https://doi.org/10.1007/978-3-030-82385-6_16

Lim, B., Jickells, T. D., Colin, J. L., & Losno, R. (1994). Solubilities of Al, Pb, Cu, and Zn in rain sampled in the marine environment over the North Atlantic Ocean and Mediterranean Sea. *Global Biogeochemical Cycles, 8*, 349–362. https://doi.org/10.1029/94GB01267

Lipiatou, E., & Albaigés, J. (1994). Atmospheric deposition of hydrophobic organic chemicals in the northwestern Mediterranean Sea: Comparison with the Rhone River input. *Marine Chemistry, 46*, 153–164. https://doi.org/10.1016/0304-4203(94)90052-3

Lipiatou, E., Tolosa, I., Simó, R., Bouloubassi, I., Dachs, J., Marti, S., Sicre, M.-A., Bayona, J. M., Grimalt, J. O., Saliot, A., & Albaiges, J. (1997). Mass budget and dynamics of polycyclic aromatic hydrocarbons in the Mediterranean Sea. *Deep Sea Research Part II: Topical Studies in Oceanography, 44*, 881–905. https://doi.org/10.1016/S0967-0645(96)00093-8

Losno, R. (1989). *Chimie d'éléments minéraux en traces dans les pluies méditerranéennes* (PhD dissertation, 159 pp.). University of Paris VII - Paris-Diderot - Paris Cité, https://tel.archives-ouvertes.fr/tel-00814327/document, last access 8 July 2022.

Losno, R., Bergametti, G., & Buat-Ménard, P. (1988). Zinc partitioning in Mediterranean rainwater. *Geophysical Research Letters, 15*, 1389–1392. https://doi.org/10.1029/GL015i012p01389

Loÿe-Pilot, M. D., Guieu, C., & Ridame, C. (2001). Atmospheric bulk fluxes of natural and pollutant metals to the north western Mediterranean, their trend over the past 15 years (1985–2000). In *Atmospheric transport and deposition of pollutants into the Mediterranean Sea* (UNEP/MAP Technical Rept. Ser. 133) (pp. 35–54). United Nations Environment Program/Mediterranean Action Plan. http://wedocs.unep.org/xmlui/bitstream/handle/20.500.11822/576/mts133.pdf?sequence=2#page=41. Last access 8 July 2022.

Loÿe-Pilot, M. D., Martin, J. M., & Morelli, J. (1986). Influence of Saharan dust on the rain acidity and atmospheric input to the Mediterranean. *Nature, 321*, 427–428. https://doi.org/10.1038/321427a0

Mackey, K., Buck, K., Casey, J., Cid, A., Lomas, M., Sohrin, Y., & Paytan, A. (2012). Phytoplankton responses to atmospheric metal deposition in the coastal and open-ocean Sargasso Sea. *Frontiers in Microbiology, 3*, 359. https://doi.org/10.3389/fmicb.2012.00359

Mahowald, N. M., Hamilton, D. S., Mackey, K. R. M., Moore, J. K., Baker, A. R., Scanza, R. A., & Zhang, Y. (2018). Aerosol trace metal leaching and impacts on marine microorganisms. *Nature Communications, 9*, 2614. https://doi.org/10.1038/s41467-018-04970-7

Mandalakis, M., & Stephanou, E. G. (2002). Study of atmospheric PCB concentrations over the eastern Mediterranean Sea. *Journal of Geophysical Research, 107*, 4716. https://doi.org/10.1029/2001JD001566

Mandalakis, M., & Stephanou, E. G. (2004). Wet deposition of polychlorinated biphenyls in the eastern Mediterranean. *Environmental Science & Technology, 38*, 3011–3018. https://doi.org/10.1021/es030078q

Mason, B. (1966). *Principles of geochemistry* (3rd ed.). Wiley. ISBN 9780471575214

Mesquita, S. R., van Drooge, B. L., Reche, C., Guimarães, L., Grimalt, J. O., Barata, C., & Piña, B. (2014). Toxic assessment of urban atmospheric particle-bound PAHs: Relevance of composition and particle size in Barcelona (Spain). *Environmental Pollution, 184*, 555–562. https://doi.org/10.1016/j.envpol.2013.09.034

Mesquita, S. R., Dachs, J., van Drooge, B. L., Castro-Jiménez, J., Navarro-Martín, L., Barata, C., Vieira, N., Guimarães, L., & Piña, B. (2016). Toxicity assessment of atmospheric particulate matter in the Mediterranean and Black Seas open waters. *Science of The Total Environment, 545–546*, 163–170. https://doi.org/10.1016/j.scitotenv.2015.12.055

Migon, C., & Nicolas, E. (1998). The trace metal recycling component in the Northwestern Mediterranean. *Marine Pollution Bulletin, 36*, 273–277. https://doi.org/10.1016/S0025-326X(98)00160-X

Migon, C., Morelli, J., Nicolas, E., & Copin-Montégut, G. (1991). Evaluation of total atmospheric deposition of Pb, Cd, Cu and Zn to the Ligurian Sea. *Science of The Total Environment, 105*, 135–148. https://doi.org/10.1016/0048-9697(91)90336-D

Migon, C., Journel, B., & Nicolas, E. (1997). Measurement of trace metal wet, dry, and total atmospheric fluxes over the Ligurian Sea. *Atmospheric Environment, 31*, 889–896. https://doi.org/10.1016/S1352-2310(96)00242-7

Migon, C., Robin, T., Dufour, A., & Gentili, B. (2008). Decrease of lead concentrations in the Western Mediterranean atmosphere during the last 20 years. *Atmospheric Environment, 42*, 815–821. https://doi.org/10.1016/j.atmosenv.2007.10.078

Morel, F. M. M., & Price, N. M. (2003). The biogeochemical cycles of trace metals in the oceans. *Science, 300*, 944–947. https://doi.org/10.1126/science.1083545

Muezzinoglu, A., & Cizmecioglu, S. C. (2006). Deposition of heavy metals in a Mediterranean climate area. *Atmospheric Research, 81*, 1–16. https://doi.org/10.1016/j.atmosres.2005.10.004

Özsoy, T., & Örnektekin, S. (2009). Trace elements in urban and suburban rainfall, Mersin, Northeastern Mediterranean. *Atmospheric Research, 94*, 203–219. https://doi.org/10.1016/j.atmosres.2009.05.017

Pinedo-González, P., West, A. J., Tovar-Sánchez, A., Duarte, C. M., Marañón, E., Cermeño, P., González, N., Sobrino, C., Huete-Ortega, M., Fernández, A., López-Sandoval, D. C., Vidal, M., Blasco, D., Estrada, M., & Sañudo-Wilhelmy, S. A. (2015). Surface distribution of dissolved trace metals in the oligotrophic ocean and their influence on phytoplankton biomass and productivity. *Global Biogeochemical Cycles, 29*, 1763–1781. https://doi.org/10.1002/2015GB005149

Pirrone, N., Costa, P., & Pacyna, J. M. (1999). Past current and projected atmospheric emissions of trace elements in the Mediterranean region. *Water Science and Technology, 39*, 1–7. https://doi.org/10.1016/S0273-1223(99)00311-X

Remoudaki, E., Bergametti, G., & Buat-Ménard, P. (1991a). Temporal variability of atmospheric lead concentrations and fluxes over the northwestern Mediterranean Sea. *Journal of Geophysical Research, 96*, 1043–1055. https://doi.org/10.1029/90JD00111

Remoudaki, E., Bergametti, G., & Losno, R. (1991b). On the dynamic of the atmospheric input of copper and manganese into the Western Mediterranean Sea. *Atmospheric Environment, 25A*, 733–744. https://doi.org/10.1016/0960-1686(91)90072-F

Ridame, C., Guieu, C., & Löye-Pilot, M. D. (1999). Trend in total atmospheric deposition fluxes of aluminium iron and trace metals in the northwestern Mediterranean over the past decade (1985-1997). *Journal of Geophysical Research, 104*, 30127–30138. https://doi.org/10.1029/1999JD900747

Ridame, C., Le Moal, M., Guieu, C., Ternon, E., Biegala, I. C., L'Helguen, S., & Pujo-Pay, M. (2011). Nutrient control of N2 fixation in the oligotrophic Mediterranean Sea and the impact of Saharan dust events. *Biogeosciences, 8*, 2773–2783. https://doi.org/10.5194/bg-8-2773-2011

Rudnick, R. L., & Gao, S. (2003). 4.1 - Composition of the continental crust. In H. D. Holland & K. K. Turekian (Eds.), *Treatise on geochemistry* (2nd ed., pp. 1–64). Elsevier. https://doi.org/10.1016/B978-0-08-095975-7.00301-6

Ruiz-Pino, D. P., Jeandel, C., Bethoux, J.-P., & Minster, J.-F. (1990). Are the trace metal cycles balanced in the Mediterranean Sea? *Global and Planetary Change, 2*, 369–388. https://doi.org/10.1016/0921-8181(90)90009-2

Sandroni, V., & Migon, C. (2002). Atmospheric deposition of metallic pollutants over the Ligurian Sea: Labile and residual inputs. *Chemosphere, 4*, 753–764. https://doi.org/10.1016/S0045-6535(01)00337-X

Schmidt, N., Thibault, D., Galgani, F., Paluselli, A., & Sempéré, R. (2018). Occurrence of microplastics in surface waters of the Gulf of Lion (NW Mediterranean Sea). *Progress in Oceanography, 163*, 214–220. https://doi.org/10.1016/j.pocean.2017.11.010

Shelley, R. U., Landing, W. M., Ussher, S. J., Planquette, H., & Sarthou, G. (2018). Regional trends in the fractional solubility of Fe and other metals from North Atlantic aerosols (GEOTRACES cruises GA01 and GA03) following a two-stage leach. *Biogeosciences, 15*, 2271–2288. https://doi.org/10.5194/bg-15-2271-2018

The MerMex group. (2011). Marine ecosystems' responses to climatic and anthropogenic forcings in the Mediterranean. *Progress in Oceanography, 91*, 97–166. https://doi.org/10.1016/j.pocean.2011.02.003

Theodosi, C., Markaki, Z., Tselepides, A., & Mihalopoulos, N. (2010). The significance of atmospheric inputs of soluble and particulate major and trace metals to the Eastern Mediterranean Sea. *Marine Chemistry, 120*, 154–163. https://doi.org/10.1016/j.marchem.2010.02.003

Theodosi, C., Parinos, C., Gogou, A., Kokotos, A., Stavrakakis, S., Lykousis, V., Hatzianestis, J., & Mihalopoulos, N. (2013). Downward fluxes of elemental carbon metals and polycyclic aromatic hydrocarbons in settling particles from the deep Ionian Sea (NESTOR site) Eastern Mediterranean. *Biogeosciences, 10*, 4449–4464. https://doi.org/10.5194/bg-10-4449-2013

Tolosa, I., Readman, J. W., Fowler, S. W., Villeneuve, J. P., Dachs, J., Bayona, J. M., & Albaiges, J. (1997). PCBs in the western Mediterranean. Temporal trends and mass balance assessment. *Deep Sea Research Part II: Topical Studies in Oceanography, 44*, 907–928. https://doi.org/10.1016/S0967-0645(96)00104-X

Tovar-Sánchez, A., Duarte, C. M., Arrieta, J. M., & Sañudo-Wilhelmy, S. A. (2014). Spatial gradients in trace metal concentrations in the surface microlayer of the Mediterranean Sea. *Frontiers in Marine Science, 1*, 79. https://doi.org/10.3389/fmars.2014.00079

Tsapakis, M., & Stephanou, E. G. (2005). Polycyclic aromatic hydrocarbons in the atmosphere of the Eastern Mediterranean. *Environmental Science & Technology, 39*, 6584–6590. https://doi.org/10.1021/es0505321

Tsapakis, M., Apostolaki, M., Eisenreich, S., & Stephanou, E. G. (2006). Atmospheric deposition and marine sedimentation fluxes of polycyclic aromatic hydrocarbons in the eastern Mediterranean basin. *Environmental Science & Technology, 40*, 4922–4927. https://doi.org/10.1021/es060487x

Wedepohl, K. H. (1995). The composition of the continental crust. *Geochimica et Cosmochimica Acta, 59*, 1217–1239. https://doi.org/10.1016/0016-7037(95)00038-2

WHO (2004). *Health aspects of air pollution results from the WHO project "Systematic review of health aspects of air pollution in Europe"*. Tech. Rep. EUR/04/5046026, World Health Organization, Regional Office for Europe, Copenhagen, VI+24 pp., https://apps.who.int/iris/handle/10665/107571

Part IX
Impacts of Air Pollution on Precipitation Chemistry and Climate

Coordinated by ***Maria Kanakidou***
Univ. of Crete (UOC), Department of Chemistry, Environmental Chemical Processes Laboratory, 70013 Crete, Greece

Reviewed partly by ***Lucia Mona*** *and partly by* ***Simone Lolli*** *(CNR/IMAA, Controda S. Loja snc, 85050 Tito (PZ), Italy)*

Abstract

In this section, we review various impacts of atmospheric composition and its changes focusing on precipitation chemistry and climate in the Mediterranean region. The first chapter is dedicated to current knowledge on aerosol and tropospheric ozone direct radiative impacts in the region, including radiation extinction relevant to renewable energy production. The second chapter summarizes knowledge on the indirect climatic effects of aerosol through cloud condensation and ice nuclei properties. The third chapter discusses the involvement of aerosols in precipitation chemistry and impact on atmospheric composition through multiphase reactions. The effects of atmospheric acidity on the composition and amounts of semi-volatile aerosol and the concentration of trace nutrients and toxic soluble metals are also discussed. All chapters are based on experimental results from chamber, ground based, aircraft and remote sensing observations, as well as numerical modeling.

Aerosol and Tropospheric Ozone Direct Radiative Impacts

Marc Mallet, Pierre Nabat, Alcide Giorgio di Sarra, Fabien Solmon, Claudia Gutiérrez, Sylvain Mailler, Laurent Menut, Dimitris Kaskaoutis, Matthew Rowlinson, Alexandru Rap, and François Dulac

Contents

Abstract This chapter describes the direct radiative forcing (DRF) over the Mediterranean region exerted by aerosols and tropospheric ozone. Recent results on the regional aerosol DRF at the surface and at the top of the atmosphere (TOA) are

*Chapter reviewed by **Olivier Boucher** (Laboratoire de Météorologie Dynamique (LMD), Paris, France), as part of the book Part IX Impacts of Air Pollution on Precipitation Chemistry and Climate also reviewed by **Lucia Mona** and **Simone Lolli** (CNR/IMAA, Tito Scalo (PZ), Italy)*

M. Mallet (✉) · P. Nabat
Centre National de Recherches Météorologiques (CNRM), Université de Toulouse, Météo-France, CNRS, Toulouse, France
e-mail: marc.mallet@meteo.fr

A. G. di Sarra
Laboratory for Observations and Measurements for Environment and Climate, Italian National Agency for New Technologies, Energy, and Sustainable Economic Development (ENEA), Rome, Italy

F. Solmon
Laboratoire d'Aérologie (LAERO), Université de Toulouse III Paul Sabatier, CNRS, Toulouse, France

C. Gutiérrez
Environmental Science Institute, University of Castilla-La Mancha (UCLM), Toledo, Spain

F. Dulac et al. (eds.), *Atmospheric Chemistry in the Mediterranean Region*,
https://doi.org/10.1007/978-3-030-82385-6_19

presented, together with trends in surface solar radiation. Absorption by aerosol particles within the troposphere affects heating rates and atmospheric stability, therefore playing a key role in the regional radiative impact of aerosols. In addition, the impact of aerosols on photochemistry and solar energy production over the Mediterranean region is also discussed with a focus on recent advances on the impact of the aerosol dimming on photovoltaic (PV) panels. Finally, the last section describes the regional radiative forcing (RF) of tropospheric ozone and drivers of its uncertainty.

1 Introduction

Among the various impacts (air quality, biogeochemical cycle, snow deposition, etc.) of atmospheric aerosols, their radiative effect has been recognized of paramount importance on the climate (e.g., Ramanathan et al., 2001; Crutzen et al., 2003; Boucher et al., 2013). Indirect radiative effects through aerosol-cloud interactions are analyzed in the following chapter of this volume (Nabat et al., 2022) and Mediterranean aerosol optical properties are reviewed in another chapter (Mallet et al., 2022). In this chapter, we focus on the direct radiative forcing (DRF) exerted by different aerosols types observed in the Mediterranean region. Quantifying the radiative forcing (RF) of aerosols is very important because it can lead to climate change (surface temperature, surface-atmosphere exchange fluxes, precipitation) even if these feedbacks are complex and not necessarily linear. Most of the studies are based on a 1D radiative transfer model using ground-based and aircraft in situ measurements as input data. Some estimates are provided by regional climate models and satellite data. We first consider the aerosol DRF exerted at the surface (Section 2.1) and at the top of the atmosphere (TOA) (Sect. 2.2), and the trends in

S. Mailler · L. Menut
Laboratoire de Météorologie Dynamique (LMD), Ecole Polytechnique, Ecole Normale Supérieure, Université Paris-Saclay, Sorbonne Université, CNRS, Ecole des Ponts ParisTech, IPSL, Palaiseau, France

D. Kaskaoutis
Institute for Environmental Research and Sustainable Development, National Observatory of Athens (NOA/IERSD), Athens, Greece

M. Rowlinson
National Centre for Atmospheric Science, University of York, York, UK

A. Rap
School of Earth and Environment, University of Leeds, Leeds, UK

F. Dulac
Laboratoire des Sciences du Climat et de l'Environnement (LSCE), CEA-CNRS-UVSQ, Université Paris-Saclay, IPSL, CEA Paris-Saclay, Gif-sur-Yvette, France

surface solar radiation (Sect. 2.3). In the following Section, we discuss the effect of aerosols on atmospheric photolysis rates (Sect. 3.1) and photovoltaic production (PV) (Sect. 3.2). Then, we examine the regional RF of tropospheric ozone (Sect. 4). In the last part (Sect. 5), conclusions and recommendations for future research are drawn.

2 Aerosol Direct Radiative Forcing

In the literature, aerosol DRF is classically defined at different levels, namely, at the surface or bottom of atmosphere (BOA), at the tropopause or top of the atmosphere (TOA), and within the atmosphere (ATM). The first forcing represents the effect of particles on the net radiation fluxes reaching the surface, and the second one, on the radiation fluxes reflected back to space by aerosols. The last term ATM indicates the part of solar energy which is absorbed by aerosols. Through absorption and scattering, aerosols typically induce a decrease in the solar energy reaching the surface, thereby possibly cooling it. At TOA, the aerosol particles generally produce an increase in the reflectivity of the Earth-Atmosphere system, inducing a cooling or parasol effect (Crutzen et al., 2003; IPCC, 2013). The atmospheric forcing results, for a part, from the possible absorption of solar radiation by particles. In case of purely scattering aerosols (e.g., pure sulfate or sea salt), the single scattering albedo of particles (SSA) tends toward 1, and the loss of energy at the surface is mostly scattered upward to space. In case of particles absorbing light either from biomass burning (BB), anthropogenic urban/industrial (UI) pollution, or mineral dust (D), the SSA is lower than 1, and a part of this loss at the surface is due to absorption within the aerosol layer which is consequently heated (Alpert et al., 1998; Ramanathan et al., 2007). Large particles, such as dust, also produce a measurable impact on the longwave radiation budget, through radiation absorption, scattering, and emission. The longwave radiative forcing at BOA is generally positive (i.e., aerosols induce an increase in downwelling IR radiation due to IR emission by suspended particles), while it is positive at TOA. Although this effect is smaller than in the shortwave spectral range, it may offset a significant part of the shortwave effect when large particles are present (e.g., Nabat et al., 2012).

2.1 Direct Radiative Effect at the Surface

By scattering and absorbing solar (shortwave) and infrared (longwave) radiation, natural and anthropogenic aerosols are able to perturb the net radiative fluxes at the surface in the Mediterranean basin. Perturbations in the shortwave can be strong as illustrated in Fig. 1, they are of a lesser extent in the longwave.

As an example, observations performed at the island of Lampedusa in the western central Mediterranean (35.5°N, 12.6°E) have been used to provide computations

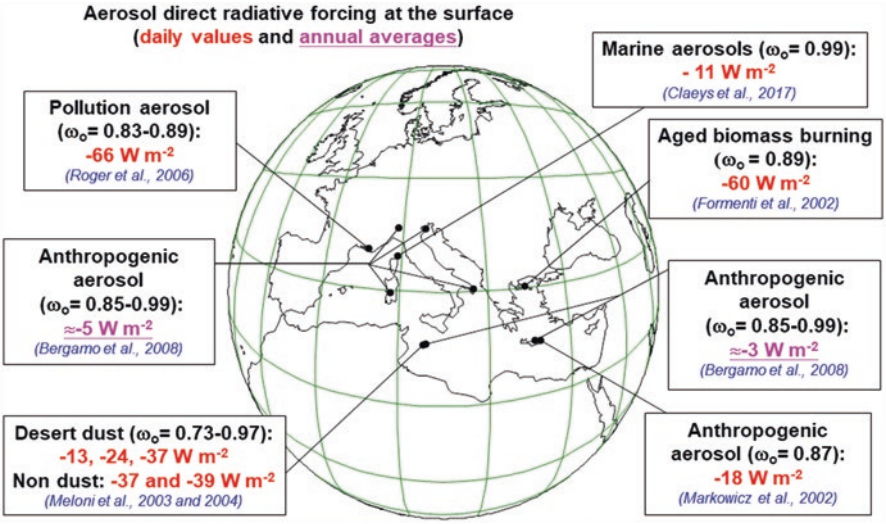

Fig. 1 Examples of literature-reported estimates of the direct radiative effect exerted by different aerosol species (mineral dust, smoke, anthropogenic, and sea spray) at the surface in the Mediterranean region. Daily and yearly (underlined) estimates are indicated for different locations. ω_o is the aerosol single scattering albedo. See Table 1 for more results

of the direct radiative forcing for three Saharan dust episodes, which occurred on May 18, 1999 (Meloni et al., 2003) and July 14–16, 2002 (Meloni et al., 2004). Radiative transfer computations denote a significant surface cooling, with respective instantaneous BOA forcings (Fig. 1; Table 1) of −13, −24, and −70.8 W m^{-2} for July 14–16 and May 18. At the same location, di Sarra et al. (2008) report surface aerosol effects obtained measuring the shortwave fluxes and aerosol optical properties in the period May–November of 2003 and 2004 (the pristine flux is considered here as the one occurring in the absence of atmospheric aerosols). They indicate that the daily surface forcing of mineral dust is much larger with respect to other aerosol species, with a mean value at the summer solstice and equinox of −30 and −24 W m^{-2}, respectively. Compared to the previous seasonal averages of about −85 W m^{-2}, a significantly higher daily DRF was measured at Lampedusa Island in late March 2010 during a very intense dust event (aerosol optical depth (AOD) up to 1.9 at 500 nm; di Sarra et al., 2011), while it was about −29 W m^{-2} during a less intense dust event (AOD of 0.5 at 500 nm) in spring 2008 (Meloni et al., 2015). At a different site (coastal French Mediterranean region), Saha et al. (2008) have also calculated a significant diurnal reduction of the downward shortwave radiation by about −62 W m^{-2} (daily mean) due to the presence of dust. As previously noted, regional climate models used to compute the direct radiative forcing of aerosols over the Mediterranean put in evidence important values, e.g. ranging between −5 and −20 W m^{-2} using the RegCM model (Nabat et al., 2012), with maximum values during the dusty season. In parallel, Nabat et al. (2015) have reported higher values of the DRF at the surface ranging from −10 to −30 W m^{-2} using the CNRM-RCSM regional climate model (period 2003–2009). Spyrou et al. (2013) have also shown

Table 1 Daily (unless specified) shortwave (SW) direct radiative forcing (DRF, in W m^{-2}) and forcing efficiency (FE, in W m^{-2} per unit AOD) of aerosols in the Mediterranean region, at the bottom or top of the atmosphere (BOA or TOA subscript, respectively), and within the atmosphere (ATM subscript)

Localization	Period	Aerosol species	DRF_{BOA} (FE_{BOA})	DRF_{TOA} (FE_{TOA})	DRF_{ATM}(FE_{ATM})	References
Eastern Mediterranean (STAAARTE-MED Exp.)	14/8/1998	Biomass burning	−64 (−164.1)	−22 (−56.4)	42 (107.7)	Formenti et al. (2002)
Ionian Sea	24–27/8/2007		−55	−20	35	Kaskaoutis et al. (2011)
Barcelona (NE Spain)	07/2009		–	−13(1)	–	Sicard et al. (2012)
Almeria (S Spain)	06/1999	Continental urban	−23.1 (−57.7)	−4.2 (−10.5)	18.9 (47.2)	Horvath et al. (2002)
Marseille (ESCOMPTE Exp.)	06/2001		−34.3 (−114.3)	−7.7 (−25.7)	26.6 (88.7)	Roger et al. (2006)
Toulon (SE France)	06/2006		−24.9 (−83.0)	−5.1 (−17)	19.8 (66)	Saha et al. (2008)
Realtor (ESCOMPTE)	24/6/2001	Continental industrial	−66[a] (−165.0[a])	−9[a] (−22.5[a])	57[a] (142.5[a])	Mallet et al. (2006)
Lampedusa Isl.	25/5/1999	Anthropogenic	−18.8 (−117.5)	+1.1 (+6.9)	19.9 (124.4)	Meloni et al. (2003)
	27/5/1999		−20.0 (−90.9)	−0.6 (−2.7)	19.4 (88.2)	
Finokalia, Crete Isl. (MINOS Exp.)	07/2001		−17.9 (−85.2)	−6.6 (−31.4)	11.3 (53.8)	Markowicz et al. (2002)
Whole Mediterranean	1996–2007		–	~−5	–	Zanis et al. (2012)
	1979–2016	Anthropogenic nitrate	−1.7	−1.3	0.4	Drugé et al. (2019)
Vinon-Sur-Verdon (ESCOMPTE Exp.)	24/6/2001	Continental rural	−61[a] (−164.9[a])	−8[a] (−21.6[a])	53[a] (143.2[a])	Mallet et al. (2006)
Toulon (SE France)	19/6/2006	Continental dust	−61.8 (−77.2)	−7.7 (−9.6)	54.1 (67.6)	Saha et al. (2008)

Localization	Period	Aerosol species	DRF_{BOA} (FE_{BOA})	DRF_{TOA} (FE_{TOA})	DRF_{ATM}(FE_{ATM})	References
Eastern Med. (24.5–34.5 °E and 32.5–35.5 °N)	June–Aug. 2010	Polluted continental	−17.41[b] (–)	−10.27[b] (–)	7.14[b] (–)	Mishra et al. (2014)
		Polluted dust	−39.95[b] (–)	−20.60[b] (–)	19.35[b] (–)	
		Saharan dust	−21.95[b] (–)	−11.05[b] (–)	10.90[b] (–)	
-Barcelona (NE Spain)	22–23/07/2009		–	−8(1)	–	Sicard et al. (2012)
Lampedusa Isl.	18/5/1999		−36.7 (−72.0)	−1.6 (−3.1)	35.1 (68.8)	Meloni et al. (2003)
	May–Nov. 2003 and 2004		−(24–30) (−(68.8–86.4))	–	–	di Sarra et al. (2008)
	14/7/2002		−13.1[a] (−56.9[a])	−5.7[a] (−24.8[a])	7.4[a] (32.2[a])	Meloni et al. (2004)
	16/7/2002	North African dust	−24.1[a] (−92.7[a])	−1.5[a] (−5.8[a])	22.6[a] (86.9[a])	
Western Mediterranean	Summer 2013	Marine	−11 (–)	−8 (–)	+3 (–)	Claeys et al. (2017)
7 km downwind Etna (Sicily)	Summer 2016–2017	Volcanic aerosol	−4.5 (–)	−7 (–)	2.5 (–)	Sellitto et al. (2020)
Lecce (South Italy)	Summer 2003–2004	Not specified	−15 (–)	−9.0 (–)	6 (–)	Tafuro et al. (2007)

[a]Instantaneous values

[b]For a solar zenith angle of 60° (overestimates the daytime value at the surface and top of atmosphere, underestimates it within the atmosphere; see suppl. Fig. S8 by Mishra et al., 2014)

the crucial effect of dust aerosols on the Mediterranean budget through the dust SKYRON model radiative transfer scheme for a 6-year simulation, with an annual maxima over the basin in the southern part of the western and central basins. Lastly, for specific case studies, Santese et al. (2010) indicated a daily-mean SW direct radiative effect of about ~−24 W m^{-2} at the surface and at a large regional scale, during two dust outbreaks. Using the NMMB-MONARCH model, Gkikas et al. (2018) assessed the regional dust radiative effect during the most intense identified dust events in the Mediterranean in the period 2000–2013 (maximum dust AOD ranging from about 2.5 to 5.5). They found that dust outbreaks affect the radiation budget at BOA, with values of the mean regional DRF from −22.2 to +2.2 W m^{-2}.

Similar effects have been observed and/or calculated for urban/industrial aerosols over the Mediterranean region (Table 1). Horvath et al. (2002), Markowicz et al. (2002), Meloni et al. (2003), Roger et al. (2006), Saha et al. (2008), and Mallet et al. (2016) show a decrease in surface solar fluxes of 23, 18, 19, 34, 24, and 15 W m^{-2} (daily mean) at Almeria (South Mediterranean coast of Spain), Finokalia (Crete Island in the eastern Mediterranean; 35.3°N, 25.6°E), Lampedusa Island, Marseilles (southeastern France), Toulon (South Mediterranean coast of France), and Barcelona, respectively. More recently, for continental pollution in the western basin observed in summer 2013, di Biagio et al. (2016) have suggested up to a 50% change in the aerosol radiative forcing efficiency (FE), i.e., the DRF per unit of optical depth, at the surface (from −160 to −235 W m^{-2} AOD^{-1} at 60° solar zenith angle) for an *SSA* varying between its maximum and minimum value.

By considering annual mean values of the measured AOD at Lampedusa for the different aerosol types, and the corresponding estimates of FE, Di Biagio et al. (2010) estimated a surface shortwave daily average DRF at the equinox of about −22 W m^{-2} for desert dust, −17 W m^{-2} for polluted/biomass burning particles, and −13 W m^{-2} for marine-mixed aerosol types. Volcanic aerosols originating from Etna have also been shown to produce a non-negligible DRF during active phases. Sellitto et al. (2016) estimated daily shortwave FE between −39 and −48 W m^{-2} AOD^{-1} at the TOA and between −66 and −49 W m^{-2} AOD^{-1} at the surface. Recently, Sellitto et al. (2020) have reported a daily average radiative forcing of −7 W m^{-2} at the surface for a volcanic plume with an ultraviolet AOD of 0.12–0.14.

At a regional scale, Zanis (2009) has also studied the radiative forcing of anthropogenic aerosols for summer 2000 and indicated significant values from −30 to −80 W m^{-2} over the Central Europe (mainly due to sulfates particles) and lowest (between 0 and −10 W m^{-2}) over the Mediterranean basin. In addition, the COSMO-CLM version has been used to study the dimming/brightening phenomenon over Europe for the period 1958–2001 (Zubler et al., 2011). Recently, Drugé et al. (2019) have proposed a first estimate of the nitrate direct radiative forcing at the surface. Over the period 1979–2016, the DRF is found to be about −1.7 W m^{-2} over Europe. Although only few studies have been dedicated to the radiative effect of biomass burning aerosols over the region, calculations performed by Formenti et al. (2002) during STAAARTE-MED reveal a significant surface dimming by smoke particles. Based on chemical, physical, and optical measurements within a large aged BB plume on board a research aircraft, they calculated a shortwave radiative forcing of

−64 W m^{-2} at the surface. Finally, for primary sea spray aerosols, Claeys et al. (2017) have reported values of ~−11 W m^{-2} during summer 2013.

Numerous studies underline the fact that the LW radiative effect of large particles, in particular mineral dust, can offset for a part the one exerted in the SW (Santese et al., 2010; di Sarra et al., 2011; Nabat et al., 2012, 2015; Spyrou et al., 2013; Meloni et al., 2018). At the surface, during desert dust events at Lampedusa, the longwave forcing has been computed to offset about 50% of the shortwave forcing (di Sarra et al., 2011; Meloni et al., 2015). It has been estimated that longwave radiation scattering by desert dust contributes by 18% to the LW direct radiative forcing (Sicard et al., 2014). As discussed by Gómez-Amo et al. (2011) and Gkikas et al. (2018), while the shortwave forcing is more intense during daytime (SZA of 50–60°) and zero in nighttime, the longwave forcing acts continuously. The combination of the two may produce a modulation of the overall effect, producing time varying effects on the surface radiation budget and on the atmospheric temperature.Although estimations of the surface radiative effects over the Mediterranean Sea are scarce at this time, the results presented here clearly display a non-negligible surface dimming at different locations. In regard to such surface cooling, it appears now crucial to investigate its potential impact in terms of changes in regional Mediterranean climate. First, there is a need to better quantify how the change in solar irradiance at the sea/continental surface influences regional water cycles through modifications in evaporative, heat fluxes, and SST. Secondly and since the percentage reduction in the UV and the visible region is as large as 10–20%, effects on terrestrial and marine biogeochemical cycles need to be examined. In particular, it should be interesting to study how the change in solar irradiance at the sea surface influences the carbon cycle and marine biological productivity through photosynthesis changes.

2.2 Aerosol Direct Radiative Forcing at TOA

Unless specified, results in this subsection are for the shortwave domain. As reported in Table 1 and Fig. 1, large differences are observed between the surface and top of the atmosphere forcing over the Mediterranean region. Concerning dust aerosols, the radiative transfer computations performed at Lampedusa show that the presence of dust increases the part of incident radiation that is scattered back to space but in magnitudes significantly lower than the surface energy losses (Meloni et al., 2003, 2004). Similarly, Saha et al. (2008) indicate a diurnal direct TOA forcing of −7.7 W m^{-2}, which is significantly lower than the one estimated at the surface. At the regional scale and using the RegCM3 regional climate model, Santese et al. (2010) have indicated a daily-mean SW DRF for mineral dust outbreak of about ~−3 W m^{-2} at top of the atmosphere. For some specific cases, model computation results put in evidence positive values of (SW) dust DRF at TOA for extremely absorbing mixed dust particles (Sicard et al., 2012). Di Biagio et al. (2010) estimated a shortwave daily average DRF at TOA at the equinox at Lampedusa.

They found that the DRF_{TOA} is about -14 W m^{-2} for desert dust, -5 W m^{-2} for polluted/biomass burning particles, and -4 W m^{-2} for marine-mixed aerosol types.

For polluted aerosols, results are quite similar and radiative transfer computations performed by Roger et al. (2006) indicate a mean TOA DRF four times lower compared to the surface one, consistently with computations performed by Horvath et al. (2002), Markowicz et al. (2002), Meloni et al. (2003), and Saha et al. (2008). Over Crete Island, Vrekoussis et al. (2005) indicated a radiative effect ranging from -12.6 to -2.3 W m^{-2} at TOA for summer and winter (March 2001–June 2002), respectively. Over the Po Valley, where nitrate is an important source of aerosol emissions and over the Adriatic Sea, Highwood et al. (2007) report an instantaneous TOA aerosol forcing of -4 ± 2 W m^{-2} over vegetation and -8 ± 4 W m^{-2} over ocean during the Aerosol Direct Radiative Impact Experiment (ADRIEX) project in late summer 2004.

Bergamo et al. (2008) indicate that anthropogenic particles produce a significant cooling effect over coastal and land sites of the central Mediterranean. At the TOA, the monthly average DRF is -4 ± 1 W m^{-2} during spring-summer and -2 ± 1 W m^{-2} during autumn-winter at the polluted sites. In parallel and based on MODIS Level 2 data in the eastern Mediterranean (Crete), Benas et al. (2011) report that anthropogenic aerosol forcing can reach values of -4 W m^{-2} at TOA (monthly mean instantaneous values).

Based on RegCM3 climatological computations, Zanis et al. (2012) have indicated a DRF of -3 W m^{-2} over the Iberian Peninsula and about -5 W m^{-2} (from their figure 2b) over the Mediterranean for anthropogenic (sulfate + carbonaceous) aerosols from 1996 to 2007. Recently, Drugé et al. (2019) have proposed a first estimate of the nitrate DRF at TOA. On average over the period 1979–2016, it is found to be about -1.4 W m^{-2} over Europe. Formenti et al. (2002) indicate that,

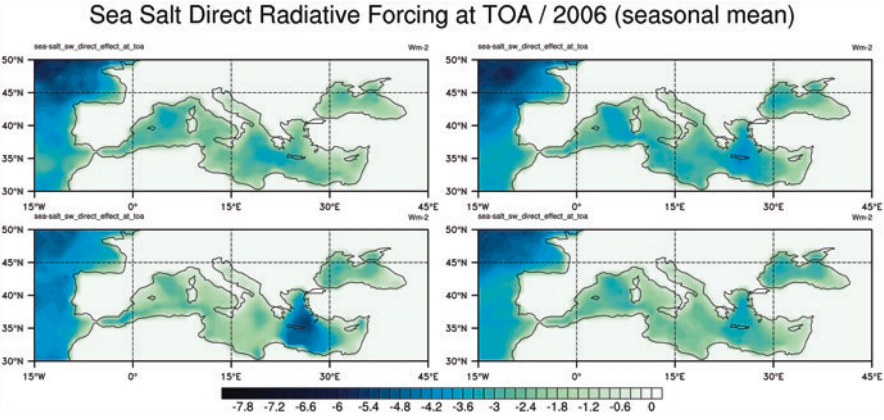

Fig. 2 Shortwave seasonal mean direct radiative forcing (W m^{-2}) exerted by primary sea-spray aerosols at TOA: *up left* December–February; *up right* March–May; *bottom left* June–August; *bottom right* September–November. MACC reanalysis data for the year 2006 from Inness et al. (2013)

over the sea, the SW radiative forcing is up to −64 W m^{-2} at the surface and up to −22 W m^{-2} at TOA during an event of smoke aerosols. Sicard et al. (2012) have also documented smoke particles and showed significant instantaneous radiative forcing at TOA of about −13 W m^{-2} (at 17 UT) observed over Barcelona. Finally, Di Biagio et al. (2010) have reported a value of diurnal average DRF at the equinox and summer solstice, respectively, of about −5 (−13) and −6.5 (−17) W m^{-2} at the TOA (and surface) for urban-industrial plus biomass burning aerosols, corresponding to a FE of −19.2 ± 3.3 (−59.0 ± 4.3) W m^{-2} AOD^{-1} at the equinox and −23.3 ± 4.1−75.6 ± 7.9) W m^{-2} AOD^{-1} at the summer solstice. During the EPL-RADIO campaigns (summer 2016–2017), Sellitto et al. (2020) have reported a daily radiative forcing of about −4.5 W m^{-2} for volcanic aerosols 7 km downwind the Etna degassing craters.

Di Biagio et al. (2009) have highlighted a significant sensitivity of the direct radiative effects exerted by aerosols over the Mediterranean to the varying SSA of particles. Similarly to what happens at the surface, for desert dust, the longwave effects compensate part of the shortwave radiative perturbation (Santese et al., 2010; di Sarra et al., 2011; Nabat et al., 2015; Meloni et al., 2018). The dust longwave radiative forcing at TOA is generally positive. Measurements at Lampedusa show that on a daily basis over the Mediterranean, the longwave effects offsets 26–35% of the shortwave radiation cooling (di Sarra et al., 2011; Meloni et al., 2015). As shown by Meloni et al. (2015), the longwave radiation emission by dust may lead to a net cooling of the atmosphere at specific altitude ranges even in daytime.

Concerning primary sea-spray aerosols, Nabat et al. (2015) reported a mean DRF at the regional scale in the Mediterranean basin around −1 W m^{-2} at the surface and at the TOA using the CNRM-RCSM4 model (simulation covering the period from 2003 to 2009). In addition, the (daytime) DRF of marine aerosols has been estimated during summer 2010 over the eastern Mediterranean (clear-sky conditions) by Mishra et al. (2014) using satellite, in situ observations, and radiative transfer modeling. The direct radiative forcing exerted at the surface and at TOA are found to be between −5 and −10 W m^{-2} (wavelength range 0.25–20 μm). In parallel, Lundgren et al. (2013) carried out a three-day computation (from July 24 to 26, 2006) over the whole Mediterranean basin with the COSMO-ART model. For clear-sky conditions and over the whole area (continental and oceanic surfaces), the solar DRF was about −0.62 ± 3.71 W m^{-2} at the surface and −0.47 ± 3.21 W m^{-2} at TOA. More recently, Claeys et al. (2017) reported higher DRF (at local scale) of −11 ± 4 W m^{-2} at the surface and −8 ± 3 W m^{-2} at TOA during summer 2013. Marine aerosols also have the ability to interact with longwave radiation, but few estimates are available over the Mediterranean basin. Lundgren et al. (2013) have reported an estimate of the LW forcing of +0.19 ± 1.08 W m^{-2} at the surface and +0.05 ± 0.54 W m^{-2} at TOA.

Figure 2 shows the seasonal-averaged SW DRF exerted by primary sea-spray particles at TOA as derived from the MACC reanalysis data (Inness et al., 2013) for 2006. Results indicate a significant seasonal variability with a maximum occurring during spring and summer. During the summer (JJA) season, DRF can reach ~6 W m^{-2} over the eastern Mediterranean basin, notably due to the strong dry north

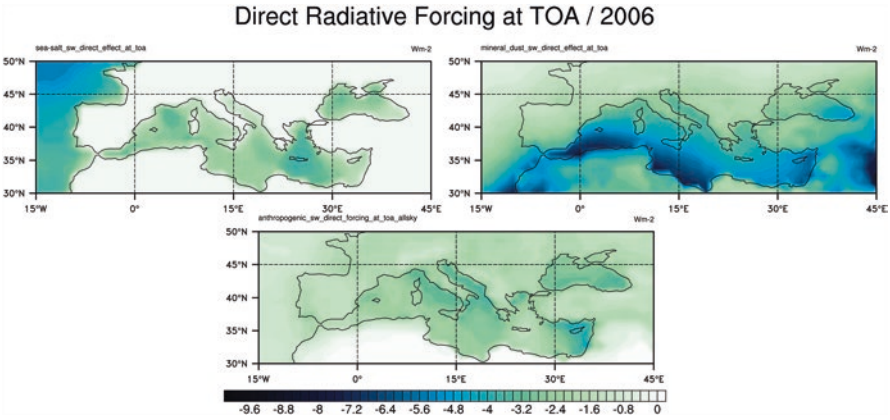

Fig. 3 Shortwave yearly-mean direct radiative forcing at TOA (W m^{-2}) due to various aerosols in the Mediterranean region: *up left* primary sea spray; *up right* mineral dust; *bottom* anthropogenic aerosols. MACC reanalysis data for the year 2006 from Inness et al. (2013)

winds over the Aegean Sea. During spring (MAM), important DRF is also observed over the western basin with values around −2 to −3 W m^{-2}. Compared to other aerosol regimes observed over the Mediterranean, the DRF due to marine particles is found to be similar to DRF exerted by anthropogenic aerosols. Figure 3 indicates yearly-mean (2006) DRF around −1 to −2 W m^{-2} at TOA for primary sea spray consistently with estimates provided by Nabat et al. (2015). Compared to other natural aerosols, the DRF at TOA over the sea by marine aerosols is lower than the mineral dust solar forcing (~−5 to −8 W m^{-2}; Fig. 3).

2.3 *Trends in Surface Solar Radiation over the Mediterranean Basin*

In parallel to the direct radiative forcing, the surface solar radiation (SSR) plays a vital role for the life on Earth as it controls the surface energy balance, the meteorological and climatic conditions, the water cycle, the plant photosynthesis and carbon cycle, and the diurnal and seasonal temperature variations (Mercado et al., 2009; Sanchez-Lorenzo et al., 2009; Wild et al., 2013). In addition to the greenhouse gas increase effect on the longwave radiative budget, the multi-decadal trends in solar radiation (global dimming/brightening phenomena) partly control (in addition to the global climate) the regional climate change, but the Mediterranean basin, as a whole area, has not been studied extensively. A recent work (Kambezidis et al., 2016) examined the evolution and trends of the surface net solar radiation. The solar dimming/brightening phenomenon is temporally and spatially analyzed over the Mediterranean basin based on MERRA (Modern Era Retrospective Analysis for Research and Applications) datasets. Results show an increase in the spatially

averaged SSR over the whole Mediterranean basin of +0.36 W m^{-2} per decade during the period 1979–2012. The SSR for all-sky conditions exhibited an overall increase of +2.1% from 1979 to 2012 over the whole Mediterranean basin in spring, while the respective variations in the other seasons were below 1%. However, statistically significant trends in onthly SSR, either for all-sky or clear-sky conditions, were observed only in May (Kambezidis et al., 2016). The higher increase in SSR in spring was common for all Mediterranean regions (west: 6.67°W–7°E, central: 7°E–21°E, east: 21–35°E), whereas the central part exhibited slight negative trends during autumn and winter. However, these tendencies were not statistically significant except for June (west part), May (central and east parts), and spring (east part). Annual mean variations of SSR for all-sky conditions in the west, central, and east Mediterranean regions exhibited an increasing tendency, with a higher rate in the western region, which is statistically significant at 95% confidence level (+0.82 W m^{-2} per decade). The other two regions reveal slight and not statistically significant increasing trends in SSR. However, these trends presented less increasing rates in the 2000s, in accordance with the results obtained in south Europe (Sanchez-Lorenzo et al., 2015). In general, the trends were higher (more positive or less negative) over the western Mediterranean, except in spring when the eastern Mediterranean exhibited higher increasing rates in SSR. An overall negative trend in SSR over the Mediterranean basin (2000–2007) was found by Hatzianastassiou et al. (2012) based on satellite data, mostly detected over the sea and the north African coasts, while positive trends were observed over the Iberian Peninsula and Balkan countries during 2001–2006. In addition, a solar brightening was observed after the late 1990s over Europe (Ohmura, 2009; Wild et al., 2009) including Spain (Sanchez-Lorenzo et al., 2009), Greece (Zerefos et al., 2009), Israel (Stanhill & Cohen, 2009), and Italy (Manara et al., 2015, 2016). The comparison between the results from the various studies indicates a large variation or even reversible signs in the SSR trends attributed to the different periods used in the analysis, the different stations or spatial domains that are involved, and the various techniques, making the study of the solar dimming/brightening phenomenon over the Mediterranean a really difficult task (Kambezidis et al., 2016).

At local scales, long-term actinometric measurements verified the increasing tendencies in solar radiation computed via satellite observations and reanalysis. Recent analysis in Athens (Kambezidis, 2018) showed that the global solar radiation exhibited a trend of +0.40% per decade during 1992–2017. For the case of clear skies, the trends were found to be +2.38% per decade, implying also a declining trend in cloudiness. Furthermore, it was found that the solar radiation in Athens had a winter trend of −2.46% per decade and a summer trend of +1.91% per decade during 1992–2017 (Kambezidis, 2018), whereas Kazadzis et al. (2018) revealed a +1.5% per decade in SSR in Athens during the brightening period (1980–2012). It was also found that the diffuse irradiance exhibited a trend of −5.19% per decade during 1992–2017 (Kambezidis, 2018), while under clear skies, the trend became −6.77% per decade. The declining trend in the diffuse radiation implies a decrease in aerosol amount or in cloudiness or/even both over the study location.

3 Implication for Photochemical Processes and Solar Energy Production

3.1 Impact on Photolysis

Impact of aerosols on photochemistry in the Mediterranean is a relevant question due to the presence of persistent, occasionally strong loads of aerosols over the area together with strong concentrations of tropospheric ozone over the Mediterranean Sea (Richards et al., 2013; Dulac et al., 2023). Using lidar and total ozone observations at Thessaloniki, Greece, Balis et al. (2004) found that aerosols can change by 10–25% the UV irradiance, thus being able to mask its changes due to total O_3 perturbations. The observational studies of Casasanta et al. (2011) and Gerasopoulos et al. (2012) have shown that the effect of aerosols on photolysis rates in this region is substantial. Both studies show a strong impact of aerosol screening on two key photolysis rates, namely, JO^{1}D and JNO$_2$. From sun photometer measurements at Lampedusa, Casasanta et al. (2011) have found a relatively linear effect of AOD at 416 nm on ground-level JO^{1}D, with a reduction of 62% in measured JO^{1}D for a unit AOD when the solar zenithal angle is 60°. From long-term measurements at the site of Finokalia, Gerasopoulos et al. (2012) found a substantial climatological effect of aerosols, from −6% in both JNO$_2$ and JO^{1}D when the aerosol load is low down to −30% to −40% when the AOD exceeds 0.5, which is consistent with the findings of Casasanta et al. (2011). At the same location in the eastern Mediterranean, Benas et al. (2013) identified maxima in the aerosol effect on JO^{1}D in springtime and autumn, corresponding to the season of maximal occurrence of mineral dust plumes in this basin. They computed daily surface JO^{1}D based on Terra MODIS aerosol optical depth data and total ozone MODIS and found a 13% decrease over a period of 11 years (2000–2010) at Finokalia station in the east Mediterranean, while daily effects of dust aerosol on JO^{1}D as high as 10% reduction were found. Note that a stronger impact of dust aerosols on the actinic flux and the photolysis rates has been recorded in Beijing by Wang et al. (2019).

The effect of aerosols on photolysis rates is nowadays relatively well known and included in many chemistry-transport models such as Polyphemus (Real & Sartelet, 2011) or CHIMERE (Mailler et al., 2016). It has been shown by Mailler et al. (2016) that the dominant aerosol species affecting photolysis rates at the station of Lampedusa during the ChArMEx/ADRIMED campaign was mineral dust, a conclusion similar to that for Crete from Gerasopoulos et al. (2012). Mailler et al. (2016) show that including the effect of aerosols on photolysis rates reduces CHIMERE model errors in the calculation of these rates and considerably improves the ability of the model to reproduce the observed day-to-day variations of the photolysis rate of ozone. Including the aerosol effects on photolysis rates has a double-edged impact on tropospheric ozone, reducing ozone production through NO_2 photolysis but also reducing ozone destruction through ozone photolysis. Using a chemical box model, Gerasopoulos et al. (2012) calculated that a 24% and 5% reduction in JO^{1}D and JNO$_2$ noon values, respectively, results in 12% reduction in

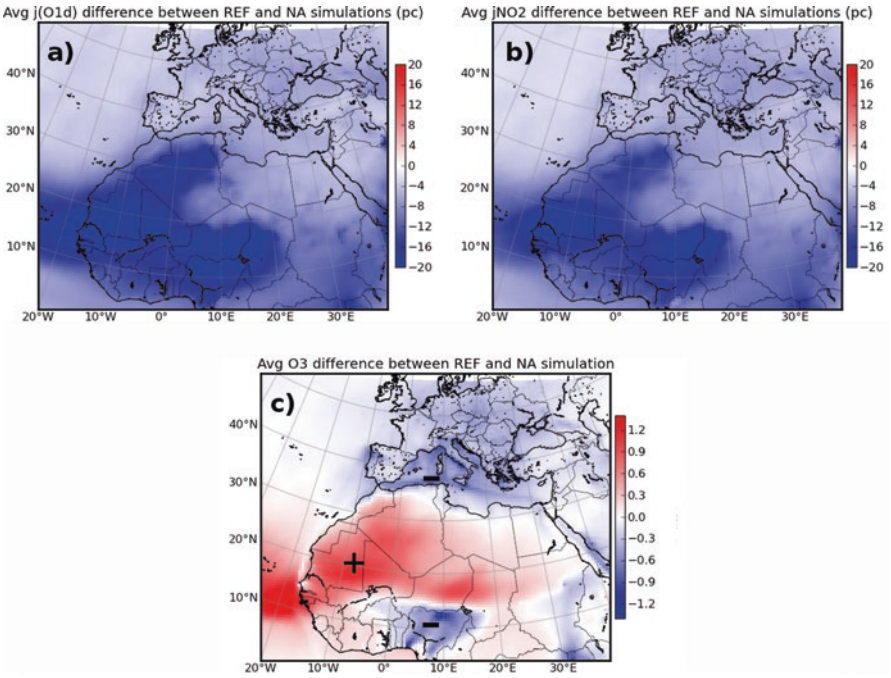

Fig. 4 CHIMERE model simulations between June 6 and July 15, 2013, of (**a**) average effect of aerosols on JO^1D (in %), (**b**) average effect of aerosols on JNO_2 (in %), and **c** average difference of low-level ozone concentration (in ppbv) due to the aerosol radiative effect on photolysis. (Adapted from Mailler et al., 2016)

the mean diurnal net chemical production of O_3 at Finokalia. The results of Mailler et al. (2016) with the CHIMERE model for their 6-week study period in June–July 2013 suggest, as a result of these competing effects, (i) a slight reduction in ozone concentrations over the Mediterranean Sea, stronger over the east-west shipping highway that crosses the Mediterranean between the Suez Canal and the Gibraltar Strait, (ii) a reduction as well over the surrounding land in Europe, and (iii) an ozone concentration increase further south over the Saharan desert. According to these authors, the net effect of aerosols on ozone concentrations through modulation of the photolysis rates would be relatively weak, hardly more than 1 ppb on average during their study period (Fig. 4).

3.2 Impact of Aerosol Dimming on the Solar Energy Production

The Mediterranean region is highly influenced by aerosols coming from different sources (e.g., Lelieveld et al., 2002), which affects the radiative budget (through the direct/indirect effect), climate, deposition, and cloudiness in the region, so in the

end, the amount of solar energy available at the surface. Despite being a region with a high solar resource due to its latitude, there are areas highly impacted by aerosols, like desert areas or some polluted areas in northern countries whose solar energy production potential could increase with a reduction of these anthropogenic aerosols emissions (Gutiérrez et al., 2018). Evaluation of the solar potential has been usually done using satellite-derived products (Sengupta et al., 2017), due to the lack of solar irradiance measurements at the surface. Satellite products have a high spatial resolution and have proven an accurate performance with low bias thresholds of errors (Posselt et al., 2012). However, aerosol retrieval from satellites performs worse in areas of high reflectivity, making the resource assessment more difficult in arid areas, which are abundant around the Mediterranean basin and are also sources of natural dust aerosols (Sengupta et al., 2017). The state-of-the-art approach for the evaluation of long-term solar resources consists of a solar irradiance retrieval algorithm from satellite, which is usually completed with a clear-sky model. The latter accounts mostly for the aerosol's impact on solar irradiance. The AOD is the variable usually considered in these algorithms, and it is generally included, as a monthly climatology, which means that they cannot account for the interannual or short-term variabilities of aerosols (Ruiz-Arias et al., 2016; Sanchez-Lorenzo et al., 2017). Products with higher temporal resolution in aerosol input are becoming more frequent (Gschwind et al., 2019). A sensitivity of some satellite-based methods for solar irradiance to aerosols input was analyzed by Polo et al. (2014). An overestimation of 50% in AOD causes an error in the global horizontal irradiance of 3%–5% in southeastern Spain. Long-term trends in solar irradiance caused by an increase or reduction of aerosol concentrations, e.g., from anthropogenic sources like during the brightening period observed in Europe since the 1980s (Wild, 2012; Nabat et al., 2014), have an impact on the potential PV power output. Changes in solar irradiance of up to about 3% by decade in areas of Central Europe on the horizontal plane and even higher for tilted and tracked panels,increase the resource and have an important impact on the PV production estimates over the lifetime of a power plant (Müller et al., 2014; Gutiérrez et al., 2018).

PV Forecasting and Aerosol Impact over the Mediterranean Area

In order to manage the photovoltaic production intermittency, an energy forecast needs to be made by power plant owners and operators of the systems. The forecast can be made at different timescales ranging from minutes to several weeks ahead, and different methods are applied from statistical to physical models, usually depending on the forecasting horizon (Wild et al., 2015). Each model deals with aerosols in a different way (Inman et al., 2013). In the statistical methods, which are usually applied to a specific place, the availability of measurements of different atmospheric components at that location is important. Usually, some AOD satellite products, as well as aerosol type, are used but they are limited by their temporal resolution (Ruiz-Arias et al., 2016). On the other hand, numerical weather prediction models (NWP) that are accurate to forecast solar irradiance from intra-daily (beyond 4 h) to several

days ahead (Perez et al., 2010) only include an AOD climatology, which has led to forecasting errors that generated big economic losses. For instance, the dust outbreak of April 14, 2014, over continental Europe ended in an overestimation of 5.3 GW of the PV electricity production in Germany (Rieger et al., 2017). The need to buy this missing energy at short notice in the intra-daily energy market caused a big economic damage. A combination of earth observation techniques and machine learning algorithms is applied to estimate the impact of particulate matter in Egypt (Kosmopoulos et al., 2018), finding a reduction in daily energy of more than 4 kWh m^{-2} in a 10 MW plant, which can lead to important loss in daily revenues. Other studies have shown the impact on daily PV yield of different aerosol events around the Mediterranean area. In the Sahel zone, aerosols can potentially reduce the PV yield by 14%, and extreme events like dust storms can reach a −48% reduction (Neher et al., 2017). Other values are found in Romania, where the estimations show an impact of around 20% in PV energy produced due to different types of aerosols: volcanic ash, desert dust, biomass burning, and urban aerosols (Calinoiu et al., 2013). In the western Mediterranean, extreme events of dust and smoke have caused a sporadic decrease in PV daily yield of 34% and 5%, respectively (Gómez-Amo et al., 2019).

Dust Deposition on PV Panels

Large-scale PV projects are sometimes developed in arid and semiarid areas, where a high concentration of atmospheric dust can be found. Apart from the reduction of solar irradiance from atmospheric aerosols, deposition (and accumulation) of dust over the optical surfaces also affects transmission and reflection of solar irradiance, causing a drop in the PV electricity production (El-Shobokshy and Hussein, 2013a; Sayyah et al., 2016). Several review articles on these soiling effects have been carried out on this topic (Mani and Pillai, 2010; Sarver et al., 2013; Costa et al., 2016). In general, the impact of soiling on a PV power plant depends on different factors like the dust properties, the frequency of different dust episodes and rain events, and the tilt of the panels. A wide range of reduction in cell performance have been reported in different studies in the Mediterranean and Middle-East region (Mekhilef et al., 2012): 40% in a 6-month period in Saudi Arabia (Nimmo et al., 1981) or 32% in an 8-month period (Mani and Pillai, 2010). In Egypt, 66% reductions in performance have been reported after 6 months exposure (Hassan et al., 2005), and in Algeria, 32-deg tilted panels have an 8% daily energy loss after several months (Semaoui et al., 2015). On the populated and relatively wet Algerian coast, a significant soiling effect is produced by the dirt from deposition of dust and carbonaceous particles (Semaoui et al., 2020). From laboratory tests El-Shobokshy and Hussein (2013b) have shown that deposited particles consisting in small mineral dust and especially combustion-derived carbon generate a higher loss in power production. Other studies in Spain have presented average daily energy losses around 4% in a year and higher for long periods without rain (Zorrilla-Casanova et al., 2011). The accumulation of particles on the surface depends on the tilt of the panels, the rate of deposition, and the removal due to enough wind speed. Strategies to prevent decrease in PV output and degradation due to soiling are needed.

Future PV Projections and the Role of Aerosols

Planification of future photovoltaic power plants, made by different stakeholders of the industry, can take advantage of modeling tools like climate model projections instead of relying on historical data. In Gaetani et al. (2014), the impact of future trends in anthropogenic aerosol emissions on photovoltaic potential is shown using a global climate model (ECHAM5-HAM) with simulations between 2000 and 2030 for the scenario SRES B2. In general, the future reduction in aerosols results in an increase in the projected global warming. This indirectly results in an increase in PV productivity with more clear and less cloudy conditions in western Europe and eastern Mediterranean (10%). A reduction in PV productivity is projected in northern Africa due to augmented cloudiness (Gaetani et al., 2014). A positive trend has also been projected in Europe for the midcentury, using CMIP5 models and the RCP8.5 scenario, partly due to a positive trend in clear-sky radiation that is likely related to a decrease in aerosol burdens (Wild et al., 2015). Different studies have also evaluated photovoltaic future potential in the Euro-Mediterranean area using higher-resolution regional climate models (RCMs), and they project an overall decrease in PV productivity over the Mediterranean area, more important in central and northern Europe. However, the limited representation of aerosols in the simulations makes it impossible to evaluate their impact on future PV potential, and it adds uncertainty to the power projections presented. Nevertheless, RCMs including evolving aerosols have simulated an increase in near-future PV potential of up to +10% in summer in central and eastern Europe with uncertainty in magnitude related to the model (Gutiérrez et al., 2020).

4 Radiative Forcing of Tropospheric Ozone

Tropospheric ozone is a secondary anthropogenic pollutant (see Kalabokas et al., 2023 for a review of ozone studies in the Mediterranean region) and a short-lived greenhouse gas. The Intergovernmental Panel on Climate Change (IPCC) current best estimate for global mean tropospheric ozone RF over the industrial era is 0.4 ± 0.2 W m^{-2} with a 5–95% confidence interval, making tropospheric ozone the third most important anthropogenic greenhouse gas after CO_2 and CH_4 (Myhre et al., 2013). This is also confirmed by the recent Copernicus Atmosphere Monitoring Service (CAMS) RF estimate for tropospheric ozone based on the CAMS Reanalysis (Huijnen et al., 2020), which is 0.32 W m^{-2}. The concentration and distribution of tropospheric ozone in the present day are well constrained by satellite observations, resulting in robust estimates of the present-day RF of tropospheric ozone (Rap et al., 2015). Estimates of present-day tropospheric ozone annual mean radiative effect using the TOMCAT-GLOMAP model are 1.17 ± 0.03 W m^{-2} globally and 1.63 W m^{-2} over the Mediterranean region (defined here as 28°N–47°N, 9°W–36°E) (Rap et al., 2015; Rowlinson et al., 2019). The large uncertainty range in global mean RF (0.2–0.6 W m^{-2}) is primarily caused by the poor understanding of preindustrial ozone concentrations, due to a lack of reliable pre-industrial (PI) measurements (Myhre et al., 2013; Stevenson et al., 2013). Ozone is not stable in ice or

snow, meaning proxy records are not available, and although measurements of tropospheric ozone exist as far back as the late nineteenth, the accuracy and coverage of these early measurements are limited (Volz & Kley, 1988; Cooper et al., 2014). As well as anthropogenic sources, ozone precursors such as CH_4, CO, and NO_x have natural emission sources such as wildfires, wetlands, lightning, and biogenic emissions. The role of these natural sources in the PI era is highly uncertain, introducing a large uncertainty when attempting to simulate tropospheric ozone in the PI atmosphere. Checa-Garcia et al. (2018) found that differences in PI estimates between Coupled Model Intercomparison Project phase 5 (CMIP5) and CMIP6 cause an 8%–12% variation in ozone RF estimates but did not explicitly assess uncertainty in natural PI emissions. A recent analysis of oxygen isotopes in polar ice cores by Yeung et al. (2019) indicates that tropospheric ozone in the northern hemisphere increased by less than 40% between 1850 and 2005, suggesting that global mean tropospheric ozone RF is likely lower than the 0.4 W m^{-2} IPCC estimate.

Annual mean tropospheric ozone in the Mediterranean basin is characterized by high concentrations in the east Mediterranean, with lower ozone in the north Mediterranean and Adriatic Sea (Fig. 5a). Background tropospheric ozone concentrations in the eastern Mediterranean are among the highest in the world due to

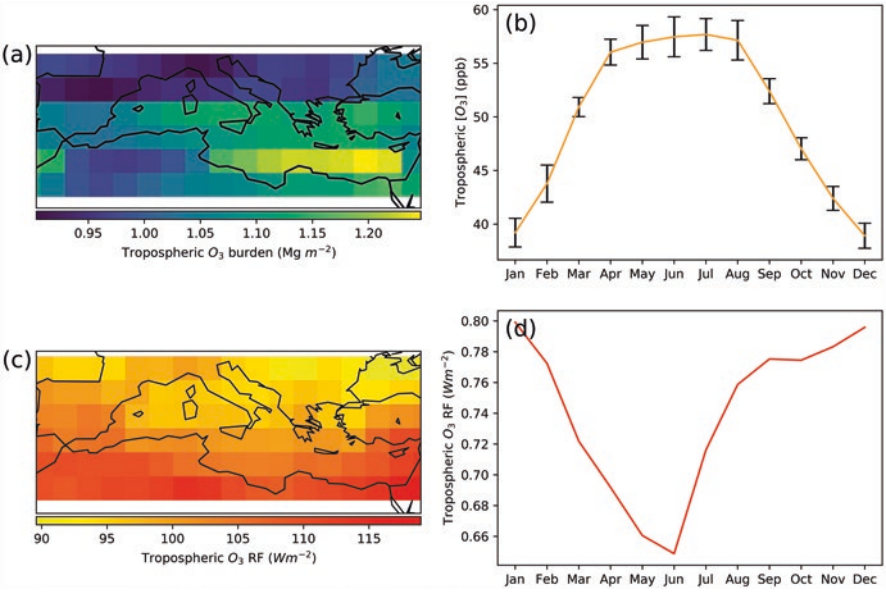

Fig. 5 TOMCAT-GLOMAP simulated tropospheric ozone in the Mediterranean region: (**a**) Annual mean tropospheric ozone burden (Mg m^{-2} averaged over 1997–2015). (**b**) Seasonal cycle of simulated mean tropospheric ozone concentrations (ppbv), with error bars showing one standard deviation of the monthly means over the period. (**c**) Geographical distribution of the annual mean preindustrial to present-day stratospherically adjusted radiative forcing (W m^{-2}) of tropospheric ozone. (**d**) Seasonal cycle of the global mean preindustrial to present-day tropospheric ozone radiative forcing (W m^{-2}). (Adapted from Rowlinson et al., 2020)

enhanced photochemical production (Zanis et al., 2014), stratospheric injection of ozone (Akritidis et al., 2016), and being at the "crossroad" of emissions from Europe, Asia, and Africa (Lelieveld et al., 2002; Zerefos et al., 2002). High solar intensity and low cloud cover conditions mean the Mediterranean region exhibits a pronounced summertime maximum in tropospheric ozone concentration (Fig. 5b; Kanakidou et al., 2011; Richards et al., 2013; Zanis et al., 2014; Kopanakis et al., 2016). In situ observations show that summer concentrations regularly exceed European Union (EU) target levels, up to 88% of the time over a 7-year period at the Akrotiri monitoring station in Greece (Kopanakis et al., 2016). Richards et al. (2013) found that tropospheric ozone in the Mediterranean region is sensitive to natural volatile organic compounds emissions, whereas surface ozone is most sensitive to local anthropogenic NO_x emissions.

Tropospheric ozone RF since the preindustrial era is largest over the south and eastern Mediterranean (Fig. 5c), with a TOMCAT-GLOMAP model estimated Mediterranean region mean of 0.74 W m^{-2} when using CMIP6 present-day and preindustrial emissions (Rowlinson et al., 2020). Uncertainty in preindustrial conditions (Hamilton et al., 2018; Rowlinson et al., 2020) means that this estimate might be in fact substantially lower. Using the TOMCAT-GLOMAP simulations from Rowlinson et al. (2020), we estimate this could be as low as 0.49 W m^{-2} when accounting for uncertainty in biogenic and biomass burning emissions in 1750. Strong localized forcing due to high tropospheric ozone production in the central and southeast Mediterranean may cause changes in atmospheric dynamics. Richards et al. (2013) showed that ozone in the upper troposphere, where ozone has the largest radiative effect, is most sensitive to global emissions rather than local sources, necessitating global action on emissions to mitigate the regional climate impact. Interestingly, unlike the seasonal cycle of present-day regional tropospheric ozone concentrations (Fig. 5b), the tropospheric ozone RF over the Mediterranean region is larger in winter (Fig. 5d). Therefore, while the summer tropospheric ozone maximum is problematic for air quality, the climatic impact due to anthropogenic emissions is relatively larger during the winter months.

5 Conclusion and Recommendations

The direct radiative effects exerted by aerosols and tropospheric ozone are now well documented at the local and regional scales by a large number of studies. Most of the direct aerosol effect estimates have been done in the solar spectral range. Based on the available literature, there is a clear consensus showing that Mediterranean aerosols exert a large and variable direct radiative effect at the surface and TOA. At the basin scale, this negative annual mean DRF is even larger in absolute value than the greenhouse gas positive forcing. However, the decrease in sulfate aerosol during the last decades has contributed by about 20–25% to the surface warming in the Euro-Mediterranean region between 1980 and 2012 (Nabat et al., 2014).

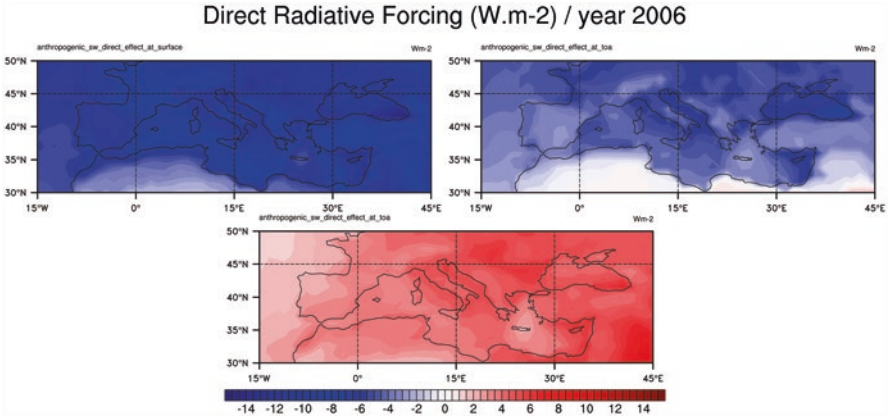

Fig. 6 Annual average shortwave direct radiative effect (in W m^{-2}) of anthropogenic tropospheric aerosols: *Top left* at the surface; *top right* at the TOA; and *bottom* within the atmosphere. MACC reanalysis data for the year 2006 from Inness et al. (2013)

The direct radiative forcing exerted by desert aerosols in the longwave spectral range has been demonstrated locally, but few studies have been carried out at regional and climatic scales. An effort could be made using updated optical properties (Di Biagio et al., 2020). In addition, the analysis of current decadal time series of dust data over the Mediterranean from research infrastructures and satellites (in particular CALIPSO) would be very informative.

A lot of studies report important differences between the surface and the TOA DRF of aerosols, indicating that an important part of solar radiation is absorbed within absorbing aerosol layers (anthropogenic, mineral dust, and smoke, typically), producing an important heating. Figure 6 indicates that the yearly-mean atmospheric forcing due to anthropogenic particles can reach important values of about 5–10 W m^{-2} over the Mediterranean basin. In that context, more mesoscale and RCM simulations are needed to quantify the semi-direct effect of natural/anthropogenic aerosols on the thermodynamic properties of the atmosphere and the circulation at regional and event/climatic scales. It appears also crucial to investigate more deeply the impact of the DRF of aerosols over both continental and marine surfaces on the Mediterranean climate, and more specifically the impact on humidity fluxes between the sea and the atmosphere and more largely the hydrological cycle. For this, coupled atmosphere-ocean models seem necessary because they can account for changes in sea surface temperature and evaporation due to the aerosol dimming at the surface (Nabat et al., 2014, 2015).

It would also be very interesting to study the effects of aerosol radiative forcing on air quality through the impact of absorbing polluted aerosols on the boundary layer development (Péré et al., 2011).

In parallel, investigating the possible link between the aerosol DRF and some characteristics of the Mediterranean heat waves (intensity, duration), especially for mineral dust and anthropogenic particles, should also be a priority for future research given the expected regional climate change and positive aerosol feedback

on heat waves (Pace et al., 2005; Hodzic et al., 2007; Nabat et al., 2015). The aerosol radiative impact on PV production is an issue of recent concern, especially driven by the need of energy production and distribution networks to have accurate forecasts of the daily production yield. More studies dedicated to the impact of aerosols on solar energy production (by both reduction of surface solar radiations and wet/dry deposition) are needed in the context of the energy transition toward renewable energy sources, especially over the southern Mediterranean and islands.

The radiative effect of tropospheric ozone is the strongest in the eastern Mediterranean during the summer maximum, but the influence of anthropogenic emissions is the greatest in winter, as the summer maximum is primarily driven by meteorological conditions. Further research is needed to understand the impact of strong regional forcing due to tropospheric ozone on atmospheric dynamics and chemistry, including how elevated ozone and OH production interact with other pollutants. Studies should also focus on how effective future emissions reduction scenarios will be at decreasing tropospheric ozone in the Mediterranean basin, contrasting the projected changes in climate which may enhance ozone production and counteract mitigation measures (Meleux et al., 2007; Jaidan et al., 2018).

References

Akritidis, D., Pozzer, A., Zanis, P., Tyrlis, E., Škerlak, B., Sprenger, M., & Lelieveld, J. (2016). On the role of tropopause folds in summertime tropospheric ozone over the eastern Mediterranean and the Middle East. *Atmospheric Chemistry and Physics, 16*, 14025–14039. https://doi.org/10.5194/acp-16-14025-2016

Alpert, P., Kaufman, Y., Shay-El, Y., Tanre, D., da Silva, A., Schubert, S., & Joseph, J. H. (1998). Quantification of dust-forced heating of the lower troposphere. *Nature, 395*, 367–370. https://doi.org/10.1038/26456

Balis, D. S., Amiridis, V., Zerefos, C., Kazantzidis, A., Kazadzis, S., Bais, A. F., Meleti, C., Gerasopoulos, E., Papayannis, A., Matthias, V., Dier, H., & Andreae, M. O. (2004). Study of the effect of different type of aerosols on UV-B radiation from measurements during EARLINET. *Atmospheric Chemistry and Physics, 4*, 307–321. https://doi.org/10.5194/acp-4-307-2004

Benas, N., Hatzianastassiou, N., Matsoukas, C., Fotiadi, A., Mihalopoulos, N., & Vardavas, I. (2011). Aerosol shortwave direct radiative effect and forcing based on MODIS Level 2 data in the Eastern Mediterranean (Crete). *Atmospheric Chemistry and Physics, 11*, 12647–12662. https://doi.org/10.5194/acp-11-12647-2011

Benas, N., Mourtzanou, E., Kouvarakis, G., Bais, A., Mihalopoulos, N., & Vardavas, I. (2013). Surface ozone photolysis rate trends in the Eastern Mediterranean: Modeling the effects of aerosols and total column ozone based on Terra MODIS data. *Atmospheric Environment, 74*, 1–9. https://doi.org/10.1016/j.atmosenv.2013.03.019

Bergamo, A., Tafuro, A. M., Kinne, S., De Tomasi, F., & Perrone, M. R. (2008). Monthly-averaged anthropogenic aerosol direct radiative forcing over the Mediterranean based on AERONET aerosol properties. *Atmospheric Chemistry and Physics, 8*, 6995–7014. https://doi.org/10.5194/acp-8-6995-2008

Boucher, O., Randall, D., Artaxo, P., Bretherton, C., Feingold, G., Forster, P., Kerminen, V.-M., Kondo, Y., Liao, H., Lohmann, U., Rasch, P., Satheesh, S. K., Sherwood, S., Stevens, B., & Zhang, X. Y. (2013). Clouds and aerosols. In Stocker, T. F., D. Qin, G.-K. Plattner, M. Tignor, S. K. Allen, J. Boschung, A. Nauels, Y. Xia, V. Bex, & P. M. Midgley (Eds.), *Climate change*

2013: The physical science basis. Contribution of working group I to the fifth assessment report of the intergovernmental panel on climate change, 571–657. Cambridge University Press. https://www.ipcc.ch/site/assets/uploads/2018/02/WG1AR5_all_final.pdf. Last access 21 July 2022.

Calinoiu, D., Paulescu, M., Ionel, I., Stefu, N., Pop, N., Boata, R., Pacurar, A., Gravila, P., Paulescu, E., & Trif-Tordai, G. (2013). Influence of aerosols pollution on the amount of collectable solar energy. *Energy Conversion and Management, 70*, 76–82. https://doi.org/10.1016/j.enconman.2013.02.012

Casasanta, G., di Sarra, A., Meloni, D., Monteleone, F., Pace, G., Piacentino, S., & Sferlazzo, D. (2011). Large aerosol effects on ozone photolysis in the Mediterranean. *Atmospheric Environment, 45*, 3937–3943. https://doi.org/10.1016/j.atmosenv.2011.04.065

Checa-Garcia, R., Hegglin, M. I., Kinnison, D., Plummer, D. A., & Shine, K. P. (2018). Historical tropospheric and stratospheric ozone radiative forcing using the CMIP6 database. *Geophysical Research Letters, 45*, 3264–3273. https://doi.org/10.1002/2017GL076770

Claeys, M., Roberts, G., Mallet, M., Arndt, J., Sellegri, K., Sciare, J., Wenger, J., & Sauvage, B. (2017). Optical, physical and chemical properties of aerosols transported to a coastal site in the western Mediterranean: A focus on primary marine aerosols. *Atmospheric Chemistry and Physics, 17*, 7891–7915. https://doi.org/10.5194/acp-17-7891-2017

Cooper, O., Parrish, D., Ziemke, J., Balashov, N., Cupeiro, M., Galbally, I., Gilge, S., Horowitz, L., Jensen, N., Lamarque, J.-F., Naik, V., Oltmans, S., Schwab, J., Shindell, D., Thompson, A., Thouret, V., Wang, Y., & Zbinden, R. (2014). Global distribution and trends of tropospheric ozone: An observation-based review. *Elementa: Science of the Anthropocene, 2*, 000029. https://doi.org/10.12952/journal.elementa.000029

Costa, S. C. S., Diniz, A. S. A. C., & Kazmerski, L. L. (2016). Dust and soiling issues and impacts relating to solar energy systems: Literature review update for 2012–2015. *Renewable and Sustainable Energy Reviews, 63*, 33–61. https://doi.org/10.1016/j.rser.2016.04.059

Crutzen, P. J., Ramanathan, V., Anderson, T. L., Charlson, R. J., Schwartz, S. E., Knutti, R., Boucher, O., Rodhe, H., & Heintzenberg, J. (2003). The parasol effect on climate. *Science, 302*, 1679–1681. https://doi.org/10.1126/science.302.5651.1679

Di Biagio, C., di Sarra, A., Meloni, D., Monteleone, F., Piacentino, S., & Sferlazzo, D. (2009). Measurements of Mediterranean aerosol radiative forcing and influence of the single scattering albedo. *Journal of Geophysical Research, 114*, D06211. https://doi.org/10.1029/2008JD011037

Di Biagio, C., di Sarra, A., & Meloni, D. (2010). Large atmospheric shortwave radiative forcing by Mediterranean aerosol derived from simultaneous ground-based and spaceborne observations, and dependence on the aerosol type and single scattering albedo. *Journal of Geophysical Research, 115*, D10209. https://doi.org/10.1029/2009JD012697

Di Biagio, C., Formenti, P., Doppler, L., Gaimoz, C., Grand, N., Ancellet, G., Attié, J.-L., Bucci, S., Dubuisson, P., Fierli, F., Mallet, M., & Ravetta, F. (2016). Continental pollution in the Western Mediterranean basin: Large variability of the aerosol single scattering albedo and influence on the direct shortwave radiative effect. *Atmospheric Chemistry and Physics, 16*, 10591–10607. https://doi.org/10.5194/acp-16-10591-2016

Di Biagio, C., Balkanski, Y., Albani, S., Boucher, O., & Formenti, P. (2020). Direct radiative effect by mineral dust aerosols constrained by new microphysical and spectral optical data. *Geophysical Research Letters, 47*, e2019GL086. https://doi.org/10.1029/2019GL086186

di Sarra, A., Pace, G., Meloni, D., De Silvestri, L., Piacentino, S., & Monteleone, F. (2008). Surface shortwave radiative forcing of different aerosol types in the Central Mediterranean. *Geophysical Research Letters, 35*, L02714. https://doi.org/10.1029/2007GL032395

di Sarra, A., Di Biagio, C., Meloni, D., Monteleone, F., Pace, G., Pugnaghi, S., & Sferlazzo, D. (2011). Shortwave and longwave radiative effects of the intense Saharan dust event of 25–26 March, 2010, at Lampedusa (Mediterranean Sea). *Journal of Geophysical Research, 116*, D23209. https://doi.org/10.1029/2011JD016238

Drugé, T., Nabat, P., Mallet, M., & Somot, S. (2019). Radiative and climatic effects of ammonium-nitrate aerosols over the Euro-Mediterranean region. *Atmospheric Chemistry and Physics, 19*, 3707–3731. https://doi.org/10.5194/acp-19-3707-2019

Dulac, F., Sauvage, S., Hamonou, E., & Dayan, U. (2023). Scientific importance of atmospheric reactive gases and aerosols and the particular case of the Mediterranean region. In F. Dulac, S. Sauvage, & E. Hamonou (Eds.), *Atmospheric chemistry in the Mediterranean Region* (Vol. 1, Background information and pollutant distribution). Springer.

El-Shobokshy, M. S., & Hussein, F. M. (1993a). Degradation of photovoltaic cell performance due to dust deposition on to its surface. *Renewable Energy, 3*, 585–590. https://doi.org/10.1016/0960-1481(93)90064-N

El-Shobokshy, M. S., & Hussein, F. M. (1993b). Effect of dust with different physical properties on the performance of photovoltaic cells. *Solar Energy, 51*, 505–511. https://doi.org/10.1016/0038-092X(93)90135-B

Formenti, P., Boucher, O., Reiner, T., Sprung, D., Andreae, M. O., Wendisch, M., Wex, H., Kindred, D., Tzortziou, M., Vasaras, A., & Zerefos, C. (2002). STAAARTE-MED 1998 summer airborne measurements over the Aegean Sea, 2. Aerosol scattering and absorption, and radiative calculations. *Journal of Geophysical Research, 107*, 4451. https://doi.org/10.1029/2001JD001536

Gaetani, M., Huld, T., Vignati, E., Monforti-Ferrario, F., Dosio, A., & Raes, F. (2014). The near future availability of photovoltaic energy in Europe and Africa in climate-aerosol modeling experiments. *Renewable and Sustainable Energy Reviews, 38*, 706–716. https://doi.org/10.1016/j.rser.2014.07.041

Gerasopoulos, E., Kazadzis, S., Vrekoussis, M., Kouvarakis, G., Liakakou, E., Kouremeti, N., Giannadaki, D., Kanakidou, M., Bohn, B., & Mihalopoulos, N. (2012). Factors affecting O_3 and NO_2 photolysis frequencies measured in the eastern Mediterranean during the five-year period 2002–2006. *Journal of Geophysical Research, 117*, D22305. https://doi.org/10.1029/2012JD01762

Gkikas, A., Obiso, V., Pérez García-Pando, C., Jorba, O., Hatzianastassiou, N., Vendrell, L., Basart, S., Solomos, S., Gassó, S., & Baldasano, J. M. (2018). Direct radiative effects during intense Mediterranean desert dust outbreaks. *Atmospheric Chemistry and Physics, 18*, 8757–8787. https://doi.org/10.5194/acp-18-8757-2018

Gómez-Amo, J. L., Pinti, V., Di Iorio, T., di Sarra, A., Meloni, D., Becagli, S., Bellantone, V., Cacciani, M., Fuà, D., & Perrone, M. R. (2011). The June 2007 Saharan dust event in the central Mediterranean: Observations and radiative effects in marine, urban, and suburban environments. *Atmospheric Environment, 45*, 5385–5393. https://doi.org/10.1016/j.atmosenv.2011.06.045

Gómez-Amo, J. L., Freile-Aranda, M. D., Camarasa, J., Estellés, V., Utrillas, M. P., & Mártinez-Lozano, J. A. (2019). Empirical estimates of the radiative impact of an unusually extreme dust and wildfire episode on the performance of a photovoltaic plant in Western Mediterranean. *Applied Energy, 235*, 1226–1234. https://doi.org/10.1016/j.apenergy.2018.11.052

Gschwind, B., Wald, L., Blanc, P., Lefèvre, M., Schroedter-Homscheidt, M., & Arola, A. (2019). Improving the McClear model estimating the downwelling solar radiation at ground level in cloud-free conditions–McClear-v3. *Meteorologische Zeitschrift, 28*(2), 147–163. https://doi.org/10.1127/metz/2019/0946

Gutiérrez, C., Somot, S., Nabat, P., Mallet, M., Gaertner, M. Á., & Perpiñán, O. (2018). Impact of aerosols on the spatiotemporal variability of photovoltaic energy production in the Euro-Mediterranean area. *Solar Energy, 174*, 1142–1152. https://doi.org/10.1016/j.solener.2018.09.085

Gutiérrez, C., Somot, S., Nabat, P., Mallet, M., Corre, L., van Meijgaard, E., Gartner, M. A., & Perpiñán, O. (2020). Future evolution of surface solar radiation and photovoltaic potential in Europe: Investigating the role of aerosols. *Environmental Research Letters, 15*, 034035. https://doi.org/10.1088/1748-9326/ab6666

Hamilton, D. S., Hantson, S., Scott, C. E., Kaplan, J. O., Pringle, K. J., Nieradzik, L. P., Rap, A., Folberth, G. A., Spracklen, D. V., & Carslaw, K. S. (2018). Reassessment of pre-industrial fire emissions strongly affects anthropogenic aerosol forcing. *Nature Communications, 9*, 3182. https://doi.org/10.1038/s41467-018-05592-9

Hassan, A. H., Rahoma, U. A., Elminir, H. K., & Fathy, A. M. (2005). Effect of airborne dust concentration on the performance of PV modules. *Journal of the Astronomical Society of Egypt, 13*, 24–38.

Hatzianastassiou, N., Papadimas, C. D., Matsoukas, C., Pavlakis, K., Fotiadi, A., Wild, M., & Vardavas, I. (2012). Recent regional surface solar radiation dimming and brightening patterns: Inter-hemispherical asymmetry and a dimming in the Southern Hemisphere. *Atmospheric Science Letters, 13*, 43–48. https://doi.org/10.1002/asl.361

Highwood, E. J., Haywood, J. M., Coe, H., Cook, J., Osborne, S., Williams, P., Crosier, J., Bower, K., Formenti, P., McQuaid, J., Brooks, B., Thomas, G., Grainger, R., Barnaba, F., Gobbi, G. P., de Leeuw, G., & Hopkins, J. (2007). Aerosol Direct Radiative Impact Experiment (ADRIEX) overview. *Quarterly Journal of the Royal Meteorological Society, 133*, 3–15. https://doi.org/10.1002/qj.89

Hodzic, A., Madronich, S., Bohn, B., Massie, S., Menut, L., & Wiedinmyer, C. (2007). Wildfire particulate matter in Europe during summer 2003: meso-scale modeling of smoke emissions, transport and radiative effects, *Atmospheric Chemistry and Physics, 7*, 4043–4064. https://doi.org/10.5194/acp-7-4043-2007

Horvath, H., Alados Arboledas, L., Olmo, F. J., Jovanovic, O., Gangl, M., Sanchez, C., Sauerzopf, H., & Seidl, S. (2002). Optical characteristics of the aerosol in Spain and Austria and its effect on radiative forcing. *Journal of Geophysical Research, 107*, 4386. https://doi.org/10.1029/2001JD001472

Huijnen, V., Miyazaki, K., Flemming, J., Inness, A., Sekiya, T., & Schultz, M. G. (2020). An intercomparison of tropospheric ozone reanalysis products from CAMS, CAMS interim, TCR-1, and TCR-2. *Geoscientific Model Development, 13*, 1513–1544. https://doi.org/10.5194/gmd-13-1513-2020

Inman, R. H., Pedro, H. T. C., & Coimbra, C. F. M. (2013). Solar forecasting methods for renewable energy integration. *Progress in Energy and Combustion Science, 39*, 535–576. https://doi.org/10.1016/j.pecs.2013.06.002

Inness, A., Baier, F., Benedetti, A., Bouarar, I., Chabrillat, S., Clark, H., Clerbaux, C., Coheur, P., Engelen, R. J., Errera, Q., Flemming, J., George, M., Granier, C., Hadji-Lazaro, J., Huijnen, V., Hurtmans, D., Jones, L., Kaiser, J. W., Kapsomenakis, J., … Zerefos, C. (2013). The MACC team: The MACC reanalysis: An 8 yr data set of atmospheric composition. *Atmospheric Chemistry and Physics, 13*, 4073–4109. https://doi.org/10.5194/acp-13-4073-2013

IPCC. (2013). Climate change 2013: The physical science basis. Contribution of working group I to the fifth assessment report of the intergovernmental panel on climate change. In T. F. Stocker, D. Qin, G.-K. Plattner, M. M. B. Tignor, S. K. Allen, J. Boschung, A. Nauels, Y. Xia, V. Bex, & P. Midgley (Eds.). Cambridge University Press, 1535 pp. https://www.ipcc.ch/site/assets/uploads/2018/02/WG1AR5_all_final.pdf. LAst access 20 July 2022.

Jaidan, N., El Amraoui, L., Attié, J.-L., Ricaud, P., & Dulac, F. (2018). Future changes in surface ozone over the Mediterranean Basin in the framework of the Chemistry-Aerosol Mediterranean Experiment (ChArMEx). *Atmospheric Chemistry and Physics, 18*, 9351–9373. https://doi.org/10.5194/acp-18-9351-2018

Kalabokas, P., Zanis, P., Akritidis, D., Georgoulias, A. K., Kapsomenakis, J., Zerefos, C. S., Dufour, G., Gaudel, A., Sellitto, P., Armengaud, A., Ancellet, G., Gheusi, F., & Dulac, F. (2023). Ozone in the Mediterranean atmosphere. In F. Dulac, S. Sauvage, & E. Hamonou (Eds.), *Atmospheric chemistry in the Mediterranean Region* (Vol. 1, Background information and pollutant distribution). Springer.

Kambezidis, H. D. (2018). The solar radiation climate of Athens: Variations and tendencies in the period 1992-2017, the brightening era. *Solar Energy, 173*, 328–347. https://doi.org/10.1016/j.solener.2018.07.076

Kambezidis, H. D., Psiloglou, B. E., Karagiannis, D., Dumka, U. C., & Kaskaoutis, D. G. (2016). Recent improvements of the meteorological radiation model for solar irradiance estimates under all-sky conditions. *Renewable Energy, 93*, 142–158. https://doi.org/10.1016/j.jastp.2016.10.006

Kanakidou, M., Mihalopoulos, N., Kindap, T., Im, U., Vrekoussis, M., Gerasopoulos, E., Dermitzaki, E., Unal, A., Koçak, M., Markakis, K., Melas, D., Kouvarakis, G., Youssef, A. F., Richter, A., Hatzianastassiou, N., Hilboll, A., Ebojie, F., Wittrock, F., von Savigny, C., … Moubasher, H. (2011). Megacities as hot spots of air pollution in the East Mediterranean. *Atmospheric Environment, 45*, 1223–1235. https://doi.org/10.1016/j.atmosenv.2010.11.048

Kaskaoutis, D. G., Kharol, S. K., Sifakis, N., Nastos, P. T., Sharma, A. R., Badarinath, K. V. S., & Kambezidis, H. D. (2011). Satellite monitoring of the biomass burning aerosols during the wildfires of August 2007 in Greece: Climate implications. *Atmospheric Environment, 45*, 716–726. https://doi.org/10.1016/j.atmosenv.2010.09.043

Kaskaoutis, D. G., Dumka, U. C., Rashki, A., Psiloglou, B. E., Gavriil, A., Mofidi, A., Petrinoli, K., Karagiannis, D., & Kambezidis, H. D. (2019a). Analysis of intense dust storms over the eastern Mediterranean in March 2018: Impact on radiative forcing and Athens air quality. *Atmospheric Environment, 209*, 23–39. https://doi.org/10.1016/j.atmosenv.2019.04.025

Kaskaoutis, D. G., Rashki, A., Dumka, U. C., Mofidi, A., Kambezidis, H. D., Psiloglou, B. E., Karagiannis, D., Petrinoli, K., & Gavriil, A. (2019b). Atmospheric dynamics associated with exceptionally dusty conditions over the eastern Mediterranean and Greece in March 2018. *Atmospheric Research, 218*, 269–284. https://doi.org/10.1016/j.atmosres.2018.12.009

Kazadzis, S., Founda, D., Psiloglou, B. E., Kambezidis, H., Mihalopoulos, N., Sanchez-Lorenzo, A., Meleti, C., Raptis, P. I., Pierros, F., & Nabat, P. (2018). Long-term series and trends in surface solar radiation in Athens, Greece. *Atmospheric Chemistry and Physics, 18*, 2395–2411. https://doi.org/10.5194/acp-18-2395-2018

Kopanakis, I., Glytsos, T., Kouvarakis, G., Gerasopoulos, E., Mihalopoulos, N., & Lazaridis, M. (2016). Variability of ozone in the Eastern Mediterranean during a 7-year study. *Air Quality, Atmosphere and Health, 9*, 461–470. https://doi.org/10.1007/s11869-015-0362-3

Kosmopoulos, P. G., Kazadzis, S., El-Askary, H., Taylor, M., Gkikas, A., Proestakis, K. C., & El-Khayat, M. M. (2018). Earth-observation-based estimation and forecasting of particulate matter impact on solar energy in Egypt. *Remote Sensing, 10*(12), 1870. https://doi.org/10.3390/rs10121870

Lelieveld, J., Berresheim, H., Borrmann, S., Crutzen, P. J., Dentener, F. J., Fischer, H., Feichter, J., Flatau, P. J., Heland, J., Holzinger, R., Korrmann, R., Lawrence, M. G., Levin, Z., Markowicz, K. M., Mihalopoulos, N., Minikin, A., Ramanathan, V., de Reus, M., Roelofs, G. J., … Ziereis, H. (2002). Global air pollution crossroads over the Mediterranean. *Science, 298*, 794–799. https://doi.org/10.1126/science.1075457

Lundgren, K., Vogel, B., Vogel, H., & Kottmeier, C. (2013). Direct radiative effects of sea salt for the Mediterranean region under conditions of low to moderate wind speeds. *Journal of Geophysical Research – Atmospheres, 118*, 1906–1923. https://doi.org/10.1029/2012JD018629

Maghami, M. R., Hizam, H., Gomes, C., Radzi, M. A., Rezadad, M. I., & Hajighorbani, S. (2016). Power loss due to soiling on solar panel: A review. *Renewable and Sustainable Energy Reviews, 59*, 1307–1316. https://doi.org/10.1016/j.rser.2016.01.044

Mailler, S., Menut, L., di Sarra, A. G., Becagli, S., Di Iorio, T., Bessagnet, B., Briant, R., Formenti, P., Doussin, J.-F., Gómez-Amo, J. L., Mallet, M., Rea, G., Siour, G., Sferlazzo, D. M., Traversi, R., Udisti, R., & Turquety, S. (2016). On the radiative impact of aerosols on photolysis rates: Comparison of simulations and observations in the Lampedusa island during the ChArMEx/ADRIMED campaign. *Atmospheric Chemistry and Physics, 16*, 1219–1244. https://doi.org/10.5194/acp-16-1219-2016

Mallet, M., Pont, V., Liousse, C., Roger, J. C., & Dubuisson, P. (2006). Simulation of aerosol radiative properties with the ORISAM-RAD model during a pollution event (ESCOMPTE 2001). *Atmospheric Environment, 40*, 7696–7705. https://doi.org/10.1016/j.atmosenv.2006.08.031

Mallet, M., Dulac, F., Formenti, P., Nabat, P., Sciare, J., Roberts, G., Pelon, J., Ancellet, G., Tanré, D., Parol, F., Denjean, C., Brogniez, G., di Sarra, A., Alados-Arboledas, L., Arndt, J., Auriol, F., Blarel, L., Bourrianne, T., Chazette, P., … Zapf, P. (2016). Overview of the Chemistry-Aerosol Mediterranean Experiment/Aerosol Direct Radiative Forcing on the Mediterranean Climate (ChArMEx/ADRIMED) summer 2013 campaign. *Atmospheric Chemistry and Physics, 16*, 455–504. https://doi.org/10.5194/acp-16-455-2016

Mallet, M., Chazette, P., Dulac, F., Formenti, P., Di Biagio, C., Denjean, C., & Chiapello, I. (2022). Aerosol optical properties. In F. Dulac, S. Sauvage, & E. Hamonou (Eds.), *Atmospheric chemistry in the Mediterranean Region* (Vol. 2, From air pollutant sources to impacts). Springer, this volume. https://doi.org/10.1007/978-3-030-82385-6_14

Manara, V., Beltrano, M. C., Brunetti, M., Maugeri, M., Sanchez-Lorenzo, A., Simolo, C., & Sorrenti, S. (2015). Sunshine duration variability and trends in Italy from homogenized

instrumental time series (1936–2013). *Journal of Geophysical Research – Atmospheres, 120*, 3622–3641. https://doi.org/10.1002/2014JD022560

Manara, V., Brunetti, M., Celozzi, A., Maugeri, M., Sanchez-Lorenzo, A., & Wild, M. (2016). Detection of dimming/brightening in Italy from homogenized all-sky and clear-sky surface solar radiation records and underlying causes (1959–2013). *Atmospheric Chemistry and Physics, 16*, 11145–11161. https://doi.org/10.5194/acp-16-11145-2016

Mani, M, & Pillai, R. (2010). Impact of dust on solar photovoltaic (PV) performance: Research status challenges and recommendations. *Renewable and Sustainable Energy Reviews, 14*, 3124–3131. https://doi.org/10.1016/j.rser.2010.07.065

Matthew J., Rowlinson Alexandru, Rap Douglas S., Hamilton Richard J., Pope Stijn, Hantson Steve R., Arnold Jed O., Kaplan Almut, Arneth Martyn P., Chipperfield Piers M., Forster Lars, Nieradzik (2020) Tropospheric ozone radiative forcing uncertainty due to pre-industrial fire and biogenic emissions. *Atmospheric Chemistry and Physics 20*(18), 10937–10951. https://doi.org/10.5194/acp-20-10937-2020

Markowicz, K. M., Flatau, P. J., Ramana, M. V., Crutzen, P. J., & Ramanathan, V. (2002). Absorbing Mediterranean aerosols lead to a large reduction in the solar radiation at the surface. *Geophysical Research Letters, 29*, 1968. https://doi.org/10.1029/2002GL015767

Mekhilef, S., Saidur, R., & Kamalisarvestani, M. (2012). Effect of dust humidity and air velocity on efficiency of photovoltaic cells. *Renewable and Sustainable Energy Reviews, 16*, 2920–2925. https://doi.org/10.1016/j.rser.2012.02.012

Meleux, F., Solmon, F., & Giorgi, F. (2007). Increase in summer European ozone amounts due to climate change. *Atmospheric Environment, 41*, 7577–7587. https://doi.org/10.1016/j.atmosenv.2007.05.048

Meloni, D., di Sarra, A., DeLuisi, J., Di Iorio, T., Fiocco, G., Junkermann, W., & Pace, G. (2003). Tropospheric aerosols in the Mediterranean: 2. Radiative effects through model simulations and measurements. *Journal of Geophysical Research, 108*, 4317. https://doi.org/10.1029/2002JD002807

Meloni, D., di Sarra, A., Di Iorio, T., & Fiocco, G. (2004). Direct radiative forcing of Saharan dust in the Mediterranean from measurements at Lampedusa Island and MISR space-borne observations. *Journal of Geophysical Research, 109*, D08206. https://doi.org/10.1029/2003JD003960

Meloni, D., Junkermann, W., di Sarra, A., Cacciani, M., De Silvestri, L., Di Iorio, T., Estellés, V., Gómez-Amo, J. L., Pace, G., & Sferlazzo, D. M. (2015). Altitude-resolved shortwave and long-wave radiative effects of desert dust in the Mediterranean during the GAMARF campaign: Indications of a net daily cooling in the dust layer. *Journal of Geophysical Research – Atmospheres, 120*, 3386–3407. https://doi.org/10.1002/2014JD022312

Meloni, D., di Sarra, A., Brogniez, G., Denjean, C., De Silvestri, L., Di Iorio, T., Formenti, P., Gómez-Amo, J. L., Gröbner, J., Kouremeti, N., Liuzzi, G., Mallet, M., Pace, G., & Sferlazzo, D. M. (2018). Determining the infrared radiative effects of Saharan dust: A radiative transfer modelling study based on vertically resolved measurements at Lampedusa. *Atmospheric Chemistry and Physics, 18*, 4377–4401. https://doi.org/10.5194/acp-18-4377-2018

Mercado, L. M., Bellouin, N., Sitch, S., Boucher, O., Huntingford, C., Wild, M., & Cox, P. M. (2009). Impact of changes in diffuse radiation on the global land carbon sink. *Nature, 458*, 1014–1018. https://doi.org/10.1038/nature07949

Mishra, A. K., Klingmueller, K., Fredj, E., Lelieveld, J., Rudich, Y., & Koren, I. (2014). Radiative signature of absorbing aerosol over the eastern Mediterranean basin. *Atmospheric Chemistry and Physics, 14*, 7213–7231. https://doi.org/10.5194/acp-14-7213-2014

Müller, B., Wild, M., Driesse, A., & Behrens, K. (2014). Rethinking solar resource assessments in the context of global dimming and brightening. *Solar Energy, 99*, 272–282. https://doi.org/10.1016/j.solener.2013.11.013

Myhre, G., Shindell, D., Bréon, F.-M., Collins, W., Fuglestvedt, J., Huang, J., Koch, D., Lamarque, J.-F., Lee, D., Mendoza, B., Nakajima, T., Robock, A., Stephens, G., Takemura, T., & Zhang, H. (2013). Anthropogenic and natural radiative forcing. In T. F. Stocker, D. Qin, G.-K. Plattner, M. Tignor, S. K. Allen, J. Boschung, A. Nauels, Y. Xia, V. Bex, & P. M. Midgley (Eds.),

Climate change 2013: The physical science basis, contribution of working group I to the fifth assessment report of the intergovernmental panel on climate change (pp. 659–740). Cambridge University Press.

Nabat, P., Solmon, F., Mallet, M., Kok, J. F., & Somot, S. (2012). Dust emission size distribution impact on aerosol budget and radiative forcing over the Mediterranean region: A regional climate model approach. *Atmospheric Chemistry and Physics, 12*, 10545–10567. https://doi.org/10.5194/acp-12-10545-2012

Nabat, P., Somot, S., Mallet, M., Sanchez-Lorenzo, A., & Wild, M. (2014). Contribution of anthropogenic sulfate aerosols to the changing Euro-Mediterranean climate since 1980. *Geophysical Research Letters, 41*, 5605–5611. https://doi.org/10.1002/2014GL060798

Nabat, P., Somot, S., Mallet, M., Sevault, F., Chiacchio, M., & Wild, M. (2015). Direct and semi-direct aerosol radiative effect on the Mediterranean climate variability using a coupled regional climate system model. *Climate Dynamics, 44*, 1127–1155. https://doi.org/10.1007/s00382-014-2205-6

Nabat, P., Kanji, Z., Mallet, M., Denjean, C., & Solmon, F. (2022). Aerosol-cloud interactions and impact on the regional climate. In F. Dulac, S. Sauvage, & E. Hamonou (Eds.), *Atmospheric chemistry in the Mediterranean Region* (Vol. 2, From air pollutant sources to impacts). Springer, this volume. https://doi.org/10.1007/978-3-030-82385-6_20

Neher, I., Buchmann, T., Crewell, S., Evers-Dietze, B., Pfeilsticker, K., Pospichal, B., Schirrmeister, C., & Meilinger, S. (2017). Impact of atmospheric aerosols on photovoltaic energy production scenario for the Sahel zone. *Energy Procedia, 125*, 170–179. https://doi.org/10.1016/j.egypro.2017.08.168

Nimmo, B. G., & Said, S. A. M. (1981). Effects of dust on the performance of thermal and photovoltaic flat-plate collectors in Saudi Arabia – Preliminary results. In *Proceedings of the 2nd Miami International Conference on Alternative Energy Sources*, Miami Beach, Fla., December 10–13, 1979, T. N. Veziroglu (Ed.), Hemisphere Publishing Corp., 1, 145–152.

Ohmura, A. (2009). Observed decadal variations in surface solar radiation and their cause. *Journal of Geophysical Research, 114*, D00D05. https://doi.org/10.1029/2008JD011290

Pace, G., Meloni, D., & di Sarra, A. (2005). Forest fire aerosol over the Mediterranean basin during summer 2003. *Journal of Geophysical Research, 110*, D21202. https://doi.org/10.1029/2005JD005986

Péré, J. C., Mallet, M., Pont, V., & Bessagnet, B. (2011). Impact of aerosol direct radiative forcing on the radiative budget, surface heat fluxes, and atmospheric dynamics during the heat wave of summer 2003 over Western Europe: A modeling study. *Journal of Geophysical Research, 116*, D23119. https://doi.org/10.1029/2011JD016240

Perez, R., Kivalov, S., Schlemmer, J., Hemker, K., Jr., Renné, D., & Hoff, T. E. (2010). Validation of short and medium term operational solar radiation forecasts in the US. *Solar Energy, 84*, 2161–2172. https://doi.org/10.1016/j.solener.2010.08.014

Polo, J., Antonanzas-Torres, F., Vindel, J. M., & Ramirez, L. (2014). Sensitivity of satellite-based methods for deriving solar radiation to different choice of aerosol input and models. *Renewable Energy, 68*, 785–792. https://doi.org/10.1016/j.renene.2014.03.022

Posselt, R., Mueller, R. W., Stöckli, R., & Trentmann, J. (2012). Remote sensing of solar surface radiation for climate monitoring — The CM-SAF retrieval in international comparison. *Remote Sensing of Environment, 118*, 186–198. https://doi.org/10.1016/j.rse.2011.11.016

Ramanathan, V., Crutzen, P. J., Kiehl, J. T., & Rosenfeld, D. (2001). Aerosols, climate, and the hydrological cycle. *Science, 294*, 2119–2124. https://doi.org/10.1126/science.1064034

Ramanathan, V., Ramana, M., Roberts, G., Kim, D., Corrigan, C., Chung, C., & Winker, D. (2007). Warming trends in Asia amplified by brown cloud solar absorption. *Nature, 448*, 575–578. https://doi.org/10.1038/nature06019

Rap, A., Richards, N. A. D., Forster, P. M., Monks, S. A., Arnold, S. R., & Chipperfield, M. P. (2015). Satellite constraint on the tropospheric ozone radiative effect. *Geophysical Research Letters, 42*, 5074–5081. https://doi.org/10.1002/2015GL064037

Real, E., & Sartelet, K. (2011). Modeling of photolysis rates over Europe: Impact on chemical gaseous species and aerosols. *Atmospheric Chemistry and Physics, 11*, 1711–1727. https://doi.org/10.5194/acp-11-1711-2011

Richards, N. A. D., Arnold, S. R., Chipperfield, M. P., Miles, G., Rap, A., Siddans, R., Monks, S. A., & Hollaway, M. J. (2013). The Mediterranean summertime ozone maximum: Global emission sensitivities and radiative impacts. *Atmospheric Chemistry and Physics, 13*, 2331–2345. https://doi.org/10.5194/acp-13-2331-2013

Rieger, D., Steiner, A., Bachmann, V., Gasch, P., Förstner, J., Deetz, K., Vogel, B., & Vogel, H. (2017). Impact of the 4 April 2014 Saharan dust outbreak on the photovoltaic power generation in Germany. *Atmospheric Chemistry and Physics, 17*, 13391–13415. https://doi.org/10.5194/acp-17-13391-2017

Roger, J. C., Mallet, M., Dubuisson, P., Cachier, H., Vermote, E., Dubovik, O., & Despiau, S. (2006). A synergetic approach for estimating the local direct aerosol forcing during the ESCOMPTE campaign. *Journal of Geophysical Research – Atmospheres, 111*, D13208. https://doi.org/10.1029/2005JD006361

Rowlinson, M. J., Rap, A., Arnold, S. R., Pope, R. J., Chipperfield, M. P., McNorton, J., Forster, P., Gordon, H., Pringle, K. J., Feng, W., Kerridge, B. J., Latter, B. L., & Siddans, R. (2019). Impact of El Niño–Southern Oscillation on the interannual variability of methane and tropospheric ozone. *Atmospheric Chemistry and Physics, 19*, 8669–8686. https://doi.org/10.5194/acp-19-8669-2019

Rowlinson, M. J., Rap, A., Hamilton, D. S., Pope, R. J., Hantson, S., Arnold, S. R., Kaplan, J. O., Arneth, A., Chipperfield, M. P., Forster, P. M., & Nieradzik, L. (2020) Tropospheric ozone radiative forcing uncertainty due to pre-industrial fire and biogenic emissions. *Atmospheric Chemistry and Physics, 20*, 10937–10951. https://doi.org/10.5194/acp-20-10937-2020

Ruiz-Arias, J. A., Gueymard, C. A., Santos-Alamillos, F. J., & Pozo-Vázquez, D. (2016). Worldwide impact of aerosol's time scale on the predicted long-term concentrating solar power potential. *Scientific Reports, 6*, 30546. https://doi.org/10.1038/srep30546

Saha, A., Mallet, M., Roger, J. C., Dubuisson, P., Piazzola, J., & Despiau, S. (2008). One year measurements of aerosol optical properties over the urban coastal zone. Effect on the local radiative effects. *Atmospheric Research, 90*, 195–202. https://doi.org/10.1016/j.atmosres.2008.02.003

Sanchez-Lorenzo, A., Brunetti, M., & Deser, C. (2009). Dimming/brightening over the Iberian Peninsula: Trends in sunshine duration and cloud cover and their relations with atmospheric circulation. *Journal of Geophysical Research, 114*, D00D09. https://doi.org/10.1029/2008JD011394

Sanchez-Lorenzo, A., Wild, M., Brunetti, M., Guijarro, J. A., Hakuba, M. Z., Calbó, J., Mystakidis, S., & Bartok, B. (2015). Reassessment and update of long-term trends in downward surface radiation over Europe (1939-2012). *Journal of Geophysical Research, 120*, 9555–9569. https://doi.org/10.1002/2015JD023321

Sanchez-Lorenzo, A., Enriquez-Alonso, A., Wild, M., Trentmann, J., Vicente-Serrano, S. M., Sanchez-Romero, A., Posselt, R., & Hakuba, M. Z. (2017). Trends in downward surface solar radiation from satellites and ground observations over Europe during 1983–2010. *Remote Sensing of Environment, 189*, 108–117. https://doi.org/10.1016/j.rse.2016.11.018

Santese, M., Perrone, M. R., Zakey, A. S., De Tomasi, F., & Giorgi, F. (2010). Modeling of Saharan dust outbreaks over the Mediterranean by RegCM3: Case studies. *Atmospheric Chemistry and Physics, 10*, 133–156. https://doi.org/10.5194/acp-10-133-2010

Sarver, T., Al-Qaraghuli, A., & Kazmerski, L. L. (2013). A comprehensive review of the impact of dust on the use of solar energy: History investigations results literature and mitigation approaches. *Renewable and Sustainable Energy Reviews, 22*, 698–733. https://doi.org/10.1016/j.rser.2012.12.065

Sayyah, A., Horenstein, M. N., & Mazumder, M. K. (2016). Energy yield loss caused by dust deposition on photovoltaic panels. *Solar Energy, 107*, 576–604. https://doi.org/10.1016/j.solener.2014.05.030

Sellitto, P., di Sarra, A., Corradini, S., Boichu, M., Herbin, H., Dubuisson, P., Sèze, G., Meloni, D., Monteleone, F., Merucci, L., Rusalem, J., Salerno, G., Briole, P., & Legras, B. (2016). Synergistic use of Lagrangian dispersion and radiative transfer modelling with satellite and

surface remote sensing measurements for the investigation of volcanic plumes: The Mount Etna eruption of 25–27 October 2013. *Atmospheric Chemistry and Physics, 16*, 6841–6861. https://doi.org/10.5194/acp-16-6841-2016

Sellitto, P., Salerno, G., La Spina, A., Caltabiano, T., Scollo, S., Boselli, A., Leto, G., Zanmar Sanchez, R., Crumeyrolle, S., Hanoune, B., & Briole, P. (2020). Small-scale volcanic aerosols variability, processes and direct radiative impact at Mount Etna during the EPL-RADIO campaigns. *Scientific Reports, 10*, 15224. https://doi.org/10.1038/s41598-020-71635-1

Semaoui, S., Hadj Arab, A., Boudjelthia, E. K., Bacha, S., & Zeraia, H. (2015). Dust effect on optical transmittance of photovoltaic module glazing in a desert region. *Energy Procedia, 74*, 1347–1357. https://doi.org/10.1016/j.egypro.2015.07.781

Semaoui, S., Abdeladim, K., Taghezouit, B., Hadj Arab, A., Razagui, A., Bacha, S., Boulahchiche, S., Bouacha, S., & Gherbi, A. (2020). Experimental investigation of soiling impact on grid connected PV power. *Energy Reports, 6, Suppl. I*, 302–308. https://doi.org/10.1016/j.egyr.2019.08.060

Sengupta, M., Habte, A., Gueymard, C., Wilbert, S., Renné, D., & Stoffel, S., (Eds.). (2017). *Best practices handbook for the collection and use of solar resource data for solar energy applications: Second Edition* (Tech. Rep. NREL/TP-5D00-68886). Golden, CO: National Renewable Energy Lab. 238 pp., https://doi.org/10.2172/1411856.

Sicard, M., Mallet, M., García-Vizcaíno, D., Comerón, A., Rocadenbosch, F., Dubuisson, P., & Muñoz-Porcar, C. (2012). Intense dust and extremely fresh biomass burning outbreak in Barcelona, Spain: Characterization of their optical properties and estimation of their direct radiative forcing. *Environmental Research Letters, 7*, 034016. https://doi.org/10.1088/F1748-9326/2F7/2F3/2F034016

Sicard, M., Bertolín, S., Mallet, M., Dubuisson, P., & Comerón, A. (2014). Estimation of mineral dust longwave radiative forcing: Sensitivity study to particle properties and application to real cases in the region of Barcelona. *Atmospheric Chemistry and Physics, 14*, 9213–9231. https://doi.org/10.5194/acpd-14-8533-2014

Spyrou, C., Kallos, G., Mitsakou, C., Athanasiadis, P., Kalogeri, C., & Iacono, M. (2013). Modeling the radiative effects of desert dust on weather and regional climate. *Atmospheric Chemistry and Physics, 13*, 5489–5504. https://doi.org/10.5194/acp-13-5489-2013

Stanhill, G., & Cohen, S. (2009). Is solar dimming global or urban? Evidence from measurements in Israel between 1954 and 2007. *Journal of Geophysical Research, 114*, D00D17. https://doi.org/10.1029/2009JD011976

Stevenson, D. S., Young, P. J., Naik, V., Lamarque, J. F., Shindell, D. T., Voulgarakis, A., Skeie, R. B., Dalsoren, S. B., Myhre, G., Berntsen, T. K., Folberth, G. A., Rumbold, S. T., Collins, W. J., MacKenzie, I. A., Doherty, R. M., Zeng, G., van Noije, T. P. C., Strunk, A., Bergmann, D., … Archibald, A. (2013). Tropospheric ozone changes, radiative forcing and attribution to emissions in the Atmospheric Chemistry and Climate Model Intercomparison Project (ACCMIP). *Atmospheric Chemistry and Physics, 13*, 3063–3085. https://doi.org/10.5194/acp-13-3063-2013

Tafuro, A. M., Kinne, S., De Tomasi, F., & Perrone, M. R. (2007). Annual cycle of direct radiative effect over southeast Italy and sensitivity studies. *Journal of Geophysical Research, 112*, D20202. https://doi.org/10.1029/2006JD008265

Volz, A., & Kley, D. (1988). Evaluation of the Montsouris series of ozone measurements made in the nineteenth century. *Nature, 332*, 240–242. https://doi.org/10.1038/332240a0

Vrekoussis, M., Liakakou, E., Koçak, M., Kubilay, N., Oikonomou, K., Sciare, J., & Mihalopoulos, N. (2005). Seasonal variability of optical properties of aerosols in the Eastern Mediterranean. *Atmospheric Environment, 39*, 7083–7094. https://doi.org/10.1016/j.atmosenv.2005.08.011

Wang, W., Li, X., Shao, M., Hu, M., Zeng, L., Wu, Y., &, Tan, T. (2019). The impact of aerosols on photolysis frequencies and ozone production in Beijing during the 4-year period 2012–2015. *Atmospheric Chemistry and Physics, 19*, 9413–9429. https://doi.org/10.5194/acp-19-9413-2019

Wild, M. (2012). Enlightening global dimming and brightening. *Bulletin of the American Meteorological Society, 93*, 27–37. https://doi.org/10.1175/BAMS-D-11-00074.1

Wild, M., Trüssel, B., Ohmura, A., Long, C. N., König-Langlo, G., Dutton, E. G., & Tsvetkov, A. (2009). Global dimming and brightening: An update beyond 2000. *Journal of Geophysical Research, 114*, D00D13. https://doi.org/10.1029/2008JD011382

Wild, M., Folini, D., Schär, C., Loeb, N., Dutton, E. G., & König-Langlo, G. (2013). The global energy balance from a surface perspective. *Climate Dynamics, 40*, 3107–3134. https://doi.org/10.1007/s00382-012-1569-8

Wild, M., Folini, D., Henschel, F., Fischer, N., & Müller, B. (2015). Projections of long-term changes in solar radiation based on CMIP5 climate models and their influence on energy yields of photovoltaic systems. *Solar Energy, 116*, 12–24. https://doi.org/10.1016/j.solener.2015.03.039

Yeung, L. Y., Murray, L. T., Martinerie, P., Witrant, E., Hu, H., Banerjee, A., Orsi, A., & Chappellaz, J. (2019). Isotopic constraint on the twentieth-century increase in tropospheric ozone. *Nature, 570*, 224–227. https://doi.org/10.1038/s41586-019-1277-1

Zanis, P. (2009). A study on the direct effect of anthropogenic aerosols on near surface air temperature over southeastern Europe during summer 2000 based on regional climate modeling. *Annales Geophysicae, 27*, 3977–3988. https://doi.org/10.5194/angeo-27-3977-2009

Zanis, P., Ntogras, C., Zakey, A., Pytharoulis, I., & Karacostas, T. (2012). Regional climate feedback of anthropogenic aerosols over Europe using RegCM3. *Climate Research, 52*, 267–278. https://doi.org/10.3354/cr01070

Zanis, P., Hadjinicolaou, P., Pozzer, A., Tyrlis, E., Dafka, S., Mihalopoulos, N., & Lelieveld, J. (2014). Summertime free-tropospheric ozone pool over the eastern Mediterranean/Middle East. *Atmospheric Chemistry and Physics, 14*, 115–132. https://doi.org/10.5194/acp-14-115-2014

Zerefos, C. S., Kourtidis, K. A., Melas, D., Balis, D., Zanis, P., Katsaros, L., Mantis, H. T., Repapis, C., Isaksen, I., Sundet, J., Herman, J., Bhartia, P. K., & Calpini, B. (2002). Photochemical Activity and Solar Ultraviolet Radiation (PAUR) modulation factors: An overview of the project. *Journal of Geophysical Research, 107*, 8134. https://doi.org/10.1029/2000jd000134

Zerefos, C. S., Eleftheratos, K., Meleti, C., Kazadzis, S., Romanou, A., Ickoku, C., Tselioudis, G., & Bais, A. (2009). Solar dimming and brightening over Thessaloniki, Greece, and Beijing, China. *Tellus B: Chemical and Physical Meteorology, 61*, 657–665. https://doi.org/10.1111/j.1600-0889.2009.00425.x

Zubler, E. M., Folini, D., Lohmann, U., Lüthi, D., Schär, C., & Wild, M. (2011). Simulation of dimming and brightening in Europe from 1958 to 2001 using a regional climate model. *Journal of Geophysical Research, 116*, D18205. https://doi.org/10.1029/2010JD015396

Zorrilla-Casanova, J., Piliougine, M., Carretero, J., Bernaola, P., Carpena, P., Mora-López, L., & Sidrach-de-Cardona, M. (2011). Analysis of dust losses in photovoltaic modules. In *Proceedings of the World Renewable Energy Congress*, B. Moshfeg (Ed.), Linköping University Electronic Press, 2985–2992. https://doi.org/10.3384/ecp110572985

Aerosol-Cloud Interactions and Impact on Regional Climate

Pierre Nabat, Zamin A. Kanji, Marc Mallet, Cyrielle Denjean, and Fabien Solmon

Contents

Abstract Aerosols interact with clouds through radiative and microphysical mechanisms in addition to their direct radiative effects of scattering and absorbing of solar and thermal radiation. Aerosol indirect effects consist of the modification of cloud droplet number concentrations, cloud albedo, and ice-nucleating particle concentrations with ensuing effects on precipitation through aerosol perturbations. Different aerosol types present over the basin, notably dust, sea salt, and anthropogenic, contribute to the formation of cloud condensation and ice-nucleating particles, thus modifying cloud parameters. These processes notably occur during the

Chapter reviewed by ***Daniel Rosenfeld*** *(Institute of Earth Sciences, The Hebrew University of Jerusalem, Israel), as part of the book Part IX Impacts of Air Pollution on Precipitation Chemistry and Climate also reviewed by* ***Simone Lolli*** *(CNR/IMAA, Tito Scalo (PZ), Italy)*

P. Nabat (✉) · M. Mallet · C. Denjean
Centre National de Recherches Météorologiques (CNRM), Université de Toulouse, Météo-France, CNRS, Toulouse, France
e-mail: pierre.nabat@meteo.fr

Z. A. Kanji
Swiss Federal Institute of Technology (ETH), Zurich, Switzerland

F. Solmon
Laboratoire d'Aérologie (LAERO), Université de Toulouse III Paul Sabatier, CNRS, Toulouse, France

F. Dulac et al. (eds.), *Atmospheric Chemistry in the Mediterranean Region*,
https://doi.org/10.1007/978-3-030-82385-6_20

frequent dust outbreaks over the Mediterranean Sea. Besides, the semi-direct aerosol effect, namely, changes in cloud cover and atmospheric dynamics due to aerosol absorption, is another impact on regional climate. Regional climate simulations including aerosol-cloud interactions highlight the importance of considering aerosols, even if uncertainties are still important notably with regard to effects on cloud microphysics. To date, the direct and semi-direct effects seem to have larger impacts on the average radiative budget over the Mediterranean than the cloud-albedo indirect effect, but the question remains open concerning other indirect effects. Therefore, more observations of these interactions coupled with numerical simulations considering all these processes are needed to reduce uncertainties.

1 Introduction

1.1 Climate-Aerosol Interactions

Atmospheric aerosols play an essential role in the climate system through different mechanisms. First of all, they interact with radiation insofar as they are able to absorb and scatter solar radiation and absorb and emit thermal radiation. This is known as the direct effect (Haywood & Boucher, 2000) and has been documented in the previous chapter (Mallet et al., 2022). The second, main impact of aerosols on climate is due to their interactions with clouds. Indeed, aerosols are known to act as cloud condensation nuclei (CCN) and ice-nucleating particles (INP) and thus impact the formation and the life cycle of clouds (Pruppacher & Klett, 1980). These effects are known as indirect aerosol effects (Lohmann & Feichter, 2005) and belong to what is now called aerosol-cloud interactions (Boucher et al., 2013). In addition to these direct and indirect effects, atmospheric circulation and dynamics can also be affected by local warming due to aerosol absorption of solar light, with ensuing effects on cloud cover and precipitation. These processes are referred to as semi-direct effects (Hansen et al., 1997; Johnson et al., 2004). All these effects have significant consequences on global and regional climate. This chapter will specifically deal with aerosol-cloud interactions and their impact on the regional climate over the Mediterranean area.

1.2 Aerosol Indirect Effects

Aerosol indirect effects are a generic term to refer to all effects arising from processes involving aerosol particles and cloud microphysics. They include notably cloud droplet activation and ice nucleation which lead to the formation of cloud droplets and ice crystals, respectively. Aerosols can alter warm, ice, and mixed-phase cloud formation processes by increasing droplet number concentrations and

ice particle concentrations. The various identified aerosol indirect effects are complex and interlinked. The first one has been identified by Twomey (1959), consisting of an enhanced number of cloud droplets due to the presence of aerosols. These cloud droplets have reduced sizes for a similar liquid water path (LWP), resulting in an increased cloud optical thickness, that is to say an increase in the cloud albedo, which could lead to surface cooling. Besides, the more numerous but smaller cloud droplets inhibit precipitation formation efficiency and therefore increase the cloud lifetime, LWP, and cloud fraction (CF), which is referred to as the Albrecht effect or second indirect effect (Albrecht, 1989). This effect could be as large as the Twomey effect. This change in droplet size can also induce changes in the cloud top height (Pincus & Baker, 1994). Aerosols may thus lead to an increase in cloud optical thickness due to a combination of reduction in cloud droplet radius and increased water content. However, this simple chain of events has been challenged for warm stratocumulus clouds (Ackerman et al., 2004) and shallow cumulus (Jiang et al., 2006). The latter studies confirmed a reduction in precipitation with increasing aerosol but showed both positive and negative responses of parameters such as LWP and CF. Aerosols perturbing pristine convective clouds have also been proposed to result in the same amount of surface precipitation due to convective invigoration despite the slower conversion of cloud droplets to precipitation in polluted conditions (Rosenfeld et al., 2008). Furthermore, Koren et al. (2012) have shown that aerosols could intensify precipitation events in the lower and midlatitudes. As a matter of fact, these different studies show that it is difficult to establish climatically meaningful relationships between aerosols, clouds, and precipitation (Stevens & Feingold, 2009). More recently, Fan et al. (2018) have highlighted the role of ultrafine aerosol particles (less than 50 nm in diameter) in enhancing convection and precipitation although they are too small to serve as CCN at cloud base.

Moreover, the complex interactions between particles and clouds depend on the characteristics of particles in question (concentration, size distribution, chemical composition, hygroscopic properties, mixing state) and the type of clouds involved (continental or maritime, convective or stratiform, cold or warm). Aerosols, on which cloud droplets form, determine the initial concentration and sizes of the droplets, influence the effectiveness of precipitation production, and affect cloud radiative properties. For instance, even insoluble particles like dust and biomass burning aerosols may affect convective clouds if coated with a small amount of soluble material (Levin et al., 1996; Kaufman & Fraser, 1997; Ackerman et al., 2000; Roberts et al., 2003; Levin et al., 2005). In return, the clouds affect the aerosols by modifying their size, concentration, and chemical composition due to heterogeneous reactions (see also the chapter by Michoud, 2022). Particles are modified by various chemical reactions that take place in the drops (or in ice crystals), and their concentration in the atmosphere is modified through various scavenging processes. Since most clouds evaporate and do not precipitate, aerosols of different compositions are released back into the atmosphere after droplet evaporation (Levin et al., 1996; Wurzler et al., 2000; Yin et al., 2002). For example, the study of Wurzler et al. (2000) shows that the interaction of insoluble mineral dust particles with clouds modifies the composition and size of the particles that are released into the

atmosphere following cloud evaporation. Laboratory measurements indicate that dust particles may become better CCN after cloud processing (Kumar et al., 2011; see also the chapters by Becagli, 2022 and Denjean, 2022). These modified particles can serve as giant cloud condensation nuclei (GCCN) and thus can have a significant impact on the microphysical characteristics and the formation of precipitation in subsequent clouds (Rosenfeld et al., 2001).

It must be borne in mind that the treatment of aerosols and clouds in climate models encounters large uncertainties because of the complexity of these mechanisms and the large range of scales of these interactions (Seinfeld et al., 2016). Numerous observations of various types (remote sensing, in situ) are increasingly being used to constrain model simulations. The use of fine-scale models is helpful to represent clouds, aerosols, and aerosol-cloud interactions with high fidelity and to consider specificities of regions such as the Mediterranean area. The interactions with the larger scale are however absent from these regional models.

1.3 Other Cloud-Aerosol Interactions

With regard to the semi-direct effect of aerosols, several studies have focused on the inhibition of cloud formation (Ackerman et al., 2000; Ramanathan et al., 2001; Koren et al., 2004; Johnson et al., 2004; Ramanathan et al., 2007). This aerosol effect has a strong impact on the radiative balance but is also very sensitive to the vertical distribution of aerosols and clouds (Penner et al., 2003; Johnson et al., 2004). Studies have shown that absorbing aerosol particles in a cloud layer could increase evaporation of droplets, whereas an absorbing aerosol layer warming the air above a cloud deck (e.g., stratocumulus) could result in a thicker cloud via the reduction of above cloud subsidence and dry intrusions (Wilcox, 2010). The cloud adjustments to absorbing aerosol such as black carbon can thus partially offset or reinforce the cooling due to the indirect aerosol effect (Penner et al., 2003; Johnson et al., 2004). Both the second indirect effect and the semi-direct effect involve feedback because of cloud lifetime and liquid water content changes.

1.4 Clouds and Aerosols Over the Mediterranean

Undoubtedly, the aerosol types, seasons, and regions of interest influence the impacts of aerosols on regional climate. As the Mediterranean is a crossroads of various natural and anthropogenic aerosol types (Lelieveld et al., 2002), their interactions with clouds and climate are all the more complex. For example, the presence of mineral dust and especially the high percentage of mixtures of mineral dust and sea salt raise questions about the potential effects of these particles in cloud formation processes and precipitation development. Previous works have shown that large dust particles coated with soluble material are efficient CCN (Levin et al., 1996) and

that mineral dust particles are also efficient INPs (Grosch & Georgii, 1976; DeMott et al., 2003). Anthropogenic particles coming from European sources (transport, industries) as well as ship transport are also responsible for the presence of CCN over the Mediterranean Sea. All these issues will be discussed in the following paragraphs, based on both observation (in situ, satellite data) and modeling studies.

2 Aerosol-Cloud Interactions By Aerosol Type

2.1 The Case of Dust Particles

Mineral dust is the major source of coarse aerosol particles in the Mediterranean, together with sea-salt particles. They mainly come from the Saharan desert, from which they are frequently transported over the Mediterranean Sea (Moulin et al., 1998; Israelevich et al., 2012; Gkikas et al., 2013). Their optical properties make them able to both scatter and absorb solar radiation, which leads to a reduction in incoming solar radiation at the surface, with ensuing cooling as shown by several studies over the Mediterranean area (e.g., Spyrou et al., 2013; Flamant et al., 2015; Nabat et al., 2015a; Gkikas et al., 2018). Dust aerosols also have the ability to affect cloud microphysics through ice particle formation and to act as CCN through their coating by other aerosol types such as sea salt and sulfate (for more details, see Denjean, 2022).

In particular, dust aerosols play a role in the formation of giant cloud condensation nuclei (GCCN) as shown by Levin et al. (2005). These GCCN can notably enhance the development of the large drops, leading to enhanced growth by collection and rapid development of the rain (Johnson, 1982; Cooper et al., 1997; Yin et al., 2000; Teller & Levin, 2006). They have thus a positive effect on the amount of rain in continental clouds but have a negligible (even slightly negative) effect in maritime clouds. Levin et al. (2005) have used size distribution and chemical composition of the aerosols measured during a dust storm in the Mediterranean region as initial conditions for simulating cloud development. They concluded that the amount of rain falling from a maritime cloud is generally much higher than from a continental cloud. However, the development of the warm rain process in the latter case is enhanced when allowing the soluble component of the mixed aerosols to act as an efficient GCCN and ignoring the ice-nucleating ability of the mineral dust. They also infer that the role of mineral dust particles acting as efficient INP reduces the amount of rain on the ground compared to the case when they are inactive. When the dust particles are active as both GCCN and effective INP, the continental clouds become wider, while the effects on the more maritime clouds are very small. It was also found that the rapid growth of large drops enhances ice formation in colder convective clouds through the more efficient freezing of drops. This efficient production of large drops and ice particles modifies the time, the amount, and the distribution of the precipitation. In contrast, when the concentration of small nuclei is low, as that in maritime clouds, the effect of these GCCN is insignificant and the total precipitation remains unaltered. On the other hand, for both marine and

continental clouds, inclusion of the effects of INP by dust particles tends to delay the initiation of the rain and leads to a reduction in the total rainfall amount as compared with the cases having only GCCN.

Satellite observations and in situ measurements have also been used to show that desert dust aerosols might also suppress precipitation in marine clouds (Rosenfeld et al., 2001; Mahowald & Kiehl, 2003). The latter two studies found a strong relationship between thin cloud properties and mineral dust concentrations over North Africa. In fact, the introduction of modified dust into the clouds has two competing effects (Yin et al., 2002). The large particles acting as GCCN produce larger drops which tend to rapidly form precipitation by collecting small drops formed on the large number of small CCN particles. At the same time, the larger concentrations of drops compete for the available water vapor. Thus, the drops may be smaller, reducing the efficiency of precipitation.

More recent studies have relied on regional climate simulations to confirm the role of dust in CCN and INP formation. Bangert et al. (2012) reproduced a strong Saharan dust outbreak over Europe in May 2008 using the regional climate model COSMO-ART, including a two-moment cloud microphysics scheme coupled with comprehensive parameterizations of aerosol activation and ice nucleation. Even if dust aerosols do not significantly modify the cloud droplet number concentration, the simulation highlights the impact of dust on clouds under specific temperature conditions, namely, between the freezing level and the level of homogeneous freezing. In this case, the number concentration of ice crystals is found to be strongly related to dust particles because of their efficient heterogeneous freezing. Dust aerosols thus modify the glaciation of mixed phase clouds, with ensuing effects on cloud optical properties that lead to optically thicker clouds, which scatter more efficiently shortwave radiation. As a result, Bangert et al. (2012) have found that the combined direct and indirect effects of dust aerosols caused a decrease in the incoming shortwave radiation at the surface of up to -75 W m^{-2} and a cooling of -0.2 to -0.5 K (locally -1.0 K) during this dust outbreak. However, at lower temperatures, the effects of dust particles are weaker because of a competition with the homogeneous freezing of liquid aerosol particles for water vapor during the ice nucleation. The same kind of dust outbreak was also studied by Bègue et al. (2015), who simulated the transport of dust over the Mediterranean and Europe with Meso-NH in May 2008 during the EUCAARI campaign. Their analysis puts forward heterogeneous reactions between dust and inorganic salts, making dust particles soluble enough to impact hygroscopic growth and cloud droplet activation. Another study by Abdelkader et al. (2015) focused on two dust events over the eastern Mediterranean in September 2011 has highlighted the role of synoptic disturbances and frontal systems in the transport of dust particles in this region. Using simulations with the atmospheric chemistry model ECHAM5/MESSy2 and back trajectory analysis, these authors have shown that frontal systems associated with precipitation control dust removal processes, thus impacting dust aging, increasing particle size, dust deposition, and scavenging efficiency during transport.

Beyond these case studies, Hande et al. (2015) have studied the impact of dust on ice nucleation at a seasonal timescale. They used the COSMO-MUSCAT regional climate model to estimate dust concentrations and their role as ice-nucleating particles during 2008. Dust concentrations are indeed highly variable over Europe and the Mediterranean between seasons, with the highest concentrations and variability in the lower to mid-troposphere, where the increase of potential INP concentrations is exponential with height. Spring has been found to be the season with the highest dust concentrations over Europe, and therefore the highest potential INP, contrary to summer, about an order of magnitude weaker.

2.2 The Case of Sea-Salt Particles

Sea-salt aerosols constitute the other main natural aerosol type present over the Mediterranean region. Like other aerosol particles, they are able to scatter solar radiation (de Leeuw et al., 2011) and to a lesser extent thermal radiation (Li et al., 2008). In addition, they can act as CCN because of their size and hygroscopic properties and thus impact marine cloud properties and lifetime (Pierce & Adams, 2006; Korhonen et al., 2008). Sea-salt aerosols are more CCN active than sulfate particles because of their larger size and lower supersaturation threshold required for their activation (O'Dowd et al., 1999). At the global scale, the direct radiative effect of sea-salt aerosols is well established, ranging from -0.38 to -0.65 W m^{-2} (Reddy et al., 2005; Ma et al., 2008; Ayash et al., 2008; Partanen et al., 2014) with stronger values over the Southern Ocean. On the contrary, the estimation of the indirect effect is more uncertain. While Ma et al. (2008) have found a larger negative indirect forcing of sea-salt aerosols (-2.9 W m^{-2}), Ayash et al. (2008) have shown that indirect sea-salt aerosol effects were weaker than their direct radiative effects, and Partanen et al. (2014) have even identified a positive global indirect effect, putting forward competition effects. All these uncertainties argue for a better estimate of sea-salt climate effects at the regional scale.

Over the Mediterranean, the direct sea-salt aerosol effects have been estimated by Zakey et al. (2008) using the regional climate model and by Lundgren et al. (2013) using the nonhydrostatic online-coupled regional-scale model system COSMO-ART for case studies under conditions of low to moderate wind speeds. The resulting clear-sky shortwave and longwave radiative budgets are found to be of the same order of magnitude but with opposite signs. Therefore, the net radiative effect of sea salt is close to zero, hence a weak impact of sea salt on surface temperature. However, this conclusion is only relevant for clear-sky conditions without considering the indirect effects of sea salt. The latter has been discussed by Kallos et al. (2016), focusing on low cloud formation over the southern Aegean and eastern coast of the Mediterranean. High sea-salt loads are indeed observed in this area. Using the modeling system RAMS/ICLAMS, they simulate the cloud formation of mixed stratiform clouds and low-level cumulonimbus around Crete. The combination of sea-salt and dust particles can lead in deep convection through orographic lifting

and activation of ice nucleation processes. The authors conclude that in this case with slow lifting and thermal updrafts, sea-salt particles influence mainly the cloud droplet number concentration.

2.3 The Case of Anthropogenic Particles

Anthropogenic particles are also known to have both direct (Charlson et al., 1992) and indirect effects (Boucher, 1995). As for sea-salt particles, their direct radiative forcing is better understood than their indirect forcing, probably because of the complexity of cloud system responses to aerosol perturbations that complicates the estimation of indirect effects (Boucher et al., 2013). Sulfate particles brought the highest contribution to the anthropogenic aerosol forcing which is negative at the global scale (Myhre et al., 2013), but nitrates (Bellouin et al., 2011; Drugé et al., 2019) and secondary organic aerosols (Scott et al., 2014) also have significant impacts, which consist also in negative radiative forcing. The role of black carbon particles is however different because of their absorbing properties that tend to warm the atmosphere (Chin et al., 2009; Myhre & Samset, 2015). The Mediterranean region is also affected by all these anthropogenic particles, coming essentially from European sources, Middle East and North African cities, and ship transport.

The effective radiative forcing (ERF) of anthropogenic aerosols can be estimated with global simulations from the sixth Coupled Model Intercomparison Project (CMIP6), in which specific simulations using preindustrial (1850) and 2014 aerosol concentrations have been carried out (Smith et al., 2020). The ERF is calculated according to the Ghan (2013) methodology, which enables us to retrieve separately the aerosol-radiation and the aerosol-cloud interactions (ERFari and ERFaci, respectively). Figure 1 presents the average over the Mediterranean from six CMIP6 models, for which this calculation of ERF is possible, thanks to available radiation

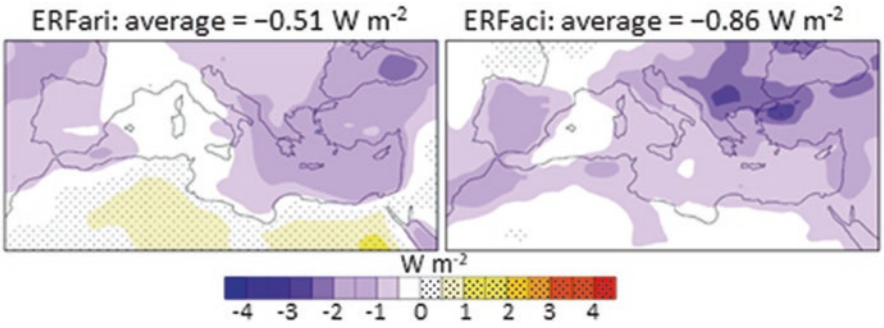

Fig. 1 Effective radiative forcing of anthropogenic aerosols at the top of the atmosphere estimated from multi-model CMIP6 simulations by difference between 2014 and 1850, separated between aerosol-radiation (ERFari) and aerosol-cloud (ERFaci) interactions. (Adapted from Smith et al., 2020)

fluxes with and without aerosols (double-call radiation). The resulting ERFari at the top of the atmosphere is on average −0.51 W m^{-2}, in addition to −0.86 W m^{-2} for ERFaci. The highest forcing is located over the eastern basin. Note that these ERF values are in absolute values lower than the one of anthropogenic greenhouse gases (2.85 W m^{-2}). It can also be inferred that anthropogenic aerosol-cloud interactions could have a larger radiative forcing over the Mediterranean than aerosol-radiation interactions, even if we must bear in mind that uncertainties are important since the respective confidence intervals at 95% of ERFari and ERFaci calculated for this ensemble of six CMIP6 models are ±0.76 and ± 0.96 W m^{-2}, respectively.

Because aerosols show much more variability at smaller time and space scales than greenhouse gases (e.g., Le Treut et al., 1998), it is of interest to study their radiative forcing at the regional scale with higher-resolution models. The first modeling study using a regional model to estimate the anthropogenic aerosol effects over Europe and the Mediterranean area was carried out by Ekman and Rodhe (2003). They used the RCA2 regional climate model including tropospheric sulphate particles and a parameterization of their cloud-albedo effect to estimate the Twomey effect during 1993. The result was an anthropogenic sulfate indirect effect between −2.7 and −2.5 W m^{-2}, and a corresponding annual mean surface temperature response of −0.4 K over the model domain (western Europe and northern Mediterranean). With regard to direct and semi-direct effects, Zanis (2009) has found a negative radiative forcing over Europe and the Mediterranean during summer 2000, using RegCM3 regional simulations. This negative forcing leads to a decrease in surface temperature by sulfate particles of up to 1.2 K over the Balkan Peninsula and southern Europe. Semi-direct mechanisms have also been identified insofar as sulfate aerosols induced changes in the circulation with a southward shift of the subtropical jet stream. These climate effects were better assessed in Zanis et al. (2012), using the same model but over a longer period (1996–2007). The annual average effect of anthropogenic aerosols on near-surface temperature was smaller (up to −0.2 K over the Balkan Peninsula) than in previous case studies, but it is associated with changes in atmospheric circulation. The maxima in aerosol loads are indeed uncorrelated with effects on surface temperature.

3 Implications for Regional Climate

3.1 Impact of Aerosol-Cloud Interactions on Regional Radiative Budget

After analyzing the aerosol effects on clouds and climate by aerosol species, this section aims at summarizing these effects at the scale of the Mediterranean area for the whole aerosol load. First of all, it is worth mentioning that the average direct effect of aerosols over the Mediterranean area has been estimated with both satellite and model data. Papadimas et al. (2012) have used MODIS data to find a direct

radiative forcing of aerosols of −16.5 W m^{-2} at the surface and −2.4 W m^{-2} at the top of the atmosphere (TOA). These values are close to those given by regional climate models: Nabat et al. (2012) have, respectively, found at the surface and at TOA −10.3 and −3.1 W m^{-2}; Nabat et al. (2015b), −19.9 and −7.8 W m^{-2}; and more recently, Drugé et al. (2019), −8.7 and −2.4 W m^{-2}. Differences in model estimates may be attributed to the way aerosols are represented in the models (e.g., with monthly mean AOD values or interactive variables) and/or to the representation of radiation and clouds.

In addition to these direct effects, the semi-direct effect has also been estimated but in fewer studies. It consists of changes in cloud cover and atmospheric circulation due to aerosol absorption. Nabat et al. (2015b) have found a positive semi-direct effect over the Mediterranean of 5.7 W m^{-2} on average, counterbalancing partly the negative direct forcing. A similar positive semi-direct forcing has been identified by Meier et al. (2012) in Europe in the case of absorbing aerosols in summer. In some cases, this semi-direct can even become stronger than the direct effect, as found by Forkel et al. (2012) in June to July 2006 in Europe.

Finally, the estimation of the aerosol indirect forcing is the most difficult to quantify. Using CERES and MODIS satellite data, Quaas et al. (2008) have estimated the average direct and indirect aerosol effects. Their maps show that the direct aerosol effect is an order of magnitude higher than the first indirect effect (cloud-albedo effect) over the Mediterranean area. From surface measurements over 1981–2005, Ruckstuhl et al. (2010) have underlined that the contribution of the first indirect aerosol effect to surface solar radiation changes over Europe was small compared to the direct effect. The same conclusion was drawn by Nabat et al. (2014). However, it should be noted that this comparison concerns only the first indirect aerosol effect, while the other aerosol-cloud interactions are more complex to quantify. Their impact on the radiative budget may not be negligible and needs to be studied in the future.

3.2 Implications for Surface Temperatures

All the effects of aerosols on the radiative budget including cloud-aerosol interactions have an impact on surface temperature, which generally leads to a cooling of the surface. Climate model simulations with and without aerosols are useful to quantify this impact on temperature. Ekman and Rodhe (2003) have first shown an average cooling of 0.4 K over Europe due to the first indirect effect of sulfate particles. This order of magnitude was confirmed by the studies of Zanis (2009) and Zanis et al. (2012) as far as the direct and semi-direct effects of sulfate are concerned. Dust aerosols also contribute to this cooling over the Mediterranean, as noted by Santese et al. (2010), Bangert et al. (2012), and Nabat et al. (2015a). However, most of these studies concern only specific aerosol types and/or seasons.

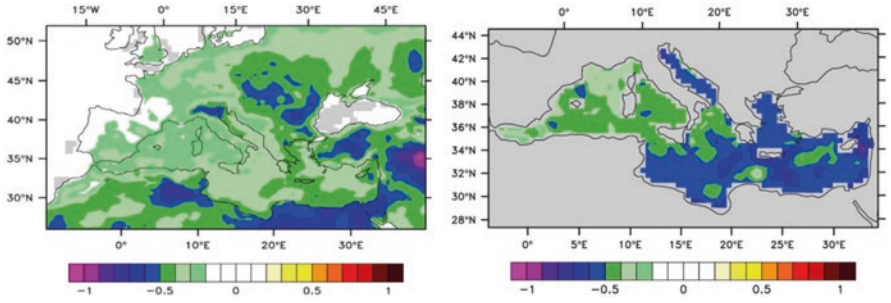

Fig. 2 Annual average aerosol impact on near-surface (2 m) temperature **(left)** and on sea surface temperature (**right**) in CNRM-RCSM simulations (2003–2009 average, in K). Only significant values at level 0.05 are shown (grey indicates non meaningful values). All resulting values are negative. (Adapted from Fig. 11 in Nabat et al., 2015b)

A more complete study dealing with the impact of aerosols on surface temperature was carried out by Nabat et al. (2015b). They have used the fully coupled regional climate system model CNRM-RCSM including the main natural and anthropogenic aerosol types, as well as ocean-atmosphere coupling for the Mediterranean region. They concluded that the negative radiative forcing of aerosols at the surface was responsible for an annual average cooling of 0.5 K in near-surface temperature over the Mediterranean, and the same value for the Mediterranean Sea surface temperature (SST), an effect that atmospheric models forced with external SST cannot consider (Fig. 2). This cooling is stronger in spring and summer when aerosol loads are higher. Indeed, the temperature decrease can be much more important during episodes of strong aerosol concentrations, for instance, as shown by Gkikas et al. (2019) during dust outbreaks over the central Mediterranean.

3.3 Aerosol Impact on Cloud Parameters

Both satellite data and model simulations have been used to show the impact of aerosols on cloud parameters. Myhre et al. (2007) have used MODIS data to study possible relationships between aerosol optical depth (AOD) and different atmospheric parameters. Their results over the Mediterranean area show a tendency for a weak increase in liquid water path (LWP) with AOD (Fig. 3a), a sharper increase in cloud fraction with AOD (Fig. 3b), and a more surprising increase in cloud droplet radius with AOD (Fig. 3c). With regard to LWP, this relationship is poorly reproduced by global models, making it difficult to draw conclusions from this observation to know whether anthropogenic or mineral aerosols impact the hydrological cycle. Tests performed with a non-hydrostatic large eddy simulation (LES) model (Sandu et al., 2005) demonstrate that the diurnal evolution of the cloud LWP is very sensitive to the type and amount of aerosol particles in the boundary layer. The increase in cloud fraction with AOD could be related to the role of aerosols as CCN

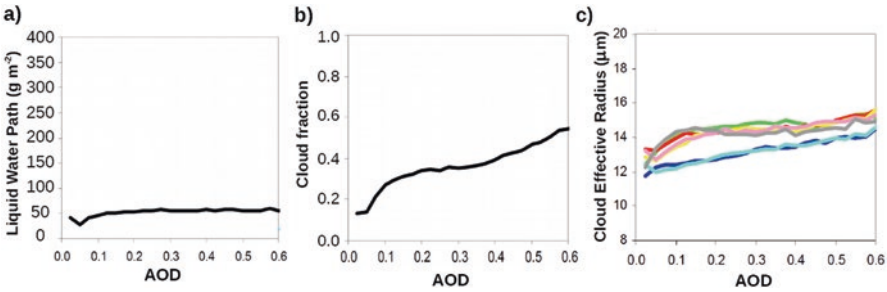

Fig. 3 (**a**) Liquid water path, (**b**) cloud fraction, and (**c**) cloud effective radius, as a function of the aerosol optical depth for the Mediterranean region. In (**a**) and (**b**), data are from the standard MODIS Terra product for the year 2001. Every line in (**c**) represents a different year from MODIS Aqua (2003 and 2004, in blue) or MODIS Terra (2000–2004). (Adapted from Figs. 5, 7 and 13 in Myhre et al., 2007)

but also to their effects on cloud lifetime which are very complex. Jiang et al. (2006) have explored this impact for shallow cumulus clouds by using models including size-resolved treatment of drop size distributions and warm microphysical processes and a variety of sounding representing marine trade cumulus and continental convective clouds. Contrary to expectation, it was shown that an increase in aerosol concentration from very clean to very polluted conditions does not increase cloud lifetime even though precipitation is suppressed. This could be due to competing effects between precipitation suppression and enhanced evaporation. For a Mediterranean sounding adapted from measurements in the central Mediterranean Sea, individual cloud lifetimes may even show a decrease in lifetime of 10–40% for polluted conditions. It is proposed that an enhanced evaporation tends to dominate in these shallow clouds. Absorption of incoming solar radiation by aerosols (like smoke and dust) can reduce cloud cover (Ramanathan et al., 2001; Kaufman et al., 2005). This effect can even be amplified if absorption of solar radiation by these aerosol particles occurs within cloud droplets (Chýlek et al., 1996). In fact, absorption of solar radiation, which is dependent on the chemical composition of the aerosol particles incorporated in cloud droplets, has a significant impact on the diurnal cycle of boundary layer clouds (Sandu et al., 2005).

With regard to the relationship between cloud droplet radius and AOD, the classical theory (Twomey, 1959) would imply a decrease in effective radius with the aerosol load, associated with an increase in cloud droplet number concentration. This is the basis of some parametrizations of the first indirect aerosol effect (e.g., Menon et al., 2002). At the global scale, this relationship between cloud droplet number concentration and AOD is observed in both satellite data (MODIS) and global models (Quaas et al., 2009). However, as mentioned previously, Myhre et al. (2007) found the opposite result with MODIS data over the Mediterranean.

This could be due to the observed decrease in cloud top pressure with AOD, given that cloud droplet radius increases with a decreasing cloud top pressure of convective clouds (Rosenfeld & Lensky, 1998). This specificity of the Mediterranean area needs to be confirmed in the future by more observations and modelling studies. Besides, Calmer et al. (2019) have recently highlighted the role of entrainment on cloud optical properties and cloud-aerosol interactions, and this variability in entrainment mixing also needs to be constrained in order to improve climate models.

3.4 Aerosol Impact on Precipitation

The impact on precipitation and hydrological cycle of the direct and semi-direct radiative effects has been studied by Nabat et al. (2015b). Using regional ocean-atmosphere coupled simulations, they concluded in a decrease of −0.2 mm yr^{-1} in precipitation over the Mediterranean due to the increase in atmospheric stability caused by aerosols. It represents a reduction of about 10% of the activity of the hydrological cycle, which is also noted in evaporation.

In addition to the reduction of precipitation caused by the reduced incoming solar radiative flux due to the direct aerosol effects, the sign and magnitude of the aerosol indirect forcing effect on precipitation is still controversial because of various processes competing with each other. Solomos et al. (2011) have carried out RAMS/ICLAMS simulations to deal with the effects of pollution on precipitation in clean and polluted environments in the eastern Mediterranean. The onset of precipitation in hazy clouds is shown to be delayed compared to cleaner conditions. In particular, hygroscopic dust particles contribute to more vigorous convection and more intense updrafts. In a case study, the simulated clouds extended about 3 kilometers higher, thus delaying the initiation of precipitation by one hour.

Using WRF simulations including an aerosol-aware microphysics scheme, Da Silva et al. (2018) have studied aerosol effects on summer precipitation in the Euro-Mediterranean area. They have found that increased aerosol loads lead to a reduction in precipitation, both with and without convection-permitting configurations. They propose a causal chain between aerosol effects on microphysics and their effects on precipitation (Fig. 4). These relationships involve the negative aerosol radiative forcing at the surface due to changes in cloud microphysics making clouds optically thicker (left part of the scheme), which increases atmospheric stability and thus reduces convection (right part of the scheme).

Global climate models (GCM) can also be used to identify the aerosol effects on precipitation, taking advantage from the higher number of available simulations despite coarser horizontal simulations. Tang et al. (2018) have compared the GCM responses of Mediterranean precipitation to greenhouse gases and aerosols. Both of them can indeed cause a drying of the Mediterranean, but they conclude that precipitation is more sensitive to black carbon forcing than to greenhouse gases and sulfate aerosol. Black carbon has the ability to strongly absorb solar radiation, thus

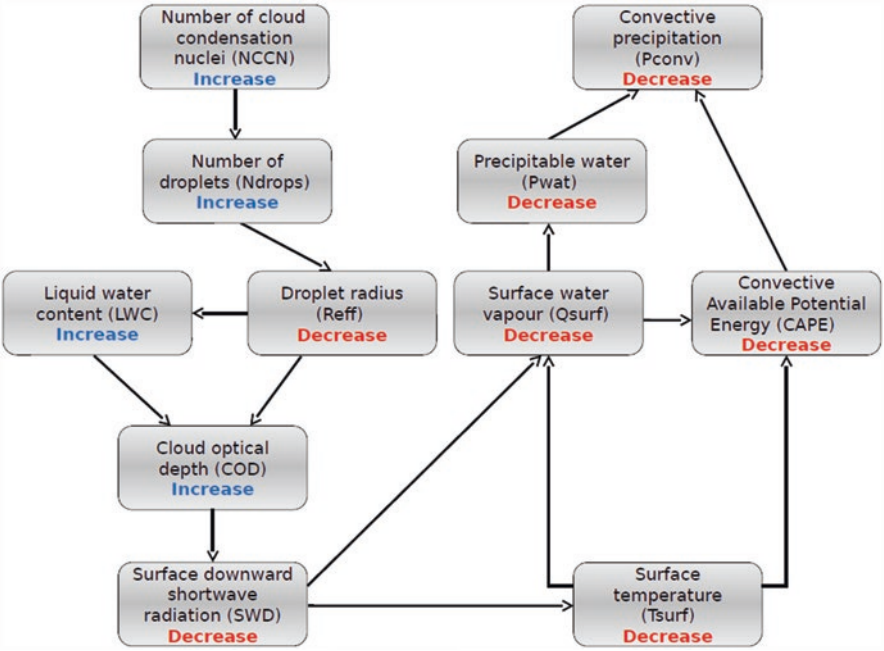

Fig. 4 Schematic summary of the proposed aerosol causal chain sequence for the indirect effect of aerosols on convective precipitation. (Reprinted from Da Silva et al., 2018)

heating the atmosphere locally. However, this is not the only mechanism that explains the impact of aerosols. An enhanced positive sea-level pressure pattern similar to the North Atlantic Oscillation-Arctic Oscillation has been shown because of black carbon particles, characterized by higher pressures over the Mediterranean and lower pressures at northern latitudes. Greenhouse gases can lead to similar pressure changes. Due to both factors, the northward diversion of the jet stream and storm tracks tend to decrease precipitation in the Mediterranean while increasing precipitation in northern Europe. Finally, the authors warn of a possible underestimation of the aerosol-cloud interactions in these GCMs because many of them did not fully include such processes.

3.5 Trends in Aerosol-Cloud Interactions

As described in the preceding chapter (Mallet et al., 2022), an increasing trend in surface solar radiation has been observed since 1980, which has been attributed to the decrease in anthropogenic aerosols over the same period reported by Nabat et al. (2014). This study also underlines that the role of clouds and of the indirect aerosol effect in this brightening seems to be negligible compared to the direct effect of aerosols at the scale of the Mediterranean area. However, weak trends in cloud cover and

other cloud parameters have been noted in the same period. Using the MERRA reanalysis, Kambezidis et al. (2016) have shown that the brightening over the Mediterranean during the last decades was mostly associated with decreasing trends in cloud optical depth (COD), especially for the low (<700 hPa) clouds and during the spring season. On a monthly basis, those low clouds contributed 58–87% to the total spatially averaged COD in the Mediterranean. This decreasing trend in cloudiness and cloud thickness over southern Europe and the Mediterranean is also supported by other studies. In this respect, the slight brightening observed over Europe by Hatzianastassiou et al. (2012) was associated with a decrease of 5–10% in cloud cover.

As for precipitation, a slight decrease of −0.56 mm per month per decade (−1.3%) has been noted during 2002–2014 by Floutsi et al. (2016), in consistence with the decrease of convection and low-level cloudiness observed by Kambezidis et al. (2016).

4 Conclusion and Recommendations

All these studies put forward the various and strong effects of natural and anthropogenic aerosols on the Mediterranean regional climate. In addition to the direct radiative effects, the interactions between clouds and aerosols also modify the radiative budget and regional climate over the Mediterranean. Absorbing aerosols such as dust and carbonaceous particles can modify cloud formation and atmospheric dynamics, which leads to semi-direct aerosol effects. Many aerosol types can also act as CCN and/or INP, with ensuing impacts on cloud cover, cloud lifetime, and precipitation. However, there remains large uncertainties about the role of aerosols in modifying cloud microphysics, cloud radiative properties, and precipitation. More research in terms of both field experiments, laboratory studies, and modeling efforts is clearly needed in order to better understand and quantify the effects of aerosol on clouds and the hydrological cycle and predict future evolution. Most of the results presented above, which rely on numerical simulations, must be taken with caution because of the uncertainties associated with the different parameterizations used in models. In order to better understand and quantify the microphysical impact of aerosols on clouds, and thus better predict climate change, it is critical to particularly seek information on aerosol-cloud interactions in observations (Seinfeld et al., 2016). For that, the Mediterranean region appears as an excellent natural laboratory for studying the interactions between clouds and aerosols because this region is affected by air masses from different sources containing anthropogenic pollution from Europe, marine aerosols from the sea, mineral dust particles from the Saharan desert, biomass burning from summertime forest fires, and biogenic material from various land and marine sources.

Representation of cloud microphysical processes in climate models is challenging because fundamental microphysical details are poorly understood. Although there are several parameterizations that correlate the aerosol concentration and the CCN and INP concentrations as a function of aerosol properties, too many unknowns exist in order to accurately predict the cloud droplet and ice crystal number

concentrations. To date, in situ observations of the latter in the different cloud regimes over the Mediterranean are lacking. Calls for observations of cloud droplet and ice crystal number concentrations in the different cloud regimes have already been expressed (Kanji et al., 2017; Grosvenor et al., 2018), specifically to provide a more complete assessment of the relationship between CCN or INP concentration and cloud droplet or ice crystal number concentrations. To accomplish this, the next generation of field experiments should focus on extended characterization of aerosol and enhanced cloud observations (e.g., mixed-phase and ice clouds developing in different air masses) by combined in situ and remote sensing observations. These observations would be very helpful to improve climate models over the Mediterranean and notably better understand the specificities of this region in terms of aerosol-cloud interactions described in this chapter.

Acknowledgements We would like to thank our late colleague Laurent Gomes who initiated the writing of this chapter in the early phase of the ChArMEx project. We are also grateful to François Dulac for his valuable comments on this chapter.

References

Abdelkader, M., Metzger, S., Mamouri, R. E., Astitha, M., Barrie, L., Levin, Z., & Lelieveld, J. (2015). Dust–air pollution dynamics over the eastern Mediterranean. *Atmospheric Chemistry and Physics, 15*, 9173–9189. https://doi.org/10.5194/acp-15-9173-2015

Ackerman, A. S., Toon, O. B., Taylor, J. P., Johnson, D. W., Hobbs, P. V., & Ferek, R. J. (2000). Effects of aerosols on cloud albedo: Evaluation of Twomey's parameterization of cloud susceptibility using measurements of ship tracks. *Journal of the Atmospheric Sciences, 57*, 2684–2695. https://doi.org/10.1175/1520-0469(2000)057<2684:EOAOCA>2.0.CO;2

Ackerman, A., Kirkpatrick, M., Stevens, D., & Toon, O. B. (2004). The impact of humidity above stratiform clouds on indirect aerosol climate forcing. *Nature, 432*, 1014–1017. https://doi.org/10.1038/nature03174

Albrecht, B. A. (1989). Aerosols, cloud microphysics, and fractional cloudiness. *Science, 245*, 1227–1230. https://doi.org/10.1126/science.245.4923.1227

Ayash, T., Gong, S., & Jia, C. Q. (2008). Direct and indirect shortwave radiative effects of sea salt aerosols. *Journal of Climate, 21*, 3207–3220. https://doi.org/10.1175/2007JCLI2063.1

Bangert, M., Nenes, A., Vogel, B., Vogel, H., Barahona, D., Karydis, V. A., Kumar, P., Kottmeier, C., & Blahak, U. (2012). Saharan dust event impacts on cloud formation and radiation over Western Europe. *Atmospheric Chemistry and Physics, 12*, 4045–4063. https://doi.org/10.5194/acp-12-4045-2012

Becagli, S. (2022). Aerosol composition and reactivity. In F. Dulac, S. Sauvage, & E. Hamonou (Eds.), *Atmospheric chemistry in the Mediterranean Region* (Vol. 2, From air pollutant sources to impacts). Springer, this volume. https://doi.org/10.1007/978-3-030-82385-6_13

Bègue, N., Tulet, P., Pelon, J., Aouizerats, B., Berger, A., & Schwarzenboeck, A. (2015). Aerosol processing and CCN formation of an intense Saharan dust plume during the EUCAARI 2008 campaign. *Atmospheric Chemistry and Physics, 15*, 3497–3516. https://doi.org/10.5194/acp-15-3497-2015

Bellouin, N., Rae, J., Jones, A., Johnson, C., Haywood, J., & Boucher, O. (2011). Aerosol forcing in the Climate Model Intercomparison Project (CMIP5) simulations by HadGEM2-ES and the role of ammonium nitrate. *Journal of Geophysical Research, 116*, D20206. https://doi.org/10.1029/2011JD016074

Boucher, O. (1995). GCM estimate of the indirect aerosol forcing using satellite-retrieved cloud droplet effective radii. *Journal of Climate, 8*, 1403–1409. https://doi.org/10.1175/1520-0442(1995)008<1403:GEOTIA>2.0.CO;2

Boucher, O., Randall, D., Artaxo, P., Bretherton, C., Feingold, G., Forster, P., Kerminen, V.-M., Kondo, Y., Liao, H., Lohmann, U., Rasch, P., Satheesh, S. K., Sherwood, S., Stevens, B., & Zhang, X. Y. (2013). Clouds and aerosols. In T. F. Stocker, D. Qin, G.-K. Plattner, M. Tignor, S. K. Allen, J. Boschung, A. Nauels, Y. Xia, V. Bex, & P. M. Midgley (Eds.), *Climate change 2013: The physical science basis. Contribution of Working Group I to the Fifth Assessment Report of the Intergovernmental Panel on Climate Change*, 571–657. Cambridge University Press. https://www.ipcc.ch/site/assets/uploads/2018/02/WG1AR5_all_final.pdf. Last access 21 July 2022.

Calmer, R., Roberts, G. C., Sanchez, K. J., Sciare, J., Sellegri, K., Picard, D., Vrekoussis, M., & Pikridas, M. (2019). Aerosol–cloud closure study on cloud optical properties using remotely piloted aircraft measurements during a BACCHUS field campaign in Cyprus. *Atmospheric Chemistry and Physics, 19*, 13989–14007. https://doi.org/10.5194/acp-19-13989-2019

Charlson, R. J., Schwartz, S. E., Hales, J. M., Cess, R. D., Coakley-Junior, J. A., Hansen, J. E., & Hofmann, D. J. (1992). Climate forcing by anthropogenic aerosols. *Science, 255*, 423–430. https://doi.org/10.1126/science.255.5043.423

Chin, M., Diehl, T., Dubovik, O., Eck, T. F., Holben, B. N., Sinyuk, A., & Streets, D. G. (2009). Light absorption by pollution, dust, and biomass burning aerosols: A global model study and evaluation with AERONET measurements. *Annales de Geophysique, 27*, 3439–3464. https://doi.org/10.5194/angeo-27-3439-2009

Chýlek, P., Lesins, G. B., Videen, G., Wong, J. G. D., Pinnick, R. G., Ngo, D., & Klett, J. D. (1996). Black carbon and absorption of solar radiation by clouds. *Journal of Geophysical Research, 101*, 23365–23371. https://doi.org/10.1029/96JD01901

Cooper, W. A., Bruintjes, R. T., & Mather, G. K. (1997). Calculations pertaining to hygroscopic seeding with flares. *Journal of Applied Meteorology, 36*, 1449–1469. https://doi.org/10.1175/1520-0450(1997)036<1449:CPTHSW>2.0.CO;2

Da Silva, N., Mailler, S., & Drobinski, P. (2018). Aerosol indirect effects on summer precipitation in a regional climate model for the Euro-Mediterranean region. *Annales de Geophysique, 36*, 321–335. https://doi.org/10.5194/angeo-36-321-2018

de Leeuw, G., Andreas, E. L., Anguelova, M. D., Fairall, C. W., Lewis, E. R., O'Dowd, C., Schulz, M., & Schwartz, S. E. (2011). Production flux of sea spray aerosol. *Reviews of Geophysics, 49*, RG2001. https://doi.org/10.1029/2010RG000349

DeMott, P. J., Sassen, K., Poellot, M. R., Baumgardner, D., Rogers, D. C., Brooks, S. D., Prenni, A. J., & Kreidenweis, S. M. (2003). African dust aerosols as atmospheric ice nuclei. *Geophysical Research Letters, 30*(14), 1732. https://doi.org/10.1029/2003GL017410

Denjean, C. (2022). Aerosol hygroscopicity. In F. Dulac, S. Sauvage, & E. Hamonou (Eds.), *Atmospheric chemistry in the Mediterranean Region* (Vol. 2, From air pollutant sources to impacts). Springer, this volume. https://doi.org/10.1007/978-3-030-82385-6_15

Drugé, T., Nabat, P., Mallet, M., & Somot, S. (2019). Model simulation of ammonium and nitrate aerosols distribution in the Euro-Mediterranean region and their radiative and climatic effects over 1979–2016. *Atmospheric Chemistry and Physics, 19*, 3707–3731. https://doi.org/10.5194/acp-19-3707-2019

Ekman, A. M. L., & Rodhe, H. (2003). Regional temperature response due to indirect sulfate aerosol forcing: Impact of model resolution. *Climate Dynamics, 21*, 1–10. https://doi.org/10.1007/s00382-003-0311-y

Fan, J., Rosenfeld, D., Zhang, Y., Giangrande, S. E., Li, Z., Machado, L. A., Martin, S. T., Yang, Y., Wang, J., Artaxo, P., & Barbosa, H. M. (2018). Substantial convection and precipitation enhancements by ultrafine aerosol particles. *Science, 359*, 411–418. https://doi.org/10.1126/science.aan8461

Flamant, C., Chaboureau, J.-P., Chazette, P., Di Girolamo, P., Bourrianne, T., Totems, J., & Cacciani, M. (2015). The radiative impact of desert dust on orographic rain in the Cévennes–Vivarais

area: A case study from HyMeX. *Atmospheric Chemistry and Physics, 15*, 12231–12249. https://doi.org/10.5194/acp-15-12231-2015

Floutsi, A. A., Korras-Carraca, M. B., Matsoukas, C., Hatzianastassiou, N., & Biskos, G. (2016). Climatology and trends of aerosol optical depth over the Mediterranean basin during the last 12 years (2002–2014) based on Collection 006 MODIS aqua data. *Science of the Total Environment, 551–552*, 292–303. https://doi.org/10.1016/j.scitotenv.2016.01.192

Forkel, R., Werhahn, J., Hansen, A. B., McKeen, S., Peckham, S., Grell, G., & Suppan, P. (2012). Effect of aerosol-radiation feedback on regional air quality – A case study with WRF/Chem. *Atmospheric Environment, 53*, 202–211. https://doi.org/10.1016/j.atmosenv.2011.10.009

Ghan, S. J. (2013). Technical note: Estimating aerosol effects on cloud radiative forcing. *Atmospheric Chemistry and Physics, 13*, 9971–9974. https://doi.org/10.5194/acp-13-9971-2013

Gkikas, A., Hatzianastassiou, N., Mihalopoulos, N., Katsoulis, V., Kazadzis, S., Pey, J., Querol, X., & Torres, O. (2013). The regime of intense desert dust episodes in the Mediterranean based on contemporary satellite observations and ground measurements. *Atmospheric Chemistry and Physics, 13*, 12135–12154. https://doi.org/10.5194/acp-13-12135-2013

Gkikas, A., Obiso, V., Pérez García-Pando, C., Jorba, O., Hatzianastassiou, N., Vendrell, L., Basart, S., Solomos, S., Gassó, S., & Baldasano, J. M. (2018). Direct radiative effects during intense Mediterranean desert dust outbreaks. *Atmospheric Chemistry and Physics, 18*, 8757–8787. https://doi.org/10.5194/acp-18-8757-2018

Gkikas, A., Giannaros, T. M., Kotroni, V., & Lagouvardos, K. (2019). Assessing the radiative impacts of an extreme desert dust outbreak and the potential improvements on short-term weather forecasts: The case of February 2015. *Atmospheric Research, 226*, 152–170. https://doi.org/10.1016/j.atmosres.2019.04.020

Grosch, M., & Georgii, H. W. (1976). Elemental composition of atmospheric aerosols and natural ice forming nuclei. *Journal de Recherches Atmospheriques, 10*, 227–232.

Grosvenor, D. P., Sourdeval, O., Zuidema, P., Ackerman, A., Alexandrov, M. D., Bennartz, R., Boers, R., Cairns, B., Christine Chiu, J., Christensen, M., Deneke, H., Diamond, M., Feingold, G., Fridlind, A., Hünerbein, A., Knist, C., Kollias, P., Marshak, A., McCoy, D., … Quaas, J. (2018). Remote sensing of droplet number concentration in warm clouds: A review of the current state of knowledge and perspectives. *Reviews of Geophysics, 56*, 409–453. https://doi.org/10.1029/2017RG000593

Hande, L. B., Engler, C., Hoose, C., & Tegen, I. (2015). Seasonal variability of Saharan desert dust and ice nucleating particles over Europe. *Atmospheric Chemistry and Physics, 15*, 4389–4397. https://doi.org/10.5194/acp-15-4389-2015

Hansen, J., Sato, M., & Ruedy, R. (1997). Radiative forcing and climate response. *Journal of Geophysical Research, 102*, 6831–6864. https://doi.org/10.1029/96JD03436

Hatzianastassiou, N., Papadimas, C. D., Matsoukas, C., Pavlakis, K., Fotiadi, A., Wild, M., & Vardavas, I. (2012). Recent regional surface solar radiation dimming and brightening patterns: Inter-hemispherical asymmetry and a dimming in the Southern Hemisphere. *Atmospheric Science Letters, 13*, 43–48. https://doi.org/10.1002/asl.361

Haywood, J., & Boucher, O. (2000). Estimates of the direct and indirect radiative forcing due to tropospheric aerosols: A review. *Reviews of Geophysics, 38*, 513–543. https://doi.org/10.1029/1999RG000078

Israelevich, P., Ganor, E., Alpert, P., Kishcha, P., & Stupp, A. (2012). Predominant transport paths of Saharan dust over the Mediterranean Sea to Europe. *Journal of Geophysical Research, 117*, D02205. https://doi.org/10.1029/2011JD016482

Jiang, H., Xue, H., Teller, A., Feingold, G., & Levin, Z. (2006). Aerosol effects on the lifetime of shallow cumulus. *Geophysical Research Letters, 33*, L14806. https://doi.org/10.1029/2006GL026024

Johnson, D. B. (1982). The role of giant and ultragiant aerosol particles in warm rain initiation. *Journal of the Atmospheric Sciences, 39*, 448–460. https://doi.org/10.1175/1520-0469(1982)039<0448:TROGAU>2.0.CO;2

Johnson, B. T., Shine, K. P., & Forster, P. M. (2004). The semi-direct aerosol effect: Impact of absorbing aerosols on marine stratocumulus. *Quarterly Journal of the Royal Meteorological Society, 130*, 1407–1422. https://doi.org/10.1256/qj.03.61

Kallos, G., Nenes, A., Patlakas, P., Drakaki, E., Koukoula, M., Rosenfeld, D., & Mihalopoulos, N. (2016). Aerosols in the Mediterranean region and their role in cloud formation. In C. Mensink & G. Kallos (Eds.), *Air pollution modeling and its application XXV, ITM 2016* (pp. 551–557). Springer. https://doi.org/10.1007/978-3-319-57645-9_86

Kambezidis, H. D., Psiloglou, B. E., Karagiannis, D., Dumka, U. C., & Kaskaoutis, D. G. (2016). Recent improvements of the Meteorological Radiation Model for solar irradiance estimates under all-sky conditions. *Renewable Energy, 93*, 142–158. https://doi.org/10.1016/j.jastp.2016.10.006

Kanji, Z. A., Ladino, L. A., Wex, H., Boose, Y., Burkert-Kohn, M., Cziczo, D. J., & Krämer, M. (2017). Overview of ice nucleating particles. *Meteorological Monographs, 58*, 1.1–1.33. https://doi.org/10.1175/AMSMONOGRAPHS-D-16-0006.1

Kaufman, Y. J., & Fraser, R. S. (1997). The effect of smoke particles on clouds and climate forcing. *Science, 277*, 1636–1639. https://doi.org/10.1126/science.277.5332.1636

Kaufman, Y. J., Boucher, O., Tanré, D., Chin, M., Remer, L. A., & Takemura, T. (2005). Aerosol anthropogenic component estimated from satellite data. *Geophysical Research Letters, 32*, L17804. https://doi.org/10.1029/2005GL023125

Koren, I., Kaufman, Y. J., Remer, L. A., & Martins, J. V. (2004). Measurement of the effect of Amazon smoke on inhibition of cloud formation. *Science, 303*(5662), 1342–1345. https://doi.org/10.1126/science.1089424

Koren, I., Altaratz, O., Remer, L., Feingold, G., Martins, J. V., & Heiblum, R. H. (2012). Aerosol-induced intensification of rain from the tropics to the mid-latitudes. *Nature Geoscience, 5*, 118–122. https://doi.org/10.1038/ngeo1364

Korhonen, H., Carslaw, K. S., Spracklen, D. V., Mann, G. W., & Woodhouse, M. T. (2008). Influence of oceanic dimethyl sulfide emissions on cloud condensation nuclei concentrations and seasonality over the remote Southern Hemisphere oceans: A global model study. *Journal of Geophysical Research, 113*, D15204. https://doi.org/10.1029/2007JD009718

Kumar, P., Sokolik, I. N., & Nenes, A. (2011). Measurements of cloud condensation nuclei activity and droplet activation kinetics of fresh unprocessed regional dust samples and minerals. *Atmospheric Chemistry and Physics, 11*, 3527–3541. https://doi.org/10.5194/acp-11-3527-2011

Le Treut, H., Forichon, M., Boucher, O., & Li, Z.-X. (1998). Sulfate aerosol indirect effect and CO_2 greenhouse forcing: Equilibrium response of the LMD GCM and associated cloud feedbacks. *Journal of Climate, 11*, 1673–1684. https://doi.org/10.1175/1520-0442(1998)011<1673:SAIEAC>2.0.CO;2

Lelieveld, J., Berresheim, H., Borrmann, S., Crutzen, P. J., Dentener, F. J., Fischer, H., Feichter, J., Flatau, P. J., Heland, J., Holzinger, R., Korrmann, R., Lawrence, M. G., Levin, Z., Markowicz, K. M., Mihalopoulos, N., Minikin, A., Ramanathan, V., de Reus, M., Roelofs, G. J., … Ziereis, H. (2002). Global air pollution crossroads over the Mediterranean. *Science, 298*, 794–799. https://doi.org/10.1126/science.1075457

Levin, Z., Ganor, E., & Gladstein, V. (1996). The effects of desert particles coated with sulfate on rain formation in the eastern Mediterranean. *Journal of Applied Meteorology, 35*, 1511–1523. https://doi.org/10.1175/1520-0450(1996)035<1511:TEODPC>2.0.CO;2

Levin, Z., Teller, A., Ganor, E., & Yin, Y. (2005). On the interactions of mineral dust, sea-salt particles, and clouds: A measurement and modeling study from the Mediterranean Israeli Dust Experiment campaign. *Journal of Geophysical Research, 110*, D20202. https://doi.org/10.1029/2005JD005810

Li, J., Ma, X., von Salzen, K., & Dobbie, S. (2008). Parameterization of sea-salt optical properties and physics of the associated radiative forcing. *Atmospheric Chemistry and Physics, 8*, 4787–4798. https://doi.org/10.5194/acp-8-4787-2008

Lohmann, U., & Feichter, J. (2005). Global indirect aerosol effects: A review. *Atmospheric Chemistry and Physics, 5*, 715–737. https://doi.org/10.5194/acp-5-715-2005

Lundgren, K., Vogel, B., Vogel, H., & Kottmeier, C. (2013). Direct radiative effects of sea salt for the Mediterranean region under conditions of low to moderate wind speeds. *Journal of Geophysical Research – Atmospheres, 118*, 1906–1923. https://doi.org/10.1029/2012JD018629

Ma, X., von Salzen, K., & Li, J. (2008). Modelling sea salt aerosol and its direct and indirect effects on climate. *Atmospheric Chemistry and Physics, 8*, 1311–1327. https://doi.org/10.5194/acp-8-1311-2008

Mahowald, N. M., & Kiehl, L. M. (2003). Mineral aerosol and cloud interactions. *Geophysical Research Letters, 30*, 1475. https://doi.org/10.1029/2002GL016762

Mallet, M., di Sarra, A., Nabat, P., Solmon, F., Gutierrez, C., Mailler, S., Menut, L., Kaskaoukis, D., Rowlinson, M., & Rap, A. (2022). Tropospheric aerosol and ozone direct radiative forcing. In F. Dulac, S. Sauvage, & E. Hamonou (Eds.), *Atmospheric chemistry in the Mediterranean Region* (Vol. 2, From air pollutant sources to impacts). Springer, this volume. https://doi.org/10.1007/978-3-030-82385-6_19

Meier, J., Tegen, I., Heinold, B., & Wolke, R. (2012). Direct and semi-direct radiative effects of absorbing aerosols in Europe: Results from a regional model. *Geophysical Research Letters, 39*, L09802. https://doi.org/10.1029/2012GL050994

Menon, S., Genio, A. D., Koch, D., & Tselioudis, G. (2002). GCM simulations of the aerosol indirect effect: Sensitivity to cloud parameterization and aerosol burden. *Journal of the Atmospheric Sciences, 59*, 692–713. https://doi.org/10.1175/1520-0469(2002)059<0692:GSOTAI>2.0.CO;2

Michoud, V. (2022). Particle-gas multiphasic reactions. In F. Dulac, S. Sauvage, & E. Hamonou (Eds.), *Atmospheric chemistry in the Mediterranean Region* (Vol. 2, From air pollutant sources to impacts). Springer, this volume. https://doi.org/10.1007/978-3-030-82385-6_11

Moulin, C., Lambert, C. E., Dayan, U., Masson, V., Ramonet, M., Bousquet, P., Legrand, M., Balkanski, Y. J., Guelle, W., Marticorena, B., Bergametti, G., & Dulac, F. (1998). Satellite climatology of African dust transport in the Mediterranean atmosphere. *Journal of Geophysical Research, 103*, 13137–13144. https://doi.org/10.1029/98JD00171

Myhre, G., & Samset, B. H. (2015). Standard climate models radiation codes underestimate black carbon radiative forcing. *Atmospheric Chemistry and Physics, 15*, 2883–2888. https://doi.org/10.5194/acp-15-2883-2015

Myhre, G., Stordal, F., Johnsrud, M., Kaufman, Y. J., Rosenfeld, D., Storelvmo, T., Kristjansson, J. E., Berntsen, T. K., Myhre, A., & Isaksen, I. S. A. (2007). Aerosol-cloud interaction inferred from MODIS satellite data and global aerosol models. *Atmospheric Chemistry and Physics, 7*, 3081–3101. https://doi.org/10.5194/acp-7-3081-2007

Myhre, G., Samset, B. H., Schulz, M., Balkanski, Y., Bauer, S., Berntsen, T. K., Bian, H., Bellouin, N., Chin, M., Diehl, T., Easter, R. C., Feichter, J., Ghan, S. J., Hauglustaine, D., Iversen, T., Kinne, S., Kirkevåg, A., Lamarque, J.-F., Lin, G., … Zhou, C. (2013). Radiative forcing of the direct aerosol effect from AeroCom Phase II simulations. *Atmospheric Chemistry and Physics, 13*, 1853–1877. https://doi.org/10.5194/acp-13-1853-2013

Nabat, P., Solmon, F., Mallet, M., Kok, J. F., & Somot, S. (2012). Dust emission size distribution impact on aerosol budget and radiative forcing over the Mediterranean region: A regional climate model approach. *Atmospheric Chemistry and Physics, 12*, 10545–10567. https://doi.org/10.5194/acp-12-10545-2012

Nabat, P., Somot, S., Mallet, M., Sanchez-Lorenzo, A., & Wild, M. (2014). Contribution of anthropogenic sulfate aerosols to the changing Euro-Mediterranean climate since 1980. *Geophysical Research Letters, 41*, 5605–5611. https://doi.org/10.1002/2014GL060798

Nabat, P., Somot, S., Mallet, M., Sevault, F., Chiacchio, M., & Wild, M. (2015a). Direct and semi-direct aerosol radiative effect on the Mediterranean climate variability using a coupled regional climate system model. *Climate Dynamics, 44*, 1127–1155. https://doi.org/10.1007/s00382-014-2205-6

Nabat, P., Somot, S., Mallet, M., Michou, M., Sevault, F., Driouech, F., Meloni, D., Di Sarra, A., Di Biagio, C., Formenti, P., Sicard, M., Léon, J.-F., & Bouin, M.-N. (2015b). Dust aerosol radiative effects during summer 2012 simulated with a coupled regional aerosol-atmosphere-ocean

model over the Mediterranean region. *Atmospheric Chemistry and Physics, 15*, 3303–3326. https://doi.org/10.5194/acp-15-3303-2015

O'Dowd, C. D., Lowe, J. A., Smith, M. H., & Kaye, A. D. (1999). The relative importance of non-sea-salt sulphate and sea-salt aerosol to the marine cloud condensation nuclei population: An improved multi-component aerosol-cloud droplet parametrization. *Quarterly Journal of the Royal Meteorological Society, 125*, 1295–1313. https://doi.org/10.1002/qj.1999.49712555610

Papadimas, C. D., Hatzianastassiou, N., Matsoukas, C., Kanakidou, M., Mihalopoulos, N., & Vardavas, L. (2012). The direct effect of aerosols on solar radiation over the broader Mediterranean basin. *Atmospheric Chemistry and Physics, 12*, 7165–7185. https://doi.org/10.5194/acp-12-7165-2012

Partanen, A.-I., Dunne, E. M., Bergman, T., Laakso, A., Kokkola, H., Ovadnevaite, J., Sogacheva, L., Baisnée, D., Sciare, J., Manders, A., O'Dowd, C., de Leeuw, G., & Korhonen, H. (2014). Global modelling of direct and indirect effects of sea spray aerosol using a source function encapsulating wave state. *Atmospheric Chemistry and Physics, 14*, 11731–11752. https://doi.org/10.5194/acp-14-11731-2014

Penner, J. E., Zhang, S. Y., & Chuang, C. C. (2003). Soot and smoke aerosol may not warm climate. *Journal of Geophysical Research, 108*(D21), 4657. https://doi.org/10.1029/2003JD003409

Pierce, J. R., & Adams, P. J. (2006). Global evaluation of CCN formation by direct emission of sea salt and growth of ultrafine sea salt. *Journal of Geophysical Research, 111*, D06203. https://doi.org/10.1029/2005JD006186

Pincus, R., & Baker, M. B. (1994). Effect of precipitation on the albedo susceptibility of clouds in the marine boundary layer. *Nature, 372*, 250–252. https://doi.org/10.1038/372250a0

Pruppacher, H. R., & Klett, J. D. (1980). *Microphysics of clouds and precipitation*. Kluwer.

Quaas, J., Boucher, O., Bellouin, N., & Kinne, S. (2008). Satellite-based estimate of the direct and indirect aerosol climate forcing. *Journal of Geophysical Research, 113*, D05204. https://doi.org/10.1029/2007JD008962

Quaas, J., Ming, Y., Menon, S., Takemura, T., Wang, M., Penner, J. E., Gettelman, A., Lohmann, U., Bellouin, N., Boucher, O., Sayer, A. M., Thomas, G. E., McComiskey, A., Feingold, G., Hoose, C., Kristjánsson, J. E., Liu, X., Balkanski, Y., Donner, L. J., … Schulz, M. (2009). Aerosol indirect effects – general circulation model intercomparison and evaluation with satellite data. *Atmospheric Chemistry and Physics, 9*, 8697–8717. https://doi.org/10.5194/acp-9-8697-2009

Ramanathan, V., Crutzen, P. J., Kiehl, J. T., & Rosenfeld, D. (2001). Aerosols, climate, and the hydrological cycle. *Science, 294*, 2119–2124. https://doi.org/10.1126/science.1064034

Ramanathan, V., Ramana, M., Roberts, G., Kim, D., Corrigan, C., Chung, C., & Winker, D. (2007). Warming trends in Asia amplified by brown cloud solar absorption. *Nature, 448*, 575–578. https://doi.org/10.1038/nature06019

Reddy, M. S., Boucher, O., Balkanski, Y., & Schulz, M. (2005). Aerosol optical depths and direct radiative perturbations by species and source type. *Geophysical Research Letters, 32*, L12803. https://doi.org/10.1029/2004GL021743

Roberts, G. C., Nenes, A., Seinfeld, J. H., & Andreae, M. O. (2003). Impact of biomass burning on cloud properties in the Amazon Basin. *Journal of Geophysical Research, 108*, 4062. https://doi.org/10.1029/2001JD000985

Rosenfeld, D., & Lensky, I. M. (1998). Satellite-based insights into precipitation formation processes in continental and maritime convective clouds. *Bulletin of the American Meteorological Society, 79*, 2457–2476. https://doi.org/10.1175/1520-0477(1998)079<2457:SBIIPF>2.0.CO;2

Rosenfeld, D., Rudich, Y., & Lahav, R. (2001). Desert dust suppressing precipitation: A possible desertification feedback loop. *Proceedings of the National Academy of Sciences of the United States of America, 98*, 5975–5980. https://doi.org/10.1073/pnas.101122798

Rosenfeld, D., Lohmann, U., Raga, G. B., O'Dowd, C. D., Kul-mala, M., Fuzzi, S., Reissell, A., & Andreae, M. O. (2008). Flood or drought: How do aerosols affect precipitation? *Science, 312*, 1309–1313. https://doi.org/10.1126/science.1160606

Ruckstuhl, C., Norris, J. R., & Philipona, R. (2010). Is there evidence for an aerosol indirect effect during the recent aerosol optical depth decline in Europe? *Journal of Geophysical Research, 115*, D04204. https://doi.org/10.1029/2009JD012867

Sandu, I., Tulet, P., & Brenguier, J.-L. (2005). Parameterization of the cloud droplet single scattering albedo based on aerosol chemical composition for LES modelling of boundary layer clouds. *Geophysical Research Letters, 32*, L19814. https://doi.org/10.1029/2005GL023994

Santese, M., Perrone, M. R., Zakey, A. S., De Tomasi, F., & Giorgi, F. (2010). Modeling of Saharan dust outbreaks over the Mediterranean by RegCM3: Case studies. *Atmospheric Chemistry and Physics, 10*, 133–156. https://doi.org/10.5194/acp-10-133-2010

Scott, C. E., Rap, A., Spracklen, D. V., Forster, P. M., Carslaw, K. S., Mann, G. W., Pringle, K. J., Kivekäs, N., Kulmala, M., Lihavainen, H., & Tunved, P. (2014). The direct and indirect radiative effects of biogenic secondary organic aerosol. *Atmospheric Chemistry and Physics, 14*, 447–470. https://doi.org/10.5194/acp-14-447-2014

Seinfeld, J. H., Bretherton, C., Carslaw, K. S., Coe, H., DeMott, P. J., Dunlea, E. J., Feingold, G., Ghan, S., Guenther, A. B., Kahn, R., & Kraucunas, I. (2016). Improving our fundamental understanding of the role of aerosol-cloud interactions in the climate system. *Proceedings of the National Academy of Sciences of the United States of America, 113*, 5781–5790. https://doi.org/10.1073/pnas.1514043113

Smith, C. J., Kramer, R. J., Myhre, G., Alterskjær, K., Collins, W., Sima, A., Boucher, O., Dufresne, J.-L., Nabat, P., Michou, M., Yukimoto, S., Cole, J., Paynter, D., Shiogama, H., O'Connor, F. M., Robertson, E., Wiltshire, A., Andrews, T., Hannay, C., Miller, R., Nazarenko, L., Kirkevåg, A., Olivié, D., Fiedler, S., Pincus, R., & Forster, P. M. (2020). Effective radiative forcing and adjustments in CMIP6 models. *Atmospheric Chemistry and Physics. 20*, 9591–9618. https://doi.org/10.5194/acp-20-9591-2020

Solomos, S., Kallos, G., Kushta, J., Astitha, M., Tremback, C., Nenes, A., & Levin, Z. (2011). An integrated modeling study on the effects of mineral dust and sea salt particles on clouds and precipitation. *Atmospheric Chemistry and Physics, 11*, 873–892. https://doi.org/10.5194/acp-11-873-2011

Spyrou, C., Kallos, G., Mitsakou, C., Athanasiadis, P., Kalogeri, C., & Iacono, M. (2013). Modeling the radiative effects of desert dust on weather and regional climate. *Atmospheric Chemistry and Physics, 13*, 5489–5504. https://doi.org/10.5194/acp-13-5489-2013

Stevens, B., & Feingold, G. (2009). Untangling aerosol effects on clouds and precipitation in a buffered system. *Nature, 461*, 607–613. https://doi.org/10.1038/nature08281

Tang, T., Shindell, D., Samset, B. H., Boucher, O., Forster, P. M., Hodnebrog, Ø., Myhre, G., Sillmann, J., Voulgarakis, A., Andrews, T., Faluvegi, G., Fläschner, D., Iversen, T., Kasoar, M., Kharin, V., Kirkevåg, A., Lamarque, J.-F., Olivié, D., Richardson, T., … Takemura, T. (2018). Dynamical response of Mediterranean precipitation to greenhouse gases and aerosols. *Atmospheric Chemistry and Physics, 18*, 8439–8452. https://doi.org/10.5194/acp-18-8439-2018

Teller, A., & Levin, Z. (2006). The effects of aerosols on precipitation and dimensions of subtropical clouds: A sensitivity study using a numerical cloud model. *Atmospheric Chemistry and Physics, 6*, 67–80. https://doi.org/10.5194/acp-6-67-2006

Twomey, S. (1959). The nuclei of natural cloud formation part II: The supersaturation in natural clouds and the variation of cloud droplet concentration. *Geofisica Pura e Applicata, 43*, 243–249. https://doi.org/10.1007/BF01993560

Wilcox, E. M. (2010). Stratocumulus cloud thickening beneath layers of absorbing smoke aerosol. *Atmospheric Chemistry and Physics, 10*, 11769–11777. https://doi.org/10.5194/acp-10-11769-2010

Wurzler, S., Reisin, T. G., & Levin, Z. (2000). Modification of mineral dust particles by cloud processing and subsequent effects on drop size distributions. *Journal of Geophysical Research, 105*, 4501–4512. https://doi.org/10.1029/1999JD900980

Yin, Y., Levin, Z., Reisin, T., & Tzivion, S. (2000). Seeding convective clouds with hygroscopic flares: Numerical simulations using a cloud model with detailed microphysics. *Journal of*

Applied Meteorology, 39, 1460–1472. https://doi.org/10.1175/1520-0450(2000)039<1460:SCCWHF>2.0.CO;2

Yin, Y., Wurzler, S., Levin, Z., & Reisin, T. G. (2002). Interactions of mineral dust particles and clouds: Effects on precipitation and cloud optical properties. *Journal of Geophysical Research, 107*, 4724. https://doi.org/10.1029/2001JD001544

Zakey, A. S., Giorgi, F., & Bi, X. (2008). Modeling of sea salt in a regional climate model: Fluxes and radiative forcing. *Journal of Geophysical Research, 113*, D14221. https://doi.org/10.1029/2007JD009209

Zanis, P. (2009). A study on the direct effect of anthropogenic aerosols on near surface air temperature over Southeastern Europe during summer 2000 based on regional climate modeling. *Annales de Geophysique, 27*, 3977–3988. https://doi.org/10.5194/angeo-27-3977-2009

Zanis, P., Ntogras, C., Zakey, A., Pytharoulis, I., & Karacostas, T. (2012). Regional climate feedback of anthropogenic aerosols over Europe using RegCM3. *Climate Research, 52*, 267–278. https://doi.org/10.3354/cr01070

Aerosol Impacts on Atmospheric and Precipitation Chemistry

Maria Kanakidou, Stelios Myriokefalitakis, Vassileios C. Papadimitriou, and Athanasios Nenes

Contents

Abstract This chapter summarizes current knowledge on the impact of aerosols on atmospheric chemistry and composition combining recent chamber, field, and modeling results focusing on the Mediterranean region. Particularly, the chapter addresses issues related to heterogeneous reactions on aerosol surfaces, attenuation

Chapter reviewed by ***Frank J. Dentener*** *(Joint Research Centre (JRS), European Commission,Ispra (VA), Italy), as part of the book Part IX Impacts of Air Pollution on Precipitation Chemistry and Climate also reviewed by* ***Lucia Mona*** *(CNR/IMAA, Tito Scalo (PZ), Italy)*

M. Kanakidou (✉)
Environmental Chemical Processes Laboratory (ECPL), Department of Chemistry, University of Crete, Heraklion, Greece
e-mail: mariak@uoc.gr

S. Myriokefalitakis
Institute for Environmental Research and Sustainable Development, National Observatory of Athens (NOA/IERSD), Lofos Koufou, Greece

V. C. Papadimitriou
Laboratory of Photochemistry and Chemical Kinetics, Department of Chemistry, University of Crete, Heraklion, Greece

A. Nenes
School of Architecture, Civil and Environmental Engineering, Ecole Polytechnique Fédérale de Lausanne, Lausanne, Switzerland

Institute for Chemical Engineering Sciences, Foundation for Research and Technology Hellas, Patras, Greece

F. Dulac et al. (eds.), *Atmospheric Chemistry in the Mediterranean Region*,
https://doi.org/10.1007/978-3-030-82385-6_21

of solar radiation and its effect on key atmospheric species, and aerosol formation from gaseous precursors. Finally, the effects of strong acidity on the composition and amounts of semi-volatile aerosol and the concentration of trace nutrients and toxic soluble metals are discussed.

1 Introduction

The Mediterranean region is affected by large amounts of aerosols of various origins (see Kaskaoutis et al., 2023). In particular, desert dust, biomass burning aerosol, and anthropogenic aerosols can be found in large quantities depending on season and location. Dust aerosol, mainly originating from the African continent, is abundant in the Mediterranean atmosphere and readily mixes with air masses containing aerosol and gas pollutants (Kanakidou et al., 2011). This mixture of natural and anthropogenic trace compounds fundamentally changes dust aerosol properties (chemical, physical, optical), as well as oxidant levels. The large amounts of dust aerosol present in the Mediterranean atmosphere (as well as globally) have motivated several laboratory and field studies to investigate the role of dust as a reactive substrate (see Becagli, 2022). The quantitative understanding of these heterogeneous chemical reactions has readily been integrated in numerical modelling for dust impact assessments. Furthermore, all types of atmospheric aerosols affect atmospheric composition by attenuation of solar radiation that is driving central photo dissociation reactions for atmospheric chemistry (see Mallet et al., 2022). They also act as substrates for reactions that modify the composition of both the gas and the aerosol phases in the atmosphere through multiphase reactions (Kanakidou et al., 2018). Multiphase reactions also depend on atmospheric acidity and liquid water content, modify the solubility of nutrients or toxic components, and are present in the aerosols with impacts on human health (see Kalivitis et al., 2022) and ecosystems through their deposition to surfaces (see Guieu and Ridame, 2022; Kanakidou et al., 2022). In turn, these reactions and aerosol components affect atmospheric acidity in all media of the atmosphere (gaseous acidic compounds, aerosol water, cloud water, precipitation) and precipitation chemistry (Pye et al., 2020).

Atmospheric aerosol particles constitute an important and reactive medium, which strongly interacts with the gas and aqueous phases in the atmosphere. These interactions, besides their effect on aerosol composition and physical and optical properties, have been also shown to affect levels of other atmospheric constituents, such as nitrogen oxides (NO_x), ozone (O_3), nitric acid (HNO_3), and sulfate (SO_4^{2-}) (e.g., Dentener & Crutzen, 1993; Dentener et al., 1996; Liao et al., 2003; Bauer et al., 2004; Zhu et al., 2010, 2011; Tang et al., 2017; Wang et al., 2019). Thus, they have an effect on climate via altering anthropogenic aerosols and ozone radiative forcing (e.g., Liao & Seinfeld, 2005). For instance, Dentener et al. (1996) estimated that heterogeneous reactions on dust aerosol can reduce O_3 levels up to 10% in the vicinity of dust source regions. They also suggested that neglecting sulfate presence in the coarse mode aerosol, where sulfate could be formed via heterogeneous

oxidation of SO_2 on aerosol surfaces, leads to an overestimate of the negative radiative forcing of sulfate, in particular over Asia. In line with these results, Liao and Seinfeld (2005) estimated that reactions of NO_x and hydrogen peroxy radicals (HO_2·) radicals on dust aerosol affect tropospheric O_3 levels and reduce the top-of-the-atmosphere present-day anthropogenic radiative forcing of O_3 by 20–45% at mid to high latitudes in the northern Hemisphere.

Because of the potential importance of atmospheric aerosols for atmospheric and precipitation chemistry, a number of laboratory studies have investigated heterogeneous reactions on various aerosols. The majority of them have been focused on mineral dust and sea salt, which are the most abundantly emitted aerosols into the atmosphere. Particularly, the uptake of oxidants O_3, hydroxyl radical (OH), and nitrate radical (NO_3) as well as other directly related species such as HO_2, hydrogen peroxide (H_2O_2), formaldehyde (HCHO), nitrous acid (HONO), and dinitrogen pentoxide (N_2O_5) on mineral dust particles has been extensively studied and quantitatively determined, being also the subject of several reviews (e.g., Rossi, 2003; Usher et al., 2003; Crowley et al., 2010; George et al., 2015). In addition, it is well known that acid displacement reactions occurring on sea-salt aerosol surface lead to halogens release, via hydrochloric acid (HCl) substitution by a stronger and/or less volatile acid, i.e., sulfuric acid (H_2SO_4) and HNO_3. In the same line, N_2O_5 reactions on Cl-enriched sulfate aerosols result in 10–15 times higher chlorine nitrite ($ClNO_2$) release (Pechtl & von Glasow, 2007; von Glasow, 2008). Such reactions lead to a measurable deficit in halogen in the aerosol phase compared to the seawater composition that provides evidence of their occurrence (Kouvarakis et al., 2002). Acid displacement reactions on dust aerosols release carbon dioxide (CO_2) when H_2SO_4, HNO_3, HCl, or organic acids attack calcium carbonate ($CaCO_3$) and attach sulfate and nitrate on dust aerosol (e.g., Ragosti & Sarin, 2005; Drozd et al., 2014). In the case of sulfate, the displacement reactions (Fig. 1) attach sulfate to the coarse mode aerosol, where most of the dust and sea-salt mass is present, weakening the radiative forcing efficiency of sulfate aerosol (Dentener et al., 1996).

Furthermore, due to their low water content, aerosols are characterized by extremely high ionic strengths and unusually strong and persistent acidity (e.g., Weber et al., 2016; Guo et al., 2018) although there are many regions of the globe – especially near strong sea-salt, dust, or ammonia sources – where the acidity is much lower and pH is higher (see Pye et al., 2020 for a review). Therefore, combined with the effects of acidity, the aerosol water is a suitable medium for acidity-sensitive gas-particle partitioning (Seinfeld & Pandis, 2016; Guo et al., 2018; Nenes et al., 2020, 2021) and multiphase reactions (Herrmann et al., 2015; Carlton et al., 2007; Lim et al., 2010; Myriokefalitakis et al., 2011; Kanakidou et al., 2018). A typical example is SO_2 partitioning into water aerosol that is favored in a basic aqueous environment. The subsequent O_3-induced oxidation of SO_3^{2-} (second dissociation product of hydrated SO_2) in the aqueous phase is more efficient at higher pH values (Seinfeld & Pandis, 2016). On the opposite, the reactive uptake of peroxides is acid-catalyzed. Organics can also be involved in pH-driven reactions like esterification of carboxylic acids, aldol condensation, and hemiacetal and acetal formation, resulting in a significant formation of secondary organic aerosol, in aerosol water

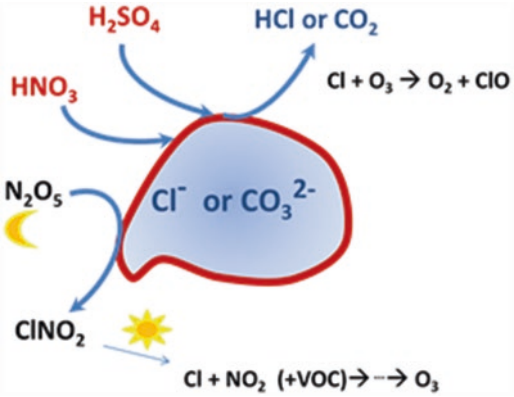

Fig. 1 Acid displacement reaction will partition H_2SO_4 as SO_4^{2-} and HNO_3 as nitrate ion (NO_3^-) to the aerosol phase and will release halogen or CO_2, from sea-salt (Cl^-) and dust (CO_3^{2-}) aerosol, respectively. During night in polluted regions, the N_2O_5 reactions with sea-salt halogens will release $ClNO_2$ into the atmosphere that can be photolyzed during the day to produce halogen and NO_2, which will ultimately produce O_3 in the presence of volatile organic compounds (VOC). On the opposite, the halogen released during the day can lead to O_3 depletion in remote marine environments

(Hermann et al., 2015; Xu et al., 2015, 2016; Budisulistiorini et al., 2017; Pye et al., 2020).

In this chapter, we summarize recent findings with regard to aerosols impacts on atmospheric chemistry, acidity, and precipitation chemistry in the Mediterranean region, as well as global modeling studies when these provide additional insights into the topic.

2 Aerosol Impacts on Tropospheric Chemistry

Aerosols impact on tropospheric chemistry through two different mechanisms: alteration of photolysis rates (by extinction of light by particles; see also the chapter by Mallet et al., 2022) and multiphase reactions (where aerosols act as a substrate for chemical reactions and sink for trace gases of importance for tropospheric chemistry; see also the chapter by Becagli, 2022).

2.1 Impact of Aerosols on Oxidants Through Interactions with Light

Aerosol particle interactions with solar radiation via absorption or scattering lead to a solar flux attenuation that is significant enough to affect the photodissociation efficiency of chemically important atmospheric trace constituents. It has been

demonstrated that the presence of clouds leads to changes in the O_3 and NO_2 photolysis rates (JO, JNO_2). Depending on location and cloud optical thickness, they can either be higher (mainly above clouds) or lower (below clouds) (Landgraf & Crutzen, 1998; Tang et al., 2004), as observed in several occasions in the Mediterranean (e.g., Berresheim et al., 2003; Gerasopoulos et al., 2012). The impact of aerosols on the photolysis rates is a complex phenomenon because most aerosols vary on long enough timescales that make it difficult to unravel their effect, contrary to the cloud cover, which can change much faster and thus has a noticeable impact on actinic fluxes. Therefore, statistical analysis and modelling is required along with field observations to attribute changes in the photolysis rates to the effect of aerosols (Gerasopoulos et al., 2012; Mailler et al., 2016). Increase in the atmospheric aerosol leads to a reduction in near-surface O_3 and NO_2 photolysis rates. However, likewise clouds, the effect of scattering aerosols on the photolysis rates can be positive or negative depending on the location of the aerosol layers in the atmosphere. These changes affect both the chemical loss (through O_3 photolysis) and production (through NO_2 photolysis) of O_3, respectively.

On a global scale, the modeling study by Liao et al. (2003) employing online coupling between gas and aerosol chemistry and accounting for heterogeneous reactions and impact of aerosols on photolysis rates has shown that both gases and aerosols levels have a nonlinear response to changes in emissions of aerosol precursors. This study also showed that photolysis rates decrease due to solar radiation attenuation by aerosols has a small effect on O_3 concentrations (<1 ppbv) corresponding to 2–3% change. The effect maximizes over central Africa, India, and central and northeast Asia, where although HNO_3 reduction is the highest, it is still very small in relative scale (<3%). In particular, the reduction of photolysis rates by mineral dust was calculated to lead to an increase in global annual mean O_3 concentration by about 0.2% (Zender et al., 2003). Bian and Zender (2003) global modeling study evaluated the impact of dust on oxidant levels through changes in the photolysis rates to be higher in the northern than in the southern hemisphere due to the spatial distribution of dust. However, the overall calculated global annual impacts were as low as +0.2% for O_3 and −2.4% for OH radicals, with the maximum differences found in regions where dust loads are high.

In the eastern Mediterranean, Gerasopoulos et al. (2012) used long-term observations from the Finokalia monitoring station in Crete, Greece, along with a chemical box model to show that reduction of O_3 and NO_2 photolysis rates by 24% and 5%, respectively, due to actinic flux attenuation by aerosols leads to an overall 12% reduction in O_3 net chemical production. In the Central Mediterranean, Mailler et al. (2016) elaborated observations at Lampedusa during the ChArMEx/ADRIMED campaign of summer 2013 and, with the CHIMERE model, demonstrated that the impact of aerosols through changes in the photolysis rates led to slightly decreased averaged O_3 levels close to the sources while a slight increase was calculated over all North Africa. Astitha et al. (2007, 2008) and Astitha and Kallos (2009) conducted regional-scale modeling studies for the Mediterranean including heterogeneous reactions of reactive nitrogen species and O_3 with mineral dust aerosol as well as the impact of aerosols on photolysis efficiency. They investigated three periods

with intensive dust outbreaks in the East Mediterranean, and they calculated a 15% reduction in photolysis efficiency of O_3 and NO_2 over Athens, where a dust layer was present at PM_{10} levels of about 750 μg m^{-3} (aerosol optical depth, AOD, at 340 nm of 0.55) and about 20% reduction when AOD was 0.7–0.8. They also simulated a contribution of those reactions to aerosol nitrate by about 20–40 μg m^{-3} (calculated as a 2-hour average) and a reduction in O_3 by up to 10–30 ppb.

2.2 Heterogeneous Reactions on Aerosol Surfaces

Heterogeneous chemical processes may also strongly affect O_3 budget through their impacts on sources and sinks of HO_x (OH and HO_2) and NO_x (NO and NO_2) (Dentener & Crutzen, 1993; Dentener et al., 1996; Jacob, 2000; Zhu et al., 2010), halogen radicals, and nitryl chloride ($ClNO_2$) production (Thornton et al., 2010; Phillips et al., 2012, 2016; Wang et al., 2016). A direct removal pathway for O_3 via heterogeneous uptake has also been proposed as a plausible explanation of observations (de Reus et al., 2000). Usher et al. (2003) and Crowley et al. (2010) provided comprehensive reviews of heterogeneous reactions on dust aerosol particles. Reactions of O_3 and NO_2 on mineral dust surface have been reviewed by Cwiertny et al. (2008). In particular, they discussed the reduction in apparent O_3 uptake at increased levels of relative humidity up to 58%, and no obvious surface saturation effect is observed during water layer formation, as a result of the more rapid uptake of water than O_3. They also discussed HONO formation by heterogeneous reactions involving humic substances, heterogeneous hydrolysis of NO_2, and TiO_2 photocatalysis. They finally pinpointed the need to study non-photochemical nitrate reduction that can occur in regions like the Mediterranean where dust plumes mix with anthropogenic pollutants. Shen et al. (2013) have, in particular, summarized multiphase reactions that act as sinks of volatile organics and can affect aerosol growth by formation of bicarbonyls and organic acids, changing the physicochemical and optical properties of the aerosols. Chen et al. (2012) summarized reactions for TiO_2 as a substrate and George et al. (2015) for other minerals. George et al. (2015) pointed out that metal oxides contained in dust aerosol act as atmospheric photocatalysts leading to OH radical formation, in the gas phase, which results from the oxidation of water absorbed on dust. This dust-associated OH formation can initiate SO_2 oxidation to H_2SO_4 nearby dust aerosol, providing, thus, a path to sulfate formation, additional to the more common heterogeneous reaction of SO_2 on dust that does not require light. Furthermore, George et al. (2015) suggested that this photocatalytically initiated formation of H_2SO_4 could lead to nucleation events in the atmosphere under low-dust conditions, i.e., when only few particles are present and thus nucleation dominates over condensation. Rossi (2003) provides a synthetic view of the reactions involving sea-salt aerosol, and Finlayson-Pitts (2003) summarizes the solid- and aqueous-phase sea-salt reactions providing evidence from field studies for the contributions of halogens to tropospheric chemistry and the acid displacement reactions.

Tang et al. (2017) summarized the laboratory determinations of reactive uptake coefficients (γ_X) of oxidants (O_3 and H_2O_2), HCHO, HONO, N_2O_5, and free radicals (OH, HO_2, and NO_3) pointing out the dependence of γ_X on the substrate as well as on light and relative humidity (RH). At this point, it is worth noting the difference between the mass accommodation coefficient, α, which defines the probability for a gas molecule striking the aerosol surface to enter the condensed phase, and the uptake coefficient, γ, which defines the probability of the molecule to be removed by the condensed phase, including both physical and chemical processes (Kolb et al., 1995). For reactive removal of the absorbed species X, the uptake coefficient, depending on the stage and on the nature of interaction, may be defined as initial uptake coefficient, γ_0 (negligible adsorbates on the surface), steady-state uptake coefficient, γ_{ss} (saturated surface), and reactive uptake coefficient, γ_X (irreversible reactive uptake). Tang et al. (2017) reported the initial uptake coefficient (γ_0) for OH and HO_2 radicals on various mineral surfaces to be inversely dependent on relative humidity and to be independent of temperature. The steady-state uptake of HO_2 (γ_{ss}) on mineral surfaces was found to increase with increasing RH, and Tang et al. (2017) and James et al. (2017) suggested a catalytic role of Fe in this uptake. Two potential pathways for the fate of HO_2 on aerosol particles have been proposed: formation of H_2O_2, which will recycle reactive hydrogen in the troposphere, and decomposition to H_2O and O_2, which will be a net sink for reactive hydrogen (see references in Tang et al., 2017). Variable response to RH was found for H_2O_2 uptake on mineral surfaces, with negative dependence for TiO_2 and positive for Saharan and Gobi desert aerosol, with dust aerosol from Sahara being more reactive than from Gobi desert (Pradhan et al., 2010a, b). On dust aerosol, H_2O_2 can be decomposed to H_2O and O_2, converted to HO_2 (Romanias et al., 2012a), or undergo simple partitioning (Zhao et al., 2013). The reactive uptake coefficient of O_3 was measured to decrease with increasing RH, both on iron and aluminum oxides, pointing to the importance of aerosol water and subsequently of multiphase reactions; in darkness, reactive uptake of O_3 on TiO_2 was independent of RH. Interestingly, organic materials coated on mineral dust can be subject to heterogeneous ozonolysis by O_3 uptake on the particles (Tang et al., 2017). Such reactions have been found to be photosensitized and to proceed via electron transfer to O_3 forming an ozonide anion (O_3^-) and subsequently OH radicals (De Laurentiis et al., 2013).

With regard to nitrogen reactive species, HONO initial uptake on mineral surfaces was determined to be independent of temperature and inversely dependent on RH followed by HONO conversion to NO and NO_2 (Romanias et al., 2012b). Uptake of NO_3 radicals on dust resulted in the release of both N_2O_5, produced from NO_3 reaction with NO_2 on aerosol surface, and HNO_3 produced by heterogeneous reaction of N_2O_5 on the aerosol surface, in the gas phase (Karagulian & Rossi, 2005). Heterogeneous uptake of N_2O_5 can proceed both via heterogeneous hydrolysis or via on-surface reaction with OH radical (Seisel et al., 2005), forming HNO_3 and nitrate aerosol as end products, thus substantially modifying dust aerosol properties and atmospheric composition. Remarkably, surface deactivation related to water uptake and/or to decrease of N_2O_5 update due to the produced nitrate in the aqueous phase, the so-called nitrate effect, has been also observed, while in several

cases, increased levels of relative humidity and coating by aerosol water led to increased reactivity, as outlined previously.

Limited studies with controversial behavior have been reported for black carbon/soot aerosol, which can provide substrate for reduction reactions. Nienow and Roberts (2006) have summarized kinetic studies of heterogeneous reactions on carbonaceous aerosols and pointed out that the chemical reactivity strongly depends on the carbon type and on experimental conditions, hampering extrapolation of the laboratory experiments to the ambient conditions. Interestingly, soot has been proposed to interact with O_3 and H_2O leading to increased hydrophilicity by the formation of oxygenated surface functional groups. Soot can also reduce NO_2 to NO or HONO, and HNO_3 to HONO, providing hints to improve the simulations of NO_x in the troposphere and to understand HONO tropospheric budget (see references in Nienow & Roberts, 2006).

2.3 Evidence of Heterogeneous Reactions in Field Studies

In most of the kinetics laboratory measurements, the nature of the studied particles is simple compared to the ambient dust particles of more complex mineralogy. Keeping this in mind, atmospheric observations of trace gases and aerosol in the troposphere can be used to determine steady-state lifetimes of short-lived pollutants like NO_3 radical and N_2O_5, due to their losses on aerosol surfaces and the associated reactive uptake coefficients γ_x (e.g., Brown et al., 2006, 2009; Morgan et al., 2015). In particular, Brown et al. (2006) measured ambient NO_3 radical, N_2O_5, and aerosol surface concentrations during nighttime aircraft flights in the northeast USA and found that the uptake of N_2O_5 on aerosols was strongly dependent on aerosol composition, being more intense onto sulfate aerosol. Such behavior could be explained by the acidic character of sulfate aerosol, which constrains the partitioning of nitrate to the aerosol phase that inhibits N_2O_5 uptake. They suggested potentially strong interactions at regional scale between nitrogen oxides and sulfur dioxide anthropogenic emissions. Further determinations of reactive uptake of N_2O_5 on aerosols based on aircraft measurements in the USA by Brown et al. (2009) suggested that nocturnal chemistry of N_2O_5 could produce similar amounts of HNO_3 to those from direct production of HNO_3. In line with these findings, Vrekoussis et al. (2007), analyzing 2 years of long-path Differential Optical Absorption Spectroscopy (DOAS) observations of NO_3 radical in the gas phase along with auxiliary O_3, NO_2, and meteorological data recorded in Finokalia monitoring station in Crete, in the East Mediterranean, have inferred that, overall, the major sink of NO_3 radical was its conversion to N_2O_5, which was subsequently subject to heterogeneous losses on aqueous particles. The reactions of NO_3 in the gas phase were found to be more important during spring and summer. Nighttime production of HNO_3 plus particulate NO_3^-, as initiated by NO_3 radicals, accounted for about 50–65% of the total production rate, depending also on the season of reference (Vrekoussis et al., 2006). They have also found that on a yearly mean basis, oxidation of dimethylsulfide of

marine origin by NO_3 radicals, which are mainly of anthropogenic origin, contributed about 17% to the HNO_3 plus particulate NO_3^- formation. This result points to important interactions between natural and anthropogenic emissions that lead to acid and nutrient formation. Using airborne observations over the eastern and southern regions of the UK and in situ observations in the greater London area, Morgan et al. (2015) highlighted the significant contribution of reactive uptake of N_2O_5 as a source of nitrate aerosol as well as the importance of ammonium nitrate (NH_4NO_3) in that region. They have found higher uptake than previously reported over the USA, and this uptake was favored under high RH conditions. On the contrary, higher ratios of particulate NO_3^- concentrations to aerosol water were found to suppress N_2O_5 uptake.

It is known that the presence of the semi-volatile nature of NH_4^+ in aerosol depends on the aerosol pH and aerosol liquid water content (which in turn depends on relative humidity and liquid water content) (Seinfeld & Pandis, 2016). Nitrate also depends on pH (Guo et al., 2018); NH_4NO_3 formation is therefore favored for aerosol pH above 2.5–3.0 for typical atmospheric conditions, although this acidity range can change with liquid water and temperature (Nenes et al., 2020). Indeed, the recent regional modeling study over Europe by Kakavas et al. (2021) predicted the highest average particulate NO_3^- levels for the $PM_{2.5–5}$ range to be over locations where aerosol pH exceeds 3. In line with these findings, Guo et al. (2018) have discussed the role of soluble nonvolatile cations (NVCs), like those present in sea-salt, dust, and biomass burning aerosols (e.g., Na^+, Ca^{2+}, K^+, Mg^{+2}) in modulating aerosol pH, which depends on the relative abundance of anions and cations, and can therefore reach values favoring the partitioning of nitrate to the aerosol phase. Vasilakos et al. (2018) pointed out that because of this effect of NVCs on pH and its subsequent effect on nitrate uptake by aerosols, models can exhibit unrealistic sensitivity to nitrate availability if the emissions and treatment of NVCs contain biases.

Sea-salt aerosol containing NVCs also favors acid displacement reactions that can partition nitrate (and sulfate) into the aerosol phase, releasing halogens to the gas phase. Such reactions have been evidenced in the Mediterranean atmosphere by the observations of halogen deficit in the aerosol phase compared to the seawater composition. During the PAUR II experiment on Crete, observations by Kouvarakis et al., (2002) have indicated on average 8% and 55% deficit in Cl^- and Br^-, respectively, in the aerosol phase that was anticorrelated with the net aerosol acidity inferred by the difference between acidic and basic ions in the aerosol. Further, supportive for the potential importance of halogen chemistry in the marine environment in the Mediterranean are also the reported observations about hydrocarbons of various reactivities, which have been used as indicators of OH and Cl levels in the region (Arsene et al., 2007).

As far as the aerosol impact on surface levels of O_3 is concerned, it was demonstrated during aircraft flights near Tenerife, Canary Islands, in July 1997 (Second Aerosol Characterization Experiment, ACE 2) and also from surface measurements in July–August 2002 (MINeral dust Aerosol and TROpospheric Chemistry, MINATROC) that at high aerosol mass ranging between 400 and 500 μg m^{-3}, the dust layers were associated with low O_3 levels (de Reus et al., 2000, 2005).

Photochemical box model simulations suggested heterogeneous losses of O_3 and its precursors on aerosol surfaces. De Reus et al. (2000) estimated this loss to be 4 ppbv of O_3 per day, which is in relatively good agreement with the more recent finding (de Reus et al., 2005) of a 0.14 ppb hr^{-1} decrease in the mean daytime net ozone production. However, these box model results rely on assumptions made on O_3 levels and other trace gases in the dust source area, and the heterogeneous removal of HO_2 and H_2O_2 assumed in their model has not been able to explain the low peroxy radical levels observed during the MINATROC campaign.

2.4 *Biomass Burning Products Impacts on Trace Pollutants*

Forest fires and more generally open biomass burning, constitute an additional important source of tropospheric aerosols in the Mediterranean atmosphere, particularly during the summer (Pace et al., 2005; Bougiatioti et al., 2014, 2016a) contributing to the available substrate load for heterogeneous processes, such as surface reactions or condensation of organic matter. Biomass burning produces carbonaceous aerosols (black, organic, and brown carbon) in addition to a number of trace gases that are potent environmental contributors to secondary organic aerosol (SOA) (Fig. 2; Akagi et al., 2011; Bougiatioti et al., 2016a; Liu et al., 2017).

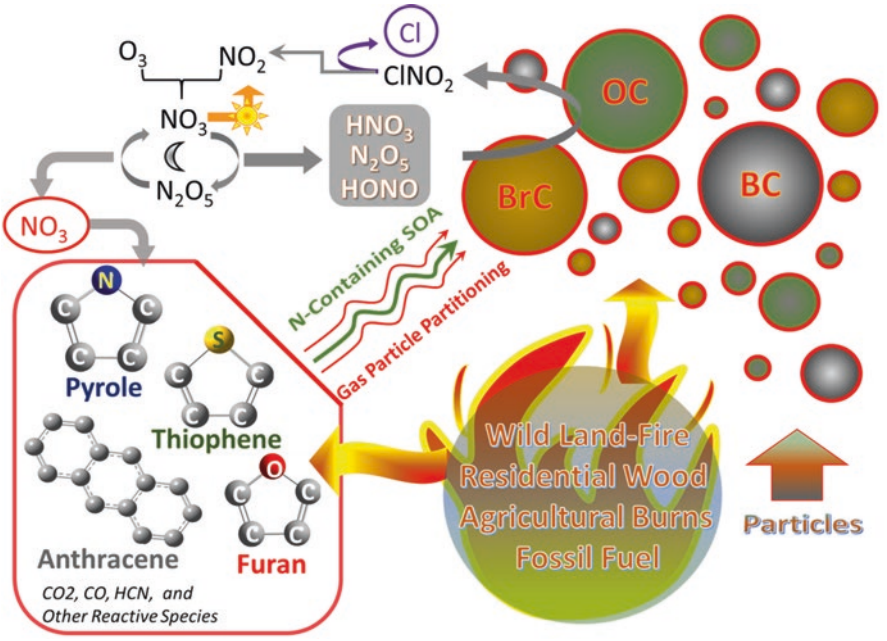

Fig. 2 Simplified scheme of biomass burning impact on atmospheric composition (gas-phase, secondary organic aerosols formation and particulate matter) via atmospheric processing involving gas to particle partitioning and multiphase reactions

The nonvolatile cations present in biomass burning aerosol tend to increase aerosol pH and, depending on if the acidity is in the right range (the so-called sensitivity window of nitrate partitioning; Vasilakos et al., 2018; Nenes et al., 2020), may promote nitrate to further partition to the aerosol phase, thus increasing aerosol water and reducing the sensitivity of aerosol amount to gas-phase ammonia levels. However, the photochemistry and the atmospheric impacts of these SOA precursors are understudied.

Bougiatioti et al. (2016a) observed, at Finokalia monitoring station in the East Mediterranean, the transformation of freshly emitted biomass burning aerosol to more oxidized organic aerosol and the associated doubling of aerosol hygroscopicity. Bougiatioti et al. (2016b) also found that biomass burning aerosols was by 1–1.5 pH unit less acidic than other types of aerosol in the region. Wong et al. (2019) found that brown carbon (BrC) aerosol (i.e., light-absorbing organic particles) from hardwood burning is composed from high (>400 Da) and low (<400 Da) molecular weight molecules with different lifetimes. The low molecular weight BrC components' lifetime, due to photolysis and oxidation by OH radical, is estimated to be about 1 h, while the high molecular weight components, have longer lifetimes around a day. They also measured BrC in samples collected from Heraklion, Crete, Greece, during open wildfire events and estimated a mean lifetime for all BrC components between 15 and 28 days, which is consistent with the lifetime of the high molecular weight BrC components observed in chamber experiments. The same study concluded that the BrC associated with the high molecular weight components, which are most stable against photochemical bleaching, can be subject to long-range transport.

Important biomass burning products with significant atmospheric abundance are various aromatic compounds known for their direct adverse effects to human health, including furans (Crutzen & Andreae, 1990; Akagi et al., 2011; Majdi et al., 2019), nitrogen, and sulfur-containing compounds, as well as polyaromatic hydrocarbons (Samburova et al., 2016) that have been detected during domestic and wildland fires, agricultural burns, and domestic fuels use. Biomass burning products are strongly dependent on fuel type and fire characteristics, and many different VOCs are produced in the fire plume. These are photochemically converted to secondary pollutants, in the presence of NO, and they eventually lead to increased tropospheric ozone levels and nitrogen containing secondary organic aerosols (SOA) formation (Jiang et al., 2019). Polycyclic aromatic hydrocarbons (PAHs), on the other hand, constitute important brown carbon sources in the atmosphere (Samburova et al., 2016). Even though efforts have been recently made (Shrivastava et al., 2017) to develop analytical methods to quantify emissions from continuous monitoring of non-methane organic gases in biomass burning events and episodes, there are still obstacles. The atmospheric levels of furans due to domestic and wild fires, relative to 1 ppm of CO formation, are between 68 and 118 ppb (Gilman et al., 2015). Models estimate that furans contribute 9–14% to the OH reactivity of the total biomass burning mixture. However, the detailed chemistry of the SOA precursors gas-phase formation is currently not well understood (Hatch et al., 2017). Therefore, there is an urgent need for integrating laboratory and field studies of biomass

burning products with regard to their reactivity, their contribution on SOA, and the on-surface heterogeneous or multiphase reactions in modelling to improve our understanding and to evaluate their role as oxidants sinks or pollutants sources, along with their effect on Earth's radiation balance.

2.5 Insights from Global Modeling Studies

Liao et al. (2003) estimated the impact of heterogeneous chemistry on modeled O_3 concentrations to be a decrease of about 30%, near the surface at the high latitudes of the northern hemisphere (NH), while they suggested that the aforementioned effect is less intense, 10–15%, in the southern hemisphere (SH). In particular, they calculated a 20–25% reduction in surface O_3 and a spatially very variable reduction in surface NO_x (about 20–50%), over the Mediterranean region. They also calculate an overall 16% reduction in global O_3 burden due to O_3 uptake by dust and to NO_x heterogeneous removal on all aerosols. The O_3 removal on dust aerosol was calculated to be very efficient compared to other modeling studies, reducing the global O_3 burden by 7%. These impacts are almost an order of magnitude larger compared to the estimated effect of aerosol-induced photolysis rates change from the same authors. They are also larger than earlier estimates by Dentener and Crutzen (1993) mainly due to the larger NO_x removal in the high latitude of the NH resulting from the heterogeneous losses on non-dust aerosol particles. Lower effects of aerosols on O_3 have also been computed by Bian and Zender (2003), who also compared the impact of dust aerosols on tropospheric oxidants stemming from changes in photolysis rates and heterogeneous reactions. Their study suggested that although aerosol-induced photolysis rates change is the determinant process for dust aerosol effects on tropospheric oxidant concentrations in the low to middle troposphere, and more specifically in the SH, heterogeneous reactions dominate everywhere else. These two mechanisms have opposite effects on global annual mean tropospheric O_3 and odd nitrogen abundances, with the photolysis rates perturbations and heterogeneous reactions leading to increase and decrease O_3 levels, respectively. Thus, they result in weak overall changes on global annual mean tropospheric concentration levels (-0.7% for O_3 and -3.5% for HNO_3), except in the cases of hydroxyl (OH) and hydrogen peroxy (HO_2) radicals (-11.1% and -5.2%, respectively), both mechanisms affecting their concentration in the same direction. Bian and Zender (2003) also found seasonal patterns of this effect close to dust sources, where the coupling of these two mechanisms is responsible for about 20% of the calculated O_3 changes. They also pointed to the importance of temperature dependence of the uptake rates, and thus of the vertical structure of dust plumes, with regard to the impact of heterogeneous reactions on tropospheric composition.

Bauer et al. (2004) accounted for the heterogeneous reactions of O_3, HNO_3, NO_3, and N_2O_5 on dust aerosol in a global model and investigated the dust events during the summer 2000 MINATROC campaign, focusing on Mount Cimone in northern Italy. They have shown that these reactions, acting as sinks of O_3 and the reservoir

species NO and NO_2, can reduce the global levels of tropospheric O_3 by about 5%. Contrary to the study of Bian and Zender (2003), Bauer et al. (2004) did neither account for the impact of aerosols on photolysis rates nor for heterogeneous reactions of OH and HO_2 radicals and H_2O_2 onto dust. Bauer et al. (2004), however, used a higher horizontal resolution for their model simulations than Bian and Zender (2003). These differences in the modeling framework, including potential differences in the dust particle size distribution and thus in the associated dust aerosol surface, can explain the higher impact of dust on O_3 calculated in the study of Bauer et al. (2004).

Stadtler et al. (2018) used two different global chemistry transport (CTM) models to evaluate the impact of heterogeneous reactions of N_2O_5, NO_3, NO_2, HNO_3, O_3, and HO_2, on dust and sea-salt, among which that of N_2O_5 was identified by both models as the most important process for the observed oxidant levels, globally. The major impact was determined to be during springtime, when levels of N_2O_5 are high and photochemistry is significant. In particular, this reaction leads to a reduction in surface O_3, which, on continental scale, varies between 5–6% for South Asia and North America, 7% for Europe, and 8–9% for East Asia. Over the Mediterranean region, reductions related to this reaction were calculated to be about 3 ppb for O_3 and 0.5 ppb for NO_2. The heterogeneous reactions of NO_2, HNO_3, and HO_2 gained relevance in East Asia due to the high levels of aerosol surfaces and NO_2, while the direct loss of O_3 on dust aerosol was found to be of minor importance. The two global model results are in reasonable agreement. It is worth to note that both global models considered heterogeneous reactions that substantially improved the comparison with surface O_3 observations in the northern hemisphere, alluding to the need of their inclusion in tropospheric composition modeling.

The impact of mineral dust on nitrate formation has been simulated mainly due to the global importance of dust aerosol, which is transported downwind of the major desserts, namely, the African Sahara and the Gobi desert, as well as desert regions in North and South America, including the Patagonian desert, and that in Australia. Karydis et al. (2016) calculated a 44% increase in particulate NO_3^- tropospheric burden (53% increase in near-surface concentrations in the coarse mode) due to interactions of gases with mineral dust. In the Mediterranean region, they calculated about 10–20% increase in total surface particulate NO_3^-. They also calculated a 41% decrease in ammonium global concentrations attributed to reduction in the available HNO_3 in the atmosphere, which is captured in the aerosol phase by the nonvolatile mineral cations and thus leading to a decrease of the potentially formed NH_4NO_3. Interestingly, Karydis et al. (2016) found a 7% increase in SO_4^{2-} levels related to changes in the aerosol pH comprising the most favorable conditions for SO_2 oxidation by O_3 and a 9% increase in Cl^- tropospheric burden as a result of reactions with mineral dust cations.

Mao et al. (2013) have also investigated the importance of copper (Cu) and iron (Fe) redox chemistry in aerosol water as a potent radical sink in the global atmosphere. Redox reactions involve the reduction of a molecule via electron transfer from the electron donor (metal oxide) to the electron acceptor, a molecule of O_2, which is thus converted to the extremely reactive superoxide radical (O_2^-). This can

oxidize the water absorbed on the surface of the mineral to hydroxyl radical, which will further oxidize possible absorbed organics leading to several products formation, some of them having been identified in both chambers and field studies (George et al., 2015). Mao et al. (2013) global modeling study with regard to the coupling of the transition metal ions Cu and Fe has shown the rapid conversion of HO_2 to H_2O by HO_2 uptake in aqueous aerosol. This process can affect tropospheric oxidants levels, as well as carbon monoxide, improving comparison between model results and observations and providing an additional pathway of aerosol impact on radiative forcing through changes in ozone levels or the lifetime of reactive greenhouse gases, such as methane and hydrofluorocarbons. Myriokefalitakis et al. (2015, 2016) global modeling of Fe and phosphorus (P) atmospheric cycles, also accounting for Fenton reactions in the atmospheric aerosol phases (cloud and aerosol water), have shown that multiphase chemistry is able to mobilize significant amounts of Fe and P from the mineral-aerosol phase to the aqueous phase, thus increasing the Fe and P solubility. This mobilization also involves ligands, like oxalate, for which carbonyl multiphase chemistry is the major formation pathway (Myriokefalitakis et al., 2011).

Table 1 summarizes the main mechanisms discussed herein, through which aerosols are affecting tropospheric chemistry and nutrients solubility, and associated impact estimates for the Mediterranean.

3 Aerosols and Atmospheric Acidity

3.1 Aerosol pH in the Mediterranean

Since direct observations of ambient aerosol pH are only recently emerging (Pye et al., 2020), the most reliable indirect information on the aerosol acidity is derived from thermodynamic analysis of observation data (that include major aerosol and semi-volatile species, e.g., NH_3/NH_4, HNO_3/NO_3) with equilibrium model calculations like E-AIM (Clegg et al., 1998) and ISORROPIA II (Fountoukis & Nenes, 2007). This approach enabled the evaluation of ambient aerosol pH in the East Mediterranean (Bougiatioti et al., 2016b) and in the Central Mediterranean (Squizzato et al., 2013; Masiol et al., 2020). Additional acidity inferences were carried out by Nenes et al. (2011) and Ingall et al. (2018) for the East Mediterranean to understand the potential role of dust acidification on bioavailable trace nutrient levels. A few global models are also able to compute aerosol and cloud acidity distributions (Myriokefalitakis et al., 2015; a review is provided in Pye et al., 2020). Recently, Kakavas et al. (2021) published the first mesoscale chemistry transport modeling study over Europe of aerosol pH with a detailed sectional description of the aerosol size distribution, chemical composition, and acidity calculation (carried out with the embedded ISORROPIA II model).

Table 1 Summary of main mechanisms here discussed through which aerosols are affecting tropospheric chemistry and nutrients solubility and associated impact estimates for the Mediterranean

Mechanism	Impacts	Importance for the Mediterranean	References
Photolysis rates changes	Reduction in photolysis rates near-surface and impact on O_3 net production	15–20% lower JNO_2, JO_3 reduction up to 10–30 ppb O_3 (Athens) −24% in O_3 net production (Finokalia) Up to −20% in JO_3 and JNO_2; up to −2 ppb of O_3 (Lampedusa)	Astitha et al., (2007, 2008) Gerasopoulos et al. (2012) Mailler et al. (2016)
Acid displacement reactions	Deficit of halogens in aerosols and more halogens in the gas phase	8% Cl deficit 55% Br deficit 0.6×10^4–4.7×10^4 Cl cm^{-3}	Kouvarakis et al. (2002) Arsene et al. (2007) for indications of Cl presence
Heterogeneous reactions on aerosol surfaces	Depletion of HO_x (HO_2, OH), N_2O_5, HNO_3, O_3, and NO_x and formation of HONO, HNO_3, and $ClNO_2$	$HNO_3 + NO_3^-$ night-time formation = 50–65% of total Loss of up to 4 ppb d^{-1} of O_3 due to dust	Vrekoussis et al. (2007) de Reus et al. (2000, 2005)
VOC multiphase reactions	Carbonyl loss and formation and SOA formation	Oxalate net chemical production over the Med. Sea: 53 Gg yr^{-1}; concentrations: 0.10–0.15 μg m^{-3}	Derived from Kanakidou et al., (2020) and ref therein
Aerosol acidity	Solubilization of Fe and P changing dust lifetime; nitrate formation and reactive nitrogen deposition	Solubilization flux over the Med Sea: 11 Gg(Fe) yr^{-1} and 1 Gg(P) yr^{-1} Increase in aerosol nitrate by about 20–40 μg m^{-3}	Derived from Kanakidou et al. (2020) Nenes et al. (2011) Astitha et al. (2007, 2008) Myriokefalitakis et al. (2018) Nenes et al., (2020a, b)

Squizzato et al. (2013), using fine ($PM_{2.5}$) aerosol composition observations in the Venice area in the Po Valley during four periods representative of the different seasons in 2009 and the E-AIM thermodynamic model, derived an average aerosol pH of 3.02 with maximum in winter (3.62) when aerosol water maximizes and minimum (2.27) in summer. The higher aerosol pH in winter over summer can be attributed to the higher relative humidity and thus aerosol water content in winter. Similar seasonality in aerosol pH is found for five cities in the lower end of the Po Valley by Masiol et al. (2020), who used aerosol composition measurements and the thermodynamic ISORROPIA II model to infer aerosol acidity, which varied between 1.5 and 4.5. They found that sulfate and fossil fuel use reduces aerosol pH and

nitrate, while biomass burning increases pH. The role of biomass burning and of water uptake by aerosols for aerosol acidity has also been discussed by Bougiatioti et al. (2016b) who used aerosol chemical composition measurements at Finokalia, Crete, Greece in the East Mediterranean and the thermodynamic model ISORROPIA II to evaluate the submicron (PM_1) aerosol pH. They found submicron aerosol to be very acidic with pH varying from 0.5 to 2.8 during the 6-month period of the study (June to November 2012), with biomass burning aerosols presenting the highest pH and the lowest total aerosol water. This pattern is in line with the presence of non-volatile cations in the biomass burning aerosol and the presence of relatively high amounts of nitrate and ammonia. They have also found a clear daily pattern with the most acidic aerosol around noon when temperature is the highest, relative humidity the lowest, and thus aerosol water low. During that period of the day, the aerosol water is mainly associated with inorganic aerosol components, while during night, organics contribute significantly to aerosol water. Overall, organics were found to contribute about 27.5% to the total aerosol water at this location.

Kakavas et al. (2021) modeling study over Europe simulated aerosol pH with a comprehensive representation of different aerosol sizes. They have found the same trend in aerosol pH with the global TM4-ECPL model (Myriokefalitakis et al., 2015; Pye et al., 2020) with the smaller particles being more acidic than the larger ones, reflecting the chemical composition of the aerosols and the associated amount of aerosol water. Figure 3 depicts annual mean aerosol pH computed by the TM4-ECPL model and shows differences by about 2 pH units between sub- and super-micron particles, with the submicron aerosol being the most acidic. It is also found that the aerosol acidity increases with altitude due to changes in water vapor

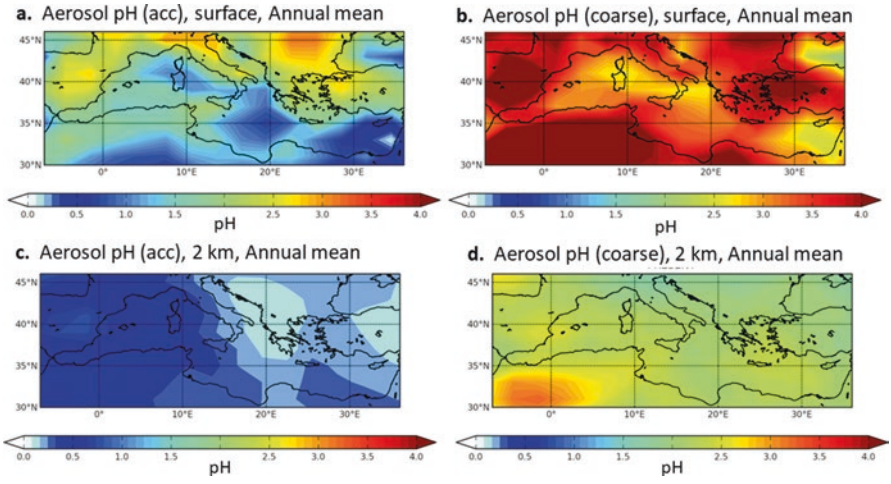

Fig. 3 Average predicted aerosol pH as a function of size and altitude: (**a**) and (**c**) for accumulation aerosol (PM_1 in the model) and (**b**) and (**d**) for coarse mode aerosol at surface (top) and 2 km in altitude (bottom) for the base case simulation annual mean values. (Data from the simulation by Kanakidou et al., 2020)

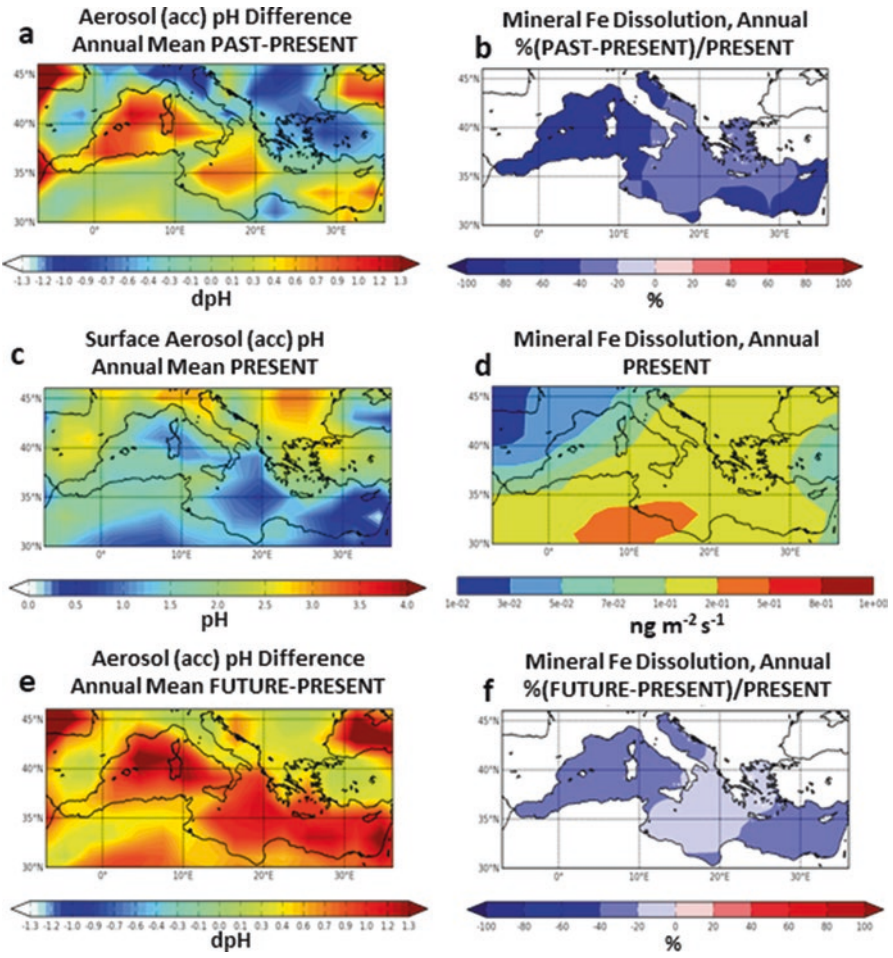

Fig. 4 Evolution due to anthropogenic and biomass burning emissions changes of the pH of the near-surface submicron aerosol in the Mediterranean (**left**) and dissolution flux of Fe from minerals (**right**): (**a**) differences in pH units (PAST-PRESENT); (**b**) absolute pH calculated for PRESENT; (**c**) differences in pH units (PAST-PRESENT); (**d**) percent changes from the past relative to present ((PAST-PRESENT)/PRESENT); (**e**) absolute dissolution fluxes of Fe calculated for PRESENT in ng m^{-2} s^{-1}; (**f**) projected percent changes in the future relative to present ((FUTURE-PRESENT)/PRESENT). Calculations are done with the TM4-ECPL global model using CMIP5 and RCP6.0 emissions (parameterizations by Myriokefalitakis et al., 2015; simulation shown is described in Kanakidou et al., 2020). In these calculations, K^+ from biomass burning is not considered in the thermodynamic model calculations. PAST, PRESENT, and FUTURE with emissions for 1850, 2010, and 2100, respectively

availability (0.5–2 units pH over 2 km) (Fig. 3), a trend which is consistent with pH inferences from aircraft measurement in the East USA (Guo et al., 2017). Myriokefalitakis et al. (2015) calculated an increase in submicron aerosol acidity from the anthropogenic and biomass burning emissions in the region, while a reduction is projected in the future due to mitigation of air pollution (Fig. 4 left column).

3.2 Dust Acidification and Nutrients

Acid processing of atmospheric aerosols is affecting the solubility of trace nutrients, like iron, phosphorus, and copper, present in the aerosols, which can then become readily available to the ecosystems (Ito et al., 2016; Kanakidou et al., 2018; Pye et al., 2020). Indeed, nutrient's mobilization from mineral dust strongly depends on the aerosol pH (Shi et al., 2012) as well as the mineralogy of the dust. Similarly to Fe, P is also solubilized under acidic conditions in aqueous atmospheric media (Myriokefalitakis et al., 2016) (Fig. 4). Pollutants alter the levels of atmospheric acidity via the formation of strong acids, such as sulfuric (H_2SO_4) and nitric (HNO_3) acid, that eventually transform, partly, dust insoluble minerals, e.g., hematite and apatite, into soluble Fe(II) or Fe(III) and PO_4^{3-}, respectively (e.g., Meskhidze et al., 2003; Nenes et al., 2011; Shi et al., 2011; Stockdale et al., 2016; Ingall et al., 2018). Mineral Fe solubilization may also be enhanced by multiphase reactions in the presence of organic ligands, such as the oxalic acid, under favorable atmospheric conditions (e.g., Saydam & Senyuva, 2002; Paris et al., 2011; Paris & Desboeufs, 2013).

In an effort to explain the observed solubility of atmospheric phosphorus in the Mediterranean region, Nenes et al. (2011) performed laboratory experiments demonstrating the ability of acidification to increase Saharan soil and dust solubility (bioavailability) by an order of magnitude. They proposed that the atmospheric acidification of aerosol particles increases the bioavailability of phosphorus in soil dust when dust is mixed with atmospheric pollutants. Similar results were obtained by Stockdale et al. (2016) via simulation studies, in which dust and dust precursor soil samples collected from the south part of the Mediterranean (Greece, Israel, Algeria, Morocco, and Libya) were exposed to similar acidic conditions with the ones observed in the atmosphere. They also found a pH threshold above which surface-bounds forms are dissolved, while at lower pH values, phosphorus dissolution is proportional to the amount of H^+ exposure. Combining their kinetics findings with numerical simulations, they suggested that the observed variability in soluble inorganic phosphorus in the Mediterranean (and other ocean regions of the globe like North Central Atlantic) can be interpreted by dust acidification.

Atmospheric acidity, over the Mediterranean, is substantially enhanced during summertime due to the increased photochemical activity, which further leads to increased NO_x and SO_x oxidation and reduced aerosol water. These, together with heterogeneous reactions of acidic gases (NO_x, SO_x) on dust particles surface that also increase the acidity of dust, enhance proton dissolution of mineral dust-associated nutrients and thus dust solubility. In line with these findings, Theodosi et al. (2010) found a positive correlation of acidity with Fe that has been either dissolved in rainwater or subject to dry deposition. Samples processed in this study were collected in Crete in the East Mediterranean, and the solubility ranged from 27.2% for polluted rainwater (pH of 4–5) to 0.5% for Saharan dust episodes (pH close to 8). Similarly, observed solubilities of the inorganic fraction of P in aerosols over the Mediterranean ranges between 20% and 45%, with the lowest values being associated with dust-influenced air masses and the highest ones with air masses

from Central Europe (Herut et al., 1999; Markaki et al., 2003, 2010). Myriokefalitakis et al. (2015, 2016) and Kanakidou et al. (2020) calculated enhanced mineral Fe and P dissolution fluxes over the eastern Mediterranean basin and the Middle East. Overall, an increase in the soluble Fe and P deposition fluxes over the Mediterranean Sea resulting from the acidity-driven dissolution of dust is calculated to be about 11 Gg-(Fe) yr^{-1} and 1 Gg(P) yr^{-1}, respectively (Kanakidou et al., 2020; Table 1). Additionally, it is suggested that emissions from biomass burning and anthropogenic origin oil combustion also contribute to the soluble Fe levels (Ito et al., 2019), and through deposition, they can impact ocean biogeochemistry (Ito et al., 2016). Oxalate aqueous-phase formation, and therefore the organic ligand-promoted Fe dissolution, is also favored by the higher biogenic NMVOC emissions during the warm season, which are precursors of organic ligands (e.g., Myriokefalitakis et al., 2011).

The aforementioned dust aerosol chemical aging is reducing the lifetime of dust, which also depends on the aerosol size distribution (the smaller the particles, the longer they stay in the atmosphere). Indeed, the lifetime of Fe-containing aerosols has been estimated between less than 1 day for the super-micron aerosol and weeks for the submicron aerosol (Kok et al., 2017), while the overall dust aerosol lifetime has been estimated between 1.6 and 7.1 days (Huneeus et al., 2011). However, evaluation of the lifetime of dust and how it is changing during atmospheric transport and processing remains challenging (Renard et al., 2018). Large differences have been found between models of the atmospheric Fe cycle due to both the aerosol size distribution and solubilization parameterization of dust (as a measure of model divergence, the ratio of the standard deviation to the ensemble model mean was examined and found regionally larger than 2; Myriokefalitakis et al., 2018). Future emission scenarios (van Vuuren et al., 2011) show that the sources of the main acidic atmospheric species, such as nitrogen (NO_x) and sulfur (SO_x) oxides, are expected to decrease by 34–59% and 75–88%, respectively, between 2010 and 2100, but ammonia (NH_3) will most probably increase by 3–55%. This heterogeneity in the projection of acidic and alkaline emissions will, overall, nonlinearly perturb both atmospheric aerosol acidity (Weber et al., 2016) and dust acidification, and the produced nutrients will be transferred into the ocean. Particularly for the Mediterranean region, Kanakidou et al. (2020) demonstrated that the preindustrial soluble P and soluble Fe deposition rates were lower compared to modern times (i.e., 35% and 54%, respectively), but they will almost return to the present-day levels, in the foreseeable future. The aforementioned differences, however, integrate changes of both direct emissions and atmospheric processing (Fig. 4). Overall, these changes may be of particular importance and play a key role in ecosystems like in the Mediterranean and particularly its eastern basin, where phytoplankton growth is limited by P availability.

Furthermore, nitrate and ammonium partitioning to the aerosol phase are also affected by acidity, and since gases are more efficiently exhibiting dry deposition compared to submicron aerosols, changes in acidity lead to changes in the deposition patterns of those nutrients (Nenes et al., 2021). Interestingly, nitrate partitioning to the aerosol phase is favored at higher pH, while NH_4^+ partitioning shows

opposite dependence on the pH and is favored in an acidic environment. Thus, transport and deposition of reduced nitrogen response to aerosol acidity changes are different from those of the oxidized nitrogen (Nenes et al., 2021). In addition, the aforementioned heterogeneous reactions, which favor partitioning of nitrate onto the coarse mode aerosol, reduce the residence time of nitrate and therefore affect its atmospheric deposition patterns through increased sedimentation.

Following the methodology by Nenes et al. (2020, 2021), Fig. 5 provides policy-relevant information on the sensitivity of particulate matter (PM_1) levels and of dry reactive inorganic nitrogen deposition fluxes, respectively, to total ammonia and nitrate availability. The figure depicts chemical domain classifications based on model results for grid cells of 2 deg in latitude by 3 deg in longitude over an extended Mediterranean region (southern Europe and northern Africa; Kanakidou et al., 2020).

According to these calculations, in more than 60% of the area, the aerosol (Fig. 5a) is exclusively sensitive to NH_3, another 15% exclusively sensitive to HNO_3, 5% insensitive, and the remainder sensitive to both HNO_3 and NH_3. Thus although policies for PM_1 reduction may differ among areas, PM_1 is sensitive to NH_3 over about 80% of the area, and PM_1 is sensitive to HNO_3 over about 35% of the areas. These results support the great potential of reduction in PM_1 levels by controlling NH_3 emissions. Figure 5b shows that dry deposition of reactive nitrogen is fast both for the oxygenated and the reduced inorganic nitrogen forms, which are thus rapidly lost by dry deposition in the boundary layer.

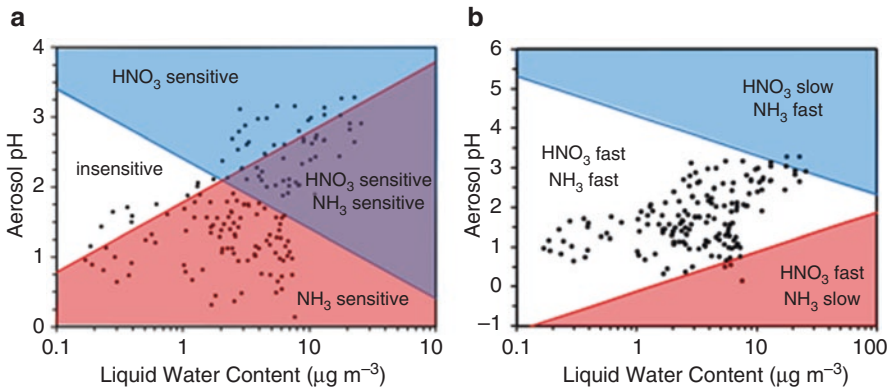

Fig. 5 (**a**) Diagram denoting the regimes of particulate matter (PM_1) sensitivity to total ammonia and nitrate (marked in the figure by HNO_3) availability. Note that for most cases, aerosol is either exclusively sensitive to total ammonia (red region) or sensitive to both total ammonia and nitrate (purple region). (**b**) Diagram of dry deposition regimes of reactive nitrogen. For most conditions simulated by TM4-ECPL, the combination of liquid water content and pH ensures that most of the reactive nitrogen dry deposition is rapid (close to the gas deposition velocity limit), meaning that it does not allow accumulation of nitrate or ammonia in the boundary layer and that nitrogen deposits close to the region it is emitted (for ammonia) and/or produced (for nitrate). Dots show the annual mean results from the TM4-ECPL model (Kanakidou et al., 2020) in grids of 2° × 3° for the region from 28°N to 48°N and 9°W to 36°E

4 Conclusion and Perspectives

Aerosols have diverse impacts on atmospheric and precipitation chemistry that have been discussed in this chapter. The major ones are related to heterogeneous reactions on aerosol particle surfaces that affect nitrogen reactive species and subsequently atmospheric oxidant levels, sulfur dioxide oxidation in the atmosphere, secondary organic aerosol formation, and atmospheric acidity. The latter is driving solubilization of nutrients or toxic metals, present in aerosols, and overall, precipitation chemistry.

While reactions on dust and sea-salt aerosol have been reasonably well documented by laboratory and field studies over the past decades, these are not routinely integrated in atmospheric modeling owing to difficulties regarding the treatment, model setup (e.g., emissions), and computational expense associated with the rigorous treatment and representation of size-segregated aerosol composition and processes. Furthermore, the uncertainty associated with studying size-resolved processes in the laboratory and field poses additional and significant challenges.

The importance of biomass burning gaseous and particulate products for the levels of atmospheric oxidants and aerosol, which have impacts on climate and health, has been pointed out and is of major concern for the scientific and broader community. To understand the rapid chemistry that is involved in biomass burning emissions and their aging, fast measuring techniques need to be applied in chamber and field experiments that include nocturnal conditions. These will provide information on SOA formation and primary carbonaceous aerosol aging as well as on the properties of the resulting aged aerosols in the atmosphere. Such information is needed to improve model simulations of atmospheric aerosols.

Aerosol composition observations and thermodynamic modeling have shown that aerosol acidity exhibits significant regional and temporal variability that depends on aerosol size, composition, ambient relative humidity, and temperature. In the Mediterranean, fine aerosol is strongly acidic, particularly in the absence of biomass burning, while the size dependence of aerosol acidity is considerable, up to 4 pH units. Given that the species found in aerosol is also strongly size dependent – and that key processes exhibit pH sensitivity – many of the impacts of aerosol require a comprehensive understanding of the pH and liquid water distributions across particle size.

Atmospheric chemical processing of aerosol particles converts insoluble minerals to soluble nutrients (or toxic components) that are transported into the ecosystems following the atmospheric deposition of aerosols. The latter is of importance since it supports ecosystem growth and carbon sequestration. The same soluble metal species can also have a significant negative impact on human health. Therefore, chemical aging of atmospheric aerosol is changing the key properties of aerosols that notably affect the ecosystems. Our understanding of those processes needs to be significantly improved and their effects quantified by integrating them into Earth system modeling. Given the high concentration of acids and dust in the Mediterranean, understanding these interactions is critical for fully appreciating the broader impacts of human activities on people, ecosystems, and climate throughout the Mediterranean.

Acknowledgments We acknowledge support of this work by the project "PANhellenic infrastructure for Atmospheric Composition and climatE change" (MIS 5021516), which is implemented under the action "Reinforcement of the Research and Innovation Infrastructure" funded by the operational program "Competitiveness, Entrepreneurship and Innovation" (NSRF 2014-2020) and cofinanced by Greece and the European Union (European Regional Development Fund). We also acknowledge support by the project PyroTRACH (ERC-2016-COG) funded by H2020-EU.1.1. – Excellent Science – European Research Council (ERC), project ID 726165 and from the European Union Horizon 2020 project FORCeS under grant agreement No 821205.

References

Akagi, S. K., Yokelson, R. J., Wiedinmyer, C., Alvarado, M. J., Reid, J. S., Karl, T., Crounse, J. D., & Wennberg, P. O. (2011). Emission factors for open and domestic biomass burning for use in atmospheric models. *Atmospheric Chemistry and Physics, 11*, 4039–4072. https://doi.org/10.5194/acp-11-4039-2011

Arsene, C., Bougiatioti, A., Kanakidou, M., Bonsang, B., & Mihalopoulos, N. (2007). Tropospheric OH and Cl levels deduced from non-methane hydrocarbon measurements in a marine site. *Atmospheric Chemistry and Physics, 7*, 4661–4673. https://doi.org/10.5194/acp-7-4661-2007

Astitha, M., & Kallos, G. (2009). Gas-phase and aerosol chemistry interactions in South Europe and the Mediterranean region. *Environmental Fluid Mechanics, 9*, 3–22. https://doi.org/10.1007/s10652-008-9110-7

Astitha, M., Kallos, G., Katsafados, P., Pytharoulis, I., & Mihalopoulos, N. (2007). Chapter 5.7 Radiative effects of natural PMs on photochemical processes in the Mediterranean region. In C. Borrego & E. Renner (Eds.), Dev. Environ. Sci., 6, 548–559 *Air pollution modeling and its application XVIII*. Elsevier. https://doi.org/10.1016/S1474-8177(07)06057-3

Astitha, M., Kallos, G., Katsafados, P., & Mavromatidis, E. (2008). Heterogeneous chemical processes and their role on particulate matter formation in the Mediterranean region. In C. Borrego & A. I. Miranda (Eds.), NATO Science for Peace and Security Series Series C *Air pollution modeling and its application XIX*. Springer. https://doi.org/10.1007/978-1-4020-8453-9_55

Becagli, S. (2022). Aerosol composition ad reactivity. In F. Dulac, S. Sauvage, & E. Hamonou (Eds.), *Atmospheric chemistry in the Mediterranean Region* (Vol. 2, From air pollutant sources to impacts). Springer, this volume. https://doi.org/10.1007/978-3-030-82385-6_13

Bauer, S. E., Balkanski, Y., Schulz, M., Hauglustaine, D. A., & Dentener, F. J. (2004). Global modeling of heterogeneous chemistry on mineral aerosol surfaces: Influence on tropospheric ozone chemistry and comparison to observations. *Journal of Geophysical Research, 109*, D02304. https://doi.org/10.1029/2003JD003868

Berresheim, H., Plass-Dülmer, C., Elste, T., Mihalopoulos, N., & Rohrer, F. (2003). OH in the coastal boundary layer of Crete during MINOS: Measurements and relationship with ozone photolysis. *Atmospheric Chemistry and Physics, 3*, 639–649. https://doi.org/10.5194/acp-3-639-2003

Bian, H., & Zender, C. S. (2003). Mineral dust and global tropospheric chemistry: Relative roles of photolysis and heterogeneous uptake. *Journal of Geophysical Research, 108*, 4672. https://doi.org/10.1029/2002JD003143

Bougiatioti, A., Stavroulas, I., Kostenidou, E., Zarmpas, P., Theodosi, C., Kouvarakis, G., Canonaco, F., Prévôt, A. S. H., Nenes, A., Pandis, S. N., & Mihalopoulos, N. (2014). Processing of biomass burning aerosol in the Eastern Mediterranean during summertime. *Atmospheric Chemistry and Physics, 14*, 4793–4807. https://doi.org/10.5194/acp-14-4793-2014

Bougiatioti, A., Bezantakos, S., Stavroulas, I., Kalivitis, N., Kokkalis, P., Biskos, G., Mihalopoulos, N., Papayannis, A., & Nenes, A. (2016a). Biomass-burning impact on CCN number, hygroscopicity and cloud formation during summertime in the eastern Mediterranean. *Atmospheric Chemistry and Physics, 16*, 7389–7409. https://doi.org/10.5194/acp-16-4579-2016

Bougiatioti, A., Nikolaou, P., Stavroulas, I., Kouvarakis, G., Weber, R., Nenes, A., Kanakidou, M., & Mihalopoulos, N. (2016b). Particle water and pH in the eastern Mediterranean: Source variability and implications for nutrient availability. *Atmospheric Chemistry and Physics, 16*, 4579–4591. https://doi.org/10.5194/acp-16-4579-2016

Brown, S. S., Ryerson, T. B., Wollny, A. G., Brock, C. A., Peltier, R., Sullivan, A. P., Weber, R. J., Dube, W. P., Trainer, M., Meagher, J. F., Fehsenfeld, F. C., & Ravishankara, A. R. (2006). Variability in nocturnal nitrogen oxide processing and its role in regional air quality. *Science, 311*, 67–70. https://doi.org/10.1126/science.1120120

Brown, S. S., Dube, W. P., Fuchs, H., Ryerson, T. B., Wollny, A. G., Brock, C. A., Bahreini, R., Middlebrook, A. M., Neuman, J. A., Atlas, E., Roberts, J. M., Osthoff, H. D., Trainer, M., Fehsenfeld, F. C., & Ravishankara, A. R. (2009). Reactive uptake coefficients for N_2O_5 determined from aircraft measurements during the Second Texas Air Quality Study: Comparison to current model parameterizations. *Journal of Geophysical Research, 114*, D00F10. https://doi.org/10.1029/2008JD011679

Budisulistiorini, S. H., Nenes, A., Carlton, A. G., Surratt, J. D., McNeill, V. F., & Pye, H. O. T. (2017). Simulating aqueous-phase isoprene-epoxydiol (IEPOX) secondary organic aerosol production during the 2013 Southern Oxidant and Aerosol Study (SOAS). *Environmental Science & Technology, 51*(9), 5026–5034. https://doi.org/10.1021/acs.est.6b05750

Carlton, A. G., Turpin, B. J., Altieri, K. E., Seitzinger, S., Reff, A., Lim, H.-J., & Ervens, B. (2007). Atmospheric oxalic acid and SOA production from glyoxal: Results of aqueous photooxidation experiments. *Atmospheric Environment, 41*, 7588–7602. https://doi.org/10.1016/j.atmosenv.2007.05.035

Chen, H. H., Nanayakkara, C. E., & Grassian, V. H. (2012). Titanium dioxide photocatalysis in atmospheric chemistry. *Chemical Reviews, 112*(11), 5919–5948. https://doi.org/10.1021/cr3002092

Clegg, S. L., Brimblecombe, P., & Wexler, A. S. (1998). A thermodynamic model of the system H^+–NH_4^+–SO_4^{2-}–NO_3^-–H_2O at tropospheric temperatures. *The Journal of Physical Chemistry. A, 102*, 2137–2154. https://doi.org/10.1021/jp973042r

Crowley, J. N., Ammann, M., Cox, R. A., Hynes, R. G., Jenkin, M. E., Mellouki, A., Rossi, M. J., Troe, J., & Wallington, T. J. (2010). Evaluated kinetic and photochemical data for atmospheric chemistry: Volume V – heterogeneous reactions on solid substrates. *Atmospheric Chemistry and Physics, 10*, 9059–9223. https://doi.org/10.5194/acp-10-9059-2010

Crutzen, P. J., & Andreae, M. O. (1990). Biomass burning in the tropics: Impact on atmospheric chemistry and biogeochemical cycles. *Science, 250*, 1669–1678. https://doi.org/10.1126/science.250.4988.1669

Cwiertny, D. M., Young, M. A., & Grassian, V. H. (2008). Chemistry and photochemistry of mineral dust aerosol. *Annual Review of Physical Chemistry, 59*, 27–51. https://doi.org/10.1146/annurev.physchem.59.032607.093630

De Laurentiis, E., Socorro, J., Vione, D., Quivet, E., Brigante, M., Mailhot, G., Wortham, H., & Gligorovski, S. (2013). Phototransformation of 4-phenoxyphenol sensitised by 4-carboxybenzophenone: Evidence of new photochemical pathways in the bulk aqueous phase and on the surface of aerosol deliquescent particles. *Atmospheric Environment, 81*, 569–578. https://doi.org/10.1016/j.atmosenv.2013.09.036

de Reus, M., Dentener, F., Thomas, A., Borrmann, S., Ström, J., & Lelieveld, J. (2000). Airborne observations of dust aerosol over the North Atlantic Ocean during ACE-2: Indications for heterogeneous ozone destruction, *Journal of Geophysical Research*, *105*, 15263–15275, https://doi.org/10.1029/2000JD900164

de Reus, M., Fischer, H., Sander, R., Gros, V., Kormann, R., Salisbury, G., Van Dingenen, R., Williams, J., Zöllner, M., & Lelieveld, J. (2005). Observations and model calculations of trace gas scavenging in a dense Saharan dust plume during MINATROC. *Atmospheric Chemistry and Physics, 5*, 1787–1803. https://doi.org/10.5194/acp-5-1787-2005

Dentener, F. J., & Crutzen, P. J. (1993). Reaction of N_2O_5 on tropospheric aerosols: Impact on the global distributions of NOx, O_3, and OH. *Journal of Geophysical Research, 98*, 7149–7163. https://doi.org/10.1029/92JD02979

Dentener, F. J., Carmichael, G. R., Zhang, Y., Lelieveld, J., & Crutzen, P. J. (1996). Role of mineral aerosol as a reactive surface in the global troposphere. *Journal of Geophysical Research, 101*, 22869–22889. https://doi.org/10.1029/96JD01818

Drozd, G., Woo, J., Häkkinen, S. A. K., Nenes, A., & McNeill, V. F. (2014). Inorganic salts interact with oxalic acid in submicron particles to form material with low hygroscopicity and volatility. *Atmospheric Chemistry and Physics, 14*, 5205–5215. https://doi.org/10.5194/acp-14-5205-2014

Finlayson-Pitts, B. J. (2003). The Tropospheric chemistry of sea salt: A molecular-level view of the chemistry of NaCl and NaBr. *Chemical Reviews, 103*(12), 4801–4822. https://doi.org/10.1021/cr020653t

Fountoukis, C., & Nenes, A. (2007). ISORROPIA II: A computationally efficient thermodynamic equilibrium model for K+-Ca2+-Mg2+-NH4+-Na+-SO42−-NO3−-Cl--H2O aerosols. *Atmospheric Chemistry and Physics, 7*, 4639–4659. https://doi.org/10.5194/acp-7-4639-2007

George, C., Ammann, M., D'Anna, B., Donaldson, D. J., & Nizkorodov, S. A. (2015). Heterogeneous photochemistry in the atmosphere. *Chemical Reviews, 115*, 4218–4258. https://doi.org/10.1021/cr500648z

Gerasopoulos, E., Kazadzis, S., Vrekoussis, M., Kouvarakis, G., Liakakou, E., Kouremeti, N., Giannadaki, D., Kanakidou, M., Bohn, B., & Mihalopoulos, N. (2012). Factors affecting O_3 and NO_2 photolysis frequencies measured in the eastern Mediterranean during the five-year period 2002–2006. *Journal of Geophysical Research, 117*, D22305. https://doi.org/10.1029/2012JD017622

Gilman, J. B., Lerner, B. M., Kuster, W. C., Goldan, P. D., Warneke, C., Veres, P. R., Roberts, J. M., de Gouw, J. A., Burling, I. R., & Yokelson, R. J. (2015). Biomass burning emissions and potential air quality impacts of volatile organic compounds and other trace gases from fuels common in the US. *Atmospheric Chemistry and Physics, 15*, 13915–13938. https://doi.org/10.5194/acp-15-13915-2015

Guieu, C., & Ridame, C. (2022) Impact of atmospheric deposition on marine chemistry and biogeochemistry. In F. Dulac, S. Sauvage, & E. Hamonou (Eds.), *Atmospheric chemistry in the Mediterranean Region* (Vol. 2, From air pollutant sources to impacts). Springer, this volume. https://doi.org/10.1007/978-3-030-82385-6_23

Guo, H., Liu, J., Froyd, K. D., Roberts, J. M., Veres, P. R., Hayes, P. L., Jimenez, J. L., Nenes, A., & Weber, R. J. (2017). Fine particle pH and gas-particle phase partitioning of inorganic species in Pasadena, California, during the 2010 CalNex campaign. *Atmospheric Chemistry and Physics, 17*, 5703–5719. https://doi.org/10.5194/acp-17-5703-2017

Guo, H., Nenes, A., & Weber, R. J. (2018). The underappreciated role of nonvolatile cations in aerosol ammonium-sulfate molar ratios. *Atmospheric Chemistry and Physics, 18*, 17307–17323. https://doi.org/10.5194/acp-18-17307-2018

Hatch, L. E., Yokelson, R. J., Stockwell, C. E., Veres, P. R., Simpson, I. J., Blake, D. R., Orlando, J. J., & Barsanti, K. C. (2017). Multi-instrument comparison and compilation of non-methane organic gas emissions from biomass burning and implications for smoke-derived secondary organic aerosol precursors. *Atmospheric Chemistry and Physics, 17*, 1471–1489. https://doi.org/10.5194/acp-17-1471-2017

Herrmann, H., Schaefer, T., Tilgner, A., Styler, S. A., Weller, C., Teich, M., & Otto, T. (2015). Tropospheric aqueous-phase chemistry: Kinetics, mechanisms, and its coupling to a changing gas phase. *Chemical Reviews, 115*, 4259–4334. https://doi.org/10.1021/cr500447k

Herut, B., Krom, M. D., Pan, G., & Mortimer, R. (1999). Atmospheric input of nitrogen and phosphorus to the Southeast Mediterranean: Sources, fluxes, and possible impact. *Limnology and Oceanography, 44*, 1683–1692. https://doi.org/10.4319/lo.1999.44.7.1683

Huneeus, N., Schulz, M., Balkanski, Y., Griesfeller, J., Prospero, J., Kinne, S., Bauer, S., Boucher, O., Chin, M., Dentener, F., Diehl, T., Easter, R., Fillmore, D., Ghan, S., Ginoux, P., Grini, A., Horowitz, L., Koch, D., Krol, M. C., … Zender, C. S. (2011). Global dust model intercomparison in AeroCom phase I. *Atmospheric Chemistry and Physics, 11*, 7781–7816. https://doi.org/10.5194/acp-11-7781-2011

Ingall, E. D., Feng, Y., Longo, A. F., Lai, B., Shelley, R. U., Landing, W. M., Morton, P. L., Nenes, A., Mihalopoulos, N., Violaki, K., Gao, Y., Sahai, S., & Castorina, E. (2018). Enhanced iron solubility at low pH in global aerosols. *Atmosphere, 9*, 201. https://doi.org/10.3390/atmos9050201

Ito, T., Nenes, A., Johnson, M. S., Meskhidze, N., & Deutsch, C. (2016). Acceleration of oxygen decline in the tropical Pacific over the past decades by aerosol pollutants. *Nature Geoscience, 9*, 443–447. https://doi.org/10.1038/NGEO2717

Ito, A., Myriokefalitakis, S., Kanakidou, M., Mahowald, N. M., Scanza, R. A., Hamilton, D. S., Baker, A. R., Jickells, T., Sarin, M., Bikkina, S., Gao, Y., Shelley, R. U., Buck, C. S., Landing, W. M., Bowie, A. R., Perron, M. M. G., Guieu, C., Meskhidze, N., Johnson, M. S., … Duce, R. A. (2019). Pyrogenic iron: The missing link to high iron solubility in aerosols. *Science Advances, 5*, eaau7671. https://doi.org/10.1126/sciadv.aau7671

Jacob, D. J. (2000). Heterogeneous chemistry and tropospheric ozone. *Atmospheric Environment, 34*, 2131–2159. https://doi.org/10.1016/S1352-2310(99)00462-8

James, A. D., Moon, D. R., Feng, W., Lakey, P. S. J., Frankland, V. L., Heard, D. E., & Plane, J. M. C. (2017). The uptake of HO_2 on meteoric smoke analogues. *Journal of Geophysical Research – Atmospheres, 122*, 554–565. https://doi.org/10.1002/2016JD02588

Jiang, H., Frie, A. L., Lavi, A., Chen, J. Y., Zhang, H., Bahreini, R., & Lin, Y.-H. (2019). Brown carbon formation from nighttime chemistry of unsaturated heterocyclic volatile organic compounds. *Environmental Science & Technology Letters, 6*, 184–190. https://doi.org/10.1021/acs.estlett.9b00017.s001

Kakavas, S., Patoulias, D., Zakoura, M., Nenes, A., & Pandis, S. N. (2021). Size-resolved aerosol pH over Europe during summer, *Atmospheric Chemistry and Physics, 21*, 799–811. https://doi.org/10.5194/acp-21-799-2021

Kalivitis, N., Papatheodorou, S., Maesano, C. N., & Annesi-Maesano, I. (2022). Air quality and health impacts. In F. Dulac, S. Sauvage, & E. Hamonou (Eds.), *Atmospheric chemistry in the Mediterranean Region* (Vol. 2, From air pollutant sources to impacts). Springer, this volume. https://doi.org/10.1007/978-3-030-82385-6_22

Kanakidou, M., Mihalopoulos, N., Kindap, T., Im, U., Vrekoussis, M., Gerasopoulos, E., Dermitzaki, E., Unal, A., Kocak, M., Markakis, K., Melas, D., Kouvarakis, G., Youssef, A. F., Richter, A., Hatzianastassiou, N., Hilboll, A., Ebojie, F., Wittrock, F., von Savigny, C., & Burrows, J. P. (2011). Megacities as hot spots of air pollution in the East Mediterranean. *Atmospheric Environment, 45*, 1223–1235. https://doi.org/10.1016/j.atmosenv.2010.11.048

Kanakidou, M., Myriokefalitakis, S., & Tsigaridis, K. (2018). Aerosols in atmospheric chemistry and biogeochemical cycles of nutrients. *Environmental Research Letters, 13*, 063004. https://doi.org/10.1088/1748-9326/aabcdb

Kanakidou, M., Myriokefalitakis, S., & Tsagkaraki, M. (2020). Atmospheric inputs of nutrients to the Mediterranean Sea. *Deep-Sea Research Part II, 171*, 104606. https://doi.org/10.1016/j.dsr2.2019.06.014

Kanakidou, M., Sfakianaki, M., & Probst, A. (2022). Impact of air pollution on terrestrial ecosystems. In F. Dulac, S. Sauvage, & E. Hamonou (Eds.), *Atmospheric chemistry in the Mediterranean Region* (Vol. 2, From air pollutant sources to impacts). Springer, this volume. https://doi.org/10.1007/978-3-030-82385-6_24

Karagulian, F., & Rossi, M. J. (2005). The heterogeneous chemical kinetics of NO_3 on atmospheric mineral dust surrogates. *Physical Chemistry Chemical Physics, 7*, 3150–3162. https://doi.org/10.1039/B506750M

Karydis, V. A., Tsimpidi, A. P., Pozzer, A., Astitha, M., & Lelieveld, J. (2016). Effects of mineral dust on global atmospheric nitrate concentrations. *Atmospheric Chemistry and Physics, 16*, 1491–1509. https://doi.org/10.5194/acp-16-1491-2016

Kaskaoutis, D., Liakakou, E., Grivas, G., Gerasopoulos, E., Mihalopoulos, N., Alastuey, A., Dulac, F., Pandolfi, M., Sciare, J., & Titos, G. (2023). Chemical composition and levels of concentrations of aerosols in the Mediterranean. In F. Dulac, S. Sauvage, & E. Hamonou (Eds.), *Atmospheric chemistry in the Mediterranean Region* (Vol. 1, Background information and pollutants distribution). Springer.

Kok, J. F., Ridley, D. A., Zhou, Q., Zhao, C., Miller, R. L., Heald, C. L., Ward, D. S., Albani, S., & Haustein, K. (2017). Smaller desert dust cooling effect estimated from analysis of desert dust size and abundance. *Nature Geoscience, 10*, 274–278. https://doi.org/10.1038/NGEO2912

Kolb, C. E., Worsnop, D. R., Zahniser, M. S., Davidovits, P., Keyser, L. F., Leu, M.-T., Molina, M. J., Hanson, D. R., Ravishankara, A. R., Williams, L. R., & Tolbert, M. A. (1995) Laboratory studies of atmospheric heterogeneous chemistry. In *Progress and problems in atmospheric chemistry*, J. R. Barker (Ed.), *Advanced Series in Physical Chemistry*, *3*, 771-875, World Science, River Edge, NJ, https://doi.org/10.1142/9789812831712_0018

Kouvarakis, G., Doukelis, Y., Mihalopoulos, N., Rapsomanikis, S., Sciare, J., & Blumthaler, M. (2002). Chemical, physical, and optical characterization of aerosols during PAUR II experiment. *Journal of Geophysical Research, 107*, 8141. https://doi.org/10.1029/2000JD000291

Landgraf, J., & Crutzen, P. J. (1998). An efficient method for online calculations of photolysis and heating rates, *Journal of the Atmospheric Sciences*, 55863–55878, https://doi.org/10.1175/1520-0469(1998)055<0863:AEMFOC>2.0.CO;2

Liao, H., & Seinfeld, J. H. (2005). Global impacts of gas-phase chemistry-aerosol interactions on direct radiative forcing by anthropogenic aerosols and ozone. *Journal of Geophysical Research, 110*, D18208. https://doi.org/10.1029/2005JD005907

Liao, H., Adams, P. J., Chung, S. H., Seinfeld, J. H., Mickley, L. J., & Jacob, D. J. (2003). Interactions between tropospheric chemistry and aerosols in a unified general circulation model. *Journal of Geophysical Research, 108*, 4001. https://doi.org/10.1029/2001JD001260

Lim, Y. B., Tan, Y., Perri, M. J., Seitzinger, S. P., & Turpin, B. J. (2010). Aqueous chemistry and its role in secondary organic aerosol (SOA) formation. *Atmospheric Chemistry and Physics, 10*, 10521–10539. https://doi.org/10.5194/acp-10-10521-2010

Liu, X., Huey, L. G., Yokelson, R. J., Selimovic, V., Simpson, I. J., Müller, M., Jimenez, J. L., Campuzano-Jost, P., Beyersdorf, A. J., Blake, D. R., Butterfield, Z., Choi, Y., Crounse, J. D., Day, D. A., Diskin, G. S., Dubey, M. K., Fortner, E., Hanisco, T. F., Hu, W., … Wolfe, G. M. (2017). Airborne measurements of western U.S. wildfire emissions: Comparison with prescribed burning and air quality implications. *Journal of Geophysical Research – Atmospheres, 122*, 6108–6129. https://doi.org/10.1002/2016JD026315

Mailler, S., Menut, L., di Sarra, A. G., Becagli, S., Di Iorio, T., Bessagnet, B., Briant, R., Formenti, P., Doussin, J.-F., Gómez-Amo, J. L., Mallet, M., Rea, G., Siour, G., Sferlazzo, D. M., Traversi, R., Udisti, R., & Turquety, S. (2016). On the radiative impact of aerosols on photolysis rates: Comparison of simulations and observations in the Lampedusa island during the ChArMEx/ADRIMED campaign. *Atmospheric Chemistry and Physics, 16*, 1219–1244. https://doi.org/10.5194/acp-16-1219-2016

Majdi, M., Sartelet, K., Lanzafame, G. M., Couvidat, F., Kim, Y., Chrit, M., & Turquety, S. (2019). Precursors and formation of secondary organic aerosols from wildfires in the Euro-Mediterranean region. *Atmospheric Chemistry and Physics, 19*, 5543–5569. https://doi.org/10.5194/acp-19-5543-2019

Mallet, M., di Sarra, A., Nabat, P., Solmon, F., Gutierrez, C., Mailler, S., Menut, L., Kaskaoutis, D., Rowlinson, M., & Rap, A. (2022). Aerosol and ozone direct radiative impact. In F. Dulac, S. Sauvage, & E. Hamonou (Eds.), *Atmospheric chemistry in the Mediterranean Region* (Vol. 2, From air pollutant sources to impacts). Springer, this volume. https://doi.org/10.1007/978-3-030-82385-6_19

Mao, J., Fan, S., Jacob, D. J., & Travis, K. R. (2013). Radical loss in the atmosphere from Cu-Fe redox coupling in aerosols. *Atmospheric Chemistry and Physics, 13*, 509–519. https://doi.org/10.5194/acp-13-509-2013

Markaki, Z., Oikonomou, K., Kocak, M., Kouvarakis, G., Chaniotaki, A., Kubilay, N., & Mihalopoulos, N. (2003). Atmospheric deposition of inorganic phosphorus in the Levantine Basin, eastern Mediterranean: Spatial and temporal variability and its role in seawater productivity. *Limnology and Oceanography, 48*, 1557–1568. https://doi.org/10.4319/lo.2003.48.4.1557

Markaki, Z., Loÿe-Pilot, M. D., Violaki, K., Benyahya, L., & Mihalopoulos, N. (2010). Variability of atmospheric deposition of dissolved nitrogen and phosphorus in the Mediterranean and possible link to the anomalous seawater N/P ratio. *Marine Chemistry, 120*, 187–194. https://doi.org/10.1016/j.marchem.2008.10.005

Masiol, M., Squizzato, S., Formenton, G., Md Badiuzzaman, K., Hopke, P. K., Nenes, A., Pandis, S. N., Tositti, L., Benetello, F., Visin, F., & Pavoni, B. (2020). Hybrid multiple-site mass closure and source apportionment of $PM_{2.5}$ and aerosol acidity at major cities in the Po Valley. *The Science of the Total Environment, 704*, 135287. https://doi.org/10.1016/j.scitotenv.2019.135287

Meskhidze, N., Chameides, W. L., Nenes, A., & Chen, G. (2003). Iron mobilization in mineral dust: Can anthropogenic SO_2 emissions affect ocean productivity? *Geophysical Research Letters, 30*, 2085. https://doi.org/10.1029/2003GL018035

Morgan, W. T., Ouyang, B., Allan, J. D., Aruffo, E., Di Carlo, P., Kennedy, O. J., Lowe, D., Flynn, M. J., Rosenberg, P. D., Williams, P. I., Jones, R., McFiggans, G. B., & Coe, H. (2015). Influence of aerosol chemical composition on N_2O_5 uptake: Airborne regional measurements in northwestern Europe. *Atmospheric Chemistry and Physics, 15*, 973–990. https://doi.org/10.5194/acp-15-973-2015

Myriokefalitakis, S., Tsigaridis, K., Mihalopoulos, N., Sciare, J., Nenes, A., Kawamura, K., Segers, A., & Kanakidou, M. (2011). Incloud oxalate formation in the global troposphere: A 3-D modeling study. *Atmospheric Chemistry and Physics, 11*, 5761–5782. https://doi.org/10.5194/acp-11-5761-2011

Myriokefalitakis, S., Daskalakis, N., Mihalopoulos, N., Baker, A. R., Nenes, A., & Kanakidou, M. (2015). Changes in dissolved iron deposition to the oceans driven by human activity: A 3-D global modelling study. *Biogeosciences, 12*, 3973–3992. https://doi.org/10.5194/bg-12-3973-2015

Myriokefalitakis, S., Nenes, A., Baker, A. R., Mihalopoulos, N., & Kanakidou, M. (2016). Bioavailable atmospheric phosphorous supply to the global ocean: A 3-D global modeling study. *Biogeosciences, 13*, 6519–6543. https://doi.org/10.5194/bg-13-6519-2016

Myriokefalitakis, S., Ito, A., Kanakidou, M., Nenes, A., Krol, M. C., Mahowald, N. M., Scanza, R. A., Hamilton, D. S., Johnson, M. S., Meskhidze, N., Kok, J. F., Guieu, C., Baker, A. R., Jickells, T. D., Sarin, M. M., Bikkina, S., Shelley, R., Bowie, A., Perron, M. M. G., & Duce, R. A. (2018). Reviews and syntheses: The GESAMP atmospheric iron deposition model intercomparison study. *Biogeosciences, 15*, 6659–6684. https://doi.org/10.5194/bg-15-6659-2018

Nenes, A., Krom, M. D., Mihalopoulos, N., Van Cappellen, P., Shi, Z., Bougiatioti, A., Zarmpas, P., & Herut, B. (2011). Atmospheric acidification of mineral aerosols: A source of bioavailable phosphorus for the oceans. *Atmospheric Chemistry and Physics, 11*, 6265–6272. https://doi.org/10.5194/acp-11-6265-2011

Nenes, A., Pandis, S. N., Weber, R. J., & Russell, A. (2020). Aerosol pH and liquid water content determine when particulate matter is sensitive to ammonia and nitrate availability. *Atmospheric Chemistry and Physics, 20*, 3249–3258. https://doi.org/10.5194/acp-20-3249-2020

Nenes, A., Pandis, S. N., Kanakidou, M., Russell, A., Song, S., Vasilakos, P., & Weber, R. J. (2021) Aerosol acidity and liquid water content regulate the dry deposition of inorganic reactive nitrogen, *Atmospheric Chemistry and Physics, 21*, 799–811, https://doi.org/10.5194/acp-21-799-2021

Nienow, A. M., & Roberts, J. T. (2006). Heterogeneous chemistry of carbon aerosols. *Annual Review of Physical Chemistry, 57*, 105–128. https://doi.org/10.1146/annurev.physchem.57.032905.104525

Pace, G., Meloni, D., & di Sarra, A. (2005). Forest fire aerosol over the Mediterranean basin during summer 2003. *Journal of Geophysical Research, 110*, D21202. https://doi.org/10.1029/2005JD005986

Paris, R., & Desboeufs, K. V. (2013). Effect of atmospheric organic complexation on iron-bearing dust solubility. *Atmospheric Chemistry and Physics, 13*, 4895–4905. https://doi.org/10.5194/acp-13-4895-2013

Paris, R., Desboeufs, K., & Journet, E. (2011). Variability of dust iron solubility in atmospheric waters: Investigation of the role of oxalate organic complexation. *Atmospheric Environment, 45*, 6510–6517. https://doi.org/10.1016/j.atmosenv.2011.08.068

Pechtl, S., & von Glasow, R. (2007). Reactive chlorine in the marine boundary layer in the outflow of polluted continental air: A model study. *Geophysical Research Letters, 34*, L11813. https://doi.org/10.1029/2007GL029761

Phillips, G. J., Tang, M. J., Thieser, J., Brickwedde, B., Schuster, G., Bohn, B., Lelieveld, J., & Crowley, J. N. (2012). Significant concentrations of nitryl chloride observed in rural continental Europe associated with the influence of sea salt chloride and anthropogenic emissions. *Geophysical Research Letters, 39*, L10811. https://doi.org/10.1029/2012GL051912

Phillips, G. J., Thieser, J., Tang, M., Sobanski, N., Schuster, G., Fachinger, J., Drewnick, F., Borrmann, S., Bingemer, H., Lelieveld, J., & Crowley, J. N. (2016). Estimating N_2O_5 uptake coefficients using ambient measurements of NO_3, N_2O_5, $ClNO_2$ and particle-phase nitrate. *Atmospheric Chemistry and Physics, 16*, 13231–13249. https://doi.org/10.5194/acp-16-13231-2016

Pradhan, M., Kalberer, M., Griffiths, P. T., Braban, C. F., Pope, F. D., Cox, R. A., & Lambert, R. M. (2010a). Uptake of gaseous hydrogen peroxide by submicrometer titanium dioxide aerosol as a function of relative humidity. *Environmental Science & Technology, 44*, 1360–1365. https://doi.org/10.1021/es902916f

Pradhan, M., Kyriakou, G., Archibald, A. T., Papageorgiou, A. C., Kalberer, M., & Lambert, R. M. (2010b). Heterogeneous uptake of gaseous hydrogen peroxide by Gobi and Saharan dust aerosols: A potential missing sink for H2O2 in the troposphere. *Atmospheric Chemistry and Physics, 10*, 7127–7136. https://doi.org/10.5194/acp-10-7127-2010

Pye, H. O. T., Nenes, A., Alexander, B., Ault, A. P., Barth, M. C., Clegg, S. L., Collett, J. L., Jr., Fahey, K. M., Hennigan, C. J., Herrmann, H., Kanakidou, M., Kelly, J. T., Ku, I.-T., McNeill, V. F., Riemer, N., Schaefer, T., Shi, G., Tilgner, A., Walker, J. T., … Zuend, A. (2020). The acidity of atmospheric particles and clouds. *Atmospheric Chemistry and Physics, 20*, 4809–4888. https://doi.org/10.5194/acp-20-4809-2020

Ragosti, N., & Sarin, M. M. (2005). Long-term characterization of ionic species in aerosols from urban and high-altitude sites in western India: Role of mineral dust and anthropogenic sources. *Atmospheric Environment, 39*, 5541–5554. https://doi.org/10.1016/j.atmosenv.2005.06.011

Renard, J.-B., Dulac, F., Durand, P., Bourgeois, Q., Denjean, C., Vignelles, D., Couté, B., Jeannot, M., Verdier, N., & Mallet, M. (2018). In situ measurements of desert dust particles above the western Mediterranean Sea with the balloon-borne Light Optical Aerosol Counter/sizer (LOAC) during the ChArMEx campaign of summer 2013. *Atmos. Chem. Phys., 18*, 3677–3699. https://doi.org/10.5194/acp-18-3677-2018

Romanias, M. N., El Zein, A., & Bedjanian, Y. (2012a). Heterogeneous interaction of H_2O_2 with TiO_2 surface under dark and UV light irradiation conditions. *The Journal of Physical Chemistry. A, 116*, 8191–8200. https://doi.org/10.1021/jp305366v

Romanias, M. N., El Zein, A., & Bedjanian, Y. (2012b). Reactive uptake of HONO on aluminium oxide surface. *Journal of Photochemistry and Photobiology A-Chemistry, 250*, 50–57. https://doi.org/10.1016/j.jphotochem.2012.09.018

Rossi, M. (2003). Heterogeneous reactions on salts. *Chemical Reviews, 103*, 4823–4882. https://doi.org/10.1021/cr020507n

Samburova, V., Connolly, J., Gyawali, M., Yatavelli, R. L. N., Watts, A. C., Chakrabarty, R. K., Zielinska, B., Moosmüller, H., & Khlystov, A. (2016). Polycyclic aromatic hydrocarbons in biomass-burning emissions and their contribution to light absorption and aerosol toxicity, *Science of the Total Environment*, 391–401, https://doi.org/10.1016/j.scitotenv.2016.06.026

Saydam, A. C., & Senyuva, H. Z. (2002). Deserts: Can they be the potential suppliers of bioavailable iron? *Geophys. Res. Lett., 29*, 1524. https://doi.org/10.1029/2001GL013562

Seinfeld, J. H., & Pandis, S. N. (2016). *Atmospheric chemistry and physics: From air pollution to climate change* (3rd ed., 1152 pp.). Wiley. ISBN 978-1-118-94740-1.

Seisel, S., Börensen, C., Vogt, R., & Zellner, R. (2005). Kinetics and mechanism of the uptake of N2O5 on mineral dust at 298 K. *Atmospheric Chemistry and Physics, 5*, 3423–3432. https://doi.org/10.5194/acp-5-3423-2005

Shen, X., Zhao, Y., Chen, Z., & Huang, D. (2013). Heterogeneous reactions of volatile organic compounds in the atmosphere. *Atmospheric Environment, 68*, 297–314. https://doi.org/10.1016/j.atmosenv.2012.11.027

Shi, Z., Bonneville, S., Krom, M. D., Carslaw, K. S., Jickells, T. D., Baker, A. R., & Benning, L. G. (2011). Iron dissolution kinetics of mineral dust at low pH during simulated atmospheric

processing. *Atmospheric Chemistry and Physics, 11*, 995–1007. https://doi.org/10.5194/acp-11-995-2011

Shi, Z., Krom, M. D., Jickells, T. D., Bonneville, S., Carslaw, K. S., Mihalopoulos, N., Baker, A. R., & Benning, L. G. (2012). Impacts on iron solubility in the mineral dust by processes in the source region and the atmosphere: A review. *Aeolian Research, 5*, 21–42. https://doi.org/10.1016/j.aeolia.2012.03.001

Shrivastava, M., Cappa, C. D., Fan, J., Goldstein, A. H., Guenther, A. B., Jimenez, J. L., Kuang, C., Laskin, A., Martin, S. T., Ng, N. L., Petaja, T., Pierce, J. R., Rasch, P. J., Roldin, P., Seinfeld, J. H., Shilling, J., Smith, J. N., Thornton, J. A., Volkamer, R., … Zhang, Q. (2017). Recent advances in understanding secondary organic aerosol: Implications for global climate forcing. *Reviews of Geophysics, 55*, 509–559. https://doi.org/10.1002/2016RG000540

Squizzato, S., Masiol, M., Brunelli, A., Pistollato, S., Tarabotti, E., Rampazzo, G., & Pavoni, B. (2013). Factors determining the formation of secondary inorganic aerosol: A case study in the Po Valley (Italy). *Atmospheric Chemistry and Physics, 13*, 1927–1939. https://doi.org/10.5194/acp-13-1927-2013

Stadtler, S., Simpson, D., Schröder, S., Taraborrelli, D., Bott, A., & Schultz, M. (2018). Ozone impacts of gas–aerosol uptake in global chemistry transport models. *Atmospheric Chemistry and Physics, 18*, 3147–3171. https://doi.org/10.5194/acp-18-3147-2018

Stockdale, A., Krom, M. D., Mortimer, R. J. G., Benning, L. G., Carslaw, K. S., Herbert, R. J., Shi, Z., Myriokefalitakis, S., Kanakidou, M., & Nenes, A. (2016). Understanding the nature of atmospheric acid processing of mineral dusts in supplying bioavailable phosphorus to the oceans. *Proceedings of the National Academy of Sciences USA, 113*, 14639–14644. https://doi.org/10.1073/pnas.1608136113

Tang, Y., Carmichael, G. R., Kurata, G., Uno, I., Weber, R. J., Song, C. H., Guttikunda, S. K., Woo, J. H., Streets, D. G., Wei, C., Clarke, A. D., Huebert, B., & Anderson, T. L. (2004). Impacts of dust on regional tropospheric chemistry during the ACE-Asia Experiment: A model study with observations. *Journal of Geophysical Research, 109*, D19S21. https://doi.org/10.1029/2003jd003806

Tang, M., Huang, X., Lu, K., Ge, M., Li, Y., Cheng, P., Zhu, T., Ding, A., Zhang, Y., Gligorovski, S., Song, W., Ding, X., Bi, X., & Wang, X. (2017). Heterogeneous reactions of mineral dust aerosol: Implications for tropospheric oxidation capacity. *Atmospheric Chemistry and Physics, 17*, 11727–11777. https://doi.org/10.5194/acp-17-11727-2017

Theodosi, C., Markaki, Z., & Mihalopoulos, N. (2010). Iron speciation, solubility and temporal variability in wet and dry deposition in the Eastern Mediterranean. *Marine Chemistry, 120*, 100–107. https://doi.org/10.1016/j.marchem.2008.05.004

Thornton, J. A., Kercher, J. P., Riedel, T. P., Wagner, N. L., Cozic, J., Holloway, J. S., Dube, W. P., Wolfe, G. M., Quinn, P. K., Middlebrook, A. M., Alexander, B., & Brown, S. S. (2010). A large atomic chlorine source inferred from mid-continental reactive nitrogen chemistry. *Nature, 464*, 271–274. https://doi.org/10.1038/nature08905

Usher, C. R., Michel, A. E., & Grassian, V. H. (2003). Reactions on mineral dust. *Chemical Reviews, 103*, 4883–4940. https://doi.org/10.1021/cr020657y

van Vuuren, D. P., Edmonds, J., Kainuma, M., Riahi, K., Thomson, A., Hibbard, K., Hurtt, G. C., Kram, T., Krey, V., Lamarque, J.-F., Masui, T., Meinshausen, M., Nakicenovic, N., Smith, S. J., & Rose, S. K. (2011). The representative concentration pathways: An overview. *Climatic Change, 109*, 5–31. https://doi.org/10.1007/s10584-011-0148-z

Vasilakos, P., Russell, A., Weber, R., & Nenes, A. (2018). Understanding nitrate formation in a world with less sulfate. *Atmospheric Chemistry and Physics, 18*, 12765–12775. https://doi.org/10.5194/acp-18-12765-2018

von Glasow, R. (2008). Pollution meets sea salt. *Nature Geoscience, 1*, 292–293. https://doi.org/10.1038/ngeo192

Vrekoussis, M., Liakakou, H., Mihalopoulos, N., Kanakidou, M., Crutzen, P. J., & Lelieveld, J. (2006). Formation of HNO_3 and NO_3^- in the anthropogenically-influenced eastern Mediterranean marine boundary layer. *Geophysical Research Letters, 33*, L05811. https://doi.org/10.1029/2005GL025069

Vrekoussis, M., Mihalopoulos, N., Gerasopoulos, E., Kanakidou, M., Crutzen, P. J., & Lelieveld, J. (2007). Two-years of NO_3 radical observations in the boundary layer over the Eastern Mediterranean. *Atmospheric Chemistry and Physics, 7*, 315–327. https://doi.org/10.5194/acp-7-315-2007

Wang, T., Tham, Y. J., Xue, L., Li, Q., Zha, Q., Wang, Z., Poon, S. C. N., Dubé, W. P., Blake, D. R., Louie, P. K. K., Luk, C. W. Y., Tsui, W., & Brown, S. S. (2016). Observations of nitryl chloride and modeling its source and effect on ozone in the planetary boundary layer of southern China. *Journal of Geophysical Research – Atmospheres, 121*, 2476–2489. https://doi.org/10.1002/2015JD024556

Wang, W., Li, X., Shao, M., Hu, M., Zeng, L., Wu, Y., & Tan, T. (2019). The impact of aerosols on photolysis frequencies and ozone production in Beijing during the 4-year period 2012–2015. *Atmospheric Chemistry and Physics, 19*, 9413–9429. https://doi.org/10.5194/acp-19-9413-2019

Weber, R. J., Guo, H., Russell, A. G., & Nenes, A. (2016). High aerosol acidity despite declining atmospheric sulfate concentrations over the past 15 years. *Nature Geoscience, 9*, 282–285. https://doi.org/10.1038/ngeo2665

Wong, J. P. S., Tsagkaraki, M., Tsiodra, I., Mihalopoulos, N., Violaki, K., Kanakidou, M., Sciare, J., Nenes, A., & Weber, R. J. (2019). Atmospheric evolution of molecular-weight-separated brown carbon from biomass burning. *Atmospheric Chemistry and Physics, 19*, 7319–7334. https://doi.org/10.5194/acp-19-7319-2019

Xu, L., Guo, H., Boyd, C., Bougiatioti, A., Cerully, K., Hite, J., Isaacman, G., Olson, K., Goldstein, A., Kosse, A., Gouw, J. D., Baumann, K., Knote, C., Lee, S., Weber, R., Nenes, A., & Ng, N. L. (2015). Effects of anthropogenic emissions on aerosol formation from isoprene and monoterpenes in the Southeastern United States: Insights from SOAS and beyond. *Proceedings of the National Academy of Sciences of the United States of America, 112*, 37–42. https://doi.org/10.1073/pnas.1417609112

Xu, L., Middlebrook, A. M., Liao, J., deGouw, J., Guo, H., Weber, R. J., Nenes, A., Lee, B. H., Thornton, J. A., Brock, C., Trainer, M. K., Neuman, J. A., Nowak, J. B., Pollack, I. B., Ryerson, T. B., Hanisco, T. F., Wennberg, P. O., Schwarz, J. P., Welti, A., … Ng, N. L. (2016). Enhanced formation of isoprene-derived organic aerosol in power plant plumes during Southeast Nexus (SENEX). *Journal of Geophysical Research-Atmospheres, 121*, 11137–11153. https://doi.org/10.1002/2016JD025156

Zakoura, M., Kakavas, S., Nenes, A., & Pandis, S. N. (2020) Size-resolved aerosol pH over Europe during summer, *Atmospheric Chemistry and Physics Discussions*, https://doi.org/10.5194/acp-2019-1146, accepted.

Zender, C. S., Bian, H., & Newman, D. (2003). Mineral Dust Entrainment and Deposition (DEAD) model: Description and 1990s dust climatology. *Journal of Geophysical Research, 108*, 4416. https://doi.org/10.1029/2002JD002775

Zhao, Y., Chen, Z., Shen, X., & Huang, D. (2013). Heterogeneous reactions of gaseous hydrogen peroxide on pristine and acidic gas-processed calcium carbonate particles: Effects of relative humidity and surface coverage of coating. *Atmospheric Environment, 67*, 63–72. https://doi.org/10.1016/j.atmosenv.2012.10.055

Zhu, S., Butler, T., Sander, R., Ma, J., & Lawrence, M. G. (2010). Impact of dust on tropospheric chemistry over polluted regions: A case study of the Beijing megacity. *Atmospheric Chemistry and Physics, 10*, 3855–3873. https://doi.org/10.5194/acp-10-3855-2010

Zhu, T., Shang, J., & Zhao, D. F. (2011). The roles of heterogeneous chemical processes in the formation of an air pollution complex and gray haze. *Science China. Chemistry, 54*, 145–153. https://doi.org/10.1007/s11426-010-4181-y

Part X
Impacts of Air Pollution on Human Health and Ecosystems

Coordinated by ***Maria Kanakidou***

Environmental Chemical Processes Laboratory, Department of Chemistry, University of Crete (UOC), Vassilika Vouton, 70013 Heraklion, Greece

Reviewed by ***Semia Cherif*** *(ISSBAT, University of Tunis El Manar, Tunisia)*

Abstract
This section reviews current knowledge on the impacts of air pollution on human health as well as marine and terrestrial ecosystems in the Mediterranean. The first chapter summarizes the human health studies in the region, with special focus on the impact of dust and biomass burning events. The last two chapters concentrate on the impact of air quality on the marine and terrestrial ecosystems summarizing relevant knowledge from studies performed in the Mediterranean. Results from process studies and observations at sea that have been conducted over the past decade are summarized along with recent findings from a numerical marine biogeochemical model that accounts for atmospheric deposition. Effects of air pollution on vegetation occurring either indirectly through changes in the physical state of the atmosphere (temperature, diffuse radiation) or directly through phytotoxicity, as well as plant physiological responses to an excess of critical nutrient levels are presented and discussed.

Air Quality and Health Impacts

Nikolaos Kalivitis, Stefania Papatheodorou, Cara Nichole Maesano, and Isabella Annesi-Maesano

Contents

Abstract Associations between air pollution and overall morbidity and mortality have long been identified in Europe. Epidemiological studies have shown that there is an increased risk of cardiovascular and respiratory morbidity and mortality due to exposures from both particulate and gaseous pollutants such as ozone. The Mediterranean basin is under the influence of both transported and locally emitted primary and secondary air pollutants. The region is particularly susceptible to Saharan dust transport episodes, and there are several studies linking these with

*Chapter reviewed by **Laurent Alleman** (IMT Nord Europe, Institut Mines-Télécom Univ. de Lille, Lille, France), as part of the book Part X Impacts of Air Pollution on Human Health and Ecosystems also reviewed by **Semia Cherif** (ISSBAT, University of Tunis El Manar, Tunisia)*

N. Kalivitis (✉)
Environmental Chemical Processes Laboratory (ECPL), Department of Chemistry, University of Crete, Heraklion, Greece
e-mail: nkalivitis@uoc.gr

S. Papatheodorou
Department of Epidemiology, Harvard TH Chan School of Public Health, Boston, MA, USA

C. N. Maesano · I. Annesi-Maesano
INSERM, Université de Montpellier, DESP IURC, Montpellier, France

F. Dulac et al. (eds.), *Atmospheric Chemistry in the Mediterranean Region*,
https://doi.org/10.1007/978-3-030-82385-6_22

increased all-cause and respiratory mortality. However, there is a need for in-depth studies of these events and their connection to public health. Associations between air pollution resulting from biomass burning and morbidity and mortality have also been highlighted. Recent data show that air pollution, through various mechanisms, impacts not only the lungs and heart but other organs as well. Additionally, climate change is expected to introduce further challenges, including impacts on air quality and the synergistic effects of heat and air pollution, especially in areas already vulnerable to climate change. This chapter summarizes the exposure of the population to atmospheric pollutants, the short- and long-term health effects of air quality, and mitigation and adaptation strategies for the Mediterranean region.

1 Introduction

The Mediterranean region is greatly affected by the long-range transport of natural and anthropogenic pollution. This includes anthropogenic pollutants from industrialized continental Europe and the densely urbanized coastline, frequent desert dust from the arid areas of northern Africa and the Middle East, and biomass burning products from combustion sources and wildfires (Lelieveld et al., 2002). The European Environment Agency (EEA) estimates that air pollution in Europe continues to be responsible for 412,000 premature deaths attributed to $PM_{2.5}$ exposure, 71,000 to NO_2 exposure, and 15,100 to O_3 exposure (EEA, 2019). In the eastern Mediterranean, it is estimated that almost 200,000 people lost their lives in 2012 because of air pollution (WHO, 2016). Associations between short-term air pollution and overall mortality have long been identified in the Mediterranean (Katsouyanni et al., 1990). Epidemiological studies have shown that there is an increased risk of cardiovascular and respiratory mortality due to both particulate (e.g., Perez et al., 2008; Neophytou et al., 2013) and gaseous pollutants (e.g., Parodi et al., 2005). Saharan dust transport episodes are also important in the Mediterranean region, and there are several studies linking them with adverse health impacts. However, a detailed review has emphasized the need for an in-depth study of these events and their connection to public health (Karanasiou et al., 2012). Biomass burning pollutants and mortality have also been associated in the region (Faustini et al., 2015). Furthermore, effects of long-term exposure to ambient air pollution, especially due to fine particulate matter, have been associated with natural-cause mortality (Beelen et al., 2014) and cardiovascular- and respiratory-related fatalities (Sanyal et al., 2018). Strong relationships between the frequency of hospitalizations due to respiratory and cardiovascular diseases and air pollution have been reported as well (Middleton et al., 2008), especially with regard to children (Samoli et al., 2011). Air pollution also may further contribute to lung cancer incidence (Raaschou-Nielsen et al., 2013).

This section presents data on the relationship between air pollution and health effects at the population level in the Mediterranean region by addressing the

assessment and quantification of individual exposure to atmospheric pollutants, the short- and long-term effects of air quality on health, and mitigation and adaptation strategies. Priority will be given to cardiopulmonary diseases for which evidence is greater.

2 Assessing Air Pollution Exposure at the Individual Level

2.1 Level of Exposure

In Europe, the major air pollutants monitored and regulated include gases, such as nitrogen dioxide (NO_2), ozone (O_3), sulfur dioxide (SO_2), and particulate matter (PM), namely, PM_{10}, with a 50% cutoff aerodynamic diameter of 10 μm, and $PM_{2.5}$, with a cutoff diameter of 2.5 μm (fine particles), including the particulate benzo[a]pyrene (BaP) (Table 1). Long- and short-term exposure to these air pollutants have different adverse health impacts on humans including respiratory and cardiovascular diseases, neuropsychiatric complications, metabolic conditions, cancer, fetal growth, and low birth weight. Of relevance in terms of health implications due to its increased ability to travel deep into the lungs and permeate the bloodstream, smaller particulate matter, known as ultrafine particles (UFPs), with an aerodynamic diameter of less than 0.1 μm is also beginning to be monitored but is not yet regulated in Europe.

NO_2 pollutes the air mainly as a result of road traffic and energy production through fossil fuel combustion. While stratospheric O_3 acts as a beneficial filter for UV radiation from the sun, tropospheric O_3 is considered a pollutant and has negative consequences for human health. It is generated from other air pollutants, such

Table 1 European Union (EU) reference values and World Health Organization (WHO) air quality guidelines (AQGs) for the main air pollutants (Annesi-Maesano, 2017). PM_x particles with a 50% cutoff aerodynamic diameter of x μm, NO_2 nitrogen dioxide, O_3 ozone, SO_2 sulfur dioxide, BaP benzo[a]pyrene

Compound	EU reference value	WHO AQGs
$PM_{2.5}$	25 μg m^{-3} annual mean	10 μg m^{-3} annual mean 25 μg m^{-3} 24-h mean
PM_{10}	40 μg m^{-3} annual mean 50 μg m^{-3} 24-h mean (not to be exceeded on >35 days per year)	20 μg m^{-3} annual mean 50 μg m^{-3} 24-h mean
NO_2	40 μg m^{-3} annual mean 200 μg m^{-3} 1-h mean	40 μg m^{-3} annual mean 200 μg m^{-3} 1-h mean
O_3	120 μg m^{-3} 8-h mean	100 μg m^{-3} 8-h mean
SO_2	125 μg m^{-3} 24-h mean (not to be exceeded on >3 days per year)	20 μg m^{-3} 24-h mean 500 μg m^{-3} 10-min mean
BaP	1 ng m^{-3} annual mean	

as oxides of nitrogen (NO_x), carbon monoxide (CO), and non-methane volatile organic compounds (NMVOCs), through UV photochemical reactions, resulting in higher ozone levels during summer months. O_3 can also vanish when it reacts with other pollutants; hence, in Europe, O_3 levels tend to be lower in urban polluted areas than in semi-urban regions. SO_2 has disappeared in the Mediterranean except nearby sources.

Particulate matter is the sum of all solid and liquid particles suspended in air and is produced from both anthropogenic (traffic, domestic combustion, agricultural operations, industrial processes, combustion of wood and fossil fuels, and construction and demolition activities) and natural (windblown dust, wildfires and volcano eruptions) activities. Particles range in both size and chemical composition. Particles are considered primary or secondary, according to whether they are directly emitted from a source (primary particles) or formed in the air by transformation of gaseous emissions (secondary particles). The contaminants, namely, oxides of sulfur, NOx, VOCs, and ammonia (NH_3), form secondary particulate matter as a result of both human and natural activities (see the chapter by Sartelet, 2022). In Europe, sulfates, nitrates, and organic matter are the primary components of particulate air pollution in terms of particle mass, whereas in North Africa, the main contributor to particle mass is crustal matter of desert dust (Kchih et al., 2015; Terrouche et al., 2016). As reported by the European Environmental Agency (EEA), even though air quality in Europe has improved over recent decades, the levels of air pollutants still exceed EU standards and, a fortiori, the most stringent World Health Organization guidelines. In addition, in some sites, concentrations of monitored air pollutants have never significantly diminished (Annesi-Maesano, 2017).

According to the EEA, estimations from the period 2014 to 2016 showed that a significant proportion of the urban population in the EU-28 was exposed to concentrations of certain air pollutants above EU limit or target values, despite prior reductions in emissions. The number of people exposed was even higher when more stringent WHO air quality guidelines were applied (Table 1). For $PM_{2.5}$, 6–8% of the EU-28 urban population was exposed to concentrations in excess of the EU limit value of 25 μg m^{-3}, while 74–85% was exposed to concentrations above the former WHO guideline value of 10 μg m^{-3}. For PM_{10}, the respective exposure estimates were 13–19% above the EU limit value of 40 μg m^{-3} and 42–52% above the former WHO guideline value of 20 μg m^{-3}. For NO_2, the estimates were 7–8% above both the EU limit and the WHO guideline values, and for O_3, the estimates were 7–30% above the EU target value and 95–98% above the WHO guideline value.

2.2 Methods for Assessing Exposure

Studies assessing the health impact of air pollution require accurate exposure assessments at the individual level. Unfortunately, a precise measurement of exposure for any given person at a particular moment in time or for a specific duration is complicated and often unfeasible. Instead, several methods have been used to estimate

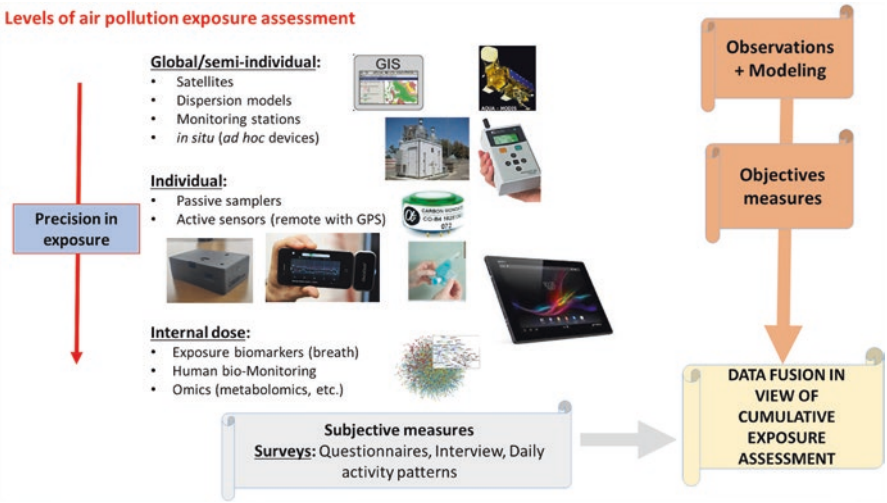

Fig. 1 Methods for assessing air pollution in health impact investigations

exposure and approximate averages over the course of a defined period. These methods range from satellite observations of the earth to personal measurements of specific biomarkers (Fig. 1). They are divided into "semi-individual," i.e., attributing the same exposure assessment to several individuals at once, and "individual" when a measurement for a given pollutant can be done for a specific person. Additionally, while direct measurements of pollutant concentration values may be obtained and applied to anyone within a given radius in some locations, there are many regions, cities, and countries that do not have the capacity for such measurements, and concentration values are produced instead through modeling.

Earth-observing satellite measurements have been found to be an important source of data for modeling PM concentrations in places where air pollution is not monitored and indeed can cover the entire globe (van Donkelaar et al., 2010). Satellites measure a quantity called aerosol optical depth (AOD), which is a measure of the extinction of reflected sunlight by dust, haze, and other aerosols, including particulate matter. AOD is a dimensionless number that is related to the amount of aerosol in the vertical column of atmosphere over the observation location. Models can then combine this information with ground-based measurements in order to extrapolate an assessment of $PM_{2.5}$, for example, at a fixed spatial and temporal resolution.

Some studies have provided estimates of $PM_{2.5}$ using a combined geophysical-statistical method with information from satellites, models, and monitors providing ground-based observations of $PM_{2.5}$ concentrations (van Donkelaar et al., 2016). Additional sources of information have been used to estimate PM speciation, for example, with the GEOS-Chem chemical transport model. Multiple studies have reliably shown the use of exposure assessment from satellite-based models to general (Hu, 2009; Andersen et al., 2012), as well as to specific, health disorders due to

distinct dust events (Goudie, 2014). However, the most important application of long-term exposure to $PM_{2.5}$ to health, as assessed by satellite, is provided by the GBD assessment, the World Health Organization (WHO, 2016) assessment (http://www.who.int/gho/phe/outdoor_air_pollution/burden/en/), and the Environmental Performance Index (http://epi.yale.edu).

Both individual and semi-individual assessments can be made starting from fixed monitoring stations, which are often scattered throughout an urban area and maintained by a governmental organization. Most of the investigations on the health impacts of air pollution in Europe have been done using values obtained from monitoring stations (Samoli et al., 2011). These air pollutant concentrations are combined with models and in situ temporary device measurements to get higher resolution and to include unmonitored locations to study the health impact of air pollution, as in the case of national dispersion models (Gandini et al., 2018; Sanyal et al., 2018).

One approach largely used in many European epidemiological investigations covering unmonitored locations is the land-use regression (LUR) model. This model is based on monitored patterns of the air pollutant of interest to estimate its concentrations in a particular area. LUR requires input on the environmental characteristics of the area, especially those that influence air pollutant emission intensity and dispersion efficiency such as traffic, topography, and other geographic variables. The LUR algorithm uses a multivariate regression model with the monitored levels of the air pollutant of interest as the dependent variable and all the other variables as the independent variables. LUR often relies on geographic information systems (GIS) to collect measurements. Using the parameter estimates derived from the regression model, levels of air pollution are predicted for any location, even for individual homes, thus providing individual assessments. As an example, LUR has been used in the ESCAPE (http://www.escapeproject.eu) project (Wang et al., 2014).

True individual assessments have recently become a reality. The field of small or individual portable air quality sensors is of growing interest within the scientific community, especially because this new technology is expected to both improve air pollutant monitoring by aggregating data from multiple devices, as well as be used for personal exposure quantification. While these sensors are not as robust or as accurate as those at fixed stations, they allow for monitoring real-time exposure to major air pollution, and collectively, they can provide much more detail for a given region and cover a larger area, as well as provide useful comparisons between one location and another. Because they are cheaper and easier to maintain, these sensors can be deployed in greater numbers in places where air pollution monitors have been lacking.

In terms of personal exposure, measurements from these sensors, despite the variability in performance, may potentially be able to determine a more accurate assessment of one's individual exposure than that of a fixed monitor by virtue of considering location-dependent variations, time spent indoors, and other factors that vary from person to person. In Europe, one example of a personal air pollution monitor used in epidemiological studies is the Canarin, a portable device carried by the individual that continuously measures exposures to $PM_{2.5}$ at 60 second intervals

automatically sending data in real time to a cloud-based server (Languille et al., 2020). These devices have allowed individuals in a given epidemiological cohort to have their own unique exposure assessment rather than a blanket value given to everyone living in a specific area.

Previously, many epidemiological studies have also considered various proxies to air pollution exposure for an individual, including proximity to air pollution sources, such as major roads, freeways, or industrial sites, with different size buffers assessed using a GIS, responses to questionnaires on the amount of traffic near the home, or percentages of the urban space near their residence or place of work. These surrogate parameters have shown their value in epidemiology by allowing assessments of adverse effects of air pollutants (Ranzi et al., 2014).

3 Short-Term Effects

3.1 The Effect of Particulate Matter on Human Health

The relationship between particulate matter and daily mortality and hospital admissions has been well documented in various geographic areas worldwide, (i.e., Katsouyanni et al., 2009). To explore associations between specific atmospheric pollutants and health, models consider confounding environmental variables such as temperature, relative humidity, and levels of other pollutants. Adjustments are also usually performed for days of the week, holidays, seasonality, information on influenza epidemics, and possible long-term trends. It should be noted that in the studies henceforth described in the following sections, the associations between pollution levels generally refer to an increase in particulate mass concentration in steps of 10 μg m^{-3} and to a lag time between exposure and health outcome of zero or one day unless stated otherwise.

Mortality Studies

There are several studies across the Mediterranean providing evidence for the adverse effects of particulate atmospheric pollutants. In one of the earliest studies of the Air Pollution on Health: European Approach (APHEA) project, in which data from Athens and Barcelona were included, Katsouyanni et al. (1997) showed strongly significant associations between particulate matter (PM) and increased total (all-cause) mortality. In a follow-up project (APHEA2), additional data from Tel Aviv and Rome were analyzed, showing that for the Mediterranean region, a PM_{10} increase was associated with an increase in the total daily number of natural deaths (Katsouyanni et al., 2001). The effects were consistently higher for the elderly category (>65 years old) compared to those for all ages (Aga et al., 2003). With respect to specific causes of mortality, a PM_{10} increase of 10 μg m^{-3} was

associated with 0.76% (95% confidence intervals (CI_{95}): 0.47–1.05%) and 0.58% (CI_{95}: 0.21–0.95%) increase in cardiovascular and respiratory related deaths, respectively (Analitis et al., 2006). A meta-analysis of data from eight Italian cities (project MISA, Meta-analysis of the Italian studies of short-term effects of air pollution) on the effects of PM_{10} on mortality showed that older people (>75 years) are more vulnerable to higher particulate mass loadings in the atmosphere, especially during the warmer months (Biggeri et al., 2001). In a follow-up project in 15 Italian cities (MISA-2), it was found that an increase in PM_{10} was associated with an increase in natural mortality of 0.31% (CI_{95}: 0.19–0.74%; Bellini et al., 2007). An evaluation of the short-term impacts of air pollution on mortality in 13 Spanish cities showed that both total suspended particulates (TSP) and PM_{10} have an association with daily mortality, the coefficients obtained for cardiovascular and respiratory causes being greater than for all-cause mortality (Ballester et al., 2002). An increase for TSP and PM_{10} was associated with a 0.7% (CI_{95}: 0.1–1.4%) and 1.2% (CI_{95}: 0.5–1.8%) increase in cardiovascular mortality, respectively. And a 1.3% (CI_{95}: 0.1–2.4%) and 1.3% (CI_{95}: 0.1%, 2.6%) increase in respiratory mortality, respectively, was also observed. In France, a significant effect of PM_{10} (0.8% risk increase, CI_{95}: 0.2–1.5%) and $PM_{2.5}$ (0.7%, CI_{95}: 0.1–1.6%) on all-ages non-accidental mortality was observed in nine cities during the period 2000–2006 (Pascal et al., 2014).

Samoli et al. (2013) investigated the effect of the size of atmospheric aerosol particles on mortality in 12 European Mediterranean cities (LIFE+/MED-PARTICLES project), a parameter that reflects the source and hence the composition of atmospheric aerosols. They found that health effects of PM are driven mainly by the size of $PM_{2.5}$. For an interquartile range (IQR) increase in PM_{10}, $PM_{2.5}$ (fine particles), and $PM_{10-2.5}$ (coarse particles) in the eight cities with data on all three PM metrics (namely, Athens, Barcelona, Emilia Romagna (region), Madrid, Marseille, Milan, Rome, and Thessaloniki), increases in all-cause mortality were 0.64%, 0.76%, and 0.33% for the three particle size classes, respectively, and 2.4%, 3.8%, and 0.84% for respiratory mortality, when accounting for cumulative exposure through the previous 5 days (5-day lag; Fig. 2).

Interestingly, for an increase in 10 μg m^{-3}, it was found that there was a stronger association between $PM_{10-2.5}$ and mortality among those <75 years old (0.76%, CI_{95}: 0.03–1.49%) in contrast with stronger associations with $PM_{2.5}$ in the elderly (versus ≥75 years old) category (0.77%, CI_{95}: 0.43–1.10%). Samoli et al. (2014) further investigated the associations between $PM_{2.5}$, $PM_{10-2.5}$, and PM_{10} with specific cause of mortality considering diabetes, cardiac diseases, cerebrovascular diseases, lower respiratory tract infections (LRTI), and chronic obstructive pulmonary disease (COPD) as the main mortality diagnoses in the European Mediterranean cities of the MED-PARTICLES project. $PM_{2.5}$ had an adverse effect on all mortality outcomes considered. The highest effect was observed for deaths due to COPD for cumulative exposure after 6 days (2.5% increase in mortality for an increase in $PM_{2.5}$; CI_{95}: −0.01–5.1%), followed by an LRTI death increase by 1.4% (CI_{95}: −1.9–4.8%) and cardiac death increase by 1.3% (CI_{95}: 0.27–2.4%). The highest increase estimate on deaths was observed due to diabetes, both for fine (1.2%, CI_{95}: 1.6–4.2%) and coarse particles (1.3%, CI_{95}: −7.1–10.4%). It is worth noticing that

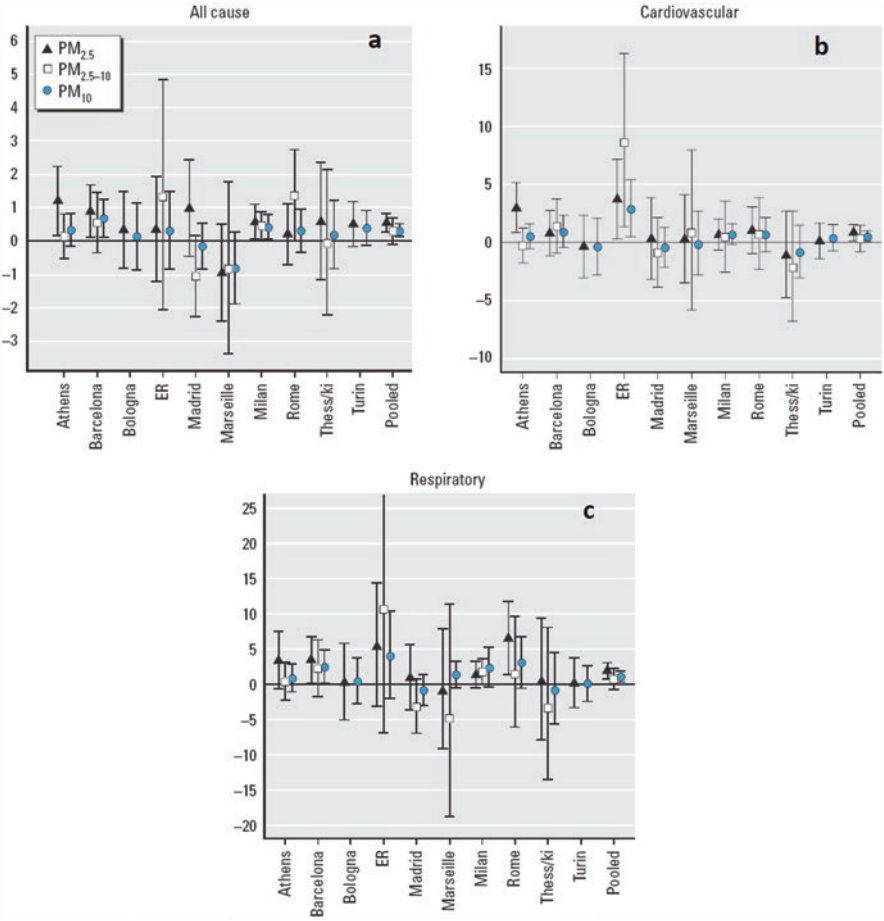

Fig. 2 Percent increase (CI_{95}) in mortality outcomes associated with 10 μg m^{-3} increases in PM for each metropolitan area. Mortality results from models for (**a**) all causes (lag 0–1), (**b**) cardiovascular causes (lag 0–5), and (**c**) respiratory causes (lag 0–5). Abbreviations: ER Emilia Romagna, Thess/ki Thessaloniki. (Reprinted from Samoli et al., 2013)

in Rome, although mean concentrations of air pollutants have decreased over the last two decades, effect estimates for a fixed increment in each exposure were generally consistent (Matteo et al., 2020). These findings suggest that there has been little or no change in the overall toxicity of the air pollution mixture over time.

Morbidity Studies

Several studies provide evidence for associations between PM levels in the atmosphere and hospitalizations in the Mediterranean region. A 10-year analysis in Nicosia showed that for an increase in daily PM_{10}, there was an increase of 0.90%

(CI_{95}: 0.6–1.2%) in all-cause and 1.2% (CI_{95}: 0.0–2.4%) in cardiovascular admissions (Middleton et al., 2008). For Mediterranean European cities (project MED-PARTICLES), both PM_{10} and $PM_{2.5}$ were associated with cardiovascular admissions the same day as the exposure and with respiratory admissions 1 or 2 days afterward (Basagaña et al., 2015). Short-term health effects of air pollution were studied in Beirut in the frame of the BAPHE (Beirut Air Pollution and Health Effects) project (Nakhlé et al., 2015a). Relative risks of admissions for respiratory and cardiovascular diseases were calculated for the year 2012. Total respiratory admissions were significantly associated with an increase in daily mean pollutant concentration for PM_{10} (1.2%, CI_{95}: 0.4–2.0%) and for $PM_{2.5}$ (1.6%, CI_{95}: 0.0–3.2%). Regarding susceptible groups, total respiratory admissions were associated with $PM_{2.5}$ and PM_{10} on the same day for children (increase 1.3%, CI_{95}: −1.5–4.2% and 1.4%, CI_{95}: 0.0–2.9% for $PM_{2.5}$ and PM_{10}, respectively; Nakhlé et al., 2015b). Moreover, a nearly significant association was found between particles and total circulatory admissions for adults and elderly groups on the same day. Significant associations between hospitalizations and PM_{10} levels increase have also been reported (0.70%, CI_{95}: 0.58–0.81%) even for smaller scale studies as in the semi-urban touristic Greek peninsula of Magnesia (Kalantzi et al., 2011).

Desert Dust and Health Effects

Desert dust originating from either North Africa or the Middle East is an atmospheric pollutant that greatly affects the Mediterranean basin. Dust transport can lead to particulate mass levels that substantially exceed the established legal limit values and result in the highest observed values across the Mediterranean. Methods for dust quantification may rely on dust concentration modeling results, air mass back trajectory analysis, in situ measurements of particulate mass or chemical composition of particles, space- and ground-based remote sensing techniques, and combinations among these methods. As the identification of dust in PM has been based on several diverse methods, it must be considered when discussing the health effects of desert dust that the results may vary solely due to the different approaches for defining desert dust particles or dust episodes. Another limitation is the different dust source regions in the various desert areas of the Sahara or Middle East (in the easternmost Mediterranean region), produce dust with distinct mineralogical compositions, and hence distinct toxicities (Querol et al., 2019).

There are several studies presenting associations between the occurrences of desert dust in the atmosphere and mortality rate increases. For the city of Rome, Mallone et al. (2011) found that during dust episodes, the cardiac mortality increase per IQR increase of PM_{10} was enhanced (9.6%, CI_{95}: 3.8–15.6%) compared to dust-free days (2.1%, CI_{95}: −0.76–5.0%). Jiménez et al. (2010) reported statistically significant increases in mortality rates for the elderly in Madrid during dust days similar to those reported for $PM_{2.5}$ for non-dust days; however, they found no effect of coarse particles on mortality during days with or without the presence of dust. For the same area, Tobias et al. (2011a) found that during dust days, the 10 μg m^{-3}

increase in $PM_{10–2.5}$ raised total mortality by 2.8% (CI_{95}: 0.1–5.8%) compared with 0.6% (CI_{95}: −1.1–2.4%) during non-dust days. In Barcelona, mortality was found to increase to 8.4% (CI_{95}: 1.5–15.8%) compared to 1.4% (CI_{95}: −0.8–3.4%) for dust-free conditions (Perez et al., 2008).

With regard to cause-specific mortality, the strongest cardiovascular effects were found during Saharan dust episodes with an indication of effect modification by the presence of dust (Perez et al., 2012). Non-accidental mortality was found to increase by 2.3% (CI_{95}: 1.4–3.1%) and 3.8% (CI_{95}: 3.2–4.4%) in non-desert dust and desert dust periods in Sicily, Italy, associated with an increase in PM_{10} at lag 0–5 days (Renzi et al., 2018), with more pronounced effects during the warm season (April to September). A high increase of respiratory-related mortality in the region of Emilia-Romagna, Italy, was found for people aged 75 or older, reaching 22% (CI_{95}: 4.0–43%), reaching up to 34% (CI_{95}: 8.4–65%) in the warm period (Zauli Sajani et al., 2010). In a study covering several southern European cities in the frame of the MED-PARTICLES project, significant associations were found for both dust and non-dust periods with mortality: a PM_{10} increase was associated with increases in natural mortality of 0.55% (CI_{95}: 0.24–0.87%) and 0.65% (CI_{95}: 0.24–1.06%), respectively. The association with desert dust appeared stronger for cardiovascular than for respiratory mortality (Stafoggia et al., 2016). It is worth mentioning that they found that 15% of days were affected by desert dust at ground level with a gradient from north to south and west to east. In the eastern Mediterranean, Neophytou et al. (2013) found a 2.4% (CI_{95}: 0.53–4.4%) increase in daily cardiovascular mortality on dusty days in Cyprus. In urban areas where other important sources of atmospheric pollutants are abundant, however, the health impacts of desert dust particles may not be as clear. Samoli et al. (2011) found that traffic-related particles in Athens, which prevail on non-desert dust days, have more toxic effects than dust particles.

There are also several studies linking the long-range transport of desert dust to hospitalizations in the Mediterranean region. During dust storms in Cyprus, it was found that all-cause and cardiovascular admissions were, respectively, 4.8% (CI_{95}: 0.7–9.0%) and approximately 10% (CI_{95}: −4.7–28%) higher for a PM_{10} increase (Middleton et al., 2008). Samoli et al. (2011) reported PM_{10}-enhanced effects on emergency hospital admissions for pediatric asthma during desert dust days. The presence of dust in the atmosphere increased the effect of the $PM_{10–2.5}$ on hospitalizations due to respiratory causes to approximately 15% (CI_{95}: 5.3–25%) against 0.32% (CI_{95}: −6.3–6.1%) for dust-free days per IQR increase in Rome. It also increased the effect of PM_{10} on cerebrovascular diseases (5.0% with CI_{95}: 0.39–9.9%, against 0.90% with CI_{95}: −2.3–4.3%; Alessandrini et al., 2013). Admissions due to respiratory causes have also been associated with dust periods regarding increased levels of PM_{10} and $PM_{10–2.5}$ in Madrid (Reyes et al., 2014) and only of PM_{10} in Athens (Trianti et al., 2017). Dadvand et al. (2011) focused on the impact of Saharan dust episodes on pregnancy complications and the subsequent outcomes at delivery (birth weight and gestational age) without finding any significant effects. Tobías et al. (2011b) suggested potential risk of meningococcal meningitis linked to desert dust episodes.

Overall, the most consistent patterns between dust presence in the atmosphere and health impacts seem to be the increase in daily cardiovascular mortality and the hospitalizations for respiratory causes. There are profound differences reported in the literature, however, that are likely due to the different approaches in the epidemiological studies and to the quantification and characterization of desert dust (Querol et al., 2019).

Health Impacts of Combustion Products

In a meta-analysis for the fine atmospheric particle constituents that have the highest association with mortality, traffic and wood combustion products (elemental carbon (EC) and K) had a stronger association with mortality (Achilleos et al., 2017). There are few studies covering the Mediterranean region focused on the health outcome of the inhalation of particulate matter originating from combustion processes. The health impact of forest fires in several European cities in the Mediterranean region was studied by Faustini et al. (2015). They identified forest fire events based on smoke surface concentration maps supplied by the NAAPS Navy Aerosol Analysis and Prediction System—US Naval Research Laboratory Marine Meteorology Division, http://www.nrlmry.navy.mil/aerosol model using aerosol optical depth (AOD) from satellite measurements and the fire-related smoke plumes. Smoky days were associated with an increase of 1.8% (CI_{95}: −0.91–4.5%) in natural mortality and of 6.3% (CI_{95}: 1.0–12%) in cardiovascular mortality. A PM_{10} increase was likely to enhance mortality rates by 0.53% (CI_{95}: 0.30–0.76%). Dhaini et al. (2017) estimated an average mortality fraction of 7.8–10% for EC from $PM_{2.5}$ measured during two intensive campaigns in winter and in summer in Beirut (Lebanon). The average attributable number of deaths (AD) and years of life lost (YLL) were found to be 257–327 and 3086–3923, respectively. Similar findings were reported by Analitis et al. (2012) for the city of Athens where they used black smoke (BS) data, a measure of the particulate mass determined by reflectometry and highly correlated to elemental carbon (Heal & Beverland, 2017). They found that the effect of BS on mortality is greater for respiratory causes and proportional to the size of the fire affecting the city. Their findings were almost identical for the number of cardiovascular deaths (6.0%, CI_{95}: 0.3–12.6%) but were substantially higher for the number of total (4.9%, CI_{95}: 0.3–9.6%) and respiratory (16%, CI_{95}: 1.3–33%) deaths.

Associations between BS concentrations and relative risks of mortality have also been reported for the Iberian Peninsula. In the framework of the project EMECAM (Spanish multicenter study on air pollution and mortality), a 10 μg m^{-3} increase in the BS concentration across seven cities in Spain was associated with a 0.8% (CI_{95}: 0.4–1.1%) increase in total mortality (Ballester et al., 2002). In a more detailed analysis covering only Athens and Barcelona, Ostro et al. (2015) used black carbon concentration (BC) in situ data, derived from optical instruments to investigate the association between daily concentrations of BC and total cardiovascular and respiratory mortality. Combining the data for the two cities using the 3-day moving BC average concentrations, associations were found with excess risks of 2.5% (CI_{95}:

0.7–4.3%), 3.6% (CI_{95}: 0.6–6.5%), and 8.9% (CI_{95}: 3.4–14.4%) per μg m^{-3} increase in BC for all-cause, cardiovascular, and respiratory mortality, respectively. Overall estimates were generally highest for respiratory mortality, with both cities reaching statistical significance for the same day exposure and a 3-day cumulative lag structure, and for mortality, among those older than 65.

Basagaña et al. (2015) examined the relationship between particulate constituents and hospitalizations and mortality in five southern European cities, three in Spain (Barcelona, Madrid, and Huelva) and two in Italy (Rome and Bologna), for a period of 10 years (2003–2013). Several individual species, namely, Elemental Carbon EC, SO_4^{2-}, SiO_2, Ca, Fe, Zn, Cu, Ti, Mn, V, and Ni, were associated with increased percent changes in hospital admissions. Most associations saw a 1% or 2% increase for one IQR increase in pollutant levels, reaching almost 3% for EC from $PM_{2.5}$ for cardiovascular admissions and for EC and Ni from $PM_{2.5}$ for respiratory admissions. EC as a product of combustion processes was found to cause consistent increased risks for mortality and hospitalizations. Increases in respiratory mortality and hospitalizations and cardiovascular hospitalizations were associated with SO_4^{2-}. Health effects were also associated with metals contained in atmospheric particles. SiO_2, Ca, Fe, and Ti had strong effects in all cities and have a mineral origin. Their abundance may be attributed either to road dust or to desert dust. Effects of Ni and V on respiratory admissions and of Ni on respiratory mortality were found. These particulate constituents are commonly linked to the combustion of fuel oil. However, it should be noted that some of the constituents resulting in adverse health effects in this study were highly correlated, and hence, it was not possible to identify the exact responsible pollutant.

3.2 Impacts of Gaseous Pollutants

The health impacts of air quality have been widely studied assuming mainly ambient particles as pollution indicators, but gaseous pollutants have also been associated with adverse effects on morbidity and mortality. Within the framework of the APHEA project, a coordinated study of the short-term effect of the atmospheric oxidant exposure on mortality for six European cities took place. O_3 and NO_2 were used as indicators of exposure (Touloumi et al., 1997). Significant positive associations were found between daily deaths and both NO_2 and O_3. Increases of 50 μg m^{-3} in NO_2 (1-h maximum) or O_3 (1-h maximum) were associated with a 1.3% (95% confidence interval 0.9–1.8) and 2.9% (95% confidence interval 1.0–4.9) increase in the daily number of deaths, respectively. Athens and Barcelona, representing the Mediterranean environment, presented significant increased risk for mortality. Gryparis et al. (2004) investigated short-term effects of O_3, both annual and seasonal, on daily total natural, respiratory, and cardiovascular mortality for the cities of APHEA2 project. For cardiovascular mortality, the effect was higher in southern European cities (0.8% increase in the daily number of deaths per 10 μg m^{-3} increase in O_3) compared with northwestern (0.54%) and central eastern (0.19%) Europe.

Accounting only for the summer period when O_3 concentrations are higher, the percentage increase in the total daily number of natural deaths was found to be highest in Athens. Parodi et al. (2005) also found a stronger effect in summer for the city of Genoa, where a synergistic effect between O_3 and temperature on cardiovascular mortality was observed. Short-term effects of photochemical air pollutants on mortality were investigated in seven Spanish cities involved in the EMECAM project. Significant positive associations were found between daily mortality and NO_2, once the rest of atmospheric pollutants were considered. A 10 μg m^{-3} increase in the daily average concentrations was associated with an increase in the daily number of deaths of 0.43% (CI_{95}: 0.0–0.86%) for all causes and 1.00% (CI_{95}: 0.24–1.85%) for cardiovascular mortality. O_3 was only related to cardiovascular daily mortality, with a 0.56% (CI_{95}: 0.07–1.13%) increase for a 10 μg m^{-3} increase in the 8-hr maximum O_3 level (Saez et al., 2002). In a study of 10 Italian cities, significant associations between NO_2 and natural, cardiac, and respiratory mortality were also found, especially among subjects with cardiovascular preexisting chronic conditions and diabetes (Chiusolo et al., 2011).

Mortality rate enhancements have also been associated with SO_2. In the frame of the APHEA project, Katsouyanni et al. (1997) were among the first to show that for Europe, associations between higher SO_2 levels and increases in daily mortality may be of a casual nature. Adverse effects of SO_2 were also shown in the EMECAM project (Ballester et al., 2002). Interestingly, peak values of SO_2 concentrations showed different relations with mortality than did daily concentrations (0.2% (CI_{95}: −0.4–0.9%) against 0.5% (CI_{95}: 0.1–1.0%) increase in total "deaths". SO_2 concentration increases have been associated with the number of daily emergency admissions for asthma in children in several European cities (APHEA2 project), Rome included (Sunyer et al., 2003a). For an increase of 10 μg m^{-3} of SO_2, the daily number of admissions increased by 1.3% (CI_{95}: 0.4–2.2%). For the same increase, they also found an increase of 0.7% (CI_{95}: 0.1–1.3%) of all cardiovascular admissions on the same and the next day (Sunyer et al., 2003b). It must be noted that these studies could not distinguish the impact of SO_2 from the effect of other pollutants. Samoli et al. (2011) reported that the same increase in SO_2 was associated with a 6.0% (CI_{95}: 0.88–11.3%) increase in pediatric asthma hospital admissions in Athens.

Samoli et al. (2007) found adverse effects of CO on mortality from all causes, and specifically cardiovascular causes, using an extensive European database (APHEA2 project). With respect to Mediterranean cities, data from Athens, Barcelona, Valencia, and Rome were included in the study. For Athens, an increase of 1 mg m^{-3} in CO was associated with 1.0% (CI_{95}: 0.7–1.3%) increase in total mortality in agreement with the earlier study of Touloumi et al. (1996) who reported an increase of 1.0% (CI_{95}: 0.5–1.5%). Additionally, gaseous pollutants have been associated with daily admissions for respiratory diseases (Anderson et al., 1997; Sunyer et al., 1997).

Dhaini et al. (2017) conducted field campaigns during summer and winter seasons in Beirut with the measurement of 70 non-methane hydrocarbons. The US EPA fraction-based approach was used to assess non-cancer hazard and cancer risk for the hydrocarbon mixture. Benzene was found to be the highest contributor to cancer

risk (39–43%), followed by 1,3-butadiene (25–29%), both originating from traffic gasoline evaporation and combustion.

4 Long-Term Effects

Long-term exposure to polluted air can result in chronic health effects. The long-term effects of atmospheric pollution presumably exceed those of short-term exposures and have a larger impact in terms of years of life lost. Early studies in Europe assigned about 6% of annual deaths to outdoor air pollution (Künzli et al., 2000). One of the earliest studies to include a city from the Mediterranean region (Marseille) showed an association between air pollution levels assessed in the 1970s and long-term mortality in France (Filleul et al., 2005).

The European Study of Cohorts for Air Pollution Effects (ESCAPE) was a 13-nation study of long-term health effects of air pollution based on subjects pooled from up to 22 cohorts, originally intended for other purposes, cohorts in Rome and Athens included. Overall, it was concluded that an increase of 10 μg m^{-3} in $PM_{2.5}$ was associated with an increased hazard ratio of 1.14 (CI_{95}: 1.04–1.26) for all-cause mortality (Lipfert 2017). Long-term exposure to fine particulate air pollution was associated with natural-cause mortality, even within concentration ranges well below the present European legislated values (Beelen et al., 2014). A meta-analysis for PM_{10} and $PM_{2.5}$ showed associations with risk for lung cancer. The overall meta-analysis hazard ratio estimates of 1.22 (CI_{95}: 1.03–1.45%) per 10 μg m^{-3} in PM_{10} and 1.18 (CI_{95}: 0.96–1.46%) per 5 μg m^{-3} in $PM_{2.5}$, respectively, were representative for the Mediterranean cohorts (Raaschou-Nielsen et al., 2013).

In a study analyzing data from cohorts in Italy, Spain, and Greece, associations between exposure to air pollution and low birth weight at term were investigated (Pedersen et al., 2013). They showed that an increase in risk of low birth weight at term was associated with a 5 μg m^{-3} increase in $PM_{2.5}$ during pregnancy (adjusted odds ratio 1.18%, CI_{95}: 1.06–1.33%), and reductions in birth weight and birth head circumference were also reported. On the other hand, in an analysis including cohorts from France, Greece, and Italy in the Mediterranean region, no statistically significant association between long-term exposure to specific atmospheric particulate constituents and total cardiovascular mortality was found (Wang et al., 2014). Long-term exposure had a nonsignificant association with exposure to air pollutants for nonmalignant respiratory mortality as well (Dimakopoulou et al., 2014).

In the framework of the LIFE MED HISS project, there were studies in France, Italy, Slovenia, and Spain investigating the potential links between long-term exposure to outdoor air pollution and adverse health effects using previously available cohorts. The outcomes of these studies have direct implications for the Mediterranean region. In a countrywide study in Italy, long-term effects of air pollution on a large series of causes of hospitalization were studied (Gandini et al., 2018). For 10 μg m^{-3} increases in $PM_{2.5}$ and NO_2 levels, positive health risks were found. They estimated hazard ratios associated with the two pollutants were, respectively, for circulatory

system diseases, 1.05 (CI_{95}: 1.03–1.06) for $PM_{2.5}$ and 1.05 (CI_{95}: 1.03–1.07) for NO_2; for myocardial infarction, 1.15 (CI_{95}: 1.12–1.18) and 1.15 (CI_{95}: 1.12–1.18); for lung cancer, 1.18 (CI_{95}: 1.10–1.26) and 1.20 (CI_{95}: 1.12–1.28); for kidney cancer, 1.24 (CI_{95}: 1.11–1.29) and 1.20 (CI_{95}: 1.07–1.33), for all cancers (but lung) 1.06 (CI_{95}: 1.04–1.08) and 1.06 (CI_{95}: 1.04–1.08); and for low respiratory tract infections, 1.07 (CI_{95}: 1.04–1.11) and 1.05 (CI_{95}: 1.02–1.08). Also significant was the association of NO_2 and hospital admissions for atherosclerosis (hazard ratio of 1.10, CI_{95}: 1.03–1.17).

A nationwide study in France confirmed the adverse effects of long-term exposure to air pollutants on respiratory, cardiovascular, and all-cause mortality and morbidity, from the analysis of results from two different surveys, the ESPS (Health Care and Insurance Survey) survey data and the CepiDc (French Epidemiology Center on Medical Causes of Death) database (Sanyal et al., 2018). The first survey supported long-term effects of air pollutants on all-cause mortality, and relative risks of 1.032 (CI_{95}: 1.021–1.065) for $PM_{2.5}$ and 1.072 (CI_{95}: 1.052–1.092) for PM_{10} were found. Additionally, a significant effect was seen for NO_2 (1.041, CI_{95}: 1.024–1.058) and O_3 (1.018, CI_{95}: 1.002–1.035). From the second dataset, exposure to both $PM_{2.5}$ and PM_{10} had a significant 12-year long-term effect on mortality from natural causes (relative risks of 1.024, CI_{95}: 1.022–1.026 for $PM_{2.5}$ and 1.029, CI_{95}: 1.027–1.031 for PM_{10}), cardiovascular diseases (1.022, CI_{95}: 1.015–1.029 and 1.047, CI_{95}: 1.045–1.051), and respiratory diseases (1.037, CI_{95}: 1.029–1.031 and 1.056, CI_{95}: 1.043–1.069). NO_2 was also related to a higher risk for all-cause mortality and cardiovascular diseases and O_3 to all-cause and respiratory mortality. Another study was focused on potential associations between residential exposure to greenness and mortality throughout Spain (de Keijzer et al., 2017). Overall, they found a reduction of 10 months of life for a 5 μg m^{-3} increase of PM_{10}, while an increase in greenness was associated with lower mortality and higher life expectancy only in areas with lower socioeconomic status.

A detailed study for the effect of long-term exposure to NO_2 and $PM_{2.5}$ on mortality was conducted by Cesaroni et al. (2013) in Italy. They analyzed a population-based cohort in Rome from 2001 with 9 years of follow-up, considering residential exposures to NO_2 and $PM_{2.5}$, as well as distance to roads and traffic intensity. Statistically significant positive associations between long-term exposure to NO_2 and $PM_{2.5}$ and non-accidental mortality were found, with hazard ratios of 1.03 (CI_{95}: 1.02–1.03) and 1.04 (CI_{95}: 1.03–1.05) per 10-μg m^{-3} increase in pollutant concentration, respectively. The strongest association was found for ischemic heart diseases, followed by cardiovascular diseases and lung cancer. Proximity to high traffic roads and high traffic intensity were also associated with non-accidental, cardiovascular, and ischemic heart disease mortality. Long-term health effects of air pollutant concentrations in the Maltese Islands were reported by Fenech and Aquilina (2020). The attributable mortality associated with long-term exposure to $PM_{2.5}$ and NO_2 ranges from 0.67% (CI_{95}: 0.27–1.07%) to 11.8% (CI_{95}: 7.8–15.5%) depending on the location. Meta-analyses have provided evidence that long-term exposure to air pollution, especially metrics of traffic-related air pollution such as nitrogen dioxide

and black carbon, is associated with the onset of childhood asthma (Thurston et al., 2020).

5 Modeling and Projections

The Mediterranean region is considered a hot spot for climate change, and air quality will be subject both to environmental changes and any adopted mitigation policies. Human activities have greatly altered atmospheric composition in the region. Compared to preindustrial levels, long-term exposures to PM_{10}, $PM_{2.5}$, and O_3 contributed to 313 and 2186 excess premature non-accidental deaths (cardiovascular diseases accounted for 45–55% of air pollution-related deaths) in Marseille and Rome, respectively, as well as 889 and 8978 additional hospital admissions for cardiovascular diseases in 2015 (Sicard et al., 2019). EU policies have greatly affected atmospheric pollution in the Mediterranean since the 1990s with a direct impact on human health. Ciarelli et al. (2019) used $PM_{2.5}$ concentrations over Europe to perform a Health Impact Assessment during the 1990–2015 period. A substantial reduction in the number of premature deaths from $PM_{2.5}$ exposure in the Mediterranean countries was estimated, almost 42% fewer premature deaths per year. For the year 2015, it has been calculated that in Europe, the mean per capita mortality rate attributable to ambient air pollution by $PM_{2.5}$ and O_3 exceeds the global mean with 133 deaths per year per 100,000 inhabitants, resulting in 790,000 excess deaths overall, while the loss of life expectancy for Europeans due to air pollution was calculated to be 2.2 years (Lelieveld et al., 2019). Of these excess deaths, 48% may be attributed to cardiovascular diseases. The Mediterranean is among the regions with significant excess deaths attributed to air pollution (Fig. 3).

It is expected that climate change will have a negative effect on air quality in the Mediterranean region and will therefore impact public health. Cholakian et al. (2019) investigated the effect of different drivers on total PM and PM_{10} components in future scenarios for the Mediterranean. They found a maximum change of +25% for winter and −19% for spring, indicating different behaviors than in other European regions. Emission reduction policies will reduce $PM_{2.5}$ components, but as the PM_{10} concentration in this area is dominated by dust and salt, these policies will not significantly lessen the overall Mediterranean PM_{10} burden, especially as scenarios show increased dust concentrations, particularly in the eastern part of the basin. Colette et al. (2015) conducted a meta-analysis for 25 ozone pollution projections in Europe and concluded that climate change is very likely to enable enhanced summertime concentrations, especially across the Mediterranean basin. Additionally, the synergistic effects of heat and air pollution on mortality have been highlighted in the Mediterranean region and Europe overall (Analitis et al., 2018; Scortichini et al., 2018). There are potentially large complementary benefits between air pollution and climate change mitigation strategies that would result in improving human health in the Mediterranean.

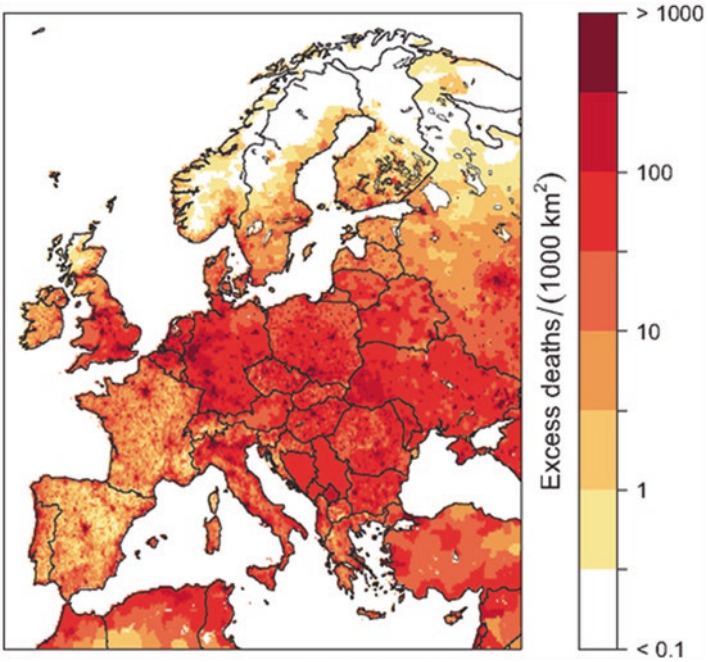

Fig. 3 Regional distribution of estimated annual excess mortality rates from cardiovascular diseases attributed to air pollution. (Reprinted from Lelieveld et al., 2019)

6 Other Diseases Related to Air Pollution

Health conditions other than cardiopulmonary diseases have been associated with air pollution as shown by European studies, among others. These include lung cancer and other malignancies such as bladder cancer and childhood leukemia; vascular diseases such as stroke; autoimmune diseases including diabetes mellitus, lupus, polyarthritis, allergic sensitization, and allergic rhinitis; neurodegenerative conditions, reduced cognitive function, and increased risk of dementia; delayed psychomotor development; and indicators of lower intelligence in children (Schraufnagel et al., 2019). In addition, air pollution exposure in pregnant mothers is significantly associated with lower birth weight and prematurity in newborns (Schraufnagel et al., 2019). In another example, proximity to high traffic roads and high traffic intensity in Rome were also associated with mental health (Cesaroni et al., 2013). Vert et al. (2017) analyzed the association between long-term exposure to air pollution and self-reported history of depression and anxiety disorders and of medication use in an adult population (from 45 to 74 years old) in Barcelona. Levels of NO_x, NO_2, PM_{10}, and $PM_{2.5}$ showed a statistically significant association with self-reported history of depression and, additionally, an increase in the odds of taking medication for anxiety and depression with increasing pollutant levels. In most cases, however, causality has not yet been established, and the relationships may be

due to other factors, such as stress, smoking, lower socioeconomic status, and neighborhood factors.

7 Mitigation and Adaptation

Human exposure to air pollution can be managed through mitigation and adaptation. Mitigation measures are those actions that are taken to reduce and curb air pollutant emissions, while adaptation measures are based on reducing vulnerability to the effects of air pollution. Mitigation, therefore, attends to the causes and sources of air pollution, while adaptation addresses its impacts at population and individual levels. Existing studies have shown that both mitigation and adaptation are effective.

The benefits of reducing air pollution, by either eliminating the source of air pollution or by lowering emissions from a particular source, have been demonstrated in several real situations. In a classic example from Ireland in the 1950s, a significant decrease in standardized respiratory mortality rates in Dublin coincided with the ban on the sale of coal (Dockery et al., 2013). Similarly, in the Swiss SAPALDIA cohort of adults, a reduction of PM_{10} concentrations was associated with a slowdown in lung function impairment (Downs et al., 2007) and the improvement of respiratory symptoms (Schindler et al., 2009). In another natural experiment, the reduction in the use of asthma care and hospital admissions was observed during the Atlanta and Beijing Summer Olympics due to temporary, but strict, restrictions on traffic (Friedman et al., 2001; Li et al., 2010). On a smaller scale, intervention studies involving changes in fuel used for public buses from diesel to cleaner fuels show reductions in premature cardiopulmonary morbidity and mortality (Adar et al., 2015).

In addition, on a theoretical level, using "Health Impact Assessment (HIA)"-type calculations, the European study APHEKOM (Improving Knowledge and Communication for Decision Making on Air Pollution and Health in Europe) conducted in nine European cities made it possible to assess the potential benefits linked to the improvement of air quality (www.aphekom.org). Life expectancy at 30 years increased by 3.6–7.5 months depending on the city, the equivalent of postponing approximately 3000 deaths per year, assuming average annual concentrations of $PM_{2.5}$ were lower than the protection values indicated by WHO (10 $\mu g\ m^{-3}$).

Also, through HIA, the recently conducted PARTLESS study showed that in the XIVth arrondissement of Paris, the improvement of emission standards, the increase in the use of electric vehicles, and the elimination of diesel vehicles can prevent more than 148 deaths per year for that single neighborhood alone (Maesano et al., 2020).

Certain population groups, such as children, the elderly, and those suffering from chronic diseases, including cardiopulmonary diseases, diabetes, and obesity, have been identified as more susceptible to the effects of air pollution. In addition, certain genetic deficits, as in the case of GST (glutathione superoxide dismutase), have been implicated, and those who have it suffer from a reduction of the response to air pollutants via an antioxidant mechanism. Besides genetically sensitive individuals, there are also people who are more vulnerable to the effects of air pollution simply because of excessive exposure due to their employment or socioeconomic position.

In general, the inhabitants of large cities can be considered a vulnerable population due to the heavy traffic, industrial discharges, lack of green space, and the urban environment in which they live, particularly those living close to highways. In addition, it has been shown that even long-term, frequent exposure to pollution levels below the former WHO guidelines but frequently found in cities can engender adverse effects (Thurston et al., 2020).

Personal-level interventions can include personal respirators or face masks. The efficacy of such protections is difficult to evaluate due to their heterogeneity. Respirators used in occupational settings generally capture only large particles (4–20 μm), while N95, FFP2, and FFP3 devices are more effective against smaller particles. Their efficacy, however, varies between experimental tests and environmental conditions (Pacitto et al., 2019). Simple observations of the spatial dispersion of air pollution and variations in concentration levels show that avoiding highly trafficked roads and streets allow people to be less exposed. Indoors, air pollution such as that from cooking or smoking cigarettes can be reduced through behavior change, such as new methods in cooking or abstention of smoking, as well as by opening windows and allowing for a cross breeze on a regular basis. Significant results from intervention studies have shown that it is important to advise patients on how they can protect themselves from air pollution effects (Schraufnagel et al., 2019).

In summary, the analysis of the effects of measures to reduce air pollution shows their effectiveness with a significant reduction in associated health events. However, many of these studies consider only one reduction measure at a time, and further studies considering several prevention and avoidance measures simultaneously are necessary.

8 Conclusion and Recommendations

The frequency and accuracy of air pollution exposure assessment has improved greatly over recent decades. It is currently possible to get spatial-temporal exposure values at the individual level. Exposure to air pollution in the Mediterranean region is associated with adverse health effects in various organs, even for low concentrations of air pollutants. Despite the European policies for clean air and the decrease of pollutant levels during past decades, the reference values are often exceeded, and there has been little or no change in the overall toxicity of the air pollution mixture over time as concluded from analyzing 17 years of data from Rome (Renzi et al., 2017). In some cases, as in Athens, socioeconomic conditions may have a direct effect on exposure to poor air quality, and the associated mortality risk for those with low socioeconomic status may have even increased (Tzima et al., 2018). It is therefore a persistent problem that so far has yet to be adequately addressed. To defend the population from the effects of air pollution, it is necessary to reduce emissions of gases and particles by limiting their sources (especially diesel in cities) and by modifying the behavior of individuals through the use of intelligent applications and pollution sensors. More precise studies are expected that consider the concept of the exposome, which is the lifetime sum of all exposures, including air

pollution, to study the effects of several simultaneous prevention measures. The health challenges emerging due to climate change demand mitigation approaches that go beyond emission control.

Acknowledgments We acknowledge support of this work by the project "PANhellenic infrastructure for Atmospheric Composition and climatE change" (MIS 5021516), which is implemented under the action "Reinforcement of the Research and Innovation Infrastructure" funded by the operational program "Competitiveness, Entrepreneurship and Innovation" (NSRF 2014–2020) and cofinanced by Greece and the European Union (European Regional Development Fund).

References

Achilleos, S., Kioumourtzoglou, M.-A., Wu, C.-D., Schwartz, J. D., Koutrakis, P., & Papatheodorou, S. I. (2017). Acute effects of fine particulate matter constituents on mortality: A systematic review and meta-regression analysis. *Environment International, 109*, 89–100. https://doi.org/10.1016/j.envint.2017.09.010

Adar, S. D., D'Souza, J., Sheppard, L., Kaufman, J. D., Hallstrand, T. S., Davey, M. E., Sullivan, J. R., Jahnke, J., Koenig, J., Larson, T. V., & Liu, L. J. S. (2015). Adopting clean fuels and technologies on school buses. Pollution and health impacts in children. *American Journal of Respiratory and Critical Care Medicine, 191*, 1413–1421. https://doi.org/10.1164/rccm.201410-1924OC

Aga, E., Samoli, E., Touloumi, G., Anderson, H. R., Cadum, E., Forsberg, B., Goodman, P., Goren, A., Kotesovec, F., Kriz, B., Macarol-Hiti, M., Medina, S., Paldy, A., Schindler, C., Sunyer, J., Tittanen, P., Wojtyniak, B., Zmirou, D., Schwartz, J., & Katsouyanni, K. (2003). Short-term effects of ambient particles on mortality in the elderly: Results from 28 cities in the APHEA2 project. *The European Respiratory Journal, 21*, 28s–33s. https://doi.org/10.1183/09031936.03.00402803

Alessandrini, E. R., Stafoggia, M., Faustini, A., Gobbi, G. P., & Forastiere, F. (2013). Saharan dust and the association between particulate matter and daily hospitalisations in Rome, Italy. *Occupational and Environmental Medicine, 70*, 432–434. https://doi.org/10.1136/oemed-2012-101182

Analitis, A., Katsouyanni, K., Dimakopoulou, K., Samoli, E., Nikoloulopoulos, A. K., Petasakis, Y., Touloumi, G., Schwartz, J., Anderson, H. R., Cambra, K., Forastiere, F., Zmirou, D., Vonk, J. M., Clancy, L., Kriz, B., Bobvos, J., & Pekkanen, J. (2006). Short-term effects of ambient particles on cardiovascular and respiratory mortality, *Epidemiology*, *17*, 230–233. https://doi.org/10.1097/01.ede.0000199439.57655.6b

Analitis, A., Georgiadis, I., & Katsouyanni, K. (2012). Forest fires are associated with elevated mortality in a dense urban setting. *Occupational and Environmental Medicine, 69*, 158–162. https://doi.org/10.1136/oem.2010.064238

Analitis, A., De' Donato, F., Scortichini, M., Lanki, T., Basagana, X., Ballester, F., Astrom, C., Paldy, A., Pascal, M., Gasparrini, A., Michelozzi, P., & Katsouyanni, K. (2018). Synergistic effects of ambient temperature and air pollution on health in Europe: Results from the PHASE project. *International Journal of Environmental Research and Public Health, 15*, 1856. https://doi.org/10.3390/ijerph15091856

Andersen, Z. J., Raaschou-Nielsen, O., Ketzel, M., Jensen, S. S., Hvidberg, M., Loft, S., Tjønneland, A., Overvad, K., & Sørensen, M. (2012). Diabetes incidence and long-term exposure to air pollution: A cohort study. *Diabetes Care, 35*, 92–98. https://doi.org/10.2337/dc11-1155

Anderson, H. R., Spix, C., Medina, S., Schouten, J. P., Castellsague, J., Rossi, G., Zmirou, D., Touloumi, G., Wojtyniak, B., Ponka, A., Bacharova, L., Schwartz, J., & Katsouyanni, K. (1997). Air pollution and daily admissions for chronic obstructive pulmonary disease in 6 European

cities: Results from the APHEA project. *The European Respiratory Journal, 10*, 1064–1071, https://erj.ersjournals.com/content/10/5/1064.full.pdf,

Annesi-Maesano, I. (2017). The air of Europe: Where are we going? *European Respiratory Review, 26*, 170024. https://doi.org/10.1183/16000617.0024-2017

Ballester, F., Sáez, M., Pérez-Hoyos, S., Iñíguez, C., Gandarillas, A., Tobías, A., Bellido, J., Taracido, M., Arribas, F., Daponte, A., Alonso, E., Cañada, A., Guillén-Grima, F., Cirera, L., Pérez-Boíllos, M. J., Saurina, C., Gómez, F., & Tenías, J. M. (2002). The EMECAM project: A multicentre study on air pollution and mortality in Spain: Combined results for particulates and for sulfur dioxide. *Occupational and Environmental Medicine, 59*, 300–308. https://doi.org/10.1136/oem.59.5.300

Basagaña, X., Jacquemin, B., Karanasiou, A., Ostro, B., Querol, X., Agis, D., Alessandrini, E., Alguacil, J., Artiñano, B., Catrambone, M., de la Rosa, J. D., Díaz, J., Faustini, A., Ferrari, S., Forastiere, F., Katsouyanni, K., Linares, C., Perrino, C., Ranzi, A., … Stafoggia, M. (2015). Short-term effects of particulate matter constituents on daily hospitalizations and mortality in five South-European cities: Results from the MED-PARTICLES project. *Environment International, 75*, 151–158. https://doi.org/10.1016/J.ENVINT.2014.11.011

Beelen, R., Raaschou-Nielsen, O., Stafoggia, M., Andersen, Z. J., Weinmayr, G., Hoffmann, B., Wolf, K., Samoli, E., Fischer, P., Nieuwenhuijsen, M., Vineis, P., Xun, W. W., Katsouyanni, K., Dimakopoulou, K., Oudin, A., Forsberg, B., Modig, L., Havulinna, A. S., Lanki, T., … Hoek, G. (2014). Effects of long-term exposure to air pollution on natural-cause mortality: An analysis of 22 European cohorts within the multicentre ESCAPE project. *Lancet, 383*, 785–795. https://doi.org/10.1016/S0140-6736(13)62158-3

Bellini, P., Baccini, M., Biggeri, A., & Terracini, B. (2007). The meta-analysis of the Italian studies on short-term effects of air pollution (MISA): Old and new issues on the interpretation of the statistical evidences. *Environmetrics, 18*, 219–229. https://doi.org/10.1002/env.836

Biggeri, A., Bellini, P., & Terracini, B. (2001). Meta-analysis of the Italian studies on short-term effects of air pollution–MISA 1996–2002 (in Italian). *Epidemiologia e Prevenzione, 25*, 1–71.

Cesaroni, G., Badaloni, C., Gariazzo, C., Stafoggia, M., Sozzi, R., Davoli, M., & Forastiere, F. (2013). Long-term exposure to urban air pollution and mortality in a cohort of more than a million adults in Rome. *Environmental Health Perspectives, 121*, 324–331. https://doi.org/10.1289/ehp.1205862

Chiusolo, M., Cadum, E., Stafoggia, M., Galassi, C., Berti, G., Faustini, A., Bisanti, L., Vigotti, M. A., Dessì, M. P., Cernigliaro, A., Mallone, S., Pacelli, B., Minerba, S., Simonato, L., Forastiere, F., & Group, E. C. (2011). Short-term effects of nitrogen dioxide on mortality and susceptibility factors in 10 Italian cities: The EpiAir study. *Environmental Health Perspectives, 119*, 1233–1238. https://doi.org/10.1289/ehp.1002904

Cholakian, A., Colette, A., Coll, I., Ciarelli, G., & Beekmann, M. (2019). Future climatic drivers and their effect on PM_{10} components in Europe and the Mediterranean Sea. *Atmospheric Chemistry and Physics, 19*, 4459–4484. https://doi.org/10.5194/acp-19-4459-2019

Ciarelli, G., Colette, A., Schucht, S., Beekmann, M., Andersson, C., Manders-Groot, A., Mircea, M., Tsyro, S., Fagerli, H., Ortiz, A. G., Adani, M., Briganti, G., Cappelletti, A., D'Isidoro, M., Cuvelier, C., Couvidat, F., Meleux, F., & Bessagnet, B. (2019). Long-term health impact assessment of total $PM_{2.5}$ in Europe during the 1990–2015 period. *Atmospheric Environment: X, 3*, 100032. https://doi.org/10.1016/j.aeaoa.2019.100032

Colette, A., Andersson, C., Baklanov, A., Bessagnet, B., Brandt, J., Christensen, J. H., Doherty, R., Engardt, M., Geels, C., Giannakopoulos, C., Hedegaard, G. B., Katragkou, E., Langner, J., Lei, H., Manders, A., Melas, D., Meleux, F., Rouïl, L., Sofiev, M., … Young, P. (2015). Is the ozone climate penalty robust in Europe? *Environmental Research Letters, 10*, 84015. https://doi.org/10.1088/1748-9326/10/8/084015

de Keijzer, C., Agis, D., Ambrós, A., Arévalo, G., Baldasano, J. M., Bande, S., Barrera-Gómez, J., Benach, J., Cirach, M., Dadvand, P., Ghigo, S., Martinez-Solanas, È., Nieuwenhuijsen, M., Cadum, E. & Basagaña, X. (2017). The association of air pollution and greenness with mortality and life expectancy in Spain: *A small-area study, Environ. Int., 99*, 170–176. https://doi.org/10.1016/j.envint.2016.11.009

Dadvand, P., Basagaña, X., Figueras, F., Amoly, E., Tobias, A., de Nazelle, A., Querol, X., Sunyer, J., & Nieuwenhuijsen, M. J. (2011). Saharan dust episodes and pregnancy. *Journal of Environmental Monitoring, 13*, 3222–3228. https://doi.org/10.1039/C1EM10579E

Dhaini, H. R., Salameh, T., Waked, A., Sauvage, S., Borbon, A., Formenti, P., Doussin, J.-F., Locoge, N., & Afif, C. (2017). Quantitative cancer risk assessment and local mortality burden for ambient air pollution in an eastern Mediterranean City. *Environmental Science and Pollution Research, 24*, 14151–14162. https://doi.org/10.1007/s11356-017-9000-y

Dimakopoulou, K., Samoli, E., Beelen, R., Stafoggia, M., Andersen, Z. J., Hoffmann, B., Fischer, P., Nieuwenhuijsen, M., Vineis, P., Xun, W., Hoek, G., Raaschou-Nielsen, O., Oudin, A., Forsberg, B., Modig, L., Jousilahti, P., Lanki, T., Turunen, A., Oftedal, B., … Katsouyanni, K. (2014). Air pollution and nonmalignant respiratory mortality in 16 cohorts within the ESCAPE project. *American Journal of Respiratory and Critical Care Medicine, 189*, 684–696. https://doi.org/10.1164/rccm.201310-1777OC

Dockery, D. W., Rich, D. Q., Goodman, P. G., Clancy, L., Ohman-Strickland, P., George, P., & Kotlov, T. (2013). Effect of air pollution control on mortality and hospital admissions in Ireland. Research Report 176, Health Effects Institute, Boston, MA.

Downs, S. H., Schindler, C., Liu, L.-J. S., Keidel, D., Bayer-Oglesby, L., Brutsche, M. H., Gerbase, M. W., Keller, R., Künzli, N., Leuenberger, P., Probst-Hensch, N. M., Tschopp, J.-M., Zellweger, J.-P., Rochat, T., Schwartz, J., & Ackermann-Liebrich, U. (2007). Reduced exposure to PM_{10} and attenuated age-related decline in lung function. *The New England Journal of Medicine, 357*, 2338–2347. https://doi.org/10.1056/NEJMoa073625

EEA. (2019). Air quality in Europe—2019 Report, European Environment Agency, Publications Office of the European Union, Copenhagen, Denmark. https://doi.org/10.2800/822355

Faustini, A., Alessandrini, E. R., Pey, J., Perez, N., Samoli, E., Querol, X., Cadum, E., Perrino, C., Ostro, B., Ranzi, A., Sunyer, J., Stafoggia, M., & Forastiere, F. (2015). Short-term effects of particulate matter on mortality during forest fires in Southern Europe: Results of the MED-PARTICLES Project. *Occupational and Environmental Medicine, 72*, 323–329. https://doi.org/10.1136/oemed-2014-102459

Fenech, S., and Aquilina, N. J. (2020). Trends in ambient ozone, nitrogen dioxide, and particulate matter concentrations over the Maltese Islands and the corresponding health impacts. *The Science of the Total Environment, 700*, 134527. https://doi.org/10.1016/j.scitotenv.2019.134527

Filleul, L., Rondeau, V., Vandentorren, S., Le Moual, N., Cantagrel, A., Annesi-Maesano, I., Charpin, D., Declercq, C., Neukirch, F., Paris, C., Vervloet, D., Brochard, P., Tessier, J.-F., Kauffmann, F., & Baldi, I. (2005). Twenty five year mortality and air pollution: Results from the French PAARC survey. *Occupational and Environmental Medicine, 62*, 453–460. https://doi.org/10.1136/oem.2004.014746

Friedman, M. S., Powell, K. E., Hutwagner, L., Graham, L. M., & Teague, W. G. (2001). Impact of changes in transportation and commuting behaviors during the 1996 Summer Olympic Games in Atlanta on air quality and childhood asthma. *JAMA, 285*, 897–905. https://doi.org/10.1001/jama.285.7.897

Gandini, M., Scarinzi, C., Bande, S., Berti, G., Carnà, P., Ciancarella, L., Costa, G., Demaria, M., Ghigo, S., Piersanti, A., Rowinski, M., Spadea, T., Stroscia, M., & Cadum, E. (2018). Long term effect of air pollution on incident hospital admissions: Results from the Italian Longitudinal Study within LIFE MED HISS project. *Environment International, 121*, 1087–1097. https://doi.org/10.1016/j.envint.2018.10.020

Goudie, A. S. (2014). Desert dust and human health disorders. *Environment International, 63*, 101–113. https://doi.org/10.1016/j.envint.2013.10.011

Gryparis, A., Forsberg, B., Katsouyanni, K., Analitis, A., Touloumi, G., Schwartz, J., Samoli, E., Medina, S., Anderson, H. R., Niciu, E. M., Wichmann, H.-E., Kriz, B., Kosnik, M., Skorkovsky, J., Vonk, J. M., & Dörtbudak, Z. (2004). Acute effects of ozone on mortality from the "Air Pollution and Health: A European approach" project. *American Journal of Respiratory and Critical Care Medicine, 170*, 1080–1087. https://doi.org/10.1164/rccm.200403-333OC

Heal, M. R., and Beverland, I. J. (2017). A chronology of ratios between black smoke and PM_{10} and $PM_{2.5}$ in the context of comparison of air pollution epidemiology concentration-response functions. *Environmental Health, 16*, 44. https://doi.org/10.1186/s12940-017-0252-2

Hu, Z. (2009). Spatial analysis of MODIS aerosol optical depth, PM2.5, and chronic coronary heart disease. *International Journal of Health Geographics, 8*, 27. https://doi.org/10.1186/1476-072X-8-27

Jiménez, E., Linares, C., Martínez, D., & Díaz, J. (2010). Role of Saharan dust in the relationship between particulate matter and short-term daily mortality among the elderly in Madrid (Spain). *Science of the Total Environment, 408*, 5729–5736. https://doi.org/10.1016/j.scitotenv.2010.08.049

Kalantzi, E. G., Makris, D., Duquenne, M. N., Kaklamani, S., Stapountzis, H., & Gourgoulianis, K. I. (2011). Air pollutants and morbidity of cardiopulmonary diseases in a semi-urban Greek peninsula. *Atmospheric Environment, 45*, 7121–7126. https://doi.org/10.1016/j.atmosenv.2011.09.032

Karanasiou, A., Moreno, N., Moreno, T., Viana, M., de Leeuw, F., & Querol, X. (2012). Health effects from Sahara dust episodes in Europe: Literature review and research gaps. *Environment International, 47*, 107–114. https://doi.org/10.1016/j.envint.2012.06.012

Katsouyanni, K., Karakatsani, A., Messari, I., Touloumi, G., Hatzakis, A., Kalandidi, A., & Trichopoulos, D. (1990). Air pollution and cause specific mortality in Athens. *Journal of Epidemiology and Community Health, 44*, 321–324. https://doi.org/10.1136/jech.44.4.321

Katsouyanni, K., Touloumi, G., Spix, C., Schwartz, J., Balducci, F., Medina, S., Rossi, G., Wojtyniak, B., Sunyer, J., Bacharova, L., Schouten, J. P., Ponka, A., & Anderson, H. R. (1997). Short term effects of ambient sulphur dioxide and particulate matter on mortality in 12 European cities: Results from time series data from the APHEA project. *BMJ, 314*, 1658. https://doi.org/10.1136/bmj.314.7095.1658

Katsouyanni, K., Samet, J., Anderson, H. R., Atkinson, R., Le Tertre, A., Medina, S., Samoli E., Touloumi, G., Burnett, R. T., Krewski, D., Ramsay, T., Dominici, F., Peng, R. D., Schwartz, J., & Zanobetti, A. (2009). Air pollution and health: A European and north American approach (APHENA), *HEI Research Report, 142*, 5–90, Health Effects Institute, Boston, MA. https://europepmc.org/article/med/20073322. Last access 20 July 2022.

Katsouyanni K, Touloumi G, Samoli E, Gryparis A, Le Tertre A, Monopolis Y, Rossi G, Zmirou D, Ballester F, Boumghar A, Anderson HR, Wojtyniak B, Paldy A, Braunstein R, Pekkanen J, Schindler C, Schwartz J. (2001). Confounding and effect modification in the short-term effects of ambient particles on total mortality: results from 29 European cities within the APHEA2 project. Epidemiology. 2001 Sep;12(5):521–31. https://doi.org/10.1097/00001648-200109000-00011. PMID: 11505171.

Kchih, H., Perrino, C., & Cherif, S. (2015). Investigation of desert dust contribution to source apportionment of PM_{10} and $PM_{2.5}$ from a southern Mediterranean coast. *Aerosol and Air Quality Research, 15*, 454–464. https://doi.org/10.4209/aaqr.2014.10.0255

Künzli, N., Kaiser, R., Medina, S., Studnicka, M., Chanel, O., Filliger, P., Herry, M., Horak, F., Jr., Puybonnieux-Texier, V., Quénel, P., Schneider, J., Seethaler, R., Vergnaud, J.-C., & Sommer, H. (2000). Public-health impact of outdoor and traffic-related air pollution: A European assessment. *Lancet, 356*, 795–801. https://doi.org/10.1016/S0140-6736(00)02653-2

Languille, B., Gros, V., Bonnaire, N., Pommier, C., Honoré, C., Debert, C., Gauvin, L., Srairi, S., Annesi-Maesano, I., Chaix, B., & Zeitouni, K. (2020). A methodology for the characterization of portable sensors for air quality measure with the goal of deployment in citizen science. *The Science of the Total Environment, 708*, 134698. https://doi.org/10.1016/j.scitotenv.2019.134698

Lelieveld, J., Berresheim, H., Borrmann, S., Crutzen, P. J., Dentener, F. J., Fischer, H., Feichter, J., Flatau, P. J., Heland, J., Holzinger, R., Korrmann, R., Lawrence, M. G., Levin, Z., Markowicz, K. M., Mihalopoulos, N., Minikin, A., Ramanathan, V., de Reus, M., Roelofs, G. J., … Ziereis, H. (2002). Global air pollution crossroads over the Mediterranean. *Science, 298*, 794–799. https://doi.org/10.1126/science.1075457

Lelieveld, J., Klingmüller, K., Pozzer, A., Pöschl, U., Fnais, M., Daiber, A., & Münzel, T. (2019). Cardiovascular disease burden from ambient air pollution in Europe reassessed using novel hazard ratio functions. *European Heart Journal, 40*, 1590–1596. https://doi.org/10.1093/eurheartj/ehz135

Li, Y., Wang, W., Kan, H., Xu, X., & Chen, B. (2010). Air quality and outpatient visits for asthma in adults during the 2008 Summer Olympic Games in Beijing. *The Science of the Total Environment, 408*, 1226–1227. https://doi.org/10.1016/j.scitotenv.2009.11.035

Lipfert, F. W. (2017). A critical review of the ESCAPE project for estimating long-term health effects of air pollution. *Environment International, 99*, 87–96. https://doi.org/10.1016/j.envint.2016.11.028

Maesano, C. N., Morel, G., Matynia, A., Ratsombath, N., Bonnety, J., Legros, G., Da Costa, P., Prud'homme, J., & Annesi-Maesano, I. (2020). Impacts on human mortality due to reductions in PM_{10} concentrations through different traffic scenarios in Paris, France. *The Science of the Total Environment, 698*, 134257. https://doi.org/10.1016/j.scitotenv.2019.134257

Mallone, S., Stafoggia, M., Faustini, A., Gobbi, G. P., Marconi, A., & Forastiere, F. (2011). Saharan dust and associations between particulate matter and daily mortality in Rome, Italy. *Environmental Health Perspectives, 119*, 1409–1414. https://doi.org/10.1289/ehp.1003026

Matteo, R., Massimo, S., Annunziata, F., Giulia, C., Giorgio, C., & Francesco, F. (2020). Analysis of temporal variability in the short-term effects of ambient air pollutants on nonaccidental mortality in Rome, Italy (1998–2014). *Environmental Health Perspectives, 125*, 67019. https://doi.org/10.1289/EHP19

Middleton, N., Yiallouros, P., Kleanthous, S., Kolokotroni, O., Schwartz, J., Dockery, D. W., Demokritou, P., & Koutrakis, P. (2008). A 10-year time-series analysis of respiratory and cardiovascular morbidity in Nicosia, Cyprus: The effect of short-term changes in air pollution and dust storms. *Environmental Health, 7*, 39. https://doi.org/10.1186/1476-069X-7-39

Nakhlé, M. M., Farah, W., Ziade, N., Abboud, M., Coussa-Koniski, M.-L., & Annesi-Maesano, I. (2015a). Beirut air pollution and health effects – BAPHE study protocol and objectives. *Multidisciplinary Respiratory Medicine, 10*, 21. https://doi.org/10.1186/s40248-015-0016-1

Nakhlé, M. M., Farah, W., Ziadé, N., Abboud, M., Salameh, D., & Annesi-Maesano, I. (2015b). Short-term relationships between emergency hospital admissions for respiratory and cardiovascular diseases and fine particulate air pollution in Beirut, Lebanon. *Environmental Monitoring and Assessment, 187*, 196. https://doi.org/10.1007/s10661-015-4409-6

Neophytou, A. M., Yiallouros, P., Coull, B. A., Kleanthous, S., Pavlou, P., Pashiardis, S., Dockery, D. W., Koutrakis, P., & Laden, F. (2013). Particulate matter concentrations during desert dust outbreaks and daily mortality in Nicosia, Cyprus. *Journal of Exposure Science & Environmental Epidemiology, 23*, 275–280. https://doi.org/10.1038/jes.2013.10

Ostro, B., Tobias, A., Karanasiou, A., Samoli, E., Querol, X., Rodopoulou, S., Basagaña, X., Eleftheriadis, K., Diapouli, E., Vratolis, S., Jacquemin, B., Katsouyanni, K., Sunyer, J., Forastiere, F., Stafoggia, M., & the MED-PARTICLES Study Group. (2015). The risks of acute exposure to black carbon in Southern Europe: Results from the MED-PARTICLES project. *Occupational and Environmental Medicine, 72*, 123–129. https://doi.org/10.1136/oemed-2014-102184

Pacitto, A., Amato, F., Salmatonidis, A., Moreno, T., Alastuey, A., Reche, C., Buonanno, G., Benito, C., & Querol, X. (2019). Effectiveness of commercial face masks to reduce personal PM exposure. *The Science of the Total Environment, 650*, 1582–1590. https://doi.org/10.1016/j.scitotenv.2018.09.109

Parodi, S., Vercelli, M., Garrone, E., Fontana, V., & Izzotti, A. (2005). Ozone air pollution and daily mortality in Genoa, Italy between 1993 and 1996. *Public Health, 119*, 844–850. https://doi.org/10.1016/j.puhe.2004.10.007

Pascal, M., Falq, G., Wagner, V., Chatignoux, E., Corso, M., Myriam, B., Host, S., Pascal, L., & Larrieu, S. (2014). Short-term impacts of particulate matter (PM_{10}, $PM_{10-2.5}$, $PM_{2.5}$) on mortality in nine French cities. *Atmospheric Environment, 95*, 175–184. https://doi.org/10.1016/j.atmosenv.2014.06.030

Pedersen, M., Giorgis-Allemand, L., Bernard, C., Aguilera, I., Andersen, A.-M. N., Ballester, F., Beelen, R. M. J., Chatzi, L., Cirach, M., Danileviciute, A., Dedele, A., van Eijsden, M., Estarlich, M., Fernández-Somoano, A., Fernández, M. F., Forastiere, F., Gehring, U., Grazuleviciene, R., Gruzieva, O., … Slama, R. (2013). Ambient air pollution and low birthweight: A European cohort study (ESCAPE). *The Lancet Respiratory Medicine, 1*, 695–704. https://doi.org/10.1016/S2213-2600(13)70192-9

Perez, L., Tobias, A., Querol, X., Künzli, N., Pey, J., Alastuey, A., Viana, M., Valero, N., González-Cabré, M., & Sunyer, J. (2008). Coarse particles from Saharan dust and daily mortality, *Epidemiology, 19*, 800–807, https://doi.org/10.1097/EDE.0b013e31818131cf

Perez, L., Tobías, A., Querol, X., Pey, J., Alastuey, A., Díaz, J., & Sunyer, J. (2012). Saharan dust, particulate matter and cause-specific mortality: A case–crossover study in Barcelona (Spain). *Environment International, 48*, 150–155. https://doi.org/10.1016/j.envint.2012.07.001

Querol, X., Tobías, A., Pérez, N., Karanasiou, A., Amato, F., Stafoggia, M., Pérez García-Pando, C., Ginoux, P., Forastiere, F., Gumy, S., Mudu, P., & Alastuey, A. (2019). Monitoring the impact of desert dust outbreaks for air quality for health studies. *Environment International, 130*, 104867. https://doi.org/10.1016/J.ENVINT.2019.05.061

Raaschou-Nielsen, O., Andersen, Z. J., Beelen, R., Samoli, E., Stafoggia, M., Weinmayr, G., Hoffmann, B., Fischer, P., Nieuwenhuijsen, M. J., Brunekreef, B., Xun, W. W., Katsouyanni, K., Dimakopoulou, K., Sommar, J., Forsberg, B., Modig, L., Oudin, A., Oftedal, B., Schwarze, P. E., … Hoek, G. (2013). Air pollution and lung cancer incidence in 17 European cohorts: Prospective analyses from the European Study of Cohorts for Air Pollution Effects (ESCAPE). *The Lancet Oncology, 14*, 813–822. https://doi.org/10.1016/S1470-2045(13)70279-1

Ranzi, A., Porta, D., Badaloni, C., Cesaroni, G., Lauriola, P., Davoli, M., & Forastiere, F. (2014). Exposure to air pollution and respiratory symptoms during the first 7 years of life in an Italian birth cohort. *Occupational and Environmental Medicine, 71*, 430–436. https://doi.org/10.1136/oemed-2013-101867

Renzi, M., Faustini, A., Cesaroni, G., Cattani, G., & Forastiere, F. (2017). Analysis of temporal variability in the short-term effects of ambient air pollutants on nonaccidental mortality in Rome, Italy (1998–2014), *Environmental Health Perspectives*, *125*. https://doi.org/10.1289/EHP19

Renzi, M., Forastiere, F., Calzolari, R., Cernigliaro, A., Madonia, G., Michelozzi, P., Davoli, M., Scondotto, S., & Stafoggia, M. (2018). Short-term effects of desert and non-desert PM_{10} on mortality in Sicily, Italy. *Environment International, 120*, 472–479. https://doi.org/10.1016/j.envint.2018.08.016

Reyes, M., Díaz, J., Tobias, A., Montero, J. C., & Linares, C. (2014). Impact of Saharan dust particles on hospital admissions in Madrid (Spain). *International Journal of Environmental Health Research, 24*, 63–72. https://doi.org/10.1080/09603123.2013.782604

Saez, M., Ballester, F., Barceló, M. A., Pérez-Hoyos, S., Bellido, J., Tenías, J. M., Ocaña, R., Figueiras, A., Arribas, F., Aragonés, N., Tobías, A., Cirera, L., Cañada, A., & EMECAM. (2002). A combined analysis of the short-term effects of photochemical air pollutants on mortality within the EMECAM project. *Environmental Health Perspectives, 110*, 221–228. https://doi.org/10.1289/ehp.02110221

Samoli, E., Touloumi, G., Schwartz, J., Anderson, H. R., Schindler, C., Forsberg, B., Vigotti, M. A., Vonk, J., Kosnik, M., Skorkovsky, J., & Katsouyanni, K. (2007). Short-term effects of carbon monoxide on mortality: An analysis within the APHEA project. *Environmental Health Perspectives, 115*, 1578–1583. https://doi.org/10.1289/ehp.10375

Samoli, E., Nastos, P. T., Paliatsos, A. G., Katsouyanni, K., & Priftis, K. N. (2011). Acute effects of air pollution on pediatric asthma exacerbation: Evidence of association and effect modification. *Environmental Research, 111*, 418–424. https://doi.org/10.1016/j.envres.2011.01.014

Samoli, E., Stafoggia, M., Rodopoulou, S., Ostro, B., Declercq, C., Alessandrini, E., Díaz, J., Karanasiou, A., Kelessis, A. G., Le Tertre, A., Pandolfi, P., Randi, G., Scarinzi, C., Zauli-Sajani, S., Katsouyanni, K., Forastiere, F., & the MED-PARTICLES Study Group. (2013). Associations between fine and coarse particles and mortality in Mediterranean cities: Results from the MED-PARTICLES project. *Environmental Health Perspectives, 121*, 932–938. https://doi.org/10.1289/ehp.1206124

Samoli, E., Stafoggia, M., Rodopoulou, S., Ostro, B., Alessandrini, E., Basagaña, X., Díaz, J., Faustini, A., Gandini, M., Karanasiou, A., Kelessis, A. G., Le Tertre, A., Linares, C., Ranzi, A., Scarinzi, C., Katsouyanni, K., & Forastiere, F. (2014). Which specific causes of death are associated with short term exposure to fine and coarse particles in Southern Europe? Results from the MED-PARTICLES project. *Environment International, 67*, 54–61. https://doi.org/10.1016/j.envint.2014.02.013

Sanyal, S., Rochereau, T., Maesano, C. N., Com-Ruelle, L., & Annesi-Maesano, I. (2018). Long-term effect of outdoor air pollution on mortality and morbidity: A 12-year follow-up study for metropolitan France. *International Journal of Environmental Research and Public Health, 15*, 2487. https://doi.org/10.3390/ijerph15112487

Sartelet, K. (2022). Secondary aerosol formation and their modeling. In F. Dulac, S. Sauvage, & E. Hamonou (Eds.). *Atmospheric chemistry in the Mediterranean Region* (Vol. 2, From air pollutant sources to impacts). Springer, this volume. https://doi.org/10.1007/978-3-030-82385-6_10

Schindler, C., Keidel, D., Gerbase, M. W., Zemp, E., Bettschart, R., Brändli, O., Brtsche, M. H., Burdet, L., Karrer, W., Knöpfli, B., Pons, M., Rapp, R., Bayer-Oglesby, L., Künzli, N., Schartz, J., Liu, L.-J. S., Ackermann-Liebrich, U., Rochat, T., & the SAPALDIA Team. (2009). Improvements in PM_{10} exposure and reduced rates of respiratory symptoms in a cohort of Swiss adults (SAPALDIA). *American Journal of Respiratory and Critical Care Medicine, 179*, 579–587. https://doi.org/10.1164/rccm.200803-388OC

Schraufnagel, D. E., Balmes, J. R., Cowl, C. T., De Matteis, S., Jung, S. H., Mortimer, K., Perez-Padilla, R., Rice, M. B., Riojas-Rodriguez, H., Sood, A., Thurston, G. D., To, T., Vanker, A., & Wuebbles, D. J. (2019). Air pollution and noncommunicable diseases: A review by the forum of International Respiratory Societies' Environmental Committee, Part 2: Air pollution and organ systems. *Chest, 155*, 417–426. https://doi.org/10.1016/j.chest.2018.10.041

Scortichini, M., De Sario, M., De' Donato, F. K., Davoli, M., Michelozzi, P., & Stafoggia, M. (2018). Short-term effects of heat on mortality and effect modification by air pollution in 25 Italian cities. *International Journal of Environmental Research and Public Health, 15*, 1771. https://doi.org/10.3390/ijerph15081771

Sicard, P., Khaniabadi, Y. O., Perez, S., Gualtieri, M., & De Marco, A. (2019). Effect of O_3, PM_{10} and $PM_{2.5}$ on cardiovascular and respiratory diseases in cities of France, Iran and Italy. *Environmental Science and Pollution Research, 26*, 32645–32665. https://doi.org/10.1007/s11356-019-06445-8

Stafoggia, M., Zauli-Sajani, S., Pey, J., Samoli, E., Alessandrini, E., Basagaña, X., Cernigliaro, A., Chiusolo, M., Demaria, M., Díaz, J., Faustini, A., Katsouyanni, K., Kelessis, A. G., Linares, C., Marchesi, S., Medina, S., Pandolfi, P., Pérez, N., Querol, X., … the MED-PARTICLES Study Group: Desert dust outbreaks in southern Europe. (2016). Contribution to daily PM_{10} concentrations and short-term associations with mortality and hospital admissions. *Environmental Health Perspectives, 124*, 413–419. https://doi.org/10.1289/ehp.1409164

Sunyer, J., Spix, C., Quénel, P., Ponce-de-León, A., Pönka, A., Barumandzadeh, T., Touloumi, G., Bacharova, L., Wojtyniak, B., Vonk, J., Bisanti, L., Schwartz, J., & Katsouyanni, K. (1997). Urban air pollution and emergency admissions for asthma in four European cities: The APHEA Project. *Thorax, 52*, 760–765. https://doi.org/10.1136/thx.52.9.760

Sunyer, J., Atkinson, R., Ballester, F., Le Tertre, A., Ayres, J. G., Forastiere, F., Forsberg, B., Vonk, J. M., Bisanti, L., Anderson, R. H., Schwartz, J., & Katsouyanni, K. (2003a). Respiratory effects of sulphur dioxide: A hierarchical multicity analysis in the APHEA 2 study. *Occupational and Environmental Medicine, 60*, e2. https://doi.org/10.1136/oem.60.8.e2

Sunyer, J., Ballester, F., Le Tertre, A., Atkinson, R., Ayres, J. G., Forastiere, F., Forsberg, B., Vonk, J. M., Bisanti, L., Tenías, J. M., Medina, S., Schwartz, J., & Katsouyanni, K. (2003b). The association of daily sulfur dioxide air pollution levels with hospital admissions for cardiovascular diseases in Europe (The Aphea-II study). *European Heart Journal, 24*, 752–760. https://doi.org/10.1016/S0195-668X(02)00808-4

Terrouche, A., Ali-Khodja, H., Kemmouche, A., Bouziane, M., Ahmed Derradji, A., & Charron, A. (2016). Identification of sources of atmospheric particulate matter and trace metals in Constantine, Algeria. *Air Quality, Atmosphere and Health, 9*, 69–82. https://doi.org/10.1007/s11869-014-0308-1

Thurston, G. D., Balmes, J. R., Garcia, E., Gilliland, F. D., Rice, M. B., Schikowski, T., Van Winkle, L. S., Annesi-Maesano, I., Burchard, E. G., Carlsten, C., Harkema, J. R., Khreis, H., Kleeberger, S. R., Kodavanti, U. P., London, S. J., McConnell, R., Peden, D. B., Pinkerton, K. E., Reibman, J., & White, C. W. (2020). Outdoor air pollution and new-onset airway disease. An official American Thoracic Society workshop report. *Annals of the American Thoracic Society, 17*, 387–398. https://doi.org/10.1513/AnnalsATS.202001-046ST

Tobías, A., Pérez, L., Díaz, J., Linares, C., Pey, J., Alastruey, A., & Querol, X. (2011a). Short-term effects of particulate matter on total mortality during Saharan dust outbreaks: A case-crossover analysis in Madrid (Spain). *The Science of the Total Environment, 412–413*, 386–389. https://doi.org/10.1016/j.scitotenv.2011.10.027

Tobías, A., Caylà, J. A., Pey, J., Alastuey, A., & Querol, X. (2011b). Are Saharan dust intrusions increasing the risk of meningococcal meningitis? *International Journal of Infectious Diseases, 15*, e503. https://doi.org/10.1016/j.ijid.2011.03.008

Touloumi, G., Samoli, E., & Katsouyanni, K. (1996). Daily mortality and "winter type" air pollution in Athens, Greece–a time series analysis within the APHEA project. *Journal of Epidemiology and Community Health, 50*(Suppl 1), s47–s51. https://doi.org/10.1136/jech.50.suppl_1.s47

Touloumi, G., Katsouyanni, K., Zmirou, D., Schwartz, J., Spix, C., De Leon, A., Tobias, A., Quennel, P., Rabczenko, D., Bacharova, L., Bisanti, L., Vonk, J., & Ponka, A. (1997). Short-term effects of ambient oxidant exposure on mortality: A combined analysis within the APHEA project. *American Journal of Epidemiology, 146*, 177–185. https://doi.org/10.1093/oxfordjournals.aje.a009249

Trianti, S.-M., Samoli, E., Rodopoulou, S., Katsouyanni, K., Papiris, S. A., & Karakatsani, A. (2017). Desert dust outbreaks and respiratory morbidity in Athens, Greece. *Environmental Health, 16*, 72. https://doi.org/10.1186/s12940-017-0281-x

Tzima, K., Analitis, A., & Samoli, E. (2018). Has the risk of mortality related to short-term exposure to particles changed over the past years in Athens, Greece? *Environment International, 113*, 306–312. https://doi.org/10.1016/j.envint.2018.01.002

van Donkelaar, A., Martin, R. V., Brauer, M., Kahn, R., Levy, R., Verduzco, C., & Villeneuve, P. J. (2010). Global estimates of ambient fine particulate matter concentrations from satellite-based aerosol optical depth: Development and application. *Environmental Health Perspectives, 118*, 847–855. https://doi.org/10.1289/ehp.0901623

van Donkelaar, A., Martin, R. V., Brauer, M., Hsu, N. C., Kahn, R. A., Levy, R. C., Lyapustin, A., Sayer, A. M., & Winker, D. M. (2016). Global estimates of fine particulate matter using a combined geophysical-statistical method with information from satellites, models, and monitors. *Environmental Science & Technology, 50*, 3762–3772. https://doi.org/10.1021/acs.est.5b05833

Vert, C., Sánchez-Benavides, G., Martínez, D., Gotsens, X., Gramunt, N., Cirach, M., Molinuevo, J. L., Sunyer, J., Nieuwenhuijsen, M. J., Crous-Bou, M., & Gascon, M. (2017). Effect of long-term exposure to air pollution on anxiety and depression in adults: A cross-sectional study. *International Journal of Hygiene and Environmental Health, 220*, 1074–1080. https://doi.org/10.1016/j.ijheh.2017.06.009

Wang, M., Beelen, R., Stafoggia, M., Raaschou-Nielsen, O., Jovanovic Andersen, Z., Hoffmann, B., Fischer, P., Houthuijs, D., Nieuwenhuijsen, M., Weinmayr, G., Vineis, P., Xun, W. W., Dimakopoulou, K., Samoli, E., Laatikainen, T., Lanki, T., Turunen, A. W., Oftedal, B., Schwarze, P., … Hoek, G. (2014). Long-term exposure to elemental constituents of particulate matter and cardiovascular mortality in 19 European cohorts: Results from the ESCAPE and TRANSPHORM projects. *Environment International, 66*, 97–106. https://doi.org/10.1016/j.envint.2014.01.026

WHO. (2016). *Ambient air pollution: A global assessment of exposure and burden of disease*. World Health Organization, 131 pp. https://apps.who.int/iris/bitstream/handle/10665/250141/9789241511/9789241511/9789241511353-eng.pdf. Last access 20 July 2022.

Zauli Sajani, S., Miglio, R., Bonasoni, P., Cristofanelli, P., Marinoni, A., Sartini, C., Goldoni, C., De Girolamo, G., & Lauriola, P. (2010). Saharan dust and daily mortality in Emilia-Romagna (Italy). *Occupational and Environmental Medicine, 68*, 446–451. https://doi.org/10.1136/oem.2010.058156

Impact of Atmospheric Deposition on Marine Chemistry and Biogeochemistry

Cécile Guieu and Céline Ridame

Contents

Abstract This chapter presents the current knowledge on the impact of atmospheric deposition from natural sources, such as Saharan dust, and from anthropogenic activities, on marine chemistry and biogeochemistry of the open Mediterranean Sea. Results from process studies and observations at sea that have been conducted over the past decade are summarized along with recent findings from a numerical biogeochemical model of the ocean that accounts for atmospheric deposition.

Chapter reviewed by ***Emilio Marañon*** *(Dept. of Ecology and Animal Biology, Univ. of Vigo, Spain), as part of the book Section X Impacts of Air Pollution on Human Health and Ecosystems also reviewed by* ***Semia Cherif*** *(ISSBAT, University of Tunis El Manar, Tunisia)*

C. Guieu (✉)
Laboratoire d'Océanographie de Villefranche (LOV), UMR 7093 CNRS, Sorbonne Universitén Chemin du Lazaret, Villefranche-sur-Mer, France
e-mail: cecile.guieu@imev-mer.fr

C. Ridame
Laboratoire d'Océanographie et du Climat: Expérimentations et Approches Numériques (LOCEAN), UMR 7159 CNRS, IRD, MNHN, Sorbonne Université, IPSL, Paris, France

F. Dulac et al. (eds.), *Atmospheric Chemistry in the Mediterranean Region*,
https://doi.org/10.1007/978-3-030-82385-6_23

1 Introduction

The Mediterranean Sea is considered as an oligotrophic sea representative of a low-nutrient and low-chlorophyll system (LNLC). Due to high deposition fluxes of desert dust and anthropogenic aerosols (whose sources are close to the Mediterranean basin and numerous), atmospheric inputs impact the cycles of chemical elements of biological interest in the open Mediterranean Sea which can affect the regional ecosystem. From about May to October, the upper water column is stratified (D'Ortenzio et al., 2005), and the sea surface mixed layer (SML) is nutrient-depleted, inducing a low productivity (e.g., Bosc et al., 2004). Consequently, during these 6 months, the atmosphere is considered as an important source of new nutrients for the SML of the open sea (as derived from in situ and experimental evidences, e.g., Migon et al., 2002; Ridame & Guieu, 2002, and from the modelling approach considering vertical transfers of nutrients by diffusion, by Richon et al., 2018). When comparing with available diffusive fluxes quantified at the upper nutricline limits (>60 m, i.e., much deeper than the base of the SML at about 10–15 m), recent estimates (Table 1) for the western basin show that atmospheric deposition of soluble nitrogen is of the same order of magnitude as diffusive flux. For soluble phosphorus, these deep diffusive fluxes are much higher. For a better comparison between the different nutrient fluxes entering the SML, the atmospheric fluxes should be compared to the diffusive fluxes through the pycnocline at the base of the SML. Unfortunately, such fluxes are not yet available in the literature.

The NO_3:PO_4 molar ratio in deep Mediterranean waters, of the order of 22–28, is higher than the molar Redfield ratio of 16:1, indicating that P is the controlling factor of primary production (PP) in the open surface waters during the stratification period (e.g., Krom et al., 1991; Kress & Herut, 2001; Marty et al., 2002; Thingstad et al., 2005). Yet PP can also be limited by N (Tanaka et al., 2011) or co-limited by both N and P (Zohary et al., 2005; Tanaka et al., 2011). It has to be noted that,

Table 1 Comparison of soluble atmospheric and diffusive N and P fluxes in mmol m^{-2} d^{-1}. The diffusive fluxes were quantified during the stratified period, across the nutricline

Atmospheric soluble N	N diffusive flux	Atmospheric soluble P	P diffusive flux
Whole Mediterranean: 0.10 Kanakidou et al. (2020) 0.084 Guerzoni & Molinaroli (2005)	*Northwestern Mediterranean Sea:* 0.09–0.4 Mouriño-Carballido et al. (2016) *Tyrrhenian Sea:* 0.42–0.70 Taillandier et al. (2020) *Algerian Basin:* 0.07–0.118 Taillandier et al. (2020)	*Whole Mediterranean:* (0.15–2.16) 10^{-3} Kanakidou et al. (2020)	*Algerian Basin:* 2 10^{-3} *Tyrrhenian Sea:* 13 10^{-3} Vincent Taillandier Personal Comm. (2020)

during the stratified period, the concentrations of dissolved iron (*[dFe]*) are relatively high due to atmospheric Fe accumulation in the SML (Bonnet & Guieu, 2004), suggesting that Fe is not a limiting factor for PP. Heterotrophic bacterial activity is also limited by P or NP co-limited (Sala et al., 2002; Tanaka et al., 2011), suggesting a competition for nutrient uptake between heterotrophic bacteria and autotrophic phytoplankton. Dinitrogen fixation (N_2 fixation) is not limited by Fe or co-limited by P and Fe in the open surface waters. It is rather P limited in the western and eastern basins (Rees et al., 2006; Ridame et al., 2011). Interestingly, in the central basin, N_2 fixation could be limited or co-limited by a trace element released by dust different from Fe and dissolved inorganic phosphorus (DIP) (Ridame et al., 2011).

Atmospheric deposition is a major source of nutrients for the eastern basin, supplying N and P (wet + dry) far in excess of the Redfield ratio (e.g., Herut et al., 2002; Carbo et al., 2005; Markaki et al., 2010). The detailed nutrient budget of inputs to the basin shows a major contribution from atmospheric origin and a high N:P ratio in all other input sources (Krom et al., 2004). This observation suggests that the atmospheric input of nutrients may contribute significantly to the high NO_3:PO_4 ratios in the deep East Mediterranean waters, which is preserved because of insignificant denitrification in such an oligotrophic basin (Krom et al., 2004).

This situation makes the open Mediterranean Sea an excellent natural laboratory to study the biogeochemical effect of atmospheric inputs on the water column. Through some examples, we show hereafter how atmospheric inputs impact marine cycles of elements, and from recent investigations, we establish the link between atmospheric deposition and ecosystem responses in such LNLC areas.

The importance of atmospheric inputs for marine chemistry in the Mediterranean Sea has been revealed during the past ~30 years (e.g., first review by Guerzoni et al., 1999; Richon et al., 2018). For metals, to our knowledge, only one study provided a budget taking into account inputs from the atmosphere, the rivers, and the straits at the scale of the western Mediterranean Sea (Elbaz-Poulichet et al., 2001). This budget is particularly interesting as it considered the inputs under dissolved form (concentration of the fraction below 0.2 or 0.4 μm) that likely includes the bioavailable fraction. It shows that for all the metals considered in that study (Mn, Fe, Ni, Co, Cu, Zn, Cd, and Pb), the atmospheric inputs significantly dominate the river inputs over annual timescales. In the case of Fe, the atmospheric source even dominates the inputs from the straits. Such facts imply that atmospheric deposition plays a key role in the marine cycle of pollutants (such as Pb) and key biogeochemical elements (such as Fe). Concerning macronutrients, at the small scale of the Gulf of Lions, the atmosphere does not represent a significant source of dissolved inorganic phosphorus (DIP) and dissolved inorganic nitrogen (DIN) (Durrieu de Madron et al., 2003). However, at the scale of the western and eastern basins and at the scale of the whole Mediterranean Sea, experimental approaches and models show the significance of atmospheric deposition for both budgets. Loÿe-Pilot et al. (1990) and Guerzoni et al. (1999) concluded that atmospheric DIN input is of the same order of magnitude as the riverine input for the northwestern Mediterranean and for the whole Mediterranean Sea. For DIP, at the annual scale and for the western

Table 2 Comparison of atmospheric and riverine nutrients annual fluxes at the scale of the whole Mediterranean Sea

Species	Atmosphere (Kanakidou et al., 2020)	Rivers (Ludwig et al., 2009)
Soluble N (Tg-N yr^{-1})	1.28	1.08
Soluble P (Gg-P yr^{-1})	4.31–61.27	49.4

Mediterranean Sea, the inputs from the atmosphere represent 8–30% (Bergametti et al., 1992; Ridame, 2001) and 37% (Guerzoni et al., 1999) of the riverine inputs. For the eastern Mediterranean, according to Krom et al. (2004), atmospheric inputs of DIN and DIP account for 61% and 28% of the total budget of N and P, respectively. The most recent estimates at the scale of the whole Mediterranean Sea are reported in Table 2 and show that the same orders of magnitude are found for both soluble N and soluble P from atmosphere and rivers.

A recent modelling study simulating the period 1997–2012 (Richon et al., 2018) concluded that atmospheric deposition accounts on average for, respectively, 10% of total nitrate and for 5–30% of DIP external inputs to the entire water column at the basin scale.

These figures demonstrate the importance of the fraction originating from the atmosphere, particularly for the open seawaters, outside of the direct influence of the riverine inputs. Atmospheric inputs reach the sea surface by means of wet and dry deposition. Partitioning between dissolved and particulate phase in rainwaters depends on many factors and is described in another chapter (Desboeufs, 2022). Dissolved atmospheric fraction is the sum of actual dissolved fraction in wet deposition plus a fraction that will possibly dissolve in surface seawater from dry deposition. This is what is likely bioavailable and both bacteria and phytoplankton will compete to uptake these nutrients in such an oligotrophic system (Ridame et al., 2014; Pulido-Villena et al., 2014; Guieu et al., 2014a; Pitta et al., 2017). Dust deposition can also result in removal of DIP and nitrate (Louis et al., 2015) and trace elements (Fe, Al) in seawater (Wagener et al., 2010; Bressac & Guieu, 2013; Wuttig et al., 2013) linked to particle dynamics, governed by the quality/quantity of dissolved organic matter (DOM). Such findings were made possible by the use of mesocosms and large minicosms where dust was sprayed at the surface and the dynamics of the settling particles can be taken into account contrary to batch approaches where the dust concentration is homogenized (Fig. 1a) (de Leeuw et al., 2014).

There is thus a suite of processes that rules the availability of new nutrients depending on in situ conditions at the time of the deposition (Fig. 1b). The "realistic view" experiments can be carried out in situ (mesocosms) or in the laboratory (minicosms) and result in the parameterization of the processes involved while the particles are sinking. Such parameterization can improve complex biogeochemical models that make it possible to better quantify the impacts of atmospheric deposition at different scales of time and space (see, e.g., Richon et al., 2018).

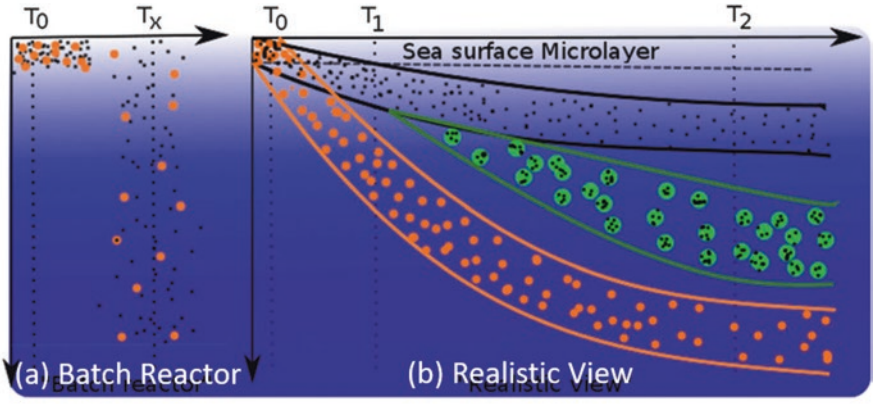

Fig. 1 Conceptual view of the fate of atmospheric particles after their deposition: (**a**) "batch reactor" point of view with atmospheric particles perfectly mixed over the SML; (**b**) hypothetical dynamics of atmospheric particles in the water column; at T_0, particles are in the surface microlayer; after T_0, bigger particles (orange) settle faster than smaller particles (black) which form aggregates with organic matter (green) at an intermediate depth. (Reprinted from de Leeuw et al., 2014)

2 Water Body Impacted by Atmospheric Inputs

A key question concerns the water body actually impacted by both dry and wet atmospheric deposition. The way chemicals, after a rain, dilute in time and space in the surface waters remains very poorly known, and so far, to our knowledge, dilution calculations are based on simple mixing of fresh water at the top of the surface water. Such calculations simulate short-term conditions in the surface few meters of seawater following a rain event (see, for ex., Klein et al., 1997), but the actual situation seems to be much more complicated because of atmospheric forcing such as wind that can upwell nutrients from below (Guieu et al., 2010a). The way atmospheric particles are transported across the surface mixed layer is also crucial regarding the dissolution/scavenging processes that will occur in seawater and thus regarding the bioavailability of elements associated with those particles. The Stokes' law (Stokes, 1851) was used as a first approach (see, e.g., Ridame & Guieu, 2002) to estimate the sedimentation rate of atmospheric particles in surface seawater as a function of particle size. For example, the sedimentation rates of the size fraction <1 μm that represents at least 90% of the total number of particles (Guieu et al., 2010b) are very low (<5 cm d^{-1}). In theory, small particles with diameter of 1 μm would take several months to sink over a 10 m depth mixed layer, meaning that their residence time is long enough to have them accumulated in the SML during the whole stratified period (maximum stratification in June and July when the mixed layer depth is about 10–15 m over most of the basin according to D'Ortenzio et al., 2005). This is indeed a very simplistic view as we know that the biota may also play a role in the sedimentation of those particles. Indeed, atmospheric dust particles can

be rapidly removed from the surface waters together with large organic particles produced by biological packaging (Buat-Ménard et al., 1989) or dissolved organic matter forming mineral-organic aggregates (Bressac et al., 2012, 2014; Louis et al., 2017). The role of the sea surface organic microlayer in this complex scheme is also unknown, although it can accumulate atmospheric particles (Tovar-Sánchez et al., 2014) and favors photochemical and biological processes that may affect the transformation of aerosols at the air-sea interface.

3 Particle Dissolution in Seawater and Impacts on Marine Chemistry

In all the studies performed within the Mediterranean context, the authors have shown that dissolution of atmospheric particles in seawater depends on several parameters, among which, the most important are the particles origin, concentration, and size distribution. For experiments conducted in seawater, the "new" nutrients released from atmospheric particles depend also on the DOM present at the time of the deposition.

3.1 Batch Experiments

In batch experiments (Fig. 1a) that cannot take into account the impact of sinking particles, it was shown, that the percentage of dissolved Fe (Bonnet & Guieu, 2004) and DIP (Ridame & Guieu, 2002; Bonnet et al., 2005) was inversely proportional to the amount of particles introduced in Mediterranean-filtered seawater and that this percentage was higher for anthropogenic particles than for crustal particles. In those experiments, while those percentages could reach up to 15% for inorganic P associated with Saharan dust, they were shown to be extremely low for Fe (0.05–2%). Mendez et al. (2010) have shown that the amount of dissolved iron released when using the same Saharan dust and the same dust concentrations as in Bonnet and Guieu (2004) was smaller when the dissolution was performed in surface-filtered seawater collected in the Pacific. Authors argued that Fe dissolution was dependent on the water's ligand field rather than the type or quantity of dust deposited at the surface. The role of Fe binding ligands was confirmed by Wagener et al. (2008), who showed that the dust Fe dissolution rates were linearly dependent on iron binding ligands (Fig. 2a) and dissolved organic carbon concentrations (not shown).

Concerning DIN release from Saharan dust, results depended on whether experiments used evapo-condensed (EC) dust (dust enriched in nitrogen due to the simulation of cloud water processes involving HNO_3 to mimic the mixing between dust and pollution during transport; see details in Guieu et al., 2010b and Desboeufs, 2022) or non-EC dust. Abiotic batch dissolution experiments in filtered seawater have shown that non-EC dust (<20 mg L^{-1}) are a negligible source of NO_x ($NO_3^- + NO_2^-$) and NH_4^+ (Ridame

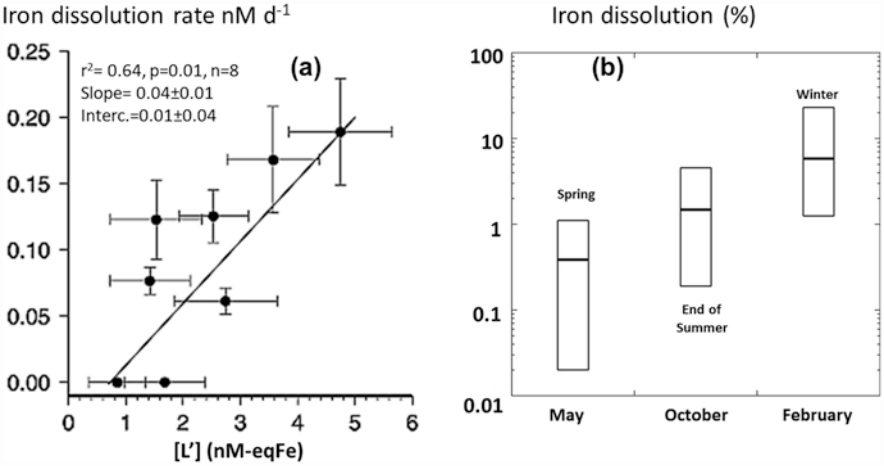

Fig. 2 (**a**) Results from "batch experiments" performed using the same dust in filtered seawater sampled each month at the DYFAMED time series site in the Ligurian Sea. They confirmed that Fe dissolution from dust is controlled by the concentration of Fe binding ligands [L']. (Reprinted from Wagener et al., 2008). (**b**) Results from "realistic view" dissolution experiment: same dust, dust flux, and protocol were used in three different experiments conducted in minicosms at different seasons characterized by contrasted in situ DOM. (Reprinted from Bressac & Guieu, 2013)

et al., 2014). In contrast, the percentage of NO_x dissolution reached 100% for EC dust concentrations higher than 0.5 mg L^{-1} (3-h contact time). However, EC dust additions (<20 mg L^{-1}) did not significantly change the ambient concentration of NH_4^+.

3.2 Mesocosm and Minicosm Experiments

In "realistic view" experiments, dust seeding on top of large pelagic mesocosms with the natural assemblage allowed to better evidence of the role of DOM and ligands, in relation to biological activity. During the first DUNE experiment in June 2008 (Guieu et al., 2010a), the dust seeding at the surface of the mesocosms was immediately followed by a decrease in *[dFe]* in the 0–10 m water column due to dissolved iron scavenging by settling dust particles and mineral organic aggregates (Wagener et al., 2010). During the second DUNE experiment (June 2010), two successive dust seedings were performed and both dissolved and particulates Al, Mn, and Fe were monitored (Wuttig et al., 2013). Dissolved Al and Mn showed clear increases directly after both seedings with dissolution of (1.44 ± 0.19)% and (0.91 ± 0.83)% for Al and (41 ± 9)% and (27 ± 19)% for Mn for the first and the second dust addition, respectively. Interestingly, 3 days after the second dust seeding, dissolved Al concentrations decreased as a consequence of scavenging by sinking biogenic particles related to the high increase in planktonic material. As for DUNE 1, the first dust addition resulted in a scavenging of dissolved Fe by sinking dust particles (net solubility = 0). On the

contrary, the second seeding induced dissolution of Fe (0.12% net solubility) from the dust particles due to the excess Fe binding ligand concentrations following the first seeding that induced fertilization (see following section on biological impacts), allowing maintaining higher *[dFe]*. Following these experiments, Bressac and Guieu (2013) conducted several dust seeding experiments on top of minicosms filled with filtered Mediterranean seawater and using the same dust and flux as in DUNE. Experiments were conducted at three different seasons when the surface seawater has very contrasted biogeochemical properties in terms of type and concentration of DOM. Depending on the season when the sampling was performed, up to one order of magnitude difference in atmospheric Fe dust dissolution was observed (Fig. 2b). Indeed, when the seawater was characterized by high and fresh DOM conditions (spring, end of summer), the rapid formation of aggregates led to both scavenging of dissolved iron and organic complexation, resulting in low dissolution. On the contrary, in winter when seawater was characterized by low-DOM conditions, there was no aggregation, and a very large transient increase in *[dFe]* was observed before being removed by re-adsorption onto settling particles.

In large pelagic mesocosms (DUNE) seeded with EC dust mimicking a dust wet event, results agreed that 100% of N attached to dust was released in seawater a few hours after dust addition (Ridame et al., 2014); same results were obtained in minicosms using 0.2-μm filtered seawater (Louis et al., 2018). This indicates that wet deposition is a major pathway for this essential nutrient to the Mediterranean Sea. Dry deposition simulated by non-EC dust seeding (that has a N content about tenfold lower than EC dust) was shown on the contrary to be a negligible source of NO_3^- (Ridame et al., 2014). In presence of the natural planktonic assemblage (DUNE mesocosms), a transient increase in DIP was observed few hours after the EC dust seeding increasing the top layer of the mesocosms of 13 nM DIP (corresponding to a 32.5% increase) (Pulido-Villena et al., 2010, 2014). This was attributed to 35% dissolution of the total P content in the dust, a dissolution percentage comparable to the one established in Ridame and Guieu (2002) from an abiotic experiment. The DIP released from dust during DUNE was completely lost 24 h after the seeding, interpreted mainly as biological uptake from the natural assemblage limited in P or NP co-limited (Pulido-Villena et al., 2010, 2014). This was indeed followed by a strong and rapid biological response (increase in both bacterial and phytoplanktonic production) (Ridame et al., 2014; Guieu et al., 2014a). Similar DIP transient increase followed by a total removal was also observed in Louis et al. (2015, 2018) in abiotic condition, indicating that biological uptake is not the only process decreasing DIP concentration and that new DIP released from dust could also be re-adsorbed by the particles within few days if not uptaken rapidly by biota.

3.3 In Situ Measurements

Simultaneous in situ measurement in both the atmosphere and seawater is another interesting approach. The recent advent of the new nanomolar techniques to measure nutrients in oligotrophic environments, such as the Mediterranean Sea, has

greatly improved our knowledge on the role of atmospheric nutrients in the nutrient stocks in the surface marine mixed layer. A pioneer study by Pulido-Villena et al. (2010) reported the first 1-year time series of concomitant measurements of nanomolar DIP at the DYFAMED site (Ligurian Sea) and atmospheric measurements at a nearby site (see those site locations in Fig. 5). During the stratification period, DIP concentration was 1–6 nM in the SML, and interestingly, no increase could be observed although the atmosphere was frequently bringing new DIP to the surface seawater. This suggests that this biologically available DIP was rapidly taken up by the biological activity, which was confirmed during a dust seeding experiment (Pulido-Villena et al., 2010).

Contribution of the organic fraction to the total soluble nitrogen (SON) and phosphorus (SOP) atmospheric deposition and its contribution to surface mixed layer stocks was recently simultaneously quantified in the NW Mediterranean Sea (Djaoudi et al., 2018). The proportions of SON and SOP to total soluble N and P in the atmospheric deposition was 40% and 25%, respectively, indicating the importance of the organic fraction. However, the contribution of atmospheric deposition to the DOC, DON, and DOP pools in the SML, estimated for the stratification period, was low for P (4.5%) and moderate for N (12%). For iron, the temporal pattern of *[dFe]* in surface waters is controlled by atmospheric deposition. For example, Bonnet and Guieu (2006) observed that the Fe enrichment in the SML that takes place all along the stratified period was of the same order of magnitude as the cumulative atmospheric inputs for the same period. This is explained by the fact that during the stratified period, the reduced marine mixed layer acts as an almost "closed" reservoir: the surface waters are isolated from deeper ones by the physical barrier generated by the thermocline, and the atmosphere becomes the main pathway of Fe supply for the surface waters. In fact, the particulate atmospheric material accumulates along the thermocline, and during the stratification period, the export of atmospheric material towards the deeper layers is reduced (Migon et al., 2002; Ternon et al., 2010). It is important to note that in the study by Bonnet and Guieu (2006), the anthropogenic contribution during the stratification period was 44% of the total atmospheric [DFe]. In the same area, it was shown in summer 2003 (during the heat wave that made the fire season longer) that biomass burning was also a significant source of dissolved iron for surface seawater (Guieu et al., 2005).

4 Impact on Ecosystems: From Experiments to In Situ Observations and Models

4.1 Direct Impact (Fertilization)

Artificial Fertilization Experiments

The dominant impacts of twelve different aerosol addition experiments conducted in the Mediterranean Sea surface waters over the past decade are summarized in Fig. 3. These studies were either performed in bottles, minicosms (300 L), or large

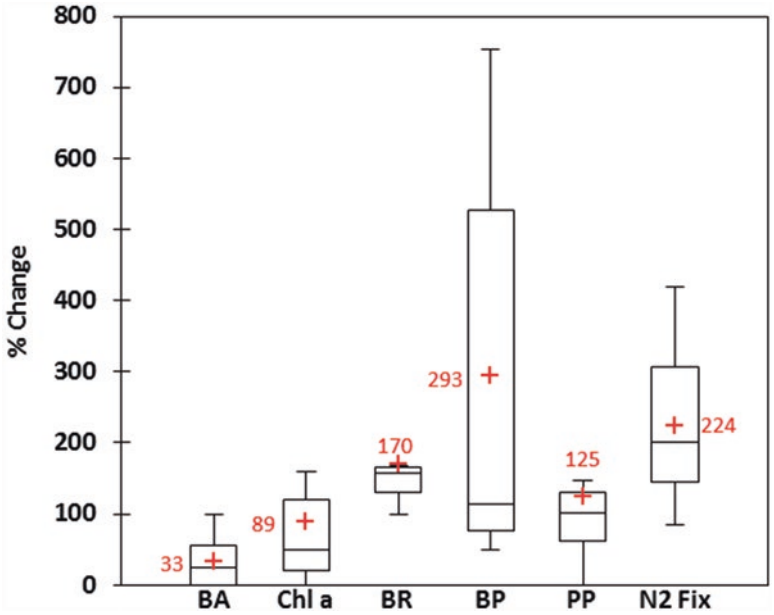

Fig. 3 Synthesis of available data on the impact on Mediterranean surface waters biological activity of natural and anthropogenic additions of aerosols obtained from field studies, and experiments performed in laboratories, minicosms and mesocosms. Box-Whisker plots: the box portion shows the interquartile range (25th to 75th percentile) of the data set; the horizontal bar within the box is the median value; the red cross and number show the mean value. The responses are % changes in the aerosol treatment relative to the control after 2–8 days, with zero indicating no difference between the aerosol treatment and the control and a positive response indicating an increase in the parameter in the aerosol treatment relative to the control. Stocks: BA Bacterial Abundance and Chl*a* Chlorophyll *a*. Fluxes: BR Bacterial Respiration, BP Bacterial Production, PP primary production, and N2Fix N_2 fixation. Details on experiments can be found in Table 1 in Guieu et al. (2014b): only the experiments conducted in the Mediterranean are considered here; original data in Bonnet et al. (2005), Guieu et al. (2014a), Herut et al. (2005, 2016), Laghdass et al. (2011), Lekunberri et al. (2010), Marín-Beltrán et al. (2019), Pulido-Villena et al. (2008, 2014), Rahav et al. (2016), Ridame (2001), Ridame et al. (2011, 2013, 2014), Ternon et al. (2011)

mesocosms, either pelagic or on-land. Different types and amounts of aerosols have been added to surface waters with different initial chemical and biological conditions (natural assemblage, limitations), and impacts have been followed during different incubation times.

In spite of these important differences in methodology, all the tested parameters indicate a positive response to aerosols addition of both bacterial and phytoplanktonic (in particular diazotrophic) communities. The lowest impact was found for the stocks (+33% in average of bacteria abundance (BA) and +89% of chlorophyll *a* (Chl*a*)) compared to the biological rates. The strongest impact was for bacteria production (BP) with, on average, a factor 4 increase with an important variability between experiments. In the ten distinct experiments, the response of N_2 fixation was high with an average increase of 224%. N_2 fixation was more stimulated after

aerosols addition than PP. This discrepancy is likely due to different nutrient limitations for PP and N_2 fixation. This was shown during the DUNE experiments where PP was likely DIN limited or co-limited by both DIN and DIP while N_2 fixation was likely limited or co-limited by DIP and/or a trace element other than Fe and released by dust (Ridame et al., 2013). Despite the strong stimulation by dust inputs, N_2 fixation rates remained low (<1.31 nmol L^{-1} d^{-1}) and its contribution to primary production was low (maximum of 8% in Rahav et al., 2016), confirming that N_2 fixation is not a key process to provide new N to the surface waters of the Mediterranean Sea (e.g., Ridame et al., 2013). The change in the phytoplanktonic biomass (Chl*a*) was also associated with important changes in plankton diversity (Laghdass et al., 2011; Herut et al., 2005; Lekunberri et al., 2010; Giovagnetti et al., 2013). Relying only on stocks to assess the effect of atmospheric deposition could lead to a very partial vision as bacteria and phytoplankton biomass are also controlled by grazing. Best example is given from phosphate addition to surface waters in the eastern Mediterranean Sea during a Lagrangian experiment. The addition caused a negative Chl*a* response and an increase in abundance of heterotrophs (both bacteria and zooplankton) (Thingstad et al., 2005). The metabolic fluxes are thus more robust indicators of the effect, and it can be seen that bacterial production is more responsive than primary production. As previously stated for other oligotrophic environments (Marañón et al., 2010), this indicates an increase in organic matter remineralization and a corresponding reduction in organic carbon export. How much the stimulation of heterotrophic bacteria would impact carbon export in the Mediterranean Sea and other LNLC environments is an important question. To our knowledge, only the DUNE experiments allowed one to establish a carbon budget following dust deposition because metabolic fluxes were measured together with carbon export at the base of the large pelagic mesocosm.

The change induced by the dust addition on the total organic carbon pool inside the mesocosm over the 7 days of the DUNE experiments was an organic carbon loss dominated by bacteria respiration that was at least 5–10 times higher than any other term involved in the budget. Although dominated by heterotrophy, a net export of particulate organic carbon was measured in the sediment traps partly due to the DOM-dust aggregation process. This carbon exported by the "lithogenic carbon pump" is detailed hereafter in Sect. 4.2.

Satellite Observations

Several attempts to observe dust fertilization effects using satellite observations have been performed over the Mediterranean basin with contrasting results. Dulac et al. (1996) have searched for evidence of the impact of Saharan dust inputs on phytoplankton based on daily satellite observations of ocean color (CZCS) and dust transport (Meteosat) near the DYFAMED station in the Ligurian Sea in summer 1983. A careful selection of Chl*a* concentration data was done to avoid data with large uncertainties due to the cloud cover and aerosol-induced biases which limited the time series. However, one particularly intense dust event in late July was

observed to be followed by a small but significant increase in phytoplankton concentration starting to increase about one week after the dust event from the background value <0.2 mg Chl*a* m^{-3} to an observed maximum of about 0.5 mg Chl*a* m^{-3} 3 weeks after the dust event (with missing Chl*a* data in-between). This case met the conditions necessary to connect atmospheric deposition and phytoplankton development during the oligotrophic season: (i) a significant increase in Chl*a*, (ii) a realistic time lag between the deposition and the increase in Chl*a,* and (iii) a wind speed not strong enough during the period (<30 km h^{-1}) to destroy the stratification and allow the nutrients to upwell from below. The authors concluded that this was likely the first observation of the impact of desert dust deposition on marine biology. This pioneer work was followed by a study over a longer period using a combination of SeaWiFS ocean color data and dust deposition from models during 2 years over the even more oligotrophic eastern Mediterranean Sea (<0.10 mg Chl*a* m^{-3} from May to September) and with a better temporal coverage (Dulac et al., 2004). Authors observed a low (0.02–0.16 mg Chl*a* m^{-3}) but systematic increase in Chl*a* concentration shortly following dust deposition, supporting possible dust fertilization of photoautotrophs organisms of the eastern Mediterranean Sea. On the other hand, the authors also showed the occurrence of high winds during dust events. Such winds, also responsible for mixing of the waters, could bring nutrients from below to the SML. In addition, Claustre et al. (2002) have shown that absorption and scattering by mineral dust particles suspended in surface waters after a deposition event likely produced a bias in SeaWiFS-derived Chl*a*, resulting in a small but significant overestimation of the biomass in such an oligotrophic environment. It is thus very difficult, if not impossible, to disentangle both effects using only satellite images. Mixed conclusions were also reached in Volpe et al. (2009) based on 5 years of satellite data (ocean color and aerosol optical thickness) who also argued that short-term responses observed from space after dust events were due to an artifact of the satellite data processing. The authors recommended using such satellite data carefully to test fertilization hypotheses. Several more recent studies reported small up to significant Chl*a* peaks following dust events, but no clear correlation pattern or rules could be inferred from satellite time series (e.g., Gallisai et al., 2014, 2016). Another recent study (Kotta & Kitsiou, 2019) focusing on the Hellenic Seas showed that the Chl*a* increase following a strong dust episode could be of the same order of magnitude compared to those reported from experimental studies (see previous section) in a limited area. Yet, authors emphasize also on the difficulty of using this approach to discriminate between dust and other meteorological effects.

In addition to issues regarding methodological consideration (Volpe et al., 2009), such studies based on ocean color, a proxy of the phytoplankton biomass, preclude observation of any possible effect on metabolic fluxes (such as primary production or respiration), and "fertilization effect" is only seen as an increase in phytoplankton biomass. Yet, experimental approaches have clearly shown the predominance of changes for rates rather than stocks as emphasized in the above Section 1.1), and that biomass is not a good proxy to test fertilization mainly because biomass is strongly influenced by grazing losses. It has to be noted that chlorophyll is not simply a measure of phytoplankton biomass but also reflects cellular pigmentation

arising from photo acclimation and nutrient-driven physiological responses. This constitutes an additional caveat when using Chl*a* from satellites as a proxy for biomass responses to dust deposition. Indeed, during and after dust storms, cells likely experience lower irradiance levels which could induce higher Chl*a* content but not related to an increase in biomass (Behrenfeld et al., 2016).

Models

Models can also bring a synoptic view of the effects at the Mediterranean Sea scale. As shown in the previous sections, our knowledge on deposition impact on marine (biogeo)chemistry was improved, mainly thanks to studies conducted over the past 15 years. This knowledge is still limited in space and time, and models can help fill quantification gaps at the scale of the Mediterranean Sea and help investigate the extent and locations of atmospheric deposition of nutrients and their impacts on nutrient(s) (co-)limitation. Recently, Palmiéri (2014) developed a regional Mediterranean configuration of the coupled model NEMOMED12/PISCES (see Aumont et al. (2015) for the global PISCES biogeochemical model configuration). In PISCES, atmospheric deposition is included as a source of nutrients (nitrate, ammonium, phosphate, silicate, and iron), and Richon et al. (2018) considered atmospheric deposition forcing of nitrogen (nitrate and ammonium) from both natural and anthropogenic sources modelled with LMDz-INCA (Hauglustaine et al., 2014) and phosphate inputs from Saharan dust modelled with ALADIN-Climate (Nabat et al., 2015). They used both monthly averages of deposition and intense 1-day fluxes uniformly distributed over the whole Mediterranean Sea to simulate the effect of extreme events (strong fluxes on short timescale as explained in Guieu et al. (2014b) for the global scale) that are observed in the Mediterranean region. Although some processes, such as the heterotrophic bacterial activity, that have been shown to be important from experimental approaches (see previous section) are not explicitly represented in the model, interesting results have been obtained. Both monthly climatology and extreme events show visible effects during the stratification period, and the impacts of anthropogenic N deposition on biology was more important than natural dust deposition of P. Although the highlighted impacts are much lower than those obtained from experimental setups (e.g., at maximum, a 30% increase in Chl*a*, mainly attributed to N deposition), the model identified where the different (co-)limitations occured at the scale of the whole Mediterranean Sea and for each month and how atmospheric deposition relieved these limitations. They showed, for example, that P deposition can alone increase primary production in the Adriatic Sea, indicating that this region is P-limited, whereas both N and P deposition are needed to increase primary production in the Tyrrhenian and Ionian seas, indicating that those regions are N-P co-limited (Fig. 4).

The study confirms the transitory effect of high dust deposition previously observed using PISCES at the global scale (Guieu et al., 2014b) with a maximum response occurring 4–10 days and 1–5 days after the N and P deposition, respectively. A more regional model study in the eastern Mediterranean Sea (Christodoulaki

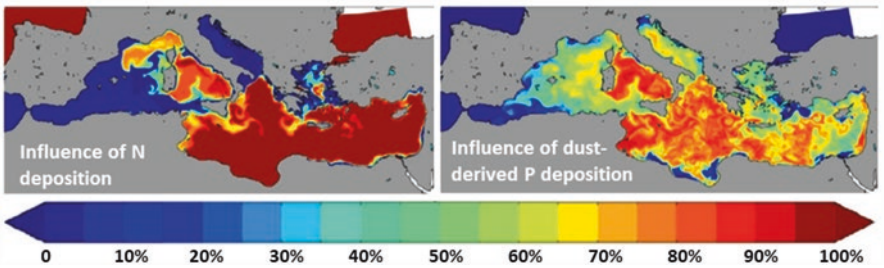

Fig. 4 Maximal relative impacts (%) of atmospheric deposition of N (left) and P (right) on primary production observed for the month of June using NEMOMED12/PISCES model. (Adapted from Richon et al., 2018)

et al., 2013) also showed significant effects of N and P deposition on primary production and phytoplankton biomass but, there again, to a lesser extent than experimental results.

4.2 Indirect Impact on Carbon Export ("Lithogenic Carbon Pump")

In the Mediterranean Sea, based on averaged atmospheric and riverine inputs, the aeolian flux of insoluble particles contributes to 50–80% of the deep-sea sedimentation in offshore waters (Guerzoni et al., 1999). Another fraction of sedimentation that is often omitted concerns the particulate organic carbon exported by DOM-dust aggregation processes. Earlier studies (e.g., Armstrong et al., 2002) have shown a strong association between fluxes of organic carbon and fluxes of ballast minerals in the deep sea. Those minerals include biogenic silicate and carbonate and dust, and the specific role of dust has been emphasized in several studies (e.g., Dunne et al., 2007). The Mediterranean Sea is an interesting laboratory to study specifically the effect of dust ballast on the export of organic carbon and several studies have recently documented both the processes involved and the resulting fluxes. We will illustrate this section with two examples showing how the pulsed dust inputs can have a quantitative impact on the export of particulate organic carbon not linked to an enhancement of primary production but due to the "lithogenic carbon pump" (following the name given in Bressac et al., 2014). The first example detailed in Ternon et al. (2010) is from simultaneous measurements of a large dust deposition that occurred in February 2004 in the Ligurian region and the sediment export in the water column at the DYFAMED time series station. This intense dust pulse (25 g m^{-2}) was particularly interesting because it occurred during a season when the nutrients were not limiting the primary productivity. The effect of that deposition to the export of particulate organic carbon (POC) in the water column was thus likely dominated by a ballast effect from the dust rather than due to an increase in

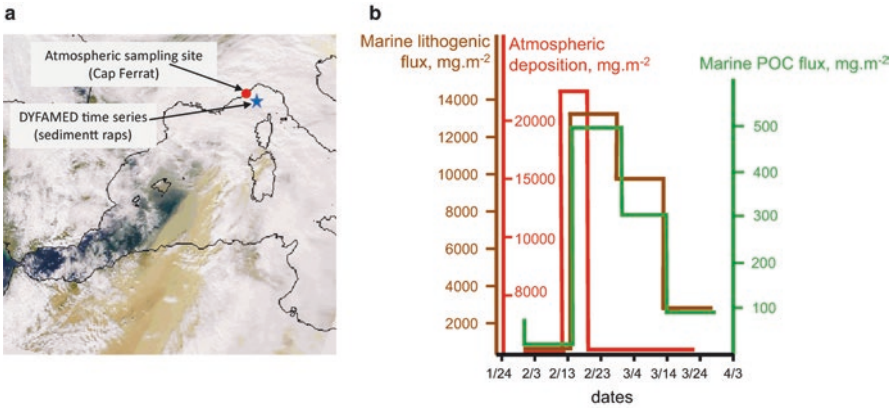

Fig. 5 An example of an extreme dust deposition event and its impact on marine lithogenic material and particulate organic carbon exports in the water column: (**a**) satellite image showing the transport of Saharan dust across the western Mediterranean Sea (SeaWiFS, NASA); (**b**) total atmospheric deposition mass flux (in red) measured at the Cap Ferrat sampling site (French Riviera) along with time series of fluxes from sediment traps at 200 m at the nearby DYFAMED stations (43°25'N, 07°52′E; http://www.obs-vlfr.fr/sodyf/) showing the huge increase in both lithogenic (in brown) and POC (in green) flux following the event. (Reprinted from de Leeuw et al., 2014)

production. A strong increase in POC export was concomitant to the marine lithogenic flux that was collected in the traps right after the event (Fig. 5).

This POC exported from the surface layer to deeper layers following the dust event represented ~45% of the total annual POC exported over the whole year 2004 at 200 m in the water column at the DYFAMED site. It showed, for the first time, the high potential of the "lithogenic carbon pump" to export substantial amounts of POC to the ocean depth. During the DUNE experiment, the POC export was linked with both the CO_2 fixation induced by the fertilization after artificial dust seeding and the dust ballasting DOM present in the water (Bressac et al., 2014). By normalizing POC export collected in the sediment traps to the primary production measured in the water column, Bressac et al. were able to quantify the contribution of the lithogenic carbon pump to the total organic carbon export. They showed that 42–50% of POC fluxes were strictly associated with lithogenic particles. Process studies conducted in 0.2-μm filtered seawater later showed that the introduction of Saharan dust actually triggered the abiotic formation of transparent exopolymer particles (TEP) leading to the formation of organic mineral aggregates and export (Louis et al., 2017). It is important to note that, so far, this fraction of carbon export in the water column is not considered in biogeochemical models indicating that a significant part of carbon export following dust pulse could be missed in budgets in oceanic regions impacted by dust deposition such as the Mediterranean Sea and the North Atlantic gyre (Pabortsava et al., 2017).

5 Conclusions and Perspectives

The results presented here demonstrate the need to consider the atmospheric compartment as a marine ecosystem forcing that must be included in biogeochemical models. Global warming may have strong effects on the stratification of surface waters in the Mediterranean Sea by increasing its vertical extent and its duration and thus enhancing the fertilizing role of the atmosphere during the whole stratification period. A concomitant effect is the possible increase in atmospheric inputs from anthropogenic (due to an increasing pressure around the whole Mediterranean basin) and natural (from Sahara but also biomass burning) sources. Open Mediterranean surface pH is projected to decline by up to around 0.3 pH unit by the end of the century. One consequence could be a change in atmospheric nutrient inputs through a potential increase in their solubility. The role of atmospheric inputs in the functioning of the Mediterranean ecosystem could be altered through modification of the plankton assemblages with possible consequences for higher trophic levels.In light of the results described here, a large experimental effort was set up to go further in our understanding of the processes at play at the air-sea interface in the Mediterranean by combining in situ observations and processes studies. A cruise took place in spring 2017 and, thanks to a dedicated strategy, the scientific team was able to study in situ the effects of dust deposition (Guieu et al., 2020). In the frame of the PEACETIME project (http://peacetime-project.org/, last access 16 Jan. 2022), an oceanographic campaign took place in spring 2017 (Guieu et al., 2020; https://campagnes.flotteoceanographique.fr/campagnes/17000300/, last access 16 Jan. 2022). More than twenty publications from PEACETIME are available in the joint special issue of the journals Biogeosciences and Atmospheric Chemistry and Physics (atmospheric deposition in the low-nutrient, low-chlorophyll (LNLC) ocean: effects on marine life today and in the future, https://www.biogeosciences.net/special_issue1040.html, last access 16 Jan. 2022). In summary, thanks to a dedicated strategy, the scientific team was able to study in situ the effects of two dust wet deposition events and dry deposition along a 4300 km transect. Impacts on the metal concentrations in the surface microlayer (Tovar-Sánchez et al., 2020) and water column (Bressac et al., 2021) and on the nitrogen budget (van Wambeke et al., 2021) were quantified. Interestingly for phosphorus, Pulido-Villena et al. (2021) have shown that external inputs of dissolved inorganic phosphorus (DIP) from both atmospheric deposition and deeper marine layer, into the DIP-depleted surface layer contributed little to the biological DIP requirement that was rather sustained by in situ hydrolysis of dissolved organic phosphorus. In situ chemical and biological stocks and fluxes over several days before-during and after a Saharan rain revealed complex competition between heterotrophic bacteria and phytoplankton for the 'new' deposited nutrient resources (van Wambeke et al., 2021) and community changes up to the zooplankton level (Feliú et al., 2020) were observed. Experimental process studies in climate reactors during the PEACETIME cruise have investigated the impact of simulated dust deposition under present and future projected conditions of seawater temperature and pH at three stations located in different basins of the western Mediterranean Sea (Gazeau et al., 2021a). The impact of dust addition

on biological communities appeared different between stations. For example, no stimulation of the autotrophic community (biomass and primary production) was observed in the Tyrrhenian Sea under present climate conditions, whereas heterotrophic bacterial production was enhanced. This could be due to an increased grazing pressure of phytoplankton by zooplankton grazers and/or competition for nutrients uptake with heterotrophic prokaryotes. A strong dust deposition that occurred 10 days before this experiment (Bressac et al., 2021) could have stimulated the growth of phytoplankton and subsequently increased the abundance and activity of the heterotrophic compartment (bacteria, micro- and meso-zooplankton). Differences in the biological response between the three experiments appear to be a consequence of the initial metabolic states of the community (autotrophy vs. heterotrophy). At the three sites, nutrients released from dust addition did not strongly alter but rather exacerbated this initial state (Gazeau et al., 2021b). While acidification and warming had no detectable impact on nutrient inputs released from dust, they induced an increase in most stocks and metabolic activities (Gazeau et al., 2021a; Ridame et al., 2022) with a stronger impact on heterotrophic remineralization relative to photosynthesis. This suggests that, in the future, phytoplanktonic communities in Mediterranean surface waters may have a reduced capacity to sequester atmospheric CO_2 after atmospheric dust deposition (Gazeau et al., 2021a).

Future works dealing with the impact of atmospheric deposition in the Mediterranean Sea will improve present knowledge only with strong collaboration between experimental scientists and modellers from the atmosphere and marine biogeochemistry. Indeed, an important perspective is to improve the representation of key processes involved in models. The characterization and quantification of the processes that have to be considered (such as bacterial production and the lithogenic carbon pump) should be provided by "realistic view" experiments taking into account the fate of the particles in order to allow their accurate parameterization. Experiments should cover a large spectrum of realistic atmospheric forcing (duration, type (i.e., wet and dry), origin, and composition), marine biogeochemical conditions (variety of organic matter, different states of nutrient limitation), and physical oceanic conditions (temperature, pH). The objective is to improve not only the quantification of current effects but also their evolution in the future. Indeed, the question of future atmospheric deposition of nutrients of both anthropogenic and natural origins and especially of Saharan origin, remains a great unknown. Here again, modelling is a necessary tool and different future scenarios should be simulated.

References

Armstrong, R. A., Lee, C., Hedges, J. I., Honjo, S., & Wakeham, S. G. (2002). A new, mechanistic model for organic carbon fluxes in the ocean: Based on the quantitative association of POC with ballast minerals. *Deep-Sea Research Part II, 49*, 219–236. https://doi.org/10.1016/S0967-0645(01)00101-1

Aumont, O., Éthé, C., Tagliabue, A., Bopp, L., & Gehlen, M. (2015). PISCES-v2: An ocean biogeochemical model for carbon and ecosystem studies. *Geoscientific Model Development, 8*, 2465–2513. https://doi.org/10.5194/gmd-8-2465-2015

Behrenfeld, M., O'Malley, R., Boss, E., Westberry, T. K., Graff, J. R., Halsey, K. H., Milligan, A. J., Siegel, D. A., & Brown, M. B. (2016). Revaluating ocean warming impacts on global phytoplankton. *Nature Climate Change, 6*, 323–330. https://doi.org/10.1038/nclimate2838

Bergametti, G., Remoudaki, E., Losno, R., Steiner, E., Chatenet, B., & Buat-Menard, P. (1992). Source, transport and deposition of atmospheric phosphorus over the northwestern Mediterranean. *Journal of Atmospheric Chemistry, 14*, 501–513. https://doi.org/10.1007/BF00115254

Bonnet, S., & Guieu, C. (2004). Dissolution of atmospheric iron in seawater. *Geophysical Research Letters, 31*, L03303. https://doi.org/10.1029/2003GL018423

Bonnet, S., & Guieu, C. (2006). Atmospheric forcing on the annual iron cycle in the Mediterranean Sea: A one-year survey. *Journal of Geophysical Research, 111*, C09010. https://doi.org/10.1029/2005JC003213

Bonnet, S., Guieu, C., Chiaverini, J., Ras, J., & Stock, A. (2005). Effect of atmospheric nutrients on the autotrophic communities in a low nutrient, low chlorophyll system. *Limnology and Oceanography, 6*, 1810–1819. https://doi.org/10.4319/lo.2005.50.6.1810

Bosc, E., Bricaud, A., & Antoine, D. (2004). Seasonal and interannual variability in algal biomass and primary production in the Mediterranean Sea, as derived from 4 years of SeaWiFS observations. *Global Biogeochemical Cycles, 18*, GB1005. https://doi.org/10.1029/2003GB002034

Bressac, M., & Guieu, C. (2013). Post-depositional processes: What really happens to new atmospheric iron in the ocean surface? *Global Biogeochemical Cycles, 27*. https://doi.org/10.1002/gbc.20076

Bressac, M., Guieu, C., Doxaran, D., Bourrin, F., Obolensky, G., & Grisoni, J.-M. (2012). A mesocosm experiment coupled with optical measurements to assess the fate and sinking of atmospheric particles in clear oligotrophic waters. *Geo-Marine Letters, 32*, 153–164. https://doi.org/10.1007/s00367-011-0269-4

Bressac, M., Guieu, C., Doxaran, D., Bourrin, F., Leblond, N., Desboeufs, K., & Ridame, C. (2014). Quantification of the lithogenic carbon pump following a simulated dust deposition event in large mesocosm. *Biogeosciences, 11*, 1007–1020. https://doi.org/10.5194/bg-11-1007-2014

Bressac, M., Wagener, T., Leblond, N., Tovar-Sánchez, A., Ridame, C., Taillandier, V., Albani, S., Guasco, S., Dufour, A., Jacquet, S. H. M., Dulac, F., Desboeufs, K., & Guieu, C. (2021). Subsurface iron accumulation and rapid aluminum removal in the Mediterranean following African dust deposition. *Biogeosciences, 18*, 6435–6453. https://doi.org/10.5194/bg-18-6435-2021

Buat-Ménard, P., Davies, P. J., Remoudaki, E., Miquel, J. C., Bergametti, G., Lambert, C. E., Ezat, E., Quétel, C. R., La Rosa, J., & Fowler, S. W. (1989). Non-steady-state biological removal of atmospheric particles from Mediterranean surface waters. *Nature, 340*, 131–133. https://doi.org/10.1038/340131a0

Carbo, P., Krom, M. D., Homoky, W. B., Benning, L. G., & Herut, B. (2005). Impact of atmospheric deposition on N and P geochemistry in the southeastern Levantine basin. *Deep-Sea Research Part II, 52*, 3041–3053. https://doi.org/10.1016/j.dsr2.2005.08.014

Christodoulaki, S., Petihakis, G., Kanakidou, M., Mihalopoulos, N., Tsiaras, K., & Triantafyllou, G. (2013). Atmospheric deposition in the Eastern Mediterranean. A driving force for ecosystem dynamics. *Journal of Marine Systems, 109–110*, 78–93. https://doi.org/10.1016/j.jmarsys.2012.07.007

Claustre, H., Morel, A., Hooker, S. B., Babin, M., Antoine, D., Oubelkheir, K., Bricaud A., Leblanc K., Quéguiner B., & Maritorena, S. A. (2002). Is desert dust making oligotrophic waters greener? *Geophysical Research Letters, 29*, 1469. https://doi.org/10.1029/2001GL014056

D'Ortenzio, F., Iudicone, D., de Boyer Montegut, C., Testor, P., Antoine, D., Marullo, S., Santoleri, R., & Madec, G. (2005). Seasonal variability of the mixed layer depth in the Mediterranean Sea as derived from in situ profiles. *Geophysical Research Letters, 32*, L12605. https://doi.org/10.1029/2005GL022463

de Leeuw, G., Guieu, C., Arneth, A., Bellouin, N., Bopp, L., Boyd, P., Denier van der Gon, H., Desboeufs, K., Dulac, F., Facchini, C., Gantt, B., Langmann, B., Mahowald, N., Marañón, E., O'Dowd, C., Olgun, N., Pulido-Villena, E., Rinaldi, M., Stephanou, E. G., & Wagener,

T. (2014). Ocean–atmosphere interactions of particles. In: P.S. Liss, & M. T. Johnson (Eds.), *Ocean-Atmosphere Interactions of Gases and Particles*. Springer, 171–246. https://doi.org/10.1007/978-3-642-25643-1_4

Desboeufs, K. (Coord.). (2022). Deposition. In F. Dulac, S. Sauvage, & E. Hamonou (Eds.), *Atmospheric chemistry in the Mediterranean Region* (Vol. 2, From air pollutant sources to impacts, Part VIII). Springer, this volume. https://doi.org/10.1007/978-3-030-82385-6

Djaoudi, K., Van Wambeke, F., Barani, A., Hélias-Nunige, S., Sempéré, R., & Pulido-Villena, E. (2018). Atmospheric fluxes of soluble organic C, N, and P to the Mediterranean Sea: Potential biogeochemical implications in the surface layer. *Progress in Oceanography, 163*, 59–69. https://doi.org/10.1016/j.pocean.2017.07.008

Dulac, F., Moulin, C., Lambert, C. E., Guillard, F., Poitou, J., Guelle, W., Quétel, C. R., Schneider, X., & Ezat, U. (1996). Quantitative remote sensing of African dust transport to the Mediterranean. In The Impact of Desert Dust Across the Mediterranean, Kluwer, 25–49, https://doi.org/10.1007/978-94-017-3354-0_3

Dulac, F., Moulin, C., Planquette, H., Schulz, M., & Tartar, M. (2004). African dust deposition and ocean colour in the eastern Mediterranean. *Rapp. Comm. Int. Mer Médit, Rept Comm. Int. Mer Médit., Monaco, 37*, 190.

Dunne, J. P., Sarmiento, J. L., & Gnanadesikan, A. (2007). A synthesis of global particle export from the surface ocean and cycling through the ocean interior and on the seafloor. *Global Biogeochemical Cycles, 21*, GB4006. https://doi.org/10.1029/2006GB002907

Durrieu de Madron, X., Denis, L., Diaz, F., Garcia, N., Guieu, C., Grenz, C., Loÿe-Pilot, M.-D., Ludwig, W., Moutin, Y., Raimbault, P., & Ridame, C. (2003). Nutrients and carbon budget budgets for the Gulf of Lion during the MOOGLI cruises. *Oceanologica Acta, 26*, 421–433. https://doi.org/10.1016/S0399-1784(03)00024-0

Elbaz-Poulichet, F., Guieu, C., & Morley, N. H. (2001). A reassessment of trace metal budgets in the Western Mediterranean Sea. *Marine Pollution Bulletin, 42*, 623–627. https://doi.org/10.1016/S0025-326X(01)00065-0

Feliú, G., Pagano, M., Hidalgo, P., & Carlotti, F. (2020). Structure and function of epipelagic mesozooplankton and their response to dust deposition events during the spring PEACETIME cruise in the Mediterranean Sea. *Biogeosciences, 17*, 5417–5441. https://doi.org/10.5194/bg-17-5417-2020

Gallisai, R., Peters, F., Volpe, G., Basart, S., & Baldasano, J. M. (2014). Saharan Dust deposition may affect phytoplankton growth in the Mediterranean Sea at ecological time scales. *PLoS One, 9*, e110762. https://doi.org/10.1371/journal.pone.0110762

Gallisai, R., Volpe, G., & Peters, F. (2016). Large Saharan dust storms: Implications for chlorophyll dynamics in the Mediterranean Sea. *Global Biogeochemical Cycles, 30*, 1725–1737. https://doi.org/10.1002/2016GB005404

Gazeau, F., Ridame, C., Van Wambeke, F., Alliouane, S., Stolpe, C., Irisson, J.-O.,Marro, S., Grisoni, J.-M., De Liège, G., Nunige, S., Djaoudi, K., Pulido-Villena, E., Dinasquet, J., Obernosterer, I., Catala, P., & Guieu, C. (2021a). Impact of dust addition on Mediterranean plankton communities under present and future conditions of pH and temperature: an experimental overview. *Biogeosciences, 18*, 5011–5034. https://doi.org/10.5194/bg-18-5011-2021

Gazeau, F., Van Wambeke, F., Marañón, E., Pérez-Lorenzo, M., Alliouane, S., Stolpe, C., Blasco, T., Leblond, N., Zäncker, B., Engel, A., Marie, B., Dinasquet, J., &Guieu, C. (2021b). Impact of dust addition on the metabolism of Mediterranean planktoncommunities and carbon export under present and future conditions of pH andtemperature. *Biogeosciences, 18*, 5423–5446. https://doi.org/10.5194/bg-18-5423-2021

Giovagnetti, V., Brunet, C., Conversano, F., Tramontano, F., Obernosterer, I., Ridame, C., & Guieu, C. (2013). Assessing the role of dust deposition on phytoplankton ecophysiology and succession in a low-nutrient low-chlorophyll ecosystem: A mesocosm experiment in the Mediterranean Sea. *Biogeosciences, 10*, 2973–2991. https://doi.org/10.5194/BG-10-2973-2013

Guerzoni, S., & Molinaroli, E. (2005). Input of various chemicals transported by Saharan dust and depositing at the sea surface in the Mediterranean Sea. In A. Saliot (Ed.), *The Mediterranean Sea. Handbook of Environmental Chemistry* (Vol. 5K). Springer. https://doi.org/10.1007/b107149

Guerzoni, S., Chester, R., Dulac, F., Herut, B., Loÿe-Pilot, M.-D., Measures, C., Migon, C., Molinaroli, E., Moulin, C., Rossini, P., Saydam, C., Soudine, A., & Ziveri, P. (1999). The role of atmospheric deposition in the biogeochemistry of the Mediterranean Sea. *Progress in Oceanography, 44*, 147–190. https://doi.org/10.1016/S0079-6611(99)00024-5

Guieu, C., Bonnet, S., Wagener, T., & Loÿe-Pilot, M.-D. (2005). Biomass burning as a source of dissolved iron to open ocean? *Geophysical Research Letters, 32*, L19608. https://doi.org/10.1029/2005GL022962

Guieu, C., Loÿe-Pilot, M.-D., Benyaya, L., & Dufour, A. (2010a). Spatial and temporal variability of atmospheric fluxes of metals (Al, Fe, Cd, Zn and Pb) and phosphorus over the whole Mediterranean from a one-year monitoring experiment: Biogeochemical implications. *Marine Chemistry, 120*, 164–178. https://doi.org/10.1016/j.marchem.2009.02.004

Guieu, C., Dulac, F., Desboeufs, K., Wagener, T., Pulido-Villena, E., Grisoni, J.-M., Louis, F., Ridame, C., Blain, S., Brunet, C., Bon Nguyen, E., Tran, S., Labiadh, M., & Dominici, J.-M. (2010b). Large clean mesocosms and simulated dust deposition: A new methodology to investigate responses of marine oligotrophic ecosystems to atmospheric inputs. *Biogeosciences, 7*, 2765–2784. https://doi.org/10.5194/BG-7-2765-2010

Guieu, C., Ridame, C., Pulido-Villena, E., Bressac, M., Desboeufs, K., & Dulac, F. (2014a). Impact of dust deposition on carbon budget: A tentative assessment from a mesocosm approach. *Biogeosciences, 11*, 5621–5635. https://doi.org/10.5194/bg-11-5621-2014

Guieu, C., Aumont, O., Paytan, A., Bopp, L., Law, C. S., Mahowald, N., Achterberg, E. P., Marañón, E., Salihoglu, B., Crise, A., Wagener, T., Herut, B., Desboeufs, K., Kanakidou, M., Olgun, N., Peters, F., Pulido-Villena, E., Tovar-Sanchez, A., & Völker, C. (2014b). The significance of episodicity in atmospheric deposition to Low Nutrient Low Chlorophyll regions. *Global Biogeochemical Cycles, 28*, 1178–1198. https://doi.org/10.1002/2014GB004852

Guieu, C., D'Ortenzio, F., Dulac, F., Taillandier, V., Doglioli, A., Petrenko, A., Barrillon, S., Mallet, M., Nabat, P., and Desboeufs, K. (2020). Process studies at the air-sea interface after atmospheric deposition in the Mediterranean Sea: Objectives and strategy of the PEACETIME oceanographic campaign (May-June 2017), *Biogeosciences Discussions*. https://doi.org/10.5194/bg-2020-44

Hauglustaine, D. A., Balkanski, Y., & Schulz, M. (2014). A global model simulation of present and future nitrate aerosols and their direct radiative forcing of climate. *Atmospheric Chemistry and Physics, 14*, 11031–11063. https://doi.org/10.5194/acp-14-11031-2014

Herut, B., Collier, R., & Krom, M. D. (2002). The role of dust in supplying nitrogen and phosphorus to the Southeast Mediterranean. *Limnology and Oceanography, 47*, 870–878. https://doi.org/10.4319/lo.2002.47.3.0870

Herut, B., Zohary, T., Krom, M. D., Mantoura, R. F., Pitta, P., Psarra, S., Rassoulzadegan, F., Tanaka, T., & Thingstad, T. F. (2005). Response of East Mediterranean surface water to Saharan dust: On-board microcosm experiment and field observations. *Deep-Sea Research Part II, 52*, 3024–3040. https://doi.org/10.1016/j.dsr2.2005.09.003

Herut, B., Rahav, E., Tsagaraki, T. M., Giannakourou, A., Tsiola, A., Psarra, S., Lagaria, A., Papageorgiou, N., Mihalopoulos, N., Theodosi, C. N., Violaki, K., Stathopoulou, E., Scoullos, M., Krom, M. D., Stockdale, A., Shi, Z., Berman-Frank, I., Meador, T. B., Tanaka, T., & Paraskevi, P. (2016). The potential impact of Saharan dust and polluted aerosols on microbial populations in the East Mediterranean Sea, an overview of a mesocosm experimental approach. *Frontiers in Marine Science, 3*, 226. https://doi.org/10.3389/fmars.2016.00226

Kanakidou, M., Myriokefalitakis, S., & Tsagkaraki, M. (2020). Atmospheric inputs of nutrients to the Mediterranean Sea. *Deep-Sea Research Part II, 171*, 104606. https://doi.org/10.1016/j.dsr2.2019.06.014

Klein, C., Dolan, J. R., & Rassoulzadegan, F. (1997). Experimental examination of the effects of rainwater on microbial communities in the surface layer of the NW Mediterranean Sea. *Marine Ecology Progress Series, 158*, 41–50. https://doi.org/10.3354/meps158041

Kotta, D., & Kitsiou, D. (2019). Exploring possible influence of dust episodes on surface marine chlorophyll concentrations. *Journal of Marine Science and Engineering, 7*, 50. https://doi.org/10.3390/jmse7020050

Kress, N., & Herut, B. (2001). Spatial and seasonal evolution of dissolved oxygen and nutrients in the Southern Levantine Basin (Eastern Mediterranean Sea): Chemical characterization of the water masses and inferences on the N:P ratios. *Deep-Sea Research Part I, 48*, 347–2372. https://doi.org/10.1016/S0967-0637(01)00022-X

Krom, M. D., Kress, N., Brenner, S., & Gordon, L. I. (1991). Phosphorus limitation of primary productivity in the eastern Mediterranean Sea. *Limnology and Oceanography, 36*, 424–432. https://doi.org/10.4319/lo.1991.36.3.0424

Krom, M. D., Herut, B., & Mantoura, R. F. C. (2004). Nutrient budget for the Eastern Mediterranean: Implications for phosphorus limitation. *Limnology and Oceanography, 49*, 1582–1592. https://doi.org/10.4319/lo.2004.49.5.1582

Laghdass, M., Blain, S., Besseling, M., Catala, P., Guieu, C., & Obernosterer, I. (2011). Impact of Saharan dust deposition on the bacterial diversity and activity in the NW Mediterranean Sea. *Aquatic Microbial Ecology, 62*, 201–213. https://doi.org/10.3354/ame01466

Lekunberri, I., Lefort, T., Romero, E., Vázquez-Domínguez, E., Romera-Castillo, C., Marrasé, C., Peters, F., Weinbauer, M., & Gasol, J. M. (2010). Effects of a dust deposition event on coastal marine microbial abundance and activity, bacterial community structure and ecosystem function. *Journal of Plankton Research, 32*, 381–396. https://doi.org/10.1093/plankt/fbp137

Louis, J., Bressac, M., Pedrotti, M. L., & Guieu, C. (2015). Dissolved inorganic nitrogen and phosphorus dynamics in abiotic seawater following an artificial Saharan dust deposition. *Frontiers in Marine Science, 2*, 27. https://doi.org/10.3389/fmars.2015.00027

Louis, J., Pedrotti, M. L., Gazeau, F., & Guieu, C. (2017). Experimental evidence of formation of Transparent Exopolymer Particles (TEP) and POC export provoked by dust addition under current and high pCO_2 conditions. *PLoS One, 12*, e0171980. https://doi.org/10.1371/journal.pone.0171980

Louis, J., Gazeau, F., & Guieu, C. (2018). Atmospheric nutrients in seawater under current and high pCO_2 conditions after Saharan dust deposition: Results from three minicosm experiments. *Progress in Oceanography, 163*, 40–49. https://doi.org/10.1016/j.pocean.2017.10.011

Loÿe-Pilot, M. D., Martin, J. M., & Morelli, J. (1990). Atmospheric input of inorganic nitrogen to the Western Mediterranean. *Biogeochemistry, 9*, 117–134. https://doi.org/10.1007/BF00692168

Ludwig, W., Dumont, E., Meybeck, M., & Heussner, S. (2009). River discharges of water and nutrients to the Mediterranean and Black Sea: Major drivers for ecosystem changes during past and future decades? *Progress in Oceanography, 80*, 199–217. https://doi.org/10.1016/j.pocean.2009.02.001

Marañón, E., Fernández, A., Mourino-Carballido, B., MartÍnez-GarcÍa, S., Teira, E., Cermeno, P., Choucino, P., Huete-Ortega, M., Fernandez, E., Calvo-Diaz, A., Morán, X. A. G., Bode, A., Moreno-Ostos, E., Varela, M. M., Patey, M. D., & Achterberg, E. P. (2010). Degree of oligotrophy controls the response of microbial plankton to Saharan dust. *Limnology and Oceanography, 55*, 2339–2352. https://doi.org/10.4319/lo.2010.55.6.2339

Marín-Beltrán, I., Logue, J. B., Andersson, A. F., & Peters, F. (2019). Atmospheric deposition impact on bacterial community composition in the NW Mediterranean. *Frontiers in Microbiology, 10*, 858. https://doi.org/10.3389/fmicb.2019.00858

Markaki, Z., Loÿe-Pilot, M. D., Violaki, K., Benyahya, L., & Mihalopoulos, N. (2010). Variability of atmospheric deposition of dissolved nitrogen and phosphorus in the Mediterranean and possible link to the anomalous seawater N/P ratio. *Marine Chemistry, 120*, 187–194. https://doi.org/10.1016/j.marchem.2008.10.005

Marty, J.-C., Chiavérini, J., Pizay, M.-D., & Avril, B. (2002). Seasonal and interannual dynamics of nutrients and phytoplankton pigments in the western Mediterranean Sea at the DYFAMED time-series station (1991–1999). *Deep-Sea Research Part II, 49*, 1965–1985. https://doi.org/10.1016/S0967-0645(02)00022-X

Mendez, J., Guieu, C., & Adkins, J. (2010). Atmospheric input of manganese and iron to the ocean: Seawater dissolution experiments with Saharan and North American dusts. *Marine Chemistry, 120*, 34–43. https://doi.org/10.1016/j.marchem.2008.08.006

Migon, C., Sandroni, V., Marty, J. C., Gasser, B., & Miquel, J. C. (2002). Transfer of atmospheric matter through the euphotic layer in the northwestern Mediterranean: Seasonal pattern and driving forces. *Deep-Sea Research Part II, 49*, 2125–2141. https://doi.org/10.1016/S0967-0645(02)00031-0

Mouriño-Carballido, B., Hojas, E., Cermeño, P., Chouciño, P., Fernández-Castro, B., Latasa, M., Marañón, E., Morán, X. A. G., & Vidal, M. (2016). Nutrient supply controls picoplankton community structure during three contrasting seasons in the northwestern Mediterranean Sea. *Marine Ecology Progress Series, 543*, 1–19. https://doi.org/10.3354/meps11558

Nabat, P., Somot, S., Mallet, M., Michou, M., Sevault, F., Driouech, F., Meloni, D., di Sarra, A., Di Biagio, C., Formenti, P., Sicard, M., Léon, J.-F., & Bouin, M.-N. (2015). Dust aerosol radiative effects during summer 2012 simulated with a coupled regional aerosol atmosphere ocean model over the Mediterranean. *Atmospheric Chemistry and Physics, 15*, 3303–3326. https://doi.org/10.5194/acp-15-3303-2015

Pabortsava, K., Lampitt, R., Benson, J., Crowe, C., McLachlan, R., Le Moigne, F. A. C., Moore, C. M., Pebody, C., Provost, P., Rees, A. P., Tilstone, G. H., & Woodward, E. M. S. (2017). Carbon sequestration in the deep Atlantic enhanced by Saharan dust. *Nature Geoscience, 10*, 189–194. https://doi.org/10.1038/ngeo2899

Palmiéri, J. (2014). Modélisation biogéochimique de la mer Méditerranée avec le modèle régional couplé NEMO-MED12/PISCES, PhD dissertation, Univ. Versailles-St Quentin en Yvelines, 2014VERS0061, 203 pp. https://tel.archives-ouvertes.fr/tel-01221529/document. Last access 21 July 2022.

Pitta, P., Kanakidou, M., Mihalopoulos, N., Christodoulaki, S., Dimitriou, P. D., Frangoulis, C., Giannakourou, A., Kagiorgi, M., Lagaria, A., Nikolaou, P., Papageorgiou, N., Psarra, S., Santi, I., Tsapakis, M., Tsiola, A., Viollaki, K., & Petihakis, G. (2017). Saharan dust deposition effects on the microbial food web in the Eastern Mediterranean: A study based on a mesocosm experiment. *Frontiers in Marine Science, 4*, 117. https://doi.org/10.3389/fmars.2017.00117

Pulido-Villena, E., Wagener, T., & Guieu, C. (2008). Bacterial response to dust pulses in the western Mediterranean: Implications for carbon cycling in the oligotrophic ocean. *Global Biogeochemical Cycles, 22*, GB1020. https://doi.org/10.1029/2007GB003091

Pulido-Villena, E., Rerolle, V., & Guieu, C. (2010). Transient fertilizing effect of dust in P-deficient LNLC surface ocean. *Geophysical Research Letters, 37*, L01603. https://doi.org/10.1029/2009GL041415

Pulido-Villena, E., Baudoux, A.-C., Obernosterer, I., Landa, M., Caparros, J., Catala, P., Georges, C., Harmand, J., & Guieu, C. (2014). Microbial food web dynamics in response to a Saharan dust event: Results from a mesocosm study in the oligotrophic Mediterranean Sea. *Biogeosciences, 11*, 5607–5619. https://doi.org/10.5194/bg-11-5607-2014

Pulido-Villena, E., Desboeufs K., Djaoudi, K., Van Wambeke, F., Barrillon, S., Doglioli, A., Petrenko, A., Taillandier, V., Fu, F., Gaillard, T., Guasco, S., Nunige, S., Triquet, S., & Guieu, C. (2021). Phosphorus cycling in the upper waters of the Mediterranean Sea (PEACETIME cruise): relative contribution of external and internal sources. Biogeosciences, 18, 5871–5889. https://doi.org/10.5194/bg-18-5871-2021

Rahav, E., Shun-Yan, C., Cui, G., Liu, H., Tsagaraki, T. M., Giannakourou, A., Tsiola, A., Psarra, S., Lagaria, A., Mulholland, M. R., Stathopoulou, E., Paraskevi, P., Herut, B., & Berman-Frank, I. (2016). Evaluating the impact of atmospheric depositions on springtime dinitrogen fixation in the Cretan Sea (eastern Mediterranean)—A mesocosm approach. *Frontiers in Marine Science, 3*, 180. https://doi.org/10.3389/fmars.2016.00180

Rees, A. P., Law, C. S., & Woodward, E. M. S. (2006). High rates of nitrogen fixation during an in-situ phosphate release experiment in the Eastern Mediterranean Sea. *Geophysical Research Letters, 33*, L10607. https://doi.org/10.1029/2006GL025791

Richon, C., Dutay, J. C., Dulac, F., Wang, R., Balkanski, Y., Nabat, P., Aumont, O., Desboeufs, K., Laurent, B., Guieu, C., Raimbault, P., & Beuvier, J. (2018). Modeling the impacts of atmospheric deposition of nitrogen and desert dust-derived phosphorus on nutrients and biologi-

cal budgets of the Mediterranean Sea. *Progress in Oceanography, 163*, 21–39. https://doi.org/10.1016/j.pocean.2017.04.009

Ridame, C. (2001). Rôle des apports atmosphériques d'origine continentale dans la biogéochimie marine: Impact des apports sahariens sur la production primaire en Méditerranée, PhD dissertation, Univ. Paris 6, 297 pp. Villefranche sur Mer, France.

Ridame, C., & Guieu, C. (2002). Saharan input of phosphorus to the oligotrophic water of the open western Mediterranean. *Limnology and Oceanography, 47*, 856–869. https://doi.org/10.4319/lo.2002.47.3.0856

Ridame, C., Le Moal, M., Guieu, C., Ternon, E., Biegala, I. C., L'Helguen, S., & Pujo-Pay, M. (2011). Nutrient control of N_2 fixation in the oligotrophic Mediterranean Sea and the impact of Saharan dust events. *Biogeosciences, 8*, 2773–2783. https://doi.org/10.5194/bg-8-2773-2011

Ridame, C., Guieu, C., & L'Helguen, S. (2013). Strong stimulation of N_2 fixation in oligotrophic Mediterranean Sea: Results from dust addition in large in situ mesocosms. *Biogeosciences, 10*, 7333–7346. https://doi.org/10.5194/bg-10-7333-2013

Ridame, C., Dekaezemacker, J., Guieu, C., Bonnet, S., L'Helguen, S., & Malien, F. (2014). Phytoplanktonic response to contrasted Saharan dust deposition events during mesocosm experiments in LNLC environment. *Biogeosciences, 11*, 4783–4800. https://doi.org/10.5194/bg-11-4783-2014

Ridame, C., Dinasquet, J., Hallstrøm, S., Bigeard, E., Riemann, L., Van Wambeke, F., Bressac, M., Pulido-Villena, E., Taillandier, V., Gazeau, F., Tovar-Sanchez, A., Baudoux, A-C., & C. Guieu (2022). N_2 fixation in the Mediterranean Sea related to the composition of the diazotrophic community and impact of dust under present and future environmental conditions. *Biogeosciences, 19*, 415–435. https://doi.org/10.5194/bg-19-415-2022

Sala, M. M., Peters, F., Gasol, J. M., Pedrós-Alió, C., Marrasé, C., & Vaqué, D. (2002). Seasonal and spatial variations in the nutrient limitation of bacterioplankton growth in the northwestern Mediterranean. *Aquatic Microbial Ecology, 27*, 47–56. https://doi.org/10.3354/ame027047

Stokes, G. G. (1851). On the effect of the internal friction of fluids on the motion of pendulums. *Transactions of the Cambridge Philosophical Society, 9*, 8–106.

Taillandier, V., Prieur, L., D'Ortenzio, F., Ribera d'Alcalà, M., & Pulido-Villena, E. (2020). Profiling float observation of thermohaline staircases in the western Mediterranean Sea and impact on nutrient fluxes. *Biogeosciences, 17*, 3343–3366. https://doi.org/10.5194/bg-17-3343-2020

Tanaka, T., Thingstad, T. F., Christaki, U., Colombet, J., Cornet-Barthaux, V., Courties, C., Grattepanche, J.-D., Lagaria, A., Nedoma, J., Oriol, L., Psarra, S., Pujo-Pay, M., & Van Wambeke, F. (2011). Lack of P-limitation of phytoplankton and heterotrophic prokaryotes in surface waters of three anticyclonic eddies in the stratified Mediterranean Sea. *Biogeosciences, 8*, 525–538. https://doi.org/10.5194/bg-8-525-2011

Ternon, E., Guieu, C., Loÿe-Pilot, M.-D., Leblond, N., Bosc, E., Gasser, B., Miquel, J.-C., & Martin, J. (2010). The impact of Saharan dust on the particulate export in the water column of the North Western Mediterranean Sea. *Biogeosciences, 7*, 809–826. https://doi.org/10.5194/bg-7-809-2010

Ternon, E., Guieu, C., Ridame, C., L'Helguen, S., & Catala, P. (2011). Longitudinal variability of the biogeochemical role of Mediterranean aerosols in the Mediterranean Sea. *Biogeosciences, 8*, 1067–1080. https://doi.org/10.5194/bg-8-1067-2011

Thingstad, T. F., Krom, M. D., Mantoura, R. F. C., Flaten, G. A. F., Groom, S., Herut, B., Kress, N., Law, C. S., Pasternak, A., Pitta, P., Psarra, S., Rassoulzadegan, F., Tanaka, T., Tselepides, A., Wassmann, P., Woodward, E. M. S., Wexels Riser, C., Zodiatis, G., & Zohary, T. (2005). Nature of phosphorus limitation in the ultraoligotrophic eastern Mediterranean. *Science, 309*, 1068–1071. https://doi.org/10.1126/science.1112632

Tovar-Sánchez, A., Arrieta, J. M., Duarte, C. M., & Sañudo-Wilhelmy, S. A. (2014). Spatial gradients in trace metal concentrations in the surface microlayer of the Mediterranean Sea. *Frontiers in Marine Science, 1*, 79. https://doi.org/10.3389/fmars.2014.00079

Tovar-Sánchez, A., Rodríguez-Romero, A., Engel, A., Zäncker, B., Fu, F., Marañón, E.,Pérez-Lorenzo, M., Bressac, M., Wagener, T., Triquet, S., Siour, G., Desboeufs,K., & Guieu, C. (2020). Characterizing the surface microlayer in the MediterraneanSea: trace metal concentrations and microbial plankton abundance. *Biogeosciences, 17*, 2349–2364. https://doi.org/10.5194/bg-17-2349-2020

Van Wambeke, F., Taillandier, V., Desboeufs, K., Pulido-Villena, E., Dinasquet, J., Engel, A., Marañón, E., Ridame, C., & Guieu, C. (2021). Influence of atmospheric deposition on biogeochemical cycles in an oligotrophic ocean system. *Biogeosciences, 18*, 5699–5717. https://doi.org/10.5194/bg-18-5699-2021

Volpe, G., Banzon, V. F., Evans, R. H., Santoleri, R., Mariano, A. J., & Sciarra, R. (2009). Satellite observations of the impact of dust in a low-nutrient, low chlorophyll region: Fertilization or artifact? *Global Biogeochemical Cycles, 23*, GB3007. https://doi.org/10.1029/2008GB003216

Wagener, T., Pulido-Villena, E., & Guieu, C. (2008). Dust iron dissolution in seawater: Results from a one-year time-series in the Mediterranean Sea. *Geophysical Research Letters, 35*, L16601. https://doi.org/10.1029/2008GL034581

Wagener, T., Guieu, C., & Leblond, N. (2010). Effects of dust deposition on iron cycle in the surface Mediterranean Sea: Results from a mesocosm seeding experiment. *Biogeosciences, 7*, 3769–3781. https://doi.org/10.5194/bg-7-3769-2010

Wuttig, K., Wagener, T., Bressac, M., Dammshäuser, A., Streu, P., Guieu, C., & Croot, P. L. (2013). Impacts of dust deposition on dissolved trace metal concentrations (Mn, Al and Fe) during a mesocosm experiment. *Biogeosciences, 10*, 2583–2600. https://doi.org/10.5194/bg-10-2583-2013

Zohary, T., Herut, B., Krom, M. D., Mantoura, R. F. C., Pitta, P., Psarra, S., Rassoulzadegan, F., Stambler, N., Tanaka, T., Thingstad, T. F., & Woodward, E. M. S. (2005). P-limited bacteria but N and P co-limited phytoplankton in the Eastern Mediterranean – A microcosm experiment. *Deep Sea Research, 52*, 3011–3023. https://doi.org/10.1016/j.dsr2.2005.08.011

Impact of Air Pollution on Terrestrial Ecosystems

Maria Kanakidou, Maria Sfakianaki, and Anne Probst

Contents

Abstract This chapter summarizes the current state of knowledge on the impacts of air pollution on terrestrial vegetation in general and in the Mediterranean region. These impacts occur either indirectly through changes in the physical state of the atmosphere, such as increase in the temperature (caused by greenhouse gases), and in the diffuse radiation (caused by aerosols) that reaches vegetation, or directly through phytotoxicity resulting from ozone, sulfur, nitrogen, and other pollutants' stomatal and non-stomatal uptake by the plants, nutrient balance modification by atmospheric deposition, transfer of plant diseases by aerosols, and pollution by

Chapter reviewed by Panayiotis Nektarios (School of Agricultural Sciences, Department of Agriculture, Hellenic Mediterranean University, Heraklion, Greece), as part of the book Section X Impacts of Air Pollution on Human Health and Ecosystems also reviewed by Semia Cherif (ISSBAT, University of Tunis El Manar, Tunisia)

M. Kanakidou (✉) · M. Sfakianaki
Environmental Chemical Processes Laboratory (ECPL), Department of Chemistry, University of Crete, Heraklion, Greece
e-mail: mariak@uoc.gr

A. Probst
Laboratoire Ecologie Fonctionnelle et Environnement, Observatoire Midi-Pyrénées, Université de Toulouse, CNRS, Toulouse, France

F. Dulac et al. (eds.), *Atmospheric Chemistry in the Mediterranean Region*,
https://doi.org/10.1007/978-3-030-82385-6_24

persistent pollutants and metals. Abiotic and biotic stresses can also alter the composition, amounts, and functioning of volatile organic compounds that are emitted by the plants and play known ecological roles. These impacts are summarized, and plant physiological responses to an excess of critical nutrient levels are presented and discussed.

1 Introduction

The Mediterranean Basin is among the world's regions hosting the highest biodiversity of both marine and terrestrial ecosystems. The Mediterranean's flora is highly diverse with 15,000–25,000 species, among which 60% are native and endemic species unique to the region (Vlachogianni et al., 2012). Globally, terrestrial vegetation is responsible for more than half of the atmospheric oxygen production. Regionally, vegetation interacts with the atmospheric water cycle through photosynthesis, respiration, and transpiration. In urban regions, vegetation has the capacity to partially counterbalance the heat island effect and improve microclimate through the reduction of both noise and intensity of atmospheric ionization. Furthermore, vegetation is an efficient recycling energy source, and plant products provide raw material for various constructions, clothing, as well as nutrients for humans and fauna.

Due to the mild weather conditions and the fertility of most soils, agriculture has always been an integral part of human activities and an important contributor to the economy of the Mediterranean countries. However, vegetation in the region is at risk due to land use changes and the occurrence of environmental stresses and air pollution combined with climate change. Mediterranean vegetation is known to be highly resilient to disturbances, which is tentatively attributed to its historical evolution under various stresses and to its increased biodiversity, although the mechanisms associated with the resilience of ecosystems remain to be understood (Lavorel, 1999). Severe man-driven land use changes, like urban extension, agricultural abandonment, and afforestation, have led to flora redistribution within the Mediterranean region and to the increase of invasive alien plant species (Mosher et al., 2009; Vilà et al., 2003). In addition, human interference to nature has resulted to several side effects such as extreme climatic events, including prolonged droughts and increased occurrence of wildfires, along with elevated ozone (O_3) and particulate matter levels (Avila et al., 1997; Kanakidou et al., 2011).

Air pollutants affect the physiology of the plants in several ways and through different pathways: (a) by absorption through the leaf stomata or epidermis (Heath, 2008; Hill, 1971), (b) through the root system after air pollutant deposition onto the soils (Cataldo & Wildung, 1978; Gandois & Probst, 2012), (c) by adsorption of aerosols onto the leaves thus reducing the penetrating light and blocking the opening of stomata (Gheorghe & Ion, 2011), and (d) by changing the Photosynthetically Active Radiation (PAR) that reaches the plant (Rap et al., 2015). Air pollutants can

also cause acute damage to the vegetation whenever absorption of high pollutant concentrations is performed in a relatively short time interval, while chronic injuries occur due to long-term absorption of pollutants at sublethal concentrations (Gheorghe & Ion, 2011). In addition, plants (both above- and below-ground plant components) emit a variety of volatile organic compounds (VOC) (Agathokleous et al., 2020; Guenther et al., 2012; Yuan et al., 2009) that have several ecological functions in the plant cycle, serving, for instance, for pollinator attraction, plant defense against insects, plant-plant communication, thermotolerance, and removing reactive oxygen species like ozone (Yuan et al., 2009). Biotic and abiotic stresses to the plants can lead to changes in the emitted VOC composition (e.g., VOCs emitted as a plant response to pathogen or herbivore attacks; Hopke et al., 1994), and thus in their contribution to the abovementioned functions (Yuan et al., 2009). Mills et al. (2018) estimated a global loss in wheat yields due to exposure to O_3 of 6–9% on average in the south and north hemisphere, respectively, that results in actual total grain losses of approximately 85 Tg per year.

In the 80s, acid rain emerged as a major problem for European forests (Grennfelt et al., 2020). The acid rain facilitated solubilization and leaching of mineral elements, like calcium (Ca), potassium (K), and magnesium (Mg), from the soil and led to the removal of vital minerals and nutrients for plant growth resulting in profound yellowing of the leaves due to deficiencies (Landmann & Bonneau, 1995). The applied legislation for air pollution abatement resulted in the reduction of pollutants' emissions (Lamarque et al., 2013) that subsequently led to substantial decrease of sulfate concentrations in atmospheric aerosols over the past 30 years (Aas et al., 2019) and reduced atmospheric deposition to distant forests (Pierret et al., 2019). However, deposition fluxes of reactive nitrogen remain high and affect ecosystem's health (Aguillaume et al., 2016; Im et al., 2013; Kanakidou et al., 2020; Markaki et al., 2010; Ochoa-Hueso et al., 2011). Nevertheless, eutrophication and acidification issues persist, and they are of high concern since they affect biodiversity leading to a loss of species richness (Duprè et al., 2010). Analyzing 70 years of species richness in acidic grasslands of Northern Europe, Duprè et al. (2010) found that changes in vegetation species spatial distribution were mainly related to soil acidity, which affects solubilization of metal oxides and releases toxic metal ions, and to the cumulative amounts of nitrogen (N) and sulfur (S) deposition. It is worth noting that N atmospheric deposition has been proposed to be the main driver for variation in plant species richness (Stevens et al., 2004), phytocommunity composition (Bobbink et al., 2010), and relative plant species abundance (Gilliam, 2006). The interaction between N deposition and air temperature increase under climate change has been predicted to impact soil functioning and to cause vegetation species and spatial changes for the next decades (Gaudio et al., 2015; Rizzetto et al., 2016).

Furthermore, aerosol pollution also affects vegetation by scattering light and thus increasing the fraction of diffuse radiation and the efficiency of photosynthesis (Rap et al., 2015) and by providing nutrients and/or toxic substances to the ecosystem through dry or wet deposition (Kanakidou et al., 2018; Ochoa-Hueso et al., 2011). Adsorption of aerosols on the leaf surface causes negative effects to the

plants since aerosols cover the leaves surface, reduce the penetrating light, and block the opening of stomata (Gheorghe & Ion, 2011). The vicinity of the Mediterranean Basin with the African desert results in frequent dust outbreaks that increase aerosol levels and nutrient deposition over the Mediterranean (Kanakidou et al., 2020; Guieu and Ridame, 2022). In addition, dust outbreaks can also carry pathogens to Mediterranean (Polymenakou et al., 2008) and other ecosystems causing them to degrade as has been suggested for Caribbean ecosystems (Garrison et al., 2003, 2006).

Finally, intensification of agriculture activities so as to cover human needs for nutrition has led to soil contamination through the excessive use of fertilizers and pesticides. Spraying of several pesticides in the atmosphere against insects, plant pathogens, or other pests in order to improve product quality and to increase the yields of various crops has contributed to air pollution of agricultural regions. Pesticides include a wide range of compounds: insecticides, herbicides, fungicides, plant growth regulators, and others (Aktar et al., 2009). They are sprayed on the crops, and thus they partially remain in the atmosphere, transported by the wind, and deposited to the nearby soils, thus expanding contamination and providing an additional pathway for pesticides to penetrate into the plants through the soil. Toxic metals form another category of important air pollutant present in the atmosphere in low concentrations, which once are deposited can accumulate in the soils (Hernandez et al., 2003), sediments (N'Guessan et al., 2009), and organisms (EMEP, 2018; Kabata-Pendias, 2010). Persistent organic compounds and toxic metals tend to accumulate in plants, resulting in an increase of their concentration within the tissues of organisms at successively higher levels, entering the food chain (Liu et al., 2005). Metal enrichments of soils in agricultural and urban areas of Greece (Kelepertzis, 2014) and Spain (Acosta et al., 2011) have been attributed to accumulation processes resulting from prolonged applications of large amounts of fertilizers and pesticides–fungicides (copper (Cu), zinc (Zn), cadmium (Cd), lead (Pb), and arsenic (As)), as well as from industrial activities, and metal deposition due to the high volume of vehicular traffic (Pb and Cd). Pollution of vegetation both by metals and pesticides can be harmful to human health since these pollutants can penetrate in the food chain (Nasreddine & Parent-Massin, 2002). Finally, more or less biodegradable detergents that are discharged into the sea can then be transported to the atmosphere through the production of sea spray leading to air pollution. The deposition of sea spray loaded with detergent on the leaves of the plants promotes the penetration of salt into the plants causing their death. Impacts of the aforementioned pollution can be observed on certain coastal forests around the Mediterranean Sea (Garrec, 2019).

In this chapter, we first outline general information regarding the mechanisms of air pollutants pathways into the plants and the phytotoxicity effects caused by the most common atmospheric pollutants. Subsequently, we discuss the impact of the major pollutants, namely, ozone, sulfur, nitrogen, and metals on the vegetation, spanning from forests to crops in the Mediterranean region.

2 Pollutant Uptake by the Plants

Penetration of air pollutants into the plant occurs either from the aerial or from the underground organs of the plants. From the aerial organs, air pollutant absorption into plants occurs mainly through the leaves, although a slight absorption through stems and trunk might also be possible (Garrec, 2019; Kabata-Pendias, 2010). Air pollutants can also be absorbed by the roots of the plants after being deposited onto the soil in their deposited chemical form or after being chemically transformed. Before reaching the cuticle of the leaf, the pollutant passes through a thin zone of calm air that surrounds each leaf, the atmospheric interfacial leaf/atmosphere sublayer. The resistance to air pollution absorption through the interfacial atmospheric layer varies according to numerous parameters, such as leaf size, shape, and orientation, presence and shape of trichomes, and wind speed (Garrec, 2019; Gupta, 2016; Heath et al., 2009).

The interfacial leaf/atmosphere layer contains three phases: (a) the gas phase, where the air pollutants reaching the plant are present together with the emissions of the leaf; (b) the aqueous phase, which contains the water film located at the surface of the leaf and water that is bound to the cuticle through its polar groups; and (c) the lipid phase, which contains the waxes that are located on the surface of or inside the cuticle. The pollutant may react in one of these phases and could produce additional secondary phytotoxic products to the initial pollutant itself (Percy et al., 1994). Organic matter exudation by the leaves can lead to a complete dissolution of dry deposition of metals at the leaf surface and make them easier to be absorbed by the leaves (Hou et al., 2005).

The air pollutants can be transported into the plant following various pathways (Fig. 1): penetration mainly by stomata (*gases*), which are present in the leaf surface (Gupta, 2016), surface deposits (aerosols), and trapping in epicuticular waxes (lipophilic and high molecular weight gases). Following dry and wet atmospheric deposition, *metals* can be found in wax and inside the coniferous needles depending on the metal and its particulate or dissolved form (Gandois & Probst, 2012). The main plant absorption route for *organic pollutants* is via the lipid structure of the cuticle. However, from the pollutant concentration found in the interfacial leaf/atmosphere layer, only a small portion will finally enter into the plant. There, they will react within the different plant compartments, both in the outer and the inner sides of the plasma membrane (apoplast and symplast) (Faulkner, 2018; Garrec, 2019; Kundu et al., 2018; Oparka, 2005). Meteorological conditions such as amount of sun irradiance, wind, and rain, as well as leaf microstructure and vegetation macrostructure, influence the characteristics of *aerosol deposition* on the surface of the leaves (Leonard et al., 2016). Moreover, O_3 absorption by stomata depends on water availability during the growing season, plant morphological characteristics such as the existence and the shape of the leaf trichomes, and also on the sensitivity of the plants, which may vary strongly according to both the species and the varieties (Lombard et al., 2015; Saitanis et al., 2014; Saitanis & Karandinos, 2002). The physiological response of plants to air pollutants after their absorption will depend

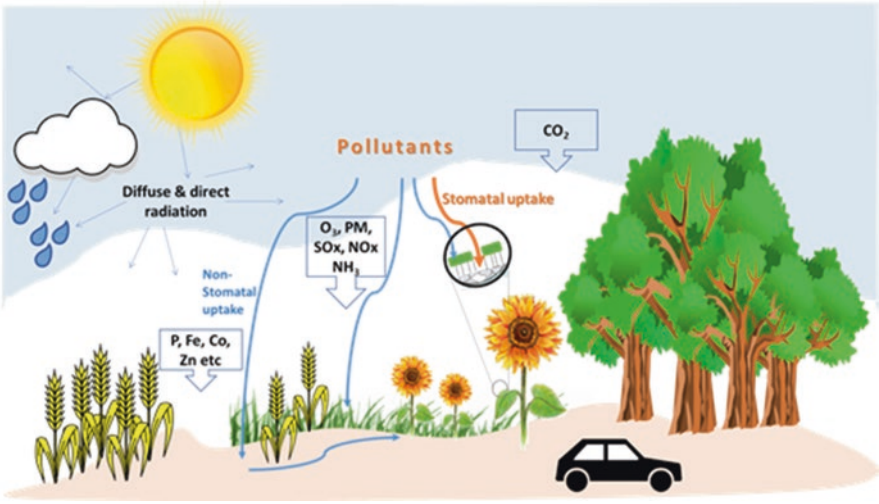

Fig. 1 Gaseous and particulate atmospheric pollutants are transported in the plants through stomatal and non-stomatal uptake by the leaves as well as via deposition onto the soil and subsequent uptake by the roots

on both the characteristics of the plant and the nature of the air pollutant (Wolfenden & Mansfield, 1990).

3 Pollutant Reactions Inside the Plant

Once the pollutant enters the plant, it causes an oxidative stress producing reactive oxygen species (ROS), including free hydroxyl radicals, which can cause damage to the plants at different levels. ROS induce oxidative damage to lipids, proteins, and DNA (Sharma et al., 2012). The pollutant will cause specific stress to the plant depending on its physicochemical characteristics (Table 1).

Ozone enters the plants through stomatal and non-stomatal uptake from the leaf cuticle via thermal decomposition or aqueous reactions in water films on plant surfaces (Fowler et al., 2009; Heath, 2008). Inside the plant, O_3 contributes to ROS production, but since it is very short-lived, it is quickly converted to more stable ROS, such as hydrogen peroxide, superoxide, and hydroxyl radical (Health 2008). If O_3 concentration exceeds the detoxification capacity of the apoplastic antioxidants, it will negatively affect plant's physiological processes, such as photosynthesis and/or respiration (Emberson et al., 2018; Musselman et al., 2006).

Nitrogen dioxide (NO_2) dissolved in cells produces nitrite ions (NO_2^-), which are toxic at high concentrations and nitrate ions (NO_3^-) that enter nitrogen metabolism. Nitrogen dioxide pollution is detectable on leaves and seedlings and is more

Table 1 Main categories of atmospheric short-lived pollutants, the pathways through which they enter into the plants, and their main effects on the plants

Pollutant	Transport pathway	Effects on plant
Ozone (O_3)	Stomata, non-stomatal pathway, deposition on leaves	Increase in reactive oxygen species Changes in plant's physiological processes Reduction of photosynthesis Reduction of crop yields Emissions of VOC, plant reproduction, plant-to-plant and plant-soil-microbe interactions Changes in C and N cycling Changes in Diversity of plant communities
Reactive nitrogen (N) (mainly NOx, NH_3, HNO_3, ammonium, and nitrate)	Stomata, deposition on leaves	Low levels→ amino acids/protein synthesis High levels → reduced photosynthetic activity Changes in plant and soil stoichiometry (N/P) N-induced P limitation Soil and water eutrophication leading to plant toxicities or deficiencies and biodiversity losses
Sulfur (S) (mainly SO_2, H_2SO_4, sulfate)	Stomata, deposition on leaves	Low levels → protein synthesis High levels → stomata opening reduction, water stress, O_2 replacement in cellular material Chlorophyll degradation Acidification after deposition to plants and soils Soil acidification/nutrient losses
Acid deposition (mainly N, S)	Deposition on leaves and soil	Acidification of soil: nutrient losses through leaching of plant growth minerals and nutrients, resulting in yellowing of leaves, increase vulnerability of plants, dying trees, and solubilization of toxic metals; loss of plant diversity
Aerosols (also containing S, N, and metals)	Deposition on leaves and soil	Diffuse radiation, closing of stomata Acidification of soils, leaching of minerals, mineral and nutrient deficiency Accumulation of pollutants into plants Carriers of plant diseases
Trace metals	Deposition on leaves and soil, with uptake by the roots	Accumulation into plants and leave edges Disturbance of plant's physiological processes depending on the metal Contamination of food chain
Pesticides	Deposition on leaves and soil, with uptake by roots	Accumulation into plants Contamination of food chains
Halogens (Cl_2, HCl, HF)	Stomata, deposition on leaves	Interfere with enzymes activity Damage cell membranes of plants Disruption of the cellular metabolism of calcium Necrosis, plant death

profound in conifer older needles where tipburn is observed. It forms crystalloid structures in the stroma of chloroplasts and bloats the thylakoid membrane within the plant cells, resulting in the reduction of photosynthetic activity (Gheorghe & Ion, 2011).

Sulfur enters the leaves as sulfur dioxide (SO_2) through the stomata. Sulfur, at low concentrations, is used by the plant in protein synthesis, but at high concentrations, it interferes with electron transport chain, leading to stomatal opening reduction, water stress, and oxygen replacement in cellular material (Mudd, 1975). It also affects structural proteins in the cell membrane leading to alterations in the permeability of the membranes (Nieboer et al., 1976). In high concentrations, SO_2 will lead to chlorophyll's degradation (Brahmachari & Kundu, 2017).

Halogens (Cl_2, HCl, HF) enter the plants through the stomata and move to the margins and edges of the leaves, where they tend to accumulate. Inside the plants, fluorides interfere with the activity of many enzymes, by inhibiting the functioning of proteins through combination with the metal components of the proteins or otherwise (Gheorghe & Ion, 2011). It is worth mentioning that hydrofluoric acid (HF) pollution is also inducing a disruption of the cellular metabolism of calcium (Garrec, 2019).

The phytotoxicity of the various pollutants depends on their chemical identity (Table 1). The main air pollutants have been classified by laboratory experiments according to their decreasing phytotoxicity impact as follows:

Hydrofluoric acid (HF) > ozone (O_3) > sulfur dioxide (SO_2) > nitrogen dioxide (NO_2).

However, this trend is only indicative, since different plants have different sensitivity to the various pollutants (Smith et al., 1989; Yu et al., 2011). In addition to the phytotoxic potential of the pollutant, the plant's response depends on the cumulative amount of the pollutant that entered the plant. Furthermore, the time period over which a certain amount of pollutant is transported into the plant is also important for its phytotoxic response. For the same amount of pollutant, a shorter transportation time will result in a greater pollutant impact. The so-called peak effect is usually explained by the fact that over short periods of time, the plant does not have adequate time to acclimatize, adapt, and initiate its defense systems response.

The large number of pollutants (e.g., HF, O_3, SO_2, NO_2, aerosols, metals) that affect plants can also be classified according to the extent of their impact zone, which depends on their lifetime in the atmosphere and thus on the distance in which they can affect vegetation after emission or formation and transport in the atmosphere (Garrec, 2019). Short-lived pollutants, like nitrogen oxides and ammonia, with lifetimes of a few hours to a day exhibit impacts on the plants within a radius of a few tens of kilometers from their emission sources. Nitrogen oxides (NOx) are mainly originating from transport and other combustion sources, while ammonia (NH_3) is mainly from agriculture and transport. In contrast, pollutants with atmospheric lifetimes ranging from few days to weeks can have impacts over several hundred kilometers around their emission sources. These include mainly acidic compounds, such as sulfuric acid (H_2SO_4) and nitric acid (HNO_3), deposited by dry or wet removal processes. Since these acids are formed via the oxidation of primary pollutants (SO_2 and NO_2) by oxidants like ozone, hydroxyl radicals, and nitrate radicals, they are considered as secondary pollutants (Graedel & Crutzen, 1993). Pollutants with lifetime of several years have global impacts and mainly include carbon dioxide (CO), which is linked to the massive use of fossil fuels by transport

and industry. Carbon dioxide has direct beneficial effects on plant growth via its essential role in photosynthesis, while at the same time, it has indirect harmful effects on plants through enhancing the greenhouse effect that results in climate change (Farquhar, 1997). Other global pollutants, which have an indirect effect on vegetation via their contribution to the greenhouse effect, include: methane (CH_4), a component of natural gas, which is also produced by ruminants and in anaerobic environments such as wetlands and rice fields and which has phytotoxic effects on plants whenever its concentration is increased such as in the case of landfills (Peer et al., 1993); nitrous oxide (N_2O), resulting from the massive use of fertilizers in agriculture; halocarbons, having several applications such as solvents, refrigerants and in insulation materials; or even soil disinfectants such as methyl bromide which was in use until the beginning of the century. Halocarbons are also ozone-depleting gases with the possibility of an additional negative impact on plants as a result of the increased UV-B solar flux that reaches Earth's surface due to their contribution to the enlargement of the ozone hole.

4 Plant's Response to Pollution Exposure

Plants respond to air pollution by developing different defensive mechanisms through anatomical, morphological, and physiological changes (Darrall, 1989; Dineva, 2004; Gravano et al., 2003), aiming to limit the uptake of the pollutant and thus increase plant's tolerance to the pollutant. Such mechanisms can be physiological (i.e., falling leaves, closing stomata) or chemical and biochemical (i.e., production of insoluble precipitates, emission of reduced forms of pollutant (e.g., H_2S, NH_3), enzymatic degradations or on-enzymatic antioxidant compounds) (Heck et al., 1988). When the plant confronts pollution stress, these additional defense mechanisms are activated and added to the existing ones, in an effort to strengthen the plant's tolerance to imposed pollution stress.

Damages caused by air pollution can be irreversible, such as cell death and leaf necrosis of the plant, which correspond to the so-called visible injury. In contrast, the injuries could be "invisible" whenever the defense system of the plants manages to limit the damage or the pollution impact is low. In those cases, either a physiological plant change is observed, such as decreases in size and yield (Guderian, 1985; Garrec, 2019), or changes in phenology (Honour et al., 2009).

Wang et al. (2003) suggested that the impact of abiotic stresses related to climate and air pollution, such as heat, drought, cold, salinity, and nutrient deficiencies or toxicity, can cause a reduction on worldwide agriculture average yields by >50% for most major crop plants. Imposition of stress conditions may also alter the emissions of biogenic volatile compounds from the vegetation (Guenther et al., 2012; Rinnan et al., 2014). Each emitted compound has a specific role in the plant tolerance and defense (Yuan et al., 2009). For instance, isoprene emissions from plants were found to attribute an antioxidant role in the presence of high O_3 levels (Loreto et al., 2001) and to contribute to the thermotolerance of the plants (Hanson et al., 1999;

Velikova & Loreto, 2005). Furthermore, plant exposure to high O_3 levels affects the above- and below-ground analogy of plant biomass, generally inhibiting the allocation to roots and decreasing C cycling and N fixation (Agathokleous et al., 2020). Tiiva et al. (2007) also found that exposure of subarctic fens to high UV-B radiation resulting from stratospheric O_3 depletion was leading to isoprene emissions increase.

5 Symptomatology of Plants Affected by Air Pollution

Upon air pollution imposition, a variety of symptoms are induced and expressed by plants. Therefore, the symptomatology, which is the analysis of such symptoms, could serve as the basis of air quality biomonitoring methods by utilizing plants' responses to pollutants.

5.1 Symptoms

Depending on the plant species and the type of pollutant, the injury symptoms are different. Generally, air or soil pollution by pesticides have similar symptoms on vegetation, which are mainly expressed on foliage in the form of chlorosis, necrosis, burns, and twisting of leaves (Sharma et al., 2018). Reactive nitrogen species, in the form of nitrate (NO_3^-) and ammonium (NH_4^+), act as fertilizers promoting plant's growth. However, they can also have a negative impact on vegetation (and fauna) when they accumulate inducing ecosystems eutrophication, acidification, and mineral deficiencies. The latter affects biodiversity and leads to a decrease in resilience resistance to various stresses (European Commission, 2013; European Environment Agency, 2019; Garrec, 2019). In most cases, injury by NO_2 is shown as burn at the edge of the conifer needle and chlorosis in the leaves of angiosperms. Leaves first exhibit water-soaked areas that at later stages become necrotic (Gheorghe & Ion, 2011). Injury by halogens is commonly visible on conifers by chlorosis, which later on is changing to red/brown discoloration and burns of the edges of the needles, eventually evolving to necrosis of the entire needle. Similar symptoms are common in the leaves of angiosperms (Gheorghe & Ion, 2011). In most cases, plants' injury by SO_2 is initially seen by the appearance of water-soaked leaves, which later become necrotic, changing into brown spots (Gheorghe & Ion, 2011). Yellowing of conifer needles and decrease in tree vitality are the impacts of acid deposition on plants (Altshuller & Linthurst, 1984). This is mainly an indirect effect of acid atmospheric deposition on soil acidification, which leads to soil base cation depletion and, consequently, to needle magnesium deficiency evidenced by needle yellowing (Landmann & Bonneau, 1995). Acidity is mainly induced by HNO_3 and H_2SO_4 acids and releases soluble forms of metals into the environment, which may be in toxic forms. For instance, Cu toxicity is increased in acidic environments and affects primarily the plant roots leading to growth reduction and chlorosis of mature leaves

(Alva et al., 1995). Finally, Pb and Cd affect the biodiversity of soil fauna species and microorganisms and reduce plant growth (European Environment Agency, 2019).

Injury due to exposure to elevated concentrations of O_3 is commonly expressed by necrotic spots on the leaves of the plants that have irregular shape and are often tan, brown, or black colored. Some of the leaves change their color to bronze or red, which is usually a precursor sign to necrosis. Ozone is the most worrying pollutant currently affecting vegetation and ecosystems, since it is well established that it causes leaf necrosis and results in yield losses reaching 5–19% (Feng & Kobayashi, 2009). Ozone also has indirect effects on vegetation since it is a greenhouse gas linked to climate change (see the chapter by Mallet et al., 2022). Holland et al. (2006) estimated that ozone is responsible for 90% of the plants yield losses related to air pollution. However, the negative effects of ozone are very often masked by the positive effects on photosynthesis due to CO_2 increase in the atmosphere.

5.2 Biotic and Abiotic Indicators and Biomonitoring of Air Quality

Due to this significant role of O_3, a number of indicators have been developed in order to describe the sensitivity of plants to O_3 in different natural or anthropogenic environments (forests, grasslands, field crops, etc.), depending on the climatic zones (Western and Central Europe, Mediterranean coast of Europe, and other). The most used indicator for plant's exposure to O_3 is AOT40, which is a measure of the accumulated daylight ozone concentrations in excess above a threshold of 80 μg m^{-3} (40 ppbv), using only the daily O_3 levels per hour between 8:00 and 20:00 (CET) in the months of the growth season. This is also used for legislation purposes in European Union (EU Directive 2008/50/EC). Other O_3 metrics include the daylight average ozone concentrations during the growing season (M7 for 7 hours daylight period or M12 for 12 hours daylight period) or cumulative exposure indexes over the growing season with weights on hourly average O_3 concentrations that favor the higher hourly average concentrations, while retaining the mid and lower concentrations (Emberson et al., 2018).

Plants can also be used as indicators of metals air pollution. Riga-Karandinos and Saitanis (2004) suggested that trace metal concentration measurements in the leaves of Laurel (*Laurus nobilis* L.) could be used as indicators of urban traffic in Athens. Riga-Karandinos et al. (2006) have further found high concentrations of platinum (Pt) and Pb, known to be used in catalytic converters, together with other traffic metals (Pb, Cu, and Zn) at roadside topsoil in the greater Athens area where pollutants can penetrate the plants through their roots. Furthermore, Rodríguez Martin et al. (2018) suggested that metal content in tree rings could be used as a pollution registry.

Biomonitoring is using both the visible (by observing necroses) or invisible (by biochemical analyses) disturbances of the plants caused by air pollution to deduce

air pollutant levels (de Temmerman et al., 2004; Garrec & Van Haluwyn, 2002). The use of bioindicators might be complicated by the nonlinear response of ecosystems to air pollution and climate change. In addition, it requires an unambiguous relationship between the cause and the bioindicator symptom.

Cryptogams (lichens and bryophytes) , which are important components of the Mediterranean vegetation, are often used as indicators of air pollution and climate change relative to a set of contaminants (Agnan et al., 2015; Gandois et al., 2014; Loppi et al., 1997). Due to their high sensitivity to environmental changes, they are often employed as early-warning indicators of such impacts in particular for N (Ochoa-Hueso et al., 2017). In addition, the potential utility of the N content in mosses as an indicator of total N deposition has been demonstrated by Munzi et al. (2012), and they have also been used as critical load indicators for nitrogen (Geiser et al., 2010). However, cryptogams in the Mediterranean are not effective biomarkers for changes in water availability induced by climate change because they are affected by several stress factors in similar ways (Pirintsos et al., 2011). Lichens have been efficiently used to identify local sources of atmospheric contamination in urban or highly contaminated industrial sites of the Mediterranean countries (Llop et al., 2017; Paoli et al., 2006; Ratier et al., 2018). More rarely used in distant areas, lichen and mosses were successfully used as metal biomonitors in various environmental situations in France and over the last century. This allowed identification of present-day and past sources of contaminants and dust, and their variation in time and space (Agnan et al., 2014, 2015), revealing a regional atmospheric signal, including both soils derived and industrially influenced atmospheric deposition. Moreover, in three different mountainous forest sites in France, lichens and mosses contents in trace metals, of which Rare Earth Elements, were compared to various compartments of the forest ecosystem (bulk deposition and throughfall, soil, and bedrock) (Gandois et al., 2014). The different accumulation of trace metals as monitored by lichens and mosses indicated a different influence of forest ecosystems. Mosses were representative of local throughfall content, since they were enriched in elements from the accumulation of dry deposition inside the canopy, either due to leaching (Mn), direct uptake (Ni), or dry deposition dissolution (Pb, Cu, Cs) contrary to lichens growing on tree barks where transfer was observed only for major elements. Agnan et al. (2017) has improved the bioindication scale using lichens collected in eight distinct French and Swiss forest areas. This also enabled the evaluation of the metal resistance or sensitivity of lichens. Furthermore, the index of atmospheric purity and the lichen diversity value were calculated based on the estimation of various ecological variables (including lichen diversity and abundance) and average ecological features for each site and variable (light, temperature, humidity, substrate pH, and eutrophication) that corresponded to lichen communities. Furthermore, tobacco plant varieties have been used as O_3 bioindicators in Greece (Saitanis, 2008; Saitanis et al., 2003) and have shown high injuries in all studied regions indicating high phytotoxicity by O_3 levels.

5.3 Eutrophication, Acidification, Critical Loads

Eutrophication refers to ecosystem conditions with an excess in nutrients (often referring to N compounds) resulting from increased input rates. Nitrate and ammonium inputs through atmospheric deposition are of particular interest in the present section. In concern to air pollution, eutrophication is related to the ability of an ecosystem to optimally use the reactive nitrogen atmospheric deposition fluxes for its growth. Eutrophication happens when the ecosystem is saturated in N, and thus additional N input is not leading to further growth optimization but instead is leading to N and biodiversity losses (Bobbink et al., 2010; Schmitz et al., 2019). Acidification is related to eutrophication and refers to the lowering of the soil pH due to deposition of acidic compounds, such as HNO_3 and H_2SO_4 that are produced from the oxidation of NO_x and SO_x emissions. Under the Convention of Long-Range Transboundary Air Pollution (LRTAP) within the United Nations, the critical loads of S and N have been used as indicators for ecosystem sensitivity to acidification and eutrophication (Reinds et al., 2008). Thus, critical N load levels are the threshold values above which damage occurs to the ecosystem (Hettelingh et al., 2001). These thresholds were initially determined using mass balance steady-state models or from empirical models. The latter are experimentally derived models studying different types of vegetation and are specific to habitat classes. Ammonia and NO_x critical levels are based on the response of vegetation types like lichens and bryophytes (Ochoa-Hueso et al., 2017), often based on very little information. Thus, for European-Mediterranean habitats, empirical critical N loads have been proposed to vary between 3 and 25 Kg N ha^{-1} yr^{-1} for four different ecosystems with the highest values corresponding to xeric grasslands and the lowest ones to the *Pinus* woodlands (Bobbink & Hettelingh, 2011).

Recently, it was stated that while steady-state models are compatible with the critical loads concept (CLRTAP, 2015), they are not suitable for simulating temporal air pollutant changes, particularly for nitrogen. Therefore, dynamic biogeochemical-ecological coupled models have been developed (de Vries et al., 2010; Rowe et al., 2015; Wallman et al., 2005), based on the impact of atmospheric deposition of S and N on soil functioning and in cascade to forest underground vegetation, using the loss of biodiversity as an indicator of change (Belyazid et al., 2011; Probst et al., 2015). However, the adequacy of critical loads as indicators of N deposition effects has been recently questioned by Payne et al. (2019), who proposed that the cumulative deposition over a 30-year window should be considered as the metric for the ecological damage caused by nitrogen deposition. This suggestion was further supported by the observed slow recovery of ecosystems from N deposition effects (Schmitz et al., 2019). Similarly, although N deposition has decreased in several regions over Europe due to declined NO_x and NH_3 emissions (>50% and < 30%, respectively, between 1990 and 2015), the required timescale to observe the effect of these changes on the ecosystems is uncertain. Dirnböck et al. (2018) investigated 23 European forest research sites, including sites in Italy and the Balkans, and they concluded that reduction of NO_x and NH_3 emissions have to be

significantly higher than projected under current legislation scenarios to allow recovery from chronically high N deposition. Thus, current reduction in N deposition is expected to lead only to limited species recovery in European forests.

6 Interactions and Covariates Between Plants, Air Pollutants, and Environment

Air pollution and climate have concurrent impacts on vegetation. Temperature increases accelerate the dryness of vegetated soils, which retain less water for evapotranspiration, and, thus, cannot effectively contribute to the cooling of the atmosphere. In a warmer and dryer environment, plants close their stomata in order to reduce their water losses, thus minimizing the entrance of O_3 within the plant, therefore reducing O_3 uptake and subsequent reactive oxygen species formation. Gao et al. (2017) suggested that accounting for water stress effects on stomatal O_3 flux can better explain biomass losses on poplar (*Populus deltoides Marsh*) than without consideration of such effects. Lin et al. (2020) pointed out the significant O_3/vegetation/climate interactions since reduced O_3 absorption or uptake by vegetation is increasing surface O_3 concentrations, leading to further atmosphere warming through escalation of greenhouse effect by O_3. They further discussed the importance of soil moisture effect on O_3 reduction by stomatal uptake and its consequent increase for the overall O_3 dry deposition. These effects are currently not considered in O_3 deposition modeling although they could help to improve our understanding of the observed O_3 concentration trends. Lin et al. (2020) have used measurements of O_3 fluxes by eddy correlation and derived O_3 deposition velocities over an oak forest in Italy, and over a spruce-dominated forest in Denmark. These observations were performed for two different study periods: 1 year characterized by heat wave and drought and a second year with normal precipitation events. They reported significant decreases in O_3 deposition velocity during the year characterized by heat waves and drought periods. More specifically, in the Mediterranean study site, a 70% reduction in O_3 deposition velocity was reported and was attributed to plants' stomatal response to the reduced soil moisture, suggesting that vegetation response is expected to worsen peak O_3 episodes during mega-droughts periods. However, multiple stresses on vegetation do not result in additive effects since, for instance, the signalling pathways of biotic and abiotic stresses can act antagonistically as reported by Atkinson and Urwin (2012). Therefore, understanding the mechanisms of the interactions of the responses to various stress factors at a molecular level is fundamental for future development of stress-tolerant crop plants (Atkinson & Urwin, 2012).

Ainsworth (2008) meta-analysis of vegetation response to combined increases in temperature, CO_2, and O_3 showed that high temperature damage negated any yield benefits resulting from elevated CO_2. A large number of studies have been conducted in major food crops (potato, barley, wheat, rice, bean and soybean) to

investigate concurrent effects of drought and ozone on vegetation (see Feng and Kobayashi (2009) for a comprehensive review). Such studies have exhibited that the positive impact of O_3 limitation by stomata closing was often outweighed by the damages on yield due to drought stress (Fangmeier et al., 1994). High temperatures induce faster maturation and hence a shorter grain fill period, reducing the overall yield (Erda et al., 2005), and can induce floret sterility in cereals such as rice (Matsui et al., 2014), wheat, and maize (Craufurd & Wheeler, 2009; Wheeler et al., 1996). However, physiological responses differ among crops (Eyshi Rezaei et al., 2015). Yield losses varied from 5.3% for potato to 19% for beans and soya beans when exposed to O_3 concentrations between 30 and 50 ppbv compared to 26 ppbv or less (Feng & Kobayashi, 2009). Avnery et al. (2011) evaluated crop losses reaching up to 15% for the year 2000 due to O_3 exposure, corresponding to an annual loss of 79–121 million metric tons of global crop yields or 11–18 billion dollars annually, while Mills et al. (2018) estimated that exposure to O_3 led to wheat grain losses to cost 24.2 billion dollars annually for the period 2010–2012.

In addition to O_3, climate is affecting other pivotal air pollutants (such as SO_2, N reactive species, and aerosols), due to their temperature-dependent photochemical production or depletion and their deposition dependence on precipitation and wind patterns. In particular, atmospheric N deposition due to the semi-volatile character of NH_4NO_3 is strongly dependent on relative humidity and temperature conditions (Fowler et al., 2009; Nenes et al., 2021). Thus, atmospheric deposition of nitrogen is affected by climatic changes and will impact vegetation habitats (Dirnböck et al., 2003). Dynamic biogeochemical-ecological chain models for critical loads have thus tested these covariant effects. They were able to detect the joined influence of climate and nitrogen deposition on biodiversity loss, following scenarios of current legislation or maximum feasible reduction of N emissions or/and temperature increase (Gaudio et al., 2015; Rizzetto et al., 2016).

7 Impacts of Air Pollutants on Terrestrial Vegetation of the Mediterranean Region

The natural and seminatural ecosystems in the Mediterranean Basin have much higher plant biodiversity (hosting 4.3% of the global endemic plants) and biologically relevant heterogeneity in space and time compared to those in temperate and boreal areas of Europe (Myers et al., 2000; Ochoa-Hueso et al., 2017). The Mediterranean climate, characterized by drought summer periods and mild winter temperatures, plays a critical role in the behavior of plants, allowing their growing season to be extended over the whole course of the calendar year. Therefore, it has been suggested that the entire ecosystem exposure to pollutants should be calculated based on an annual basis, while the actual growing season period is more suitable for determining single species exposure to pollutants (Schenone, 1993). These particularities support a separate discussion of air pollution impact on Mediterranean vegetation. This separation is further supported by the existence of multiple plant

adaptation mechanisms to the climatic conditions of the Mediterranean Basin, where heat waves and droughts are occurring frequently. Such mechanisms include foliage loss during the water stress periods; physiological responses such as closing of the stomata to limit water losses; changes in the metabolic pathways such as instead of C_3 photosynthesis utilizing the Crassulacean acid metabolism (CAM), which is a typical ecophysiological adaptation of plants to arid conditions (Grams & Thiel, 2002); and changes in the depth and distribution pattern of the root systems. All the above mechanisms develop plant adaptation and ensure their survival under stressful climatic extremes (Schenone, 1993). Furthermore, due to natural evolution and adaptation to their environment, the Mediterranean forests have developed cross-tolerance to the environmental conditions dominating the region (Paoletti, 2006).

7.1 Vegetation Exposure to Ground Level Ozone

Due to the sunny and warm weather conditions of the Mediterranean region, there is a potential for high O_3 deposition rates throughout the year (Kanakidou et al., 2011). Consequently, higher O_3 stomatal uptake may take place during winter than summer months, in spite of the lower winter ozone concentrations (Cieslik, 2009; Gerasopoulos et al., 2006). In addition, plants emit different compositions of VOC, which are oxidized by ozone reducing the oxidative stress and thereby protecting the plants (Yuan et al., 2009). However, these reactions are also reducing the distance to which VOC can be transported to enable plant communication and pollinator attraction. Ozone pollution can also alter the timing of flowering, the number and biomass of flowers, and weed development. The susceptibility of plants to O_3 levels depends on genotype and varies among plant functional groups (Agathokleous et al., 2020). Therefore, exposure to high O_3 levels affects plant community composition and also threatens terrestrial biodiversity at various trophic levels. Agathokleous et al. (2020) using climate scenarios for 2100 warned that the Mediterranean Basin, one of the higher endemic richness regions globally, is among the most threatened regions by high O_3 levels. Gerosa et al. (2005) found that in an Italian oak forest, which represented a typical Mediterranean ecosystem, the average O_3 stomatal uptake was less than half of the total O_3 deposition flux and that non-stomatal deposition was increasing with leaf wetness and air humidity during the fall season. The increased non-stomatal fluxes of O_3 observed in Mediterranean forests (Gerosa et al., 2005, 2009) and their diurnal and seasonal variations were different in many aspects when compared to those observed in the northern European forests (Fowler et al., 2009). Furthermore, measurements above oak forests in central Italy (Gerosa et al., 2005, 2009; Cieslik, 2009) and southeastern France (Michou et al., 2005) showed that dry and hot conditions can significantly affect the diurnal variation of O_3 deposition velocity. The Mediterranean vegetation is more tolerant to high O_3 levels than the mesophillic broad-leaf trees (Paoletti, 2006) because of its better antioxidant defense (Nali et al., 2004), although biomass losses and changes

in biomass distribution in the various plant compartments due to exposure to high O_3 cannot be excluded. However, deciduous broad-leaf trees are less tolerant to oxidative stress compared to evergreen broad-leaf trees due to their physiology with higher stomatal conductance and thinner leaves (Calatayud et al., 2010). Indeed, Calatayud et al. (2007) investigated the sensitivity to O_3 of four maple trees (*A. campestre, Acer opalus subsp. granatense, A. monspessulanum, and A. pseudoplatanus*), which are present in humid parts of the Mediterranean. They found differences (e.g., in CO_2 assimilation, stomatal conductance, transpiration rate, and water use efficiency), which may be partly related to higher stomatal conductance. On the other hand, Li et al. (2016) examining the O_3 sensitivity of 29 deciduous and evergreen species in China detected correlation to both low leaf mass per area and low leaf area-based antioxidant levels, but not to stomatal conductance. Moreover, Manes et al. (2007) evidenced that O_3 uptake varies within a Holm oak (*Quercus ilex* L.) canopy and attributed this fluctuation to the influence of microclimatic conditions on plants' physiological activity related to stomatal opening, which in turn is affected by internal and external effectors (e.g., plant hormones, water availability, hydraulic conductance). Sanz and Millan (2000) suggested a complex interaction between high radiation, drought, and O_3 response in Mediterranean tree species such as Aleppo pine (*Pinus halepensis* Mill.). Tree species sensitivity to O_3 as revealed by functional leaf traits has to be considered (Calatayud et al., 2011). Saitanis et al. (2003) observed stomatal conductance in leaves of tobacco, grape wines, and needles of Aleppo pine at various locations in Greece and found them peaking in midday hours when O_3 was high. They also observed injuries due to O_3 air pollution which were more severe at the high-altitude location. Fumagalli et al. (2001) performed studies with open-top chambers in 24 agricultural and horticultural crops grown in commercial fields in the Mediterranean. They reported that ambient O_3 resulted in 17–39% yield loss in crops such as wheat, bean, watermelon, and tomato. Nitrogen fixing legumes were also found to be less tolerant to O_3 exposure compared to grasses, which could eventually reduce their economic value (Sanz et al., 2007).

7.2 Vegetation Exposure to Nitrogen Oxides

Dry deposition onto the ecosystems can contribute up to 58–67% of the total N deposition in the Mediterranean Basin (Rodà et al., 2002). Due to the difficulty of measuring the actual dry deposition, this flux is commonly inferred from observations of atmospheric concentrations from representative stations (Sanz et al., 2002) coupled with deposition modeling (García-Gómez et al., 2018). Nitrogen is deposited in the forms of reduced or oxidized, inorganic, or organic N. The contribution of organic N was found to vary between 34% and 56% of total deposition (Im et al., 2013; Izquieta-Rojano et al., 2016; Kanakidou et al., 2020; Mace et al., 2003; Violaki et al., 2010) and can be a substantial contributor to N critical loads in

Mediterranean agricultural areas. Several studies have been performed in the Mediterranean to investigate the impact of N deposition on individual plants, lichens, and soil properties as reviewed by Ochoa-Hueso et al. (2017). Few studies, such as NitroMed (Ochoa-Hueso & Manrique, 2011), investigated the integrated responses at the ecosystem level using statistical methods. Their results indicate that N availability in soils is increased by N deposition, but concurrently, soil becomes more acidic, which affects the microbial community by reducing the fungi to bacteria ratio and impact the overall enzymatic activity (Ochoa-Hueso et al., 2017). Changes in the stoichiometry of the plants (higher N/P ratio of the leaves) (Sardans et al., 2016) as well as changes in biomass partitioning and allometric ratios (Cambui et al., 2011) have been observed as a response to the increased N deposition. Furthermore, the effect of concurrent O_3 and N deposition in the Mediterranean can change composition and reproductive structure of the annual pastures (Gonzalez-Fernandez et al., 2013).

7.3 Accumulation of Toxic Metal Air Pollutants on Vegetation and Soil

Only limited number of studies have investigated metals in agricultural soils in the Mediterranean region (Stanners & Bourdeau, 1995) and mainly at regional level in some countries such as Greece (Stalikas et al., 1997), Italy (Abollino et al., 2002; Facchinelli et al., 2001), and Spain (Andreu & Gimeno-García, 1996; Boluda et al., 1988). Riga-Karandinos et al. (2006) measurements of trace metals at roadside topsoil in the greater Athens area indicated the penetration of pollution metals into the soils, from where they can be potentially transferred to the plants (Gandois et al., 2010). Evergreen shrubs were tested for their capacity to accumulate a large set of metals on the surface of their current season leaves in a Mediterranean environment. The results showed a common temporal pattern with elements increasing from early summer to midsummer and then decreasing to early autumn. Deposition was also linked to meteorological parameters. Rain decreased the accumulation of metals on leaves, while increasing wind speed was enhancing the presence of elements on leaves (Mori et al., 2015).

Furthermore, Rodríguez Martin et al. (2018) have found significant enrichments of metals in Aleppo pine wood compared to the natural environment. More specifically, they measured 2.5 times higher Pb in tree wood close to burning power plants and 25 times higher Cd near mining areas compared to natural areas. Based on measurements of aerosols deposited on the leaves of *Platanus acerifolia* tree from 23 European cities over 20 countries, Baldacchini et al. (2017) concluded that this tree could be used to monitor aerosols, using the morphology and elemental composition of leaf-deposited particles, together with the leaf magnetic content, i.e., in ferromagnetic minerals coming from dust deposited on the leaves (Leng et al., 2018).

7.4 Plant Nutrient Uptake Limitations Induced by Air Pollution

Ochoa-Hueso et al. (2011) suggested that the effect of N deposition inputs and the susceptibility of the Mediterranean ecosystems to exotic plant invasion may be controlled by P availability. In their study, Herut et al. (1999) indicated that atmospheric inputs of bioavailable N and P represent an imbalanced contribution to the new carbon production and reinforce the unusual N:P ratios (∼27) and possible P limitation in the southeast Mediterranean Sea. Ochoa-Hueso and Manrique (2013) and Ochoa-Hueso et al. (2017) reported a shift from N to P limitation in the terricolous moss *Tortella squarrosa* in the Iberian Peninsula due to increased N deposition. In addition, the epiphytic lichen communities in Portugal and Spain have shifted from oligotrophic-dominated to nitrophytic-dominated species (Aguillaume, 2016; Pinho et al., 2008). The impact of anthropogenic N emissions on these shifts is supported by the ^{15}N isotopic signature of the N composition of mosses, which is shifted to more positive $\delta^{15}N$ values, while the agricultural activities are reducing $\delta^{15}N$ (e.g., Delgado et al., 2013). Human-induced imbalance in N and P deposition has been also reported for other regions and ecosystems, like the Chinese forests, leading to P limitation of the forest ecosystem (Du et al., 2016).

8 Conclusions and Perspectives

Air pollution has significant direct (after uptake by the plant) and indirect (through changes in climate and diffuse solar radiation) effects on terrestrial vegetation that lead to visible and invisible vegetation damages. These effects, mostly from exposure to high O_3, have been observed to reduce crop yields, thus affecting agriculture effectiveness and its ability to feed the Earth's population. Plant phenology, functional type, and the seasonality of O_3 have to be taken into account when evaluating the impact of air pollution on the Mediterranean vegetation. Understanding of the interaction between the various stress factors, in particular climate (temperature, droughts, and other extremes) and air pollution (O_3, aerosol, CO_2) and how these factors once combined affect vegetation, is critical for the definition of actions in order to preserve biodiversity and sustain agricultural production.

Atmospheric deposition of pollutants provides nutrients and toxic compounds or their products to the vegetation via either direct uptake by the foliage or by indirect uptake through plants' roots. Accumulation of pollutants in the environment has long-term effects on vegetation and soil; thus, it demands long recovery periods after the accumulation has stopped. This is particularly true for N deposition, which leads to N accumulation more than the optimal ecosystem levels in the soils, implies soil acidification, leads to biodiversity reduction, and changes the composition of phytocommunities. Indeed, changes in nutrient stoichiometry have been observed in plants exposed to excessively high N levels in the soil resulting from deposition

of anthropogenic reactive nitrogen. As in other locations, human-induced P limitation has been observed in Europe and the Mediterranean due to anthropogenic N deposition. Such alterations of the ecosystem's composition must be carefully evaluated, particularly under conditions of climate change that are potentially increasing the occurrence of severe drought events. Indeed, interactive effects between climate change and N deposition on vegetation have been shown and predicted.

Finally, plants' response to air pollution is expressed by symptoms that vary depending on the plant species and variety and the type of pollutant. Thus, plant disturbances caused by air pollution can be utilized to deduce air pollution levels, through the so-called biomonitoring procedure. However, since the use of bioindicators requires an unambiguous relationship between the cause and the plant response, this approach becomes complicated by the nonlinear response of ecosystems to air pollution and climate change. Despite this complexity, the power of biomonitoring to reconstruct past pollution influence, by using, for example, well-preserved herbariums compared with present-day situations, can contribute to the effort to obtain a spatial view of the impact of atmospheric pollution around the Mediterranean regions.

Further research is needed in all abovementioned fields. Observatories for long-term monitoring of all compartments of the environment and key drivers are essential to understand and evaluate the impact of air pollution on Earth's vegetation. This need is specifically urgent for the Mediterranean region, due to its susceptibility to various stresses induced either by climate change or air pollution or by other expressions of human activities footprint on the environment.

Acknowledgments We acknowledge support of this work by the project "PANhellenic infrastructure for Atmospheric Composition and climatE change" (MIS 5021516), which is implemented under the action "Reinforcement of the Research and Innovation Infrastructure" funded by the operational program "Competitiveness, Entrepreneurship and Innovation" (NSRF 2014–2020) and cofinanced by Greece and the European Union (European Regional Development Fund). We also thank the reviewers for detailed comments that helped improve this chapter significantly.

References

Aas, W., Mortier, A., Bowersox, V., Cherian, R., Faluvegi, G., Fagerli, H., Hand, J., Klimont, Z., Galy-Lacaux, C., Lehmann, C. M. B., Myhre, C. L., Myhre, G., Olivié, D., Sato, K., Quaas, J., Rao, P. S. P., Schulz, M., Shindell, D., Skeie, R. B., … Xu, X. (2019). Global and regional trends of atmospheric sulfur. *Scientific Reports, 9*, 1–11. https://doi.org/10.1038/s41598-018-37304-0

Abollino, O., Aceto, M., Malandrino, M., Mentasti, E., Sarzanini, C., & Petrella, F. (2002). Heavy metals in agricultural soils from Piedmont, Italy. Distribution, speciation and chemometric data treatment. *Chemosphere, 49*, 545–557. https://doi.org/10.1016/S0045-6535(02)00352-1

Acosta, J. A., Faz, A., Martínez-Martínez, S., & Arocena, J. M. (2011). Enrichment of metals in soils subjected to different land uses in a typical Mediterranean environment (Murcia City, southeast Spain). *Applied Geochemistry, 26*, 405–414. https://doi.org/10.1016/j.apgeochem.2011.01.023

Agathokleous, E., Feng, Z., Oksanen, E., Sicard, P., Wang, Q., Saitanis C.J., Araminiene, V., Blande, J. D., Hayes, F., Calatayud, V., Domingos, M., Veresoglou, S. D., Peñuelas J., Wardle, D.A., De Marco, A., Li, Z., Harmens, H., Yuan, X., Vitale, M., Paoletti, E.: (2020) Ozone

affects plant, insect, and soil microbial communities: A threat to terrestrial ecosystems and biodiversity. Sci Adv, 6, eabc1176, https://doi.org/10.1126/sciadv.abc1176,

Agnan, Y., Séjalon-Delmas, N., & Probst, A. (2014). Origin and distribution of rare earth elements in various lichen and moss species over the last century in France. *Sci Total Environ, 487*, 1–12. https://doi.org/10.1016/j.scitotenv.2014.03.132

Agnan, Y., Séjalon-Delmas, N., Claustres, A., & Probst, A. (2015). Investigation of spatial and temporal metal atmospheric deposition in France through lichen and moss bioaccumulation over one century. *Science of the Total Environment, 529*, 285–296. https://doi.org/10.1016/j.scitotenv.2015.05.083

Agnan, Y., Probst, A., & Séjalon-Delmas, N. (2017). Evaluation of lichen species resistance to atmospheric metal pollution by coupling diversity and bioaccumulation approaches: A new bioindication scale for French forested areas. *Ecological Indicators, 72*, 99–110. https://doi.org/10.1016/j.ecolind.2016.08.006

Aguillaume, L. (2016). La deposición de nitrógeno en encinares Mediterráneos: Cargas e indicadores. *Ecosistemas: Revista Cietifica y Tecnica de Ecologia y Medio Ambiente, 25*, 110–113. https://doi.org/10.7818/ECOS.2016.25-2.15

Aguillaume, L., Rodrigo, A., & Avila, A. (2016). Long-term effects of changing atmospheric pollution on throughfall, bulk deposition and stream waters in a Mediterranean forest. *Sci Total Environ, 544*, 919–928. https://doi.org/10.1016/j.scitotenv.2015.12.017

Ainsworth, E. A. (2008). Rice production in a changing climate: A meta-analysis of responses to elevated carbon dioxide and elevated ozone concentration. *Global Change Biology, 14*, 1642–1650. https://doi.org/10.1111/j.1365-2486.2008.01594.x

Aktar, W., Sengupta, D., & Chowdhury, A. (2009). Impact of pesticides use in agriculture: Their benefits and hazards. *Interdisciplinary Toxicology, 2*, 1–12. https://doi.org/10.2478/v10102-009-0001-7

Altshuller, A. P., & Linthurst, R. A. (1984). Acidic deposition phenomenon and its effects: Critical assessment review papers, Volume 1, Tech. Rept. PB-85-100030/XAD, North Carolina State Univ., Raleigh, USA.

Alva, A. K., Graham, J. H., & Anderson, C. A. (1995). Soil pH and copper effects on young 'Hamlin' orange trees. *Soil Science Society of America Journal, 59*, 481–487. https://doi.org/10.2136/sssaj1995.03615995005900020031x

Andreu, V., & Gimeno-García, E. (1996). Total content and extractable fraction of cadmium, cobalt, copper, nickel, lead, and zinc in calcareous orchard soils. *Communications in Soil Science and Plant Analysis, 27*, 2633–2648. https://doi.org/10.1080/00103629609369728

Atkinson, N. J., & Urwin, P. E. (2012). The interaction of plant biotic and abiotic stresses: From genes to the field. *Journal of Experimental Botany, 63*, 3523–3544. https://doi.org/10.1093/jxb/ers100

Avila, A., Queralt-Mitjans, I., & Alarcón, M. (1997). Mineralogical composition of African dust delivered by red rains over northeastern Spain. *Journal of Geophysical Research, 102*, 21977–21996. https://doi.org/10.1029/97jd00485

Avnery, S., Mauzerall, D. L., Liu, J., & Horowitz, L. W. (2011). Global crop yield reductions due to surface ozone exposure: 1. Year 2000 crop production losses and economic damage. *Atmospheric Environment, 45*, 2284–2296. https://doi.org/10.1016/j.atmosenv.2010.11.045

Baldacchini, C., Castanheiro, A., Maghakyan, N., Sgrigna, G., Verhelst, J., Alonso, R., Amorim, J. H., Bellan, P., Breuste, J., Bühler, O., Cântar, I. C., Cariñanos, P., Carriero, G., Churkina, G., Dinca, L., Esposito, R., Gawronski, S. W., Kern, M., Le Thiec, D., … Samson, R. (2017). How does the amount and composition of PM deposited on Platanus acerifolia leaves change across different cities in Europe? *Environmental Science & Technology, 51*, 1147–1156. https://doi.org/10.1021/acs.est.6b04052

Belyazid, S., Kurz, D., Braun, S., Sverdrup, H., Rihm, B., & Hettelingh, J. P. (2011). A dynamic modelling approach for estimating critical loads of nitrogen based on plant community changes under a changing climate. *Environmental Pollution, 159*, 789–801. https://doi.org/10.1016/j.envpol.2010.11.005

Bobbink, R., Hicks, K., Galloway, J., Spranger, T., Alkemade, R., Ashmore, M., Bustamante, M., Cinderby, S., Davidson, E., Dentener, F., Emmett, B., Erisman, J. W., Fenn, M., Gilliam, F., Nordin, A., Pardo, L., & De Vries, W. (2010). Global assessment of nitrogen deposition effects on terrestrial plant diversity: A synthesis. *Ecological Applications, 20*, 30–59. https://doi.org/10.1890/08-1140.1

Bobbink, R., & Hettelingh, J.-P. (Eds.) (2011). Review and revision of empirical critical loads response relationships. In Proc. Expert Workshop, Noordwijkerhout, the Netherlands, 23–25 June 2010, Coordination Centre for the Effects, Rijksinstituut voor Volksgezondheid en Milieu, 246 pp. https://rivm.openrepository.com/bitstream/handle/10029/260510/680359002.pdf.

Boluda, R., Andreu, V., Pons, V., & Sánchez, J. (1988). Contenido de metales pesados (Cd, Co, Cr, Cu, Ni, Pb y Zn) en suelos de la comarca La Plana de Requena-Utiel (Valencia). *Anales de Edafología y Agrobiología, 47*, 1485–1502.

Brahmachari, S., & Kundu, S. (2017). SO_2 stress: Its effect on plants, plant defence responses and strategies for developing enduring resistance. *International Advanced Research Journal in Science, Engineering and Technology, 4*, 303–309. https://doi.org/10.17148/IARJSET.2017.4752

Calatayud, V., Cerveró, J., & Sanz, M. J. (2007). Foliar, physiological and growth responses of four maple species exposed to ozone. *Water, Air, and Soil Pollution, 185*, 239–254. https://doi.org/10.1007/s11270-007-9446-5

Calatayud, V., Marco, F., Cerveró, J., Sánchez-Peña, G., & Sanz, M. J. (2010). Contrasting ozone sensitivity in related evergreen and deciduous shrubs. *Environmental Pollution, 158*, 3580–3587. https://doi.org/10.1016/j.envpol.2010.08.013

Calatayud, V., Cerveró, J., Calvo, E., García-Breijo, F. J., Reig-Arminana, J., & Sanz, M. J. (2011). Responses of evergreen and deciduous Quercus species to enhanced ozone levels. *Environmental Pollution, 159*, 55–63. https://doi.org/10.1016/j.envpol.2010.09.024

Cambui, C. A., Svennerstam, H., Gruffman, L., Nordin, A., Ganeteg, U., & Näsholm, T. (2011). Patterns of plant biomass partitioning depend on Nitrogen source. *PLoS ONE, 6*, 1–7. https://doi.org/10.1371/journal.pone.0019211

Cataldo, D. A., & Wildung, R. E. (1978). Soil and plant factors influencing the accumulation of heavy metals by plants. *Environmental Health Perspectives, 27*, 149–159. https://doi.org/10.2307/3428874

Cieslik, S. (2009). Ozone fluxes over various plant ecosystems in Italy: A review. *Environmental Pollution, 157*, 1487–1496. https://doi.org/10.1016/j.envpol.2008.09.050

CLRTAP. (2015). Mapping critical loads for ecosystems, Chapter V of Manual on methodologies and criteria for modelling and mapping critical loads and levels and air pollution effects, risks and trends. Umweltbundesamt/German Environment Agency, Berlin, 116 pp., https://www.umweltbundesamt.de/sites/default/files/medien/4292/dokumente/ch5-mapman-2017-09-10.pdf. Last access 20 July 2022.

Craufurd, P. Q., & Wheeler, T. R. (2009). Climate change and the flowering time of annual crops. *Journal of Experimental Botany, 60*, 2529–2539. https://doi.org/10.1093/jxb/erp196

Darrall, N. M. (1989). The effect of air pollutants on physiological processes in plants. *Plant, Cell & Environment, 12*, 1–30. https://doi.org/10.1111/j.1365-3040.1989.tb01913.x

de Temmerman, L., Bell, J. N. B., Garrec, J. P., Klumpp, A., Krause, G. H. M., & Tonneijck, A. E. G. (2004). Biomonitoring of air pollutants with plants – Considerations for the future. In A. Klumpp, W. Ansel, & G. Klumpp (Eds.), *Urban air pollution, bioindication and environmental awareness* (pp. 337–373). Cuvillier Verlag. ISBN 978–3736910782.

de Vries, W., Wamelink, G. W. W., Van Dobben, H., Kros, J., Reinds, G. J., Mol-Dijkstra, J. P., Smart, S. M., Evans, C. D., Rowe, E. C., Belyazid, S., Sverdrup, H. U., Van Hinsberg, A., Posch, M., Hettelingh, J. P., Spranger, T., & Bobbink, R. (2010). Use of dynamic soil – Vegetation models to assess impacts of nitrogen deposition on plant species composition: An overview. *Ecological Applications, 20*, 60–79. https://doi.org/10.1890/08-1019.1

Delgado, V., Ederra, A., & Santamaría, J. M. (2013). Nitrogen and carbon contents and $\delta^{15}N$ and $\delta^{13}C$ signatures in six bryophyte species: Assessment of long-term deposition changes

(1980–2010) in Spanish beech forests. *Global Change Biology, 19*, 2221–2228. https://doi.org/10.1111/gcb.12210

Dineva, S. B. (2004). Comparative studies of the leaf morphology and structure of white ash *Fraxinus americana* L. and London plane tree *Platanus acerifolia* Willd growing in polluted area. *Dendrobiology*, 52, 3–8, http://yadda.icm.edu.pl/yadda/element/bwmeta1.element.agro-article-c95f1f7a-69a8-48dd-9331-224b19949fa7/c/52_3_8.pdf. Last access 20 July 2022.

Dirnböck, T., Dullinger, S., & Grabherr, G. (2003). A regional impact assessment of climate and land-use change on alpine vegetation. *Journal of Biogeography, 30*, 401–417. https://doi.org/10.1046/j.1365-2699.2003.00839.x

Dirnböck, T., Pröll, G., Austnes, K., Beloica, J., Beudert, B., Canullo, R., De Marco, A., Fornasier, M. F., Futter, M., Goergen, K., Grandin, U., Holmberg, M., Lindroos, A. J., Mirtl, M., Neirynck, J., Pecka, T., Nieminen, T. M., Nordbakken, J. F., Posch, M., … Forsius, M. (2018). Currently legislated decreases in nitrogen deposition will yield only limited plant species recovery in European forests. *Environmental Research Letters, 13*, 125010. https://doi.org/10.1088/1748-9326/aaf26b

Du, E., De Vries, W., Han, W., Liu, X., Yan, Z., & Jiang, Y. (2016). Imbalanced phosphorus and nitrogen deposition in China's forests. *Atmospheric Chemistry and Physics, 16*, 8571–8579. https://doi.org/10.5194/acp-16-8571-2016

Duprè, C., Stevens, C. J., Ranke, T., Bleeker, A., Peppler-Lisbach, C., Gowing, D. J. G., Dise, N. B., Dorland, E., & Diekmann, M. (2010). Changes in species richness and composition in European acidic grasslands over the past 70 years: The contribution of cumulative atmospheric nitrogen deposition. *Global Change Biology, 16*, 344–357. https://doi.org/10.1111/j.1365-2486.2009.01982.x

Emberson, L. D., Pleijel, H., Ainsworth, E. A., van den Berg, M., Ren, W., Osborne, S., Mills, G., Pandey, D., Dentener, F., Büker, P., Ewert, F., Koeble, R., & Van Dingenen, R. (2018). Ozone effects on crops and consideration in crop models. *European Journal of Agronomy, 100*, 19–34. https://doi.org/10.1016/j.eja.2018.06.002

Erda, L., Wei, X., Hui, J., Yinlong, X., Yue, L., Liping, B., & Liyong, X. (2005). Climate change impacts on crop yield and quality with CO_2 fertilization in China. *Philosophical Transactions of the Royal Society B, 360*, 2149–2154. https://doi.org/10.1098/rstb.2005.1743

European Commission. (2013). Science for Environment Policy, IN-DEPTH REPORT, Nitrogen Pollution and the European Environment: Implications for Air Quality Policy, 28 pp., https://ec.europa.eu/environment/integration/research/newsalert/pdf/IR6_en.pdf. Last access 20 July 2022.

European Environment Agency. (2019). Eutrophication of terrestrial ecosystems due to air pollution. Annual Indicator Report Series (AIRS), 1–9, retrieved from https://www.eea.europa.eu/airs/2016/natural-capital/eutrophication-of-terrestrial-ecosystems. Last access 20 July 2022.

EMEP. (2018). Transboundary particulate matter, photo-oxidants, acidifying and eutrophying components, European Monitoring and Evaluation Programme Status Report 2018, 1–204, ISSN 1504–6192, https://emep.int/publ/common_publications.html.

Eyshi Rezaei, E., Webber, H., Gaiser, T., Naab, J., & Ewert, F. (2015). Heat stress in cereals: Mechanisms and modelling. *European Journal of Agronomy, 64*, 98–113. https://doi.org/10.1016/j.eja.2014.10.003

Facchinelli, A., Sacchi, E., & Mallen, L. (2001). Multivariate statistical and GIS-based approach to identify heavy metal sources in soils. *Environmental Pollution, 114*, 313–324. https://doi.org/10.1016/S0269-7491(00)00243-8

Fangmeier, A., Brockerhoff, U., Grüters, U., & Jäger, H. J. (1994). Growth and yield responses of spring wheat (Triticum aestivum L. CV. Turbo) grown in open-top chambers to ozone and water stress. *Environmental Pollution, 83*, 317–325. https://doi.org/10.1016/0269-7491(94)90153-8,

Farquhar, G. D. (1997). Carbon dioxide and vegetation. *Science, 278*, 1411. https://doi.org/10.1126/science.278.5342.1411

Faulkner, C. (2018). Plasmodesmata and the symplast. *Current Biology, 28*, R1374–R1378. https://doi.org/10.1016/j.cub.2018.11.004

Feng, Z., & Kobayashi, K. (2009). Assessing the impacts of current and future concentrations of surface ozone on crop yield with meta-analysis. *Atmospheric Environment, 43*, 1510–1519. https://doi.org/10.1016/j.atmosenv.2008.11.033

Fowler, D., Pilegaard, K., Sutton, M. A., Ambus, P., Raivonen, M., Duyzer, J. D., Simpson, D., Fagerli, H., Fuzzi, S., Schjoerring, J. K., Granier, C., Neftel, A., Isaksen, I. S. A., Laj, P., Maione, M., Monks, P. S., Burkhardt, J., Daemmgen, U., Neirynck, J., … Erisman, J. W. (2009). Atmospheric composition change: Ecosystems-atmosphere interactions. *Atmospheric Environment, 43*, 5193–5267. https://doi.org/10.1016/j.atmosenv.2009.07.068

Fumagalli, I., Gimeno, B. S., Velissariou, D., De Temmerman, L., & Mills, G. (2001). Evidence of ozone-induced adverse effects on crops in the Mediterranean region. *Atmospheric Environment, 35*, 2583–2587. https://doi.org/10.1016/S1352-2310(00)00468-4

Gandois, L., Nicolas, M., VanderHeijden, G., & Probst, A. (2010). The importance of biomass net uptake for a trace metal budget in a forest stand in north-eastern France. *Sci Total Environ, 408*, 5870–5877. https://doi.org/10.1016/j.scitotenv.2010.07.061

Gandois, L., & Probst, A. (2012). Localisation and mobility of trace metal in silver fir needles. *Chemosphere, 87*, 204–210. https://doi.org/10.1016/j.chemosphere.2011.12.020

Gandois, L., Agnan, Y., Leblond, S., Séjalon-Delmas, N., Le Roux, G., & Probst, A. (2014). Use of geochemical signatures, including rare earth elements, in mosses and lichens to assess spatial integration and the influence of forest environment. *Atmospheric Environment, 95*, 96–104. https://doi.org/10.1016/j.atmosenv.2014.06.029

Gao, F., Calatayud, V., Paoletti, E., Hoshika, Y., & Feng, Z. (2017). Water stress mitigates the negative effects of ozone on photosynthesis and biomass in poplar plants. *Environmental Pollution, 230*, 268–279. https://doi.org/10.1016/j.envpol.2017.06.044

García-Gómez, H., Izquieta-Rojano, S., Aguillaume, L., González-Fernández, I., Valiño, F., Elustondo, D., Santamaría, J. M., Avila, A., Bytnerowicz, A., Bermejo, V., & Alonso, R. (2018). Joining empirical and modelling approaches to estimate dry deposition of nitrogen in Mediterranean forests. *Environmental Pollution, 243*, 427–436. https://doi.org/10.1016/j.envpol.2018.09.015

Garrec, J. P., & Van Haluwyn, C. (2002). Biosurveillance Végétale de la Qualité de l'Air. Concepts, Méthodes et Applications, Editions Tec et Doc, Lavoisier, Paris, 116 pp., ISBN 2-7430-0540-8.

Garrec, J. P. (2019). What is the impact of air pollutants on vegetation? In J. Joyard, R. Moreau, & J. Sommeria (Eds.), *Encyclopedia of the environment*, 14 pp. online ISSN 2555–0950, Uni. Grenoble Alpes, Saint-Martin-d'Hères, France. https://www.encyclopedie-environnement.org/en/life/impact-air-pollutants-on-vegetation/. Last access 21 July 2022.

Garrison, V. H., Shinn, E. A., Foreman, W. T., Griffin, D. W., Holmes, C. W., Kellogg, C. A., Majewski, M. S., Richardson, L. L., Ritchie, K. B., & Smith, G. W. (2003). African and Asian Dust: From desert soils to coral reefs. *BioScience, 53*, 469–480. https://doi.org/10.1641/0006-3568(2003)053[0469:AAADFD]2.0.CO;2

Garrison, V. H, Foreman, W. T, Genualdi, S, Griffin, D. W, Kellogg, C. A, Majewski, M. S, Mohammed, A, Ramsubhag, A, Shinn, E. A, Simonich, S. L, & Smith, G. W. (2006). Saharan dust – A carrier of persistent organic pollutants, metals and microbes to the Caribbean? Saharan dust – a carrier of persistent organic pollutants, metals and microbes to the Caribbean? *Revista de Biologia Tropical, 54* (Suppl. 3), 9–21. https://www.scielo.sa.cr/scielo.php?script=sci_arttext&pid=S0034-77442006000600007. Last access 21 July 2022.

Gaudio, N., Belyazid, S., Gendre, X., Mansat, A., Nicolas, M., Rizzetto, S., Harald Sverdrup, H., & Probst, A. (2015). Combined effect of atmospheric nitrogen deposition and climate change on temperate forest soil biogeochemistry: A modeling approach. *Ecological Modelling, 306*, 24–34. https://doi.org/10.1016/j.ecolmodel.2014.10.002

Geiser, L. H., Jovan, S. E., Glavich, D. A., & Porter, M. K. (2010). Lichen-based critical loads for atmospheric nitrogen deposition in Western Oregon and Washington Forests, USA. *Environmental Pollution, 158*, 2412–2421. https://doi.org/10.1016/j.envpol.2010.04.001

Gerasopoulos, E., Kouvarakis, G., Vrekoussis, M., Donoussis, C., Mihalopoulos, N., & Kanakidou, M. (2006). Photochemical ozone production in the Eastern Mediterranean. *Atmospheric Environment, 40*, 3057–3069. https://doi.org/10.1016/j.atmosenv.2005.12.061

Gerosa, G., Vitale, M., Finco, A., Manes, F., Denti, A. B., & Cieslik, S. (2005). Ozone uptake by an evergreen Mediterranean Forest (Quercus ilex) in Italy. Part I: Micrometeorological flux measurements and flux partitioning. *Atmospheric Environment, 39*, 3255–3266. https://doi.org/10.1016/j.atmosenv.2005.01.056

Gerosa, G., Finco, A., Mereu, S., Vitale, M., Manes, F., & Denti, A. B. (2009). Comparison of seasonal variations of ozone exposure and fluxes in a Mediterranean Holm oak forest between the exceptionally dry 2003 and the following year. *Environmental Pollution, 157*, 1737–1744. https://doi.org/10.1016/j.envpol.2007.11.025

Gheorghe, I. F., & Ion, B. (2011). The effects of air pollutants on vegetation and the role of vegetation in reducing atmospheric pollution. In M. K. Khallaf (Ed.), *The impact of air pollution on health, economy, environment and agricultural sources* (pp. 241–280). IntechOpen. https://doi.org/10.5772/17660

Gilliam, F. S. (2006). us layer of forest ecosystems to excess nitrogen deposition. *Journal of Ecology, 94*(6), 1176–1191. https://doi.org/10.1111/j.1365-2745.2006.01155.x

Gonzalez-Fernandez, I., Gerosa, G., & Bermejo, V. (2013). Ozone effects on vegetation biodiversity in a biodiversity "hotspot" (southern Europe). In G. Mills, S. Wagg, & H. Harmens (Eds.), *Ozone pollution: Impacts on ecosystem services and biodiversity* (38–42). NERC Centre for Ecology and Hydrology, Bangor. https://nora.nerc.ac.uk/id/eprint/502675/1/N502675CR.pdf. Last access 20 July 2022.

Graedel, T. E., & Crutzen, P. J. (1993). *Atmospheric change: An Earth system perspective*. W. H. Freeman & Co., ISBN 978-0716723325, xiii+446 pp.

Grams, T. E. E., & Thiel, S. (2002). High light-induced switch from C3-photosynthesis to Crassulacean acid metabolism is mediated by UV-A/blue light. *Journal of Experimental Botany, 53*, 1475–1483. https://doi.org/10.1093/jexbot/53.373.1475

Gravano, E., Giulietti, V., Desotgiu, R., Bussotti, F., Grossoni, P., Gerosa, G., & Tani, C. (2003). Foliar response of an Ailanthus altissima clone in two sites with different levels of ozone-pollution. *Environmental Pollution, 121*, 137–146. https://doi.org/10.1016/S0269-7491(02)00180-X

Grennfelt, P., Engleryd, A., Forsius, M., Hov, Ø., Rodhe, H., & Cowling, E. (2020). Acid rain and air pollution: 50 years of progress in environmental science and policy. *Ambio, 49*, 849–864. https://doi.org/10.1007/s13280-019-01244-4

Guderian, R. (Ed.) (1985): *Air Pollution by Photochemical Oxidants: Formation, Transport, Control, and Effects on Plants*, Springer, ISBN 978–3–642-70118-4.

Guenther, A. B., Jiang, X., Heald, C. L., Sakulyanontvittaya, T., Duhl, T., Emmons, L. K., & Wang, X. (2012). The Model of Emissions of Gases and Aerosols from Nature version 2.1 (MEGAN2.1): An extended and updated framework for modeling biogenic emissions. *Geoscientific Model Development, 5*, 1471–1492. https://doi.org/10.5194/gmd-5-1471-2012

Guieu, C., & Ridame, C. (2022). Impact of atmospheric deposition on marine chemistry and biogeochemistry. In F. Dulac, S. Sauvage, & E. Hamonou (Eds.), *Atmospheric chemistry in the Mediterranean Region* (Vol. 2, From air pollutant sources to impacts). Springer, this volume. https://doi.org/10.1007/978-3-030-82385-6_23

Gupta, A. (2016). Effect of air pollutants on plant gaseous exchange process: Effect on stomata and respiration. In U. Kulshrestha, & P. Saxena, (Eds.), *Plant responses to air pollution* (pp. 85–92). Springer. https://doi.org/10.1007/978-981-10-1201-3_8.

Hanson, D. T., Swanson, S., Graham, L. E., & Sharkey, T. D. (1999). Evolutionary significance of isoprene emission from mosses. *American Journal of Botany, 86*, 634–639. https://doi.org/10.2307/2656571

Heath, R. L. (2008). Modification of the biochemical pathways of plants induced by ozone: What are the varied routes to change? *Environmental Pollution, 155*, 453–463. https://doi.org/10.1016/j.envpol.2008.03.010

Heath, R. L., Lefohn, A. S., & Musselman, R. C. (2009). Temporal processes that contribute to nonlinearity in vegetation responses to ozone exposure and dose. *Atmospheric Environment, 43*, 2919–2928. https://doi.org/10.1016/j.atmosenv.2009.03.011

Heck, W. W., Taylor, O. C., & Tingey, D. T. (1988). Assessment of crop loss from air pollutants. *The Journal of Agricultural Science, 113*, 414. https://doi.org/10.1017/S0021859600070209

Hernandez, L., Probst, A., Probst, J. L., & Ulrich, E. (2003). Heavy metal distribution in some French forest soils: Evidence for atmospheric contamination. *Science of the Total Environment, 312*, 195–219. https://doi.org/10.1016/S0048-9697(03)00223-7

Herut, B., Krom, M. D., Pan, G., & Mortimer, R. (1999). Atmospheric input of nitrogen and phosphorus to the Southeast Mediterranean: Sources, fluxes, and possible impact. *Limnology and Oceanography, 44*, 1683–1692. https://doi.org/10.4319/lo.1999.44.7.1683

Hettelingh, J. P., Posch, M., & De Smet, P. A. M. (2001). Multi-effect critical loads used in multi-pollutant reduction agreements in Europe. *Water, Air, and Soil Pollution, 130*, 1133–1138. https://doi.org/10.1023/A:1013935907768

Hill, A. C. (1971). Vegetation: A sink for atmospheric pollutants. *Journal of the Air Pollution Control Association, 21*, 341–346. https://doi.org/10.1080/00022470.1971.10469535

Holland, M., Kinghorn, S., Emberson, L., Cinderby, S., Ashmore, M., Mills, G., & Harmens, H. (2006). Development of a framework for probabilistic assessment of the economic losses caused by ozone damage to crops in Europe, Natural Environment Research Council) CEH project C02309NEW Defra contract EPG, 1, 3–205.

Honour, S. L., Bell, J. N. B., Ashenden, T. W., Cape, J. N., & Power, S. A. (2009). Responses of herbaceous plants to urban air pollution: Effects on growth, phenology and leaf surface characteristics. *Environmental Pollution, 157*, 1279–1286. https://doi.org/10.1016/j.envpol.2008.11.049

Hopke, J., Donath, J., Blechert, S., & Boland, W. (1994). Herbivore induced volatiles – The emission of acyclic homoterpenes from leaves of Phaseolus lunatus and Zea mays can be triggered by a β-glucosidase and jasmonic acid. *FEBS Letters, 352*, 146–150. https://doi.org/10.1016/0014-5793(94)00948-1

Hou, H., Takamatsu, T., Koshikawa, M. K., & Hosomi, M. (2005). Copper complexing capacity of throughfall and its environmental effect. *Water, Air, and Soil Pollution, 162*, 229–245. https://doi.org/10.1007/s11270-005-6439-0

Im, U., Christodoulaki, S., Violaki, K., Zarmpas, P., Kocak, M., Daskalakis, N., Mihalopoulos, N., & Kanakidou, M. (2013). Atmospheric deposition of nitrogen and sulfur over southern Europe with focus on the Mediterranean and the Black Sea. *Atmospheric Environment, 81*, 660–670. https://doi.org/10.1016/j.atmosenv.2013.09.048

Izquieta-Rojano, S., García-Gomez, H., Aguillaume, L., Santamaría, J. M., Tang, Y. S., Santamaría, C., Valiño, F., Lashera, E., Alonso, R., Avila, A., Cape, J. N., & Elustondo, D. (2016). Throughfall and bulk deposition of dissolved organic nitrogen to holm oak forests in the Iberian Peninsula: Flux estimation and identification of potential sources. *Environmental Pollution, 210*, 104–112. https://doi.org/10.1016/j.envpol.2015.12.002

Kabata-Pendias, A. (2010*). Trace elements in soils and plants* (4th ed, 550 pp). Taylor and Francis. https://doi.org/10.1201/b10158.

Kanakidou, M., Mihalopoulos, N., Kindap, T., Im, U., Vrekoussis, M., Gerasopoulos, E., Dermitzaki, E., Unal, A., Koçak, M., Markakis, K., Melas, D., Kouvarakis, G., Youssef, A. F., Richter, A., Hatzianastassiou, N., Hilboll, A., Ebojie, F., Wittrock, F., von Savigny, C., … Moubasher, H. (2011). Megacities as hot spots of air pollution in the East Mediterranean. *Atmospheric Environment, 45*, 1223–1235. https://doi.org/10.1016/j.atmosenv.2010.11.048

Kanakidou, M., Myriokefalitakis, S., & Tsigaridis, K. (2018). Aerosols in atmospheric chemistry and biogeochemical cycles of nutrients. *Environmental Research Letters, 13*, 063004. https://doi.org/10.1088/1748-9326/aabcdb

Kanakidou, M., Myriokefalitakis, S., & Tsagkaraki, M. (2020). Atmospheric inputs of nutrients to the Mediterranean Sea. *Deep-Sea Research Part II, 171*, 104606. https://doi.org/10.1016/j.dsr2.2019.06.014

Kelepertzis, E. (2014). Accumulation of heavy metals in agricultural soils of Mediterranean: Insights from Argolida basin, Peloponnese, Greece. *Geoderma, 221–222*, 82–90. https://doi.org/10.1016/j.geoderma.2014.01.007

Kundu, P., Gill, R., Ahlawat, S., Anjum, N. A., Sharma, K. K., Ansari, A. A., Hasanuzzaman, M., Ramakrishna, A., Chauhan, N., Tuteja, N., & Gill, S. S. (2018). Targeting the redox regulatory mechanisms for abiotic stress tolerance in crops. In S. H. Wani (Ed.), *Biochemical, physiological and molecular avenues for combating abiotic stress in plants* (pp. 151–220). Academic Press. https://doi.org/10.1016/B978-0-12-813066-7.00010-3

Lamarque, J. F., Shindell, D. T., Josse, B., Young, P. J., Cionni, I., Eyring, V., Bergmann, D., Cameron-Smith, P., Collins, W. J., Doherty, R., Dalsoren, S., Faluvegi, G., Folberth, G., Ghan, S. J., Horowitz, L. W., Lee, Y. H., MacKenzie, I. A., Nagashima, T., Naik, V., … Zeng, G. (2013). The atmospheric chemistry and climate model intercomparison Project (ACCMIP): Overview and description of models, simulations and climate diagnostics. *Geoscientific Model Development, 6*, 179–206. https://doi.org/10.5194/gmd-6-179-2013

Landmann, G., Bonneau, M., & Kaennel, M. (Eds.) (1995). *Forest decline and atmospheric deposition effects in the French mountains*, 461 pp. Springer. https://doi.org/10.1007/978-3-642-79535-0

Lavorel, S. (1999). Ecological diversity and resilience of Mediterranean vegetation to disturbance. *Diversity and Distributions, 5*, 3–13. https://doi.org/10.1046/j.1472-4642.1999.00033.x

Leng, X., Qian, X., Yang, M., Wang, C., Huiming Li, H., & Wang, J. (2018). Leaf magnetic properties as a method for predicting heavy metal concentrations in $PM_{2.5}$ using support vector machine: A case study in Nanjing, China. *Environmental Pollution, 242*, 922–930. https://doi.org/10.1016/j.envpol.2018.07.007

Leonard, R. J., McArthur, C., & Hochuli, D. F. (2016). Particulate matter deposition on roadside plants and the importance of leaf trait combinations. *Urban Forestry & Urban Greening, 20*, 249–253. https://doi.org/10.1016/j.ufug.2016.09.008

Li, P., Calatayud, V., Gao, F., Uddling, J., & Feng, Z. (2016). Differences in ozone sensitivity among woody species are related to leaf morphology and antioxidant levels. *Tree Physiology, 36*, 1105–1116. https://doi.org/10.1093/treephys/tpw042

Lin, M., Horowitz, L. W., Xie, Y., Paulot, F., Malyshev, S., Shevliakova, E., Finco, A., Gerosa, G., Kubistin, D., & Pilegaard, K. (2020). Vegetation feedbacks during drought exacerbate ozone air pollution extremes in Europe. *Nature Climate Change, 10*, 444–451. https://doi.org/10.1038/s41558-020-0743-y

Liu, H., Probst, A., & Liao, B. (2005). Metal contamination of soils and crops affected by the Chenzhou lead/zinc mine spill (Hunan, China). *Sci. Total Environ., 339*, 153–166. https://doi.org/10.1016/j.scitotenv.2004.07.030

Llop, E., Pinho, P., Ribeiro, M. C., Pereira, M. J., & Branquinho, C. (2017). Traffic represents the main source of pollution in small Mediterranean urban areas as seen by lichen functional groups. *Environmental Science and Pollution Research, 24*, 12016–12025. https://doi.org/10.1007/s11356-017-8598-0

Lombard, L., van der Merwe, N. A., Groenewald, J. Z., & Crous, P. W. (2015). Generic concepts in Nectriaceae. *Studies in Mycology, 80*, 189–245. https://doi.org/10.1016/j.simyco.2014.12.002

Loppi, S., Nelli, L., Ancora, S., & Bargagli, R. (1997). Passive monitoring of trace elements by means of tree leaves, epiphytic lichens and bark substrate. *Environmental Monitoring and Assessment, 45*, 81–88. https://doi.org/10.1023/A:1005770126624

Loreto, F., Mannozzi, M., Maris, C., Nascetti, P., Ferranti, F., & Pasqualini, S. (2001). Ozone quenching properties of isoprene and its antioxidant role in leaves. *Plant Physiology, 126*, 993–1000. https://doi.org/10.1104/pp.126.3.993

Mace, K. A., Kubilay, N., & Duce, R. A. (2003). Organic nitrogen in rain and aerosol in the eastern Mediterranean atmosphere: An association with atmospheric dust. *Journal of Geophysical Research, 108*, 4320. https://doi.org/10.1029/2002jd002997

Mallet, M., Nabat, P., di Sarra, A. G., Solmon, F., Gutierrez, C., Mailler, S., Menut, L., Kaskaoutis, D., Rowlinson, M., Rap, A., & Dulac, F. (2022). Aerosol and ozone direct radiative impacts.

In F. Dulac, S. Sauvage, & E. Hamonou (Eds.), *Atmospheric chemistry in the Mediterranean Region* (Vol. 2, From air pollutant sources to impacts). Springer, this volume. https://doi.org/10.1007/978-3-030-82385-6_19

Manes, F., Vitale, M., Maria Fabi, A., De Santis, F., & Zona, D. (2007). Estimates of potential ozone stomatal uptake in mature trees of Quercus ilex in a Mediterranean climate. *Environmental and Experimental Botany, 59*, 235–241. https://doi.org/10.1016/j.envexpbot.2005.12.001

Markaki, Z., Loÿe-Pilot, M. D., Violaki, K., Benyahya, L., & Mihalopoulos, N. (2010). Variability of atmospheric deposition of dissolved nitrogen and phosphorus in the Mediterranean and possible link to the anomalous seawater N/P ratio. *Marine Chemistry, 120*, 187–194. https://doi.org/10.1016/j.marchem.2008.10.005

Matsui, T., Kobayasi, K., Nakagawa, H., Yoshimoto, M., Hasegawa, T., Reinke, R., & Angus, J. (2014). Lower-than-expected floret sterility of rice under extremely hot conditions in a flood-irrigated field in New South Wales, Australia. *Plant Production Science, 17*, 245–252. https://doi.org/10.1626/pps.17.245

Michou, M., Laville, P., Serça, D., Fotiadi, A., Bouchou, P., & Peuch, V. H. (2005). Measured and modeled dry deposition velocities over the ESCOMPTE area. *Atmospheric Research, 74*, 89–116. https://doi.org/10.1016/j.atmosres.2004.04.011

Mills, G., Sharps, K., Simpson, D., Pleijel, H., Frei, M., Burkey, K., Emberson, L., Uddling, J., Broberg, M., Feng, Z., Kobayashi, K., & Agrawal, M. (2018). Closing the global ozone yield gap: Quantification and cobenefits for multistress tolerance. *Global Change Biology, 24*, 4869–4893. https://doi.org/10.1111/gcb.14381

Mori, J., Sæbø, A., Hanslin, H. M., Teani, A., Ferrini, F., Fini, A., & Burchi, G. (2015). Deposition of traffic-related air pollutants on leaves of six evergreen shrub species during a Mediterranean summer season. *Urban Forestry & Urban Greening, 14*, 264–273. https://doi.org/10.1016/j.ufug.2015.02.008

Mosher, E. S., Silander, J. A., & Latimer, A. M. (2009). The role of land-use history in major invasions by woody plant species in the northeastern north american landscape. *Biological Invasions, 11*, 2317–2328. https://doi.org/10.1007/s10530-008-9418-8

Mudd, J. B. (1975). Sulfur dioxide. In J. B. Mudd, & T. T. Kozlowski (Eds), *Responses of plants to air pollution*. Academic Press New York, 9–22, ISBN 978 0125094504.

Munzi, S., Paoli, L., Fiorini, E., & Loppi, S. (2012). Physiological response of the epiphytic lichen Evernia prunastri (L.) Ach. to ecologically relevant nitrogen concentrations. *Environmental Pollution, 171*, 25–29. https://doi.org/10.1016/j.envpol.2012.07.001

Musselman, R. C., Lefohn, A. S., Massman, W. J., & Heath, R. L. (2006). A critical review and analysis of the use of exposu re- and flux-based ozone indices for predicting vegetation effects. *Atmospheric Environment, 40*, 1869–1888. https://doi.org/10.1016/j.atmosenv.2005.10.064

Myers, N., Mittermeler, R. A., Mittermeler, C. G., Da Fonseca, G. A. B., & Kent, J. (2000). Biodiversity hotspots for conservation priorities. *Nature, 403*, 853–858. https://doi.org/10.1038/35002501

Nali, C., Paoletti, E., Marabottini, R., Della Rocca, G., Lorenzini, G., Paolacci, A. R., Ciaffi, M., & Badiani, M. (2004). Ecophysiological and biochemical strategies of response to ozone in Mediterranean evergreen broadleaf species. *Atmospheric Environment, 38*, 2247–2257. https://doi.org/10.1016/j.atmosenv.2003.11.043

Nasreddine, L., & Parent-Massin, D. (2002). Food contamination by metals and pesticides in the European Union. Should we worry? *Toxicology Letters, 127*, 29–41. https://doi.org/10.1016/S0378-4274(01)00480-5

Nenes, A., Pandis, S. N., Kanakidou, M., Russell, A., Song, S., Vasilakos, P., & Weber, R. J. (2021). Aerosol acidity and liquid water content regulate the dry deposition of inorganic reactive nitrogen. *Atmospheric Chemistry and Physics, 21*, 799–811. https://doi.org/10.5194/acp-21-799-2021

Nieboer, N., Richardson, D. H. S., Pukett, K. J., & Tomassini, F. D. (1976). The phytotoxicity of sulfur dioxide in relation to measurable responses in lichens. In Soc. Exp. Biol. Sem. Ser., Vol. 1, Cambridge University Press, ISBN 0521 29039, 61–86.

N'Guessan, Y. M., Probst, J. L., Bur, T., & Probst, A. (2009). Trace elements in stream bed sediments from agricultural catchments (Gascogne region, S-W France): Where do they come from? *Sci Total Environ, 407*, 2939–2952. https://doi.org/10.1016/j.scitotenv.2008.12.047

Ochoa-Hueso, R., Allen, E. B., Branquinho, C., Cruz, C., Dias, T., Fenn, M. E., Manrique, E., Pérez-Corona, M. E., Sheppard, L. J., & Stock, W. D. (2011). Nitrogen deposition effects on Mediterranean-type ecosystems: An ecological assessment. *Environmental Pollution, 159*, 2265–2279. https://doi.org/10.1016/j.envpol.2010.12.019

Ochoa-Hueso, R., & Manrique, E. (2011). Effects of nitrogen deposition and soil fertility on cover and physiology of *Cladonia foliacea* (Huds.) Willd., a lichen of biological soil crusts from Mediterranean Spain. *Environmental Pollution, 159*, 449–457. https://doi.org/10.1016/j.envpol.2010.10.021

Ochoa-Hueso, R., & Manrique, E. (2013). Effects of nitrogen deposition on growth and physiology of *Pleurochaete squarrosa* (Brid.) Lindb., a terricolous moss from Mediterranean ecosystems. *Water, Air, and Soil Pollution, 224*, 1492. https://doi.org/10.1007/s11270-013-1492-6

Ochoa-Hueso, R., Munzi, S., Alonso, R., Arróniz-Crespo, M., Avila, A., Bermejo, V., Bobbink, R., Branquinho, C., Concostrina-Zubiri, L., Cruz, C., de Carvalho, R. C., De Marco, A., Dias, T., Elustondo, D., Elvira, S., Estébanez, B., Fusaro, L., Gerosa, G., Izquieta-Rojano, S., … Theobald, M. R. (2017). Ecological impacts of atmospheric pollution and interactions with climate change in terrestrial ecosystems of the Mediterranean Basin: Current research and future directions. *Environmental Pollution, 227*, 194–206. https://doi.org/10.1016/j.envpol.2017.04.062

Oparka, K. J. (Ed.) (2005). Plasmodesmata. Oxford Blackwell Publishing Ltd, XV+313 pp. https://doi.org/10.1002/9780470988572

Paoletti, E. (2006). Impact of ozone on Mediterranean forests: A review. *Environmental Pollution, 144*, 463–474. https://doi.org/10.1016/j.envpol.2005.12.051

Paoli, L., Guttová, A., & Loppi, S. (2006). Assessment of environmental quality by the diversity of epiphytic lichens in a semi-arid Mediterranean area (Val Basento, South Italy). *Biologia, 61*, 353–359. https://doi.org/10.2478/s11756-006-0064-2

Payne, R. J., Campbell, C., Britton, A. J., Mitchell, R. J., Pakeman, R. J., Jones, L., Ross, L. C., Stevens, C. J., Field, C., Caporn, S. J. M., Carroll, J., Edmondson, J. L., Carnell, E. J., Tomlinson, S., Dore, A. J., Dise, N., & Dragosits, U. (2019). What is the most ecologically-meaningful metric of nitrogen deposition? *Environmental Pollution, 247*, 319–331. https://doi.org/10.1016/j.envpol.2019.01.059

Peer, R. L., Thorneloe, S. A., & Epperson, D. L. (1993). A comparison of methods for estimating global methane emissions from landfills. *Chemosphere, 26*, 387–400. https://doi.org/10.1016/0045-6535(93)90433-6

Pierret, M. C., Viville, D., Dambrine, E., Cotel, S., & Probst, A. (2019). Twenty-five year record of chemicals in open field precipitation and throughfall from a medium-altitude forest catchment (Strengbach – NE France): An obvious response to atmospheric pollution trends. *Atmospheric Environment, 202*, 296–314. https://doi.org/10.1016/j.atmosenv.2018.12.026

Pinho, P., Augusto, S., Martins-Loução, M. A., Pereira, M. J., Soares, A., Máguas, C., & Branquinho, C. (2008). Causes of change in nitrophytic and oligotrophic lichen species in a Mediterranean climate: Impact of land cover and atmospheric pollutants. *Environmental Pollution, 154*, 380–389. https://doi.org/10.1016/j.envpol.2007.11.028

Pirintsos, S. A., Paoli, L., Loppi, S., & Kotzabasis, K. (2011). Photosynthetic performance of lichen transplants as early indicator of climatic stress along an altitudinal gradient in the arid Mediterranean area. *Climatic Change, 107*, 305–328. https://doi.org/10.1007/s10584-010-9989-0

Percy, K. E., Cape, J. N., Jagels, R., and Simpson C. J. (Eds.) (1994). Air pollutants and the leaf cuticle, NATO ASI Series (Vol. 236, 398 pp). https://doi.org/10.1007/978-3-642-79081-2.

Polymenakou, P. N., Mandalakis, M., Stephanou, E. G., & Tselepides, A. (2008). Particle size distribution of airborne microorganisms and pathogens during an intense African dust event

in the eastern Mediterranean. *Environmental Health Perspectives, 116*, 292–296. https://doi.org/10.1289/ehp.10684

Probst, A., Obeidy, C., Gaudio, N., Belyazid, S., Gégout, J. C., Alard, D., Corket, E., Party, J. P., Gauquelin, T., Mansat, A., Nihlgård, B., Leguédois, S., & Sverdrup, H. U. (2015). Evaluation of plant-responses to atmospheric nitrogen deposition in France using integrated soil-vegetation models. In W. de Vries, J.-P. Hettelingh, & M. Posch (Eds.), *Critical loads and dynamic risk assessments – Nitrogen, acidity and metals in terrestrial and aquatic ecosystems* (Environmental pollution) (Vol. 255, pp. 359–379). Springer. https://doi.org/10.1007/978-94-017-9508-1_13

Rap, A., Spracklen, D. V., Mercado, L., Reddington, C. L., Haywood, J. M., Ellis, R. J., Phillips, O. L., Artaxo, P., Bonal, D., Restrepo Coupe, N., & Butt, N. (2015). Fires increase Amazon forest productivity. *Geophysical Research Letters, 42*, 4654–4662. https://doi.org/10.1002/2015GL063719

Ratier, A., Dron, J., Revenko, G., Austruy, A., Dauphin, C. E., Chaspoul, F., & Wafo, E. (2018). Characterization of atmospheric emission sources in lichen from metal and organic contaminant patterns. *Environmental Science and Pollution Research, 25*, 8364–8376. https://doi.org/10.1007/s11356-017-1173-x

Reinds, G. J., Posch, M., De Vries, W., Slootweg, J., & Hettelingh, J. P. (2008). Critical loads of sulphur and nitrogen for terrestrial ecosystems in Europe and northern Asia using different soil chemical criteria. *Water, Air, and Soil Pollution, 193*, 269–287. https://doi.org/10.1007/s11270-008-9688-x

Riga-Karandinos, A. N., & Saitanis, C. (2004). Biomonitoring of concentrations of platinum group elements and their correlations to other metals. *International Journal of Environment and Pollution, 22*, 563–579. https://doi.org/10.1504/IJEP.2004.005910

Riga-Karandinos, A. N., Saitanis, C. J., & Arapis, G. (2006). First study of anthropogenic platinum group elements in roadside top-soils in Athens, Greece. *Water, Air, and Soil Pollution, 172*, 3–20. https://doi.org/10.1007/s11270-005-9016-7

Rinnan, R., Steinke, M., McGenity, T., & Loreto, F. (2014). Plant volatiles in extreme terrestrial and marine environments. *Plant, Cell & Environment, 37*, 1776–1789. https://doi.org/10.1111/pce.12320

Rizzetto, S., Belyazid, S., Gégout, J. C., Nicolas, M., Alard, D., Corcket, E., Gaudio, N., Sverdrup, H., & Probst, A. (2016). Modelling the impact of climate change and atmospheric N deposition on French forests biodiversity. *Environmental Pollution, 213*, 1016–1027. https://doi.org/10.1016/j.envpol.2015.12.048

Rodà, F., Avila, A., & Rodrigo, A. (2002). Nitrogen deposition in Mediterranean forests. *Environmental Pollution, 118*, 205–213. https://doi.org/10.1016/s0269-7491(01)00313-x

Rodríguez Martin, J. A., Gutiérrez, C., Torrijos, M., & Nanos, N. (2018). Wood and bark of *Pinus halepensis* as archives of heavy metal pollution in the Mediterranean Region. *Environmental Pollution, 239*, 438–447. https://doi.org/10.1016/j.envpol.2018.04.036

Rowe, E. C., Wamelink, G. W., Smart, S. M., Butler, A., Henrys, P. A., van Dobben, H. F., Reinds, G. J., Evans, C. D., Kros, J., & de Vries, W. (2015). Field survey based models for exploring nitrogen and acidity effects on plant species diversity and assessing long-term critical loads. In W. de Vries, J.-P. Hettelingh, & M. Posch (Eds.), *Critical loads and dynamic risk assessments – Nitrogen, acidity and metals in terrestrial and aquatic ecosystems* (Environmental pollution) (Vol. 255, pp. 297–326). Springer. https://doi.org/10.1007/978-94-017-9508-1_11

Saitanis, C. (2008). Tropospheric ozone: a menace for crops and natural vegetation in Greece. *Italian Journal of Agronomy, 3*, 71–77. https://doi.org/10.4081/ija.2008.71

Saitanis, C. J., & Karandinos, M. G. (2002). Effects of ozone on tobacco (Nicotiana tabacum L.) varieties. *Journal of Agronomy and Crop Science, 188*, 51–58. https://doi.org/10.1046/j.1439-037x.2002.00539.x

Saitanis, C., Karandinos, M. G., Riga-Karandinos, A. N., Lorenzini, G., & Vlassi, A. (2003). Photochemical air pollutant levels and ozone phytotoxicity in the region of Mesogia-Attica, Greece. *International Journal of Environment and Pollution, 19*, 197–208. https://doi.org/10.1504/IJEP.2003.003748

Saitanis, C. J., Bari, S. M., Burkey, K. O., Stamatelopoulos, D., & Agathokleous, E. (2014). Screening of Bangladeshi winter wheat (*Triticum aestivum* L.) cultivars for sensitivity to ozone. *Environmental Science and Pollution Research, 21*, 13560–13571. https://doi.org/10.1007/s11356-014-3286-9

Sanz, M. J., & Millán, M. M. (2000). Ozone in the Mediterranean region: evidence of injury to vegetation, in Forest Dynamics in Heavily Polluted Regions, Innes, J. L., Ed., IUFRO Research Series 1, CABI Publishing, Wallingford, UK, 165–192.

Sanz, M. J., Carratalá, A., Gimeno, C., & Millán, M. M. (2002). Atmospheric nitrogen deposition on the east coast of Spain: Relevance of dry deposition in semi-arid Mediterranean regions. *Environmental Pollution, 118*, 259–272. https://doi.org/10.1016/S0269-7491(01)00318-9

Sanz, J., Bermejo, V., Gimeno, B. S., Elvira, S., & Alonso, R. (2007). Ozone sensitivity of the Mediterranean terophyte Trifolium striatum is modulated by soil nitrogen content. *Atmospheric Environment, 41*, 8952–8962. https://doi.org/10.1016/j.atmosenv.2007.08.016

Sardans, J., Alonso, R., Carnicer, J., Fernández-Martínez, M., Vivanco, M. G., & Peñuelas, J. (2016). Factors influencing the foliar elemental composition and stoichiometry in forest trees in Spain. *Perspectives in Plant Ecology, Evolution and Systematics, 18*, 52–69. https://doi.org/10.1016/j.ppees.2016.01.001

Schenone, G. (1993). Air pollution and vegetation in the Mediterranean area. *Méditerranée, 4*, 49–52.

Schmitz, A., Sanders, T. G. M., Bolte, A., Bussotti, F., Dirnböck, T., Johnson, J., Peñuelas, J., Pollastrini, M., Prescher, A., Sardans, J., Verstraeten, A., & Vries, W. (2019). Responses of forest ecosystems in Europe to decreasing nitrogen deposition. *Environmental Pollution, 244*, 980–994. https://doi.org/10.1016/j.envpol.2018.09.101

Sharma, P., Jha, A. B., Dubey, R. S., & Pessarakli, M. (2012). Reactive oxygen species, oxidative damage, and antioxidative defense mechanism in plants under stressful conditions. *Journal of Botany, 2012*, 1–26. https://doi.org/10.1155/2012/217037

Sharma, A., Kumar, V., Kumar, R., Shahzad, B., Thukral, A. K., & Bhardwaj, R. (2018). Brassinosteroid-mediated pesticide detoxification in plants: A mini-review. *Cogent Food & Agriculture, 4*, 1436212. https://doi.org/10.1080/23311932.2018.1436212

Smith, R. I., Fowler, D., & Cape, J. N. (1989). The statistics of phytotoxic air pollutants. *Journal of the Royal Statistical Society: Series A, 152*, 183–198. https://doi.org/10.2307/2982914

Stalikas, C. D., Mantalovas, A. C., & Pilidis, G. A. (1997). Multielement concentrations in vegetable species grown in two typical agricultural areas of Greece. *Science of the Total Environment, 206*, 17–24. https://doi.org/10.1016/S0048-9697(97)00213-1

Stanners, D., & Bourdeau, P. (1995). Europe's Environment: The Dobris Assessment, Paperback – 31, Office for Official Publications of the European Communities, Luxembourg, 712 pp.

Stevens, C. J., Dise, N. B., Owen Mountford, J., & Gowing, D. J. (2004). Impact of nitrogen deposition on the species richness of grasslands. *Science, 303*, 1876–1879. https://doi.org/10.1126/science.1094678

Tiiva, P., Rinnan, R., Faubert, P., Räsänen, J., Holopainen, T., Kyrö, E., & Holopainen, J. K. (2007). Isoprene emission from a subarctic peatland under enhanced UV-B radiation. *The New Phytologist, 176*, 346–355. https://doi.org/10.1111/j.1469-8137.2007.02164.x

Velikova, V., & Loreto, F. (2005). On the relationship between isoprene emission and thermotolerance in Phragmites australis leaves exposed to high temperatures and during the recovery from a heat stress. *Plant, Cell & Environment, 28*, 318–327. https://doi.org/10.1111/j.1365-3040.2004.01314.x

Vilà, M., Burriel, J. A., Pino, J., Chamizo, J., Llach, E., Porterias, M., & Vives, M. (2003). Association between Opuntia species invasion and changes in land-cover in the Mediterranean region. *Global Change Biology, 9*, 1234–1239. https://doi.org/10.1046/j.1365-2486.2003.00652.x

Violaki, K., Zarbas, P., & Mihalopoulos, N. (2010). Long-term measurements of dissolved organic nitrogen (DON) in atmospheric deposition in the Eastern Mediterranean: Fluxes, origin and biogeochemical implications. *Marine Chemistry, 120*, 179–186. https://doi.org/10.1016/j.marchem.2009.08.004

Vlachogianni, T., Vogrin, M., & Scoullos, M. (2012) Biodiversity in the Mediterranean, The Regional Activity Centre for Specially Protected Areas (RAC/SPA), 1–10, Retrieved from http://www.rac-spa.org/publications

Wallman, P., Svensson, M. G. E., Sverdrup, H., & Belyazid, S. (2005). ForSAFE – An integrated process-oriented forest model for long-term sustainability assessments. *Forest Ecology and Management, 207*, 19–36. https://doi.org/10.1016/j.foreco.2004.10.016

Wang, W., Vinocur, B., & Altman, A. (2003). Plant responses to drought, salinity and extreme temperatures: Towards genetic engineering for stress tolerance. *Planta, 218*, 1–14. https://doi.org/10.1007/s00425-003-1105-5

Wheeler, T. R., Hong, T. D., Ellis, R. H., Batts, G. R., Morison, J. I. L., & Hadley, P. (1996). The duration and rate of grain growth, and harvest index, of wheat (Triticum aestivum L.) in response to temperature and CO_2. *Journal of Experimental Botany, 47*, 623–630. https://doi.org/10.1093/jxb/47.5.623

Wolfenden, J., & Mansfield, T. A. (1990). Physiological disturbances in plants caused by air pollutants. *Royal Society of Edinburgh. Section B: Biology, 97*, 117–138. https://doi.org/10.1017/s0269727000005315

Yu, M. H., Tsunoda, H., & Tsunoda, M. (2011). *Environmental toxicology: Biological and health effects of pollutants* (3rd ed., 397 pp). CRC press. https://doi.org/10.1201/b11677

Yuan, J. S., Himanen, S. J., Holopainen, H. K., Chen, F., & Stewart, C. N., Jr. (2009). Smelling global climate change: Mitigation of function for plant volatile organic compounds. *Trends in Ecology & Evolution, 24*, 323–331. https://doi.org/10.1016/j.tree.2009.01.012

Summary of Recent Progress and Recommendations for Future Research Regarding Air Pollution Sources, Processes, and Impacts in the Mediterranean Region

François Dulac, Eric Hamonou, Stéphane Sauvage, Maria Kanakidou, Matthias Beekmann, Karine Desboeufs, Paola Formenti, Silvia Becagli, Claudia di Biagio, Agnès Borbon, Cyrielle Denjean, François Gheusi, Valérie Gros, Cécile Guieu, Wolfgang Junkermann, Nikolaos Kalivitis, Benoît Laurent, Marc Mallet, Vincent Michoud, Pierre Nabat, Karine Sartelet, and Karine Sellegri

Contents

Reviewed by Oksana Tarasova (Atmospheric Environment Research Division, World Meteorological Organization, Geneva, Switzerland) and commented by Jos Lelieveld (Max Planck Institute for Chemistry, Mainz, Germany, and Climate and Atmosphere Research Center (CARE-C), The Cyprus Institute, Aglantzia, Nicosia, Cyprus)

F. Dulac (✉) · V. Gros
Laboratoire des Sciences du Climat et de l'Environnement (LSCE), CEA-CNRS-UVSQ, IPSL, Université Paris-Saclay, Gif-sur-Yvette, France
e-mail: francois.dulac@cea.fr

E. Hamonou
Science-Partners, Paris, France

S. Sauvage
IMT Nord Europe, Institut Mines-Télécom, Univ. Lille, Centre for Energy and Environment, F-59000 Lille, France

M. Kanakidou · N. Kalivitis
Environmental Chemical Processes Laboratory (ECPL), Department of Chemistry, University of Crete, Heraklion, Greece

F. Dulac et al. (eds.), *Atmospheric Chemistry in the Mediterranean Region*,
https://doi.org/10.1007/978-3-030-82385-6_25

Abstract Mediterranean atmospheric pollution sources, processes, and impacts are summarized in this chapter. The companion Volume 1 describes the context and the distribution of gaseous and particulate pollutants. The present volume is composed of six sections that make the synthesis of our knowledge on air pollutant sources (Part V), atmospheric chemical processes (VI), aerosol properties (VII), atmospheric deposition fluxes (VIII), and the impacts of air pollution on the chemical composition of precipitation and climate (IX) and on human health and ecosystems (X). The conclusions presented in this volume demonstrate large variety of impacts of air pollution on the environment in the Mediterranean, including the impacts on human health, ecosystems, and climate. Accurate emission evaluation of gaseous and particulate pollutants and understanding of their chemical transformation are critical for representation and prediction of atmospheric pollution and climate change in this region. Long-term observations of physical and chemical parameters describing atmospheric composition together with climate variables are essential to constrain models and to better quantify interactions between climate change and air quality. Addressing the impacts of pollution and supporting mitigation measures require holistic and integrated approach to the related studies, putting together scientific communities working on atmosphere, on health, as well as on both terrestrial and marine ecosystems.

M. Beekmann · K. Desboeufs · P. Formenti · C. di Biagio · B. Laurent · V. Michoud
Université Paris Cité and Univ. Paris Est Créteil, CNRS, LISA, Paris, France

S. Becagli
Department of Chemistry Ugo Schiff, University of Florence, Florence, Italy

A. Borbon · K. Sellegri
Université Clermont Auvergne, CNRS, Laboratoire de Météorologie Physique UMR 6016 (LaMP), Clermont-Ferrand, France

C. Denjean · M. Mallet · P. Nabat
Centre National de Recherches Météorologiques (CNRM), Université de Toulouse, Météo France, CNRS, Toulouse, France

F. Gheusi
Laboratoire d'Aérologie (LAERO), Université de Toulouse III Paul Sabatier, CNRS, Observatoire Midi-Pyrénées, Toulouse, France

C. Guieu
Laboratoire d'Océanographie de Villefranche (LOV), UMR 7093, CNRS, Sorbonne Université, Chemin du Lazaret, Villefranche-sur-Mer, France

W. Junkermann
Institute of Meteorology and Climate Research (IMK-IFU), Karlsruhe Institute of Technology, Campus-Alpine, Garmisch-Partenkirchen, Germany

K. Sartelet
Centre d'Enseignement et de Recherche en Environnement Atmosphérique (CEREA), École des Ponts ParisTech, EDF R&D, Marne-la-Vallée, France

1 Introduction

The lower Earth atmosphere composition has been recognized as an important component of the Earth system, especially at the regional scale. Its changes have many impacts on human health and mortality, on climate, and on terrestrial as well as freshwater and marine ecosystems. Changes in atmospheric chemical composition are driven by increasing anthropogenic pressure on the environment and climate change. In the Mediterranean region, human activities and long-range transport affect also the marine atmospheric environment. Atmospheric pollution is often higher over the Mediterranean basin than over most European continental regions, especially during the long Mediterranean summer season, due to (i) the convergence of long-range transported continental air masses that adds to local sources of air pollution, (ii) the lack of precipitation scavenging, (iii) intense photochemistry, and (iv) local circulations that recycle polluted air layers in the western basin and poor ventilation rates. The Mediterranean basin is the recipient of anthropogenic emissions from continental Europe and densely populated coastal urban areas around the basin, and from the intense maritime ship traffic, combined with natural emissions from the surrounding vegetation, the sea surface, and the African and Middle East deserts. In addition, the Mediterranean region is highly sensitive to climate change, which already altered, in a substantial way, natural emissions, photochemical processes, pollutant transport, dispersion, and wet and dry deposition in the region.

This is the second of the two volumes. The first volume (Dulac et al., 2023) addresses the importance of the Mediterranean atmospheric chemistry and the general context of the Mediterranean atmospheric environment, including climate and its predicted evolution and anthropogenic drivers (book Part I; Dulac, 2023). The role of the atmospheric dynamics in the distribution of atmospheric pollutants is then depicted (Part II; Dayan, 2023). The volume also includes the characterization of the distribution of aerosols (Part III; Mihalopoulos, 2023a) and reactive gases (Part IV; Mihalopoulos, 2023b) and their spatial and temporal variability and trends. This second volume (Dulac et al., 2022) first presents an update on regional emissions of natural and anthropogenic pollutants (Part V; Sauvage, 2022). Sections on chemical processes (Part VI; Beekmann, 2022), aerosol properties and their connections with atmospheric chemistry and climate (Part VII; Formenti, 2022), and deposition (Part VIII; Desboeufs, 2022) are following. The last two sections review the main impacts of air pollutants, including the effects on chemical composition of precipitation, radiation and climate (Part IX; Kanakidou, 2022a) and the effects on human health and marine and terrestrial ecosystems (Part X; Kanakidou, 2022b). In the following, we first summarize the main conclusions presented in the different chapters of Volume 2 and then put forward a number of recommendations for future research on air pollutant sources and fates, aerosol properties, deposition, and various important impacts of the atmospheric composition on the Mediterranean region.

2 Main Conclusions

2.1 Anthropogenic and Natural Emissions of Air Pollutants

The volume starts by making accurate emission assessments of gaseous and particulate pollutants as a prerequisite to the study of the interplay between atmospheric pollution and climate change in the Mediterranean (Sauvage, 2022). Numerous natural and anthropogenic source types have been identified and evaluated in terms of chemical composition of emitted pollutants as well as their emission processes.

Sea spray which originates from the action of the wind stress on the sea surface, creating waves and bubbles, constitutes one of the most important natural components of the global aerosol. These particles are traditionally assumed to be mainly composed of inorganic sea salt, an organic fraction, and water. Recent studies in the Mediterranean have shown that the chemical composition of the inorganic fraction is very similar to the composition of the seawater. Much more uncertainties are associated with the emission of marine organic matter. Such knowledge is critical, since several laboratory experiments have shown that higher number of sea spray particles are emitted when seawater is enriched in biologically derived organics. This is also true in the Mediterranean oligotrophic sea, where recent findings have identified a clear relationship between the number of emitted sea spray particles and the abundance of nanophytoplankton cells in the water. The findings also indicate that Mediterranean seawater contains biologically originated organic material with the same properties as found in the global ocean. The Mediterranean Sea is oligotrophic, and hence, sea spray particles emitted from its surface waters normally contain a low level of biologically originating carbon except during phytoplanktonic bloom conditions. Under environmental conditions specific to the Mediterranean Sea, the relationships between sea spray and the seawater biogeochemical properties are complex and depend on the interplay of physical, (photo) chemical, and biological processes. Studies have found that concentrations of marine organic aerosol particles are highly dependent on the biological productivity at the ocean surface and follow the seasonal blooming cycle. Nowadays, parameterizations of sea spray aerosol fluxes include an organic component that is at best a function of Chlorophyll-a in the seawater, although a recent modelling study has integrated the different classes of organic substances in the seawater (originating from proteins, lipids, polysaccharides, or humic-like substances) and their surfactant properties, for prescribing their transfer to the atmosphere.

The Mediterranean vegetation is another large contributing source to atmospheric reactive gases and particles including “bioaerosols.” Due to the high vegetation biodiversity and favorable climatic conditions, the Mediterranean area is a huge source of biogenic VOCs (BVOCs), which are precursors of tropospheric ozone and secondary organic aerosols (SOA). In the Mediterranean basin, BVOCs could be responsible for an additional 5–15 ppb of tropospheric ozone formation in summertime and could also contribute significantly to the SOA formation. The countries located at the border of the Mediterranean Sea have BVOCs emission rates (by

surface unit) 2–3 times higher than other European countries. Based on measurement campaigns in remote areas, more than 20% of VOCs were attributed to biogenic sources (primary or secondary) in the western Mediterranean (Corsica) in summer, whereas this biogenic contribution to the total VOCs load has been evaluated up to 40% of VOCs in the eastern part of the basin (Cyprus). The determination of the speciation and emissions of BVOCs (especially isoprene and terpenes) have been performed in several Mediterranean ecosystems at different scales (leaf, branch, and canopy). The development of new measurement technologies, based in particular on mass spectrometry (e.g., PTR-MS) during the last 20 years, allowed for canopy flux measurements as well as the measurements of BVOC classes neglected so far, especially methanol and other oxygenated compounds that can be emitted in large quantities by the terrestrial vegetation. These measurements have enabled good progress in modelling capacity and the development of different simulation approaches. Studies emphasized that VOC emissions largely depend on the species ability to withstand drought.

Mineral dust is a major component of the Mediterranean aerosol. Sporadic dust events result in strong spatial and temporal gradients of dust concentrations with concentrations that may vary over several orders of magnitude, from several tens to several thousands of $\mu g\ m^{-3}$, in less than 48 h or over hundreds of km. Dust emissions result from complex interactions between meteorological parameters and the soil surface including a surface wind threshold effect, making them very sensitive to climate change and intensification of high surface winds. Mineral dust emissions also result from soil disturbances due to changes in human activities and desertification. Observations and models suggest that the entire Sahara, even its southernmost part to a lesser extent, can contribute to the dust events observed in the Mediterranean basin. It seems that the northern sources, especially those located on the border of the Atlas Mountains, in Tunisia, Libya, and Egypt are the most frequent dust source areas for the western and central Mediterranean. However, it is also likely that large-scale dust events, originating from well-known active dust sources like the Bodélé depression or the Western Sahara, are responsible for the most intense dust events happening in the Mediterranean basin. The Middle East deserts also appear to be seasonal sources of dust in the easternmost Mediterranean basin.

Both gases and particulate pollutants can be directly emitted by numerous anthropogenic sources. Identifying emission sources and quantifying their contributions to the atmospheric pollution levels are essential steps for environmental management. There is no specific emission inventory for the Mediterranean region, and emission can be estimated either using gridded emissions from global inventories like the Atmospheric Chemistry and Climate Model Intercomparison Project (ACCMIP) or regional inventories such as EMEP. Some of the non-European countries of the basin have developed local emission inventories at the national level (e.g., Lebanon) or institutional levels (e.g., Egypt and Turkey). Composite emission inventories available for the Mediterranean region show a decrease in emissions since the 1990s for most of the gaseous compounds. However, $PM_{2.5}$ increased slightly at the end of last century with a slight decreasing trend after the year 2000. Road transport is one of the important anthropogenic emission sectors for gaseous

emissions like NO_x, VOCs, and CO. The Mediterranean Sea is an important path of the world network of maritime shipping, especially with the Suez Canal. Almost 4% of the total global shipping emissions occur in the Mediterranean with higher emissions in the eastern than in the western part of the basin. Biomass burning in this region became more frequent and more intense in the recent years in comparison with climatological average. ACCMIP shows an increase in emissions from this sources category in the Mediterranean countries in the years 1990–2000 for NO_x and non-methane VOCs (NMVOCs), with a contribution of biomass burning to total emissions of 1% and 2%, respectively. Anthropogenic emission inventories usually show consistent trends with discrepancies generally not exceeding 40%. However, beside high uncertainties for some pollutants, different patterns are depicted between the western, eastern, northern, and southern basins. For inventory evaluation, source apportionment based on field observations was made possible by the development of source-receptor models and the continuous improvement of analytical technologies. First experimental initiatives were performed in large cities around the basin (Marseille, Athens, Barcelona) bringing new inputs to emission inventory development as well as model evaluation. A study conducted in Athens has shown that in addition to traffic, residential heating is also an important source of NMVOC in winter. More recently, observation campaigns in Beirut (2011) and Istanbul (2014) and Positive Matrix Factorization analysis (PMF) allowed an assessment of the spatiotemporal variability of those large city emissions. Traffic is the major source of NMVOCs in Beirut , whereas in Istanbul, the traffic, including exhaust and fuel evaporation, only contributes to 16% of NMVOC ambient mixing ratio after natural gas evaporation (26%). From comparison with the PMF results in Beirut, the national emission inventory for Lebanon is found to underestimate by 20% to 39% the road transport emissions of NMVOCs in Beirut . The global emission inventories (ACCMIP, EDGARv4.2) even show more significant differences reaching a factor of 10. These results demonstrate the inconsistency between global and national inventories as well as the need to consider both the speciation and absolute emissions.

Finally, ultrafine particles (UFP, size below 100 nm) have recently been investigated regarding their high potential impacts. They cover the “nucleation” particle size mode, <1–20 nm, and the “Aitken” mode, 20–100 nm. In the upper range of the Aitken mode (>40 nm) and further extending into the “accumulation” mode (>100 nm), ultrafine particles may act as cloud condensation nuclei (CCN) and therefore may strongly impact weather and climate. UFP in the atmosphere originate mainly from nucleation of gas phase molecules or gas to particle conversion. Their main sources are industrial and residential combustion processes as well as traffic, especially in large urban areas. Their emission evaluation remains quite uncertain and includes only continental sources, leaving out the contribution from ship traffic yet intense over the Mediterranean basin. From source areas along the coast, UFP are easily transported over the whole Mediterranean basin even beyond 500 km. The physical and chemical processes (aging) along transport ways lead changes in particle size distribution, mainly toward CCN sizes and to the accumulation mode. As a consequence, the fraction of particles acting as CCN is increasing

up to 100% in aged particles over Corsica. Single event observations together with back trajectories allowed for identification of some major sources of CCN such as fossil fuel power plants and the Suez to Gibraltar major shipping route. Nowadays, shipping appears as a major source of ultrafine particulate matter, especially in the marine environment of the central Mediterranean, which was originally remote or only moderately polluted (at least up to the 1970s). From a maximum of 600–800 CCN cm^{-3} in 1970, more than 2000 CCN cm^{-3} are encountered nowadays over the Mediterranean.

2.2 Chemical Processes

Once emitted, air pollutants undergo physicochemical transformations which are particularly favored in the Mediterranean region due to its meteorological conditions supporting photochemistry. These processes strongly impact the tropospheric chemical composition. Depending on the oxidative capacity, they may lead to the formation of secondary pollutants such as ozone or secondary aerosols. Several important processes are addressed in this volume (Beekmann, 2022).

The hydroxyl radical (OH) is the main atmospheric oxidant during daytime. The recent progress in the total OH reactivity measurement provides a relevant estimate of the total load of reactive molecules in the atmosphere as well as a constraint of the total OH source when the concentration of the OH radical is known. Moreover, this information is of interest to evaluate remaining unmeasured atmospheric constituents that play a role in atmospheric chemistry, to derive the ozone production potential, and to understand the formation of new particles. Only a few studies have been performed so far in the Mediterranean area on OH reactivity, but nevertheless, they have documented OH behavior in various environments, from unperturbed natural environment to anthropogenically impacted areas. Studies performed at remote sites located in the western and eastern Mediterranean basins have shown that the western basin has a larger OH reactivity for these specific sites, which was mainly attributed to biogenic VOCs, specifically terpenes, and possibly to their oxidation products. The VOC speciation and the intensity of the emissions depend on the type of vegetation but also on the meteorological conditions such as sunlight and temperature. Biogenic VOCs are very reactive compounds; therefore, their influence on OH reactivity is mainly local, although they can have a wider impact through the transport of their oxidation products. However, anthropogenic sources (urban, industrial, and from oil and gas production and processing) can lead to high reactivity like it was demonstrated in the Arabian Gulf, Gulf of Suez, and Suez Canal.

As shown in Vol. 1 of this book, the Mediterranean basin is a summer hot spot for surface and tropospheric ozone. Because the marine lower troposphere remained largely unexplored, 16 drifting balloon flights were conducted to monitor ozone during three ChArMEx field campaigns in summer 2012 and 2013. In situ net ozone production was found over sea during daytime in both the marine boundary layer and the free troposphere at lower rates than generally observed over the land in polluted coastal

areas in the Mediterranean basin but however higher than those found in very remote marine environments. Despite the lack of precursor measurements, it was assumed that after being launched from relatively polluted areas, the balloons flew in air masses with limited levels of ozone precursors leading to an observed daytime ozone buildup of ~10 ppbv in 6 h in the absence of surface deposition and titration at night.

Secondary aerosols can be organic or inorganic and may represent a large fraction of fine particles especially over the Mediterranean. In summer, organics are mostly of biogenic origin, water soluble, and highly oxidized. The secondary aerosol is mainly formed from biogenic organic compounds (see the chapter by Sartelet, 2022). Anthropogenic pollutants also constitute a part of the process through the formation of oxidants and by providing an absorbing support for condensation. Despite the large uncertainties in BVOCs emissions, 3D air-quality models can now well simulate the formation processes, the concentrations, and properties of organic aerosol (OA) at remote sites and over forests. For these models, it was shown that extremely low-volatility VOCs (ELVOCs) from the oxidation of monoterpenes contribute up to 10% to organic compounds in the western Mediterranean and still partly explain the high observed oxidation state of OA. For anthropogenic organic precursors, intermediate and semi-volatile organic compounds (I/S-VOCs) are found to contribute about 20% or less to total OA in summer, while their contribution is major in winter (about 80%). VOCs emitted from residential wood combustion may especially influence the OA formation. Wildfires contribute as well to high OA loading with I/S-VOCs contributing up to 70% of OA during severe fire episodes. Primary sea-salt organic emissions are estimated to have a low contribution to OA. However, sea-salt emissions strongly enhance the formation of organic aerosols by providing an absorbing aqueous mass to the hydrophilic semi-volatile organics formed from the oxidation of biogenic precursors. The concentrations of secondary organic aerosols have been simulated to increase in the Mediterranean by 2050 because of climate change. Increased temperatures lead to an increase in biogenic VOC emissions and to a shift of the gas-particle phase equilibrium toward the gas phase. Over cities, the increase in secondary aerosols may also be due to an increase in oxidant concentrations, because of NO_x emission reductions. Sulfate particles represent a large fraction of fine aerosol over the Mediterranean region. While the contribution of sea-salt sulfate to PM_1 is low, sulfate is highly sensitive to primary emissions and specially to ship emissions. Several simulation studies showed the strong influence of maritime traffic, meteorology, and sea-salt emissions on inorganic aerosol concentrations in the western Mediterranean region.

Recent observation campaigns showed covariations between OA and the oxygenated component of the gas phase, suggesting that similar processes lead to the formation and aging of organics in the gas and particulate phases. That makes the partitioning of oxygenated compounds of importance to better understand these processes and predict atmospheric composition, especially over the Mediterranean basin where air masses under anthropogenic and biogenic influences are mixed and the atmospheric constituents undergo intense photooxidation. The gas-particle partitioning of the semi-volatile compounds depends on several factors such as ambient conditions (temperature, humidity), the state of particles (viscosity, water content,

organic fraction concentrations, acidity, etc.), as well as the properties of the compounds themselves (solubility, vapor pressure, reactivity, etc.). This leads to differences between experimental and theoretical partitioning coefficients, which have important implications for organic aerosol modelling. However, the secondary OA (SOA) models previously mentioned have been improved in the framework of ChArMEx to consider the formation of nonvolatile organic aerosols from biogenic precursors and the viscosity of particles in order to account for deviations from ideal partitioning theory.

Among the formation pathways of secondary aerosols, nucleation is the process responsible for the formation of new nanoparticle clusters observed in a variety of environments, as opposed to the process of condensation onto preexisting particles. The processes of nucleation and early growth were found to be ubiquitous in the Mediterranean atmosphere, from coastal sites to the open Mediterranean Sea atmospheric boundary layer and free troposphere. The identification of new particle formation (NPF) precursors remains complex. A study in the eastern part of the Mediterranean basin demonstrated that the availability of SO_2 and sulfuric acid cannot explain NPF events alone. NPF were, in some cases, strongly correlated to availability of biogenic organic precursors. In coastal areas, compounds from different origins are mixed under sea/land breeze that may induce an enhanced production of condensable vapors. The large spatial extent of NPF events over the Mediterranean Sea, independent of the air mass origin, suggests the potential contribution of marine precursors to nucleation. Experiments were performed with mesocosms in the western Mediterranean basin in order to derive direct fluxes of nanoparticles formed from seawater. It was demonstrated that new particle clusters can be formed with a high formation rate from marine emissions in nontidal waters in a confined volume. The concentrations of new clusters correlate with concentration of iodine that have condensed onto larger particles. Iodine is thus a key precursor, itself dependent on the phytoplanktonic activity. Amines of biological origin are linked to the early growth of newly formed clusters. On the other hand, no correlation has been found between dimethyl sulfide (DMS) or methane sulfonic acid (MSA) or a proxy of sulfuric acid and cluster concentrations. The high level of ozone may also favor the formation of new particle clusters from iodine oxides rather than from DMS oxidation products, which might be a specificity of the region compared to other oceanic environments. However, in the southwestern part of the central basin (Lampedusa), less influenced by coastal anthropogenic activities, NPF events were associated only with Atlantic air masses with, for the most pronounced event, a signature of MSA in the accumulation mode, possibly linked to the condensation of marine biogenic vapors.

2.3 Aerosol Properties

Recent scientific progress in the observation of aerosol properties allowed a better characterization of atmospheric aerosols in the Mediterranean region over the last twenty years. Observation-based knowledge has been improved by longtime series

and intensive field campaigns using in situ airborne and spaceborne observations as described in this volume (Formenti, 2022). While historical observations and analysis of longtime series have been essential in assessing the fundamental and climate-relevant characteristics of aerosol particles, the most recent observational effort within the ChArMEx project has provided new way for integration and cross-validation of satellite products and in situ observations supporting model evaluation and constraints. We now have a reliable knowledge of the chemical composition, size distribution, scattering, absorption, and cloud-forming properties of lower and mid-tropospheric aerosols over the Mediterranean.

New particle formation events are observed at the regional scale, regardless of the air mass origin, both in the boundary layer and the free troposphere, and ultrafine particles of less than 100 nm in diameter are ubiquitous over the basin. Particle mixing and reactivity leading to new particles formation and growth are favored due to the presence of gaseous precursors, the high irradiance, and the specific boundary layer dynamic. Sulfate aerosols are abundant, and the atmosphere is generally ammonium-poor. Elemental carbon is often present in internal mixture, with important implications for optical properties. As a matter of fact, solar radiation absorption by aerosol particles is a prominent feature of the Mediterranean aerosols, as shown by new observations of the single scattering albedo of mineral dust, biomass, and fossil fuel burning aerosols. The development of novel instrumentation has allowed significant progress in measuring the capability of lower-troposphere aerosol particles, mostly mineral dust and biological carbonaceous particles, to act as ice nuclei (IN). Numerous new measurements of cloud condensation nuclei (CCN) for chemically resolved particles have also become available.

Finally, a key result was highlighted, thanks to the recent ChArMEx experiment, showing the conservation of a very coarse mode of mineral dust aerosols during the transport above the Mediterranean basin regardless of transport time after emission. Dust particles as large as 30 μm were detected in lofted layers in the free troposphere. The results of drifting balloon measurements in the Mediterranean are consistent with airborne observations in elevated layers across the North Atlantic and are, therefore, suggestive of a universal mechanism, possibly involving internal turbulence, strong thermal inversions, and/or electrical processes, counteracting and preventing size-dependent sedimentation of large desert dust particles.

2.4 Atmospheric Deposition

Atmospheric deposition, one of the largest processes through which atmospheric composition impacts ecosystems, is reviewed in this volume for the Mediterranean region (Desboeufs, 2022). Dry and wet deposition constitute a major external source of nutrients and contaminants for Mediterranean terrestrial and marine ecosystems. Historical measurements dating back to the 1960s and the recent unprecedented effort conducted in the framework of ChArMEx to operate a network of several stations in the western Mediterranean to measure weekly total deposition fluxes over

several years have provided a realistic picture of the dust deposition in the Mediterranean basin. Mineral dust, which controls annual to short-term aerosol mass deposition fluxes in this region, was specifically studied. Long-term simulations point out an important interannual variability of dust deposition and no significant trend in the southern part of the basin. However, long-term direct dust (insoluble mass) or Al deposition measurements in the northwestern Mediterranean indicate an order of magnitude decrease in the deposition fluxes in the 2010s compared to the 1980s.

The importance of atmospheric deposition for the biogeochemical cycling of N and P in the Mediterranean spurred several longtime series of nutrient deposition measurements across the basin, some of which are 30 years long. The results demonstrate no clear long-term trend for P but a decreasing trend for dissolved inorganic nitrogen fluxes possibly associated with the anthropogenic emission mitigation. However, it is difficult to analyze long-term trends due to the uncertainties in N measurements. The usual devices to measure N deposition still neglect the gaseous part of nitrogen by dry deposition (in particular of NO_x), which could significantly contribute to the atmospheric input of N in the Mediterranean system. Moreover, although the contribution of organic forms is often similar to, or even higher than, the inorganic fraction in the totally deposited amounts of both N and P, the lack of relevant data constitutes another factor that greatly increases the uncertainties and hinders our knowledge of the nitrogen and phosphorus cycles in this region. A high interannual variability has been observed in N and P fluxes at all Mediterranean sampling locations. This variability is mainly linked to the frequency of both dust intrusion and precipitation events. The spatial variability of nutrient fluxes is related to the presence of potential anthropogenic sources with no clear north-south or longitudinal gradient observed. The variability between measurement sites is usually related to the vicinity of local anthropogenic sources or to arrival of anthropogenically influenced air masses. The temporal dynamics of marine N and P concentrations since 1985 show a high sensitivity to atmospheric deposition of anthropogenic compounds and are expected to decline in the coming decades due to pollutant emissions control and mitigation.

Atmospheric deposition also brings traces of heavy metals and organic contaminants to the Mediterranean waters. Recent studies used statistical methods to address the source apportionment of deposited metals. They generally show that anthropogenic sources dominate the deposition fluxes of trace and heavy metals, although atmospheric mineral dust deposition during strong desert dust events contributes strongly to the deposition fluxes of elements such as silicon, titanium, aluminum, iron, and nickel in a lesser extent. Atmospheric metal fluxes are typically too low to have a toxicological impact on the Mediterranean marine biosphere. Organic contaminants show low deposition fluxes due to the air-sea equilibrium and degradation processes in the water column and, hence, may only have a small impact on marine ecosystems.

2.5 Impacts

Air pollutant impacts on weather and climate, human health, and marine and terrestrial ecosystems in the Mediterranean region are finally reviewed in this volume (Kanakidou, 2022a; Kanakidou, 2022b). Aerosol particles and tropospheric ozone are both short-lived pollutants and radiative forcers with direct and indirect radiative forcing of paramount importance to climate. Tropospheric ozone is both an important reactive (oxidative) air pollutant and the third most important greenhouse gas after CO_2 and CH_4, while most atmospheric particles, except the absorbing ones (namely, black, brown carbon, and mineral dust), exert a cooling effect to the atmosphere, i.e., an opposite effect to that of the greenhouse gases. However, the ultrafine fraction, too small to interfere directly with shortwave radiation, might impact the budget of greenhouse gases and their vertical distribution via aerosol cloud interactions, e.g., by increasing cloud droplet evaporation in mid elevations of the troposphere. This effect also contributes to the latent heat energy budget.

Tropospheric ozone radiative effect is the strongest in the eastern Mediterranean during the summer ozone concentration maximum, which is primarily driven by meteorological conditions that favor long-range transport to the region, low precipitation, and intensive photochemistry. The contribution of anthropogenic emissions to tropospheric ozone formation is the greatest in winter resulting in high anthropogenic radiative forcing of tropospheric ozone.

At the basin scale, the annual mean direct forcing by coarse and fine atmospheric particles is larger than the effect of greenhouse gases but with an opposite sign. As a result, the observed decrease in sulfate aerosol due to the enforcement of clean air policies in Europe that is beneficial for air quality and human health led to about 20%–25% increase in the surface warming in the Euro-Mediterranean region between 1980 and 2012. Aerosols can strongly modulate both the net shortwave and longwave radiation fluxes reaching the surface in the Mediterranean basin, by scattering and absorbing solar and infrared radiations. For large particles, as is the case of mineral dust, the warming from the absorption of longwave radiation can partially offset the cooling from scattering of the shortwave radiation, as seen at Lampedusa where the longwave forcing has been shown to offset about 50% of the shortwave forcing at the surface during desert dust events. Furthermore, over the Mediterranean region, absorption of radiation by aerosol particles within the troposphere provides a key contribution to the regional direct radiative impact of aerosols and affects atmospheric heating rates and stability. For absorbing aerosols including mineral dust, radiative forcing at the top of the atmosphere is generally much smaller than the forcing at the surface, and it is negative. For some extremely absorbing mixed dust and carbonaceous particles, however, models simulate positive values of the direct forcing at the top of the atmosphere (note that the albedo can significantly impact the forcing over bright surfaces such as clouds and deserts).

The surface solar radiation (SSR) controls the heating rates and surface energy balance, the meteorological and climatic conditions, the diurnal and seasonal temperature variations, the water cycle, the plant photosynthesis, and the carbon cycle.

It is therefore important for life on Earth. Large heterogeneities are found in the amount and trends in SSR that partially reflect differences in the amount, seasonality, and year-to-year variability of aerosol loads, water vapor, and clouds presence over the various parts of the Mediterranean.

Aerosols have been shown to be able to significantly reduce UV irradiance in the Mediterranean. Their impact on the Mediterranean is thus a relevant question due to the presence of persistent, occasionally high loads of aerosols over the area together with high concentrations of tropospheric ozone. Experimental studies have shown strong impacts of aerosol on two key photolysis rates, that of O_3 to singlet oxygen (O^1D) and of NO_2, respectively, leading to O_3 loss and O_3 formation. Long-term observations at Finokalia (Crete) revealed a reduction of −6% in both photolysis rates at low aerosol load and a larger reduction of −30% to −40% for aerosol optical depth exceeding 0.5. Including the aerosol effects on photolysis rates in models reduces both the production and the destruction of tropospheric ozone, by reducing the photolysis of NO_2 and of O_3, respectively, resulting in a relatively weak net effect of aerosols on O_3 concentrations.

Extinction of radiation by aerosols impacts the photovoltaic energy production (PV) in the Mediterranean. The brightening trend observed in Europe since 1980 in relation to the implementation of air-quality policies could potentially have increased PV production by more than 10% in the lifetime of a power plant. On a shorter timescale, however, aerosol outbreaks causing high aerosol optical depth (dust, biomass burning, etc.) can lead to drastic reduction of PV production. In the Sahel zone, the reduction of PV production due to aerosols can approach 50% under extreme events, like dust storms. Similarly, in the western Mediterranean, extreme aerosol loadings caused by dust and smoke have decreased PV daily yield by 34% and 5%, respectively. In Romania, volcanic ashes, desert dust, biomass burning, and urban aerosols are found responsible for a loss of around 20% in PV energy production. Accumulation of dust after deposition over the optical surfaces (soiling effect) also affects transmission and reflection of solar irradiance, reducing the PV electricity production. The impact of soiling on a PV power plant depends on the dust properties, the frequency of different dust episodes, the rain events, and the tilt of the panels. Finer particles have large specific surface areas, meaning that when they are deposited on the panels, energy loss is higher in comparison to the same mass concentration of larger particles. Future projections do not always agree on the impact of aerosol on PV productivity. However, the most recent studies using regional climate models accounting for evolving aerosols simulated a summertime increase in future PV potential in central and eastern Europe by up to +10%.

In addition to their direct effects on solar and terrestrial radiations, aerosols also affect climate and weather through their impact on cloud formation and properties via radiative and microphysical mechanisms. In particular, aerosols modify cloud droplet and ice particle number concentrations and cloud albedo with consequences for precipitation. Over the Mediterranean basin, different aerosol types, namely, dust, sea-salt, bioaerosols, and anthropogenic aerosols contribute to the formation of cloud condensation and ice nucleating particles, thus modifying cloud properties. Furthermore, absorbing aerosols frequently present in the Mediterranean

atmosphere, with biomass burning aerosol as a major contributor, are modifying atmospheric dynamics and cloud cover, thus impacting regional climate, the so-called semi-direct aerosol effect. Despite the large uncertainties in the current parameterizations of aerosol impact on cloud microphysics, aerosol-cloud interactions have been shown an important component to be considered in the regional climate simulations. Keeping in mind the large uncertainties associated with these simulations, larger impacts on the average radiative budget over the Mediterranean are found from the direct and semi-direct effects than from the cloud-albedo indirect effect.

Aerosols also have diverse impacts on atmospheric and precipitation chemistry. Their surfaces serve as substrates for heterogeneous reactions that affect reactive nitrogen species and subsequently atmospheric oxidant levels, sulfur dioxide oxidation in the atmosphere, atmospheric acidity, and secondary organic aerosol formation. Atmospheric acidity of aerosol water, cloud water, and precipitation is driving solubilization of nutrients and/or toxic metals present in aerosols and, overall, precipitation chemistry. Because of the challenges in measuring aerosol acidity, this parameter is inferred from observations of aerosol chemical composition, relative humidity, temperature, and thermodynamic modelling. Studies have shown that aerosol acidity exhibits significant regional and temporal variability that also depends on aerosol size. Indeed, the size dependence of aerosol acidity is considerable with the fine aerosol being strongly acidic, particularly in the absence of biomass burning, and the coarse aerosol demonstrating larger pH values by about 2 pH units. Therefore, evaluation of the aerosol impacts requires a comprehensive understanding of the variations of pH and liquid water content across particle size.

During transport in the atmosphere, aerosol particles are chemically processed resulting in conversion of insoluble minerals to soluble nutrients (or toxic components) that are then entering into the ecosystems following the atmospheric deposition of aerosols. Thus, key properties of atmospheric aerosols that affect the ecosystems and human health are changing during physicochemical aging of aerosols in the Mediterranean atmosphere, where dust and acids are mixed. Atmospheric deposition of soluble material is important because of the stimulation of ecosystem growth and carbon sequestration. At the same time, soluble metal species can have a significant negative impact on human health. Therefore, our understanding of the aerosol aging processes and impacts of soluble material availability needs to be improved and quantified by integrating them into Earth system modelling. Understanding of interactions between aerosol, chemical aging, and chemical composition of deposition is critical to fully appreciate the broader impacts of human activities on people, ecosystems, and climate throughout the Mediterranean.

Adverse health effects in various human organs have been associated with exposure to air pollution in the Mediterranean region, even at low concentrations of air pollutants. The improvement of the accuracy of air pollution exposure assessment over recent decades has enabled the acquisition of spatiotemporal exposure values at the individual level. Therefore, in the Mediterranean, significant associations between particulate matter (PM) load and increased all-cause mortality have been found by several studies with the biggest toll on the elderly. Evidence for

associations between PM levels in the atmosphere and hospitalizations has been provided by several studies in the Mediterranean region, for instance, in Lebanon, Cyprus, Greece, Italy, and Spain. Older people (>75 years) show also higher susceptibility than younger people to high atmospheric PM loadings, especially when combined with warm weather. Studies also show that the size of PM is mainly driving the health effects of PM, fine particles having larger adverse effects on diabetes, cardiac diseases, cerebrovascular diseases, lower respiratory tract infections (LRTI), and chronic obstructive pulmonary disease (COPD).

The relationship between particulate chemical composition and hospitalizations and mortality has also been investigated over a period of 10 years (2003–2013) in several large Spanish and Italian cities. Increased hospital admissions were associated with the increased presence of various chemical species in aerosol particles such as elemental carbon (EC), SO_4^{2-}, SiO_2, Ca, Fe, Zn, Cu, Ti, Mn, V, and Ni. For instance, EC, a product of combustion processes, increased risks of mortality and hospitalizations by up to 3% for one interquartile increase in its concentration. SO_4^{2-} increased respiratory mortality and hospitalizations and cardiovascular hospitalizations. Metals contained in atmospheric particles were also pointed to cause health effects. SiO_2, Ca, Fe, and Ti that have a mineral origin and are associated either with road or desert dust had strong health effects in all studied cities. Ni and V, commonly linked to the combustion of fuel oil, increased respiratory hospital admissions, and in particular, Ni increased respiratory mortality. Note, however, the fact that presence of some of the health-damaging constituents was highly correlated, prohibiting the identification of the exact responsible pollutant. Exposure to gaseous pollutants was also studied in several European cities, and significant positive correlations were found between daily deaths and both exposure to NO_2 and O_3. For cardiovascular mortality, this association was higher for southern Europe in agreement with previous findings that showed a synergistic effect of O_3 and temperature on cardiovascular mortality.

Despite the European policies on clean air and the decrease of some atmospheric pollutant levels during past decades, the regulatory limit values for heath are still often exceeded, and little or no change in the overall toxicity of the air pollution has been found in Rome from 17 years of data. In addition, socioeconomic conditions together with stress, smoking, and neighborhood factors (traffic proximity) may have a direct effect on exposure to poor air quality. Such issues persist over time and must be adequately addressed by the society. In addition to human health, air pollution jointly with climate change also affects ecosystems. Climate change impacts the ocean-atmosphere exchange especially through a change of the surface water stratification and, as consequence, the ocean fertilization by atmospheric species. Models predict that open Mediterranean surface seawater pH could decrease by up to about 0.3 pH unit by the end of the century due to ocean uptake of the atmospheric CO_2, leading to a change in atmospheric nutrient availability as consequence of the potential increase in their solubility. On the other hand, predictions for atmospheric aerosol pH and precipitation show a potential decrease in atmospheric acidity (i.e., increase in pH), following the observed trend of the recent years, thus leading to smaller differences in acidity between the atmospheric inputs and the

surface seawater. Future changes in atmospheric inputs of the main nutrients could affect the functioning of the Mediterranean ecosystem through modification of the plankton assemblages with possible consequences for higher trophic levels. A 1-month oceanographic cruise (PEACETIME) that combined in situ observation of the atmospheric chemical composition and process studies was set up in spring 2017 to go further in our understanding of processes at the air-sea interface in the western and central Mediterranean. An African dust wet deposition event could be targeted by the research vessel between Baleares and Algeria and monitored in both air and sea (Guieu et al., 2020), and the water column was also sampled a few days after another high dust deposition event in the Tyrrhenian Sea. Both events were associated with different behaviors of marine Al and Fe (Bressac et al., 2021).

Nutrients and toxic compounds are also provided through atmospheric deposition to the continental vegetation via either direct uptake by the foliage or by indirect uptake through plants' roots. Impacts of air pollution on vegetation are either direct or indirect. Direct impacts occur through (i) phytotoxicity resulting from ozone, sulfur, nitrogen, and other pollutants stomatal and non-stomatal uptake by the plants, (ii) nutrient balance modification by atmospheric deposition, (iii) transfer of plant diseases by aerosols, and (iv) pollution by metals and persistent pollutants. Indirect impacts occur through changes in the physical state of the atmosphere and changes in ambient temperature and relative humidity as well as in the diffuse solar radiation that reaches vegetation (impacted by greenhouse gases and aerosols). Air pollution leads to visible and invisible damages of terrestrial vegetation. Exposure to air pollutants, especially to high O_3, have been observed to reduce crop yields, thus agriculture's ability to feed the Earth's population. The evaluation of the impact of air pollution on the Mediterranean vegetation requires consideration of plant phenology, functional type, and the seasonality of O_3. Various stress factors, in particular climate (temperature, droughts, and other extremes) and air pollution (O_3, aerosol), have combined effects on vegetation. Understanding these effects is a prerequisite for the definition of actions to preserve biodiversity and sustain agricultural production.

It is noticeable that long-term effects on vegetation and soil, induced by pollutants accumulation, require long periods of recovery after the accumulation has stopped. Nitrogen accumulation in excess of the optimal ecosystem levels in the soils, induced by atmospheric deposition, implies soil acidification and leads to change in the composition of phytocommunities and biodiversity reduction. Exposure of plants to excessively high nitrogen levels in the soil resulting from deposition of anthropogenic reactive nitrogen has been found to induce changes in nutrient stoichiometry in the plants. This imbalance in N and P deposition has been observed to result in phosphorus limitation of ecosystems in Europe and the Mediterranean, as also found elsewhere, for instance, in China's forests and in Alpine lakes. Such alterations of the available nutrient balance induced by air pollution impact vegetation and must be carefully examined, particularly under conditions of climate change that is potentially increasing the occurrence of severe drought events and exacerbates the impacts of air pollution on vegetation.

3 Main Recommendations

In this subchapter, we issue several recommendations for future research on natural and anthropogenic source identification and apportionment, atmospheric processes, aerosols properties, as well as research strategies for the mitigation of air pollution impacts in the Mediterranean region.

3.1 Safeguard the Regional Integration of the Mediterranean Scientific Community

Five ChArMEx international workshops were held in France, Spain, Italy, and Cyprus from 2009 to 2016, gathering between about 60 and 90 participants from up to 19 countries at a time. The sixth one to be held in Greece in fall 2019 was cancelled for funding reasons, and we suggest supporting a new workshop, possibly jointly organized with other more recent projects in the eastern basin such as A-LIFE, AQABA, EMME-CARE, EXCELSIOR, PANACEA, etc., in order to encourage further international scientific cooperation on atmospheric chemistry and its impacts in the region.

3.2 Improve Emission Data

Improve our Knowledge of Natural Emission Sources

Mesoscale models are unable to reproduce the number concentrations of aerosol particles in the marine boundary layer and their impact on cloud properties. Large uncertainties in the projection of future climate can be attributed to a lack of knowledge on marine aerosols. In the Mediterranean area, the marine aerosol emission pathways may be different from those in other parts of the world due to the specific temperature range and oligotrophic properties of the seawater, and high radiation and ozone levels in the atmosphere, which lead to intense photochemical activity throughout the year. Furthermore, the Mediterranean Sea receives a large amount of radiation, with effects on emissions which are largely unknown. Hence, future research should be the focus on sea spray aerosol emissions. Further experiments have to be designed to study marine emission pathways under specific Mediterranean conditions.

We still miss measurements to characterize Biogenic Volatile Organic Compounds (BVOC) emissions and chemistry. There are still plenty of Mediterranean species which are poorly investigated, and we recommend extending measurements to a larger number of plant species. Although emissions from bare soil are very low, VOC emissions from the litter may also need to be considered. More flux measurements are needed to better characterize this source and enable its implementation in

emission models. Airborne measurements can be recommended in the Mediterranean area for a good representation of BVOCs emissions at the landscape scale. Our capability to correctly assess the impact of drought on VOC emission inventories is especially crucial for regions like the Mediterranean, that are covered with a large quantity of strong VOC emitters and that experience frequent drought episodes. We still need more data (1) to refine our knowledge on drought effects on BVOC emissions and (2) to parameterize and validate empirical approaches over a broader range of environmental stress conditions and of emitters. Therefore, we recommend expanding field experiments, like the one performed recently at the Oak Observatory at Observatoire de Haute-Provence (O3HP) in southern France with a controlled reduction of natural precipitation received, to other Mediterranean ecosystems to better understand their responses to climate change. All these improvements in BVOC emission characterization will help as well to improve modelling of the secondary species (ozone, secondary organic aerosols) and to better assess biosphere-atmosphere interactions in the context of regional climate change.

A more systematic identification of the source regions of mineral dusts should be performed in a context of semiarid area evolution under climate change. The improvement of remote sensing techniques and meteorological data analysis together with chemical and mineralogical approaches provides efficient tools for mineral dust source identification.

Improve Anthropogenic Air Pollutant Emission Inventories

Anthropogenic emission inventories are still associated with large uncertainties. There is a need for highly spatially and temporally resolved local emission inventories that consider Mediterranean region heterogeneities in terms of environment, level of technology, and regulations. Harmonized methodology and quality assurance/quality control of the inventories are recommended to maintain a minimum level of reliability. Evaluation of emission inventories must be performed using chemical-transport modelling as well as remote sensing and in situ measurements. Sustained projects like TRANSEMED or EMME-CARE are much needed especially in the southern part of the basin to favor collaborations with decision-makers with the help of the northern countries to enhance policy making related to emission regulations and the future of the atmospheric environment in the Mediterranean basin.

3.3 Better Evaluate Ozone Production and Characterize Impacts

Study the Atmospheric Oxidant Budget

For a complete understanding of OH reactivity and budget in the Mediterranean basin, measurements of the missing reactivity in different natural and anthropogenic environments and seasons are needed together with a complete speciation of the

gaseous phase. That would allow the identification of unmeasured compounds leading to a significant missing OH reactivity, to better constraining the OH budget and estimate the O_3 production potential, as well as to compare total reactivity derived from atmospheric chemistry models and from measurements.

Study the Impact of Ozone Forcing on Atmospheric Dynamics and Chemistry and the Future Evolution of Ozone

Further research is needed to understand the impact of strong regional forcing due to tropospheric ozone on the regional atmospheric dynamics and chemistry, including how high ozone and OH production interacts with other pollutants. Ozone levels and derived ozone net production rates should be considered as an important observational constraint for numerical chemistry-transport modelling studies. A better understanding of ozone chemistry should improve air-quality models and forecasts around the Mediterranean basin. This is important in a context of changing climate and emissions that will affect regional ozone levels. Studies should also focus on how effective future emission reduction scenarios will be for decreasing tropospheric ozone in the Mediterranean basin, contrasting the projected changes in climate, which may further increase ozone production and counteract mitigation measures.

3.4 Conduct Multiparametric Investigations of Aerosols

Improve the Understanding of Secondary Aerosol Formation Processes

The mechanisms leading to formation of secondary aerosols are complex, nonlinear, and still not fully understood. Therefore, there is a need for long-term monitoring of the aerosol precursors both organic and inorganics, together with the composition of the aerosol, in particular of its finest fraction.

The measurement of the concentration of nanometric particles, simultaneously with potential precursor gases of low volatility, is a prerequisite to understand the contribution from the different sources (marine, anthropogenic, vegetation, or a combined effect of different sources) to the process of nucleation. More modelling studies on nucleation in the Mediterranean atmosphere will help in testing different hypotheses for potential nucleating species in such an environment.

Document and Model the Gas-Particle Partitioning and Aerosol Surface Reactions

An accurate representation of the gas-particle partitioning is required to better characterize aerosol concentrations. The study of experimental partitioning coefficients should be carried on in various types of environments and systematically compared

to theoretical ones considering thermodynamic and aerosol mixing state. Moreover, hypotheses of multilayer particles of various viscosities and/or phases or reactivity in the particulate phase should be investigated by comparing measurements and simulations.

While reactions at the surface of dust and sea-salt aerosol particles have been reasonably well documented by laboratory and field studies over the past decades, they are not routinely integrated in atmospheric modelling owing to difficulties regarding the treatment, model setup (e.g., emissions), and computational expense associated with the rigorous representation of size-segregated aerosol composition and processes. Furthermore, the uncertainty associated with studying size-resolved processes in the laboratory and field poses additional and worth addressing challenges.

Improve Understanding of Relationships between Aerosol Composition and Optical Properties

Assessment of the chemical composition, particle size distribution, optical and hygroscopic properties of particles, and their mixtures needs to be combined in "closure" studies, including inverse methods and numerical modelling.

A better assessment of the aerosol spectral single scattering albedo is needed, especially for biomass burning particles, based on observations from satellites and both in situ at the surface and airborne platforms, to encompass the limitations of columnar data. The effect of the mixing state (external and/or internal) of absorbing aerosols (urban/industrial black carbon, biomass burning, and even mineral dust) should be better understood and parameterized.

Use Satellite Observations to Broaden Perspective on Aerosol Spatial and Temporal Variabilities

An advanced use of new satellite observations is crucial to improve the regional, seasonal, annual, and long-term description of aerosol parameters. This is especially true for the aerosol size distribution which is measured during field campaigns, limited in scope and time, and retrieved at fixed, distributed but relatively sparse AERONET sites that provide column averages. A broader picture, including seasonality of the aerosol size distribution, is needed, and it would require advanced analysis of spaceborne products beyond the column-averaged aerosol Angström exponent or the effective aerosol diameter.

Perform New Laboratory Studies that Simulate the Mediterranean Atmosphere in Addition to Field Experiments, to Investigate Aerosol Particle Reactivity and Evolution

The reactivity of aerosol particles in air masses relevant to Mediterranean conditions should be investigated. Field observations of particle aging due to surface reactivity and gas-phase uptake are complex in the real environment where the initial state of the air mass is unknown. Traditional laboratory experiments have been performed on single species (both in the aerosol and gas phase). We recommend that new laboratory studies simulating the Mediterranean atmosphere should be performed in flow tubes and large-scale reactors to investigate the reactivity as well as its induced changes in the particle optical and hygroscopic properties.

The new generation of fast measuring techniques needs to be applied in chamber and field experiments that include nocturnal conditions and the detection of more comprehensive sets of species within both gaseous and particulate phases. These should provide information on SOA formation and primary carbonaceous aerosol aging as well as on the properties of the resulting aged aerosols in the atmosphere. Such information is needed to improve model simulations of fine atmospheric aerosols.

Investigate the Connection between the Concentration of Cloud Condensation Nuclei (CCN) and the Cloud Droplet Number Concentration

A better connection between the concentration of CCN particles and the ambient cloud droplet number concentration should be sought. That would improve the quantification of precipitation from shallow convection and more generally foster our understanding of the processes and feedbacks in the aerosol-cloud-climate system for the improvement of climate models in the Mediterranean region.

Investigate the Chemical Speciation of Particles Serving as Ice Nuclei by Combining Field and Laboratory Experiments

The chemical speciation of particles serving as ice nuclei and the extent to which anthropogenic aerosols can play a role in ice cloud formation are still open questions. Combined field experiments and targeted laboratory investigations should be designed.

UFP are suspected to strongly impact climate through aerosol-cloud interactions. Increasing emissions of UFP have likely contributed to the observed modification of rainfall patterns in the region within the last decades. There is also experimental evidence that in other areas with reported exceptional rainfall deficiencies, the number concentrations of UFP were enhanced in a similar way to the Mediterranean and that rainfall decline timely correlates with an increase in ultrafine particles. There is therefore a need for observations of this aerosol fraction and further sophisticated

climate modelling of its impacts with updated primary emission inputs as well as detailed physical characteristics of aerosols and clouds.

Enlarge the Bioaerosol Measurement Network

Bioaerosols is an emerging important topic due to its potential impact on human health and on climate. The situation is contrasted. While pollen measurements are routinely performed in the western part of the Mediterranean basin, the eastern part is much less documented. In addition, measurements of fungal spores and bacteria are still very scarce in the whole basin. Therefore, current efforts to extend the bioaerosol measurement network should be encouraged, in parallel with the implementation of bioaerosols in regional models.

3.5 Pursue the Monitoring of Atmospheric Deposition to Better Constrain Models

Evaluate the Contribution of Aerosol Particle Types to the Total Mass Deposition

Long-term simulations and observations of mineral dust deposition fluxes since the 1980s do not seem to agree on trends. Simulations point out an important interannual variability of dust deposition and no overall trend, whereas measurements indicate a strong decrease in dust deposition. This illustrates the need to pursue a combined monitoring of both atmospheric dust load and deposition. These direct observations and model simulations must be better combined to document a possible evolution in the Mediterranean region. The estimation of the relative contribution of the different aerosol particles to the total mass deposition in the Mediterranean requires joint studies of air mass trajectories and chemical composition of the deposition. Deposition fluxes can provide an improved constraint to the dust transport models compared to the current validation by surface PM concentrations and aerosol optical depth. This will allow a more accurate computing of the desert dust mass budget and associated transfers of chemical elements from arid areas to the marine and terrestrial ecosystems of the Mediterranean basin.

Reinforce Long-Term Measurements of Nutrient Deposition over the Basin

The regulation of pollutant emissions from anthropogenic activities could be a key driver affecting the Mediterranean oligotrophic seawater nutrient cycles and hence the marine ecosystem in the future. Moreover, atmospheric trace metal sources and ecosystem impacts need to be better understood to provide high-quality projections in a context of future changes. Modelling is the optimal method to differentiate

spatial and temporal variations of anthropogenic deposition. However, the model quantification of the atmospheric nutrient deposition over the Mediterranean basin has still to be considered with caution. Aerosol and dust atmospheric transport and deposition simulations differ widely from model to model regarding the total mass of nutrient deposition as well as its spatial and temporal patterns. The observational time series are spatially spotty and tend to exist for relatively short time periods (a few years at best). We underline the need for more long-term deposition measurements in order to better constrain the modelling of important nutrient sources for the Mediterranean.

Better Represent Spatial and Temporal Variabilities of Trace Metal and Organic Contaminant Deposition

Due to their environmental impact, emissions of metals and organic contaminants have been targeted by different regulations in Europe. Similar regulations are underway in North Africa. In the near future, fluxes of metals could decrease by orders of magnitude so that they would not anymore represent a contamination source. But atmospheric fluxes of some trace metals might become too low to support the needs of ecosystems. Moreover, due to climate change, the Mediterranean is expected to experience a dryer and warmer climate that could impact the soluble (bioavailable) inputs of metals by wet deposition. Thus, the future evolution of the atmospheric trace metals sources and deposition in a changing climate should be investigated. The limited available deposition observations do not enable us to observe and quantify the potential impact of emission regulations on the atmospheric deposition fluxes of metals and organic contaminants. We still lack information on the recent deposition fluxes of metals as well as on the spatial distribution of these fluxes. Current monitoring sites are also not equipped enough to documents emerging contaminants. For organic contaminants, the deposition measurements are often limited to one or two studies for each persistent organic pollutant or associated pollutants. In addition, most deposition measurements are carried out at coastal sites, where local or regional contamination is often present. We thus recommend increasing representative measurements of atmospheric concentrations and wet deposition of these compounds in isolated islands and during oceanographic cruises in remote waters of the Mediterranean basin.

Further Investigate New Emerging Organic Contaminants

New emerging organic contaminants, including flame retardants, perfluoroalkyl substances, surfactants, personal care products, and pharmaceutical compounds, have been identified and could prove to be problematic for marine ecosystems in the coming years but have received little consideration yet. In addition, phosphorus is a limiting nutrient in the oligotrophic Mediterranean Sea. The contribution of organophosphate esters and other potential families of organic compounds containing P as

a source of phosphorus could be a relevant aspect of the atmospheric deposition of organic chemicals in the Mediterranean Sea. The studies of these emerging and P-rich contaminants are also key to estimate the effect of atmospheric deposition on marine biogeochemistry.

Provide more Robust Data of Nitrogenous and Phosphorus Compound Deposition

It is difficult to analyze long-term trends of nitrogen (N) deposition due to the uncertainties in its measurements. The usual devices to measure N deposition still neglect the gaseous part of its dry deposition, which could be a significant form of atmospheric input of N in Mediterranean systems. The synopsis of survey data is complicated by a strong dependence of the results on sampling and analytical methods. Hence, we encourage the use of common procedures for total deposition sampling between the different longtime series sites, as it is the case of the harmonized method for monitoring of air pollution effects on European forests (http://icp-forests.net/; last access 20 July 2022).

Recent efforts to estimate the deposition of organic forms of nitrogen (N) and phosphorus (P) have shown that it is often similar to, or even higher than, the inorganic fraction in the total deposition, both for N and P. Despite this evidence, data are still fragmented. Moreover, the exact source of these organic forms remains unknown. The lack of data constitutes a great source of uncertainties and hinders our knowledge of the nitrogen and phosphorus cycles in this region. Efforts to better characterize the organic fraction in the total deposition of N and P need to be continued.

3.6 Further Study the Impacts of the Aerosol Direct and Indirect Radiative Forcing

Include the Impact of Longwave Direct Radiative Forcing in Regional Climate Modelling

The direct radiative forcing exerted by desert aerosols in the longwave spectral range has been demonstrated locally. Further studies for quantifying this effect must be carried out at the regional scale.

Study the Impact of Aerosol Direct Radiative Forcing Using Coupled Atmosphere-Ocean Models

It appears crucial to investigate more deeply the impact of the direct radiative effect of aerosols over both continental and marine surfaces on the Mediterranean climate. The yearly-mean direct aerosol radiative forcing at the surface ranges from −10 to

−30 W m^{-2} over the Mediterranean basin. This direct radiative effect impacts humidity fluxes between the sea and the atmosphere and more largely the hydrological cycle. For this, coupled atmosphere-ocean models are necessary because they can account for changes in sea surface temperature and evaporation due to the aerosol dimming at the surface.

Study the Impact of Absorbing Aerosols

A lot of studies report important differences between the surface and the top of atmosphere (TOA) direct forcing, indicating that an important part of solar radiation is absorbed within absorbing aerosol layers (anthropogenic, mineral dust, and smoke, typically) heating the atmosphere. The yearly-mean atmospheric forcing due to anthropogenic particles can reach as high as 5–10 W m^{-2} over the Mediterranean basin. In that context, more mesoscale and RCM simulations are needed to quantify at different timescale, the semi-direct effect of natural/anthropogenic aerosols on the thermodynamic properties of the atmosphere, and the circulation at regional scale.

In-depth investigation of the link between the aerosol direct forcing and some characteristics of the Mediterranean heat waves (intensity, duration), especially for mineral dust and anthropogenic particles, which absorb solar radiation, should also be a priority for future research given the expected regional climate change and demonstrated positive aerosol feedback on heat waves.

It would also be interesting to study the effects of aerosol radiative forcing on air quality through the possible impact of heating by absorbing aerosols on the boundary layer development and mixing.

Study the Impact of Aerosol Radiative Impacts on Photovoltaic Production

The aerosol radiative impact on photovoltaic production is an issue of recent concern, especially driven by the need of energy production and distribution networks to have accurate forecasts of the daily production yield. More studies dedicated to the impact of aerosols on solar energy production (by both reduction of surface solar radiations and wet/dry deposition) are needed in the context of the energy transition toward renewable energy sources, especially over the southern Mediterranean and islands.

Study the Impact on Marine Productivity of Surface Solar Irradiance Modification Due to Aerosol Dimming

Although estimations of the surface radiative forcing over the Mediterranean Sea are scarce at this time, the results presented here clearly display a non-negligible surface dimming at different locations. In regard to such surface cooling, it appears now crucial to investigate its potential impact in terms of change in regional

Mediterranean climate. First, there is a need to better quantify how does the change in solar irradiance at the sea/continental surface influence regional water cycles through modifications in evaporative, heat fluxes and SST. Secondly, since the reduction in the UV and the visible region is as large as 10% to 20%, effects on terrestrial and marine biogeochemical cycles need to be examined. It would be interesting to study how the change in solar irradiance at the sea surface influences the carbon cycle and marine biological productivity through photosynthesis changes.

Design New Field Campaigns Focused on the Characterization of Aerosol and Clouds in Different Air Masses by Combining in Situ and Remote Sensing Observations for a Better Assessment of the Regional Aerosol Indirect Radiative Forcing

More research in terms of both field experiments, laboratory studies, and modelling efforts is clearly needed to better understand and quantify the effects of aerosol on clouds and the hydrological cycle and predict future evolution of impacts. Representation of cloud microphysical processes in climate models is challenging because fundamental microphysical details are poorly understood. Although there are several parameterizations that correlate the aerosol concentration and the CCN/INP concentrations as a function of aerosol properties, too many unknowns exist to accurately predict the cloud droplet and ice crystal number concentrations. To date, in situ observations of the latter in the different cloud regimes over the Mediterranean are lacking. Calls for observations of cloud droplet and ice crystal number concentrations in the different cloud regimes have already been expressed, requesting to provide a more complete assessment of the relationship between CCN/INP concentration and cloud droplet/ice crystal number concentrations. To accomplish this, the next generation of field experiments should focus on extended characterization of aerosol and enhanced cloud observations (e.g., mixed-phase and ice clouds developing in different air masses) by combining in situ and remote sensing platforms. These observations would be extremely helpful to improve climate models over the Mediterranean and better understand the specificities of this region in terms of aerosol-cloud interactions. A key issue would be to get more statistically sound knowledge about the conditions at cloud level. One or two observation sites at elevations up to 3000 m above sea level in the central Mediterranean could improve our database significantly.

3.7 Further Assess Atmospheric Pollution Impacts in this Sensitive Region

Better Understand the Relationships between Aerosols Properties and their Impacts

Modelling the potential impacts of aerosols on atmospheric chemistry requires a comprehensive understanding of the pH and aerosol liquid water distributions across particle size. Concurrent gas and aerosol size segregated information that provides input to thermodynamic modelling can enable the documentation of the levels and variability of aerosol pH and aerosol liquid water content, until appropriate operational methods of direct observations of these aerosol properties will become available.

Key properties of aerosols that affect the ecosystems are changing during physicochemical aging of aerosols in the atmosphere. There is a need for improving the understanding of those processes and for integrating their effects into Earth system modelling.

Integrative Approaches to Take up the Health Challenge in a Changing Climate

Reduction of air pollution by limiting the emissions of gases and particles (especially diesel in cities) is a prerequisite for population's health protection. There is also a need for behavioral changes of individuals that can be guided by using intelligent applications and pollution sensors. New studies accounting for the exposome, which is the lifetime sum of all exposures, including air pollution and climate change variables, are needed to provide better constraints to the effects of several simultaneous prevention measures.

Encourage Collaboration between Experimental Scientists and Modellers from the Atmosphere and Marine Biogeochemistry

Future works dealing with the impact of atmospheric deposition in the Mediterranean Sea will improve knowledge only through strong collaboration between experimental scientists and modellers from the atmosphere and marine biogeochemistry communities. Indeed, an important perspective is to improve the representation of key processes included in models. The characterization and quantification of the processes that have to be considered (such as bacterial production and the lithogenic carbon pump) should be provided by "realistic view experiments" considering the fate of the particles, in order to allow their accurate parameterizations. Experiments should cover a large spectrum of realistic atmospheric forcing (duration, type (i.e., wet and dry), origin, and composition), marine biogeochemical conditions (variety

of organic matter, different states of nutrient limitation), and physical oceanic conditions (temperature, pH). The objective is to improve not only the quantification of current impacts of atmospheric pollution but also their evolution in the future. A great unknown remains concerning future atmospheric deposition of nutrients, both those of anthropogenic origin and especially those of Saharan origin. Here again, modelling is a necessary tool, and different future scenarios should be simulated.

Study the Impact of Various Stress Factor and their Combination on Terrestrial Vegetation

Understanding of the interaction between the various stress factors, in particular climate (temperature, droughts, and other extremes) and air pollution (O_3, aerosol, CO_2), and how these factors combined affect vegetation is critical for the definition of actions in order to preserve biodiversity and sustain agricultural production. Observatories for long-term monitoring of all compartments of the environment and key drivers of climate change and air pollution are essential to understand and evaluate the complex impacts of air pollution on vegetation. This need is urgent for the Mediterranean region due to its susceptibility to various stresses induced either by climate change or air pollution or by other expressions of human activities footprint on the environment.

References

Beekmann, M. (Coord.) (2022). Recent progress on chemical processes. In F. Dulac, S. Sauvage, & E. Hamonou (Eds.), *Atmospheric chemistry in the Mediterranean Region* (Vol. 2, From air pollutant sources to impacts, Part VI). Springer, this volume. https://doi.org/10.1007/978-3-030-82385-6

Bressac, M., Wagener, T., Leblond, N., Tovar-Sánchez, A., Ridame, C., Taillandier, V., Albani, S., Guasco, S., Dufour, A., Jacquet, S. H. M., Dulac, F., Desboeufs, K., and Guieu, C. (2021). Subsurface iron accumulation and rapid aluminum removal in the Mediterranean following African dust deposition. *Biogeosciences, 18*, 6435–6453. https://doi.org/10.5194/bg-18-6435-2021

Dayan, U. (2023). Synoptic and dynamic conditions affecting pollutant concentrations over the Mediterranean basin. In F. Dulac, S. Sauvage, & E. Hamonou, (Eds.), *Atmospheric chemistry in the mediterranean Region* (Vol. 1, Context and pollutant distribution, Part II). Springer.

Desboeufs, K. (Coord.) (2022). Deposition. In F. Dulac, S. Sauvage, & E. Hamonou (Eds.), *Atmospheric chemistry in the Mediterranean Region* (Vol. 2, From air pollutant sources to impacts, Part VIII). Springer, this volume. https://doi.org/10.1007/978-3-030-82385-6

Dulac, F. (Coord.) (2023). The Mediterranean atmospheric chemistry hotspot. In F. Dulac, S. Sauvage, & E. Hamonou (Eds.), *Atmospheric chemistry in the Mediterranean Region* (Vol. 1, Context and pollutant distribution, Part I). Springer.

Dulac, F., Sauvage, S., & Hamonou, E. (2022). *Atmospheric chemistry in the Mediterranean Region* (Vol. 2, From air pollutants sources to impacts). Springer, this volume. https://doi.org/10.1007/978-3-030-82385-6

Dulac, F., Sauvage, S., & Hamonou, E. (2023). *Atmospheric chemistry in the Mediterranean Region* (Vol.1, Context and pollutant distribution). Springer.

Formenti, P. (Coord.) (2022). Mediterranean aerosol properties. In F. Dulac, S. Sauvage, & E. Hamonou (Eds.), *Atmospheric chemistry in the Mediterranean Region* (Vol. 2, From air pollutant sources to impacts, Part VII). Springer, this volume. https://doi.org/10.1007/978-3-030-82385-6

Guieu, C., D'Ortenzio, F., Dulac, F., Taillandier, V., Doglioli, A., Petrenko, A., Barrillon, S., Mallet, M., Nabat, P., & Desboeufs, K. (2020). Introduction: Process studies at the air–sea interface after atmospheric deposition in the Mediterranean Sea – Objectives and strategy of the PEACETIME oceanographic campaign (May–June 2017). *Biogeosciences, 17*, 5563–5585. https://doi.org/10.5194/bg-17-5563-2020

Kanakidou, M. (Coord.) (2022a). Impact of air pollution on precipitation chemistry and climate. In F. Dulac, S. Sauvage, & E. Hamonou (Eds.), *Atmospheric chemistry in the Mediterranean Region* (Vol. 2, From air pollutant sources to impacts, Part IX). Springer, this volume. https://doi.org/10.1007/978-3-030-82385-6

Kanakidou, M. (Coord.) (2022b). Impact of air pollution on human health and ecosystems. In F. Dulac, S. Sauvage, & E. Hamonou (Eds.), *Atmospheric Chemistry in the Mediterranean Region* (Vol. 2, From air pollutant sources to impacts, Part X) Springer, this volume. https://doi.org/10.1007/978-3-030-82385-6

Mihalopoulos, N. (Coord.) (2023a). Aerosol concentrations and variability. In F. Dulac, S. Sauvage, & E. Hamonou (Eds.), *Atmospheric Chemistry in the Mediterranean Region* (Vol. 1, Context and pollutant distribution, Part III). Springer.

Mihalopoulos, N. (Coord.) (2023b). Reactive gas concentrations and variability. In F. Dulac, S. Sauvage, & E. Hamonou (Eds.), *Atmospheric chemistry in the Mediterranean Region* (Vol. 1, Context and pollutant distribution, Part IV). Springer.

Sartelet, K. (2022). Secondary aerosol formation and their modeling. In F. Dulac, S. Sauvage, & E. Hamonou (Eds.), Atmospheric chemistry in the Mediterranean Region (Vol. 2, From air pollutant sources to impacts). Springer, this volume. https://doi.org/10.1007/978-3-030-82385-6_10

Sauvage, S. (Coord.) (2022). Emissions and sources. In F. Dulac, S. Sauvage, & E. Hamonou (Eds.), *Atmospheric chemistry in the Mediterranean Region* (Vol. 2, From air pollutant sources to impacts, part V). Springer, this volume. https://doi.org/10.1007/978-3-030-82385-6

Appendix

Maps of ChArMEx and Related Observations in the Mediterranean

The following full-page Google Earth-based maps provide an overview of the location of ChArMEx (the Chemistry-Aerosol Mediterranean Experiment) and ChArMEx-related observations in the Mediterranean region over the period 2010–July 2020, hereafter referred to as the "ChArMEx decade". ChArMEx data are available from a dedicated database (https://mistrals.sedoo.fr/ChArMEx/). Note that some early measurements started in 2008 in Corsica as part of the preparatory phase of ChArMEx and that earlier measurements such as AERONET maritime measurements at sea, which started in 2007 in the Mediterranean, are also reported for providing an extensive view of available data in the region. The five main ChArMEx intensive field campaigns performed with airborne means in summers 2012, 2013, and 2014 at the regional scale are called Special Observation Periods (SOPs). Those figures are an annex to the introduction chapter of Vol. 1 of this book and should be referred to as Dulac et al. (2023). They include:

F. Dulac et al. (eds.), *Atmospheric Chemistry in the Mediterranean Region*,
https://doi.org/10.1007/978-3-030-82385-6

Fig. A1 Google Earth map of the AERONET sun and sky automated photometers operated in the Mediterranean region for more than two years during the ChArMEx decade. Those set up in the framework of ChArMEx are in yellow and underlined. Markers of those no more operated in July 2020 include a black diamond. Data from http://aeronet.gsfc.nasa.gov

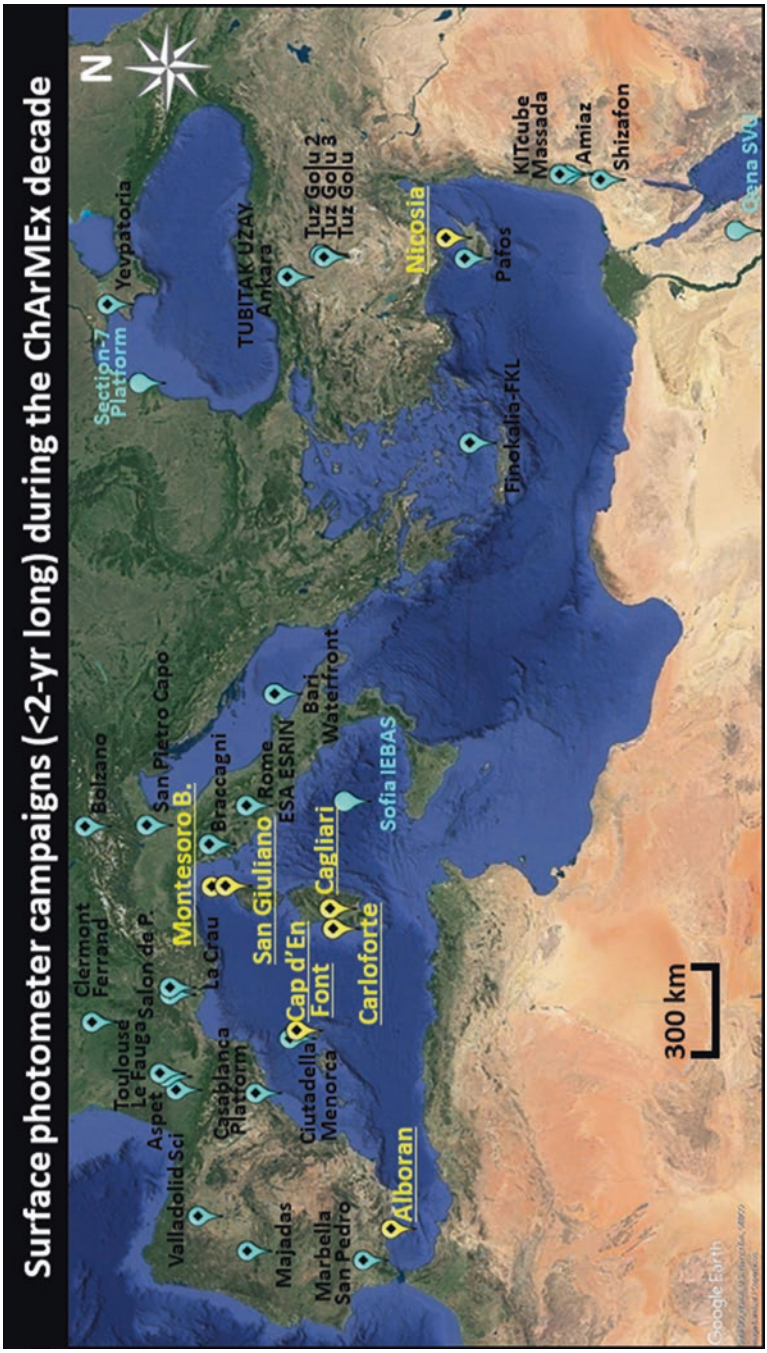

Fig. A2 Google Earth map of the AERONET sun and sky automated photometers operated in the Mediterranean during the period January 2010-July 2020 for less than 2 years. Stations in yellow and underlined are those set up in the framework of ChArMEx. Some of these sites have been set up at the end of the ChArMEx period (08/2018-12/2019) and are still operated in July 2020 (blue pins) while the others were only set-up for short periods (blue pins with a black diamond). Data from http://aeronet.gsfc.nasa.gov

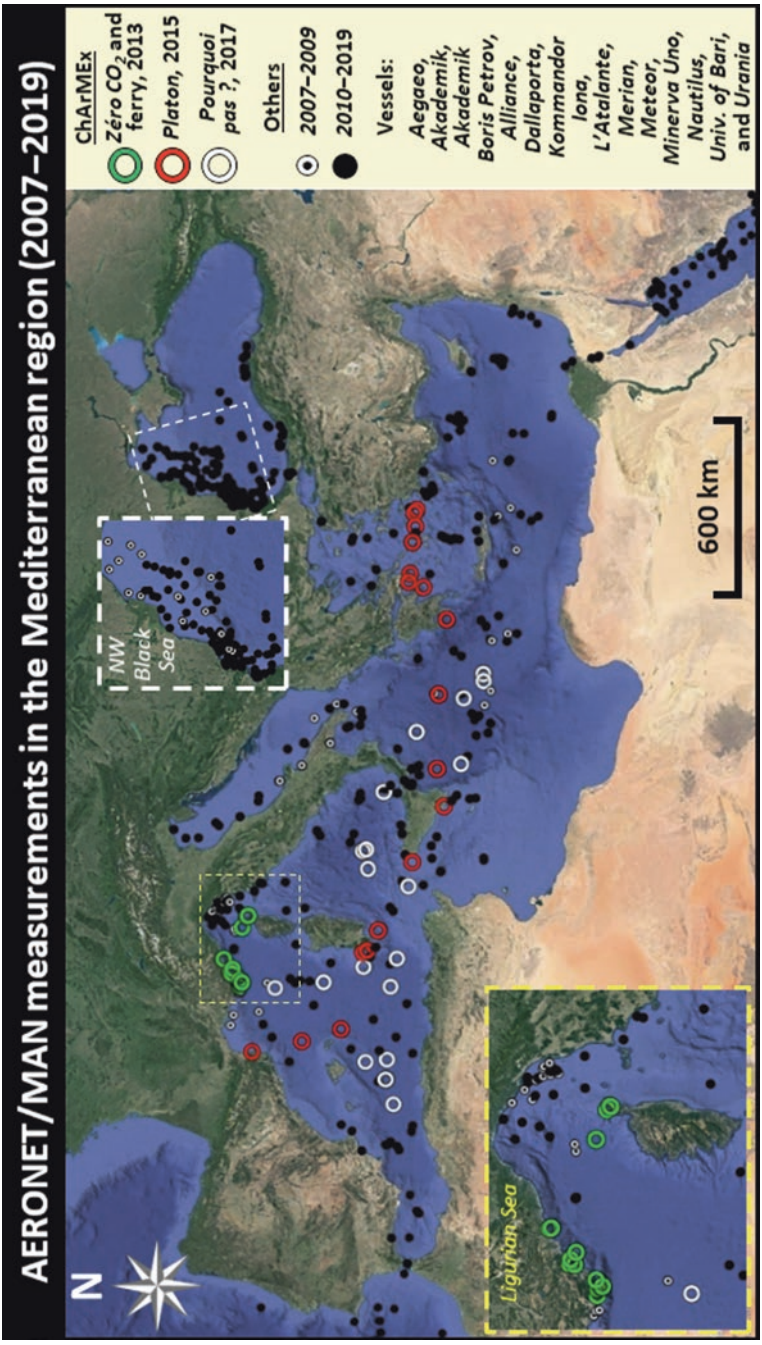

Fig. A3 Google Earth map of the AERONET/MAN shipborne photometric aerosol optical depth measurements (level 1.5 daily average values) in the Mediterranean and adjacent marine areas. The period covered extends from 21 April 2007 to 3 June 2019 (no campaign from mid-2019 to mid-2020). Some 2007-2009 markers are masked by more recent data in the main map. The top central insert is a zoom on the northwestern Black Sea, and the bottom left one, on the Ligurian Sea. Data from https://aeronet.gsfc.nasa.gov/new_web/maritime_aerosol_network.html

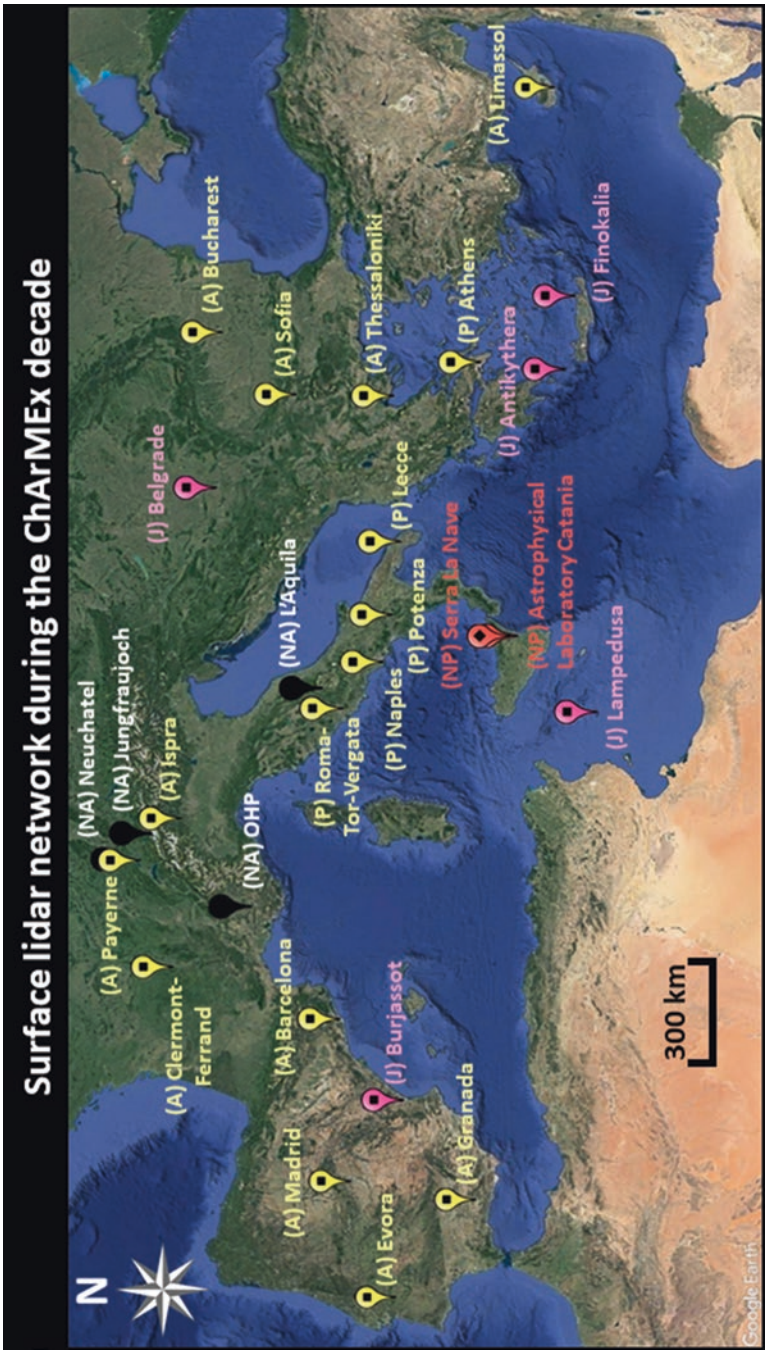

Fig. A4 Google Earth map of the ACTRIS/EARLINET lidar systems operated during the ChArMEx period (2010-2020). In July 2020, the EARLINET network in the Mediterranean region includes 16 active (A, yellow markers), 5 joining (J, pink markers), 2 non permanent (NP, red markers) and 4 not active (NA, black markers/white labels) stations with measurements provided during part of the period. Data from https://www.earlinet.org

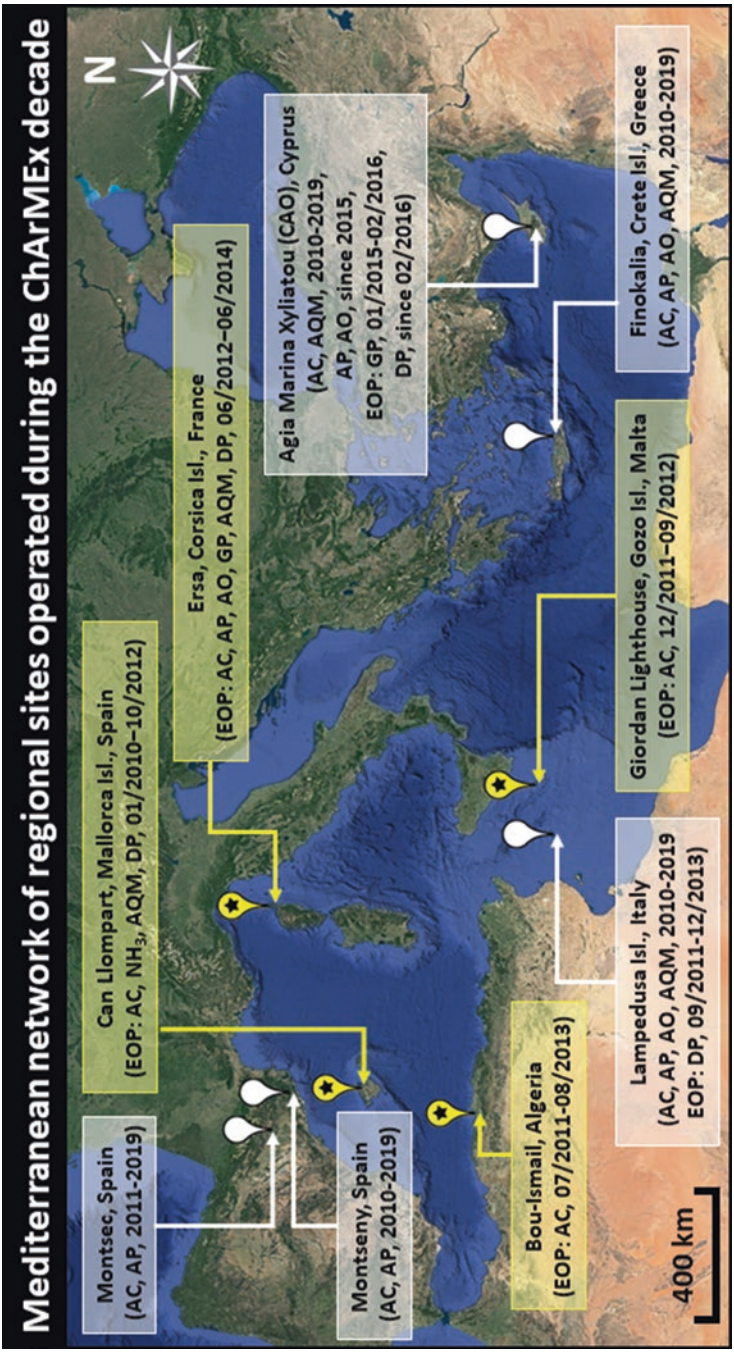

Fig. A5a Network of ChArMEx monitoring stations for the characterization of aerosols from multi-year observations at remote marine sites of the Mediterranean. Yellow starred markers represent aerosol stations specifically operated in the framework of the ChArMEx enhanced observation periods (EOPs). White markers represent other aerosol stations running during the ChArMEx decade. AC: aerosol chemistry; AP: aerosol physics; AO: aerosol optical parameters; GP: gaseous precursors; AQM: air quality measurements; DP: atmospheric deposition (see also Fig. A6 for more information on the deposition network)

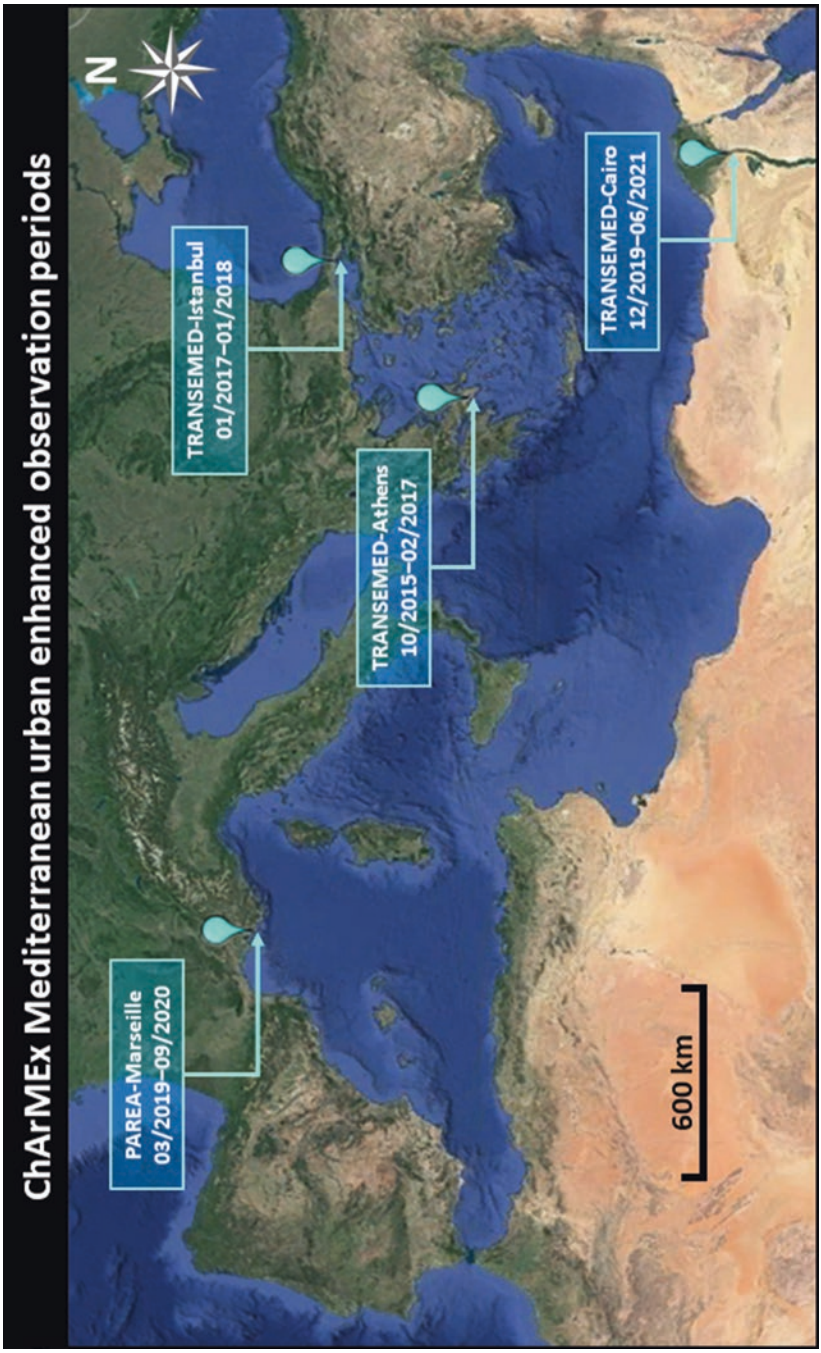

Fig. A5b Map of the ChArMEx Enhanced Observation Periods (EOPs) of at least 1-yr long monitoring that took place in different Mediterranean megapoles in order to investigate emissions, pollutant variability, and chemical processes

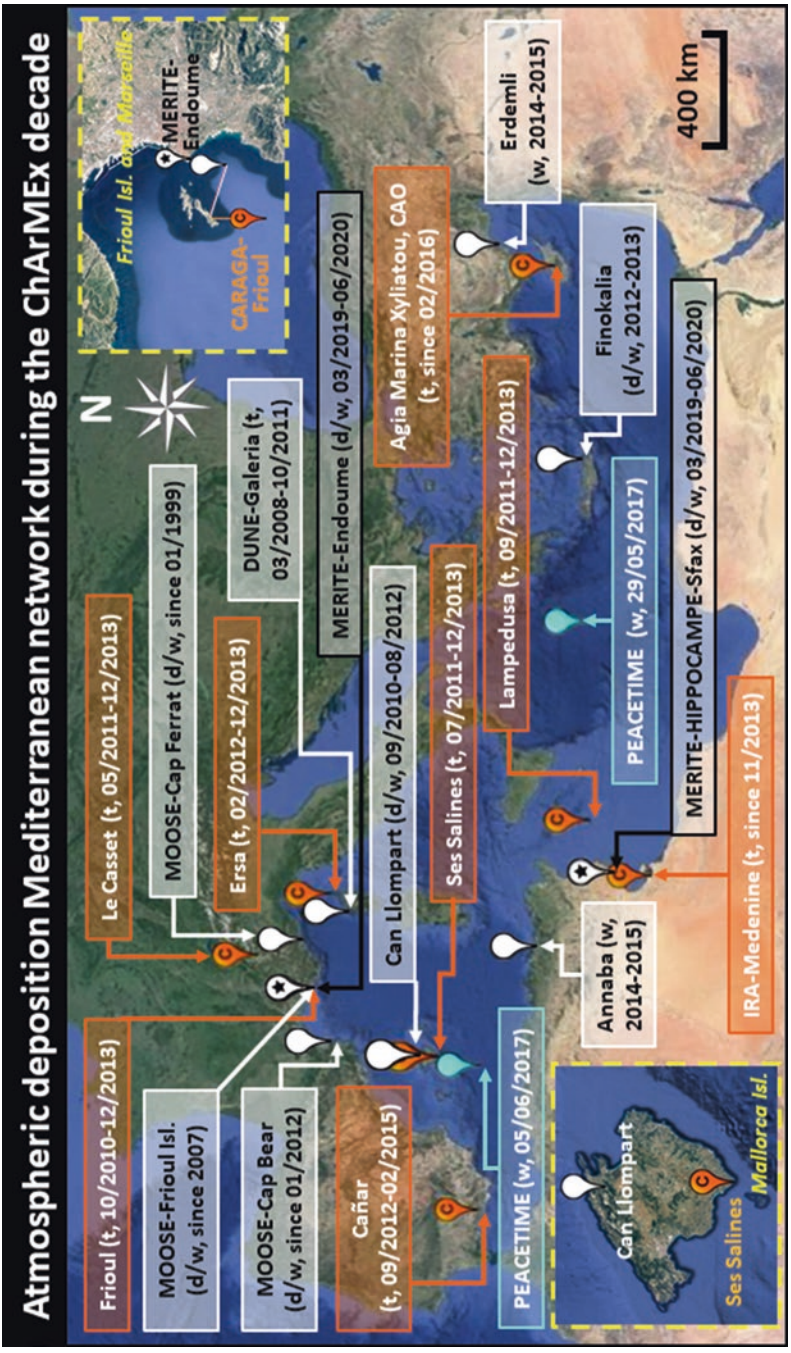

Fig. A6 Mediterranean stations for assessing soil dust or major aerosol chemical constituents in total (t), wet (w) or dry (d) atmospheric deposition. Orange pins with a "C" inside indicate CARAGA samplers (Laurent et al., 2015), and blue pins, two rain events collected at sea during the PEACETIME cruise (Desboeufs et al., 2022). The two inserts show a zoom on Mallorca (bottom left) and Marseille (top right)

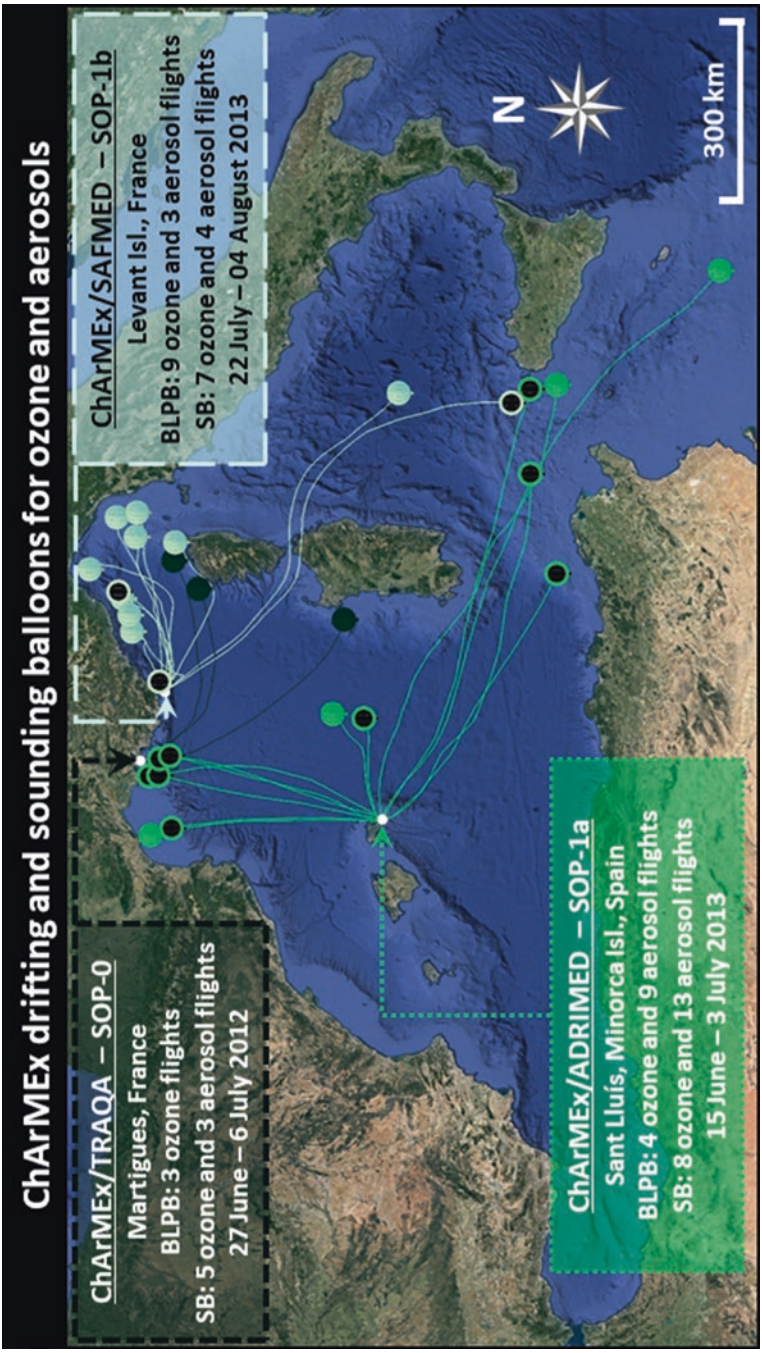

Fig. A7 Google Earth map of CNES drifting balloon (BLPB) trajectories with ozone or aerosol objectives (full or circled discs at end of flight, respectively) during ChArMEx special observation periods (SOPs). Three campaigns were performed in summer 2012 (from Martigues, France) and 2013 (from Minorca Isl;, Spain, and Levant Isl., France). Ceiling altitudes ranged between 0.2 and 3.3 km. Sounding balloons (SB) launched from the three sites up to the lower stratosphere ($\leq$36 km) are also listed (trajectories not shown). See Gheusi et al. (2016) for ozone balloons, and Renard et al. (2018) for dust

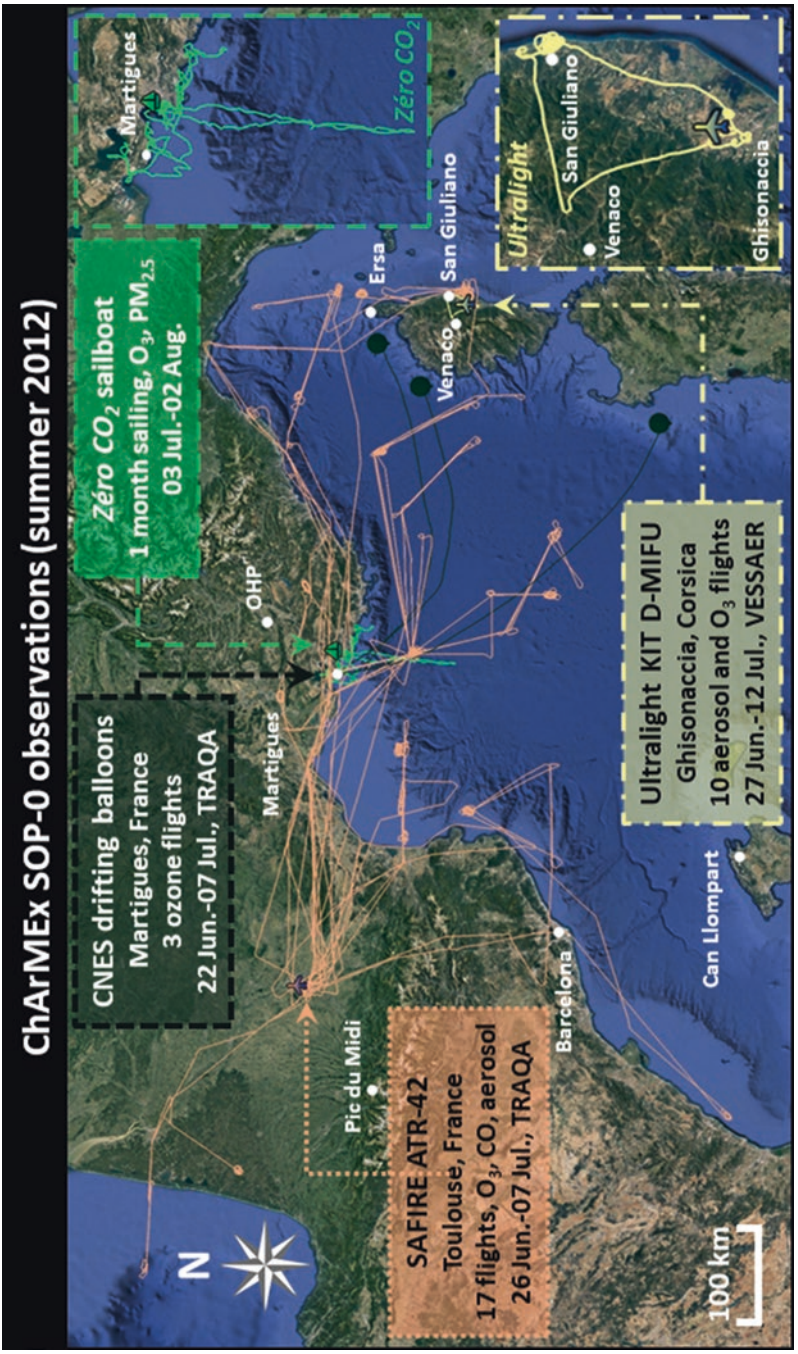

Fig. A8 Google Earth map of the surface (white disks) and airborne (black lines: drifting balloons; orange: ATR-42; yellow: ultralight aircraft) field observations during the ChArMEx pre-campaign in summer 2012 (Special Observation Period 0). Top right insert is a zoom on the *ZéroCO*$_2$ sailing boat cruise off Marseille and bottom right insert, on a typical ultralight flight from Ghisonaccia airfield

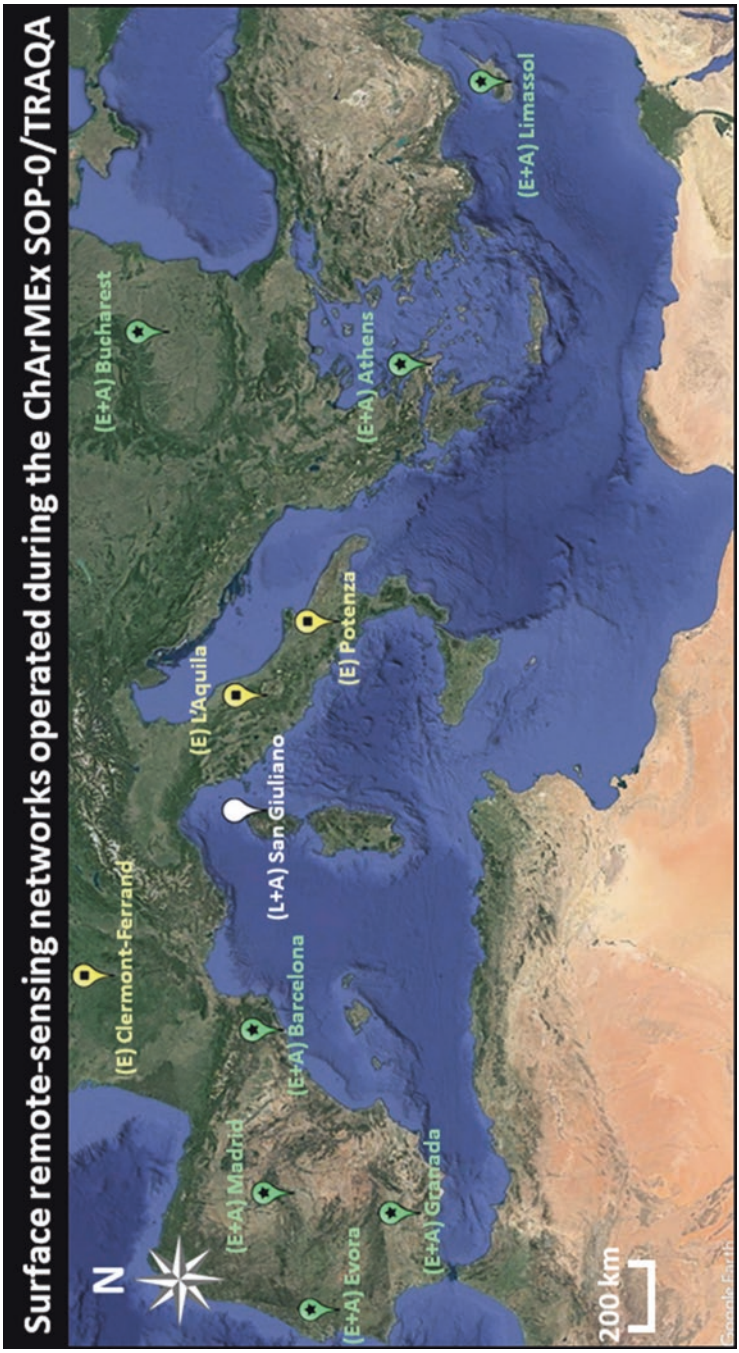

Fig. A9 Google Earth map of the surface lidar systems operated during the ChArMEx pre-campaign TRAQA in summer 2012 (Special Observation Period 0 or SOP-0), including ten ACTRIS/EARLINET lidar systems (E, green and yellow pins) and an additional ChArMEx lidar (L, white pin). At most areas, the lidar was co-located with an AERONET sun-photometer (A, black star inside the pin), at the exception of 3 areas (yellow pins). In particular, the EARLINET lidars were operated continuously for 72 h on 9–12 July in view of a model assimilation exercise (Wang et al., 2014)

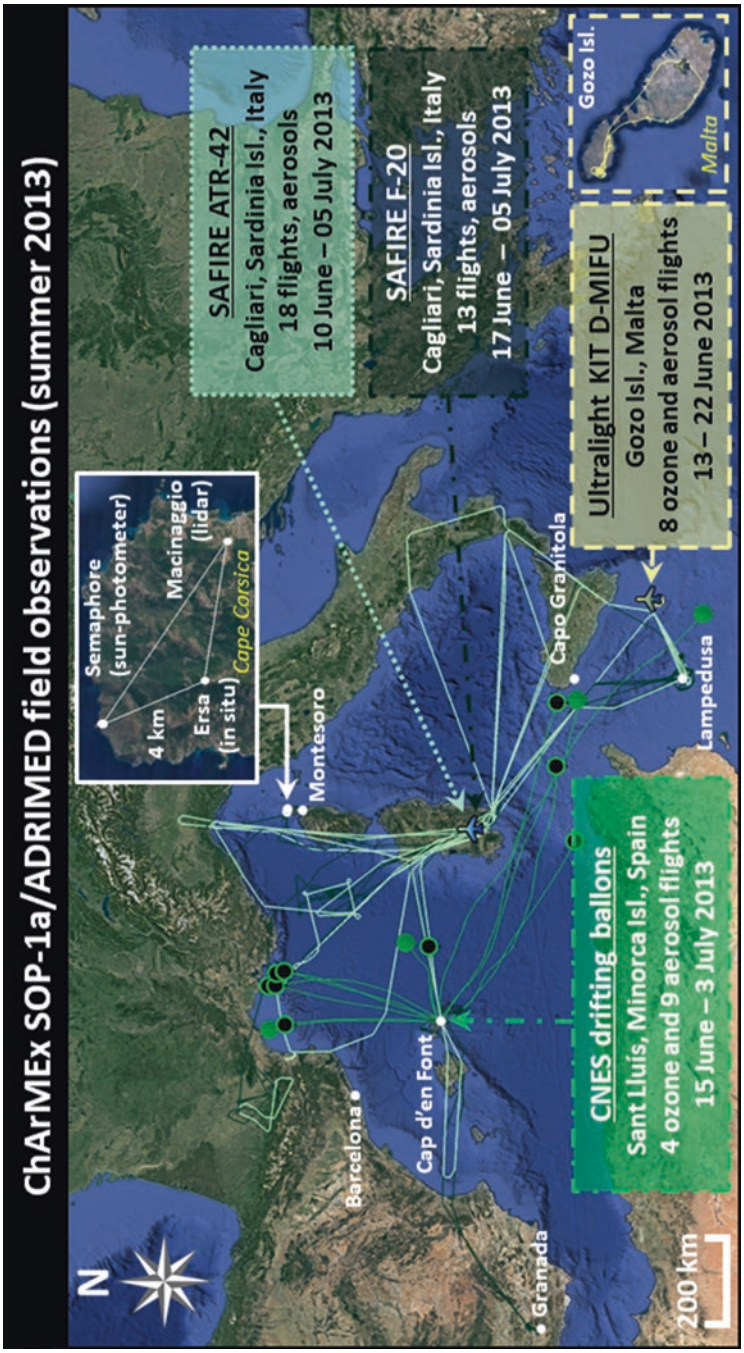

Fig. A10 Google Earth map of the surface (white dots) and airborne (colored trajectories) field observations deployment during the ChArMEx June-early July 2013 ADRIMED campaign (Special Observation Period 1a). CNES drifting balloon flights were flown with ozone (full discs) or aerosol (circled discs) objectives. Top insert is a zoom on three closed sites situated on the northern tip of Corsica Isl., and bottom right insert, a zoom with a typical ultralight aircraft flight (yellow line) from Malta airport with a vertical profile over the Gozo Isl. An overview of the campaign is given by Mallet et al. (2016)

Fig. A11 Google Earth map of PHOTONS/AERONET sun photometers (A; blue markers/black diamond) and ACTRIS/EARLINET lidars (E; yellow markers/black square) operated in the western Mediterranean during the ChArMEx/ADRIMED summer campaign (Special Observation Period 1a or SOP-1a, 13 June–05 July 2013). At four AERONET stations, an ACTRIS/EARLINET lidar was located near an AERONET sun-photometer (A+E; green markers/black star). At three others, a lidar was especially deployed for the field campaign (L+A, blue markers/white diamond). Lidars at Naples, Serra La Nave, Potenza, and Lecce were only operated on 22–24 June 2013

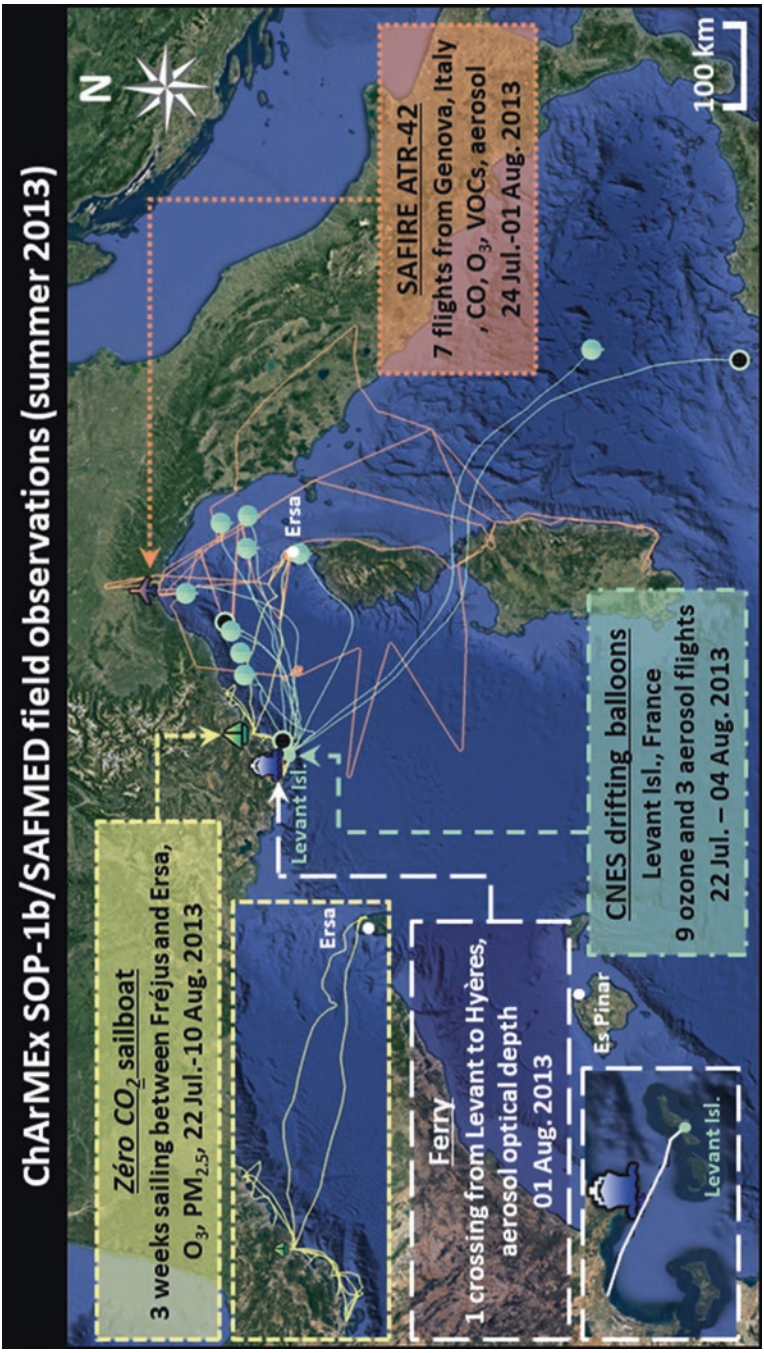

Fig. A12 Google Earth map of the field observations during the ChArMEx summer 2013 SAFMED campaign (Special Observation Period 1b). White disks: surface stations of Ersa (Corsica Isl.) and Es Pinar (Mallorca Isl.). Yellow lines: sailboat cruise in the Ligurian Sea (also in the centre left embedded zoom). White line in bottom left embedded zoom: ferry cruise. Turquoise lines: drifting balloon flights from Levant Isl., with ozone (full discs) or aerosol (circled discs) objectives. Orange lines: aircraft flights from Genova flights from Levant Isl., with ozone (full discs) or aerosol (circled discs) objectives. Orange lines: aircraft flights from Genova

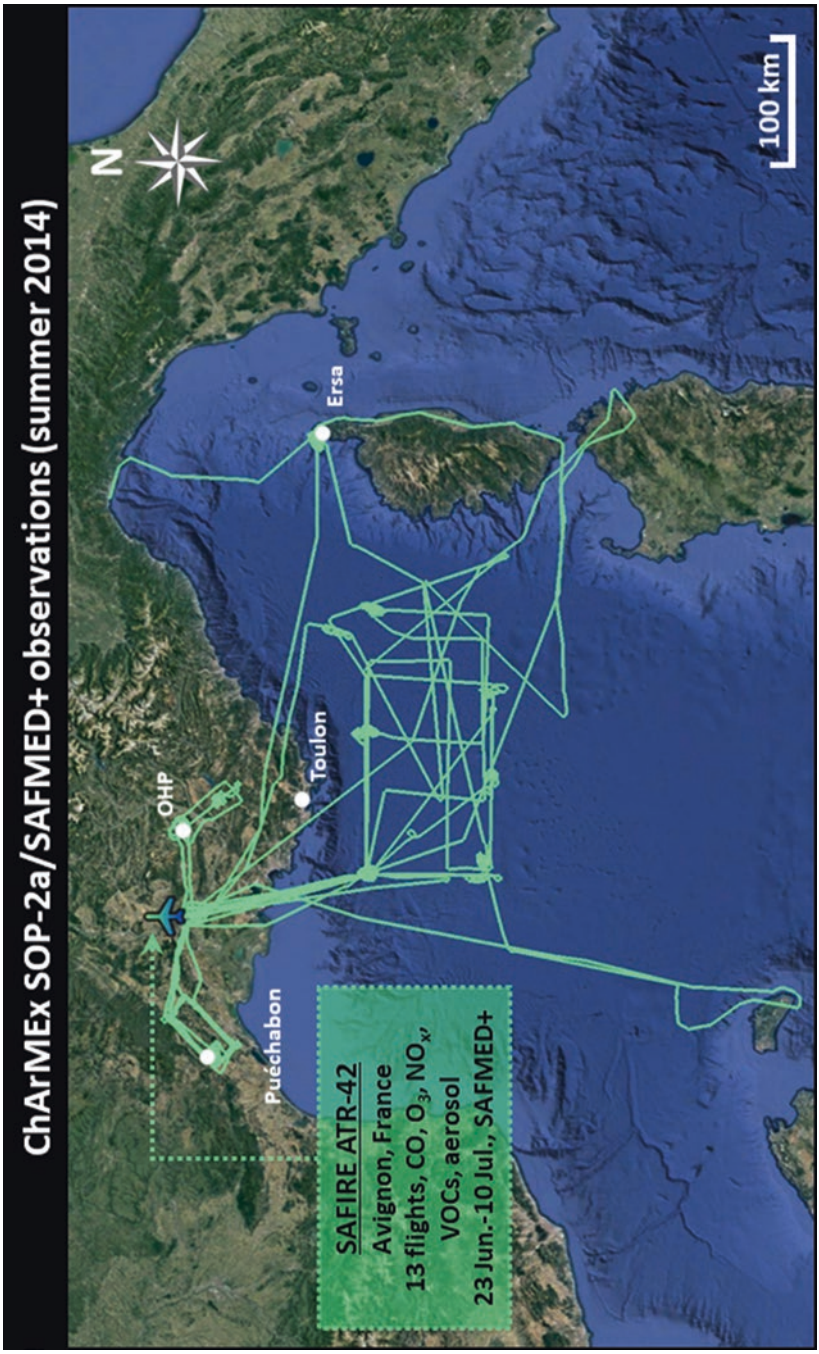

Fig. A13 Google Earth map of the surface (white disks) and airborne (colored lines) field observations during the ChArMEx summer 2014 SAFMED+ campaign (Special Observation Period 2a)

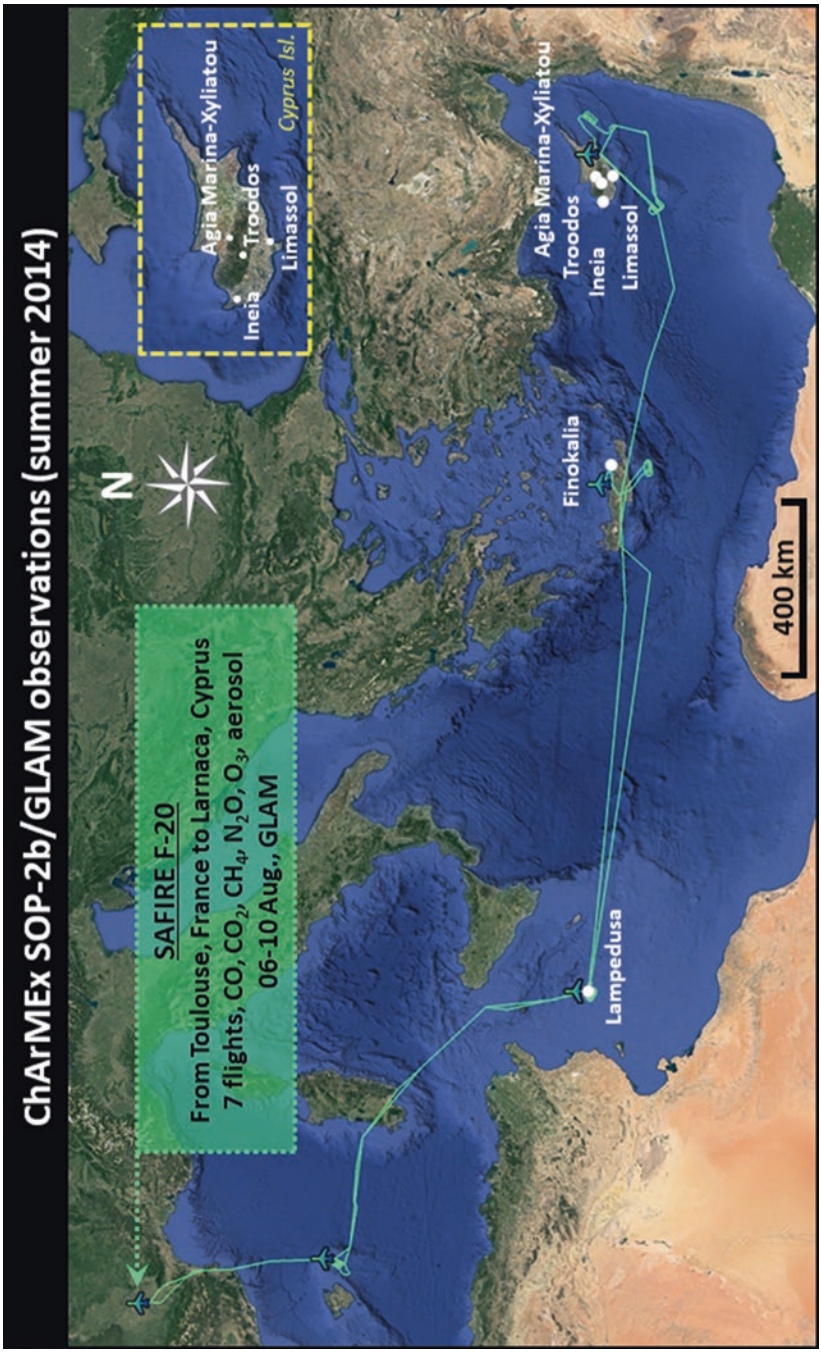

Fig. A14 Google Earth map of the surface (white disks) and airborne (colored lines) field observations deployment during the ChArMEx summer 2014 GLAM campaign (Special Observation Period 2b) (top right: embedded zoom on Cyprus Island). An overview of the campaign is given by Ricaud et al. (2018)

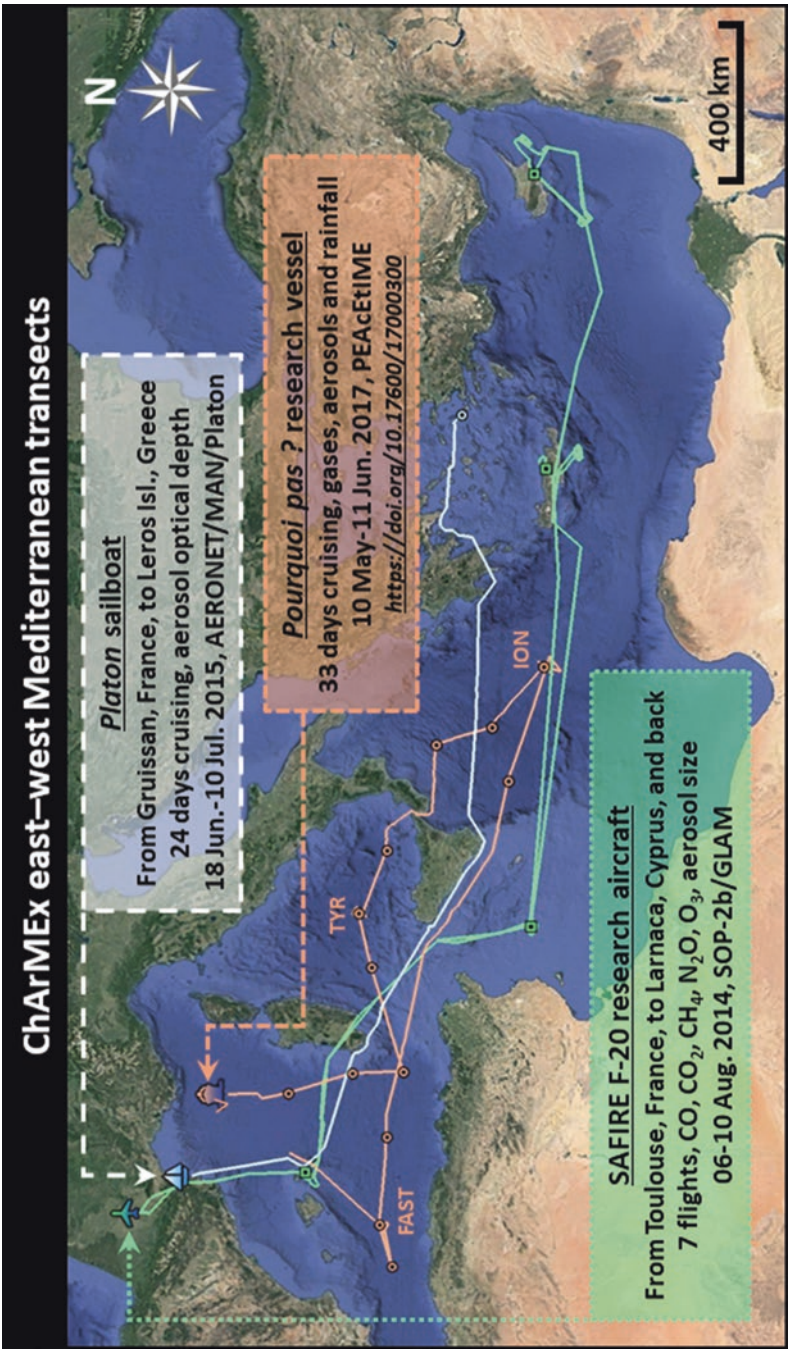

Fig. A15 Google Earth map of the ChArMEx transects across the Mediterranean, including a Falcon transect in the mid and upper troposphere with intermediate column profiles (GLAM campaign; Ricaud et al., 2018), a sailboat transect with aerosol optical depth measurements (PLATON campaign; https://aeronet.gsfc.nasa.gov/new_web/cruises_new/Platon_15.html), and an oceanographic cruise to study the air sea interface, with 11 short stations and 3 long stations for experimenting dust deposition effects (PEACETIME campaign; Guieu et al., 2020)

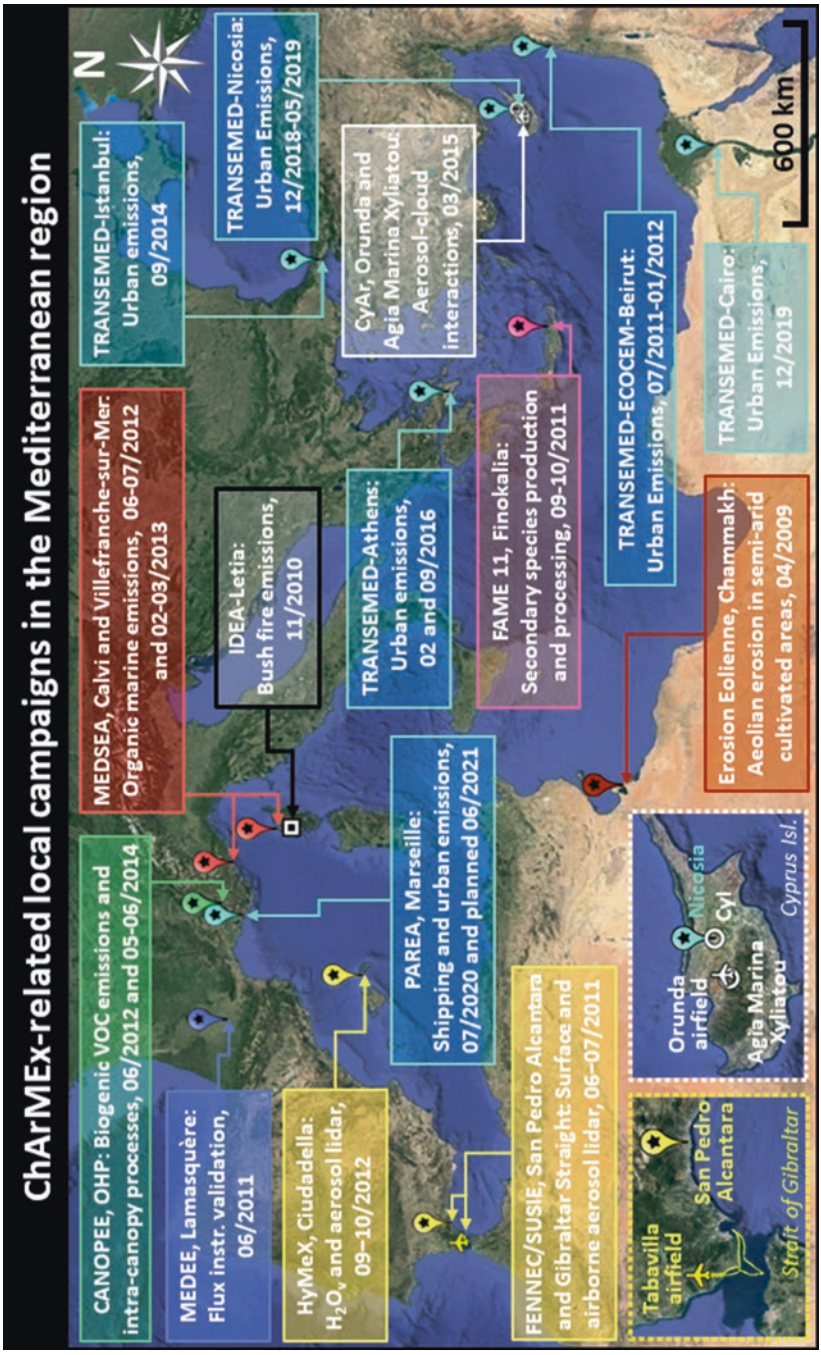

Fig. A16 Google Earth map of ChArMEx-related local campaignsto investigate selected processes and/or specific Mediterranean environments. Bottom left: embedded zooms on the Strait of Gibraltar (with a ULA airfield; Chazette, 2020) and Cyprus Island (with a UAV airfield; Calmer et al., 2019) highlight airborne observations

References

Calmer, R., Roberts, G. C., Sanchez, K. J., Sciare, J., Sellegri, K., Picard, D., Vrekoussis, M., & Pikridas, M. (2019). Aerosol–cloud closure study on cloud optical properties using remotely piloted aircraft measurements during a BACCHUS field campaign in Cyprus. *Atmospheric Chemistry and Physics, 19*, 13989–14007. https://doi.org/10.5194/acp-19-13989-2019

Chazette, P. (2020). Aerosol optical properties as observed from an ultralight aircraft over the Strait of Gibraltar. *Atmospheric Measurement Techniques, 13*, 4461–4477. https://doi.org/10.5194/amt-13-4461-2020

Desboeufs, K., Fu, F., Bressac, M., Tovar-Sánchez, A., Triquet, S., Doussin, J.-F., Giorio, C., Chazette, P., Disnaquet J., Feron, A., Formenti, P., Maisonneuve, F., Rodríguez-Romero, A., Zapf, P., Dulac, F., & Guieu, C. (2022). Wet deposition in the remote western and central Mediterranean as a source of trace metals to surface seawater. *Atmospheric Chemistry and Physics, 22*, 2309–2332. https://doi.org/10.5194/acp-22-2309-2022

Dulac, F., Hamonou, E., Sauvage, S., & Debevec, C. (2023). Introduction to the volume 1 of Atmospheric chemistry in the mediterranean region and to the ChArMEx experimental effort. In *Atmospheric chemistry in the Mediterranean* (Vol. 1, Background information and pollutants distribution). Springer, in press.

Gheusi, F., Durand, P., Verdier, N., Dulac, F., Attié, J.-L., Commun, P., Barret, B., Basdevant, C., Clenet, A., Derrien, S., Doerenbecher, A., El Amraoui, L., Fontaine, A., Hache, E., Jambert, C., Jaumouillé, E., Meyerfeld, Y., Roblou, L., & Tocquer, F. (2016). Adapted ECC ozonesonde for long-duration flights aboard boundary-layer pressurised balloons. *Atmospheric Measurement Techniques, 9*, 5811–5832. https://doi.org/10.5194/amt-9-5811-2016

Guieu, C., D'Ortenzio, F., Dulac, F., Taillandier, V., Doglioli, A., Petrenko, A., Barrillon, S., Mallet, M., Nabat, P., & Desboeufs, K. (2020). Introduction: Process studies at the air–sea interface after atmospheric deposition in the Mediterranean Sea – objectives and strategy of the PEACETIME oceanographic campaign (May–June 2017). *Biogeosciences, 17*, 5563–5585. https://doi.org/10.5194/bg-17-5563-2020

Laurent, B., Losno, R., Chevaillier, S., Vincent, J., Roullet, P., Bon Nguyen, E., Ouboulmane, N., Triquet, S., Fornier, M., Raimbault, P., & Bergametti, G. (2015). An automatic collector to monitor insoluble atmospheric deposition: Application for mineral dust deposition. *Atmospheric Measurement Techniques, 8*, 2801–2811. https://doi.org/10.5194/amt-8-2801-2015

Mallet, M., Dulac, F., Formenti, P., Nabat, P., Sciare, J., Roberts, G., Pelon, J., Ancellet, G., Tanré, D., Parol, F., Denjean, C., Brogniez, G., di Sarra, A., Alados-Arboledas, L., Andt, J., Auriol, F., Blarel, L., Bourrianne, T., Chazette, P., … Zapf, P. (2016). Overview of the Chemistry-Aerosol Mediterranean Experiment/Aerosol Direct Radiative Forcing on the Mediterranean Climate (ChArMEx/ADRIMED) summer 2013 campaign. *Atmospheric Chemistry and Physics, 16*, 455–504. https://doi.org/10.5194/acp-16-455-2016

Renard, J.-B., Dulac, F., Durand, P., Bourgeois, Q., Denjean, C., Vignelles, D., Couté, B., Jeannot, M., Verdier, N., & Mallet, M. (2018). In situ measurements of desert dust particles above the western Mediterranean Sea with the balloon-borne Light Optical Aerosol Counter/sizer (LOAC) during the ChArMEx campaign of summer 2013. *Atmospheric Chemistry and Physics, 18*, 3677–3699. https://doi.org/10.5194/acp-18-3677-2018

Ricaud, P., Zbinden, R., Catoire, V., Brocchi, V., Dulac, F., Hamonou, E., Canonici, J.-C., El Amraoui, L., Massart, S., Piguet, B., Dayan, U., Nabat, P., Sciare, J., Ramonet, M., Delmotte, M., di Sarra, A., Sferlazzo, D., di Iorio, T., Piacentino, S., ... Théron, P. (2018). The GLAM airborne campaign across the Mediterranean Basin. *Bulletin of the American Meteorological Society, 99*, 361–380. https://doi.org/10.1175/BAMS-D-16-0226.1

Wang, Y., Sartelet, K. N., Bocquet, M., Chazette, P., Sicard, M., D'Amico, G., Léon, J. F., Alados-Arboledas, L., Amodeo, A., Augustin, P., Bach, J., Belegante, L., Binietoglou, I., Bush, X., Comerón, A., Delbarre, H., García-Vízcaino, D., Guerrero-Rascado, J. L., Hervo, M., … Dulac, F. (2014). Assimilation of lidar signals: application to aerosol forecasting in the western Mediterranean basin. *Atmospheric Chemistry and Physics, 14*, 12031–12053. https://doi.org/10.5194/acp-14-12031-2014

Index

F. Dulac et al. (eds.), *Atmospheric Chemistry in the Mediterranean Region*,
https://doi.org/10.1007/978-3-030-82385-6